WOODS HOLE OCEANOGRAPHIC INSTITUTION

COLLECTED REPRINTS

1956

SEP 1957
LIBRARY
BOFI
FISH & WILDLIFE
SERVICE

JULY, 1957

DATE OF MAGAZINE
BORROWER'S NAME

PERIODICAL
WOODS HOLE
OCEANOGR.
INSTITUTION

COLLECTED
REPRINTS

1956

LIBRARY
BUREAU OF COMMERCIAL FISHERIES
U. S. FISH AND WILDLIFE SERVICE
P. O. BOX 3830
HONOLULU 12, HAWAII

LIBRARY
BUREAU OF COMMERCIAL FISHERIES
U. S. FISH AND WILDLIFE SERVICE
P. O. BOX 3830
HONOLULU 12, HAWAII

WOODS HOLE OCEANOGRAPHIC INSTITUTION

COLLECTED REPRINTS

1956

SEP 1957
LIBRARY
POFI
FISH & WILDLIFE
SERVICE

GC1
W71
2007

JULY, 1957

This volume contains contributions from the WOODS HOLE OCEANOGRAPHIC INSTITUTION which were published in 1956; also the Annual Report of the Director for the year 1956.

TABLE OF CONTENTS

Contribution No.

ARONS, A. B. and HENRY STOMMEL
A β-Plane Analysis of Free Periods of the Second Class in Meridional and Zonal Oceans 855

AYERS, JOHN C.
Population Dynamics of the Marine Clam, *Mya arenaria* 766
A Dynamic Height Method for the Determination of Currents in Deep Lakes . 823

✓ BACKUS, RICHARD H. and J. B. HERSEY
Echo-Sounder Observations of Midwater Nets and their Towing Cables . . . 834

BACKUS, RICHARD H., STEWART SPRINGER and EDGAR L. ARNOLD, JR.
A Contribution to the Natural History of the White-Tip Shark, *Pterolamiops longimanus* (Poey) 814

✓ BULLIS, HARVEY R., JR. and F. J. MATHER, III
Tunas of the Genus *Thunnus* of the Northern Caribbean 774

BUNKER, A. F.
Measurements of Counter-Gradient Heat Flows in the Atmosphere 682

✓ CLARKE, GEORGE L. and RICHARD H. BACKUS
Measurements of Light Penetration in Relation to Vertical Migration and Records of Luminescence of Deep-Sea Animals 858

✓ CLARKE, GEORGE L. and GUNTHER K. WERTHEIM
Measurements of Illumination at Great Depths and at Night in the Atlantic Ocean by Means of a New Bathyphotometer 821

EDWARDS, RICHARD S. and FRANCIS A. RICHARDS
A Bottom-Water Sampler 865

FAIRBANK, NORA GLADWIN
Methods and Preliminary Results in a Study of Minerals from the Eastern Gulf of Mexico 798

✓ FALLER, ALAN J.
A Demonstration of Fronts and Frontal Waves in Atmospheric Models . . 754

FRIEDMAN, IRVING, DANIEL R. NORTON, DOUGLAS B. CARTER and ALFRED C. REDFIELD
The Deuterium Balance of Lake Maracaibo 867

HULBURT, E. M.
The Phytoplankton of Great Pond, Massachusetts 764

✓ ISELIN, C. O'D.
Recent Advances in our Understanding of the Circulation Problem and their Implications (Dated 1955) 765

Contribution No.

✓ JOHNSON, HENRY R., RICHARD H. BACKUS, J. B. HERSEY and D. M. OWEN
Suspended Echo-Sounder and Camera Studies of Midwater Sound Scatterers . 841

✓ KNOTT, S. T. and J. B. HERSEY
Interpretation of High-Resolution Echo-Sounding Techniques and their Use in Bathymetry, Marine Geophysics, and Biology 863

MACKIEWICZ, JOHN and RICHARD H. BACKUS
Oceanic Records of *Lasionycteris noctivagans* and *Lasiurus borealis* 805

MALKUS, JOANNE STARR
On the Maintenance of the Trade Winds 827

MALKUS, W. V. R.
Outline of a Theory of Turbulent Shear Flow 804

MILLER, ROBERT L.
Trend Surfaces: Their Application to Analysis and Description of Environments of Sedimentation. 1. The Relation of Sediment-Size Parameters to Current-Wave Systems and Physiography 826

✓ MOORE, H. B. and E. G. CORWIN
The Effects of Temperature, Illumination and Pressure on the Vertical Distribution of Zooplankton 864

✓ MORGAN, G. W.
On the Wind-Driven Ocean Circulation 811

MOULTON, JAMES M.
Influencing the Calling of Sea Robins (*Prionotus* spp.) with Sound 862

NUTT, DAVID C. and LAWRENCE K. COACHMAN
The Oceanography of Hebron Fjord, Labrador 831

RICHARDS, FRANCIS A.
On the State of our Knowledge of Trace Elements in the Ocean 840

RICHARDS, FRANCIS A. and NATHANIEL CORWIN
Some Oceanographic Applications of Recent Determinations of the Solubility of Oxygen in Sea Water 852

RICHARDS, FRANCIS A. and RALPH F. VACCARO
The Cariaco Trench, an Anaerobic Basin in the Caribbean Sea 830

RYTHER, JOHN H.
Photosynthesis in the Ocean as a Function of Light Intensity 819
The Measurement of Primary Production 825
Interrelation between Photosynthesis and Respiration in the Marine Flagellate, *Dunaliella euchlora* 842

Contribution No.

SCHELL, IRVING I.
Interrelations of Arctic Ice with the Atmosphere and the Ocean in the North Atlantic — Arctic and Adjacent Areas 745
Further Evidence of Dynamic Persistence and of its Application to Foreshadowing 797
On the Nature and Origin of the Southern Oscillation 853

SCHEVILL, WILLIAM E.
Lagenorhynchus acutus off Cape Cod 815

SCHEVILL, WILLIAM E. and BARBARA LAWRENCE
Food-Finding by a Captive Porpoise (*Tursiops truncatus*). 832

✓ SCHLEICHER, KARL E. and ALVIN BRADSHAW
A Conductivity Bridge for Measurement of the Salinity of Sea Water . . . 810

SCHOLANDER, P. F.
Observations on the Gas Gland in Living Fish 880

SCHOLANDER, P. F., JOHN W. KANWISHER and D. C. NUTT
Gases in Icebergs 818

SCHOLANDER, P. F. and L. VAN DAM
Micro Gasometric Determination of Oxygen in Fish Blood 879

SCHOLANDER, P. F., L. VAN DAM and THEODORE ENNS
Nitrogen Secretion in the Swimbladder of Whitefish 816
The Source of Oxygen Secreted into the Swimbladder of Cod 881

SOULE, FLOYD M. and J. E. MURRAY
Physical Oceanography of the Grand Banks and the Labrador Sea in 1955 . . 801

SPILHAUS, ATHELSTAN
Control of the World Environment 847

✓ STOMMEL, HENRY
On the Determination of the Depth of No Meridional Motion 846

STOMMEL, HENRY, ARNOLD B. ARONS and DUNCAN BLANCHARD
An Oceanographical Curiosity: the Perpetual Salt Fountain 799

TRASK, PARKER D.
The *Atlantis* Marine Geological Expedition to Peru and Chile 824

TURNER, HARRY J., CARL J. GEORGE and JOSEPH H. CONNELL
Eighth Report on Investigations of the Shellfisheries of Massachusetts (Dated 1955) 876

✓ VERONIS, G. and HENRY STOMMEL
The Action of Variable Wind Stresses on a Stratified Ocean 859

VISHNIAC, HELEN S.
On the Ecology of the Lower Marine Fungi 869

Contribution No.

VOLKMANN, GORDON, JOHN KNAUSS and ALLYN VINE
The Use of Parachute Drogues in the Measurement of Subsurface Ocean Currents 856

von ARX, WILLIAM S.
Some Techniques for Laboratory Study of the Primary Ocean Circulation . . 681

WOODCOCK, A. H.
Dimorphism in the Portuguese Man-of-War 837

WORTHINGTON, L. V.
The Temperature Increase in Caribbean Deep Water since 1933 666

THE WOODS HOLE OCEANOGRAPHIC INSTITUTION
Report for the Year 1956

LIST OF CONTRIBUTIONS

The following contributions, published in 1956, are not included in this volume.

COACHMAN, LAWRENCE K., E. HEMMINGSEN and P. F. SCHOLANDER
Gas Enclosures in a Temperate Glacier 873

LAWRENCE, BARBARA and WILLIAM E. SCHEVILL
The functional Anatomy of the Delphinid Nose 793

Contribution No. 666

Deep-Sea Research, 1956, Vol. 3, pp. 234 and 235. Pergamon Press Ltd., London.

LETTER TO THE EDITORS

The temperature increase in Caribbean deep water since 1933

IN a recent paper in this journal (WORTHINGTON, 1955) I presented a chronology, based on oxygen consumption, in which a date (1790) was assigned to the isolation of the deep water in the Caribbean Basin from that in the Cayman Basin. For this chronology the observed rate of oxygen loss in the Caribbean deep water over the last twenty years was presumed to have been the same since the time when this water was saturated with oxygen. As we knew the amount of oxygen that this water can contain, it was a simple calculation to arrive at a date for its formation.

The admitted weakness in this dating system was that, if the water were much below its saturation point when it flowed over the sill, the filling of the basin would have to be moved into the more recent past. At the time this paper was submitted no great attention was paid to the increase in temperature (WORTHINGTON, 1955) which accompanied this oxygen loss, other than that its existence was attributed to eddy diffusion from higher levels. A more recent study of this temperature increase has provided some evidence that the Caribbean Basin was indeed cut off at a more recent date than the one assigned in the chronology.

The oceanographic section which provided the new temperature and oxygen data closely followed a section made in 1933. In the following table are listed the average potential temperatures at various levels in both sections. Figures in parentheses are the number of stations which were used.

Depth, M	*Potential Temperature °C*		
	March, 1933	*December*, 1954	*Gain*
1500	4·028 (9)	4·075 (6)	0·047
1600	3·973 (9)	4·009 (6)	0·036
1750	3·928 (9)	3·952 (6)	0·024
2000	3·886 (9)	3·901 (6)	0·015
2500	3·842 (5)	3·850 (5)	0·008
3000	3·832 (5)	3·837 (5)	0·005

In spite of the small number of observations at each level the curve of temperature gain versus depth is surprisingly smooth.

The minimum potential temperature found on both sections was 3·80°. This occurred at the greatest depth sampled on each section (4960 m in 1933, 5445 m in 1954). No change in temperature can be detected at these depths. It is not unreasonable to assume that at the time the deep waters of the Caribbean were cut off from the outside they had a potential temperature of 3·80° from the sill depth down to the bottom – in other words that they were neutrally stable – and that the increasingly stable conditions which are found nowadays are due to the supply of heat from above.

If the measured rate of temperature increase at each level has remained the same since the basin waters were cut off, it is possible to arrive at a date for that occurrence. For instance, at the 1500 m level the temperature in 1954 was 4·075°, or 0·275° more than 3·80°, the assumed temperature at the cut-off date. The rate of gain in temperature was 0·047° in 21¾ years, so

$$T = 21{\cdot}75 \times \frac{0{\cdot}275}{0{\cdot}047} = 127 \text{ years before } 1954.$$

If the same calculation is carried out for the other levels we get the following answers :

1500 m	1827
1600 m	1828
1750 m	1816
2000 m	1808
2500 m	1818
3000 m	1793

The value at 3000 m seems out of line, but an increase of 0·001° at this level would change the answer to 1816. The others hold pretty close to the average, around 1819. This method can probably be refined, but there seems little use in doing so until there are more modern observations. According to this average the water which filled the deep Caribbean Basin was about 30 years old when it passed over the sill, if we accept the formation date set by oxygen consumption.

No great accuracy can be claimed for either method of dating but the important thing seems to be that both methods agree in order of magnitude. The question of whether this water is 150 or 1,500 years old is the fundamental one at present, and the new evidence favours the more youthful ocean, on the basis of both temperature gain and oxygen loss.

L. V. WORTHINGTON

Contribution No. 666 *from the Woods Hole Oceanographic Institution, Woods Hole, Massachusetts.*

REFERENCE

WORTHINGTON, L. V. (1955), A new theory of Caribbean bottom-water formation. *Deep-Sea Res.*, **3**, 82-87.

Printed in Great Britain by The Salisbury Press Ltd., Publicity House, Wilton Road, Salisbury, Wilts. (96505)

Contribution No. 681

REPRINTED FROM

FLUID MODELS IN GEOPHYSICS

Proceedings of the First Symposium on the Use of Models in Geophysical Fluid Dynamics

Held at
The Johns Hopkins University
September 1–4, 1953

Editor
ROBERT R. LONG
The John Hopkins University

Sponsored by
The Office of Naval Research
with the Cooperation of
The Geophysics Research Directorate
and
The U. S. Weather Bureau

SOME TECHNIQUES FOR LABORATORY STUDY OF THE PRIMARY OCEAN CIRCULATION

William S. von Arx

Woods Hole Oceanographic Institution
Woods Hole, Massachusetts

A laboratory study of the northern hemisphere oceans was begun at Woods Hole in the latter part of 1950. Several experimental arrangements were tried. The most recent of these is described in a paper which appeared in 1952 (*1*). Therefore, except for some comments on the history of the apparatus not mentioned in that earlier paper, this discussion will be concerned primarily with the results of the experiments, their interpretation, and experiments that may be undertaken in the future.

The use of models in connection with the circulation of the open ocean has been delayed, I think, mainly by the technically forbidding prospect of maintaining a suitable density distribution in a rotating system which would lead to associated geostrophic flow patterns within more or less realistically shaped physical boundaries. The density differences could be provided experimentally through use of two or more immiscible liquids, but these produce unrealistically sharp gradients of density and interfacial tension. Surface heating seems more suitable because it produces continuous gradients of density, resembles insolation, and provides a source of energy by which the model ocean might be driven. However it introduces the problems of controlling evaporation, and phase changes, and the particularly difficult matter of holding appropriately related scales of horizontal motion and turbulent mixing. In these "geostrophic" views of ocean modeling, the effect of the zonal wind stress is considered only secondarily.

A fresh point of view was suggested by a paper by Mr. Henry Stommel (*2*) concerning the vorticity theory of the primary ocean circulation. According to this, the essential factors determining the characteristic pattern of the circulation of oceans in tropical and temperate latitudes are wind stress, friction and the rotation of the earth. Heating and density differences in the ocean are neglected as contributing only secondary effects. The term "westward intensification" is introduced to describe the marked narrowing and acceleration of the flow away from the equator into higher tropical and temperate latitudes by way of the westernmost portions of particularly the North Atlantic and North Pacific Oceans. This effect is much less conspicuous in southern hemisphere oceans.

In qualitative terms the vorticity theory concerns itself with the balance of frictional (shearing) vorticity, against the sum of the planetary vorticity tendency and curl of the zonal wind stress. In the cases of the North Atlantic and North Pacific Oceans, as the clearest examples, the curl of the wind stress imparts an anticyclonic spin to vertical water columns which augments the tendency for anticyclonic spin (planetary vorticity) to accompany northward flow in the western portions of these oceans. In order for the frictional vorticity tendency to cancel the sum of these two vorticity tendencies, the northward-flowing currents must lie close against the western continental masses to produce strong cyclonic shear. In the eastern portions of these oceans where the flow is southward, the planetary vorticity tendency is re-

---

Note: This is contribution No. 681, from the Woods Hole Oceanographic Institution. This work has been supported by the Office of Naval Research under Contract N6onr-27701 (NR-083-004) with the Woods Hole Oceanographic Institution.

versed (cyclonic) and is itself opposed and nearly equal to the vorticity associated with the curl of the wind stress. Thus friction against the eastern continental boundaries is almost unnecessary and the flow there can be broad and consequently slow. A definitive discussion of these ideas may be found in the paper by Stommel (*2*), already referred to, and their quantitative aspects in another by Munk (*3*).

To date three models have been constructed on the basis of the vorticity principle. The first was a hemispherical bowl 20 cm in diameter floating in a pan of water and given northern hemisphere rotation by three jets of water striking its outside surface. Wind stress was applied zonally from three nozzles attached to the laboratory compressed air line. The interior of the bowl was divided with sponge rubber strips into 30, 60, 90 and 180° compartments. A crude but encouraging sort of westward intensification was noted in each water-filled compartment but even in the largest of these the narrow and swift current along the western margin was unrealistically broad compared with the width of the compartment. A larger bowl was tried.

This bowl, also hemispherical, was 80 cm in diameter and rotated on the end of a vertical shaft driven by a synchronous motor. The same experiments were performed. In this case westward intensification was more nearly in scale (0.05 the width of the 90° compartment) compared with the size of the compartments but in absolute terms the western currents were almost as wide as in the smaller model, due perhaps to there being the same minimum level of turbulence.

Since increasing the scale of the apparatus seemed to be the simplest way to increase the geometrical realism of the experiments it was decided to build a basin as large as permitted by the dimensions of the laboratory doorway. This basin is a paraboloid 200 cm in diameter having a focal length of 50 cm, i. e., the paraboloid is terminated at the latus rectum. The discussion from here on will be concerned with the results of some experiments with this apparatus, shown in Fig. 1.

Originally it was not expected that the paraboloidal model could represent more than the topography and wind systems approximately 53° away from the geographic pole, since this is the arc of a sphere that would most closely approximate the paraboloid. But these limits cut away the interesting parts of the oceans in temperate and tropical latitudes. It was therefore decided to attempt to model a full hemisphere and to determine empirically what time, length, velocity and derivative scales seemed to yield best results. To this end the continents were projected gnomonically from the center of a terrestrial globe imagined to have been placed at the solar focus of the paraboloid, as shown in Fig. 2.

In the first few tests the apparatus was rotated with great care at that angular velocity which would maintain a uniform depth of water measured parallel with the axis of rotation. There was no trace of westward intensification in the circulation. It was then thought that the depth should perhaps be maintained constant along normals to the free surface by increasing the rate of rotation. Westward intensification appeared but in a very distorted pattern. A realistic pattern developed only when the basin was rotating at a certain critical speed some 3 per cent above the first rate.

These interesting effects were interpreted by Professor C. G. Rossby who pointed out that when the depth of water is constant, measured parallel with the axis of rotation, the depth of water measured along normals to the free surface increases poleward (that is, in the direction of the vertex of the paraboloid) and that the relative vorticity accompanying vertical stretching and shrinking had, in this case, exactly canceled the planetary vorticity due to meridional curvature of the basin. He also computed at the time that if the depth of water measured along normals to the free surface were greater over the equator than over the pole by $1+1/\sqrt{2}$, that the relative vorticity due to stretching and shrinking would augment that due to the basin curvature to produce results similar to what might be obtained were the model truly hemispherical.

This result has been approached in experiments wherein the ratio of equatorial to polar depths has been found to range from 1.8 to 2.0 when the rate of rotation has been adjusted to give an acceptable approximation of the known ocean circulation patterns. Exact agreement could not be expected because it was not then known how to locate the latitude circles (and topography) in the model so that the meridional change in relative vorticity between given points in the model could be made similar to the change in planetary vorticity between corresponding points on the earth. Stated symbolically

$$\left(\frac{\partial f}{\partial \phi}\right)_{\text{earth}}=\left(\frac{\partial f}{\partial \phi}+\left(\frac{f+\zeta}{D}\right)\frac{\partial D}{\partial \phi}\right)_{\text{model}}, \tag{1}$$

where f is the Coriolis parameter, ϕ is the latitude, ζ is the relative vorticity (usually neglected), and D is the depth of fluid.

The spacing of latitude circles can be established in either of two ways: (1) through calculation of the divergence due to stretching and shrinking for columns parallel to the axis of rotation, or (2) through calculation of divergence in fluid columns measured normal to the local free surface and the added effects of meridional curvature. In the first case the columns are regarded as having some of the properties of Taylor "walls," (*4*) and not so in the second case. There are insufficient experimental data to choose between these two alternatives at present.

There is, nevertheless, a way to avoid this dilemma through the use of flat, rather than paraboloidal models, in which divergence is the only effect called upon to simulate the planetary vorticity of the spherical earth. This possibility[1] is being looked into both experimentally and theoretically at present and seems to offer promise from both points of view.

Substitution of divergence for part of the effects required to simulate variation of the Coriolis parameter with latitude in the paraboloidal model leads to the interesting possibility that the balance of the planetary and wind stress vorticities by frictional vorticity can be altered by changing the rate of rotation to produce strange as well as familiar patterns of oceanic circulation. When the effective planetary vorticity is reduced to zero, one has merely a balance of the wind stress vorticity against frictional vorticity. Since both are uniformly distributed but of opposite sign, the ocean circulation becomes symmetrical around the center of the ocean basin. When the sign of the planetary vorticity tendency is reversed (that is, made cyclonic for northward displacements) it is found that the ordinary zonal wind pattern results in eastward intensification of the ocean currents.

The model experiments were undertaken primarily to extend the consequences of the vorticity theory of the ocean circulation to the case of realistically shaped ocean boundaries which are geometrically too complex to be managed mathematically. In simulating the horizontal boundaries of the ocean basins of the northern hemisphere it was conceivable that the experimental results might have shown that the marked resemblance between the wind-driven circulations within regular geometrical shapes (squares and triangles) might vanish when these boundaries were more realistically contorted. Since we now know that the experimental circulations become more like the actual ocean circulation patterns, indeed even in some detail, the experiments suggest that results may be improved further when the geography of the ocean basins is reproduced with even greater fidelity.

Beyond vorticity similarity and the Rossby number (*5*), the scaling[2] of rotating models is but a starting point. As with ordinary hydraulic models verification is essential; hence it is necessary to know the nature of at least the kinetic behavior of the prototype so that through simple comparison of the model with the prototype, one can tell whether or not the model is behaving properly. This is difficult in the case of the ocean because relatively little is known of other than the average features of the circulation and even the average pattern is somewhat uncertain. For example, there is disagreement concerning the very existence of the

---

[1] Originally suggested by Fultz in discussion at the Symposium.

[2] The vorticity criterion, Eq. (1), implies that for terrestrial models one revolution is equivalent to one revolution of the earth, thereby establishing a time scale. The length scale is presumed to be identical with the mapping scale, hence the velocity scale is also known. In the case of the 200 cm. model at Woods Hole the time scale $T_r=2\times10^{-3}$ approximately, and $L_r=10^{-7}$ the approximate ratio of quadrantal lengths on the earth and in the basin. The velocity scale is simply $L_r/T_r=1/50$. Other ratios such as eddy diffusivity L_r^2/T_r, etc. can be found in terms of these length and time scales. The Rossby number $U/\Omega A$ for the model is approximately 0.3×10^{-2}, which matches closely that of the ocean prototype.

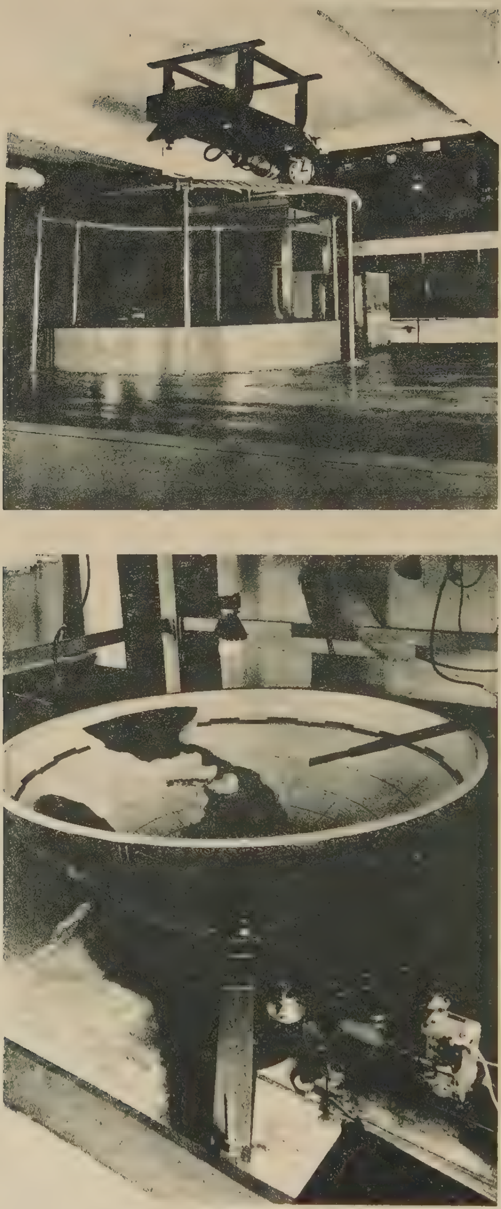

FIGURE 1—General arrangement of the rotating basin apparatus.

(a) The observing platform showing the control panel at the extreme right, accessible from the observer's desk at the eye end of the optical train.

(b) Directly beneath the observation platform is the basin mounted in a concrete sump. The drive machinery can be seen at the lower right. The main light source at the effective center of curvature of the basin and the blowers around the basin are suspended from the observing platform. The continental modeling is 6 cm high and cemented in place.

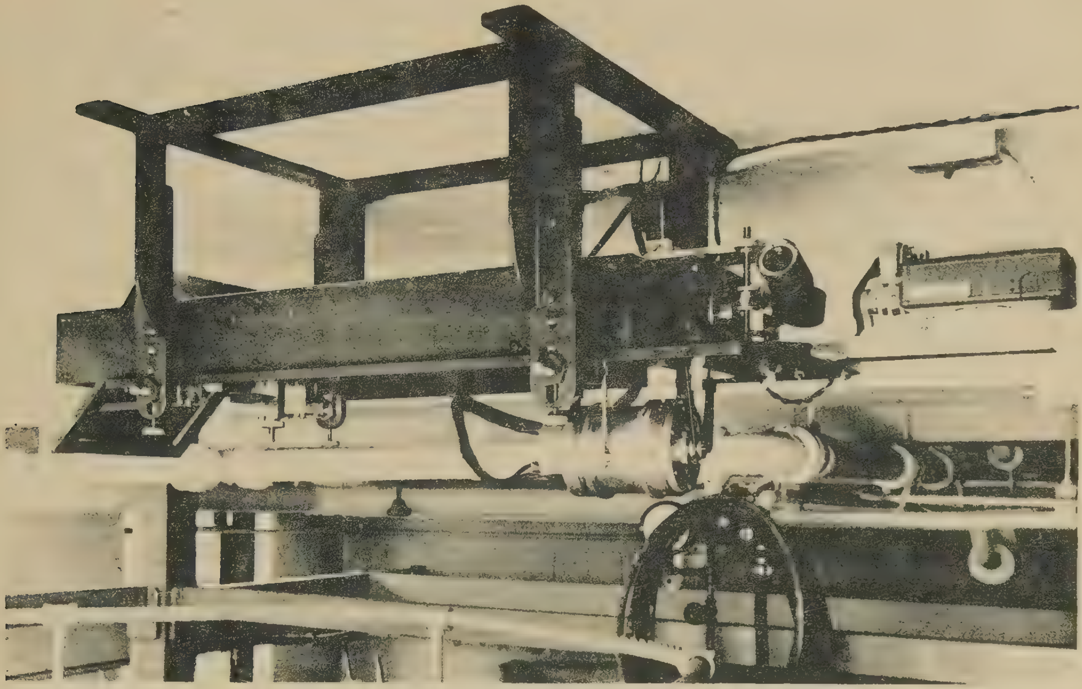

FIGURE 1 (c)—View of the observer's end of the wide-field optical train and "rotoscope" used to produce a stationary image of the rotating basin The selsyn repeater motor which drives the Dove prism of the rotoscope is shown mounted below the bed plate of the system. The elbow telescope shown in place, can be swung away from the Dove prism box allowing the time-lapse 16-mm motion picture camera or a 35-mm still camera to be used. The optical system has a true field of 65°.

Antilles current which is supposed to flow in the Atlantic Ocean along the northern limits of the island arc enclosing the Caribbean Sea. In the rotating model it is found that this current can be made to appear and disappear at will by changing the planetary vorticity gradient. When the effective planetary vorticity gradient is less marked than similarity requires, the center of the North Atlantic circulation is found to move eastward and somewhat northward from its normal position, allowing motions of the sort to be expected in an Antilles current to appear. Under these conditions the flow in the Caribbean and Yucatan Channel becomes abnormal. If the planetary vorticity is increased to the point where the flow through the Caribbean appears normal, the Antilles current becomes of negligible importance or disappears. Less than ½ per cent change of angular velocity of the apparatus will produce these effects.

Another question in verification concerns the exchange of water between the North Atlantic Ocean and the Arctic Ocean. In order for the Gulf Stream system in the model to extend branches along the Norwegian coast in agreement with the conclusions of some oceanographers, it is necessary to vent the Arctic Ocean and return this discharge to the Gulf of Guinea in the bight of the West African coast. If this discharge is not permitted, the Gulf Stream system in the model does not extend branches north of approximately latitude 53°.

Within the last few months Fuglister (*6*), has completed a study of the temperature distribution at the 200 meter level in the North Atlantic Ocean. This study indicates that the warm water flowing with the eastward extensions of the Gulf Stream system may not join the warm water of the Norwegian coast. In view of this result it may be a mistake to require the Gulf Stream system to enter the Norwegian Sea. However, when this flow is stopped, the modeled circulation of the North Atlantic and particularly in the Gulf Stream becomes extremely slow compared with the Kuroshio in the North Pacific. Evidently realism requires that there be some additional return flow route in the North Atlantic compartment of the model.

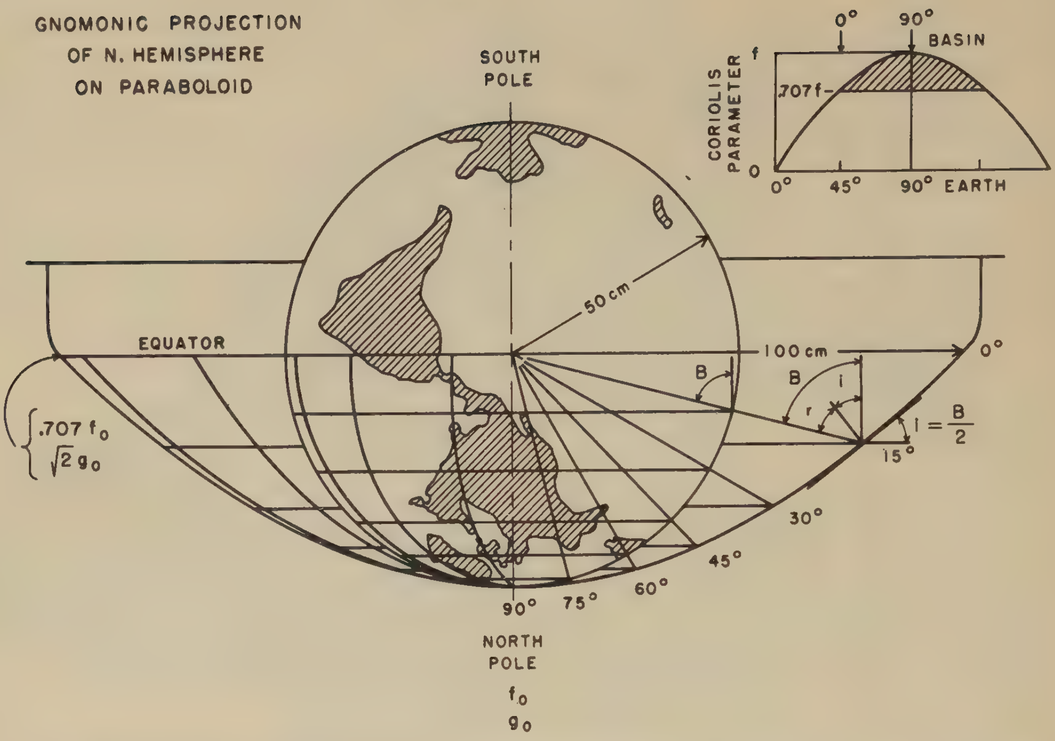

FIGURE 2—Gnomonic projection of the land masses of the northern hemisphere on the interior of the paraboloidal basin. The meridional variation of the Coriolis parameter due to the curvature of the basin, and the change of the combined gravitational and centrifugal accelerations, are indicated for the equilibrium speed of rotation.

Another difference between the North Atlantic and North Pacific circulations in the model is that the intensity of wind stress does not influence the circulation of the North Atlantic appreciably while noteworthy effects occur in the North Pacific. East of the 180° meridian in the North Pacific the Kuroshio extension becomes folded in a most complicated way filling the region between Hawaii and the Gulf of Alaska with narrow ribbons of water moving NNE and SSW relative to a general motion of the whole complex, southeastward. When the wind stress is reduced this complex fills the Eastern Pacific but as the wind stress is increased the path of the complex moves westward and a current (Davidson current?) flows northward along the North American coast from the Gulf of Panama.

As a further problem in verification it is found that when the topography below the depth of the main thermocline is reproduced in the main ocean basins, the circulation is influenced by more than acceptable amounts.[3] A model of the mid-Atlantic ridge, for example, causes a marked deviation of the circulation pattern in the North Atlantic which in the light of present knowledge seems entirely too great. Still, the patterns obtained seem to require something more than a smooth floor provided by the plastic surface of the basin. Perhaps the main thermocline should be modeled. The main thermocline lies at a depth of approximately 100 meters near the equator, deepens gradually to approximately 1000 to 1500 meters in mid-latitudes and rises again to very near the surface at subarctic latitudes. In terms of Rossby's point of view the deepening in nature of the main thermocline northward from the tropical regions would introduce some cyclonic vorticity due to horizontal convergence accompanying northward transport. Similarly, further progress from mid-latitudes toward the north would induce anticyclonic vorticity which, added to the planetary vorticity, may in effect postpone the maximum westward intensification to the region of temperate latitudes. Presumably the vertical scale required to model the thermocline could be calculated on a basis of the vorticity change due to vertical stretching and shrinking for currents moving over the earth, and then simulated in the model.

---

[3] There is a possibility that this is a consequence of the Taylor (4) effect for, in very small areas, the flow is approximately two-dimensional; but near the continental boundaries, in the centers of the ocean gyres and due to the poleward diminution of depth, vertical motions are significant.

In view of the encouraging realism of the circulation patterns produced by wind stress in the model, question arises concerning the role of the thermohaline processes in the actual temperate and tropical oceans. One is tempted to think that since the circulation produced under wind stress in homogeneous water in the model is so like the observed mean circulation of the oceans that the establishment of density fields must be a consequence of the wind-driven circulation. But, once established, the density structure in nature may have an important influence in sustaining the circulation geostrophically in times of fluctuation of the wind stress. The response of the model to fluctuations in wind stress is far more extensive and much more rapid than is the known response of the actual oceans.

The wind stress pattern applied to the model has taken the form shown in Fig. 3 and is discussed in an earlier paper (*1*). Experimentally, at least, the intensity of the blast in the Trade Wind zone is of less importance to the pattern of water motions than is the latitude of the inflection point of the zonal wind profile. Since the intensity of the wind torque does influence the velocity of the water in the Gulf Stream and Kuroshio, adjustments of wind force have been in the directions required to hold the water velocities to the scale $V_r = L_r/T_r = 1/50$, while keeping the turbulence due to surface ripples at a minimum. It seems remarkable that an acceptably detailed circulation pattern can be produced in the water by so crude an approximation of the zonal wind field. Attempts to improve the degree of this approximation, such as adding a blower to provide polar easterlies, or to mask the Trade Wind blower nozzles so that the wind falls off rapidly in the zone of doldrums have had very little effect on the overall pattern of water motions. However, all these matters require much more study and technical improvement.

Thus far no comment has been made concerning the deep circulation which may be related to the wind-driven motions in the upper levels by thermohaline as well as frictional and other

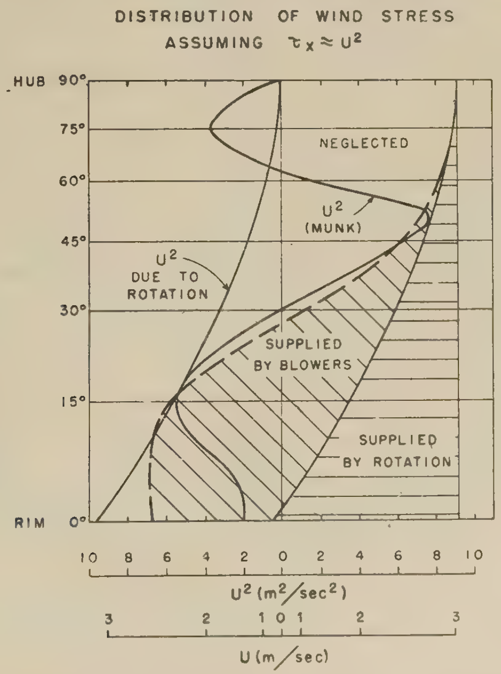

FIGURE 3—Experimental distribution of zonal wind stress (dashed line) compared with that derived by Munk (solid line) from records of the average zonal wind stress over the northern hemisphere of the earth.

influences. It is premature to discuss this involved and highly speculative problem but the model experiments may eventually have bearing and on it.

For example, the contributions of the thermohaline processes to the otherwise wind-driven motions of the North Atlantic and North Pacific may depend, to some extent, on atmospheric transport of water. There is a gradient of insolation between the northern and southernmost extremities of these oceans. There is also a zone of persistently high pressure composed of warm, clear, dry air near 30° north that encourages evaporation in excess of precipitation. Farther north there are persistent low pressure centers and storm tracks with which there is associated an excess of precipitation. Recent studies by Riehl, et al. (*7*), Malkus (*8*), and others of the heat budget in the northern parts of the Trade Wind zone indicate that the total transport of liquid water by evaporation and advection from the Trade Wind zone and horse latitudes in each ocean may amount to the order of 1×10^6 m^3/sec which is a small (2%) but appreciable fraction of the transport normally accredited to major ocean currents such as the Gulf Stream and Kuroshio. This volume of fresh water distilled away in the horse latitudes must increase the salinity and density of surface water there and cause it to sink. In order for the specific volume of the highly saline surface water to remain large under these conditions, fresh supplies of lower salinity water must flow into the region of intense evaporation.

Suitable motions occur in the rotating basin to account for this replenishment, although the mechanism is not the same. There is a centrifugal flow of water in the bottom boundary layer beneath the ocean gyres and a centripetal flow at the free surface. Dr. Henry Kierstead (*9*), has discussed the nature of both of these in an analytical study of the motions of a homogeneous liquid in a rotating paraboloid. The centrifugal motion in the bottom boundary layer is antitriptic; a consequence of the pressure field at higher levels in the liquid (where the flow is quasi-geostrophic) being transmitted to the bottom boundary layer where the circulation is retarded by friction and geostrophic balance is not maintained. The centripetal flow in the surface layer of frictional influence is approximately orthogonal to that in the bottom boundary layer, and extends downward through perhaps the first millimeter of depth. This centripetal flow at the free surface compensates the discharge in the bottom layer and offers a reasonable pattern of motions which may exist for the refreshment of the areas of intense evaporation in the real oceans. This is all very close to the idealized case treated by Ekman (*10*).

It would be difficult to produce these effects by employing the same physical forces in a small model. The scaled rate of evaporation would require not only steep temperature gradients but temperature extremes verging on the boiling and freezing points of water. There are further technical difficulties, for studies of the thermal circulation of oceans would require that Bjerknes' theorem (*11*) be taken into account, i. e., that which concerns the effects of the levels of sources and sinks on the conversion of thermal energy into mechanical energy. To apply heat and extract it again only at the free surface, it would seem necessary to employ larger (cylindrical) models in order to obtain a longer time scale. In a very large or slowly rotating model it might also be possible to drive a gas such as CO_2 by thermal convection which could exert a suitable wind stress on an ocean model underneath.

Discussion up to this point has been concerned with the representation of the average circulation and the processes that contribute to its maintenance. I think it is also important for the future to try to gain some insight into the nature of the unsteady departures of the circulation from an average condition. This, too, must be a speculative undertaking for it cannot be forgotten that the models so far studied are not models of the ocean at all, but rather an experimental analogue of the climatological mean circulation to be expected in terms of the vorticity theory of Stommel and Munk. Since this theory was conceived in terms of the average pattern of motions deduced from observations made more or less at random over a long period of time, there is probably a fair correspondence between the theoretical model and the ocean prototype. More than this, the experimental model is apparently capable of differentiating dyed water masses in a manner resembling in many ways the density differentiation observed in the actual oceans (Fig. 4). The coastal regions in the model have well developed water

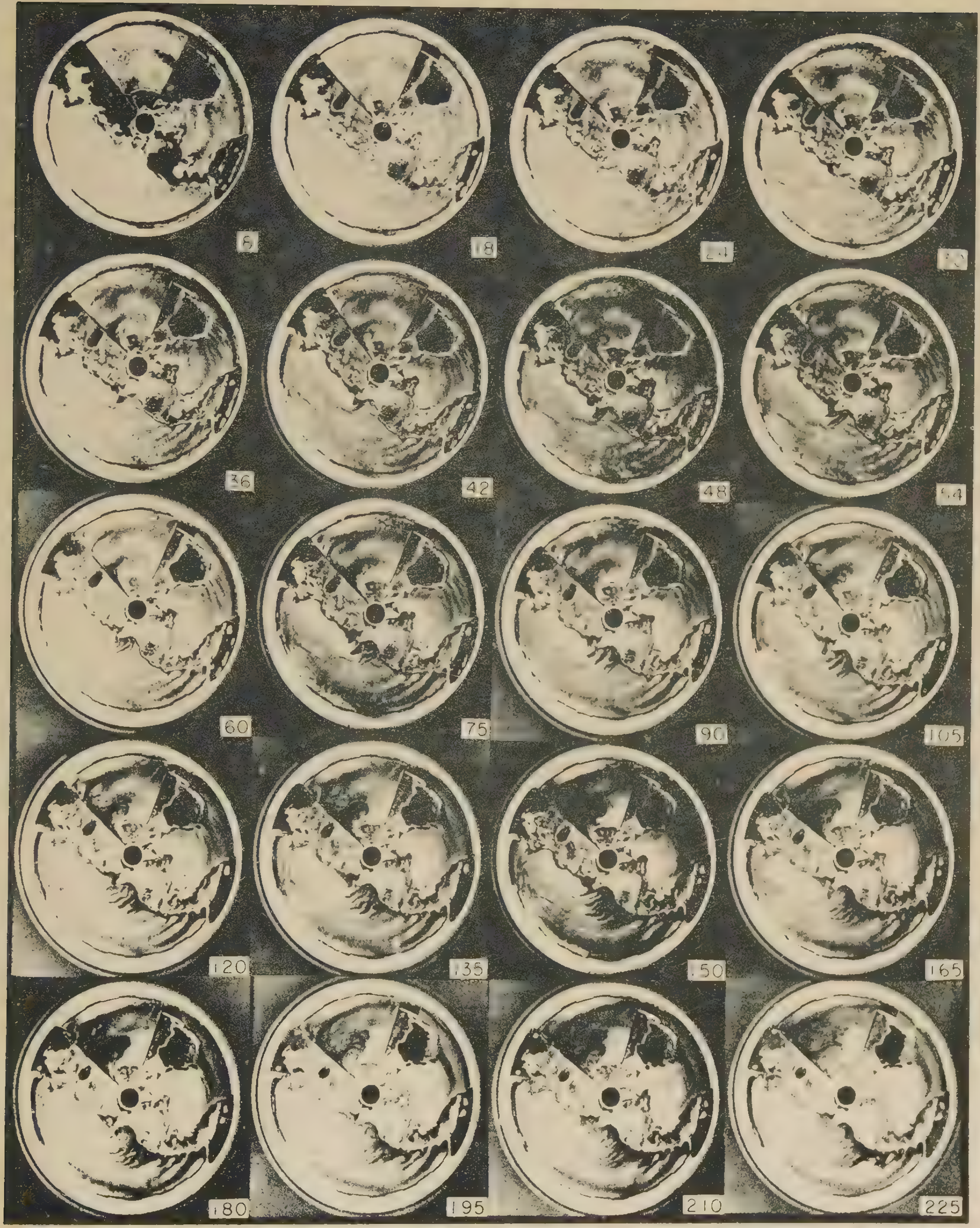

FIGURE 4—Successive patterns of $KMnO_4$ dye produced by the wind-driven circulation. The number of revolutions of the basin following introduction of the permanganate crystals is shown in the lower right corner of each photograph. The antitriptic circulation over the bottom is shown in the first two rows of photographs and the accumulation of bottom water in coastal water masses is shown in the lower rows. Ink (not shown) introduced in the equatorial zone follows the outer margins of these water masses.

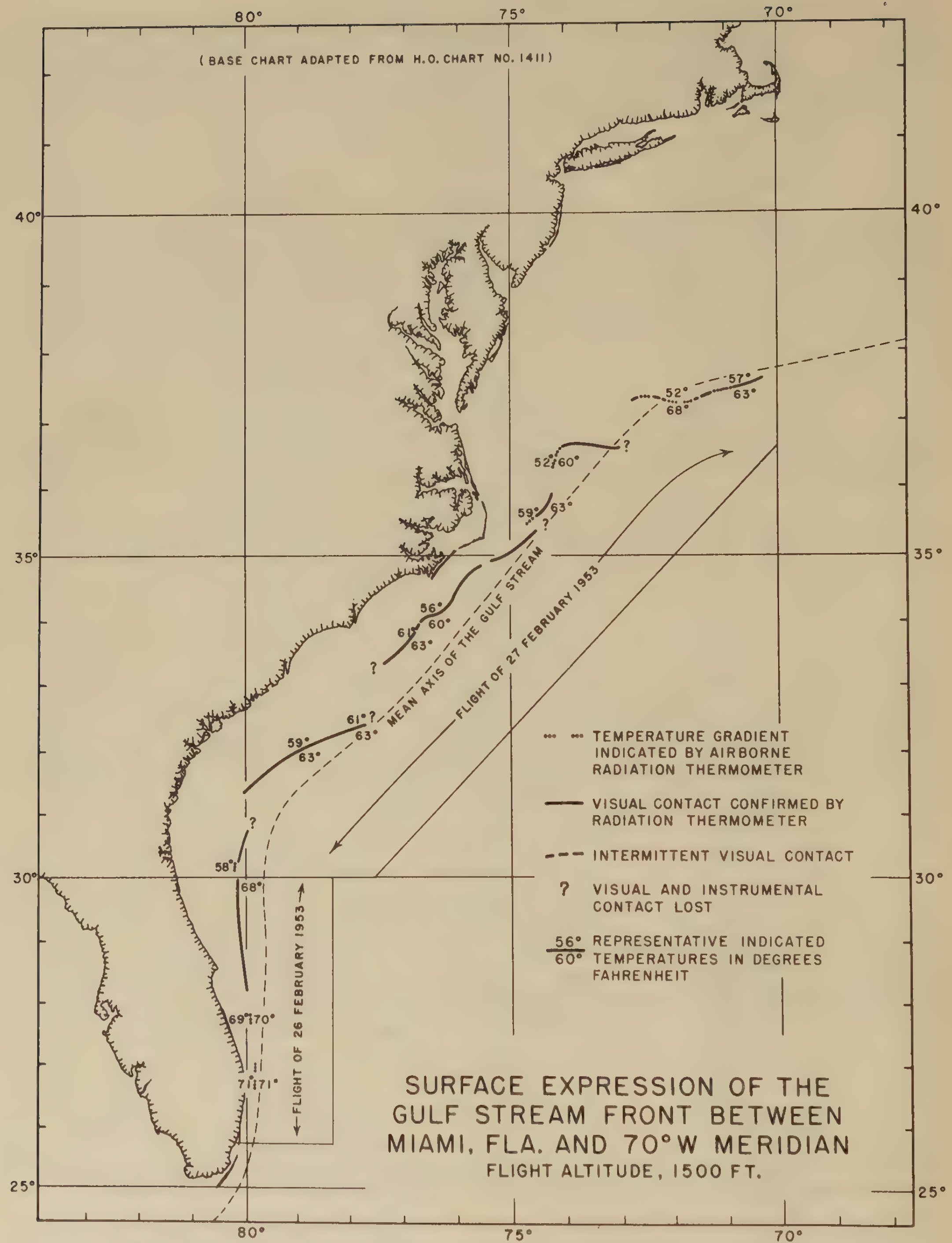
(BASE CHART ADAPTED FROM H.O. CHART NO. 1411)
80°
75°
70°
40°
35°
30°
25°
MEAN AXIS OF THE GULF STREAM
FLIGHT OF 27 FEBRUARY 1953
FLIGHT OF 26 FEBRUARY 1953
57°
63°
52°
68°
52°
60°
59°
63°
56°
60°
61°
63°
61°
63°
59°
63°
58°
68°
69°
70°
71°
71°
?
TEMPERATURE GRADIENT INDICATED BY AIRBORNE RADIATION THERMOMETER
VISUAL CONTACT CONFIRMED BY RADIATION THERMOMETER
INTERMITTENT VISUAL CONTACT
? VISUAL AND INSTRUMENTAL CONTACT LOST
56° / 60° REPRESENTATIVE INDICATED TEMPERATURES IN DEGREES FAHRENHEIT
SURFACE EXPRESSION OF THE GULF STREAM FRONT BETWEEN MIAMI, FLA. AND 70°W MERIDIAN
FLIGHT ALTITUDE, 1500 FT.

FIGURE 5—The surface outcrop of the Gulf Stream front traced by visual and thermometric means from an aircraft during 26 and 27 February 1953. This together with other evidence obtained from shipboard during May and June 1953 suggests that the Gulf Stream is a pulsating current due to causes not yet determined but possibly related to the tides in the Gulf of Mexico. Both tidal modulation and the possibility that pulsation of the current might be apparent along the coast were suggested by the rotating basin experiments, and later explored in the field

masses accumulated from the bottom boundary layer which resemble geographically the coastal and slope water masses in nature and, like them, do not participate actively in the main oceanic circulation.

The swift western currents (corresponding to the Gulf Stream and Kuroshio) flow along the eastern margins of these zones of coastal water. Both in nature and in the model these currents are very unsteady features. There is no assurance that the character of this unsteadiness bears any resemblance to that of the real oceans. However, since we have no other sources of information such as synoptic observations or firm physical intuition concerning the nature of these unsteady processes, a model may provide a basis for a working hypothesis in the field. As the model can be used to prompt programs of field study, the results of field study may be used in turn to verify the model, and so to extend its usefulness. One study of the frontal structure (Fig. 5) and short term fluctuations of the velocity and transport of the Gulf Stream has already been suggested by the model (*12*) and the field work carried on with both ships and aircraft.

Finally, it is conceivable that some of the major features of the less well known wind-driven oceans may be revealed if experimental variables can be properly adjusted to agree with the facts of observation. To this end Mr. Robert T. Ward, lately of Amherst College, has spent the past summer on careful quantitative experiments with the northern hemisphere model to study in some detail the effects on the circulation of changes in planetary vorticity and the distribution of zonal wind stress. Once it is clear how each of these experimental variables affects the circulation in the northern hemisphere, it then may be safe to undertake experiments with southern hemisphere oceans where the details of circulation of both the oceans and atmosphere are far less well known. In the southern hemisphere, for example, there is the Antarctic circumpolar ocean which is unique among oceans, but like the atmosphere in having no meridional interruptions to zonal flow. The southern hemisphere is also a region in which the principle of westward intensification appears to have exceptions.

In view of the encouraging results already obtained it seems probable that vorticity models may become useful adjuncts to research on problems of the primary ocean circulation and its fluctuations just as Froude and Reynolds models of rivers and estuaries have been useful in their places. It is also conceivable that as the behavior of ocean models is understood theoretically, some of the theory may be adapted to discussion of the actual ocean circulation.

REFERENCES

1. **von Arx, W. S.,** "A Laboratory Study of the Wind-Driven Ocean Circulation," Tellus, 4: 311–318, 1952
2. **Stommel, Henry,** "The Westward Intensification of Wind-Driven Ocean Currents," Trans. Am. Geophys. Un. 29 (No. 2): 202–206, 1948
3. **Munk, Walter H.,** "On the Wind-Driven Ocean Circulation," J. Meteorol. 7 (No. 2): 79–93, 1950
4. **Taylor, G. I.,** "Experiments with Rotating Fluids," Proc. Roy. Soc. A100: 114–121, 1921
5. **Fultz, D.,** "Non-Dimensional Equations and Modeling Criteria for the Atmosphere," J. Meteorol. 8: 262–267, 1951
6. **Fuglister, Frederick C.,** "Average Temperature and Salinity at a Depth of 200 Meters in the North Atlantic," Tellus, 6: 46–58, 1954
7. **Riehl, H., Yeh, T. C., Malkus, J. S.,** and **La Seur, N. E.,** "The North-East Trade of the Pacific Ocean," Quart. J. Roy. Meteorol. Soc. 77 (No. 334): 598–626, 1951
8. **Malkus, Joanne S.,** "Some Results of a Trade Cumulus Cloud Investigation," Woods Hole Oceanogr. Inst. Ref. No. 53–30 (unpublished manuscript), 1953
9. **Kierstead, Henry,** "The Wind-Driven Ocean on a Rotating Basin," Woods Hole Oceanogr. Inst. Ref. No. 52–87 (unpublished manuscript), 1952
10. **Ekman, V. Walfrid,** "On the Influence of the Earth's Rotation on Ocean Currents," Arkiv. Mat. Astron. Fysik 2 (No. 11): 51–52, 1905
11. **Bjerknes, V., Bjerknes, J., Solberg, H.,** and **Bergeron, T.,** Physikalische Hydrodynamik, p. 184, Berlin: Springer, 1933
12. **von Arx, W. S., Bumpus, D. F.,** and **Richardson, W. S.,** "Short Term Fluctuations in the Structure and Transport of the Gulf Stream System," Woods Hole Oc. Inst. Ref. No. 54–76 (unpublished manuscript), 1954

Contribution No. 682

Reprinted from the Australian Journal of Physics, Volume 9, Number 1, pp. 133–143, 1956

MEASUREMENTS OF COUNTER-GRADIENT HEAT FLOWS IN THE ATMOSPHERE*

By A. F. Bunker†

[*Manuscript received November* 7, 1955]

Summary

Heat flows and temperature gradients were measured in a stable atmosphere heated by the water during a United States east coast to Bermuda aeroplane flight. The flux was computed from $c_p\rho\overline{w'T'}$, where w' and T' are the vertical velocities and temperature deviations of the individual gusts. It is found that the heat flow is directed up the gradient as predicted by Priestley (1954). The expression for the maximum heat flow to be expected derived by Priestley in terms of the standard deviation of the temperature fluctuations and the temperature gradient gives the correct order of magnitude for the observed flow.

I. Introduction

The generally accepted theory of turbulent diffusion of momentum, heat, and water vapour was modelled after the molecular diffusion theory and considers the transport to be accomplished by turbulent eddies which carry the average properties of the fluid at the level of origin through some reference level. Whenever a gradient of the properties exists a net turbulent transport of the property results from the summation of all the eddies passing through the surface, provided there is no mass transport through the surface. This theory shows that the flux is proportional to both the gradient and the coefficient of turbulent mass exchange and the flux is directed down the gradient. It is concerning the point of the necessity for heat flow to be down the gradient even in a gravitational field that the theory fails to describe the actual flow of heat through the atmosphere. It has been observed that in certain cases upward flows of heat exist in the face of potential temperatures increasing with height.

The idea of warmer parcels of air rising through the atmosphere and contributing to a counter-gradient flow of heat was incorporated into the classical diffusion theory by Priestley and Swinbank (1947). They differed in their approach by considering that, at the point of origin of the eddy, the air did not necessarily have the mean temperature of that level but had the temperature T_0+T'', where T_0 is the average temperature of the level and T'' is a deviation from that temperature. Treating this temperature sum in much the same manner as the authors of the classical mixing length theory, they develop the heat flow equation

$$F=\rho_0 c_p[-K(\partial T_0/\partial z+\Gamma)+\overline{wT''}]. \qquad \ldots\ldots\ldots\ldots\, (1)$$

---

* Contribution No. 682 from the Woods Hole Oceanographic Institution. Work supported by the Office of Naval Research, U.S. Navy, under contract number Nonr 1721 (00) (NR–082–021).

† Woods Hole Oceanographic Institution, Woods Hole, Massachusetts, U.S.A.

Here ρ_0 is the density corresponding to T_0, K is the diffusion coefficient, Γ is the dry adiabatic lapse rate, and w is the vertical velocity of the eddy at the reference level. The authors point out that the $\overline{wT''}$ term results in a systematic upward flux of heat irrespective of the sign of $(\partial T_0/\partial z+\Gamma)$. This equation cannot be checked directly because of the impossibility of observing T''. Because of this difficulty the equation is not quantitatively useful and remained without further development although it was recognized as a great advance toward a true description of heat flow in the atmosphere.

Following the presentation of the Priestley-Swinbank theory, several studies of the properties of buoyant parcels moving through an environmental air were made. One of these by Houghton and Cramer (1951) studied the effects of entrainment of environmental air upon columns of air rising as a result of its buoyancy. Equations are derived that give mass entrainment, temperature deviations, and velocities as functions of the height. These equations were set up for both dry air and saturated air from which the water vapour condenses as the air rises. Thus, assuming that the only interaction with the environment comes from the entrainment of air which carries with it its characteristic momentum and temperature anomaly, the life history of a warm parcel of air can be determined. This approach to the study of buoyant parcels was developed further by Bunker (1953), who followed the general development of Houghton and Cramer but added the effects of a turbulent atmospheric environment and a dynamic pressure drag upon the rising bubble. Equations are found which give temperature deviations and vertical velocities as functions of height when the turbulent mass exchange coefficients of the environmental air and the size of the parcels are known or assumed as functions of the height. Numerical integration of the equations is required in both of these treatments.

A theory presented by Scorer and Ludlam (1953) described a mechanism of convective rise of bubbles which erode as they penetrate the atmosphere. This mechanism is modelled after the tank experiments of Davies and Taylor (1950) and experiments of the authors with bubbles rising through tinted water. Particular emphasis is placed upon the effects of the wake of the bubble in aiding subsequent parcels to penetrate to greater heights of the atmosphere.

An extremely valuable treatment of the problem of buoyant parcels was developed by Priestley (1953). Time derivative equations of the vertical velocity and temperature excess T' of the parcel following the mean motion are developed taking into account mixing of momentum and heat of the parcel air with the environment, which has the temperature T_e. The simultaneous equations are:

$$\dot{w}=(g/T_e)T'-k_1w, \quad \dots\dots\dots\dots \quad (2)$$

$$\dot{T}'=-w(\partial T_e/\partial z+\Gamma)-k_2T'. \quad \dots\dots\dots\dots \quad (3)$$

Here k_1 and k_2 are mixing rates of momentum and heat. They are defined in terms of the radius R of the parcel and the diffusivity coefficient K by the following relations, where c_1 and c_2 depend upon the form of the parcel:

$$k_1=c_1K_1/R^2, \quad k_2=c_2K_2/R^2. \quad \dots\dots\dots\dots \quad (4)$$

The second order differential equation was formed

$$\ddot{w}+(k_1+k_2)\dot{w}+\varkappa^2 w=0 \quad \ldots\ldots\ldots\ldots\ldots\ldots (5)$$

and solved in conjunction with the previous equations for w and T'/T_e as functions of time and the mixing rates. When these solutions are examined for various combinations of environmental lapse rates and mixing rates it is clear that the parcels may have three modes of motion: oscillatory, asymptotic, and absolute buoyancy.

In a subsequent paper, Priestley (1954) has developed the equations describing the motion and temperature relations of a buoyant parcel to the point where heat flows can be calculated under given conditions. Using either the oscillatory motion or the asymptotic motion case, the products of wT' and T'^2 are averaged over the path of the parcel to get the heat flow and the standard deviation (σ_T) of the temperature. The relation is found

$$F_H/\rho c_p=\sigma_T^2(g/T_e)\frac{2k_1}{(g/T_e)(\partial T_e/\partial z+\Gamma)+k_1k_2+2k_1{}^2}, \quad \ldots\ldots (6)$$

which gives the heat flow in terms of the temperature fluctuations, the lapse rate, and the mixing rates.

To investigate the dependence of the convective heat flow as a function of lapse rate and other quantities, several parameters are defined and substituted into the above equation. From a plot of these parameters it is apparent that a maximum value of the heat flow exists for a given mixing rate ratio. This is interpreted to mean that an optimum size of parcel exists which can transport a maximum amount of heat for a given degree of turbulence and thermal stability. The upper limit for the heat flux can now be expressed as

$$F_H=\frac{\rho c_p \sigma_T^2}{\sqrt{\{(3T_e/g)(\partial T_e/\partial z+\Gamma)\}}}, \quad \ldots\ldots\ldots\ldots\ldots (7)$$

when the reasonable assumption is made that $k_1=k_2$.

In view of these theories set forth by the various workers, which have had little confirmation or checking with observations, it is desired to obtain data that can be used for this purpose. The flow of cool air over warm water offers circumstances ideal for the study of the gravitational effect upon heat flow and the application of the concepts and equations of Priestley. Usually in these cases, the turbulence in the lowest 50 m is too small to transport all of the heat crossing the air-water interface, with the result that a large super-adiabatic lapse rate is established. The resulting instability allows warm buoyant parcels of varying sizes to rise through the air, thereby transporting heat upward at a faster rate than that of turbulent diffusion. This system carries the heat to higher levels where it is finally mixed into the environmental air. As a result of the small heat diffusion in the lowest levels and the greater transport to higher levels, a potential temperature minimum can be established in the 50–300 m level in the cool air. As a temperature inversion usually exists at the top of the mixed layer the stability of the air is increased further by downward diffusion of heat from this source. Under the conditions just described and at altitudes up to the inversion many of the various types of heat flow will be large and easily measured.

The major technique employed in this study is the measurement of heat flow from an aeroplane by averaging the cross products of the temperature and vertical velocity deviations. Such values have been obtained at numerous heights and localities where counter-gradient fluxes are suspected to exist. Observations were obtained from an aeroplane flying at levels from 30 to 1700 m and to distances up to 1100 km off shore. Radiosonde and radiowinds observed at land, ship, and island stations were used as supplementary sources of information. The instrumentation of the aeroplane and the technique of obtaining vertical and horizontal turbulent fluctuations of the air velocity have been described by Bunker (1955), hence only the briefest mention of these topics will be made. A modification of the reduction system is used now which gives reliable values over flight paths of many kilometres in length. This change involves the use of deviations of the airspeed and attitude from a mean over the entire run rather than over 10 sec. The fluctuations are determined from the measured responses of a vertically mounted accelerometer, a gyroscope, and a pressure gauge connected to a pitot-static tube. Temperature fluctuations are found from the response of a thermopile. Once a time series of w_i, the vertical turbulent component of the wind, and T_i, the temperature fluctuations, read to 0·1 °C are obtained, then cross products and root mean square deviations can be formed, giving $(\overline{w'^2})^{\frac{1}{2}}$, $(\overline{T'^2})^{\frac{1}{2}}$, and $c_p\bar{\rho}\overline{w'T'}$, the heat flux. Particular attention will be paid here to the heat flow calculation, and an interpretation of this observed quantity in terms of diffusion and buoyant transport will be discussed. Heat flows into the air mass averaged over all or part of the distance covered by the air in its travel over the water surface have been calculated from observed individual temperature changes, local changes, and mean vertical velocities in the air mass. From the mean temperatures observed at various heights by the aeroplane, the gradients of the potential temperature can be found and the way is clear for a discussion of Priestley's maximum buoyant heat flow and associated problems of turbulent mass exchange.

II. OBSERVATIONAL DATA OBTAINED DURING THE POLAR OUTBREAK OVER THE ATLANTIC OCEAN, JANUARY 18, 1955, RHODE ISLAND TO BERMUDA

This flight to Bermuda was made at about the middle of a 3-week period of predominant north-westerly flow off the east coast of North America. A low pressure system passed to the north of New England on the morning of January 17 and north-west winds prevailed until a coastal storm interrupted them temporarily on the afternoon of the 19th. The skies were clear over the land at take-off time and remained so as the air passed over the shallow coastal waters. As warmer waters were reached, a few cumulus clouds appeared and rapidly built up to a complete overcast of stratocumulus as the air flowed over the very warm waters of the Gulf Stream. In this region the aeroplane was flying in and out of scud at 500 m. No showers were noted at any time. Some 300 km beyond the Gulf Stream breaks in the overcast appeared and grew until only six-tenths of the sky was covered by cumulus clouds at Bermuda.

The resistances of a thermistor mounted in a housing attached ahead of the nose of the aeroplane were recorded continuously throughout the flight. From these resistances the air temperatures were found, corrected for the dynamic heating of the aeroplane's motion, and potential temperatures computed. Water temperatures were obtained from mean maps and the intake water temperatures of the R.V. *Atlantis* which travelled the course to Bermuda January 19–22, 1955. These water temperatures are treated as air temperatures and reduced to potential temperatures. This procedure is justified on the basis that the air immediately in contact with the water takes on the water's temperature.

Five times *en route* to Bermuda the aeroplane was flown from the cloud base down to 90 m above the water to obtain vertical temperature gradients, turbulence, and heat flow data. The temperatures obtained during these descents had to be corrected for the horizontal gradients since 30–40 km was traversed during a descent and ascent. The temperatures, corrected to mean off-shore distances, have been plotted on a height-temperature diagram, and presented in Figure 1. As conclusions of considerable importance will be drawn from the nature of these gradients great care was taken that no systematic errors were introduced by the reduction system and the flight procedure of flying faster at the lowest elevations. From numerous flight tests performed it is concluded that if any systematic errors exist they are less than 0·1 °C. An uncertainty of 0·1 °C over a 500 m height range is equivalent to an uncertainty of 2×10^{-6} cm^{-1} in the gradient determination. The observed gradients are several times this amount. It is noted that a slight but real stability exists in the upper 90 per cent. of the sub-cloud layer. Although no temperatures other than the water temperatures were obtained below the 30 m level it is obvious that the air in this region is very unstable.

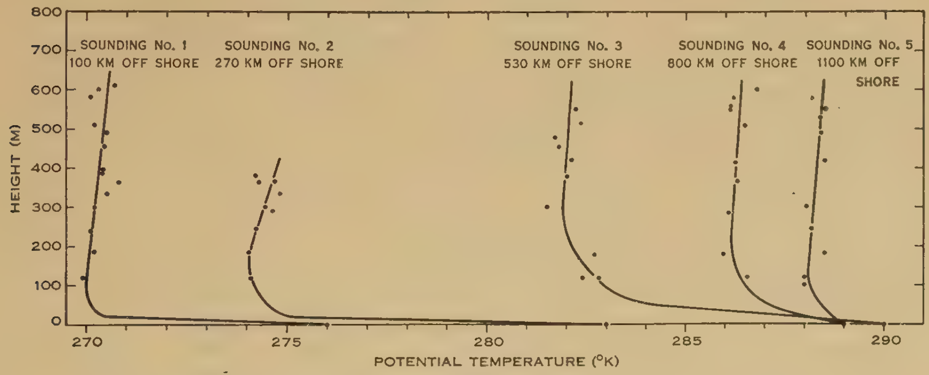

Fig. 1.—Potential temperature gradients, Rhode Island to Bermuda.

Fluctuation data obtained from 17 horizontal runs made during the five descents already mentioned were reduced to time series of w_i and T_i and subsequently to series of w' and T'. From these series values of $(\overline{w'})^{\frac{1}{2}}$, $(\overline{T'})^{\frac{1}{2}}$, and $c_p\rho\overline{w'T'}$ have been computed and tabulated in Table 1. With these values are listed information concerning an identifying run number, distance off shore, height above the sea surface, and the vertical gradients of the potential temperature measured from the temperature-height diagram, Figure 1. The last column gives the maximum heat flow as computed from Priestley's theory. This will be discussed later.

A potential temperature cross section of the atmosphere between Rhode Island and Bermuda, presented here as Figure 2, has been drawn to show the temperature changes taking place in the air mass as it moves over the water and to show other observed quantities. The ordinate of the diagram is atmospheric pressure in millibars, while the abscissa is the double entry of the Greenwich Mean Time of a particular observation made from the aeroplane, and of the off shore distance from the Rhode Island coast. The heavy lines are isopleths of potential temperature computed from both aeroplane measurements, represented here by dots, and radiosonde measurements, represented by crosses within circles. Cloud reports are entered along the top and at the flight level. The potential temperature of the air in contact with the water is entered in the ellipses at the sea-level pressure line. The turbulence encountered during the flight is indicated by the root-mean-square vertical velocities in cm sec^{-1} entered in the boxes located at the proper pressure and time. Lastly the heat flows in mcal cm^{-2} sec^{-1} computed from the cross products of the vertical velocities and the temperature deviations are entered with an arrow representing the direction of flow.

TABLE 1

HEAT FLOWS COMPUTED FROM FLUCTUATION DATA, JANUARY 18, 1955

Atlantic Ocean, Rhode Island to Bermuda. 1820–2210 hr G.M.T.

Run Number	Distance (km)	Height (m)	$(\overline{w'^2})^{\frac{1}{2}}$ (cm sec^{-1})	$(\overline{T'^2})^{\frac{1}{2}}$ (°C)	$c_p\rho\overline{w'T'}$ (mcal cm^{-2} sec^{-1})	$d\theta/dz$ (cm$^{-1}\times10^5$)	$F_{H\max.}$ (mcal cm^{-2} sec^{-1})
974	100	520	86	0·05	0·1	1·1	0·2
975	100	335	121	0·07	1·7	1·1	0·4
976	100	150	94	0·08	1·1	1·1	0·6
977	270	305	107	0·08	1·1	3·0	0·4
978	270	150	135	0·19	3·9	−1·0	—
979	530	460	174	0·10	2·1	0·5	1·3
980	530	120	177	0·18	1·3	−8·0	—
981	800	550	122	0·09	1·1	0·6	1·0
982	800	305	134	0·10	2·0	0·6	1·2
983	800	120	138	0·11	2·1	−7·0	—
984	1100	550	129	0·07	0·8	0·8	0·5
987	1100	305	151	0·08	1·1	0·8	0·7
990	1100	90	138	0·13	2·4	?	—

The sensible heat flowing into the moving air column has been calculated by measuring the temperature change per 100 km as observed from the aeroplane and by measuring local changes and subsidence rates by use of radiosonde and

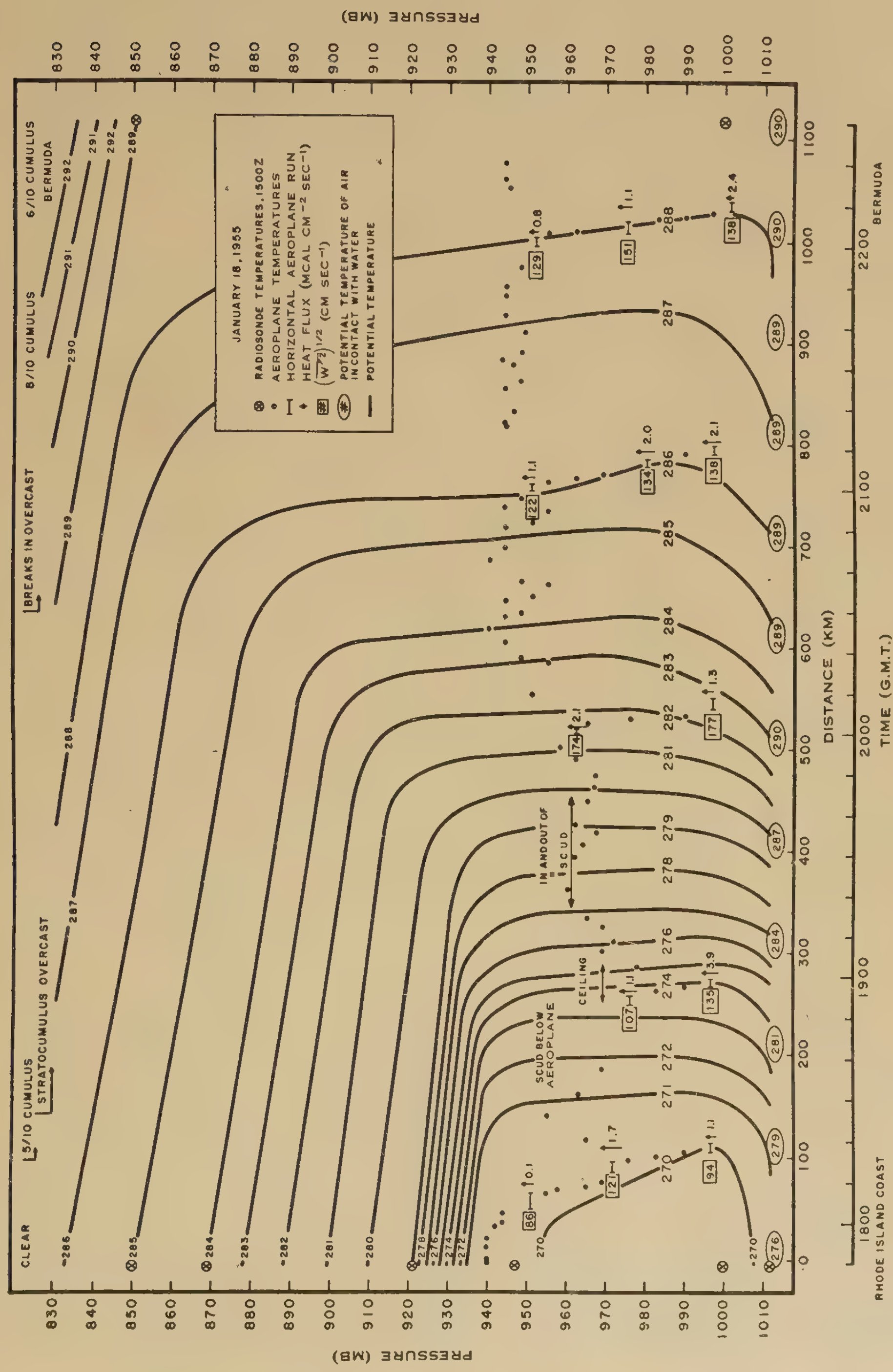

Fig. 2.—Atmospheric cross section from Rhode Island to Bermuda.

radiowind reports. The temperature changes were measured in two height ranges, one below the inversion and one in the inversion. From these figures the amount of heat added was found and the rate of addition calculated by dividing by the time of transit, 8×10^3 sec. Adding the rates of heating for the two regions gives the total heating assuming no subsidence and no local changes of temperature. The average over the entire area was found to be $5 \cdot 3$ mcal $\text{cm}^{-2}\ \text{sec}^{-1}$. To evaluate the heating arising from the neglected effects the terms in the following equation were determined

$$\left.\frac{\mathrm{d}Q}{\mathrm{d}t}\right)_{l\ \&\ s} = \left(\frac{\mathrm{d}p}{g}\right)c_p\left[\frac{\mathrm{d}T}{\mathrm{d}t} + \left(\frac{p}{10^6}\right)^{R/c_p} w\frac{\mathrm{d}\theta}{\mathrm{d}z}\right], \qquad \ldots\ldots\ldots\ldots (8)$$

where $\mathrm{d}Q/\mathrm{d}t)_{l\ \&\ s}$ is the heating due to subsidence and local changes in temperature where $\mathrm{d}p$ is the change in pressure in baryes through the layer concerned. The $\mathrm{d}T/\mathrm{d}t$ term was measured by using the Bermuda radiosonde for two times 12 hr apart. The vertical velocity, w, was computed from the radiowinds from Nantucket, Mass., Washington, D.C., and Bermuda, by computing mass divergences. These divergences were calculated by the Bellamy (1949) method. Assuming the vertical velocity to be zero at the 1000 mb level, it is found that the air is subsiding at the rate of $0 \cdot 6$ cm sec^{-1} at 850 mb over the entire region. While it is admitted that the computation of divergences and velocities from so few wind observations is generally inaccurate, in the present case the wind field was steady for long periods and over large areas, so the computed velocity is considered reasonably reliable. The average rate of heating due to these two terms is $1 \cdot 3$ mcal $\text{cm}^{-2}\ \text{sec}^{-1}$ in the 1000–800 mb layer. When this is subtracted from the average total heat flow measured for the same layer, we get $4 \cdot 0$ mcal $\text{cm}^{-2}\ \text{sec}^{-1}$. The maximum heat flow found for the 100 km regions was found to be $8 \cdot 0$ mcal $\text{cm}^{-2}\ \text{sec}^{-1}$ for the 200–300 km region. It is of interest to compare these values with those entered in Table 1. The average for the total area, $4 \cdot 0$ mcal $\text{cm}^{-2}\ \text{sec}^{-1}$, represents satisfactory agreement, all difficulties considered, with $2 \cdot 4$ mcal $\text{cm}^{-2}\ \text{sec}^{-1}$, the average of the five cross product heat flows taken at the lowest level of a given series. Likewise the heat flow for the 200–300 km region computed from the change in heat content, $8 \cdot 0$ mcal $\text{cm}^{-2}\ \text{sec}^{-1}$, shows satisfactory agreement with the cross products method value of $3 \cdot 9$ mcal $\text{cm}^{-2}\ \text{sec}^{-1}$.

III. DESCRIPTION OF CONVECTIVE PARCELS AND ENVIRONMENT

Before checking the heat flows computed according to any theory against the observed heat flows, a few values and averages have been assembled that will give a clearer conception of the convective regime existing in the study area. First it should be pointed out that at the levels at which the aeroplane was flying it is easy to pick out the individual buoyant parcels from the environmental air. Visual inspection of the horizontal w', T' time series shows clearly that the environmental air is relatively quiet and homogeneous and that the convective parcels break through this quiet air as isolated well-defined turbulent disturbances of warmer updrafts and colder downdrafts. This regime contrasts strongly with a wind field characterized by mechanical turbulence in which no warm updrafts or cool downdrafts can be recognized although w', T' cross products show that an appreciable heat flow exists. In the present study, the existence of these parcels is much more obvious at the lower levels (150–300 m) where the temperature fluctuations are greater, than at the higher levels (600 m). At the higher levels the cool downdrafts disappear so that only the environmental air and the warm updrafts are observable by inspection.

Table 2

OBSERVED SIZES OF COOL AND WARM AIR PARCELS

Size Range (m)	Number of Cool Air Parcels	Number of Warm Air Parcels
50	6	7
50–100	7	7
100–200	3	6
200–300	1	6
300–400	0	3
400–500	0	1

Three temperature deviation groups have been defined by $T' \leqslant -0{\cdot}2$ °C, $-0{\cdot}1$ °C$\leqslant T' \leqslant 0{\cdot}1$ °C, and $0{\cdot}2$ °C$\leqslant T'$, to aid in describing the observed parcels. These groups are intended to represent cool descending parcels, environmental air, and warm rising parcels respectively. The diameters of these cool and warm parcels have been determined for all 13 horizontal runs made during the flight to Bermuda. During these runs which totalled about 40 km only 47 parcels were observed. Their sizes are tabulated in Table 2.

Table 3

ANALYSIS OF TEMPERATURE CLASS PROPERTIES

Run Number	Temperature Class (°C)	Number of 20 m Intervals	Average Temperature (°C)	Average Vertical Velocity (cm sec^{-1})	Heat Flow (mcal cm^{-2} sec^{-1})
977	$-0{\cdot}2\leqslant T\leqslant 0{\cdot}3$	165	0·006	− 4·9	1·13
977	$0{\cdot}2\leqslant T\leqslant 0{\cdot}3$	45	0·11	15	0·41
977	$-0{\cdot}2=T$	15	−0·18	−60	0·25
977	$-0{\cdot}1\leqslant T\leqslant 0{\cdot}1$	105	−0·013	− 5·5	0·50
978	$-0{\cdot}3\leqslant T\leqslant 0{\cdot}6$	165	0·004	0·6	3·92
978	$0{\cdot}2\leqslant T\leqslant 0{\cdot}6$	28	0·346	162	2·88
978	$-0{\cdot}3\leqslant T\leqslant 0{\cdot}2$	9	−0·244	−96	0·36
978	$-0{\cdot}1\leqslant T\leqslant 0{\cdot}1$	128	−0·053	−28	0·71
982	$-0{\cdot}2\leqslant T\leqslant 0{\cdot}3$	165	0·002	2·0	1·99
982	$0{\cdot}2\leqslant T\leqslant 0{\cdot}3$	15	0·25	186	1·15
982	$-0{\cdot}2=T$	2	−0·20	−64	0·08
982	$-0{\cdot}1\leqslant T\leqslant 0{\cdot}1$	148	−0·02	−16	0·80

It should be noted in interpreting these size distributions that parcels larger than 1000 m would be difficult to recognize by the method used. This is true since the defined temperature groups are with respect to a line of regression of temperature upon time along the 3000 m flight path. Also it is likely that parcels of greater size have smaller amplitudes of the temperature deviations and hence may be unobservable with the present thermopile. In any case these parcels contribute the major portion of the heat flows tabulated in Table 1.

The sensible heat transported by air parcels belonging to each of the defined temperature classes has been computed for three horizontal runs picked at random from the 13 available. For each run and class, the number of 20 m intervals of the run occupied by each class, the average temperature deviation, the average vertical velocity, and the heat flow computed from the w', T' cross product have been tabulated in Table 3.

This collection of data gives a clear picture of the properties of the convective parcels and their environment, but is too incomplete to serve as a check upon the merits of the several parcel theories already discussed.

IV. Comparison of Theories of Heat Flow with the Data

A study of Figure 1 shows that the gradient of the potential temperature, except for the lowest 100 m or so, was positive throughout all of its journey from the mainland to Bermuda in spite of heating from the bottom. The discussion of systematic errors in the previous section shows that the gradients are real and that the classical heat flow theory can break down as has been pointed out previously by Priestley and Swinbank (1947).

The heat flow of the environmental air ($-0{\cdot}1 \leqslant T \leqslant 0{\cdot}1$) was computed with the idea in mind that the correlation between the vertical velocity deviations and the temperature deviations might be negative in accordance with the classical diffusion theory, which says that heat should flow down the gradient. The heat flow was found to be positive in all three cases, two of these cases having positive gradients, thus giving additional confirmation of the inadequacy of classical theory in the presence of a gravitational field. As already stated, it has been anticipated that if a temperature class with sufficiently small limits had been analysed a negative correlation would have been found. This was based on the concept that this temperature class represented the undisturbed environmental air and that for small deviations neither organized overturning nor the weak buoyancy forces of Priestley and Swinbank would cause the $w'T''$ term of (1) to predominate over the diffusion term. As the thermopile could not resolve temperature variations of less than 0·1 °C, no answer could be obtained to this question.

The present set of observations is not well adapted to shed light upon the validity or weaknesses of the three parcel theories of Houghton and Cramer, Bunker, and Scorer and Ludlum in their present form. No definitive statistical study of the sizes, velocities, and temperature amplitudes at various heights and distances off shore has been attempted. This was not done because, after a brief inspection of the records, it was evident that a very large range existed in these variables and that a very small sample had been taken in each location. It was felt that no conclusions could be drawn concerning the validity of the equations from this type of data without further development of the equations on a statistical basis.

As Priestley's equation (7) for the heat flow is expressed in observable statistical parameters, a comparison between his predicted maximum heat flows and $c_p\bar{\rho}\overline{w'T'}$ can be made. It is assumed that in the present case the heat flow mechanism of the atmosphere became adjusted in such a manner that a close approximation to maximum flow is attained. The maximum heat flow has been computed from (7) by substituting the observed value of $\overline{T'^2}$ for σ_T^2 as defined. In substituting $\overline{T'^2}$ for σ_T^2, one is replacing σ_T^2 by a value that is a time-weighted average of the temperature deviations of both parcels moving through the flight path and the environmental air. Equation (7) then gives the time-weighted maximum heat flow rather than the heat flow due to a given parcel of the optimum size. The value obtained in this manner is equivalent to the heat flow determined from $c_p\bar{\rho}\overline{w'T'}$. These values have been tabulated in the last column of Table 1. A glance will show that these are values of the same order of magnitude but smaller than the values of $c_p\bar{\rho}\overline{w'T'}$ listed in column 6 of the table.

The agreement as to sign and order of magnitude proves that the theory is sound and that the underlying assumptions must be basically correct. The fact that the predicted values are smaller than the observed values may be caused by discrepancies between the assumptions made concerning impressed temperatures in a stable atmosphere and the condition of the temperatures and vertical velocities of the buoyant parcels obtaining at the base of the stable region of the atmosphere. If this is the case then a different expression for the original conditions of the parcel might be developed that would fit the observed conditions even better. Similarly, a more carefully controlled experiment might fit the conditions treated by Priestley more exactly and lead to a closer agreement.

V. ACKNOWLEDGMENTS

The author wishes to acknowledge the help of Mr. J. G. Fraser in servicing the instruments used in the aircraft and in operating many of them during the observational flight. The author is indebted also to Mrs. Martha Vaccaro for reading and reducing the vertical velocity and temperature data and computing the heat flows.

VI. REFERENCES

BELLAMY, J. C. (1949).—*Bull. Amer. Met. Soc.* **30**: 45–9.
BUNKER, A. F. (1953).—*J. Met.* **10**: 212–18.
BUNKER, A. F. (1955).—*J. Met.* **12**: 445–55.
DAVIES, R. M., and TAYLOR, G. I. (1950).—*Proc. Roy. Soc.* A **200**: 375–90.
HOUGHTON, H. G., and CRAMER, H. E. (1951).—*J. Met.* **8**: 95–102.
PRIESTLEY, C. H. B. (1953).—*Aust. J. Phys.* **6**: 279–90.
PRIESTLEY, C. H. B. (1954).—*Aust. J. Phys.* **7**: 202–19.
PRIESTLEY, C. H. B., and SWINBANK, W. C. (1947).—*Proc. Roy. Soc.* A **189**: 543–61.
SCORER, R. S., and LUDLUM, F. H. (1953).—*Quart. J. R. Met. Soc.* **79**: 94–103.

AUSTRALASIAN MEDICAL PUBLISHING CO. LTD.
SEAMER AND ARUNDEL STS., GLEBE, SYDNEY

Contribution No. 745

INTERRELATIONS OF ARCTIC ICE WITH THE ATMOSPHERE AND THE OCEAN IN THE NORTH ATLANTIC — ARCTIC AND ADJACENT AREAS

By Irving I. Schell

Woods Hole Oceanographic Institution[1,2,3]

(Manuscript received 20 January 1955)

ABSTRACT

It is shown that the mean sea-ice limit in the Greenland and Barents Seas during the period April–August is a substantial measure of both the sea-surface temperature near the Faroes and the east coast of Iceland, and the air temperature at Iceland, during the subsequent period September–February.

Furthermore, it is shown that decadal variations of Arctic ice are a measure of decadal trends of ocean phenomena and weather in the region of the northern North Atlantic Ocean.

1. Introduction

The aim of this study is to outline the degree of interrelation between the severity of the Arctic ice in the northern North Atlantic and: the seasonal, annual and longer-period variations in ocean and air temperatures, precipitation, and storm frequencies and mean storm tracks in that general area.

The problem of Arctic ice relationships may be divided into two phases: relationships of the ice with the preceding ocean and air circulations, and relationships of the ice with the contemporary and subsequent ocean and weather conditions. Although the two phases are interrelated, they can be treated separately. The second phase will be treated here. Because the Arctic ice record considerably antedates the earliest meteorological and oceanographic observations in the Arctic and adjacent areas, an outline of the relationships of the Arctic ice with air and ocean temperatures, *etc.*, would provide valuable information on earlier oceanographic and meteorological conditions in those areas.

2. Data and method of study

The ocean areas from which Arctic ice data are available for long periods of time are: (1) the waters off Iceland (1750's on) and the Greenland Sea in general (since 1877); (2) the Barents Sea (since 1895); (3) the waters off southwest Greenland (since 1820), (4) the waters off Newfoundland (since 1861, approximately; principally iceberg counts); and (5) the Bering and Chuckchee Seas (since 1899) and others.

Only the ice data from areas (1), (2) and (3), embracing the Greenland and Barents Seas, could be treated in this investigation. The southerly limits of the ice in these areas were taken from compilations made by the Danish Meteorological Institute. The values designating the severity of the ice off Iceland were taken from a recent compilation by Koch (1945). The air temperature and precipitation data were, for the most part, taken from *World weather records*. The sea-temperature data came mainly from a series of recent papers by Smed (1947 to 1953) and from a paper by Brown (1953). Further details about the data, including the storm frequencies also studied here, will be found in the appropriate sections dealing with them. Many data for recent years were obtained by correspondence; and the writer wishes to express his gratitude to all those who have contributed in this respect.

The various ice data were then correlated with oceanographic and meteorological data from the Arctic and adjacent areas by season, year and decade; and the results of the correlation are shown in the tables below. In those instances where use was made of the correlation coefficient r, it was only to measure an association, anticipated in general terms from physical considerations; and as the question of the significance level of the derived coefficients did not apply, it was not considered. Were these coefficients compared with the "largest possible by chance," it would have led to misleading results, since the coefficients that fall below this value indicate a relationship as real as those that match it or exceed it.

3. Brief statement of problem

Because the two large polar ice areas in the Arctic and Antarctic are a prominent factor in the general circulation of the atmosphere and the hydrosphere, significant changes in their areal extent might be as-

---

[1] Contribution No. 745 from the Woods Hole Oceanographic Institution.

[2] Present affiliation: Tufts University.

[3] This article has been prepared under a research contract between the Office of Naval Research and the Woods Hole Oceanographic Institution.

sociated with changes in the atmosphere and the ocean in the high latitudes and, although to a lesser extent, with changes in the circulation in lower latitudes.

In general, severe ice conditions off Iceland and a more southerly extension of the Arctic ice pack in the Greenland Sea, for example, might be expected to be associated with an unusually well developed polar high and a less developed North Atlantic low shifted southward. Presumably there would be a more southward extension of the colder polar water and, therefore, a southerly displacement of the zone of sharp temperature contrasts between the southward-flowing cold polar water and the northward-flowing warm Atlantic water. In addition, since the mean storm track in the northern North Atlantic is presumably associated with the zone of sharp temperature contrasts, we might expect also a shift of this storm track southward and, consequently, an increase in the storminess in lower (and a decrease in higher) latitudes. Thus, the pressure could be expected to be lower (higher) and the precipitation higher (lower) in the zone of increased (decreased) storminess to the south (north). Because of persistence, one may also expect the subsequent ocean circulation and weather patterns to be related to the Arctic ice.

4. Previous investigations

For earlier work in this field, the reader is referred primarily to a paper by Wiese (1924) and, for a recent extension, to a work by this writer (1947; see also 1940) in which the relationship between the variations of the ice in the Greenland Sea (April-August) and the subsequent precipitation in northwestern Europe was considered on the basis of 56 years of data then available. In conformance with the pattern of Arctic ice-weather relationships drawn above, the average October-December precipitation following severe ice conditions was found heavier than usual south of 60°N (in the area of the British Isles, Denmark, northern France, southern Norway, and Holland), where an excess of storminess would be expected, but lighter than usual over northern Norway, where a deficiency would be expected following the same type of ice conditions.

In addition to the earlier indicated relationships of the Arctic ice with the contemporary and subsequent seasons' pressure distributions, mean storm tracks and storm frequencies, temperatures and precipitation, a similar relation between the decadal character of the ice off Iceland[4] and the temperatures of several Arctic fringe areas and other areas in lower latitudes was determined (Schell, 1952). The results covering the period 1831–1950 showed the severe (light) ice decades during this 120-yr period to be associated with negative (positive) temperature deviations, the relation of the ice with the temperatures of the stations in the Arctic fringe areas being the closer. In addition, a relation was also found with the following decadal temperature in Stykkisholm, Archangel, and to a lesser extent, Vardo. At Archangel, where the effect of local persistence of severe ice conditions and the associated cold water may be expected to be strengthened by a greater dilution of the northeastward-flowing warm Atlantic water by a stronger East Icelandic polar current during severe ice periods, the temperature deviation (negative sign) of the decade following a severe ice decade was found to be actually greater than the deviation corresponding to the severe ice decade itself (Schell, 1952).

5. Present investigation

The plan of the current investigation was to broaden the relationships of Arctic ice with the contemporary and subsequent ocean and air temperature, *etc.*, by employing (1) longer records of the Arctic ice, temperature, precipitation, *etc.*, that have since become available, (2) observations from additional areas, and (3) observations for additional seasons. In addition to the Greenland-Sea-ice and the ice-off-Iceland series that were previously generally employed, a series combining the Greenland and Barents Seas ice limits was also used. The respective ice series were next correlated with the contemporary and the subsequent seasons' temperatures and precipitation of Iceland. A separate investigation was also made of the relationships between the Greenland Sea ice and the large body of sea-surface temperature data of the northern North Atlantic (north of 50°N) that has recently become available, and the data from the fixed stations along the coasts of Norway, Iceland, *etc.* Additionally, a correlation was made of the month-to-month change in the net air transfer in the Arctic with the changes in the ice area. Also, the character of the decadal relationships with the ice was further investigated by treating the sea-surface temperatures, and the precipitation of Iceland, southern Greenland, Spitzbergen and northern Europe, as well as the storminess over the northern North Atlantic.

Relationships with contemporary and subsequent temperature of Iceland.—We should expect the temperature of Iceland and adjacent areas during (and also for a period of months following) a severe (light) ice season to show a tendency for below (above) normal values. In an attempt to measure this relationship, the Greenland Sea ice series (dating from 1881), as well as the shorter Greenland Sea and Barents Sea ice series combined (dating from 1895), were correlated with the mean temperatures of the March-May and June-August quarters (contemporary with the ice season) and with the temperatures of the following

---

[4] The decadal character of the ice off Iceland usually reflects the ice conditions over a much wider area.

September-November, December-February and March-May quarters at Berufjord on the east coast and at Stykkisholm on the west coast of Iceland; and then correlated with the temperature of the two contemporary and the two immediately following seasons, and for both stations together. Another correlation was carried out with the annual air temperatures. The two sets of correlation coefficients, based on data ranging from 64 to 50 yr, are shown for each of the quarters, *etc.*, in table 1.

It is evident from the negative sign of the correlation coefficients that there is a tendency for below (above) normal temperatures contemporary with and followa severe (light) ice season. It also appears that when the temperatures of these two stations are considered together, as well as when the values of the temperatures are averaged for the two seasons that are contemporary with and the two that follow the ice season, the correlation coefficients obtained are frequently higher than those obtained with each of the seasons or stations singly. The frequent closer associations between the Arctic ice and the temperature data from two related (with respect to the ice) stations and two similarly related seasons together are no doubt due to the smoothing out of local influences and to automatic smoothing introduced when combining initially homogeneous time intervals. On the same principle, the annual correlation coefficients also frequently came out higher than any of those for a single quarter. Also, the correlations of the temperature with the ice of the Greenland and Barents Seas combined came out on the whole closer than those with the Greenland Sea ice alone, indicating that the ice of the larger area is a better index of the contemporary and subsequent circulation processes in that general area than the Greenland Sea ice alone. (The present definition of the association between the temperature and the ice of the Greenland Sea alone must be regarded as better, however, since the Greenland Sea ice series is longer by 13 yr. Nevertheless, one would expect that a larger ice area would reflect conditions more faithfully than a smaller area; and for want of contradictory evidence, we must accept the finding that the ice of the Greenland and Barents Seas combined is apparently the better index of the two.)

Relationship with the contemporary and subsequent precipitation of Iceland.—As previously suggested, severe (light) ice conditions in the Arctic are presumed to be associated with a greater (lesser) development of the polar high-pressure field and a southerly (northerly) displacement of the mean storm track in the northern North Atlantic from its usual position. Thus, with a tendency towards higher pressure and fewer storms over Iceland with severe as compared with light ice conditions, we should expect lower (higher) than usual precipitation during and following severe (light) ice conditions.

A correlation of the two ice series was made, in the same manner as before, with the contemporary and subsequent precipitation at Stykkisholm and Berufjord, beginning with the March-May quarter. The results are also shown in table 1. It is again evident, from the negative sign of the correlation coefficients throughout, that a tendency exists for below (above) normal precipitation during and following a severe (light) ice season, as anticipated.

As in the case of the temperature, the association of the precipitation with the Arctic ice is frequently closer when the two stations, or the two contemporary seasons (March-May, June-August), or the two seasons following the ice seasons (September-November, December-February) are treated together. Also, the

TABLE 1. Correlation coefficients of April-August Greenland Sea ice (A), and Greenland Sea and Barents Sea ice combined (B), with contemporary and following March-May, June-August, etc., temperature and precipitation of Iceland.

	Contemp. Mar.-May	Jun.-Aug.	Mar.-Aug.	Sep.-Nov.	Dec.-Feb.	Sep.-Feb.	Follow. Mar.-May	Annual
A. Greenland Sea ice (1881-1892, 1895-1939, 1946-1949)								
Temperature								
Berufjord	−.18	−.33	−.25	−.24	−.37	−.38	−.20	−.32
Stykkisholm	−.44	−.61	−.52	−.23	−.35	−.34	−.33	−.60
Berufjord and Stykkisholm	−.23	−.36	−.36	−.33	−.37	−.41	−.23	−.41
Precipitation								
Berufjord	−.19	−.37	−.39	−.05	.09	−.04	−.15	−.22
Stykkisholm	−.13	−.42	−.36	−.31	−.35	−.34	−.31	−.50
Berufjord and Stykkisholm	−.22	−.42	−.41	−.23	−.13	−.22		−.42
B. Greenland Sea and Barents Sea ice (1895-1939, 1946-1949)								
Temperature								
Berufjord	−.25	−.32	−.31	−.31	−.51	−.49	−.22	−.42
Stykkisholm	−.35	−.43	−.41	−.38	−.50	−.56	−.23	−.50
Berufjord and Stykkisholm	−.29	−.36	−.36	−.40	−.53	−.54	−.27	−.50
Precipitation								
Berufjord	−.20	−.34	−.45	−.19	−.17	−.23	−.06	−.40
Stykkisholm	−.18	−.37	−.32	−.34	−.41	−.42	−.39	−.55
Berufjord and Stykkisholm	−.26	−.43	−.45	−.34	−.31	−.43	−.30	−.58

association on the whole is closer with the ice of the Greenland and Barents Seas combined, than with the ice of the Greenland Sea alone. It is interesting to note that the association of the temperature with the ice generally diminishes after the December-February quarter following the ice season, the correlation coefficients between the ice and the following March-May quarter temperatures being smaller than those with the temperatures of the September-November and December-February seasons before. Thus, the persistence of the processes associated with different types of ice conditions appears to extend for a limited number of months following the ice season.

The above results of the association of the ice with the precipitation in Iceland are not very different from those previously obtained for northern Norway (Schell, 1947), which lies in more or less the same zone of interrelation with respect to the Arctic ice. Thus, the correlation of the ice in the Greenland Sea with the following October-December precipitation of northern Norway becomes $r = -0.50$ ($n = 61$), after recomputation with five additional years of data recently made available (1939, 1946–1949).

The pattern of correlations obtained between the temperature and precipitation and the Arctic ice conforms with that expected from theoretical considerations. At the same time, the size of the correlation coefficient tells us that the ice of the northern North Atlantic is but a partial index of the contemporary and subsequent temperature and precipitation. To what extent more adequate observations of the Arctic ice might alter the indications obtained at present, remains to be seen.

Relationship with preceding, contemporary, and subsequent sea-surface temperatures in northern North Atlantic.—In outlining the general relationship of the ice in the Arctic with the ocean circulation in that general area, it has been assumed that the fluctuations in the ice are associated also with changes in the temperature of the Arctic waters. A more southerly limit of the ice in the Greenland Sea is associated with a well-developed flow of cold water from the north and lower temperatures; and, on the other hand, a more northerly limit of the ice, *etc.*, is associated with a stronger Irminger Current sweeping round to the north coast of Iceland from the south and with higher temperatures. It was further assumed that, because of persistence of the circulation processes, the sea temperatures following the ice season would show the same trend as the temperatures contemporary with the ice season.

As the severity of the Arctic ice season off Iceland probably reflects the intensity of the East Icelandic Polar Current, we may expect a greater southeastward penetration of this current in severe than in light ice years. Thus, Knudsen (1906) found that the 10C isotherm and 35.00 per mille isohaline, which he took as an index of the southeastward extension of the East Icelandic Polar Current, lay between the Faroes and the Shetlands in 1902, a severe ice year, but well to the northwest of this position in 1903, a normal ice year off Iceland. More recently, Hermann (1948) showed that the eastern boundary of the East Icelandic Polar Current (35.00 per mille isohaline at 100 m) in August 1948, a very light ice year, intersected latitude 65°N at longitude 7°W, while in July-September 1900, a less light ice year, this isohaline intersected the same latitude at longitude 2°30′W; and in August-September 1903, a normal ice year, the point of intersection was at longitude 1°W.

In an attempt to define the Arctic ice as an index of the circulation in the Arctic and adjacent waters, it becomes necessary (for lack of sufficient data on currents in these waters) to examine this question indirectly by studying the longer series of sea-surface temperatures now available. Accordingly, correlations were carried out between the ice of the Greenland Sea and the contemporary, subsequent, and the preceding annual sea-surface temperatures of a number of areas in the North Atlantic north of 50°N (fig. 1) that have recently been tabulated by Smed (1947–1953), and also with the temperatures from a number of stations along Iceland's coasts as well as Thorshavn, *etc.* An attempt at differentiation of the water characteristics of the individual areas within this large area (fig. 1) suggests that the waters in areas F, G, H, K, L, M, N, and Marsden Squares 252A, 252B, 251C, 251D (fig. 1) are of warm Atlantic origin; the waters in areas A, B, C and I, mainly of polar origin; and the waters in areas D, E and J, in greater or lesser proportions of both origins.

Similarly, the waters at Papey off the east coast of

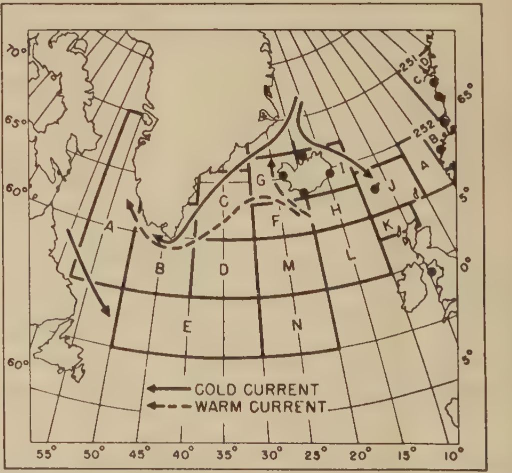

FIG. 1. Location of sea areas A to N (after Smed), and Marsden Squares 252A, 252B, 251C and 251D, and of coastal and island stations (dots).

TABLE 2. Correlation coefficients of Greenland Sea ice with annual sea surface-temperature of North Atlantic.

Areas	Years −2	−1	0	1	2	3	4	5
A		−.13	−.33	−.35	−.40	−.40	−.26	
B		−.07	−.26	−.25	−.30	−.46	−.28	
C	−.35	−.37	−.56	−.33	−.37	−.58	−.54	−.38
D		−.04	−.22	−.19	−.29	−.38	−.18	
E		−.06	−.01	−.14	−.05			
F		.03	−.27	−.20	−.29	−.43	−.26	
G		.08	−.23	−.21	−.21	−.33	−.34	−.16
H		−.15	−.27	−.33	−.34	−.44	−.45	−.36
I		−.20	−.42	−.42	−.25	−.27		
J	−.14	−.30	−.27	−.30	−.15			
K		−.23	−.32	−.35	−.33	−.24		
L		−.19	−.38	−.33	−.27	−.39	−.29	
M		−.09	−.20	−.25	−.25	−.30	−.16	
N		.09	.01	−.03	−.02			
Grimsey		−.16	−.37	−.45	−.09			
Papey		−.25	−.47	−.49	−.20			
Vestmanno		−.24	−.43	−.34	−.27			
Stykkisholm		.03	−.07	−.09				
Thorsh./Myg.		−.24	−.35	−.22	−.11			
Ona		−.16	−.20	−.07				
Nordoyen		−.29	−.25	−.20				
Port Erin	−.09	−.39	−.29	−.29				

Iceland are mainly of polar origin, those at Vestmanno on the south coast and Stykkisholm on the west coast are warm Atlantic in origin, while those at Grimso off the north coast show an intermingling of both polar and relatively warm Atlantic waters. All four stations reflect to some extent the influence of the land mass on whose rim they lie. Equally, the waters at Thorshavn-Myggenaes, Port Erin, and along the coast of Norway are warm Atlantic in origin, and, except for Thorshavn, are to a greater or lesser degree influenced by the adjacent land masses.

The data for the areas A to N, except for area C which begins with the year 1905, generally cover the years 1876 to 1949, minus the 6-yr period 1940–1945 and a portion of the World War I period. They thus provide approximately six decades of record in most cases. However, the material is sparse and quite uneven in that much fewer observations were made for most areas in the earlier than in later years, and practically no observations were available for the winter months until fairly recently from the more northerly areas. This shortcoming is to a considerable extent offset by the conservativeness of the ocean processes. A more serious drawback, as seen from fig. 1, is the mainly geographical delimitation of these areas, many of them representing water masses of mixed origin — warm Atlantic and Arctic.

Coefficients of correlation of the Greenland Sea ice with the ocean-surface temperatures of the various areas were computed for time lags ranging from −2 to +5 years. These are shown in table 2 together with the separate set of coefficients based on the data from the four stations along the northern (Grimso), southern (Vestmanno), western (Stykkisholm), and eastern (Papey) coasts of Iceland, Thorshavn-Myggenaes in the Faroes, and others.

Because of the limiting nature in which the large area was divided, no strong association of the sea-temperature series with the Arctic ice could be expected; and it is perhaps no surprise that, with a few exceptions, the correlation coefficients obtained were quite small. It is significant, however, that the sign of the coefficients is negative throughout, showing a tendency for below (above) normal temperatures with severe (light) ice conditions, as was to be expected. To a certain extent, the negative sign of the correlation coefficients obtained is probably due to the recent climatic trend, since the correlation here examined is

TABLE 3. Correlation coefficients of Greenland Sea ice, and Greenland and Barents Seas ice combined, with specified sea-surface temperatures.

	Contemp. Mar.–May	Jun.–Aug.	Mar.–Aug.	Sep.–Nov.	Dec.–Feb.	Sep.–Feb.	Follow. Mar.–May
A. Greenland and Barents Seas ice combined							
Papey (1895–1949)*	−.35	−.39	−.45	−.49	−.50	−.64	−.37
Thors.-Myg. (1895–1949)*	−.19	−.38	−.32	−.50	−.46	−.57	−.26
B. Greenland Sea ice							
Papey (1877–1949)**	−.36	−.45	−.45	−.42	−.31	−.46	−.36
Thors.-Myg. (1877–1949)**	−.21	−.32	−.32	−.32	−.26	−.35	−.22

* 1940–1945 missing.
** 1893–1894 and 1940–1945 missing.

not limited to the more northerly areas but includes the warm-water areas.

The fact that in several instances the coefficient of correlation increases following the year of the ice season, and that with one or two exceptions the coefficients are smallest for the year before the ice season, would lead us to conclude that the Arctic ice is more a precursor of the future sea-surface temperature than an index of the temperature contemporary with the ice season, and that the preceding sea-surface temperature bears little relation to the Arctic ice transport. It can be assumed that it would take the Arctic water longer to travel to the south and to assert its influence there than it would take the ice to cover the same distance.

In addition to these correlations, a separate set of correlation coefficients was obtained of the Greenland Sea ice, as well as the Greenland Sea and Barents Sea ice combined, with Papey and Thorshavn-Myggenaes sea-surface temperature for each season contemporary with (March-May, *etc.*) and following the ice season (September-November, *etc.*) (table 3). Papey was chosen because it lies close to an area with a single well-defined Arctic flow (East Icelandic Polar Current), while the choice of Thorshavn-Myggenaes in the Faroes was determined by the consideration that the East Icelandic Current approaches these islands. The results obtained indeed show a close correlation of the ice with the Papey sea-surface temperature and also indicate, as before, that the association of the ice with the polar water temperatures is closer, not with the season contemporary with the ice (March-August), but with the season following it (September-February). Similarly, the correlations obtained with the Thorshavn-Myggenaes sea-surface temperature, which are only a little less than those with Papey, additionally indicate that the ice of the Greenland and Barents Seas markedly reflects the intensity of the East Icelandic Polar Current as it approaches the Faroes. Thus, the ice during April-August is a significant index of the following fall-winter sea-surface temperature along the East Icelandic Polar Current.

Relationship with longer-period variations in ocean temperature, precipitation, and cyclonic distribution in northern North Atlantic and adjacent areas.—The longer series of ocean-surface temperatures from the 14 areas in the open northern North Atlantic and from the four stations in Iceland, *etc.* (fig. 1), were also examined in relation to the ice variations over longer periods. Before discussion of the results, it is desirable to examine the general trend in sea-surface temperature in recent decades.

Considerable evidence exists by now that the water temperatures in many areas have undergone a marked rise, much the same as the air temperature has in recent decades over a wide portion of the globe, though a rise of smaller magnitude. Evidence of this temperature rise over the North Atlantic north of 50°N has been most fully given by Smed (1947; 1949). The upward temperature trend is also evident along the east coast of the United States where, at Boston, for example, the average annual sea-surface temperature rose from 49.0F for the first half (1922–1937) of the period examined to 50.9F the second half (1938–1953). Similarly, at Cristobal (Panama Canal Zone), where regular water-surface temperature observations have been made since 1908, the annual temperature rose from an average of 82.0F for the period 1908–1930 to a value of 82.9F for the more recent period 1931–1952. As the standard deviation of this temperature series is only 0.76F, the rise experienced fully attests to the significance of the change.

It would appear from a study by Sandstrom (1942) of the interdecadal changes in the mean January sea-surface temperatures in the northern North Atlantic that, for the areas as a whole, the net change from the 10-yr period 1900–1909 to the period following it, 1910–1919, was approximately nil; that from 1910–1919 to 1920–1929, markedly positive; and that from 1920–1929 to 1930–1939, also positive though not as marked. Similarly, from a more recent study by Brown (1953), giving the mean decadal anomalies of the sea-surface temperature in four 5-deg squares in the area 60–70°N, 20–0°E, it appears (table 4) that the average change in the sea-surface temperature was 0.1C from the period 1900–1909 to 1910–1919; 0.3C from the period 1910–1919 to 1920–1929; 1.2C from the period 1920–1929 to 1930–1939; and −0.2C from the latter 10-yr period to the 1940–1949 period, the last finding suggesting a reversal of the upward trend of the sea-surface temperature in that area in the late 1940's.[5]

An examination of the interdecadal variations in the ocean-surface temperatures in the northern North Atlantic based on all the data from the various areas, *etc.*, discussed above, shows the temperatures for the broad area as a whole to have risen from the preceding decade in each of the decades 1891–1900, 1921–1930 and 1931–1940 (table 4); to have fallen from the preceding decade in the decade 1901–1910, and partially in the decades 1911–1920 and 1941–1950.

Examining the results in more detail, one finds that the rise in temperature in the decade 1891–1900 from the decade preceding it held for all but two of the areas (table 4) and for four of the six stations existing at the time, while the rise in the decades 1921–1930 and 1931–1940 held for all areas and stations but three and was also considerably greater than for the earlier decades.

Similarly, the fall in ocean temperatures in the decade 1901–1910 from the preceding decade was almost as widespread but not as large as the temperature rise in the 1921–1940 periods; while for the decade 1911–1920 and the recently ended decade 1941–1950 there were areas, in almost equal numbers, both with a rise and a fall in the temperature from the preceding decade. Thus, while the same temperature trend appears to have generally prevailed almost throughout the entire area irrespective of origin of the water masses in most of the earlier decades, the decade 1941–1950 and to a certain extent the decade 1911–1920 represent periods with conflicting tendencies in the temperature trend, and therefore a steeper temperature gradient between some of the areas. Much the same results were obtained on the basis of the more numerous observations provided by the coastal or island stations (table 4).

---

[5] Both the decades 1910–1919 and 1940–1949 were deficient in observations due to military operations.

To what extent the temperature rise in recent decades in the northern North Atlantic has been due to a greater inflow of warmer water from the south, the very marked increase in the temperature of the air above, or a possible increase in local insolation, is impossible to say. Some evidence that the warming of the waters in the high latitudes was in fact due to a greater inflow of warmer water appears from a consideration of the warming pattern in recent years. If it is supposed that in the areas where the inflow of warmer water occurs earlier, the temperature rise would be greater than the simultaneous rise in the areas where the warmer water reaches in full strength later, the rise in the sea-surface temperatures off northern Norway would be expected to be greater than in the same period off southern Norway, where the warmer Atlantic water would be expected to reach later. Thus, Hesselberg found (1940) that the recent rise in the sea-surface temperature off northern Norway ranged from 0.7 to 1.0C, as compared with only 0.2 to 0.4C in the same period off southern Norway. Similarly, Smed (1947) found that the maximum rise in the surface temperature occurred later in the North Sea than in the area farther to the north where the warm Atlantic water would be expected to arrive first (before sweeping southward).

The probability that the rise in the ocean temperatures in the northern North Atlantic was largely due to a greater transport of warmer water from the south agrees with the fact that the atmospheric circulation pattern over the northern North Atlantic has altered markedly in recent decades and a marked increase of

TABLE 4. Interdecadal variations in sea-surface temperature (deg C) in northern North Atlantic, and interdecadal variations in character of ice off Iceland and in southerly limit of ice in Greenland and Barents Seas combined.

	Period					
Area	1881–90 to 1891–00	1891–00 to 1901–10	1901–10 to 1911–20	1911–20 to 1921–30	1921–30 to 1931–40	1931–40 to 1941–50
A	−0.1	−0.1	−0.1	0.9	−0.1	−0.1
B	0.1	−0.3	−0.1	0.7	0.0	−0.4
C	—	—	—	0.4	0.5	−0.3
D	0.3	−0.6	0.1	0.2	0.4	−0.1
E	0.2	−0.7	−0.1	0.2	0.6	−0.8
F	0.2	−0.3	−0.2	0.2	0.5	0.1
G	0.3	−0.3	0.0	0.0	0.7	0.1
H	0.1	−0.1	−0.2	0.2	0.4	0.4
I	0.4	−0.1	0.1	0.1	0.7	0.2
J	−0.1	0.0	−0.1	0.1	0.5	0.4
K	0.1	−0.3	0.0	0.2	0.3	0.4
L	0.2	−0.4	0.0	0.1	0.5	0.2
M	0.4	−0.6	−0.1	0.1	0.6	−0.2
N	0.5	−0.6	−0.1	−0.1	—	—
Average	0.2	−0.3	−0.1	0.2	0.4	0.0
252A	—	—	0.1	0.4	0.9	−0.2
252B	—	—	0.1	−0.1	1.6	−0.4
251C	—	—	0.2	0.5	1.1	−0.3
251D	—	—	0.0	0.4	1.3	0.1
Average	—	—	0.1	0.3	1.2	−0.2
Vestmanno	0.4	0.1	0.1	0.6	0.4	0.1
Stykkisholm	−0.4	0.1	0.3	0.2	0.1	−0.3
Grimsey	0.3	−0.4	0.5	0.9	0.6	−0.6
Papey	0.4	0.1	0.0	1.0	0.5	−0.3
Port Erin	—	—	−0.2	0.4	0.1	−0.1
Myken	—	—	—	—	0.4	−0.3
Nordoyan	—	−0.1	0.4	0.1	0.4	−0.3
Skomvaer	—	—	—	—	0.7	−0.3
Ona	−0.1	0.1	0.0	0.1	0.5	−0.2
Thorsh./Myg.	0.2	−0.3	0.1	0.3	0.2	0.2
Average	0.1	−0.1	0.2	0.4	0.4	−0.2
Ice limit (deg lat)*	—	—	0.6	−1.1	−0.2	0.7**
Ice off Iceland	Sv./Md.	Md./Md.	Md./Md.	Md./Lt.	Lt./Lt.	Lt./Md.**

* Minus sign signifies northward displacement.

** Provisional.

southerly winds has taken place (Eriksson, 1943). Additional evidence is provided by the increase in the salinities of these waters for the same period, as reported by Smed (1943) and Helland-Hansen (1949).

It has been shown that during the period under consideration, as well as previous to it, the character of the ice off Iceland has similarly undergone considerable changes from decade to decade, as has the southerly limit of the ice in the Greenland and Barents Seas during the shorter period beginning with the 1901–1910 decade, the first full decade for which information for this larger area is available. Table 4 gives the interdecadal variations in the character of the ice off Iceland earlier determined by the writer (1952), and in the mean position of the decadal ice limit drawn from the individual ice limits given by the Danish Meteorological Institute. The table shows that the severity of the ice off Iceland has decreased from the preceding decade (or was so much below the normal that no further substantial decrease could occur) in the decades 1891–1900 (from severe to moderate), 1921–1930 (moderate to light) and 1931–1940 (light to light), and has probably increased in the decade 1941–1950[6] (light to moderate), though not in the decades 1901–1910 and 1911–1920. Similarly, the average southerly ice limit in the Greenland and Barents Seas lay farther north (minus change in latitude) in the decades 1921–1930 (−1.1 deg lat) and 1931–1940 (−0.2 deg lat) than in each of the preceding decades, and correspondingly lay farther south in the decade 1911–1920 (0.6 deg lat) and during the 1946–1950 period (0.7 deg lat), the portion of the 1941–1950 decade for which information on the ice limit is at present available.

Comparing the above pattern of changes in the ice with the changes in the sea-surface temperatures given in table 4, one notes that an increase in the decadal ocean temperature for the area as a whole generally coincided with the particular character of the ice off Iceland and the ice limit of the Greenland and Barents Seas. The increases in the ocean-surface temperature in the northern North Atlantic during the decades 1891–1900, 1921–1930 and 1931–1940 from the preceding decade correspond to ice decreases. No such clear-cut relationship is evident, however, for the two decades 1901–1910 and 1911–1920.

In attempting to outline the possible relations of the ocean-surface temperatures of the individual areas and stations with the Arctic ice, we are confronted as before with the question of the origin of the water masses of the different areas, *etc.* We might reasonably expect that the colder waters of this large area would show closer correlation with the ice than would the warmer waters.

An examination of table 4 shows that, except for the recent decade 1941–1950, this is not the case. Virtually all areas, irrespective of the type of water masses, showed either a simultaneous increase or decrease in the temperature for the same period. This would suggest that, by and large, the longer-period variations in the Arctic ice and in the ocean-surface temperatures in the northern North Atlantic are part of the same general longer-period changes in the circulation in that large area, the Arctic ice and the sea-surface temperature reflecting these deep-seated changes together.

The trends in the decadal sea temperatures discussed above and in the air temperature earlier (Schell, 1952) might be expected to be associated with corresponding trends in the decadal precipitation. As a result of the fall in pressure (Petterssen, 1949) and increase in southerly winds (Eriksson, 1943) over the northern North Atlantic and adjacent areas in recent decades, higher precipitation would be expected during the same period in that general area, inasmuch as wetness and warmth over longer periods tend to coincide north of 55°N (Willett, 1952). Table 5 shows that in the region embracing Iceland, southernmost Greenland, Spitsbergen, and northernmost Europe, represented by 10 to 14 stations (except by only two during the period 1861–1880), the precipitation was, in fact, above normal in the last three decades (1921–1950) and close to normal or below in the decades before.

In an attempt to determine the existence of a general relationship between the ice in the Arctic and longer-period precipitation, a comparison of the available decadal precipitation data from Iceland[7], southernmost Greenland[8], Spitsbergen[9] and northernmost Europe[10] was made with the ice off Iceland, and then with the average latitude of the ice limit in the Greenland and Barents Seas combined. Although the general character of the ice in the Greenland and Barents Seas when considered by decade is very similar to the character of the ice off Iceland, it was thought desirable to take advantage of the areally more extensive though shorter ice series since become available, to study the relation of the precipitation with the ice in the Arctic on a broader basis. Accordingly, our comparison of the precipitation with the severity of the ice off Iceland begins with the decade 1861–70, the first full decade with corresponding precipitation observations; that with the average latitude of the ice limit in the Greenland and Barents Seas combined starts with the 1901–1910 decade, the first full decade when ice values for this larger area are available.

---

[6] No figures comparable to those obtained for the previous decades have yet been published, but it is known that the ice of this decade was not as light as that of the decade before and probably was moderate.

[7] Stykkisholm, Berufjord and Vestmanno.

[8] Ivigtut, whose record for the decade 1921–1930 was too incomplete to be included; and Angmagsalik, whose record begins with 1898.

[9] Record begins with 1912, and values are missing for a number of years including the World War II period.

[10] Bodo, Tromso, Bronnoysund and Vardo in northern Norway; Karesuando and Haparanda in northern Sweden; Kaajani and Sodankyla in northern Finland; and Archangel in northern Russia.

Table 5 shows that the precipitation in the two consecutive decades with light-ice conditions off Iceland (1921–1940), coinciding also with a less southerly extension of the ice in the Greenland and Barents Seas, was above the long-term average, as follows (average of both decades): Iceland, 109.5 per cent; southernmost Greenland, 108.5 per cent; Spitsbergen, 105.5 per cent; northernmost Europe, 105.5 per cent; region as a whole, 106.5 per cent. On the contrary, the precipitation in the severe-ice decade 1881–1890 was, except for Greenland, below the average as follows: Iceland, 94 per cent; southernmost Greenland, 104 per cent; northernmost Europe, 92 per cent; region as a whole, 94 per cent. Similarly, in the other severe-ice decade, 1861–1870, the precipitation was also below the average: Stykkisholm, 92 per cent; Haparanda, 75 per cent.

Although none of the decades after 1881–1890 can be considered as having had severe ice conditions as in Iceland, the average limit of the ice in the combined Greenland and Barents Seas in the decade 1911–1920 extended farther south than in any of the other four decades for which similar measurements are available. Table 5 shows that the precipitation of this decade was indeed below the average (95 per cent for the region as a whole).

From the foregoing, it is evident that the decadal precipitation in the Icelandic, *etc.*, areas varies with the southerly extent of the ice in the sector of the Arctic examined. A more southerly (northerly) position of the ice limit is accompanied by lighter (heavier) precipitation over that area.

It has been shown (Schell, 1952), that following a decade with extreme ice conditions the temperature departure of Iceland and northernmost Europe tends to retain the sign of the departure of the previous decade, below (above) normal temperatures being maintained following severe (light) ice conditions. It was suggested at the time that this relationship is due to the persistence of the circulation associated with one or another type of extreme ice conditions and presumably with a greater or lesser outpouring of Arctic water, the water, and to a lesser extent the ice, contributing to the maintenance of the time-lag relationship.

From this we may infer that the precipitation pattern will also show a similar relation with the Arctic ice. Hence, following severe ice conditions, for example, the below-normal precipitation trend in the northern North Atlantic and adjacent areas that is associated with severe ice would be maintained for some time afterwards, provided no radical change in the circulation and in the corresponding ice character from the previous decade has occurred.

Table 5 shows that the precipitation in the decades 1871–1880 and 1891–1900, both following the severe ice decades 1861–1870 and 1881–1890, respectively, was below the average, as follows: Iceland (Stykkisholm only), 93 per cent; northernmost Europe (Haparanda only), 79 per cent, all for the decade 1871–1880; and Iceland, southernmost Greenland, and northernmost Europe combined (11 stations), 98 per cent for the decade 1891–1900.

Similarly, the precipitation in the decades 1931–1940 and 1941–1950, following the light ice decades 1921–1930 and 1931–1940, respectively, was above the average, as follows: Iceland, 110 per cent; southernmost Greenland, 108 per cent; Spitsbergen, 98 per cent; northernmost Europe, 108 per cent; region as a whole, 109 per cent, all for the decade 1931–1940; region as a whole, 102 per cent for the decade 1941–1950.

TABLE 5. Character of ice off Iceland, average latitude (°N) of ice limit in Greenland and Barents Seas combined, and annual precipitation (per cent of normal) at indicated locations (*n* = number of stations).

	Ice		Precipitation					
Decade	off Iceland	Greenland and Barents Seas	Iceland	Southern Greenland	Spitsbergen	Northernmost Europe	Region	*n*
1861–70	Severe	—	92	—	—	75	84	2
1871–80	Moderate	—	93	—	—	79	86	2
1881–90	Severe	—	94	104**	—	92	94	10
1891–00	Moderate	—	95	102**	—	98	98	11
1901–10	Moderate	71.8	100*	102	—	100	100	13
1911–20	Moderate	71.2	91*	99**	89**	96	95	13
1921–30	Light	72.3	109	89**	113**	103	104	14
1931–40	Light	72.5	110	128**	98**	108	109	14
1941–50	Moderate°	71.8°	100	98	—	104	102	11
Average (1881–1940) (mm):			1107	1008	322	678	960	

° Provisional.

* Values of Iceland's precipitation for 1911–1920, and to lesser extent for 1901–1910, are too low due to poor exposure of rain-gauge at Stykkisholm. ("A considerable amount of precipitation occurring during periods of east and south winds got lost." Personal communication from Mr. H. Sigtryggsson, Icelandic Weather Service.)

** All Spitsbergen and Greenland values for 1881–1900 and 1911–1940 are single-station values.

The higher value of the precipitation for the decade 1931–1940 than for the decade 1941–1950 is probably due to the decade 1931–1940 having had light ice and followed a decade with light ice. (The decade 1941–1950 followed one with light ice but was, it appears, a decade with moderate ice.) We may, therefore, conclude that the precipitation trend in the northern North Atlantic and adjacent areas follows a pattern similar to that followed by the temperature, *etc.;* namely, the pattern associated with extreme ice conditions tends to persist for some time afterwards.

The relation of the ice in the Greenland and Barents Seas with the air and sea temperatures and precipitation would be expected to involve also a relation with the storminess. In accordance with the pattern of interrelations drawn above, we may expect a more southerly extension of the ice boundary, for example, to be associated with a less northerly position of the mean northern North Atlantic storm track and, on the assumption that a more polar development in the North Atlantic-Arctic would lead to less steep meridional pressure gradients, also expect fewer storms. Additionally, with a tendency towards persistence in the circulation associated with different ice extremes, we may expect the storminess pattern corresponding to severe and light ice conditions, respectively, similarly to persist.

Evidence of a relation between the latitude of the mean storm track in the northern North Atlantic during the ice season (and the season following it) and the variations in the ice of the Greenland Sea was previously given by Wiese (1924), the average latitude of the storm track in the summer contemporary with a heavy ice season (and in the fall following it) being several degrees farther south than in the summer and fall contemporary with and following a light ice season and, similarly, the frequency of storms being smaller with a severe than with a light ice season.

We might expect the relation of the storminess with the Arctic ice to hold for ice variations over longer time intervals as well. As a test, decadal values of the annual storm frequency and mean latitude of the storm track, based on a compilation of annual frequencies of closed low-pressure systems recently obtained by Pollack and O'Brien (1951) for the period 1901–1938, were first prepared for the area 45–70°N, 0–70°W. Table 6 shows, however, a marked decrease in the annual frequency of the storms in this particular area from the first part (1901–1920) to the second part (1921–1938) of this period, with the lowest annual frequency being registered for the years 1931–1938. Thus, for this area as a whole, the annual frequency has decreased from a high of 626.8 per annum for the decade 1911–1920 to a value of 541.3 for the period 1931–1938, and from an annual value of 619.4 for the first two decades 1901–1920 to a value of 567.4 as the average of the period 1921–1938.

Table 6. Annual frequency* of storms (closed low-pressure systems) for each 5-deg zone of latitude, and mean latitude of storm track, in area from 0 to 70°W, by decade, *etc.*, during 1901–1938.

Zone (°N):	70–65	65–60	60–55	55–50	50–45	70–45	Mean lat.
1901–10:	105.6	131.0	122.6	135.9	116.8	611.9	57.3
1911–20:	100.4	153.1	115.3	140.9	117.1	626.8	57.3
1921–30:	103.3	127.0	115.6	133.6	114.1	593.6	57.3
1931–38:	95.7	125.4	103.2	112.3	104.7	541.3	57.5
1901–20:	103.0	142.0	119.0	138.4	117.0	619.4	57.3
1921–38:	99.5	126.2	109.4	123.0	109.4	567.4	57.4
Difference:	3.5	15.8	9.6	15.4	7.6	52.0	−0.1

* Because a low appearing in one section of this zone may appear later in another section, the figures often represent repetitions.

No perceptible variation from one decade to another, *etc.*, is shown in the mean latitude of the storm track (table 6), however. Neither result based on the values of storminess in the area appears consistent with the premises and earlier findings referred to above, which call for a greater frequency of storms and for a more northerly position of the mean latitude of the storm track during the period 1921–1938 (light ice conditions) than during the preceding two decades 1901–1920 (relatively heavy ice conditions).

A special feature is the much smaller decrease, from the first to the second part of the period, in the annual frequency of storms in the zone from 65 to 70°N, especially as compared with the neighboring zone (3.5 units as compared with 15.8). This sharp northward tapering off in the storm-frequency difference from the first to the second part of the period, in the zone from 60 to 70°N, permits us to suppose that, if this trend were to continue north of 70°N, an increase rather than a decrease in the annual frequency would be the result. Hence, the mean path of the storm track would lie farther north in the more recent period with light ice conditions (1921–1938) than in the preceding period with heavier ice conditions (1901–1920), as was to be expected originally.

As the values made available from the tabulations by Pollak and O'Brien (1951) do not go beyond 70°N, we cannot test this point in the manner employed above. We can, however, make a partial test by examining the differences in the winter cyclonic frequencies between the 1900–1919 and 1920–1939 periods recently given by Petterssen (1949) for substantially the same area as used here, but which fortunately includes the zone from 70 to 75°N as well. The presentation of the results by Petterssen is somewhat different than employed here. Nonetheless, we find for the quadrilateral, bounded by 70°N, 75°N, 10°E and 30°W, a very substantial increase in the winter cyclonic frequency in the 1920–1939 period over the 1900–1919 period, all the other areas south of

TABLE 7. Mean monthly average pressure change (mb) (running means of three months) from one month to next in Arctic sector and in northern hemisphere (20–90°N) as whole.

Sector	Jan*	Feb	Mar	Apr	May	Jun	Jul	Aug	Sep	Oct	Nov	Dec
60–90°N:	0.6	0.6	0.6	0.0	−1.0	−1.2	−1.0	−0.3	0.0	0.5	0.8	0.8
20–90°N:	0.0	−0.2	−0.6	−0.6	−1.1	−0.9	−0.5	0.4	0.8	1.0	0.8	0.6

* Month to which change is reckoned; thus, change from December to January.

this zone showing a decrease in the cylconic frequency as was the case with our own findings. This would suggest that, if the results for the remaining three seasons (March-May, *etc.*) similarly show an increase in cyclonic frequency, the frequency of storms in the North Atlantic north of 70°N would indeed have been greater with light than with heavy ice conditions, and that the mean latitude of the storm track in the same area would have followed the northward retreat of the southerly limit of the ice in recent years, as was to be expected.

The above result is to a certain extent corroborated also by the experience of the more recent expeditions in the Arctic (North Pole station, Sedov) which have recorded storms with a frequency far greater than that observed by members of the Fram and other expeditions of an earlier period.

Relationship with mean monthly net air transfer in the Arctic.—Because of the apparent relation of the pressure in the North Atlantic — Arctic and adjacent areas to the ice in the Greenland and Barents Seas, we might expect that the mean monthly net air transfer, or inflow and outflow of air, from the Arctic would be related to the variations in the ice.

To probe this, values of the net change in the mean monthly pressure from one month to the next, based on northern-hemisphere pressure-profile data (1899–1939, inclusive, prepared at the Massachusetts Institute of Technology) were computed for the Arctic sector (60–90°N) and for the northern hemisphere as a whole (north of 20°N), due allowance being made for the decrease in total mass of air with increase in latitude. Values of the monthly net air transfer (average pressure change), derived as running means of three consecutive months, are shown in table 7.

It appears that the net inflow of air into the Arctic sector begins approximately in October and continues through March, which are the times of the year with the least and the greatest ice cover in the Arctic, respectively. On the other hand, for the northern hemisphere as a whole (20–90°N), the inflow begins in August and the outflow in February.

The apparent over-all relation between the development of the ice cover in the Arctic and monthly transfer of air to and from the Arctic sector suggests that there may also be a relation between the changes in the yearly and longer-period variations in the ice cover and the corresponding air transfer. Lacking yearly values of air transfer for the Arctic sector, we may examine the possibility of such a relation for the northern hemisphere as a whole, fully expecting the relation with the hemisphere as a whole to be far less close than with the Arctic sector alone.

On correlating the yearly values of the ice in the Barents and Greenland Seas with the corresponding norther-hemisphere pressures (north of 20°N) based on the 41-yr period from 1899 to 1939, we obtain the coefficient of correlation $r = 0.38$, indicating some tendency for more ice in the North Atlantic — Arctic to be associated with higher pressures in the northern hemisphere (north of 20°N). Again, the average pressure or total mass of air over the northern hemisphere (north of 20°N) for the 20-yr period from 1901 to 1920, with relatively severe ice conditions (average latitude of ice limit: 71.6°N) was 0.28 mb above the 39-yr (1901–1939) average of 1015.20 mb, as against 0.29 mb below the average for the 19-yr (1921–1939[11]) period with light ice conditions (ice limit: 72.5°N) (table 8).

6. Discussion

It was assumed above that the relationships of the Arctic ice with the weather are due primarily to varying outflows of water from the Arctic, and that the ice reflects the intensity of these outflows. An indirect attempt to corroborate these relationships was also made by correlating the Greenland Sea and Barents Sea ice with the sea-surface temperature of the northern North Atlantic. It would be reasonable to assume, therefore, that by employing the ocean temperatures directly in the correlation with the precipitation of Iceland, for example, we should obtain at least as good a correlation as was obtained with the Arctic ice itself. As a test, we have selected the mean March-August Papey sea-surface temperatures which, owing to this

TABLE 8. Departure from average pressure in northern hemisphere (north of 20°N) and mean latitude of ice limit in Barents and Greenland Seas.

Period	Pressure (mb)	Ice limit (°N)
1901–20	0.28	71.6
1921–39	−0.29	72.5*

* The difference of only 0.9 deg lat between the two periods is in part due to the very small fluctuations in the ice limit between Cape Farewell and west of Iceland. For the area from west of Iceland to Novaya Zemlya, the average difference is nearly 2 deg lat.

---

[11] For the year 1939, only the first six months' pressures were available.

station's location on an island 6 mi off the east coast of Iceland, may be assumed better to reflect the changes in the Arctic water outflow (East Icelandic Polar Current) than the temperatures of any of the other stations in that general area. Later we correlated these temperatures with the following September-November and September-February precipitation of Iceland. The correlation coefficients obtained had values less than 0.2.

The reason for the apparent lack of a relationship between the sea-surface temperatures and the following precipitation of Iceland becomes clear, perhaps, if we remember that the coldness of the water off the east coast of Iceland is probably only partially a measure of the intensity of the East Icelandic Polar Current. What has been regarded as most significant was, we may recall, the degree of penetration of Arctic water southward. Presumably this is reflected better by the presence or absence of Arctic ice, which is associated with a movement of the water and air, rather than simply with the temperature of the water which, in addition to reflecting the intensity of the Arctic outflow, also reflects chilling from above, mixing with subsurface water, *etc.*, all of which may be little related to the degree of penetration of the cold water to lower latitudes.

Strangely, to date no attention has been paid to the question of relationships of the weather, *etc.*, with ice in the North Pacific — Arctic (Bering Sea, Chuckchee Sea). The variations in the ice of the North Atlantic — Arctic (Greenland and Barents Seas combined) and in the ice of the North Pacific — Arctic (Bering and Chuckchee Seas combined) might be expected to be similar.

As a preliminary test of a possible relationship between the southerly extensions of the ice of the two regions, the annual values of the North Pacific — Arctic ice for the 43-yr period, 1901 to 1939 and 1946–1949 were correlated with the simultaneous values of the North Atlantic — Arctic. The correlation coefficient obtained is −0.45, which suggests some tendency for the southern boundary of the ice in the North Atlantic — Arctic to retreat while its boundary in the North Pacific — Arctic extends southward, and vice versa[12]. This is unlikely to involve a shift in the pack itself, but probably reflects the tendency earlier indicated by Walker (1932) for the North Pacific and North Atlantic circulations to act not necessarily in unison with each other.

The results obtained here are, on the whole, favorable for the theory that the Arctic ice can serve as an index of the contemporary and also the subsequent ocean and air temperatures, precipitation, *etc.*, in the Arctic and adjacent areas; and they also show that in some instances, as in the cases of Papey and Thorshavn-Myggenaes, for example, the Arctic ice is a better index of the subsequent sea-surface temperatures than of those contemporary with the ice. It is equally apparent from the results obtained to date that the ice is not a complete index of the ocean and air circulation.

In assuming that with a better developed than usual Polar High associated with a more southerly extension of the Arctic ice, for example, we should expect a lesser exchange of air between the high and low latitudes and, therefore, a decrease in storminess, we have omitted saying that with severe ice conditions a need also arises for a greater exchange of air between the same latitudes due to a steepening of the meridional temperature gradient. Thus, two opposing tendencies come into being, though not simultaneously. The evidence submitted in this article and in earlier ones indicates the initial tendency for fewer storms with severe ice, *etc.* The effect of the opposing tendency for an increase in storminess, *etc.*, with severe ice, however, prevents the Arctic ice from becoming a broader index of the circulation and weather in the Arctic and adjacent areas.

It has been suggested earlier that the relation of the longer-period variations in the Arctic ice with the temperature, precipitation, *etc.*, may serve as a guide to the conditions in earlier years, when only ice observations were made. We find that a period as poor in ice off Iceland as that from 1919 to 1943 has not occurred since the middle of the 18th century, and if we can trust the records prior to the 1750's as well, it would then be more accurate to say since the middle of the 17th century. This would suggest that the recent relatively warm and wet period in the North Atlantic — Arctic and adjacent areas may not have been duplicated earlier for 200 years or more.

Acknowledgments.—The writer is indebted to the Misses Carolyn Donohue and Barbara Shearer and to Mrs. Robert F. Malkemes for carrying out the computations.

REFERENCES

Brown, P. R., 1953: Climatic fluctuations in the Greenland and Norwegian Seas. *Quart. J. r. meteor. Soc.*, **79**, 272–281.

Eriksson, B. E., 1943: Till kännedomen om den nutida klimatändringen inom omradena kring nordligaste Atlanten. *Geograf. Ann.*, **25**, 170–201.

Helland-Hansen, B., 1949: Remarks on some variations in atmosphere and sea. *Geograf. Ann.*, **31**, 75–82.

Hermann, F., 1949: Hydrographic conditions in the southwestern part of the Norwegian Sea. *Cons. perm. internatl. Explor. Mer, Ann. Biol.*, **5**, 19–21.

Hesselberg, T., 1940: Secular variation of the surface temperature of the sea along the Norwegian coast. *Internatl. Union Geod. Geophys., Ocean., Proc.-Verb. 1939*, **3**, 179–181.

---

[12] For longer-period ice variations, the tendency for the ice in the North Pacific — Arctic not to vary in the same sense as in the North Atlantic — Arctic appears more marked. Thus, while the average ice limit in the North Atlantic — Arctic appears to have decreased by 18 per cent from the 1901–1920 to the 1921–1939 period, it has apparently increased by 22 per cent during the second period on the North Pacific side of the Arctic.

Knudsen, M., 1905: On the influence of the East Icelandic Polar Stream on the climatic changes of the Faroes Isles, the Shetlands, and the North of Scotland. *Cons. perm. internatl. Explor. Mer, Rapp. Proc.-Verb.*, **3**, 1–8.

Koch, L., 1945: The East Greenland Ice. *Meddel. Grønland*, **130**, No. 3, 374 pp.

Pollak, L. W., and N. O'Brien, 1951: Frequencies of centers of closed low-pressure systems over the North Atlantic Ocean. *Dublin Inst. adv. Study, Geophys. Bull.*, No. 3, 45 pp.

Petterssen, S., 1949: Changes in the general circulation associated with the recent climatic variation. *Geograf. Ann.*, **31**, 212–221.

Sandstrom, J. W., 1942: On the relation of the surface temperature of the sea to the air temperature. *Arkiv Mat., Astr. Fyz.*, **28**, 1–24.

Schell, I. I., 1940: Polar ice as a factor in seasonal weather. *Mon. Wea. Rev.*, Suppl. 39, pp. 27–51.

——, 1947: Dynamic persistence and its application to long-range foreshadowing. *Harvard meteor. Stud.*, No. 8, 80 pp.

——, 1952: On the role of the ice off Iceland in the decadal air temperatures of Iceland and some other areas. *J. Cons. perm. internatl. Explor. Mer*, **18**, 1–36.

Smed, J., 1943: Annual and seasonal variations in the salinity of the North Atlantic Surface Water. *Cons. perm. internatl. Explor. Mer, Rapp. Proc.-Verb.*, **112**, 77–94.

——, 1947, 1948, 1949, 1950, 1951, 1952, 1953: Monthly anomalies of the surface temperature. *Cons. perm. internatl. Explor. Mer, Ann. Biol.*, **2**, 17–22; **3**, 12–24; **4**, 11–26; **5**, 10–15; **6**, 18–27; **7**, 9–13; **8**, 19–20; **9**, 16–19.

——, 1947: The inflow of Atlantic water into the North Sea through the Orkney-Shetland Channel. *J. Cons. perm. internatl. Explor. Mer*, **15**, 27–38.

———, 1949: The increase in the sea temperature in northern waters during recent years. *Cons. perm. internatl. Explor. Mer, Rapp. Proc.-Verb.*, **125**, 21–25.

——, 1953: Variation of the surface temperature in the northern North Atlantic during 1876–1952. *Cons. perm. internatl. Explor. Mer, Ann. Biol.*, **9**, 19–21.

Walker, E. W., and G. T. Bliss, 1932: World weather, V. *Mem. r. meteor. Soc.*, No. 4, 53–84.

Wiese, W., 1924: Polareis und atmosphärische Schwankungen. *Geograf. Ann.*, **6**, 273–299.

Willett, H. C., 1951: Extrapolation of sunspot-climate relationships. *J. Meteor.*, **8**, 1–6.

Contribution No. 754

VOL. 13, NO. 1 JOURNAL OF METEOROLOGY FEBRUARY 1956

A DEMONSTRATION OF FRONTS AND FRONTAL WAVES IN ATMOSPHERIC MODELS

By Alan J. Faller

Massachusetts Institute of Technology and Woods Hole Oceanographic Institution[1,2]

(Original manuscript received 16 February 1955; revised manuscript received 13 May 1955)

ABSTRACT

The remarkable similarity between the motions in a heated rotating tank of water (dishpan experiments) and the large-scale motions of the atmosphere has raised the question of the similarity of the details of the motion. It has been found possible to demonstrate visually the existence of frontal systems and associated wave cyclones. Analyses and photographs showing the relationships of these systems to the large-scale circulations are presented. It is concluded that similarity in laboratory models is not confined to that scale of motion commonly referred to as the general circulation.

1. Introduction

Considerable progress has been made in recent years in the development of models of the large-scale atmospheric motions (see Fultz, 1951b). The present article describes some new developments which seem to extend the usefulness of such experimental models.

Some preliminary work by the writer with a 2-ft (diameter) rotating tank suggested that a still larger apparatus would be desireable so that the frontal structures noted by the writer in smaller models and by Fultz (1952) could be studied in greater detail. The effects of scale upon the general characteristics of the motion and the experimental practicability of larger models were also to be investigated.

2. Experimental apparatus

The model outlined in fig. 1 was provided a stable variable-speed drive by setting it upon the rotating paraboloid used by Von Arx (1952) for oceanographic model experiments. The cylinder consisted of a brass rim, 4 in. high, fastened around a plywood base. A central cooling system was provided by circulating cold water through a stationary piping system to the underside of a copper plate set in the center of the base. Heat was applied near the rim by means of twelve 250-watt heat lamps fixed 1 ft above the tank. For these experiments, the angular rotation rate was 0.140 sec^{-1}, and the depth was 3 cm.

One of the important and difficult problems in such experiments is that of tracing the motion of the fluid. The following methods were found useful in this case:

1. The motion at the top surface of the water was determined by photographing the displacements of floating particles in a measured interval of time. Small discs of waterproof paper were found to be most practical as floating particles.
2. Crystals of potassium-permanganate dye were scattered uniformly over the tank. These fell to rest on the bottom and dissolved slowly, so that the plumes from the diffusing dye indicated the direction of the flow at the bottom.
3. Several revolutions after the introduction of the dye, regions of convergence were indicated by concentrations of dye at the bottom of the fluid. This seemed to be a consequence of the fact that the dye was heavier than the water and tended to concentrate in regions of low-level convergence and upward motion. Fronts and associated wave cyclones were clearly seen. After the initial effects of the convergence, however, it was somewhat fortuitous whether dye was available to indicate any newly developing regions of convergence.

3. Results

Fig. 2 illustrates the circulations at the bottom and at the free surface at a particular time. The left-hand portion shows the bottom circulation as

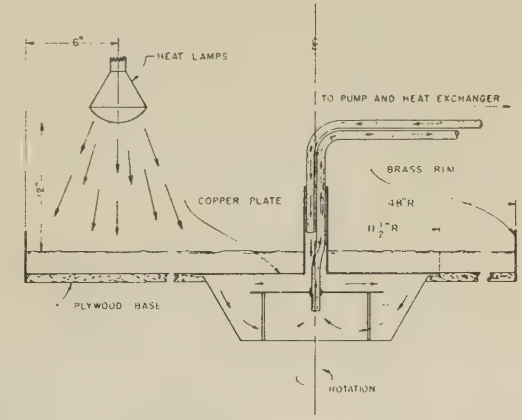

Fig. 1. Schematic diagram of rotating apparatus.

---

[1] The research reported in this article has been sponsored in part by the Geophysics Research Directorate, Air Force Cambridge Research Center, under Contract AF 19(604)-1000, and in part by a fellowship from the Woods Hole Oceanographic Institution.

[2] Contribution No. 754 from the Woods Hole Oceanographic Institution.

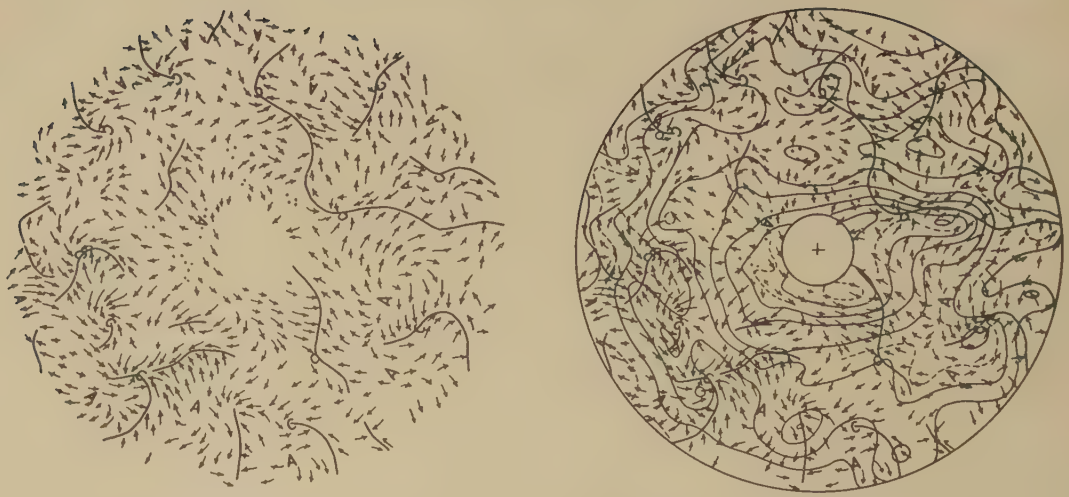

FIG. 2. Analysis of bottom circulation (left) and free-surface circulation superimposed upon bottom circulation (right).

indicated by the plumes of dissolving dye. Distinct lines of convergence and cyclonic shear, apparently fronts, are denoted by solid lines. Regions of clearly cyclonic or anticyclonic motion are labeled *C* or *A* respectively. Some attempt was made to indicate speeds by the lengths of the arrows, even though no accurate measurements could be made. The right-hand diagram illustrates the free-surface circulation superimposed upon the bottom circulation. To obtain the representation used here, velocity vectors were derived from the displacements of the paper discs in a 10-sec interval, and the velocity field was converted to an equivalent isobaric chart by constructing approximate streamlines with a spacing inversely proportional to the speeds. Due to observational difficulties close to the rim of the tank, the limit of the diagrams is taken a short distance from the rim. The tilt of cyclones with height, and the relationships of fronts to the upper-level pattern, are very similar to those in the atmosphere.

Fig. 3 shows a representation of the circulation seven revolutions after that shown in fig. 2. The frontal systems are made clear by the bands of dye and, again, the close connection with the free-surface circulation is evident.

An example of the development of wave cyclones is shown in fig. 4. The time interval between photographs is one revolution, and the sequence proceeds

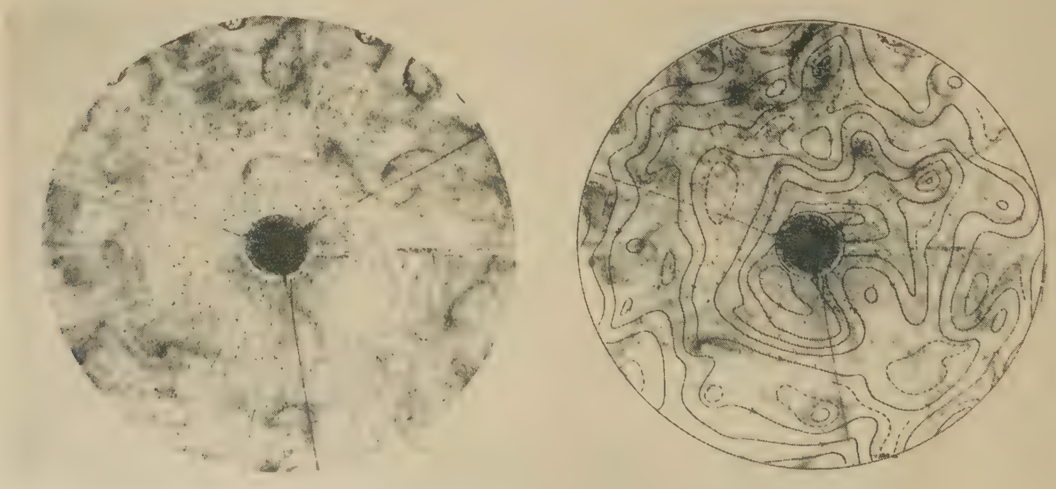

FIG. 3. Bottom circulation seven revolutions after fig. 2 as indicated by dye fronts (left), and corresponding free-surface circulation (right).

from left to right and from top to bottom. The development of two waves may be seen on the principal front. The one in the centers of the frames reached occlusion rapidly, while the cyclone near the bottoms developed more slowly. Moving cold fronts, other than those in the principal frontal system, may be

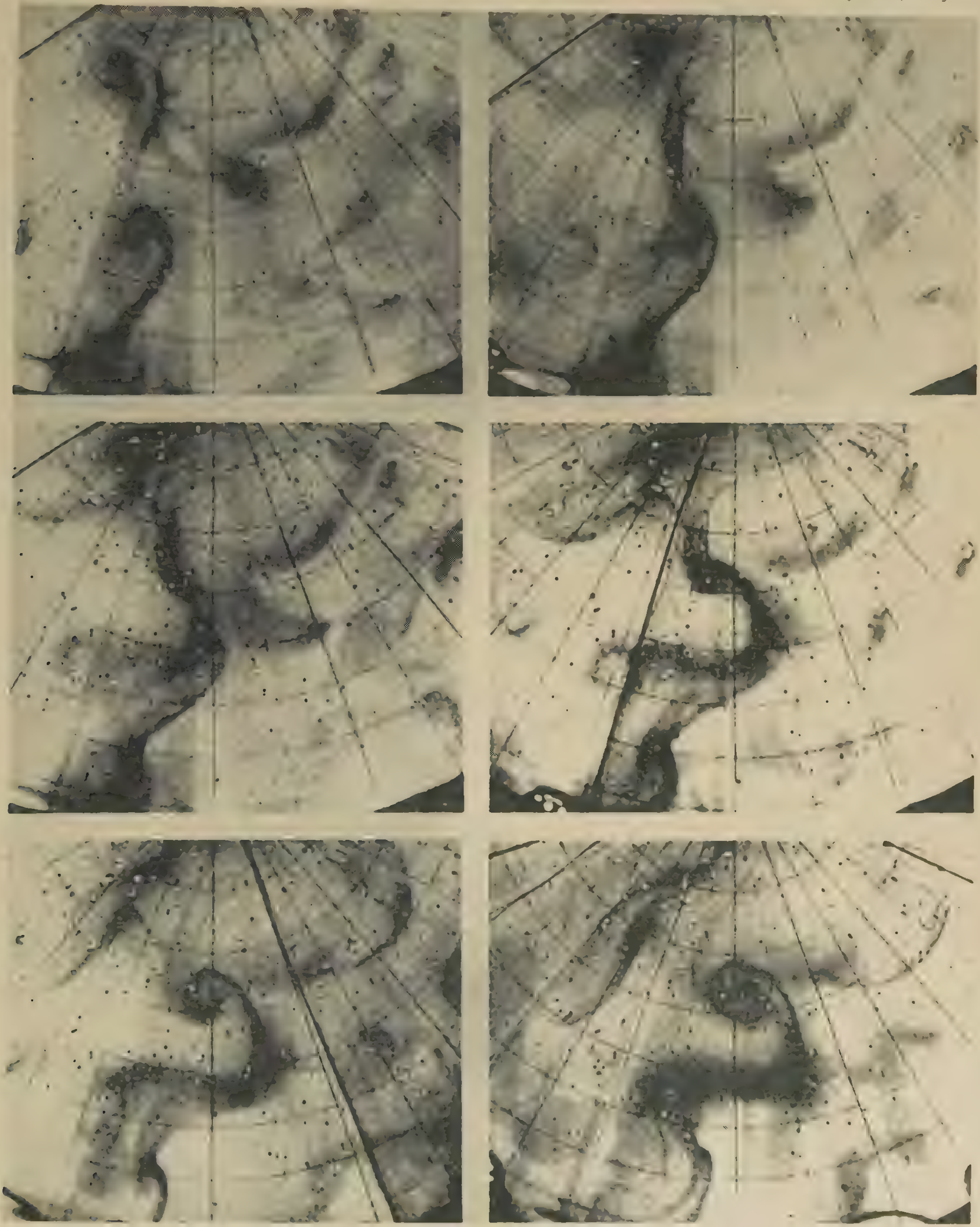

FIG. 4. Example of development of wave cyclones and movement of fronts. Read from top left to top right to center left *etc.*

detected in the upper left and upper right of each photograph.

To establish the presence of thermal contrast at the fronts indicated by the dye, a line of stationary thermocouples was immersed $\frac{1}{2}$ cm beneath the free surface from the center to the rim of the cylinder. In one revolution, each thermocouple, therefore, described a complete circle at its particular radius, and the overall thermal pattern was revealed. Despite the time lag inherent in the thermocouples and recording system, and the rapid movement of the thermocouples through the water, very sharp temperature changes associated with the dye fronts were evident.

4. Conclusions

One may note certain dissimilarities between the configurations of fronts as indicated in the model and those found on weather charts. In view of the simplicity of the apparatus, these discrepancies are not surprising; rather, the similarity is considered to be remarkable. A sufficient condition for the generation of fronts which bear marked resemblences to those envisioned in the atmosphere seems to be a proper combination of the rotation rate and the meridional temperature gradient. Since the meridional temperature gradient is related to the velocities, this condition of similarity may be attained by requiring equality in the model and in the prototype of the non-dimensional ratio $v/rf = \mathrm{Ro}$ (the Rossby number, see Fultz, 1951a), where v is a representative velocity, r a representative length, and f is the Coriolis parameter. For the model, using values of $v = 1$ cm/sec, $f = 2 \times 0.140\ \mathrm{sec}^{-1}$, and $r = 122$ cm (the radius of the model), one obtains $\mathrm{Ro} = 0.003$. For the atmosphere, using $f = 10^{-4}\ \mathrm{sec}^{-1}$ ($2\omega \sin \varphi$ at $\varphi = 45°$), $r = 6400$ km (the radius of the earth), and a velocity of 50 m/sec, one finds $\mathrm{Ro} = 0.008$. In view of the lack of geometric similarity and the indefinite specification of a representative velocity, the similarity in this respect is satisfactory.

The exact manner of production of the meridional temperature gradient does not appear to affect the qualitative results appreciably. Although in the apparatus a large fraction of the applied radiant energy was absorbed in the top layers of the water (50 per cent in the top 2 mm, 27 per cent in the remainder of the 3 cm, and 23 per cent transmitted to the bottom), similar circulation was obtained in other apparatus when heated from below. In addition, substantially the same results were obtained by using either the heat source near the rim or the cooling mechanism near the pole alone, except that in those cases a steady-state mean temperature distribution could not easily be obtained.

It is evident, however, that to attempt a model more similar in detail it would be necessary to pay strict attention to the distribution of heating, and disturbing influences such as evaporation from the free surface would have to be eliminated or kept under control.

A more complete analysis of the results of these experiments is not warranted at the present time. However, the results demonstrate that complete frontal systems may be produced in models and suggest that much may be learned from experiments concerning their atmospheric counterparts. Indeed, they suggest that the similarity of laboratory models is not confined to the larger-scale circulation.

Acknowledgment.—The writer is indebted to the Woods Hole Oceanographic Institution, and in particular to Mr. William Von Arx, for permission to use the facilities available at that laboratory.

REFERENCES

Fultz, D., 1951a: Non-dimensional equations and modeling criteria for the atmosphere. *J. Meteor.*, **8**, 262–267.

——, 1951b: Experimental analogies to atmospheric motions. *Compendium Meteor.*, Boston, Amer. meteor. Soc., 1235–1248.

——, 1952: On the possibility of experimental models of the polar-front wave. *J. Meteor.*, **9**, 379–384.

Von Arx, W. S., 1952: A laboratory study of the wind-driven ocean circulation. *Tellus*, **4**, 311–319.

Contribution No. 764

Reprinted from Biological Bulletin, Vol. 110, No. 2, 157–168, April, 1956
Printed in U. S. A.

THE PHYTOPLANKTON OF GREAT POND, MASSACHUSETTS[1]

E. M. HULBURT

Hydrographic Office, Navy Department, Washington, D. C.

Although the plankton flora of moderately deep estuaries has been studied to some degree (Braarud and Bursa, 1939; Cowles, 1930; Gran and Braarud, 1935; Lohmann, 1908; Morse, 1947) very little quantitative study of phytoplankton in very shallow estuaries has been done. Several investigators in Belgium and Holland (Conrad, 1926a, 1926b; Massart, 1920; Van Goor, 1925a, 1925b, 1925c) have studied taxonomically the phytoplankton of very shoal estuaries. The forms they describe are almost entirely flagellates. It would be of great interest to learn whether these taxonomic studies indicate a distinctly different flora composed primarily of flagellates or whether diatoms, as well as flagellates, thrive in very shallow estuaries. Further, in the event that flagellates should dominate in shoal estuaries, it would be of interest to characterize the conditions associated with their dominance.

The Embayment Investigated

Figure 1 shows the form and depth of Great Pond. A narrow gut admits water from Vineyard Sound at one end and a small river, the Coonamessett, empties at the other end. It is divided into a wider seaward portion, the main pond, and a narrower landward portion, the arm. Its depth is nowhere greater than 9 feet at highest high tide. The hydrography of the Pond has been well studied by Barlow (in press), but a few of the salient features are reviewed here. The mean salinity indicates that the Pond water is 83 parts sea water and 17 parts river water. Surface salinity decreases from 32‰ in the Sound to 1–2‰ near the mouth of the River. Bottom salinity decreases from 32‰ to 24‰ near the mouth of the River, indicating marked stratification in the arm. The effect of wind blowing toward the Sound is to move the surface water seaward, resulting in upwelling of deep water and increase of surface salinities to 24‰ or above all the way to the River.

Water samples were taken at the stations indicated in Figure 1 from the shore in February and March and from a rowboat during the rest of the year. Samples were taken within several inches of the surface and approximately ten inches from the bottom. Phytoplankton cell counts and phosphate, turbidity, and salinity determinations were made on each sample.

Methods

Cell counts were made from four to forty-eight hours after samples were collected. Cell concentrations were determined by counting living cells in a very shallow chamber, so that a high power microscope objective could be used. Usually the water sample was concentrated on a smooth-surfaced porcelain filter with a pore

---

[1] Contribution No. 764 from the Woods Hole Oceanographic Institution.

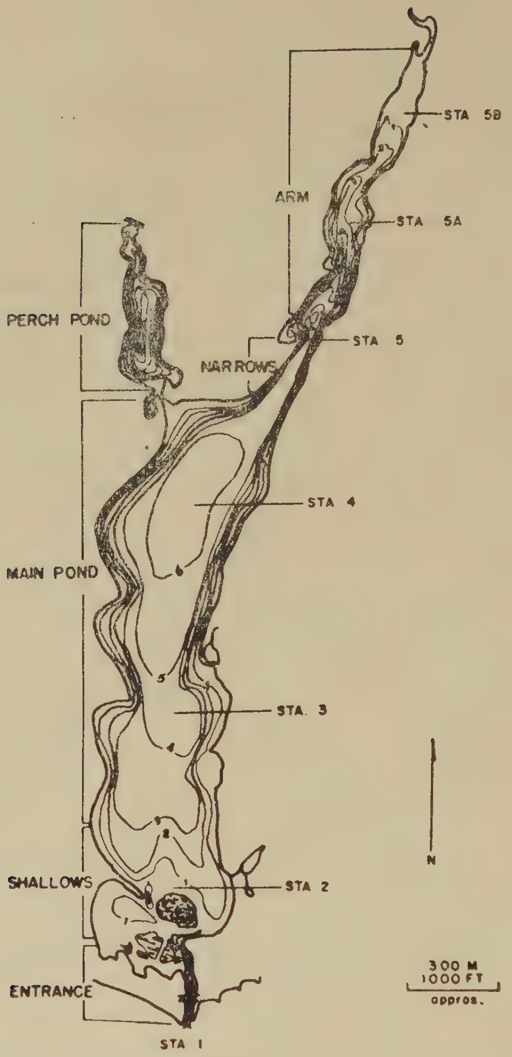
STA 5B
ARM
STA 5A
PERCH POND
STA 5
NARROWS
STA 4
MAIN POND
6
5
STA. 3
4
2
SHALLOWS
STA 2
1
ENTRANCE
STA 1
N
300 M
1000 FT
approx.

Figure 1. The morphometry of Great Pond. Depths are in feet.

diameter of 0.5 μ, manufactured by the Selas Corporation. Occasionally counts were made without filtration. Comparison of filtered and unfiltered counts showed that a large proportion of the cells was lost in filtration. Therefore, all filtered counts were multiplied by 1.81 to give the true concentration of cells in the water. All cells from 2–3 μ in diameter to about 50 μ in diameter were counted.

Results

Figure 2 shows the distribution of total phytoplankton. In the surface waters greater concentrations occurred within the Pond, and this difference was greater

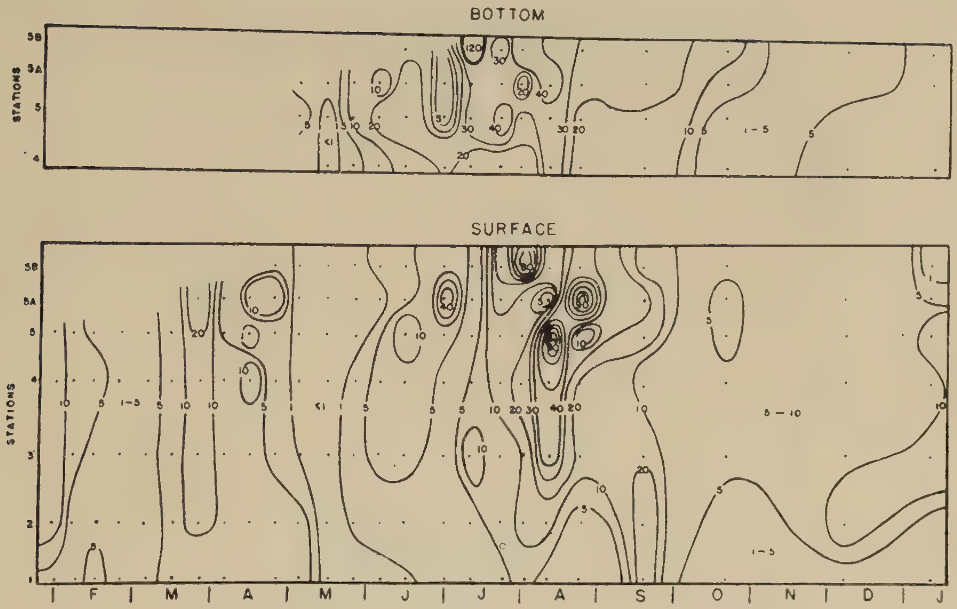

FIGURE 2. The distribution of total phytoplankton. Values × 10⁶ are numbers of cells per liter.

during the summer than during the rest of the year. In summer there was, at a maximum, a 20-fold increase from the Sound to the surface waters of the arm. Between mid-September and the end of May, by contrast, the greatest increase from Sound to Pond was four-fold. The highest concentration in the surface waters, over 90,000,000 cells per liter, occurred in the summer at Station 5, well up the Pond. It is noteworthy that much greater fluctuations in cell concentrations occurred during summer than during the rest of the year. This feature was particu-

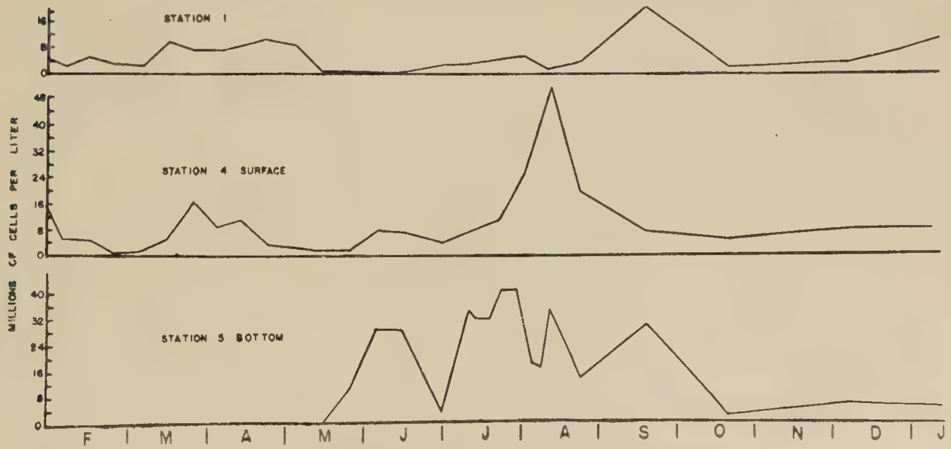

FIGURE 3. The seasonal cycle of total phytoplankton.

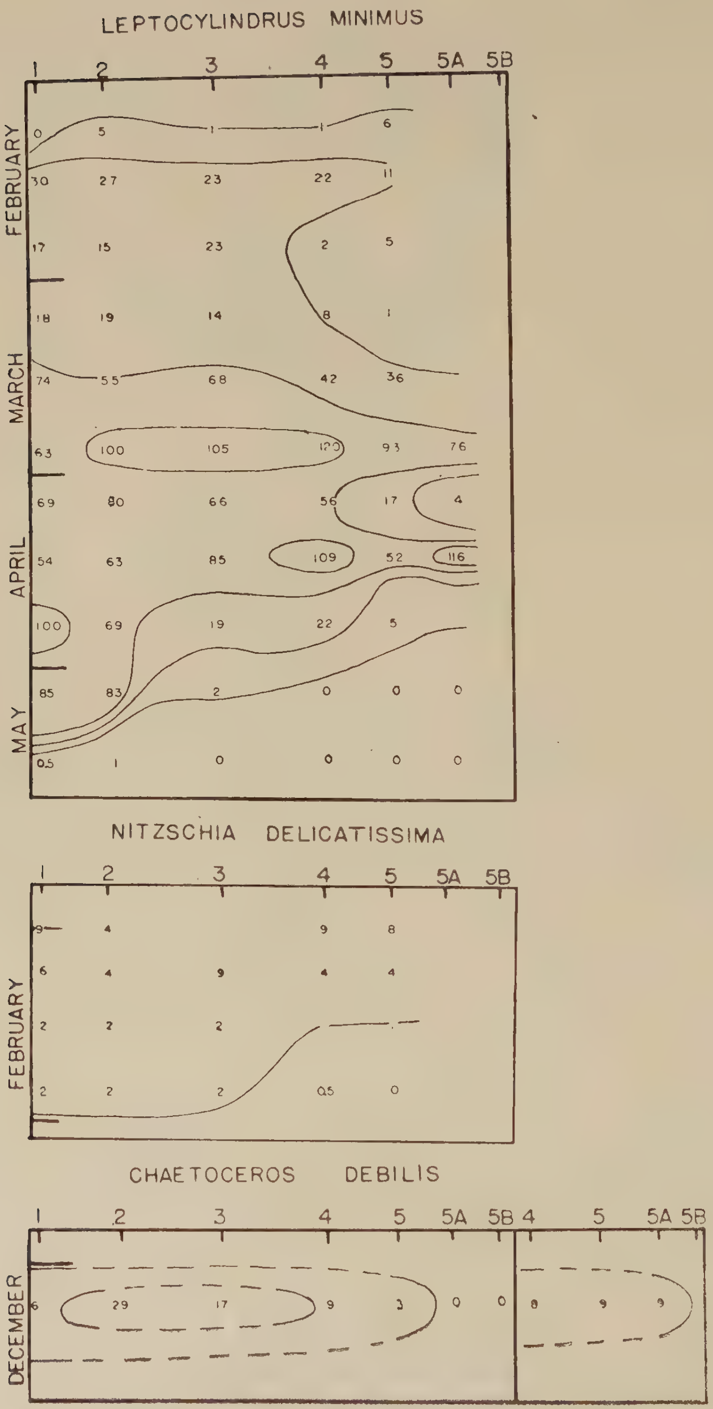

FIGURE 4. The distribution of Sound-derived species. Values × 10^5 are numbers of cells per liter. Station numbers, 1–5b, cross the figure.

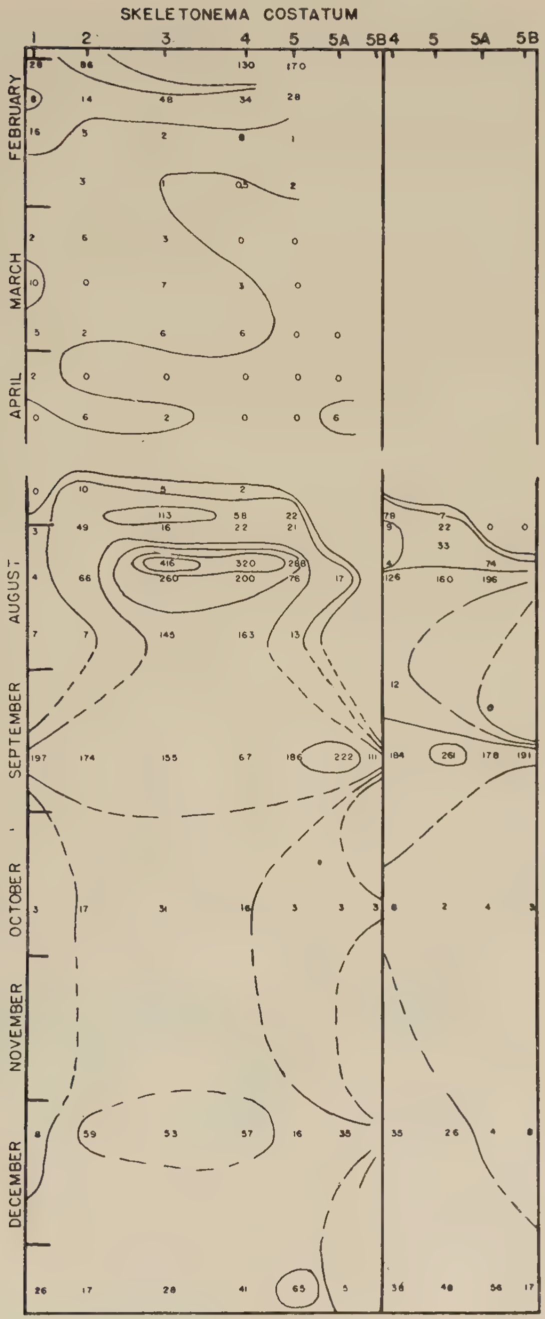

Figure 5. The distribution of *Skeletonema costatum.* Values × 10^5 are numbers of cells per liter. Station numbers, 1–5b, cross the figure.

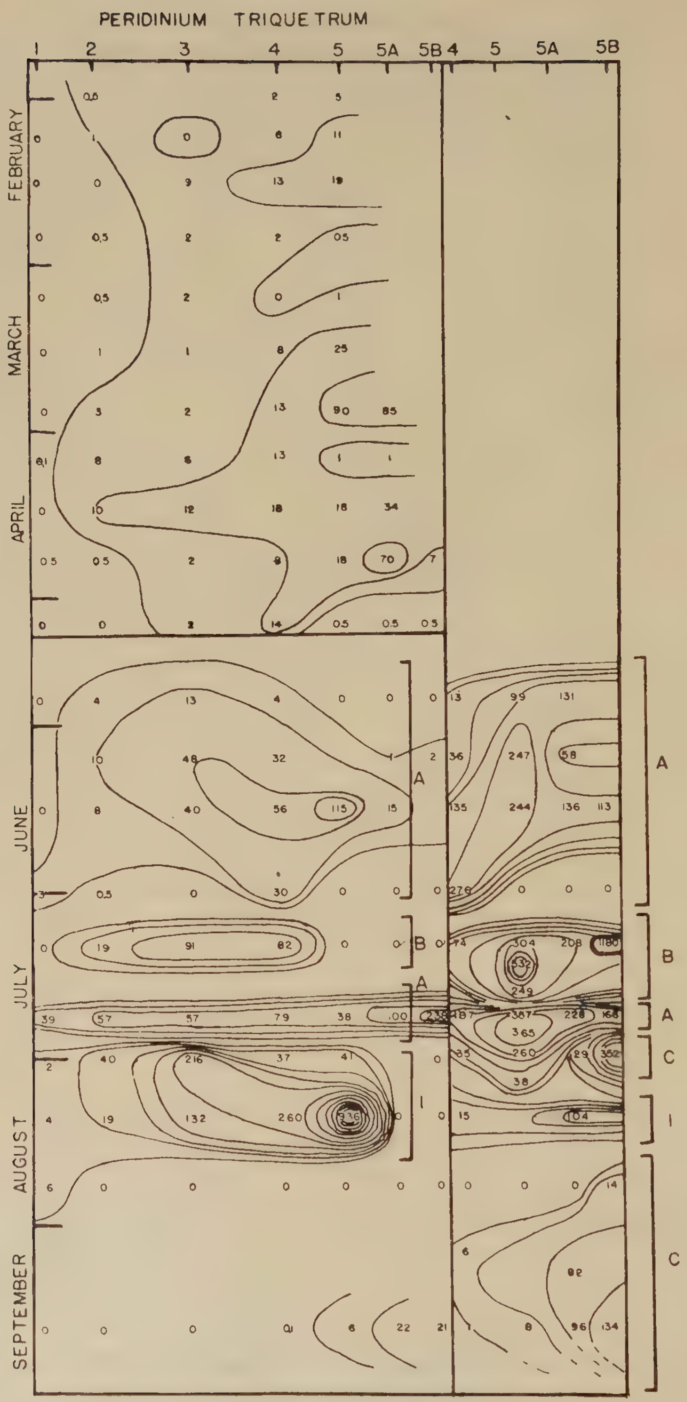
PERIDINIUM TRIQUETRUM
1
2
3
4
5
5A
5B
4
5
5A
5B
FEBRUARY
MARCH
APRIL
JUNE
JULY
AUGUST
SEPTEMBER
A
B
A
C
I
C

FIGURE 6.

larly noticeable in the surface waters of the arm, where isolated pools of high concentrations occurred on June 30 and on August 1, 11, and 23.

Cell concentrations along the bottom were, in a gross way, similar to those at the surface, being greater in summer than in fall or winter. However, with the exception of a brief period at the beginning of July, cell concentrations remained at high levels throughout the summer. The highest concentration observed, 120, 000,000 cells per liter, was at Station 5b, far from the Sound.

Seasonal cycles for several stations are shown in Figure 3. In the Sound there was a bimodal cycle, with moderate concentrations in late winter and spring and high concentrations in early fall. The surface waters of mid-pond showed a bimodal curve, also, with roughly the same concentrations in late winter and spring, as in the Sound, but, unlike the Sound, with very high concentrations in later summer. Deep water at mid-pond had high concentrations throughout summer and September and moderate concentrations in fall and winter. Sound and Pond both showed lowest concentrations at the end of May.

Figure 4 shows the distributions of three species of diatoms, *Leptocylindrus minimus, Nitzschia delicatissima,* and *Chaetoceros debilis.* These were observed only during the cooler months and were found to extend from the Sound far into the Pond. *Leptocylindrus minimus* showed a relatively uniform distribution in the Sound and seaward portion of the Pond. Though concentrations were occasionally somewhat greater in the Pond than in the Sound, they never showed a variation that was more than two-fold. In the surface waters of the arm concentrations were about the same as those in the seaward portion of the Pond on days of upwelling, March 26 and April 15, but were much lower on a normal day, April 5, when no upwelling occurred. In the Sound and main pond *Leptocylindrus minimus* increased rapidly to become the dominant species by February 15, attained a maximum on March 25, and decreased abruptly early in May. *Nitzschia delicatissima* showed a similar distribution to *Leptocylindrus minimus* during February. Its concentrations were about one-tenth those of *Leptocylindrus minimus. Chaetoceros debilis* resembled *Leptocylindrus* in distribution.

Skeletonema costatum, the distribution of which is shown in Figure 5, was the only species of diatom that was present during summer as well as during the rest of the year. At times it exhibited a uniform distribution from the Sound far into the Pond, as on September 18, January 10 and February 25. At various other times it was more abundant in the Pond than in the Sound, the variation being eight-fold on October 20, December 7 and January 30 and as high as one hundred-fold in August. During fall and winter it was the dominant species, attaining a maximum on September 18. In February it declined as *Leptocylindrus minimus* became the dominant species. Although *Skeletonema* was not clearly a dominant organism in August, it reached its greatest concentration at that time.

In spring the dinophycean *Peridinium triquetrum* rose to considerable prominence (see Figure 6), its concentrations being as high as one-fifth of those of *Leptocylindrus* on April 15. It was more abundant within the Pond than in the Sound. There was a hundred-fold increase from the Sound to the mid-reaches of

FIGURE 6. The distribution of Pond-derived species. Values × 10^5 are numbers of cells per liter. Station numbers, 1–5b, cross the figure. A represents undetermined chrysophycean, B *Bipedinomonas pyriformis,* C *Nephrochloris salina,* and I *Chaetoceros simplex.*

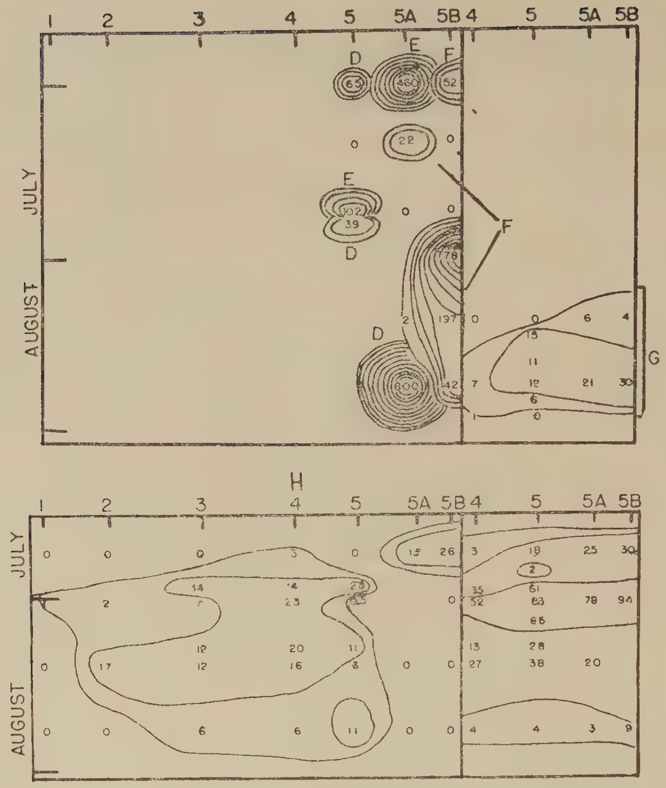

THALASSIOSIRA NANA

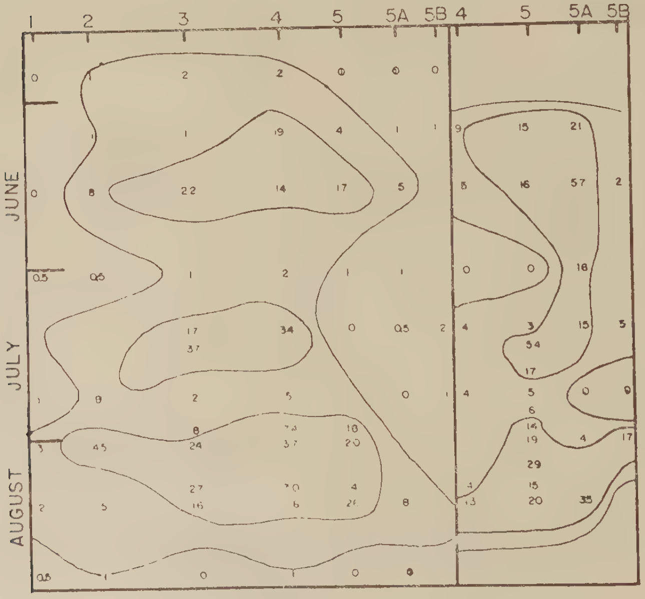

FIGURE 7.

the Pond on March 26. This difference was greater than any observed for the four diatoms so far described in the period between mid-September and the end of May.

Figure 6 shows the distributions of several species found primarily in summer. They were always far more abundant in the Pond than in the Sound. During June the dominant species was an undetermined chrysophycean flagellate. Its numbers were usually greater along the bottom than at the surface. The surface waters at the ends of the Pond had smaller concentrations than the waters of mid-pond, the difference being as much as one hundred-fold. Only in mid-pond did concentrations approach those along the bottom. Abrupt decrease of the chrysophycean was followed in early July by a growth of the flagellate *Bipedinomonas pyriformis*. Its distribution was identical to that of the chrysophycean. By late July *Bipedinomonas* had disappeared completely and the undetermined chrysophycean flagellate was dominant again throughout the Pond. On July 22 the chrysophycean showed an exceptional abundance at the surface of the arm due to upwelling. In August the small diatom *Chaetoceros simplex* became extremely abundant, more so in the surface waters of mid-pond than in the deeper water. On August 11 it showed a two hundred-fold difference between Sound and Station 5. The flagellate *Nephrochloris salina* was moderately abundant in August and September in bottom water at the extreme landward end of the Pond.

Figure 7 shows the distributions of several less important species of summer. The flagellate *Gyrodinium estuariale* and the minute diatom *Thalassiosira nana* exhibited the same type of distribution as described for the undetermined chrysophycean. In the surface waters of the arm contours are close-packed around the flagellate *Chlamydomonas* in the surface waters at the outlet of the river and around the flagellates, *Massartia rotundata* and *Rhodomonas minuta,* farther down the arm. The growth of these species was sporadic and attained very great concentrations. It is noteworthy that when these species grew in the surface waters, no traces of the species were found in the bottom water only five or six feet below.

DISCUSSION

The species can be divided into Sound-, Pond-, and River-derived types. The Sound-derived type was abundant in the Sound and Pond alike. The Pond-derived type was abundant only in the Pond, particularly in the inner reaches and along the bottom. The river type was found primarily in the surface water at the outlet of the River. The two principal Sound-type species were the diatoms *Leptocylindrus minimus* and *Skeletonema costatum*. *Nitzschia delicatissima* and *Chaetoceros debilis* represented well-defined Sound types, but were of minor importance. Principal Pond types were the undetermined chrysophycean flagellate; the heterokontan flagellate *Nephrochloris salina;* the chlorophycean flagellate *Bipedinomonas pyriformis;* the dinophycean flagellates *Peridinium triquetrum, Massartia rotundata,* and *Gyrodinium estuariale;* the cryptophycean flagellate *Rhodomonas minuta;* and the diatoms *Chaetoceros simplex* and *Thalassiosira nana.* The River type was repre-

FIGURE 7. The distribution of Pond- and River-derived species. Values × 10^5 are numbers of cells per liter. Station numbers, 1–5b, cross the figure. D represents *Massartia rotunda,* E *Rhodomonas minuta,* F *Chlamydomonas* sp., G *Gyrodinium dominans,* and H *Gyrodinium estuariale.*

sented by chlorophycean flagellates, consisting of two unidentified species of *Chlamydomonas*.

The Sound-derived species thrived during fall, winter, and spring primarily and in summer to a small degree. The Pond-derived species flourished in summer primarily and in spring to a small degree. All of the Sound-derived forms were non-motile; the majority of the Pond-derived forms were motile.

During the fall, winter, and spring the water of the Sound, which fills 83% of the Pond at any time, carried its plankton far into the Pond. Within the estuary changes in this plankton were slight or negligible, indicated by the small difference in total plankton between Sound and Pond, by the change from dominance of *Skeletonema* to *Leptocylindrus* simultaneous in Sound and Pond, and finally by the intrusion of Sound species far into the Pond. During summer the Sound water carried with it little plankton, and once within the estuary the identity of this plankton was lost to a large degree. Plankton from the River could be identified only in the surface waters where the River emptied into the Pond. Throughout the greater portion of the Pond an indigenous plankton flourished.

TABLE I

Concentrations of diatoms and flagellates and statistics of physical features along the length of Great Pond

	Diatoms $\times 10^4$/1	Flagellates $\times 10^4$/1	Six-hour mean tidal velocity, knots	Salinity difference between surface and bottom, $^0/_{00}$
Sound	34	43	1.60	—
Mid-Pond, Station 4	633	598	0.01	6.38
Arm, Station 5a	319	1492	0.02	17.90

During the transport of water through the Pond, rapid changes in the plankton occurred in summer, as indicated by the abrupt changes in dominant species from place to place on the same survey. In the surface waters of the arm such changes caused large fluctuations in total phytoplankton. These changes indicate a rapid growth rate. During the remainder of the year abrupt changes in dominant species and extreme variations in total phytoplankton did not occur and hence growth rates were less than in summer. Thus, when conditions for growth in the Pond were good, Pond species rather than Sound species flourished. When growth conditions were less favorable, during the cool months, the plankton of the Sound drifted into the Pond, replacing the endemic flora that had previously flourished.

It has been pointed out that during summer the dominant members of the plankton included seven flagellates and three diatoms. In order to account for the preponderance of motile forms within the Pond, its association with low current velocities and great vertical stability of the water will be investigated. Averages of the dominant species as flagellates or diatoms are given for various stations in Table I. Surface and bottom values are averaged for stations 4 and 5a. Current velocities were taken from surface current measurements for Vineyard Sound one mile south of Great Pond (U. S. Coast and Geodetic Survey, 1949) and were computed for Great Pond by dividing the intertidal volume landward of a station by the cross-sectional area at the station. Surface current measurements may be higher than computed currents estimates by as much as 50% (Riley, 1952). The salinity difference between surface and bottom was the average difference of all observations during summer. Both diatoms and flagellates increased from the Sound to mid-pond, but flagellates increased at the expense of the diatoms from mid-pond to the headwaters. Tidal currents were much less from mid-pond to headwaters than in the Sound; while the vertical salinity gradient became progressively greater up-pond.

The moderate success of the motile cell from Sound to mid-pond can be attributed to a decrease in vertical turbulence, as a result of lessened tidal current. The greater success from mid-pond to the headwaters can be attributed to further decrease in turbulence, as a result of both weak currents and marked stability. Settling out of non-motile cells in the quiet waters of the Pond, particularly the arm, would place the motile cell at an advantage. In addition, cells destined to settle out would have less time to divide and replace the stock in the shallow waters of the Pond than in the deep waters of the Sound, so that the motile cell would be at a still greater advantage in the Pond. Thus, when growth conditions favor an endemic flora, the quietness and shoalness of the Pond water should favor motility as a characteristic of the flora.

The Pond flora may have been better adapted than the Sound flora to lowered salinity, high temperature, or nutrient products of the intermediate metabolism of the pond water. Adaptations of these sorts may have been effective in favoring the successive blooms of different species and in fostering the occasional dominance of non-motile forms.

In conclusion, the summer conditions at Great Pond furnish an example of the dominance of flagellates rather than diatoms in the phytoplankton. This dominance appears to result in part from a coupling of good growth conditions, which foster an endemic flora, with a quiet, very shallow habitat, which should favor the non-settling, motile cell.

The author wishes to express the greatest gratitude to Dr. A. C. Redfield and to Dr. W. R. Taylor for their help during this study. The best of thanks go to Dr. John Barlow, for use of salinity data and help in collecting samples, and to Mr. Harry Turner, for use of the chart of Great Pond prepared by him.

Summary

1. Determinations of phytoplankton concentrations were made throughout 1950 in Great Pond, a small estuary near Falmouth, Massachusetts.

2. Greater concentrations occurred within Great Pond than in the ocean water at its entrance. This difference was greatest in summer.

3. During fall, winter, and spring the same species populated the waters of the ocean and the Pond, but during the summer an assemblage of species flourished within the Pond that was never found in the ocean water and was not characteristic of the river water.

4. The Pond-derived flora of summer contained a large proportion of flagellates, whereas the Sound-derived flora was composed completely of diatoms.

5. The preponderance of motile forms within the Pond during summer was attributed to good growth conditions, which stimulated an endemic flora, and to shoal, quiet water, which should favor the non-settling type of cell.

LITERATURE CITED

Barlow, J. The hydrography of Great Pond, a tidal estuary. *J. Mar. Res.*, in press.

Braarud, T., and A. Bursa, 1939. The phytoplankton of the Oslo fjord, 1933–1934. *Det. Norske Vid. -Akad. i. Oslo, Hval. Scri.*, **19**: 1–63.

Conrad, W., 1926a. Recherches sur les Flagellates de nos eaux saumâtres. Ie partie, Dinoflagellates. *Arch. f. Protist.*, **55**: 63–100.

Conrad, W., 1926b. Recherches sur les Flagellates de nos eaux saumâtres. 2° partie, Chrysomonadines. *Arch. f. Protist.*, **56**: 167–231.

Cowles, R. P., 1930. A biological study of the offshore waters of Chesapeake Bay. *Bull. Bur. Fish.*, **46**: 277–381.

Gran, H. H., and T. Braarud, 1935. A quantitative study of the phytoplankton in the Bay of Fundy and the Gulf of Maine (including observations on hydrography, chemistry and turbidity). *J. Biol. Bd. Canada,* **1** (5) : 279–467.

Lohmann, H., 1908. Untersuchungen zur Feststellung des vollständigen Gehaltes des Meeres an Plankton. *Wiss. Meeresunters. Abt. Kiel. N. F.*, **10**: 129–370.

Massart, J., 1920. Recherches sur les organismes inférieurs, VIII. Sur la motilité des Flagellates. *Bull. Acad. Roy. Belgique, Cl. de Sc., 5^{me}. Sér.* **6** (4–5) : 116–141.

Morse, D. C., 1947. Some observations on seasonal variations in plankton population, Patuxent River, Maryland, 1943–1945. State of Maryland Board of Natural Resources. Pub. No. 65: 1–31.

Riley, G. A., 1952. Hydrography of the Long Island and Block Island Sounds. *Bull. Bingham Oceano. Coll.*, **13** (3) : 5–39.

U. S. Coast and Geodetic Survey, 1949. Tidal Current Charts, Narragansett Bay to Nantucket Sound. Serial No. 628. Washington, D. C.

Van Goor, A. C. J., 1925a. Einige bemerkenswerte Peridineen des holländischen Brackwassers. *Rec. Trav. Bot. Néerl.*, **22**: 275–291.

Van Goor, A. C. J., 1925b. Die Euglenineae des holländischen Brachwassers mit besonderer Berücksichtigung ihrer Chromatophoren. *Rec. Trav. Bot. Néerl.*, **22**: 292–314.

Van Goor, A. C. J., 1925c. Über einige bemerkenswerte Flagellaten der holländischen Gewasser. *Rec. Trav. Bot. Néerl.*, **22**: 315–319.

Contribution No. 765

RECENT ADVANCES IN OUR UNDERSTANDING OF THE CIRCULATION PROBLEM AND THEIR IMPLICATIONS[1]

By

C. O'D. ISELIN
Woods Hole Oceanographic Institution
Woods Hole, Massachusetts

When I was first asked to prepare a paper for this program, although it was obviously an honor, I hesitated to accept, for it seemed to me doubtful that a regular staff member of the Woods Hole Oceanographic Institution should be asked to express his views. After all, one of the chief purposes of this Convocation was to gain the benefit of your collective advice as to future scientific policy. The occasion of the dedication of the new laboratory was to be used to give us a new start and some encouragement to embark on novel, and perhaps more fruitful, directions. For nearly 25 years I have been intimately associated with our efforts to advance the circulation problem. I have written or helped to write many annual reports. What could I possibly say here that would be new or helpful to the main purpose of these meetings?

However, after considerable hesitation I came around to the idea that at least one paper in this series might well review the factors on which our present program is based and might try to set forth our plans and expectations for the future. If we are to gain the benefit of sound advice, those who have been asked to help us should at least know what we now think the problems are and how, until now, we have been planning to meet them.

Under the term circulation problem I include a wide variety of phenomena, both large scale and small scale. It has been emphasized many times that the movements of the water constitute the central theme in oceanography and that we are justified in considering this as a separate and somewhat specialized field of science. Few aspects of oceanography can be successfully divorced from the consequences of water movements, either the slow ones or the swift ones.

In 1931, when the ATLANTIS became available for full time operation, the underlying reasoning of the geostrophic equation was just becoming generally understood. It seemed that here at last

---

[1] Contribution No. 765 from the Woods Hole Oceanographic Institution.

Reprint from SEARS FOUND. JOURN. MAR. RES.

was a way to make physical oceanography three dimensional and at the same time put it more nearly on a synoptic basis. When our field work was planned, our first idea was to follow the highly successful lead of the International Ice Patrol Service and compute water movements from networks of discrete observations of temperature and salinity. If we could only occupy a large enough number of hydrographic stations, we could then solve for the water movements over a considerable area. In those days the circulation problem seemed just a matter of patience, hard work at sea, and arithmetic. Because the Gulf Stream was near at hand and because it was obviously a major factor in the circulation of the North Atlantic, we began collecting temperature and salinity profiles across this exceptionally swift current when the ATLANTIS was ready. We had little comprehension of the magnitude of the task and of the limitations of the then available observational techniques.

The first few Gulf Stream profiles seemed to agree rather well with the simplifying assumptions of the geostrophic equation. Computed surface velocities on the whole agreed with available navigational experience, but even after several years of sailing back and forth across the Gulf Stream we had gained little comprehension of how crude our navigation was. The interpolation between the points of observation of temperature and salinity smoothed out the picture of the current system to about the same degree as the necessary averaging of the surface current, as observed by celestial navigation. In neither case were we able to see any of the fine-scale structure that today makes the circulation problem seem so much more complex.

It is amusing to note that in 1934, after about three years' work in deep water in the western North Atlantic, we considered that the ATLANTIS had gathered enough data on the Gulf Stream System and that we should resume systematic surveys of the Gulf of Maine, where the interests of biologists were traditionally centered. It was a rude shock when, after nearly two years of monthly surveys of the Gulf of Maine area, the physical oceanographers here could not even write one paper that added anything of significance to what Dr. Bigelow had worked out on the basis of much less systematic and more widely spaced observations. Although we came to realize in this way that the circulation problem in shallow water is an extremely difficult one, we still thought that in deep water the movements were broad and relatively steady and that they could be generally explained on the basis of the then available theory.

Thus, in 1937, the ATLANTIS returned to making Gulf Stream profiles, this time on the line between Montauk Point and Bermuda. Internal waves became somewhat of a worry, but if enough stations were occupied these could be smoothed out. We began to encounter more and more "eddies" on either side of the Gulf Stream. Usually these involved transports equivalent to the Gulf Stream, but sometimes they were considerably weaker. Where do eddies leave off and internal waves begin? This became the doubt which indicated that all was not well.

At this point World War II intervened, and for four or five years the circulation problem was neglected. On the other hand, during the war years we acquired several new techniques, but, perhaps more important, we attracted some new people. As most of you know, after the war, under the leadership of Mr. F. C. Fuglister, an entirely new approach to the problems of the Gulf Stream System was developed. By exploiting the capabilities of the bathythermograph and of Loran navigation it became possible to gain measurements of the surface velocity and at the same time observe approximately the temperature distribution in three dimensions, at least down to moderate depths. At once the Gulf Stream became surprisingly narrow and swift. The theoreticians, led by Mr. Henry Stommel, quickly advanced a plausible explanation. The effects of the change of the Coriolis force with latitude were for the first time included in the theory. But after a year or so of further field work to the eastward, it became evident that the currents were not only narrow and streaky in the west, where they have a northward component, but that they also retain these characteristics in flowing from west to east.

It soon became evident also that for the type of survey so successfully initiated by Mr. Fuglister a single ship was inadequate. To gain a picture of the large scale pattern of the Gulf Stream System, several vessels should be used simultaneously. Operation Cabot was organized and that more or less terminated a stage in our thinking. It is the nearest approach to synoptic deep sea oceanography that has yet been attempted, but it is now abundantly clear that even six ships are too few to gain a clear picture of a phenomenon as large as the Gulf Stream.

In retrospect, Operation Cabot had some other serious deficiencies. It was planned with a preconceived idea of what would be encountered. It concentrated on what might be called "Gulf Stream Number One," and only one of the ships obtained a few observations in the overlapping "jetlet." From this and other experiences, Fuglister's multiple current hypothesis was born. It would require a survey considerably more elaborate and extensive than Operation Cabot to demonstrate conclusively the existence of the sort of current system that he has postulated. A major question today is whether or not such a survey should soon be attempted. If so, are we ready for it and should we again survey a considerable area of the Gulf Stream System or should we focus attention on some other major current? After all, the Gulf Stream may turn out to be a special case. There is growing evidence that the North Atlantic is not a typical ocean. The reconnaissance phase of North Atlantic physical oceanography can be considered completed. Should we continue to study these relatively well explored currents or should we turn our attention to a contrasting region?

Opportunities for multi-ship surveys will not come frequently. We should plan the next one with the greatest of care. Were precise navigation available, there would be little doubt in my mind that the next major effort should be in the Antarctic Circumpolar Current, for I believe that the so-called convergences are nothing more than overlapping jet streams. Yet, without something comparable to Loran navigation, a co-operative survey in southern latitudes might fail. Nevertheless, this is surely the only ocean current system that is relatively free of continental boundaries.

Since Operation Cabot, we have been casting about for new techniques that would be helpful in gaining a better understanding of Gulf Stream phenomena and we have also had a good look at the currents in the trade wind latitudes. I will elaborate on some of the new techniques, but the best that can be said of our efforts in low latitudes during 1952 and 1953 is that they were inconclusive. For lack of precise navigation, the surveys were too open to yield a unique solution. Mr. Fuglister's principle that the current always appears to follow the ship was once again in operation. How to contour temperature data gained in the course of widespread surveys is still a major problem in physical oceanography. The most direct and simple solution to the contouring problem may yield most misleading results, as he showed recently.

Several years ago Dr. Willem Malkus made a direct attack on the old problem of how velocity varies with depth. How deep is the Gulf Stream and how does the velocity profile change in the downstream direction and how does it differ in landward and seaward meanders? He has evolved a variety of devices which we call bathypitotmeters. The development stage has just about been completed. New tactics have evolved, and the first cruise using these new techniques has just terminated.

It is too early to predict what will come out of these new methods, but at least it can be said that they should help to fill a long felt need. Dr. Malkus has set himself the problem of observing how the velocity structure in a given water mass changes with time. He simply drifts with the current, observing the crosscurrent components, the path of the axis of the current, and the velocity-depth changes. For the remainder of this summer we plan to monitor the Gulf Stream almost continuously in these and other ways. What happens to the end of the current after a meander has broken off? How long does the resulting eddy persist? These are critical questions and I do not see how to proceed until they are answered.

Meanwhile, the hope that a plane can monitor the broad synoptic situation while a ship examines a limited part of it in three dimensions is being partially realized. Dr. William S. Richardson has greatly improved the radiation thermometer, first devised by Stommel and Parsons. He has flown it many miles, and what he sees of the temperature pattern of the sea surface adds greatly to our present difficulties. While the ships have shown that the Gulf Stream is discontinuous on a large scale, the plane seems to indicate that, at the surface at least, it is also discontinuous on a small scale.

As most of you know, a few years ago Mr. W. S. von Arx took a new and radical tack. Our vessels are confronted with the difficulty that the ocean is too big. He proposed to make a small one. He started very small indeed, for his first model was no larger than a good sized salad bowl. He is now planning one 24 feet in diameter. It would be feasible to operate a model 100 feet or so in diameter and still spend less money than that consumed by a single vessel. There is little doubt today that model techniques in the earth sciences are embarking on a rapid development. The model integrates much more easily and more cheaply than electronic computors, and it is much more fun to watch.

The future of the circulation problem would be bright were it not for the uncertainty that all important factors operating in the prototype could be included in a reasonably sized model. If the model has to be 100 yards in diameter rather than 100 feet, then we are out of luck. Meanwhile, the model technique will clearly be helpful to the development of somewhat simplified theories of oceanic circulation, and it should also show the critical areas in the southern hemisphere where field observations should be concentrated.

It is my belief that the model technique constitutes an essential link between field observations and theory. Only by using all three approaches simultaneously and wisely are we likely to succeed.

Now, what can be said about the future of theories? We have some very good and satisfactory theory that is based on the idea that the average winds over the ocean provide most of the energy necessary to maintain the horizontal currents. Theories that include the obvious major effects of seasonal production of large amounts of surface water of different densities are just being born. Theories that can deal simultaneously with thermo-haline processes and a variable wind field have yet to be devised, although it is clear that in the ocean we have currents that range all the way from pure wind currents to currents deriving all of their energy from density differences. Most currents appear to be of an intermediate character, and it may be many years before we can assign values to the relative importance of these two causes of the circulation.

Meanwhile one very important lesson has been learned in shallow water. After the war, when interest was developing in estuarine circulation, rapid progress was made because in general a continuous record of one factor was available, namely the freshwater inflow. The analysis of the shallow water surveys had to account for the varying contribution of energy from the river. We were no longer dealing with spot observations alone. The spot observations had to be so analyzed as to transmit a measured amount of fresh water out of the estuary. Undoubtedly our deep water observations could be made to yield more convincing results if they too had to allow for some continuingly measured variable.

Several recent efforts in this direction have produced encouraging results. Mr. Wertheim's electrodes on either side of the Florida Straits presumably give a record of the energy available to the beginnings of the Gulf Stream. Changes in the initial energy should be reflected in future happenings downstream. We are dealing with a system that has both short period and gradual variations. Our attempts to analyze synoptic data must admit to this fact and should be directed so as to advance our ability to predict what will happen off New England, for example, following radical changes in the Florida Straits.

In this respect I believe we are somewhat ahead of meteorolcgy, for we have stumbled on means of getting continuous measurements of the variations in energy available to parts of the marine system. I feel that a considerable effort to gain continuous data on oceanic circulation is well justified and will yield increasingly valuable results, especially after really long records become available.

The long term approach is really the responsibility of the institution rather than of the individual researchers on its staff. Few of us have the patience to wait for accumulation of even a 10 year record. The Woods Hole Oceanographic Institution has now been in existence nearly 25 years, yet today we do not even have a continuous record of winter temperature in Woods Hole Harbor for the whole of this period.

Only recently, through Mr. Stommel's enthusiasm, has the idea of a continuing oceanographic observatory been born. No doubt he will soon turn his attention to other matters, yet it is clear that some organized effort to secure long series of data will in time pay big dividends. More of our present effort should be directed toward a selection of critical places where continuous observations will yield the most significant results and also toward methods of devising inexpensive means of recording a number of types of information simultaneously.

Too few oceanographic instruments that can obtain long continuing records comparable to those of a tide gauge ever become fully developed. The inventor, in satisfying the needs of his particular research problem, nurses the instrument so long as it is critical to his particular study and then puts it on the shelf. We have no organization at present to refine the design of such instruments and to put them to work gathering long series of data that may become of great interest to future investigators. This has been a serious deficiency in our past program and I hope that something can be done about it in the future. The idea that an oceanographic laboratory should maintain a few permanent points of observation in the ocean seems to me a sound one and it is high time that suitable equipment was developed.

To summarize: our experience indicates that it will be a long time before we are able to develop adequate synoptic pictures of the circulation pattern of considerable areas of the ocean in three dimensions. The more detailed our surveys, the more difficult the problem has become. The hope is that models can be developed that can be trusted. Our ships, supplemented by buoys and submerged recorders of various kinds, can observe what goes on at a given spot or in a given water mass as a function of time, and perhaps the model can interpolate between these few points of continuous observation. The outstanding characteristic of oceanic circulation is that it is variable over a very wide time scale. It varies significantly from week to week, from month to month, from year to year, and probably over periods of 100 years or so as Mr. L. V. Worthington has recently pointed out. Combining observations widely separated in space and time usually obscures the very factors we are trying to understand.

We still have exploratory survey work to carry out in large areas, especially in the southern hemisphere. Before this is undertaken on any considerable scale I feel that we should first develop a means of precise navigation. To survey new areas by using conventional techniques perhaps would seem satisfactory to a geographer. It would fill in areas that are now more or less blank on our charts. But so far as the circulation problem is concerned, I doubt that we would learn much that is new, except possibly through multi-ship operations. Meanwhile, awaiting a better and more universal means of navigation, I believe that we should continue to study the limited areas where Loran navigation at least is available.

When one looks back on the history of the circulation problem, advances in our understanding of a large scale phenomenon has always depended on major improvements in navigation. Maury's contributions depended on the chronometer coming into general use. He developed the climatological, two dimensional ocean that was the starting point of modern oceanography. The next hundred years were consumed in trying to understand a three dimensional, statistical ocean. Only when Loran navigation became available did we begin to appreciate the pitfalls of the averaging and interpolating procedure. We need something much better than Loran and we need to have all parts of the system under our control. If any of you doubt this statement I suggest that you spend a few hours aboard the ATLANTIS while she is tied up to the dock. You will find that Woods Hole moves in sudden and unpredictable ways as some technician at Halifax or Nantucket decides that it is advisable to alter the timing between the master and the slave station.

At present our only means of proving out either developments in theory or in models is through navigation. Until we have improved navigation by another order of magnitude we will remain in danger of confusing the average ocean with the one that exists at any one time. In this respect meteorologists are ahead of us, although in the long run we have an advantage, for our system changes so much more slowly.

Contribution No. 766

Reprinted from Limnology and Oceanography
Vol. 1, No. 1, January, 1956
Printed in U.S.A.

Population Dynamics of the Marine Clam, *Mya arenaria*[1]

John C. Ayers

Department of Conservation, Cornell University and Woods Hole Oceanographic Institution

ABSTRACT

From present spawning and survival data, it is calculated that stable local populations of *Mya* require an average annual production, per spawning pair, of 40 spat which both survive and remain in the spawning area. The sizes of larva populations which survive and remain in the area under various flushing rates and mortalities are calculated. From this and the 40 spat/pair/year level the suitability of estuaries or embayments as sites for *Mya* cultivation may be judged when local flushing rates and mortality coefficients are known. A formula for estimating the harvestable fraction of the existing population under local flushing rate and mortality conditions has been derived. The method, combined with the local oceanography, adequately explains the anomalous history of *Mya* production in the harbor of Barnstable, Massachusetts.

INTRODUCTION

The soft-shelled or "steamer" clam, *Mya arenaria*, formerly a wildlife resource of great value, has been reduced by over-exploitation to such an extent that a high degree of management practice must be developed and put into effect if this food delicacy is not to disappear from the market. A few empirical management practices are employed but underlying fundamental studies, to serve as their guides, are lacking.

Certain principles for determination of environmental suitability and size of the harvestable fraction of the population evolved in this study appear to be applicable not only to *Mya* but, with modification, also to other species both marine and freshwater.

In the waters of Massachusetts *Mya* larvae spend about a fortnight in a weakly-swimming pelagic larval stage prior to settling to the bottom as spat and assuming their burrowing mode of life. During their swimming stage they are at the mercy of the currents and are subject to enormous mortality from a variety of causes, including predation. *Mya* is primarily an inhabitant of estuaries and tidal embayments where its larva populations are reduced by being flushed out to sea by the tides, in addition to the mortality from all causes which would occur regardless of tidal action.

This study is concerned with the reductions in numbers of larvae that result from the combined effects of flushing-out and mortality. From consideration of these matters come indications of some of the criteria by which we may judge the suitability of estuaries or embayments as localities for *Mya* cultivation. A formula for the size of the harvestable fraction of existing populations is derived. The considerations are finally applied to an embayment whose *Mya*-producing history is known. In conjunction with knowledge of the local oceanography, they appear to explain this history adequately.

The author is sincerely grateful for advice and constructive criticism received from Dr. A. C. Redfield, Dr. B. H. Ketchum, and Mr. Harry J. Turner, all of the Woods Hole Oceanographic Institution; Dr. Wilson F. Clark, Department of Conservation, Cornell University (now at Eastern Montana State College, Billings, Montana); and Dr. L. B. Slobodkin, Department of Zoology, University of Michigan. Financial support during the field phases of this study was received from the Division of Marine Fisheries, Massachusetts Department of Conservation.

GENERAL CONSIDERATIONS

Mya Biology

Adults of *Mya* are not hermaphroditic; male and female individuals are separate. Spawning is presumed to occur in massive bursts probably involving all the adults of an area. For the purposes of this paper the annual spawning is considered to be complete in the one major burst per year. Belding (1930) calculated that a single female *Mya* produces three million eggs per year. Since the author knows of no evidence of abnormal sex ratios in this species, it is assumed that spawning involves equal numbers of males and females, and further, the mass spawning is presumed to result in fertilization of all the eggs. A single spawning pair is considered to produce three million larvae per annual spawning.

---

[1] Contribution No. 766 from the Woods Hole Oceanographic Institution.

The studies of H. J. Turner (personal communication) indicate that only about 1% of the spat which settle to the bottom at the end of the 14-day swimming stage will survive to become sexually mature. If two second-generation adults (to replace the original parent pair) are to result from this 1% survival, 200 spat must settle.

Observations by the author indicate that five years is a conservative estimate of the period of sexual maturity in *Mya*. In a stable population each pair of parent *Mya* must, during its period of sexual maturity, replace itself with a second-generation pair. The production of a second-generation pair would require 200 settled spat during five years, or an annual production of 40 settled spat.

The biological statistics of a stable *Mya* population appear to be:

3×10^6 eggs/spawning/parent pair
3×10^6 larvae/spawning/parent pair
200 spat must settle during five years
40 spat must settle per year
1 second-generation adult pair produced in five years

Subsequent research may modify these figures and necessitate recalculations, but the principles involved will not be changed.

Mortality

As used here, mortality includes predation and all other causes of death. Calculation of the size of a population after a time, t, during which mortality has taken place involves only the fundamental equation:

$$P_t = P_0 e^{-kt} \qquad (1)$$

in which P_0 and P_t are the initial and final population sizes, e is the base of the natural logarithms, t is time, and k is the coefficient of mortality; when $k = 1$ the population will drop to the $1/e$th fraction per unit of time. The factor e^{-kt} represents the fraction of the population surviving after time t. Substitution of 3×10^6 larvae for P_0, 28 tidal cycles (two weeks) for t, and various values for k, allows calculation of the size of the larva population (resulting from a single spawning pair) which will survive, under various mortality rates, to settle as spat at the end of the 14-day swimming phase. The results of these calculations are shown in Figure 1 and in the $f = 0$ section of Table 1.

Dilution

Dilution is a general term applied by Ketchum, Ayers, and Vaccaro (1952) to all those processes, such as flushing-out to sea or dilution by the addition of extra water, which produce a decrease in population density without any of the population dying. In the situations where *Mya* lives, flushing-out to sea is probably the common mechanism of dilution.

Recent discoveries in coastal oceanography have produced mathematical techniques and field methods which make possible calculation of the effects of dilution. The mathematical techniques were developed by Ketchum (1951) and Ketchum, Ayers, and Vaccaro (1952). The field methods have been developed in large part by these authors and are described in the Appendices of this paper.

The mathematical considerations derive the equation for the effect of dilution:

$$P_t = P_0(1 - f)^t \qquad (2)$$

where P_0 and P_t are the original and final populations remaining in their natal estuary or embayment after time, t (in tidal cycles of 12.4 hours each), during which the population has been subject to intermittent flushing out to sea; and f is the fraction of water lost from the estuary or embayment during one complete tidal cycle, also called the flushing rate. The factor $(1 - f)^t$ represents the fraction retained in the estuary or embayment after time t. The calculation of f for Barnstable Harbor, Massachusetts is given in Appendix I.

Substitution of 3×10^6 larvae for P_0, 28 tidal cycles for t, and various values between 0 and 1 for f, permits calculation of the size of the larva population (stemming from a single spawning pair) which will remain in the area until they settle as spat at the end of the 14-day swimming stage. The results of these calculations are shown in Figure 1 and in the $k = 0$ portions of Table 1.

Combined Dilution and Mortality

Under estuarine or embayment conditions dilution and mortality proceed simultaneously and produce a greater decrease in population than could be achieved by either process alone. Of the fraction which remains in the area, only a further fraction survives. The equation for combined dilution and mortality is:

$$P_t = P_0(1 - f)^t e^{-kt} \qquad (3)$$

where P_t is the size of the population which *both* survives *and* remains in the spawning area, all other factors as above. Substitution of 3×10^6 larvae for P_0, 28 tidal cycles for t, and letting k vary from 0 to 1.0 at each level of f as f goes from 0 to 0.5 (Table 1) produces a family of curves summarizing the combined effects of dilution and mortality on the larva population, resulting from a single spawning pair, during the two-week swimming phase. The results of these calculations are presented in Table 1 and Figure 2.

RESULTS

Dilution-Mortality Relations of Mya Populations

The production of 40 larvae per year which both remain in the spawning area and survive to settle as spat appears to be the minimum which will allow one parent pair of *Mya* to replace itself, during its period of sexual maturity, with a single pair of second-generation adults, i.e., give a stable local population. More than forty retained and surviving larvae per pair per year represents a population in which there is at least a potentiality for increase. Fewer than forty retained and surviving larvae per pair per year indicates a population which is at least potentially declining.

TABLE 1

Size of final larva population (from three million fertilized eggs produced by a single spawning pair) both retained in the spawning area and surviving at the end of the 28-tidal-cycle swimming stage as mortality, k, *varies at various levels of flushing rate,* f.

f	Retention $P_0(1-f)^t$	k	Surviving fraction e^{-kt}	Final population P_t	Harvestable fraction $(P_t - 40)/P_t$
					%
0	3×10^6	0	1.00	3×10^6	99.9
		0.2	37×10^{-4}	1.1×10^4	99.6
		0.4	135×10^{-7}	41	2.5
		0.5	82×10^{-8}	2.5	0
		0.6	50×10^{-9}	0.15	0
		0.8	18×10^{-11}	5.6×10^{-4}	0
		1.0	67×10^{-14}	2.1×10^{-6}	0
0.1	1.6×10^5	0	1.00	1.6×10^5	99.9
		0.2	37×10^{-4}	592	93.1
		0.3	22×10^{-5}	35	0
		0.4	135×10^{-7}	2	0
		0.6	50×10^{-9}	8.0×10^{-3}	0
		0.8	18×10^{-11}	2.9×10^{-5}	0
		1.0	67×10^{-14}	1.1×10^{-7}	0
0.2	5.8×10^3	0	1.00	5.8×10^3	99.3
		0.1	0.0608	353	88.3
		0.2	37×10^{-4}	21	0
		0.4	135×10^{-7}	0.08	0
		0.6	50×10^{-9}	2.9×10^{-4}	0
		0.8	18×10^{-11}	1.04×10^{-6}	0
		1.0	67×10^{-14}	3.9×10^{-9}	0
0.3	138	0	1.00	138	71.0
		0.05	0.2466	34	0
		0.2	37×10^{-4}	0.5	0
		0.4	135×10^{-7}	1.8×10^{-3}	0
		0.6	50×10^{-9}	6.9×10^{-6}	0
		0.8	18×10^{-11}	2.5×10^{-8}	0
		1.0	67×10^{-14}	9.2×10^{-11}	0
0.4	1.84	0	1.00	1.84	0
		0.2	37×10^{-4}	6.8×10^{-3}	0
		0.4	135×10^{-7}	2.5×10^{-5}	0
		0.6	50×10^{-9}	9.2×10^{-8}	0
		0.8	18×10^{-11}	3.3×10^{-10}	0
		1.0	67×10^{-14}	1.2×10^{-12}	0
0.5	0.012	0	1.00	0.012	0
		0.2	37×10^{-4}	4.4×10^{-5}	0
		0.4	135×10^{-7}	1.6×10^{-7}	0
		0.6	50×10^{-9}	6.0×10^{-10}	0
		0.8	18×10^{-11}	2.2×10^{-12}	0
		1.0	67×10^{-14}	8.0×10^{-15}	0

In the absence of mortality, an estuary or embayment may retain 40 larvae per pair per year to the end of their swimming stage provided the flushing rate does not exceed $f = 0.33$ per tidal cycle (Table 2). In the

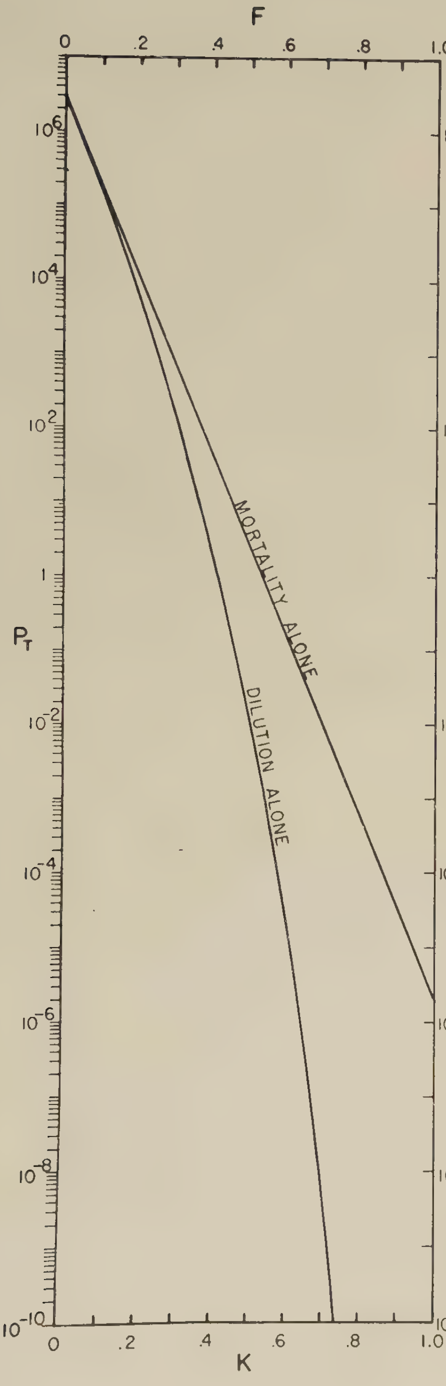

FIG. 1

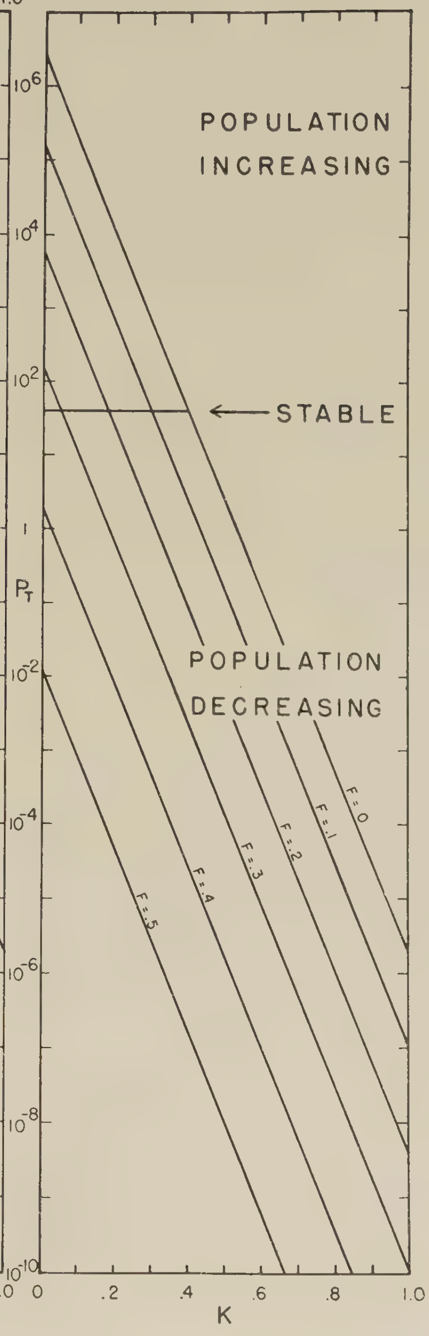

FIG. 2

FIG. 1. Size of larva population, from a single spawning pair, after 28 tidal cycles at various levels of mortality or dilution alone.

FIG. 2. Size of larva population after 28 tidal cycles as mortality, k, goes from 0 to 1 at flushing rates, f, of 0 to 0.5. The 40 spat/pair/year level of a stable local population is indicated.

as spat just ready to settle at the end of a 14-day drift in this current must have traveled 26.6 nautical miles. Retracing the curving path of the current for 26.6 miles brings one to the harbor of Plymouth, Massachusetts. It thus seems both possible and probable that the occasional enormous *Mya* sets formerly received by Barnstable Harbor were larvae produced in Plymouth Harbor, which under occasional unusually fortuitous conditions were able to complete the journey to Barnstable. Such fortuitous sets, indeed, appear to have been the only significant recruitment to the harbor's *Mya* population.

The observed effects of the economic depression of 1929 in no way disagree with these conclusions. During the depression clamming afforded the only livelihood available to many of the people of both Plymouth and Barnstable. The *Mya* stocks of both harbors were heavily depleted during this period, and Barnstable then gradually lost the remainder of its population.

Since the heavy digging-out of the harbors' stocks during the depression, the enormous sets that Barnstable formerly received have been virtually absent; a moderate set in 1941 survived, grew, and supported a commercial clamming industry through 1947; a set in 1946 did not survive, nor did a small set in 1951. Failure of these sets to survive has been shown by Turner *et al* (1948–1951) to be due to the harbor's normally-large predator populations, which lead a marginal existence in the absence of clams and which seek out and completely destroy any small sets. A set sufficient to repopulate Barnstable Harbor must be so large that it can support the predators and still have a residue surviving to maturity. The history of the *Mya* populations of Barnstable and Plymouth is reviewed in detail by Turner *et al* (op. cit.).

SUMMARY

From currently accepted information on the spawning and survival of *Mya arenaria* it is calculated that stable populations can be maintained if each pair of spawning adults produces an annual average of 40 spat which *both* survive *and* remain in the spawning area. Populations would tend to increase if more than 40 such spat per pair per year are produced, to decrease if production is less than 40.

The sizes of larva populations (from a single pair of spawners) which both survive and remain in the spawning locality until spatfall, under various conditions of flushing rate and mortality, are calculated. The graph of these results expresses the overall relationship between flushing rate, mortality, and size of larva population retained in the area and surviving until spatfall. The position at which the level of 40 spat per pair per year falls across this overall relationship provides a criterion for judging whether an existing adult population is potentially increasing, stable, or decreasing under the conditions of flushing rate and mortality which prevail.

Field measurements of flushing rate and mortality may be compared to the overall relationship as a means of estimating the suitability of essentially *Mya*-less localities as places for the cultivation of the shellfish.

A formula for estimating the harvestable fraction of the existing population (under local flushing rate and mortality conditions) has been derived.

Additional determinations of natural coefficients of *Mya*-larva mortality, of survival from spatfall to maturity, of egg production per spawning pair, and field tests of the method as a whole, are needed for the refinement of the method; it is not anticipated that these will modify the underlying principles.

The method, combined with the local oceanography, adequately explains the recorded history of *Mya* production in Barnstable Harbor, Massachusetts.

APPENDIX I

The flushing time is defined as the average number of tidal cycles required for the total freshwater inflow (see Appendix II) to replace the quantity of freshwater which is present in an estuary or embayment at any high water during constant runoff conditions. It is determined by computing the volume of freshwater in the area at high water, dividing by the volume of total freshwater inflow per tidal cycle to obtain the flushing time. The reciprocal of the flushing time is the flushing rate, f.

In small estuaries or tidal embayments where there is no *vertical* gradient in salinity (although

TABLE 3

Freshwater accumulation in Barnstable Harbor, high water, 29 August 1947

No vertical salinity gradient. Base salinity = greatest salinity = 31.64 ‰. Fresh water fraction = (base salinity minus inter-contour average salinity)/base salinity

Salinity		Area ft^2	Average depth, ft	Volume ft^3	Freshwater fraction	Freshwater volume, ft^3
Range	Average					
31.60–31.50	31.55	58.7×10^6	15	880×10^6	0.003	2.6×10^6
31.50–31.02	31.26	37.2×10^6	10	372×10^6	0.012	4.4×10^6
Total freshwater accumulation						7.0×10^6

an extensive horizontal gradient may exist along the length of the area), the areas between adjacent salinity contours (drawn on navigation charts) are determined by planimetry and each area is multiplied by the average of all the depth soundings it encloses; an inter-contour volume is thus obtained for each area. Each inter-contour volume is multiplied by the freshwater fraction (see Table 3) represented by its average salinity to obtain the inter-contour volume of freshwater. Summation of these freshwater volumes gives the total freshwater volume; this is divided by the total freshwater inflow per tidal cycle to give the flushing time.

This method has been used in Barnstable Harbor; the results are shown in Table 3.

The average flushing time of Barnstable Harbor is, then,

$$\frac{7.0 \times 10^6 \text{ ft}^3 \text{ accumulated freshwater}}{1.4 \times 10^6 \text{ ft}^3 \text{ total inflow/tidal cycle (Appendix II)}} = 5.0 \text{ tidal cycles}$$

and the flushing rate is 0.2 per tidal cycle. Ketchum (1954) using a different method, has estimated Barnstable's flushing rate to be 0.3.

APPENDIX II

In sandy soils ground-water seepage contributes freshwater which cannot be measured directly. This acquisition is apt to be a significant part of the total freshwater inflow in tidal embayments (characterized by the absence of a river; runoff entering from small streams) and less so in estuaries (characterized by the presence of a river whose flow usually constitutes the major part of the freshwater inflow). Measurements of stream runoff and water transports into and out of Barnstable Harbor in August 1948 during a period of low rainfall comparable to that of August 1947 allow an analysis of the hydrology of the area.

The Barnstable watershed acquired from a 0.14 inch rainfall on 30 August 1948:

$$22.8 \text{ mi}^2 \text{ watershed} \times 5280 \text{ ft}^2/\text{mi}^2 \times \frac{.011 \text{ ft rain/day}}{2 \text{ tidal cycles/day}} = 3.4 \times 10^6 \text{ ft}^3/\text{tidal cycle.}$$

After the rainfall, measured stream flow was only 0.3×10^6 ft^3/tidal cycle and the net transport seaward through the harbor mouth was 1.4×10^6 ft^3 of freshwater/tidal cycle. The latter was determined from a series of stations across the harbor mouth which were occupied at each hour of the tidal cycle; at each station surface, mid-depth, and bottom current velocities and salinity samples were obtained. From the hourly areas of the section, the hourly current velocities, and the hourly freshwater fractions, the total inward and outward transports of freshwater were determined. The excess of ebb-tide freshwater outflow over flood-tide return of freshwater represents the sum of runoff and groundwater seepage.

The results may be summarized as follows:

	(all $\times 10^6$ ft^3/tidal cycle)	
Rainfall		3.4
Transport seaward (runoff plus seepage)	1.4	
Subtract runoff	0.3	
Seepage	1.1	
Runoff plus seepage		1.4
Evaporation, interception, soil-retention and retention in harbor (by difference)		2.0

Since inflow of freshwater by seepage is as effective in displacing the accumulated freshwater of the harbor as is runoff via streams, the sum of the two must be used as the total freshwater inflow in the determination of the flushing time—from which flushing rate is obtained.

REFERENCES

BELDING, D. L. 1930. The soft-shelled clam fishery of Massachusetts. Commonwealth of Massachusetts, Dept. of Conservation, Div. Fish. and Game, Mar. Fish. Sect., Mar. Fish. Series No. 1. Boston, Mass.

BIGELOW, H. B. 1927. Physical oceanography of the Gulf of Maine. Bull. U. S. Bur. Fish., **40** (Part II): 511–1027.

BOUSFIELD, E. L. 1954. The distribution and spawning seasons of barnacles on the Atlantic coast of Canada. Department of Northern

Affairs and National Resources. Canada. Bulletin No. 132, Annual Report of the National Museum for 1952–53, pp. 112–154.

Ketchum, B. H. 1951. The exchanges of fresh and salt water in tidal estuaries. J. Mar. Res., **10:** 18–38.

———. 1954. Relation between circulation and planktonic populations in estuaries. Ecology, **35:** 191–200.

Ketchum, B. H., J. C. Ayers, and R. F. Vaccaro. 1952. Processes contributing to the decrease of coliform bacteria in a tidal estuary. Ecology, **33:** 247–258.

Turner, H. J., *et al.* 1948. Report on investigations of the propagation of the soft-shelled clam, *Mya arenaria.* Commonwealth of Massachusetts, Dept. of Conservation, Div. Mar. Fish. Boston, Mass. 61 pp.

———. 1949. Report on investigations of methods of improving the shellfish resources of Massachusetts. Ibid. 22 pp.

———. 1950. Third report on investigations of methods of improving the shellfish resources of Massachusetts. Ibid. 31 pp.

———. 1951. Fourth report on investigations of the shellfisheries of Massachusetts. Ibid. 21 pp.

Contribution No. 774

American Museum Novitates

PUBLISHED BY THE AMERICAN MUSEUM OF NATURAL HISTORY
CENTRAL PARK WEST AT 79TH STREET, NEW YORK 24, N.Y.

NUMBER 1765 APRIL 6, 1956

Tunas of the Genus *Thunnus* of the Northern Caribbean

By Harvey R. Bullis, Jr.,[1] and F. J. Mather, III[2]

During Cruise 30 of the United States Fish and Wildlife Service exploratory fishing vessel "Oregon," in April, 1955, six species of tuna were caught on longlines in the northern Caribbean. The species of tunas taken at the 11 stations occupied (see fig. 1) are listed in table 1. Additional information on the distribution of tunas was obtained from Captain Archie Cross of the M/V "Santo Antonino" and Captain Ed Saarinen of the M/V "Hermes II," who have been fishing with longlines in this area.

The yellowfin tuna, *Thunnus*[3] *albacares* (Bonnaterre), the blackfin tuna, *Thunnus atlanticus* (Lesson), and the oceanic bonito, *Katsuwonus pelamis* (Linneaus), are well-known indigenes of the region (Beebe and Tee Van, 1928, 1936; Rivas, 1951; Mather and Schuck, 1952; Rawlings, 1953). Most reports of the albacore, *Thunnus alalunga* (Gmelin), have been based on *T. atlanticus,* and there are no records of this species, substantiated by specimens, from the western North Atlantic (Rivas, 1951, pp. 220, 222, 223). Specific data on the presence of bluefin tuna, *Thunnus thynnus* (Linneaus), in the Caribbean area are lacking, although there is one known capture from the northern coast of Jamaica (personal communication). We know of no previous records of the Atlantic big-

---

[1] United States Fish and Wildlife Service, Pascagoula, Mississippi.

[2] Woods Hole Oceanographic Institution, Woods Hole, Massachusetts (Contribution No. 774, Woods Hole Oceanographic Institution).

[3] We have followed Fraser-Brunner (1950) and Rivas (1951) in considering the genera *Neothunnus, Parathunnus,* and *Germo* as either synonyms of the genus *Thunnus* or subgenera of that genus.

TABLE 1

Catches of Tuna by Stations

"Oregon" Station Number	Date April, 1955	North Latitude	West Longitude	*Thunnus obesus*	*Thunnus alalunga*	*Thunnus thynnus*	*Thunnus albacares*	*Thunnus atlanticus*	*Katsuwonus pelamis*
1286	11	21° 15′	84° 05′	—	—	—	—	1	—
1287	12	20° 01′	81° 50′	—	—	1	—	—	—
1288	14	18° 15′	78° 30′	—	—	—	—	—	—
1289	19	17° 10′	74° 20′	—	1	—	10	—	1
1290	20	16° 15′	73° 30′	—	6	—	3	—	—
1291	21	17° 50′	72° 00′	2	1	—	4	—	—
1292	22	18° 08′	74° 35′	—	—	—	—	—	—
1293	23	19° 55′	74° 10′	—	2	8	10	—	—
1295	24	19° 45′	74° 45′	—	2	8	3	—	—
1296	25	19° 30′	76° 50′	—	1	3	7	7	1
1297	28	20° 50′	86° 10′	—	—	1	—	1	—

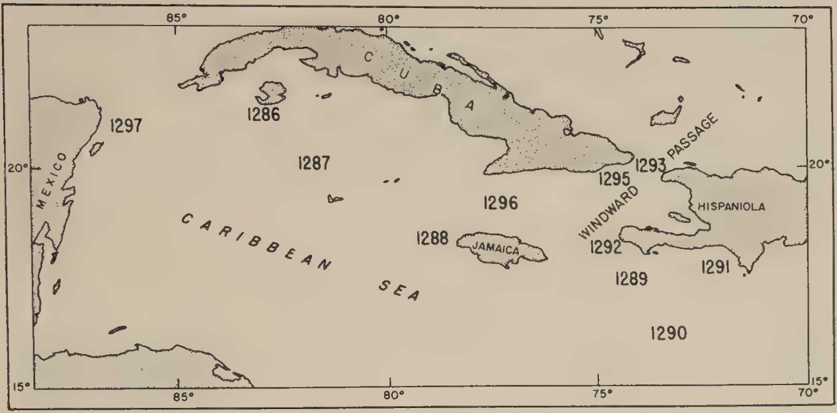

FIG. 1. Positions of longline stations in the northern Caribbean.

eye tuna, *Thunnus obesus* (Lowe), from west of the Azores. The listing of this little-known species among the fishes of Port-au-Prince Bay by Beebe and Tee Van (1928) was later (1936) placed in the synonymy of *T. atlanticus* by those authors. Morice and Cadenat (1952) and Morice (1953) synonymized *T. atlanticus* with *T. obesus,* and it appears that the species to which they refer as occurring off the West Indies was the former.

Beebe and Tee Van (1936) showed clearly that *T. atlanticus* (placed in the genus *Parathunnus* by them) was a valid species. Fraser-Brunner (1950) incorrectly placed it in the synonymy of *T. alalunga.* Having examined freshly caught specimens of *T. obesus, T. atlanticus,* and *T. alalunga,* we have no doubt that they are different and valid species. A decisive character in separating *T. atlanticus* from the others is its gill-raker count. Beebe and Tee Van counted the gill rakers on both the left and right arches of 58 blackfins and found the following range of counts: for the lower limb, 15 to 18; for the upper limb, four to six; total number, 20 to 24. One of us (Mather) has taken gill-raker counts from many *T. atlanticus* captured between Rio de Janeiro and Cape Cod. These are in very close agreement with those of Beebe and Tee Van, ranging from 15 to 18 for the lower limb, four to seven for the upper, and from 20 to 23 in total number. Rivas (1951) gives a slightly higher range of lower rakers (15–19), but states that his studies are in complete accord with those of Beebe and Tee Van. In contrast, the count given by Fraser-Brunner for *T. obesus* is 18 to 25 lower, and eight to 13 upper, and that for *T. alalunga* by Letaconnoux (1950) is 18 to 22 lower, seven to 10 upper, and 26 to 31 total. The counts obtained by us are consistent

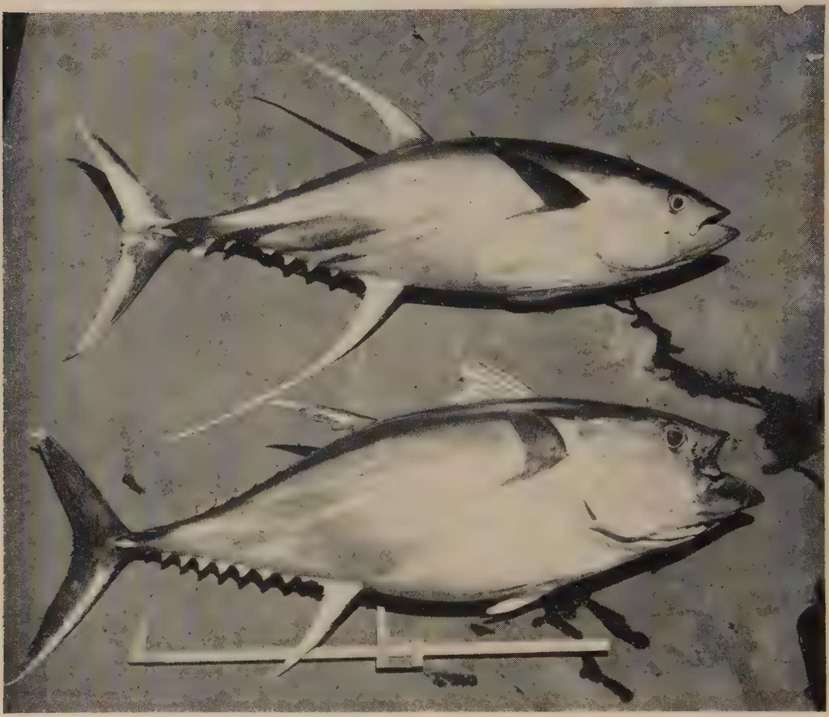

FIG. 2. A yellowfin tuna, *Thunnus albacares* (upper), compared with the heavier big-eye tuna, *Thunnus obesus* (lower). The fork length of each fish is approximately 150 cm.

with these figures, being 19 lower, eight to nine upper, and 27 to 28 total for *T. obesus,*[1] and 19 to 22 lower, seven to nine upper, and 27 to 31 total for *T. alalunga.* Thus *T. atlanticus* is readily separable from both *T. obesus and T. alalunga* on the basis of total gill-raker counts, and in most cases by the lower limb count.

The pectoral of the albacore is usually much longer (1 to 1.6[2] times head length) than that of the blackfin tuna (0.8 to 1.2 times head length), but the species intergrade in this respect.

In addition, the color of the finlets distinguishes *T. atlanticus* from the other species. All the finlets of *T. obesus* and the dorsal ones of *T.*

---

[1] Rivas obtained counts of 20 to 22 lower, nine upper, and 29 to 31 total for two eastern Atlantic specimens (personal communication).

[2] From measurements of Bay of Biscay specimens 51 to 80 cm. long (Navaz, 1950). For the larger specimens measured by us, the pectoral varied from 1.35 to 1.6 times head length.

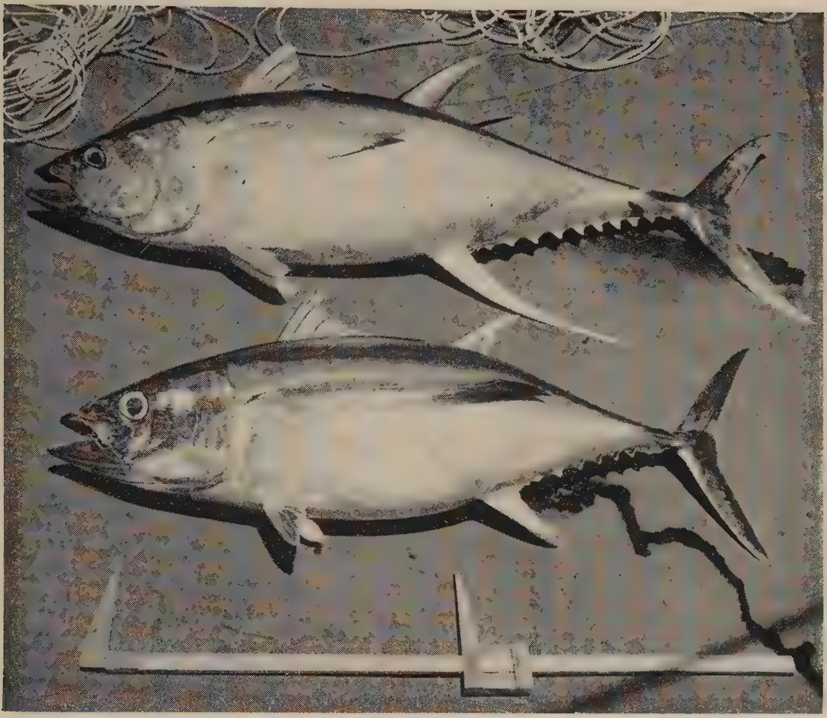

FIG. 3. A yellowfin tuna (upper) compared with an albacore, *Thunnus alalunga* (lower). The yellowfin is about 100 cm., and the albacore about 96 cm., in fork length.

alalunga are predominantly yellow. Those of *T. atlanticus* are not yellow, the dorsal ones usually being of a dusky brown color, and the anals dusky steel.

The total size range of *T. atlanticus* also appears to preclude the possibility that it is identical with *T. obesus*. The maximum size attributed to *T. atlanticus* is 60 pounds (Mowbray, 1935), but our own observations lead us to believe that individuals weighing over 25 pounds are very rare. On the other hand, our specimens of *T. obesus* weighed about 175 pounds each, and Frade (1931) examined individuals up to 188 cm. long, probably weighing about 275 pounds. In addition to this disparity in recorded sizes, the fact that *T. atlanticus* spawns at a very small size (less than 10 pounds) suggests that its maximum size cannot compare with that attained by *T. obesus*.

We believe that the capture of two Atlantic big-eye tunas at Station 1291 off the south central coast of Hispaniola constitutes the first record

TABLE 2

MEASUREMENTS (IN PERCENTAGE OF FORK LENGTH) OF TUNAS FROM THE NORTHWESTERN CARIBBEAN[a]
(Measurements were taken with calipers following the method of Marr and Schaefer, 1949, except that the orbit was measured instead of the iris.)

Measurements	*Thunnus albacares*					*Thunnus obesus*		*Thunnus alalunga*				*Katsuwonus pelamis*
Fork length in mm.	1006	1281	1523	1550	1699	1503	1519	958	969	1025	1050	801
Snout to first dorsal	.286	.268	.250	.269	.279	.294	.292	.322	.326	.310	.327	.342
Snout to second dorsal	.509	.495	.480	.492	.485	.529	.535	.576	.591	.563	.576	.625
Snout to anal	.567	.549	.545	.540	.536	.595	.600	.625	.641	.630	.626	.684
Snout to ventral	.295	.280	.305	.282	.284	.342	.339	.326	.340	.342	.325	.350
Head	.260	.250	.252	.255	.258	.294	.296	.287	.302	.296	.288	.305
Maximum depth	.241	.244	.259	.258	.269	.296	.292	.279	.282	.270	.277	.281
Maximum width	.183	.193	.199	.201	.191	.212	.211	.219	.221	.212	.212	.231
Largest first dorsal spine	.109	.115	.123	.135	.122	.120	.127	.111	.123	.119	.113	.162
Base first dorsal	.232	.230	.223	.224	.219	.238	.246	.252	.262	.239	.246	.281
Length second dorsal	.199	.290	.390	.386	.290	.168	.161	.132	.127	.140	.139	.115
Base second dorsal	.093	.095	.088	.101	.093	.090	.090	.094	.094	.101	.101	.092
Length anal	.210	.314	.411	.465	mut.	.198	.179	.127	.130	.128	.137	.108
Base anal	.075	.080	.086	.088	.084	.070	.071	.074	.093	.094	.077	.085
Pectoral	.293	.258	.246	.258	.220	.262	.244	.409	.412	.428	.450	.156
Ventral	.117	.102	.110	.115	.103	.119	.114	.109	.102	.099	.097	.121
Caudal spread	.350	.379	.378	.414	.433	.416	.404	.336	.369	.361	.369	.308
Longest dorsal finlet	.033	.036	—	.039	.037	.035	—	.031	.033	.032	.034	.036
Ventral insert to vent	.283	.271	.260	.266	.268	.278	.283	.310	.312	.309	.313	.334
Least depth caudal peduncle	.024	.025	.023	.026	.024	.028	.026	.023	.024	.024	.024	.021
Maximum width at caudal keels	.093	.101	.093	.098	.093	.094	.099	.079	.073	.079	.074	.071
Snout	.088	.091	.087	.092	.092	.106	.104	.094	.102	.098	.100	.101

TABLE 2—(*Continued*)

Measurements	*Thunnus albacares*					*Thunnus obesus*		*Thunnus alalunga*				*Katsuwonus pelamis*
Maxillary	.101	.096	.095	.099	.098	.117	.117	.103	.115	.106	.105	.118
Interorbital	.093	.094	.102	.101	.103	.122	.113	.095	.099	.094	.100	.089
Diameter orbit	.036	.032	.032	.031	.029	.045	.045	.049	.054	.050	.056	.037
Longest gill raker	.033	.030	.039	—	—	.047	.049	.037	.035	.035	.039	.039

[a]The 1699-mm. *T. albacares* was taken in May, 1955, in the Gulf of Mexico.

TABLE 3

COUNTS OF TUNAS FROM THE NORTHWESTERN CARIBBEAN

Counts	*Thunnus albacares*					*Thunnus obesus*		*Thunnus alalunga*				*Katsuwonus pelamis*
First dorsal spines	14	14	14	14	14	14	14	14	14	13	13	15
Second dorsal spines and rays	14	14	14	15	14	14	14	15	15	15	15	14
Dorsal finlets	9	9	9	8	9	9	9	8	8	8	8	7
Anal spines and rays	13	14	14	14	14	11	13	15	15	15	14	14
Anal finlets	9	9	8	8	9	9	9	7	7	7	8	7
Pectoral	36	35	36	36	35	34	33	33	34	34	33	27
Upper gill rakers	10	9	8		9	9	8	8	9	8	7	16
Lower gill rakers	22	20	21		20	19	19	19	20	19	20	35

of the species, substantiated by adequate descriptive data, from the western Atlantic. These fish and four yellowfin tuna which were caught along with them all fell within a size grouping of 150.0 to 154.6 cm. (fork length), and, when compared side by side, the two species were readily distinguishable (see fig. 2). The Atlantic big-eyes could be quickly separated by their much shorter second dorsal and anal fins, much wider and deeper bodies, and larger eyes.[1] The second dorsal and anal showed dull yellow in the distal portions only, and just a trace of yellow was present on the first dorsal and ventrals. The finlets had a heavy band of glossy black edging, centrally a dull yellow turning to a sienna brown proximally, and black along the base. The finlets of the yellowfin were uniformly bright lemon yellow, with thin black edging. Three of the yellowfin and one big-eye were caught on adjacent hooks, indicating mixed schooling of large individuals of the two species. Captain Cross told us that he has occasionally found these two species mixed in his catches taken south of Ponce, Puerto Rico, and in the vicinity of St. Croix.

Thirteen albacore were taken at seven stations in the area south of and between western Hispaniola and eastern Cuba, and north and east of Jamaica. Their lengths ranged from 95 to 105 cm. Furthermore, Cross had been catching albacore at a rate of one or two per 100 hooks south of Ponce, Puerto Rico, and in the vicinity of St. Croix, from January through April. Thus this valuable species appears to have been fairly abundant and widely distributed in the northern Caribbean from midwinter through April. The albacore were easily distinguishable from yellowfin (fig. 3). Several differences in proportions between the species are indicated by table 2. Among the most notable were the longer pectorals, shorter and more posteriorly located second dorsal and anal fins, larger eye, and deeper and wider body of the albacore. The species also differed markedly in coloration. The albacore showed little yellow on its fins, except the dorsal finlets, and the median area of its body had a brownish bronze tint rather than the golden yellow of a fresh yellowfin. The finlets of the yellowfin were, as mentioned above, a bright lemon yellow, thinly edged with black. The dorsal finlets of the albacore were of a much darker yellow, with a wider black anterior edge and a clear whitish area beyond the black at the tip and along the posterior edge. The anals were usually of dull metallic hue, with the same whitish tips and posterior edges as the dorsals. On some individuals, however, one or two of the largest anal finlets were similar in color to the dorsals. In addition to the finlets, the caudal, the second dorsal, the anal, the ventrals, and the proximal part of the pectorals all had clear whitish posterior edges. This was especially noticeable on the caudal, and this character seems sufficient to separate the albacore from all other western Atlantic members of the genus *Thunnus,* in cases where the length of the pectoral of the albacore[1] fails to do so. The albacore also differed notably in body form from the yellowfin, being heavy posteriorly and tapering abruptly to the caudal peduncle, in a manner reminiscent of *Katsuwonus,* in contrast to the very long and gradual taper of the posterior half of the yellowfin.

---

[1] Tables 2 and 3 list caliper measurements and counts (by the method of Marr and Schaefer, 1949) of tunas of various species taken during this cruise.

Twenty-one giant bluefin tuna were caught at five stations, 19 of them in the Windward Passage and its southwestern approaches, one 45 miles northwest of Grand Cayman Island, and one 30 miles northeast of Cozumel Island. The fish ranged from 209 to 245 cm., with most of them near 225 cm. in length, or about 475 pounds in weight. Gear damage indicated that at least as many more were hooked and lost. In addition, Saarinen reported releasing a giant bluefin 65 miles northwest of South Negril Point, Jamaica, April 16. He believed, on the evidence of lost equipment, that several more had been hooked. Thus it appears that in April giant bluefins were abundant in the Windward Passage and off Guantanamo, moderately abundant from there to a point somewhat west of Jamaica, and scattered from there to the Yucatan Peninsula. The estimated numbers of bluefins hooked in the respective areas are 3.5, 1.3, and less than 0.5, per 100 hooks. Thirteen of the fish taken at Stations 1293, 1295, and 1296 were opened. Ten of them were females, and three were males. The testes of a 245-cm. bluefin taken April 12 weighed 26 pounds and appeared to be fully ripe and ready for spawning.[2] Some milt ran without external pressure from two of the males taken April 24–25. The testes of one of these weighed 12 pounds.

---

[1] The data of Navaz (1950) indicate that the pectorals of small albacore taken in the Bay of Biscay are sometimes as short as those of some western Atlantic yellowfins.

[2] One of us (Mather) in a discussion delivered jointly with Howard A. Schuck on bluefin tuna at the Oceanic Fisheries Conference, Bermuda, June, 1951 (recorded but not published), stated that most of the giant bluefins taken off Bimini and Cat Cay in May and June probably had spawned somewhat earlier, possibly in April or early May, and not far south of these places. This opinion was based on the condition of the gonads of fish examined at Bimini, the direction in which the fish were observed to be traveling, and back calculations based on European data (Heldt, 1930) of the probable dates of hatching of juveniles. Rivas (1954) discussed the spawning of bluefins in the Straits of Florida.

Although the total number of yellowfins taken was small (37), some evidence of size segregation between the open Caribbean and the Windward Passage was noted. Seventeen fish from the open Caribbean averaged 148 cm. (fork length), while the 16 from the Windward Passage averaged only 112 cm. (four yellowfins were partially eaten by sharks, and lengths were unobtainable). Previous observations on longline catches by the "Oregon" in the Gulf of Mexico have also shown indications of size segregation, particularly during the summer months. The only school of tuna which appeared to be yellowfin was sighted on April 23 between Cape Maisi and Guantanamo Bay. The weight of these fish was estimated to be 10 to 20 pounds each, the same as that of yellowfins caught on longlines in that area. As the *Katsuwonus pelamis* from Station 1289 represents the largest specimen of the species we have seen, we have included its measurements in table 2.

Although the blackfin tuna is known to range widely throughout the area fished (Mather and Day, 1954) and supports a small tuna fishery on the southwestern coast of Cuba (Rawlings, 1953), few captures were made on longline gear (see table 1). Schools believed to consist of small blackfins were frequently sighted between the Windward Passage and the Yucatan Channel. These were seen surfacing and feeding on small carangids and nomeids that gathered under the buoys of the longline gear during fishing operations. In the vicinity of Station 1297 northeast of Cozumel Island, 10 small blackfins were caught on trolling lines. These ranged from 34.2 to 40.5 cm., fork length, and averaged 36.9.

One specimen of the Atlantic big-eye tuna has been placed in the collection of the United States National Museum (U.S.N.M. No. 157791), together with one of the albacore (U.S.N.M. No. 157790). The United States National Museum also has a short series of the blackfin and small bluefin tunas collected in the Gulf of Mexico on other "Oregon" cruises.

These observations show that all five species of the genus *Thunnus* known to occur in the Atlantic may be found in the Caribbean. Three of these, the yellowfin, the albacore, and the Atlantic big-eye, were encountered in sizes which may be fished efficiently by the longline method and utilized in canneries. This may be a factor of some importance to the new tuna industry that is being started in Puerto Rico, as dependence on a single species might result in serious fluctuations in supply. A further implication that may be drawn from these observations is that the yellowfin tuna, the albacore, and the Atlantic big-eye, which are known to be abundant in the eastern Atlantic as far west as the Azores, may be distributed all the way across the tropical and subtropical parts of that ocean. This suggests the possibility of an extenive tuna resource in the tropical Atlantic.

We wish to thank Mr. W. C. Schroeder of the Woods Hole Oceanographic Institution and Prof. Luis Rivas of Miami University for their valued suggestions in regard to this paper.

TENTATIVE KEY TO FISHES OF THE GENUS *Thunnus* OF THE WESTERN ATLANTIC

1. Pectoral less than four-fifths[1] of head length, usually reaching to tenth to twelfth dorsal spine. Lower gill rakers, first arch, 24 to 28 . . . . bluefin tuna, *thynnus*
   Pectoral more than four-fifths[1] of head length, usually reaching almost to second dorsal fin or beyond. Lower gill rakers, first arch, 15 to 22 . . . 2
2. Pectoral more than one and one-fifth[1] of head length, usually reaching to anal fin or beyond. Caudal distinctly edged with white posteriorly . . . . albacore, *alalunga*
   Pectoral less than one and one-fifth[1] of head length, usually not reaching anal fin. Caudal not edged with white posteriorly 3
3. Total gill-raker count on first arch 20 to 24 (usually 15–18 on lower limb). Finlets not yellow . . . . blackfin tuna, *atlanticus*
   Total gill-raker count on first arch 24 to 33 (usually 18–22 on lower limb). Finlets predominantly yellow 4
4. Body robust (depth usually less than three and three-quarters in length), second dorsal and anal fins not greatly elongate (usually less than three-fifths of depth), fins without large yellow areas, finlets dull or brownish yellow, with extensive dusky edging. Posterior ventral margin of liver striated . . . . Atlantic big-eye tuna, *obesus*
   Body slender (depth usually more than three and three-quarters in length in individuals over 2 feet long), fins with large yellow areas, finlets bright lemon yellow, with narrow dusky edging. Liver not striated . . . . yellowfin tuna, *albacares*

BIBLIOGRAPHY

BEEBE, WILLIAM, AND J. TEE VAN
1928. The fishes of Port-au-Prince Bay, Haiti. Zoologica, vol. 10, pp. 1–279.
1936. Systematic notes on the Bermudian and West Indian tunas of the genera *Parathunnus* and *Neothunnus*. *Ibid.*, vol. 21, pp. 177–194.

FRADE, F.
1931. Données biométriques sur trois espèces de thon de l'Atlantique oriental. Rapp. Cons. Explor. Mer, Copenhagen, vol. 70, pp. 117–126.

FRASER-BRUNNER, A.
1950. The fishes of the family *Scombridae*. Ann. Mag. Nat. Hist., ser. 12, vol. 3, pp. 131–163.

---

[1] Proportions based on head length were measured with calipers. These may not hold for tunas less than 2½ feet long, which usually have relatively short pectorals. It is, therefore, especially important to use the gill-raker count and other characters for small individuals.

Ginsburg, Isaac

1953. The taxonomic status and nomenclature of some Atlantic and Pacific populations of yellowfin and bluefin tunas. Copeia, no. 1, pp. 1–10.

Heldt, Henri

1930. Le thon rouge et sa pêche (*Thunnus thynnus* L.) nouveaux aspects de la question. Bull. Sta. Océanogr. Salammbo, no. 18, pp. 1–69.

Letaconnoux, R.

1950. Le germon (*Germo alalunga* Gmelin). Examen du nombre de branchiospines. Ann. Biol., Copenhagen, vol. 7, p. 63.

Marr, J. C., and M. B. Schaefer

1940. Definitions of body dimensions used in describing tunas. Fish. Bull. U. S. Fish and Wildlife Service, no. 47, pp. 241–244.

Mather, Frank J., III, and C. Godfrey Day

1954. Observations of pelagic fishes of the tropical Atlantic. Copeia, no. 3, pp. 181–188.

Mather, Frank J., III, and Howard A. Schuck

1952. Additional notes on the distribution of the blackfin tuna *Parathunnus atlanticus*. Copeia, no. 4, p. 267.

Morice, Jean

1953. Un essai systematique sur les familles des Cybiidae, Thunnidae, et Katsuwonidae, poissons Scrombroides. Rev. Trav. Inst. Sci. Tech. Pêches Maritimes, vol. 8, fasc. 1, pp. 35–63.

Morice, Jean, and J. Cadenat

1952. Distribution of fish species in the French West Indies. *In appendix 5 of* Fisheries in the Caribbean. Report of the Fisheries Conference held at Kent House, Trinidad, March 24–28, 1952. Port-of-Spain, Kent House, no. 7, pp. 102–122.

Mowbray, Louis L.

1935. Description of the Bermuda large-eyed tuna *Parathunnus ambiguus*, n. sp. Bermuda, Government Aquarium. (Privately printed pamphlet of three pages, no page numbers.)

Navaz, Jose Maria

1950. Contribucion al estudio de las Escombridos de la costa vasca (atun, bonitos y melva). Bol. Inst. Español Oceanogr., no. 31, pp. 1–21.

Rawlings, John E.

1953. A report on the Cuban tuna fishery. Comm. Fish. Rev., no. 15, pp. 8–21.

Rivas, Luis Rene

1951. A preliminary review of the western North Atlantic fishes of the family Scombridae. Bull. Marine Sci. Gulf and Caribbean, vol. 1, pp. 209–230.

1954. A preliminary report on the spawning of the western North Atlantic bluefin tuna (*Thunnus thynnus*) in the Straits of Florida. *Ibid.*, vol. 4, pp. 302–322.

Contribution No. 797

FURTHER EVIDENCE OF DYNAMIC PERSISTENCE AND OF ITS APPLICATION TO FORESHADOWING

By Irving I. Schell

Tufts University and Woods Hole Oceanographic Institution[1]

(Original manuscript received 18 August 1955; revised manuscript received 26 March 1956)

ABSTRACT

Detailed evidence is presented of the relationship of the winter and preceding fall pressure in the Philippines and adjacent areas with the winter precipitation of the North Pacific and North America, affirming the principle of dynamic persistence. An examination of several dynamic-persistence relationships during the 17-year period from 1939–1940 to 1955–1956 shows their foreshadowing performance to be appreciably better than could be obtained from probability and simple persistence considerations.

1. Introduction

The principle of dynamic persistence (Schell, 1947), briefly stated, is as follows: given area B whose weather during a given season is synoptically linked to another area A, where conditions are markedly similar to conditions in this area the season before, the weather in area B must also be related to conditions in area A the season before. For example, if the pressure and storminess in area A are characterized by marked persistence from the September-November quarter to the following December-February quarter and if, furthermore, the December-February pressure and storminess are synoptically linked to the storminess and precipitation in area B the same season, it must follow that the storminess and precipitation in area B during December-February are related to the pressure and storminess in area A during September-November (fig. 1). Thus, dynamic persistence exists when the general circulation meets two conditions: (1) local persistence over a certain area from a season t to the following season $t+1$, and (2) a contemporary synoptic connection between the weather of the area of local persistence and the weather of another area during the season $t+1$. In the sense that an effect of local persistence is translated to another area, the term "dynamic persistence" was chosen to define this property of the general circulation.

In the earlier paper (Schell, 1947), four broad dynamic-persistence relationships were identified. Of these, one will be considered in detail here: the relationship of the September-November pressure in the general area of the Philippines including northern Australia (hereafter referred to as tropical Australasia or simply as tAA) with the following December-February weather over the North Pacific, North America, and adjacent areas.

2. Relationships with the winter precipitation

Philippines, Midway Island, Hawaii, southwest Canada, and northwest United States.—The persistence in the pressure from September-November to the following December-February in the general tAA area, expressed with the aid of the simple correlation coefficient, is $r = 0.77$ (1887–1888 to 1940–1941, $N = 54$) for the area as a whole (Schell, 1947). This considerable local persistence in tAA pressure thus establishes the first condition required for possible dynamic persistence.

We may now assume that the lower the December-February pressure in tAA, for example, the greater the storminess tendency and precipitation in that general area and in the areas traversed by the storms as they subsequently move northeastward across the North Pacific and into southwest Canada and the northwestern United States. Thus, the correlation of the December-February tAA pressures with the con-

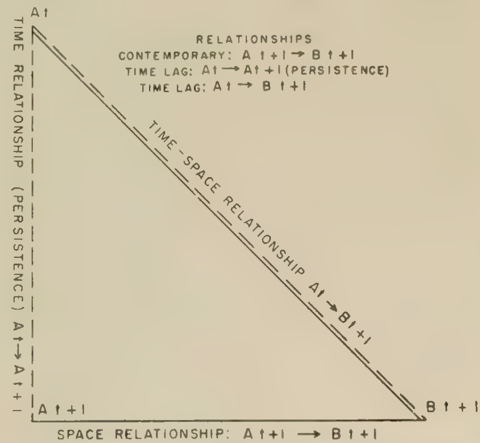
A t
RELATIONSHIPS
CONTEMPORARY: A t+1 → B t+1
TIME LAG: A t → A t+1 (PERSISTENCE)
TIME LAG: A t → B t+1
TIME-SPACE RELATIONSHIP A t → B t+1
TIME RELATIONSHIP (PERSISTENCE) A t → A t+1
A t+1
B t+1
SPACE RELATIONSHIP: A t+1 → B t+1

FIG. 1. Structure of a dynamic-persistence relationship: conditions in area $B(t+1)$ with respect to area $A(t+1)$ and $A(t)$.

---

[1] Contribution No. 797 from the Woods Hole Oceanographic Institution. The research was supported in part by the Geophysics Research Directorate, Air Force Cambridge Research Center.

TABLE 1. Correlation of December-February tAA pressure with contemporary precipitation in North Pacific, southwest Canada, and northwest United States.

Location	r	Period	N
Philippines *	−0.73	1902–1903 to 1939–1940	38
Midway Island	−0.51	1917–1918 to 1940–1941	24
Hawaii (Territory)	−0.52	1905–1906 to 1940–1941	36
SW Canada **	−0.53	1882–1883 to 1940–1941	59
NW United States ***	−0.55	1895–1896 to 1940–1941	46

* Combination of four stations: Manila, Iloilo, Aparri, Legaspi.
** Combination of eight stations: Edmonton, Prince Albert, Calgary, Victoria, Qu'Apelle, Winnipeg, Kamloops, Barkerville.
*** Combination of four states: Washington, Idaho, Montana, Wyoming.

temporary precipitation in these areas yields negative coefficients throughout (table 1). This establishes the second condition required for dynamic persistence.

Next, from these two links, it should follow that below-normal pressure over tAA in the September-November quarter is followed by above-normal precipitation in the areas here considered during the following quarter. The results of the correlation obtained between September-November tAA pressure and the following winter precipitation are shown in table 2.[2] The signs of the coefficients are again negative throughout, and the magnitudes are appreciable. This group of relationships is the foreshadowing member of the two that was to be obtained according to our definition of dynamic persistence.

Of the areas whose winter precipitation has thus far been considered, the Philippines are different from all others in that they are included in tAA. Here the first and third links comprise the entire relationship, the second link being obviated by virtue of the fact that areas A and B are the same.

We are able to consider the relationship with respect to Hawaii in some detail, as a result of several recent studies of precipitation in that area by Solot (1948), Landsberg (1950) and others. The heaviest winter rains in Hawaii are associated with cyclones whose southerly portions pass over Hawaii. Thus it appears, from the mean monthly pressure distributions over that general area prepared by Solot (1948), that heavy winter precipitation is accompanied by a shallow trough of low pressure extending from the Aleutians to the subtropical high-pressure belt. Conversely, with light precipitation, the islands are close to a ridge of high pressure, and a strongly developed Aleutian low is far to the north. Accordingly, the average pressure difference between Hawaii (25°N, 160°W) and Dutch Harbor is approximately 29 mb for dry winter months, as compared with a difference of only approximately 9 mb for wet winter months.

TABLE 2. Correlation of September-November tAA pressure with subsequent winter precipitation in North Pacific, southwest Canada, and northwest United States.

Location	r	Period	N
Philippines *	−0.63	1902–1903 to 1939–1940	38
Midway Island	−0.67	1917–1918 to 1940–1941	24
Kauai Island **	−0.73	1905–1906 to 1940–1941	36
Oahu Island **	−0.74	1905–1906 to 1940–1941	36
Hawaii Island **	−0.56	1905–1906 to 1940–1941	36
All Hawaii **	−0.72	1905–1906 to 1940–1941	36
Hawaii (Territory)	−0.49	1905–1906 to 1940–1941	36
SW Canada *	−0.59	1884–1885 to 1940–1941	57
NW United States *	−0.67	1895–1896 to 1940–1941	46

* See corresponding footnotes to table 1.
** Based on values taken from Solot (1950).

TABLE 3. Correlation of December-February tAA pressure with contemporary precipitation in Aleutian Islands and Alaska.

Location	r	Period	N
Aleutian Islands *	0.02	1911–1912 to 1940–1941	22
Alaska (north)	−0.18	1907–1908 to 1940–1941	34
Alaska (south)	0.24	1907–1908 to 1940–1941	34

* St. Paul and Dutch Harbor combined.

Table 2 shows the individual correlation coefficients for the islands of Kauai and Oahu to be essentially the same, while that for Hawaii Island is appreciably less. This last island is the most southeasterly of the three and, therefore, farthest from the influence of the depressions crossing in a northeasterly direction to the northwest of the island group.

Table 2 also shows the value of r for Hawaii precipitation as derived from Solot's figures to differ from that based on the usual combination of observations for the Territory as a whole. Although the correlation coefficient between the two precipitation series is high ($r = 0.95$, $N = 37$, 1905–1906 to 1941–1942), their difference is sufficient to permit the emergence of a closer relationship with tAA pressures for Solot's than for the standard series. This suggests that Solot's representation of Hawaiian winter precipitation is more revealing of the processes that determine it, at least insofar as the variations in tAA pressures are concerned.

Aleutian Islands and Alaska.—Application of dynamic persistence to the winter precipitation of the Aleutian Islands would be of special interest, as they lie directly in the path of the normal winter North Pacific storms (Haurwitz and Austin, 1944). In contrast to an area well to the north or south of a storm track, however, we cannot expect a storm-track shift of a few degrees of latitude to have an appreciable

TABLE 4. Correlation of September-November tAA pressure with subsequent winter precipitation in Aleutian Islands and Alaska.

Location	r	Period	N
Aleutian Islands *	−0.10	1911–1912 to 1940–1941	22
Alaska (north)	−0.03	1907–1908 to 1940–1941	34
Alaska (south)	+0.26	1907–1908 to 1940–1941	34

* St. Paul and Dutch Harbor combined.

---

[2] The use of the data to 1940 only in the early tables is due in part to the break in record in 1940 at Manila, one of the areas included in the network of tAA pressures. A discussion of the results after 1940 is given below.

Table 5. Correlation of December-February tAA pressure with contemporary precipitation in southeastern United States, Bahamas and Bermuda.

Location	r	Period	N
SE United States *	0.48	1892–1893 to 1940–1941	49
Florida	0.57	1891–1892 to 1940–1941	50
Bahamas	0.58	1882–1883 to 1940–1941 **	55
Bermuda	0.26	1887–1888 to 1940–1941	54

* Florida and coastal portions of North Carolina, South Carolina, Georgia, Alabama, Louisiana and Texas.
** Less 1891–1892 to 1894–1895.

effect on precipitation; the normal extent of a storm area encompasses a much broader zone. Hence, a correlation of the Aleutians' winter precipitation with the contemporary December-February and preceding September-November tAA pressure might be expected to be neutral. The values of the correlations of the tAA pressure with the winter precipitation of Dutch Harbor and St. Paul combined are (tables 3 and 4), indeed, negligible.

Owing to its size and configuration, the position of Alaska as a whole in relation to the northern North Pacific storm track is complex. It would appear, however, that the northern North Pacific storm track, after having passed the Aleutians, runs south and east away from the mainland due to the high mountain ranges along the coast. Accordingly, with below normal pressure in tAA and a southerly shift in the storm track, we would expect a decrease in the precipitation in southern and southeastern Alaska. As is seen from tables 3 and 4, the correlation of winter precipitation in southern Alaska with tAA pressure does yield positive coefficients, in contrast to the negative ones for the Philippines, Midway, Hawaii and southwestern Canada.

Southeastern United States, Bahamas, Bermuda.—It may be expected that an important change in the circulation over the vast area of the North Pacific and adjacent land areas would be reflected in the weather of more distant areas. The writer pointed out earlier (Schell, 1947) that the application of dynamic persistence to the winter precipitation in the North Pacific and northwestern United States, based on tAA pressures, should lead to similar relationships between tAA pressure and winter precipitation in the southeastern United States; an increase in storminess in the northwest United States during winter is associated with diminished storminess over the Gulf of Mexico and the southeast. Thus, a correlation of the December-February precipitation of Florida with the preceeding September-November tAA pressure gave $r = 0.58$ ($N = 50$, 1891–1892 to 1940–1941); lesser values of r were obtained for the Gulf and southeastern Atlantic states or their combination (tables 5 and 6).

Table 6. Correlation of September-November tAA pressure with subsequent winter precipitation in southeastern United States, Bahamas and Bermuda.

Location	r	Period	N
SE United States *	0.48	1892–1893 to 1940–1941	49
Florida	0.58	1891–1892 to 1940–1941	50
Bahamas	0.71	1877–1878 to 1940–1941 **	60
Bermuda	0.40	1887–1888 to 1940–1941	54

* Florida and coastal portions of North Carolina, South Carolina, Georgia, Alabama, Louisiana and Texas.
** Less 1891–1892 to 1894–1895.

We may also assume, from the fact that the winter precipitation of the Gulf and the southeast Atlantic states is markedly influenced by Gulf lows, that the sections bordering on the Gulf would be more strongly influenced than the states as a whole by tAA pressure. Accordingly, a value of $r = 0.48$ ($N = 49$, 1892–1893 to 1940–1941) is obtained between the September-November tAA pressure and the subsequent winter precipitation of the combination: Florida and the coastal portions of North Carolina, South Carolina, Georgia, Alabama, Louisiana and Texas. If these states are included in their entirety, the value drops to $r = 0.34$ ($N = 49$, 1892–1893 to 1940–1941).

Further, since the average position of the polar front extends eastward from the Gulf of Mexico across Florida and thence northeasterly over the Atlantic (Willett, 1944), and as the normal track of Gulf lows follows a course roughly parallel to this position of the front but some distance northward, the winter precipitation of the ocean area east and northeast of Florida would bear the same relation to the September-November tAA pressure as does the precipitation of Florida. Thus, correlation of the winter precipitation of Nassau (Bahamas) and Bermuda with the preceding September-November tAA pressure (table 6) yields $r = 0.71$ ($N = 60$) and $r = 0.40$ ($N = 56$), respectively.

Other United States areas.—From the application of dynamic persistence, on the basis of variations in tAA pressure, to the winter precipitation in the Northwestern United States (negative correlations) and in the southeastern United States (positive correlations), it must follow that the correlation is close to zero for the large area between these two (Schell, 1947). This does not mean, however, a total lack of relationship. With precipitation above normal in the northwest and simultaneously below normal in the southeast, for example, subsequent to a tAA pressure below normal, the precipitation in the area between would tend to be close to normal. Similarly, with precipitation close to normal in the northwest and southeast, subsequent to tAA pressures near normal, the precipitation in the area between would tend to be either above or below normal.

3. Synoptic consideration of relationships with winter precipitation and temperature

Sea-level pressure distribution.—The relationships considered above were assumed to arise through realignments in the pressure field over the North Pacific and adjacent areas following different values of departure from normal of September-November tAA pressure. For a test of this assumption, we have constructed (from the historical series of sea-level charts for 1899 to 1939) composite mean September-November and December-February pressure distributions corresponding to those cases when the September-November tAA pressure markedly differed from normal ($|\Delta| \geqslant 0.7\,\sigma$). The total number of cases in each of the two groups (group A, $\Delta \geqslant 0.7\,\sigma$; group B, $\Delta \leqslant -0.7\,\sigma$) came to eight and six, respectively. Group A included the autumns of 1899, 1902, 1911, 1913, 1914, 1918, 1925, 1930, and the following winters. Group B included the falls of 1906, 1909, 1910, 1915, 1916, 1917, and the following winters. The charts for winter are shown in figs. 2 and 3.

Reference was made earlier to Solot's (1948) study of the composite mean monthly pressure distributions associated with heavy and light winter rainfall over Hawaii. He showed, it will be recalled, very significant differences in the meridional pressure gradient over the North Pacific for the two rainfall groups, the winter months with heavy rain being associated with a weak and diffuse Aleutian low, those with light rains being associated with an intense but constricted Aleutian low far to the north. In accord with the relationship between autumn tAA pressure and the following winter precipitation in Hawaii, we similarly find the group A map (fig. 2) showing a northward displacement of the Aleutian low. The group B map (fig. 3) shows a weaker and diffuse Aleutian low.

Thus, in winters with a weak Aleutian low extending southward (fig. 3), precipitation in Midway and Hawaii tends to be above normal. Also, from the west-to-east trend of the isobars over the Gulf of Alaska and near the Pacific northwest and southwest Canada, the winter precipitation of the latter two areas tends to be above normal.

With lower winter pressures over Mexico (fig. 2), following after autumn tAA pressures well above normal, there would be a greater procession of lows across the Gulf of Mexico and above-normal precipitation over the southern sections of the Gulf states and Florida.

Figs. 4 and 5 give the autumn sea-level pressure distribution associated, respectively, with simultaneous tAA pressures well below (group B) and well above (group A) normal. One notes that the corresponding pressure patterns during the following winter are suggested by the pressure distribution during autumn. Thus, fig. 4 ($\Delta \leqslant -0.7\,\sigma$) shows a higher pressure over the Beaufort Sea and the McKenzie Valley area than is shown on fig. 5 ($\Delta \geqslant 0.7\,\sigma$).

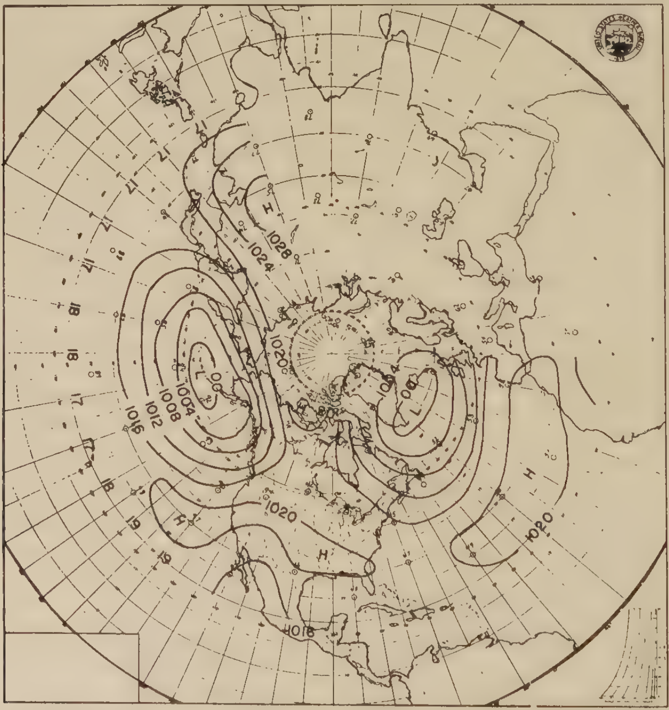

FIG. 2. Composite sea-level winter pressure. Class A, following autumn tAA pressure departure of $\Delta \geqslant 0.7\sigma$.

Another feature distinguishing these two pressure distributions is the difference in pressure along 20°N between the area east of Hawaii (20°N, 150°W) and that immediately to the east of the Philippines. In the case of group B (fig. 4), this difference is 7 mb; it is only 4 mb for group A (fig. 5). It would appear as if the steeper zonal pressure gradient in that region for the cases with $\Delta \leqslant -0.7\sigma$ predisposes a more southerly movement of lows from east of the Philippines northeastward during the subsequent winters.

With reference to the higher winter pressures over the Beaufort Sea and the McKenzie Valley subsequent to autumns with tAA pressure well below normal (fig. 3), it appears that the section of the circumpolar high facing eastern Siberia and western North America is better developed in this instance. Thus, in winters following $\Delta \leqslant -0.7\sigma$, a 1028-mb isobar is seen to reach the McKenzie Valley (fig. 3); this is in contrast to an isobar of only 1020 mb in the winters included in fig. 2. In a winter with strong development of the pressure over the Beaufort Sea, everything else being equal, more cold air would be expected to move southward. Therefore, positive correlation coefficients would be expected between the autumn tAA pressures and the following winter temperatures of Alaska, western Canada, and the northwestern United States (table 7). The positive coefficients obtained are in agreement with the negative coefficients earlier obtained with the winter precipitation, or with the normal tendency for lower temperatures and heavier precipitation to be associated in that general area in winter.

Table 7. Correlation of September-November tAA pressure with subsequent December–February temperature in Alaska, western Canada, Montana, North Dakota, and Minnesota.

Location	r	Period	N
Alaska (north)	0.41	1907–1908 to 1952–1953	46
Alaska (south)	0.54	1907–1908 to 1952–1953	46
Dawson	0.48	1902–1903 to 1952–1953	51
Calgary	0.55	1884–1885 to 1953–1954	70
Edmonton	0.47	1885–1886 to 1953–1954	69
Prince Albert	0.46	1885–1886 to 1953–1954	69
Victoria	0.50	1891–1892 to 1953–1954	63
Winnipeg	0.52	1885–1886 to 1953–1954	69
SW Canada *	0.55	1891–1892 to 1953–1954	63
Montana	0.38	1895–1896 to 1953–1954	59
North Dakota	0.45	1891–1892 to 1953–1954	63
Minnesota	0.42	1891–1892 to 1953–1954	63
3-state area	0.42	1895–1896 to 1953–1954	59

* Combination of Calgary, Edmonton, Prince Albert, Victoria and Winnipeg.

Upper-air pressure anomalies.—Based on Solot's values derived by him for an abbreviated northern-hemisphere network of stations, composite maps of the winter pressure anomalies at the 20,000-ft level were prepared for groups B (fig. 6) and A (fig. 7). Though Solot's figures must be regarded as rather

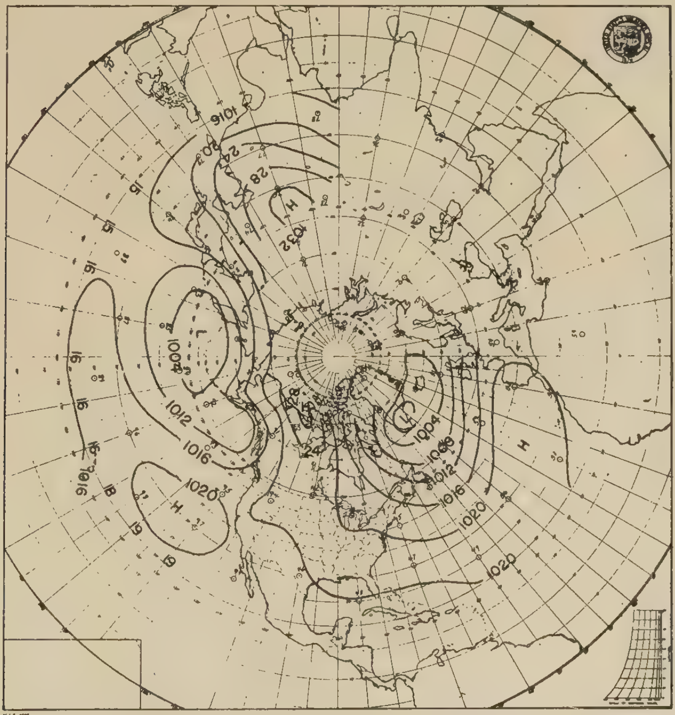

Fig. 3. Composite sea-level winter pressure. Class B, following autumn tAA pressure departure of $\Delta \leqslant -0.7\sigma$.

approximate, it is seen from fig. 6 that the anomalies are negative over the Pacific Northwest and positive over the Gulf and neighboring areas after autumns in which the tAA pressure was well below normal. In contrast, a large positive anomaly over much of the United States, and a field of negative pressure anomalies over the Gulf and adjacent areas, are observed (fig. 7) after autumns in which the tAA pressure was well above normal. Similarly, a negative anomaly is shown over Hawaii and Midway in fig. 6, a positive one in fig. 7. Also, sharp differences between the two cases are noted over the Gulf of Alaska and adjacent areas.

On the whole, the composite upper-level winter pressure distribution for $\Delta \leqslant -0.7\,\sigma$ (fig. 6) indicates a low zonal-index pattern over the general area, in general agreement with the sea-level patterns discussed above. The distribution for $\Delta \geqslant 0.7\,\sigma$ (fig. 7) tends more towards a high zonal index over the general area.

4. Comparison with local persistence

The dynamic persistence relationships shown in tables 2 and 6, when considered for foreshadowing, should turn out closer than relationships that follow from simple or local persistence. Thus, the correlation coefficient $r = -0.72$ (table 2), describing the relationship with the winter precipitation in Hawaii, for example, should be greater than the value of r obtained from correlation of Hawaii's winter precipitation with that during the preceding fall or, simply, November. Table 8 shows a comparison of the values of r thus obtained for Hawaii and some of the other regions here considered with the values of r obtained from a consideration of dynamic persistence. Little local persistence exists in the precipitation of the areas here considered.

5. Performance of relationships from 1939–1940 to 1954–1955

From the evidence presented above, foreshadowings of the winter precipitation appear possible for large areas. Actually, the first attempt to foreshadow the winter precipitation of one of the areas discussed in this article (Montana) was made for the winter 1939–1940 (Schell, 1947). Altogether we have, as this is being written, beginning with the foreshadowing for that winter, a total of 16 years since this type of analysis was first made. Shown in figs. 8 to 10 are the computed and actual departures in the winter precipitation for three of the areas treated here. As might have been expected, the computed and observed values show considerable agreement.

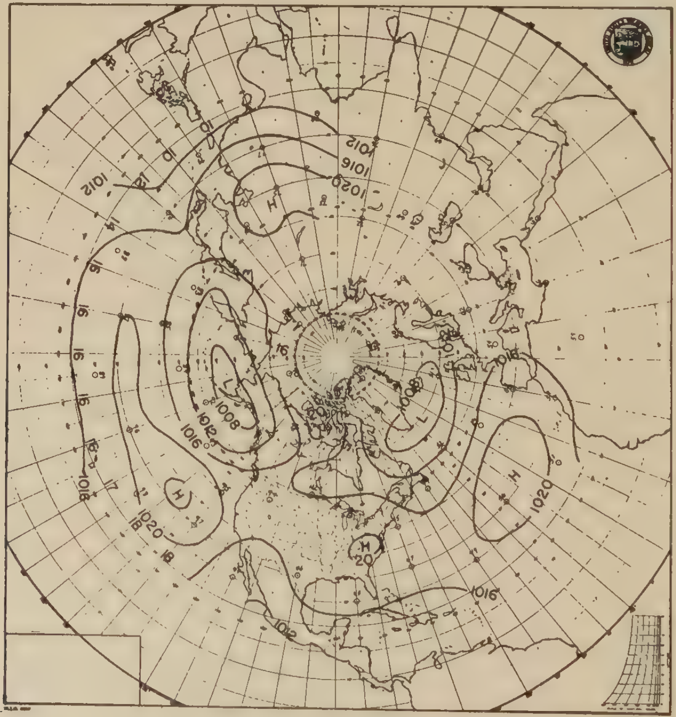

FIG. 4. Composite sea-level autumn pressure, class B.

Table 8. Correlation coefficients of winter precipitation with preceding September-November tAA pressure (dynamic persistence), and with preceding September-November and preceding November precipitation (local persistence).

Location	Sept.–Nov. tAA pressure	Sept.–Nov. precip.	Nov. precip.	Period	N
Midway Is.	−0.67	−0.06	0.09	1920/21–1952/53	32*
Hawaii (Solot)	−0.72	0.00	0.02	1905/06–1945/46	41
NW United States	−0.67	−0.22	0.00	1895/96–1940/41	46
SW Canada	−0.59	−0.15	0.01	1887/88–1940/41	54
Florida	0.58	−0.07	0.10	1891/92–1938/39	48

* Less 1941–1942.

6. Data, methods and computations

The data used in this study were obtained from Clayton (1927; 1934), Clayton and Clayton (1944), U. S. Weather Bureau climatological data, scattered publications, and by correspondence. As a rule, regional values of precipitation and temperature were used. Where these were lacking, use was made of the generally longer records from individual stations.

The effect of skewness of the rainfall data on the precipitation correlation coefficients here computed may, as a rule, be regarded as small. In general, the greater the number of stations within the area and the longer the time interval considered, the less the skewness of a precipitation series; both factors operate to "normalize" the data. Some idea of the relative normality of the precipitation series employed here can be had from a consideration of their extreme values. For example, the extremes in the winter precipitation of Florida, during the 58-yr period from 1891–1892 to 1953–1954, were 70 per cent below and 74 per cent above the long-term average of 8.61 in. Similarly, the extreme December-February precipitation values in the northwestern United States during the period from 1895–1896 to 1953–1954 were 44 per cent below and 58 per cent above the normal. Again, the regional values for southwest Canada (mean of eight stations) winter precipitation, during the period from 1895–1896 to 1953–1954, ran from a low of 56 per cent below the normal for one winter to a high of 57 per cent above normal for another.

We can expect that tropical regions, which are often characterized by very heavy rainfall, would show marked skewness. But here, too, the skewness is decisively reduced when precipitation is considered

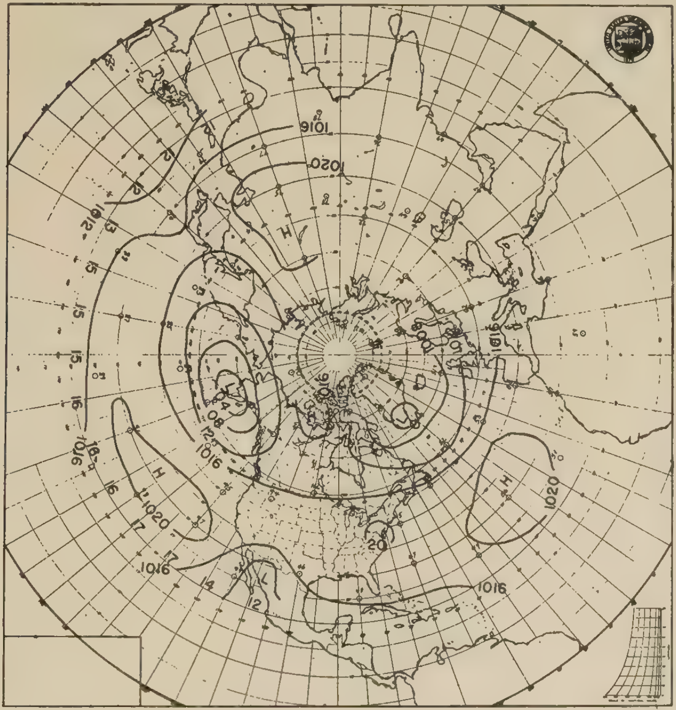

Fig. 5. Composite sea-level autumn pressure, class A.

on a regional basis. Thus, the range in winter precipitation for Hawaii (Solot's index), during the period from 1905–1906 to 1945–1946, is from 56 units below to 45 units above the normal. Although the precipitation distributions of single stations may be considerably skewed, within certain limits they might nevertheless be representative of the regional rainfall, provided rainfall is considered on a seasonal or longer time-interval basis. For, also in the tropics, the basic cause of the year-to-year variations in the seasonal rainfall generally overshadows the local causes; as a result, a small network of stations, or even a single station, is often representative of a wide area. Thus, a correlation of Honolulu's winter rainfall with the corresponding values of the rainfall of Hawaii as a whole (Solot's index) gave $r = 0.88$ ($N = 41$, 1905–1906 to 1945–1946).

TABLE 9. Correlation coefficients of winter precipitation with preceding September-November tAA pressure based on series of years ending with 1940–1941 winter and 1954–1955 winter, except Hawaii, where latter series ends with 1945–1946 winter. Manila not included in tAA pressures for 1941 to 1945, inclusive.

Location	Ending 1940–1941	N	Ending 1954–1955	N
Midway	−0.67	24	−0.64	38
Hawaii *	−0.72	27	−0.67	32
NW United States	−0.67	46	−0.57	60
SW Canada	−0.59	57	−0.48	71
Florida	0.58	50	0.57	64

* Based on Solot's index (27 stations).

7. Stability of relationships

In table 9 are shown the correlation coefficients of September-November tAA pressure with the following December-February precipitation of Midway, Hawaii, northwestern United States, southwestern Canada, and Florida, based on (1) the period ending with the 1940–1941 winter and on (2) the period ending with the 1954–1955 winter. Hawaii is an exception, the data in the required form being available only through the 1945–1946 winter. It appears that the absolute values of r obtained upon inclusion of the data after 1940–1941 show a marked decrease in some cases. The northwestern United States, for example, changes from −0.67 to −0.57.

It has previously been noted that a disturbance in the tAA pressure network occurred in 1941 with the loss of the Manila record, which was not restored until near the end of 1945. But this circumstance could not in any real sense account for the marked change in the values of r that was found. For a correlation of September-November tAA pressure including Manila observations with a form of tAA pressure without Manila gave $r = 0.96$ ($N = 59$, 1882–1940). The decrease in absolute values of r

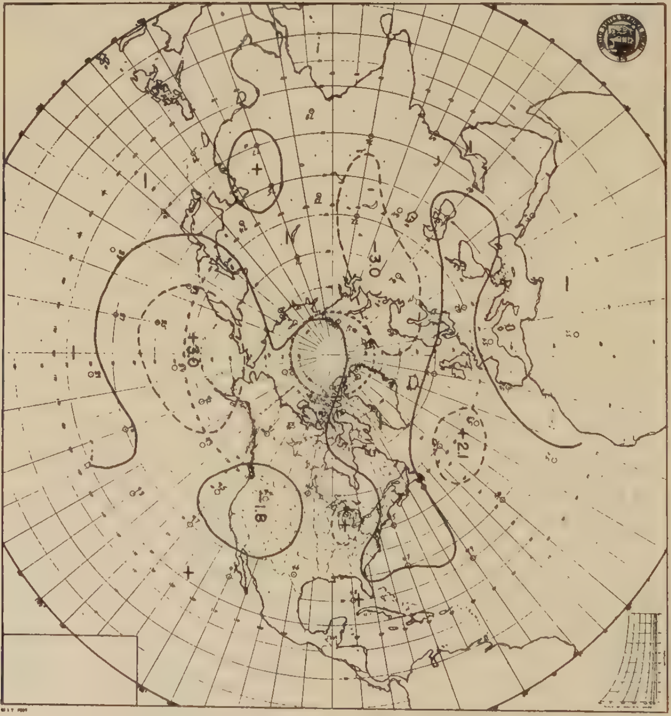

FIG. 6. Composite upper-level winter pressure anomalies, class B.

must therefore be due to other causes. Study of the values of the departures in tAA pressure during the period from 1941 to 1954 revealed only one year in which the departure exceeded the value of the standard deviation. This compares with 15 cases during the preceding 50 years (1891 to 1940). The probability of a departure in excess of σ is 0.32. Such a distribution as was observed during 1941 to 1954 could automatically reduce the large correlation coefficients computed earlier.

On the other hand, the change in the northwestern United States correlation coefficient from −0.67 to −0.57 is not as serious for the relationship as might appear. Fig. 9 shows that, out of the 14 cases covered by the period from 1941–1942 to 1954–1955, agreement as to sign of computed and observed departures occurred in eight cases, disagreement in three cases; the remaining three cases had either an observed or a computed departure of zero. Actually, neither in the case of Midway[3] nor in the cases of the northwestern United States, Florida,[4] and the other areas here considered, have we sufficiently explored the possibilities. The primary objective of this investigation was to find additional confirmation for the principle of dynamic persistence. Insofar as deriving bases for foreshadowing the winter weather is concerned, we would obviously not limit ourselves to simple means of September-November tAA pressure. We would consider in detail the pressure distribution and the pressure development during the season, as well as the extensive background of synoptic and other information of the areas involved. We are likely to obtain a higher score than the one shown by figs. 8 to 10.

8. Discussion

In attempting to explain the variations in the winter precipitation of the various areas through the application of one dynamic-persistence relationship, we have succeeded in accounting for only a part of these variations. This was to be expected, inasmuch as by treating the changes in tAA pressure we have dealt with but one cause of the precipitation of each of these areas. This cause, presumably, is disturbances developing from winter interaction of cold air breaking out from the Asiatic mainland with the warm moist air it encounters in the southwest Pacific. However, while a considerable part of Hawaii's winter precipitation, for example, is due to the southerly extensions of storms whose centers cross the North Pacific in higher latitudes, an important part of the

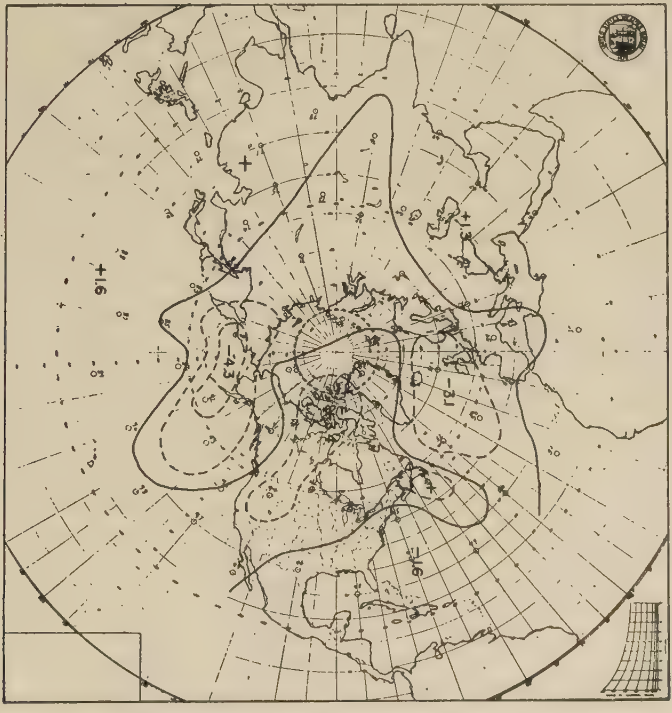

Fig. 7. Composite upper-level winter pressure anomalies, class A.

---

[3] Number of cases of agreement as to sign of departure was nine. There were one disagreement and four neutral cases. See fig. 9.

[4] Number of cases of agreement as to sign of departure was eleven. There were one disagreement and two neutral cases. See fig. 10.

area's winter precipitation is due to storms appearing over Hawaii from the south (Palmer, 1951). Thus, to secure a broader application of the principle of dynamic persistence to Hawaii's winter precipitation, for example, additional relationships must be determined.

Furthermore, the effects of below-normal tAA pressure, for example, on the winter precipitation of each of the considered areas need not always be the same. With the same lower pressure we may have (1) more storms heading northeastward across the North Pacific, or (2) more storms taking a less northerly course, or (3) both. In the specific case of an intense North Pacific high that is associated with below-normal tAA pressure, lower tAA pressure can mean a greater number of storms heading northeastward but not on a less northerly course. In that case, the precipitation of Hawaii would be below normal, while that of the area to the north and west of Hawaii would be above normal. Additionally, with the same below-normal tAA pressure we can have either (1) a small number of deep lows or (2) a large number of shallow lows which can develop into intense storms as they progress to higher latitudes. The simple tracing of the winter precipitation to the preceding mean autumn tAA pressure is, therefore, to be regarded as the initial basic step in the relationship that can be developed. The next stage would be to express the relationships discussed here in terms of detailed indices of circulation.

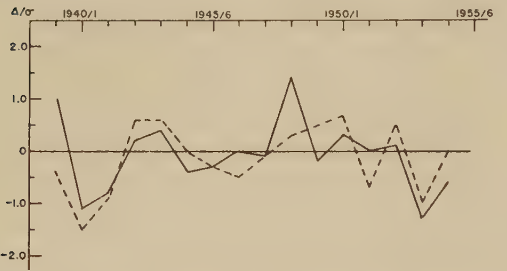

FIG. 8. Computed (dashed) and observed (solid) departures (Δ/σ) from average winter precipitation at Midway Island (1917–1918 to 1938–1939).

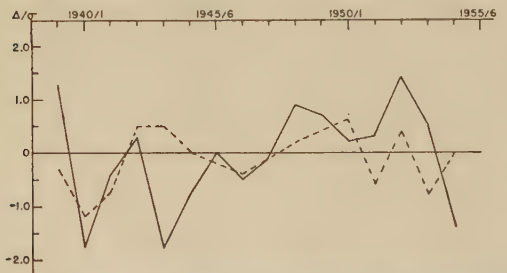

FIG. 9. Computed (dashed) and observed (solid) departures (Δ/σ) from average winter precipitation (1895–1896 to 1938–1939) in northwest United States (Washington, Idaho, Montana and Wyoming combined).

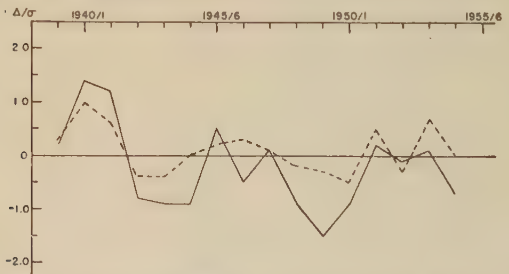

FIG. 10. Computed (dashed) and observed (solid) departures (Δ/σ) from average winter precipitation (1891–1892 to 1938–1939) in Florida.

The principle of dynamic persistence is, by its definition, independent of time scale. It can, therefore, be considered for either a longer or shorter time interval than a season. [See also Schell (1947).] However, by selecting a long time interval for analysis and by first determining the broad sweep of the weather, we can hope more readily to arrive subsequently at the details within this interval through a consideration of additional information.

This does not mean that the longer the time interval considered, the more uncertain the result. As only the average temperature or total rainfall for that interval is considered, the week, month and season become single units of time much the same as the day in daily weather analysis. The difference between the approaches used in daily, weekly, monthly or seasonal analysis lies in the conditions which control the weather peculiar to each interval. In general, the longer the time interval, the greater the area that must be considered for determining the factors exercising control. Size alone is not the sole criterion, however. The tropics and the southern hemisphere appear to exercise a greater control of the winter weather of many areas in the northern hemisphere than the weather in that hemisphere itself. For those areas where the application of dynamic persistence cannot be considered directly, relationships could be sought indirectly, *i.e.*, from their interrelation with areas to which dynamic persistence can be applied, as is the case with the winter precipitation of Florida, for example.

As every area of simple persistence is potentially an area of dynamic persistence, and every area of dynamic persistence may be related to the weather of some other areas, it follows that the approach used here could be employed for possible discovery of many additional foreshadowing relationships. Thus, for example, to the extent to which the December-February precipitation of southern South America, which is produced by lows crossing the South Pacific, could be traced to the contemporary and preceding tAA pressure, the precipitation of a large part of that continent could be foreshadowed in the same manner as the precipitation of some of the areas considered here. Also, for some large areas in the world where no stations exist, the possibility of applying dynamic persistence may be granted from indirect considerations. Thus, the relationship with the winter precipitation of Hawaii and Midway, for example, must hold equally well for hundreds of thousands of square miles of open ocean between and adjacent to them.

The use of tAA pressure, rather than the pressure of the Philippines alone, for correlation with winter precipitation and temperature in the considered areas raises a question. Actually, some correlations of the winter precipitation with the Philippines pressure were carried out. They showed the same kind of relationship as those based on the pressure of the large area, which also includes northern Australia. In every case, however, the correlations based on tAA pressures were better than those using the Philippines pressure alone. This suggests that some of the weak easterly waves, which develop into storms that cross the North Pacific into North America, have their origin south of the equator.

Acknowledgments.—The writer is indebted to Mrs. James F. Hughes, Jr., Mr. Robert F. Malkemes, and Mr. Thomas J. Rockett for carrying out many of the computations.

Note added in proof.—The computed and observed departures of the precipitation for the winter 1955–1956, in continuation of figs. 8 to 10, are, respectively: Midway, 0.5 Δ/σ and -0.1; northwestern United States, 0.4 and 1.3; Florida, -0.3 and -0.8.

REFERENCES

Clayton, H. H., 1927: World weather records. *Smithsonian misc. Coll.*, **79**, 1189 pp.

——, 1934: World weather records. *Smithsonian misc. Coll.*, **90**, 616 pp.

——, and F. L. Clayton, 1944: World weather records. *Smithsonian misc. Coll.*, **105**, 646 pp.

Haurwitz, B., and J. M. Austin, 1944: *Climatology*. New York, McGraw-Hill, 410 pp.

Landsberg, H., 1951: Statistical investigations into climatology of rainfall on Oahu (TH). *Meteor. Monogr.*, **1**, No. 3, 7–23.

Palmer, C. E., 1951: On high level cyclones originating in the tropics. *Trans. Amer. geophys. Union*, **32**, 683–696.

Schell, I. I., 1947: Dynamic persistence and its applications to long-range foreshadowing. *Harvard meteor. Stud.*, No. 8, 80 pp.

Solot, S. B., 1948: Possibility of long-range precipitation forecasting for the Hawaiian Islands. *U. S. Wea. Bureau Res. Pap.*, No. 28, 52 pp.

——, 1950: Further studies in Hawaiian precipitation. *U. S. Wea. Bureau Res. Pap.*, No. 32, 37 pp.

Walker, G. T., 1924: Correlations in seasonal variations in weather, IX. *Mem. India meteor. Dept.*, **24**, 275–345.

Willett, H. C., 1944: *Descriptive meteorology*. New York, Academic Press, 310 pp.

Contribution No. 798

METHODS AND PRELIMINARY RESULTS IN A STUDY OF MINERALS FROM THE EASTERN GULF OF MEXICO

BY

NORA GLADWIN FAIRBANK

Reprinted from the Journal of Sedimentary Petrology for September, 1956

JOURNAL OF SEDIMENTARY PETROLOGY, VOL. 26, NO. 3, PP. 268–275
FIGS. 1–4, SEPTEMBER, 1956

METHODS AND PRELIMINARY RESULTS IN A STUDY OF MINERALS FROM THE EASTERN GULF OF MEXICO[1]

NORA GLADWIN FAIRBANK
Woods Hole Oceanographic Institution, Woods Hole, Massachusetts

ABSTRACT

The special problems of mineralogical studies of ocean bottom sediments are discussed, and methods of preparation and study described which are particularly applicable to these problems. The abundance of minerals in samples from the eastern Gulf of Mexico varies greatly, and their distribution in relation to fragments of organic origin can be correlated with the bottom topography.

INTRODUCTION

The study of minerals found in ocean-bottom sediments is complicated by a number of special conditions not found in dry-land or river samples. These difficulties arise from the large areas to be covered and the practical problems of getting a sample from under water. In spite of many recent developments by which we can accurately locate the position of the ship, sampling is still somewhat a matter of chance. The coring tube drops through the water, is driven into the ocean bottom below the ship, and with luck an undisturbed core from the sea-floor is hauled up at the end of a wire which may be more than a mile long. Meanwhile the ship is drifting, and it is never possible to go back and get another sample at precisely the same spot. In an area where the slopes are steep or the lithology changes, one never has enough samples to make as detailed a study as one would like; the significance of small changes in slope or in the character of the sediments does not appear until the material has been brought back and studied in the laboratory.

SPECIFIC PROBLEMS IN MARINE MINERALOGY

Although much work has been done in mapping and describing marine sediments, there still remain vast areas of the ocean where we have no knowledge of the character of the bottom, and even in regions where studies have been made, our information is scanty by dry-land standards. The writer is at present engaged in a study of minerals from the eastern Gulf of Mexico, covering an area about the size of New England. The *Atlantis*, research vessel of the Woods Hole Oceanographic Institution, cruised in these waters in 1951, taking observations and samples at a total of 225 stations, but at some of these, no sample could be obtained, either because the bottom was hard rock, or because of mechanical or weather troubles. The best coverage of an area would be obtained by locating the stations in a grid pattern, with the size of the grid determined by the problems to be studied, but that is not practical at sea. The track chart (fig. 1) shows the various courses sailed in order to locate the stations along lines which are continuous from close inshore out into the deep water of the central Gulf. The number of traverses which can be made is limited by the time available; along each traverse the stations are closer together inshore because of the increasing mechanical difficulties as the water deepens.

METHODS OF PREPARATION

A mineralogist approaching the study of such an area as the eastern Gulf of

---

[1] Contribution No. 798 from the Woods Hole Oceanographic Institution.

Mexico must bear these factors in mind in his choice of methods of preparation and analysis of the material. In most cases, oceanography being still a young field of science, he will start with a blank map; the nautical charts have such notations as "Mud," "Sandy," "Rocky," but that will be the extent of his information about the character of the sediments he is to study. In an area of any size, there will necessarily be a wide range of material to handle: coarse and fine, uniform and mixed. In order to arrive at results which will be

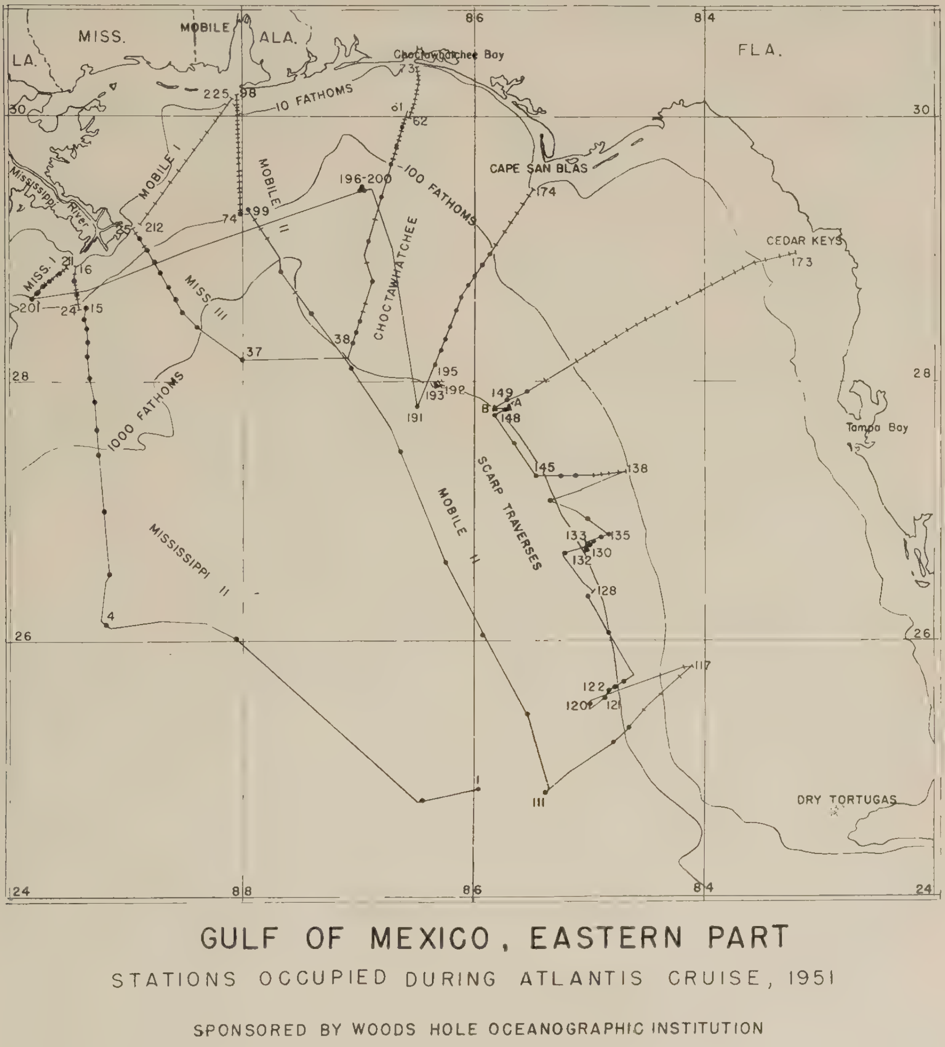
MISS.
MOBILE
ALA.
LA.
FLA.
Choctawhatchee Bay
10 FATHOMS
100 FATHOMS
1000 FATHOMS
CAPE SAN BLAS
CEDAR KEYS
Tampa Bay
DRY TORTUGAS
Mississippi River
MOBILE I
MOBILE II
MOBILE III
MISS. I
MISS. III
MISSISSIPPI II
CHOCTAWHATCHEE
SCARP TRAVERSES
30
28
26
24
88
86
84
225
98
73
61
62
196-200
174
173
74
99
212
21
16
201
24
15
37
38
195
193
192
191
149
A
B
148
145
138
133
135
130
132
128
117
122
120
121
111
1
4
GULF OF MEXICO, EASTERN PART
STATIONS OCCUPIED DURING ATLANTIS CRUISE, 1951
SPONSORED BY WOODS HOLE OCEANOGRAPHIC INSTITUTION

FIG. 1.—Traverses along which samples were taken. At those stations represented by round dots, long cores (not included in the present study) were taken as well as Phleger cores or scoop samples. At stations marked by triangles, a rock dredge was used. At the remaining stations, either short cores or scoop samples were collected. The stations are numbered in the order in which they were occupied, so that they are not necessarily consecutive along any one traverse.

comparable over the whole area, each sample must be treated in a similar way. Due to the small size of the coring tube and the fineness of deep water sediments, the material available for mineralogical study is often very small in quantity. This unfortunately makes it impossible to use procedures such as feldspar staining or magnetic separation which are so useful in most mineralogical studies. Where the total weight of heavy minerals is one milligram or less, for example, it is impractical to try to separate the magnetic grains and weigh them separately, as mechanical losses will be far too large in proportion to the total sample. Fortunately optical methods can be applied to samples of any size, and have the added advantage that they do not affect the sample itself, as chemical methods do. For these reasons the writer has come to depend chiefly on the polarizing microscope, with which it is possible, in most cases, to identify even single grains.

In the literature on sedimentary petrography there are many different methods described for the preparation of samples, but they assume an ample supply of material, and advise choosing a method of treatment particularly suitable to the kind of sediment to be studied. For the reasons given above, it is considered preferable in this case to use the same basic procedure for all samples, of whatever kind or size. As interest in submarine geology increases, more and more workers will be drawn into this field, so that the following account of the preparation procedures worked out by one "submarine mineralogist" may be of interest to others who have met or will have to solve similar problems.

The samples being considered here have been collected by two different devices: the Phleger bottom sampler (described in Phleger and Parker, 1951, pp. 3–4) which provides cores one inch in diameter and up to $1\frac{1}{2}$ feet long, of which the top half inch is being studied at present; and a scoop (either a commercial orange peel or the dredge described in Stetson, 1938, pp. 7–8) which brings up as much as a pint of material, but this is mixed and not a stratified core. Cores are taken wherever possible, but the tube will only penetrate soft sediments, and the scoop must be used whenever hard sand is found. In practice this is usually close to shore.

In the laboratory, the samples are first sieved, weighed, and a mechanical analysis done in the usual way; this is outside the province of the strictly mineralogical study. Similarly, the organic material, although of great importance, has here been ignored as far as possible, and the identification of shells and foraminifera has been carried out by others. The mineralogist, then, begins with a dry, clean sample of all the material larger than .074 mm; the grains smaller than that, which passed through the 200-mesh sieve, have in this study been discarded after the mechanical analysis and would in any case be too fine for satisfactory microscopic identification.[2]

The first step is to look over the samples and see if any of them have large pieces of material which would stick in the funnel and make trouble later. If they do, pass the sample through a 20-mesh sieve; if this coarse fraction is all shells, the mineralogist can ignore it, but if it appears to be rock fragments, it will have to be broken up, using such methods as described by Krumbein and Pettijohn (1938, pp. 310–314) and added to the original sample.

Next, separate the light and heavy minerals, by floating the light minerals in bromoform. As this is a standard procedure (Krumbein and Pettijohn,

---

[2] X-ray diffraction methods have not yet been applied to material from this area. It is hoped that a correlated study, using optical methods as described here on the fraction coarser than .074 mm in diameter, and X-rays on the finer fraction from the same cores, can be carried out in the near future.

1938, p. 343) there is no need to describe it here.

If the light fraction is made up chiefly of foraminifera, they will mask any minerals present. Some of the foraminifera, particularly those in which air is trapped, will float in a liquid of specific gravity 2.51. Although there are minerals with a lower specific gravity than this, they are not those which are likely to occur in significant amounts in ocean bottom sediments. Therefore, with samples in which foraminifera predominate it is worth while to make a second separation in the same manner as the first, using a mixture of bromoform and acetone such that the specific gravity is 2.51. This is a good use for the bromoform washings from the first separation, as bromoform can seldom be recovered pure enough to have its standard specific gravity of 2.87.

Then the separate fractions must be weighed; in the case of very small samples, the danger of loss in handling can be reduced by the following procedure: weigh the empty bottle or vial in which the sample is to be kept, add the sample from the filter paper on which it was caught after separation, and weigh the bottle plus the sample. This requires an extra weighing as compared with using a weighed beaker for measuring the samples, but is more accurate with very small samples.

METHODS OF STUDY

The final problems remaining before one actually begins to identify and count minerals, are to decide in what medium to mount the samples, and how to select that part of the sample to be examined. Krumbein & Pettijohn (1938, p. 343) recommend permanent mounts of canada balsam and piperine for the light and heavy minerals respectively. These have obvious advantages and are widely used. The writer feels, however, that where identifications must often be made on the basis of very few, or even single grains, the greater flexibility of immersion oils makes them preferable. A grain can often be turned so that it can be observed in different orientations, and if necessary it can be removed from one liquid to another until the indices of refraction are determined. Also, if it seems advisable to make X-ray studies of some baffling mineral or to dissolve the sample in acid to eliminate organic material, it is far easier to wash off the oils than to remove grains from a hard mount. As each slide is finished, it is washed with acetone onto a filter paper, and the grains put back in the bottle when they are dry.

The method used to select the grains for study is determined by the size of the sample. Where the sample is very small, one simply taps the entire contents of the bottle into a drop of oil on the slide. Where the sample is large, a microsplitter[3] can be used to bring it to a manageable size. But most of the samples from the eastern Gulf of Mexico are too big to examine all at once and yet so small that even a microsplitter is too crude. A number of methods have been tried, and the one used by the author for most samples has been quick and easy to do and at the same time seems to obtain a sample representative of the whole. If the depth of the sample in its bottle is not more than about a quarter of an inch, one can moisten a fine needle by rolling it in the drop of oil standing ready on a slide, and dip the needle straight into the bottle, being sure to go to the bottom. The needle must be withdrawn carefully, so that all the grains which have stuck to it will be transferred to the slide. This is repeated until a large enough sample is on the slide, perhaps one or two thousand grains.

In order to test the validity of this method as compared with splitting, in one sample several slides were prepared by each method, and detailed counts made of every slide. The variation between slides was noticeably less in the group of slides where the needle had been used than in that prepared with the splitter. However, if the depth of the sample in the bottle was over a quarter of an inch, the variation between slides increased rapidly so that the sampling error became too great.

---

[3] Similar to a Jones sample splitter (Krumbein & Pettijohn, 1938, p. 45) but smaller, with the splitting compartments about 3 mm in width and pans $5\frac{1}{2} \times 2\frac{1}{2} \times 1$ cm.

All the minerals in a slide are then identified, and a count made. The number of grains counted depends on the number of mineral species present, and their abundance with respect to organic material. At least 200 grains of the light and of the heavy minerals are counted (Dryden, 1931), but where the slide is mostly organic remains (shells and shell fragments, sponge spicules, worm tubes, fecal pellets, and so forth) it may be necessary to examine thousands of grains in order to find even a few minerals. The writer begins the count (after the minerals present have been identified) by counting every particle. If after several hundred have been counted it appears that the organic-mineral ratio is greater than 100 to 1, only minerals are counted, and an estimate made of the total number of grains in the slide. If necessary, more than one slide is made in order to find a reasonable number of minerals.

In some cases, the amount of organic material is so overwhelming that the minerals must be concentrated chemically. Dissolving the sample in dilute hydrochloric acid unfortunately does not solve the problem as neatly as one would hope. Many shells or tests contain

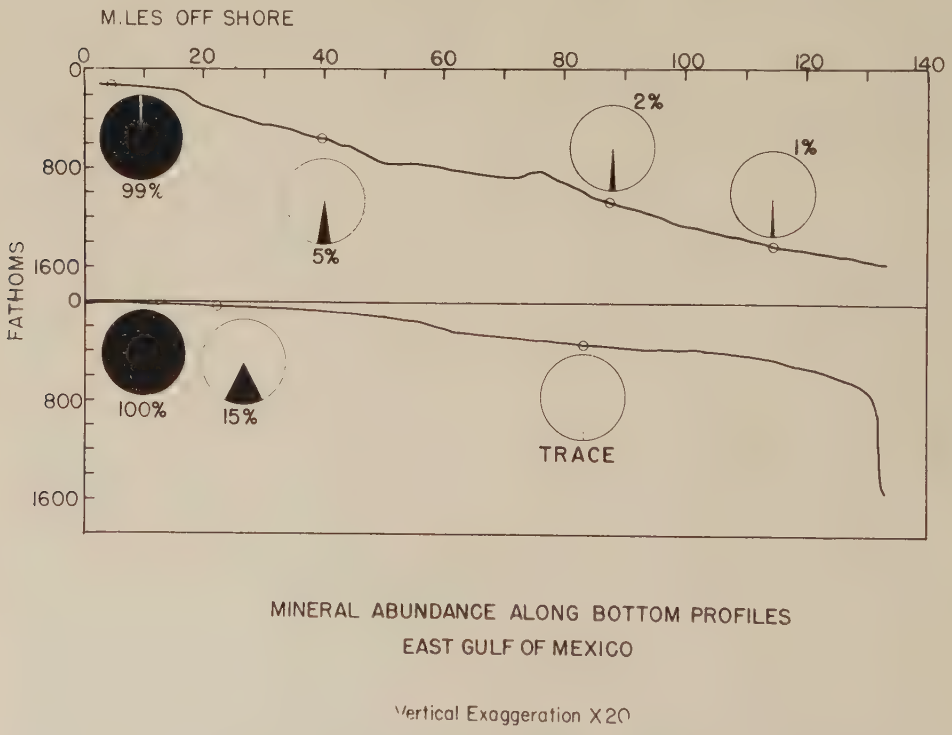

FIG. 2.—Minerals are represented by the black portions of the circles, and fragments of organic origin by the white segments. The upper profile is along the Mississippi II traverse (See fig. 1), and the lower one is Choctawhatchee; for the sake of clarity not all the stations on either line are indicated in this figure.

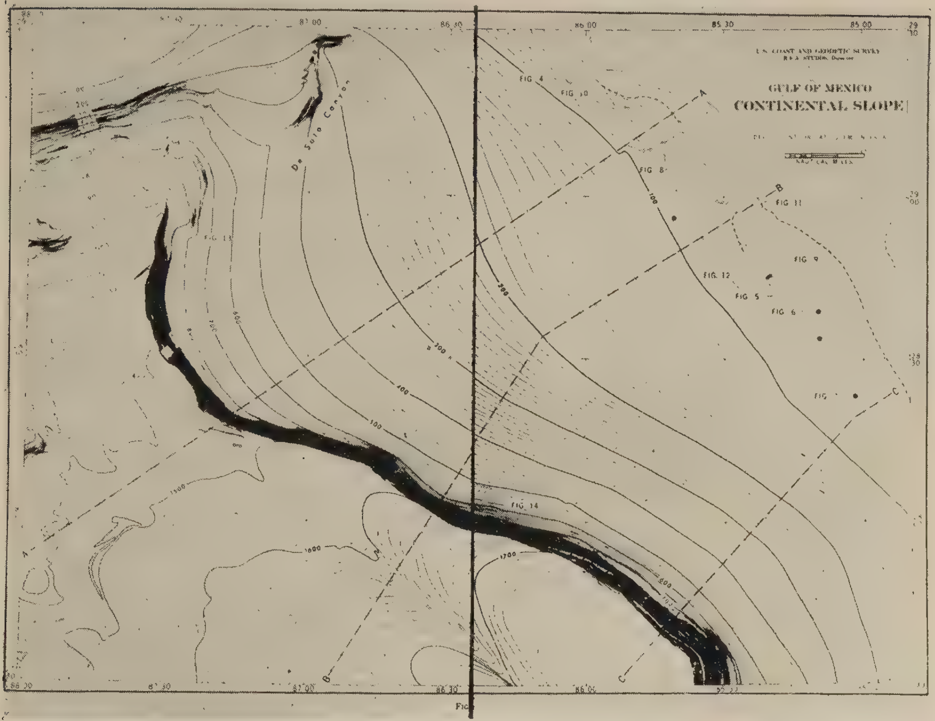

FIG. 3.—A portion of the scarp off the west Florida coast (After Jordan, 1951).

chitinous or other material which is insoluble in acid; hence the residue after acid treatment is so full of a very fine brown sludge that the minerals are still quite effectively masked. The following procedure is not ideal, but is the best that the writer has been able to find. The sample, after microscopic examination as described above, is put in dilute hydrochloric acid (1:10). After effervescence has stopped, most of the cloudy liquid is decanted, and the remainder, solid and some liquid, put in a separatory funnel. If the sample is small enough, the acid treatment can be done right in the funnel. Water is added, and the whole shaken. A few minutes are allowed for settling; as soon as all the material which looks coarser than 200-mesh has settled, the sediment is drawn off onto filter paper and the remainder discarded. The paper is washed several times with fresh water and allowed to dry. The residue is weighed and studied under the microscope as before, and the ratio of minerals to organic remains determined again. The dissolved material is assumed to be all organic, unless acid-soluble minerals were found in the first microscopic examination.

PRELIMINARY RESULTS

In drawing any conclusions from a study of this sort, one must keep in mind the fact that one is dealing with only a part of the whole sample: that fraction coarser than .074 mm diameter. The following statements apply only to this relatively coarse material, and may be severely modified by future studies of the clay fraction.

The ratio between minerals and material of organic origin has proved to be significant in the eastern Gulf, where the proportion of minerals decreases with increasing distance from the coast. The circle diagrams and percentages in figure 2 illustrate this distribution: near the coast, minerals predominate, while about thirty miles and more off shore, shells make up more than ninety percent of the samples; in some cases the mineral-organic ratio is more than one to a thousand. Not enough samples have yet been studied to determine how distance from shore, river discharge, depth, and steepness of slope affect the change from coarse, rounded quartz sand about a half millimeter in diameter near the beach, to a fine sediment of shell fragments off shore.

Figure 2 also shows the two main kinds of bottom topography found in this area: an irregular but steady downward curve with no marked break in slope, such as is found off the Mississippi Delta, and a smooth, nearly flat plain ending abruptly in a major fault scarp, which is characteristic of most of the northern Florida Gulf coast (fig. 3 and Jordan, 1951). The *Atlantis* traversed this scarp seven times in order to cover as much of the

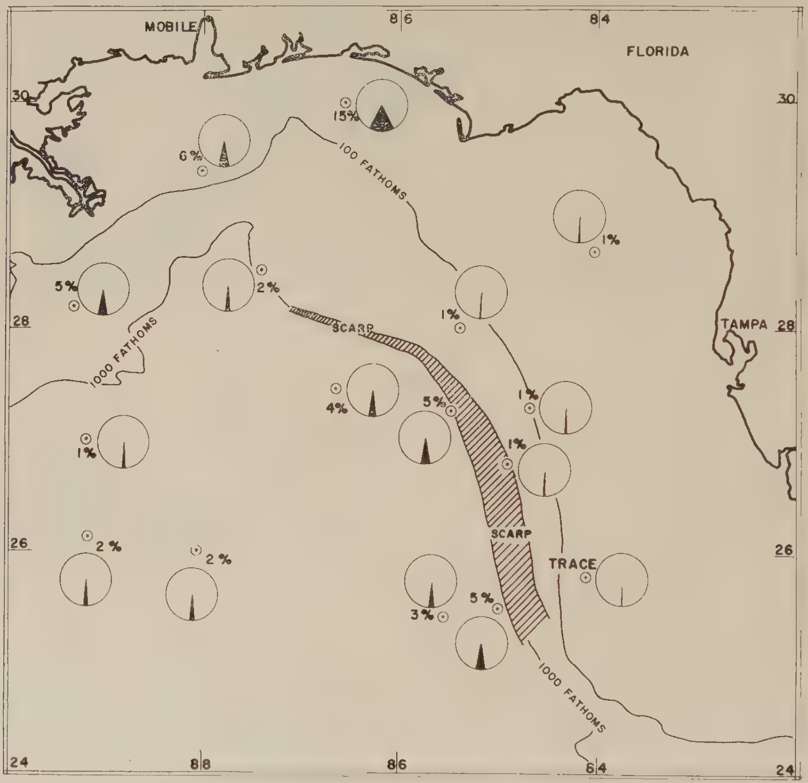

GULF OF MEXICO, EASTERN PART

RATIOS OF MINERAL GRAINS TO SHELL FRAGMENTS

FIG. 4.—Minerals are represented by the black portions of the circles, and fragments of organic origin by the white segments. The scarp area is represented by hatching; it extends further to the east and south beyond the area covered by this study. For the sake of clarity not all the samples studied have been represented by circle diagrams, but they all, so far, follow this pattern of distribution.

area as possible. But where on land such a cliff with rock outcropping all along it would be a mine of information, and would be intensively mapped, here it is covered by over a mile of water, and we must content ourselves for the present with 34 samples from a scarp 300 miles long and 3000 to 7000 feet high.

So far, minerals from only ten samples in this area have been studied, but they suggest an unexpected mineral-shell relationship (fig. 4). In this area, as is usual off shore, the minerals comprise five percent or less of the total. But even though there are few minerals available, their distribution varies significantly. Above the scarp to the east, minerals are almost absent: in one case there are more than a thousand grains of organic origin for each small chip of quartz, and there is no other mineral species at all. But immediately below the scarp, minerals are more abundant, ranging from three to five percent of the total sample; there is also a large variety of minerals, as many as twenty different species being found in one sample.

CONCLUSION

Where do these minerals come from? If they had been washed over the scarp from the Florida coast they should also be present above the scarp. If they are derived from the west, from the Mississippi and the other rivers of the central Gulf coast they should increase steadily in abundance up to the river's mouth. That is not the case in the samples studied so far; in the deep water samples the mineral frequency decreases toward the west, and a higher mineral concentration only reappears near the coast. The most likely source seems at present to be the rocks of the scarp itself; the few rock fragments collected are a fine limestone marl made up of foraminifera, but much of the Florida section may be present. Future work will have to confirm this relationship or lead to some other hypothesis. As more of the samples are examined, detailed comparisons will be made of the distribution of different mineral species, and a clearer picture should emerge of the mineralogy of the eastern Gulf of Mexico.

BIBLIOGRAPHY

Dryden, A. L., Jr., 1931, Accuracy in percentage representation of heavy mineral frequencies: Nat. Acad. Sci. Proc., v. 17, no. 5, pp. 233–238.

Jordan, G. F., 1951, Continental slope off Apalachicola River, Florida: Am. Assoc. Petroleum Geologists Bull., v. 35, no. 9, pp. 1978–1993.

Krumbein, W. C., and Pettijohn, F. J., 1938, Manual of sedimentary petrography. D. Appleton-Century Co., New York. 549 pp.

Phleger, F. B., and Parker, F. L., 1951, Ecology of Foraminifera, northwest Gulf of Mexico: Geol. Soc. America Memoir 46, 46 pp.

Stetson, H. C., 1938, The sediments of the continental shelf off the eastern coast of the United States. Papers in Physical Oceanography and Meteorology. Massachusetts Inst. Technology and Woods Hole Oceanographic Institution. v. 5, no. 4, 48 pp.

Contribution No. 799

Deep-Sea Research, 1956, Vol. 3, pp. 152 and 153. Pergamon Press Ltd., London.

LETTER TO THE EDITORS

An oceanographical curiosity : the perpetual salt fountain

In many tropical and subtropical regions of the ocean the warm surface layers have a salinity exceeding that found in the colder waters of polar origin below. If a long tube were lowered from the surface to depth of low salinity water, and the deep water were slowly pumped to the surface through the tube, and the pump then disconnected, the water would continue to flow, by itself, forever. This remarkable phenomenon occurs because slow motion through the tube allows the water inside to attain the same temperature as the surrounding water. Its salinity, and hence density, is therefore less than that of its surroundings outside the tube, and hence the entire column of water inside the tube is buoyant with respect to the fluid outside at the same level. If the direction of pumping is reversed, so that the fluid initially goes downward, it will of course continue to flow downward forever on account of its excess in density over that of the water outside the tube.

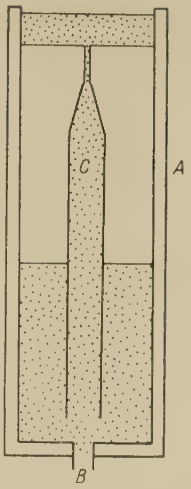

Fig. 1. Laboratory experiment to demonstrate the salt fountain, showing outside glass tube *A*, with hole in the bottom for filling *B*, and inner glass tube *C* to produce the fountain. The shading indicates the coloured water after the fountain has been in operation for some time.

Although the attempt has not been made it is likely that in the Central North Atlantic with a tube 2,000 meters long, one might develop a pressure head of as much as two meters at the surface. A simple experiment on a laboratory scale will demonstrate the principle, however. A vertical glass tube, about three inches in diameter (A in Fig. 1) is filled halfway with hot fresh water. Then the same quantity of slightly coloured cold fresh water is introduced through a hole in the bottom (B) care being taken not to produce too much mixing at the interface between the two fluids. An inner tube, *C*, slightly restricted at the top to suppress secondary flows that tend to develop inside it, is now gently lowered into the fluid. The operator keeps his finger over the upper end until the lower end is below the interface so as to fill the inner tube entirely with the lower fluid. If this is done slowly enough so that the coloured water in the inner tube equalizes temperature with the fluid outside at the same level, it will stay above the outside interface even after the top of the tube *C* is below the surface of the upper layer. After the system has stood for a few minutes there will be evidence of small secondary motions and circulations inside tube *C*, but these appear to be associated with the slow cooling and warming of the system as a whole. Up until this stage of the demonstration there has been no salinity difference involved. Now we add with gentle stirring a little hot salt water to the upper layer outside tube *C*, but not enough to upset the overall stability of the two layered system outside tube *C*. Immediately a strong jet of coloured bottom water starts to flow from the nozzle at the top of tube *C*. A third layer – fresh, warm and coloured – forms at the very top. The flow continues until the conditions of the experiment break down. In the ocean, however, the stratification is maintained by large scale climatological influences, and the tube could have no reaction upon the external situation, so that it would flow forever.

It seems premature to speculate upon the improbable practical importance of this phenomenon for pumping up nutrient rich deep water to the surface for fish-farming applications, or its inverse for removing waste products to the deep water. As a power source it is quite unpromising. Thus it remains essentially a curiosity.

HENRY STOMMEL
ARNOLD B. ARONS
DUNCAN BLANCHARD

Contribution No. 799 of The Woods Hole Oceanographic Institution, Woods Hole, Mass., U.S.A.

Printed in Great Britain by The Salisbury Press Ltd., Publicity House, Wilton Road, Salisbury, Wilts. (95255)

Contribution No. 801

PHYSICAL OCEANOGRAPHY OF THE GRAND BANKS AND THE LABRADOR SEA IN 1955[1]

By Floyd M. Soule and J. E. Murray
(U. S. Coast Guard)

As in each of the seasons since 1948, in 1955 the USCGC *Evergreen* served as the oceanographic vessel of the ice patrol. Descriptions of the equipment in the laboratory and on deck for carrying out the mission of ice patrol oceanography are to be found in earlier bulletins of this series. The only change in 1955 was the addition of equipment for taking 40-gallon water samples from subsurface levels down to depths of 150 meters. A continuous length of polyethelene plastic pipe was joined to an axial brass pipe and this ended externally at a packed slip joint where connection was made to a gear pump and valving system which permitted priming of the pump and plastic pipe with water from the ship's fire main. The plastic pipe was rove through a light 30-inch diameter fairlead sheave and the intake end lashed to the manila leader between the sinker and the 5/32-inch wire rope which is normally used for handling Nansen water bottles. A bathythermograph was suspended from a bridle just below the sinker. It was found necessary to control the plastic pipe by securing it to the wire rope at intervals of about 15 meters as the pipe and wire were paid out. This was accomplished by means of snap hooks lashed to the pipe and snapped around the wire at points where clamps from Nansen water bottles were clamped to the wire Priming was completed before submerging the intake end of the pipe. Once submerged, pumping continued until all desired levels were sampled. At each sampling level, it was of course necessary to flush the pipe and pump system before taking the sample Because of the friction head involved the pumping rate was slow with 3/4-inch pipe. Trials of a 1½-inch diameter pipe resulted in little saving in time as the increased pumping rate was overbalanced by the necessity of flushing four times the volume of pipe. Buoyancy of the pipe was a consideration and it was found that about 200 pounds of bronze sinkers were necessary with the 1½-inch pipe. The method described was found to be feasible in quiet water for depths down to about 150 meters. For deeper samples other methods of collection are more likely to be productive.

---

[1] To be reprinted as Contribution No. 801 in the Collected Reprints of the Woods Hole Oceanographic Institution.

(Extract from U. S. Coast Guard Bulletin No. 41. Pages 59–114.)

Partly because of the small quantity and disposition of the ice and partly because of a boiler casualty on the *Evergreen*, only three dynamic topographic surveys were made during the 1955 season and of these only one covered the usual area between Flemish Cap and the Tail of the Grand Banks. As the *Evergreen* left Argentia on 30 March to begin the survey work no bergs had yet been reported except in the northern part of the Grand Banks area and as a result even the major features of the current pattern were unknown. The first survey was planned to explore the probable areas of hazard should bergs enter the area along the northeastern slope of the Grand Banks. Surface temperature reports prior to the beginning of the survey work had been atypically warm and in the neighborhood of the Tail of the Banks lacked the contrast usually present there in the early part of the season. Hence it appeared that Labrador Current water did not extend much to the west of the 50th meridian in that vicinity. The first survey was planned to extend from just west of the Tail of the Banks northward along the eastern slope to about the latitude of Flemish Cap. The work of collection of data began at the southern end of the area at station 5741 on 1 April and progressed northward. On 6 April, shortly after leaving station 5770, it was necessary to heave to to await better weather for continuing the oceanographic work. Work was resumed about 8 hours later. Again on the evening of 7 April after completion of station 5775 it was necessary to heave to on account of weather, this time for 27½ hours. It was necessary to heave to on account of weather a third time, after completion of station 5818, on the evening of 13 April. Work was resumed on the evening of 14 April and no further interruptions occurred. The collection of data was completed on the afternoon of 15 April, 87 stations having been coccupied. The *Evergreen* then proceeded to Argentia, arriving there on 16 April.

The *Evergreen* departed Argentia on the morning of 25 April to begin a second survey. This survey was planned to cover the area seaward of the northeastern slope of the Grand Banks from the northern end of the area covered by the first survey northwestward as far as sea ice conditions permitted. The Bonavista triangle was encumbered by ice. For about a week previous to the beginning of the second survey a stationary barometric pressure low had been centered near the eastern edge of the Bonavista triangle and it was surmised that, with the movement of the low northward out of the area, the ice might spread southeastward. Accordingly the survey was begun at the southeastern edge of the Bonavista triangle and progressed southeastward. The work of collection of data began on the morning of 26 April at station 5828. On the afternoon of 28 April a fire which disabled the heating boiler and evaporator left the ship without heat, and the ensuing cold and condensation posed problems of maintaining health and reasonable comfort which dictated the curtailment of the survey.

On 1 May the quiet weather came to an end. By noon it was too rough to carry out the GEK jog pattern and by 1210 it was necessary to heave to. At 0400 the next morning it was possible to proceed toward the next station, 5868, but progress was slow and the GEK program could not be resumed until nearly noon on 2 May upon departure from station 5870. No further extended delays were encountered and the last station, 5877, was completed on the morning of 3 May. The *Evergreen* then proceeded to Argentia, arriving there on 4 May. During the survey 50 stations were occupied.

The *Evergreen* proceeded to Boston, where repairs to the heating boiler and evaporator were accomplished, and then returned to Argentia. On the morning of 1 June departure was taken from Argentia for the purpose of making a survey of the area northward of the Grand Banks. The northern limit of the survey was set at about the latitude of the Strait of Belle Isle and was determined by the southern limit of the sea ice. The eastern limit of the survey was far enough east to include the eastern margin of the Labrador Current and to include an adequate number of deep water stations to serve as reference stations for the numerous sections of anomaly of specific volume necessary for the determination of the dynamic heights of the shallow water stations. The Bonavista triangle was included in this survey and a network extended the surveyed area from the triangle to Flemish Cap. The work of collection of data began at the offshore end of the northernmost section, station 5878, on the morning of 3 June and progressed from north toward south. Very nearly ideal conditions of wind and sea prevailed throughout the survey and no delays were encountered other than that occasioned by the necessity of skirting the edge of field ice along the northern and western edges of the surveyed area. The collection of data at the 106 stations comprising the survey was completed on the morning of 14 June at station 5983. The *Evergreen* then proceeded to Argentia, arriving there on 15 June.

On 17 June the *Evergreen* proceeded to Boston and on 7 July departed Boston to begin the post-season cruise. This was to consist of the occupation of the Bonavista triangle and a section across the Labrador Sea from South Wolf Island, Labrador, to Cape Farewell, Greenland. The work of collection of data began at station 5984 at the off-shore corner of the triangle on the morning of 11 July and progressed without incident, working around the triangle in a counter-clockwise direction to the point of beginning and completing the work of collection for the triangle at station 6013 on the morning of 14 July. South Wolf Island was reached on the morning of 15 July and the work on the section across the Labrador Sea progressed without incident until station 6036 where field ice was encountered about 10½ miles off Cape Farewell. Visual and radar observation confirmed the expectation from the previous several days of on-shore winds that the coastal belt of ice would be compact. Thus the work of collection of data was completed at station 6036 on the evening of 18 July with the omission of only the last of the planned stations. The *Evergreen* then proceeded to Woods Hole, stopping briefly at Argentia on 22 July to pick up spare oceanographic equipment stored there during the season. Woods Hole was reached on 25 July and oceanographic equipment and personnel were off-loaded to complete the oceanographic field work for 1955. During the post-season cruise 53 stations were cocupied.

The oceanographic work was under the supervision of Oceanographer Floyd M. Soule who was assisted by LT John E. Murray. During the third survey LCDR Harry H. Carter also assisted. Other assistants in the observational work were Francis N. Brown, yeoman first class; Elwood C. Gray, aerographer's mate first class; Lewis M. Lawday, aerographer's mate second class; Hugh R. McCartney Jr., aerographer's mate second class; and Bruce M. McCluskey, boatswain's mate third class.

Of the 296 stations occupied during the season and post-season surveys the 23 stations forming the section across the Labrador Sea were occupied from the surface to as near bottom as was practicable, and at the other 273 stations the observations extended to a depth of about 1500 meters where the depth of water permitted. As in previous years, the intended depths of observation, in meters, were 0, 25, 50, 75, 100, 150, 200, 300, 400, 600, 800, 1000 and thence by 500-meter intervals. The dynamic heights have been referred to the 1000-decibar surface, except for the section across the Labrador Sea where the 1500-decibar surface has been used for reference.

In addition to the usual measurements of temperature and salinity 264 samples were taken during the occupation of the South Wolf Island-Cape Farewell section for subsequent determination of total phosphorus concentration.

Temperatures were measured with deep-sea reversing thermometers. Most of the protected thermometers used were of Richter and Wiese manufacture but a small percentage were made by Negretti and Zambra, G. M. Manufacturing Co., and the Kahl Scientific Instrument Corp. The depths of observation were based on unprotected thermometers made by Richter and Wiese and by Kahl. As described in earlier bulletins of this series a program of intercomparison of the protected thermometers was carried out. From a total of 1994 comparisons, the probable difference between the corrected readings of a pair of thermometers was 0.010° C. As many of the thermometers had recent laboratory comparisons with thermometers tested by the National Bureau of Standards, and as in most cases the temperatures are the means of the corrected readings of a pair of thermometers, it is considered that the observed temperatures listed in the table of oceanographic data have a probable error of about ±0.01° C.

As in previous years, routine salinity measurements were made with a Wenner salinity bridge. Measurements and tests of the instrument, made prior to the beginning of the 1955 field work, indicated no requirement for the redetermination of its calibration curve. During the routine measurements standardizations were made with water from an oil-sealed carboy of sea water and at least twice during each run a sample of Copenhagen water of the batch P17 was measured as an unknown. At the end of each survey these measurements of Copenhagen water were used to compute such corrections as had to be made to the salinities measured during the survey. For the first survey and the post-season cruise the indicated corrections did not exceed 0.005°/₀₀ so no corrections have been made to those salinities. For the second and third surveys corrections of −0.007°/₀₀ and +0.008°/₀₀ respectively have been applied. The dynamic topographic charts, however, were not redrawn and the dynamic heights shown in figures 14 and 15 consequently are respectively too low and too high by 5.2 and 6 dynamic mm. The relative topography and derived velocities and transports are not affected.

The determinations of the total phosphorus concentration were carried out by personnel of the Woods Hole Oceanographic Institution as described in Bulletin No. 40 of this series.

Figures 13, 14, 15 and 16 show, in chronological order, the current charts resulting from the three surveys made during the season and the post-season occupation of the Bonavista triangle. Figure 13 shows that at the time of the first survey the dynamic heights on the Grand Banks were about normal and the dynamic heights in the valley east of the Labrador Current were nearly normal. The dynamic heights on the seaward margin of the surveyed area were decidedly less than usual with the maximum heights about 30 dynamic centimeters less than usual. Thus, for the most part, the border of the Atlantic Current was outside the surveyed area. The Labrador Current was flowing with normal vigor from the northernmost section to the Tail of the Banks. From this survey it was expected that any bergs which might follow this path would not get further west than about 50°40′ W., south of the Grand Banks before recurving eastward. It was expected, further, that the southernmost point which such bergs might reach would be south of the southern limits of the survey and could only be estimated as about 40°20′ N., occurring at about the 48th meridian. The areas in which bergs might approach the North Atlantic Track Agreement tracks were along the southern margin of the surveyed area between 49° W., and 47° W., and along the eastern margin of the surveyed area between 43° N., and 44° N. Eastward of the Labrador Current north of about 43°30′ N., the gradients in the dynamic topography were so slight that if any bergs reached this area their movements would have been greatly affected by winds and transient wind

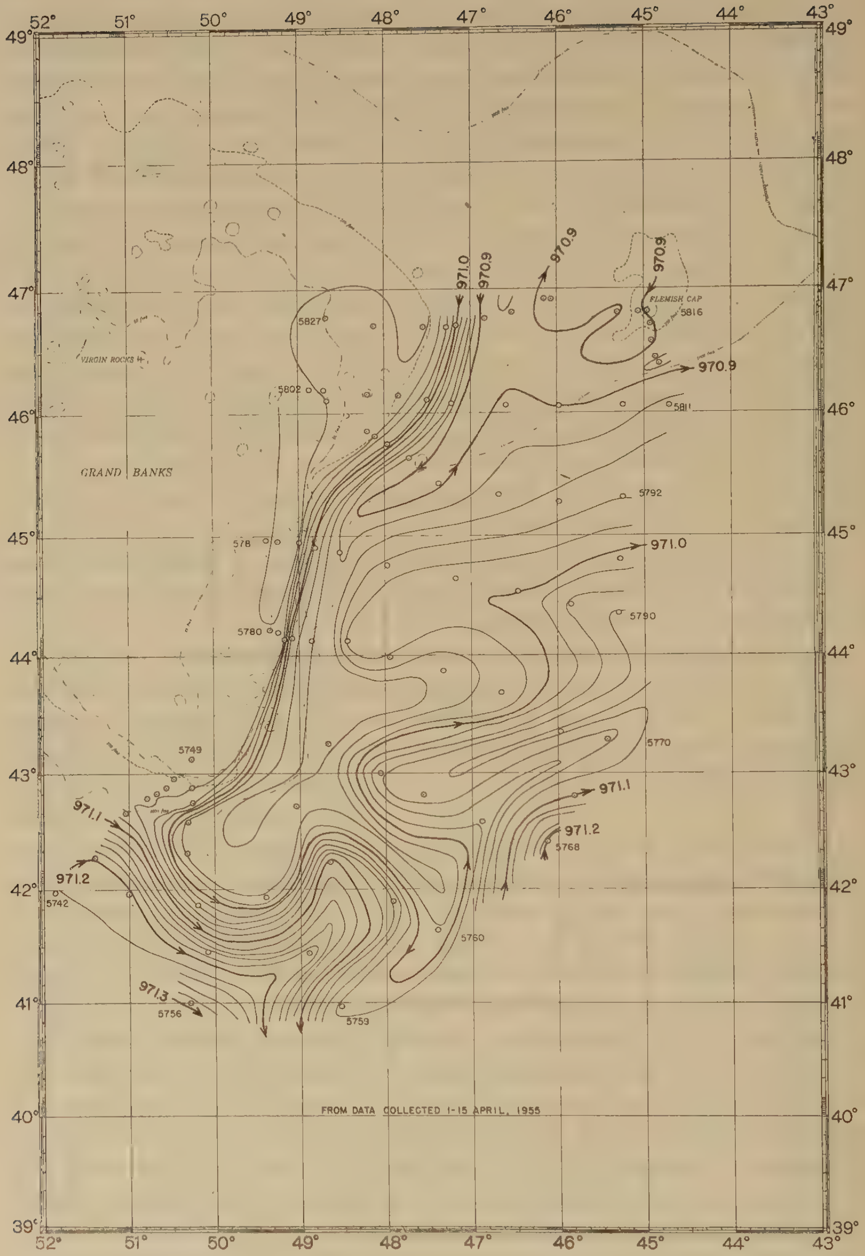
52°
51°
50°
49°
48°
47°
46°
45°
44°
43°
39°
40°
41°
42°
VIRGIN ROCKS
GRAND BANKS
FLEMISH CAP
971.0
970.9
970.9
970.9
970.9
971.0
971.1
971.1
971.2
971.2
971.3
5827
5802
5816
5811
5792
578
5780
5790
5770
5749
5742
5756
5759
5760
5768
FROM DATA COLLECTED 1-15 APRIL, 1955

Figure 13.—Dynamic topography of the sea surface relative to the 1000-decibar surface from data collected 1–15 April 1955. Oceanographic station positions are indicated and the station numbers given at turning points.

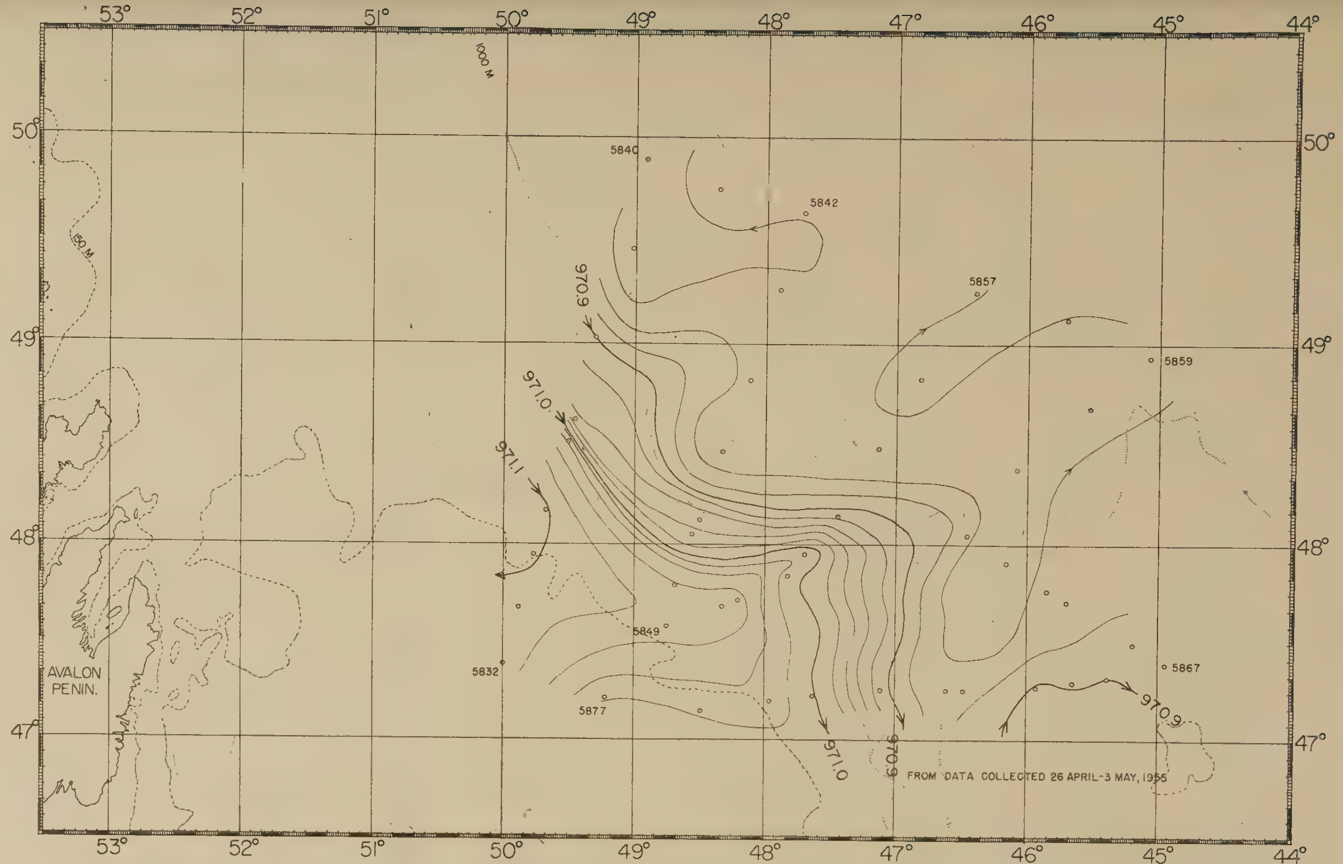
53°
52°
51°
50°
49°
48°
47°
46°
45°
44°
50°
49°
48°
47°
1000 M
150 M
5840
5842
5857
5859
5849
5832
5877
5867
970.9
971.0
971.1
AVALON
PENIN.
FROM DATA COLLECTED 26 APRIL-3 MAY, 1955

FIGURE 14.—Dynamic topography of the sea surface relative to the 1000-decibar surface from data collected 26 April–3 May 1955. Oceanographic station positions are indicated and the station numbers given at turning points.

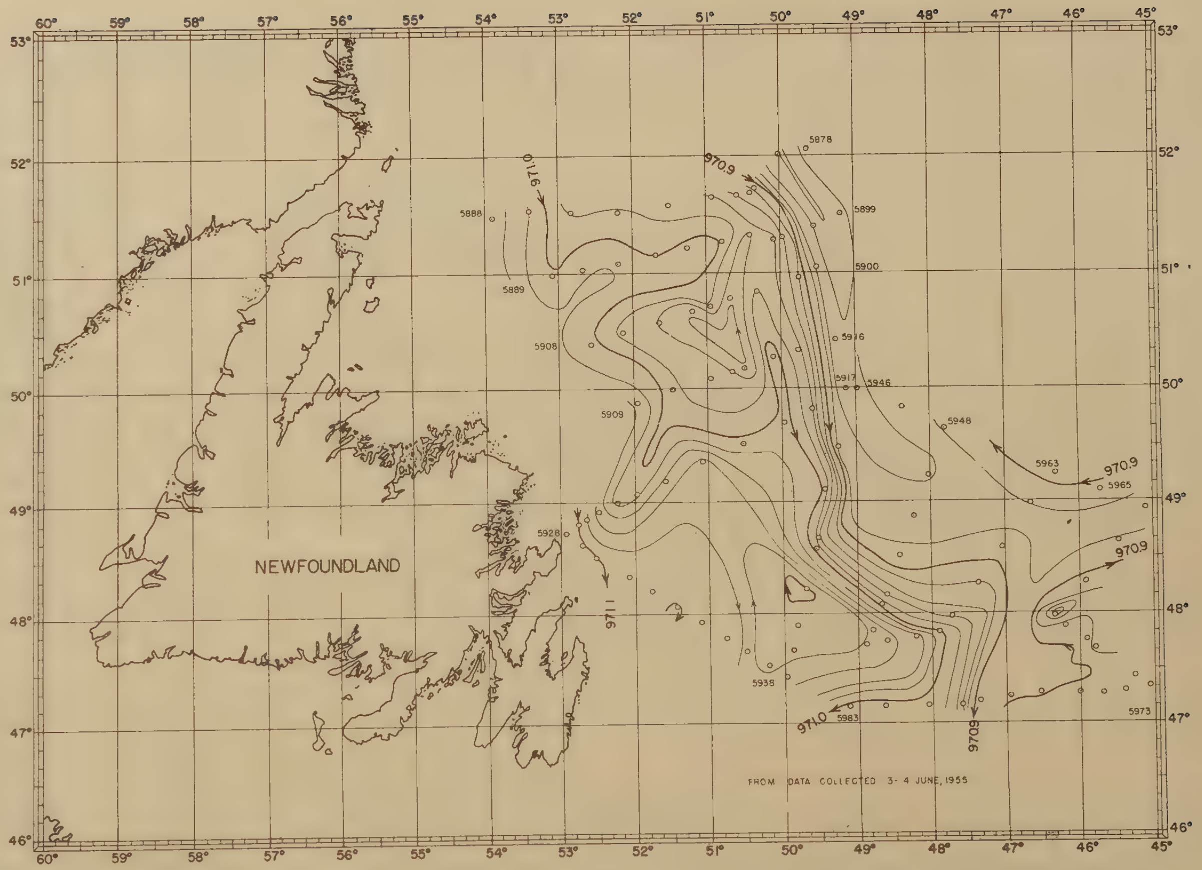
60°
59°
58°
57°
56°
55°
54°
53°
52°
51°
50°
49°
48°
47°
46°
45°
NEWFOUNDLAND
5878
5888
5889
5899
5900
5908
5909
5916
5917
5928
5938
5946
5948
5963
5965
5973
5983
970.9
971.0
9711
FROM DATA COLLECTED 3- 4 JUNE, 1955

FIGURE 15.—Dynamic topography of the sea surface relative to the 1000-decibar surface from data collected 3–14 June 1955. Oceanographic station positions are indicated and the station numbers given at turning points.

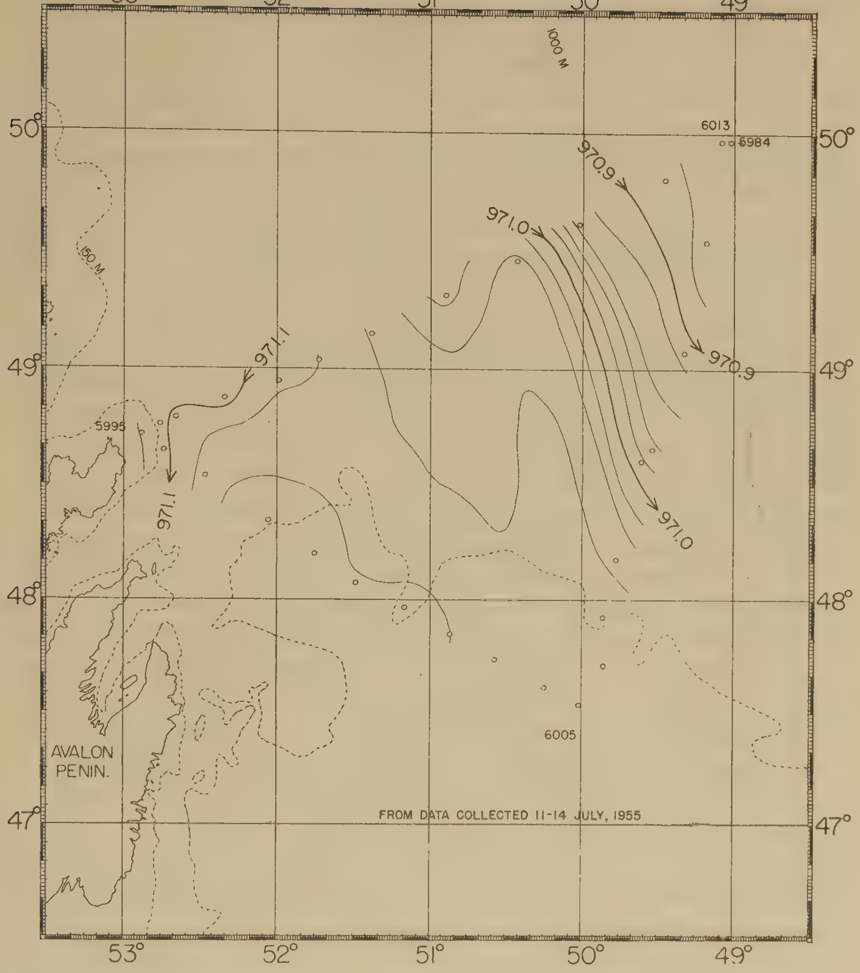
1000 M
6013
6984
970.9
971.0
971.0
970.9
971.1
971.1
150 M
5995
AVALON PENIN.
6005
FROM DATA COLLECTED 11-14 JULY, 1955
50°
49°
48°
47°
50°
49°
48°
47°
53°
52°
51°
50°
49°

Figure 16.—Dynamic topography of the sea surface relative to the 1000-decibar surface from data collected 11–14 July 1955. Oceanographic station positions are indicated and the station numbers given at turning points.

currents. There was evidence that exceptionally vigorous wind stirring took place prior to this survey and over nearly the entire surveyed area there was a mixed surface layer about 50 meters in thickness. The northward moving water at the extreme western part of the survey is regarded as a compensating eddy associated with an increase in the strength of the Labrador Current. The temperatures support the presumption of an increase in the Labrador Current prior to this survey if it is also assumed that the initially weak current had warmer temperatures than usual and that a strengthening of the current would tend to erase such anomalies. The minimum temperatures observed in the several sections across the Labrador Current were, from south to north, —0.05, —0.73, —0.74, —1.16, —1.20 and —1.42° C.

While there is no overlap in surveyed area between the first and second, surveys, comparison of the southern end of figure 14 with the northern part of the first survey presented in figure 13 shows marked similarity from the 970.9-dynamic meter contour near 46°10′ W., westward to the 971.0-dynamic meter contour. Westward of this, however, figure 14 shows a movement westward onto the banks in dynamic heights greater than about 971.01 dynamic meters. Thus the chances of a deep draft berg moving south of the 47th parallel along the eastern edge of the Grand Banks were much less than usual. The swiftest current found during the second survey, both as indicated by GEK and dynamic topography, was in the axis of the Labrador Current as it crossed the first section between stations 5836 and 5837. In an area more than 60 by 150 miles in extent, in the northeastern part of the surveyed area, the steady currents were practically nonexistent with a total range in dynamic height of about 4 centimeters.

Figure 15 shows the dynamic topography found during the third survey. Since no previous network survey of the area on the Newfoundland shelf north of the Bonavista triangle has ever been made there exists no basis for comparison of this portion of figure 15 with normal conditions. A few earlier sections, widely spaced, have suggested the presence of an eddy. The principal interest, from a standpoint of practical application of oceanography to Ice Patrol, lay in the core of the Labrador Current near the continental slope and the area southeastward of the Bonavista triangle at and just northward of the latitude of Flemish Cap. Here figure 15, like figure 14, shows a pronounced set onto the Grand Banks. This movement into shoaler depths began as far north as 50° N., but was of practical magnitude only south of 48° N. The colder water of the temperature minimum of the Labrador Current apparently followed this path since the lowest temperature found in the section from Flemish Cap to the Grand Banks was —0.6° C. whereas temperatures as low as —1.48° C. were observed in the southeastern section of the Bonavista triangle. Thus the current in the water which is deep enough to permit passage of a large berg had temperatures warmer than the optimum for lengthy survival. In comparison to figure 14, there was an apparent westward shift of the current pattern in the vicinity of the valley between Flemish Cap and the Grand Banks.

Figure 15 indicates that only such bergs as might cross the 49th parallel west of about 52°30′ W., would follow the western branch of the Labrador Current and that any bergs crossing this parallel between 52°30′ W., and about 49°30′ W., would strand on the northern and northeastern slopes of the Grand Banks. Of those crossing the 49th parallel eastward of 49°30′ W., it was expected that most would recurve eastward north of the latitude of Flemish Cap. Figure 16 shows the dynamic topography found at the Bonavista triangle during the postseason cruise about a month later. During this interval there was an eastward shift of the current pattern along the northwest section of the triangle and this topography was interpreted to mean that any bergs entering the area from the north and crossing the 49th parallel west of about 51°30′ W., would follow the western branch, that those crossing this parallel between 51°30′ W., and 49°50′ W., would strand on the Grand Banks and that those crossing eastward of about 49°40′ W., would recurve eastward and northeastward without reaching latitude 47° N.

In the Grand Banks region Labrador Current water and Atlantic Current water have characteristic temperature-salinity relationships which identify them as water masses. Here also these parent water masses usually mix in a sufficiently constant proportion so that the mixed water can be regarded as a virtual water mass. In 1955 only the first survey was located in the area which has been the source of the T-S data considered in the past. The relationships found during this survey are shown as solid lines in figure 17 and are compared with averages for the 8-year period 1934–41, shown in broken lines. The 1955 T-S curve for Labrador Current water is like that for the 8-year mean but is fresher than the mean below about 400 meters. The mixed water in 1955 was fresher than the mean and slightly warmer throughout. In 1955 the Atlantic Current water was slightly saltier than the mean above 600 meters and fresher below that level. It was also slightly warmer than the mean above about 800 meters. In 1955, level for level, all the water masses were lighter than the mean at all levels. Geographically, the northern sections show normal Labrador Current water. In the southern sections there was some mixing of Labrador Current water with mixed water in the area usually occupied by Labrador Current water. Also the southern sections showed some mixing of mixed water with Atlantic Current water. The Flemish Cap area was occupied by normal mixed water.

For the first and only 1955 survey which extended far enough south to include a portion of the cold wall its position was determined as in other years using as a criterion the horizontal projection of the line along which a temperature of 6° C corresponds to a salinity of $34.95\,^{\circ}/_{\circ\circ}$. The area included between this boundary and rhumb lines of the 45th parallel, the 49th meridian from 45° N., to 43° N., and a line from 43° N., 49° W., through 42° N., 47° W., extended to the boundary, was 8.5×10^4 square kilometers. This area, adjusted for the volume transport of the Labrador Current entering the area past the 45th parallel, reduced to 5.16. This adjusted area, A, did not compare well with the 2.30 computed from the prediction formula, $A=6.97(H-5.07)+1.67$ in which A is the adjusted area and H, expressed in feet, is the sea level at Charleston, minus the departure from average sea level at Bermuda 11½ months earlier. As only one

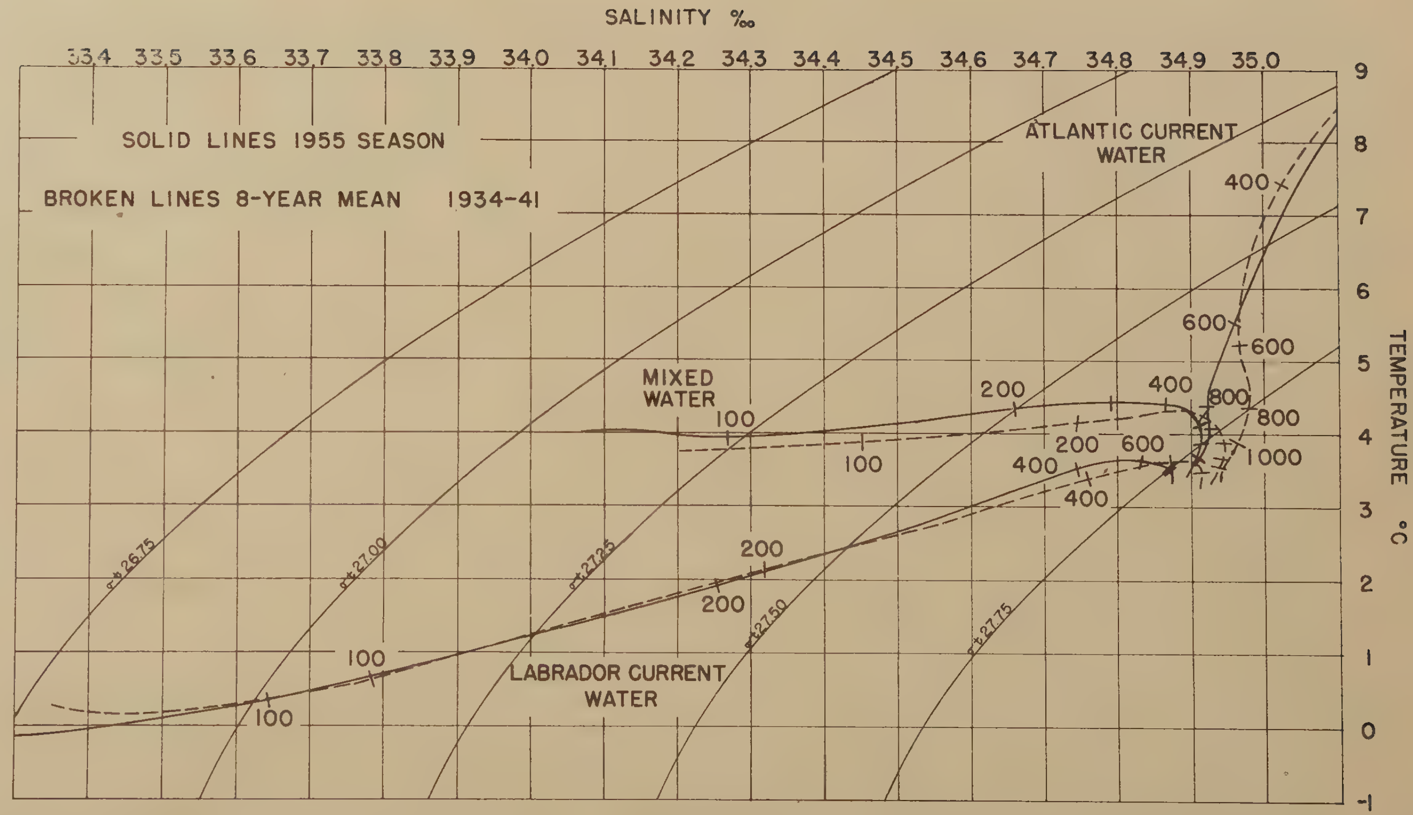

FIGURE 17.—Temperature-salinity relationships for Labrador Current water, Atlantic Current water, and mixed water found in the Grand Banks region. Solid lines show conditions found during the first survey, 1955, and broken lines represent the 8-year mean for the period 1934–41. An approximate depth scale in meters is given.

survey was made in 1955 it is not possible to judge whether the time lag of 11½ months, which has been found in the post-war years, was still effective or whether the prewar lag of 13½ months should have been used.

For a number of years the circulation in the upper layers of the waters in the vicinity of the Grand Banks has been studied in some detail through examination of the distribution of velocity and temperature in selected vertical sections across the Labrador Current. The values of volume transport, mean temperature, minimum observed temperature and heat transport so derived from observations made in 1955 are given in table 1. In this table and in the discussion volume transport is in millions of cubic meters per second, heat transport is in millions of cubic meter degrees Centigrade per second and mean temperature and minimum observed temperature are in degrees Centigrade. Sections T, U, and W are located as follows: T extending southeasterly from about 46°20′ N., 49°00′ W.; U extending easterly from the Grand Banks at about 45° N.; and W extending southerly from the Grand Banks at about 50° W. Sections NW, SW and SE are the sides of a triangle the corners of which are located near Cape Bonavista, Newfoundland, about 50° N., 49° W., and about 47°20′ N., 50° W. Section F extends easterly from the Grand Banks to Flemish Cap and sections G, H and HN radiate seaward from the northeastern shoulder of the Grand Banks successively northward between section F and the Bonavista triangle. The South Wolf Island section extends northeasterly from South Wolf Island, Labrador. Rough approximations to seasonal normal variations have been developed and published for sections T, U and W in bulletin number 36 of this series and for sections NW, SW and SE in bulletin number 39 Such seasonal normal values have been given in table 1. The several occupations of the South Wolf Island section have all taken place at about the same time of year and average values are given for this section in lieu of normals. Sections F, G, H and HN have not been occupied a sufficient number of times to provide either seasonal normals or useful average values.

In the first survey the volume transport of the Labrador Current decreased southward from sections F to T to U as portions recurved northeastward. At section W the increase over section U is considered to be the effect of a recirculatory closed eddy between the supply from the north and the off-lying Atlantic Current. The mean temperature at section T was below normal, at section U about normal and at section W above normal. While at section T the minimum observed temperature was about a quarter of a degree above normal, at sections U and W it was about a half degree warmer than normal. These temperature variations are interpreted as indicating that an increase in flow of colder water from the north was taking place at about the time of the survey.

Table 1.—Summary of velocity sections across Labrador Current occupied in 1955

Section	Volume transport			Mean temperature			Minimum observed temperature			Heat transport		
	1955	Normal	Anomaly	1955	Normal	Anomaly	1955	Normal	Anomaly	1955	Normal	Anomaly
1st Survey:												
F	4.58	------	------	1.42	------	------	−1.40	------	------	6.51	------	------
T	4.44	3.33	+1.11	1.56	1.95	−0.39	−1.16	−1.40	+0.24	6.94	6.49	+0.45
U	3.62	5.31	−1.69	1.49	1.51	−0.02	−0.74	−1.22	+0.48	5.40	8.02	−2.62
W	4.32	4.25	+0.07	2.22	2.02	+0.20	−0.05	−0.50	+0.45	9.60	8.58	+1.02
2d Survey:												
HN	3.51	------	------	1.10	------	------	−1.42	------	------	3.87	------	------
H	4.17	------	------	1.48	------	------	−1.30	------	------	6.15	------	------
G	2.75	------	------	1.90	------	------	−0.98	------	------	5.23	------	------
3d Survey:												
NW	4.18	3.62	+0.56	1.40	1.14	+0.26	−1.44	−1.69	+0.25	5.86	4.13	+1.73
SW	0.35	0.48	−0.13	−0.01	−0.41	+0.40	−1.54	−1.63	+0.09	0.00	−0.20	+0.20
SE	3.72	3.09	+0.63	1.82	1.67	+0.15	−1.48	−1.53	+0.05	6.77	5.16	+1.61
HN	3.69	------	------	2.20	------	------	−1.18	------	------	8.11	------	------
H	3.47	------	------	1.89	------	------	−1.09	------	------	6.57	------	------
G	0.99	------	------	1.62	------	------	−1.20	------	------	1.61	------	------
Postseason:												
NW	2.79	4.05	−1.26	1.00	1.41	−0.41	−1.66	−1.61	−0.05	2.78	5.71	−2.93
SW	0.40	0.62	−0.22	0.51	0.06	+0.45	−1.47	−1.64	+0.17	0.20	0.04	+0.16
SE	2.96	3.32	−0.36	1.89	1.98	−0.09	−1.07	−1.58	+0.51	5.60	6.57	−0.97
South Wolf Island	5.02	4.75	+0.27	2.62	2.49	+0.13	−1.66	−1.49	−0.17	13.15	12.35	+0.80

The second survey took place in an area for which no normals are available. A comparison of the volume passing section G with that which was found at section F during the first survey, however, shows a marked decrease in volume of water passing southward between the Grand Banks and Flemish Cap. Further comparison of the volume transport past sections HN, H, and G for the second and third surveys shows a continuation of this trend as well as a seasonally increasing recurvature of water north of the latitude of Flemish Cap. Also a large part of the decrease in volume from sections H to G in both the second and third surveys is attributable to an anamolous set onto the Grand Banks between these sections (see figures 14 and 15).

Table 1 also shows that the volume transport passing the Bonavista triangle during the third survey was greater than normal and with a larger than normal proportion following the eastern branch. At each of the three sides of the triangle the mean temperature was warmer than normal but with the minimum observed temperatures close to normal. In the postseason cruise occupation of the Bonavista triangle the volume transport had dropped off decidedly to subnormal values accompanied by a drop in mean temperature of the Labrador Current passing the NW and SE sections. The minimum observed temperatures dropped to about normal at the NW section and rose to about a half degree above normal at the SE section. At the South Wolf Island section, occupied only a few days later, the minimum observed temperature was the same as that found at the Bonavista triangle, whereas the situation usually found is that of a colder minimum temperature at the Bonavista triangle than at the South Wolf Island section.[2] The volume transport, mean temperature and heat transport at the South Wolf Island section were close to average values for the first time in several years. The volume transport was the lowest found since 1948 and approximately the same as found in 1949, the beginning of the seven-year sequence of exceptionally active circulation in the Labrador Sea. The volume transports found in 1955 have been shown schematically in figure 18. The tabulated values ot volume of flow have been rounded off to the nearest tenth and in the case of the Bonavista triangle it has been assumed that there was no vertical volume transport across the 1,000-decibar reference surface. This figure will be referred to again after discussion of the Greenland end of the South Wolf Island-Cape Farewell section.

---

[2] See Soule, Bush and Murray "International Ice Observation and Ice Patrol Service in the North Atlantic Ocean—Season of 1953" U. S. Coast Guard Bull. No. 39, page 64.

The dynamic topography of the sea surface in the neighborhood of the section from South Wolf Island, Labrador, to Cape Farewell, Greenland, is shown in figure 19. This topography is relative to the 1500-decibar surface, and since it is not supported by an adjacent network of stations much has been inferred from temperature and salinity distribution within the section and from the results of earlier surveys. Figure 20 shows the temperature distribution along this section and figure 21 gives the salinity distribution in the Greenland half of the section. In figure 20 the frigid water of the Labrador Current is apparent over the inner part of the shelf grading to the warmer offshore part of the Labrador Current above the continental slope. This warmer water of greater than 3.3° extends to the bottom at intermediate depths along the slope and between depths of 1,000 and 2,000 meters is traceable seaward as a temperature maximum as far as station 6026. A similar tongue of water warmer than 3.3° is traceable seaward from the Greenland side. The resulting minima at intermediate depths above these maxima include temperatures of from 3.11° to 3.17° thus classifying 1955 as one of the colder years. Of the years for which data are available 1934–39, 1950 and 1954–55 were years when the temperature minimum was about 3.17°. During the other years for which data are available, 1940–41, 1948–49 and 1951–53, the minimum was about 0.10° to 0.15° warmer. At the Greenland end of the section the warmer water was disposed similarly to the distribution found in 1954 and the cross sectional areas between successive isotherms from the 3.5° isotherm to the 6° isotherm were much the same as in 1954 even though the 1955 occupation of the section was about 6 weeks earlier in the summer than the 1954 occupation.

The salinities shown in figure 21 show a general distribution similar to that found in 1954. The extent and magnitude of the salinity maximum, however, are less than in 1954, the highest salinity being only 34.96°/₀₀. There is a possibility that a somewhat higher salinity may have been missed in the interval between stations 6031 and 6032.

As on the Labrador side, the Greenland end of the section showed a decrease from the abnormally active circulation in the Labrador Sea

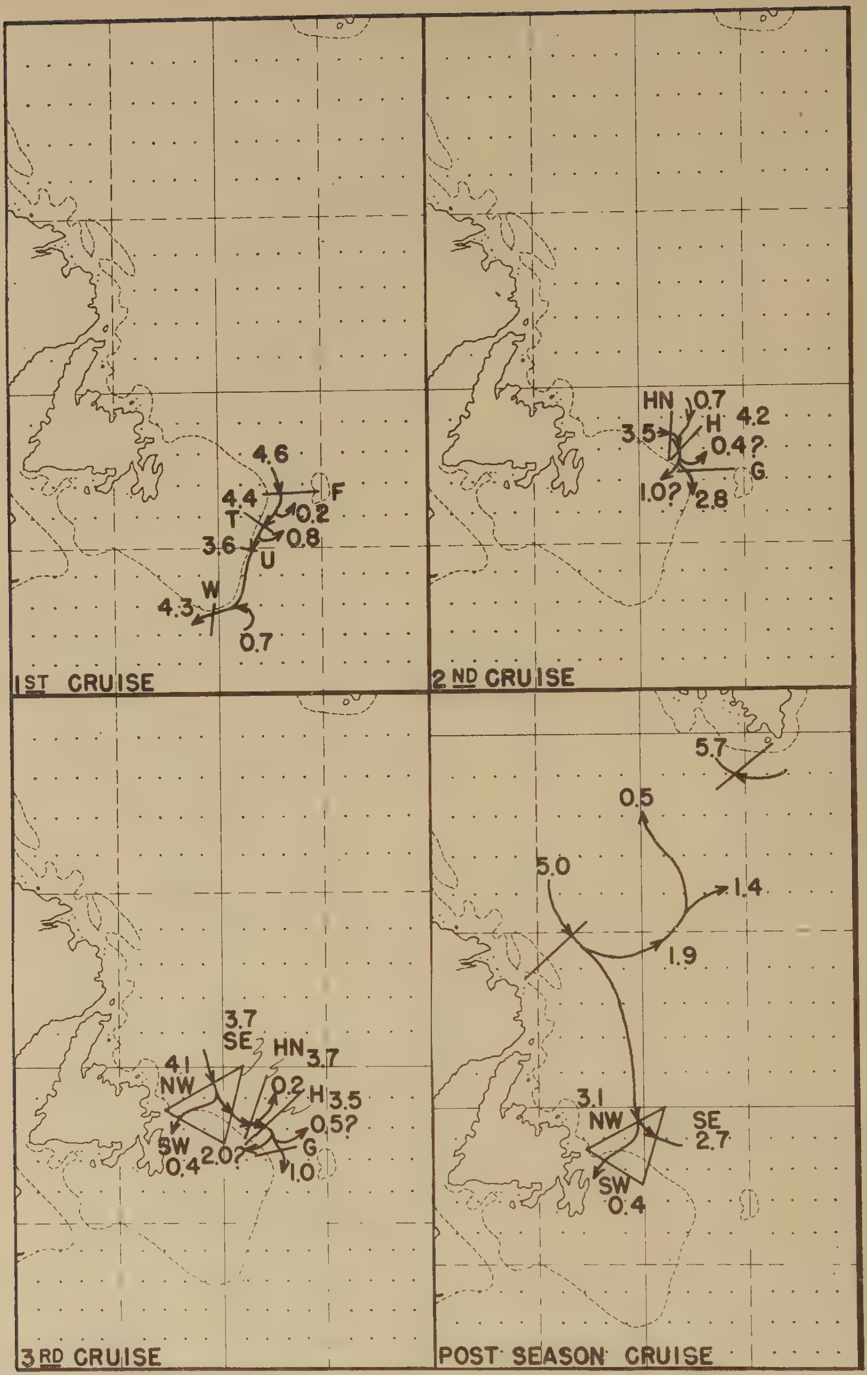
4.6
F
4.4
0.2
T
0.8
3.6
U
W
4.3
0.7
1ST CRUISE
HN
0.7
H
4.2
3.5
0.4?
G
1.0?
2.8
2ND CRUISE
3.7
SE
HN
3.7
4.1
NW
0.2
H
3.5
0.5?
SW
2.0?
G
0.4
1.0
3RD CRUISE
5.7
0.5
5.0
1.4
1.9
3.1
NW
SE
2.7
SW
0.4
POST SEASON CRUISE

FIGURE 18.—Schematic representation of circulation deduced from sections occupied during 1955. Numerals indicate volume transport in units of cu.m/sec X 10^{-6}.

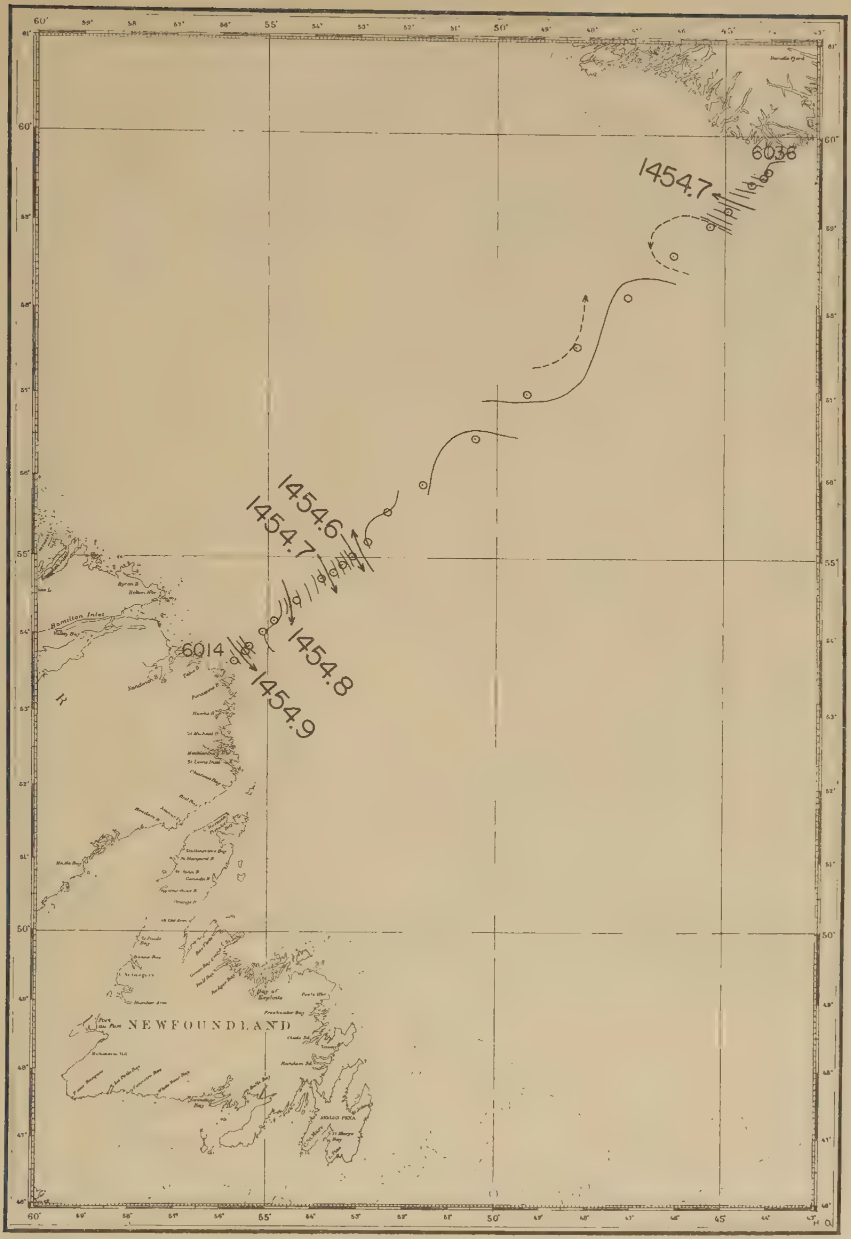
60°
55°
50°
45°
60°
55°
50°
6036
1454.7
1454.6
1454.7
1454.8
1454.9
6014
Hamilton Inlet
NEWFOUNDLAND
Bay of Exploits
AVALON PENA

FIGURE 19.—Dynamic topography of the sea surface relative to the 1500-decibar surface from data collected 15–18 July 1955. Oceanographic station positions are indicated and the station numbers given at turning points.

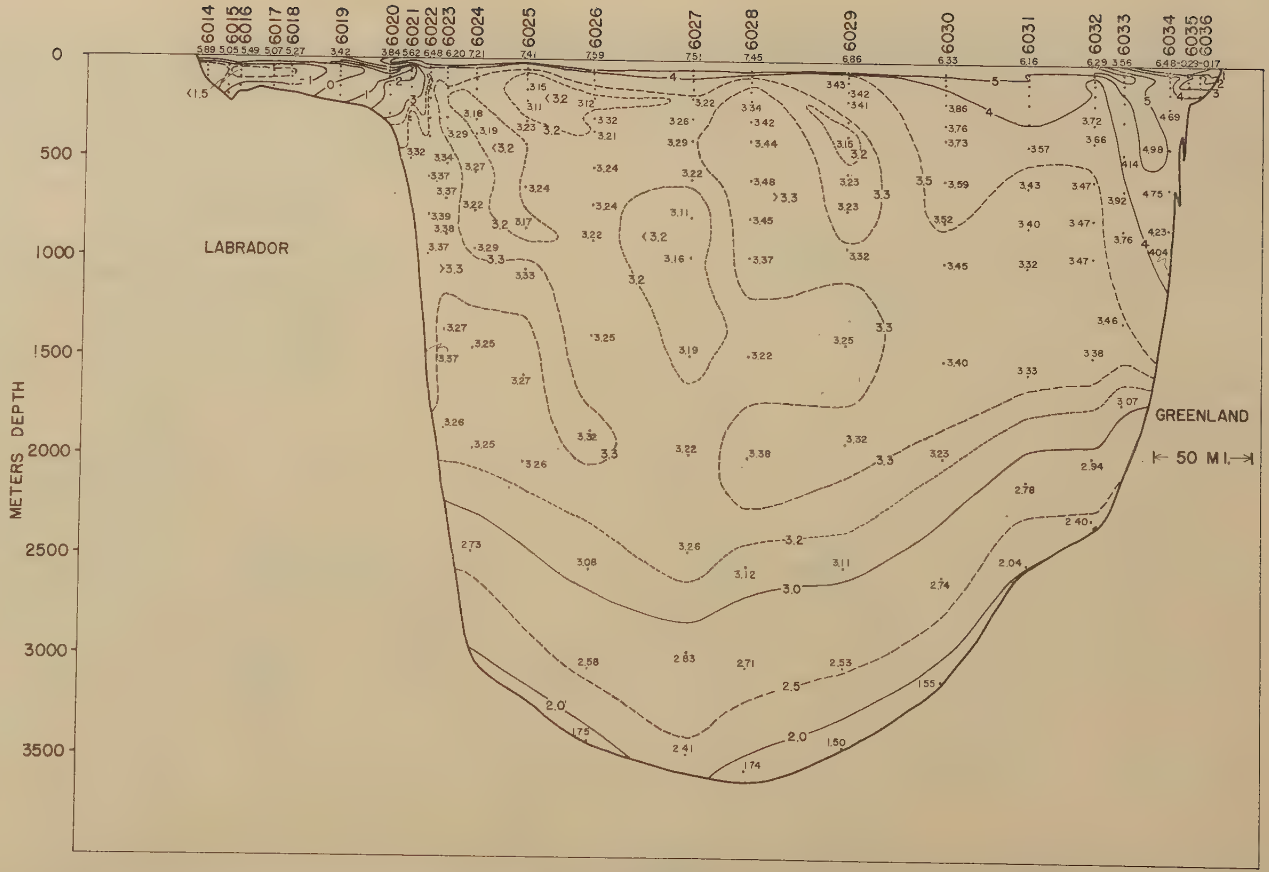

FIGURE 20.—Temperature distribution between South Wolf Island, Labrador, and Cape Farewell, Greenland, 15–18 July 1955.

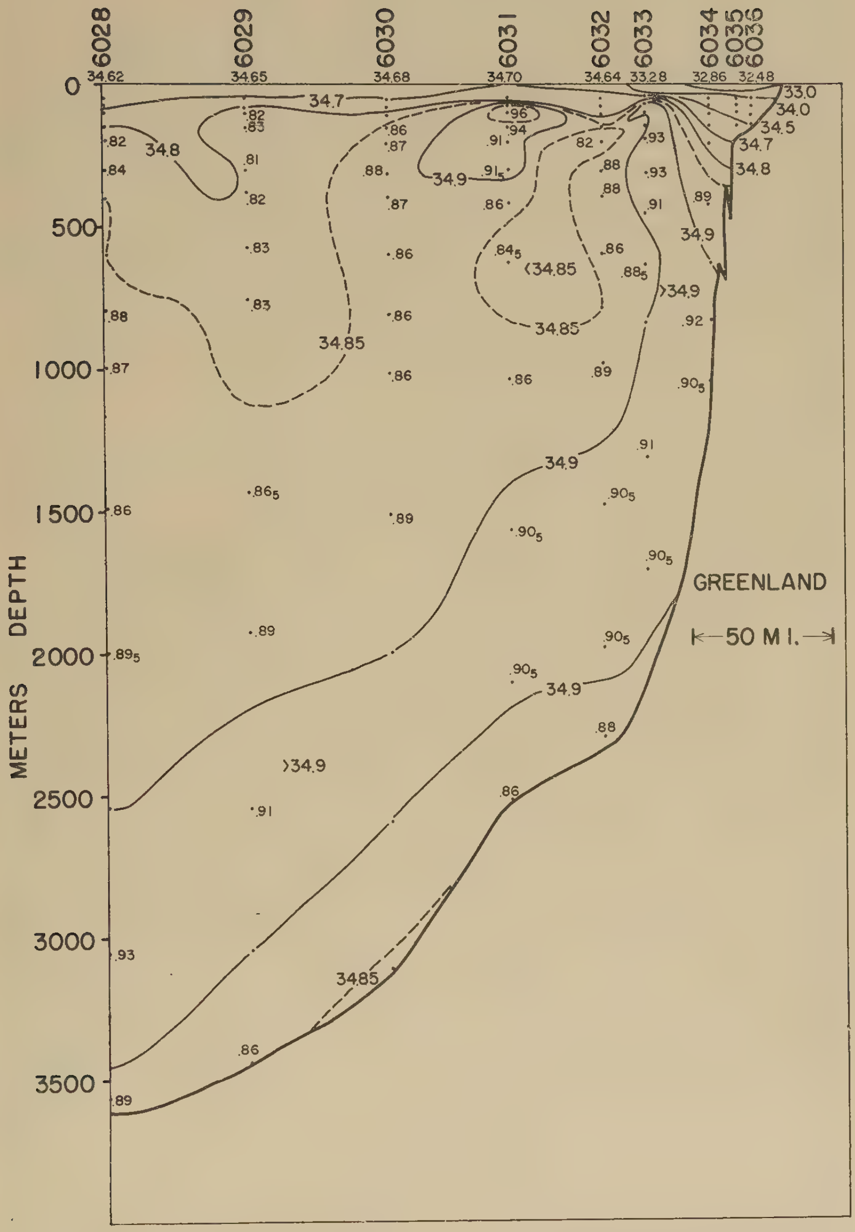

Figure 21.—Salinity distribution southwest of Cape Farewell, Greenland, 17–18 July 1955.

which has characterized the last several years. The volume transport of the West Greenland Current was computed to be 5.66 with a mean temperature of 4.74 compared to seasonal normals of 4.55 and 4.65 respectively. The resulting heat transport of 26.85 was 5.69 above the seasonal normal. On the basis of constant mean temperatures of 3.2° and 5.5° for the East Greenland Current and Irminger Current components of the West Greenland Current the volume transport found was made up of 1.87 and 3.79 for these components, being 0.19 and 0.92 greater than the respective seasonal normals. Once more the net transport across the complete section was found to be northwesterly, the amount being 1.24. Again the reference surface selected, 1500 decibars, appears to be about as good as any single level although it would appear that the motionless surface may have been at about 1,700 meters on the Labrador side. The 1500-decibar surface was accepted in constructing the picture of the circulation in the Labrador Sea shown in figure 18.

Again in 1955 samples were taken at all levels at all stations comprising the South Wolf Island-Cape Farewell section for subsequent determination of the concentration of total phosphorus. The distribution found in this section is shown in figure 22. In 1955, as in previous years when total phosphorus has been measured along this section, there were slight maxima at intermediate depths just seaward of the Labrador Current and just seaward of the West Greenland Current. Examination of the total phosphorus-density relationship shows station curves characteristic of the Labrador Current only over the Labrador shelf as far out as station 6019. The constant phosphorus value approached in these curves is about 1.0 μga/L compared with 1.15 in 1954 and 1.30 in 1952. In the central Labrador Sea the 1955 stations were uniformly lower in phosphorus than in earlier observations and the deep maximum occurring at a potential density of about 27.75 was about 1.1 compared with about 1.2 in 1954. The phosphorus distribution found in 1955 had smaller variations from place to place than previously found and the highest 1955 phosphorus value was 1.30. This occurred at station 6030 which was the only central Labrador Sea station that departed much from the average phosphorus-density relationship. The results of the measurements of total phosphorus concentration are given in tabular form at the end of the usual table of oceanographic data.

SUMMARY

1. The surface circulation in the Grand Banks region found during the 1955 ice patrol season has been discussed in the light of three dynamic topographic surveys, two of which were confined to the northeastern slope of the Grand Banks north of the latitude of Flemish Cap.

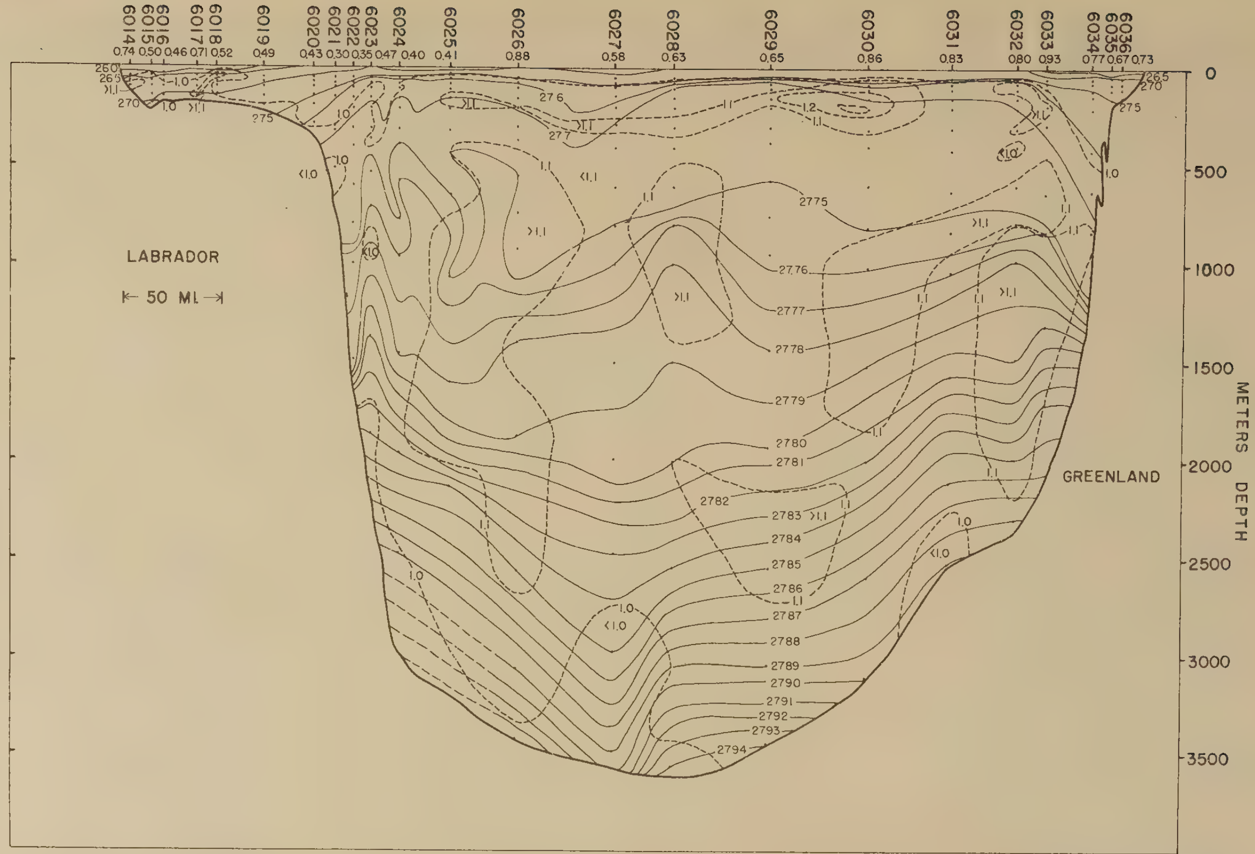

Figure 22.—Distribution of total phosphorus between South Wolf Island, Labrador, and Cape Farewell, Greenland, 15–18 July 1955. Concentration is given in microgram-atoms per liter. Solid lines show isentropic surfaces of equal $\sigma_{t\theta}$.

2. A more detailed examination of the Labrador Current in 1955 has been presented on the basis of volume and heat transport and mean and minimum observed temperatures found during the 17 occupations of 11 selected sections. The values found have been compared with seasonal normals where such normals are available.

3. The temperature-salinity relationships of the Labrador Current water, mixed water and Atlantic Current water found during the first 1955 survey have been compared with mean values for the 8-year period 1934–41.

4. Conditions found during the 1955 post-season cruise in the Labrador Sea have been described and the decreased circulation noted.

The data collected during 1955 are tabulated below. The individual station headings give the station number, date, geographical position, depth of water and the dynamic height of the sea surface used in the construction of the dynamic topographic charts shown in figures 13, 14, 15, 16 and 19. The depths of water are rough approximations, being uncorrected sonic soundings based on a sounding velocity of 800 fathoms per second and containing an additional mechanical speed error of about 1/60. Where the depths of scaled values are enclosed in parentheses, the data are based on extrapolated vertical distribution curves of temperature or salinity or both. Asterisks appearing before observed temperatures indicate that these temperatures were determined from the depth of reversal and the corrected reading of an unprotected thermometer. The symbol σ_t signifies 1,000(density−1) at atmospheric pressure and temperature t.

Table of Oceanographic Data

STATIONS OCCUPIED IN 1955

Station 5741; April 1; latitude 41°57′ N., longitude 51°00′ W.; depth 3,383 m.; dynamic height 971.204.

Observed values			Scaled values			
Depth, meters	Temperature, °C.	Salinity, °/oo	Depth, meters	Temperature, °C.	Salinity, °/oo	σ_t
0	6.71	33.74	0	6.71	33.74	26.49
23	13.23	35.66	25	13.25	35.68	26.88
46	13.43	35.72	50	13.40	35.72	26.89
70	13.40	35.72	75	13.40	35.72	26.89
93	13.27	35.68	100	13.20	35.68	26.89
139	13.42	35.70	150	13.30	35.69	26.89
185	13.02	35.61	200	12.85	35.58	26.89
278	11.84	35.44	300	11.10	35.36	27.06
336	9.90	35.24	400	8.25	35.10	27.33
481	6.83	35.01	600	5.55	34.96	27.60
610	5.46	34.96	800	4.15	34.89	27.70
781	4.16	34.89	1,000	3.90	34.89	27.73
1,241	3.73	34.90				

Station 5742; April 1: latitude 41°58′ N., longitude 51°53′ W.; depth 3,859 m.; dynamic height 971.224.

Observed values			Scaled values			
Depth, meters	Temperature, °C.	Salinity, °/oo	Depth, meters	Temperature, °C.	Salinity, °/oo	σ_t
0	13.08	35.62	0	13.08	35.62	26.87
25	13.09	35.63	25	13.09	35.63	26.87
51	13.06	35.62	50	13.05	35.62	26.87
76	13.09	35.62	75	13.10	35.62	26.87
102	13.08	35.63	100	13.05	35.63	26.88
152	13.21	35.68	150	13.20	35.68	26.89
203	13.26	35.69	200	13.25	35.69	26.89
305	*10.92	35.41	300	11.05	35.43	27.11
402	9.07	35.16	400	9.10	35.16	27.25
602	4.36	34.72	600	4.35	34.72	27.55
803	4.99	34.98	800	5.00	34.98	27.68
1,006	4.33	34.94	1,000	4.35	34.94	27.72
1,518	3.64	34.90				

Station 5743; April 1; latitude 42°16′ N., longitude 51°24′ W.; depth 3,109m.; dynamic height 971.197.

Observed values			Scaled values			
Depth, meters	Temperature, °C.	Salinity, °/oo	Depth, meters	Temperature, °C.	Salinity, °/oo	σ_t
0	11.91	35.28	0	11.91	35.28	26.84
25	13.28	35.71	25	13.28	35.71	26.90
50	13.47	35.76	50	13.47	35.76	26.90
74	13.49	35.71	75	13.45	35.76	26.91
99	13.49	35.76	100	13.40	35.76	26.92
148	13.48	35.78	150	13.45	35.77	26.92
197	13.50	35.77	200	13.45	35.77	26.92
296	11.29	35.44	300	11.15	35.42	27.10
369	9.23	35.18	400	8.65	35.15	27.31
559	6.44	35.05	600	5.95	35.03	27.60
756	4.72	34.935	800	4.60	34.94	27.69
957	4.26	34.95	1,000	4.20	34.95	27.75
1,480	3.61	34.90				

Station 5744; April 1; latitude 42°39.5′ N., longitude 51°02′ W.; depth 1,756 m.; dynamic height 971.067.

Observed values			Scaled values			
Depth, meters	Temperature, °C.	Salinity, °/oo	Depth, meters	Temperature, °C.	Salinity, °/oo	σ_t
0	3.24	32.90	0	3.24	32.90	26.21
26	1.73	33.12	25	1.75	33.11	26.50
51	0.44	33.32	50	0.45	33.32	26.75
77	0.28	33.40	75	0.25	33.39	26.82
102	2.55	33.80	100	2.25	33.76	26.98
153	3.27	34.12	150	3.25	34.11	27.17
204	2.62	34.18	200	2.65	34.17	27.28
306	5.25	34.75	300	5.10	34.73	27.47
372	5.00	34.81	400	4.90	34.83	27.57
564	4.44	34.89	600	4.30	34.89	27.68
760	3.60	34.83	800	3.60	34.83	27.71
962	3.53	34.85	1,000	3.55	34.85	27.73
1,486	3.45	34.86				

Table of Oceanographic Data—Continued

STATIONS OCCUPIED IN 1955—Continued

Observed values			Scaled values			
Depth, meters	Temperature, ° C.	Salinity ‰	Depth, meters	Temperature, ° C.	Salinity, ‰	σ_t
Station 5745; April 1; latitude 42°47′ N., longitude 50°47′ W: depth 1,000 m., dynamic height 971.068.						
0	1. 42	33. 23	0	1. 42	33. 23	26. 62
26	1. 03	33. 31	25	1. 00	33. 31	26. 71
53	1. 00	33. 32	50	1. 00	33. 32	26. 72
79	5. 64	34. 01	75	5. 00	33 97	26. 88
105	3. 24	33. 95	100	3. 50	33. 96	27. 03
157	3. 44	34. 18	150	3. 40	34. 14	27. 18
209	5. 12	34. 64	200	5. 00	34. 57	27. 36
314	5. 04	34. 71	300	5. 05	34. 71	27. 46
400	3. 83	34. 67	400	3. 85	34. 67	27. 56
604	4. 05	34. 74	600	4. 05	34. 74	27. 59
812	3. 60	34. 83	800	3. 65	34. 82	27. 70
992	3. 59	-------	1, 000	3. 60	34. 86	27. 74
Station 5746; April 1–2; latitude 42°50′ N., longitude 50°42′ W.; depth 640 m.; dynamic height 971.062.						
0	1. 38	33. 22	0	1. 38	33. 22	26. 61
25	0. 52	33. 30	25	0. 52	33. 30	26. 72
50	0. 41	33. 36	50	0. 41	33. 36	26. 78
75	0. 41	33. 40	75	0. 41	33. 40	26. 82
100	0. 44	33. 50	100	0. 44	33. 50	26. 89
150	0. 77	33. 86	150	0. 77	33. 86	27. 16
200	1. 13	34. 01	200	1. 13	34. 01	27. 27
300	1. 86	34. 26	300	1. 86	34. 26	27. 41
392	2. 87	34. 53	400	2. 95	34. 55	27. 55
534	3. 59	34. 73	(600)	3. 70	34. 78	27. 66
Station 5747; April 2; latitude 42°52.5′ N., longitude 50°35′ W.; depth 148 m.; dynamic height 971.073.						
0	1. 20	33. 25	0	1. 20	33. 25	26. 66
25	0. 95	33. 27	25	0. 95	33. 27	26. 68
50	0. 69	33. 30	50	0. 69	33. 30	26. 71
75	0. 55	33. 32	75	0. 55	33. 32	26. 74
100	0. 28	33. 45	100	0. 29	33. 45	26. 86
150	0. 68	33. 82	150	0. 68	33. 82	27. 14
Station 5748; April 2; latitude 42°57′ N., longitude 50°29′ W.; depth 98 m.; dynamic height 971.070.						
0	1. 76	33. 16	0	1. 76	33. 16	26. 54
26	1. 06	33. 27	25	1. 05	33. 27	26. 68
51	0. 57	33. 32	50	0. 60	33. 32	26. 74
77	0. 43	33. 46	75	0. 45	33. 45	26. 85
Station 5749; April 2; latitude 43°08′ N., longitude 50°16′ W.; depth 73 m.; dynamic height 971.075.						
0	1. 59	33. 16	0	1. 59	33. 16	26. 55
28	1. 46	33. 22	25	1. 50	33. 21	26. 60
55	1. 00	33. 31	50	1. 05	33. 30	26. 70
Station 5750; April 2; latitude 42°53′ N., longitude 50°16′ W.; depth 108 m.; dynamic height 971.060.						
0	1. 06	33. 35	0	1. 06	33. 35	26. 74
25	1. 02	33. 32	25	1. 02	33. 35	26. 74
51	0. 32	33. 40	50	0. 35	33. 40	26. 82
76	0. 33	33. 60	75	0. 35	33. 58	26. 96
			(100)	0. 40	33. 70	27. 06

Observed values			Scaled values			
Depth, meters	Temperature, ° C.	Salinity, ‰	Depth, meters	Temperature, ° C.	Salinity, ‰	σ_t
Station 5751; April 2; latitude 42°45′ N., longitude 50°16′ W.; depth 421 m.; dynamic height 971.045						
0	0. 21	33. 33	0	0. 21	33. 33	26. 77
25	0. 14	33. 33	25	0. 14	33. 33	26. 78
50	−0. 05	33. 50	50	−0. 05	33. 50	26. 92
75	0. 10	33. 63	75	0. 10	33. 63	27. 01
100	0. 24	33. 72	100	0. 24	33. 72	27. 09
150	0. 81	33. 99	150	0. 81	33. 99	27. 26
200	1. 23	34. 11	200	1. 23	34. 11	27. 34
300	1. 49	34. 19	300	1. 49	34. 19	27. 38
Station 5752; April 2; latitude 42°35′ N., longitude 50°19′ W.; depth 1,829 m.; dynamic height 970.952.						
0	2. 01	33. 70	0	2. 01	33. 70	26. 95
24	2. 01	33. 70	25	2. 00	33. 70	26. 95
47	2. 77	33. 87	50	2. 80	33. 89	27. 04
71	2. 74	34. 06	75	2. 70	34. 08	27. 19
95	2. 34	34. 18	100	2. 25	34. 19	27. 32
142	1. 83	34. 28	150	1. 90	34. 30	27. 44
189	2. 34	34. 43	200	2. 45	34. 46	27. 52
284	3. 31	34. 67	300	3. 40	34. 69	27. 62
357	3. 61	34. 76	400	3. 65	34. 78	27. 66
542	3. 70	34. 82	600	3. 65	34. 82	27. 70
730	3. 57	34. 83	800	3. 55	34. 84	27. 72
923	3. 55	34. 85	1,000	3. 55	34. 85	27. 73
1, 422	3. 48	34. 86				
Station 5753; April 2; latitude 42°18.5′ N., longitude 50°20′ W.; depth 2,761 m.; dynamic height 970.951.						
0	2. 16	33. 64	0	2. 16	33. 64	26. 90
26	2. 59	33. 74	25	2. 55	33. 74	26. 94
53	2. 56	33. 78	50	2. 55	33. 77	26. 97
79	2. 61	33. 94	75	2. 60	33. 91	27. 07
106	2. 47	34. 06	100	2. 50	34. 04	27. 18
157	2. 49	34. 26	150	2. 50	34. 24	27. 34
210	3. 26	34. 51	200	3. 10	34. 47	27. 48
316	3. 69	34. 73	300	3. 65	34. 70	27. 60
410	3. 66	34. 83	400	3. 70	34. 82	27. 70
616	3. 56	34. 85	600	3. 55	34. 85	27. 73
822	3. 62	34. 89	800	3. 60	34. 89	27. 76
1, 030	3. 44	34. 88	1, 000	3. 50	34. 88	27. 76
1, 552	3. 43	34. 90				
Station 5754; April 2; latitude 41°51′ N., longitude 50°12′ W.; Depth 3,695 m.; dynamic height 971.030.						
0	1. 26	33. 26	0	1. 26	33. 26	26. 65
24	0. 64	33. 31	25	0. 60	33. 31	26. 73
49	0. 44	33. 33	50	0. 45	33. 33	26. 75
73	0. 32	33. 44	75	0. 35	33. 45	26. 86
98	0. 40	33. 54	100	0. 45	33. 54	26. 92
146	0. 62	33. 81	150	0. 70	33. 83	27. 14
194	2. 05	34. 14	200	2. 10	34. 18	27. 32
292	3. 20	34. 55	300	3. 30	34. 57	27. 54
326	3. 65	34. 66	400	4. 00	34. 77	27. 63
466	4. 23	34. 83	600	4. 20	34. 88	27. 69
591	4. 18	34. 88	800	4. 20	34. 94	27. 74
759	4. 21	34. 95	1, 000	3. 80	34. 90	27. 75
1,210	3. 59	34. 88				

Table of Oceanographic Data—Continued

STATIONS OCCUPIED IN 1955—Continued

Station 5755; April 2; latitude 41°27′ N., longitude 50°06′ W.; dynamic height 971.175.

Observed values			Scaled values			
Depth, meters	Temperature, ° C.	Salinity °/oo	Depth, meters	Temperature, ° C.	Salinity, °/oo	σ_t
0	9.63	34.62	0	9.63	34.62	26.74
24	9.95	34.70	25	9.95	34.70	26.75
48	11.50	35.17	50	11.55	35.18	26.83
72	11.97	35.31	75	12.00	35.32	26.86
95	12.10	35.36	100	12.15	35.36	26.86
144	12.29	35.38	150	12.30	35.395	26.86
191	12.49	35.44	200	12.35	35.44	26.88
286	10.37	35.30	300	10.10	35.27	27.17
323	9.68	35.22	400	8.20	35.12	27.36
486	6.57	35.02	600	4.70	34.87	27.63
652	4.21	34.82	800	4.00	34.91	27.74
831	3.99	--------	1,000	3.90	34.92	27.76
1,311	3.77	34.91				

Station 5756; April 3; latitude 41°00′ N., longitude 50°17′ W.; depth 3,695 m.; dynamic height 971.294.

Observed values			Scaled values			
Depth, meters	Temperature, ° C.	Salinity °/oo	Depth, meters	Temperature, ° C.	Salinity, °/oo	σ_t
0	13.50	35.73	0	13.50	35.73	26.87
27	13.50	35.73	25	13.50	35.73	26.87
53	13.51	35.73	50	13.50	35.73	26.87
80	13.52	35.73	75	13.50	35.73	26.87
106	13.51	35.73	100	13.45	35.73	26.88
161	13.30	35.68	150	13.30	35.69	26.88
214	13.28	35.68	200	13.25	35.68	26.88
320	13.22	35.68	300	13.25	35.68	26.88
388	10.97	35.36	400	10.70	35.32	27.10
572	7.25	35.04	600	6.70	34.99	27.47
749	3.61	34.70	800	3.70	34.75	27.64
935	4.05	34.87	1,000	3.90	34.87	27.72
1,398	3.48	34.89				

Station 5757; April 3; latitude 41°56′ N., longitude 49°26′ W.; depth 3,091 m.; dynamic height 970.967.

Observed values			Scaled values			
Depth, meters	Temperature, ° C.	Salinity °/oo	Depth, meters	Temperature, ° C.	Salinity, °/oo	σ_t
0	3.32	33.63	0	3.32	33.63	26.78
26	3.23	33.63	25	3.20	33.63	26.79
53	2.43	33.64	50	2.50	33.64	26.86
79	1.77	33.91	75	1.80	33.87	27.10
106	2.52	34.10	100	2.40	34.07	27.22
157	2.67	34.34	150	2.65	34.31	27.39
210	3.23	34.52	200	3.10	34.49	27.49
316	5.22	34.94	300	5.00	34.89	27.61
443	3.87	34.83	400	4.25	34.86	27.67
663	3.56	34.84	600	3.60	34.83	27.71
883	3.99	34.94	800	3.85	34.90	27.74
1,104	3.63	34.91	1,000	3.80	34.92	27.77
1,658	3.50	34.91				

Station 5758; April 3; latitude 41°27′ N., longitude 48°54′ W.; depth 3,292 m.; dynamic height 971.193.

Observed values			Scaled values			
Depth, meters	Temperature, ° C.	Salinity °/oo	Depth, meters	Temperature, ° C.	Salinity, °/oo	σ_t
0	13.41	35.73	0	13.41	35.73	26.89
25	13.42	35.73	25	13.42	35.73	26.89
49	13.42	35.71	50	13.40	35.71	26.88
74	13.34	35.70	75	13.35	35.70	26.88
99	13.36	35.70	100	13.30	35.70	26.89
148	13.35	35.71	150	13.35	35.71	26.89
197	13.32	35.70	200	13.30	35.70	26.89
296	11.05	35.36	300	10.90	35.34	27.08
384	8.00	34.97	400	7.60	34.95	27.31
580	4.94	34.87	600	4.95	34.88	27.60
778	4.89	35.01	800	4.80	35.01	27.73
976	4.27	34.98	1,000	4.25	34.97	27.76
1,480	3.63	34.91				

Station 5759; April 3; latitude 40°58′ N., longitude 48°32′ W.; depth 3,017 m.; dynamic height 971.017.

Observed values			Scaled values			
Depth, meters	Temperature, ° C.	Salinity, °/oo	Depth, meters	Temperature, ° C.	Salinity, °/oo	σ_t
0	6.70	34.15	0	6.70	34.15	26.81
25	6.72	34.15	25	6.72	34.15	26.81
50	6.73	34.15	50	6.73	34.15	26.80
74	6.75	34.16	75	6.75	34.16	26.81
99	6.34	34.32	100	6.25	34.33	27.01
148	5.18	34.50	150	5.20	34.50	27.28
197	5.55	34.70	200	5.55	34.70	27.39
296	3.93	34.62	300	3.95	34.62	27.51
390	5.02	35.01	400	5.05	35.01	27.70
585	4.91	34.985	600	4.85	34.985	27.70
782	4.37	34.93	800	4.35	34.93	27.71
984	3.94	34.92	1,000	3.95	34.92	27.75
1,500	3.57	34.89				

Station 5760; April 4; latitude 41°39.5′ N., longitude 47°24′ W.; depth 3,932 m.; dynamic height 970.986.

Observed values			Scaled values			
Depth, meters	Temperature, ° C.	Salinity, °/oo	Depth, meters	Temperature, ° C.	Salinity, °/oo	σ_t
0	6.73	34.00	0	6.73	34.00	26.69
26	6.73	34.02	25	6.70	34.02	26.71
51	6.72	34.02	50	6.70	34.02	26.71
77	8.60	34.68	75	8.50	34.68	26.96
102	5.05	34.37	100	5.15	34.38	27.18
152	5.25	34.61	150	5.25	34.60	27.35
203	5.11	34.74	200	5.10	34.74	27.48
305	4.88	34.85	300	4.90	34.85	27.59
425	4.98	34.96	400	5.00	34.95	27.66
635	4.69	35.00	600	4.80	35.00	27.72
844	4.15	34.97	800	4.25	34.98	27.76
1,054	3.85	34.945	1,000	3.90	34.95	27.78
1,580	3.50	34.92				

Station 5761; April 4; latitude 41°53.5′ N., longitude 47°54′ W.; depth 3,841 m.; dynamic height 971.056.

Observed values			Scaled values			
Depth, meters	Temperature, ° C.	Salinity, °/oo	Depth, meters	Temperature, ° C.	Salinity, °/oo	σ_t
0	5.21	33.91	0	5.21	33.91	26.82
26	5.23	33.92	25	5.20	33.92	26.83
51	6.96	34.26	50	6.90	34.25	26.86
77	7.86	34.53	75	7.80	34.51	26.94
102	8.30	34.72	100	8.25	34.71	27.03
152	8.48	34.86	150	8.45	34.86	27.12
203	7.64	34.85	200	7.70	34.85	27.22
305	4.77	34.62	300	4.80	34.62	27.42
393	4.94	34.81	400	4.95	34.82	27.56
584	5.26	35.04	600	5.20	35.04	27.70
770	4.52	34.98	800	4.45	34.97	27.74
971	4.11	34.95	1,000	4.10	34.95	27.76
1,487	3.54	34.90				

Station 5762; April 4; latitude 42°14.5′ N., longitude 48°39′ W.; depth 3,383 m.; dynamic height 971.107.

Observed values			Scaled values			
Depth, meters	Temperature, ° C.	Salinity, °/oo	Depth, meters	Temperature, ° C.	Salinity, °/oo	σ_t
0	11.91	35.38	0	11.91	35.38	26.92
25	12.04	35.43	25	12.04	35.43	26.93
51	12.06	35.43	50	12.05	35.43	26.93
76	12.15	35.45	75	12.15	35.45	26.93
102	12.16	35.45	100	12.10	35.45	26.94
153	12.18	35.46	150	12.15	35.46	26.94
204	9.88	35.06	200	10.10	35.09	27.02
306	7.05	34.88	300	7.15	34.88	27.32
424	6.28	35.00	400	6.40	34.98	27.50
633	5.17	35.03	600	5.35	35.03	27.67
842	4.30	34.96	800	4.45	34.97	27.74
1,054	3.98	34.94	1,000	4.05	34.94	27.75
1,589	3.54	34.90				

Table of Oceanographic Data—Continued

STATIONS OCCUPIED IN 1955—Continued

Station 5763; April 4, latitude 42°43′ N., longitude 49°03′ W.; depth 2,652 m.; dynamic height 970.951.

Observed values			Scaled values			
Depth, meters	Temperature, ° C.	Salinity ‰	Depth, meters	Temperature, ° C.	Salinity, ‰	σ_t
0	3.91	33.65	0	3.91	33.65	26.75
25	3.79	33.66	25	3.79	33.66	26.77
50	3.62	33.84	50	3.62	33.84	26.92
75	2.18	34.10	75	2.18	34.10	27.26
100	2.67	34.24	100	2.67	34.24	27.33
150	3.07	34.43	150	3.07	34.43	27.44
201	3.47	34.56	200	3.45	34.56	27.51
301	3.96	34.75	300	3.95	34.75	27.61
399	5.13	34.99	400	5.10	34.99	27.67
599	4.42	34.96	600	4.40	34.96	27.73
800	4.06	34.95	800	4.05	34.95	27.76
998	3.86	34.94	1,000	3.85	34.94	27.77
1,490	3.47	34.91				

Station 5764; April 4–5; latitude 43°15′ N., longitude 48°41′W.; depth 2,103 m.; dynamic height 970.931.

Observed values			Scaled values			
Depth, meters	Temperature, ° C.	Salinity ‰	Depth, meters	Temperature, ° C.	Salinity, ‰	σ_t
0	4.03	33.71	0	4.03	33.71	26.78
25	4.02	33.71	25	4.02	33.71	26.79
50	3.53	33.82	50	3.53	33.82	26.91
76	2.32	34.03	75	2.35	34.03	27.18
101	2.74	34.17	100	2.70	34.17	27.27
151	3.24	34.45	150	3.50	34.45	27.42
202	3.98	34.72	200	3.95	34.71	27.58
303	*3.96	34.81	300	3.95	34.81	27.66
401	4.05	34.89	400	4.05	34.89	27.71
600	3.66	34.88	600	3.65	34.88	27.74
799	3.46	34.87	800	3.45	34.87	27.76
1,000	3.31	34.86	1,000	3.30	34.86	27.77
1,501	3.30	34.87				

Station 5765; April 5; latitude 43°01′ N., longitude 48°03′ W.; depth 3,338 m.; dynamic height 971.059.

Observed values			Scaled values			
Depth, meters	Temperature, ° C.	Salinity ‰	Depth, meters	Temperature, ° C.	Salinity, ‰	σ_t
0	11.90	35.50	0	11.90	35.50	27.02
22	12.01	35.51	25	12.00	35.51	27.01
44	11.99	35.50	50	11.95	35.50	27.01
67	11.91	35.49	75	11.85	35.49	27.01
89	11.85	35.49	100	11.75	35.47	27.02
133	11.21	35.32	150	10.70	35.22	27.02
177	9.78	35.05	200	9.05	35.02	27.15
266	7.47	34.95	300	5.50	34.70	27.40
298	5.56	34.70	400	4.55	34.74	27.54
451	4.30	34.78	600	4.60	34.94	27.69
608	4.62	34.95	800	4.20	34.94	27.74
776	4.26	34.94	1,000	3.95	34.92	27.75
1,222	3.66	34.91				

Station 5766; April 5; latitude 42°49′ N., longitude 47°34′ W.; depth 3,685 m.; dynamic height 971.072.

Observed values			Scaled values			
Depth, meters	Temperature, ° C.	Salinity ‰	Depth, meters	Temperature, ° C.	Salinity, ‰	σ_t
0	9.59	34.93	0	9.59	34.93	26.98
27	9.51	34.92	25	9.50	34.92	26.99
54	10.77	35.22	50	10.65	35.19	27.00
82	10.91	35.25	75	10.90	35.25	27.01
108	10.89	35.25	100	10.90	35.25	27.01
163	10.33	35.16	150	10.50	35.19	27.03
217	8.63	35.00	200	9.35	35.05	27.12
325	5.09	34.66	300	5.60	34.71	27.40
411	*5.03	34.79	400	5.05	34.77	27.51
620	4.69	34.95	600	4.70	34.94	27.68
831	4.31	34.96	800	4.40	34.96	27.73
1,046	3.98	34.94	1,000	4.05	34.94	27.75
1,596	3.40	34.89				

Station 5767; April 5; latitude 42°35′ N., longitude 46°54′ W.; depth 4,024 m.; dynamic height 971.021.

Observed values			Scaled values			
Depth, meters	Temperature, ° C.	Salinity, ‰	Depth, meters	Temperature, ° C.	Salinity, ‰	σ_t
0	7.78	34.45	0	7.78	34.45	26.90
25	8.06	34.55	25	8.06	34.55	26.93
49	8.13	34.56	50	8.15	34.56	26.93
74	7.48	34.56	75	7.45	34.56	27.03
99	6.29	34.49	100	6.25	34.49	27.14
147	5.48	34.50	150	5.50	34.50	27.24
196	5.67	34.64	200	5.65	34.64	27.33
295	4.50	34.63	300	4.50	34.63	27.45
363	4.83	34.81	400	4.80	34.84	27.59
545	4.61	34.92	600	4.55	34.94	27.70
724	4.46	34.97	800	4.40	34.97	27.74
920	4.18	34.96	1,000	4.05	34.95	27.76
1,422	3.59	34.91				

Station 5768; April 5; latitude 42°25.5′ N., longitude 46°06′ W.; depth 4,340 m.; dynamic height 971.208.

Observed values			Scaled values			
Depth, meters	Temperature, ° C.	Salinity, ‰	Depth, meters	Temperature, ° C.	Salinity, ‰	σ_t
0	15.60	36.10	0	15.60	36.10	26.71
26	15.59	36.09	25	15.60	36.09	26.70
50	15.09	35.98	50	15.10	35.98	26.72
76	13.87	35.69	75	13.90	35.69	26.75
100	13.69	35.68	100	13.69	35.68	26.80
152	12.99	35.52	150	13.00	35.52	26.81
202	13.06	35.54	200	13.05	35.54	26.82
302	8.08	34.65	300	8.15	34.66	27.00
			(400)	6.65	34.77	27.31
			(600)	5.30	35.02	27.68
			(800)	4.75	35.02	27.74
			(1,000)	4.40	34.99	27.75

Station 5769; April 5; latitude 42°48′ N., longitude 45°48′ W.; depth 4,663 m.; dynamic height 971.097.

Observed values			Scaled values			
Depth, meters	Temperature, ° C.	Salinity, ‰	Depth, meters	Temperature, ° C.	Salinity, ‰	σ_t
0	7.94	34.40	0	7.94	34.40	26.83
27	7.89	34.42	25	7.80	34.42	26.87
54	8.17	34.50	50	8.10	34.49	26.88
81	8.64	34.69	75	8.60	34.65	26.93
107	8.33	34.72	100	8.40	34.71	27.01
162	9.35	35.06	150	9.15	35.02	27.13
215	9.19	35.14	200	9.25	35.13	27.20
322	4.63	34.52	300	5.60	34.65	27.35
422	6.58	34.98	400	6.15	34.90	27.47
628	4.82	34.92	600	5.05	34.92	27.63
831	4.53	34.97	800	4.55	34.96	27.72
1,043	4.35	34.98	1,000	4.40	34.98	27.74
1,580	3.67	34.92				

Station 5770; April 6; latitude 43°17.5′ N., longitude 45°26′ W.; depth 4,572 m.; dynamic height 971.051.

Observed values			Scaled values			
Depth, meters	Temperature, ° C.	Salinity, ‰	Depth, meters	Temperature, ° C.	Salinity, ‰	σ_t
0	8.50	34.42	0	8.50	34.42	26.76
25	8.49	34.44	25	8.49	34.44	26.78
49	8.84	34.53	50	8.85	34.52	26.79
74	8.93	34.60	75	8.90	34.60	26.84
98	7.39	34.50	100	7.25	34.50	27.01
148	6.37	34.51	150	6.35	34.52	27.15
197	7.14	34.77	200	7.10	34.77	27.25
295	4.47	34.53	300	4.40	34.53	27.39
389	3.99	34.57	400	4.00	34.59	27.58
580	4.84	34.92	600	4.80	34.92	27.66
770	4.59	34.96	800	4.55	34.97	27.73
966	4.42	34.98	1,000	4.35	34.98	27.75
1,466	3.61	34.905				

Table of Oceanographic Data—Continued

STATIONS OCCUPIED IN 1955—Continued

Station 5771; April 6; latitude 43°21.5′ N.; longitude 45°58′ W.; depth 4,663 m.; dynamic height 971.087.

Observed values			Scaled values			
Depth, meters	Temperature, ° C.	Salinity °/oo	Depth, meters	Temperature, ° C.	Salinity, °/oo	σt
0	8.19	34.44	0	8.19	34.44	26.82
27	8.21	34.43	25	8.20	34.43	26.81
53	8.37	34.45	50	8.35	34.44	26.80
80	9.05	34.71	75	9.00	34.69	26.89
106	8.68	34.70	100	8.80	34.71	26.94
160	5.22	34.40	150	5.60	34.44	27.18
212	4.50	34.42	200	4.60	34.41	27.27
318	5.91	34.73	300	5.85	34.67	27.33
			(400)	5.65	34.83	27.48
			(600)	4.90	34.94	27.66
			(800)	4.65	34.99	27.73
			(1,000)	4.40	34.98	27.74

Station 5772; April 7; latitude 43°41.5′ N., longitude 46°39′ W.; depth 4,298 m.; dynamic height 970.967.

Observed values			Scaled values			
Depth, meters	Temperature, ° C.	Salinity °/oo	Depth, meters	Temperature, ° C.	Salinity, °/oo	σt
0	6.14	34.24	0	6.14	34.24	26.95
26	6.14	34.24	25	6.10	34.24	26.96
52	6.17	34.27	50	6.15	34.26	26.97
78	6.30	34.39	75	6.30	34.37	27.04
104	6.27	34.58	100	6.30	34.57	27.20
155	4.28	34.44	150	4.40	34.45	27.33
207	3.05	34.40	200	3.10	34.40	27.42
311	4.64	34.81	300	4.55	34.78	27.57
364	4.90	34.88	500	4.80	34.91	27.65
553	4.47	34.97	600	4.40	34.97	27.74
746	4.15	34.97	800	4.05	34.96	27.77
943	3.78	34.92	1,000	3.75	34.92	27.77
1,455	3.55	34.915				

Station 5773; April 7; latitude 43°52′ N., longitude 47°20′ W.; depth 4,107 m.; dynamic height 970.949.

Observed values			Scaled values			
Depth, meters	Temperature, ° C.	Salinity °/oo	Depth, meters	Temperature, ° C.	Salinity, °/oo	σt
0	4.07	33.95	0	4.07	33.95	26.96
25	4.07	33.95	25	4.07	33.95	26.96
50	4.04	33.95	50	4.04	33.95	26.96
75	4.02	33.95	75	4.02	33.95	26.97
100	2.13	34.07	100	2.13	34.07	27.24
150	2.60	34.30	150	2.60	34.30	27.38
200	3.31	34.58	200	3.31	34.58	27.54
300	4.27	34.83	300	4.27	34.83	27.64
352	4.90	34.92	400	4.70	34.93	27.67
565	4.21	34.94	600	4.15	34.94	27.74
778	3.96	34.93	800	3.95	34.93	27.75
991	3.62	34.905	1,000	3.60	34.90	27.77

Station 5774; April 7; latitude 44°00′ N., longitude 47°57′ W.; depth 3,870 m.; dynamic height 970.979.

Observed values			Scaled values			
Depth, meters	Temperature, ° C.	Salinity °/oo	Depth, meters	Temperature, ° C.	Salinity, °/oo	σt
0	6.10	34.27	0	6.10	34.27	26.99
25	6.01	34.26	25	6.01	34.26	26.99
49	6.09	34.28	50	6.10	34.28	26.99
74	6.20	34.32	75	6.20	34.32	27.01
98	5.99	34.45	100	5.90	34.45	27.15
147	4.50	34.37	150	4.50	34.37	27.26
196	5.09	34.62	200	5.10	34.63	27.39
294	4.32	34.71	300	4.35	34.73	27.55
372	5.43	34.99	400	5.25	34.98	27.65
562	4.31	34.92	600	4.20	34.92	72.73
753	3.94	34.93	800	3.90	34.93	27.76
946	3.78	34.915	1,000	3.75	34.91	27.76
1,440	3.41	34.89				

Station 5775; April 7; latitude 44°08′ N., longitude 48 27′ W.; depth 3,475 m.; dynamic height 970.982.

Observed values			Scaled values			
Depth, meters	Temperature, ° C.	Salinity, °/oo	Depth, meters	Temperature, ° C.	Salinity, °/oo	σt
0	4.99	33.90	0	4.99	33.90	26.83
26	5.14	33.94	25	5.10	33.93	26.84
51	5.66	34.10	50	5.60	34.09	26.90
77	6.97	34.40	75	6.95	34.38	26.95
103	6.46	34.46	100	6.55	34.46	27.08
153	3.32	34.27	150	3.35	34.27	27.29
205	3.43	34.47	200	3.40	34.45	27.43
308	5.35	34.93	300	5.35	34.93	27.59
282	5.35	34.93	400	5.15	34.97	27.66
442	5.02	34.99	600	4.50	34.97	27.73
615	4.43	34.97	800	3.90	34.93	27.76
788	3.94	34.93	1,000	3.70	34.91	27.77
1,250	3.43	34.89				

Station 5776; April 9; latitude 44°08′ N., longitude 48°52′ W.; depth 1,920 m.; dynamic height 970.944.

Observed values			Scaled values			
Depth, meters	Temperature, ° C.	Salinity, °/oo	Depth, meters	Temperature, ° C.	Salinity, °/oo	σt
0	−0.30	33.12	0	−0.30	33.12	26.62
26	1.18	33.58	25	1.15	33.57	26.91
52	1.24	33.65	50	1.25	33.69	26.99
78	2.39	33.90	75	2.25	33.87	27.07
104	2.97	34.29	100	2.90	34.24	27.31
155	3.39	34.48	150	3.35	34.47	27.45
207	2.57	34.46	200	2.60	34.46	27.51
311	3.66	34.75	300	3.55	34.73	27.63
405	3.89	34.85	400	3.90	34.85	27.70
605	3.62	34.85	600	3.60	34.85	27.73
804	3.66	34.88	800	3.65	34.88	27.74
1,008	3.45	34.865	1,000	3.45	34.87	27.76
1,520	3.32	34.86				

Station 5777; April 9; latitude 44°09′ N., longitude 49°05′ W.; depth 609 m.; dynamic height 970.982.

Observed values			Scaled values			
Depth, meters	Temperature, ° C.	Salinity, °/oo	Depth, meters	Temperature, ° C.	Salinity, °/oo	σt
0	−0.70	33.05	0	−0.70	33.05	26.58
25	−0.70	33.06	25	−0.70	33.06	26.59
50	−0.65	33.08	50	−0.65	33.08	26.61
75	−0.48	33.41	75	−0.48	33.41	26.87
101	−0.06	33.57	100	−0.05	33.57	26.98
150	0.63	33.90	150	0.65	33.90	27.20
201	1.18	34.13	200	1.15	34.12	27.35
302	2.55	34.50	300	2.50	34.49	27.54
403	3.04	34.62	400	3.05	34.62	27.60
589	3.64	34.80	600	3.65	34.81	27.69

Station 5778; April 9; latitude 44°09.5′ N., longitude 49°11′ W.; depth 161 m.; dynamic height 971.071.

Observed values			Scaled values			
Depth, meters	Temperature, ° C.	Salinity, °/oo	Depth, meters	Temperature, ° C.	Salinity, °/oo	σt
0	−0.52	33.17	0	−0.52	33.17	26.67
25	−0.55	33.20	25	−0.55	33.20	26.70
50	−0.54	33.33	50	−0.54	33.33	26.80
75	−0.30	33.46	75	−0.30	33.46	26.90
100	−0.29	33.47	100	−0.29	33.47	26.91
145	−0.28	33.47	150	−0.30	33.47	26.91

Station 5779; April 9; latitude 44°11.5′ N., longitude 49°16′ W.; depth 86 m.; dynamic height 971.072.

Observed values			Scaled values			
Depth, meters	Temperature, ° C.	Salinity, °/oo	Depth, meters	Temperature, ° C.	Salinity, °/oo	σt
0	−0.43	33.12	0	−0.43	33.12	26.63
26	−0.49	33.28	25	−0.50	33.28	26.76
51	−0.49	33.32	50	−0.50	33.32	26.79
72	−0.39	33.40	75	−0.40	33.41	26.87

Table of Oceanographic Data—Continued

STATIONS OCCUPIED IN 1955—Continued

Station 5780; April 9; latitude 44°13′ N., longitude 49°22′ W.; depth 57 m.; dynamic height 971.078.

Observed values: Depth, meters	Temperature, ° C.	Salinity, ‰	Scaled values: Depth, meters	Temperature, ° C.	Salinity, ‰	σ_t
0	−0.41	33.12	0	−0.41	33.12	26.63
25	−0.49	33.12	25	−0.49	33.12	26.63
45	−0.50	33.17	50	−0.50	33.18	26.68

Station 5781; April 9; latitude 44°59′ N., longitude 49°24′ W.; depth 73 m.; dynamic height 971.077.

Observed values: Depth, meters	Temperature, ° C.	Salinity, ‰	Scaled values: Depth, meters	Temperature, ° C.	Salinity, ‰	σ_t
0	−0.34	33.06	0	−0.34	33.06	26.57
25	−0.53	33.07	25	−0.53	33.07	26.59
51	−0.59	33.10	50	−0.60	33.10	26.61

Station 5782; April 9; latitude 44°58′ N., longitude 49°16′ W.; depth 110 m.; dynamic height 971.081.

Observed values: Depth, meters	Temperature, ° C.	Salinity, ‰	Scaled values: Depth, meters	Temperature, ° C.	Salinity, ‰	σ_t
0	−0.24	33.04	0	−0.24	33.04	26.56
26	−0.53	33.05	25	−0.55	33.05	26.58
52	−0.57	33.05	50	−0.55	33.05	26.58
77	−0.58	33.06	75	−0.60	33.06	26.85
93	−0.60	33.07	(100)	−0.60	33.07	26.59

Station 5783; April 9; latitude 44°57′ N., longitude 49°02′ W.; depth 696 m.; dynamic height 971.089.

Observed values: Depth, meters	Temperature, ° C.	Salinity, ‰	Scaled values: Depth, meters	Temperature, ° C.	Salinity, ‰	σ_t
0	−0.42	32.94	0	−0.42	32.94	26.49
25	−0.74	32.98	25	−0.74	32.98	26.53
51	−0.74	33.00	50	−0.75	33.00	26.55
76	−0.68	33.08	75	−0.70	33.08	26.61
101	−0.52	33.32	100	−0.50	33.31	26.78
152	−0.19	33.52	150	−0.20	33.52	26.95
203	−0.05	33.60	200	−0.05	33.59	26.99
304	1.40	34.16	300	1.35	34.14	27.35
401	3.35	34.70	400	3.35	34.70	27.63
602	3.70	34.84	600	3.70	34.84	27.71

Station 5784; April 9; latitude 44°54.5′ N., longitude 48°48′ W.; depth 1,829 m.; dynamic height 970.982.

Observed values: Depth, meters	Temperature, ° C.	Salinity, ‰	Scaled values: Depth, meters	Temperature, ° C.	Salinity, ‰	σ_t
0	−0.19	33.06	0	−0.19	33.06	26.57
24	−0.43	33.21	25	−0.45	33.21	26.71
48	−0.17	33.46	50	−0.10	33.48	26.90
72	1.18	33.76	75	1.50	33.79	27.06
95	2.41	33.94	100	2.30	33.94	27.12
143	0.87	33.94	150	1.15	33.98	27.23
191	2.71	34.38	200	2.75	34.40	27.45
286	2.96	34.57	300	3.15	34.62	27.59
327	3.61	34.74	400	3.70	34.80	27.68
493	3.74	34.83	600	3.65	34.83	27.70
659	3.58	34.83	800	3.50	34.86	27.75
839	3.47	34.86	1,000	3.40	34.86	27.76
1,316	3.34	34.86				

Station 5785; April 9; latitude 44°51.5′ N., longitude 48°33′ W.; depth 2,469 m.; dynamic height 970.922.

Observed values: Depth, meters	Temperature, ° C.	Salinity, ‰	Scaled values: Depth, meters	Temperature, ° C.	Salinity, ‰	σ_t
0	3.46	33.80	0	3.46	33.80	26.90
25	3.38	33.81	25	3.38	33.81	26.92
49	3.21	33.82	50	3.20	33.82	26.95
74	2.09	34.20	75	2.10	34.02	27.20
98	2.19	34.20	100	2.20	34.20	27.34
147	2.83	34.46	150	2.90	34.47	27.50
197	4.02	34.70	200	4.05	34.71	27.57
295	4.67	34.92	300	4.65	34.92	27.68
384	4.49	34.94	400	4.45	34.94	27.71
575	4.01	34.92	600	3.95	34.92	27.75
765	3.67	34.89	800	3.65	34.89	27.75
964	3.49	34.88	1,000	3.45	34.88	27.76
1,472	3.36	34.88				

Station 5786; April 10; latitude 44°45.5′ N., longitude 47°59′ W.; dynamic height 970.966.

Observed values: Depth, meters	Temperature, ° C.	Salinity, ‰	Scaled values: Depth, meters	Temperature, ° C.	Salinity, ‰	σ_t
0	5.80	34.17	0	5.80	34.17	26.95
25	5.76	34.17	25	5.76	34.17	26.95
50	5.76	34.17	50	5.76	34.17	26.95
76	5.40	34.16	75	5.40	34.16	26.98
101	5.59	34.46	100	5.60	34.46	27.20
151	4.61	34.50	150	4.65	34.50	27.34
202	4.47	34.60	200	4.45	34.60	27.44
303	5.18	34.91	300	5.15	34.90	27.60
409	4.89	34.96	400	4.95	34.96	27.67
614	3.93	34.90	600	4.00	34.90	27.73
817	3.79	34.90	800	3.80	34.90	27.75
1,024	3.53	34.895	1,000	3.55	34.90	27.77
1,542	3.31	34.88				

Station 5787; April 10; latitude 44°38′ N., longitude 47°12′ W.; depth 3,749 m.; dynamic height 970.990.

Observed values: Depth, meters	Temperature, ° C.	Salinity, ‰	Scaled values: Depth, meters	Temperature, ° C.	Salinity, ‰	σ_t
0	5.21	34.00	0	5.21	34.00	26.88
23	5.23	34.02	25	5.23	34.02	26.89
47	5.41	34.09	50	5.40	34.10	26.94
70	5.56	34.15	75	5.50	34.15	26.96
93	5.19	34.14	100	4.90	34.13	27.01
140	3.51	34.06	150	3.85	34.14	27.14
196	5.87	34.68	200	5.85	34.69	27.34
279	5.04	34.80	300	4.95	34.83	27.56
345	4.72	34.90	400	4.40	34.89	27.67
526	3.78	34.87	600	3.65	34.87	27.74
712	3.55	34.87	800	3.50	34.88	27.76
900	3.49	34.89	1,000	3.45	34.89	27.77
1,387	3.32	34.90				

Station 5788; April 10; latitude 44°32′ N., longitude 41°28′ W.; depth 3,749 m.; dynamic height 970.998.

Observed values: Depth, meters	Temperature, ° C.	Salinity, ‰	Scaled values: Depth, meters	Temperature, ° C.	Salinity, ‰	σ_t
0	7.15	34.23	0	7.15	34.23	26.81
26	7.11	34.23	25	7.10	34.23	26.82
51	7.10	34.25	50	7.10	34.25	26.84
77	7.68	34.56	75	7.65	34.53	26.97
103	6.27	34.62	100	6.45	34.62	27.22
153	5.44	34.56	150	5.50	34.56	27.29
205	3.93	34.42	200	4.00	34.52	27.43
308	4.72	34.74	300	4.70	34.72	27.51
391	4.61	34.84	400	4.60	34.85	27.62
588	4.44	34.945	600	4.40	34.95	27.72
787	4.32	34.975	800	4.30	34.97	27.75
992	3.95	34.94	1,000	3.95	34.94	27.76
1,521	3.53	34.92				

Table of Oceanographic Data—Continued

STATIONS OCCUPIED IN 1955—Continued

Station 5789; April 10; latitude 44°26.5′ N., longitude 45°50′ W.; depth 3,841 m.; dynamic height 971.042.

Observed values			Scaled values			
Depth, meters	Temperature, ° C.	Salinity ‰	Depth, meters	Temperature, ° C.	Salinity, ‰	σ_t
0	8.13	34.45	0	8.13	34.45	26.85
26	9.53	34.80	25	9.50	34.80	26.90
52	8.95	34.74	50	8.95	34.74	26.94
78	9.33	34.86	75	9.30	34.84	26.96
103	9.69	35.05	100	9.65	35.04	27.06
154	7.55	34.79	150	7.75	34.81	27.18
206	5.09	34.52	200	5.15	34.53	27.30
309	4.90	34.71	300	4.90	34.69	27.46
414	5.26	34.885	400	5.25	34.86	27.56
621	4.72	34.96	600	4.75	34.96	27.69
829	4.23	34.95	800	4.30	34.95	27.73
1,042	3.73	34.86	1,000	3.80	34.87	27.73
1,580	3.44	34.89				

Station 5790; April 10; latitude 44°22′ N., longitude 45°18′ W.; depth 4,298 m.; dynamic height 971.062.

Observed values			Scaled values			
Depth, meters	Temperature, ° C.	Salinity ‰	Depth, meters	Temperature, ° C.	Salinity, ‰	σ_t
0	8.57	34.42	0	8.57	34.42	26.75
24	8.55	34.41	25	8.55	34.41	26.75
48	8.35	34.54	50	8.40	34.58	26.90
72	9.63	35.00	75	9.60	35.00	27.04
96	9.18	34.96	100	9.10	34.94	27.07
144	7.65	34.80	150	7.50	34.78	27.19
193	6.55	34.68	200	6.35	34.67	27.27
289	4.83	34.60	300	5.05	34.65	27.41
357	6.87	35.07	400	6.40	35.02	27.54
544	4.69	34.88	600	4.60	34.90	27.66
738	4.56	34.96	800	4.50	34.96	27.72
930	4.25	34.96	1,000	4.15	34.96	27.76
1,423	3.72	34.92				

Station 5791; April 10; latitude 44°49′ N., longitude 45°17′ W.; depth 4,115 m.; dynamic height 971.013.

Observed values			Scaled values			
Depth, meters	Temperature, ° C.	Salinity ‰	Depth, meters	Temperature, ° C.	Salinity, ‰	σ_t
0	8.10	34.50	0	8.10	34.50	26.89
25	8.12	34.50	25	8.12	34.50	26.89
50	8.08	34.50	50	8.08	34.50	26.89
75	7.87	34.46	75	7.87	34.46	26.89
99	7.70	34.70	100	7.70	34.70	27.10
149	5.52	34.51	150	5.45	34.51	27.26
199	4.59	34.44	200	4.60	34.44	27.29
298	4.93	34.72	300	4.90	34.72	27.49
394	4.44	34.82	400	4.40	34.82	27.62
595	4.23	34.91	600	4.20	34.91	27.71
800	4.05	34.925	800	4.05	34.92	27.74
1,005	3.77	34.92	1,000	3.80	34.92	27.77
1,526	3.36	34.88				

Station 5792; April 11; latitude 45°20′ N., longitude 45°14′ W.; depth 4,061 m.; dynamic height 970.957.

Observed values			Scaled values			
Depth, meters	Temperature, ° C.	Salinity ‰	Depth, meters	Temperature, ° C.	Salinity, ‰	σ_t
0	5.49	34.18	0	5.49	34.18	26.99
25	5.48	34.18	25	5.48	34.18	26.99
51	5.48	34.18	50	5.48	34.18	26.99
76	5.15	34.18	75	5.15	34.18	27.03
102	4.38	34.19	100	4.45	34.19	27.11
153	5.28	34.57	150	5.25	34.56	27.32
204	5.17	34.72	200	5.20	34.71	27.44
306	4.86	34.89	300	4.90	34.89	27.62
417	4.25	34.88	400	4.35	34.88	27.67
617	4.21	34.96	600	4.20	34.96	27.76
813	3.86	34.92	800	3.90	34.92	27.76
1,018	3.61	34.91	1,000	3.60	34.91	27.78
1,534	3.42	34.91				

Station 5793; April 11; latitude 45°17.5′ N., longitude 45°59′ W.; depth 3,475 m.; dynamic height 970.948.

Observed values			Scaled values			
Depth, meters	Temperature, ° C.	Salinity, ‰	Depth, meters	Temperature, ° C.	Salinity, ‰	σ_t
0	6.25	34.21	0	6.25	34.21	26.92
25	6.18	34.20	25	6.18	34.20	26.92
50	5.38	34.09	50	5.38	34.09	26.93
75	5.94	34.27	75	5.94	34.27	27.01
100	5.40	34.38	100	5.40	34.38	27.15
150	5.14	34.60	150	5.14	34.60	27.36
200	5.32	34.77	200	5.32	34.77	27.48
300	4.21	34.83	300	4.21	34.83	27.65
383	4.08	34.87	400	4.05	34.87	27.70
577	3.79	34.90	600	3.80	34.90	27.75
772	3.69	34.90	800	3.65	34.90	27.76
968	3.53	34.89	1,000	3.50	34.89	27.77
1,466	3.27	34.87				

Station 5794; April 11; latitude 45°21′ N., longitude 46°42′ W.; depth 3,109 m.; dynamic height 970.929.

Observed values			Scaled values			
Depth, meters	Temperature, ° C.	Salinity, ‰	Depth, meters	Temperature, ° C.	Salinity, ‰	σ_t
0	5.25	34.10	0	5.25	34.10	26.95
25	5.20	34.09	25	5.20	34.09	26.95
50	4.14	34.03	50	4.14	34.03	.27.02
75	4.11	34.06	75	4.11	34.06	27.05
99	3.68	34.12	100	3.70	34.12	27.14
149	4.50	34.55	150	4.50	34.55	27.40
199	4.41	34.77	200	4.40	34.77	27.58
298	3.97	34.82	300	3.95	34.82	27.67
366	*3.75	34.84	400	3.70	34.84	27.71
552	3.58	34.86	600	3.55	34.87	27.75
741	3.51	34.88	800	3.50	34.88	27.76
934	3.42	34.88	1,000	3.40	34.88	27.77
1,430	3.28	34.88				

Station 5795; April 11; latitude 45°26.5′ N., longitude 47°23′ W.; depth 2,378 m.; dynamic height 970.893.

Observed values			Scaled values			
Depth, meters	Temperature, ° C.	Salinity, ‰	Depth, meters	Temperature, ° C.	Salinity, ‰	σ_t
0	2.63	34.00	0	2.63	34.00	27.14
24	2.61	34.00	25	2.60	34.00	27.14
47	2.55	34.00	50	2.55	34.00	27.15
71	2.63	34.08	75	2.80	34.13	27.23
94	3.78	34.40	100	4.00	34.45	27.37
141	4.64	34.74	150	4.60	34.75	27.54
189	4.40	34.78	200	4.35	34.79	27.60
283	4.16	34.86	300	4.15	34.87	27.69
354	4.09	34.88	400	4.00	34.88	27.71
537	3.72	34.89	600	3.60	34.89	27.76
723	3.45	34.88	800	3.40	34.88	27.77
915	3.34	34.88	1,000	3.35	34.88	27.77
1,413	3.26	34.88				

Station 5796; April 11; latitude 45°38′ N., longitude 47°43′ W.; depth 1,430 m.; dynamic height 970.916.

Observed values			Scaled values			
Depth, meters	Temperature, ° C.	Salinity, ‰	Depth, meters	Temperature, ° C.	Salinity, ‰	σ_t
0	1.09	33.70	0	1.09	33.70	27.01
25	1.26	33.76	25	1.26	33.76	27.05
50	2.04	33.97	50	2.04	33.97	27.17
74	0.74	33.88	75	0.75	33.88	27.18
99	1.37	33.98	100	1.35	33.99	27.23
148	2.75	34.39	150	2.80	34.40	27.44
197	3.36	34.61	200	3.35	34.62	27.57
296	3.79	34.83	300	3.80	34.83	27.69
360	3.63	34.83	400	3.60	34.83	27.71
542	3.52	34.85	600	3.50	34.85	27.74
726	3.45	34.86	800	3.40	34.85	27.75
919	3.35	34.845	1,000	3.35	34.85	27.75
1,300	3.26	34.84				

STATIONS OCCUPIED IN 1955—Continued

Observed values			Scaled values			
Depth, meters	Temperature, ° C.	Salinity °/oo	Depth, meters	Temperature, ° C.	Salinity, °/oo	σt
Station 5797; April 11; latitude 45°45′ N., longitude W.; depth 608 m.; dynamic height 971.026.						
0	−0.80	33.12	0	−0.80	33.12	26.64
26	−0.80	33.12	25	−0.80	33.12	26.64
51	−0.72	33.40	50	−0.70	33.39	26.86
77	−0.55	33.60	75	−0.55	33.59	27.01
102	0.34	33.72	100	0.30	33.72	27.08
153	0.43	33.80	150	0.45	33.79	27.12
204	0.54	33.88	200	0.55	33.87	27.19
306	2.14	34.41	300	2.00	34.38	27.49
406	3.49	34.72	400	3.45	34.71	27.63
592	3.57	34.82	600	3.60	34.82	27.71
Station 5798; April 11; latitude 45°49.5′ N., longitude 48°07′ W.; depth 170 m.; dynamic height 971.063.						
0	−0.97	33.07	0	−0.97	33.07	26.61
25	−0.95	33.10	25	−0.95	33.10	26.63
50	−1.01	33.36	50	−1.01	33.36	26.84
75	−0.61	33.52	75	−0.61	33.52	26.96
100	0.02	33.62	100	0.02	33.62	27.02
150	0.05	33.62	150	0.05	33.62	27.02
Station 5799; April 11; latitude 45°52′ N., longitude 48°12′ W.; depth 126 m.; dynamic height 971.074.						
0	−0.92	33.07	0	−0.92	33.07	26.61
25	−0.95	33.07	25	−0.95	33.07	26.61
50	−1.16	33.18	50	−1.16	33.18	26.70
74	−1.01	33.29	75	−1.00	33.29	26.78
99	−0.28	33.48	100	−0.25	33.49	26.92
Station 5800; April 12; latitude46°00′ N., longitude 48°27′W.; depth 102 m.; dynamic height 971.078.						
0	−0.26	33.02	0	−0.26	33.02	26.54
25	−0.25	33.03	25	−0.25	33.03	26.55
50	−0.15	33.06	50	−0.15	33.06	26.57
75	−0.13	33.07	75	−0.13	33.07	26.58
95	*−0.36	33.46	(100)	−0.40	33.50	26.94
Station 5801; April 12; latitude 46°07′ N., longitude 48°41′ W.; depth 95 m.; dynamic height 971.080.						
0	0.21	33.10	0	0.21	33.10	26.58
26	0.21	33.10	25	0.20	33.10	26.58
51	0.21	33.10	50	0.20	33.10	26.58
77	−0.03	33.22	75	0.00	33.21	26.69
Station 5802; April 12; latitude 46°13′ N., longitude 48°53′ W.; depth 77 m.; dynamic height 971.081.						
0	0.34	33.06	0	0.34	33.06	26.54
27	0.33	33.08	25	0.30	33.08	27.57
54	0.28	33.09	50	0.30	33.09	26.57
70	0.25	33.12	(75)	0.25	33.13	26.61

Observed values			Scaled values			
Depth, meters	Temperature, ° C.	Salinity, °/oo	Depth, meters	Temperature, ° C.	Salinity, °/oo	σt
Station 5803; April 12; latitude 46°12.5′ N., longitude 48°43′ W.; depth 95 m.; dynamic height 971.076.						
0	0.28	33.13	0	0.28	33.13	26.61
25	0.28	33.12	25	0.28	33.12	26.60
49	0.29	33.12	50	0.30	33.12	26.60
74	0.09	33.20	75	0.10	33.20	26.68
Station 5804; April 12; latitude 46°10.5′ N., longitude 48°12′ W.; depth 115 m.; dynamic height 971.067.						
0	−0.42	33.00	0	−0.42	33.00	26.54
25	−0.41	33.00	25	−0.41	33.00	26.54
51	−0.25	33.40	50	−0.25	33.40	26.85
76	−0.24	33.40	75	−0.25	33.40	26.85
102	−0.12	33.50	100	−0.15	33.49	26.92
Station 5805; April 12; latitude 46°09.5′ N., longitude 47°51′ W.; depth 169 m.; dynamic height 971.075.						
0	−1.19	33.03	0	−1.19	33.03	26.58
24	−1.20	33.03	25	−1.20	33.03	26.58
49	−1.20	33.04	50	−1.20	33.04	26.59
73	−0.87	33.30	75	−0.85	33.31	26.79
97	−0.67	33.44	100	−0.60	33.44	26.89
146	−0.10	33.58	150	−0.05	33.59	26.99
Station 5806; April 12; latitude 46°07.5′ N., longitude 47°31′ W.; depth 633 m.; dynamic height 971.024.						
0	−0.41	33.07	0	−0.41	33.07	26.59
24	−0.48	33.07	25	−0.45	33.07	26.59
48	−0.61	33.25	50	−0.65	33.26	26.75
72	−0.78	33.40	75	−0.80	33.41	26.88
97	−0.56	33.50	100	−0.50	33.52	26.96
145	0.46	33.87	150	0.50	33.89	27.20
193	0.82	34.03	200	0.90	34.06	27.32
290	2.27	34.44	300	2.35	34.46	27.53
394	2.96	34.61	400	3.00	34.62	27.61
600	3.66	34.85	600	3.66	34.85	27.72
Station 5807; April 12; latitude 46°06′ N., longitude 47°14′ W.; depth 1,472 m., dynamic height 970.939.						
0	−0.28	33.25	0	−0.28	33.25	26.72
26	0.07	33.57	25	0.05	33.56	26.97
51	0.37	33.86	50	0.35	33.85	27.18
77	0.92	34.03	75	0.90	34.01	27.28
103	1.01	34.12	100	1.00	34.11	27.35
153	1.67	34.27	150	1.60	34.26	27.43
204	2.22	34.42	200	2.15	34.41	27.51
307	3.45	34.71	300	3.40	34.69	27.62
424	3.86	34.83	400	3.85	34.82	27.68
637	3.63	34.84	600	3.65	34.84	27.71
851	3.45	34.84	800	3.50	34.84	27.73
1,063	3.35	34.86	1,000	3.35	34.86	27.76
1,457	3.26	34.87				

Table of Oceanographic Data—Continued

STATIONS OCCUPIED IN 1955—Continued

Station 5808; April 12; latitude 46°05′ N., longitude 46°35′ W.; depth 1,097 m.; dynamic height 970.906.

Observed values			Scaled values			
Depth, meters	Temperature, ° C.	Salinity, ‰	Depth, meters	Temperature, ° C.	Salinity, ‰	σ_t
0	3.59	34.04	0	3.59	34.04	27.08
25	3.45	34.05	25	3.45	34.05	27.11
49	3.04	34.04	50	3.05	34.04	27.13
74	3.90	34.32	75	3.95	34.33	27.28
98	4.22	34.50	100	4.25	34.51	27.39
147	4.50	34.73	150	4.50	34.74	27.54
196	4.50	34.82	200	4.50	34.82	27.61
294	4.16	24.86	300	4.15	24.86	27.68
401	3.89	34.88	400	3.90	34.88	27.72
600	3.64	34.88	600	3.65	34.88	27.74
800	3.37	34.86	800	3.60	34.86	27.74
999	3.33	34.865	1,000	3.60	34.86	27.74

Station 5809; April 12; latitude 46°04′ N., longitude 45°59′ W.; depth 1,646 m.; dynamic height 970.900.

Observed values			Scaled values			
Depth, meters	Temperature, ° C.	Salinity, ‰	Depth, meters	Temperature, ° C.	Salinity, ‰	σ_t
0	3.90	34.02	0	3.90	34.02	27.04
25	3.90	34.06	25	3.90	34.06	27.08
50	3.87	34.08	50	3.87	34.08	27.08
74	3.82	34.10	75	3.70	34.10	27.12
100	3.88	34.32	100	3.90	34.32	27.28
149	3.99	34.70	150	4.00	34.70	27.57
199	3.92	34.80	200	3.90	34.80	27.66
299	3.72	34.83	300	3.70	34.83	27.70
361	3.66	34.84	400	3.65	34.85	27.72
550	3.54	34.86	600	3.50	34.86	27.75
746	3.44	34.85	800	3.40	34.85	27.75
941	3.35	34.865	1,000	3.35	34.86	27.76
1,445	3.28	34.875				

Station 5810; April 13; latitude 46°04.5′ N., longitude 45°14′ W.; depth 2,926 m.; dynamic height 970.909.

Observed values			Scaled values			
Depth, meters	Temperature, ° C.	Salinity, ‰	Depth, meters	Temperature, ° C.	Salinity, ‰	σ_t
0	5.01	34.26	0	5.01	34.26	27.11
25	5.00	34.27	25	5.00	34.27	27.13
50	4.90	34.28	50	4.90	34.28	27.13
75	4.90	34.35	75	4.90	34.35	27.19
101	4.81	34.46	100	4.80	34.46	27.29
150	4.75	34.67	150	4.75	34.67	27.47
201	4.24	34.71	200	4.25	34.71	27.55
302	3.89	34.80	300	3.90	34.80	27.66
378	3.81	34.84	400	3.80	34.85	27.71
572	3.61	34.865	600	3.55	34.87	27.75
768	------	34.87	800	3.40	34.87	27.77
969	3.38	34.87	1,000	3.35	34.87	27.77
1,485	3.28	34.90				

Station 5811; April 13; latitude 46°04.5′ N., longitude 44°42′ W.; depth 3,510 m.; dynamic height 970.927.

Observed values			Scaled values			
Depth, meters	Temperature, ° C.	Salinity, ‰	Depth, meters	Temperature, ° C.	Salinity, ‰	σ_t
0	5.08	34.30	0	5.08	34.30	27.13
24	5.05	34.30	25	5.05	34.30	27.14
49	5.01	34.28	50	4.85	34.28	27.14
73	4.50	34.25	75	4.50	34.25	27.16
98	4.46	34.33	100	4.45	34.34	27.23
145	4.40	34.47	150	4.35	34.48	27.35
194	4.02	34.56	200	4.00	34.57	27.47
292	4.36	34.82	300	4.35	34.83	27.63
396	4.20	34.89	400	4.20	34.89	27.70
589	3.94	34.92	600	3.85	34.92	27.76
778	3.64	34.90	800	3.60	34.90	27.77
975	3.50	34.90	1,000	3.50	34.90	27.78
1,472	3.33	34.88				

Station 5812; April 13; latitude 46°25′ N., longitude 44°50′ W.; depth 1,518 m.; dynamic height 970.876.

Observed values			Scaled values			
Depth, meters	Temperature, ° C.	Salinity, ‰	Depth, meters	Temperature, ° C.	Salinity, ‰	σ_t
0	3.79	34.18	0	3.79	34.18	27.17
25	3.80	34.18	25	3.80	34.18	27.18
50	3.79	34.19	50	3.79	34.19	27.18
76	3.87	34.32	75	3.85	34.32	27.29
101	3.96	34.48	100	3.95	34.47	27.39
151	3.93	34.73	150	3.95	34.72	27.59
201	3.87	34.82	200	3.85	34.82	27.68
302	3.86	34.85	300	3.85	34.85	27.70
417	3.56	34.86	400	3.60	34.86	27.74
627	3.42	34.86	600	3.45	34.86	27.75
839	*3.38	34.87	800	3.40	34.87	27.77
1,052	3.35	34.875	1,000	3.35	34.87	27.77
1,234	3.33	34.875				

Station 5813; April 13; latitude 46°28′ N., longitude 44°52′ W.; depth 741 m.; dynamic height 970.886.

Observed values			Scaled values			
Depth, meters	Temperature, ° C.	Salinity, ‰	Depth, meters	Temperature, ° C.	Salinity, ‰	σ_t
0	3.80	34.10	0	3.80	34.10	27.11
26	3.80	34.10	25	3.75	34.10	27.12
53	3.78	34.11	50	3.80	34.11	27.12
79	3.75	34.21	75	3.75	34.19	27.19
105	4.02	34.54	100	4.00	34.48	27.39
157	3.96	34.68	150	3.95	34.66	27.54
209	3.85	34.80	200	3.85	34.78	27.64
314	3.84	34.855	300	3.85	34.85	27.70
582	3.46	34.88	400	3.70	34.86	27.73
			(600)	3.45	34.88	27.76

Station 5814; April 13; latitude 46°36′ N., longitude 44°55′ W.; depth 238 m.; dynamic height 970.903.

Observed values			Scaled values			
Depth, meters	Temperature, ° C.	Salinity, ‰	Depth, meters	Temperature, ° C.	Salinity, ‰	σ_t
0	3.81	34.06	0	3.81	34.06	27.08
25	3.81	34.05	25	3.81	34.05	27.07
49	3.81	34.07	50	3.80	34.07	27.09
74	3.70	34.13	75	3.70	34.13	27.14
98	3.65	34.22	100	3.65	34.24	27.24
147	4.22	43.66	150	4.20	34.67	27.53
196	3.99	34.78	200	3.95	34.78	27.63

Station 5815; April 13; latitude 46°43′ N., longitude 44°56′ W.; depth 174 m.; dynamic height 970.901.

Observed values			Scaled values			
Depth, meters	Temperature, ° C.	Salinity, ‰	Depth, meters	Temperature, ° C.	Salinity, ‰	σ_t
0	3.84	34.08	0	3.84	34.08	27.09
27	3.84	34.08	25	3.85	34.08	27.09
53	3.76	34.10	50	3.75	34.09	27.11
80	3.63	34.20	75	3.65	34.18	27.19
107	3.74	34.33	100	3.70	34.29	27.27
161	4.07	34.68	150	4.00	34.61	27.50

Station 5816; April 13; latitude 46°49′ N., longitude 44°57′ W.; depth 165 m.; dynamic height 970.897.

Observed values			Scaled values			
Depth, meters	Temperature, ° C.	Salinity, ‰	Depth, meters	Temperature, ° C.	Salinity, ‰	σ_t
0	3.84	34.08	0	3.84	34.08	27.10
25	3.84	34.09	25	3.84	34.09	27.11
50	3.84	34.09	50	3.84	34.09	27.10
75	3.81	34.11	75	3.81	34.11	27.12
100	3.82	34.41	100	3.82	34.41	27.36
145	4.04	34.65	(150)	4.05	34.67	27.54

STATIONS OCCUPIED IN 1955—Continued

Station 5817; April 13; latitude 46°49′ N., longitude 45°04′ W.; depth 176 m.; dynamic height 970.903.

Observed values			Scaled values			
Depth, meters	Temperature, ° C.	Salinity °/oo	Depth, meters	Temperature, ° C.	Salinity, °/oo	σt
0	3.86	34.07	0	3.86	34.07	27.09
26	3.86	34.075	25	3.85	34.08	27.09
51	3.87	34.08	50	3.85	34.08	27.09
77	3.84	34.115	75	3.85	34.11	27.12
102	3.85	34.27	100	3.85	34.25	27.23
			(150)	4.00	34.60	27.49

Station 5818; April 13; latitude 46°49′ N., longitude 45°18′ W.; depth 222 m.; dynamic height 970.899.

Observed values			Scaled values			
Depth, meters	Temperature, ° C.	Salinity °/oo	Depth, meters	Temperature, ° C.	Salinity, °/oo	σt
0	3.84	34.04	0	3.84	34.04	27.06
25	3.84	34.04	25	3.84	34.04	27.06
50	3.82	34.06	50	3.82	34.06	27.08
75	3.79	34.06	75	3.79	34.06	27.08
100	3.95	34.38	100	3.95	34.38	27.32
149	4.14	34.73	150	4.15	34.73	27.57
199	4.04	34.72	200	4.05	34.72	27.58

Station 5819; April 14; latitude 46°56′ N., longitude 46°04′ W.; depth 306 m.; dynamic height 970.913.

Observed values			Scaled values			
Depth, meters	Temperature, ° C.	Salinity °/oo	Depth, meters	Temperature, ° C.	Salinity, °/oo	σt
0	3.84	34.06	0	3.84	34.06	27.08
26	3.85	34.06	25	3.85	34.06	27.08
50	3.87	34.06	50	3.87	34.06	27.08
76	3.85	34.06	75	3.85	34.06	27.08
101	3.86	34.05	100	3.85	34.06	27.08
152	4.62	34.63	150	4.60	34.61	27.46
202	4.21	34.75	200	4.25	34.74	27.57
261	3.85	34.83	(300)	3.80	34.86	27.72

Station 5820; April 14; latitude 46°55.5′ N., longitude 46°10′ W.; depth 302 m.; dynamic height 970.908.

Observed values			Scaled values			
Depth, meters	Temperature, ° C.	Salinity °/oo	Depth, meters	Temperature, ° C.	Salinity, °/oo	σt
0	3.86	34.07	0	3.86	34.07	27.09
25	3.89	34.06	25	3.89	34.06	27.07
49	3.89	34.06	50	3.90	34.06	27.07
73	3.91	34.07	75	3.90	34.07	27.08
97	3.90	34.07	100	3.90	34.07	27.08
147	4.52	34.67	150	4.50	34.68	27.49
196	4.19	34.80	200	4.15	34.80	27.63
293	3.80	34.85	300	3.80	34.85	27.71

Station 5821; April 14; latitude 46°49.5′ N., longitude 46°32′ W.; depth 626 m.; dynamic height 970.883.

Observed values			Scaled values			
Depth, meters	Temperature, ° C.	Salinity °/oo	Depth, meters	Temperature, ° C.	Salinity, °/oo	σt
0	2.54	34.06	0	2.54	34.06	27.20
27	2.44	34.07	25	2.45	34.07	27.21
53	2.42	34.07	50	2.40	34.07	27.22
80	2.39	34.10	75	2.40	34.09	27.23
107	2.42	34.30	100	2.40	34.25	27.36
161	3.78	34.74	150	3.55	34.65	27.57
214	3.85	34.80	200	3.85	34.79	27.65
321	3.79	34.84	300	3.80	34.83	27.69
389	3.52	34.86	400	3.50	34.86	27.74
594	3.48	34.86	600	3.45	34.86	27.75

Station 5822; April 15; latitude 46°46.5′ N., longitude 46°51′ W.; depth 1,229 m.; dynamic height 970.891.

Observed values			Scaled values			
Depth, meters	Temperature, ° C.	Salinity, °/oo	Depth, meters	Temperature, ° C.	Salinity, °/oo	σt
0	1.27	34.02	0	1.27	34.02	27.27
27	1.43	34.08	25	1.40	34.07	27.29
52	1.61	34.13	50	1.60	34.12	27.32
79	1.62	34.18	75	1.65	34.17	27.36
105	1.81	34.28	100	1.75	34.26	27.42
158	2.47	34.49	150	2.35	34.46	27.53
210	2.97	34.62	200	2.85	34.60	27.60
315	3.88	34.80	300	3.75	34.78	27.65
401	3.78	34.84	400	3.80	34.84	27.70
604	3.61	34.85	600	3.60	34.85	27.73
807	3.42	34.86	800	3.40	34.86	27.76
1,173	3.31	34.86	1,000	3.35	34.86	27.76

Station 5823; April 15; latitude 46°43′ N., longitude 47°10′ W.; depth 567 m.; dynamic height 971.001.

Observed values			Scaled values			
Depth, meters	Temperature, ° C.	Salinity, °/oo	Depth, meters	Temperature, ° C.	Salinity, °/oo	σt
0	−0.41	33.41	0	−0.41	33.41	26.87
25	−0.39	33.42	25	−0.39	33.41	26.87
50	−0.36	33.41	50	−0.36	33.42	26.87
75	−0.36	33.42	75	−0.36	33.42	26.87
99	0.02	33.62	100	0.05	33.63	27.02
149	0.69	34.01	150	0.80	34.01	27.28
199	1.17	34.17	200	1.20	34.17	27.39
298	2.31	34.47	300	2.30	34.47	27.55
407	3.12	34.65	400	3.10	34.64	27.61

Station 5824; April 15; latitude 46°42′ N., longitude 47°17′ W.; depth 298 m.; dynamic height 971.047.

Observed values			Scaled values			
Depth, meters	Temperature, ° C.	Salinity, °/oo	Depth, meters	Temperature, ° C.	Salinity, °/oo	σt
0	−0.89	33.24	0	−0.89	33.24	26.75
27	−0.78	33.30	25	−0.80	33.29	26.77
53	−0.49	33.40	50	−0.55	33.39	26.85
80	−0.43	33.44	75	−0.45	33.43	26.88
106	−0.01	33.54	100	−0.10	33.51	26.93
160	0.46	33.77	150	0.40	33.72	27.08
213	0.68	34.01	200	0.60	33.96	27.25
293	1.23	34.19	(300)	1.30	34.20	27.40

Station 5825; April 15; latitude 46°43′ N., longitude 47°34′ W.; depth 178 m.; dynamic height 971.098.

Observed values			Scaled values			
Depth, meters	Temperature, ° C.	Salinity, °/oo	Depth, meters	Temperature, ° C.	Salinity, °/oo	σt
0	−1.40	32.92	0	−1.40	32.92	26.50
25	−1.40	32.95	25	−1.40	32.95	26.52
50	−1.39	32.96	50	−1.39	32.96	26.53
75	−1.37	32.98	75	−1.37	32.98	26.55
100	−1.23	33.08	100	−1.23	33.08	26.62
150	−0.13	33.48	150	−0.13	33.48	26.91

Station 5826; April 15; latitude 46°43′ N., longitude 48°08′ W.; depth 117 m.; dynamic height 971.077.

Observed values			Scaled values			
Depth, meters	Temperature, ° C.	Salinity, °/oo	Depth, meters	Temperature, ° C.	Salinity, °/oo	σt
0	−0.01	33.05	0	−0.01	33.05	26.56
25	−0.03	33.08	25	−0.03	33.08	26.58
50	−0.03	33.08	50	−0.03	33.08	26.58
75	−0.05	33.08	75	−0.05	33.08	26.58
100	−0.11	33.55	100	−0.11	33.55	26.96

STATIONS OCCUPIED IN 1955—Continued

Station 5827; April 15; latitude 46°46.5′ N., longitude 48°41′ W.; depth 93 m.; dynamic height 971.076.

Observed values			Scaled values			
Depth, meters	Temperature, ° C.	Salinity, ‰	Depth, meters	Temperature, ° C.	Salinity, ‰	σ_t
0	0.21	33.07	0	0.21	33.07	26.56
25	0.14	33.14	25	0.14	33.14	26.62
50	0.13	33.13	50	0.13	33.14	26.62
75	0.13	33.14	75	0.13	33.14	26.62

Station 5828; April 26; latitude 47°25.5′ N., longitude 50°02′ W.; depth 75 m.

Observed values			Scaled values			
Depth, meters	Temperature, ° C.	Salinity, ‰	Depth, meters	Temperature, ° C.	Salinity, ‰	σ_t
0	−0.60	33.03	0	−0.60	33.03	------
27	−0.61	-----	25	−0.60	------	------
53	−0.45	-----	50	−0.45	------	------
69	−0.49	-----	(75)	−0.50	------	------

Station 5829; April 26; latitude 47°40′ N., longitude 49°56′ W.; depth 128 m.

Observed values			Scaled values			
Depth, meters	Temperature, ° C.	Salinity, ‰	Depth, meters	Temperature, ° C.	Salinity, ‰	σ_t
0	−0.59	-----	0	− .59	------	------
25	−0.62	-----	25	−0.62	------	------
50	−0.64	-----	50	−0.64	------	------
76	−0.74	-----	75	−0.75	------	------
101	−0.32	-----	100	−0.35	------	------

Station 5830; April 26; latitude 47°55′ N., longitude 49°52′ W.; depth 169 m.

Observed values			Scaled values			
Depth, meters	Temperature, ° C.	Salinity, ‰	Depth, meters	Temperature, ° C.	Salinity, ‰	σ_t
0	−1.18	32.88	0	−1.18	32.88	26.47
26	−1.23	-----	25	−1.20	32.89	26.47
51	−1.35	-----	50	−1.35	32.90	26.48
77	−1.39	32.99	75	−1.40	32.99	26.56
103	−1.21	33.10	100	−1.25	33.09	26.63
154	−0.31	33.43	150	−0.40	33.41	26.87

Station 5831; April 26; latitude 48°10.5′ N., longitude 49°46′ W.; depth 210 m.

Observed values			Scaled values			
Depth, meters	Temperature, ° C.	Salinity, ‰	Depth, meters	Temperature, ° C.	Salinity, ‰	σ_t
0	−1.09	32.87	0	−1.09	32.87	26.45
25	−1.15	32.88	25	−1.15	32.88	26.47
50	−1.36	32.91	50	−1.36	32.91	26.49
75	−1.57	33.01	75	−1.57	33.01	26.58
100	−1.53	33.09	100	−1.53	33.09	26.64
151	−0.83	33.28	150	−0.85	33.28	26.77
201	−0.38	33.41	200	−0.40	33.41	26.87

Station 5832; April 26; latitude 47°23.5′ N., longitude 50°00′ W.; depth 114 m.; dynamic height 971.093.

Observed values			Scaled values			
Depth, meters	Temperature, ° C.	Salinity, ‰	Depth, meters	Temperature, ° C.	Salinity, ‰	σ_t
0	−0.18	33.05	0	−0.18	33.05	26.56
25	−0.29	33.06	25	−0.29	33.06	26.57
51	−0.37	33.09	50	−0.35	33.09	26.59
76	−0.44	33.12	75	−0.40	33.12	26.63

Station 5833; April 26; latitude 47°40.5′ N., longitude 49°53′ W.; depth 115 m.; dynamic height 971.096.

Observed values			Scaled values			
Depth, meters	Temperature, ° C.	Salinity, ‰	Depth, meters	Temperature, ° C.	Salinity, ‰	σ_t
0	−0.63	32.94	0	−0.63	32.94	26.50
25	−0.56	32.96	25	−0.56	32.96	26.50
51	−0.72	32.98	50	−0.70	32.98	26.53
76	−0.61	33.21	75	−0.65	33.21	26.72
102	−0.31	33.35	100	−0.30	33.34	26.80

Station 5834; April 26–27; latitude 47°57′ N., longitude 49°45′ W.; depth 178 m.; dynamic height 971.107.

Observed values			Scaled values			
Depth, meters	Temperature, ° C.	Salinity, ‰	Depth, meters	Temperature, ° C.	Salinity, ‰	σ_t
0	−1.03	32.91	0	−1.03	32.91	26.48
25	−1.12	32.92	25	−1.12	32.92	26.49
50	−1.28	32.93	50	−1.28	32.93	26.50
75	−1.36	33.01	75	−1.36	33.01	26.58
101	−1.24	33.08	100	−1.25	33.08	26.62
151	−0.71	33.31	150	−0.70	33.31	26.79

Station 5835; April 27; latitude 48°10′ N., longitude 49°40′ W.; depth 224 m.; dynamic height 971.109.

Observed values			Scaled values			
Depth, meters	Temperature, ° C.	Salinity, ‰	Depth, meters	Temperature, ° C.	Salinity, ‰	σ_t
0	−1.05	32.85	0	−1.05	32.85	26.44
25	−1.16	32.86	25	−1.16	32.86	26.44
49	−1.48	32.93	50	−1.50	32.93	26.51
74	−1.41	33.02	75	−1.40	33.02	26.58
99	−1.55	33.07	100	−1.55	33.07	26.63
148	−1.09	33.22	150	−1.05	33.23	26.74
197	−0.39	33.43	200	−0.35	33.44	26.88

Station 5836; April 27; latitude 48°30.5′ N., longitude 49°30′ W.; depth 564 m.; dynamic height 971.044.

Observed values			Scaled values			
Depth, meters	Temperature, ° C.	Salinity, ‰	Depth, meters	Temperature, ° C.	Salinity, ‰	σ_t
0	−1.06	32.98	0	−1.06	32.98	26.54
22	−1.00	33.05	25	−1.05	33.07	26.61
45	−1.18	33.15	50	−1.15	33.17	26.70
67	−0.83	33.23	75	−0.70	33.26	26.75
89	−0.55	33.33	100	−0.45	33.39	26.85
134	−0.10	33.61	150	0.10	33.72	27.09
179	0.41	33.89	200	0.60	33 95	27.24
268	1.13	34.09	300	1.50	34.19	27.38
260	1.12	34.09	400	2.50	34.54	27.58
414	2.64	34.59				

Station 5837; April 27; latitude 48°37′ N., longitude 49°27′ W.; depth 1,060 m.; dynamic height 970.952.

Observed values			Scaled values			
Depth, meters	Temperature, ° C.	Salinity, ‰	Depth, meters	Temperature, ° C.	Salinity, ‰	σ_t
0	0.05	33.43	0	0.05	33.43	26.86
25	0.05	33.48	25	0.05	33.48	26.90
50	−0.19	33.59	50	−0.19	33.59	27.00
74	0.22	33.70	75	0.25	33.70	27.07
99	0.44	33.87	100	0 45	33.87	27.19
148	1.44	34.19	150	1.45	34.19	27.38
198	1.97	34.31	200	2.00	34.31	27.44
297	2.71	34.62	300	2.75	34.62	27.63
344	2.93	34.67	400	3.25	34.73	27.66
528	3.70	34.84	600	3.70	34.86	27.73
720	3.66	34.87	800	3.60	34.88	27.75
922	3.53	34.88	(1,000)	3.50	34.85	27.76

STATIONS OCCUPIED IN 1955—Continued

Observed values			Scaled values			
Depth, meters	Temperature, ° C.	Salinity °/oo	Depth, meters	Temperature, ° C.	Salinity, °/oo	σ_t

Station 5838; April 27; latitude 49°01.5′ N., longitude 49°18′ W.; depth 1,646 m.; dynamic height 970.906.

0	0.15	33.47	0	0.15	33.47	26.89
24	1.00	33.93	25	1.00	33.93	27.20
47	0.95	33.98	50	0.95	33.99	27.25
71	1.45	34.19	75	1.50	34.22	27.41
95	1.73	34.31	100	1.80	34.32	27.47
142	2.02	34.43	150	2.10	34.45	27.54
189	2.47	34.55	200	2.50	34.56	27.60
284	2.89	34.66	300	3.00	34.68	27.65
367	3.31	34.75	400	3.35	34.77	27.69
556	3.50	34.83	600	3.45	34.82	27.72
749	3.30	34.81	800	3.35	24.82	27.73
943	3.60	34.88	1,000	3.60	34.88	27.75
1,439	3.36	34.88				

Station 5839; April 27; latitude 49°27.5′ N., longitude 49°01′ W.; depth 1,829 m.; dynamic height 970.829.

0	3.00	34.34	0	3.00	34.34	27.38
24	2.47	34.32	25	2.45	34.32	27.41
49	2.54	34.34	50	2.55	34.34	27.42
73	2.69	34.49	75	2.70	34.51	27.54
98	2.77	34.69	100	2.80	34.70	27.68
147	3.19	34.77	150	3.20	34.77	27.71
195	3.40	34.80	200	3.40	34.81	27.72
293	3.52	34.84	300	3.55	34.84	27.72
407	3.53	34.86	400	3.55	34.86	27.74
609	3.57	34.89	600	3.60	34.89	27.76
810	3.47	34.89	800	3.45	34.89	27.77
1,014	3.41	34.89	1,000	3.40	34.89	27.78
1,529	3.19	34.92				

Station 5840; April 27; latitude 49°54′ N., longitude 48°55′ W., depth 1,975 m.; dynamic height 970.839.

0	3.81	34.53	0	3.81	34.53	27.45
25	3.56	34.51	25	3.56	34.51	27.46
50	2.91	34.46	50	2.91	34.46	27.49
75	2.79	34.50	75	2.79	34.50	27.52
100	2.95	34.65	100	2.95	34.65	27.63
150	3.29	34.75	150	3.29	34.75	27.68
199	3.13	34.75	200	3.15	34.75	27.69
299	3.27	34.77	300	3.25	34.77	27.70
406	3.42	34.83	400	3.40	34.83	27.73
612	3.52	34.87	600	3.50	34.87	27.76
820	3.51	34.88	800	3.50	34.88	27.76
1,026	3.39	34.88	1,000	3.40	34.88	27.77
1,540	3.29	34.91				

Station 5841; April 28; latitude 49°45.5′ N., longitude 48°22′ W.; depth 2,378 m.; dynamic height 970.859.

0	4.60	34.49	0	4.60	34.49	27.33
25	4.56	34.49	25	4.56	34.49	27.34
50	4.25	34.45	50	4.25	34.45	27.34
75	3.54	34.44	75	3.54	34.44	27.40
100	3.25	34.51	100	3.25	34.51	27.49
150	2.89	34.63	150	2.89	34.63	27.62
201	3.53	34.77	200	3.50	34.77	27.68
301	3.49	34.81	300	3.50	34.81	27.71
408	3.45	34.83	400	3.45	34.83	27.72
609	3.62	34.88	600	3.60	34.88	27.75
807	3.49	34.885	800	3.50	34.88	27.76
1,011	3.39	34.88	1,000	3.40	34.88	27.77
1,526	3.33	34.90				

Observed values			Scaled values			
Depth, meters	Temperature, ° C.	Salinity, °/oo	Depth, meters	Temperature, ° C.	Salinity, °/oo	σ_t

Station 5842; April 28; latitude 49°38′ N., longitude 47°43′ W.; depth 2,652 m.; dynamic height 970.848.

0	3.87	34.40	0	3.87	34.40	27.35
26	3.85	34.40	25	3.85	34.40	27.35
51	3.22	34.39	50	3.25	34.39	27.39
77	2.97	34.41	75	3.00	34.41	27.44
102	2.65	34.55	100	2.65	34.54	27.57
153	3.39	34.72	150	3.40	34.71	27.64
205	3.35	34.77	200	3.35	34.76	27.68
307	3.72	34.85	300	3.70	34.85	27.72
402	3.73	34.87	400	3.75	34.87	27.73
600	3.59	34.89	600	3.60	34.89	27.76
797	3.45	34.885	800	3.45	34.885	27.77
997	3.36	34.88	1,000	3.35	34.88	27.77
1,500	3.27	34.905				

Station 5843; April 28; latitude 49°15.5′ N., longitude 47°53′ W.; depth 2,451 m.; dynamic height 970.852.

0	4.56	34.47	0	4.56	34.47	27.33
25	4.50	34.45	25	4.50	34.45	27.32
50	4.48	34.49	50	4.48	34.49	27.35
75	3.87	34.47	75	3.87	34.47	27.40
100	2.91	34.56	100	2.91	34.56	37.57
150	3.21	34.73	150	3.21	34.73	27.67
201	3.14	34.75	200	3.15	34.75	27.69
301	3.15	34.78	300	3.15	34.78	27.71
378	3.71	34.87	400	3.70	34.87	27.74
566	3.61	34.88	600	3.60	34.88	27.75
755	3.48	34.88	800	3.45	34.88	27.76
950	3.38	34.87	1,000	3.35	34.87	27.77
1,447	3.30	34.91				

Station 5844; April 28; latitude 48°49′ N., longitude 48°07′ W.; depth 2,268 m.; dynamic height 970.860.

0	2.65	34.28	0	2.65	34.28	27.36
25	2.47	34.31	25	2.47	34.31	27.40
50	2.45	34.29	50	2.45	34.31	27.40
75	2.46	34.32	75	2.46	34.32	27.41
100	2.72	34.44	100	2.72	34.44	27.48
150	3.21	34.71	150	3.21	34.71	27.66
201	3.46	34.77	200	3.45	34.77	27.68
301	3.39	34.79	300	3.35	34.79	27.70
400	3.22	34.78	400	3.25	34.78	27.70
600	3.63	34.86	600	3.65	34.86	27.73
801	3.49	34.89	800	3.50	34.89	27.77
1,001	3.37	34.875	1,000	3.35	34.75	27.77
1,504	3.33	34.89				

Station 5845; April 28; latitude 48°28′ N., longitude 48°20′ W.; depth 1,829 m.; dynamic height 970.852.

0	2.59	34.25	0	2.59	34.25	27.34
25	2.65	34.35	25	2.65	34.35	27.42
50	2.76	34.37	50	2.76	34.37	27.43
75	2.61	34.45	75	2.61	34.45	27.50
100	2.69	34.59	100	2.69	34.59	27.60
150	3.04	34.69	150	3.04	34.69	27.65
200	3.32	34.75	200	3.32	34.75	27.68
300	3.70	34.83	300	3.70	34.83	27.70
384	3.65	34.85	400	3.65	34.85	27.72
578	3.63	34.88	600	3.65	34.88	27.74
774	3.53	34.88	800	3.55	34.88	27.75
970	3.43	34.88	1,000	3.40	34.88	27.77
1,464	3.32	34.90				

STATIONS OCCUPIED IN 1955—Continued

Station 5846; April 29; latitude 48°07′ N., longitude 48°30′ W., depth 503 m.; dynamic height 970.958.

Observed values			Scaled values			
Depth, meters	Temperature, ° C.	Salinity °/oo	Depth, meters	Temperature, ° C.	Salinity, °/oo	σ_t
0	−0.15	33.31	0	−0.15	33.31	26.77
25	−0.64	33.35	25	−0.64	33.35	26.82
51	−0.35	33.52	50	−0.35	33.52	26.95
77	0.18	33.74	75	0.15	33.72	27.09
103	0.52	33.90	100	0.50	33.89	27.20
153	1.15	34.13	150	1.15	34.12	27.35
205	1.86	34.31	200	1.80	34.29	27.44
308	3.01	34.65	300	2.90	34.63	27.62
407	3.79	34.85	400	3.75	34.84	27.70
480	3.63	34.855				

Station 5847; April 29; latitude 48°03′ N., longitude 48°33′ W.; depth 324 m.; dynamic height 970.969.

Observed values			Scaled values			
Depth, meters	Temperature, ° C.	Salinity °/oo	Depth, meters	Temperature, ° C.	Salinity, °/oo	σ_t
0	−0.34	33.27	0	−0.34	33.27	26.74
25	0.27	33.50	25	0.27	33.50	26.91
51	0.14	33.56	50	0.15	33.56	26.96
76	0.32	33.69	75	0.30	33.68	27.04
102	0.53	33.91	100	0.50	33.88	27.19
153	0.96	34.05	150	0.95	34.04	27.29
203	1.49	34.26	200	1.45	34.25	27.43
305	2.68	34.56	300	2.65	34.55	27.58

Station 5848; April 29; latitude 47°47.5′ N., longitude 48°41′ W.; depth 224 m.; dynamic height 971.067.

Observed values			Scaled values			
Depth, meters	Temperature, ° C.	Salinity °/oo	Depth, meters	Temperature, ° C.	Salinity, °/oo	σ_t
0	−0.57	32.87	0	−0.57	32.87	26.44
25	−1.13	32.91	25	−1.13	32.91	26.48
51	−1.35	32.94	50	−1.35	32.94	26.52
76	−1.42	33.04	75	−1.40	33.04	26.60
102	−1.05	33.19	100	−1.10	33.18	26.70
153	−0.64	33.38	150	−0.65	33.37	26.84
204	−0.16	33.56	200	−0.20	33.54	26.96

Station 5849; April 29; latitude 47°35′ N., longitude 48°45′ W.; depth 172 m.; dynamic height 971.073.

Observed values			Scaled values			
Depth, meters	Temperature, ° C.	Salinity °/oo	Depth, meters	Temperature, ° C.	Salinity, °/oo	σ_t
0	−0.66	32.88	0	−0.66	32.88	26.45
25	−1.22	32.95	25	−1.22	32.95	26.52
51	−1.28	33.01	50	−1.30	33.01	26.57
76	−1.29	33.09	75	−1.30	33.09	26.63
102	−1.08	33.19	100	−1.15	33.18	26.70
153	−0.67	33.34	150	−0.70	33.33	26.81

Station 5850; April 29; latitude 47°41′ N., longitude 48°20′ W.; depth 220 m.; dynamic height 971.078.

Observed values			Scaled values			
Depth, meters	Temperature, ° C.	Salinity °/oo	Depth, meters	Temperature, ° C.	Salinity, °/oo	σ_t
0	−0.71	32.83	0	−0.71	32.83	26.41
24	−1.10	32.91	25	−1.15	32.91	26.48
49	−1.37	32.92	50	−1.35	32.92	26.50
73	−1.30	33.09	75	−1.30	33.10	26.64
98	−1.18	33.13	100	−1.15	33.13	26.66
146	−0.71	33.31	150	−0.65	33.33	26.81
195	−0.04	33.60	200	0.00	33.63	27.02

Station 5851; April 29; latitude 47°43′ N., longitude 48°12′ W.; depth 240 m.; dynamic height 971.071.

Observed values			Scaled values			
Depth, meters	Temperature, ° C.	Salinity, °/oo	Depth, meters	Temperature, ° C.	Salinity, °/oo	σ_t
0	−0.59	32.83	0	−0.59	32.83	26.40
25	−0.91	32.87	25	−0.91	32.87	26.45
50	−1.07	32.89	50	−1.07	32.87	26.46
75	−1.24	33.03	75	−1.24	33.03	26.58
100	−1.16	33.17	100	−1.16	33.17	26.70
149	−0.39	33.43	150	−0.40	33.44	26.89
199	0.40	33.79	200	0.40	33.80	27.14
229	1.21	34.12				

Station 5852; April 29; latitude 47°50′ N., longitude 47°50′ W.; depth 315 m.; dynamic height 971.015.

Observed values			Scaled values			
Depth, meters	Temperature, ° C.	Salinity, °/oo	Depth, meters	Temperature, ° C.	Salinity, °/oo	σ_t
0	−0.14	32.97	0	−0.14	32.97	26.50
25	−0.71	33.10	25	−0.71	33.10	26.62
50	−0.72	33.28	50	−0.72	33.28	26.77
74	−0.57	33.40	75	−0.55	33.40	26.86
99	−0.15	33.55	100	−0.15	33.55	26.97
149	0.47	33.83	150	0.45	33.83	27.15
198	0.80	34.02	200	0.80	34.03	27.29
297	3.01	35.65	300	3.05	34.67	27.64

Station 5853; April 29; latitude 47°57′ N., longitude 47°42′ W.; depth 355 m.; dynamic height 971.019.

Observed values			Scaled values			
Depth, meters	Temperature, ° C.	Salinity, °/oo	Depth, meters	Temperature, ° C.	Salinity, °/oo	σ_t
0	−0.43	33.01	0	−0.43	33.01	26.55
25	−0.90	33.14	25	−0.90	33.14	26.67
50	−0.82	33.27	50	−0.82	33.27	26.76
75	−0.43	33.42	75	−0.43	33.42	26.88
101	−0.14	33.56	100	−0.15	33.56	26.98
151	0.38	33.82	150	0.35	33.82	27.16
201	0.94	34.02	200	0.95	34.02	27.28
302	2.24	34.44	300	2.20	34.43	27.52

Station 5854; April 29; latitude 48°08.5′ N., longitude 47°27′ W.; depth 1,097 m.; dynamic height 970.917.

Observed values			Scaled values			
Depth, meters	Temperature, ° C.	Salinity, °/oo	Depth, meters	Temperature, ° C.	Salinity, °/oo	σ_t
0	0.89	33.37	0	0.89	33.37	26.76
25	0.88	33.99	25	0.88	33.99	27.26
50	0.93	34.06	50	0.93	34.06	27.31
75	1.22	34.15	75	1.22	34.15	27.37
101	1.40	34.21	100	1.40	34.21	27.41
151	1.75	34.31	150	1.70	34.31	27.46
201	2.39	34.48	200	2.40	34.48	27.54
302	3.00	34.65	300	3.00	34.65	27.63
388	3.27	34.71	400	3.30	34.72	27.66
584	3.72	34.84	600	3.70	34.85	27.72
781	3.68	34.87	800	3.65	34.87	27.74
981	3.54	34.88	1000	3.55	34.88	27.75

Station 5855; April 29; latitude 48°28.5′ N., longitude 47°09′ W.; depth 2,195 m.; dynamic height 970.856.

Observed values			Scaled values			
Depth, meters	Temperature, ° C.	Salinity, °/oo	Depth, meters	Temperature, ° C.	Salinity, °/oo	σ_t
0	2.48	34.21	0	2.48	34.21	27.32
25	2.21	34.24	25	2.21	34.24	27.37
49	2.38	34.32	50	2.40	34.32	27.42
74	3.44	34.36	75	2.45	34.36	27.44
99	2.51	34.39	100	2.50	34.39	27.46
148	3.19	34.68	150	3.20	34.69	27.64
197	3.64	34.79	200	3.65	34.79	27.67
296	3.82	34.855	300	3.80	34.85	27.71
380	3.63	34.85	400	3.65	34.85	27.72
572	3.63	34.88	600	3.60	34.88	27.75
765	3.50	34.875	800	3.50	34.88	27.76
960	3.41	34.88	1,000	3.40	34.89	27.78
1,456	3.31	34.90				

STATIONS OCCUPIED IN 1955—Continued

Station 5856; April 29; latitude 48°49.5′ N., longitude 46°50′ W.; depth 2,652 m.; dynamic height 970.874.

Observed values			Scaled values			
Depth, meters	Temperature, ° C.	Salinity °/oo	Depth, meters	Temperature, ° C.	Salinity, °/oo	σ_t
0	4.24	34.405	0	4.24	34.405	27.30
24	4.22	34.40	25	4.20	34.40	27.31
48	4.12	34.41	50	4.10	34.41	27.33
72	4.03	34.41	75	4.00	34.41	27.34
96	3.93	34.41	100	3.90	34.41	27.35
144	3.28	34.59	150	3.30	34.61	27.57
191	3.70	34.75	200	3.75	34.76	27.64
287	3.91	34.84	300	3.90	34.85	27.70
362	3.83	34.86	400	3.75	34.87	27.73
550	3.65	34.885	600	3.60	34.88	27.75
743	3.54	34.88	800	3.50	34.88	27.76
936	3.45	34.87	1,000	3.40	34.87	27.77
1,431	3.31	34.875				

Station 5857; April 30; latitude 49°15′ N., longitude 46°26′ W.; depth 3,017 m.; dynamic height 970.864.

Observed values			Scaled values			
Depth, meters	Temperature, ° C.	Salinity °/oo	Depth, meters	Temperature, ° C.	Salinity, °/oo	σ_t
0	4.09	34.36	0	4.09	34.36	27.29
26	3.65	34.36	25	3.65	34.36	27.33
51	3.46	34.37	50	3.45	34.37	27.36
77	3.35	34.37	75	3.35	34.37	27.37
102	3.47	24.51	100	3.45	34.49	27.45
152	3.77	34.74	150	3.75	34.73	27.61
203	4.02	34.83	200	4.00	34.83	27.67
305	3.82	34.86	300	3.85	34.86	27.71
409	3.71	34.87	400	3.70	34.87	27.74
610	3.55	34.88	600	3.55	34.88	27.75
810	3.44	34.87	800	3.45	34.87	27.76
1,014	3.33	34.87	1,000	3.30	34.87	27.78
1,532	3.30	34.89				

Station 5858; April 30; latitude 49°07′ N., longitude 45°44′ W.; depth 2,743 m.; dynamic height 970.865.

Observed values			Scaled values			
Depth, meters	Temperature, ° C.	Salinity °/oo	Depth, meters	Temperature, ° C.	Salinity, °/oo	σ_t
0	2.45	34.15	0	2.45	34.15	27.27
25	3.79	34.35	26	3.79	34.35	27.32
50	3.56	34.37	50	3.56	34.37	27.35
75	3.39	34.39	75	3.39	34.39	27.38
99	2.39	34.36	100	2.40	34.36	27.45
149	3.67	34.73	150	3.65	34.73	27.62
199	3.27	34.73	200	3.30	34.73	27.66
298	3.72	34.83	300	3.70	34.83	27.70
402	3.69	34.85	400	3.70	34.85	27.72
601	3.59	34.88	600	3.60	34.88	27.75
799	3.45	34.88	800	3.45	34.88	27.76
1,001	3.38	34.88	1,000	3.35	34.88	27.77
1,511	3.33	34.89				

Station 5859; April 30; latitude 48°56′N., longitude 45°05′ W.; depth 1,417 m.; dynamic height 970.859.

Observed values			Scaled values			
Depth, meters	Temperature, ° C.	Salinity °/oo	Depth, meters	Temperature, ° C.	Salinity, °/oo	σ_t
0	2.30	34.03	0	2.30	34.03	27.19
24	1.94	34.13	25	1.90	34.13	27.30
49	1.92	34.19	50	1.90	34.19	27.35
73	2.54	34.40	75	2.55	34.41	27.48
97	2.74	34.53	100	2.75	34.55	27.57
146	3.15	34.71	150	3.15	34.72	27.67
195	3.45	34.77	200	3.45	34.77	27.68
292	3.66	34.82	300	3.70	34.82	27.70
321	3.82	34.86	400	3.75	34.87	27.73
508	3.64	34.87	600	3.55	34.87	27.75
697	3.47	34.88	800	3.45	34.88	27.76
890	3.39	34.88	1,000	3.40	34.88	27.77
1,335	3.30	34.89				

Station 5860; April 30; latitude 48°40.5′ N., longitude 45°32′ W.; depth 1,186 m.; dynamic height 970.858.

Observed values			Scaled values			
Depth, meters	Temperature, ° C.	Salinity, °/oo	Depth, meters	Temperature, ° C.	Salinity, °/oo	σ_t
0	4.39	34.28	0	4.39	34.28	27.19
26	3.73	34.28	25	3.70	34.28	27.26
52	3.68	34.33	50	3.70	34.32	27.30
78	3.35	34.39	75	3.40	34.38	27.37
104	2.89	34.49	100	2.90	34.47	27.50
155	3.65	34.75	150	3.60	34.73	27.63
207	3.84	34.81	200	3.85	34.81	27.67
311	3.79	34.86	300	3.80	34.86	27.72
404	3.71	34.87	200	3.70	34.87	27.74
607	3.52	34.885	600	3.50	34.88	27.76
812	3.36	34.875	800	3.40	34.875	27.77
1,021	3.29	34.86	1,000	3.30	34.86	27.77

Station 5861; April 30; latitude 48°22.5′ N., longitude 40°06′ W., depth 1,130 m.; dynamic height 970.856.

Observed values			Scaled values			
Depth, meters	Temperature, ° C.	Salinity, °/oo	Depth, meters	Temperature, ° C.	Salinity, °/oo	σ_t
0	2.46	34.02	0	2.46	34.02	27.17
25	1.47	34.01	25	1.47	34.01	27.24
49	1.47	34.13	50	1.45	34.13	27.33
74	2.08	34.45	75	2.10	34.45	27.54
99	2.45	34.54	100	2.45	34.54	27.58
148	2.96	34.66	150	2.95	34.66	27.64
197	3.32	34.73	200	3.35	34.73	27.65
296	3.84	34.86	300	3.85	34.86	27.71
405	3.75	34.86	400	3.75	34.86	27.72
607	3.59	34.88	600	3.60	34.88	27.75
808	3.44	34.885	800	3.45	34.885	27.77
1,015	3.35	34.88	1,000	3.35	34.88	27.77

Station 5862; April 30; latitude 48°03′ N., longitude 46°28′ W.; depth 1,181 m.; dynamic height 970.873.

Observed values			Scaled values			
Depth, meters	Temperature, ° C.	Salinity, °/oo	Depth, meters	Temperature, ° C.	Salinity, °/oo	σ_t
0	2.42	34.05	0	2.42	34.05	27.20
25	1.78	34.07	25	1.78	34.07	27.27
49	2.93	34.23	50	2.95	34.23	27.29
74	3.10	34.31	75	3.10	34.31	27.35
98	2.22	34.31	100	2.25	34.31	27.42
147	2.89	34.62	150	2.90	34.63	27.62
197	3.38	34.73	200	3.40	34.73	27.65
295	3.81	34.85	300	3.80	34.85	27.71
360	3.73	34.855	400	3.70	34.855	27.72
549	3.56	34.855	600	3.55	34.86	27.74
745	3.46	34.87	800	3.45	34.87	27.76
949	3.34	34.87	1,000	3.30	34.87	27.78

Station 5863; May 1; latitude 47°54.5′ N., longitude 46°10′ W.; depth 1,060 m.; dynamic height 970.849.

Observed values			Scaled values			
Depth, meters	Temperature, ° C.	Salinity, °/oo	Depth, meters	Temperature, ° C.	Salinity, °/oo	σ_t
0	3.45	34.20	0	3.45	34.20	27.22
25	2.76	34.29	25	2.76	34.29	27.36
50	2.46	34.28	50	2.46	34.28	27.37
75	2.74	34.33	75	2.74	34.33	27.39
100	2.93	34.43	100	2.93	34.43	27.45
149	3.79	34.76	150	3.80	34.76	27.64
199	3.74	34.83	200	3.75	34.83	27.69
299	3.61	34.84	300	3.65	34.84	27.71
406	3.52	34.85	400	3.50	34.85	27.74
609	3.42	34.87	600	3.40	34.87	27.77
814	3.25	34.865	800	3.25	34.865	27.77
1,028	3.23	34.875	1,000	3.20	34.87	27.79

Station 5864; May 1; latitude 47°45.5′ N., longitude 45°52′ W.; depth 434 m.; dynamic height 970.875.

Observed values			Scaled values			
Depth, meters	Temperature, ° C.	Salinity, °/oo	Depth, meters	Temperature, ° C.	Salinity, °/oo	σ_t
0	3.73	34.05	0	3.73	34.05	27.08
25	3.71	34.07	25	3.71	34.07	27.10
49	3.30	34.14	50	3.30	34.14	27.19
74	3.02	34.23	75	3.00	34.23	27.29
99	2.99	34.33	100	3.00	34.33	27.37
147	3.46	34.60	150	3.50	34.62	27.56
196	3.82	34.795	200	3.80	34.80	27.67
295	3.69	34.84	300	3.70	34.84	27.71
402	3.39	34.86	400	3.40	34.86	27.76

Station 5865; May 1; latitude 47°42.5′ N., longitude 45°43′ W.; depth 320 m.; dynamic height 970.879.

Observed values			Scaled values			
Depth, meters	Temperature, ° C.	Salinity, °/oo	Depth, meters	Temperature, ° C.	Salinity, °/oo	σ_t
0	4.18	34.02	0	4.18	34.02	27.01
22	4.17	34.02	25	4.10	34.02	27.02
45	3.43	34.09	50	3.25	34.10	27.16
67	3.06	34.15	75	3.10	34.19	27.25
89	3.30	34.30	100	3.50	34.38	27.36
134	4.23	34.62	150	4.25	34.71	27.55
178	4.18	34.81	200	4.10	34.83	27.66
267	3.79	34.86	(300)	3.65	34.87	27.74

Station 5866; May 1; latitude 47°29.5′ N., longitude 45°12′ W.; depth 224 m.; dynamic height 970.888.

Observed values			Scaled values			
Depth, meters	Temperature, ° C.	Salinity, °/oo	Depth, meters	Temperature, ° C.	Salinity, °/oo	σ_t
0	4.21	34.03	0	4.21	34.03	27.02
25	4.17	34.05	25	4.17	34.05	27.04
50	3.81	34.12	50	3.81	34.12	27.13
75	3.63	34.17	75	3.63	34.17	27.19
100	3.48	34.29	100	3.48	34.29	27.29
150	4.13	34.66	150	4.13	34.66	27.53
200	3.99	34.77	200	3.99	34.77	27.63

Station 5867; May 1; latitude 47°23.5′ N., longitude 44°58′ W.; depth 173 m.; dynamic height 970.890.

Observed values			Scaled values			
Depth, meters	Temperature, ° C.	Salinity, °/oo	Depth, meters	Temperature, ° C.	Salinity, °/oo	σ_t
0	4.30	34.05	0	4.30	34.05	27.02
26	4.28	34.04	25	4.25	34.04	27.02
52	3.86	34.07	50	3.85	34.06	27.08
77	3.84	34.10	75	3.85	34.10	27.11
103	4.07	34.51	100	4.05	34.44	27.36
154	4.01	34.71	150	4.05	34.69	27.55

Station 5868; May 2; latitude 47°19′ N., longitude 45°24′ W.; depth 231 m.; dynamic height 970.905.

Observed values			Scaled values			
Depth, meters	Temperature, ° C.	Salinity, °/oo	Depth, meters	Temperature, ° C.	Salinity, °/oo	σ_t
0	3.83	34.09	0	3.83	34.09	27.10
26	3.83	34.08	25	3.85	34.08	27.09
52	3.84	34.10	50	3.85	34.10	27.11
79	3.84	34.10	75	3.85	34.10	27.11
105	3.86	34.12	100	3.85	34.11	27.12
157	4.06	34.63	150	4.05	34.58	27.46
209	3.93	34.65	200	4.00	34.65	27.53

Station 5869; May 2; latitude 47°18′ N., longitude 45°40′ W.; depth 274 m.; dynamic height 970.899

Observed values			Scaled values			
Depth, meters	Temperature, ° C.	Salinity, °/oo	Depth, meters	Temperature, ° C.	Salinity, °/oo	σ_t
0	3.86	34.09	0	3.86	34.09	27.10
24	3.86	34.09	25	3.85	34.09	27.10
47	3.86	34.09	50	3.85	34.09	27.10
71	3.87	34.08	75	3.85	34.09	27.10
94	3.85	34.10	100	3.85	34.16	27.16
142	4.27	34.59	150	4.25	34.65	27.50
189	4.10	34.78	200	4.05	34.79	27.63
236	3.89	34.83				

Station 5870; May 2; latitude 47°16′ N., longitude 45°56′ W., depth 318 m.; dynamic height 970.908.

Observed values			Scaled values			
Depth, meters	Temperature, ° C.	Salinity, °/oo	Depth, meters	Temperature, ° C.	Salinity, °/oo	σ_t
0	3.86	34.06	0	3.86	34.06	27.08
24	3.86	34.06	25	3.85	34.06	27.08
47	3.85	34.07	50	3.85	34.07	27.09
71	3.84	34.08	75	3.85	34.08	27.09
95	3.81	34.09	100	3.80	34.09	27.10
142	4.12	34.50	150	4.15	34.56	27.44
189	4.26	34.75	200	4.20	34.77	27.61
284	3.88	34.86	(300)	3.85	34.86	27.71

Station 5871; May 2; latitude 47°15.5′ N., longitude 46°30′ W.; depth 631 m.; dynamic height 970.877.

Observed values			Scaled values			
Depth, meters	Temperature, ° C.	Salinity, °/oo	Depth, meters	Temperature, ° C.	Salinity, °/oo	σ_t
0	2.51	34.16	0	2.51	34.16	27.28
26	2.51	34.16	25	2.50	34.16	27.28
51	2.51	34.16	50	2.50	34.16	27.28
77	2.51	34.16	75	2.50	34.16	27.28
103	2.77	34.24	100	2.70	34.22	27.31
153	3.75	34.71	150	3.70	34.68	27.58
205	3.94	34.81	200	3.90	34.81	27.67
308	3.69	34.82	300	3.75	34.82	27.69
378	3.55	34.83	400	3.50	34.83	27.72
578	3.41	34.84	600	3.40	34.84	27.74

Station 5872; May 2; latitude 47°15.5′N., longitude 46°37′W.; depth 1,134 m.; dynamic height 970.877.

Observed values			Scaled values			
Depth, meters	Temperature, ° C.	Salinity, °/oo	Depth, meters	Temperature, ° C.	Salinity, °/oo	σ_t
0	2.15	34.17	0	2.15	34.17	27.32
26	2.15	34.16	25	2.10	34.16	27.31
52	2.15	34.16	50	2.15	34.16	27.31
78	2.13	34.17	75	2.15	34.17	27.32
104	2.21	34.21	100	2.20	34.20	27.34
155	2.66	34.55	150	2.60	34.51	27.55
207	3.67	34.75	200	3.50	34.73	27.64
311	3.80	34.84	300	3.80	34.84	27.70
422	3.67	34.84	400	3.70	34.84	27.71
629	3.42	34.85	600	3.45	34.85	27.74
835	3.37	34.86	800	3.40	34.86	27.76
1,047	3.28	34.86	1,000	3.30	34.86	27.77

Station 5873; May 2; latitude 47°15.5′N., longitude 47°07′W.; depth 982 m.; dynamic height 970.917.

Observed values			Scaled values			
Depth, meters	Temperature, ° C.	Salinity, °/oo	Depth, meters	Temperature, ° C.	Salinity, °/oo	σ_t
0	0.73	33.78	0	0.73	33.78	27.10
26	0.74	33.77	25	0.70	33.77	27.10
52	0.74	33.77	50	0.75	33.77	27.10
78	0.88	33.89	75	0.85	33.87	27.17
104	1.19	34.16	100	1.15	34.12	27.35
155	1.97	34.39	150	1.90	34.37	27.50
206	2.48	34.55	200	2.40	34.53	27.58
310	3.36	34.73	300	3.30	34.71	27.65
476	3.84	34.85	400	3.70	34.82	27.70
586	3.72	34.85	600	3.70	34.85	27.72
755	3.61	34.86	(800)	3.55	34.86	27.74

Table of Oceanographic Data—Continued

STATIONS OCCUPIED IN 1955—Continued

Station 5874; May 3; latitude 47°13.5′ N., longitude 47°37′W.; depth 222 m.; dynamic height 971.008.

Observed values			Scaled values			
Depth, meters	Temperature, ° C.	Salinity °/oo	Depth, meters	Temperature, ° C.	Salinity, °/oo	σt
0	−0.54	33.15	0	−0.54	33.15	26.66
25	−0.51	33.15	25	−0.51	33.15	26.66
50	−0.58	33.17	50	−0.58	33.17	26.67
75	−0.70	33.29	75	−0.70	33.29	26.77
100	−0.36	33.50	100	−0.36	33.50	26.93
149	0.72	33.96	150	0.75	33.96	27.25
199	1.34	34.15	200	1.35	34.15	27.36

Station 5875; May 3; latitude 47°12′N., longitude 47°58′W.; depth 172 m.; dynamic height 971.036.

Observed values			Scaled values			
Depth, meters	Temperature, ° C.	Salinity °/oo	Depth, meters	Temperature, ° C.	Salinity, °/oo	σt
0	−0.98	32.98	0	−0.98	32.98	26.53
25	−0.96	32.98	25	−0.96	32.98	26.53
51	−0.96	32.97	50	−0.95	32.98	26.53
76	−0.98	33.02	75	−1.00	33.02	26.57
101	−0.81	33.24	100	−0.85	33.23	26.73
152	0.51	33.84	150	0.45	33.82	27.15

Station 5876; May 3; latitude 47°09′N., longitude 48°29′W.; depth 125 m.; dynamic height 971.030.

Observed values			Scaled values			
Depth, meters	Temperature, ° C.	Salinity °/oo	Depth, meters	Temperature, ° C.	Salinity, °/oo	σt
0	−0.51	33.03	0	−0.51	33.03	26.56
26	−0.48	33.04	25	−0.50	33.04	26.57
51	−0.47	33.04	50	−0.45	33.04	26.57
77	−0.58	33.11	75	−0.60	33.09	26.60
103	−0.27	33.50	100	−0.35	33.46	26.90

Station 5877; May 3; latitude 47°13′N.; longitude 49°13′W.; depth 91 m.; dynamic height 971.026.

Observed values			Scaled values			
Depth, meters	Temperature, ° C.	Salinity °/oo	Depth, meters	Temperature, ° C.	Salinity, °/oo	σt
0	−0.39	33.02	0	−0.39	33.02	26.55
24	−0.43	33.02	25	−0.45	33.02	26.55
49	−0.45	33.02	50	−0.45	33.02	26.55
73	−0.31	33.30	75	−0.30	33.34	26.80

Station 5878; June 3; latitude 52°03′N., longitude 49°38′W.; depth 3,127 m.; dynamic height 970.842

Observed values			Scaled values			
Depth, meters	Temperature, ° C.	Salinity °/oo	Depth, meters	Temperature, ° C.	Salinity, °/oo	σt
0	7.07	34.50	0	7.07	34.50	27.04
25	5.46	34.48	25	5.46	34.48	27.23
50	3.53	34.41	50	3.53	34.41	27.38
74	3.03	34.55	75	3.00	34.55	27.55
99	2.74	34.63	100	2.75	34.63	27.63
149	2.71	-------	150	2.70	34.70	27.69
198	3.06	34.75	200	3.05	34.75	27.70
297	3.16	34.82	300	3.15	34.82	27.75
390	3.19	34.84	400	3.20	34.84	27.76
584	3.34	34.865	600	3.35	34.865	27.76
777	3.37	34.87	800	3.40	34.87	27.77
974	3.36	34.87	1,000	3.35	34.87	27.77
1,471	3.29	34.90				

Station 5879; June 3; latitude 52°00′N.; longitude 50°01′W.; depth 2,634 m.; dynamic height 970.816.

Observed values			Scaled values			
Depth, meters	Temperature, ° C.	Salinity, °/oo	Depth, meters	Temperature, ° C.	Salinity, °/oo	σt
0	4.97	34.48	0	4.97	34.48	27.29
25	4.03	34.53	25	4.03	34.53	27.43
51	3.92	34.59	50	3.95	34.59	27.48
76	2.96	34.63	75	2.95	34.63	27.61
101	2.84	34.70	100	2.85	34.70	27.68
152	3.01	-------	150	3.00	34.78	27.73
203	3.26	34.82	200	3.25	34.82	27.74
304	3.15	34.82	300	3.15	34.82	27.75
394	3.21	34.84	400	3.20	34.84	27.76
590	3.28	34.86	600	3.30	34.86	27.77
787	3.32	34.88	800	3.30	34.88	27.78
986	3.32	34.885	1,000	3.30	34.89	27.79
1,486	3.32	34.90				

Station 5880; June 3; latitude 51°43.5′N., longitude 50°21′W.; depth 1,088 m.; dynamic height 970.913.

Observed values			Scaled values			
Depth, meters	Temperature, ° C.	Salinity, °/oo	Depth, meters	Temperature, ° C.	Salinity, °/oo	σt
0	2.17	31.75	0	2.17	31.75	25.38
25	−1.20	33.44	25	−1.20	33.44	26.92
50	−0.68	33.70	50	−0.68	33.70	27.11
75	0.07	33.92	75	0.07	33.92	27.26
99	0.64	34.09	100	0.65	34.10	27.36
149	1.67	-------	150	1.70	34.37	27.51
199	2.48	34.56	200	2.50	34.56	27.60
298	2.95	34.76	300	2.95	34.76	27.72
329	3.01	34.77	400	3.15	34.80	27.73
502	3.24	34.84	600	3.25	34.85	27.76
682	3.24	-------	800	3.30	34.86	27.77
877	3.30	34.865	(1,000)	3.30	34.87	27.78

Station 5881; June 3; latitude 51°41′N., longitude 50°25′W.; depth 608 m.; dynamic height 970.924.

Observed values			Scaled values			
Depth, meters	Temperature, ° C.	Salinity, °/oo	Depth, meters	Temperature, ° C.	Salinity, °/oo	σt
0	3.27	32.86	0	3.27	32.86	26.18
22	0.65	33.31	25	0.20	33.33	26.77
44	−1.12	33.47	50	−1.00	33.51	26.97
65	−0.62	33.63	75	−0.40	33.72	27.12
87	−0.18	33.87	100	0.10	33.96	27.28
131	0.77	34.13	150	1.05	34.21	27.43
174	1.38	34.31	200	1.80	34.42	27.55
261	2.67	34.65	300	2.90	34.70	27.68
284	2.83	34.68	400	3.15	34.79	27.72
460	3.23	34.83	(600)	3.30	34.87	27.78

Station 5882; June 3; latitude 51°39.5′N., longitude 50°36′W.; depth 318 m.; dynamic height 970.933.

Observed values			Scaled values			
Depth, meters	Temperature, ° C.	Salinity, °/oo	Depth, meters	Temperature, ° C.	Salinity, °/oo	σt
0	3.10	32.73	0	3.10	32.73	26.09
24	1.11	32.99	25	1.10	33.01	26.47
48	1.62	33.70	50	1.60	33.72	27.00
72	−0.14	33.84	75	−0.15	33.85	27.21
96	0.50	33.99	100	0.60	34.01	27.29
144	1.27	-------	150	1.35	34.19	27.39
192	1.68	34.33	200	1.75	34.35	27.49
288	2.79	34.66	300	2.95	34.71	27.68

STATIONS OCCUPIED IN 1955—Continued

Station 5883; June 3; latitude 51°39′ N., longitude 50°56′ W.; depth 332 m.; dynamic height 970.955.

Observed values			Scaled values			
Depth, meters	Temperature, ° C.	Salinity, ‰	Depth, meters	Temperature, ° C.	Salinity, ‰	σ_t
0	0.84	31.65	0	0.84	31.65	25.39
22	2.10	33.29	25	2.00	33.30	26.63
43	−0.02	33.37	50	−0.20	33.42	26.87
64	−0.38	33.53	75	−0.30	33.64	27.04
85	−0.16	33.73	100	0.05	33.84	27.19
128	0.51	34.01	150	0.90	34.12	27.37
171	1.19	34.21	200	1.60	34.31	27.47
256	2.27	34.47	(300)	2.75	34.58	27.59

Station 5884; June 3; latitude 51°34.5′ N., longitude 51°31′ W.; depth 399 m.; dynamic height 970.964.

Observed values			Scaled values			
Depth, meters	Temperature, ° C.	Salinity, ‰	Depth, meters	Temperature, ° C.	Salinity, ‰	σ_t
0	2.91	33.12	0	2.91	33.12	26.42
27	0.15	33.15	25	0.30	33.15	26.62
54	−0.76	33.19	50	−0.70	33.18	26.69
81	−0.90	33.40	75	−0.90	33.33	26.82
108	0.19	33.89	100	−0.15	33.78	27.15
163	0.46	-------	150	0.40	34.01	27.31
216	1.40	34.24	200	1.10	34.18	27.40
324	2.46	34.56	300	2.25	34.49	27.56
375	3.08	34.75	(400)	3.35	34.83	27.73

Station 5885; June 4; latitude 51°30.5′ N., longitude 52°13′ W.; depth 501 m.; dynamic height 970.978.

Observed values			Scaled values			
Depth, meters	Temperature, ° C.	Salinity, ‰	Depth, meters	Temperature, ° C.	Salinity, ‰	σ_t
0	2.84	33.15	0	2.84	33.15	26.44
24	2.39	33.19	25	2.30	33.19	26.53
47	−0.58	33.22	50	−0.60	33.23	26.72
71	−0.76	33.35	75	−0.80	33.39	26.86
95	−0.81	33.57	100	−0.80	33.60	27.03
141	0.37	33.84	150	0.60	33.90	27.20
188	1.27	34.18	200	1.45	34.23	27.41
283	2.37	-------	300	2.50	34.50	27.55
393	2.82	34.68	400	2.85	34.69	27.67

Station 5886; June 4; latitude 51°31′ N., longitude 52°50′ W.; depth 316 m.; dynamic height 970.973.

Observed values			Scaled values			
Depth, meters	Temperature, ° C.	Salinity, ‰	Depth, meters	Temperature, ° C.	Salinity, ‰	σ_t
0	2.85	33.15	0	2.85	33.15	26.44
23	2.21	33.12	25	1.90	33.12	26.50
46	−0.56	33.27	50	−0.65	33.31	26.79
70	−0.92	33.53	75	−0.90	33.57	27.02
93	−0.39	33.71	100	−0.30	33.74	27.12
139	0.12	33.85	150	0.30	33.90	27.22
185	0.99	34.08	200	1.20	34.14	27.36
278	2.21	34.44	(300)	2.45	34.52	27.57

Station 5887; June 4; latitude 51°32′ N., longitude 53°26′ W.; depth 408 m.; dynamic height 971.015.

Observed values			Scaled values			
Depth, meters	Temperature, ° C.	Salinity, ‰	Depth, meters	Temperature, ° C.	Salinity, ‰	σ_t
0	0.97	31.66	0	0.97	31.66	25.39
27	−0.64	33.09	25	−0.45	32.98	26.52
53	−1.22	33.17	50	−1.20	33.16	26.69
80	−1.36	33.31	75	−1.35	33.28	26.79
106	−1.07	33.54	100	−1.20	33.49	26.96
160	−0.24	33.79	150	−0.35	33.75	27.13
214	0.39	34.03	200	0.20	33.97	27.29
320	2.12	34.43	300	1.90	34.36	27.49
355	2.33	34.49	(400)	2.60	34.55	27.58

Station 5888; June 4; latitude 51°29′ N., longitude 53°56′ W.; depth 348 m.; dynamic height 971.046.

Observed values			Scaled values			
Depth, meters	Temperature, ° C.	Salinity, ‰	Depth, meters	Temperature, ° C.	Salinity, ‰	σ_t
0	2.15	31.83	0	2.15	31.83	25.46
25	0.92	32.95	25	0.92	32.95	26.42
50	−1.00	33.11	50	−1.00	33.11	26.64
75	−1.21	33.20	75	−1.21	33.20	26.72
100	−1.37	33.33	100	−1.37	33.33	26.83
150	−1.00	33.50	150	−1.00	33.50	26.96
200	−0.22	33.81	200	−0.22	33.81	27.18
300	1.06	34.18	300	1.06	34.18	27.40

Station 5889; June 4; latitude 50°58.5′ N., longitude 53°07′ W.; depth 434 m.; dynamic height 970.997.

Observed values			Scaled values			
Depth, meters	Temperature, ° C.	Salinity, ‰	Depth, meters	Temperature, ° C.	Salinity, ‰	σ_t
0	3.54	33.03	0	3.54	33.03	26.29
25	0.48	33.05	25	0.48	33.05	26.54
50	−1.28	33.21	50	−1.28	33.21	26.73
75	−1.39	33.39	75	−1.39	33.39	26.88
100	−0.97	33.53	100	−0.97	33.53	26.98
150	−0.05	33.83	150	−0.05	33.83	27.18
200	0.57	34.03	200	0.57	34.03	27.31
300	1.95	34.38	300	1.95	34.38	27.50
398	2.65	34.61	400	2.65	34.61	27.63

Station 5890; June 4; latitude 51°02′ N., longitude 52°41′ W.; depth 416 m.; dynamic height 971.013.

Observed values			Scaled values			
Depth, meters	Temperature, ° C.	Salinity, ‰	Depth, meters	Temperature, ° C.	Salinity, ‰	σ_t
0	3.45	33.03	0	3.45	33.03	26.30
25	1.60	33.09	25	1.60	33.09	26.49
50	−1.06	33.17	50	−1.06	33.17	26.69
75	−1.22	33.19	75	−1.22	33.19	26.71
99	−1.13	33.37	100	−1.15	33.38	26.87
149	0.05	33.81	150	0.05	33.82	27.18
199	0.80	34.07	200	0.80	34.07	27.33
298	1.85	34.29	300	1.85	34.30	27.44
386	2.53	34.56	(400)	2.65	34.61	27.63

Station 5891; June 4; latitude 51°05.5′ N., longitude 52°12′ W.; depth 279 m.; dynamic height 971.011.

Observed values			Scaled values			
Depth, meters	Temperature, ° C.	Salinity, ‰	Depth, meters	Temperature, ° C.	Salinity, ‰	σ_t
0	3.22	33.15	0	3.22	33.15	26.42
24	2.07	33.11	25	2.00	33.11	26.48
49	0.34	33.13	50	0.30	33.13	26.61
73	−0.54	33.19	75	−0.60	33.21	26.71
97	−1.00	33.46	100	−1.00	33.49	26.95
146	0.01	33.79	150	0.05	33.81	27.17
195	0.57	33.99	200	0.60	34.01	27.29
263	1.31	34.23	-------	-------	-------	-------

Station 5892; June 4; latitude 51°09′ N., longitude 51°42′ W.; depth 224 m.; dynamic height 970.994.

Observed values			Scaled values			
Depth, meters	Temperature, ° C.	Salinity, ‰	Depth, meters	Temperature, ° C.	Salinity, ‰	σ_t
0	3.11	33.14	0	3.11	33.14	26.42
25	0.81	33.17	25	0.81	33.17	26.61
51	−0.58	33.23	50	−0.55	33.23	26.72
76	−0.86	33.27	75	−0.85	33.27	26.76
102	−0.74	33.46	100	−0.80	33.44	26.90
152	0.33	33.93	150	0.30	33.91	27.23
203	1.20	34.20	200	1.15	34.20	27.41

STATIONS OCCUPIED IN 1955—Continued

Station 5893; June 4; latitude 51°13.5′ N., longitude 51°16′ W.; depth 263 m.; dynamic height 970.999.

Observed values			Scaled values			
Depth, meters	Temperature, ° C.	Salinity °/₀₀	Depth, meters	Temperature, ° C.	Salinity, °/₀₀	σ_t
0	2.92	33.15	0	2.92	33.15	26.44
25	1.55	33.15	25	1.55	33.15	26.54
51	−0.54	33.17	50	−0.50	33.17	26.67
76	−0.91	33.34	75	−0.90	33.34	26.83
102	−0.62	33.57	100	−0.65	33.55	26.99
153	0.51	33.81	150	0.45	33.80	27.13
204	1.03	34.15	200	1.00	34.12	27.36

Station 5894; June 4; latitude 51°16′ N., longitude 50°48′ W.; depth 269 m.; dynamic height 970.993.

Observed values			Scaled values			
Depth, meters	Temperature, ° C.	Salinity °/₀₀	Depth, meters	Temperature, ° C.	Salinity, °/₀₀	σ_t
0	3.11	33.13	0	3.11	33.13	26.41
25	1.62	33.14	25	1.62	33.14	26.54
51	−0.45	33.22	50	−0.45	33.21	26.71
76	−0.19	33.32	75	−0.20	33.31	26.77
102	−0.17	33.69	100	−0.15	33.66	27.06
153	0.14	33.91	150	0.10	33.89	27.22
204	1.17	34.16	200	1.10	34.14	27.37
250	1.57	34.30	--------	---- -	------	------

Station 5895; June 5; latitude 51°19.5′ N., longitude 50°26′ W.; depth 324 m.; dynamic height 970.952.

Observed values			Scaled values			
Depth, meters	Temperature, ° C.	Salinity °/₀₀	Depth, meters	Temperature, ° C.	Salinity, °/₀₀	σ_t
0	2.04	32.51	0	2.04	32.51	26.00
25	0.08	33.31	25	0.08	33.31	26.76
50	−0.92	33.47	50	−0.92	33.47	26.94
76	−0.58	33.69	75	−0.60	33.68	27.08
101	0.17	33.89	100	0.15	33.88	27.21
151	1.44	34.23	150	1.40	34.23	27.42
202	1.99	34.42	200	1.95	34.42	27.54
303	2.69	34.61	300	2.65	34.61	27.63

Station 5896; June 5; latitutude 51°17′ n., longitude 50°06′ W.; depth 619 m.; dynamic height 970.961.

Observed values			Scaled values			
Depth, meters	Temperature, ° C.	Salinity °/₀₀	Depth, meters	Temperature, ° C.	Salinity, °/₀₀	σ_t
0	0.70	31.89	0	0.70	31.89	25.59
25	1.16	33.04	25	1.16	33.04	26.49
51	−1.24	33.46	50	−1.25	33.45	26.93
76	−0.76	33.68	75	−0.80	33.67	27.09
101	−0.41	33.80	100	−0.45	33.79	27.17
152	1.04	34.18	150	0.95	34.16	27.39
203	1.74	34.38	200	1.70	34.37	27.51
304	2.67	34.67	300	2.65	34.66	27.67
395	3.21	34.80	400	3.25	34.80	27.72
595	3.24	34.80	600	3.25	34.80	27.72

Station 5897; June 5; latitude 51°18.5′ N., longitude 49°58′ W.; depth 1,060 m.; dynamic height 970.935.

Observed values			Scaled values			
Depth, meters	Temperature, ° C.	Salinity °/₀₀	Depth, meters	Temperature, ° C.	Salinity, °/₀₀	σ_t
0	−0.11	31.28	0	−0.11	31.28	25.13
25	1.23	33.15	25	1.23	33.15	26.58
51	−0.89	33.60	50	−0.90	33.60	27.04
76	−0.13	33.89	75	−0.15	33.89	27.24
101	0.48	34.04	100	0.45	34.04	27.32
152	1.41	34.28	150	1.40	34.27	27.46
203	2.04	34.47	200	2.00	34.46	27.56
304	2.78	34.71	300	2.75	34.70	27.69
400	3.16	34.80	400	3.15	34.80	27.73
599	3.27	34.85	600	3.25	34.85	27.76
797	3.28	34.86	800	3.30	34.86	27.77
1,003	3.30	34.87	1,000	3.30	34.87	27.78

Station 5898; June 5; latitude 51°24′ N., longitude 49°34′ W.; depth 2,250 m.; dynamic height 970.829.

Observed values			Scaled values			
Depth, meters	Temperature, ° C.	Salinity, °/₀₀	Depth, meters	Temperature, ° C.	Salinity, °/₀₀	σ_t
0	5.09	34.51	0	5.09	34.51	27.30
25	4.71	34.51	25	4.71	34.51	27.34
50	3.87	34.52	50	3.87	34.52	27.44
75	3.21	34.63	75	3.21	34.63	27.59
100	2.92	34.69	100	2.92	34.69	27.67
150	2.98	34.75	150	2.98	34.75	27.71
200	3.05	34.78	200	3.05	34.78	27.72
300	3.13	34.81	300	3.13	34.81	27.74
400	3.15	34.82	400	3.15	34.82	27.75
600	3.25	34.85	600	3.25	34.85	27.76
801	3.28	34.88	800	3.30	34.85	27.77
1,002	3.35	34.88	1,000	3.35	34.88	27.77
1,505	3.33	34.89				

Station 5899; June 5; latitude 51°30.5′ N., longitude 49°11′ W.; depth 2,889 m.; dynamic height 970.824.

Observed values			Scaled values			
Depth, meters	Temperature, ° C.	Salinity, °/₀₀	Depth, meters	Temperature, ° C.	Salinity, °/₀₀	σ_t
0	4.32	34.51	0	4.32	34.51	27.39
25	3.89	34.52	25	3.89	34.52	27.45
50	3.83	34.54	50	3.83	34.54	27.45
75	3.53	34.61	75	3.53	34.61	27.54
101	3.24	34.67	100	3.25	34.67	27.62
151	3.04	34.71	150	3.05	34.71	27.67
201	3.01	34.77	200	3.00	34.77	27.73
302	3.13	34.83	300	3.15	34.83	27.75
390	3.16	34.83	400	3.15	34.83	27.75
585	3.25	34.84	600	3.25	34.85	27.76
781	3.29	34.88	800	3.30	34.88	27.78
978	3.25	34.88	1,000	3.25	34.88	27.78
1,474	3.28	34.90				

Station 5900; June 5; latitude 51°02.5′ N., longitude 49°31′ W.; depth 1,426 m.; dynamic height 970,850.

Observed values			Scaled values			
Depth, meters	Temperature, ° C.	Salinity, °/₀₀	Depth, meters	Temperature, ° C.	Salinity, °/₀₀	σ_t
0	3.18	33.75	0	3.18	33.75	26.89
25	3.80	34.20	25	3.80	34.20	27.20
49	3.74	34.58	50	3.75	34.58	27.49
74	2.53	34.57	75	2.55	34.57	27.61
98	2.72	34.63	100	2.70	34.63	27.63
147	2.86	34.71	150	2.85	34.71	27.69
196	2.96	34.75	200	2.95	34.75	27.71
294	3.10	34.79	300	3.10	34.79	27.73
370	3.15	34.80	400	3.15	34.80	27.73
554	3.21	34.82	600	3.20	34.82	27.75
737	3.19	34.82	800	3.25	34.83	27.75
930	3.30	34.85	1,000	3.30	34.86	27.77
1,226	3.32	34.89				

Station 5901; June 5; latitude 50°58′ N., longitude 49°45′ W.; depth 1,037 m.; dynamic height 970.920.

Observed values			Scaled values			
Depth, meters	Temperature, ° C.	Salinity, °/₀₀	Depth, meters	Temperature, ° C.	Salinity, °/₀₀	σ_t
0	0.79	31.84	0	0.79	31.84	25.54
25	−0.71	33.21	25	−0.71	33.21	26.72
49	−0.71	33.57	50	−0.70	33.58	27.01
74	0.10	33.88	75	0.15	33.89	27.22
98	0.80	34.15	100	0.85	34.16	27.40
147	1.74	34.38	150	1.80	34.39	27.52
197	2.50	34.59	200	2.50	34.59	27.62
295	2.91	34.74	300	2.95	34.74	27.70
363	3.04	34.78	400	3.10	34.80	27.74
545	3.23	34.83	600	3.25	34.84	27.75
728	3.28	34.84	800	3.30	34.85	27.76
910	3.30		(1,000)	3.30	34.86	27.77

STATIONS OCCUPIED IN 1955—Continued

Station 5902; June 5; latitude 50°51′ N., longitude 50°20′ W.; depth 1,021 m.; dynamic height 970.974.

Observed values			Scaled values			
Depth, meters	Temperature, ° C.	Salinity, ‰	Depth, meters	Temperature, ° C.	Salinity, ‰	σ_t
0	3.09	32.73	0	3.09	32.73	26.09
25	0.24	33.19	25	0.24	33.19	26.66
51	−0.94	33.43	50	−0.95	33.42	26.90
76	−0.25	33.71	75	−0.30	33.70	27.09
101	0.21	33.88	100	0.20	33.88	27.21
152	0.51	34.04	150	0.50	34.03	27.31
203	1.70	34.27	200	1.65	34.26	27.43
304	2.51	34.55	300	2.50	34.54	27.58
404	3.31	34.76	400	3.30	34.75	27.68
602	3.58	34.86	600	3.60	34.86	27.74
797	3.53	34.87	800	3.55	34.87	27.75
986	3.39	34.89	1,000	3.35	34.89	27.78

Station 5903; June 5; latitude 50°47′ N., longitude 50°41′ W.; depth 591 m.; dynamic height 970.942.

Observed values			Scaled values			
Depth, meters	Temperature, ° C.	Salinity, ‰	Depth, meters	Temperature, ° C.	Salinity, ‰	σ_t
0	2.85	32.75	0	2.85	32.75	26.12
25	2.37	33.14	25	2.37	33.14	26.49
51	1.12	33.61	50	1.15	33.60	26.93
76	0.89	33.96	75	0.90	33.95	27.23
101	0.81	34.08	100	0.80	34.08	27.33
152	1.45	34.27	150	1.40	34.25	27.44
203	2.06	34.44	200	2.05	34.44	27.54
304	2.90	34.70	300	2.85	34.69	27.67
374	3.13	34.77	400	3.20	34.78	27.71
571	3.26	34.81				

Station 5904; June 6; latitude 50°43.5′ N., longitude 50°57′ W.; depth 352 m.; dynamic height 970.972.

Observed values			Scaled values			
Depth, meters	Temperature, ° C.	Salinity, ‰	Depth, meters	Temperature, ° C.	Salinity, ‰	σ_t
0	2.96	33.11	0	2.96	33.11	26.40
25	1.92	33.15	25	1.92	33.15	26.52
50	−0.24	33.28	50	−0.24	33.28	26.75
75	−0.60	33.45	75	−0.60	33.45	26.90
100	−0.56	33.73	100	−0.56	33.73	27.12
150	0.59	34.02	150	0.59	34.02	27.30
199	1.68	34.33	200	1.70	34.33	27.47
299	2.52	34.58	300	2.55	34.58	27.61

Station 5905; June 6; latitude 50°40′ N., longitude 51°12′ W.; depth 334 m.; dynamic height 970.937.

Observed values			Scaled values			
Depth, meters	Temperature, ° C.	Salinity, ‰	Depth, meters	Temperature, ° C.	Salinity, ‰	σ_t
0	3.76	33.00	0	3.76	33.00	26.24
24	2.59	33.07	25	2.50	33.08	26.42
48	1.32	33.69	50	1.25	33.72	27.02
72	0.95	34.00	75	0.95	34.03	27.28
96	1.32	34.17	100	1.35	34.19	27.39
144	1.64	34.33	150	1.70	34.34	27.48
193	2.16	34.44	200	2.20	34.45	27.54
289	2.79	34.65	300	2.85	34.67	27.66

Station 5906; June 6; latitude 50°34.5′ N., longitude 51°39′ W.; depth 238 m.; dynamic height 970.953.

Observed values			Scaled values			
Depth, meters	Temperature, ° C.	Salinity, ‰	Depth, meters	Temperature, ° C.	Salinity, ‰	σ_t
0	3.72	33.24	0	3.72	33.24	26.44
23	2.79	33.25	25	2.60	33.25	26.54
46	0.30	33.46	50	0.20	33.49	26.90
68	0.07	33.67	75	0.10	33.73	27.09
91	0.25	33.84	100	0.35	33.89	27.21
137	0.76	34.05	150	0.95	34.11	27.35
182	1.48	34.29	200	1.80	34.36	27.50
214	2.02	34.41				

Station 5907; June 6; latitude 50°29.5′ N., longitude 52°09′ W.; depth 225 m.; dynamic height 970.966.

Observed values			Scaled values			
Depth, meters	Temperature, ° C.	Salinity, ‰	Depth, meters	Temperature, ° C.	Salinity, ‰	σ_t
0	3.30	33.12	0	3.30	33.12	26.38
25	2.98	33.19	25	2.98	33.19	26.48
50	−0.02	33.35	50	−0.02	33.35	26.80
75	−0.54	33.60	75	−0.54	33.60	27.02
100	0.06	33.77	100	0.06	33.77	27.14
150	0.77	34.03	150	0.77	34.03	27.30
200	1.23	34.23	200	1.23	34.23	27.43

Station 5908; June 6; latitude 50°23′ N., longitude 52°35′ W.; depth 309 m.; dynamic height 970.999.

Observed values			Scaled values			
Depth, meters	Temperature, ° C.	Salinity, ‰	Depth, meters	Temperature, ° C.	Salinity, ‰	σ_t
0	4.43	32.75	0	4.43	32.75	25.98
25	2.41	33.16	25	2.41	33.16	26.49
50	0.13	33.19	50	0.13	33.19	26.66
75	−1.23	33.31	75	−1.23	33.31	26.81
100	−0.35	33.60	100	−0.35	33.60	27.01
151	0.39	33.89	150	0.40	33.89	27.21
201	0.82	34.07	200	0.80	34.06	27.32
271	1.93	34.41	(300)	2.20	34.49	27.57

Station 5909; June 6; latitude 49°52.5′ N., longitude 51°58′ W.; depth 274 m.; dynamic height 971.030

Observed values			Scaled values			
Depth, meters	Temperature, ° C.	Salinity, ‰	Depth, meters	Temperature, ° C.	Salinity, ‰	σ_t
0	3.19	31.84	0	3.19	31.84	25.38
25	0.35	33.05	25	0.35	33.05	26.54
50	−1.49	33.08	50	−1.49	33.08	26.63
75	−1.48	33.13	75	−1.48	33.13	26.67
100	−1.16	33.23	100	−1.16	33.23	26.74
151	−0.61	33.61	150	−0.60	33.61	27.03
201	0.72	34.04	200	0.70	34.04	27.31
246	1.19	34.21				

Station 5910; June 6; latitude 49°59′ N., longitude 51°30′ W.; depth 306 m.; dynamic height 970.980.

Observed values			Scaled values			
Depth, meters	Temperature, ° C.	Salinity, ‰	Depth, meters	Temperature, ° C.	Salinity, ‰	σ_t
0	3.51	33.18	0	3.51	33.18	26.41
26	1.11	33.23	25	1.25	33.23	26.63
52	0.05	33.25	50	0.05	33.24	26.71
77	−0.47	33.39	75	−0.45	33.37	26.83
103	−0.10	33.64	100	−0.15	33.61	27.02
155	0.57	33.97	150	0.50	33.94	27.24
206	1.39	34.25	200	1.30	34.22	27.42
289	2.60	34.57	(300)	2.75	34.60	27.61

Station 5911; June 6; latitude 50°06′ N., longitude 50°58′ W.; depth 315 m.; dynamic height 970.967.

Observed values			Scaled values			
Depth, meters	Temperature, ° C.	Salinity, ‰	Depth, meters	Temperature, ° C.	Salinity, ‰	σ_t
0	3.48	33.22	0	3.48	33.22	26.44
24	2.42	33.23	25	2.30	33.23	26.56
47	0.26	33.33	50	0.10	33.35	26.80
71	−0.35	33.55	75	−0.30	33.58	26.99
94	−0.06	33.73	100	0.00	33.77	27.14
141	0.59	33.99	150	0.70	34.02	27.30
188	1.24	34.16	200	1.40	34.21	27.41
282	2.63	34.58	(300)	2.90	34.66	27.65

Station 5912; June 6; latitude 50°09′ N., longitude 50°40′ W.; depth 324 m.; dynamic height 970.955.

Observed values			Scaled values			
Depth, meters	Temperature, ° C.	Salinity, ‰	Depth, meters	Temperature, ° C.	Salinity, ‰	σ_t
0	3.53	33.09	0	3.53	33.09	26.32
25	1.86	33.16	25	1.86	33.16	26.53
50	−0.67	33.36	50	−0.67	33.36	26.83
75	0.11	33.79	75	0.11	33.79	27.14
100	0.38	33.92	100	0.38	33.92	27.24
150	0.91	34.09	150	0.91	34.09	27.34
199	1.77	34.32	200	1.75	34.32	27.47
299	2.97	34.69	300	3.00	34.69	27.66

Station 5913; June 6; latitude 50°11′ N., longitude 50°30′ W.; depth 635 m.; dynamic height 970.935.

Observed values			Scaled values			
Depth, meters	Temperature, ° C.	Salinity, ‰	Depth, meters	Temperature, ° C.	Salinity, ‰	σ_t
0	3.70	33.20	0	3.70	33.20	26.41
25	2.63	33.43	25	2.63	33.43	26.69
50	−0.25	33.72	50	−0.25	33.72	27.11
75	0.38	33.90	75	0.38	33.90	27.22
100	0.70	34.03	100	0.70	34.03	27.30
150	1.49	34.23	150	1.49	34.23	27.41
200	1.92	34.38	200	1.92	34.38	27.50
300	2.91	34.65	300	2.91	34.65	27.64
403	3.57	34.84	400	3.55	34.83	27.71
536	3.41	34.87	(600)	3.60	34.87	27.75

Station 5914; June 6; latitude 50°17′ N., longitude 50°07′ W.; depth 1,075 m.; dynamic height 971.001.

Observed values			Scaled values			
Depth, meters	Temperature, ° C.	Salinity, ‰	Depth, meters	Temperature, ° C.	Salinity, ‰	σ_t
0	2.86	33.05	0	2.86	33.05	26.36
24	1.42	33.19	25	1.35	33.19	26.60
49	−0.28	33.30	50	−0.25	33.30	26.76
73	−0.68	33.49	75	−0.70	33.50	26.95
97	−0.32	33.67	100	−0.30	33.68	27.07
146	0.58	33.97	150	0.65	33.99	27.27
195	1.27	34.21	200	1.30	34.23	27.42
292	2.28	34.49	300	2.35	34.51	27.57
375	3.02	34.66	400	3.15	34.69	27.64
566	3.59	34.81	600	3.60	34.82	27.71
761	3.52	34.85	800	3.55	34.86	27.74
965	3.52	34.88	1,000	3.50	34.88	27.76

Station 5915; June 7; latitude 50°20.5′ N., longitude 49°46′ W.; depth 1,326 m.; dynamic height 970.958.

Observed values			Scaled values			
Depth, meters	Temperature, ° C.	Salinity, ‰	Depth, meters	Temperature, ° C.	Salinity, ‰	σ_t
0	3.30	32.51	0	3.30	32.51	25.89
24	2.66	33.30	25	2.55	33.33	26.61
49	0.24	33.63	50	0.20	33.65	27.03
73	0.39	33.84	75	0.40	33.86	27.19
98	0.59	33.99	100	0.60	34.00	27.28
146	1.36	34.16	150	1.40	34.17	27.38
195	1.92	34.31	200	1.95	34.32	27.46
293	2.49	34.58	300	2.55	34.59	27.62
386	2.91	34.71	400	2.95	34.72	27.69
582	3.25	34.82	600	3.25	34.82	27.74
780	3.29	34.83	800	3.30	34.83	27.74
980	3.40	34.88	1,000	3.40	34.88	27.77

Station 5916; June 7; latitude 50°26′ N., longitude 49°16′ W.; depth 2,058 m.; dynamic height 970.847.

Observed values			Scaled values			
Depth, meters	Temperature, ° C.	Salinity, ‰	Depth, meters	Temperature, ° C.	Salinity, ‰	σ_t
0	5.67	34.25	0	5.67	34.25	27.02
25	4.91	34.39	25	4.91	34.39	27.22
51	3.25	34.48	50	3.25	34.48	27.46
76	2.86	34.59	75	2.85	34.58	27.58
101	2.85	34.61	100	2.85	34.61	27.61
152	2.98	34.73	150	2.95	34.73	27.69
203	3.17	34.78	200	3.15	34.78	27.71
304	3.36	34.84	300	3.35	34.84	27.74
391	3.31	34.84	400	3.30	34.84	27.75
584	3.31	34.84	600	3.30	34.84	27.75
775	3.25	34.83	800	3.25	34.835	27.75
972	3.34	34.87	1,000	3.35	34.87	27.77
1,472	3.28	34.88				

Station 5917; June 7; latitude 50°00′ N., longitude 49°08′ W.; depth 1,719 m.; dynamic height 970.837.

Observed values			Scaled values			
Depth, meters	Temperature, ° C.	Salinity, ‰	Depth, meters	Temperature, ° C.	Salinity, ‰	σ_t
0	6.45	34.34	0	6.45	34.34	26.99
23	5.06	34.35	25	4.90	34.35	27.19
46	3.07	34.55	50	3.00	34.55	27.55
70	3.02	34.60	75	3.00	34.61	27.60
93	2.98	34.66	100	3.00	34.67	27.65
139	3.06	34.74	150	3.15	34.76	27.70
185	3.46	34.79	200	3.40	34.79	27.70
278	3.26	34.81	300	3.25	34.81	27.73
349	3.24	34.83	400	3.20	34.83	27.75
526	3.16	34.83	600	3.15	34.83	27.75
705	3.11	34.83	800	3.10	34.84	27.77
892	3.12	34.84	1,000	3.10	34.85	27.78
1,377	3.30	34.89				

Station 5918; June 7; latitude 49°50′ N., longitude 49°35′ W.; depth 1,188 m.; dynamic height 970.955.

Observed values			Scaled values			
Depth, meters	Temperature, ° C.	Salinity, ‰	Depth, meters	Temperature, ° C.	Salinity, ‰	σ_t
0	4.10	32.81	0	4.10	32.81	26.07
25	0.98	33.31	25	0.98	33.31	26.71
51	−0.23	33.59	50	−0.25	33.59	27.00
76	0.10	33.76	75	0.05	33.75	27.12
101	0.89	34.01	100	0.90	34.01	27.28
152	1.16	34.18	150	1.15	34.17	27.39
203	2.23	34.40	200	2.15	34.39	27.49
304	2.56	34.61	300	2.55	34.60	27.63
394	3.14	34.72	400	3.15	34.72	27.67
588	3.49	34.85	600	3.50	34.85	27.74
781	3.57	34.89	800	3.55	34.89	27.76
981	3.41	------	1,000	3.40	34.89	27.78

Station 5919; June 7; latitude 49°42.5′ N., longitude 49°58′ W.; depth 615 m.; dynamic height 971.003.

Observed values			Scaled values			
Depth, meters	Temperature, ° C.	Salinity, ‰	Depth, meters	Temperature, ° C.	Salinity, ‰	σ_t
0	3.43	33.18	0	3.43	33.18	26.41
24	1.52	33.19	25	1.40	33.19	26.59
48	0.28	33.24	50	0.20	33.24	26.70
72	−0.03	33.33	75	−0.05	33.36	26.80
96	−0.14	33.61	100	−0.15	33.65	27.05
144	0.35	33.91	150	0.40	33.94	27.25
192	1.05	34.12	200	1.15	34.15	27.37
288	2.27	34.47	300	2.35	34.50	27.56
397	3.02	34.67	400	3.05	34.67	27.64
587	3.66	34.86	600	3.70	34.87	27.74

Station 5920; June 7; latitude 49°32′ N., longitude 50°32′ W.; depth 329 m.; dynamic height 971.002.

Observed values			Scaled values			
Depth, meters	Temperature, ° C.	Salinity °/oo	Depth, meters	Temperature, ° C.	Salinity, °/oo	σ_t
0	4.01	32.94	0	4.01	32.94	26.17
26	1.37	33.23	25	1.40	33.23	26.62
53	−0.90	33.24	50	−0.85	33.24	26.74
79	−0.29	33.50	75	−0.35	33.46	26.90
105	−0.05	33.69	100	−0.10	33.65	27.04
157	0.77	34.01	150	0.60	33.98	27.26
210	1.42	34.16	200	1.30	34.13	27.34
315	2.91	34.62	300	2.70	34.55	27.57

Station 5921; June 7; latitude 49°21.5′ N., longitude 51°06′ W.; depth 326 m.; dynamic height 971.056.

Observed values			Scaled values			
Depth, meters	Temperature, ° C.	Salinity °/oo	Depth, meters	Temperature, ° C.	Salinity, °/oo	σ_t
0	3.79	31.78	0	3.79	31.78	25.27
26	1.39	33.11	25	1.45	33.06	26.48
52	−0.65	33.12	50	−0.60	33.12	26.63
77	−1.14	33.13	75	−1.10	33.13	26.66
103	−1.43	33.23	100	−1.40	33.23	26.75
154	−0.21	33.67	150	−0.35	33.64	27.04
206	0.73	33.99	200	0.60	33.95	27.24
309	2.53	34.50	300	2.40	34.45	27.52

Station 5922 ;June 8; latitude 49°12′ N., longitude 51°35′ W.; depth 315 m.; dynamic height 971.035.

Observed values			Scaled values			
Depth, meters	Temperature, ° C.	Salinity °/oo	Depth, meters	Temperature, ° C.	Salinity, °/oo	σ_t
0	3.88	32.45	0	3.88	32.45	25.80
25	2.21	33.03	25	2.21	33.03	26.40
50	−0.36	33.17	50	−0.36	33.17	26.66
75	−0.80	33.25	75	−0.80	33.25	26.74
100	−0.89	33.32	100	−0.89	33.32	26.81
150	−0.02	33.72	150	−0.02	33.72	27.10
200	0.76	34.00	200	0.76	34.00	27.28
300	2.82	34.61	300	2.82	34.61	27.61

Station 5923; June 8; latitude 49°05′ N., longitude 51°59′ W.; depth 303 m.; dynamic height 971.005.

Observed values			Scaled values			
Depth, meters	Temperature, ° C.	Salinity °/oo	Depth, meters	Temperature, ° C.	Salinity, °/oo	σ_t
0	3.83	32.88	0	3.83	32.88	26.14
25	2.02	33.11	25	2.02	33.11	26.48
50	0.09	33.19	50	0.09	33.19	26.67
75	0.11	33.40	75	0.11	33.40	26.84
100	−0.40	33.61	100	−0.40	33.61	27.03
150	0.60	33.94	150	0.60	33.94	27.23
199	1.36	34.19	200	1.35	34.19	27.39
289	2.76	34.59	(300)	2.90	34.64	27.63

Station 5924; June 8; latitude 49°00′ N., longitude 52°14′ W.; depth 300 m.; dynamic height 971.011.

Observed values			Scaled values			
Depth, meters	Temperature, ° C.	Salinity °/oo	Depth, meters	Temperature, ° C.	Salinity, °/oo	σ_t
0	3.44	33.07	0	3.44	33.07	26.32
24	2.10	33.13	25	2.00	33.13	26.50
49	0.49	33.20	50	0.45	33.21	26.67
73	0.22	33.35	75	0.15	33.38	26.81
98	−0.35	33.52	100	−0.35	33.54	26.96
146	0.49	33.87	150	0.50	33.90	27.21
195	1.01	34.11	200	1.05	34.14	27.37
273	2.24	34.44	(300)	2.75	34.55	27.57

Station 5925; June 8; latitude 48°55.5′ N., longitude 52°30′ W.; depth 324 m.; dynamic height 971.051.

Observed values			Scaled values			
Depth, meters	Temperature, ° C.	Salinity, °/oo	Depth, meters	Temperature, ° C.	Salinity, °/oo	σ_t
0	3.54	33.03	0	3.54	33.03	26.28
25	2.63	33.06	25	2.63	33.06	26.39
49	1.02	33.21	50	1.00	33.21	26.64
74	−0.44	33.20	75	−0.50	33.20	26.70
99	−0.24	33.34	100	−0.25	33.35	26.80
148	−0.45	33.59	150	−0.45	33.60	27.02
197	0.20	33.84	200	0.20	33.85	27.19
296	1.49	34.25	300	1.55	34.27	27.44

Station 5926; June 8; latitude 48°51.5′ N., longitude 52°40′ W.; depth 224 m.; dynamic height 971.077.

Observed values			Scaled values			
Depth, meters	Temperature, ° C.	Salinity, °/oo	Depth, meters	Temperature, ° C.	Salinity, °/oo	σ_t
0	3.41	32.83	0	3.41	32.83	26.14
26	−0.70	33.01	25	−0.70	33.01	26.56
51	−1.33	33.04	50	−1.35	33.04	26.60
77	−1.42	33.15	75	−1.45	33.14	26.68
102	−1.41	33.17	100	−1.40	33.17	26.70
154	−1.44	33.23	150	−1.45	33.22	26.74
205	−0.02	33.75	200	−0.20	33.69	27.08

Station 5927; June 8; latitude 48°48.5′ N., longitude 52°48′ W.; depth 150 m.; dynamic height 971.101.

Observed values			Scaled values			
Depth, meters	Temperature, ° C.	Salinity, °/oo	Depth, meters	Temperature, ° C.	Salinity, °/oo	σ_t
0	3.54	31.58	0	3.54	31.58	25.13
23	0.45	32.73	25	0.25	32.77	26.32
46	−0.82	32.98	50	−1.00	33.00	26.55
68	−1.30	33.09	75	−1.35	33.09	26.63
91	−1.39	33.11	100	−1.40	33.12	26.66
132	−1.44	33.15	(150)	−1.45	33.17	26.70

Station 5928; June 8; latitude 48°43.5′ N., longitude 52°57′ W.; depth 110 m.; dynamic height 971.107.

Observed values			Scaled values			
Depth, meters	Temperature, ° C.	Salinity, °/oo	Depth, meters	Temperature, ° C.	Salinity, °/oo	σ_t
0	3.22	31.74	0	3.22	31.74	25.29
22	0.10	32.57	25	−0.20	32.63	26.23
43	−0.99	32.89	50	−1.10	32.93	26.50
65	−1.23	32.99	75	−1.30	33.00	26.56
82	−1.29	33.01	(100)	−1.35	33.02	26.58

Station 5929; June 8; latitude 48°38′ N., longitude 52°44′ W.; depth 218 m.; dynamic height 971.096.

Observed values			Scaled values			
Depth, meters	Temperature, ° C.	Salinity, °/oo	Depth, meters	Temperature, ° C.	Salinity, °/oo	σ_t
0	3.78	32.01	0	3.78	32.01	25.46
25	−1.01	32.78	25	−1.01	32.78	26.38
51	−1.17	33.00	50	−1.20	33.00	26.56
76	−1.32	33.07	75	−1.35	33.07	26.62
102	−1.31	33.13	100	−1.30	33.13	26.66
151	−1.37	33.15	150	−1.35	33.15	26.68
202	−1.01	33.38	200	−1.05	33.37	26.85

Station 5930; June 8; latitude 48°31′ N., longitude 52°32′ W.; depth 225 m.; dynamic height 971.095.

Observed values			Scaled values			
Depth, meters	Temperature, ° C.	Salinity, °/oo	Depth, meters	Temperature, ° C.	Salinity, °/oo	σ_t
0	3.38	31.53	0	3.38	31.53	25.11
25	1.52	32.81	25	1.52	32.81	26.28
50	−0.78	33.10	50	−0.78	33.10	26.62
75	−1.29	33.10	75	−1.29	33.10	26.64
100	−1.32	33.14	100	−1.32	33.14	26.67
151	−1.33	-------	150	−1.35	33.18	26.71
201	−0.76	33.49	200	−0.80	33.49	26.94

STATIONS OCCUPIED IN 1955—Continued

Station 5931; June 8; latitude 48°20.5′ N., longitude 52°06′ W.; depth 199 m.; dynamic height 971.090.

Observed values			Scaled values			
Depth, meters	Temperature, ° C.	Salinity, °/oo	Depth, meters	Temperature, ° C.	Salinity, °/oo	σ_t
0	2.51	32.13	0	2.51	32.13	25.66
27	−0.04	32.71	25	0.00	32.67	26.25
56	−1.44	32.97	50	−1.35	32.94	26.52
83	−1.49	32.99	75	−1.50	32.98	26.55
110	−1.54	33.13	100	−1.55	33.07	26.63
166	−1.02	33.38	150	−1.15	33.31	26.81

Station 5932; June 8; latitude 48°13′ N., longitude 51°48′ W.; depth 196 m.; dynamic height 971.090.

Observed values			Scaled values			
Depth, meters	Temperature, ° C.	Salinity, °/oo	Depth, meters	Temperature, ° C.	Salinity, °/oo	σ_t
0	2.37	32.69	0	2.37	32.69	26.11
29	0.42	32.87	25	0.65	32.85	26.36
59	−0.83	32.92	50	−0.55	32.90	26.45
88	−1.29	33.02	75	−1.15	32.97	26.53
117	−1.24	33.13	100	−1.30	33.06	26.61
176	−1.02	33.27	150	−1.15	33.21	26.73

Station 5933; June 8; latitude 48°04′ N., longitude 51°28′ W.; depth 205 m.; dynamic height 971.096.

Observed values			Scaled values			
Depth, meters	Temperature, ° C.	Salinity, °/oo	Depth, meters	Temperature, ° C.	Salinity, °/oo	σ_t
0	2.19	32.71	0	2.19	32.71	26.15
24	2.18	-------	25	2.15	32.73	26.17
48	−0.19	32.87	50	−0.40	32.88	26.44
72	−1.22	32.96	75	−1.25	32.97	26.54
96	−1.28	33.03	100	−1.25	33.04	26.59
144	−0.95	33.21	150	−0.90	33.22	26.73
192	−0.57	33.29	200	−0.50	33.30	26.77

Station 5934; June 8; latitude 47°56′ N., longitude 51°07′ W.; depth 161 m.; dynamic height 971.079.

Observed values			Scaled values			
Depth, meters	Temperature, ° C.	Salinity, °/oo	Depth, meters	Temperature, ° C.	Salinity, °/oo	σ_t
0	1.94	32.80	0	1.94	32.80	26.24
25	1.91	32.81	25	1.91	32.81	26.26
51	0.25	32.88	50	0.35	32.87	26.39
76	−1.01	33.05	75	−0.95	33.04	26.58
102	−0.72	33.24	100	−0.80	33.22	26.72
153	−0.22	33.53	150	−0.25	33.51	26.94

Station 5935; June 8–9; latitude 47°47′ N., longitude 50°48′ W.; depth 132 m.; dynamic height 971.078.

Observed values			Scaled values			
Depth, meters	Temperature, ° C.	Salinity, °/oo	Depth, meters	Temperature, ° C.	Salinity, °/oo	σ_t
0	2.21	32.83	0	2.21	32.83	26.24
26	2.17	32.87	25	2.15	32.87	26.28
51	−0.14	32.93	50	0.00	32.93	26.46
77	−0.80	33.05	75	−0.75	33.04	26.58
103	−0.99	33.17	100	−1.00	33.15	26.68

Station 5936; June 9; latitude 47°40′ N., longitude 50°31′ W.; depth 141 m.; dynamic height 971.073.

Observed values			Scaled values			
Depth, meters	Temperature, ° C.	Salinity, °/oo	Depth, meters	Temperature, ° C.	Salinity, °/oo	σ_t
0	2.29	32.72	0	2.29	32.72	26.15
25	2.23	32.89	25	2.23	32.89	26.28
50	0.80	33.00	50	0.80	33.00	26.48
75	−0.09	33.10	75	−0.09	33.10	26.59
100	−0.56	33.33	100	−0.56	33.33	26.80

Station 5937; June 9; latitude 47°32′ N., longitude 50°14′ W.; depth 102 m.; dynamic height 971.075.

Observed values			Scaled values			
Depth, meters	Temperature, ° C.	Salinity, °/oo	Depth, meters	Temperature, ° C.	Salinity, °/oo	σ_t
0	2.08	32.87	0	2.08	32.87	26.28
25	2.02	32.90	25	2.02	32.90	26.31
50	1.18	33.02	50	1.18	33.02	26.47
76	0.14	33.13	75	0.15	33.13	26.60
101	−0.29	33.21	100	−0.25	33.21	26.70

Station 5938; June 9; latitude 47°26′ N., longitude 49°58′ W.; depth 89 m.; dynamic height 971.063.

Observed values			Scaled values			
Depth, meters	Temperature, ° C.	Salinity, °/oo	Depth, meters	Temperature, ° C.	Salinity, °/oo	σ_t
0	2.50	32.92	0	2.50	32.93	26.30
18	2.29	32.94	25	1.95	32.95	26.36
39	1.01	33.02	50	0.40	33.12	26.59
60	−0.04	33.23	(75)	−0.40	33.37	26.83

Station 5939; June 9; latitude 47°41′ N., longitude 49°53′ W.; depth 123 m.; dynamic height 971.080.

Observed values			Scaled values			
Depth, meters	Temperature, ° C.	Salinity, °/oo	Depth, meters	Temperature, ° C.	Salinity, °/oo	σ_t
0	2.19	32.85	0	2.19	32.85	26.26
25	2.15	32.87	25	2.15	32.87	26.28
50	1.31	32.97	50	1.31	32.97	26.42
76	0.78	33.05	75	0.80	33.05	26.52
101	−0.17	33.24	100	−0.15	33.23	26.71

Station 5940; June 9; latitude 47°54′ N., longitude 49°49′ W.; depth 174 m.; dynamic height 971.078.

Observed values			Scaled values			
Depth, meters	Temperature, ° C.	Salinity, °/oo	Depth, meters	Temperature, ° C.	Salinity, °/oo	σ_t
0	2.40	32.78	0	2.40	32.78	26.19
23	2.06	32.77	25	1.85	32.77	26.22
46	−0.72	33.02	50	−0.90	33.04	26.58
69	−1.21	33.13	75	−1.30	33.14	26.67
92	−1.37	33.16	100	−1.35	33.19	26.72
138	−0.47	33.41	(150)	−0.15	33.49	26.92

Station 5941; June 9; latitude 48°12′ N., longitude 49°42′ W.; depth 227 m.; dynamic height 971.100.

Observed values			Scaled values			
Depth, meters	Temperature, ° C.	Salinity, °/oo	Depth, meters	Temperature, ° C.	Salinity, °/oo	σ_t
0	2.91	32.49	0	2.91	32.49	25.91
24	0.86	32.73	25	0.80	32.73	26.26
49	−0.96	32.92	50	−1.00	32.93	26.49
73	−1.38	33.03	75	−1.30	33.04	26.59
98	−1.01	33.09	100	−1.00	33.09	26.62
146	−1.48	33.11	150	−1.45	33.13	26.67
195	−0.22	33.61	200	−0.05	33.65	27.04

Station 5942; June 9; latitude 48°35.5′ N., longitude 49°33′ W.; depth 681 m.; dynamic height 970.990.

Observed values			Scaled values			
Depth, meters	Temperature, ° C.	Salinity, °/oo	Depth, meters	Temperature, ° C.	Salinity, °/oo	σ_t
0	3.97	33.09	0	3.97	33.09	26.28
25	2.84	33.13	25	2.84	33.13	26.44
50	0.86	33.23	50	0.86	33.23	26.66
75	−0.21	33.52	75	−0.21	33.52	26.95
100	0.09	33.74	100	0.09	33.79	27.15
150	1.33	34.12	150	1.33	34.12	27.34
200	1.57	34.28	200	1.57	34.28	27.44
300	2.90	34.62	300	2.90	34.62	27.62
386	3.41	34.75	400	3.45	34.76	27.67
588	3.50	34.83	600	3.50	34.83	27.72

STATIONS OCCUPIED IN 1955—Continued

Station 5943; June 9; latitude 48°42′ N., longitude 49°31′ W.; depth 1,106 m.; dynamic height 970.960.

Observed values			Scaled values			
Depth, meters	Temperature, ° C.	Salinity, °/oo	Depth, meters	Temperature, ° C.	Salinity, °/oo	σ_t
0	4.38	33.29	0	4.38	33.29	26.40
24	2.18	33.44	25	2.15	33.45	26.75
48	1.80	33.81	50	1.80	33.84	27.07
72	1.84	33.99	75	1.80	34.00	27.21
96	1.42	34.05	100	1.35	34.06	27.29
144	1.46	34.25	150	1.50	34.26	27.44
192	1.87	34.35	200	2.00	34.37	27.49
288	2.86	34.63	300	2.90	34.64	27.63
369	3.10	34.70	400	3.20	34.72	27.67
553	3.50	34.79	600	3.55	34.81	27.70
737	3.62	34.85	800	3.60	34.86	27.74
934	3.56	--------	(1 000)	3.55	34.86	27.74

Station 5944; June 9; latitude 49°07.5′ N., longitude 49°26′ W.; depth 1,485 m.; dynamic height 970.989.

Observed values			Scaled values			
Depth, meters	Temperature, ° C.	Salinity, °/oo	Depth, meters	Temperature, ° C.	Salinity, °/oo	σ_t
0	4.04	33.07	0	4.04	33.07	26.26
23	2.28	33.22	25	2.05	33.24	26.59
46	−0.06	33.43	50	−0.15	33.46	26.90
69	−0.32	33.61	75	−0.25	33.66	27.06
92	0.28	33.81	100	0.35	33.85	27.18
138	0.82	34.03	150	1.00	34.08	27.32
185	1.52	34.26	200	1.75	34.31	27.46
277	2.54	34.53	300	2.70	34.58	27.59
365	3.13	34.70	400	3.25	34.72	27.66
558	3.43	34.77	600	3.45	34.78	27.68
759	3.60	34.85	800	3.60	34.86	27.74
953	3.61	34.87	1,000	3.60	34.87	27.75
1,344	3.41	34.86				

Station 5945; June 9–10; latitude 49°29.5′ N., longitude 49°14′ W.; depth 1,646 m.; dynamic height 970.872.

Observed values			Scaled values			
Depth, meters	Temperature, ° C.	Salinity, °/oo	Depth, meters	Temperature, ° C.	Salinity, °/oo	σ_t
0	4.78	33.86	0	4.78	33.86	26.82
25	3.79	34.21	25	3.79	34.21	27.21
51	3.03	34.33	50	3.05	34.33	27.36
76	2.37	34.45	75	2.35	34.45	27.52
102	2.32	34.53	100	2.30	34.52	27.59
152	2.60	34.61	150	2.60	34.61	27.63
203	3.10	34.65	200	3.05	34.65	27.62
305	3.24	34.77	300	3.25	34.77	27.70
405	3.34	34.81	400	3.35	34.81	27.72
601	3.30	34.835	600	3.30	34.84	27.75
793	3.33	34.86	800	3.35	34.86	27.76
993	3.40	34.86	1,000	3.40	34.86	27.76
1498	3.30	34.86				

Station 5946; June 10; latitude 50°00′ N., longitude 49°00′ W.; depth 1,866 m.; dynamic height 970.857.

Observed values			Scaled values			
Depth, meters	Temperature, ° C.	Salinity, °/oo	Depth, meters	Temperature, ° C.	Salinity, °/oo	σ_t
0	6.63	34.34	0	6.63	34.34	26.96
25	6.00	34.40	25	6.00	34.40	27.10
50	3.67	34.33	50	3.67	34.33	27.31
75	2.98	34.55	75	2.98	34.55	27.55
101	4.02	34.75	100	3.95	34.75	27.61
151	4.04	34.84	150	4.05	34.84	27.67
201	4.17	34.89	200	4.15	34.89	27.70
302	3.64	34.85	300	3.65	34.85	27.72
396	3.38	34.85	400	3.40	34.85	27.75
591	3.37	34.85	600	3.35	34.85	27.75
784	3.28	34.86	800	3.30	34.86	27.77
982	3.35	34.89	1,000	3.35	34.89	27.78
1482	3.29	34.89				

Station 5947; June 10; latitude 49°50.5′ N., longitude 48°22′ W.; depth 2,286 m.; dynamic height 970.865.

Observed values			Scaled values			
Depth, meters	Temperature, ° C.	Salinity, °/oo	Depth, meters	Temperature, ° C.	Salinity, °/oo	σ_t
0	7.57	34.40	0	7.57	34.40	26.88
25	6.65	34.40	25	6.65	34.40	27.02
49	4.65	34.46	50	4.60	34.46	27.31
74	2.88	34.46	75	2.90	34.46	27.49
98	4.38	34.74	100	4.40	34.75	27.56
148	4.34	34.82	150	4.25	34.82	27.64
197	3.16	34.69	200	3.15	34.69	27.64
295	3.95	34.89	300	3.90	34.89	27.73
390	3.41	34.85	400	3.40	34.85	27.75
575	3.40	34.85	600	3.40	34.85	27.75
752	3.40	34.89	800	3.40	34.89	27.78
947	3.38	34.895	1,000	3.35	34.90	27.79
1,447	3.29	34.905				

Station 5948; June 10; latitude 49°40′ N., longitude 47°48′ W.; depth 2,561 m.; dynamic height 970.881.

Observed values			Scaled values			
Depth, meters	Temperature, ° C.	Salinity, °/oo	Depth, meters	Temperature, ° C.	Salinity, °/oo	σ_t
0	7.21	34.33	0	7.21	34.33	26.88
25	6.76	34.40	25	6.76	34.40	27.00
50	6.12	34.51	50	6.12	34.51	27.18
75	4.47	34.47	75	4.47	34.47	27.34
100	3.08	34.47	100	3.08	34.47	27.48
150	2.85	34.63	150	2.85	34.63	27.62
199	3.26	34.74	200	3.25	34.74	27.67
299	3.71	34.85	300	3.70	34.85	27.72
403	3.38	34.81	400	3.40	34.81	27.72
592	3.34	34.85	600	3.35	34.85	27.75
789	3.29	34.87	800	3.30	34.865	27.77
987	3.36	34.87	1,000	3.35	34.87	27.77
1,487	3.29	34.89				

Station 5949; June 10; latitude 49°15′ N., longitude 48°02′ W.; depth 2,378 m.; dynamic height 970.851.

Observed values			Scaled values			
Depth, meters	Temperature, ° C.	Salinity, °/oo	Depth, meters	Temperature, ° C.	Salinity, °/oo	σ_t
0	6.25	34.03	0	6.25	34.03	26.77
25	5.22	34.32	25	5.22	34.32	27.14
50	2.99	34.41	50	2.99	34.41	27.44
76	2.64	34.49	75	2.64	34.49	27.53
101	2.53	34.54	100	2.55	34.54	27.58
151	3.13	34.71	150	3.05	34.71	27.67
202	3.10	34.75	200	3.10	34.75	27.70
303	3.27	34.83	300	3.25	34.83	27.74
397	3.36	34.84	400	3.35	34.85	27.75
595	3.40	34.86	600	3.40	34.86	27.76
792	3.38	34.87	800	3.40	34.87	27.77
991	3.36	--------	1,000	3.35	34.88	27.77
1,489	3.30	34.915				

Station 5950; June 10; latitude 48°52.5′ N., longitude 48°13′ W.; depth 2,232 m.; dynamic height 970.865.

Observed values			Scaled values			
Depth, meters	Temperature, ° C.	Salinity, °/oo	Depth, meters	Temperature, ° C.	Salinity, °/oo	σ_t
0	5.94	33.99	0	5.94	33.99	26.78
25	4.24	34.13	25	4.24	34.13	27.09
50	1.84	34.27	50	1.84	34.27	27.42
74	2.49	34.47	75	2.50	34.47	27.53
99	2.54	34.55	100	2.55	34.55	27.59
149	2.94	34.67	150	2.90	34.67	27.66
198	2.99	34.72	200	2.95	34.72	27.69
297	3.29	34.78	300	3.30	34.78	27.70
398	3.45	34.85	400	3.45	34.85	27.74
599	3.46	34.86	600	3.45	34.86	27.75
802	3.47	34.86	800	3.45	34.86	27.75
1,000	3.38	34.87	1,000	3.40	34.87	27.77
1,492	3.31	34.91				

STATIONS OCCUPIED IN 1955—Continued

Station 5951; June 10; latitude 48°31.5′ N., longitude 48°25′ W.; depth 1,829 m.; dynamic height 970.880.

Observed values			Scaled values			
Depth, meters	Temperature, ° C.	Salinity, °/oo	Depth, meters	Temperature, ° C.	Salinity, °/oo	σ_t
0	4.49	33.43	0	4.49	33.43	26.50
25	1.45	34.02	25	1.45	34.02	27.25
49	1.13	34.19	50	1.15	34.19	27.40
74	1.75	34.31	75	1.75	34.31	27.46
98	2.05	34.43	100	2.10	34.44	27.53
147	2.57	34.56	150	2.55	34.56	27.60
196	2.79	34.62	200	2.80	24.63	27.62
294	3.32	34.77	300	3.30	34.77	27.70
392	3.27	34.79	400	3.30	34.79	27.71
588	3.49	34.86	600	3.50	34.86	27.75
785	3.55	34.88	800	3.55	34.88	27.75
984	3.46	34.87	1,000	3.45	34.88	27.76
1,485	3.32	34.88				

Station 5952; June 11; latitude 48°11′ N., longitude 48°36′ W.; depth 602 m.; dynamic height 970.959.

Observed values			Scaled values			
Depth, meters	Temperature, ° C.	Salinity, °/oo	Depth, meters	Temperature, ° C.	Salinity, °/oo	σ_t
0	4.34	32.92	0	4.34	32.92	26.12
25	1.50	33.44	25	1.50	33.44	26.78
0	−0.09	33.62	50	−0.09	33.62	27.02
76	0.37	33.82	75	0.35	33.81	27.15
101	0.57	33.91	100	0.55	33.91	27.22
151	1.75	34.21	150	1.65	34.21	27.39
202	2.05	34.39	200	2.05	34.39	27.50
303	2.76	34.61	300	2.70	34.61	27.62
404	3.30	34.75	400	3.30	34.75	27.68
569	3.60	34.83	(600))	3.60	34.83	27.71

Station 5953; June 11; latitude 48°05′ N., longitude 48°40′ W.; depth 326 m.; dynamic height 970.980.

Observed values			Scaled values			
Depth, meters	Temperature, ° C.	Salinity, °/oo	Depth, meters	Temperature, ° C.	Salinity, °/oo	σ_t
0	4.31	33.11	0	4.31	33.11	26.27
25	1.89	33.23	25	1.89	33.23	26.59
51	0.09	33.51	50	0.10	33.50	26.91
76	−0.20	33.65	75	−0.20	33.65	27.05
101	0.35	33.81	100	0.30	33.80	27.14
152	1.37	34.12	150	1.30	34.11	27.33
203	1.78	34.33	200	1.75	34.32	27.47
304	2.50	34.51	300	2.45	34.51	27.56

Station 5954; June 11; latitude 47°51.5′ N., longitude 48°48′ W.; depth 224 m.; dynamic height 971.072.

Observed values			Scaled values			
Depth, meters	Temperature, ° C.	Salinity, °/oo	Depth, meters	Temperature, ° C.	Salinity, °/oo	σ_t
0	2.89	32.76	0	2.89	32.76	26.13
26	1.18	32.82	25	2.05	32.82	26.25
51	−0.96	33.03	50	−0.95	33.02	26.57
76	−1.18	33.09	75	−1.20	33.09	26.63
102	−1.15	33.15	100	−1.20	33.14	26.67
153	−0.71	33.32	150	−0.80	33.30	26.78
204	0.51	33.85	200	0.40	33.82	27.16

Station 5955; June 11; latitude 47°44′ N., longitude 48°53′ W.; depth 196 m.; dynamic height 971.073.

Observed values			Scaled values			
Depth, meters	Temperature, ° C.	Salinity, °/oo	Depth, meters	Temperature, ° C.	Salinity, °/oo	σ_t
0	2.77	32.79	0	2.77	32.79	26.17
26	2.78	32.83	25	2.80	32.83	26.20
51	−0.69	32.99	50	−0.60	32.99	26.53
77	−0.90	33.07	75	−0.95	33.06	26.60
103	−1.02	33.16	100	−1.00	33.15	26.68
154	−0.73	33.33	150	−0.80	33.31	26.79

Station 5956; June 11; latitude 47°45.5′ N., longitude 48°37′ W., depth 222 m.; dynamic height 971.061.

Observed values			Scaled values			
Depth, meters	Temperature, ° C.	Salinity, °/oo	Depth, meters	Temperature, ° C.	Salinity, °/oo	σ_t
0	2.90	32.77	0	2.90	32.77	26.14
25	1.39	32.99	25	1.39	32.99	26.43
50	−0.35	33.05	50	−0.35	33.05	26.56
75	0.04	33.15	75	0.04	33.15	26.64
100	−1.09	33.17	100	−1.09	33.17	26.69
150	−0.52	33.39	150	−0.52	33.39	26.85
200	0.25	33.75	200	0.25	33.75	27.11

Station 5957; June 11; latitude 47°48.5′ N., longitude 48°14′ W.; depth 278 m.; dynamic height 971.045.

Observed values			Scaled values			
Depth, meters	Temperature, ° C.	Salinity, °/oo	Depth, meters	Temperature, ° C.	Salinity, °/oo	σ_t
0	3.35	32.64	0	3.35	32.64	26.00
25	1.82	32.89	25	1.82	32.89	26.31
51	0.14	33.16	50	0.25	33.16	26.63
76	−0.65	33.17	75	−0.65	33.17	26.68
101	−0.72	33.27	100	−0.70	33.26	26.75
152	−0.98	33.66	150	−0.05	33.64	27.03
202	0.84	33.96	200	0.80	33.94	27.22
253	1.76	34.27				

Station 5958; June 11; latitude 47°51′ N., longitude 47°54′ W.; depth 315 m.; dynamic height 971.000.

Observed values			Scaled values			
Depth, meters	Temperature, ° C.	Salinity, °/oo	Depth, meters	Temperature, ° C.	Salinity, °/oo	σ_t
0	3.29	32.83	0	3.29	32.83	26.15
23	2.34	32.96	25	2.20	32.99	26.37
46	0.60	33.23	50	0.45	33.27	26.71
69	−0.05	33.44	75	−0.10	33.49	26.91
93	−0.20	33.63	100	−0.15	33.68	27.07
139	0.60	33.91	150	0.80	33.96	27.24
185	1.33	34.12	200	1.55	34.18	27.36
278	2.60	34.53	(300)	2.90	34.63	27.62

Station 5959; June 11; latitude 47°59′ N., longitude 47°43′ W.; depth 373 m.; dynamic height 970.954.

Observed values			Scaled values			
Depth, meters	Temperature, ° C.	Salinity, °/oo	Depth, meters	Temperature, ° C.	Salinity, °/oo	σ_t
0	4.38	32.87	0	4.38	32.87	26.08
25	2.39	33.23	25	2.39	33.23	26.55
51	0.64	33.68	50	0.65	33.67	27.02
76	0.68	33.92	75	0.65	33.91	27.21
102	1.67	34.13	100	1.60	34.12	27.32
152	1.78	34.26	150	1.70	34.25	27.41
203	2.04	34.42	200	2.00	34.41	27.52
305	2.95	34.66	300	2.90	34.65	27.64
353	3.29	34.75				

Station 5960; June 11; latitude 48°17′ N., longitude 47°22′ W.; depth 1,811 m.; dynamic height 970.915.

Observed values			Scaled values			
Depth, meters	Temperature, ° C.	Salinity, °/oo	Depth, meters	Temperature, ° C.	Salinity, °/oo	σ_t
0	4.76	33.25	0	4.76	33.25	26.34
25	3.38	33.37	25	3.38	33.37	26.57
50	2.08	33.95	50	2.08	33.95	27.14
75	2.59	34.39	75	2.59	34.39	27.45
100	2.30	34.42	100	2.30	34.42	27.51
150	2.61	34.51	150	2.61	34.51	27.55
199	3.26	34.70	200	3.20	34.70	27.65
299	3.18	34.76	300	3.20	34.76	27.70
403	3.32	34.78	400	3.30	34.78	27.70
602	3.45	34.83	600	3.45	34.83	27.72
801	3.54	34.85	800	3.55	34.85	27.73
1,001	3.47	34.88	1,000	3.45	34.88	27.76
1,503	3.31	34.87				

Table of Oceanographic Data—Continued

STATIONS OCCUPIED IN 1955—Continued

Station 5961; June 11; latitude 48°36.5′ N., longitude 47°01′ W.; depth 2,743 m.; dynamic height 970.889.

Observed values			Scaled values			
Depth, meters	Temperature, ° C.	Salinity °/oo	Depth, meters	Temperature, ° C.	Salinity, °/oo	σ_t
0	7.36	34.30	0	7.36	34.30	26.84
25	6.32	34.36	25	6.32	34.36	27.03
50	4.60	34.43	50	4.60	34.43	27.28
76	4.12	34.45	75	4.10	34.45	27.36
101	3.50	34.52	100	3.50	34.52	27.48
151	3.25	34.64	150	3.25	34.64	27.59
202	3.66	34.78	200	3.60	34.78	27.67
303	3.60	34.84	300	3.60	34.84	27.72
379	*3.50	34.82	400	3.50	34.82	27.72
569	3.58	34.84	600	3.60	34.84	27.72
759	3.51	34.86	800	3.50	34.86	27.75
954	3.39	34.875	1,000	3.40	34.88	27.77
1,449	3.31	34.90				

Station 5962; June 11; latitude 48°59′ N., longitude 46°38′ W.; depth, 2,784 m.; dynamic height 970.875.

Observed values			Scaled values			
Depth, meters	Temperature, ° C.	Salinity °/oo	Depth, meters	Temperature, ° C.	Salinity, °/oo	σ_t
0	7.32	34.26	0	7.32	34.26	26.82
25	5.97	34.33	25	5.97	34.33	27.05
49	5.01	34.31	50	4.95	34.31	27.16
74	2.94	34.37	75	2.90	34.37	27.42
99	2.50	34.45	100	2.50	34.45	27.51
148	2.58	34.57	150	2.60	34.57	27.60
197	3.02	34.68	200	3.00	34.68	27.65
296	3.22	34.78	300	3.25	34.78	27.70
381	3.34	34.79	400	3.40	34.82	27.73
575	3.42	34.87	600	3.45	34.87	27.76
772	3.43	34.875	800	3.40	34.88	27.77
971	3.36	34.88	1,000	3.35	34.88	27.77
1,478	3.28	34.91				

Station 5963; June 12; latitude 49°16′ N., longitude 46°18′ W.; depth 3,017 m.; dynamic height 970.905.

Observed values			Scaled values			
Depth, meters	Temperature, ° C.	Salinity °/oo	Depth, meters	Temperature, ° C.	Salinity, °/oo	σ_t
0	8.42	34.33	0	8.42	34.33	26.70
25	7.35	34.39	25	7.35	34.39	26.91
50	6.03	34.39	50	6.03	34.39	27.08
75	4.66	34.44	75	4.66	34.44	27.29
100	4.04	34.45	100	4.04	34.45	27.36
150	4.04	34.65	150	4.04	34.65	27.52
200	4.87	34.95	200	4.87	34.95	27.68
300	4.21	34.89	300	4.21	34.89	27.70
408	4.35	34.95	400	4.40	34.95	27.72
611	3.92	34.92	600	3.95	34.92	27.75
813	3.69	34.91	800	3.70	34.905	27.76
1,018	3.43	34.88	1,000	3.45	34.88	27.76
1,534	3.32	34.91				

Station 5964; June 12; latitude 49°07′ N., longitude 45°42′ W.; depth 2,743 m.; dynamic height 970.890.

Observed values			Scaled values			
Depth, meters	Temperature, ° C.	Salinity °/oo	Depth, meters	Temperature, ° C.	Salinity, °/oo	σ_t
0	5.59	33.58	0	5.59	33.58	26.50
25	4.89	34.16	25	5.89	34.16	27.04
51	4.28	34.36	50	4.30	34.36	27.27
76	3.83	34.41	75	3.85	34.41	27.36
102	3.29	34.48	100	3.30	34.47	27.46
152	3.67	34.69	150	3.65	34.68	27.58
203	4.35	34.85	200	4.30	34.85	27.66
305	3.60	34.82	300	3.60	34.82	27.71
391	3.89	34.88	400	3.95	34.89	27.72
590	3.67	34.89	600	3.65	34.89	27.75
790	3.51	34.87	800	3.50	34.87	27.76
989	3.38	34.89	1,000	3.40	34.89	27.78
1,488	3.33	34.91				

Station 5965; June 12; latitude 48°57.5′ N., longitude 45°05′ W.; depth 1,500 m.; dynamic height 970.866.

Observed values			Scaled values			
Depth, meters	Temperature, ° C.	Salinity, °/oo	Depth, meters	Temperature, ° C.	Salinity, °/oo	σ_t
0	7.03	34.31	0	7.03	34.31	26.90
25	5.95	34.41	25	5.95	34.41	27.12
50	4.83	34.41	50	4.83	34.41	27.25
75	3.39	34.47	75	3.39	34.47	27.45
100	3.23	34.59	100	3.23	34.59	27.55
150	3.39	34.75	150	3.39	34.75	27.67
201	3.20	34.78	200	3.15	34.78	27.71
301	3.31	34.805	300	3.30	34.80	27.72
389	3.44	34.82	400	3.50	34.82	27.72
584	3.52	34.85	600	3.50	34.85	27.74
780	3.41	34.87	800	3.40	34.87	27.77
977	3.31	34.88	1,000	3.30	34.88	27.78
1,424	3.23	34.89				

Station 5966; June 12; latitude 48°39′ N., longitude 45°27′ W.; depth 1,152 m.; dynamic height 970.875.

Observed values			Scaled values			
Depth, meters	Temperature, ° C.	Salinity, °/oo	Depth, meters	Temperature, ° C.	Salinity, °/oo	σ_t
0	7.34	34.10	0	7.34	34.10	26.68
24	5.54	34.22	25	5.50	34.22	27.02
48	4.28	34.29	50	4.20	34.30	27.23
73	3.37	34.41	75	3.35	34.43	27.41
97	3.97	34.64	100	3.95	34.65	27.53
145	4.00	34.77	150	4.00	34.77	27.63
193	3.86	34.79	200	3.80	34.79	27.66
290	3.78	34.84	300	3.75	34.84	27.70
377	3.51	34.845	400	3.50	34.85	27.74
570	3.41	34.85	600	3.40	34.85	27.75
766	3.38	34.88	800	3.35	34.88	27.77
968	3.30	34.88	1,000	3.30	34.88	27.78

Station 5967; June 12; latitude 48°17.5′ N., longitude 45°54′ W.; depth 1,115 m.; dynamic height 970.901.

Observed values			Scaled values			
Depth, meters	Temperature, ° C.	Salinity, °/oo	Depth, meters	Temperature, ° C.	Salinity, °/oo	σ_t
0	3.95	32.95	0	3.95	32.95	26.18
24	2.58	33.60	25	2.50	33.63	26.85
48	1.94	34.11	50	1.90	34.11	27.29
73	1.72	34.15	75	1.70	34.16	27.34
97	2.09	34.32	100	2.15	34.34	27.45
145	2.61	34.51	150	2.65	34.53	27.56
194	3.15	34.71	200	3.10	34.72	27.68
291	3.22	34.77	300	3.25	34.78	27.70
355	3.33	34.79	400	3.40	34.80	27.71
540	3.46	34.82	600	3.45	34.83	27.72
729	3.52	34.86	800	3.50	34.87	27.76
923	3.41	34.89	(1,000)	3.35	34.89	27.78

Station 5968; June 12; latitude 47°59′ N., longitude 46°20′ W.; depth 1,188 m.; dynamic height 970.957.

Observed values			Scaled values			
Depth, meters	Temperature, ° C.	Salinity, °/oo	Depth, meters	Temperature, ° C.	Salinity, °/oo	σ_t
0	4.24	32.99	0	4.24	32.99	26.18
26	3.65	33.43	25	3.65	33.41	26.58
51	1.01	33.79	50	1.15	33.78	27.07
77	0.77	33.89	75	0.80	33.88	27.17
102	1.18	34.01	100	1.15	33.99	27.24
154	1.73	34.17	150	1.70	34.15	27.33
205	2.21	34.35	200	2.10	34.33	27.44
307	3.82	34.81	300	3.75	34.80	27.67
360	3.73	34.83	400	3.70	34.83	27.70
549	3.48	34.84	600	3.45	34.84	27.73
745	3.46	-------	800	3.45	34.86	27.75
952	3.31	34.87	(1,000)	3.25	34.87	27.78

Table of Oceanographic Data—Continued

STATIONS OCCUPIED IN 1955—Continued

Station 5969; June 12; latitude 47°54′ N., longitude 46°11′ W.; depth 1,007 m.; dynamic height 970.904.

Observed values			Scaled values			
Depth, meters	Temperature, ° C.	Salinity °/oo	Depth, meters	Temperature, ° C.	Salinity, °/oo	σ_t
0	4.68	33.27	0	4.68	33.27	26.36
25	5.68	34.06	25	5.68	34.06	26.88
50	4.52	34.14	50	4.52	34.14	27.07
76	3.57	34.22	75	3.60	34.22	27.23
101	3.08	34.31	100	3.10	34.30	27.34
151	3.30	34.61	150	3.30	34.61	27.57
201	3.80	34.79	200	3.75	34.78	27.65
302	3.70	34.84	300	3.75	34.84	27.70
326	3.70	34.84	400	3.60	34.84	27.72
507	3.50	34.83	600	3.45	34.85	27.74
699	3.45	34.88	800	3.40	34.88	27.77
861	3.35	34.88	(1,000)	3.25	34.88	27.78

Station 5970; June 12; latitude 47°46′ N., longitude 45°54′ W.; depth 405 m.; dynamic height 970.903.

Observed values			Scaled values			
Depth, meters	Temperature, ° C.	Salinity °/oo	Depth, meters	Temperature, ° C.	Salinity, °/oo	σ_t
0	6.58	33.89	0	6.58	33.89	26.62
23	5.82	34.00	25	5.75	34.01	26.82
47	4.96	34.07	50	4.85	34.08	26.98
70	4.28	34.12	75	4.10	34.13	27.10
93	3.51	34.20	100	3.45	34.23	27.24
140	3.34	34.46	150	3.40	34.53	27.49
186	3.77	34.79	200	3.75	34.80	27.67
280	3.72	34.83	300	3.65	34.84	27.71
373	3.60	34.86	(400)	3.60	34.86	27.74

Station 5971; June 12; latitude 47°41.5′ N., longitude 45°47′ W.; depth 320 m.; dynamic height 970.919.

Observed values			Scaled values			
Depth, meters	Temperature, ° C.	Salinity °/oo	Depth, meters	Temperature, ° C.	Salinity, °/oo	σ_t
0	6.88	33.91	0	6.88	33.91	26.59
24	5.96	34.02	25	5.90	34.02	26.81
49	5.02	34.08	50	5.00	34.08	26.96
73	4.29	34.13	75	4.20	34.13	27.09
98	3.71	34.19	100	3.70	34.20	27.20
147	3.69	34.45	150	3.70	34.47	27.42
195	4.03	34.73	200	4.05	34.73	27.58
293	3.75	34.75	300	3.70	34.75	27.64

Station 5972; June 13; latitude 47°27′ N., longitude 45°15′ W.; depth 233 m.; dynamic height 970.906.

Observed values			Scaled values			
Depth, meters	Temperature, ° C.	Salinity °/oo	Depth, meters	Temperature, ° C.	Salinity, °/oo	σ_t
0	6.69	33.98	0	6.69	33.98	26.68
25	5.67	34.08	25	5.67	34.08	26.89
50	4.76	34.10	50	4.76	34.10	27.01
76	4.05	34.14	75	4.05	34.14	27.12
101	3.75	34.27	100	3.75	34.26	27.25
151	4.09	34.67	150	4.10	34.66	27.53
202	3.99	34.75	200	4.00	34.75	27.61

Station 5973; June 13; latitude 47°21′ N., longitude 45°03′ W.; depth 181 m.; dynamic height 970.908.

Observed values			Scaled values			
Depth, meters	Temperature, ° C.	Salinity °/oo	Depth, meters	Temperature, ° C.	Salinity, °/oo	σ_t
0	6.87	33.94	0	6.87	33.94	26.62
25	6.74	33.96	25	6.74	33.96	26.66
50	4.96	34.07	50	4.96	34.07	26.97
75	3.92	34.18	75	3.92	34.18	27.16
100	3.75	34.28	100	3.75	34.28	27.26
150	4.09	34.66	150	4.09	34.66	27.53

Station 5974; June 13; latitude 47°18.5′ N., longitude 45°23′ W.; depth 233 m.; dynamic height 970.905.

Observed values			Scaled values			
Depth, meters	Temperature, ° C.	Salinity, °/oo	Depth, meters	Temperature, ° C.	Salinity, °/oo	σ_t
0	6.82	33.97	0	6.82	33.97	26.66
23	6.12	34.06	25	6.05	34.06	26.83
47	5.17	34.09	50	5.05	34.09	26.97
70	4.41	34.15	75	4.30	34.16	27.11
94	3.86	34.19	100	3.85	34.22	27.21
140	3.89	34.55	150	3.85	34.62	27.52
187	4.00	34.78	200	4.05	34.81	27.65

Station 5975; June 13; latitude 47°17′ N., longitude 54°41′ W.; depth 241 m.; dynamic height 970.903.

Observed values			Scaled values			
Depth, meters	Temperature, ° C.	Salinity, °/oo	Depth, meters	Temperature, ° C.	Salinity, °/oo	σ_t
0	6.88	34.01	0	6.88	34.01	26.68
25	5.65	34.04	25	5.65	34.04	26.86
50	4.75	34.08	50	4.75	34.08	26.99
75	4.03	34.11	75	4.03	34.11	27.10
100	3.23	34.18	100	3.23	34.18	27.22
151	3.79	34.58	150	3.80	34.57	27.49
201	3.99	34.81	200	3.95	34.81	27.66
231	3.95	34.83				

Station 5976; June 13; latitude 47°17.5′ N., longitude 46°00′ W.; depth 324 m.; dynamic height 970.910.

Observed values			Scaled values			
Depth, meters	Temperature, ° C.	Salinity, °/oo	Depth, meters	Temperature, ° C.	Salinity, °/oo	σ_t
0	6.82	33.93	0	6.82	33.93	26.62
23	6.22	33.98	25	6.10	33.98	26.76
46	4.99	34.05	50	4.85	34.06	26.97
69	4.31	34.08	75	4.10	34.11	27.09
92	3.60	34.19	100	3.65	34.23	27.23
137	3.92	34.45	150	3.95	34.54	27.44
184	4.05	34.76	200	4.00	34.78	27.63
276	3.71	34.85	(300)	3.65	34.86	27.73

Station 5977; June 13; latitude 47°17.5′ N., longitude 46°32′ W.; depth 652 m.; dynamic height 970.892.

Observed values			Scaled values			
Depth, meters	Temperature, ° C.	Salinity, °/oo	Depth, meters	Temperature, ° C.	Salinity, °/oo	σ_t
0	6.62	33.89	0	6.62	33.89	26.62
26	5.12	34.01	25	5.15	34.01	26.90
53	4.00	34.15	50	4.15	34.13	27.10
79	3.29	34.31	75	3.35	34.28	27.29
105	3.08	34.41	100	3.10	34.39	27.41
157	3.95	34.73	150	3.90	34.69	27.57
209	3.83	34.81	200	3.85	34.80	27.66
314	3.58	34.81	300	3.60	34.81	27.70
415	3.48	34.82	400	3.55	34.82	27.71
623	3.41	34.88	600	3.40	34.88	27.77

Station 5978; June 13; latitude 47°15.5′ N., longitude 46°56′ W.; depth 1,162 m.; dynamic height 970.890.

Observed values			Scaled values			
Depth, meters	Temperature, ° C.	Salinity, °/oo	Depth, meters	Temperature, ° C.	Salinity, °/oo	σ_t
0	6.59	34.05	0	6.59	34.05	26.74
25	5.35	34.20	25	5.35	34.20	27.03
49	4.38	34.33	50	4.35	34.33	27.23
74	3.07	34.40	75	3.05	34.40	27.42
98	2.99	34.46	100	3.00	34.46	27.48
148	3.24	34.69	150	3.25	34.69	27.63
197	3.34	34.75	200	3.35	34.75	27.67
295	3.63	34.77	300	3.60	34.77	27.67
382	3.56	34.79	400	3.60	34.79	27.68
575	3.59	34.87	600	3.60	34.87	27.75
769	3.50	34.87	800	3.45	34.87	27.76
965	3.27	34.87	1,000	3.25	34.87	27.78

STATIONS OCCUPIED IN 1955—Continued

Observed values			Scaled values			
Depth, meters	Temperature, ° C.	Salinity °/oo	Depth, meters	Temperature, ° C.	Salinity, °/oo	σ_t
Station 5979; June 13; latitude 47°13′ N., longitude 47°21′ W.; depth 313 m.; dynamic height 970.887.						
0	4.55	33.15	0	4.55	33.15	26.28
25	6.32	34.31	25	6.32	34.31	26.99
50	5.23	34.42	50	5.23	34.42	27.21
76	1.97	34.17	75	1.95	34.17	27.34
101	3.24	34.42	100	3.25	34.42	27.42
151	2.39	34.19	150	2.40	34.47	27.54
201	3.46	34.71	200	3.45	34.71	27.63
292	3.52	34.84	(300)	3.50	34.85	27.54
Station 5980; June 13; latitude 47°11′ N., longitude 47°35′ W.; depth 224 m.; dynamic height 970.943.						
0	3.49	32.94	0	3.49	32.94	26.22
24	2.62	33.03	25	2.50	33.04	26.39
49	-0.18	33.33	50	-0.15	33.34	26.80
73	-0.01	33.56	75	0.00	33.57	26.99
98	0.44	33.81	100	0.50	33.83	27.15
146	2.62	34.27	150	2.60	34.29	27.37
195	2.46	34.47	200	2.45	34.49	27.54
Station 5981; June 13; latitude 47°10′ N., longitude 48°03′ W.; depth 169 m.; dynamic height 970.989.						
0	3.70	32.67	0	3.70	32.67	25.99
25	2.36	32.92	25	2.36	32.92	26.31
51	0.72	33.18	50	0.75	33.17	26.61
76	-0.60	33.20	75	-0.60	33.20	26.70
101	-0.60	33.33	100	-0.60	33.32	26.79
152	0.56	33.79	150	0.50	33.77	27.11
Station 5982; June 13; latitude 47°10′ N., longitude 48°39′ W.; depth 123 m.; dynamic height 970.991.						
0	3.70	32.77	0	3.70	32.77	26.07
26	2.00	32.89	25	2.05	32.89	26.30
51	0.93	32.97	50	1.00	32.97	26.44
77	-0.12	33.03	75	-0.10	33.02	26.53
103	-0.25	33.49	100	-0.25	33.44	26.88
Station 5983; June 14; latitude 47°10′ N., longitude 49°07′ W.; depth 95 m.; dynamic height 970.988.						
0	3.52	32.79	0	3.52	32.79	26.09
25	2.05	32.87	25	2.05	32.87	26.29
50	1.22	32.95	50	1.22	32.95	26.40
75	-0.27	33.17	75	-0.27	33.17	26.66
Station 5984; July 11; latitude 49°58′ N., longitude 49°02′ W.; depth 1,829 m.; dynamic height, 970.870.						
0	8.21	33.62	0	8.21	38.62	26.19
23	7.17	34.36	25	6.80	34.37	26.97
45	3.87	34.48	50	3.65	34.51	27.45
68	3.24	34.60	75	3.35	34.63	27.57
91	3.61	34.70	100	3.60	34.71	27.62
136	3.39	34.73	150	3.35	34.73	27.65
181	3.26	34.73	200	3.30	34.75	27.68
272	3.53	34.80	300	3.50	34.82	27.72
286	3.47	34.85	400	3.25	34.81	27.73
439	3.16	34.81	600	3.20	34.82	27.75
598	3.18	34.82	800	3.20	34.83	27.75
767	3.21	34.83	1,000	3.25	34.85	27.76
1,220	3.28	34.86				

Observed values			Scaled values			
Depth, meters	Temperature, ° C.	Salinity, °/oo	Depth, meters	Temperature, ° C.	Salinity, °/oo	σ_t
Station 5985; July 11; latitude 49°48′ N., longitude 49°27′ W.; depth 1,408 m.; dynamic height 970.885.						
0	7.50	32.52	0	7.50	32.52	25.42
27	3.39	33.90	25	3.60	33.82	26.91
53	2.72	34.42	50	2.75	34.39	27.44
79	2.95	34.61	75	2.90	34.59	27.59
105	2.73	34.62	100	2.75	34.62	27.63
159	3.10	34.72	150	3.00	34.70	27.67
211	3.46	34.80	200	3.40	34.79	27.70
316	3.09	34.74	300	3.10	34.75	27.70
407	3.16	--------	400	3.20	34.76	27.70
612	3.20	34.83	600	3.20	34.83	27.75
820	3.25	34.83	800	3.25	34.83	27.74
1,030	3.30	34.85	1,000	3.30	34.85	27.76
1,328	3.35	34.86				
Station 5986; July 11; latitude 49°36.5′ N., longitude 50°01′ W.; depth 653 m.; dynamic height 970.933.						
0	6.72	32.44	0	6.72	32.44	25.47
25	1.04	33.10	25	1.04	33.10	26.54
50	-0.97	33.58	50	-0.97	33.58	27.02
75	0.16	33.94	75	0.10	33.94	27.27
100	1.06	34.18	100	1.06	34.18	27.40
150	2.06	34.40	150	2.06	34.40	27.51
201	2.23	34.52	200	2.20	34.52	27.60
301	3.32	34.76	300	3.30	34.76	27.69
389	3.04	34.74	400	3.10	34.74	27.69
588	3.10	34.78	600	3.10	34.78	27.72
Station 5987; July 11; latitude 49°27.5′ N., longitude 50°26′ W.; depth 335 m.; dynamic height 971.045.						
0	8.24	32.71	0	8.24	32.71	25.46
24	-0.41	32.84	25	-0.50	32.84	26.41
48	-1.49	33.02	50	-1.55	33.03	26.59
72	-1.52	33.09	75	-1.50	33.09	26.63
95	-1.33	33.14	100	-1.30	33.16	26.69
143	-0.89	33.51	150	-0.75	33.56	27.00
191	0.10	33.82	200	0.30	33.87	27.20
286	1.92	34.37	(300)	2.20	34.46	27.55
Station 5988; July 11; latitude 49°18.5′ N., longitude 50°54′ W.; depth 342 m.; dynamic height 971.011.						
0	8.38	32.88	0	8.38	32.88	25.57
25	4.07	33.04	25	4.07	33.04	26.24
50	-0.88	33.11	50	-0.88	33.11	26.63
75	-1.28	33.32	75	-1.28	33.32	26.82
101	-0.86	33.52	100	-0.90	33.51	26.97
151	0.26	33.88	150	0.25	33.87	27.21
201	1.22	34.14	200	1.20	34.14	27.36
302	2.54	34.54	300	2.50	34.53	27.57
Station 5989; July 12; latitude 49°09′ N., longitude 51°23′ W.; depth 243 m.; dynamic height 971.059.						
0	9.26	31.90	0	9.26	31.90	24.68
25	1.08	32.97	25	1.08	32.97	26.44
50	-1.47	33.06	50	-1.47	33.06	26.61
76	-1.56	33.12	75	-1.60	33.11	26.66
101	-1.51	33.18	100	-1.50	33.17	26.70
151	-0.75	33.55	150	-0.75	33.54	26.98
202	0.19	33.88	200	0.15	33.86	27.20
303	1.87	34.37	300	1.85	34.35	27.48

STATIONS OCCUPIED IN 1955—Continued

Station 5990; July 12; latitude 49°02′ N., longitude 51°44′ W.; depth 315 m.; dynamic height 971.080.

Observed values			Scaled values			
Depth, meters	Temperature, ° C.	Salinity, °/oo	Depth, meters	Temperature, ° C.	Salinity, °/oo	σ_t
0	7.09	32.14	0	7.09	32.14	25.18
25	−0.42	32.86	25	−0.42	32.86	26.42
51	−1.35	32.97	50	−1.35	32.96	26.53
76	−1.43	33.04	75	−1.40	33.04	26.60
101	−1.58	33.10	100	−1.60	33.10	26.65
152	−1.37	33.24	150	−1.40	33.23	26.75
202	−0.47	33.64	200	−0.50	33.62	27.04
283	1.42	34.22	(300)	1.85	34.34	27.47

Station 5991; July 12; latitude 48°57′ N., longitude 51°59′ W.; depth 333 m.; dynamic height 971.082.

Observed values			Scaled values			
Depth, meters	Temperature, ° C.	Salinity, °/oo	Depth, meters	Temperature, ° C.	Salinity, °/oo	σ_t
0	7.66	32.30	0	7.66	32.30	25.23
25	−0.78	32.90	25	−0.78	32.90	26.46
50	−1.63	33.02	50	−1.63	33.02	26.59
75	−1.62	33.07	75	−1.62	33.07	26.63
100	−1.66	33.08	100	−1.66	33.08	26.63
150	−1.36	33.23	150	−1.36	33.23	26.75
200	−0.59	33.59	200	−0.59	33.59	27.01
300	1.51	34.26	300	1.51	34.26	27.44

Station 5992; July 12; latitude 48°52.5′ N., longitude 52°21′ W.; depth 362 m.; dynamic height 971.108.

Observed values			Scaled values			
Depth, meters	Temperature, ° C.	Salinity, °/oo	Depth, meters	Temperature, ° C.	Salinity, °/oo	σ_t
0	8.99	31.82	0	8.99	31.82	24.65
25	−1.12	32.90	25	−1.12	32.90	26.47
50	−1.44	33.03	50	−1.44	33.03	26.59
75	−1.41	33.08	75	−1.41	33.08	26.63
99	−1.45	33.14	100	−1.45	33.14	26.68
149	−1.43	33.22	150	−1.40	33.22	26.74
199	−1.11	33.30	200	−1.10	33.30	26.79
298	1.23	34.13	300	1.25	34.15	27.37

Station 5993; July 12; latitude 48°48′ N., longitude 52°40′ W.; depth 225 m.; dynamic height 971.097.

Observed values			Scaled values			
Depth, meters	Temperature, ° C.	Salinity, °/oo	Depth, meters	Temperature, ° C.	Salinity, °/oo	σ_t
0	9.25	31.39	0	9.25	31.39	24.28
25	−0.73	32.88	25	−0.73	32.88	26.45
50	−1.35	33.03	50	−1.35	33.03	26.59
75	−1.42	33.04	75	−1.42	33.04	26.60
100	−1.45	33.08	100	−1.45	33.08	26.63
151	−1.38	33.11	150	−1.40	33.11	26.65
201	−0.78	33.42	200	−0.80	33.41	26.88

Station 5994; July 12; latitude 48°46′ N., longitude 52°45′ W.; depth 159 m.; dynamic height 971.103.

Observed values			Scaled values			
Depth, meters	Temperature, ° C.	Salinity, °/oo	Depth, meters	Temperature, ° C.	Salinity, °/oo	σ_t
0	10.05	30.98	0	10.05	30.98	23.83
25	−1.06	32.90	25	−1.06	32.90	26.47
51	−1.35	33.00	50	−1.35	33.00	26.57
76	−1.31	33.06	75	−1.30	33.06	26.61
101	−1.35	33.07	100	−1.35	33.07	26.62
147	−1.36	33.10	150	−1.35	33.10	26.64

Station 5995; July 12; latitude 48°43′ N., longitude 52°53′ W.; depth 115 m.; dynamic height 971.119.

Observed values			Scaled values			
Depth, meters	Temperature, ° C.	Salinity, °/oo	Depth, meters	Temperature, ° C.	Salinity, °/oo	σ_t
0	11.05	30.34	0	11.05	30.34	23.16
27	−0.70	32.77	25	−0.35	32.74	26.32
53	−1.22	32.91	50	−1.20	32.89	26.47
79	−1.30	32.96	75	−1.30	32.95	26.52
103	−1.37	33.05	100	−1.35	33.04	26.60

Station 5996; July 12; latitude 48°39′ N., longitude 52°44′ W.; depth 176 m.; dynamic height 971.109.

Observed values			Scaled values			
Depth, meters	Temperature, ° C.	Salinity, °/oo	Depth, meters	Temperature, ° C.	Salinity, °/oo	σ_t
0	10.13	30.43	0	10.13	30.43	23.38
26	−0.70	32.89	25	−0.45	32.86	26.42
51	−1.28	33.00	50	−1.30	32.99	26.55
77	−1.28	33.03	75	−1.30	33.03	26.58
103	−1.38	33.09	100	−1.35	33.07	26.62
154	−1.36	33.09	150	−1.35	33.08	26.63

Station 5997; July 12; latitude 48°32′ N., longitude 52°28′ W.; depth 200 m.; dynamic height 971.075.

Observed values			Scaled values			
Depth, meters	Temperature, ° C.	Salinity, °/oo	Depth, meters	Temperature, ° C.	Salinity, °/oo	σ_t
0	9.88	32.68	0	9.88	32.68	25.19
25	1.15	32.80	25	1.15	32.80	26.30
50	−1.31	33.03	50	−1.31	33.03	26.58
74	−1.25	33.09	75	−1.25	33.09	26.63
99	−1.32	33.13	100	−1.35	33.13	26.67
149	−1.47	33.15	150	−1.45	33.14	26.68
198	−0.97	33.34	(200)	−0.95	33.35	26.84

Station 5998; July 12; latitude 48°21′ N., longitude 52°03′ W.; depth 185 m.; dynamic height 971.095.

Observed values			Scaled values			
Depth, meters	Temperature, ° C.	Salinity, °/oo	Depth, meters	Temperature, ° C.	Salinity, °/oo	σ_t
0	9.74	31.19	0	9.74	31.19	24.05
25	3.34	32.47	25	3.34	32.47	25.86
50	−1.14	33.05	50	−1.14	33.05	26.60
75	−1.35	33.10	75	−1.35	33.10	26.64
101	−1.33	33.12	100	−1.30	33.12	26.66
151	−1.22	33.23	150	−1.20	33.23	26.74

Station 5999; July 12; latitude 48°12.5′N., longitude 51°45′W.; depth 165 m.; dynamic height 971.088.

Observed values			Scaled values			
Depth, meters	Temperature, ° C.	Salinity, °/oo	Depth, meters	Temperature, ° C.	Salinity, °/oo	σ_t
0	9.57	31.63	0	9.57	31.63	24.41
24	2.67	32.59	25	2.25	32.61	26.07
49	−1.12	32.95	50	−1.15	32.96	26.52
73	−1.23	33.09	75	−1.25	33.09	26.63
97	−1.42	33.12	100	−1.45	33.12	26.66
146	−1.31	33.21	150	−1.30	33.22	26.74

Station 6000; July 12; latitude 48°04 5′N., longitude 51°29′W.; depth 242 m.; dynamic height 971.081.

Observed values			Scaled values			
Depth, meters	Temperature, ° C.	Salinity, °/oo	Depth, meters	Temperature, ° C.	Salinity, °/oo	σ_t
0	9.81	32.02	0	9.81	32.02	24.69
25	1.01	32.76	25	1.01	32.76	26.27
50	−0.88	32.90	50	−0.88	32.90	26.47
74	−1.23	32.99	75	−1.25	32.99	26.55
99	−1.13	33.10	100	−1.15	33.10	26.64
149	−0.76	33.30	150	−0.75	33.30	26.78
198	−0.47	33.43	200	−0.45	33.43	26.88

Station 6001; July 12; latitude 47°57.5′N., longitude 51°10′W.; depth 170 m.; dynamic height 971.085.

Observed values			Scaled values			
Depth, meters	Temperature, ° C.	Salinity, °/oo	Depth, meters	Temperature, ° C.	Salinity, °/oo	σ_t
0	9.63	32.11	0	9.63	32.11	24.78
24	2.94	32.62	25	2.65	32.63	26.05
48	0.00	32.90	50	−0.15	32.90	26.44
71	−0.86	32.99	75	−0.90	33.01	26.56
95	−1.02	33.10	100	−1.05	33.12	26.65
			(150)	−0.85	33.30	26.78

Table of Oceanographic Data—Continued

STATIONS OCCUPIED IN 1955—Continued

Station 6002; July 12; latitude 47°51′N., longitude 50°52′W.; depth 123 m.; dynamic height 971.080.

Observed values			Scaled values			
Depth, meters	Temperature, ° C.	Salinity, ‰	Depth, meters	Temperature, ° C.	Salinity, ‰	σ_t
0	9.49	32.14	0	9.49	32.14	24.83
24	3.78	32.75	25	3.25	32.76	26.10
49	−0.12	32.92	50	−0.15	32.93	26.47
73	−0.78	33.03	75	−0.85	33.03	26.57
97	------	33.12	(100)	−1.05	33.13	26.66

Station 6003; July 13; latitude 47°44′N., longitude 50°34′W.; depth 159 m.; dynamic height 971.064.

Observed values			Scaled values			
Depth, meters	Temperature, ° C.	Salinity, ‰	Depth, meters	Temperature, ° C.	Salinity, ‰	σ_t
0	9.21	32.45	0	9.21	32.45	25.12
22	2.51	32.85	25	1.60	32.87	26.32
44	−0.58	32.99	50	−0.60	33.03	26.56
65	------	33.17	75	−0.60	33.23	26.72
87	−0.62	33.28	100	−0.60	33.29	26.76
131	−0.58	33.31	(150)	−0.55	33.32	26.79

Station 6004; July 13; latitude 47°37′N., longitude 50°15′W.; depth 125 m.; dynamic height 971.076.

Observed values			Scaled values			
Depth, meters	Temperature, ° C.	Salinity, ‰	Depth, meters	Temperature, ° C.	Salinity, ‰	σ_t
0	7.89	32.54	0	7.89	32.54	25.38
26	5.57	32.75	25	5.70	32.74	25.83
52	−0.30	32.98	50	−0.25	32.96	26.49
78	−0.29	33.20	75	−0.30	33.17	26.66
104	−0.47	33.26	100	−0.45	33.25	26.47

Station 6005; July 13; latitude 47°32′N., longitude 50°02′W.; depth 102 m.; dynamic height 971.078.

Observed values			Scaled values			
Depth, meters	Temperature, ° C.	Salinity, ‰	Depth, meters	Temperature, ° C.	Salinity, ‰	σ_t
0	8.24	32.64	0	8.24	32.64	25.41
26	5.77	32.80	25	5.85	32.79	25.85
52	1.25	33.02	50	1.55	33.00	26.43
78	−0.28	33.14	75	−0.15	33.13	26.63
			(100)	−0.50	33.22	26.71

Station 6006; July 13; latitude 47°42.5′N., longitude 49°52′W.; depth 123 m.; dynamic height 971.069

Observed values			Scaled values			
Depth, meters	Temperature, ° C.	Salinity, ‰	Depth, meters	Temperature, ° C.	Salinity, ‰	σ_t
0	7.92	32.61	0	7.92	32.61	25.44
26	3.46	32.85	25	3.40	32.84	26.15
53	−0.60	32.99	50	−0.80	32.97	26.45
79	−0.35	33.14	75	−0.25	33.12	26.62
106	−0.64	33.33	100	−0.60	33.29	26.76

Station 6007; July 13; latitude 47°55′N., longitude 49°52′W.; depth 178 m.; dynamic height 971.076.

Observed values			Scaled values			
Depth, meters	Temperature, ° C.	Salinity, ‰	Depth, meters	Temperature, ° C.	Salinity, ‰	σ_t
0	7.90	32.52	0	7.90	32.52	25.36
25	3.14	32.62	25	3.14	32.62	26.00
51	−0.37	32.95	50	−0.30	32.93	26.47
76	−0.91	33.06	75	−0.90	33.06	26.60
101	−1.03	33.16	100	−1.05	33.15	26.68
152	−0.66	33.42	150	−0.70	33.40	26.87

Station 6008; July 13; latitude 48°10.5′N., longitude 49°47′W.; depth 224 m.; dynamic height 971.054.

Observed values			Scaled values			
Depth, meters	Temperature, ° C.	Salinity, ‰	Depth, meters	Temperature, ° C.	Salinity, ‰	σ_t
0	8.29	32.26	0	8.29	32.26	25.10
25	2.48	32.84	25	2.48	32.84	26.23
50	−0.73	33.12	50	−0.73	33.12	26.64
75	−1.07	33.18	75	−1.07	33.18	26.70
100	−1.06	33.23	100	−1.06	33.23	26.74
151	−0.21	33.67	150	−0.20	33.65	27.05
201	1.02	34.10	200	1.00	34.08	27.32

Station 6009; July 13; latitude 48°36′N., longitude 49°37′W.; depth 672 m.; dynamic height 970.987.

Observed values			Scaled values			
Depth, meters	Temperature, ° C.	Salinity, ‰	Depth, meters	Temperature, ° C.	Salinity, ‰	σ_t
0	8.33	32.41	0	8.33	32.41	25.22
24	4.71	33.04	25	4.50	33.05	26.20
48	0.76	33.26	50	0.55	33.28	26.71
72	−0.56	33.52	75	−0.55	33.55	26.98
96	0.29	33.83	100	0.35	33.86	27.19
145	0.90	34.07	150	0.95	34.10	27.34
193	1.76	34.31	200	1.85	34.35	27.48
289	3.22	34.70	300	3.30	34.72	27.66
313	3.36	34.74	400	3.50	34.81	27.71
514	3.50	34.85	(600)	3.50	34.85	27.74

Station 6010; July 13; latitude 48°39′N., longitude 49°32′W.; depth 1,073 m.; dynamic height 970.961.

Observed values			Scaled values			
Depth, meters	Temperature, ° C.	Salinity, ‰	Depth, meters	Temperature, ° C.	Salinity, ‰	σ_t
0	7.83	32.88	0	7.83	32.88	25.65
25	4.24	33.20	25	4.24	33.20	26.35
50	0.56	33.81	50	0.56	33.81	27.14
75	0.43	33.86	75	0.43	33.86	27.18
100	0.88	34.07	100	0.88	34.07	27.33
150	1.40	34.21	150	1.40	34.21	27.41
200	2.16	34.42	200	2.16	34.42	27.52
300	3.01	34.61	300	3.01	34.61	27.60
367	3.32	34.76	400	3.40	34.79	27.70
563	3.49	34.83	600	3.50	34.84	27.73
766	3.52	34.86	800	3.50	34.86	27.75
966	3.33	34.86	1,000	3.35	34.86	27.76

Station 6011; July 13; latitude 49°04′N., longitude 49°20′W.; depth 1,646 m.; dynamic height 970.915.

Observed values			Scaled values			
Depth, meters	Temperature, ° C.	Salinity, ‰	Depth, meters	Temperature, ° C.	Salinity, ‰	σ_t
0	6.81	32.50	0	6.81	32.50	25.49
25	2.92	33.17	25	2.92	33.17	26.46
50	0.03	33.76	50	0.03	33.76	27.13
75	0.98	34.12	75	0.98	34.12	27.36
99	3.08	34.50	100	3.05	34.50	27.50
199	2.83	34.70	150	2.90	34.63	27.62
298	3.17	34.77	200	2.85	34.70	27.68
422	3.21	34.80	300	3.15	34.77	27.71
623	3.25	34.83	400	3.25	34.80	27.72
820	3.25	34.83	600	3.25	34.83	27.74
1,027	3.33	34.85	800	3.25	34.83	27.74
1,545	*3.31	34.87	1,000	3.30	34.85	27.76

STATIONS OCCUPIED IN 1955—Continued

Station 6012; July 13; latitude 49°32′ N., longitude 49°11′ W.; depth 1,646 m.; dynamic height 970.872.

Observed values			Scaled values			
Depth, meters	Temperature, ° C.	Salinity ‰	Depth, meters	Temperature, ° C.	Salinity, ‰	σ_t
0	8.07	32.96	0	8.07	32.96	25.68
24	4.54	34.19	25	4.50	34.22	27.14
49	3.23	34.54	50	3.20	34.54	27.52
73	2.97	34.64	75	2.95	34.64	27.62
98	2.94	34.70	100	2.95	34.70	27.67
145	3.03	34.71	150	3.05	34.71	27.67
194	3.09	34.74	200	3.10	34.74	27.69
292	3.18	34.76	300	3.15	34.76	27.70
401	3.16	34.81	400	3.15	34.81	27.74
599	3.21	34.82	600	3.25	34.82	27.74
796	3.30	34.83	800	3.30	34.83	27.74
999	3.33	34.84	1,000	3.35	34.84	27.74
1,513	3.31	34.88				

Station 6013; July 14; latitude 49°57.5′ N., longitude 49°06′ W.; depth 1,737 m.; dynamic height 970.864.

Observed values			Scaled values			
Depth, meters	Temperature, ° C.	Salinity ‰	Depth, meters	Temperature, ° C.	Salinity, ‰	σ_t
0	8.02	33.28	0	8.02	33.28	25.94
24	5.25	34.15	25	5.20	34.18	27.02
48	3.39	34.44	50	3.30	34.45	27.44
72	2.82	34.59	75	2.80	34.59	27.59
96	2.87	34.65	100	2.90	34.66	27.65
143	3.05	34.74	150	3.10	34.75	27.70
191	3.42	34.82	200	3.40	34.82	27.73
287	3.18	34.80	300	3.15	34.80	27.73
385	3.22	34.80	400	3.20	34.80	27.73
578	3.18	34.81	600	3.20	34.81	27.74
771	3.25	34.84	800	3.25	34.84	27.75
969	3.31	34.86	1,000	3.30	34.86	27.77
1,475	3.28	34.86				

Station 6014; July 15; latitude 53°43′ N., longitude 55°46′ W.; depth 126 m.; dynamic height 1454.923.

Observed values			Scaled values			
Depth, meters	Temperature, ° C.	Salinity ‰	Depth, meters	Temperature, ° C.	Salinity, ‰	σ_t
0	5.89	27.65	0	5.89	27.65	21.79
26	−0.84	32.21	25	−0.60	32.18	25.88
51	−1.63	32.86	50	−1.60	32.84	26.44
77	−1.65	32.94	75	−1.65	32.94	26.52
103	−1.66	32.95	100	−1.65	32.95	26.53

Station 6015; July 15; latitude 53°49′ N., longitude 55°31′ W.; depth 214 m.; dynamic height 1454.880.

Observed values			Scaled values			
Depth, meters	Temperature, ° C.	Salinity ‰	Depth, meters	Temperature, ° C.	Salinity, ‰	σ_t
0	5.05	31.13	0	5.05	31.13	24.63
25	0.12	32.15	25	0.12	32.15	25.82
50	−1.43	32.83	50	−1.43	32.83	26.43
75	−1.47	32.95	75	−1.47	32.95	26.52
99	−1.45	33.04	100	−1.45	33.04	26.60
149	−1.33	33.25	150	−1.35	33.26	26.77
189	−0.96	33.54	(200)	−0.85	33.63	27.05

Station 6016; July 15; latitude 53°53.5′ N., longitude 55°25′ W.; depth 172 m.; dynamic height 1454.853.

Observed values			Scaled values			
Depth, meters	Temperature, ° C.	Salinity ‰	Depth, meters	Temperature, ° C.	Salinity, ‰	σ_t
0	5.49	31.91	0	5.49	31.91	25.20
25	2.16	32.18	25	2.16	32.18	25.72
51	−1.52	32.94	50	−1.50	32.92	26.50
76	−1.60	33.04	75	−1.60	33.03	26.59
101	−1.55	33.18	100	−1.55	33.17	26.71
152	−0.80	33.65	150	−0.85	33.63	27.05

Station 6017; July 15; latitude 54°06′ N., longitude 55°06′ W.; depth 169 m.; dynamic height 1454.842.

Observed values			Scaled values			
Depth, meters	Temperature, ° C.	Salinity, ‰	Depth, meters	Temperature, ° C.	Salinity, ‰	σ_t
0	5.07	31.60	0	5.07	31.60	25.00
25	0.52	32.54	25	0.52	32.54	26.12
50	−1.08	32.94	50	−1.08	32.94	26.51
75	−1.62	33.10	75	−1.62	33.10	26.65
101	−1.59	33.29	100	−1.60	33.28	26.79
151	−0.71	33.64	150	−0.75	33.63	27.05

Station 6018; July 15; latitude 54°13′ N., longitude 54°52′ W.; depth 187 m.; dynamic height 1454.848.

Observed values			Scaled values			
Depth, meters	Temperature, ° C.	Salinity, ‰	Depth, meters	Temperature, ° C.	Salinity, ‰	σ_t
0	5.27	31.54	0	5.27	31.54	24.92
24	0.51	32.22	25	0.35	32.25	25.89
48	−1.35	32.94	50	−1.35	32.95	26.52
73	−1.54	33.12	75	−1.55	33.13	26.67
97	−1.52	33.26	100	−1.50	33.28	26.79
145	−1.04	33.54	150	−1.00	33.57	27.02

Station 6019; July 15; latitude 54°29′ N., longitude 54°23′ W.; depth 224 m.; dynamic height 1454.788.

Observed values			Scaled values			
Depth, meters	Temperature, ° C.	Salinity, ‰	Depth, meters	Temperature, ° C.	Salinity, ‰	σ_t
0	3.42	32.72	0	3.42	32.72	26.05
25	1.17	32.99	25	1.17	32.99	26.45
49	−0.78	33.27	50	−0.80	33.28	26.77
74	−0.71	33.42	75	−0.70	33.42	26.89
98	−0.37	33.58	100	−0.35	33.60	27.01
147	0.59	34.03	150	0.60	34.03	27.30
196	0.67	34.05	200	0.70	34.05	27.32

Station 6020; July 15; latitude 54°46′ N., longitude 53°50′ W.; depth 333 m.; dynamic height 1454.725.

Observed values			Scaled values			
Depth, meters	Temperature, ° C.	Salinity, ‰	Depth, meters	Temperature, ° C.	Salinity, ‰	σ_t
0	3.84	33.39	0	3.84	33.39	26.54
23	5.15	33.89	25	5.15	33.89	26.80
47	3.16	33.88	50	3.00	33.88	27.01
70	1.82	34.00	75	1.55	34.00	27.22
93	0.49	33.99	100	0.75	34.04	27.31
140	2.57	34.38	150	2.55	34.40	27.47
187	2.28	34.46	200	2.35	34.48	27.54
280	2.87	34.61	(300)	2.95	34.64	27.62

Station 6021; July 15; latitude 54°51′ N., longitude 53°35′ W.; depth 699 m.; dynamic height 1454.685.

Observed values			Scaled values			
Depth, meters	Temperature, ° C.	Salinity, ‰	Depth, meters	Temperature, ° C.	Salinity, ‰	σ_t
0	5.62	33.72	0	5.62	33.72	26.62
25	4.43	33.96	25	4.43	33.96	26.94
50	0.95	33.99	50	0.95	33.99	27.25
76	1.33	34.24	75	1.30	34.24	27.43
101	1.73	34.32	100	1.70	34.32	27.47
151	2.51	34.52	150	2.50	34.52	27.57
302	3.38	34.79	200	2.95	34.64	27.62
318	3.36	34.78	300	3.35	34.78	27.69
504	3.32	34.80	400	3.35	34.80	27.71
			(600)	3.30	34.81	27.73

STATIONS OCCUPIED IN 1955—Continued

Station 6022; July 15; latitude 54°57′ N., longitude 53°22′ W.; depth 1,558 m.; dynamic height 1,454.655.

Observed values			Scaled values			
Depth, meters	Temperature, ° C.	Salinity ‰	Depth, meters	Temperature, ° C.	Salinity, ‰	σ_t
0	6.18	34.14	0	6.18	34.14	26.87
26	5.84	34.25	25	5.85	34.25	27.00
51	4.26	34.40	50	4.30	34.39	27.29
77	3.57	34.58	75	3.60	34.56	27.50
102	3.21	34.67	100	3.20	34.66	27.62
153	3.31	34.73	150	3.30	34.73	27.66
204	3.36	34.78	200	3.35	34.78	27.69
306	3.32	34.79	300	3.35	34.79	27.70
399	3.31	34.82	400	3.35	34.82	27.73
595	3.37	34.825	600	3.35	34.825	27.73
788	3.39	34.83	800	3.40	34.83	27.73
988	3.37	34.86	1,000	3.35	34.86	27.76
1,480	3.37	34.86	1,500	3.35	34.86	27.76

Station 6023; July 15–16; latitude 55°01.5′ N., longitude 53°09′ W., depth 2,103 m.; dyanmic height 1,454.602.

Observed values			Scaled values			
Depth, meters	Temperature, ° C.	Salinity ‰	Depth, meters	Temperature, ° C.	Salinity, ‰	σ_t
0	6.20	34.39	0	6.20	34.39	27.06
25	5.38	34.54	25	5.38	34.54	27.29
50	3.74	34.70	50	3.74	34.70	27.59
76	3.42	34.74	75	3.40	34.74	27 66
101	3.35	34.76	100	3.35	34.76	27.68
151	3.27	34.75	150	3.30	34.75	27.68
201	3.20	34.79	200	3.20	34.79	27.72
302	3.27	34.82	300	3.25	34.82	27.74
357	3.29	34.84	400	3.30	34.84	27.75
532	3.34	34.84	600	3.35	34.85	27.75
705	3.37	34.86	800	3.40	34.86	27.76
890	3.38	34.865	1,000	3.35	34.87	27.77
1,368	3.27	34.885	1,500	3.25	34.89	27.79
1,862	3.26	34.915	(2,000)	3.25	34.91	27.81

Station 6024; July 16; latitude 55°11.5′ N., longitude 52°51′ W.; depth 2.985 m.; dynamic height 1,454.623.

Observed values			Scaled values			
Depth, meters	Temperature, ° C.	Salinity ‰	Depth, meters	Temperature, ° C.	Salinity, ‰	σ_t
0	7.21	34.24	0	7.21	34.24	26.81
26	5.76	34.38	25	5.80	34.37	27.10
52	3.99	34.68	50	4.10	34.65	27.52
78	3.46	34.77	75	3.50	34.77	27.68
103	3.25	34.77	100	3.25	34.77	27.70
154	3.22	34.77	150	3.25	34.77	27.70
206	3.20	34.76	200	3.20	34.76	27.70
309	3.18	34.81	300	3.20	34.81	27.74
382	3.19	34.83	400	3.20	34.83	27.75
574	3.27	34.84	600	3.25	34.84	27.75
767	3.22	34.83	800	3.20	34.83	27.75
959	3.29	34.84	1,000	3.30	34.84	27.75
1,455	3.25	34.86	1,500	3.25	34.86	27.77
1,961	3.25	34.91	2,000	3.25	34.91	27.81
2,474	2.73	34.91	2,500	2.70	34.91	27.86

Station 6025; July 16; latitude 55°30.5′ N., longitude 52°20′ W.; depth 3,200 m.; dynamic height 1,454.619.

Observed values			Scaled values			
Depth, meters	Temperature, ° C.	Salinity ‰	Depth, meters	Temperature, ° C.	Salinity, ‰	σ_t
0	7.41	34.20	0	7.41	34.20	26.75
26	3.81	34.43	25	3.90	34.42	27.36
52	3.31	34.62	50	3.35	34.60	27.55
78	3.18	34.71	75	3.20	34.70	27.65
105	3.08	34.74	100	3.10	34.73	27.68
156	3.15	34.76	150	3.15	34.76	27.70
208	3.11	34.77	200	3.10	34.77	27.71
313	3.23	34.80	300	3.20	34.79	27.72
431	3.20	34.82	400	3.20	34.82	27.75
642	3.24	34.83	600	3.25	34.83	27.75
853	3.17	34.83	800	3.20	34.83	27.75
1,061	3.33	34.84	1,000	3.30	34.84	27.75
1,593	3.27	34.86	1,500	3.30	34.86	27.77
2,129	3.26	34.92	2,000	3.25	34.91	27.81

Station 6026; July 16; latitude 55°55′ N., longitude 51°38′ W.; Depth 3,402 m.; dynamic height 1,454.636.

Observed values			Scaled values			
Depth, meters	Temperature, ° C.	Salinity, ‰	Depth, meters	Temperature, ° C.	Salinity, ‰	σ_t
0	7.59	34.57	0	7.59	34.57	27.02
25	7.55	34.59	25	7.55	34.59	27.03
50	5.14	34.70	50	5.14	34.70	27.44
75	3.61	34.68	75	3.61	34.68	27.59
100	3.34	34.68	100	3.34	34.68	27.61
150	3.28	34.70	150	3.28	34.70	27.64
199	3.12	34.74	200	3.10	34.74	27.69
299	3.32	34.83	300	3.30	34.82	27.74
365	3.21	34.81	400	3.20	34.81	27.74
548	3.24	34.82	600	3.25	34.82	27.74
733	3.24	-------	800	3.20	34.81	27.74
918	3.22	34.81	1,000	3.20	34.82	27.75
1,392	3.25	34.86	1,500	3.25	34.86	27.77
1,875	3.32	34.88	2,000	3.30	34.89	27.79
2,561	3.08	34.91	2,500	3.10	34.91	27.83
3,064	2.58	34.91	3,000	2.65	34.91	27.87
3,421	1.75	34.87				

Station 6027; July 17; latitude 56°28.5′ N., longitude 50°30′ W.; depth 3,566 m.; dynamic height 1,454.648.

Observed values			Scaled values			
Depth, meters	Temperature, ° C.	Salinity, ‰	Depth, meters	Temperature, ° C.	Salinity, ‰	σ_t
0	7.51	34.52	0	7.51	34.52	26.99
24	7.49	34.52	25	7.45	34.52	27.00
48	5.09	34.63	50	5.05	34.63	27.39
72	4.21	34.59	75	4.15	34.59	27.46
96	3.87	34.64	100	3.85	34.64	27.53
145	3.50	34.65	150	3.45	34.65	27.58
193	3.22	34.67	200	3.20	34.67	27.63
289	3.26	34.77	300	3.25	34.78	27.70
404	3.29	34.83	400	3.30	34.83	27.74
603	3.22	34.81	600	3.20	34.81	27.74
799	3.12	34.815	800	3.10	34.82	27.76
994	3.16	34.82	1,000	3.15	34.82	27.75
1,491	3.19	34.86	1,500	3.20	34.86	27.78
1,990	3.22	34.865	2,000	3.20	34.87	27.79
2,476	3.26	34.905	2,500	3.25	34.90	27.80
2,976	2.83	34.88	3,000	2.80	34.88	27.82
3,482	2.41	34.89	(3,500)	2.40	34.89	27.87

Station 6028; July 17; latitude 57°01.5′ N., longitude 49°22′ W.; depth 3,612 m.; dynamic height 1,454.617.

Observed values			Scaled values			
Depth, meters	Temperature, ° C.	Salinity, ‰	Depth, meters	Temperature, ° C.	Salinity, ‰	σ_t
0	7.45	34.62	0	7.45	34.62	27.08
25	7.13	34.62	25	7.13	34.62	27.13
50	5.45	34.66	50	5.45	34.66	27.37
75	3.47	34.62	75	3.47	34.62	27.56
101	3.20	34.76	100	3.20	34.76	27.70
151	3.33	34.80	150	3.35	34.80	27.71
201	3.34	34.82	200	3.35	34.82	27.73
302	3.42	34.84	300	3.40	34.84	27.74
403	3.44	34.85	400	3.45	34.85	27.74
602	3.48	34.85	600	3.50	34.85	27.74
798	3.45	34.88	800	3.45	34.88	27.76
993	3.37	34.87	1,000	3.35	34.87	27.77
1,494	3.22	34.86	1,500	3.20	34.86	27.78
2,000	3.38	34.895	2,000	3.35	34.89	27.78
2,546	3.12	34.90	2,500	3.15	34.90	27.81
3,053	2.71	34.93	3,000	2.75	34.93	27.87
3,562	1.74	34.89	3,500	1.95	34.90	27.92

STATIONS OCCUPIED IN 1955—Continued

Station 6029; July 17; latitude 57°35′ N., longitude 48°16′ W.; depth 3,429 m.; dynamic height 1,454.611.

Observed values			Scaled values			
Depth, meters	Temperature, ° C.	Salinity °/oo	Depth, meters	Temperature, ° C.	Salinity, °/oo	σ_t
0	6.86	34.65	0	6.86	34.65	27.18
25	6.39	34.64	25	6.39	34.64	27.23
50	3.89	34.73	50	3.89	34.73	27.60
75	3.42	34.80	75	3.42	34.80	27.71
100	3.43	34.82	100	3.43	34.82	27.72
150	3.42	34.83	150	3.42	34.83	27.72
199	3.41	-------	200	3.40	34.83	27.73
299	3.26	34.81	300	3.25	34.81	27.73
377	3.15	34.82	400	3.15	34.82	27.75
565	3.23	34.83	600	3.25	34.83	27.74
754	3.23	34.83	800	3.25	34.83	27.74
942	3.32	-------	1,000	3.30	34.84	27.75
1,430	3.25	34.865	1,500	3.25	34.87	27.78
1,927	3.32	34.89	2,000	3.30	34.89	27.79
2,547	3.11	34.91	2,500	3.15	34.91	27.82
3,046	2.53	34.90	3,000	2.60	34.90	27.86
3,450	1.50	34.86				

Station 6030; July 18; latitude 58°10′ N., longitude 47°08′ W.; depth 3,109 m.; dynamic height, 1454.629.

Observed values			Scaled values			
Depth, meters	Temperature, ° C.	Salinity °/oo	Depth, meters	Temperature, ° C.	Salinity, °/oo	σ_t
0	6.33	34.68	0	6.33	34.68	27.27
26	6.24	34.68	25	6.25	34.68	27.28
52	5.40	34.70	50	5.50	34.70	27.40
78	4.67	34.76	75	4.75	34.75	27.53
105	4.02	34.82	100	4.15	34.81	27.64
156	3.98	34.86	150	4.00	34.86	27.70
208	3.86	34.87	200	3.90	34.87	27.72
313	3.76	34.88	300	3.75	34.87	27.73
394	3.73	34.87	400	3.75	34.87	27.73
597	3.59	34.86	600	3.60	34.86	27.74
804	3.52	34.86	800	3.50	34.86	27.75
1,014	3.45	34.86	1,000	3.45	34.86	27.75
1,510	3.40	34.89	1,500	3.40	34.89	27.78
1,997	3.23	34.90	2,000	3.25	34.90	27.80
2,591	2.74	34.90	2,500	2.85	34.90	27.84
3,113	1.55	34.83	3,000	2.00	34.86	27.88

Station 6031; July 18; latitude 58°39′ N., longitude 46°08′ W., depth 2,469 m.; dynamic height 1454.608.

Observed values			Scaled values			
Depth, meters	Temperature, ° C.	Salinity °/oo	Depth, meters	Temperature, ° C.	Salinity, °/oo	σ_t
0	6.16	34.70	0	6.16	34.70	27.32
25	6.15	34.72	25	6.15	34.72	27.34
51	4.71	34.77	50	4.75	34.77	27.55
76	5.00	34.96	75	5.00	34.96	27.67
102	4.89	34.96	100	4.90	34.96	27.68
152	4.54	34.94	150	4.55	34.94	27.70
202	4.25	34.91	200	4.25	34.91	27.71
304	4.01	34.915	300	4.00	34.91	27.74
416	3.57	34.86	400	3.60	34.87	27.75
623	3.43	34.845	600	3.45	34.85	27.74
829	3.40	34.85	800	3.40	34.85	27.75
1,034	3.32	34.86	1,000	3.35	34.86	27.76
1,565	3.33	34.905	1,500	3.35	34.90	27.79
2,104	2.78	34.905	2,000	2.95	34.90	27.83
2,521	2.04	34.86	2,500	2.10	34.87	27.88

Station 6032; July 18; latitude 58°59.5′ N., longitude 45°19′ W. depth 2,345 m. dynamic height 1454.608.

Observed values			Scaled values			
Depth, meters	Temperature, ° C.	Salinity, °/oo	Depth, meters	Temperature, ° C.	Salinity, °/oo	σ_t
0	6.29	34.64	0	6.29	34.64	27.25
25	6.29	34.70	25	6.29	34.70	27.30
51	4.48	34.77	50	4.50	34.77	27.57
76	3.83	34.77	75	3.85	34.77	27.64
101	3.58	34.78	100	3.60	34.78	27.67
151	3.93	34.85	150	3.95	34.85	27.69
202	3.66	34.82	200	3.65	34.82	27.70
303	3.72	34.88	300	3.70	44.88	27.74
396	3.66	34.88	400	3.65	34.88	27.74
592	3.47	34.86	600	3.45	34.86	27.75
786	3.47	34.85	800	3.45	34.86	27.75
978	3.47	34.89	1,000	3.45	34.89	27.77
1,478	3.38	34.905	1,500	3.35	34.90	27.79
1,982	2.94	34.905	2,000	2.90	34.90	27.84
2,294	2.40	34.88				

Station 6033; July 18; latitude 59°09′ N., longitude 44°56′ W.; depth 2,083 m.; dynamic height 1454.669.

Observed values			Scaled values			
Depth, meters	Temperature, ° C.	Salinity, °/oo	Depth, meters	Temperature, ° C.	Salinity, °/oo	σ_t
0	3.56	33.28	0	3.56	33.28	26.48
24	4.92	33.63	25	5.00	33.70	26.67
47	6.27	34.80	50	6.25	34.82	27.40
71	6.28	34.915	75	6.15	34.92	27.49
94	5.74	34.91	100	5.60	34.91	27.55
141	5.02	34.89	150	5.00	34.89	27.61
188	4.83	34.93	200	4.80	34.93	27.66
282	4.58	34.93	300	4.55	34.93	27.69
283	4.62	34.925	400	4.25	34.92	27.72
451	4.14	34.91	600	3.95	34.89	27.72
636	3.92	34.885	800	3.80	34.90	27.75
838	3.76	34.90	1,000	3.65	34.90	27.76
1,308	3.46	34.91	1,500	3.30	34.91	27.81
1,708	3.07	34.905				

Station 6034; July 18; latitude 59°27′ N., longitude 44°25′ W.; depth 1,160 m.; dymamic height 1454.756.

Observed values			Scaled values			
Depth, meters	Temperature, ° C.	Salinity, °/oo	Depth, meters	Temperature, ° C.	Salinity, °/oo	σ_t
0	0.48	32.86	0	0.48	32.86	26.38
18	0.81	33.30	25	1.95	33.68	26.94
35	4.00	34.21	50	4.30	34.33	27.24
53	4.32	34.35	75	4.65	34.46	27.31
70	4.72	34.44	100	4.20	34.63	27.49
106	4.16	34.65	150	4.55	34.69	27.52
141	4.30	34.68	200	4.65	34.76	27.55
211	4.69	34.77	300	4.90	34.84	27.58
422	4.98	34.89	400	5.00	34.88	27.60
628	4.75	34.90	600	4.80	34.90	27.64
831	4.23	34.92	800	4.20	34.92	27.73
1,048	4.04	34.905	1,000	4.05	34.91	27.73

Station 6035; July 18; latitude 59°32′ N., longitude 44°10′ W.; depth 178 m.; dynamic height 1454.785.

Observed values			Scaled values			
Depth, meters	Temperature, ° C.	Salinity, °/oo	Depth, meters	Temperature, ° C.	Salinity, °/oo	σ_t
0	−0.29	32.48	0	−0.29	32.48	26.10
25	−0.50	32.81	25	−0.50	32.81	26.39
48	3.22	34.18	50	3.20	34.19	27.24
73	2.57	34.26	75	2.60	34.27	27.36
97	2.79	34.32	100	2.85	34.35	27.40
146	4.02	34.60	(150)	4.15	34.63	27.49

Station 6036; July 18; latitude 59°35.5′ N., longtiude 44°03′ W.; depth 153 m.; dynamic height 1454.775.

Observed values			Scaled values			
Depth, meters	Temperature, ° C.	Salinity, °/oo	Depth, meters	Temperature, ° C.	Salinity, °/oo	σ_t
0	−0.17	32.48	0	−0.17	32.48	26.11
26	0.47	33.27	25	0.40	33.24	26.69
52	2.74	34.18	50	2.70	34.13	27.23
79	2.30	34.26	75	2.35	34.25	27.36
105	2.76	34.36	100	2.65	34.34	27.41
145	3.71	34.50	(150)	3.85	34.52	27.44

In the following table the potential density is represented by $\sigma_{t\theta}$ which signifies 1000 (density-1) at atmospheric pressure and potential temperature t_θ. The concentration of total phosphorus is given in microgram-atoms per liter.

TOTAL PHOSPHORUS DATA COLLECTED IN 1955

Station 6014; July 15; latitude 53°43′ N., longitude 55°46′ W.; depth 126 m.

Depth, meters	$\sigma_{t\theta}$	Total P µga/L	Depth, meters	$\sigma_{t\theta}$	Total P µga/L
0	21.80	0.74	77	26.52	1.03
26	25.91	0.69	103	26.53	1.18
51	26.46	0.98			

Station 6015; July 15; latitude 53°49′ N., longitude 55°31′ W.; depth 214 m.

Depth, meters	$\sigma_{t\theta}$	Total P µga/L	Depth, meters	$\sigma_{t\theta}$	Total P µga/L
0	24.63	0.50	99	26.60	1.08
25	25.82	0.62	149	26.76	1.07
50	26.43	1.09	189	26.99	0.99
75	26.52	1.05			

Station 6016; July 15; latitude 53°53.5′ N., longitude 55°25′ W.; depth 172 m.

Depth, meters	$\sigma_{t\theta}$	Total P µga/L	Depth, meters	$\sigma_{t\theta}$	Total P µga/L
0	25.20	0.46	76	26.60	0.92
25	25.72	0.47	101	26.71	1.01
51	26.51	0.98	152	27.07	1.06

Station 6017; July 15; latitude 54°06′ N., longitude 55°06′ W.; depth 169 m.

Depth, meters	$\sigma_{t\theta}$	Total P µga/L	Depth, meters	$\sigma_{t\theta}$	Total P µga/L
0	25.00	0.71	75	26.65	1.00
25	26.12	0.92	101	26.80	1.03
50	26.51	0.97	151	27.06	1.12

Station 6018; July 15; latitude 54°13′ N., longitude 54°52′ W.; depth 187 m.

Depth, meters	$\sigma_{t\theta}$	Total P µga/L	Depth, meters	$\sigma_{t\theta}$	Total P µga/L
0	24.92	0.52	73	26.67	1.09
24	25.86	0.63	97	26.78	0.96
48	26.52	1.24	145	26.99	0.99

Station 6019; July 15; latitude 54°29′ N., longitude 54°23′ W.; depth 224 m.

Depth, meters	$\sigma_{t\theta}$	Total P µga/L	Depth, meters	$\sigma_{t\theta}$	Total P µga/L
0	26.05	0.49	98	27.00	0.90
25	26.45	0.54	147	27.31	0.95
49	26.76	0.96	196	27.32	1.00
74	26.89	0.93			

Station 6020; July 15; latitude 54°46′ N., longitude 53°50′ W.; depth 333 m.

Depth, meters	$\sigma_{t\theta}$	Total P µga/L	Depth, meters	$\sigma_{t\theta}$	Total P µga/L
0	26.54	0.63	93	27.28	0.95
23	26.80	0.38	140	27.45	0.95
47	26.99	0.44	187	27.54	0.97
70	27.21	0.58	280	27.61	0.95

Station 6021; July 15; latitude 54°51′ N., longitude 53°35′ W.; depth 699 m.

Depth, meters	$\sigma_{t\theta}$	Total P µga/L	Depth, meters	$\sigma_{t\theta}$	Total P µga/L
0	26.61	0.30	151	27.57	0.96
25	26.93	0.39	302	27.70	1.00
50	27.25	0.76	318	27.69	1.04
76	27.43	0.95	504	27.72	0.95
101	27.47	0.94			

Station 6022; July 15; latitude 54°57′ N., longitude 53°22′ W.; depth 1,558 m.

Depth, meters	$\sigma_{t\theta}$	Total P µga/L	Depth, meters	$\sigma_{t\theta}$	Total P µga/L
0	26.87	0.35	306	27.71	1.03
26	27.00	0.45	399	27.73	1.04
51	27.30	0.55	595	27.74	1.03
77	27.51	0.78	788	27.74	1.06
102	27.62	0.97	988	27.77	1.07
153	27.66	0.98	1,480	27.77	1.08
204	27.69	1.03			

Station 6023; July 15–16; latitude 55°01.5′ N., longitude 53°09′ W.; depth 2,103 m.

Depth, meters	$\sigma_{t\theta}$	Total P µga/L	Depth, meters	$\sigma_{t\theta}$	Total P µga/L
0	27.06	0.47	302	27.74	1.03
25	27.29	0.56	357	27.75	0.92
50	27.59	0.91	532	27.75	1.04
76	27.66	0.98	705	27.76	1.05
101	27.68	1.02	890	27.77	0.97
151	27.68	1.04	1,368	27.80	1.05
201	27.72	1.00	1,862	27.83	0.97

Station 6024; July 16; latitude 55°11.5′ N., longitude 52°51′ W.; depth 2,985 m.

Depth, meters	$\sigma_{t\theta}$	Total P µga/L	Depth, meters	$\sigma_{t\theta}$	Total P µga/L
0	26.81	0.40	382	27.75	1.03
26	27.11	0.64	574	27.76	1.05
52	27.55	0.88	767	27.75	1.06
78	27.68	1.00	959	27.76	1.06
103	27.70	0.95	1,455	27.78	1.08
154	27.70	1.06	1,961	27.83	1.09
206	27.70	1.05	2,474	27.88	0.99
309	27.74	1.08			

Station 6025; July 16; latitude 55°30.5′ N., longitude 52°20′ W.; depth 3,200 m.

Depth, meters	$\sigma_{t\theta}$	Total P µga/L	Depth, meters	$\sigma_{t\theta}$	Total P µga/L
0	26.75	0.41	313	27.72	1.08
26	27.37	0.98	431	27.75	1.10
52	27.57	1.08	642	27.75	1.05
78	27.66	1.08	853	27.76	1.15
105	27.69	1.08	1,061	27.75	1.11
156	27.70	1.13	1,593	27.78	1.16
208	27.71	1.09	2,129	27.84	1.09

Depth, meters	$\sigma_{t\theta}$	Total *P* μga/*L*	Depth, meters	$\sigma_{t\theta}$	Total *P* μga/*L*
Station 6026; July 16; latitude 55°55′ N., longitude 51°38′ W.; depth 3,402 m.					
0	27.02	0.88	548	27.75	1.13
25	27.03	0.68	733	------	1.13
50	27.44	0.96	918	27.74	1.14
75	27.59	1.08	1,392	27.78	1.09
100	27.62	1.03	1,875	27.79	1.12
150	27.64	1.09	2,561	27.85	1.11
199	27.69	1.10	3,064	27.89	1.06
299	27.74	1.05	3,421	27.93	0.98
365	27.74	1.08			
Station 6027; July 17; latitude 56°28.5′ N., longitude 50°30′ W.; depth 3,566 m.					
0	26.99	0.58	603	27.74	1.07
24	26.99	0.61	799	27.75	1.09
48	27.39	0.92	994	27.76	1.05
72	27.46	0.99	1,491	27.79	1.04
96	27.53	1.01	1,990	27.79	1.07
145	27.58	1.09	2,476	27.83	1.04
193	27.62	1.08	2,976	27.85	0.96
289	27.70	1.11	3,482	27.89	0.99
404	27.74	1.06			
Station 6028; July 17; latitude 57°01.5′ N., longitude 49°22′ W.; depth 3,612 m.					
0	27.08	0.63	602	27.74	1.12
25	27.12	0.64	798	27.77	1.16
50	27.37	0.87	993	27.78	1.15
75	27.56	1.06	1,494	27.79	1.09
101	27.70	1.08	2,000	27.80	1.10
151	27.71	1.06	2,546	27.84	1.06
201	27.73	1.08	3,053	27.89	1.00
302	27.74	1.11	3,562	27.94	0.97
403	27.74	1.08			
Station 6029; July 17; latitude 57°35′ N., longitude 48°16′ W.; depth 3,429 m.					
0	27.18	0.65	377	27.75	1.03
25	27.23	0.75	565	27.75	1.08
50	27.60	1.04	754	27.75	1.04
75	27.71	1.09	942	------	1.04
100	27.72	1.04	1,430	27.78	1.07
150	27.73	1.19	1,927	27.80	1.08
199	------	1.06	2,547	27.85	1.13
299	27.73	1.06	3,046	27.89	1.06
Station 6030; July 18; latitude 58°10′ N., longitude 47°08′ W.; depth 3,109 m.					
0	27.28	0.86	394	27.73	1.05
26	27.29	0.90	597	27.74	1.08
52	27.41	1.17	804	27.75	1.08
78	27.54	1.17	1,014	27.76	1.16
105	27.66	1.18	1,510	27.79	1.12
156	27.70	1.27	1,997	27.82	1.09
208	27.72	1.30	2,591	27.87	1.08
313	27.73	1.12	3,113	27.90	1.05
Station 6031; July 18; latitude 58°39′ N., longitude 46°08′ W., depth 2,469 m.					
0	27.32	0.83	416	27.74	1.06
25	27.34	0.81	623	27.75	1.05
51	27.55	0.97	829	27.75	1.16
76	27.67	1.05	1,034	27.77	1.06
102	27.68	1.05	1,565	27.81	1.08
152	27.70	1.03	2,104	27.86	1.04
202	27.71	1.05	2,521	27.89	0.95
304	27.74	1.07			
Station 6032; July 18; latitude 58°59.5′ N., longitude 45°19′ W., depth 2,345 m.					
0	27.25	0.80	396	27.74	0.97
25	27.30	0.83	592	27.75	1.11
51	27.57	1.04	786	27.75	1.10
76	27.64	1.12	978	27.78	1.15
101	27.67	1.14	1,478	27.80	1.14
151	27.69	1.08	1,982	27.85	1.13
202	27.70	1.07	2,294	27.88	1.08
303	27.74	1.11			
Station 6033; July 18; latitude 59°09′ N., longitude 44°56′ W.; depth 2,083 m.					
0	26.47	0.93	282	27.69	1.09
24	26.62	0.86	283	27.68	1.08
47	27.38	0.93	451	27.72	1.10
71	27.47	0.96	636	27.73	1.13
94	27.54	0.99	838	27.76	1.10
141	27.61	1.05	1,308	27.80	1.14
188	27.66	1.16	1,708	27.84	1.10
Station 6034; July 18; latitude 59°27′ N., longitude 44°25′ W.; depth 1,160 m.					
0	26.38	0.77	141	27.52	0.93
18	26.71	0.85	211	27.55	0.96
35	27.18	0.85	422	27.61	0.98
53	27.26	0.83	628	27.65	1.07
70	27.28	0.89	831	27.73	1.11
106	27.51	0.94	1,048	27.73	1.09
Station 6035; July 18; latitude 59°32′ N., longitude 44°10′ W.; depth 178 m.					
0	26.10	0.67	73	27.35	0.91
25	26.39	0.74	97	27.38	0.86
48	27.23	0.87	146	27.49	0.87
Station 6036; July 18; latitude 59°35.5′ N., longitude 44°03′ W.; depth 153 m.					
0	26.10	0.73	79	27.38	0.89
26	26.70	0.81	105	27.42	0.83
52	27.27	0.83	145	27.44	0.99

U. S. GOVERNMENT PRINTING OFFICE: 1957

Contribution No. 804

Reprinted from
Journal of Fluid Mechanics, Vol. 1, Part 5, p. 521, November 1956

Outline of a theory of turbulent shear flow

By W. V. R. MALKUS
Woods Hole Oceanographic Institution, Woods Hole, Massachusetts

(*Received* 4 *June* 1956)

Summary

In this paper the spatial variations and spectral structure of steady-state turbulent shear flow in channels are investigated without the introduction of empirical parameters. This is made possible by the assumption that the non-linear momentum transport has only stabilizing effects on the mean field of flow. Two constraints on the possible momentum transport are drawn from this assumption: first, that the mean flow will be statistically stable if an Orr–Sommerfeld type equation is satisfied by fluctuations of the mean; second, that the smallest scale of motion that can be present in the spectrum of the momentum transport is the scale of the marginally stable fluctuations of the mean. Within these two constraints, and for a given mass transport, an upper limit is sought for the rate of dissipation of potential energy into heat. Solutions of the stability equation depend upon the shape of the mean velocity profile. In turn, the mean velocity profile depends upon the spatial spectrum of the momentum transport. A variational technique is used to determine that momentum transport spectrum which is both marginally stable and produces a maximum dissipation rate. The resulting spectrum determines the velocity profile and its dependence on the boundary conditions. Past experimental work has disclosed laminar, 'transitional', logarithmic and parabolic regions of the velocity profile. Several experimental laws and their accompanying constants relate the extent of these regions to the boundary conditions. The theoretical profile contains each feature and law that is observed. First approximations to the constants are found, and give, in particular, a value for the logarithmic slope (von Kármán's constant) which is within the experimental error. However, the theoretical boundary constant is smaller than the observed value. Turbulent channel flow seems to achieve the extreme state found here, but a more decisive quantitative comparison of theory and experiment requires improvement in the solutions of the classical laminar stability problem.

Introduction

The significant difficulty encountered in the theoretical study of fluid turbulence is the non-linearity of the equations of motion. The classical inquiries (e.g. Goldstein 1938), which are concerned with gross spatial features of the flow, avoid dealing with non-linearity by deducing macroscopic laws from the observations. The more recent statistical inquiries (e.g. Batchelor 1953), which are mainly restricted to homogeneous fields of motion, deal with non-linearity by various hypotheses concerning the transfer of energy from one scale of motion to another. The emphasis in these latter studies is on the local random aspects of turbulence and on those regions of the spectrum of turbulence far removed from external energy sources. Hence the spatial variations and spectral structure of momentum and heat transport, which are intimately coupled to the energy sources, receive little theoretical attention.

In this paper the emphasis is on the statistical organization of turbulent fields rather than on their statistical randomness. Hence the momentum and heat transport of a steady-state turbulent field and the dependence of these transports on boundary conditions are of primary concern. However, this will not be a detailed mechanistic study. Indeed, there is little hope that exact time-dependent solutions of the non-linear equations describing turbulence can be found. Here, as in past work, an assumption specifying the role of the non-linear processes will be made. This particular assumption is a negative one, specifying what the non-linear processes can not do. In this way the class of possible turbulent fields is restricted. The determination of an extreme member of this class reduces the mathematical problem to tractable linear form without the introduction of empirical parameters. This absence of empirical parameters permits a rigorous appraisal of the validity of the assumption. Indeed, if the quantitative solutions to the problem are to compare favourably with the observations, the assumption must embody all the significant restraints imposed by the equations of motion.

The particular physical situation to be discussed is the fully turbulent flow in channels. This flow has been studied experimentally for many years. Hence it is an excellent testing ground for theoretical models. The model evolved here has its origin in conventional laminar stability theory. Therefore a brief restatement of the conclusions of this theory is of value.

The stability of a time-independent state of a fluid field can be established by study of the growth or decay of superimposed infinitesimal disturbances. If any disturbance releases a larger amount of potential energy from the pressure field than it dissipates through the action of viscosity, it will grow. The mathematical formulation of this kind of problem usually leads to a linear characteristic value equation. The external conditions which delimit the range of stability of the initial time-independent state of the fluid are determined by the minimum characteristic value. In simple shearing flow a disturbance can abstract energy from the pressure field only through the agency of viscous stress. Hence, in this case, viscosity plays the double role of permitting the growth of disturbances and also dissipating them.

When a disturbance achieves finite amplitude, its non-linear interaction with the initial motion alters both this motion and the disturbance.

First-order stability theory tells one nothing of this alteration, while inclusion of the non-linear interaction in the problem leads to such intractable mathematics that even second-order effects have seldom been investigated. However, the physics of the non-linear effects is fairly clear. The disturbance must grow until its alteration of the initial motion reduces the rate of release of potential energy to the rate of dissipation of this energy. If the disturbance is an aperiodic turbulent motion rather than another steady laminar motion, the equalization of rates of energy release and dissipation must still occur on the average. In either the laminar or turbulent case, alteration of the initial motion is accomplished by the transport of heat or momentum, whichever was responsible for the instability. Hence the most important aspects of the non-linear interaction of disturbance and initial motion are those advective terms which readjust the energy sources of the disturbance.

In the new 'stability' that is achieved, the finite-amplitude disturbance can be looked upon as the stabilizing sink of energy for the destabilizing energy source in the pressure field. It will be assumed that this is so on the average even in the fully developed steady-state turbulence, i.e. that the mean non-linear momentum transport terms in the equations of motion are entirely stabilizing, and that the only energy source for those disturbances which enter into the mean momentum transport is the pressure field of the mean motion.

In the first section, a limiting 'statistical stability' condition on the spatial structure of the mean momentum transport is found as a consequence of this assumption. The momentum transport is then resolved into a spatial spectrum whose smallest scale of motion is the scale of the smallest statistically unstable motion. The determination of the particular spectrum satisfying these stability constraints and the boundary conditions, and also releasing the largest amount of potential energy, leads to an unusual formal problem. In this problem the non-constant cofficients of a linear characteristic value equation are varied under constraints to determine a minimum least characteristic value, also the corresponding minimum least characteristic function and the optimum form of the non-constant coefficients.

The second section outlines a variational approach designed to find these optimal functions and constants; i.e. to find the momentum transport spectrum and mean velocity profile which lead to a marginally stable mean field of maximum dissipation rate. Considerable use is made of the knowledge acquired in the past thirty years about solutions of the laminar stability equation for shearing flow. A first approximation to the spectrum is found, and a comparison is made between this theoretical extreme and the observations.

The concluding section describes other more detailed tests of this work by comparison with recent channel flow data, e.g. the observation of a smallest scale of motion. An attempt to rationalize the basic assumption of the theory raises questions concerning the uniqueness of solutions to the equations of motion, while the apparent existence of extreme states in turbulent fields suggests an explicit statistical mechanical origin. Finally, the application of this approach to quite different turbulent phenomena is outlined.

1. FORMULATION OF A TRACTABLE PROBLEM

This is a study of the steady-state fully evolved three-dimensional turbulence observed between fixed parallel surfaces. Here 'fully evolved' will mean both that the Reynolds number (based on the channel half-width and the average velocity) is far above its value for marginal stability, and that there are no variations of moments of the fluctuating field in the downstream direction. In figure 1 the coordinate frame is chosen so that the x direction is the direction of the mean velocity U, which in turn is some unknown function of the cross-stream direction z. The 'mean' will be defined here as an average in the y direction (perpendicular to the plane of figure 1). It is assumed that the effect of the distant y boundaries on real flows does not influence the nature of the motion far from those boundaries. Hence the remainder of this work deals with parallel surfaces of infinite extent.

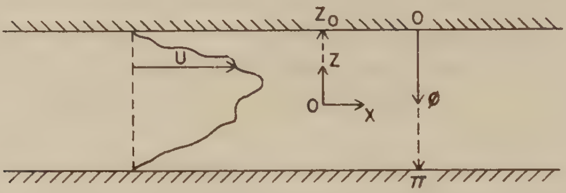

Figure 1. Coordinates chosen to describe flow between parallel surfaces.

It is also assumed in general that compressibility, heating effects and non-linear viscous effects are unimportant in the experimental situation. Therefore the equations of motion and continuity are

$$\frac{D\mathbf{v}}{Dt} = -\frac{1}{\rho}\nabla P + \nu\nabla^2\mathbf{v} \qquad \text{and} \qquad \nabla \cdot \mathbf{v} = 0, \tag{1.1}$$

where D/Dt is the substantial derivative, P the pressure, ρ the fixed density, ν the constant kinematic viscosity, and $\mathbf{v}$ the velocity vector.

A first concern will be the determination of statistical stability constraints imposed on the steady-state flow by these equations.

As implied by the name, statistical stability means the constancy in time of some space (or ensemble) average of the field of motion. Here an investigation will be made of the time dependence of the quantity

$$\bar{\mathbf{v}}(x,z,t) = \left[\frac{1}{2y_0}\int_{-y_0}^{+y_0} \mathbf{v}\,dy\right]_{y_0\to\infty} = \mathbf{v}-\mathbf{v}'. \tag{1.2}$$

Future use of the bar will indicate the mean with respect to y, as in (1.2). Expanding (1.1) with the aid of (1.2), one may write

$$\frac{\partial\bar{\mathbf{v}}}{\partial t} + \frac{\partial\mathbf{v}'}{\partial t} + \bar{\mathbf{v}}\cdot\nabla\bar{\mathbf{v}} + \bar{\mathbf{v}}\cdot\nabla\mathbf{v}' + \mathbf{v}'\cdot\nabla\bar{\mathbf{v}} + \mathbf{v}'\cdot\nabla\mathbf{v}' = -\frac{1}{\rho}\nabla P + \nu\nabla^2\bar{\mathbf{v}} + \nu\nabla^2\mathbf{v}',$$

and

$$\nabla\cdot\bar{\mathbf{v}} + \nabla\cdot\mathbf{v}' = 0. \tag{1.3}$$

The mean value of (1.3) is then

$$\frac{\partial \bar{\mathbf{v}}}{\partial t}+\bar{\mathbf{v}}\,.\,\nabla\bar{\mathbf{v}}+\overline{\mathbf{v}'\,.\,\nabla\mathbf{v}'} = -\frac{1}{\rho}\nabla_2\,\overline{P}+\nu\nabla_2^2\,\bar{\mathbf{v}}$$

and

$$\nabla_2\,.\,\bar{\mathbf{v}} = 0, \tag{1.4}$$

where ∇_2 indicates the two-dimensional (x, z) del operator. Subtracting (1.4) from (1.3), one obtains

$$\frac{\partial \mathbf{v}}{\partial t}+(\bar{\mathbf{v}}\,.\,\nabla\mathbf{v}'+\mathbf{v}'\,.\,\nabla\bar{\mathbf{v}})+(\mathbf{v}'\,.\,\nabla\mathbf{v}'-\overline{\mathbf{v}'\,.\,\nabla\mathbf{v}'}) = -\frac{1}{\rho}(\nabla P-\nabla_2\overline{P})+\nu\nabla^2\mathbf{v}',$$

and

$$\nabla\,.\,\mathbf{v}' = 0. \tag{1.5}$$

Now if the mean flow is to be stable and independent of x, i.e. if $\bar{\mathbf{v}} = U(z)\mathbf{i}$, then if follows from (1.4) that

$$\left[-\nu\frac{\partial^2 U}{\partial z^2}\right]\mathbf{i}+\left[\frac{1}{\rho}\frac{\partial P}{\partial x}\right]\mathbf{i}+\left[\frac{1}{\rho}\frac{\partial P}{\partial z}\right]\mathbf{k} = -\left[\frac{\partial}{\partial z}\overline{w'u'}\right]\mathbf{i}-\left[\frac{\partial}{\partial z}\overline{w'^2}\right]\mathbf{k}, \tag{1.6}$$

where **i** and **k** are unit vectors in the x and z directions respectively, and u' and w' are the components of $\mathbf{v}'$ in the x and z directions respectively. Equation (1.6) is, of course, the usual equation for the mean flow. Integrating the **k** equation, one finds that $\overline{P}/\rho+\overline{w'^2} = \overline{P}_0/\rho$, where $\overline{P}_0$ is the pressure at either fixed surface; and since $\partial\overline{w'^2}/\partial x = 0$ (no variation of mean flow moments in the x direction), then $\partial\overline{P}/\partial x = \partial\overline{P}_0/\partial x$. Integrating the **i** equation, one finds that, since there must be no torque on the fluid as a whole,

$$-\left(\frac{1}{\rho}\frac{\partial\overline{P}_0}{\partial x}\right)z = \nu\beta+\overline{w'u'} = \tau = \tau_0\frac{z}{z_0}, \tag{1.7}$$

where $\beta = -\partial U/\partial z$, and $\tau_0 = -\left(\frac{1}{\rho}\partial\overline{P}_0/\partial x\right)z_0$ is the stress per unit mass at the fixed surface. Equation (1.7) specifies the spatial relation of the mean gradient and the mean momentum transport. Thus it is basic to the following work.

However, the stability of any particular mean flow is not assured unless an arbitrary mean disturbance disappears in a finite time. If we take

$$\bar{\mathbf{v}} = U(z)\mathbf{i}+\epsilon\bar{\mathbf{v}}_1(x, z, t)+\epsilon^2\bar{\mathbf{v}}_2(x, z, t)+\ldots,$$

and

$$\overline{P} = \overline{P}(x, z)+\epsilon\overline{P}_1(x, z, t)+\epsilon^2\overline{P}_2(x, z, t)+\ldots, \tag{1.8}$$

where ϵ is a constant parameter, then $\bar{\mathbf{v}}_1$, $\overline{P}_1$, $\bar{\mathbf{v}}_2$,, $\overline{P}_2$, etc. must all decay in time for an arbitrary choice of ϵ. From (1.4), the zeroth-order terms in ϵ give (1.6). The first-order ϵ terms in (1.4) are

$$\frac{\partial\bar{\mathbf{v}}_1}{\partial t}+U\frac{\partial\bar{\mathbf{v}}_1}{\partial x}+\left(\bar{\mathbf{v}}_1\,.\,\mathbf{k}\frac{\partial U}{\partial z}\right)\mathbf{i}-\nu\nabla_2^2\,\bar{\mathbf{v}}_1+\frac{1}{\rho}\nabla_2\overline{P}_1 = -[\Delta\overline{\mathbf{v}'\,.\,\nabla\mathbf{v}'}]$$

and

$$\nabla_2\,.\,\bar{\mathbf{v}}_1 = 0, \tag{1.9}$$

where $[\Delta\overline{\mathbf{v}'\,.\,\nabla\mathbf{v}'}]$ signifies any first-order change that occurs in the mean non-linear stress due to the complex interaction in (1.5) of $\bar{\mathbf{v}}_1$ and $\overline{P}_1$ with the field of finite fluctuations. If arbitrary $\bar{\mathbf{v}}_1$ and $\bar{P}_1$ are to decay in time, equation (1.9) places restrictions on the form and amplitude of $U(z)$, and hence, through (1.7), on the form and amplitude of $\overline{w'u'}$.

At this point in the analysis, the mechanistic assumption that $\overline{\mathbf{v}'.\nabla\mathbf{v}'}$ plays only a stabilizing role is introduced. The conditions placed on stable forms of $U(z)$ and $\overline{w'u'}$ will be at least as severe as the actual case if the assumed stabilizing effect of $[\Delta\overline{\mathbf{v}'.\nabla\mathbf{v}'}]$ is neglected. Then, with $[\Delta\overline{\mathbf{v}'.\nabla\mathbf{v}'}]$ set equal to zero, equation (1.9) assumes the familiar linear form of the equation for the disturbance of a time-independent shearing flow. Here, however, the problem is to find the entire class of U, for given boundary conditions, which lead to marginally stable $\bar{\mathbf{v}}$ and $\bar{P}$.

Taking the curl of (1.9) to remove the pressure term, and assuming that

$$\bar{\mathbf{v}}_1.\mathbf{k} = \Phi(z)\exp i(\alpha/z_0)[x-(cU_m)t], \tag{1.10}$$

one may write

$$\left(\frac{U}{U_m}-c\right)\left(\frac{\partial^2\Phi}{\partial(z/z_0)^2}-\alpha^2\Phi\right)-\frac{\partial^2(U/U_m)}{\partial(z/z_0)^2}\Phi = \frac{i}{\alpha R}\left(\frac{\partial^4\Phi}{\partial(z/z_0)^4}-2\alpha\frac{\partial^2\Phi}{\partial(z/z_0)^2}+\alpha^4\Phi\right), \tag{1.11}$$

where α/z_0 is the downstream wave number of the disturbance of the mean, cU_m is its phase velocity, U_m is the z-averaged mean velocity, and $R = z_0U_m/\nu$ is the Reynolds number. Equation (1.11) is called the Orr–Sommerfeld equation (Orr 1906–7, Sommerfeld 1908), and has been studied for many years to determine initial instability criterion for a given laminar U. Its appearance in a problem of fully turbulent flow is due in part to the present special assumption and in part to the vanishing of explicit interaction terms between $\bar{\mathbf{v}}$ and $\mathbf{v}'$ in (1.4).

In his study of equation (1.11), Heisenberg (1924) has shown that for a given R some smallest scale of motion (largest α) is unstable. (This is also established in equation (2.41) of this paper.) In addition if $\overline{w'u'}$ is entirely stabilizing, it cannot produce motions requiring greater destabilizing force than that available in the mean flow. Hence a second consequence of the assumption is that the spectrum of $\overline{w'u'}$ cannot contain a scale of motion smaller than twice the scale of the smallest marginally stable motion according to (1.11). (We specify 'twice' since $\overline{w'u'}$ is a product of the fluctuation velocities.)

This restriction on the spectrum of $\overline{u'w'}$ is, through (1.7), a restriction on the possible spatial structure of U. Hence the class of possible U is doubly restricted by the marginal solutions of the stability equation (1.11). Within this class, for a given U_m, one function leads to the release of more potential energy per unit time than any other. This function can be thought of as the 'most stable' in the sense that any alteration of it will increase the potential energy available to disturbances. Ignorance of the detailed mechanisms of momentum transport permits one to hope that this extreme state is approached in the observed turbulence. Hence in the remainder of this section a tractable formal problem for the extreme is posed.

In the steady state, the rate of release of potential energy equals the rate at which mechanical work is done by the shearing stresses, and this equals the rate at which energy is dissipated into heat by the action of viscosity. Hence

$$(\beta\tau)_m = \nu\left[\overline{\left(\frac{\partial \mathbf{v}}{\partial x}\right)^2} + \overline{\left(\frac{\partial \mathbf{v}}{\partial y}\right)^2} + \overline{\left(\frac{\partial \mathbf{v}}{\partial z}\right)^2}\right]_m, \tag{1.12}$$

where $(\partial\mathbf{v}/\partial x)^2 = (\partial\mathbf{v}/\partial x).(\partial\mathbf{v}/\partial x)$, etc., the subscript m again indicates an average value in the z direction, and

$$(\beta\tau)_m = \tau_0(\beta z/z_0)_m = \tau_0\,\beta_0 \tag{1.13}$$

from (1.7). Also

$$\beta_0 = \frac{1}{2z_0}\int_{-z_0}^{+z_0}\beta\frac{z}{z_0}\,dz = -\frac{zU}{2z_0}\bigg|_{-z_0}^{+z_0} + \frac{1}{2z_0}\int_{-z_0}^{+z_0}\frac{U}{z_0}\,dz = \frac{U_m}{z_0}. \tag{1.14}$$

Hence the total rate of dissipation per unit mass, $\tau_0\,U_m$, will be a maximum for a given U_m when τ_0 is a maximum. In a non-dimensional form, a maximum for $(z_0/\nu)(\tau_0/U_m)$ is sought for a given $(z_0/\nu)U_m = R$. However, it is convenient to invert this problem and seek the minimum Reynolds number associated with a marginally stable solution to (1.11), holding $(z_0/\nu)(\tau_0/U_m)$ constant. This latter quantity is proportional to the ratio of the actual dissipation rate and the dissipation rate which would result from a laminar parabolic flow with the same U_m. Indeed, it is readily shown that

$$(\tau_0)_{\text{laminar}} = 3\nu\beta_0. \tag{1.15}$$

Hence the ratio

$$\frac{\tau_0}{(\tau_0)_{\text{laminar}}} = \frac{1}{3}\left(\frac{z_0}{\nu}\right)\left(\frac{\tau_0}{U_m}\right) = \frac{\beta(z_0)}{3\beta_0} \tag{1.16}$$

will be held constant during the minimization of R. The other variables in (1.11) for which optimum values will be sought are α, c and the mean velocity U. There are, however, certain geometric and boundary constraints on U which first must be determined.

One notes that since $u = v = w = 0$ and $\partial w/\partial z = 0$ (from $\nabla.\mathbf{v} = 0$) at the boundary surfaces z_0 and $-z_0$, then

$$\overline{u'w'} = \frac{\partial\overline{u'w'}}{\partial z} = \frac{\partial^2\overline{u'w'}}{\partial z^2} = 0,$$

at z_0 and $-z_0$. Hence, from (1.7), we have

$$\beta = \frac{1}{\nu}\left(\tau_0\frac{z}{z_0} - \overline{u'w'}\right) = -\frac{\partial U}{\partial z};\quad \text{thus}\quad \beta(z_0) = \frac{\tau_0}{\nu},\quad \beta(-z_0) = -\frac{\tau_0}{\nu};$$

$$\frac{\partial\beta}{\partial z} = \frac{\tau_0}{\nu z_0} - \frac{1}{\nu}\frac{\partial\overline{u'w'}}{\partial z} = -\frac{\partial^2 U}{\partial z^2}:\quad \text{thus}\quad \frac{\partial\beta}{\partial z}(z_0) = \frac{\partial\beta}{\partial z}(-z_0) = \frac{\tau_0}{\nu z_0};$$

$$\frac{\partial^2\beta}{\partial z^2} = -\frac{1}{\nu}\frac{\partial^2\overline{u'w'}}{\partial z^2} = -\frac{\partial^3 U}{\partial z^3}:\quad \text{thus}\quad \frac{\partial^2\beta}{\partial z^2}(z_0) = \frac{\partial^2\beta}{\partial z^2}(-z_0) = 0; \tag{1.17}$$

and also $U = 0$ at z_0 and $-z_0$.

Yet another constraint on U arises from certain general conclusions regarding the stability of solutions of (1.11). It has been found (Heisenberg

1924, Lin 1945–46) that a necessary, but not sufficient, requirement for stable solutions at large Reynolds numbers is that the curvature of the mean flow be always of the same sign. A type of instability called 'inflexional' can result if this is not the case. Hence one further requires of U that

$$-\frac{\partial^2 U}{\partial z^2} = \text{const.} \times d^2, \tag{1.18}$$

where d is a real quantity. It is convenient to define the dimensionless quantity

$$\mathcal{U} = \frac{U}{U_m}, \tag{1.19}$$

and choose the constant in (1.18) so that

$$\frac{\partial^2 \mathcal{U}}{d\phi^2} = -\frac{12}{\pi^2}\frac{\tau_0}{(\tau_0)_L} d^2 \equiv -K d^2, \tag{1.20}$$

where $\phi = \frac{1}{2}\pi . (1 - z/z_0)$ (see figure 1). In terms of ϕ, the boundary conditions on d^2, for equations (1.17), may be expressed as follows:

$$\left.\begin{aligned}
&(a) \quad \left(\frac{\partial d^2}{\partial \phi}\right)_0 = \left(\frac{\partial d^2}{\partial \phi}\right)_\pi = 0;\\
&(b) \quad (d^2)_0 = (d^2)_\pi = 1;\\
&(c) \quad \frac{1}{\pi}\int_0^\pi d^2\, d\phi = 1;\\
&(d) \quad \frac{2}{\pi^2}\int_0^\pi \phi\, d^2\, d\phi = 1, \quad \text{or} \quad \int_{-z_0}^{+z_0} z\, d^2\, dz = 0.
\end{aligned}\right\} \tag{1.21}$$

The definitional constraint $\pi^{-1}\int_0^\pi \mathcal{U}\, d\phi = 1$ may be written

$$\frac{2}{\pi^3}\int_0^\pi \phi^2 d^2\, d\phi = 1 - \frac{4}{\pi^2 K}. \tag{1.22}$$

Now (*d*) of (1.21) is just the requirement that d^2 be symmetric; accordingly, equation (1.22) may be written

$$\frac{1}{K} = \int_0^{\frac{1}{2}\pi}\left(\phi - \frac{\phi^2}{\pi}\right) d^2\, d\phi. \tag{1.23}$$

From (1.7) we have

$$\frac{\overline{u'w'}}{\tau_0} = \frac{2}{\pi}\int_0^\phi (d^2 - 1)\, d\phi. \tag{1.24}$$

Hence the spatial spectrum of the momentum transport is determined by d^2. We have also

$$\mathcal{U} = K\left\{\tfrac{1}{2}\pi\phi - \phi\int_0^\phi d^2\, d\phi + \int_0^\phi \phi d^2\, d\phi\right\}. \tag{1.25}$$

The final constraint on U is due to the requirement that the field of transporting motions, $\overline{u'w'}$, has some smallest scale, eventually to be determined by the stability equation. This constraint is introduced by the requirement that d has some smallest scale n_0, that is

$$d = \sum_{n=0}^{n_0} Y_n \, \psi_n(\phi), \tag{1.26}$$

where $\psi_n(\phi)$ is some real orthogonal set of functions satisfying the appropriate boundary and symmetry conditions, and the Y_n are arbitrary real amplitudes.

The formal linear problem may now be stated: First, for any U satisfying $-(\partial^2 U/\partial z^2) \geqslant 0$, find from the Orr–Sommerfeld equation (1.11) the smallest scale of motion and the relation between R, α and c for marginal stability. Second, expressing U in terms of the d from (1.18) and taking some convenient set ψ_n, vary Y_n, subject to the constraints (1.21) and (1.23), to find the minimum R for constant K. This analysis is undertaken in the next section.

2. A VARIATIONAL SOLUTION TO THE STABILITY PROBLEM

The stability equation (1.11) has been studied since 1908. A recent interesting inquiry (Lin 1945–46) contains, as a partial list, seventy references. A first purpose in all these papers was to establish the Reynolds number for the initial instability of laminar flow. Only an outline of this theory will be given here.

For a given velocity profile U, the Orr–Sommerfeld equation determines a relation $c = c(\alpha, R)$ for each solution Φ. For R and α real, and c complex, this single relation can be separated into a real and imaginary part. For marginal stability the imaginary part of c is zero and this determines $R = R(\alpha)$, the curve of marginal stability. For each point on this curve the real part of the relation $c = c(\alpha, R)$ determines the corresponding value of c. No complete solution has yet been found. However, asymptotic solutions of equation (1.11) for large values of αR have proved adequate in the study of initial laminar instability (and should be much better for the turbulence problem since αR is orders of magnitude larger). Recent quantitative work rests on the relations*:

$$\left(\Phi_3 \Big/ \frac{\partial \Phi_3}{\partial \phi}\right)_{\phi=0} = \phi_c F(\eta), \tag{2.1}$$

where Φ_3 is the highly oscillatory part of the asymptotic Φ, and ϕ_c is that value of ϕ at which $U = c$;

$$\eta = [(1+\lambda)(1-\gamma)^{1/3}] \,.\, (\tfrac{1}{4}\pi^2 K)^{-2/3} c (\alpha R)^{1/3}, \tag{2.2}$$

where

$$\gamma = \frac{2}{\pi} \int_0^{\phi_c} d^2 \, d\phi, \qquad \frac{\lambda}{1+\lambda} = \frac{1}{\phi_c} \int_0^{\phi_c} \left(\frac{2}{\pi} \int_0^{\phi} d^2 \, ds \right) d\phi; \tag{2.3}$$

and

$$F(\eta) = \frac{\int_{+\infty}^{-\eta} d\xi' \int_{+\infty}^{\xi'} \xi^{1/2} d\xi \, H_{1/3}^{(1)} \left[\tfrac{2}{3}(i\xi)^{3/2}\right]}{-\eta \int_{+\infty}^{-\eta} \xi^{1/2} d\xi \, H_{1/3}^{(1)} \left[\tfrac{2}{3}(i\xi)^{3/2}\right]} \equiv 1 - \frac{1}{J(\eta)}.$$

---

* Lin's equations (6.28), (6.29), and (12.32) correspond to (2.1), (2.2), and (2.4) in the notation used here.

The function $F(\eta)$ was first numerically calculated by Tietjens. Lin has improved and extended this calculation, of which relevant results appear in table 1 below.

η	2·6	2·8	3·0	3·2	3·4	3·6	3·8
$F_i(\eta)$	0·07203	0·12220	0·17391	0·22520	0·27193	0·30705	0·32130
$J_i(\eta)$	0·31558	0·46043	0·54872	0·58082	0·56401	0·51074	0·43560
$F_r(\eta)$	0·52773	0·49952	0·46456	0·41947	0·36110	0·28802	0·20352

Table 1

A first relation imposed by the boundary conditions on the several parts of the asymptotic Φ is written

$$J_i(\eta) = -\tfrac{1}{2}\pi^2 K(1-2\lambda)\left[\frac{\mathcal{U}\,\partial^2\mathcal{U}/\partial\phi^2}{(\partial\,\mathcal{U}/\partial\phi)^3}\right]_{\phi=\phi_c}$$
$$= 2\phi_c\, d_c^2[(1+\lambda)(1-\gamma)]^{-3} = v(c), \quad (2.4)$$

where the primary contribution to $v(c)$ is due to the pole of equation (1.11) at $U = c$, and where λ, as will be justified *a posteriori*, is assumed to be very small. The value of ϕ_c is determined from (2.4) at the first interception of $v(c)$ and $J_i(\eta)$. Equations (2.1), (2.2) and (2.4) can then be used to determine αR as a function of c; hence they determine $(\alpha R)_{\mathrm{min}}$ and the corresponding c. An important characteristic of the $R(\alpha)$ curve, used since Heisenberg first developed this approach, is that the value of R at $(\alpha R)_{\mathrm{min}}$ is very close to the minimum value of R. This property of $R(\alpha)$ will also be used here to find R_{min}. The real task of recent work has been the evaluation of α from the complicated second relation imposed by the boundary conditions on the asymptotic Φ. This will be avoided here through the use of an integral condition for stability discussed later in this section.

Turning now to the turbulence problem, one notes that the scale of motion in Φ is determined by the imaginary part of the derivative of Φ. The largest value of this derivative will occur in the sharp shear zone at the boundary. Hence

$$n_0 = \left|\left(\frac{1}{\Phi_3}\frac{\partial\Phi_3}{\partial\phi}\right)_i\right|_{\phi=0}. \quad (2.5)$$

Then, from (2.1), one may write

$$\xi_c = \frac{1}{F_i(\eta)}. \quad (2.6)$$

where $\xi_c = n_0\phi$. Equation (2.4) is now written

$$(d^2/n_0)_c = \tfrac{1}{2}[(1+\lambda)(1-\gamma)]^3 J_i(\eta) F_i(\eta). \quad (2.7)$$

To determine $(\alpha R)_{\mathrm{min}}$, Heisenberg first observed that for $\partial(\alpha R)/\partial c = 0$, one has from (2.2) and (2.4)

$$\eta J_i'(\eta) = cv'(c), \quad (2.8)$$

and

$$(\alpha R)_{\mathrm{min}} = (\tfrac{1}{4}\pi^2 K)^2\left(\frac{\eta_0}{c}\right)^3 1/(1+\lambda)^3(1-\gamma), \quad (2.9)$$

where η_0 is that η which satisfies (2.8), and where the small spatial variation of $(1+\lambda)^3(1-\gamma)$ has been neglected. Hence, if the Y_n in the expansion of d^2, equation (1.26), are constrained to satisfy (2.7) and (2.8), the resulting profile will be both marginally stable and continuously at $(\alpha R)_{\min}$, no matter what further variations of Y_n are made.

Now a convenient orthonormal set $\psi_n(\phi)$ which automatically satisfies (*a*) and (*d*) of (1.21) is

$$\psi_n(\phi) = \sqrt{2}\cos 2n\phi, \qquad \psi_0(\phi) = 1, \tag{2.10}$$

where n is any integer. Hence, to satisfy (*b*) and (*c*) of (1.21), we must have

$$\sum_{n=0}^{\frac{1}{2}n_0} Y_n^2 = 1, \tag{2.11}$$

and

$$\left(\sum_{n=0}^{\frac{1}{2}n_0} Y_n\right)^2 = \tfrac{1}{2}. \tag{2.12}$$

Equation (1.23) may be written

$$\frac{1}{K} = \sum_{n=0}^{\frac{1}{2}n_0}\sum_{m=0}^{\frac{1}{2}n_0} B_{nm} Y_n Y_m, \tag{2.13}$$

where

$$B_{nm} = \int_0^{\frac{1}{2}\pi}\left(\phi - \frac{\phi^2}{\pi}\right)[\cos 2(n+m)\phi + \cos 2(n-m)\phi]\,d\phi.$$

Also from (1.24) and (2.10) the momentum transport spectrum is

$$\frac{\overline{u'w'}}{\tau_0} = \sum_{n=1}^{n_0} T_n \sin 2n\phi,$$

where

$$T_n = \frac{1}{2n}\sum_{x=-\frac{1}{2}n_0}^{\frac{1}{2}n_0} Y_{|x|} Y_{|n-x|}. \tag{2.14}$$

It is now possible to write down a complete set of equations optimizing Y_n for a minimum $(\alpha R)_{\min}$. However, not only is this a most complicated problem, but its solution will be as approximate as the stability criteria. Thus, to establish the more significant physical consequences of the extreme state, the spectrum Y_n will be approximated to roughly the same extent that Φ is in equation (2.1). This approximation of the optimum Y_n will be done in two ways: First, only the consequences of Y_n at large n_0 will be considered, so that in expansions in powers of $1/n_0$ only the first term will be kept. Second, rather than optimize each Y_n separately, optimization will be made between sets of Y_n which satisfy the conditions (2.7), (2.8), (2.10) and (2.11).

Although other trial functions may converge more rapidly to the optimum dissipation rate, a simple power series has many mathematical advantages. Hence Y_n is expanded as

$$Y_n = \frac{A}{\sqrt{n_0}}\left[1 + \frac{C_1}{(n_0/2)}n + \frac{C_2}{(n_0/2)^2}n^2 + \frac{C_3}{(n_0/2)^3}n^3 + \ldots\right]. \tag{2.15}$$

To have even one free parameter for a variational optimization, Y_n must have five free parameters. Therefore Y_n in (2.15) will be terminated at the n^3 term, leaving A, n_0, C_1, C_2 and C_3 to be determined. From (2.15) and (1.26) one finds that

$$\begin{aligned} d = \frac{A}{(2n_0)^{1/2}}\Bigg[&\left\{1 + \frac{\sin(n_0+1)\phi}{\sin\phi}\right\} + \frac{C_1}{(n_0/2)}\left\{\left(\frac{n_0}{2}+1\right)\frac{\sin(n_0+1)\phi}{\sin\phi} - \right.\\ &\left.- \frac{1}{2}\frac{(1-\cos(n_0+1)\phi)}{\sin^2\phi}\right\} + \frac{C_2}{(n_0/2)^2}\left\{\left(\frac{n_0}{2}+1\right)^2\frac{\sin(n_0+1)\phi}{\sin\phi} + \right.\\ &\left. + \frac{(n_0+3)}{2}\frac{\cos(n_0+2)\phi}{\sin^2\phi} - \frac{1}{2}\frac{\sin(n_0+3)\phi}{\sin^3\phi}\right\} + \\ &+ \frac{C_3}{(n_0/2)^3}\left\{\left(\frac{n_0}{2}+1\right)^3\frac{\sin(n_0+1)\phi}{\sin\phi} + \frac{3}{2}\left(\frac{n_0+1}{2}\right)^2\frac{\cos(n_0+1)\phi\cos\phi}{\sin^2\phi} - \right.\\ &- \frac{3}{4}\left(\frac{n_0+1}{2}\right)\frac{\sin(n_0+1)\phi(1+\cos^2\phi)}{\sin^3\phi} + \frac{1}{4}\frac{(1+2\cos^2\phi)}{\sin^4\phi} - \\ &\left.\left. - \frac{1}{8}\frac{\cos(n_0+1)\phi\cos\phi(5+\cos^2\phi)}{\sin^4\phi}\right\}\right], \end{aligned} \tag{2.16}$$

where the various sums, $\sum_{n=0}^{\frac{1}{2}n_0} n\cos 2n\phi$, etc., have been performed by the calculus of finite differences. In keeping with the requirement of large n_0, it is convenient to divide d^2 into a function describing its complicated transition region near the boundary and a function which is important away from the boundary. These are

$$(d^2 n_0)_{\phi>>1/n_0} = \frac{A^2}{2}\left[1 + C_0\frac{\sin(n_0+1)\phi}{\sin\phi}\right]^2, \tag{2.17}$$

and

$$\begin{aligned} (d^2/n_0)_{\phi\sim 1/n_0} = \frac{A^2}{2\xi^2}\Bigg[&C_0\sin\xi + C_1\left\{-\frac{(1-\cos\xi)}{\xi}\right\} + C_2\left\{2\frac{\cos\xi}{\xi} - \frac{2\sin\xi}{\xi^2}\right\} + \\ &+ C_3\left\{3\frac{\cos\xi}{\xi} - 6\frac{\sin\xi}{\xi^2} + 6\frac{(1-\cos\xi)}{\xi^3}\right\}\Bigg] = \frac{A^2}{2\xi^2}L^2(\xi), \end{aligned} \tag{2.18}$$

where $C_0 = 1 + C_1 + C_2 + C_3$, and $\xi = n_0\phi$. Hence equation (2.7) becomes

$$AL(\xi_c) = [(1+\lambda)(1-\gamma)]^{3/2}[J_i(\eta_0)/F_i(\eta_0)]^{1/2}. \tag{2.19}$$

Moreover, if one neglects the variations of $[(1+\lambda)(1-\gamma)]^{3/2}$ with ξ_c, equation (2.8) becomes

$$\frac{L'(\xi_c)}{L(\xi_c)} = \tfrac{1}{2}F_i(\eta_0)\left[1 + \frac{\eta_0 J_i'(\eta_0)}{J_i(\eta_0)}\right]. \tag{2.20}$$

Equation (2.12) can be summed to give

$$2 = -C_1 - \tfrac{2}{3}C_2 - \tfrac{1}{2}C_3 \tag{2.21}$$

to the zeroth order in $1/n_0$, while (2.11) is summed as

$$\begin{aligned} 2 = A^2\{&1 + C_1 + \tfrac{1}{3}(2C_2 + C_1^2) + \tfrac{1}{2}(C_1C_2 + C_3) + \\ &+ \tfrac{1}{5}(2C_1C_3 + C_2^2) + \tfrac{1}{3}C_2C_3 + \tfrac{1}{7}C_3^2\}. \end{aligned} \tag{2.22}$$

Then equations (2.6), (2.19), (2.20), (2.21) and (2.22) are five relations between six independent variables A, C_1, C_2, C_3, η_0 and ξ_c. A choice for ξ_c, say, determines the other five. Actually, λ and γ are small quadratic functions of these independent variables, from equation (2.3). However, to a zeroth approximation they may be assumed to be zero, their values then computed for each ξ_c and these values used for a first approximation of A, C_1, C_2, C_3 at each ξ_c.

Before resolving these algebraic relations the remainder of the problem will be discussed. From (2.9) we have

$$(\alpha R)_{\min} = \tfrac{1}{2}\pi K^2\left(\frac{n_0}{K}\frac{\eta_0}{\xi_c}\right)^3\frac{1}{(1-\gamma)}\,; \tag{2.23}$$

i.e. $C(1+\lambda) = \frac{1}{2}\pi K/\xi_c$. Hence the dependence of n_0/K on

$$\xi_c = \xi_c(A, C_1, C_2, C_3, \eta_0)$$

must be found in order to determine that ξ_c (say $\underline{\xi_c}$) which makes $(\alpha R)_{\min}$ a minimum. Following this, to determine the relation between n_0 and R, α must be determined. Now α, the down-stream wave number, bears some (probably fixed) relation to $\frac{1}{2}\pi n_0$, the cross-stream wave number, say

$$\tfrac{1}{2}\pi n_0 = r\alpha. \tag{2.24}$$

(If $r = 1$, the smallest 'eddy' would be circular; if $r = 10$ the smallest 'eddy' would be a 10 to 1 ellipse with major axis parallel to the boundary.) Then from (2.6) and (2.23) it follows that

$$R_{\min} = \frac{r}{(1-\gamma)}\left(\frac{\eta_0}{\underline{\xi_c}}\right)^3\left(\frac{n_0}{K}\right)n_0. \tag{2.25}$$

Hence a determination of the ratio r establishes the relation $R = R(n_0)$.

To interpret the various formulae in conventional experimental terms, it is convenient to define a 'boundary Reynolds number':

$$R_{\mathrm{B}} = \frac{sU_s}{\nu}, \tag{2.26}$$

where s is a distance proportional to z_0/n_0, say $s = z_0/n_0$, and U_s is the velocity that would be due to the initial gradient at that distance from the boundary. So defined, equation (2.26) may be written as

$$R_{\mathrm{B}} = \frac{\pi^2}{4}\frac{RK}{n_0^2}, \quad \text{or} \quad n_0 = \frac{z_0}{\nu}\frac{1}{\sqrt{R_{\mathrm{B}}}}U_\tau, \quad \text{or} \quad \frac{n_0}{K} = \frac{\pi^2}{4}\frac{1}{\sqrt{R_{\mathrm{B}}}}\frac{U_m}{U_\tau}, \tag{2.27}$$

where $U_\tau \equiv \surd\tau_0$ is the conventional 'friction velocity', in terms of which most data have been described. From (2.27) and (2.25) we have

$$R_{\mathrm{B}} = \frac{\pi^2}{4}\frac{r}{(1-\gamma)}\left(\frac{\eta_0}{\underline{\xi_c}}\right)^3. \tag{2.28}$$

Finally, to find n_0/K and the velocity profile as functions of

$$\xi_c = \xi_c(A, C_1, C_2, C_3),$$

equations (1.23) and (1.26) may be integrated using (2.17) and (2.18). From

(1.26), (2.17), and (2.18), it follows that

$$\frac{n_0}{K} = \int_0^{\frac{1}{2}\pi}\left(\phi - \frac{\phi^2}{\pi}\right) d^2n_0\, d\phi \doteqdot \int_0^{\frac{1}{2}\pi-\epsilon}\left(\frac{\pi}{4} - \frac{\theta^2}{\pi}\right)(d^2n_0)_{\phi>>1/n_0} d\theta + \\ + \int_0^{n_0\epsilon}\left(\xi - \frac{\xi^2}{n_0\pi}\right)\left(\frac{d^2}{n_0}\right)_{\phi\sim 1/n_0} d\xi, \tag{2.29}$$

where $\theta = \frac{1}{2}\pi - \phi$, and $1/n_0 \ll \epsilon \ll 1$. For large n_0,

$$n_0/K = \tfrac{1}{2}A^2[\tfrac{1}{2}C_0^2(\ln \Gamma n_0 + 1) + \pi^2/12 + C], \tag{2.30}$$

where $\Gamma = 1{\cdot}78^+$ is Euler's constant, and

$$C = \frac{(2\ln 2 + 1)}{2}(1 - C_0^2) + (2\ln 2 - 1)\frac{C_2}{15}(2C_0 - 3 + \tfrac{1}{6}C_2) \tag{2.31}$$

after some condensation with the help of (2.21). From (1.25) and (2.18), the velocity field near the boundary may be determined in terms of sine and cosine integrals:

$$\frac{n_0}{K}\mathcal{U} = \tfrac{1}{2}\pi\xi - \xi\int_0^{\xi}\left(\frac{d^2}{n_0}\right)_{\phi\sim 1/n_0} ds + \int_0^{\xi} s\left(\frac{d^2}{n_0}\right)_{\phi\sim 1/n_0} ds.$$

After rising linearly, as $\frac{1}{2}\pi\xi$, from the boundary, $n_0\,\mathcal{U}/K$ turns sharply through a 'transition' region to its asymptotic value

$$n_0\,\mathcal{U}/K = \tfrac{1}{2}A^2[\tfrac{1}{2}C_0^2(\ln 2\Gamma\xi + 1) + \pi^2/12 + C]. \tag{2.32}$$

From (1.23) and (2.17), direct integration gives

$$\frac{n_0}{K}(\mathcal{U}_{\max} - \mathcal{U}) = \tfrac{1}{2}A^2[\tfrac{1}{2}\theta^2 - \tfrac{1}{2}C_0^2 \ln\cos\theta]. \tag{2.33}$$

Now combining (2.30), (2.32) and (2.33) with (2.27), one may write a theoretical form for the gross features of channel flow beyond the 'transition' region:

$$\frac{U}{U_\tau} = \sqrt{R_B}\left(\frac{AC_0}{\pi}\right)^2\left[\ln\frac{(z_0 - z)U_\tau}{\nu} + \left\{\left(1 + \ln\frac{\pi\Gamma}{\sqrt{R_B}}\right) + \right.\right. \\ \left.\left. + \frac{2}{C_0^2}\left(\frac{\pi^2}{12} + C\right)\right\}\right], \tag{2.34}$$

$$\frac{U_{\max} - U}{U_\tau} = \sqrt{R_B}\left(\frac{AC_0}{\pi}\right)^2\left[\ln\frac{1}{\cos\theta} + \frac{\theta^2}{C_0^2}\right]; \tag{2.35}$$

$$\frac{U_m}{U_\tau} = \sqrt{R_B}\left(\frac{AC_0}{\pi}\right)^2\left[\ln\frac{z_0U_\tau}{\nu} + \left\{\left(1 + \ln\frac{\Gamma}{\sqrt{R_B}}\right) + \right.\right. \\ \left.\left. + \frac{2}{C_0^2}\left(\frac{\pi^2}{12} + C\right)\right\}\right]. \tag{2.36}$$

Those readers familiar with the experimental literature will have recognized a 'velocity defect law' in equation (2.35) and a 'logarithmic boundary law' in (2.34). The usual empirical constants in these experimental laws depend here on the determination of $\xi_c = \xi_c(A, C_1, C_2, C_3, \eta_0)$ and the ratio r.

Returning to the algebraic problem of finding $\xi_c = \xi_c(A, C_1, C_2, C_3, \eta_0)$ from (2.6), (2.19), (2.20), (2.21) and (2.22), one notes that, for a particular

ξ_c, η_0 is determined from (2.6) and table 1. Resolving the other four equations, it is found that

$$C_1 = -2-\left(\frac{2}{3}+\frac{e_3}{2}\right)C_2+\tfrac{1}{2}Q; \qquad C_2 = QG_1-G_2; \qquad C_3 = Q+e_3\,C_2, \tag{2.37}$$

where

$$Q = \frac{e_1}{A}+e_2 = -\frac{q_2}{q_1}\pm\left[\left(\frac{q_2}{q_1}\right)^2-\frac{q_3}{q_1}\right]^{1/2},$$

$$q_1 = -e_5\,G_1-e_4\,G_1^2-\frac{11}{420}+\frac{2}{e_1^2},$$

$$q_2 = \tfrac{1}{2}\{e_5\,G_2+e_6\,G_1\}+e_4\,G_1\,G_2+\frac{1}{15}-\frac{2e_2}{e_1^2},$$

$$q_3 = -e_6\,G_2-e_4\,G_2^2-\frac{1}{3}+\frac{2e_2^2}{e_1^2};$$

also

$$G_1 = \frac{e_1'-1}{e_3-e_3'}, \qquad G_2 = \frac{e_1e_2-e_2'}{e_3-e_3'},$$

$$e_1 = \frac{[(1+\lambda)(1-\gamma)]^{3/2}[J_i(\eta_0)/2F_i(\eta_0)]^{1/2}}{(d_3-\frac{1}{2}d_1)},$$

$$e_2 = \frac{(2d_1-d_0)}{(d_3-\frac{1}{2}d_1)}, \qquad e_3 = \frac{(\frac{2}{3}d_1-d_2)}{(d_3-\frac{1}{2}d_1)},$$

$$e_4 = \left(\frac{2}{135}+\frac{7}{180}e_3+\frac{11}{420}e_3^2\right), \qquad e_5 = \left(\frac{7}{180}+\frac{11}{210}e_3\right),$$

$$e_6 = \left(\frac{1}{9}+\frac{2}{15}e_3\right), \qquad e_1' = \frac{\frac{1}{2}F_i(\eta)[1+\eta_0 J'(\eta_0)](d_3-\frac{1}{2}d_1)}{J(\eta_0)(d_3'-\frac{1}{2}d_1')}$$

$$e_2' = \frac{(2d_1'-d_0')}{(d_3'-\frac{1}{2}d_1')}, \qquad e_3' = \frac{(\frac{2}{3}d_1'-d_2')}{(d'-\frac{1}{2}d_1')};$$

and

$$L(\xi_c) \equiv (d_0+C_1\,d_1+C_2\,d_2+C_3\,d_3), \qquad L'(\xi_c) \equiv (d_0'+C_1\,d_1'+C_2\,d_2'+C_3\,d_3').$$

For each chosen ξ_c, the quantity $(n_0/K)(\eta_0/\xi_c)$ of equation (2.23) may be found from these relations and (2.30). However, the restriction that the first interception of $J_i(\eta)$ and $v(c)$, equation (2.4), determines ξ_c sets an upper limit on the ξ_c that may be chosen. Table 2 lists the computed values for $(n_0/K)(\eta_0/\xi_0)$, the corresponding values of γ and λ, and the maximum value of

$$I = AL(\xi)\xi^{1/2}\{[1+\lambda(\xi)]\,.\,[1-\gamma(\xi)]\}^{3/2}/[J_i(\eta_0)]^{1/2}, \qquad \xi < \xi_c,$$

at several ξ_c on either side of this upper limit. When $I = 1$, $J_i(\eta)$ marginally

ξ_c	$\left(\frac{n_0}{K}\cdot\frac{\eta_0}{\xi_c}\right)_{n_0=10^2}$	$\left(\frac{n_0}{K}\cdot\frac{\eta_0}{\xi_c}\right)_{n_0=10^4}$	γ	λ	$I(\xi)$	ξ
6·00	14·87	30·14	0·095	0·045	0·846	0·93π
350° ≡ 6·1086	14·40	28·78	0·121	0·065	1·042	0·97π
2π	13·84	27·80	0·183	0·114	1·375	1·05π

Table 2

intercepts $v(c)$ at the smaller ξ. Hence, from a graph of table 2, the minimum value of $(n_0/K)(\eta_0/\xi_c)$ occurs at $\xi_c = \underline{\xi_c} = 6{\cdot}081$. Substitution of this ξ_c into the relations (2.37) gives

$$C_2 = 25{\cdot}67, \qquad Q = -1{\cdot}630, \qquad A^2 = 11{\cdot}43;$$

and $$\frac{\eta_0}{\underline{\xi_c}} = 0{\cdot}4875, \qquad C_0^2 = 2{\cdot}308, \qquad C+\frac{\pi^2}{12} = -1{\cdot}908, \tag{2.38}$$

for $$\gamma = 0{\cdot}114, \qquad \lambda = 0{\cdot}059.$$

The ratio r can be determined from the second relation imposed by the boundary conditions on the asymptotic Φ. (Equation (2.4) was the first relation.) However, this is a difficult task involving sums of series of integrals of functions of the optimum velocity profile. Instead, an integral condition for stability due to Synge (1938) will be used. Synge observed that multiplying the Orr–Sommerfeld equation (1.11) by $\Phi^*\,d\phi$, integrating from 0 to π and adding the resulting equation to its own complex conjugate leads to

$$I_2^2+2\alpha^2I_1^2+\alpha^4I_0^2 = -\alpha R\mathcal{U}'(0)I_3-\alpha Rc_i(I_1^2+\alpha^2I_0^2), \tag{2.39}$$

where $$I_0^2 = \int_0^\pi \Phi\Phi^*d\phi, \qquad I_1^2 = \int_0^\pi \Phi'\Phi^{*\prime}d\phi, \qquad I_2^2 = \int_0^\pi \Phi''\Phi^{*\prime\prime}d\phi,$$

$$I_3 = \tfrac{1}{2}i\int_0^\pi (\mathcal{U}'/\mathcal{U}'(0))(\Phi'\Phi^*-\Phi\Phi^{*\prime})\,d\phi,$$

and the prime denotes differentiation with respect to ϕ. When Φ is stable, we have $c_i \leqslant 0$; hence

$$1/I_0^2\int_0^\pi\left[1+\frac{\mathcal{U}'(0)}{\alpha^3}R\left\{\frac{i}{2}\frac{\mathcal{U}'}{\mathcal{U}'(0)}\left(\frac{\Phi'}{\Phi}-\frac{\Phi^{*\prime}}{\Phi^*}\right)+\right.\right.$$
$$\left.\left.+\frac{2}{\alpha^2}\left(\frac{\Phi'\Phi^{*\prime}}{\Phi\Phi^*}\right)\right]\Phi\Phi^*\,d\phi+\left(\frac{I_2}{\alpha^2I}\right)^2 \geqslant 0. \tag{2.40}$$

A sufficient condition for stability is that the integral in (2.40) be greater than zero. If then $\Phi'/\Phi = A+iB$, this integral is positive definite when

$$[\mathcal{U}'(0)R]^2 = 8\alpha^4M, \qquad M = \frac{\int_0^\pi(A^2+B^2)\Phi\Phi^*d\phi\,\int_0^\pi\Phi\Phi^*d\phi}{\left[\int_0^\pi(\mathcal{U}'/\mathcal{U}'(0))B\Phi\Phi^*d\phi\right]^2}. \tag{2.41}$$

Synge noted that, since $\int B^2\Phi\Phi^*\,d\phi\int\Phi\Phi^*\,d\phi \geqslant \left[\int B\Phi\Phi^*\,d\phi\right]^2$, M in (2.41) must be greater than one. Hence, $[\mathcal{U}'(0)R]^2 = 8\alpha^4$ sets a lower limit on α for stable Φ. However, a closer condition can be set by using the asymptotic Φ to estimate M. Now at the boundary, $\phi = 0$, $A(0) \geqslant F_r(\eta_0)$ and $B(0) = F_i(\eta_0)$. From (2.38) and table 1, $F_r(\eta_0) = 0{\cdot}465$ and

$$F_i(\eta_0) = 0{\cdot}174.$$

Also from table 1 one sees that $F_r(\eta_0)/F_i(\eta_0)$ increases for smaller η (i.e. larger ϕ) through the range where $\mathcal{U}'/\mathcal{U}'(0)$ is large. Hence, in a conservative estimate, we have

$$\int_0^\pi(A^2+B^2)\Phi\Phi^*\,d\phi \geqslant \left\{1+\left[\frac{A(0)}{B(0)}\right]^2\right\}\int_0^\pi B^2\Phi\Phi^*\,d\phi,$$

and $$M \geqslant \left[1+\left(\frac{0{\cdot}465}{0{\cdot}174}\right)^2\right] \doteqdot 8.$$

Since the value of M will enter final formulae only as $M^{1/12}$, this represents only a slight improvement on Synge's condition. An extension of the preceding analysis shows that $I_2/\alpha^2 I_0$ and $I_1/\alpha I_0$ approach zero for large α and larger R; hence using (2.41), we have

$$C_i \to -\left[\frac{\alpha}{R}\left(1-\frac{2}{\alpha^2}\right)^2\right] \to 0.$$

Equation (2.41) then becomes as accurate an estimate of the marginally stable α as one could hope to attain by the tedious method mentioned earlier.

Finally, equating the R in (2.41) and (2.23), one obtains

$$r=(1-\gamma)^{1/3}\left(\frac{\xi_c}{\eta_0}\right)(8M)^{1/6}=3\cdot94 \qquad (2.42)$$

for $M = 8$, $\eta_0/\xi_c = 0\cdot4875$ and $\gamma = 0\cdot114$ from (2.38). Inserting the numerical results of (2.38) and (2.42) into (2.28) and the constants of (2.34) and (2.35), one obtains

$$R_B=\frac{\pi^2}{4}\frac{r}{(1-\gamma)}\left(\frac{\eta_0}{\xi_c}\right)^3=1\cdot271, \qquad (2.43)$$

$$\sqrt{R_B}\left(\frac{AC_0}{\pi}\right)^2=3\cdot014; \qquad \text{e.v.}=3\cdot0\pm0\cdot1, \qquad (2.44)$$

$$\left(1+\ln\frac{\pi\Gamma}{\sqrt{R_B}}\right)+\frac{2}{C_0^2}\left(\frac{\pi^2}{12}+C\right)=+1\cdot001; \qquad \text{e.v.}=1\cdot8\pm0\cdot1, \qquad (2.45)$$

where e.v. means the experimental values recently determined by Laufer (1950).

The constant of equation (2.44) (inversely proportional to von Kármán's constant) is the most important in these results since it enters into every other relation. The 'logarithmic intercept' constant, equation (2.45), involves the relatively sensitive quantity C (equation (2.31)), perhaps accounting for the error in this determination. An observation of r will be discussed in the conclusion. The dissipation rate is inversely proportional to the square of $\bar{U}_m/U_\tau$, equation (2.36); hence it is larger than observed due to the error in C. However, at large R the percentage error due to C is small, and the dissipation rate approaches the observed curve.

It should be emphasized that an extension of the technique outlined here involves considerable computational labour. In addition, further variational freedom for the Y_n spectrum may necessitate the use of R_{min} rather than the approximate $(\alpha R)_{\text{min}}$.

To summarize this section: All known gross qualitative features of turbulent flow in smooth channels result from an optimization of the dissipation rate subject to the mean stability constraints; a decisive quantitative comparison with the observations is not achieved primarily due to the mathematical difficulties encountered in finding a general solution to the Orr–Sommerfeld equation.

3. CONCLUSION

From a mathematical viewpoint the foregoing analysis is most laborious. The asymptotic solution to the Orr–Sommerfeld equation for a quite general U is described. Only then is U restricted to an optimal form.

However, the stability problem might be considerably simplified if the major restrictions on U imposed by the optimization could be made first. Some slight progress has been made along this line by performing constrained variations of U in the integral stability equations (2.39). This approach offers hope of a more complete understanding of the problem than the maze of formulae employed here permits.

On the physical side this work strongly supports the basic mechanistic assumption. Its validity can be tested by measuring the smallest scales of motion in the transport and energy spectra. Laufer (1950) has made time-spectra studies in channel flow from the boundaries to channel centre. The smallest scale of motion he detected in the energy spectrum was in the middle of the 'laminar' boundary region, and was twice as large as the observed thickness of this region. Since the energy spectrum has twice the maximum wave number of the velocity spectrum, this observation establishes that the minimum ellipticity of the smallest scale of motion is approximately four to one. Equation (2.42) gives a theoretical optimum value of 3·94. A more successful investigation of the detailed stability restrictions on the spectral transfer of energy may one day remove the assumption entirely.

Before leaving the topic of spectra, it should be noted that the spatial spectrum for the transport given by (2.14) differs in kind from the temporal spectra obtained by the experimentalist. In homogeneous turbulence, spatial and temporal spectra would be identical; but in this inhomogeneous and non-isotropic shear flow, the observed spectra are functions of position. The work presented here does not determine the temporal spectra and their spatial dependence, but does provide a framework for such an inquiry.

The apparent achievement of a statistical extreme state by the turbulent fluid raises questions of a different sort than those raised by the mechanistic assumption. It suggests that one observes the most probable of a large set of possible motions: that turbulent solutions to the equations of motion may be highly degenerate. If this is so, what determines the observed spatial and spectral structure of statistical observables, such as $\overline{\mathbf{v}'^2}$, not studied here? One might think that degeneracy implied the equal *a priori* probability of each solution, but the infinite series of higher order small corrections to the usual equations of motion remove degeneracies and couple the macroscopic field of motion to the underlying microscopic particle motion. Hence it is proposed that the probability of occurrence of a degenerate solution is directly proportional to its degree of disorganization, or entropy. The search for a useful measure of the disorganization of irreversible fluid processes involves sufficiently different formal techniques to necessitate separate discussion. However, even the usual thermostatic statistical mechanics suggests that a steady-state system with a fixed number of particles would have maximum 'entropy' when it has a maximum 'temperature' and when all the dynamic variables have, as nearly as possible, normal Gaussian distributions about their mean values. In steady-state shear flow, the mean temperature is a maximum relative to the boundary temperature for a maximum rate of dissipation of potential energy into heat. Yet to achieve this first extreme the mean momentum transport must be highly organized, as studied in this paper. Hence a completely random distribution of either macroscopic or microscopic dynamic variables is not possible. A study of possible secondary extremes for partially constrained macroscopic observables of turbulent shear flow will be presented in another paper.

Finally, it is of interest that the techniques used here are of value in the study of other forms of turbulence. Many of the laminar stability equations developed for geophysical and astrophysical problems can serve as the foundation for determining the gross statistical features of their corresponding turbulent fields. Certain of these stability problems are much easier than the Orr–Sommerfeld problem. In particular this is true of turbulence due to thermal convection. With heat flux replacing momentum transport, mean temperature profile replacing the mean velocity profile, and Rayleigh's equation replacing the Orr–Sommerfeld equation, turbulent convection may be treated just as shear flow was here. Two earlier papers (Malkus 1954) report the initial results of such a study.

The author wishes to thank Dr G. E. R. Deacon, Director of the National Institute of Oceanography, Surrey, and Professor P. A. Sheppard of the Department of Meteorology, Imperial College, London, for their kindness to him during the year in England in which this work was undertaken. He is particularly indebted to Professor C. C. Lin of the Massachusetts Institute of Technology and to Dr G. K. Batchelor of Trinity College, Cambridge, for their comments on the stability problem. This work was performed under the auspices of the Office of Naval Research, and is contribution No. 804 from the Woods Hole Oceanographic Institution.

REFERENCES

BATCHELOR, G. K. 1953 *The Theory of Homogeneous Turbulence.* Cambridge University Press.

GOLDSTEIN, S. (Ed.). 1938 *Modern Developments in Fluid Dynamics*, Vol. 2. Oxford University Press.

HEISENBERG, W. 1924 *Ann. Phys.* **74**, 577–627.

LAUFER, J. 1950 *Nat. Adv. Comm. Aero., Wash.*, no. 2123.

LIN, C. C. 1945–46 *Quart. Appl. Math.* **3**, 117–142, 218–234 & 277–301.

MALKUS, W. V. R. 1954 *Proc. Roy. Soc.* A, **225**, 185–195 & 196–212.

ORR, W. M. F. 1906–7 *Proc. Roy. Irish Acad.* **27**, 9–26, 69–138.

SOMMERFELD, A. 1908 *Proc. 4th Internat. Cong. Math., Rome,* 116–124.

SYNGE, J. L. 1938 *Semicent. Publ. Amer. Math. Soc.* **2**, 227–269.

Contribution No. 805

Reprinted from JOURNAL OF MAMMALOGY
Vol. 37, No. 3, August 1956, pp. 442–443
Printed in U.S.A.

OCEANIC RECORDS OF *LASIONYCTERIS NOCTIVAGANS* AND *LASIURUS BOREALIS*

Since the migration habits and routes of tree bats are poorly known it seems worthwhile to report the following observations made aboard the research vessel *Blue Dolphin* while she was engaged in oceanographic research by the Woods Hole Oceanographic Institution in waters off southern New England in the summer of 1953.

On August 19 at 1100 in 39°36′N, 71°03′W (about 95 miles SSE of Montauk Pt., Long I., the nearest land) a male silver-haired bat, *Lasionycteris noctivagans* (Le Conte), was collected from the rigging of the vessel. The bat had circled the ship several times before coming to rest. The junior author climbed after the bat which left the rigging, flew away a few feet, alighted on the author's back and crawled in between his thighs where it was caught with a dip net.

On August 15 hurricane "Barbara" passed through the area with strong SE, then strong

NW winds off southern New England. Weather Bureau North Atlantic charts show light and variable and 5–10 knot NW winds for the area along southern New England and offshore to the point of our observation during August 16–19.

Another lone bat was sighted on August 25 at 1100 in 39°38′N, 70°19′W (about 90 miles SSE of Montauk Pt.) and captured in the rigging after it made a brief flight around the vessel. This was a male red bat, *Lasiurus borealis* (Müller).

During August 22–24 light and variable winds blew over the area between southern New England and our observation point. On August 25 WNW winds of 5–10 knots prevailed. That both bats had come aboard the vessel while in port (August 17; Woods Hole, Mass.) does not seem probable in view of the fact that both animals were first observed flying over the water.

Griffin (Bul. Mus. Comp. Zool., 76: 217–246, 1940) in his studies of New England bats has carefully summarized the coastal and oceanic records of tree bats. He cites seven records for the red and six for the silver-haired bat with two additional accounts in which the bat was not identified. More recently Carter (Jour. Mamm., 31: 349–350, 1950) reported a red bat 65 miles off the southern New England coast. Except for a report by Merriam (Trans. Roy. Soc. Can., Sect. 4: 85–87, 1887) who includes spring records for both species, all observations at sea are for late August or September.

Joseph Chase provided us with the meteorological information.—JOHN MACKIEWICZ, *Department of Entomology, Cornell University, Ithaca, New York* AND RICHARD H. BACKUS, *Woods Hole Oceanographic Institution, Woods Hole, Massachusetts.* *(Contribution No. 805 of the Woods Hole Oceanographic Institution) Received October 8, 1955.*

Contribution No. 810

A Conductivity Bridge for Measurement of the Salinity of Sea Water[1]

By

Karl E. Schleicher and **Alvin Bradshaw**

Introduction

Among the various methods known for determining salinity of sea water in the laboratory, the KNUDSEN method, based on silver nitrate titration of halides in unknown and standard (Copenhagen) water, has the longest history and has been used the most extensively. Its advantages when compared with many of the other proposed methods have been its combination of relatively high accuracy with speed and simplicity. Around 1922, however, an instrument was built for the U.S. Coast Guard by WENNER *et al.* (WENNER, SMITH, and SOULE, 1930) for determining salinity, which used the conductivity properties of sea water. In this instrument some of the difficulties due to polarization phenomena in conductivity cells and due to bath temperature fluctuations were reduced in importance (1) by introducing a conductivity cell containing sea water in an adjacent arm of the measuring bridge, (2) by making the principle of the determination one in which the conductivity of the sample sea water is compared to that of a standard at the same temperature, and (3) by using a 1000 c.p.s. power source with low distortion. In its present form, this instrument has a precision of better than $\pm 0{\cdot}005\,^0/_{00}$ (BARNES, 1952) in salinity as compared with about $\pm 0{\cdot}02\,^0/_{00}$ (CARRITT, 1952, and ISELIN, 1936) for the KNUDSEN method.

In addition to the advantage of accuracy the Coast Guard instrument is well suited for shipboard use. The difficulties of working with fragile glassware and maintaining the laboratory at constant temperature are not present. Its suitability for use at sea is of great importance, for aside from the obvious advantages of having the salinity data complete at the conclusion of a cruise, the knowledge of salinity obtained shortly after a hydrographic station has been made can be of help in planning future stations and also makes possible the spotting of a faulty Nansen bottle.

---

[1]) Contribution No. 810 from the Woods Hole Oceanographic Institution. This work was carried out under Contract NObsr-43270 with the Bureau of Ships.

For these reasons and others it was considered desirable to build an instrument similar to the Coast Guard instrument for use on the Woods Hole Oceanographic Institution research vessels but to incorporate several improvements which were thought to be needed. Among the suggested improvements were smaller conductivity cells, at least semi-automatic balancing of the bridge and recording of the instrument reading on a chart, and a re-design of the constant-temperature bath. The design of the instrument has also been influenced by the experience of working with the STD (Jacobson, 1948).

Description of Instrument

The functional arrangement of the various component parts is shown in a block diagram (Fig. 1). The conductivity bridge is an AC impedance bridge, powered by a stabilized 1000-cycle oscillator. Arm A of the bridge is connected to any one of five conductivity cells (X or sample cells) which contain unknown samples. Arm B is connected to a sixth conductivity cell (Y cell) which contains sea water around $35\,^0/_{00}$ salinity. Arm C (the components of which are precision resistance decades) is the "standardizing" arm, variable from about 60 ohms to 1171 ohms in steps of 0·01 ohms. Before each reading this arm is set at a value which is determined when the bridge is standardized. Arm D is the "reading" arm made up of precision resistance decades and a potentiometer (appropriately shunted to minimize contact resistance effects) which is operated by a servo-motor. The decade section, variable in 1 ohm steps is set manually to a value within 1 ohm of the final resistance value of the arm for bridge balance. The servo-operated, 2 ohm range, potentiometer section completes the balance and its change in resistance is recorded on a time-driven chart. The total range of arm D is from about 260 ohms to 1370 ohms.

Neither the Wagner ground circuit to eliminate the effect of ground admittances[1]), nor the variable capacitors used to balance out the capacity effects of the cells are shown in Figure 1. That part of the bridge exclusive of the conductivity cells is contained in a steel cabinet set up above the rest of the instrument. The components are mounted so as to minimize hand capacity effects and the cabinet is heated to prevent condensation.

The output of the bridge is amplified and fed to a phase detector where the 1000-cycle signal is converted to direct current. For this purpose the necessary reference signal is taken directly from the output of the oscillator. This reference signal, after being amplified, is used as a gating voltage in a diode phase detector circuit. The output of the phase detector is a DC voltage whose polarity depends upon the direction of unbalance of the bridge and whose magnitude is zero when the bridge is balanced. This DC voltage is fed to a chopper-type servo-amplifier which controls the servo-motor mentioned above. An auxiliary monitoring circuit amplifies the unbalanced bridge output and operates a "magic eye" tuning indicator and earphones to permit checking of the servo-system.

---

[1]) See Harris, F. K., (1952) Electrical Measurements, John Wiley & Sons, Inc., New York, p. 733, for a discussion of the Wagner ground and references.

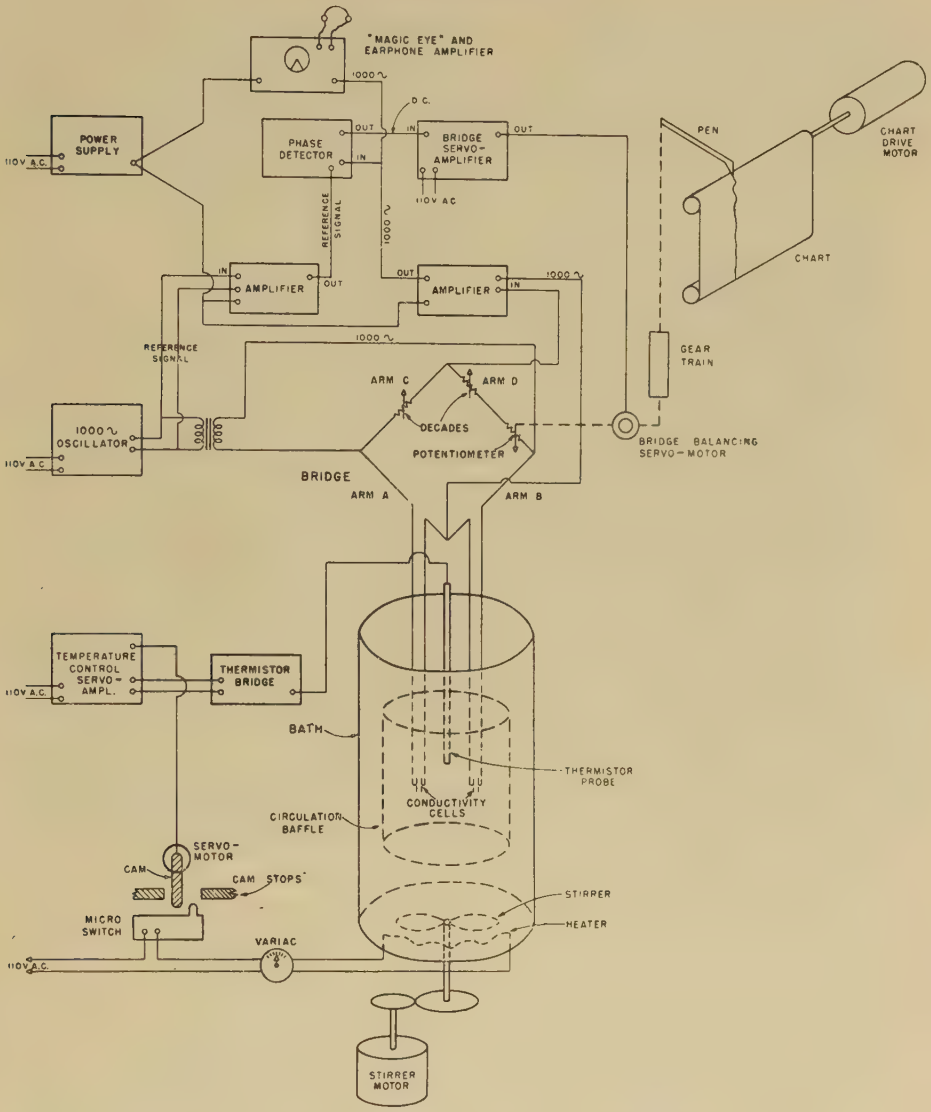
"MAGIC EYE" AND EARPHONE AMPLIFIER
1000 ~
D.C.
POWER SUPPLY
110V A.C.
PHASE DETECTOR
OUT
IN
BRIDGE SERVO-AMPLIFIER
OUT
110V AC
REFERENCE SIGNAL
1000 ~
PEN
CHART DRIVE MOTOR
CHART
IN
AMPLIFIER
OUT
OUT
AMPLIFIER
IN
1000 ~
1000 ~
REFERENCE SIGNAL
GEAR TRAIN
ARM C
ARM D
DECADES
1000 ~ OSCILLATOR
110V A.C.
POTENTIOMETER
BRIDGE BALANCING SERVO-MOTOR
BRIDGE
ARM A
ARM B
TEMPERATURE CONTROL SERVO-AMPL.
110V A.C.
THERMISTOR BRIDGE
BATH
THERMISTOR PROBE
CONDUCTIVITY CELLS
CIRCULATION BAFFLE
SERVO-MOTOR
CAM
CAM STOPS
STIRRER
HEATER
MICRO SWITCH
VARIAC
110V A.C.
STIRRER MOTOR

Figure 1. Schematic diagram, showing the general arrangement.

Since the capacity effects of the conductivity cells are not completely cancelled out by having the two cells in adjacent arms, a variable condenser is used to complete the capacitive balance. However, the phase detector used in this circuit is relatively insensitive to quadrature components and hence eliminates the need for a precise capacitive balance.

The oil bath to keep the conductivity cells at a constant and equal temperature consists of a 7-gallon galvanized steel can filled with light mineral oil. The oil is circulated by means of a stirrer at the bottom of the can and appropriate baffles are provided which cause the oil to flow down the centre of the bath and up the sides. The 500-watt immersion heater is encased in copper tubing and is laid in a circle at the bottom of the can. The cells are mounted on the lucite cover of the bath in a circular pattern and the measuring sections of the cells extend well down into the oil. This arrangement provides for a symmetrical flow of oil past the heater and cells and assures equal temperature distribution throughout the cell area. The temperature of the bath is controlled by a DC thermistor bridge which operates a servo-amplifier and motor. The servomotor actuates a microswitch in the heater circuit and a variac controls the amount of current fed to the heater. By switching in appropriate resistances in one arm of the thermistor bridge the bath can be run at 30° or 38°C. When stabilized the bath holds temperature to within about ± ·005°C.

Figure 2 is a photograph of the type of conductivity cell used. The electrodes are platinum foil fused to the inside of the glass tubing. Contacts are made to the electrodes through the sides of the tube and the leads are connected to plug-in terminals on the lucite cell mounting. The tubing between the cell electrodes is made of ¼-inch ID precision-bore tubing. The cells have a fluid capacity of about 17 cc., an electrical cell constant of about 30 cm.$^{-1}$, and are as physically similar as practicable.

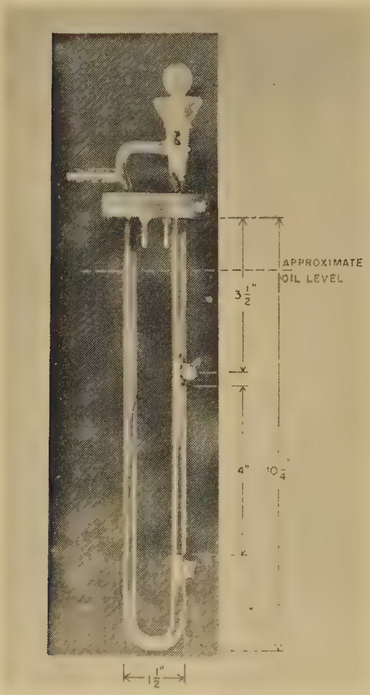

Figure 2. Conductivity cell.

The electrodes of the cell are platinized to reduce the polarization effects. The procedure of platinizing and initial cleaning was the same as given in REILLY and RAE (1944, pp. 433–4). In use, the cells are cleaned every three or four weeks with sulphuric acid and potassium dichromate cleaning solution.

All the controls which are used during routine operation of the instrument are located on the bridge panel and on the main control panel (see Figure 3). The other controls on the phase detector panel are used only for aligning the instrument and for test purposes. The bottle seen to the left of the table is a water trap used in conjunction with a small vacuum pump for emptying the cells. This pump as well as the stirrer motor, oscillator, power supply, and bridge servo-amplifier are located at the rear of the instrument and cannot be seen in this photograph. The instrument is 3 feet wide, 2 feet deep, and 4 feet high. When used in the laboratory the instrument is on casters, and when operated on shipboard shock mounts are used.

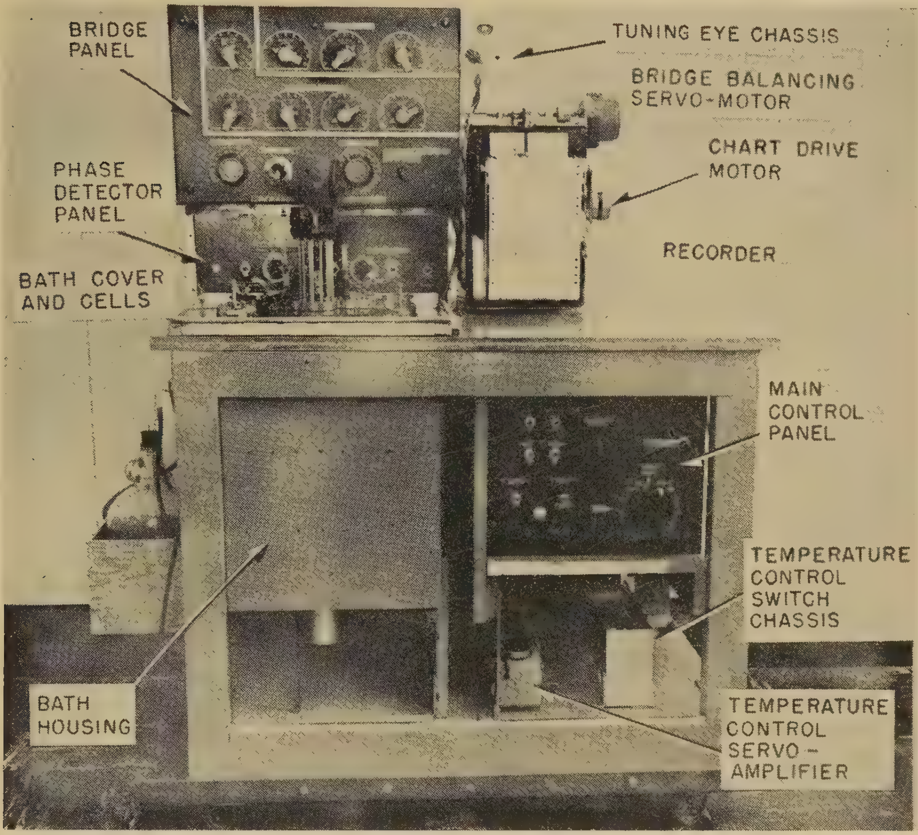
BRIDGE PANEL
TUNING EYE CHASSIS
BRIDGE BALANCING SERVO-MOTOR
CHART DRIVE MOTOR
PHASE DETECTOR PANEL
RECORDER
BATH COVER AND CELLS
MAIN CONTROL PANEL
TEMPERATURE CONTROL SWITCH CHASSIS
BATH HOUSING
TEMPERATURE CONTROL SERVO-AMPLIFIER

Figure 3. Front view of salinometer.

Operation of Instrument

Before salinities can be determined with the salinometer the Y cell is filled with sea water of about 35 $^0/_{00}$ salinity (its exact value need not be known) and the instrument is standardized. To standardize, the five sample cells are filled with Copenhagen standard water and allowed to come to bath temperature. Each cell in turn is connected into the bridge circuit and the standardizing arm adjusted to make the value of the reading arm correspond to the salinity of the standard according to the empirically determined calibration curve.

The salinities of the unknown samples of sea water can now be determined by filling the sample cells with them and allowing the cells to come to temperature equilibrium. These cells are then connected in turn into the bridge circuit and the standardizing arm set, for each cell, at the value determined for that cell by the standardizing process. The value of the reading arm for each resulting balance of the bridge is converted to salinity units by means of the calibration curve. At the end of the run the standard is again measured and the data corrected for any drift of the instrument that may have occurred.

If there are many samples to be measured, for which several days will be required, a substandard water may be used most of the time in place of the Copenhagen water. In this case the standard water is used only for the initial standardization and as an occasional check on the substandard water. The sea water in the Y cell is usually not changed until the cells require cleaning.

Theory

Figure 4 is an idealized representation of the measuring bridge of the salinity instrument, with the constant-temperature bath for conductivity cells not indicated. If the resistances Q and Y are left fixed while sea waters of different salinities are placed in the sample cell and allowed to come to bath temperature, and the bridge balanced each time with the resistance P, a relationship between the reading, P_σ, and the salinity σ of the sea water will be determined. The purpose of the following discussion is to derive a simple approximation to this relationship and to bring out some of the principles involved in this method of measurement. It will be shown that a satisfactory approximation has the form $\sigma = \alpha + \beta P_\sigma + \gamma P_\sigma^2$, where σ is the salinity in $^0/_{00}$ and P_σ the reading in ohms; and that once the reading, P_s, corresponding to the salinity S of the standard has been chosen, the relationship is a unique one, independent of Y and Q.

The Y cell contains sea water of salinity approximately 35 $^0/_{00}$ but otherwise unknown. Its presence in the bridge makes the bridge balance relatively insensitive to bath temperature variation and reduces the amount of parallel capacitance across the P or Q resistance arm required for a null balance. By platinization of the electrodes and by use of low wave-form distortion, 1000 c.p.s. power, the series resistance and capacitive reactance associated with galvanic polarization phenomena in the conductivity cells of the bridge have been reduced sufficiently to permit their neglect in the derivation¹). Also, the cell lead resistances have been found small enough to be neglected. With these things in mind we may represent the bridge as a pure resistance one, in which cell resistances are the resistances of the sea water alone.

Therefore, referring to Figure 4, let

S and σ = the salinity of standard water and the sample water, respectively;
X_s and X_σ = the resistance of the X cell when filled with standard water and the sample water, respectively;

---

1) Much information on the subject of conductivity measurements can be found in a series of papers appearing in the Journal of the American Chemical Society. In particular, two papers of the series that were of special interest and help in connexion with the galvanic polarization phenomenon were:—

JONES, G., and S. M. CHRISTIAN, 1935. "The measurement of the conductance of electrolytes. VI. Galvanic polarization by alternating current." J. Amer. Chem. Soc., 57, pp. 272–280.

JONES, G., and D. M. BOLLINGER, 1935. "The measurement of the conductance of electrolytes. VII. On platinization." Ibid., 57, pp. 280–284.

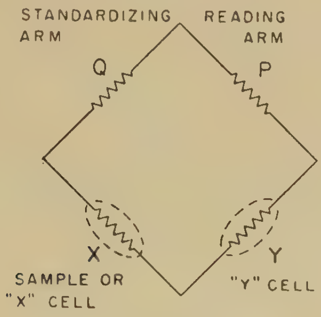

Figure 4. Idealized bridge.

Y = the resistance of the Y cell;
P_s and P_σ = the resistance of the reading arm when $X = X_s$ and $X = X_\sigma$, respectively;
Q = the resistance of the standardizing arm.

The standardization of the bridge against standard water S is made by adjusting Q until the bridge is in balance with $P = P_s$. The bridge relationship for this step is

$$X_s/Q = Y/P_s \tag{1}$$

If the sample cell is then filled with sea water of salinity σ, Q being unchanged, the bridge equation for balance becomes

$$X_\sigma/Q = Y/P_\sigma \tag{2}$$

Combining (1) and (2) we get

$$X_s/X_\sigma = P_\sigma/P_s \tag{3}$$

Since we assume that polarization and cell lead resistances can be neglected, the resistances X_s and X_σ are related to the solution conductivity C_s and C_σ by

$$X_sC_s = K \tag{4a}$$

$$X_\sigma C_\sigma = K \tag{4b}$$

where K is the cell constant of the sample cell.

Substituting equations (4a) and (4b) in (3)

$$C_\sigma/C_s = P_\sigma/P_s \tag{5}$$

With the data of THOMAS, THOMPSON, and UTTERBACK (1934), the salinity versus conductivity isotherm for 25°C. may be represented empirically by the parabola

$$\sigma = a + bC_\sigma + cC_\sigma^2 \tag{6}$$

with an accuracy of $\pm \cdot 002\,^0/_{00}$ in the salinity range of $30\,^0/_{00}$ to $40\,^0/_{00}$.

We assume this is also true for the temperatures of 30°C. and 38°C. at which the bath is operated (but for which no information is available).

Combining (5) and (6), we have

$$\sigma = a + b(C_s/P_s)P_\sigma + c(C_s/P_s)^2 P_\sigma^2 = \alpha + \beta P_\sigma + \gamma P_\sigma^2$$

which is the form of the formula approximating the bridge relationship between salinity and reading. The coefficients in this polynomial are found empirically by calibrating the bridge against samples of known salinity (by the method of least mean square). This result gives the information that the bridge calibration depends only on the bath temperature (C_s, b, c depend on temperature) and the reading P_s, chosen to correspond to the standard sea water of salinity 35 $^0/_{00}$. The temperature dependence, however, turns out to be small, a change in bath temperature from 30 to 38°C. modifying the calibration by less than ·03 $^0/_{00}$ at 30 $^0/_{00}$ and 40 $^0/_{00}$ where the temperature effect is most pronounced.

It can also be seen from the above discussion that the resistance Q of the standardizing arm is a function of the particular X cell and the sea water present in the Y cell, and will have a different value when either of these are changed. For any one combination of them Q will also change slowly with time, due to small changes in the resistance of the Y cell. This drift, however, is not great over a day's time (it varies from ·01 to ·10 ohms, which is at the most equivalent to 0·010 $^0/_{00}$) and can be corrected for by checking the bridge before and after each day's run with standard or sub-standard water.

Precision and Accuracy [1]

The precision of a single measurement for this salinity instrument has two components; (1) the precision of a single measurement for a particular standardization of the bridge, and (2) the precision of standardizing the bridge. A value for component (1) which would include the effects of flushing was obtained from a series of 50 readings, all made for a particular standardization, on sea waters of salinities ca. 35 $^0/_{00}$ and 36·5 $^0/_{00}$, alternating in sets of 5 between the two sea waters. The greatest deviations from the average and standard deviation of the 35 $^0/_{00}$ readings were 0·003 $^0/_{00}$ and 0·001 $^0/_{00}$, respectively, while the corresponding parameters in the case of 36·5 $^0/_{00}$ were 0·004 $^0/_{00}$ and 0·002 $^0/_{00}$. The largest deviation from the average found above gives a value for component (1) of ± 0·004 $^0/_{00}$. Because components (1) and (2) are equal, the precision of a single measurement was taken as ± 0·008 $^0/_{00}$ (with standard deviation $\sqrt{2} \times 0{\cdot}002 = 0{\cdot}003\,^0/_{00}$).

The accuracy of the salinometer, besides depending on the precision, is also a function of the accuracy of the salinities of the calibration samples, linearity errors in the bridge reading arms, the variation of the chlorinity-conductivity relationship at a fixed temperature in the oceans, and the accuracy of the standard water. An estimate of the accuracy of this instrument for a single measurement based on all these factors except the last two comes out to be ± ·01 $^0/_{00}$, or better, at 35 $^0/_{00}$ salinity, with a linear decrease to ± ·03 $^0/_{00}$, or better, at 30 $^0/_{00}$ and 40 $^0/_{00}$. The above accuracy figure for 30 $^0/_{00}$ and 40 $^0/_{00}$ (and thus the accuracy either side of 35 $^0/_{00}$) is subject to possible improvement by a recalibration based on independent salinity determinations which are of higher accuracy than was available for the present calibration.

---

[1]) As used here, precision means ± the maximum deviation from the *average* value; accuracy means ± the maximum deviation from the *true* value.

Copenhagen normal water has been used as the salinity standard but any other sea-water standard of about 35 $^0/_{00}$ in salinity may be used. In either case, on the assumption that the conductivity-salinity relationship in the oceans is fixed, the above accuracy limits are relative to the accuracy of the standard used. KNUDSEN (1925) does not recommend the use of Copenhagen normal water as a salinity standard in conductivity measurements because of the solution of glass from the walls of the containing ampule over long periods of time. The authors have not been able to find in the literature any estimate of magnitude of the effect of this process on the conductivity of Copenhagen water, although there has been some investigation of, and discussion on, the effect on chlorinity and density (GIRAL, 1926; MATTHEWS, 1926; DEACON, 1933; and KING, 1950).

In an attempt to get some information on the changes of conductivity with time, the authors measured the salinity (with the salinometer) of several ampules of P_{15} (bottled in 1937) after the bridge had been standardized against P_{21} (bottled in 1953). These results were that the conductivity of the P_{15} water was equivalent to that of water of about ·006 $^0/_{00}$ in salinity below the salinity calculated from the chlorinity value stated on the label. On the assumption that the glass in each case dissolves at the same constant rate, the results would indicate that the error involved in using Copenhagen water that is 3 or 4 years old is relatively small. It can also be mentioned that the determinations on deep ocean water made with the salinometer during hydrographic cruises agree to about ± 0·01 $^0/_{00}$ with the averages of values for the same areas found previously by KNUDSEN titration (compare Figure 5 of this report with Figure 25 of ISELIN, 1936).

Because of these considerations, the use of Copenhagen water seems justified until such time as a more suitable standard for conductivity measurements becomes available.

The balancing mechanism of the instrument will register a change in resistance in an arm of the bridge of less than 0·01 ohms. The reading on the chart can be estimated to 0·01 ohms, which is equivalent to a change in salinity in the "X" cell of about ·0008 $^0/_{00}$ at midscale of the calibration curve. The overall sensitivity of the instrument, therefore, is about ·001 $^0/_{00}$ in salinity, and the measurements obtained are accordingly reported to the third decimal place.

Results of Field Tests

The salinometer has been used on a two months cruise in the Sargasso and Caribbean Seas, during which about 850 salinity samples were measured, a two months cruise in northern waters, during which 450 samples were measured, and a one month cruise in waters west of Bermuda, during which 1358 samples were measured. During these cruises the instrument proved

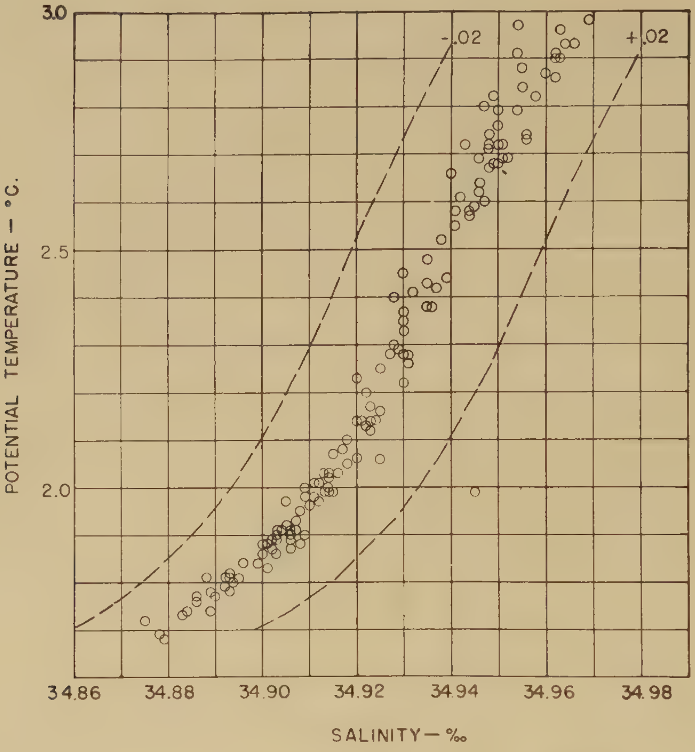

Figure 5. ϑ/S curve in deep water west of Bermuda. Salinity values obtained with salinometer.

to be seaworthy and unaffected by the rolling, pitching, or vibration of the ship, or the normal frequency and voltage variations of the ship's generator used as power supply.

Although routine measurements were made throughout the cruises some of the techniques associated with the operation of the instrument were improved. Most of these techniques had to do with the handling of the samples before analysis and the filling of the cells; both processes were found to influence greatly the precision of the results. It was found that the samples could be comfortably analysed at the rate of 20 measurements in one hour.

In order to obtain the full advantage of this type of instrument on a hydrographic cruise it may often be desirable to analyse the samples immediately after they are obtained. This would allow the oceanographer to make decisions as to bottle spacing, locations, etc., of the next station so as to obtain the greatest benefit from the cruise. From the experience gained on these first cruises it was found that the greatest factor affecting the time span between sample gathering and analysis was the need to warm the cold samples to room temperature before putting them in the cells, for otherwise the excess dissolved gases released as the sample water warmed up formed small bubbles in the cell, which caused errors. Since immediate results were not required on the cruises this difficulty was easily overcome by allowing the samples to stand in a warm place for 12 to 24 hours before analysis. Any future instrument of this kind should perhaps be supplied with a refrigerated bath so that the samples could be analysed at a lower temperature, without the necessity for this prewarming.

On these past cruises all final salinity values were determined before the ships docked. During the second cruise, spot checks were made by filling more than one cell with the same sample at the time the sample bottle was first opened. There were 65 checks made in this way and in all cases the salinity values obtained from each of these checks differed by no more than 0·01 $^0/_{00}$, the great majority (90%) differing by 0·005 $^0/_{00}$ or less. These results agree favourably with the values obtained by earlier determinations of precision made in the laboratory and already referred to.

Some of the data from the third cruise are presented in Figure 5. This figure shows the ϑ/S correlation in the deep waters (below about 2500 metres) west of Bermuda. At these depths great variations from the average ϑ/S correlation curve are not expected. The band formed by the dotted lines on either side of the points represents a total salinity spread of 0·04 $^0/_{00}$, the narrowest spread one might expect from titration.

The curve represents all the data (taken below a potential temperature of 3·0°C.) of 33 different stations. The stations were made over a period of 21 days and the salinity determination for each station made within about 24 hours of gathering the samples.

The cruises so far made have shown the practicality and general seaworthiness of the present instrument. As mentioned earlier, it seems likely that a new calibration, based on more accurate, independently determined, salinity points would improve its accuracy, particularly at the extremes of its calibrated range. Also, there are several improvements which could be incorporated in a future design which would increase the instruments versatility and ease of operation. However, it is felt that the instrument as it now stands satisfies a need for a quick and accurate method of measuring salinity on shipboard and, as such, should be useful in this phase of oceanographic work.

Acknowledgements

The authors wish to thank the various personnel of the Woods Hole Oceanographic Institution who with their advice and help contributed much towards the construction of this instrument. Special thanks are due to Mr. Allyn C. VINE, whose overall direction was most helpful, especially in formulating the requirements of the instrument as a useful sea-going tool, and to Mr. Floyd SOULE for the many discussions with him on the Coast Guard unit; to Dr. John KANWISHER for the design of the phase detector; to Mr. Paul BENNETT for help with the electronics involved; and to Mr. Valentine WORTHINGTON for his encouragement and enthusiasm, and his endeavours to use the instrument to its fullest capabilities.

Summary

A new sea-going conductivity bridge (salinometer) for measuring the salinity of sea water is described. In principle, the salinity of an unknown sample is determined by comparing its conductivity with that of a sample of known salinity at the same temperature. The calibration of the bridge is found empirically.

The instrument consists of a constant-temperature bath, a 1000-cycle impedance bridge with glass conductivity cells in two of its arms, a phase detector to convert the 1000 cycles output of the bridge to DC, and a balancing mechanism to complete automatically the "fine" adjustment in bridge balance. It operates from a 110 v. 60-cycle power source.

References

BARNES, C. A., 1952. Discussion in "Oceanographic instrumentation". Publ. Nat. Res. Counc., 309, p. 187.

CARRITT, D. E., 1952. "Chemical measurements". In "Oceanographic instrumentation". Publ. Nat. Res. Counc., 309, pp. 166–186.

DEACON, G. E. R., 1933. "An examination of 'eau de mer normale P13, 28–VI–1929" Journ. du Cons., **8**, 1, pp. 59–63.

GIRAL, J., 1926. "Quelques observations sur l'emploi de l'eau normale en océanographie". Cons. Internat. Explor. Mer, Publ. de Circ., 90, pp. 1–22.

ISELIN, C. O'D., 1936. "Study of the circulation of the North Atlantic". Pap. Phys. Oceanogr. Meteorol., **4**, 4, p. 6.

JACOBSON, A. W., 1948. "An instrument for recording continuously the salinity, temperature, and depth of sea water". Trans. American Inst. Elec. Eng., **67**, 1, pp. 714–722.

KING, J., 1950. "Some notes on the determination of the chlorinity by comparison with the international standard". Journ. du Cons., **16**, 2, pp. 167–174.

KNUDSEN, M., 1925. "L'emploi de l'eau normale dans l'océanographie". Cons. Internat. Explor. Mer, Publ. de Circ., 87, pp. 1–11.

MATTHEWS, D. J., 1926. A review of "Quelques observations sur l'emploi de l'eau normale en océanographie" by J. GIRAL. Journ. du Cons., **1**, 3, pp. 284–286.

REILLY, J., and W. N. RAE, 1944. "Physico-Chemical Methods". **2**, D. Van Nostrand Comp. Inc., New York.

THOMAS, B. D., with T. G. THOMPSON and C. L. UTTERBACK, 1934. "The electrical conductivity of sea water". Journ. du Cons., **9**, 1, pp. 28–35.

WENNER, F., E. H. SMITH, and F. M. SOULE, 1930. "Apparatus for the determination aboard ship of the salinity of sea water by the electrical conductivity method". Journ. Res. U.S. Bur. Standards, 5, pp. 711–732.

Contribution No. 811

Särtryck ur Tellus nr 3, 1956

On the Wind-Driven Ocean Circulation[1]

By G. W. MORGAN, Brown University, Providence

(Manuscript received February 8, revised June 5, 1956)

Abstract

Some aspects of existing theories of the wind-driven ocean circulation are examined with particular emphasis on the question of the need for the inclusion of lateral eddy viscosity to provide a mechanism for balancing the applied wind torque. A new model is proposed according to which the ocean is divided into a southern and a northern portion, attention being restricted to the former which is itself subdivided into an interior region and a boundary region adjacent to the western shore. The equations of motion in terms of spherical coordinates are formally integrated over depth for both a homogeneous and a two-layer ocean. Approximate equations analogous to those used in existing theories are proposed for the interior region. Conditions in the boundary region are considered in an effort to determine the relative importance of the various terms in the equations. Based on these considerations approximate equations are derived for the boundary region. These imply the predominance of the pressure terms, the nonlinear inertia terms and the terms arising from the variation of the Coriolis parameter with latitude.

The approximate equations are transformed to surface coordinates and are applied to the homogeneous ocean and a two-layer ocean subjected to a simple wind distribution, yielding reasonable results. It is shown that the variation of the Coriolis parameter plays a fundamental role in the formation of the stream on the western shore. Simple physical interpretations of the results are presented including an explanation of the facts that no similar stream can be formed on the eastern shore and that the variation of depth in a two-layer ocean, when the Coriolis parameter is assumed constant, cannot give rise to an intense stream. Appropriate curves illustrating the dependence of the solutions on certain dimensionless parameters are given. When applied to the North Atlantic the theory gives reasonable results for the Gulf Stream north to, say, Cape Hatteras.

1. Introduction

Existing theories of the wind-driven circulation in closed ocean basins (SVERDRUP, 1947; MUNK, 1950) are based on the assumption that the principal features of the flow pattern are the result of the balance between wind, Coriolis, lateral friction and pressure forces and that all other contributions to the dynamic equations are, for purposes of an approximate investigation, negligible. This assumption leads to a linear problem, an approximate solution of which is obtained most conveniently by applying boundary layer analysis to the vorticity equation (MUNK and CARRIER, 1950). Although the circulation which is predicted is, at least qualitatively, very reasonable, the theory has been criticized especially on the grounds that the value of the coefficient of lateral eddy viscosity must be chosen empirically, and further, that the value which gives the proper width to the intense current on the western shore is considerably larger than that indicated by other, independent considerations.

In the following, other aspects of the above-mentioned theories are considered and attention is devoted to the question of the importance of the lateral eddy viscosity. It has previously been argued that this must be included in every steady-state theory because it provides the forces of friction on the sides of the basin which give rise to the torque that must be present to balance the total torque exerted on the ocean by the wind. This problem is discussed in Section 2 where an equation for the balance of total moment of momentum about the center of mass of the ocean is derived and it is seen that this consideration alone is not sufficient to determine whether friction is required in the moment balance.

---

[1] Contribution No. 811 from the Woods Hole Oceanographic Institution.

In Section 3 the equation of vorticity in terms of spherical coordinates is formally integrated over the depth of a layer of water which is considered to have uniform density (either the total ocean depth, if one deals with a homogeneous model, or the depth of the upper layer in a two-layer model). Approximate equations which apply to the interior region of the ocean and stipulate the predominance of wind, Coriolis, and pressure forces are derived in Section 4. In Section 5 the conditions in the boundary region in which an intense current is expected are discussed and we return to the problem of the need for including lateral eddy viscosity. Based on this discussion a model is proposed according to which the ocean is divided into a southern and a northern region. Attention is confined to the former which is again divided into an interior region, to which the equations derived in Section 4 apply, and a boundary region, adjacent to the western shore, for which approximate equations are derived by means of boundary layer analysis. These imply the predominance of the pressure terms, the non-linear inertia terms, and the terms arising from the variation of the Coriolis parameter with latitude, friction being neglected.[1]

The approximate equations are transformed to surface coordinates in Section 6 and are applied to a homogeneous ocean in Section 7. The theory predicts an intense current flowing northward along the western shore. The reason for the existence of this current from a physical point of view is discussed and it is shown why no similar current can exist on the eastern shore.

In Section 8 the theory is applied to the upper layer of a two-layer ocean. The role of a certain parameter involving the depth of the layer, the magnitude of the westward volume transport into the boundary region, the south-north dimension of the basin, the reduced gravity constant, and the variation of the Coriolis parameter with latitude, is studied. A proof is given that the variation of the Coriolis parameter is essential to the formation of an intense current even in a two-layer system. Numerical solutions are presented and it is concluded that, for reasonable values of the physical quantities involved, the barotropic and baroclinic models are not basically different as far as the formation of the stream is concerned. When applied to the North Atlantic the theory predicts the correct order of magnitude for the width of the Gulf Stream.

2. Moment of Momentum Balance

It has frequently been asserted (e.g. MONTGOMERY, 1940) that, for steady-state conditions, friction must be present on the bounding surfaces of the basin to provide the torque required to balance the total torque applied by the wind. Since it has been held reasonable to assume that the friction on the bottom is negligible, this argument has led to the conclusion that lateral eddy viscosity must be included in the equations of motion in order to give rise to a shear stress on the sides of the basin. In view of the obvious importance of this question, it will be examined in the following. The physical quantity of interest is the total moment of momentum about the center of mass, the momentum referring to the velocity recorder by an observer who is fixed to the earth. For steady-state conditions this moment must be constant.

The equation of motion is

$$\varrho \frac{Dq}{Dt} + \varrho 2 \boldsymbol{\Omega} \times \boldsymbol{q} + \varrho \boldsymbol{\Omega} \times (\boldsymbol{\Omega} \times \boldsymbol{r}) = - \nabla p + \varrho \nabla \chi' + \boldsymbol{F} \qquad (2.1)$$

where q is the velocity of a particle as seen by an observer fixed to the earth, D/Dt is the material derivative, ϱ is the density (not necessarily uniform), $\boldsymbol{\Omega}$ is the earth's angular rotation vector, $\boldsymbol{r}$ is the position vector of the particle with respect to the center of the earth and with respect to a coordinate system which rotates with the earth, p is the pressure, χ' is the gravitational potential, and $\boldsymbol{F}$ is the net force on a unit volume due to eddy viscosity and can be written $\nabla \cdot \sigma$ where σ denotes the stress dyad minus the contribution of the pressure p.

---

[1] The probability that viscosity is unimportant in the Gulf Stream was suggested by H. Stommel in a discussion following formal papers delivered at the June 1954 Convocation at Woods Hole (the complete proceedings of which are to be published as a supplement to the Journal of Marine Research, Vol. 14, No. 4, Dec. 31, 1955), and in a privately printed pamphlet entitled "Why do our ideas about the ocean circulation have such a peculiarly dream-like quality?", April 1954.

The equation of conservation of mass is

$$\frac{\partial \varrho}{\partial t} + \operatorname{div} \varrho \boldsymbol{q} = 0. \tag{2.2}$$

Set

$$\begin{aligned} &\nabla \chi' - \boldsymbol{\Omega} \times (\boldsymbol{\Omega} \times \boldsymbol{r}) \\ &= \nabla \chi' - \nabla \left(\frac{1}{2} \Omega^2 \tilde{\omega}^2 \right) \equiv \nabla \chi \end{aligned} \tag{2.3}$$

where $\tilde{\omega}$ is the perpendicular distance of a point from the axis of rotation of the earth, Ω is the absolute value of $\boldsymbol{\Omega}$ and χ is the apparent gravitational potential. Carrying out the vector multiplication of the resulting equation with $\boldsymbol{r}_c$, the position vector of a point with respect to the center of mass, and integrating over the total volume of the ocean, one has

$$\begin{aligned} &\int_V \varrho \boldsymbol{r}_c \times \frac{D\boldsymbol{q}}{Dt} dV + \int_V \varrho \boldsymbol{r}_c \times (2\boldsymbol{\Omega} \times \boldsymbol{q})\, dV = \\ &- \int_V \boldsymbol{r}_c \times \nabla p dV + \int_V \varrho \boldsymbol{r}_c \times \nabla \chi dV + \int_V \boldsymbol{r}_c \times \nabla \sigma \cdot dV \end{aligned} \tag{2.4}$$

This equation can be transformed by making use of equation (2.2), the relations

$$\frac{D\boldsymbol{r}}{Dt} = \boldsymbol{q},$$

$$\int_V \varrho \frac{D\varphi}{Dt} dV = \frac{D}{Dt} \int_V \varrho \varphi dV, \tag{2.5}$$

φ being any arbitrary continuous function with continuous first derivatives, and the transformation formulae relating volume and surface integrals, to give

$$\begin{aligned} &\frac{D}{Dt} \int_V \boldsymbol{r}_c + \varrho \boldsymbol{q} dV + \int_V \boldsymbol{r}_c \times \varrho\, (2\, \boldsymbol{\Omega} \times \boldsymbol{q}) dV = \\ &\int_V \varrho \boldsymbol{r}_c \times \nabla \chi dV - \int_S \boldsymbol{r}_c \times \boldsymbol{n} p dS + \int_S \boldsymbol{r}_c \times \boldsymbol{T} dS \end{aligned} \tag{2.6}$$

where S is the surface enclosing the volume V, $\boldsymbol{n}$ is the unit outer normal vector on S, and $\boldsymbol{T} \equiv \boldsymbol{n} \cdot \sigma$ and denotes that portion of the surface traction which is due to the frictional mechanism. It should be noted that equation (2.6) holds irrespective of the particular nature of the eddy viscosity (or molecular viscosity), the only additional requirement for its derivation being the symmetry of the stress dyad.

The left-hand side of equation (2.6) represents the rate of change of moment of momentum and consists of the rate of change as seen by an observer fixed to the earth and the contribution by the Coriolis forces. The right-hand side represents the moment of all external forces, the gravitational attraction, the pressure on the surfaces and the forces arising from viscosity. The last integral may be split into two portions, one involving integration over the free surface and thus representing the moment due to the wind, the other involving integration over the ocean bottom and sides. The contribution of the pressures to the moment is principally due to the fact that the free surface is disturbed by the motion and that the moments due to the pressures on the sides will then not, in general, add to zero. If one deals with a circular basin having a vertical shore and uniform depth, then the moment due to the pressures acting on the shore will be very small because the center of mass will be very close to the geometrical center.

For a steady-state solution the first term on the left of equation (2.6) must vanish. The contribution of the body force to the moment is negligible. Thus the moment balance involves the contributions of the Coriolis force, the pressure, the wind, and the friction on the shores and bottom, and it is seen that no immediate conclusion can be drawn from this consideration alone concerning the need for including friction on the sides, even if friction on the bottom is neglected from the start. The moment created by the wind may possibly be balanced by the Coriolis and pressure moments, or by the former alone if the basin is circular.

The preceding considerations in no way prove that lateral friction is not required; they only demonstrate that the question cannot be decided on the basis of moment balance alone. The problem will be discussed from a different point of view in Section 5.

3. Equations of Motion in Spherical Coordinates

Since an analytical investigation of the three-dimensional problem is prohibitively complicated, we follow the usual procedure of confining our attention to the integrals over depth of the velocity components and of the vorticity.

Using the spherical coordinates (r, ϑ, φ), the origin being at the center of the earth and ϑ being the colatitude, and corresponding velocity components q_1, q_2, q_3, the momentum equations are

$$\frac{\partial q_1}{\partial t} + \text{non linear terms} - 2\,q_3 \Omega \sin\vartheta = $$
$$= -\frac{1}{\varrho}\frac{\partial p}{\partial r} - g + F_1 \qquad (3.1)$$

$$\frac{\partial q_2}{\partial t} + q_1 \frac{\partial q_2}{\partial r} + \frac{q_2}{r}\frac{\partial q_2}{\partial \vartheta} + \frac{q_3}{r\sin\vartheta}\frac{\partial q_2}{\partial \varphi} + \frac{q_1 q_2}{r} -$$
$$-\frac{q_3^{\,2}\cot\vartheta}{r} - 2\,q_3\Omega\cos\vartheta = -\frac{1}{\varrho}\frac{1}{r}\frac{\partial p}{\partial \vartheta} + F_2$$
$$(3.2)$$

$$\frac{\partial q_3}{\partial t} + q_1 \frac{\partial q_3}{\partial r} + \frac{q_2}{r}\frac{\partial q_3}{\partial \vartheta} + \frac{q_3}{r\sin\vartheta}\frac{\partial q_3}{\partial \varphi} + \frac{q_1 q_3}{r} +$$
$$+\frac{q_2 q_3}{r}\cot\vartheta + 2 q_2 \Omega\cos\vartheta + 2 q_1 \Omega \sin\vartheta =$$
$$= -\frac{1}{\varrho}\frac{1}{r\sin\vartheta}\frac{\partial p}{\partial \varphi} + F_3 \qquad (3.3)$$

Here (F_1, F_2, F_3) denote the contributions of the eddy viscosity, g denotes the gravitational acceleration, and the centrifugal force terms which give rise to the ellipticity of the undisturbed free surface of the ocean have been neglected.

We shall make either of two assumptions concerning the distribution of density; a) we consider the "homogeneous" ocean which has uniform density everywhere and is subsequently assumed to be of uniform depth when undisturbed; b) we consider a "two-layer" ocean which consists of two superposed layers each of uniform density. In the latter case we shall be concerned only with the motion in the upper, lighter layer, and the equations of motion refer to that layer alone. Hence, in both cases, the equation expressing the conservation of mass is that for an incompressible fluid:

$$\frac{\partial}{\partial r}(r^2 \sin\vartheta\, q_1) + \frac{\partial}{\partial \vartheta}(r\sin\vartheta\, q_2) + \frac{\partial}{\partial \varphi}(r q_3) = 0 \qquad (3.4)$$

The radial component of vorticity is

$$\zeta_1 = (\operatorname{curl} \boldsymbol{q})_1 =$$
$$= \frac{1}{r^2\sin\vartheta}\left[\frac{\partial}{\partial \vartheta}(r\sin\vartheta\, q_3) - \frac{\partial}{\partial \varphi}(r q_2)\right] \qquad (3.5)$$

The first component equation of the vorticity equation is obtained by performing the operation appearing on the right side of (3.5) on equations (3.3) and (3.2) in the place of q_3 and q_2, respectively, and making use of equation (3.4):

$$\frac{\partial \zeta_1}{\partial t} + q_1\frac{\partial \zeta_1}{\partial r} + \frac{q_2}{r}\frac{\partial \zeta_1}{\partial \vartheta} + \frac{q_3}{r\sin\vartheta}\frac{\partial \zeta_1}{\partial \varphi} +$$
$$+\frac{1}{r}\frac{\partial q_1}{\partial \vartheta}\frac{\partial q_3}{\partial r} + \frac{1}{r^2}\frac{\partial q_1}{\partial \vartheta} q_3 - \frac{1}{r\sin\vartheta}\frac{\partial q_1}{\partial \varphi}\frac{\partial q_2}{\partial r} -$$
$$-\frac{1}{r^2\sin\vartheta}\frac{\partial q_1}{\partial \varphi} q_2 + \frac{2}{r} q_1 \zeta_1 -$$
$$-\frac{\zeta_1}{r^2 \sin\vartheta}\frac{\partial}{\partial r}(r^2\sin\vartheta\, q_1) + \frac{4}{r}\Omega\cos\vartheta\, q_1 -$$
$$-\frac{2}{r^2}\Omega\cot\vartheta\frac{\partial}{\partial r}(r^2\sin\vartheta\, q_1) +$$
$$+\frac{2}{r}\Omega\sin\vartheta\frac{\partial q_1}{\partial \vartheta} - \frac{2}{r}\Omega\sin\vartheta\, q_2 =$$
$$= \frac{1}{r^2\sin\vartheta}\left[\frac{\partial}{\partial \vartheta}(r\sin\vartheta\, F_3) - \frac{\partial}{\partial \varphi}(r F_2)\right] \qquad (3.6)$$

The rate of change of the first component of vorticity as we follow a particle is

$$\frac{D\zeta_1}{Dt} = \frac{\partial \zeta_1}{\partial t} + q_1\frac{\partial \zeta_1}{\partial r} + \frac{q_2}{r}\frac{\partial \zeta_1}{\partial \vartheta} + \frac{q_3}{r\sin\vartheta}\frac{\partial \zeta_1}{\partial \varphi} \qquad (3.7)$$

Note that this is not the same as the first component of $D\boldsymbol{\zeta}/Dt$, $\boldsymbol{\zeta}$ being the vorticity vector. We shall find it convenient to focus our attention on that portion of the rate of change of ζ_1 which is associated with the particle's horizontal motion only and therefore define

$$\frac{d}{dt} \equiv \frac{\partial}{\partial t} + \frac{q_2}{r}\frac{\partial}{\partial \vartheta} + \frac{q_3}{r\sin\vartheta}\frac{\partial}{\partial \varphi} \qquad (3.8)$$

We now integrate equation (3.6) over the depth of the total ocean in case a) and over the upper layer in case b). In both cases the limits can be written $r = h_b(\vartheta, \varphi, t)$ on the bottom and $r = h_s(\vartheta, \varphi, t)$ on the free surface with h_b being constant in case a). Letting

$$f = 2\Omega \cos \vartheta \tag{3.9}$$

and making use of (3.8) one obtains, after some manipulation

$$\begin{aligned} &\int_{h_b}^{h_s} \frac{d\zeta_1}{dt}\, dr - (q_1\zeta_1)\Big|_{h_b}^{h_s} + 2\int_{h_b}^{h_s} q_1 \frac{\partial \zeta_1}{\partial r}\, dr + \\ &+ \int_{h_b}^{h_s} \left(\frac{1}{r}\frac{\partial q_1}{\partial \vartheta}\frac{\partial q_3}{\partial r} + \frac{1}{r^2}\frac{\partial q_1}{\partial \vartheta} q_3 - \frac{1}{r \sin \vartheta}\frac{\partial q_1}{\partial \varphi}\frac{\partial q_2}{\partial r} - \right. \\ &\left. - \frac{1}{r^2 \sin \vartheta}\frac{\partial q_1}{\partial \varphi} q_2 \right) dr + \int_{h_b}^{h_s} \frac{df}{dt}\, dr - (q_1 f)\Big|_{h_b}^{h_s} + \\ &+ 2\Omega \sin \vartheta \int_{h_b}^{h_s} \frac{1}{r}\frac{\partial q_1}{\partial \vartheta}\, dr = \\ &= \frac{1}{\sin \vartheta} \int_{h_b}^{h_s} \frac{1}{r^2}\left[\frac{\partial}{\partial \vartheta}(r \sin \vartheta F_3) - \frac{\partial}{\partial \varphi}(r F_2) \right] dr \end{aligned} \tag{3.10}$$

where the symbol $(\ )\Big|_{h_b}^{h_s}$ stands for $(\ )_{r=h_s} - (\ )_{r=h_b}$.

We now evaluate the frictional terms in (3.10). Let

$$F_i = \frac{1}{\varrho}\frac{1}{r^2}\frac{\partial}{\partial r}\left(A_r r^2 \frac{\partial q_i}{\partial r} \right) + F_i^*, \quad i = 2, 3 \tag{3.11}$$

where A_r denotes the radial eddy viscosity and F_2^*, F_3^* are used for the sake of brevity to represent the contributions due to the coefficient of lateral eddy viscosity A_L the magnitude of which is so far arbitrary. Assuming that A_r is independent of ϑ and φ and neglecting the variation of r within the range of the integration, one obtains for the right side of equation (3.10)

$$\begin{aligned} &\frac{1}{\varrho}\frac{\cot \vartheta}{r}\left(A_r \frac{\partial q_3}{\partial r} \right)\Big|_{h_b}^{h_s} + \frac{1}{\varrho}\frac{1}{r}\left(A_r \frac{\partial^2 q_3}{\partial r\, \partial \vartheta} \right)\Big|_{h_b}^{h_s} - \\ &- \frac{1}{\varrho}\frac{1}{r \sin \vartheta}\left(A_r \frac{\partial^2 q_2}{\partial r\, \partial \varphi} \right)\Big|_{h_b}^{h_s} + \\ &+ \frac{1}{\sin \vartheta}\int_{h_b}^{h_s} \frac{1}{r^2}\left[\frac{\partial}{\partial \vartheta}(r \sin \vartheta F_3^*) - \frac{\partial}{\partial \varphi}(r F_2^*) \right] dr \end{aligned} \tag{3.12}$$

The pertinent components of shear stress are

$$\begin{aligned} \tau_{r\vartheta} &= A_r \left(\frac{1}{r}\frac{\partial q_1}{\partial \vartheta} - \frac{q_2}{r} + \frac{\partial q_2}{\partial r} \right) \\ \tau_{r\varphi} &= A_r \left(\frac{1}{r \sin \vartheta}\frac{\partial q_1}{\partial \varphi} - \frac{q_3}{r} + \frac{\partial q_3}{\partial r} \right) \end{aligned} \tag{3.13}$$

Since the depth of the ocean is much smaller than the radius of the earth, only the last term in each of the brackets in equation (3.13) is important. Expression (3.12) can then be written[1]

$$\begin{aligned} &\frac{1}{\varrho}\left\{ \frac{1}{r}\frac{\partial}{\partial \vartheta}\left(\tau_{r\varphi}\Big|_{h_b}^{h_s} \right) + \frac{\cot \vartheta}{r}\left(\tau_{r\varphi}\Big|_{h_b}^{h_s} \right) - \right. \\ &- \frac{1}{r \sin \vartheta}\frac{\partial}{\partial \varphi}\left(\tau_{r\vartheta}\Big|_{h_b}^{h_s} \right) - \\ &- \frac{1}{r}\left(\left[\frac{\partial}{\partial r}\left(A_r \frac{\partial q_3}{\partial r} \right) \right] \frac{\partial h}{\partial \vartheta} \right)\Big|_{h_b}^{h_s} + \\ &\left. + \frac{1}{r \sin \vartheta}\left(\left[\frac{\partial}{\partial r}\left(A_r \frac{\partial q_2}{\partial r} \right) \right] \frac{\partial h}{\partial \varphi} \right)\Big|_{h_b}^{h_s} \right\} + \\ &+ \frac{1}{\sin \vartheta}\int_{h_b}^{h_s} \frac{1}{r^2}\left[\frac{\partial}{\partial \vartheta}(r \sin \vartheta F_3^*) - \frac{\partial}{\partial \varphi}(r F_2^*) \right] dr \end{aligned} \tag{3.14}$$

where $\left([\ ] \dfrac{\partial h}{\partial \vartheta} \right)\Big|_{h_b}^{h_s}$ is an abbriviation for

$[\ ]_{r=h_s} \dfrac{\partial h_s}{\partial \vartheta} - [\ ]_{r=h_b} \dfrac{\partial h_b}{\partial \vartheta}$ and $\dfrac{\partial}{\partial \vartheta}\left(\tau_{r\varphi}\Big|_{h_b}^{h_s} \right)$

$= \dfrac{\partial}{\partial \vartheta}\left[\tau_{r\varphi}(h_s, \vartheta, \varphi, t) - \tau_{r\varphi}(h_b, \vartheta, \varphi, t) \right]$.

---

[1] For details see: G. W. MORGAN; On the integration over depth of the equations for the wind-driven ocean circulation; Reference No. 54 – 89; unpublished manuscript of the Woods Hole Oceanographic Institution, December 1954.

Note that the three terms containing the shear stresses are approximately $\frac{1}{\varrho}(\text{curl }\tau)_1\Big|_{h_b}^{h_s}$, where τ is the shear stress vector on the surfaces h_s or h_b. The additional surface terms arise from the fact that

$$\left(\frac{\partial}{\partial\vartheta}\frac{\partial q_3}{\partial r}\right)\Bigg|_{h_b}^{h_s} + \frac{\partial}{\partial\vartheta}\left[\left(\frac{\partial q_3}{\partial r}\right)\Bigg|_{h_b}^{h}\right]$$

4. Interior Equations

In this section we derive approximate equations applicable to the interior of the ocean, i.e. to a region sufficiently far removed from all shores. A more precise definition of the "interior region" will be given in Section 5. We assume, as do other investigators, that all terms which are nonlinear in the velocity components, as well as the contributions of lateral eddy viscosity are negligibly small there. It is further assumed that the pressure is hydrostatic everywhere in the ocean, i.e. that all terms involving velocity components in (3.1) are negligible. These assumptions can be readily justified by examining the orders of magnitude of the terms in the equations. Equation (3.1) becomes

$$\frac{\partial p}{\partial r} = \varrho g \qquad (4.1)$$

Integration of equation (4.1) together with the boundary condition $p=0$ at $r=h_s$ gives

$$p = \varrho g\,(h_s - r). \qquad (4.2)$$

For the two-layer model, we assume that all velocities are negligible in the lower layer so that the pressure gradients vanish there. This leads to the two relations

$$\frac{\partial h_b}{\partial\vartheta} = -\frac{\varrho}{\Delta\varrho}\frac{\partial h_s}{\partial\vartheta},\ \frac{\partial h_b}{\partial\varphi} = -\frac{\varrho}{\Delta\varrho}\frac{\partial h_b}{\partial\varphi} \qquad (4.3)$$

where $\Delta\varrho$ is the density difference between the two layers. Letting

$$D = h_s - h_b \qquad (4.4)$$

we can write

$$\frac{\partial h_s}{\partial\vartheta} = \frac{\partial D}{\partial\vartheta},\ \frac{\partial h_s}{\partial\varphi} = \frac{\partial D}{\partial\varphi} \qquad (4.5)$$

for the homogeneous ocean (h_b having been assumed constant) and

$$\frac{\partial h_s}{\partial\vartheta} = \frac{\Delta\varrho}{\varrho}\frac{\partial D}{\partial\vartheta},\ \frac{\partial h_s}{\partial\varphi} = \frac{\Delta\varrho}{\varrho}\frac{\partial D}{\partial\varphi} \qquad (4.6)$$

for the two-layer model, where it has been assumed that $\Delta\varrho \ll \varrho$.

The momentum equations (3.2) and (3.3) become, using (3.11) and (4.2)

$$-2\Omega q_3\cos\vartheta = -g\frac{1}{r}\frac{\partial h_s}{\partial\vartheta} + \\ +\frac{1}{\varrho}\frac{1}{r^2}\frac{\partial}{\partial r}\left(A_r r^2\frac{\partial q_2}{\partial r}\right) \qquad (4.7)$$

$$2\Omega q_2\cos\vartheta + 2\Omega q_1\sin\vartheta = -g\,\frac{1}{r\sin\vartheta}\,\frac{\partial h_s}{\partial\varphi} + \\ +\frac{1}{\varrho}\frac{1}{r^2}\frac{\partial}{\partial r}\left(A_r r^2\frac{\partial q_3}{\partial r}\right) \qquad (4.8)$$

Before writing the approximate form of the vorticity equation (3.10) it is convenient to evaluate the term $(q_1 f)\Big|_{h_b}^{h_s}$. Applying the kinetic boundary conditions

$$\frac{D}{Dt}(h_s - r) = \frac{D}{Dt}(h_b - r) = 0 \qquad (4.9)$$

we have

$$(q_1 f)\Big|_{h_b}^{h_s} = f\left(\frac{q_2}{r}\frac{\partial h}{\partial\vartheta} + \frac{q_3}{r\sin\vartheta}\frac{\partial h}{\partial\varphi}\right)\Bigg|_{h_b}^{h_s} \qquad (4.10)$$

Evaluating the right side by means of equations (4.7) and (4.8), we have

$$(q_1 f)\Big|_{h_b}^{h_s} = -\left(\frac{2\Omega}{r}\sin\vartheta q_1\frac{\partial h}{\partial\vartheta}\right)\Bigg|_{h_b}^{h} + \\ +\frac{1}{\varrho}\left\{\left(\frac{1}{r^3}\frac{\partial}{\partial r}\left[A_r r^2\frac{\partial q_3}{\partial r}\right]\frac{\partial h}{\partial\vartheta}\right)\Bigg|_{h_b}^{h_s} - \\ -\left(\frac{1}{r^3\sin\vartheta}\frac{\partial}{\partial r}\left[A_r r^2\frac{\partial q_2}{\partial r}\right]\frac{\partial h}{\partial\varphi}\right)\Bigg|_{h_b}^{h_s}\right\} \qquad (4.11)$$

When this expression is substituted into equation (3.10) the last two terms cancel the corresponding terms on the right side of equation (3.10) as given by expression (3.14), provided we neglect the variation of r in equation (4.11).

The resulting vorticity equation (without nonlinear and lateral eddy viscosity terms) may be simplified further by noting that the slopes of the top and bottom surfaces will be much less than one, so that $q_1 \ll q_2$. Thus, only the term in df/dt is important on the left side and, using (3.8), equation (3.10) becomes approximately

$$-\frac{2\Omega}{r}\sin\vartheta\int_{h_b}^{h_s} q_2 dr = \frac{1}{\varrho}\left\{\frac{1}{r}\frac{\partial}{\partial\vartheta}\left(\tau_{r\varphi}\Big|_{h_b}^{h_s}\right) + \right.$$
$$\left. + \frac{\cot\vartheta}{r}\left(\tau_{r\varphi}\Big|_{h_b}^{h_s}\right) - \frac{1}{r\sin\vartheta}\frac{\partial}{\partial\varphi}\left(\tau_{r\vartheta}\Big|_{h_b}^{h_s}\right)\right\} \quad (4.12)$$

Integration of the approximate momentum equations (4.7) and (4.8) leads to

$$-2\Omega\cos\vartheta\int_{h_b}^{h_s} q_3 dr = -g'\frac{1}{r}D\frac{\partial D}{\partial\vartheta} + \frac{1}{\varrho}(\tau_{r\vartheta})\Big|_{h_b}^{h_s} \quad (4.13)$$

$$2\Omega\cos\vartheta\int_{h_b}^{h_s} q_2 dr = -g'\frac{1}{r\sin\vartheta}D\frac{\partial D}{\partial\varphi} +$$
$$+ \frac{1}{\varrho}(\tau_{r\varphi})\Big|_{h_b}^{h_s} \quad (4.14)$$

where we have used (4.4) to (4.6) and have neglected q_1, and

$$\left.\begin{array}{ll} g' \equiv g & \text{in the homogeneous ocean} \\ g' \equiv \dfrac{\Delta\varrho}{\varrho} g & \text{in the two-layer ocean} \end{array}\right\} \quad (4.15)$$

The integrated continuity equation is readily shown to be

$$\frac{\partial}{\partial\vartheta}\int_{h_b}^{h_s}\sin\vartheta\, q_2 dr + \frac{\partial}{\partial\varphi}\int_{h_b}^{h_s} q_3 dr = 0 \quad (4.16)$$

This relation is approximate in that the variation of r over the range of integration has been neglected. Introducing the "transport" components Q_2, Q_3, equation (4.16) is satisfied by defining the transport stream function ψ by the relations

$$\left.\begin{array}{l} Q_2 \equiv \displaystyle\int_{h_b}^{h_s} q_2 dr \equiv -\frac{1}{r\sin\vartheta}\frac{\partial\psi}{\partial\varphi} \\ Q_3 \equiv \displaystyle\int_{h_b}^{h_s} q_3 dr \equiv -\frac{1}{r}\frac{\partial\psi}{\partial\vartheta} \end{array}\right. \quad (4.17)$$

Equations (4.12) to (4.14) and (4.17) are the equations which we shall apply to the interior of the ocean.

5. Boundary Equations

a) Preliminary discussion.

To conform with reality, the circulation to be predicted by theory will have to exhibit relatively large velocities and velocity gradients at least near the western shore. Hence the approximations made in Section 4 for the interior region of the ocean cannot be expected to hold there. This is otherwise evident from a mathematical point of view since the approximate equations (4.12) to (4.16) do not constitute a system of a sufficiently high order to yield solutions which satisfy all boundary conditions. Hence these equations are not adequate for the entire enclosed ocean.

It has been assumed by other investigators (e.g. MUNK, 1950) that the influence of lateral eddy viscosity, while negligible in the interior, becomes important near the shore. The theory based on this assumption has led to a circulation pattern which looks remarkably realistic. As was already mentioned in the introduction, the theory has been criticized, however, because of the need for the empirical choice of the value of the coefficient of lateral eddy viscosity and the fact that the value which gives the proper width to the stream on the western shore is larger than one might expect from independent considerations. It is useful to consider the merits of this "viscous" theory from other points of view.

It was stated in the introduction that the torque due to the frictional forces on the shores has, at times, been held to be the torque which balances the torque applied by the wind. Now the viscous theory shows that the magnitude of the shore friction torque depends on the value of the viscosity (the shear stress on the shore being proportional to the viscosity and the normal derivative of the tangential velocity component, and the latter varying as viscosity to the minus two-thirds power). Hence, if the argument were correct, the value of the viscosity should be chosen so as to satisfy the torque balance! Fortunately the discussion in Section 2 relieves us of this requirement. If the friction torque is essential to the torque balance, it is certainly not the only contribution.

Consider now briefly, from a physical point of view, the role of the shore in producing an intense current. The solution of the interior vorticity and continuity equations (4.12) and (4.16) with a realistic wind distribution and neglecting bottom friction (see Section 6) leads to a southward transport component over the southern interior. The equations do not determine the direction of the other component. This evidently depends on the flow near the coast. Whichever it is, in a model which requires that the circulation be confined essentially to the northern hemisphere, the stipulation of an eastern or western shore must give rise to an intense northward current on one of the coasts, since the water which flows toward this coast has to be turned to the north to satisfy continuity. The stream will have to be narrow and hence intense if it is not to interfere with the concept of the interior region. Thus, the boundary condition of vanishing normal velocity on the shore is responsible for turning the current northward; the mechanism which accounts for the narrowness of this current (and which will determine on which of the two shores the current exists) remains to be investigated, but it appears reasonable that the usual viscous boundary condition of no slip will not have to play an essential role in the creation of the stream. This is also indicated by the viscous theory which shows that even if the extreme condition of zero normal derivative of the tangential transport is specified on the coast, the width and intensity of the stream are essentially unaffected. If, however, the no-slip condition is not essential, then the function of viscosity may not be paramount in the formation of the stream. It is only necessary to have a system of equations which is of sufficiently high order to be capable of yielding solutions which can satisfy the condition of vanishing normal transport. This, of course, can be accomplished by including the nonlinear inertia terms. The inclusion of viscosity, on the other hand, leads to a higher order system which requires another and, it seems, extraneous boundary condition.

It is important to note that the preceding discussion, having been restricted to the formative stage of the northward stream, does not necessarily suggest that lateral viscosity will not be important anywhere in the system. Since our study of the moment of momentum balance gave no conclusive answer to this question, it may be useful to examine it here from another point of view.

Imagine that the flow is contained between two solid concentric spheres and that it is created by the application of body forces uniformly distributed over the depth, rather than by surface forces. If there is no top or bottom friction we may expect the motion to be independent of r and to have vanishing radial velocity. The vorticity equation (3.6) then becomes

$$\frac{d}{dt}(\zeta_1+f) \quad = (\text{curl}\,\boldsymbol{B})_1 + \begin{array}{l}\text{lateral eddy}\\ \text{viscosity terms}\end{array} \qquad (5.1)$$

where $\boldsymbol{B}$ represents the body forces. If $(\text{curl}\,\boldsymbol{B})_1$ is everywhere positive, (as we may expect $(\text{curl}\,\boldsymbol{\tau})_1\Big|^{h_s}$, the curl of the wind stress, to be), and if viscosity is absent, then equation (5.1) says that the quantity ζ_1+f will always increase as we follow a particle. If the system is closed, this leads to a nonsteady flow. Hence, for steady flow, lateral friction must be important at least in some region through which every particle will have to pass.

This conclusion also follows immediately from energy considerations. The direction of the flow to be expected in the interior is such that the body force would do positive work on the system. In the absence of lateral eddy viscosity, however, there is no mechanism for dissipating the resulting increase in kinetic energy.

The author has so far not succeeded in carrying out an analogous examination of the variation of ζ_1+f for the actual problem. It may be noted, however, that in our formulation the transfer of the wind stress to the water occurs by means of vertical eddy viscosity and that, therefore, a mechanism for energy dissipation exists even in the absence of lateral eddy viscosity. Thus, the energy argument breaks down.

b) A new model.

The considerations presented so far suggest that we adopt a new model for our system. Let us imagine the ocean between, say, 10° latitude and 50° latitude to consist of a southern and a northern portion with the dividing circle of latitude at about 35°. The southern portion is further divided as shown. The figure also shows a typical streamline of the anticipated circulation, most, or perhaps all, of the streamlines being expected to pass through all three regions.

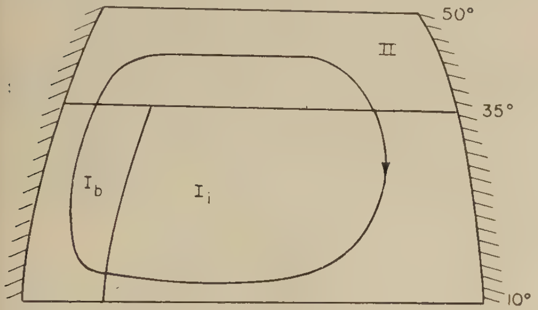

Fig. 1. The three regions of a new ocean model. I_i: interior region; I_b: frictionless stream region; II: northern region; nonsteady and lateral friction effects possibly important.

Our theory will apply to the interior region I_i and the boundary region I_b; (it will be seen that no boundary region is required on the eastern shore). In I_i the equations of Section 4 are applicable. In I_b nonlinear inertia, but not viscosity, will be included. In the Atlantic, I_b is to include the Gulf Stream north to about Cape Hatteras. In region II nonlinear, viscous and nonsteady effects may be important. This region includes the Gulf Stream meanders. If it turns out that lateral viscosity must be present somewhere in the system, its influence will be confined to region II. It is quite possible that the analysis of the problem in regions I and II together may have to include instability of the meanders, i.e. nonsteady effects. These, too, are assumed to be present in II only. The analysis of the flow in I is based on the assumption that this flow can be studied without inquiring into the conditions in II. Thus, whatever occurs in II, the flow which emerges from there into I_i is such that it obeys our interior equations. Similarly, the flow entering II from I_b is supposed to be determined by conditions in I_i and I_b alone.

c) Order of magnitude estimates.

The terms in the vorticity equation (3.10) may be grouped into three categories: (i) terms nonlinear in the velocities, (ii) terms due to the earth's rotation, (iii) terms resulting from eddy viscosity. The relative importance of each group will be examined in the following subsection by the usual procedures of boundary analysis. In the present section we carry out a preliminary simplification by comparing the relative magnitudes of the terms within each group.

(i) It will be assumed that the shores are given by two meridians. We must then expect that, in the boundary region, $|q_3| \ll |q_2|$ and derivatives parallel to the shore, $\left(\frac{\partial}{\partial\vartheta}\right)$, will be much smaller than those normal to the shore, $\left(\frac{\partial}{\partial\varphi}\right)$, Hence, from equation (3.5), $\zeta_1 \approx -(1/r \sin\vartheta)(\partial q_2/\partial\varphi)$. The magnitude of q_1 is readily estimated from the kinetic boundary condition, equation (4.9), in terms of q_2, q_3 and the slopes of h_s and h_b. For the homogeneous ocean q_1 is very small due to the small surface slope. For the two-layer ocean the principal contribution is due to the slope of h_b, the thermocline, the variation of h_b being of the order of the depth D itself.

Examining the third integral in equation (3.10), it is clear that the first, second and fourth terms are negligible compared with the third.

The contributions of $\int_{h_b}^{h_s} (d\zeta_1/dt)dr$ and $(q_1\zeta_1)\Big|_{h_b}^{h_s}$ are seen to be of equal importance in the two-layer case. To compare these terms with the remaining nonlinear terms involving radial differentiation, we must obtain an estimate of $\partial q_2/\partial r$. The second, third and fourth terms of equation (3.10) have the following orders of magnitude for a two-layer model:

$$[(q_1/r)(\partial q_2/\partial\varphi)]_{r=h_b}; \quad (q_1/r)_{r=h_b}\left[(\partial q_2/\partial\varphi)\Big|_{h_b}^{h_s}\right];$$

$$(\partial q_1/\partial\varphi)_{r=h_b}\left[(q_2/r)\Big|_{h_b}^{h_s}\right].$$

(For a homogeneous ocean q_1 is so small everywhere that all these terms are negligible.) The second and third of the above expressions involve a difference in the values at h_s and h_b of the quantities $\partial q_2/\partial\varphi$ and q_2, respectively. If these differences are of the order of the quantities themselves, then all terms must be expected to be of equal importance. We assume in the following that these differences are much smaller than the quantities themselves and hence that the term $(q_1\,\zeta_1)\Big|_{h_b}^{h_s}$, predominates. This implies that the top and bottom shear stresses which constitute the principal cause of the radial variation of q_2 are relatively unimportant in the boundary region, thus leaving q_2 essentially uniform with depth. This condition can probably be relaxed somewhat because our estimates of the third and fourth terms are likely to be on the high side, q_1 and $\partial q_1/\partial\varphi$ having been taken out of the integrals and evaluated at $r = h_b$ where they will be greatest. Nevertheless it may be important to note that the justification for omitting the terms under consideration is not beyond question.

(ii) As in (i), the first two terms involving Ω in equation (3.10) are seen to be of the same order, while the third one is negligible.

(iii) We turn to expression (3.12) for the terms due to eddy viscosity. Of the three terms involving radial eddy viscosity the last one will predominate. The principal contribution due to lateral eddy viscosity comes from F_2^* and is approximately

$$\frac{1}{\varrho r^3 \sin^3\vartheta}\int_{h_b}^{h_s} A_L \frac{\partial^3 q_2}{\partial\varphi^3}\,dr$$

A_L denoting the lateral eddy viscosity.

The simplified vorticity equation (3.10) now becomes

$$\int_{h_b}^{h_s}\frac{d}{dt}(\zeta_1 + f)\,dr - [q_1(\zeta_1 + f)]\Big|_{h_b}^{h_s} =$$

$$= -\frac{1}{\varrho}\frac{1}{r}\left(A_r\frac{\partial^2 q_2}{\partial r\partial\varphi}\right)\Big|_{h_c}^{h_s} -$$

$$-\frac{1}{r^3\sin^3\vartheta}\int_{h_b}^{h_s} A_L\,\partial^2 q_2/\partial\varphi^2\cdot dr \qquad (5.2)$$

with $\zeta_1 \cong -(1/r\sin\vartheta)\,(\partial q_2/\partial\varphi)$.

d) Boundary layer analysis.

In this subsection the technique of boundary layer analysis is employed to examine the relative magnitudes of the terms in (5.2). This technique assumes that a boundary layer type of solution exists. If it does, then the procedure readily yields an estimate of some of the properties of the solution; in this case, of the width and intensity of the stream.

We first assume that the essence of the phenomenon of interest to us will not be lost if we neglect the radial variation of the velocity components and of A_L within the boundary layer for the purpose of evaluating the integrals in equation (5.2). We also assume that the radial eddy viscosity term is not important. This assumption may not be valid for a homogeneous or a two-layer ocean, or perhaps even for a more realistic model, but an argument in its favor might be as follows. At the top surface the radial velocity gradient will be zero in the absence of a meridional wind. At the bottom surface the radial eddy viscosity may be sufficiently small to keep $(A_r\,\partial^2 q_2/\partial r\partial\varphi)_{r=h_b}$ small. We make the assumption in spite of the uncertainty of its validity because of the desirability of investigating the boundary solution in the complete absence of friction. Equation (5.2) becomes

$$D\frac{d(\zeta_1 + f)}{dt} - [q_1(\zeta_1 + f)]\Big|_{h_b}^{h_s} =$$

$$= -\frac{D}{\varrho r^3\sin^3\vartheta}A_L\frac{\partial^2 q_2}{\partial\varphi^2} \qquad (5.3)$$

or, using the kinetic boundary conditions (4.9),

$$\frac{d}{dt}\left(\frac{\zeta_1 + f}{D}\right) = -\frac{1}{D\varrho r^3\sin^3\vartheta}A_L\frac{\partial^3 q_2}{\partial\varphi^3} \qquad (5.4)$$

Equation (5.4) is rendered dimensionless by the following transformations

$$\left.\begin{array}{ll} q_2 = q^* q_2'. & q_3 = q^* q_3' \\ \dfrac{1}{r}\dfrac{\partial}{\partial\vartheta} \approx \dfrac{1}{s}\dfrac{\partial}{\partial\vartheta'} & \dfrac{1}{r}\dfrac{\partial}{\partial\varphi} \approx \dfrac{1}{s}\dfrac{\partial}{\partial\varphi'} \\ \beta = \dfrac{2\,\Omega}{r} & \end{array}\right\} \qquad (5.5)$$

where q^* is a characteristic velocity taken to be a measure of the zonal velocity in the transition region from the interior to the boundary layer, s is the south-north extent of region I, and $\sin\vartheta$ is approximated by one. We further restrict ourselves for the moment to an homogeneous ocean or to a two-layer model with such a deep upper layer that the depth may be regarded as uniform. Equation (5.4) then becomes approximately

$$\frac{q^*}{s^2\beta}\left(q_2'\frac{\partial^2 q_2'}{\partial\vartheta'\partial\varphi'}+q_3'\frac{\partial^2 q_2'}{\partial\varphi'^2}-\cos\vartheta\, q_2'\frac{\partial q_2'}{\partial\varphi'}\right)+ \\ + q_2' = \frac{A_L}{s^3\beta}\frac{\partial^3 q_2'}{\partial\varphi'^3} \qquad (5.6)$$

According to our discussion in Sections 5 a) and 5 b), we expect that the nonlinear terms will be important in the boundary layer. Since they are negligible in the interior, the parameter

$$N \equiv \frac{q^*}{s^2\beta} \qquad (5.7)$$

must be much less than one. Hence the terms cannot be important in the boundary layer unless the derivatives, and possibly the functions themselves, are large there. We therefore set

$$\varphi' = N^m\varphi'', \quad q_2' = N^{-n}q_2'' \qquad (5.8)$$

where m, n are to be determined and are expected to be positive. We hope to find a transformation (5.8) such that q_2'' $(\vartheta_1'\varphi'')$, q_3' (ϑ', φ'') and their derivatives are of order one in the boundary layer. The magnitude of each term will then be indicated by its coefficient.

The continuity equation (4.16) shows that $m = n$ and equation (5.6) becomes

$$N^{1-3m}\left(q_2''\frac{\partial^2 q_2''}{\partial\vartheta'\partial\varphi''}+q_3'\frac{\partial^2 q_2''}{\partial\varphi''^2}-\cos\vartheta\, q_2''\frac{\partial q_2''}{\partial\varphi''}\right)+ \\ + N^{-m}q_2'' = N^{-4m}\frac{A_L}{\varrho s^3\beta}\frac{\partial^3 q_2''}{\partial\varphi''^3} \qquad (5.9)$$

Since we expect nonlinear and Coriolis terms to balance, we must have $m = \frac{1}{2}$. The terms due to lateral eddy viscosity will be unimportant if $N^{-3/2}A_L/\varrho s^3\beta = \beta^{1/2}A_L/\varrho q^{*3/2} \ll 1$. The width of the stream will be of order $sN^{1/2} = (q^*/\beta)^{1/2}$, and the meridional velocity component will be of order $q^*N^{-1/2} = s(q^*\beta)^{1/2}$. With $\beta = 2\times10^{-13}\cdot(\text{cm sec})^{-1}$, $q^* = 10$ cm sec^{-1} this gives approximately 70 km for the width of the stream, which is the correct order of magnitude. The condition for smallness of the friction terms places an upper bound of approximately 5×10^6 cm^2 sec^{-1} on the magnitude of A_L. Assuming that this corresponds to actual conditions and that, therefore, lateral eddy viscosity is negligible, the vorticity equation (5.4) becomes

$$\frac{d}{dt}\left(\frac{\zeta_1+f}{D}\right) = 0 \qquad (5.10)$$

Since, in this equation, the variation of ζ_1, q_2, q_3 with depth has, effectively, been neglected, the derivative d/dt may be interpreted as the rate of change as one follows a vertical column of water in its horizontal motion, and the equation (5.10) states that the potential vorticity associated with such a column is conserved during its motion in the boundary region. Using equation (4.17), equation (5.10) can be integrated along a "transport line", i.e. a line of constant ψ, to give

$$\frac{\zeta_1+f}{D} = F(\psi) \qquad (5.11)$$

where F is a function which must be determined by matching the distribution of $(\zeta_1+f)/D$ in the boundary with the distribution in the interior near the edge of the boundary layer.

e) The momentum equations in the boundary layer.

The considerations contained in the preceding sections may now be applied to the integrals over depth of the momentum equations (3.2) and (3.3) to derive approximate equations which are consistent with the assumptions made in deriving the vorticity equation. They are

$$\int_{h_b}^{h_s}\left(\frac{q_2}{r}\frac{\partial q_2}{\partial\vartheta}+\frac{q_3}{r\sin\vartheta}\frac{\partial q_2}{\partial\varphi}\right)dr - 2\Omega\cos\vartheta\int_{h_b}^{h_s}q_3\,dr = \\ = -g'\frac{1}{r}D\frac{\partial D}{\partial\vartheta} \qquad (5.12)$$

$$2\Omega\cos\vartheta\int_{h_b}^{h}q_2\,dr = -g'\frac{1}{r\sin\vartheta}D\frac{\partial D}{\partial\varphi} \qquad (5.13)$$

We note that the meridional transport component is geostrophic, but that the zonal component is not, the nonlinear terms being as important as the Coriolis contribution.

Neglecting the variation of the integrands with depth, we derive an approximate Bernoulli equation by multiplying equation (5.12) by q_2, equation (5.13) by q_3, adding the resulting equations to obtain

$$\frac{d}{dt}\left(\frac{q_2^2}{2}\right) + g'\frac{dD}{dt} = 0, \qquad (5.14)$$

and finally integrating along a streamline (or transport line), giving

$$\frac{q_2^2}{2} + g'D = B(\psi) \qquad (5.15)$$

where B is an arbitrary function which must be determined by matching the boundary with the interior solution.

6. Transformation to Surface Coordinates

Having derived the equations in terms of spherical coordinates in an effort not to lose any important effects of the spherical ocean shape by premature introduction of plane coordinates, we are now ready to make this transformation to give the equations a more familiar appearance.

Our boundary layer analysis has been based on the assumption that the derivative $\partial/\partial\varphi$ represents differentiation normal to the coast. Hence two meridians are taken to represent the coast lines. The simplest coordinate system will then be one in which these are coordinate lines. Hence, set

$$\left.\begin{array}{lll} x = R\varphi, & y = R(K-\vartheta) & z = r - R \\ u = q_3, & v = -q_2 & \\ U = Q_3, & V = -Q_2 & \\ \tau_x = \tau_{r\varphi}, & \tau_y = -\tau_{r\vartheta} & \end{array}\right\} \qquad (6.1)$$

where K is the colatitude of the southern boundary of region I, R is the radius of the undisturbed ocean surface. Note that while y measures distance along a meridian of a sphere of radius R, x does not measure exact distance along a circle of latitude. We have

$$\frac{\partial}{\partial r} = \frac{\partial}{\partial z}; \quad \frac{\partial}{\partial\vartheta} = -R\frac{\partial}{\partial y}; \quad \frac{\partial}{\partial\varphi} = R\frac{\partial}{\partial x} \qquad (6.2)$$

If, instead of x, an alternative coordinate x' which does measure distance along a circle of latitude were chosen, (e.g. $x' = \varphi R \sin\vartheta$), then the most convenient geometrical shape in the x'—y plane, the rectangle, would represent a less realistic configuration than does the rectangle in the x—y plane which corresponds to an ocean whose east and west shores are meridians. Moreover, the velocity component v would then be an inconvenient variable since it would not represent the velocity in the direction of the constant x' curves.[1]

The interior equations (4.12), (4.13), (4.14), (4.17) become

$$\beta \sin\vartheta \int_{h_b-R}^{h_s-R} v\,dz =$$

$$= \frac{1}{\varrho}\left(-\frac{\partial\tau_x}{\partial y} + \frac{\cot\vartheta}{R}\tau_x + \frac{1}{\sin\vartheta}\frac{\partial\tau_y}{\partial x}\right)_{z=h_b-R} \qquad (6.3)$$

$$2\Omega\cos\vartheta \int_{h_b-R}^{h-R} u\,dz = -\frac{g'}{2}\frac{\partial D^2}{\partial y} + \frac{1}{\varrho}(\tau_y)_{z=h_s-R} \qquad (6.4)$$

$$-2\Omega\cos\vartheta \int_{h_b-R}^{h_s-R} v\,dz = -$$

$$-\frac{g'}{2\sin\vartheta}\frac{\partial D^2}{\partial x} + \frac{1}{\varrho}(\tau_x)_{z=h_s-R} \qquad (6.5)$$

$$V = \int_{h_b-R}^{h_s-R} v\,dz = \frac{1}{\sin\vartheta}\frac{\partial\psi}{\partial x}, \quad U = \int_{h_b-R}^{h_s-R} u\,dz = -\frac{\partial\psi}{\partial y} \qquad (6.6)$$

---

[1] The reader may wish to contrast our system with that of MUNK 1950 and MUNK-CARRIER 1950 whose x coordinate measures distance, with the result that the rectangle in the x—y plane does not correspond to a realistic ocean shape. This leads Munk-Carrier to consider a triangle. The rectangle in our x—y plane is perhaps an equally good approximation to the real ocean shape.

The agreement of corresponding terms in Munk's equations and in ours is not complete. This is due to the fact that Munk's equations have apparently not been derived by a systematic transformation of variables and coordinates from a spherical system; hence there is some question concerning the relation of Munk's variables to those in the actual spherical system.

where we have approximated $1/r$ by $1/R$ and, consistent with the assumption already made in the derivation of the boundary equations, have neglected the shear stress at the bottom surface $z = h_b - R$.

The boundary equations (5.11), (5.12), (5.13), (5.15) become

$$\frac{\dfrac{1}{\sin\vartheta}\dfrac{\partial v}{\partial x} + 2\Omega\cos\vartheta}{D} = F(\psi) \qquad (6.7)$$

$$\int_{h_b-R}^{h_s-R}\left(v\frac{\partial v}{\partial y} + \frac{u}{\sin\vartheta}\frac{\partial v}{\partial x}\right)dz + 2\Omega\cos\vartheta\int_{h_b-R}^{h_s-R} u\,dz = $$

$$= -\frac{g'}{2}\frac{\partial D^2}{\partial y} \qquad (6.8)$$

$$-2\Omega\cos\vartheta\int_{h_b-R}^{h_s-R} v\,dz = -\frac{g'}{2\sin\vartheta}\frac{\partial D^2}{\partial x} \qquad (6.9)$$

$$\frac{v^2}{2} + g'D = B(\psi) \qquad (6.10)$$

Just as in the derivation of the vorticity equation (6.7), the integrals appearing in equations (6.8) to (6.9) will be evaluated approximately by neglecting the z variation of the integrands.

7. The homogeneous Ocean with simple Wind Distribution

The homogeneous model is important principally because of the insight that will be gained into the role of density stratification in the formation of the western stream by comparing the behaviour of this model with that of a two-layer ocean. The most important question to be investigated in this connection is whether either the variation of the Coriolis parameter with latitude, or the density stratification, or both, are indispensable. Because of its simplicity, the homogeneous model also readily affords insight into the entire phenomenon of the coastal stream.

Assume the wind stresses

$$\tau_x = -W\left(1 - \frac{y^2}{s^2}\right), \quad \tau_y = 0, \quad 0 \le y \le s \qquad (7.1)$$

s being the south-north extent of region I and W being a constant. Equation (6.3) becomes

$$\beta\sin\vartheta\, V_i = \frac{W}{\varrho}\left[-\frac{2y}{s^2} + \frac{\cot\vartheta}{R}\left(1 - \frac{y^2}{s^2}\right)\right] \qquad (7.2)$$

where the subscript i is used to denote quantities in the interior region I_i. For $\vartheta \ge 55°$ and $K = 75°$, $\cot\vartheta \le .7$ and $s \approx .35\ R$, so that the second term due to the curl of the wind is considerably smaller than the first term over most of the range. Accordingly, we neglect it. Using equation (6.6)

$$\frac{\partial\psi_i}{\partial x} = -\frac{2yW}{\varrho\beta s^2} \qquad (7.3)$$

$$\psi_i = -\frac{2yW}{\varrho\beta s^2}\left[x + l(y)\right] \qquad (7.4)$$

$$U_i = \frac{2W}{\varrho\beta s^2}(x + l) + \frac{2yW}{\varrho\beta s^2}\frac{dl}{dy} \qquad (7.5)$$

where $l(y)$ is an arbitrary function. Since we do not expect a strong current on the eastern coast, (the impossibility of such a current will shortly be demonstrated), we anticipate that the interior solution will be valid all the way to this coast. Hence, we want $U = 0$ at $x = a$, $x = 0$ and $x = a$ denoting the western and eastern shores. Thus in the region I_i

$$\psi_i = \frac{2yW}{\varrho\beta s^2}(a - x) \qquad (7.6)$$

$$U_i = -\frac{2W}{\varrho\beta s^2}(a - x) \qquad (7.7)$$

We now examine the boundary equations. From equations (6.6) and (6.7) and neglecting the radial variation of v,

$$\frac{\dfrac{1}{\sin^2\vartheta}\dfrac{\partial}{\partial x}\left(\dfrac{1}{D}\dfrac{\partial\psi}{\partial x}\right) + 2\Omega\cos\vartheta}{D} = F(\psi). \qquad (7.8)$$

Since $g' = g$ in the homogeneous case, it is clear from equations (6.8) and (6.9) that the surface slopes will be very small and that, for a reasonable average depth, the depth will be essentially uniform. Expanding $\cos\vartheta$ in a power series about $\vartheta = K$ and retaining the first two terms

$$2\Omega\cos\vartheta \approx 2\Omega\cos K + 2\Omega\frac{y}{R}\sin K \qquad (7.9)$$

or

$$f \approx f_K + \beta_K y, \quad \beta_K \equiv \frac{2\Omega}{R}\sin K, \quad f_K \equiv 2\Omega\cos K \qquad (7.10)$$

and equation (7.8) becomes

$$\frac{1}{\sin^2 \vartheta}\,\frac{1}{D}\,\frac{\partial^2 \psi}{\partial x^2} + f_K + \beta_K y = G(\psi) \qquad (7.11)$$

where $G(\psi) = DF(\psi)$, D being regarded constant.

According to boundary layer analysis, as discussed in Section 5, the $\partial/\partial x$ derivatives are large only in the boundary layer and decrease as one approaches the interior. The transition from boundary to interior regions is, of course, continuous, but, to simplify the terminology, let us define some suitable distance $x = L$ as the "edge" of the boundary layer, L being large enough so that the boundary layer solution there is essentially equal to the interior solution in the same neighborhood. We then have

$$f_K + \beta_K y = G(\psi_i) \text{ at } x = L \qquad (7.12)$$

But, from equation (7.6),

$$\psi_i(L, y) \approx \frac{2 Wa}{\varrho \beta s^2}\, y \equiv U^* y \qquad (7.13)$$

since we expect $L \ll a$, and where U^* denotes the zonal transport into the boundary layer. Hence

$$f_K + \beta_K y = G(U^* y) \qquad (7.14)$$

and

$$G(\psi) = f_K + \frac{\beta_K}{U^*}\,\psi \qquad (7.15)$$

Substitution into equation (7.11) yields

$$\frac{\partial^2 \psi}{\partial x^2} - \frac{\sin^2\left(K - \frac{y}{R}\right) D\beta_K}{U^*}\,\psi =$$

$$= -\sin^2\left(K - \frac{y}{R}\right) D\beta_K y \qquad (7.16)$$

If we consider a closed ocean basin, the coast $x = 0$ and the southern boundary $y = 0$ form a continuous transport line so that $\psi(0, y) = 0$. This boundary condition together with the matching condition as the interior is approached (equation 7.13) determine the constants of integration. The solution is

$$\psi = U^* y \left[1 - e^{-\left(\frac{\sin^2 (K - y/R)\, D\beta_K}{U^*}\right)^{1/2} x}\right] \qquad (7.17)$$

and, from equation (6.6)

$$V = (U^* D\beta_K)^{1/2}\, y e^{-\left(\frac{\sin^2 (K - y/R)\, D\beta_K}{U^*}\right)^{1/2} x} \qquad (7.18)$$

Thus the theory predicts an intense northward stream on the western coast, the width of the stream being given by, say,

$$\sin\left(K - \frac{y}{R}\right) \cdot L \approx 4\left(\frac{u^*}{\beta_K}\right)^{1/2}$$

and the intensity of the northward velocity being of order $s(u^* \beta_K)^{1/2}$, where $u^* = U^*/D$. These results are seen to agree with the orders of magnitude previously derived directly from boundary analysis considerations in Section 5 d). Expressions (7.17), (7.18) are simpler and more revealing if we set

$$x \sin\left(K - \frac{y}{R}\right) = X \qquad (7.19)$$

X measuring true distance along a circle of latitude.

Curves 1 a of Figures 2 and 3 show the variation of ψ/Us and V/U^* with dimensionless distance X/s from the western shore at $y = s$ for values of U^* (10^5 cm^2 sec^{-1}) and s (2×10^8 cms) corresponding to the North Atlantic and for a depth D (or D^* in the terminology of Section 8) of 4×10^5 cms which corresponds to the total depth of the ocean. Hence the graphs may be interpreted as representing the Gulf Stream which would exist if the motion were barotropic. The stream is quite narrow (its width is about 40 km); the transport is very large near the coast and decreases very rapidly as the distance from the coast increases. The predicted flow is seen to exhibit what might be regarded as the principal qualitative property of the observed circulation—a westward interior transport being turned into a narrow, intense stream near the western coast—and the width of this stream has the appropriate order of magnitude.

The results obtained may be given a very simple physical interpretation. The vorticity equation (6.7), for D essentially constant, states that the absolute vorticity of a particle, $\zeta_1 + f$, is conserved. Since f increases as the particle travels northward, ζ_1 must decrease, and since ζ_1 $\left(\text{or } \frac{\partial v}{\partial X}\right)$ is approximately zero when the particle enters the boundary region it must become negative. Particles which approach the coast at low latitude, i.e. with small f, must undergo a large increase in f to reach a certain more northerly latitude, and hence acquire a large negative value of ζ_1 (or $\partial v/\partial X$). Those approaching with larger f need not suffer such a great change in f to reach the same northerly latitude and hence acquire less negative $\partial v/\partial X$. This gives rise to the exponential type of decline in current intensity from the coast to the interior.

It is now clear that the interior transport approaching the west coast could equally well be turned into an intense southward current if we did not stipulate that $y=0$ be a streamline in the boundary region, i.e. that the circulation be enclosed on the south. Following the same physical reasoning as before, a southward current means a decrease in f and hence positive $\partial v/\partial X$ to conserve vorticity. Further, the particles approaching the coast with larger f must acquire larger positive $\partial v/\partial X$ than must those approaching with smaller f. Hence we obtain a boundary layer solution with v having its greatest negative value at the coast and increasing to zero as the interior is approached.

Any flow pattern intermediate between the two already discussed, with a portion of the westward interior current being turned into an intense northward stream and the balance into an intense southward stream is also possible. The entire infinite family of solutions is obtained by stipulating the boundary condition

$$\psi(0, y) = \gamma s U^*, \quad 0 \le \gamma \le 1. \tag{7.20}$$

This gives

$$\psi = U^* (\gamma s - y)\, e^{-\left(\frac{D\beta_K}{U^*}\right)^{1/2} X} + U^* y \tag{7.21}$$

$$V = -(U^* D\beta_K)^{1/2} (\gamma s - y)\, e^{-\left(\frac{D\beta_K}{U^*}\right)^{1/2} X} \tag{7.22}$$

Thus all particles approaching the boundary region north of $y=\gamma s$ (but, of course, south of $y=s$ to remain within region I) turn northward, those approaching between $y=0$ and $y=\gamma s$ turn southward, the transport line $\psi=U^*\gamma s$ dividing at $x=0$ to form the shoreline both south and north of $y=\gamma s$.

Which of all these solutions is the appropriate one depends on the appropriate choice of the boundary condition and this in turn is governed by considerations of mass conservation in the overall system.

Other solutions may be obtained, for example, by giving $\psi(o, y)$ a negative value. This gives a northward stream consisting not only of the water approaching the coast from the interior and being turned north, but also of water introduced into the stream in the boundary region across $y=0$, this extra flow preventing the transport line $\psi=0$ from reaching the coast.

Another important result which is evident immediately on physical grounds is that the factors which create an intense stream on the west coast could not create a similar stream on the east coast. To show this, let us suppose that the zonal transport component in the interior is eastward. If this transport is to turn northward, f must increase along a transport line, hence $\partial v/\partial X$ must become negative. Further, particles approaching with smaller f must acquire larger negative $\partial v/\partial X$, than those approaching with greater f. Hence the solution would require positive v, negative $\partial v/\partial X$, and v tending to zero as one leaves the boundary region and approaches the interior region. Obviously, these are incompatible conditions. A similar argument rules out a southward stream. Thus we see that a boundary layer type solution is possible in region I if the zonal transport is westward, but not if the zonal transport is eastward.

Mathematically, this is seen as follows. Since ψ_i is zero on $y=0$, and since $U_i = -\partial\psi_i/\partial y > 0$ for an eastward interior current, ψ_i would be negative for $y>0$; in particular ψ_i would be negative at the edge of the intense stream on the east coast. The matching with the boundary layer solution, analogous to equation (7.12), would then lead to an expression for $G(\psi)$ analogous to (7.15) with a minus sign in front of the term containing ψ. This gives rise to a plus sign for the ψ term in the equation analogous to (7.16) for the boundary layer stream function, and hence to trigonometric instead of exponential solutions. Hence no boundary layer type solution is possible.

To avoid confusion, it should be emphasized that the above conclusion does not in any way conflict with the well known problem of ideal, irrotational fluid theory, in which a flow impinges on a solid boundary placed normal to the undisturbed flow at infinity. This flow is not of the boundary layer type and the tangential current is just as wide and no more intense than the normal current. This type of flow was excluded from our investigations as soon as we made approximations appropriate to boundary layer type solutions.

It appears that the simple homogeneous ocean model contains the essential features of the type of circulation one expects. In the following section we investigate to what extent the two-layer model alters the phenomenon.

8. The Two-Layer Ocean with Simple Wind Distribution[1]

We consider the same problem as in Section 7 and make the same approximations except that now the variation of the depth D is taken into account. The interior relations (7.3) to (7.7) remain unchanged. We shall require a relation between U^x and D_i at the edge of the boundary layer. From equations (6.4) and (7.7), and setting $2\Omega\cos\vartheta = f \approx f_K + \beta_K y$, we have

$$D_i^2 = \left(f_K y + \frac{\beta_K y^2}{2}\right)\frac{4W}{\varrho\beta s^2 g'}(a-x) + C(x) \qquad (8.1\,\mathrm{a})$$

where $C(x)$ is still arbitrary. If D^* is the depth at $y=0$ and at the edge of the boundary layer $x=L$, then $C(L)=D^{*2}$ and

$$D_i^2(L,y) = \frac{2U^x}{g'}\left(f_K y + \frac{\beta_K y^2}{2}\right) + D^{*2} \qquad (8.1\,\mathrm{b})$$

Another expression for $D_i^2(x,y)$ may be derived by using the momentum equation (6.5). It is approximately

$$D_i^2 = -\left(f_K y + \frac{\beta_K y^2}{2}\right)\frac{4W}{\varrho\beta s^2 g'}x - \frac{2W\sin K}{\varrho g'}x + C_1(y) \qquad (8.1\,\mathrm{c})$$

Comparison with equation (8.1 a) yields

$$C(x) = D_a^2 + \frac{2W\sin K}{\varrho g'}(a-x) \qquad (8.2)$$

where D_a is a constant and denotes $D_i(a,y)$.

Instead of using the vorticity equation (6.7) it is more convenient, in the two-layer case, to use the momentum equation (6.9) and the Bernoulli equation (6.10). From equations (6.9) and (6.6)

$$\psi = \frac{g'}{2f}D^2 + C_3(y) \qquad (8.3)$$

where $C_3(y)$ is arbitrary and is determined by matching ψ and D with the interior solutions. We have from equations (7.13), (8.1) and (8.3)

$$U^* y = \frac{g'}{2f}\left[\frac{2U^*}{g'}\left(f_K y + \frac{\beta_K y^2}{2}\right) + D^{*2}\right] + C_3 \qquad (8.4)$$

whence

$$C_3(y) = \frac{\beta_K y^2 U^*}{2f} - \frac{g' D^{*2}}{2f} \qquad (8.5)$$

Substituting in equation (8.3) and solving for D^2 we obtain

$$D^2 = D^{*2} + \frac{2f}{g'}\psi - \frac{\beta_K y^2 U^*}{g'} \qquad (8.6)$$

Equation (8.6) provides one relation between the unknowns ψ and D. A second relation is obtained from the Bernoulli equation (6.10). The unknown function $B(\psi)$ is again determined by matching with the interior solution. As one leaves the boundary region, equation (6.10) becomes

$$g'\left[D^{*2} + \frac{2U^*}{g'}\left(f_K y + \frac{\beta_K y^2}{2}\right)\right]^{1/2} = B(U^* y) \qquad (8.7)$$

---

[1] Some weeks following the final preparation of this paper Dr. J. G. Charney (1955) published a theory of the Gulf Stream much like the one contained in the following section. Charney's aim is to study a two-layer model which is fashioned to fit as closely as possible the observed topography of the thermocline between the Florida Straits and Cape Hatteras and the observed volume transports in the Stream, in order to determine how closely the theory can reproduce the observed flow. By contrast, this author's primary goal has been to critically analyze some of the questions connected with the formulation of a suitable theory and the development of the pertinent equations, and to investigate the mechanism which gives rise to the intense coastal current. This is done with a view to clarifying such problems as the roles of density stratification and the variation of the Coriolis parameter, the possibility of the existence of a current on the eastern boundary, the direction of the intense current, etc. In order not to obscure any of these aspects of the problem the simple model used to study the homogeneous ocean is retained in this section, where our theory is applied to the two-layer system, and no attempt is made to fit the model more closely to the Gulf Stream.

giving

$$B(\psi) = g' \left[D^{*2} + \frac{2 f_K}{g'} \psi + \frac{\beta_K}{g' U^*} \psi^2 \right]^{1/2} \qquad (8.8)$$

Substitution into equation (6.10) yields

$$\frac{v^2}{2} = g' \left\{ \left[D^{*2} + \frac{2 f_K}{g'} \psi + \frac{\beta_K}{g' U^*} \psi^2 \right]^{1/2} - D \right\} \qquad (8.9)$$

Finally, replacing v by $(1/D \sin \vartheta)\, \partial\psi/\partial x$ from equation (6.6) and eliminating D by using equation (8.6), the following equation for ψ is obtained:

$$\left(\frac{\partial \psi}{\partial x}\right)^2 =$$

$$= 2 g' \sin^2 \left(K - \frac{y}{R} \right) \left[D^{*2} + \frac{2 f}{g'} \psi - \frac{\beta_K y^2 U^*}{g'} \right]$$

$$\left\{ \left[D^{*2} + \frac{2 f_K}{g'} \psi + \frac{\beta_K}{g' U^*} \psi^2 \right]^{1/2} - \right.$$

$$\left. - \left[D^{*2} + \frac{2 f}{g'} \psi - \frac{\beta_K y^2 U^*}{g'} \right]^{1/2} \right\} \qquad (8.10)$$

The appropriate boundary condition is that $x = 0$ be a streamline. As in Section 7 the particular value to be chosen for $\psi(o, y)$ depends on continuity considerations for the entire system. We shall restrict our numerical solutions to the model discussed in Section 7, i.e. to the case where the circulation is confined to a region north of $y = 0$, so that

$$\psi(o, y) = 0 \qquad (8.11)$$

We first note the very important result $\partial\psi/\partial x = 0$ for all x if $\beta_K = 0$. Thus, if the variation of the Coriolis parameter with latitude were neglected, no boundary stream could be produced. From a different point of view, the result shows that the variation in depth alone and its effect on the potential vorticity (equation (6.7)) cannot give rise to an intense stream. Thus, in the two-layer ocean, as in the homogeneous model, the variation of f is the essential phenomenon and it remains to investigate how the resulting flow pattern is modified by density stratification. More physical insight into this conclusion can perhaps be gained by the following consideration. Consider the change of relative vorticity ζ_1 $\left(\text{or } \dfrac{1}{\sin \vartheta} \dfrac{\partial v}{\partial x} \right)$ as one follows a streamline. Since, according to equation (6.7), potential vorticity is conserved, a change in ζ_1 will be due either to a change in f or to a change in D. We see from equation (8.6), however, that a change of D along a given streamline is due solely to a change in f. Hence, if f is constant, ζ_1 is constant along each streamline and since it is approximately zero near the edge of the boundary layer it must be zero everywhere. Thus the existence of β_K is the primary cause of the phenomenon. Inasmuch as β_K together with the small value of g' in the two-layer model give rise to a considerable change of depth along a streamline, and this change in turn effects the potential vorticity and hence the current, the latter is actually dependent on the depth (and hence on the density stratification) as well as on β_K.

Proceeding now with the analysis of the differential equation (8.10), we replace x by X according to equation (7.19) and then introduce the non-dimensional quantities $\overline{X}$, $\bar{y}$, $\bar{\psi}$ by the relations

$$X = s\overline{X}, \quad y = s\bar{y}, \quad \psi = U^* s \bar{\psi}$$

so that $\bar{\psi}$ approaches $\bar{y}$ as one approaches the interior. Equation (8.10) becomes

$$\left(\frac{\partial \bar{\psi}}{\partial \overline{X}}\right)^2 = \frac{2 \beta_K^{3/2} s^3}{U^{*1/2} g'^{1/2}} [\varepsilon + \delta\bar{\psi} + 2 \bar{y} \bar{\psi} - \bar{y}^2]$$

$$\{[\varepsilon + \delta\bar{\psi} + \bar{\psi}^2]^{1/2} - [\varepsilon + \delta\bar{\psi} + 2 \bar{y} \bar{\psi} - \bar{y}^2]^{1/2}\} \qquad (8.13)$$

where

$$\varepsilon = \frac{D^{*2} g'}{U^* \beta_K s^2} = \frac{D^* g'}{u^* \beta_K s^2}, \quad \delta = \frac{2 f_K}{\beta_K s} \qquad (8.14)$$

Introducing the transformation

$$\xi = \left(\frac{\beta_K^{3/2} s^3}{U^{*1/2} g'^{1/2}} \right)^{1/2} \overline{X}, \qquad (8.15)$$

equation (8.13) becomes

$$\left(\frac{\partial \bar{\psi}}{\partial \xi}\right)^2 = 2 [\varepsilon + \delta\bar{\psi} + 2 \bar{y}\bar{\psi} - \bar{y}^2]$$

$$\{[\varepsilon + \delta\bar{\psi} + \bar{\psi}^2]^{1/2} - [\varepsilon + \delta\bar{\psi} + 2\bar{y}\bar{\psi} - \bar{y}^2]^{1/2}\} \qquad (8.16)$$

In this form all the parameters of the problem appear in the two dimensionless groupings ε and δ only. The meaning of δ is evident. The significance of ε is readily seen from equation (8.6). In terms of the dimensionless variables we have

$$D^2 = D^{*2} + \frac{2\,(f_K + \beta_K s\bar{y})}{g'}\,U^* s\bar{\psi} - \frac{U^*\beta_K s^2\bar{y}^2}{g'} \tag{8.17}$$

Thus $U^*\,\beta_K s^2/g'$ is a measure of the change of the square of the depth along a streamline and $\varepsilon^{1/2}$ is the ratio of the characteristic depth D^* to the characteristic change of depth.

In Section 7 the equations were applied to the homogeneous ocean by neglecting the variation in depth. Hence, it is to be expected that equation (8.16) will yield the solution for the homogeneous ocean when $\varepsilon \gg 1$; i.e. as far as the boundary region is concerned, a two-layer model, the depth of whose upper layer is very great compared to the change of that depth, behaves like a homogeneous model. The approximate analytical solution for $\varepsilon \gg 1$ is obtained in the following manner. The first bracket on the right-hand side of equation (8.16) is approximated by ε. The expressions inside each of the other brackets are divided by ε and the brackets expanded in binomial series retaining terms of order ε^{-1}. This yields

$$\left(\frac{\partial\bar{\psi}}{\partial\xi}\right)^2 \approx \varepsilon^{1/2}(\bar{y} - \bar{\psi})^2 \tag{8.18}$$

Imposing the boundary condition $\bar{\psi}\,(0, \bar{y}) = 0$, the solution of equation (8.18) is

$$\bar{\psi} = \bar{y}(1 - e^{-1/4\,\xi}) \tag{8.19}$$

which becomes identical with the solution obtained previously (equation 7.17) upon transformation to the appropriate variables.

If we deal with a homogeneous ocean, ε will in general be large because $g' = g$ and this quantity is of the order of 500 times as great as g' in a usual two-layer model. If we deal wthi a two-layer model ε may be made large by making D^* large. The preceding analysis

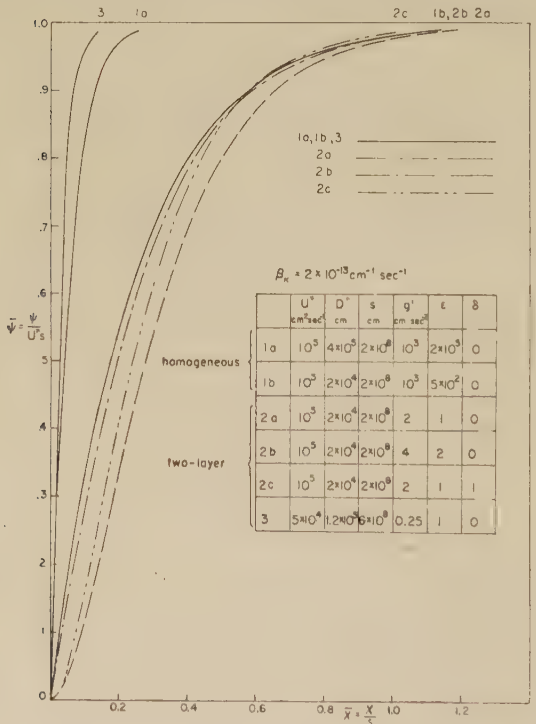

Fig. 2. Dimensionless transport function $\bar{\psi}$ vs. dimensionless distance from western coast at northern boundary of region I_b for various values of the pertinent paramaters.

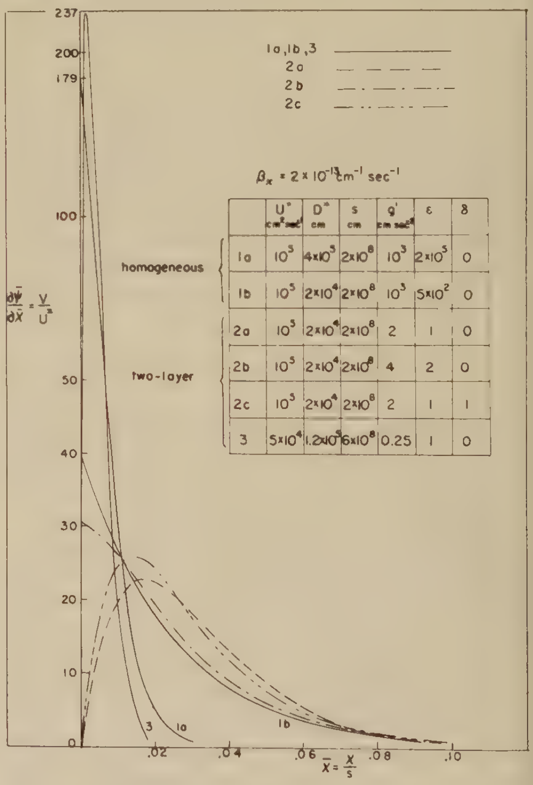

Fig. 3. Dimensionless northward transport vs. dimensionless distance from western coast at northern boundary of region I_b for various values of the pertinent parameters.

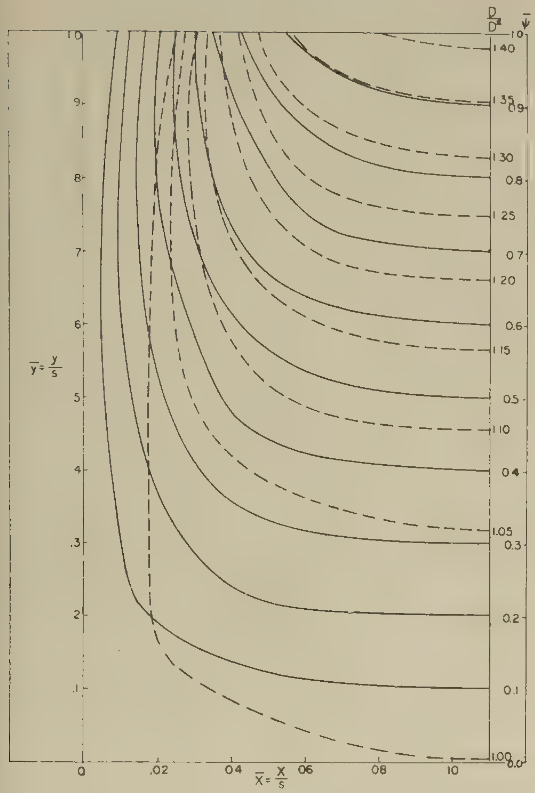

Fig. 4. Constant depth lines (dashed) and "transport" lines (solid) in region I_b for case 2a of Figs. 2 and 3 corresponding approximately of the formation of the Gulf Stream.

shows that in terms of the variables of equation (8.16) the boundary solutions $\bar{\psi}$ for a homogeneous ocean and a two-layer model are identical provided ε is large and has the same value in the two cases.

Equation (8.16) has been solved numerically for various values of ε and δ and pertinent results are plotted in Figures 2 to 4.

Figure 2 shows the variation of the dimensionless transport function $\bar{\psi}$ with dimensionless distance $\bar{X}$ from the coast at the northern boundary of region I_b. The magnitudes of β_K, U^*, s, g', D^*, ε (see legends of Figs. 2, 3) for Curve 2a correspond to a baroclinic model of the Gulf Stream except for the fact that the southern boundary of the region I is at the equator ($\delta = 0$). The width of the Stream is, say, 150 km, a very reasonable value. Curve 2c represents the same situation with $\delta = 1$, i.e. with the southern boundary at approximately 15° latitude. This northward shift of the southern boundary tends to produce a somewhat narrower stream, but the effect is quite small. Curve 1b corresponds to a homogeneous ocean with the values of U^*, D^*, s and δ equal to those of the upper layer of the two-layer model of Curve 2a. These curves thus afford a revealing comparison of the behavior of the two models. The widths of the Streams are practically the same. Thus, the question of whether the bottom surface is solid, or an interface between two layers of slightly different density in a baroclinic model, does not have much bearing on the formation of the Stream and its width. Another interesting comparison may be made between Curves 2a and 1a, the latter (see Section 7) corresponding to a homogeneous ocean whose depth is that of the total two-layer model with the same values of U^*, s, and δ and which therefore represents the Stream that would exist if the motion were barotropic.

Curve 2b represents the same situation as 2a except that the density difference is double. Comparison of the two curves demonstrates the relative insensitivity of the stream formation to this factor.

Curve 3 applies to an ocean with the same values of ε and δ as 2a but different U^*, s, g', D^*. The drastic decrease in the width of the current may be seen from equation (8.15) to be due primarily to the increase in s.

In Figure 3 the dimensionless transport $\partial\bar{\psi}/\partial\bar{X}$ is plotted against $\bar{X}$ for the systems discussed above. The transport shows a general tendency to decrease monotonically with $\bar{X}$ due to the decrease in velocity. This tendency, however, is counterbalanced by the monotonic increase of the depth, so that in some cases the transport first increases to a maximum and then decreases. This is the case in 2a, 2c and 3 where the transport starts from zero due to the fact that the depth vanishes at $\bar{y} = s$, $\bar{X} = 0$ in these cases; (see the following discussion of this point). The narrow streams of cases 1a and 3 give rise to very large transports extending over a very narrow region. The transport adjacent to the coast in the homogeneous model 1b is much greater than that in the corresponding baroclinic model 2a due to the latter's very small depth near the coast. The transport in 1b drops off much more rapidly with $\bar{X}$, however, so that the widths of the streams are about equal (Fig. 2).

Figure 4 represents a typical pattern of transport and constant depth lines (case 2 a). The transport lines near the coast tend to bend away from the latter after first approaching it due to the decrease in depth near the coast. This decrease tends to cut down the transport near the coast and hence to force the stream seawards.

Our results indicate that the density stratification influences certain aspects of the stream formation, but that it is a modifying factor rather than a fundamental one insofar as our problem is concerned. One important point must be discussed in this connection, however.

Equation (8.17) shows that, for fixed y, the depth is smallest at the boundary and that it becomes zero when

$$\bar{y} = \varepsilon^{1/2} \text{ or } y^2 = \frac{D^{*2} g'}{U^* \beta_{Ks}} \qquad (8.20)$$

Thus, if $\varepsilon < 1$, the solution cannot be valid for $\bar{y} > \varepsilon^{1/2}$ and the value $\bar{y} = \varepsilon^{1/2}$ might be interpreted as the latitude north of which a new regime of flow must take over. Since the velocity remains non-zero at that point we must actually except that the solution will break down at some distance south of $\bar{y} = \varepsilon^{1/2}$.

The preceding remarks apply to the behavior of the boundary solution when an arbitrarily fixed transport U^* with arbitrary depth D^* at $y = 0$ flows into the boundary region. If, however, we require that the boundary solution be matched to an interior solution the validity of which is to extend up to the eastern shore, then D^* and U^* are not independent. From equation (8.2)

$$C(L) = D^{*2} \approx D_a^2 + \frac{2 W a \sin K}{\varrho g'} \qquad (8.21)$$

whence, using the definitions of ε and U^x,

$$\varepsilon = \frac{D^{*2}}{D^{*2} - D_a^2} \qquad (8.22)$$

Hence, in this case $\varepsilon \geqslant 1$ and takes on its smallest value, one, only in the extreme case when $D_a = 0$. Since the meridional transport is independent of x in the interior, this extreme case would imply infinite meridional velocity at $x = a$.

It is worth noting that when the model under investigation does not represent an enclosed ocean, but rather a system in which northward flow is allowed to enter the stream across the boundary $y = 0$ so that the value of ψ on the western shore is negative, then, from equation (8.17), the depth will become zero for a value of $\bar{y}$ which is smaller than $\varepsilon^{1/2}$, so that the solution may break down for $\bar{y} < 1$ even if it is matched to an interior solution which is valid right up to $x = a$. It appears that this breakdown of the solution when ε is sufficiently small constitutes the major difference in the dynamics of the streams in a two-layer and a homogeneous model.

The theory predicts that the meridional velocity is a maximum at the western shore. This appears to violate completely the condition that a viscous fluid should adhere to a solid boundary, a condition which was specifically excluded by our approximate analysis. This violation becomes less serious than appears at first sight when one considers that the boundary may be interpreted as a water boundary with the region between the stream and the coast acting as sub-layer similar to the laminar sub-layer encountered in turbulent boundary layer flows.

Acknowledgment

The author wishes to express his gratitude to Mr. Henry Stommel of the Woods Hole Oceanographic Institution for the comments and advice offered in the course of valuable discussions without which this investigation would not have been possible.

REFERENCES

Charney, J. G., 1955: The Gulf Stream as an inertial boundary layer. *Proc. N.A.S.* (USA). **41**, No. 10, pp. 731–740.

Montgomery, R. B., 1940: The present evidence on the importance of lateral mixing processes in the Ocean. *Bull. Amer. Met. Soc.* **21**, p. 87.

Munk, W. H., 1950: On the wind-driven ocean circulation. *J. Met.* **7**, p. 79.

Munk, W. H., and Carrier, G. F., 1950: The wind-driven circulation in ocean basins of various shapes. *Tellus*, **2**, No. 3, pp. 158–167.

Stommel, H., 1955: Discussion published as a supplement to the *Journal of Marine Research*, **14**, No. 4. Also, "Why do our ideas about the ocean circulation have such a peculiarly dream-like quality?", April 1954.

Sverdrup, A. U., 1947: Wind-driven currents in a baroclinic ocean with application to the equatorial currents of the Eastern Pacific. *Proc. N.A.S.* (USA) **33**, p. 318.

PRINTED IN SWEDEN
ESSELTE, STHLM 56

Contribution No. 814

Deep-Sea Research, 1956, Vol. 3, pp. 178 to 188. Pergamon Press Ltd., London.

A contribution to the natural history of the white-tip shark, *Pterolamiops longimanus* (Poey)

RICHARD H. BACKUS*, STEWART SPRINGER† and EDGAR L. ARNOLD, Jr.‡

(*Received* 12 *January*, 1956)

Abstract—Until recently little has been known about the common, pelagic shark, *Pterolamiops longimanus*. Data gathered during recent offshore cruises show it to be abundant and widely distributed in the warm waters of the western North Atlantic. It occurs at a wide range of salinities but withdraws from some waters when the temperature gets as low as about 21°C. It is rarely present in water shallower than about 100 fathoms. In a sample of 110 sharks few were over 250 cm in total length, although the maximum size reported in the literature is much longer. Fish and cephalopods are the most frequent food items in white-tip stomachs. White-tips are cautious, persistent, and sluggish in their behaviour. They are responsible for considerable damage to long line caught tuna in the Gulf of Mexico. Geographical sexual segregation is a feature of white-tip life history. Fragmentary data indicate that the mating and pupping season is in the late spring or early summer and that the gestation period is about one year. Females probably first mate at a length of about 200 cm, and probably bear young in alternate years thereafter. The number of pups per litter varies from 2 to 9 with a mean of about 6. Shark suckers (*Remora remora*), pilotfish (*Naucrates ductor*), dolphin (*Coryphaena hippurus*) and a copepod parasite or parasites are common associates of the white-tip.

INTRODUCTION

RECENTLY, BIGELOW and SCHROEDER (1948), in their monograph " Sharks," wrote of the white-tip, " Astonishingly little is known of the habits of *longimanus*, considering that it is one of the members of its genus that has been recognized the longest."

That this is true is probably explained by the animal's rather strict oceanic habit which makes it largely unavailable to seaside naturalists. However, with an increasing number of offshore surveys it is becoming better known. MATHER and DAY (1954) found it to be widespread, abundant, and the commonest pelagic shark in the warm parts of the North Atlantic. BULLIS (1955) regards this shark as responsible for most of the damage to long line-caught tuna in the Gulf of Mexico, although it was quite unknown from that area prior to an investigation of offshore waters begun in 1950 by the U.S. Fish and Wildlife Service.

Although BIGELOW and SCHROEDER (1948) also assume the white-tip to be common in the Mediterranean on the basis of statements by MÜLLER and HENLE (1841), GÜNTHER (1870), DODERLEIN (1881), and others, TORTONESE (1951) states that its presence there is not now demonstrable by museum specimens or other verifiable records. MAUL (1955) records the species from Madeira.

The authors have been gathering data on the Atlantic white-tip shark independently during the course of other work for the past few years. BACKUS has made observations from the Research Vessels *Atlantis* and *Bear* of the Woods Hole Oceanographic

---

[*] Woods Hole Oceanographic Institution, Woods Hole, Mass. (Contribution No. 814 Woods Hole Oceanographic Institution).

[†] U.S. Fish and Wildlife Service, Washington, D.C.

[‡] U.S. Fish and Wildlife Service, Galveston, Texas.

Institution, and SPRINGER has made observations from the Exploratory Fishing Vessel *Oregon* of the U.S. Fish and Wildlife Service. ARNOLD has furnished records of captures made from the U.S.F.W.S. Vessel *Alaska* and from recent cruises of the *Oregon*. In many cases, in the absence of the authors, fishing was done and records kept by co-workers or crew members of the above vessels. Furthermore, we have used records furnished by W. W. ANDERSON of captures made from the U.S.F.W.S. Research Vessel *Theodore N. Gill*, and Mr. WILLIAM C. SCHROEDER of the Woods Hole Oceanographic Institution has given us records of captures from *Caryn* and *Cap'n Bill II*. Because of this diversity of sources, our data vary in their completeness and do not show the geographic distribution of the fishing effort which produced them.

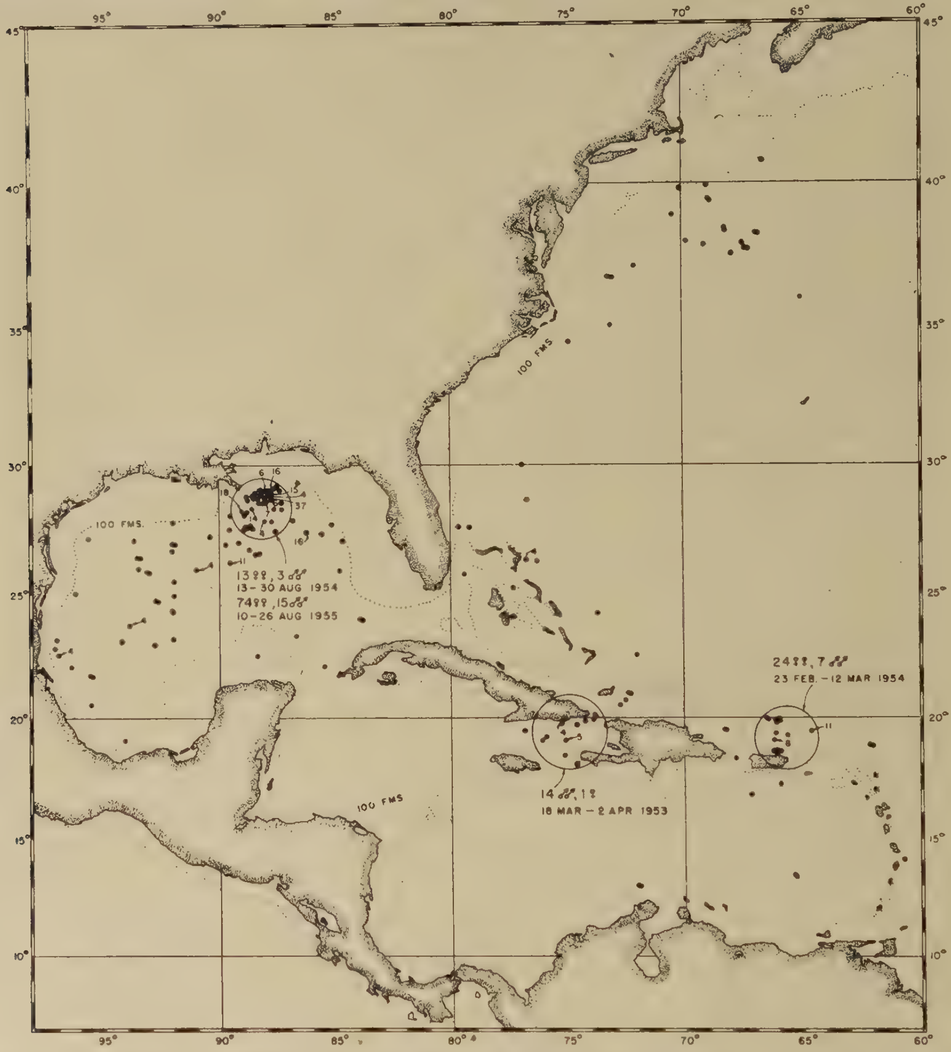
95°
90°
85°
80°
75°
70°
65°
60°
45°
40°
35°
30°
25°
20°
15°
10°
100 FMS.
100 FMS
100 FMS
6
16
18
15
37
14
16
11
13♀♀, 3♂♂
13 – 30 AUG 1954
74♀♀, 15♂♂
10 – 26 AUG 1955
24♀♀, 7♂♂
23 FEB. – 12 MAR 1954
11
8
5
14♂♂, 1♀
18 MAR – 2 APR 1953

Fig. 2. Distribution of white-tip shark captures. The scanty literature records are omitted. Three areas in which sexual segregation has been noted are encircled. All captures save one are outside the 100-fathom curve.

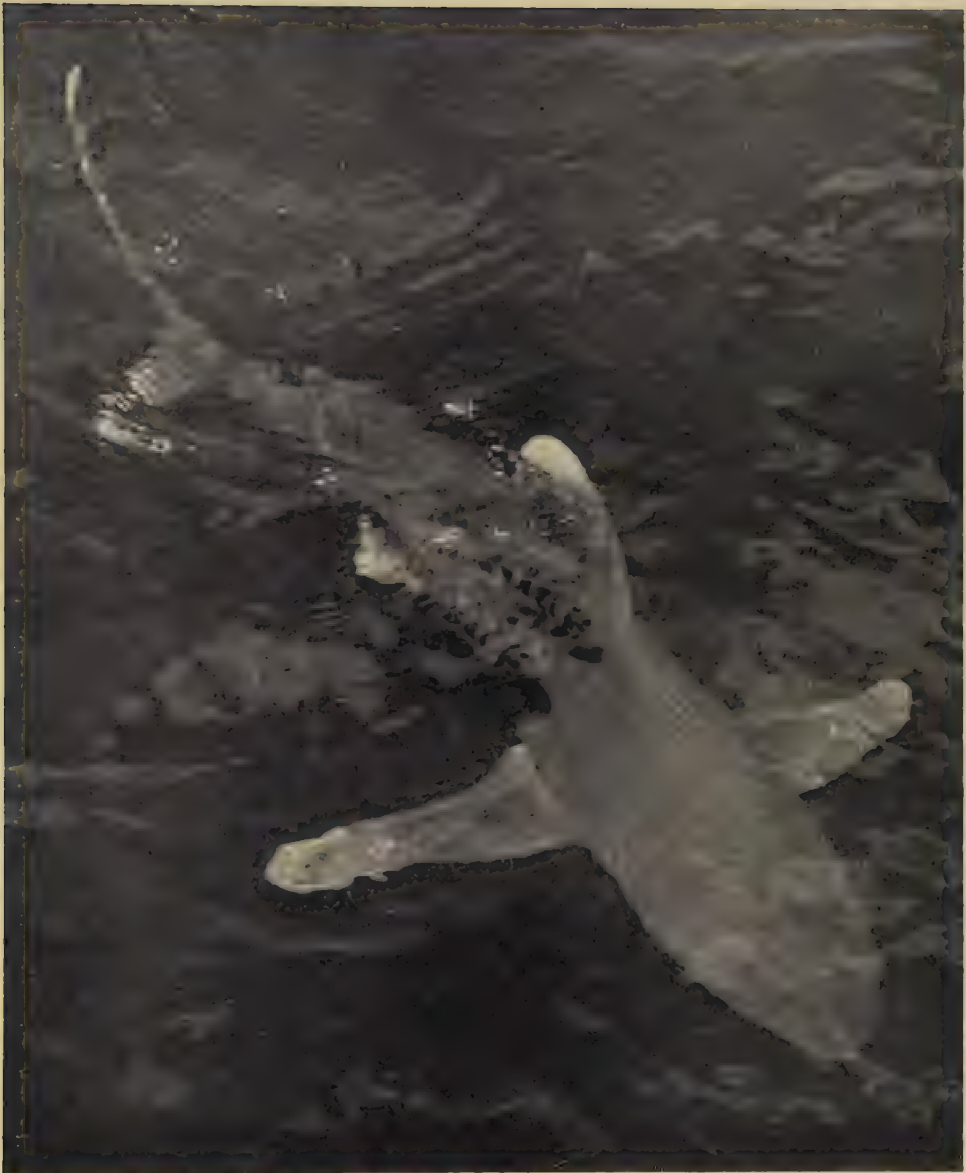

Fig. 1. White-tip shark (*Pterolamiops longimanus*) with two pilotfish, photographed at sea by JAN HAHN, Woods Hole Oceanographic Institution.

Our records (Fig. 2) are mostly from hand line and long line captures near the surface, but some sight records are included. Statements concerning the absence of white-tips from inshore waters and from parts of the Straits of Florida are largely made on the basis of SPRINGER's observations during commercial shark fishing operations on the continental shelf off Florida, in the Gulf of Mexico, off the Caribbean coasts near Nicaragua and Trinidad, and off the coasts of the Guianas between 1930 and 1949.

NOMENCLATURE

The species included in *Carcharhinus* as previously understood (see BIGELOW and SCHROEDER, 1948) were divided into three genera in a recent revision of western-Atlantic Carcharhinidae (SPRINGER, 1950a ; 1951). A primary division of these sharks was based on the presence or absence of a median, longitudinal ridge in the skin between the first and second dorsal fins. *Carcharhinus* was retained for the smooth-backed members of the older genus. The ridge-backed members were divided between *Eulamia* (with acuminate first dorsal and pectorals) and *Pterolamiops* (with broadly rounded first dorsal and pectorals). The white-tip belongs to the latter genus in this classification.

In general, though observations have not covered all species, the large ridge-back, carcharhinid sharks in the western North Atlantic are oceanic, although they may at times range into coastal waters. Conversely, western North Atlantic observations from off the shelf are lacking for any smooth-backed carcharhinids excepting two doubtful observations of *Negaprion brevirostris* (Poey). The smooth-backed species of the genus *Carcharhinus* (as restricted by SPRINGER) are shallow water species particularly abundant near mouths of large rivers. *Eulamia* contains sharks of the reefs, the outer parts of the continental shelf, and, to some extent, the high seas. *Pterolamiops* is strictly pelagic.

Field identification of the white-tip shark is easily made because it is the only large carcharhinid having a high first dorsal that is broadly and evenly rounded at its apex. The very large pectorals with broadly rounded tips are also distinctive. The middorsal ridge is readily observed in freshly caught late embryos, young, and adults, but its existence in preserved ones cannot always be demonstrated. Usually the pectorals and the first dorsal are tipped with white, but the amount of white showing is variable and its complete absence is fairly common. Black tips on the pelvics, second dorsal, anal, and lower caudal characterized a young example collected off Tampico, Mexico. This distribution of black spots is shown in MAUL's figure (1955, Fig. 9). The black spots, if regularly present in young white-tips, tend to disappear in preserved specimens, and become obscure in living white-tips as they approach maturity. The pectorals and first dorsal fin of the Tampico specimen were not white-tipped, although the first dorsal was somewhat lighter near the tip.

DISTRIBUTION

BIGELOW and SCHROEDER (1948) suggested that the physical factor which primarily determines the distribution of this " . . . more strictly pelagic . . . " shark is salinity. Data available to them indicated that this animal was not found at salinities lower than about 35·5‰. They concluded that its offshore habit was at least in part caused by an avoidance of low salinities. Thus they explained the absence of the white-tip along the east coast of the United States in summer where it might be expected on the basis of temperature alone.

Our records show that the white-tip occurs over a wide range of salinities. In 29°N, 88°W, for instance, where we have many records for July and August, the salinity may be lower than 28‰ (Dept. of Oceanography, A & M College of Texas, 1954). Furthermore, on the basis of salinity we cannot explain the absence of the white-tip from the northern and western side of the Gulf Stream in its passage through the Straits of Florida and northward along the Florida coast past the Bahamas (where the salinity is high). The area from Key West to off Palm Beach, Florida, was fished extensively by commercial shark fishermen from 1935 to 1949 using bottom set lines. Although the white-tip is apparently not available to bottom lines, regular trails of offshore fishing using floating lines were carried on. The only record of capture of a white-tip by a commercial boat was from the eastern side of the Gulf Stream near Bimini. We have caught the white-tip from early June to late October north of Cape Hatteras and west of the Gulf Stream. While we have not fished much in this region during the cold season, it seems probable that the white-tip withdraws to the south and east at this time. We have noted a withdrawl from the northern Gulf of Mexico when the waters there were cool. This may begin as early as December. In 1955 the most noticeable change in the shark fauna here occurred about 1 February. Sea surface temperatures at this time in the northern Gulf (over water deeper than 100 fathoms) are in the neighbourhood of 70°F (FUGLISTER, 1947). The withdrawal of the white-tip is accompanied by an offshore movement of some of the larger inshore sharks, notably *Galeocerdo cuvier* (Lesueur) the tiger shark, and several species of *Eulamia.*

Our records show that white-tips are ordinarily present in the surface waters where depths exceed 100 fathoms, but that they occasionally move into the adjacent shallower water. We suggest that the controlling factor is competition for food with other species of sharks which places the relatively slow-moving white-tip at a disadvantage.

The northernmost record for the white-tip in the western Atlantic, so far as we know, is for one taken in 40° 43′N, 66° 39′W on 25 July, 1953 (Fig. 2). SCHUCK and CLARK (1951) report a specimen taken in 40° 40′N, 57° 02′W on 12 June, 1950.

It has been generally supposed that the blue shark (*Prionace glauca*) is the abundant, widely-distributed, warm-water, oceanic shark. While gathering our white-tip records (Fig. 2) only one blue shark (a male, 295 cm, from between Santiago and Cabo Cruz, Cuba, 19° 30′N, 76° 50′W on 25 April, 1955) was seen by us in the area of the chart south of latitude 32°N. Published records within this area as given by BIGELOW and SCHROEDER (1948) include one each for St. Thomas, Cuba, and Miami, although HOWELL-RIVERO reported it as often seen around Cuba (in a personal communication also cited by BIGELOW and SCHROEDER). MATHER and DAY (1954) reported only 2 blue sharks (as compared with about 30 white-tips) in the wide area of the southern North Atlantic for which they had observations. This raises the point as to what the source is in the North Atlantic from which male blue sharks invade the waters off our northeast coast in such abundance in the summer.

SIZE

Very few sharks over about 250 cm or under about 150 cm in total length were caught. Since white-tips are born at a length of about 65-75 cm (BIGELOW and

SCHROEDER, 1948) it is apparent that we have not sampled a large part of the population (75-150 cm in length) (Fig. 3). It might be argued that our hooks are too large to catch the smaller sizes, but we discount this since we have caught small specimens of other species. Furthermore, it is certain that we would see the smaller sizes swimming about the vessel and nosing the baits if they were present. A young white-tip 102 cm in total length was taken near Tampico, Mexico, in late January from a long line set near the surface where the water depth was 1,200 fathoms. No long line fishing was carried on south of this point during the winter or early spring. Some other carcharhinids (e.g. *Negaprion brevirostris*, the sub-tropical lemon shark) resort to restricted nursery areas to bear young. It is possible that we would have taken more specimens in the 75-150 cm size if we had fished in the southerly parts of the species' range in the fall and early winter. The extremely rapid growth of sharks in warm-water nursery areas may well explain the absence of specimens of this size in our collections (made mostly in the spring and summer) as has been noted for *Negaprion*, (SPRINGER, 1950b).

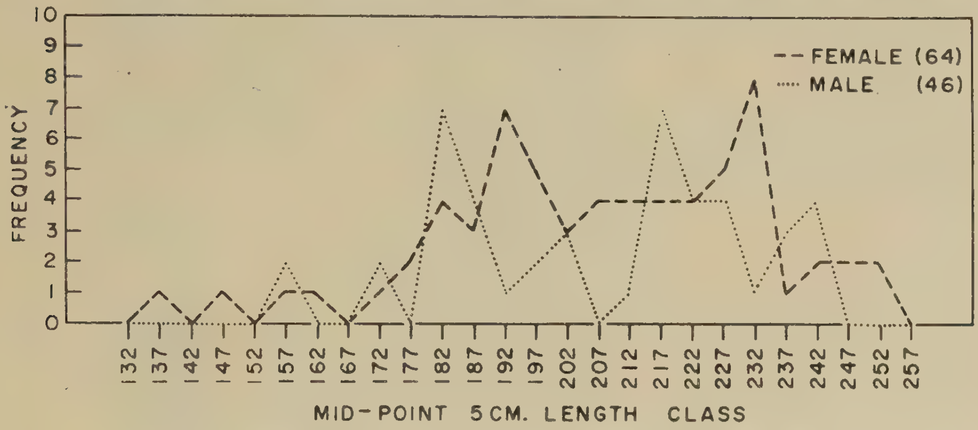

Fig. 3. Length-frequency distribution of a sample of white-tip sharks.

The longest white-tip for which BIGELOW and SCHROEDER (1948) had exact measurements was 350 cm long. This is considerably longer than our longest specimen. BIGELOW and SCHROEDER write that 12 to 13 feet (365–395 cm) is considered the maximum size, but that it is probable that an even larger size may be attained. Our data are insufficient to establish the size range of the species. However, in connection with the extremely large specimens mentioned above, a condition parallel to that found in the great hammerhead shark (*Sphyrna tudes*) is suggested. Unpublished measurements by SPRINGER of a series of adult great hammerheads show that a small percentage of the females are very much larger than the bulk of the adult breeding population. This and other observations support the possibility that some of the extreme size records for sharks persistently referred to in the literature are valid but are based on abnormal individuals, apparently always females. A false idea of the abundance of such sharks becomes established because these individuals, though solitary, eventually wander out of normal ranges into shallow water where they are easily caught. Furthermore, the capture of especially large sharks excites so much interest that they receive a disproportionate amount of attention in the literature.

A male white-tip 204 cm long weighed 60–65 kg (135–145 lb).

FOOD

Eighty-eight white-tip stomachs have been examined. Forty-one of these contain food, although a number contained only a cephalopod beak or two. It is possible that cephalopod beaks resist digestion to a greater degree than anything else that the shark ordinarily eats. This may bias the following data : Cephalopoda – in 19 stomachs ; fish – 20 (including blackfin tuna and another scombrid fish, barracuda, look-down (*Selene*), and a white marlin about 250 cm with no evidence that it had been taken from a long line) ; garbage – 13 ; sargassum and other seaweed (probably accidental) – 4 ; unidentified animal remains – 1 ; unidentified sea bird – 1 ; Crustacea – 1.

Only a few white-tips taken on tuna long lines are included above. In general the latter had empty stomachs or contained only tuna or bait used for the tuna. One stomach contained several pounds of oil.

BEHAVIOUR

White-tips almost always exhibit some suspicion of a baited hook. They generally make several passes at a bait before taking it. Between these passes they may swim away 50 to 100 yards. On 18 March, 1953, between captures (0915-1315) in the Windward Passage, there were about 6 white-tips around the vessel continuously. These were nosing baited hooks and would not take them although they immediately engulfed similar baits not on hooks.

Although white-tips exhibit a cautious approach to objects suspected of being edible they are remarkably persistent. A great deal of effort has been wasted by the crew of the *Oregon* in attempting to drive white-tips away from the vessel while long lines were being hauled. The long line is hauled as the vessel moves slowly forward and the line with the catch is taken over the side. A few white-tips usually gather within ten to fifty feet of the stern but swim forward and downward at the approach of a hooked tuna. The tuna come from ten or more fathoms and are not visible from the vessel when the sharks seem to detect their presence. The sharks meet the tuna more than thirty feet from the vessel and get one or more bites before the tuna can be landed. White-tips are commonly caught on the long lines and may occasionally attack spent or dying tuna on the lines before they are hauled. However, more of the shark damage well below the surface in the Gulf of Mexico results from attacks by silk sharks (*Eulamia floridana*), mako sharks (*Isurus oxyrinchus*), and occasionally by other species of *Eulamia*. All of these sharks are numerous enough to be a serious problem for tuna fishermen. We have not seen the mako sharks at the surface except when they come up on a hook or hanging onto a tuna, but silk sharks in the Gulf of Mexico are often numerous when sets are made near the continental shelf and permit comparative observations. The silk sharks are less bold than the white-tips but are much faster. Consequently, if baits are being thrown overboard in large quantities when both species are present, the white-tips get most of the baits close to the boat but the silk sharks get all of those that sink rapidly or drift some distance from the vessel. Several times we have seen a silk shark and a white-tip of about equal size in competition for the same discarded fish. If the white-tip was close enough, it got the fish by driving the silk shark away.

The white-tip does not leap when hooked and puts up a relatively feeble resistance to capture. In this respect it is comparable to the blue shark. The silk shark shows

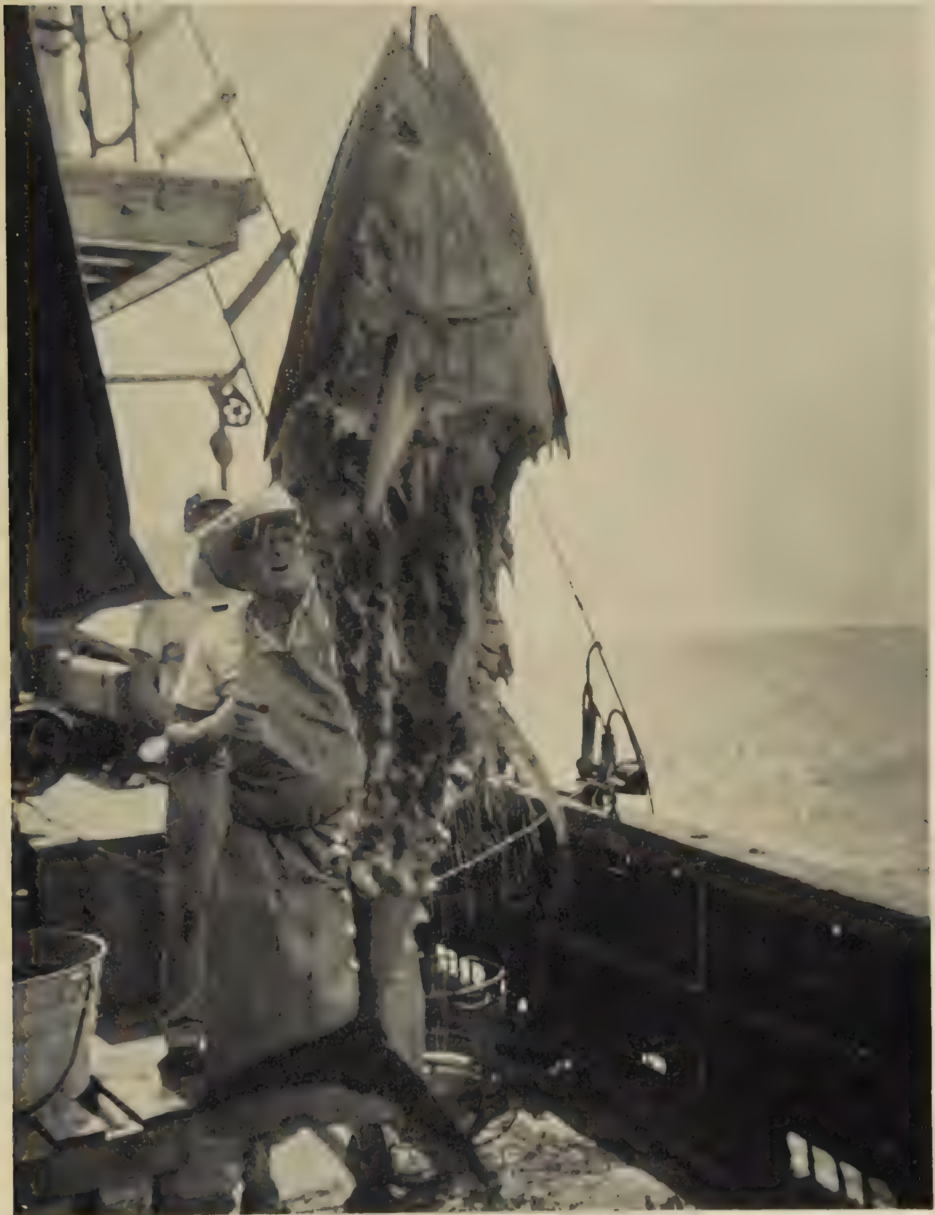

Fig. 4. Long line-caught bluefin tuna showing damage by white-tip sharks. This tuna weighed about 500 pounds before being attacked. Photo by ARNOLD.

much more speed and power than a white-tip, but once on deck the latter is more troublesome. On a few occasions white-tips have been observed to be capable of at least short bursts of speed. We have attempted to use a type of firecracker, generally known as a cherry-bomb, to drive sharks away from the vessel. The cherry-bomb was put inside a fish, the fuse lit, and the assembly tossed overboard. Due to the deliberate appraisal of the bait by the white-tip this was not often successful. The premature explosion merely caused the shark to move off a few feet, than to resume its patrol. On one occasion, however, a white-tip picked up a fish with a slow fuse and the bomb exploded in its mouth. Smoke and bits of fish blew out of its gill openings, and the shark exhibited a creditable speed in moving away.

Recently, six or seven white-tips were around the *Oregon* as long line-caught white-tips were being killed and thrown overboard. The dying specimens were never attacked although as they sank they were followed out of sight by other white-tips. Even floating livers were untouched. This reaction to livers is not typical however, as we have often used them as bait on hand lines to catch other white-tips.

When white-tips swallow objects immediately at the surface the top part of the head is lifted well out of water. On one occasion when one of us was dangling a bait in front of a shark hard by the vessel's side it made many attempts to swallow the bait before it succeeded. Such exhibitions of clumsiness make one wonder how this animal can capture live fish and cephalopods and how one (which we identified from portions of its teeth) could strike a plastic encased instrument which was being towed at night at a speed of several knots. We might say in this connection that white-tips appear to be equally active by day and night.

SEXUAL SEGREGATION

Two types of sexual segregation are known in sharks. A " behavioural " type is exemplified by the tendency of individuals of the spiny dogfish (*Squalus acanthias*) to school with others of like size, the species sorting into aggregations of large mature females ; mature males of medium size ; immature females of medium size ; or small fish of both sexes (FORD, 1921). That a given school tends to be of one sex had been noted by earlier authors (MEYER, 1875 ; SMITT, 1895 ; and BORCEA, 1906).

FORD also described what can be called " geographical " segregation in the rough-dog (*Scyliorhinus caniculus*). Several thousand specimens examined at Plymouth showed that males predominated in the winter (a peak predominance of about 65%) while females predominated in the summer (a peak of about 58%).

Geographical segregation was described by RIPLEY (1946) for the soupfin shark (*Galeorhinus zyopterus*). He showed that the sexes were generally unequally represented as a function of area or of depth in four California fishing areas. That this phenomenon exists in the blue shark (*Prionace glauca*) is indicated by BIGELOW and SCHROEDER (1948) who in writing of summering fish off northeastern United States and Canada say, " . . . few, if any, females take part in this yearly incursion . . . "

We have some information showing that geographical sexual segregation is also a feature of the life history of the white-tip. In an area in the northern Gulf of Mexico whose radius is about 75 miles, 13 females and 3 males were caught during 13–30 August, 1954. A similar ratio (74 females to 15 males) was found in the same area during 10–26 August, 1955. In an area between Cuba, Hispaniola, and Jamaica with a radius of about 90 miles, 15 white-tips were caught during 18 March – 2 April, 1953, 14 being males. In an area of about 80 miles in radius north and east of Puerto Rico 24 females and 7 males were caught during 23 February – 12 March, 1954 (see Fig. 2).

The geographical segregation phenomenon is not understood, but may be related to the existence of favoured pupping areas in which females tend to congregate seasonally.

REPRODUCTION

The fragmentary data available (Table 1, Fig. 5), suggest that both mating and pupping take place in the late spring or early summer and that the gestation period is about one year.

Table 1.

Locality	*Date*	*Number of litters*	*Total number of specimens*	*Approx. mean total length*	*Authority*
Northeastern Gulf of Mexico	13 Aug., 1951	1	7	150	Backus, Springer and Arnold
Northern Gulf of Mexico	14–16 Aug., 1951	2	16	65	,,
Northern Gulf of Mexico	26–28 Aug., 1951	2	14	160	,,
38° 25′N, 68° 07′W	24 Sept., 1955	1	4	240	,,
Central Gulf of Mexico	15 Dec., 1954	1	4	410	,,
Northern Gulf of Mexico	13 Jan., 1955	1	4	465	,,
North of Puerto Rico	23 Feb.–1 Mar., 1954	6	33	440	,,
Trinidad Islet (20°S, 29°W)	8 April, 1913	1	1	670	Nichols and Murphy (1914)
28° 40′N, 78° 46′W	3 May, 1886	1	5	520	U.S. National Museum (courtesy L. P. Schultz)

We have noted two conditions of the oviducts in females without pups. In some females (generally the smaller ones) the oviducts are approximately circular in cross-section and about 10–15 mm in diameter. The oviducts are hard and the lumen is not very evident. The oviduct is held close to the dorsal wall of the body cavity by a narrow mesentery. Females in this category, which we presume are nulliparous, measured 173, 180, 189, 192, 198 and 198 cm ($\bar{x} = 188{\cdot}3$) during 23 February – 23 March, 1954 (the only period during which we have made this type of observation).

In other females (generally the larger ones) the oviducts are flattened and measure about 30–40 mm from edge to edge. They are soft and limp, and the lumen is conspicuous. The oviduct lies loosely in the body cavity suspended by a wide mesentery. We presume these females to have previously borne young. During

23 February – 23 March, 1954, such females measured 192, 209, 215, 216, 221, 230, 232, and 246 cm ($\bar{x} = 221{\cdot}2$).

Females with pups measured during this same period were 189, 205, 207, 212, 225, and 241 cm ($\bar{x} = 213{\cdot}2$).

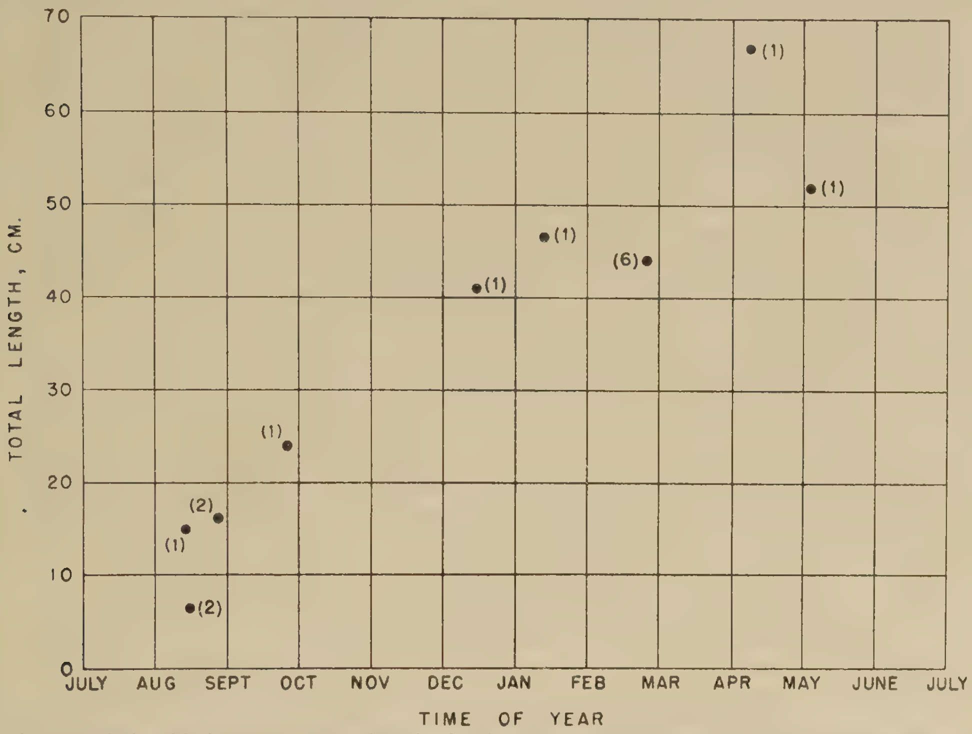

Fig. 5. Relationship between average length of embryos and time of year. The number in parentheses by each point indicates the number of litters used in arriving at the mean length.

Our original interpretation of the stretched oviducts was that females possessing them had recently dropped young. But since pregnant females at the same time were all carrying pups much smaller than the known maximum size, we no longer favour this notion. Moreover, females with stretched oviducts had large ovarian eggs measuring 25–45 mm in diameter (except one with very small eggs), while pup-bearing females had much smaller eggs (the largest being 10–15 mm in diameter). This suggests the possibility that females with stretched oviducts at this season are those that bore young the previous summer and that will mate again in the coming summer. We presume that pregnant females (with small eggs) would not mate during the coming summer.

The nulliparous females were of such a size that they could be expected to mate during the coming summer. Some of them bore ovarian eggs 10–15 mm in diameter, but some had very small eggs. None had eggs comparable in size to those of the larger non-pregnant females.

There is a good correlation (Fig. 6) between the length of the mother and the number of pups she bears ; the greater the length, the greater the number of pups. The number of pups per litter in our series (15 litters) varies from 2 to 9 with an average of about 6.

In one litter of 9, 8 embryos measured from 495 mm to 595 mm, while the ninth measured only 240 mm. It was noted that the pseudoplacental connection was lacking between the small specimen and the mother.

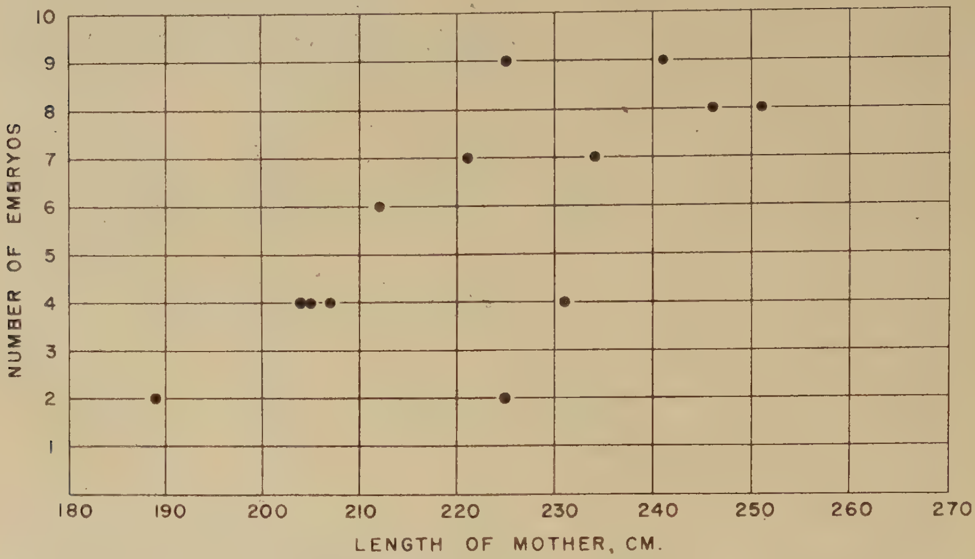

Fig. 6. Relationship between length of mother and the number of young she bears.

ANIMAL ASSOCIATES

One to 3 shark suckers (*Remora remora*) are generally attached to white-tips. They adhere so persistently that they are taken with the shark unless scraped off as the latter is pulled in over the rail. We have frequently seen them adjust their position on the shark with a rapid wriggling motion while the latter was being boated.

Often 1 or 2 pilotfish, *Naucrates ductor*, are in company with the white-tip (see Fig. 1). They generally swim a little above and behind the shark's first dorsal fin. They swim nervously back and forth near the shark after the latter has been hooked.

On several occasions we have seen one or several dolphins (*Coryphaena hippurus*) (8-10 on one occasion) swimming with the shark. They are generally to the rear or one side of the shark and by no means follow his movements as closely as the shark pilot. SCHUCK and CLARK (1951) in reporting their capture of a white-tip wrote that the stomach contained a dolphin, and they speculate as to the condition of the dolphin when captured. They also report the absence of dolphins in the immediate area of the capture of the shark, the implication being that dolphins avoid the latter.

A copepod parasite (or parasites) which is superficially attached to the white-tip's skin is frequent and often numerous.

Acknowledgements—We are indebted to Capt. W. SCOTT BRAY, First Mate A. D. COLBURN, Boatswain CARL SPEIGHT, former Radioman THOMAS LYON and many seamen of the R/V *Atlantis* for help in gathering many of the shark records.

Dr. H. B. BIGELOW, Mr. W. C. SCHROEDER, Mr. W. E. SCHEVILL, and Mr. MALCOLM S. GORDON read and helpfully criticized the manuscript.

REFERENCES

BIGELOW, H. B. and SCHROEDER, W. C. (1948), Sharks. Fishes of the western North Atlantic. Pt. 1. *Mem. Sears Found. Mar. Res.*, **1**, 59-576, 100 figs.

BORCEA, I. (1906), Recherches sur le système uro-génital des Elasmobranches. *Arch. Zool. expér. et gén.*, (4), **4**, 205.

BULLIS, H. R., Jr. (1955), Preliminary report on exploratory long-line fishing for tuna in the Gulf of Mexico and the Caribbean Sea. Pt. 1. Exploratory tuna fishing by the *Oregon*. *Comm. Fish. Rev.*, **17** (10), 1-15, 25 figs.

DEPARTMENT OF OCEANOGRAPHY, A. and M. COLLEGE OF TEXAS (1954), Oceanographic survey of the Gulf of Mexico. Ann. Rept., 30 June, 1953 – 30 June, 1954, 1-14, 7 figs. (Unpublished manuscript).

DODERLEIN, L. (1881), *Manuale Ittiologico del Mediterraneo*, Palermo, **2**, 40.

FORD, E. (1921), A contribution to our knowledge of the life-histories of the dogfishes landed at Plymouth. *J. Mar. Biol. Assoc.*, N. S., **12** (3), 468-505.

FUGLISTER, F. (1947), Average monthly sea surface temperatures of the western North Atlantic. *Pap. Phys. Ocean. Meteor.*, **10** (2), 1-25.

GÜNTHER, ALBERT (1870), *Catalogue of the fishes in the British Museum*, **8**, 372.

MATHER, F. J. and DAY, C. G. (1954), Observations of pelagic fishes of the tropical Atlantic. *Copeia*, (3), 179-188, 2 pls., 1 fig.

MAUL, G. E. (1955), Five species of rare sharks new for Madeira including two new to science. *Not. Nat. Acad. Nat. Sci. Phila.*, **279**, 1-13.

MEYER, F. (1875), Beitrag zur Anatomie des Urogenital-systems der Selachier und Amphibien. *Stizungber. Naturf. Ges.*, Leipzig, **2**, 38-44.

MÜLLER, J. and HENLE, J. (1841), *Systematische Beschreibung der Plagiostomen*. Berlin, p. 37.

NICHOLS, J. T. and MURPHY, R. C. (1914), Fishes from South Trinidad Islet. *Bull. Amer. Mus. Nat. Hist.*, **33**, 262.

RIPLEY, W. E. (1946), The soup fin shark and the fishery. *Bur. Mar. Fishes, Div. Fish and and Game, State of Calif., Fish Bull*, **64**, 7-37, 17 figs.

SCHUCK, H. A. and CLARK, J. R. (1951), Record of a white-tipped shark, *Carcharhinus longimanus*, from the western North Atlantic. *Copeia*, (2), 172.

SMITT, F. A. (1895), *A History of Scandinavian Fishes*, (2), 1161.

SPRINGER, S. (1950a), A revision of North American sharks allied to the genus *Carcharhinus*. *Amer. Mus. Novit.*, 1451, 1-13.

SPRINGER, S. (1950b), Natural history notes on the lemon shark, *Negaprion brevirostris*. *Texas J. Sci.*, **2** (3), 349-357.

SPRINGER, S. (1951), Correction for " A revision of North American sharks allied to the genus *Carcharhinus*." *Copeia*, (3), 244.

TORTONESE, E. (1951), Ulteriori considerazioni sulle specie Mediterranee dei generi *Sphyrna* e *Carcharhinus*. *Doriana*, **1** (20), 1-8.

Printed in Great Britain by The Salisbury Press Ltd., Publicity House, Wilton Road, Salisbury, Wilts. (96499)

Contribution No. 815

Reprinted from JOURNAL OF MAMMALOGY
Vol. 37, No. 1, February 1956, pp. 128–129
Printed in U.S.A.

LAGENORHYNCHUS ACUTUS OFF CAPE COD

Lagenorhynchus acutus (Gray), often called the white-sided porpoise, is a reasonably well-known form reported from both sides of the northern North Atlantic. Its northern limit is generally given as about Lat. 64° N (Godthaab, West Greenland, and Trondhjem Fjord, Norway), although Ellerman and Morrison-Scott (CHECKLIST OF PALAEARCTIC AND INDIAN MAMMALS, 1951) cite with doubt the Murman Coast. On the European side it is regularly found as far south as, say, Lat. 55° N in the British Isles, while on the American side its southern limit appears to be near Lat. 41° N, off Cape Cod. Jonsgaard and Nordli (Norwegian Whaling Gazette, 41: 229–232, 1952) have recently summarized what is known of the biology of this species. However, since it has not often been reported from our waters, and since we have noted a few particulars not previously given, we offer some remarks on a small group of perhaps a dozen encountered on September 14, 1954 near Lat. 41° 35′ N, Long. 68° 55′ W, about 50 sea miles east of Monomoy Point, Cape Cod, in 80 fathoms.

They swam briskly about ahead of the ship, but did not play at the bow, rarely approaching within 20 yards. There was at least one calf, two-thirds the length of its mother; one of the adults was very pale, almost white all over its sides and back including the upper surface of the flukes, except that some pigment was noted on the sides of the tail; the ventral surface was not seen. Much of the time they rolled high enough to show the white flank stripe; they did not expose much of the head forward of the blowhole, and the short, dark beak was not noticeable even when they swam near the ship.

One normally colored adult was collected by the skillful harpoon of Chief Engineer William J. Shields of the Woods Hole Oceanographic Institution research vessel *Bear*. It was a young female, neither pregnant or lactating, which weighed 161 kg. (about 5 kg. in the water). The following dimensions are in centimeters:

Length (snout to fluke notch, straight line), 225; length of beak (snout to melon), 4.5;

projection of tip of jaw beyond snout, 1; snout to blowhole (parallel to longitudinal axis), 29; blowhole to right eye (following surface), 20; blowhole to left eye (following surface), 18.5; snout to base of fin (parallel to longitudinal axis), 87; length of fin base, 35; maximum height of fin (perpendicular), 24; tip of jaw to origin of flipper (straight line), 40; tip of jaw to axilla (straight line), 55; length of flipper (straight line, axilla to point), 25; anus to fluke notch (parallel to longitudinal axis), 61; span of flukes, 65; depth of small (31 cm forward of fluke notch), 24; thickness of small (31 cm forward of fluke notch), 6.5; and girth (between fin and flippers), 132.

There were 8 (left)—12 (right) small dermal tubercles on the distal leading edge of the flippers (none on fins or flukes), reminiscent of those often mentioned in *Phocoena.* The dental formula (palpable teeth) was $\frac{30\text{-}30}{31\text{-}32}$. The skeleton is in the Museum of Comparative Zoology at Harvard College.

When this porpoise was harpooned, the others did not stay with her, although for nearly ten minutes they loitered near the ship, but well away from the victim. (During this time a phonograph record of their calls was made.) This apparent indifference to the troubles of one of their number recalls the statement of Jonsgaard and Nordli that no panic arose among a group of 52 *L. acutus* while they were killed one after the other. However, we need not expect them always to behave this way, as witness Janssen's report (*in* Hubbs, Jour. Mamm., 34: 498, 1953) of comradely devotion in *L. obliquidens* Gill, a closely related North Pacific form.

While being lanced, our porpoise vomited two herring; ten more, freshly swallowed, were found in her gullet and stomach. The remaining stomach contents were partially digested fish, apparently the same species, from an earlier meal, together with two squid beaks and a fragment of a squid pen. The herring, averaging about 30 cm. long, were identified as *Clupea harengus* Linnaeus by Dr. Richard H. Backus, to whom I am further grateful for active help in securing the porpoise. He jumped overboard to attach a hoisting line, and was impressed by the warmth of the body, which was conspicuous in the 15° C. water.—WILLIAM E. SCHEVILL, *Woods Hole Oceanographic Institution, Woods Hole, Massachusetts. Received April 9, 1955.*

[Contribution 815 from the Woods Hole Oceanographic Institution]

Contribution No. 816

Reprinted from Science, January 13, 1956, Vol. 123, No. 3185, pages 59–60.

Nitrogen Secretion in the Swimbladder of Whitefish

Hüfner reported in 1892 (*1*) that the swimbladder of whitefish (*Coregonus acronius*) that had been netted on the bottom of the Bodensee at a depth of 60 to 80 m contained 99 percent or more "nitrogen"—that is, unabsorbable gases. The fish were alive and distended when they reached the surface and from the amount of gas they contained one may calculate that they were in neutral buoyancy at the bottom. They could not, therefore, have filled their swimbladders with air at the surface, but the "nitrogen" must have been deposited in the swimbladder at the bottom—that is, against a pressure gradient of 5 to 7 atm (*2*). Hüfner's startling discovery was verified by Saunders (*3*) in a large series of determinations on several species of deepwater physostome fishes in Lake Huron and adjoining waters.

A similar situation exists in deep-sea physoclist fishes, in which the nitrogen tension frequently reaches 10 atm or more, although in this case the main pressure is due to oxygen. Organic gases, if any, are present only as traces (*4*), and the argon-to-nitrogen ratio is near to that in air (*5*). For physostome fishes there is no knowledge so far concerning the identity of the gas they secrete, except that it is unabsorbable. We have therefore analyzed the swimbladder gas of a deepwater coregonid (*Leucichthys johannae*) from Lake Michigan, obtaining information concerning its amount and its content of carbon dioxide, oxygen, nitrogen, organic gases, and argon (*6*).

We were able to secure samples from live fishes as they were hauled aboard the boat. The fish were caught in gill nets set at the bottom at a depth of 100 m. Only lively and externally intact fishes were used. Gas was drawn into 20-ml syringes, lubricated with concentrated lithium chloride, and analyzed in the ½-ml analyzer (*7*), accurate to ±0.015 percent, for CO_2, O_2, and "N_2." Organic gases were analyzed by fitting a combustion chamber onto the oxygen side of the Henderson-Haldane analyzer. Checks on air containing known amounts of acetylene gave satisfactory results. The argon-to-nitrogen ratio was determined by mass spectrometer at the Johns Hopkins University School of Medicine (*8*).

Buoyancy check. The gas from four fishes was pooled; it measured 188 ml. These four fishes, emptied of gas and suspended under water, weighed 15 g. Hence, neutral buoyancy would occur at a total pressure of nearly 12 atm. This is close enough to the total pressure of 11 atm at which the fishes were caught to indicate that the gas must have been deposited in the swimbladder at that depth.

Absorption analysis. The results of analyses of swimbladder gas from ten fishes taken at 100-m depth are given in Table 1. It will be seen that, in agreement with Saunders' data from similar or greater depths, the swimbladder gas in our species consisted of more than 99 percent nonabsorbable gases.

Combustion analysis. Gas from ten fishes was pooled over concentrated calcium chloride and 10-percent tank oxygen was added. Combustion resulted in zero shrinkage and zero CO_2 production. In a second lot of four pooled samples, the gas shrank in triplicate analyses by 0.10, 0.06, and 0.04 percent, with increments in CO_2 of 0.04, 0.00 and 0.01 percent. There is therefore less than 0.1 percent of combustible gas, if any, in the swimbladder, and the nonabsorbable gas consists of nitrogen and argon, with, very likely, traces of other noble gases.

Argon-nitrogen analysis. The argon-to-nitrogen ratio is of particular interest inasmuch as it may give some clue concerning how the nitrogen gets into the swimbladder. If the nitrogen were released from some chemical compound so that it attains a pressure of, say, 10 atm above the nitrogen tension in the water (0.8 atm), the argon would be left behind, so that the argon-to-nitrogen ratio in a swimbladder from a depth of 100 m would be only one-tenth of that in air—that is, 0.1 percent (*9*). Actually, we find that the argon-to-nitrogen ratio averages 0.92 percent, which is very close to the

Table 1. Composition of the swimbladder gas in whitefish taken at a depth of 100 m (combustible gases 0.00 to less than 0.10 percent).

Fish	CO_2 (%)	O_2 (%)	$N_2 + A$ (%)	Pressure of $N_2 + A$ (atm)	Ratio ($100A/N_2$)
1	0.24	0.01	99.75	11.0	
2	2.13	0.20	97.67	11.0	
3	0.47	0.00	99.53	10.9	
4	0.52	0.28	99.20	10.9	1.16
5	0.64	0.21	99.15	10.9	0.69
6	1.13	0.07	98.80	10.9	0.67
7	0.27	0.02	99.71	11.0	1.08
8	0.31	0.02	99.67	11.0	0.96
9	0.73	0.01	99.26	10.9	0.71
10	0.61	0.01	99.38	10.9	1.17
Air	0.03	20.94	79.03	0.79	1.17

1.17 percent in air and water (Table 1). In our whitefishes, the argon tension in the swimbladder was accordingly 8 to 10 times higher than it was in the water. These findings, which agree with the data from deep-sea physoclists, lend little support to the idea of a nitrogen secretion by chemical means, whether produced by the fish itself or by bacteria. We observed no free gas in the intestines of the fishes.

The swimbladder gas in our deepwater coregonid consists of some 99-percent pure nitrogen gas. This has been brought into the swimbladder against a pressure gradient of 10 atm by some process that is capable of concentrating argon as well. A similar nitrogen-argon transport is realized in deep-sea physoclist fishes, in which, however, the main action is oxygen secretion. Vascular *rete* structures have not been described for coregonid fishes, and the question therefore arises whether the epithelial cells lining the swimbladder might be the site for the secretion.

The deposition of nitrogen and argon against considerable concentration gradients in the swimbladder of fishes suggests, in the absence of other explanations, the possibility of a cellular mechanism for the secretion of inert material.

P. F. Scholander
L. van Dam
Woods Hole Oceanographic Institution, Woods Hole, Massachusetts
Theodore Enns
Department of Medicine, Johns Hopkins University, Baltimore, Maryland

References and Notes

1. G. Hüfner, *Arch. Anat. u. Physiol. Physiol. Ab.* 54 (1892).
2. P. F. Scholander *et al., Biol. Bull.* 101, 178 (1951).
3. R. L. Saunders, *Can. J. Zool.* 31, 547 (1953).
4. P. F. Scholander and I. van Dam, *Biol. Bull.* 104, 75 (1953).
5. T. Schloesing and J. Richard, *Compt. Rend.* 122, 615 (1896); P. F. Scholander, *Biol. Bull.* 107, 260 (1954).
6. Contribution No. 816 from the Woods Hole Oceanographic Institution. This investigation was supported by a grant from the National Science Foundation. We are indebted to Peter I. Tack of Michigan State University for help in arrangements to get the whitefish and for determining the species. We were able to secure samples from live fishes as they were hauled aboard the boat through the courtesy of E. L. Hill of Grand Haven, Mich.
7. P. F. Scholander, *J. Biol. Chem.* 167, 235 (1947).
8. F. P. Chinard and T. Enns, *Am. J. Physiol.* 178, 203 (1954).
9. H. Koch, *Rev. questions sci.* (*Belg. France*) 26, 385 (1934).

* Present address: Institute of Zoophysiology, University of Oslo, Oslo, Norway.

15 July 1955

Contribution No. 818

Reprinted from SCIENCE, January 20, 1956, Vol. 123, No. 3186, pages 104–105.

Gases in Icebergs

Pure ice in thick layers is bluish in color, whereas an iceberg is typically white. The whiteness is caused by tiny, closely spaced gas cavities that are dispersed all through the ice. The cavities are often elongated and oriented lengthwise; this gives a grain to the ice. The gas is usually under pressure and is liberated with a fizzing sound when a piece of berg ice melts in a pail of water. With a lens one may watch the bubbles suddenly enlarge and pop out of their cavities when the walls melt open. The pressure is also manifested by the way chips almost fly off the ice at the slightest fracture. This is undoutedly caused by the release of compressed air from the bubbles into the fracture.

Either the gas bubbles in a iceberg could be atmospheric air trapped at the time snow was compacted into glacier ice, or, since gases are insoluble in ice (*1*), the bubbles could be frozen out of air-saturated water, as they are in ice cubes from a refrigerator. Water equilibrated with air at 0°C contains 2.9 percent by volume of dissolved gases, of which 34.9 percent is oxygen. Since air has only 20.9 percent oxygen, the concentration of this gas in the bubbles may tell whether the ice was formed by compacting the snow crystals or by freezing of a body of water (*2*).

The rate of gas diffusion through ice is no more than 1/40,000 to 1/70,000 as fast as it is through water (*1*). Considering this extremely slow rate, the relatively enormous diffusion distances in the glacier, and the large quantity of gases held under pressure in the ice, it would seem possible that gas trapped in the glacier would remain unchanged for millenia. Analysis of such gas could therefore give information about the atmospheric composition at the time the ice was formed.

This article (*3*) presents studies on pieces of icebergs taken on board the research vessel *Blue Dolphin* along the Labrador coast. Most icebergs in this area are of Greenland origin. In the interior of Greenland and the Antarctic, the temperature stays below freezing all year, and the glacier ice is formed by the compacting of snow under high pressure. These are the high polar glaciers. In glaciers of warmer climates, melt water percolates through the snow in the summer and freezes deeper down, as an important part of the firnification process (*4*). The gas in such ice should accordingly be more or less enriched with oxygen. Only the polar type of glacier would therefore seem suitable for possible clues to the composition of ancient atmospheric air. Isotope distribution could probably be studied in either type.

Although the techniques for obtaining samples from bubbles in icebergs have been generally adequate, the composition of the gas has been found by several authors to be more or less close to that of the atmosphere, and it has long been known that the gas is usually under pressure (*5*). In our work, we melted a piece of ice in mercury. The gas phase and the dissolved gases in the melt water were analyzed separately and the results were totaled.

A piece of berg ice was shaved to fit snugly into the barrel of a 20-ml syringe. The plunger was set in and mercury drawn in to cover the ice. The first milliliter of melt water and bubbles was discarded. The nozzle was closed with the finger, and the ice-and-mercury volume

Table 1. Gases in iceberg ice. Air-equilibrated water at 0°C contains 2.9 percent gas by volume, of which 34.9 percent is oxygen. Clear ice contains less than 0.003 percent gas, most likely none at all (*1*). The pressure determinations are based upon from two to eight analyses in each iceberg.

Iceberg No.	Ratio of compressed gas to ice (ml/100 ml)	Ratio of gas at 1 atm to melt water (ml/100 ml)	Gas pressure in ice (atm)	O_2 in gas (%)
1	1.9 to 2.2	4.2 to 8.3	2.9 to 3.9	21.4, 21.2, 21.2
2	2.3 to 3.8	7.7 to 11.1	2.3 to 3.9	20.9
3	1.2 to 2.2	4.8 to 9.3	2.0 to 6.2	21.2
4	1.1 to 2.6	2.9 to 6.5	1.0 to 5.0	20.6
5	1.0 to 2.4	2.2 to 8.8	3.3 to 5.8	20.2, 20.4
6	2.1 to 5.2	5.6 to 9.9	1.7 to 2.6	20.0, 20.0, 20.1, 20.1

was read. The ice was quickly melted and a new volume reading taken. The gas phase was transferred to a tuberculin syringe to determine the volume, and it was analyzed for composition (*6*). The volume of meltwater w and mercury was read on the syringe and 1 ml of water was analyzed for dissolved oxygen and nitrogen (*7*). Carbon dioxide could not be determined accurately with the methods we had available. About 85 percent of the total amount of gas analyzed was in the gas phase.

The pressure of the gas in the ice was found as

$$g/x$$

where x is the volume of the compressed gas in the ice and g is the volume at 1 atm. This can be computed according to the formula

$$g/x = \frac{g}{v - 1.091w}$$

where v is the volume of ice and bubbles and $1.091w$ is the volume of ice alone.

It can be estimated that the combined accuracy of the various measurements will amount to about ± 0.2 percent by volume for the total oxygen and nitrogen. The pressure estimates are probably valid to within ± 25 percent.

Thirty pieces taken from six different icebergs were analyzed. It will be seen from Table 1 that the oxygen content in all of the bergs is close to that of the atmosphere, that is, 20.9 percent. Nevertheless, the oxygen content of iceberg No. 5 and especially No. 6 was significantly lower. One may speculate that when the snow settled on the Greenland icecap ages ago and compacted into these pieces of glacier ice (No. 5 and No. 6), an atmosphere was trapped that is slightly lower in oxygen content than our present atmosphere (*8*). Possibly this ice was formed as far back as Pleistocene time, when cold climates may have curbed photosynthetic activity of green plants over large parts of the earth, resulting in a slight lowering of the oxygen content of the air. Such a hypothesis can be verified only by better determinations of the diffusibility of gases through ice and by more accurate laboratory procedures for the extraction and analysis of the gas. No particulate matter could be detected in our ice pieces, but we cannot exclude the possibility of oxygen loss from dust oxidation. Whether or not enough organic material can be obtained from the ice for radiocarbon dating we do not know.

In our random investigation we did not encounter ice with gas bubbles rich in oxygen, which is suggestive of frozen, air-saturated water such as one might encounter in temperate-type glacier ice.

The bubbles in our icebergs were found to be under pressure, usually between 2 and 6 atm. Why the pressure seems to vary so much from one part of a berg to another is a puzzling problem. If such pressure gradients can persist in the bergs for a long time they might reflect something of the history of the berg such as the depth in the glacier from which it came.

P. F. SCHOLANDER*
JOHN W. KANWISHER
Woods Hole Oceanographic Institution,
Woods Hole, Massachusetts
D. C. NUTT
Dartmouth College,
Hanover, New Hampshire

References and Notes

1. P. F. Scholander *et al.*, *J. Cellular Comp. Physiol.* 42, suppl. 1 (1953).
2. Distilled water equilibrated at 20°C with air was frozen in a horizontal, rotating tube so that the gas and a small amount of unfrozen water collected in the center. The gas phase held 32.6 percent oxygen as against a theoretical value of 34.0 percent. The deficit undoubtedly remained dissolved in the unfrozen water.
3. Contribution No. 818 from the Woods Hole Oceanographic Institution. This work was carried out on the *Blue Dolphin* Labrador Expedition, 1954, under the auspices of the Arctic Institute of North America, project ONR-138, with funds provided by the Office of Naval Research.
4. H. W:son Ahlmann, *Geograph. Ann.* 18, 48 (1936); *Glacier Variations and Climatic Fluctuations* (American Geographical Society, New York, 1953).
5. K. J. V. Steenstrup, *Medd. Grønland* 4, 69 (1893); A. Hamberg, *Bihang Kgl. Svenska Vetenskapsakad. Handl.* 21, pt. II, No. 2, 3 (1895); J. P. Koch, *Z. Gletscherkunde* 10, No. 1, 1 (1916); C. Bernard, *Études Glaciol.* 4, 91 (1922); H. T. Barnes, *Proc. Roy. Soc. London* A114, 161 (1927) and *Ice Engineering* (Renouf, Montreal, 1928); E. H. Smith, "The Marion expedition to Davis Strait and Baffin Bay, 1928. Scientific Results, Part 3" *U.S. Coast Guard Bull. No. 19* (Washington, D.C., 1931); H. Bader, *J. Glaciol.* 1, No. 8, 443 (1950).
6. P. F. Scholander *et al.*, *Biol. Bull.* 101, 178 (1951).
7. P. F. Scholander *et al.*, *ibid.* 109, 328 (1955).
8. Analyses of the air at Point Barrow, 71°N, in Alaska showed it to be constant throughout the year and exactly the same as air in southern latitudes, namely, 20.94 percent oxygen. R. J. Hock *et al.*, *J. Meteorol.* 9, 441 (1952).

* Present address: Institute of Zoophysiology, University of Oslo, Oslo, Norway.

14 July 1955

Contribution No. 819

Reprinted from LIMNOLOGY AND OCEANOGRAPHY
Vol. 1, No. 1, January, 1956
Printed in U.S.A.

Photosynthesis in the Ocean as a Function of Light Intensity[1]

JOHN H. RYTHER

Woods Hole Oceanographic Institution

ABSTRACT

Photosynthesis was measured in 14 species of marine plankton algae in relation to light intensites within the entire range to which natural phytoplankton populations may be exposed. A mean curve was constructed showing relative photosynthesis in marine phytoplankton as related to light intensity. From this curve and surface radiation data, relative values for photosynthesis were determined throughout the day at the surface and at depths in the ocean at which the surface intensity is reduced by given amounts. Integration of these values over the entire day gave values for daily relative photosynthesis at each depth considered, and integration of the daily values with depth resulted in a single figure for daily relative photosynthesis beneath a unit of sea surface.

An empirically derived relationship was discovered between daily surface radiation and daily relative photosynthesis within the water column. From this relationship the effect of light intensity upon photosynthesis throughout the year at a temperate latitude was demonstrated.

A preliminary method is described for estimating absolute daily photosynthesis beneath a square meter of sea surface from measurement of (1) photosynthesis of a sample of the population at light saturation, (2) the extinction coefficient of light in the water, and (3) the daily surface radiation.

From an estimate of the ratio of photosynthesis to respiration at light saturation, the daily ratio $P:R$ for the entire population is calculated. It is shown that phytoplankton populations cannot photosynthesize sufficiently to compensate for their own respiration during periods of low solar radiation, as may occur in the winter months at temperate or northern latitudes.

INTRODUCTION

Although light is the most important limiting factor to photosynthesis in the ocean, the effects of light intensity upon the photosynthetic rate of the principal group of marine plants, the plankton algae, has never been adequately investigated. Laboratory studies appear to be confined to some experiments by Barker (1935) with the diatoms *Nitzschia closterium* and *N. palea* in which both light intensity and photosynthesis are expressed in relative units. In the field, Jenkin (1937) measured simultaneously light intensity and photosynthesis by the diatom *Coscinodiscus excentricus* at various depths in the English Channel, producing what has persisted as the only quantitatively useful information on the subject with respect to marine phytoplankton.

There exists a large literature dealing with the relationship between light intensity and photosynthesis in terrestrial plants, aquatic phanerogams, and a few freshwater algae, notably *Chlorella*. This has been reviewed by Rabinowitch (1951, chap. 28), showing the same general trend in every case of a linear increase of photosynthesis with light intensity up to a saturation point, beyond which higher intensities do not increase photosynthesis but eventually result in an inhibition, the physiology of which is discussed by Steemann Nielsen (1952). The majority of laboratory studies with terrestrial or freshwater plants have not been concerned with the high intensities at which this inhibition occurs, but the phenomenon has been clearly demonstrated in all measurements of photosynthesis in natural waters by a marked depression at or near the surface where the organisms are exposed to nearly full incident solar radiation (Marshall and Orr 1928, Jenkin 1937, Steemann Nielsen 1951, 1952).

---

[1] Contribution No. 819 from the Woods Hole Oceanographic Institution. These studies were carried out with the aid of a research grant from the National Science Foundation.

The following report will describe some experiments in which the relationship between photosynthesis and light intensity has been investigated in 14 species of marine plankton algae within the wide range of light intensities to which they may be exposed in nature. On the basis of these experiments an attempt will be made to construct a general photosynthesis-light curve for marine phytoplankton, which in turn will serve as a basis for some speculation on the effect of light upon total photosynthesis and the ratio of photosynthesis to respiration within the euphotic layer of the ocean.

EXPERIMENTAL METHODS

Photosynthesis measurements were made on the roof of the Woods Hole Oceanographic Institution during June and July, 1955, using solar radiation as a light source. Incident light measurements were made with a calibrated Weston Model 594RR photoelectric cell and are reported in foot-candles. Experiments were conducted for four-hour periods consisting of the two hours before and after noon, and were confined to bright sunny days with no appreciable cloud cover. The incident solar intensity increased during the first half and decreased during the latter half of the experiments, but did not vary from the mean intensity within the four-hour period by more than 8%.

Photosynthesis was measured in 20-ml glass-stoppered bottles which were placed in a light-tight box divided into 9 compartments. Each compartment held three bottles so that three experiments could be conducted simultaneously. The compartments were then covered with a graded series of neutral density filters prepared from exposed photographic plates. The absorptive indices of the filters were determined by photometric measurements made within each compartment, which thereby also took into account influences of the container itself upon the radiation.

The bottles were suspended on wire rods above a flat, black surface so that reflected light was negligible. The bottom of the compartments were open to the air but shielded from the light by a system of baffles. The temperature in the entire series of experiments ranged from 18–23°C but did not vary between bottles in any one experiment by more than 1°C.

Photosynthesis was measured by the uptake of $C^{14}O_3^{=}$ using essentially the same technique described by Steemann Nielsen (1952). However, to permit comparison of the different species, photosynthesis at each intensity (P_l), as determined by the activity of the organisms after exposure, is reported relative to the maximum photosynthesis (P_{max}) observed in the same experiment (P_l/P_{max}).

The cultures used for the experiments were routinely grown at 20°C under 1000 foot-candles of illumination provided by daylight fluorescent lamps. They were approximately one week old when used, at which time they were diluted with enriched Millipore-filtered seawater to such a density that no appreciable absorption of light could be detected through the thickness of the experimental vessel (3.2 cm). In order to eliminate any short-term effects of suddenly exposing the organisms to light intensities different from those at which they had grown, the bottles containing the algal suspensions were placed in their appropriate compartments in the experimental box and exposed to the sun for approximately two hours before the start of the experiment at which time the C^{14} was added with a hypodermic syringe.

In addition to 28 experiments with organisms grown in the manner described above, three additional experiments were made with cultures which were grown on the roof of the building and hence exposed to full sunlight.

Finally a third type of experiment consisted of measuring photosynthesis by the same method as described above and during the same four-hour, mid-day period, at various depths in Woods Hole Harbor. The simultaneous measurements of incident radiation and the extinction coefficient of the water permitted the calculation of the light intensity at each depth at which photosynthesis was measured. These experi-

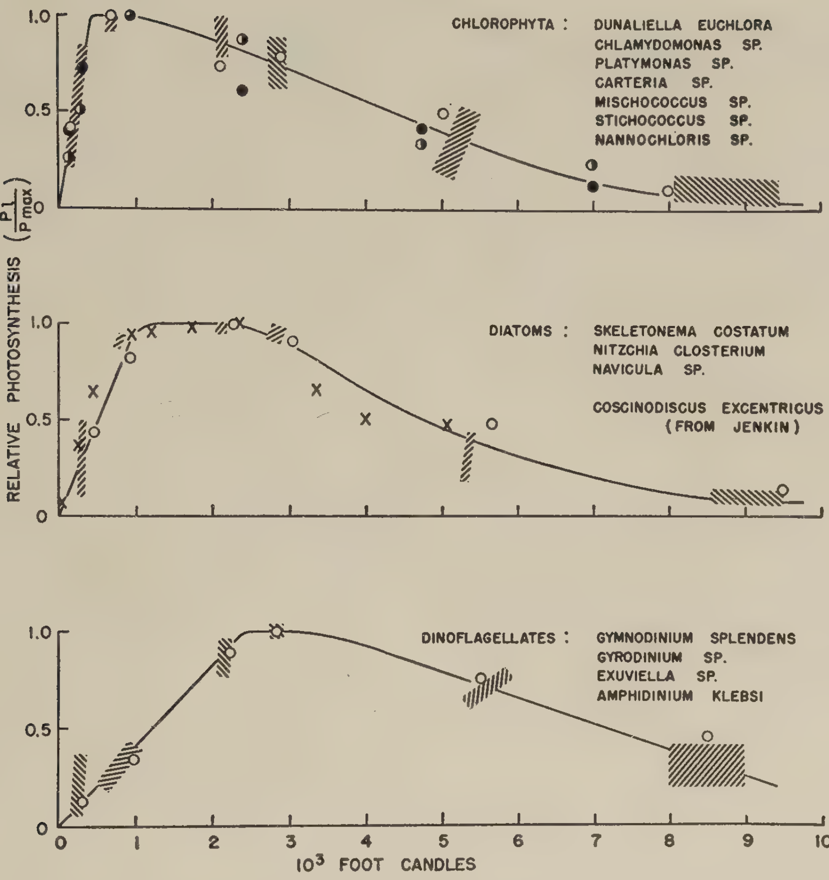

FIG. 1. The relation between photosynthesis and light intensity in some marine phytoplankton. Rectangles represent scatter of points in experiments using cultures grown at 1000 fc and measured with neutral density filters. Opên circles are cultures grown under natural sunlight. Filled and half-filled circles are cultures grown at 350 and 1500 fc and measured in Woods Hole Harbor. Crosses from Jenkin (1937).

ments were made with the green flagellate, *Dunaliella euchlora*, which had been grown in the laboratory at light intensities of 350 and 1200 foot-candles.

A total of 14 species of phytoplankton were used in these experiments including seven green algae, three diatoms, and four dinoflagellates. The species are listed in Figure 1. *Gymnodinium splendens* was obtained from Dr. Beatrice Sweeney, *Gyrodinium* sp. and *Exuviella* sp. from Dr. Luigi Provasoli, and *Amphidinium Klebsi* and *Dunaliella euchlora* from Dr. R. R. L. Guillard. The remaining organisms were isolated by the author from marine or brackish water near Woods Hole.

INTERPRETATION OF THE DATA

The uptake of C^{14} measures only photosynthesis above compensation, or photosynthesis minus respiration (Ryther 1954). Thus the point of zero apparent photosynthesis occurs at the compensation intensity, or somewhere between 50 and 100 foot-candles, and the resulting curve shows the relationship between light intensity and net photosynthesis. However, since respiration is constant, the curve for total photosynthesis lies parallel to the net photosynthesis curve and passes through the origin. The curves relating intensity and total photosynthesis which will be described below were constructed on the basis of this relationship from net photosynthesis measurements.

Although there is evidence that photosynthesis below the compensation intensity proceeds with twice the efficiency as that above that point (Kok 1951), the increase is shown here as being linear from zero light intensity to saturation. However, the error resulting from this assumption is negligible and photosynthesis below 50 foot-candles has been considered as insignificant for the purposes of this report.

RESULTS

There was a remarkable similarity in the behavior of the organisms within each of the three taxonomic groups (green algae, diatoms, and dinoflagellates) and a rather striking difference between those of different groups. For this reason the data for each group are shown separately (Fig. 1). Within each group, the scatter of data in different experiments with the same species was as great as that between different species, so the results for the individual species are not shown.

Saturation intensity was reached for the Chlorophyta at 500–750 foot-candles, for the dinoflagellates at 2500–3000 foot-candles, and at intermediate intensities for the diatoms. Inhibition of photosynthesis became apparent in all three groups within about 1000 foot-candles of saturation. At intensities of 8000–10000 foot-candles, comparable to full noon sunlight, photosynthesis in the Chlorophyta and diatoms was only 5–10% of that at saturation, while photosynthetic activity in the dinoflagellates was reduced somewhat less to 20–30% of maximum.

Cultures of one species of each group—the green flagellate, *Dunaliella euchlora*, the diatom *Skeletonema costatum*, and the dinoflagellate, *Amphidinuim Klebsi*—were grown on the roof of the laboratory where they were exposed to full incident radiation. During their growth period of one week there were one rainy day, two overcast days, and four bright, clear days. The cultures grew slowly and showed marked chlorosis, but both flagellates remained motile and all were later successfully subcultured under normal laboratory conditions.

Photosynthesis-light intensity experiments similar to those discussed above were made with these cultures at the end of seven days. Although their uptake of C^{14} was low, the relative rates at different light intensities were essentially the same as that of the same organisms grown in the laboratory under 1000 foot-candles (see Fig. 1). There was no indication of adaptation to the high intensities to which they had been exposed.

Photosynthesis of the flagellate, *Dunaliella euchlora*, was also measured at depths of 0, 1, 2.5, 5, 7.5 and 10 meters in Woods Hole Harbor. The extinction coefficient was obtained by lowering a submarine photometer (a Weston Model 594RR photoelectric cell) and measuring the reduction of light. The water was homogeneous with respect to light extinction within the upper 10 meters with a coefficient (k) of 0.40. No significant loss of radiation through reflection at the surface could be detected. Incident radiation was measured as before with a recording Weston photoelectric cell.

Cultures were used which had grown for two weeks in the laboratory at light intensities of 350 and 1200 foot-candles. Those which were grown at the lower light intensity contained 4.3 times as much chlorophyll *a* per cell, and their photosynthetic rate per cell was 3–4 times that of the cells grown at light saturation. But the relative response of the two cultures to different light intensities was essentially identical and comparable to that found in the roof experiments with neutral density filters and with cultures grown at 1000 fc (Fig. 1: Chlorophyta).

Figure 1 also shows for comparison some of Jenkin's data for the diatom, *Coscinodiscus excentricus*. The data were taken from her Figure 9 (p. 333) showing oxygen production per hour plotted against average energy per hour. The July 25 measurements were chosen for the comparison since on that day "the sea was calm, the light was very bright, and conditions were relatively constant throughout the exposure".

Light values, which were originally

measured in photometric units and converted to energy units by Jenkin, were reconverted to foot-candles to permit comparison with the present data, using the same conversion factors employed by Jenkin. A reasonably good fit of Jenkin's data to the author's diatom curve is obvious.

Despite the variability of the photosynthetic response to light intensity of the different taxonomic groups, an attempt has been made to construct a general photosynthesis-light intensity curve for marine phytoplankton. This has been done by averaging the relative photosynthesis values at each light intensity for the three groups of algae as given by the curves in Figure 1. Because the Chlorophyta are relatively unimportant in the marine phytoplankton, they have been weighted only one-half as heavily as the other organisms in obtaining the average. The resultant curve is given in Figure 2.

RELATIVE DAILY PHOTOSYNTHESIS IN THE OCEAN AS A FUNCTION OF LIGHT INTENSITY

If one knows the incident radiation falling on the surface of the ocean throughout the day and the extinction coefficient (k) of the water, it is possible to calculate from this information and the data in Figure 2 the daily relative photosynthetic rate at any depth in a water column in which the phytoplankton is distributed homogeneously.

A continuous record of incident radiation as measured by a 50-junction Epply pyrheliometer is kept by the Epply Laboratories of Newport, Rhode Island and was made available to the author through the kindness of Mr. Hedley Greer of that organization. According to Forsythe (1954) 50.4–52.3% of solar radiation falls within the range of 4000–7700 A, while according to List (1951) 42.5–45.25% falls within the range 4000–7000 Å. The present author has followed Edmondson (1955) in considering 50% of the total incident solar radiation as photosynthetically active.

Pyrheliometer values are expressed in energy units as gram calories per cm². These have been converted to units of luminosity using Jenkin's figures of 240 lumens per watt as suggested to her by Poole and Atkins, and results in the relationship 1 gram calorie per cm² per min (photosynthetically active radiation) = 15500 foot-candles.

The reflection of light from the surface of the water varies with cloud cover, surface roughness, and the altitude of the sun, but is normally rather small (Powell and Clarke 1936, Harvey 1955). For present considerations the light just penetrating the water has been taken as 95% of that incident to the surface. This is obviously an oversimplification and results in some overestimation of submarine light intensity, particularly in the early morning and late afternoon.

Figure 3 shows the light intensity in the surface layers of the ocean at the same latitude and under similar weather conditions which prevailed at Newport, Rhode Island, on June 17 and December 14, 1954, which were respectively the brightest and darkest days of the year. Mean intensities are given for half-hour intervals throughout

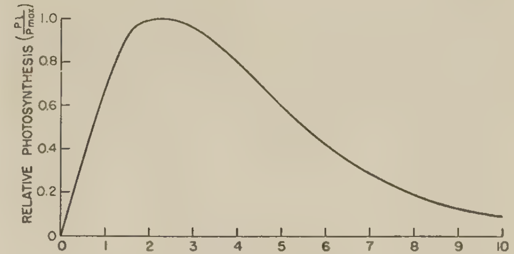

FIG. 2. Mean curve from Figure 1 showing relationship between photosynthesis and light intensity in marine phytoplankton.

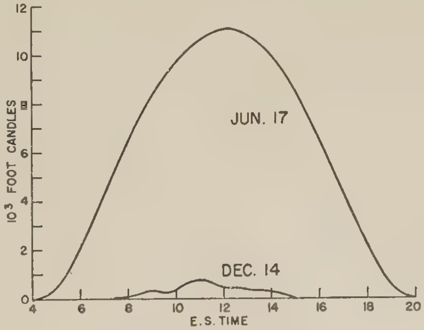

FIG. 3. Daily incident surface radiation at Newport, Rhode Island, on June 17 and December 14, 1954.

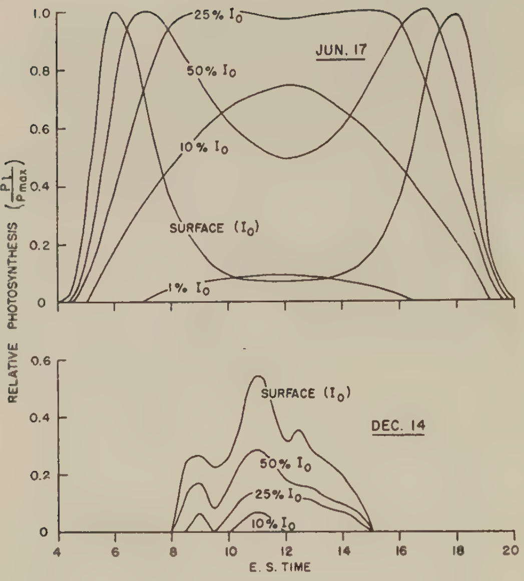

FIG. 4. Daily relative photosynthesis (P_l/P_{max}) at various depths in the ocean on June 17 and December 14, 1954, at a latitude and under weather conditions comparable to Newport, Rhode Island.

the day. Figure 4 shows relative photosynthesis also plotted at half-hour intervals at the surface and at the depths where the surface intensity is reduced to 50%, 25%, 10% and 1% of its initial value for the same two days, as obtained from Figures 2 and 3. Relative photosynthesis values may now be integrated over the entire day thereby giving daily relative photosynthesis at each depth considered (Fig. 5). The depth scale is given here as a function of the extinction coefficient of the water (km) as derived from the expression:

$$I_m = I_0 e^{-km}$$

where I_0 is the surface intensity and I_m the intensity at depth m. The curves in Figure 5 may, in turn, be integrated giving total daily relative photosynthesis within the entire euphotic zone.[2] These

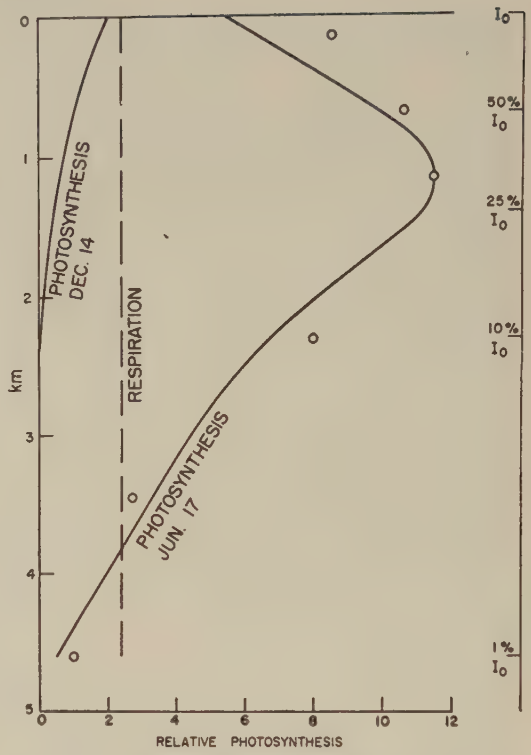

FIG. 5. Integrated daily relative photosynthesis (P_l/P_{max} × hrs. daylight/day) from surface to depth of penetration of 1% of surface light on June 17 and December 14, 1952. Dotted line represents respiration where $P:R$ at light saturation is 10:1 (see Text). Open circles from Steemann Nielsen (1952).

relative values, for the same value of k, are 29.2 and 1.8 for June 17 and December 14, respectively.

A COMPARISON BETWEEN THEORETICAL AND MEASURED DAILY PHOTOSYNTHESIS CURVES IN THE OCEAN

In December, 1950, Steemann Nielsen measured C^{14} uptake in water collected from 10 meters and suspended at various depths in the Benguela Current of Luando, Angola, S. W. Africa (see Steemann Nielsen 1952: 129). The experiment was carried out on a bright, sunny day. According to Kimball (1928) the total daily radiation on a cloudless day at that time and latitude is 720 g.cal/cm². The length of the day was 12 hours and the altitude of the zenith sun 67°.

On June 17, 1954, at Newport, Rhode

---

[2] Defined here as limited by the depth of penetration of 1% of the radiation incident to the surface. This is a constant depth (in water of the same transparency) but receives illumination which varies with the surface radiation. Thus the euphotic zone, as used here, has no biological significance other than defining the water mass below which no appreciable photosynthesis can occur.

Island, the total radiation was 802 g.cal/cm², the length of the day about 15 hours, and the sun's altitude also 67°. The two days were thus quite similar with respect to radiation, with the exception of the somewhat longer period of daylight at Newport.

Since Steemann Nielsen was dealing with a homogeneously distributed population (i.e. in using water collected from a single depth) it is possible to compare his curve of daily photosynthesis with the theoretical curve for June 17 at Newport. To do this, the depth scales must be equilibrated, which may be done by superimposing the points of maximum photosynthesis of the two curves. Thus maximum photosynthesis in the Benguela Current (at 10 meters) is arbitrarily assumed to occur where $km = 1.15$, k then becomes 0.115, and the remaining points may be plotted on Figure 5 using the same depth scale.

Photosynthesis is expressed in relative units. The rather good fit of Steemann Nielsen's data to the theoretical curve, considering that radiation in the two cases was not identical, lends some support to the preceding theoretical treatment and suggests that the response of the phytoplankton to light intensity was similar in the two cases.

THE RELATIONSHIP BETWEEN DAILY INCIDENT SURFACE RADIATION AND RELATIVE PHOTOSYNTHESIS WITHIN THE WATER COLUMN

In addition to the two days considered above (June 17 and December 14) the daily relative photosynthesis within the euphotic zone was calculated by the same method for 6 additional days in 1954. The 8 days chosen for this purpose were characterized by total incident radiation ranging at more-or-less even intervals from the darkest to the brightest day of the year. Relative photosynthesis was then plotted against total daily incident surface radiation for the 8 days (Fig. 6). The resulting smooth curve which may be drawn through the 8 points clearly indicates an empirically derived relationship between the two variables.

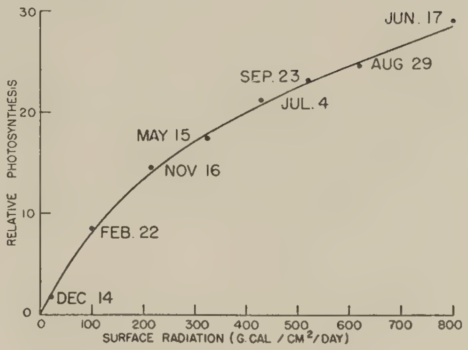

FIG. 6. The relation between total daily surface radiation and daily relative photosynthesis within the euphotic zone ($P_l/P_{\max}$ × hrs. daylight/day × k × m).

Records maintained at the Epply Laboratories include weekly averages of the total daily radiation at Newport, Rhode Island. These figures may be converted to photosynthesis values from the curve in Figure 6 to illustrate the effect of the seasonal variation of light intensity upon photosynthesis (Fig. 7). It should be emphasized here that this treatment considers only the factor of light and applies only to a hypothetical phytoplankton population which remains constant with respect to both time and depth within the euphotic zone. The actual magnitude of photosynthesis throughout the year varies as well with fluctuations in the population size, nutrient concentrations, and other limiting factors.

THE DETERMINATION OF ABSOLUTE PHOTOSYNTHESIS IN THE OCEAN

An absolute value for total photosynthesis (P), in mg of carbon assimilated per day beneath a square meter of sea surface, may now be obtained for a homogeneously distributed population from the expression:

$$P = \frac{R_s}{k} \times P_{\text{sat}}$$

where R_s = total relative photosynthesis within the euphotic zone for the appropriate value for total daily surface radiation (S), from Figure 6

k = extinction coefficient per meter, as measured

P_{sat} = measured total or "gross" photosynthesis at light satu-

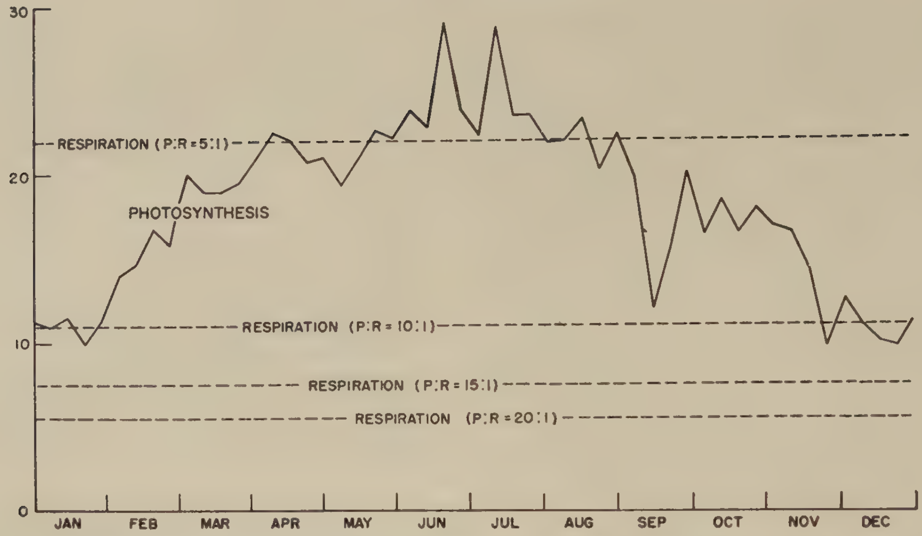

FIG. 7. Seasonal variation in daily relative photosynthesis and respiration within the euphotic zone. Different curves for respiration represent different ratios of $P:R$ at light saturation. Units as in Figure 6.

ration of a sample of the population, expressed as mg carbon/m^3/hour.

The value for (S) may be determined by measurement on the day in question, or may be taken from the published tables of Kimball (1928). The latter not only eliminates the necessity for measuring radiation, but also provides a mean value for the particular time and place under consideration. For purposes of a general survey of marine productivity, this is generally more significant than direct measurements on any single day, which cannot make allowance for the day-to-day variations in radiation resulting from local meteorological conditions.

The procedure outlined above may be used only under highly restricted conditions and is presented at this time merely to illustrate the ultimate applicability of the methods described herein. Procedures for estimating both total and net photosynthesis under varying natural conditions, based upon the same general approach as developed in this paper, will be described in a subsequent publication.

THE RATIO OF PHOTOSYNTHESIS TO RESPIRATION

At light saturation the ratio $P:R$ varies depending upon the state of nutrition of the algae. During exponential growth of *Dunaliella euchlora*[3] a maximum ratio of 12.1:1 was observed which decreased to about unity in cultures highly deficient in nitrogen and phosphorus (Ryther 1954). Kok (1952) found ratios in *Chlorella* as high as 20:1, but under "bad conditions" reported values as low as 1.4:1. In short term manometric measurements of photosynthesis, ratios of 20:1 or higher are commonly encountered, but the behavior of organisms under the highly artificial and idealized conditions of such experiments cannot be assumed to prevail over extended periods of growth.

It is not possible to measure the ratio directly in natural populations, since the respiration of the plants cannot be separated from that of the associated non-photosynthetic forms. At best it probably falls somewhat short of that observed under ideal conditions in laboratory experiments. Let us consider for the present a hypothetical situation in which the ratio of photosynthesis to respiration is 10:1 at light saturation. Respiration then assumes a value of 0.1 relative to maximum photosynthesis.

---

[3] Reported in that publication as *Chlamydomonas* sp. and correctly identified by Dr. Ralph Lewin.

Since respiration is essentially independent of light (Brown 1952) it remains constant throughout the day. Furthermore we are considering a population which is distributed homogeneously throughout the water column, so that R also remains constant with depth if we may disregard the effects of temperature. Except under conditions of extreme thermal stratification, which will be discussed below, temperature does not normally vary by more than a few degrees within the euphotic zone.

Daily respiration throughout the euphotic zone is then $0.1 \times 24 \times 4.6 = 11.04$ relative units, and this remains constant as long as the ratio $P{:}R$ at light saturation does not change. While absolute values for P and R are dependent upon the size of the population, their values relative to each other are independent of this factor.

In Figure 5, which shows the vertical distribution of daily relative photosynthesis within the euphotic zone on June 17 and December 14, the straight vertical line represents respiration. The point at which the curves for photosynthesis and respiration cross is the daily compensation depth. On June 17, this occurred at $3.83/k$ meters, which in clear oceanic water ($k \sim 0.04$) is about 95 meters and in coastal water ($k \sim 0.1$) is about 38 meters. On December 6 the curves never cross indicating that the plants could not compensate even at the surface. The daily ratio of $P{:}R$ for the euphotic zone was roughly 2.6:1 on June 17 and 0.2:1 on December 14, even though $P{:}R$ at light saturation was 10:1 in both cases.

In Figure 7, showing the seasonal pattern of photosynthesis, the horizontal lines represent respiration where $P{:}R$ at light saturation is respectively 5:1, 10:1, 15:1 and 20:1. This illustrates the fact that if a maximum ratio of 10:1 is reasonable, phytoplankton populations living at a latitude and under weather conditions comparable to Newport, Rhode Island, are unable to do more than compensate for their own respiration within the euphotic zone during the winter months. This, then, may account for the winter minimum of plankton algae in temperate and northern ocean waters.

DISCUSSION

We have discussed above the relationship between light and the ability of phytoplankton populations to maintain themselves or produce excess cellular material. Losses to the population by predation or sinking are not included in the scope of this report. Such permanent losses remove individuals from the population and hence affect the magnitude of photosynthesis and respiration, but not their relative rates with respect to each other.

For the purposes of this discussion the phytoplankton population must be considered to consist of those individuals which, through vertical mixing, spend at least some time in the euphotic zone. But the population, so defined, may extend considerably below the depth at which any photosynthesis can occur. In the open ocean this depth is of the order of 100–150 meters, in coastal waters 25–50 meters. The so-called "mixed layer" of surface water (i.e. water of the same density) may be and usually is considerably greater than these depths except in summer when thermal stratification occurs.

If one considers the entire population, as defined above, rather than that within an arbitrary depth, it is obvious that the $P{:}R$ ratio is even smaller than indicated above, at least during the late fall, winter and early spring when the mixed layer extends below the euphotic zone.

In summer the surface layers may be thermally stratified and mixing greatly reduced. Under these conditions the photosynthetically active population may not extend below the euphotic zone. But the reduction of mixing also prevents the homogeneous distribution of organisms in the upper layers and, due to the negative buoyancy of the cells, the population density increases with depth to a maximum somewhere below the depth of maximum photosynthesis (see Riley *et al* 1949: 73). This, too, will have the effect of increasing respiration relative to photosynthesis for the population as a whole. However, the effect here may be somewhat counteracted by the temperature gradient which results in lower respiratory rates near the bottom of the euphotic zone as compared with that near the surface, whereas photosynthesis at the low light intensities found at these levels is essentially independent of temperature.

From these considerations it would appear that the $P:R$ ratio for the population may be considerably lower than indicated in the preceding calculations in which only the euphotic zone was considered. This leads to a reconsideration of the choice of a $P:R$ ratio at light saturation of 10:1. Since there are always some plankton algae in the surface layer of the ocean as well as animals which are dependent upon them for food, it would seem unlikely that there would be any extended period of the year in which no net photosynthesis can occur. Thus the $P:R$ ratio at light saturation is probably somewhat greater than 10:1. For reasons stated above, it is probably not consistently as great as 20:1, and a mean value probably lies somewhere between these limits. In Figure 7 the relative curve for annual respiration is shown where $P:R$ at light saturation is 15:1. If this curve is somewhat low for the entire population, as indicated above, the population would approach or reach compensation perhaps only in extreme conditions in mid-winter.

We have thus attributed the winter minimum of phytoplankton in temperate or northern latitudes to the limitation of light. In the normal course of events, this is followed by a spring maximum and a secondary fall peak interspersed by a mid-summer low. The latter has been attributed, at least in part, to nutrient depletion of the surface waters.

As soon as the limiting nutrient concentrations fall to the level at which exponential growth of the organisms can no longer occur at optimum light intensity, the rate of photosynthesis decreases and the ratio $P:R$ falls to 5:1 or less (Ryther 1954). Under these conditions photosynthesis by the entire population is able to compensate for its respiration only on days of the highest incident radiation, as is indicated in Figure 7. Thus light is always limiting to the photosynthesis of natural plankton populations and the effect of nutrient deficiency is at most additive to the light factor.

REFERENCES

Barker, H. A. 1935. Photosynthesis in diatoms. Arch. f. Mikrob., **6**: 141–156.

Edmondson, W. T. 1955. Factors affecting productivity in fertilized salt water. Pap. Mar. Biol. and Oceanogr. Deep-Sea Res. Suppl. to Vol. **3**: 451–463.

Forsythe, W. W., ed. 1954. Smithsonian Physical Tables 9th Ed., p. 725.

Harvey, H. W. 1955. The chemistry and fertility of sea water. The University Press, Cambridge.

Jenkin, P. M. 1937. Oxygen production by the diatom *Coscinodiscus excentricus* Ehr. in relation to submarine illumination in the English Channel. J. Mar. Biol. Assoc. U. K., **22**: 301–343.

Kimball, H. H. 1928. Amount of solar radiation that reaches the surface of the earth on the land and on the sea, and methods by which it is measured. Mon. Weath. Rev., Wash., **56**: 393–398.

Kok, B. 1951. Photo-induced interactions in metabolism of green plant cells. Symp. Soc. Exp. Biol. No. 5. Carbon dioxide fixation and photosynthesis. Academic Press, Inc., N. Y.

———. 1952. On the efficiency of *Chlorella* growth. Acta. Botan. Meerl., **1**: 445–467.

List, R. J., ed. 1951. Smithsonian Meteorological Tables, p. 438.

Marshall, S., and A. P. Orr. 1928. The photosynthesis of diatom cultures in the sea. J. Mar. Biol. Assoc. U. K., **15**: 321–360.

Powell, W. M., and G. L. Clarke. 1936. The reflection and absorption of daylight at the surface of the ocean. J. Optic. Soc. Ann., **26**: 1–23.

Rabinowitch, E. I. 1951. Photosynthesis and related processes. Vol. II, Part 1. Interscience Publ. Inc., N. Y.

Riley, G. A., H. Stommel, and D. F. Bumpus. 1949. Quantitative ecology of the plankton of the western North Atlantic. Bull. Bing. Oceanogr. Coll., **12**(3): 1–169.

Ryther, J. H. 1954. The ratio of photosynthesis to respiration in marine plankton algae and its effect upon the measurement of productivity. Deep-Sea Res., **2**: 134–139.

———. 1956. The measurement of primary production. Limnology and Oceanography. (In press)

Steemann Nielsen, E. 1951. The marine vegetation of the Isefjord. Medd. Komm. Danmarks Fish, og Havunders., Ser. Plankton, **2**(4): 1–114.

———. 1952a. On detrimental effects of high light intensities on the photosynthetic mechanism. Physiol. Plant., **5**: 334–344.

———. 1952b. The use of radio-active carbon (C^{14}) for measuring organic production in the sea. J. du Cons. Internat. Explor. Mer., **19**: 117–140.

Contribution No. 821

Deep-Sea Research, 1956, Vol. 3, pp. 189 to 205. Pergamon Press Ltd., London.

Measurements of illumination at great depths and at night in the Atlantic Ocean by means of a new bathyphotometer

GEORGE L. CLARKE and GUNTHER K. WERTHEIM

(*Received 9th January*, 1956)

Abstract—The bathyphotometer described is a combination of a light-meter employing a photomultiplier tube and a depthmeter employing a bourdon tube. The spectral sensitivity of the instrument extends approximately from 320 mμ to 650 mμ with a maximum at 480 mμ. Illumination as low as 10^{-7} μw/cm^2 (about 10^{-12} of full sunlight) and depths as great as 610 m can be read directly on deck. The instrument thus permits the direct investigation of the light factor in the sea at depths and intensities far below those measurable by photovoltaic photometers.

Measurements of transparency made in the Florida Current off Miami gave extinction coefficients ranging from ·031 to ·056 for various strata between depths of 20 and 580 m. In the slope water about 200 miles SE of New York extinction coefficients of ·062 to ·072 were obtained for the upper 90 m and of ·032 to ·041 for layers extending to 596 m. These results, together with previous meagre information, indicate a uniform and high transparency for the water between 100 m and 600 m.

Measurements made at night in both localities showed that the illumination decreased with depth in the upper layers at about the same rate as during the day. Flashes of light, presumably from luminescent animals, were observed, particularly in the lower strata. At depths greater than 300 m the background light remained about constant or tended to increase. In one instance the general illumination at night at 600 m was about as great as during the day with individual flashes almost one thousand times greater.

INTRODUCTION

THE penetration of light into natural waters is of vital concern not only for the growth of green plants but also for the photic reactions of animals. In addition, a knowledge of transparency has many practical applications. Previous measurements of illumination in natural waters have provided us with considerable information on the intensity and quality of light in the upper water layers during the daytime, and the ecological significance of these has been summarized elsewhere (CLARKE, 1954). However, most of the instruments employed heretofore have been incapable of measuring accurately light weaker than 0·1% to 0·01% of full sunlight, and hence the observations have been limited to depths and times at which the natural illumination has exceeded this limit, or have depended on light from an artificial source.

Although the sensitivity of previous instruments is sufficient for investigating the growth of green plants, since photosynthesis generally requires about 1% of sunlight, earlier methods fell far short of measuring the minimum intensities of light significant for animals. Certain pond fish have been shown to be able to see small objects under an illumination of only 10^{-10} of sunlight, and this is also the approximate threshold of vision for man (CLARKE, 1936). Fish and other animals adapted to very deep water may be able to see in even weaker light. Certain animals find moonlight or starlight sufficient for vision, and the activities of many species are controlled by changes in light before sunrise or after sunset. A host of marine animals respond to the light from luminescent organisms ; in some instances they may be attracted, in others repelled, or guided by a recognition of the pattern of light. For certain species luminescence perhaps provides sufficient general illumination for vision, as will be discussed in a subsequent report (CLARKE and BACKUS, 1956). The minium intensity of light which will affect photokinesis or phototaxis may be lower than the threshold for vision, and animals can undoubtedly respond to differences in light and shade, or day and night, at lower illuminations. The vertical migrations of plankton and of fish, which have become of special interest in relation to the movement of the deep scatting layers in the ocean, also occur at depths where the light is very weak (CLARKE and BACKUS, 1956).

Since all of the animal reactions mentioned above are affected by light intensities below the range of underwater photometers commonly used in previous investigations, a much more sensitive instrument was constructed in order to explore the problems involved as well as to add to our general knowledge of underwater optics. Previous discussions of possible light reactions in deep or turbid water, or during the dark part of the day, were based on extrapolations of shallow measurements under various assumptions as to the optical conditions in deeper layers.

The depth to which direct measurements can be made depends upon the type of photometer, the clarity of the water, and the intensity of the incident radiation. Underwater photometers employing photo-voltaic cells, such as the Weston photonic cell, are not serviceable for intensities much below 0·0005 g cal/cm^2/min or 35 μw/cm^2 (visible radiation). The energy of summer sunlight received on a horizontal surface at the Blue Hill Observatory, Boston, Mass., reaches a maximum of about 1·6 g cal/cm^2/min or 112,000 μw/cm^2 for total radiation, or about 0·75 g cal/cm^2/min or 53,000 μw/cm^2 for visible radiation. This is approximately equivalent to a light intensity of 11,000 ft. can. (HAND, 1937). Since the surface layers of the clearest ocean water cause a reduction in light of approximately ten fold for each 50 m of depth, as shown by earlier measurements, it is understandable that photronic cell photometers could not be used at depths greater than about 200 m under the best of circumstances.

Greater sensitivity and hence greater depth range has been attained by using photographic methods, but these are slow and are objectionable both because of the ship's time consumed and because changes in daylight and other conditions take place during the long period of exposure. JERLOV and KOCZY (1951) was able to carry out only a few measurements at depths greater than 200 m with a deep-sea camera. Their deepest measurement at 500 m made in the extremely clear water of the Sargasso Sea required an exposure of 2 h.

To satisfy the need for great sensitivity together with a rapid response, a photometer was designed which contains a photomultiplier tube and is capable of measuring intensities ranging down to less than 10^{-7} μw/cm^2 or about 10^{-12} of full sunlight. In most previous observations of light penetration the depth of the photometer has been calculated from the length of the supporting cable and the wire angle at the surface. Since this procedure becomes unreliable at depths greater than 200 m, a depth meter was attached to the photometer head and the unit provided with insulated leads running to a deck unit where direct simultaneous readings could be made of the depth of the photometer and the light intensity at that depth. The combined instrument, termed the bathyphotometer, and measurements made with it in the Atlantic Ocean, are described below.

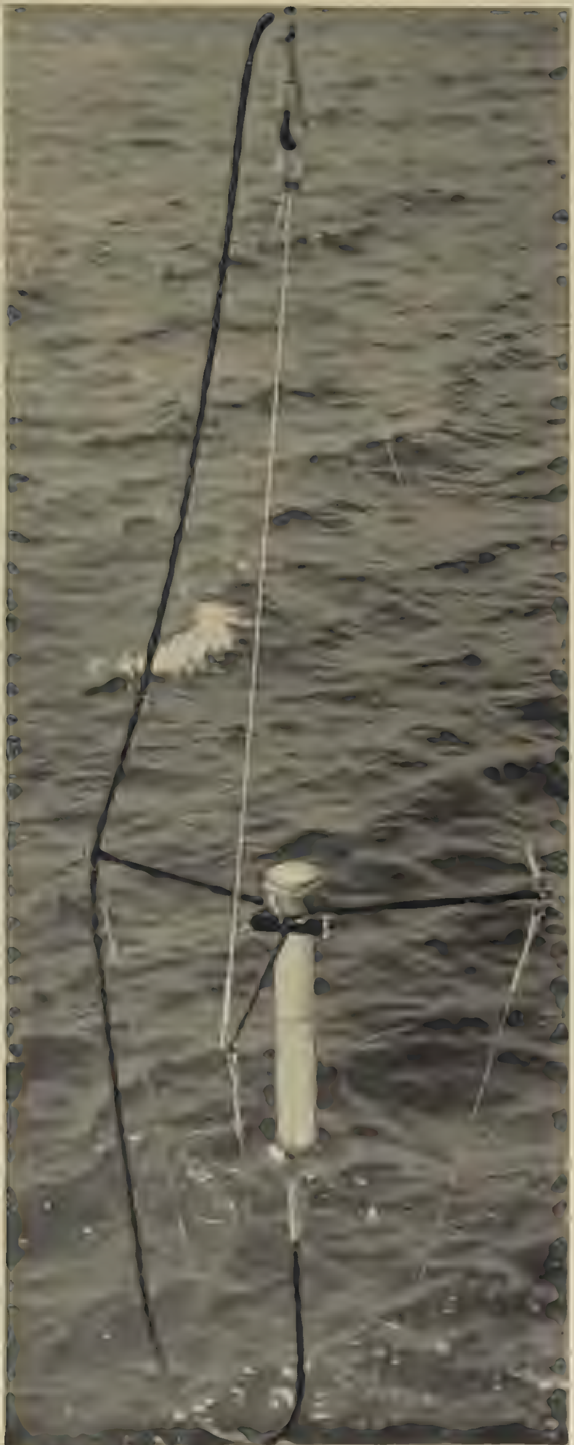

Fig. 1. Submerged unit before lowering. The hood for near-surface measurements has been placed over the photometer head. A 50 kg cylindrical lead weight was hung below the photometer

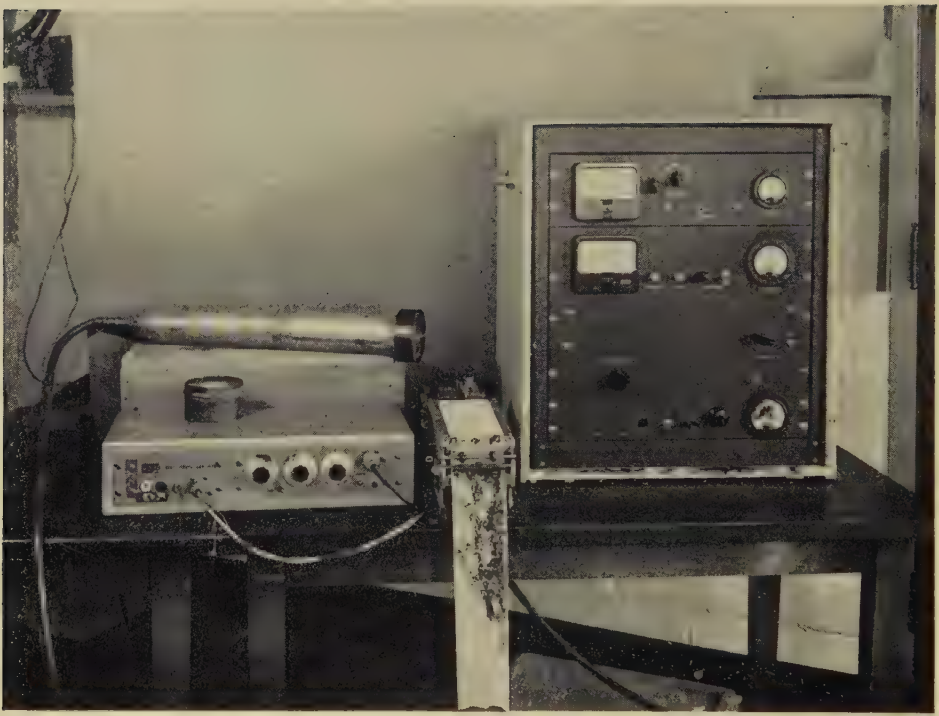

Fig. 2. Deck unit (right) showing microammeter for measuring light and depth, Brush recorder (centre) with Edin oscillograph amplifier (left) and submerged unit (rear) with hood removed.

DESCRIPTION OF BATHYPHOTOMETER

The bathyphotometer consists of two basic elements : a submerged unit (Fig. 1) carrying the photomultiplier tube and the depthmeter sensing element, and a deck unit (Fig. 2) consisting primarily of a high-voltage supply, a depthmeter indicator, and a vacuum tube microammeter. Supplementary equipment includes an Edin oscillograph amplifier and Brush recorder, on which flashes of light from luminescent animals can be recorded, and a field calibration unit. The size of the submerged unit has been kept small to reduce the drag and tilt of the instrument when lowered into water moving relative to the ship, and to enable it to be lowered on its own power-signal cable. The case is designed to operate to a depth of 750 metres.

The use of photomultiplier tubes to extend the range of underwater light measurements introduces a number of new considerations. Photronic cells are directly connected to a low impedance microammeter, or galvanometer, and have a stable, though low, sensitivity. Photomultiplier tubes, on the other hand, have remarkably high sensitivity, but possess certain inherent disadvantages. The tubes require a high supply voltage, of the order of 1,000 volts, and produce a signal current which ranges from ·01 microampere to 1 milliampere. The output at constant light level is strongly dependent on the supply voltage so that a well-regulated power source is necessary. The signal at constant light level and constant voltage is also a function of the orientation of the tube in the earth's magnetic field, and hence requires magnetic shielding.

Further difficulty arises from the fact that both the 1,000-volt supply and the small signal current must pass through the same cable and connectors. It has been found, however, that the use of shielded leads and guard rings will maintain adquately low leakage to the signal wire.

The spectral response of photomultiplier tubes, unlike that of the photronic cell, is not similar to the standard luminosity curve for the human eye ; so that direct readings of illuminance, if desired, can only be obtained through the use of filters with attendant loss of sensitivity. However, the spectral response of certain photomultiplier tubes has a broad maximum in the region of transmission of sea water, so that they may be employed for measurements of energy flux under suitable conditions.

Photometer. The photometer utilizes the linearity of the current response of photomultiplier tubes operated at constant supply voltage to obtain an extended scale of inherently higher precision than can be obtained by operating at constant anode current (Sweet, 1946 ; Kampa and Boden, 1954). The photometer circuit comprises a high-voltage supply, the phototube, and the vacuum tube microammeter (Fig. 3).

The high-voltage supply utilizes a chain of special Amperex 0G3 regulator tubes, characterized by stability and low drain, and allows selection of the high voltage in steps of 83 volts, which is the operating voltage of a single 0G3. Line voltage fluctuations at the input to the supply are controlled manually since line frequency instability on board ship makes the use of constant voltage transformers unreliable. In the absence of input voltage control fractional output voltage fluctuations are 1/50 of the fractional input voltage fluctuations.

An end window phototube is used for compactness and improved light collection geometry. An RCA 5819 was selected because of its favourable spectral response, which is high and relatively broad in the region of maximum transmission of sea water (Fig. 4). Its 3·75 cm diameter photocathode presents a large, well exposed area for the collection of light. The supply voltage required by this tube is lower than that of other similar types. It is protected against the earth's magnetic field by a Mu-metal shield.

The output of the phototube anode is brought to the deck unit by a shielded cable, and is there measured by a vacuum tube microammeter in which the various ranges are obtained by switching precision load resisters across the current to be measured.

Depthmeter. The depthmeter and associated circuit are identical with those used with cable-suspended hydrophones and described by Knott (1953). The sensing element is a helical bourdon tube which drives a wire-wound potentiometer. The meter has a full-scale deflection equivalent to 610 m and depths can be read to within ± 2 m.

Cable. The cable used was specially designed for this application and was constructed by the Okonite Co. Four conductors were cabled around a central core of aircraft steel (rated breaking strength 216 kg), and the whole was covered with a natural rubber compound for low-temperature flexibility, giving an outside diameter of 1·5 cm. Two of the conductors are of No. 14 tinned copper, are unshielded, and carry the depthmeter signal. The other two conductors are of No. 18 tinned copper, are shielded with copper braid, and carry the high-voltage and phototube signal respectively.

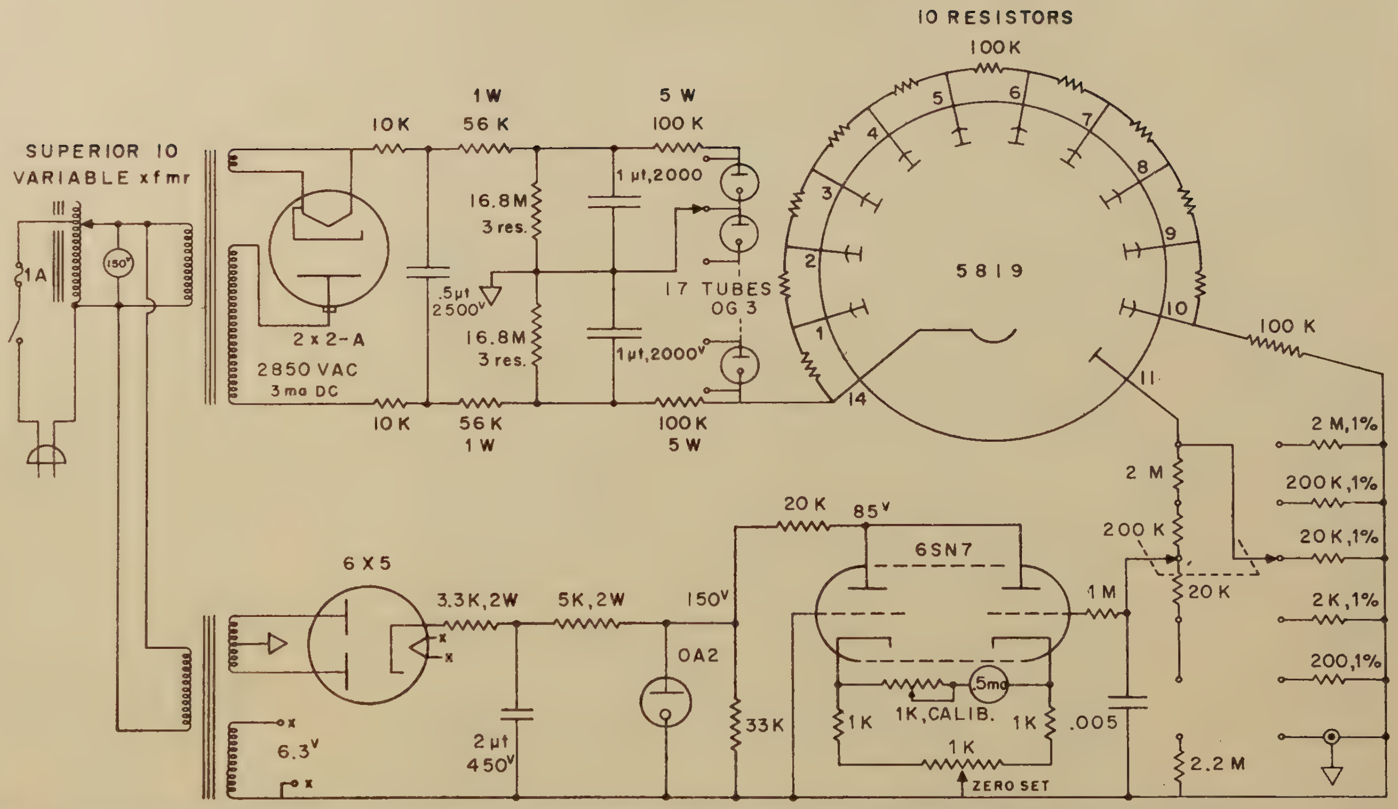
10 RESISTORS
100K
1
2
3
4
5
6
7
8
9
10
11
14
5819
100 K
SUPERIOR 10
VARIABLE xfmr
1A
150V
10K
1W
56 K
5 W
100 K
16.8M
3 res.
1 μf,2000
.5μf
2500V
16.8M
3 res.
1μf,2000V
17 TUBES
OG 3
2 x 2-A
2850 VAC
3 ma DC
10K
56K
1 W
100K
5 W
2 M,1%
200K,1%
20K,1%
2K,1%
200,1%
2 M
200 K
20 K
1 M
.005
2.2 M
20 K
85V
6SN7
5ma
1K
1K,CALIB.
1K
1K
ZERO SET
6 X 5
3.3K,2W
5K,2W
150V
OA2
33K
6.3V
2 μf
450V

Fig. 3. The photometer circuit showing the regulated high-voltage supply powered originally from the ship's 115 A.C. current, the R.A.C. 5819 photomultiplier tube, and the vacuum tube microammeter. All resisters are ½ W., 10% unless otherwise designated.

The shields are used as ground return for the depthmeter and photometer and, being at ground potential, prevent leakage to the signal lead.

The total length of cable available was 760 m, and a vertical depth of slightly over 600 m was reached with the photometer in calm weather. The whole cable weighed 234 kg in air or about 100 kg in water, but a stress greater than the weight of the cable can be caused by the drift and roll of the ship. The effect of the latter was reduced by using 5 stands of 1·3 cm shock cord in the attachment of the block over which the cable was paid out. The breaking strength of a sample section of the cable was found to be about 338 kg in a laboratory test ; at sea the cable was used at tensions up to 250 kg as measured by a Dillon dynamometer. The use of a multiconductor cable of this sort has the disadvantage of its bulk and weight in handling and its considerable drag in the water, but it provides the great advantage of allowing the voltage regulation and measurements of light and depth to be made directly and continuously in the deck laboratory.

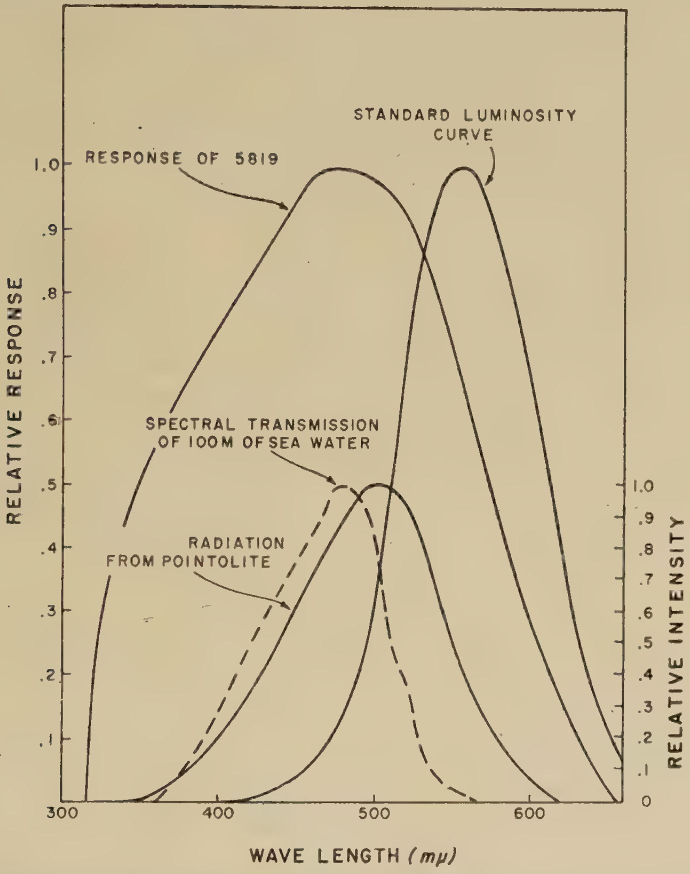

Fig. 4. Comparison of the response of R.C.A. photomultiplier cell 5819 with the standard luminosity curve (from the *Handbook of Chemistry and Physics*), the spectral transmission of the clearest sea water (CLARKE, 1939a), and the emission of the Point-o-lite lamp passing through Corning filter No. 4303.

Calibrating Unit. The calibrating unit consists of a 30 c/p " Point-o-Lite " bulb operated at 450 ma (Fig. 5) placed in a light-tight box at a distance of 37 cm from a door at one end into which the head of the photometer may be inserted. The radiation from the bulb is filtered through a Corning No. 4303 blue-green filter, yielding a computed irradiance of 12·5 microwatts/cm^2. This may be attenuated in known steps by interposing Kodak neutral density filters between the blue-green filter and the photometer head, *Calibration.* A photometer will read in units of illuminance, independent of the spectral distribution of the incident light, only if the response of the detector is identical with the standard luminosity curve (Fig. 4). In underwater photometry it is not desirable to measure the flux of radiant energy in these terms, which reflect the sensitivity of the human eye and are not necessarily pertinent to marine organisms. The measured transmission of sea water extends below 400 millimicrons, a region where a device reading in units of illuminance would be insensitive.

Calibration in terms of energy flux is possible because of the broad maximum in the response of the photomultiplier tube in the region of transmission of sea water. The actual calibration in terms of irradiance in microwatts/cm^2 is made by exposing the instrument to a known amount of radiant energy whose spectral distribution is similar to that of submarine daylight. The calibration is valid for light which falls in the range from 400 to 580 millimicrons, and thus is appropriate for measurements in the subsurface layers of the ocean where the radiation is confined within these limits (Clarke, 1954). For measurements near the surface allowance must be made for the fact that the photomultiplier tube is sensitive to longer wavelengths than those encountered in the deeper strata. Consequently, measurements with the bathyphotometer in the upper layers would be expected to yield a larger extinction coefficient than that obtained in the deeper layers, assuming that the water is homogeneous. Actually the value would not be expected to be much larger, because the spectral sensitivity of the photomultiplier tube cuts off rapidly. Since the bathyphotometer is relatively less sensitive than the Weston photronic cell to the longer wavelengths, the former would be expected to produce a somewhat smaller extinction coefficient than the latter in the upper strata of the same water body.

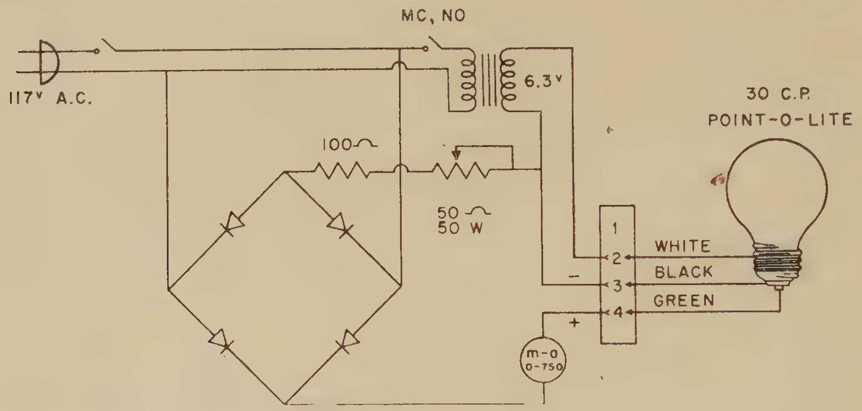

Fig. 5. Circuit for controlling the current supplied to the Point-o-lite lamp.

Since the linearity of the bathyphotometer has been demonstrated by careful laboratory calibration, it suffices in practice to establish one or two points on the calibration curve of current as a function of light intensity for each of the supply voltage used at sea.

Operating Limitations. The inherent linearity of the response of a photomultiplier tube is subject to two limitations. These are readily apparent in the complete calibration curves (Fig. 6). The nonlinearity at the high current level is due to the limited current flowing in the dynode voltage divider, and is not due to the tube itself. However, it serves as a safety device which prevents the anode rating of 750 μa from being appreciably exceeded. For the sake of gain stability it is desirable not to exceed 500 μa. Failure to observe the current rating of the anode may result in destruction of the tube, but long before this takes place fatigue of the last dynode stages will temporarily or permanently change the amplification of the photomultiplier tube (Engstrom, 1947).

In the practical use of the bathyphotometer the minimum light intensity which can be measured depends upon a minimal signal current which is significantly greater than the sum of the dark current and electrical leakage. During measurements at sea the dark current ranged between 0·01 and 0·04 μa when using the highest supply voltage for greatest sensitivity. A direct test with the photometer head shielded from all light showed that the dark current was no greater when the cable was

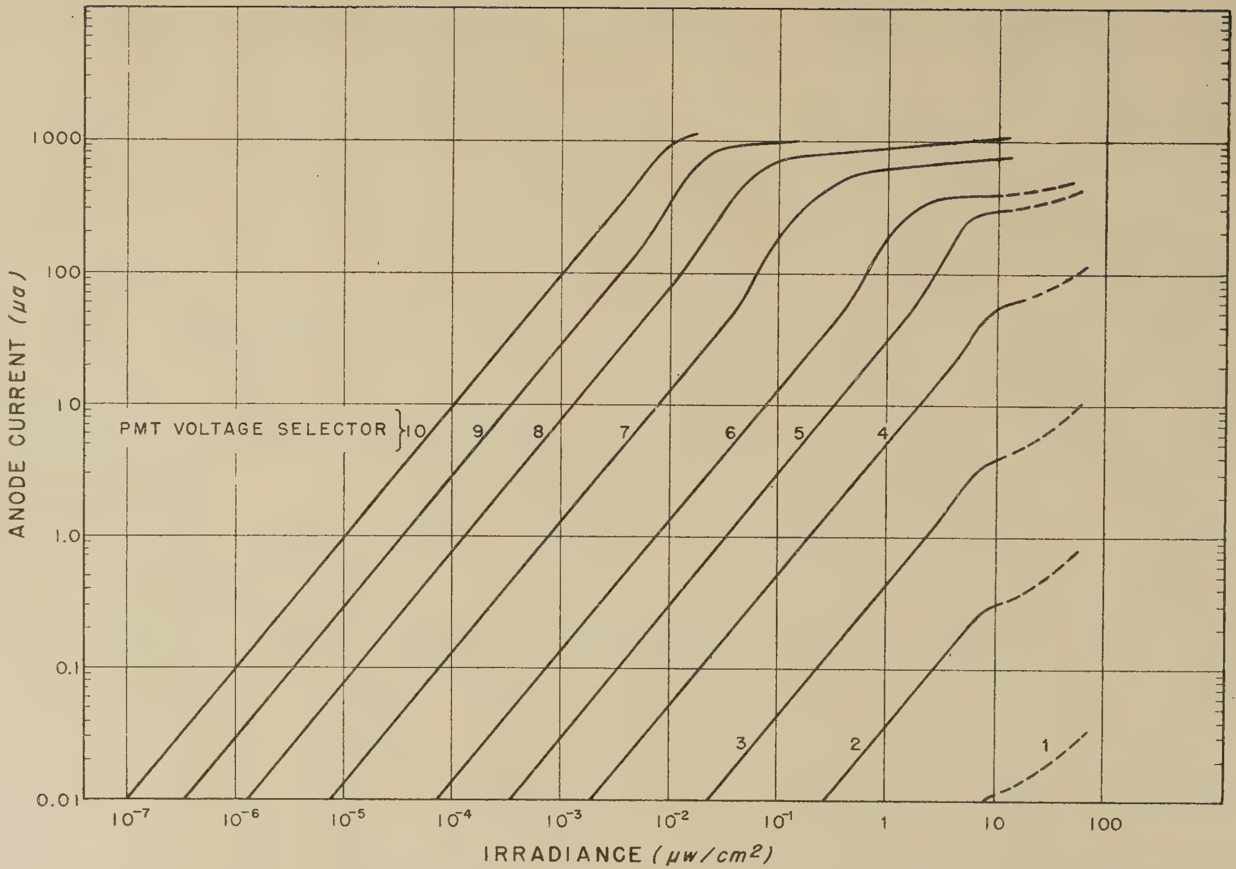

Fig. 6. Calibration curves for the bathyphotometer showing the relation between anode current and irradiance.

lowered into the water to its entire length than when it was reeled up on deck. As a result of the low and relatively steady dark current, illumination was measurable to a minimum of about 10^{-7} μw/cm^2.

The departure from linearity at high levels of illumination is caused by the internal resistance of the photocathode. It becomes noticeable when the illumination exceeds 3×10^{-4} of full sunlight. Consequently reliable readings of light of greater intensity than this cannot be made with the unprotected photometer. For measurements near the sea surface involving intensities extending up to full sunlight a hood containing a neutral filter of density 4 is placed over the photometer head. The filter is sealed between a disc of lucite below and a disc of No. 2254 Plexiglas above. The space between the lucite disc and the photometer head is filled with sea water to reduce reflection loss. This type of Plexiglas is a semi-translucent white material, equivalent to the opal glass used on older photometers. The Plexiglas disc forms the receiving surface of the hood and through its diffusing qualities minimizes the effect of solar angle, wave refraction, and photometer tilt. This arrangement follows the standard practice for the measurement of subsurface illumination (ATKINS, CLARKE, PETTERSSON, POOLE, UTTERBACK and ANGSTROM, 1938).

During observations at sea a record of changes in the radiation incident on the surface was kept by means of a deck photometer containing a Weston photronic cell. Suitable corrections were made in the calculations of transparency from the subsurface measurements. On the basis of the precision of the depth meter and lightmeter the values for the extinction coefficient obtained in this investigation are believed to be accurate to about 2%.

RESULTS OF MEASUREMENTS

One set of measurements with the bathyphotometer was made in the spring of 1955 at stations in the Florida Current located 10 and 40 miles off Miami, Florida, and another set was made the following summer at stations located in the slope water about 200 miles SE of New York. The dates, positions, and other data relating to the measurements are summarized in Table 1 together with the values of the extinction

Table 1. Summary of Measurements of Light Penetration.

Series	*Date* 1955	*Latitude N*	*Longitude W*	*Bottom depth (metres)*	*Depth range for measurements (metres)*	*Extinction coefficient k**	*Time E.S.T.*	*Sky*	*Wind (miles/hr)*
10	Mar. 4	25° 44′	79° 56′	311	20–75	·031	1100–1200	Clear	12
					75–152	·056			
12	Mar. 31	25° 35′	79° 24′	777	0–490	—	2000–2100	Halfmoon	18
13	Apr. 1	25° 35′	79° 24′	777	30–160	·043	0940–1040	Clear	12
					160–460	·034			
					460–580	·038			
20	July 18	38° 56′	70° 24′	3036	10–91	·072	1510–1715	Foggy	10
					91–427	·038			
21	July 19	38° 28′	68° 45′	3931	10–91	·072	1315–1545	Hazy	8
					91–363	.038			
					363–596	·041			
22	July 19	38° 25′	68° 48′	3950	0–610	—	2115–0030	Overcast	10
23	July 20	38° 24′	69° 10′	3840	0–290	—	1800–2035	Clear	8
24	July 21	38° 21′	69° 09′	3840	30–92	·062	1350–1530	Clear	12
					92–400	·039			
					400–554	·032			
25	July 21	38° 21′	69° 09′	3840	30–270	—	1725–1950	Clear	8

*Extinction coefficient = k in the equation $I/I_0 = e^{-kL}$ where light is reduced from I_0 to I by a stratum of water L metres thick.

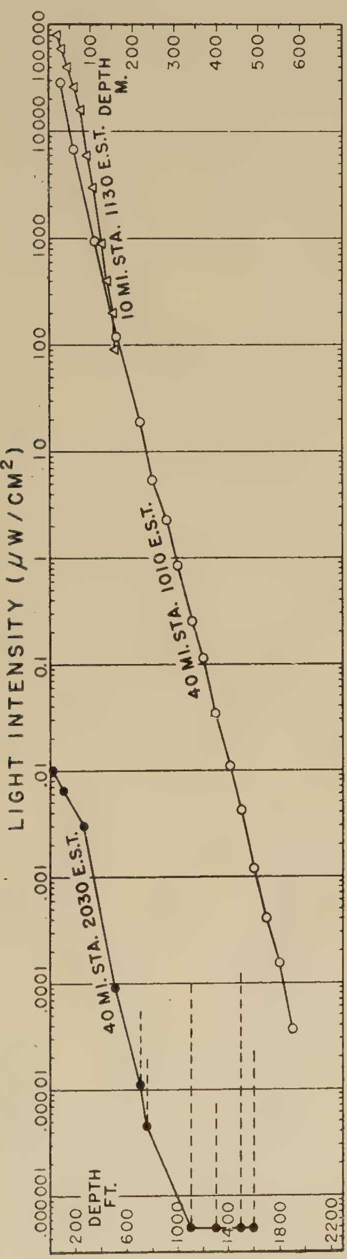

Fig. 7. Relation between depth and light intensity (logarithmic scale) at stations 10 miles off Miami (Series 10, Table 1) and 40 miles off Miami in daytime (Series 13) and at night (Series 12). Dashed lines indicate the approximate magnitude of flashes from luminescent animals.

coefficients for the indicated strata. Graphs of certain series of light penetration measurements are presented in Figs. 7 to 9. Details of the measurements made in relation to movements of deep scattering layers and in relation to luminescent flashes will be discussed separately (Clarke and Backus, 1956).

Measurements in the Florida Current

Transparency. The station occupied 10 miles off Miami was located in the western part of the Florida Current (Gulf Stream) where the water is a variable mixture from several sources, including the Yucatan Channel and the Gulf of Mexico. Measurements with the Clarke marine photometer containing a Weston photronic cell gave an extinction coefficient of k = ·050 on 4 March, 1955 for the water layer from 5 m to 25 m. Miller, Moore and Kvammen (1953) reported coefficients varying from k = ·041 to ·075 (with one observation of k = ·095) for the surface stratum at the same station between August, 1950 and February, 1952, using the same type of photometer.

Our measurements on 4 March, 1955 with the bathyphotometer (Series 10) gave an even lower value for the extinction coefficient for the stratum from 20 m to 75 m (k = ·031), but the value for the layers below 75 m was about the same as for the surface stratum. This indication of lower extinction values in the subsurface layer may be due to differences in the instruments, or a real difference in transparency may have existed. The observation of water clearer above 75 m than below that depth may be due to a direct and rapid movement of water at that level from the known clear water masses to the south (Clarke, 1938), whereas the deeper strata may have been mixed with less clear water from the Gulf of Mexico. Further observations will be necessary to determine whether the factors suggested above are actually effective, or whether other causes underlie the differences in transparency observed.

The station 40 miles off Miami was located east of the swiftest part of the Florida Current and only a few miles west of Gun Cay and Cat Cay. The water here, derived from among the Bahaman Islands and the Sargasso Sea, is relatively homogeneous and changes little from season to season. On 1 April the temperature in the upper 100 m was between 24° and 25°C and decreased at a uniform rate to 7·6°C at 645 m. Our daytime measurements with the bathyphotometer (Series 13) gave an extinction coefficient of k = ·043 for the stratum 30 to 160 m, and values varying from k = ·034 to ·038 down to 580 m. The water thus displayed a rather uniform transparency down to this great depth. The higher value for the extinction coefficient above 160 m may be due partly to the fact that the spectral sensitivity of the photometer includes the longer wavelengths which are absorbed rapidly in the upper strata. However, according to the calculations of Jerlov (1951) this selective action has little effect on the extinction coefficient at depths greater than 50 m in the clearest water. Since the graph for series 13 shows no noticeable change in slope down to 160 m., the lower transparency represented probably means that the water in this stratum had been modified more than the deeper water.

The transparency value for the stratum extending to 160 m may be compared with values obtained in neighbouring areas by Clarke using photronic cells and by Jerlov using selenium rectifier photoelectric cells. Measurements by Clarke (1938), in the Cayman Sea west of Jamaica, gave an extinction coefficient of ·045 for the stratum 2 to 95 m and of ·038 from 95 to 185 m. Values ranging from ·039 to ·049 for the upper 100 m were found at stations east of the Bahamas (CLARKE, 1941). Near the same area, using a photometer limited to the blue region of the spectrum (465 mμ), JERLOV (1951) obtained values of ·041 to ·043 for the stratum extending from 100 to 200 m. For the upper 100 m the extinction coefficient ranged from ·028 to ·039 for radiation limited to the blue region, but calculations showed that a value of about $k = \cdot 042$ would characterize the extinction for the whole spectrum for 25 to 100 m. Although the different sensitivities of the photometer used complicates the picture, it appears that the transparency of the water in the upper 200 m is generally uniform in the Caribbean region, and that our measurement on 1 April (Series 13) was representative.

Our measurements at deeper levels are the first that have been reported using direct reading photometers, but they may be compared with two measurements made with a deep-sea camera by JERLOV and KOCZY (1951) south of Bermuda. These investigators reported values of $k = \cdot 039$ and ·038 for strata extending from the surface to 400 m and to 500 m respectively. These values agree very closely with our measurements, which extended to 580 m.

Observations at Night. Measurements were made during the night of 31 March (Series 12) at the same station as that at which the daylight observations were made on 1 April. During the period of measurement a half moon was shining and the ship's lights were extinguished. From Fig. 7 it will be observed that under these conditions the light at night at the surface was roughly 10^{-7} of that during the middle of the day. As the bathyphotometer was lowered into the water, the light intensity dropped off at about the same rate as it did during the day until a depth of 335 m was reached.

When the photometer was suspended at depths greater than 200 m, the light meter recorded large but very brief increases in current at irregular intervals. These are almost certainly to be interpreted as flashes of luminescence from deep sea fishes, crustaceans, or other animals. On this occasion the first flashes were observed at a depth of 212 m. They were relatively infrequent at this level but became much more frequent at greater depths, until below about 300 m flashing was practically continual.

The approximate intensities of the flashes as they reached the photometer are indicated by the extent of the broken horizontal lines. Between 200 and 300 m the magnitude of the flashes was only about two to five times as great as the illumination penetrating from the surface. At depths greater than 300 m there was no further detectable diminution of light in the water, presumably because the general illumination from bioluminescence had become greater than the light reaching these depths from the surface. The intensity of individual flashes of luminescence was more than 200 times the magnitude of the background illumination. The flashes may have been produced by animals with brilliant photophores at some distance from the bathyphotometer, or by animals producing weaker luminescence at closer range, either stationary or moving past. Indeed, in some instances the photometer or its bridle may have actually come in contact with passing animals and thereby caused a luminescent discharge.

During the daytime measurements at the same station on 1 April, the needle of the light meter dropped steadily without irregularities at all levels down to 580 m.

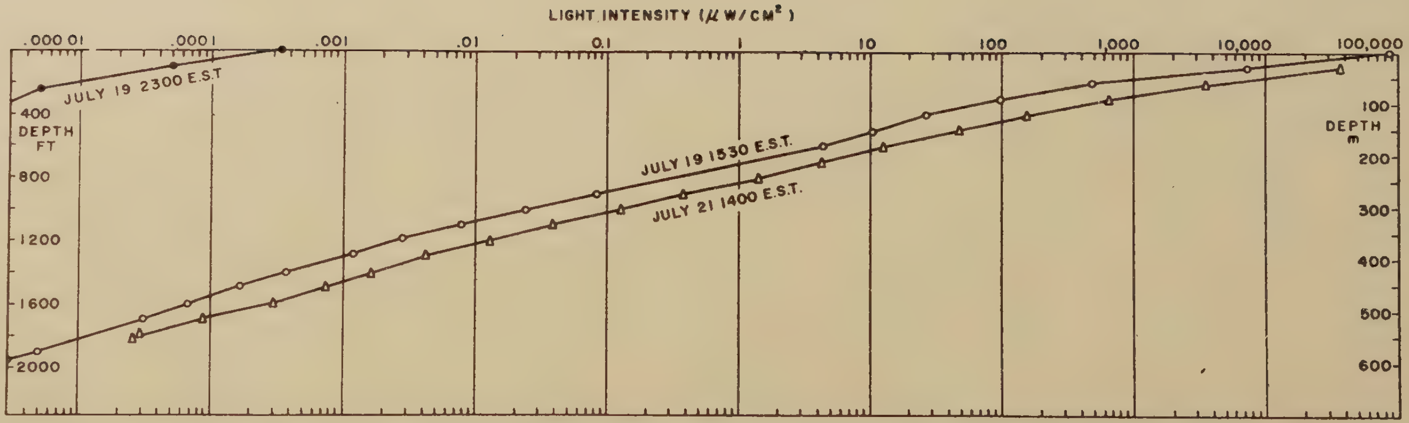

Fig. 8. Relation between depth and light intensity (logarithmic scale) at stations 200 miles S.E. of New York. The entire extent of daytime measurements on 19 July (Series 21) and on 21 July (Series 24) is shown, and the upper portion of nighttime measurements on 19 July (Series 22).

At this depth a few weak flashes were observed. Failure to observe flashes of luminescence at levels above this may have resulted from the fact that the higher intensity of illumination from the surface would render the animal light undetectable ; but it may also have been due to a migration of luminescent animals to greater depths during the day, or to a diurnal rhythm involving the cessation of luminescent discharge in the day period. Further investigation will be necessary to settle these questions.

Measurements in the slope water

Transparency. Measurements were made in the slope water between the continental shelf and the northern edge of the Gulf Stream at stations located about 200 miles SE of New York. At these stations the temperature in the upper 15 metres was about 24°C and dropped uniformly to 13°C at 65 m. Below this the temperature remained roughly constant to 150 m and then dropped to 4·7°C at 600 m. This thermal structure shows the effect of seasonal warming and reflects the fact that the upper layers of the slope water have received admixtures of coastal water. Differences in the origin of the various strata of the slope water may be correlated with vertical differences in transparency. Our measurements made on 18 to 21 July (Series 20, 21 and 24) reveal a stratum about 90 m thick with a higher extinction coefficient ($k = \cdot 062$ to ·072), overlying water considerably more transparent ($k = \cdot 032$ to ·041) Table 1 and Fig. 8).

The transparency found for the upper stratum may be compared with earlier observations in this general region. Measurements were made throughout the year 1937-38 at Stations *A*, *B* and *C* located respectively in the coastal water, the slope water, and the Sargasso water on a line between Long Island, N.Y. and Bermuda (CLARKE, 1939b). Station *B* was located about 20 miles north of the location of our present Series 20, and yielded values ranging from $k = \cdot 050$ to ·10 for the extinction coefficient. Our 18 July, 1955 value of ·072 falls in the middle of this range. A measurement on 7 March, 1941 (CLARKE, 1941 ; Station 4174, Series 556) at a point about half way between our Series 20 and 21 and only about 20 miles from Series 24 gave an extinction coefficient of ·077 for the upper 86 m, thus indicating close agreement with our present observations. At a station in the Gulf Stream about 50 miles south of our Series 21 and 24 occupied on 24 July, 1934, a value of $k = \cdot 049$ for the upper 140 m was obtained for wavelengths 490 to 620 mμ, and of $k = \cdot 048$ for the upper 180 m for wavelengths 310 to 450 mμ (OSTER and CLARKE, 1935 ; Station 2245, Series 311 and 310). At station *C* farther to the southeast in the Sargasso water coefficients varied between $k = \cdot 042$ and ·066 during 1937-38. Although these measurements are not entirely comparable because of differences in methods, a consistent change in transparency for the upper 100 m in this region is discernible from values averaging about $k = \cdot 08$ in the centre of the slope water to values of about $k = \cdot 05$ in the Sargasso water.

The much deeper extent of our present measurements makes it possible to compare the transparency of the upper stratum discussed above with the underlying water. The curves of light penetration for all three daytime series in this region show a change of slope at about 90 m. The underlying water down to about 400 m has an extinction coefficient of $k = \cdot 038$ or ·039. The water below this was characterized by a slightly higher value ($k = \cdot 041$) in Series 21 and a somewhat lower value ($k = \cdot 032$) in series 24.

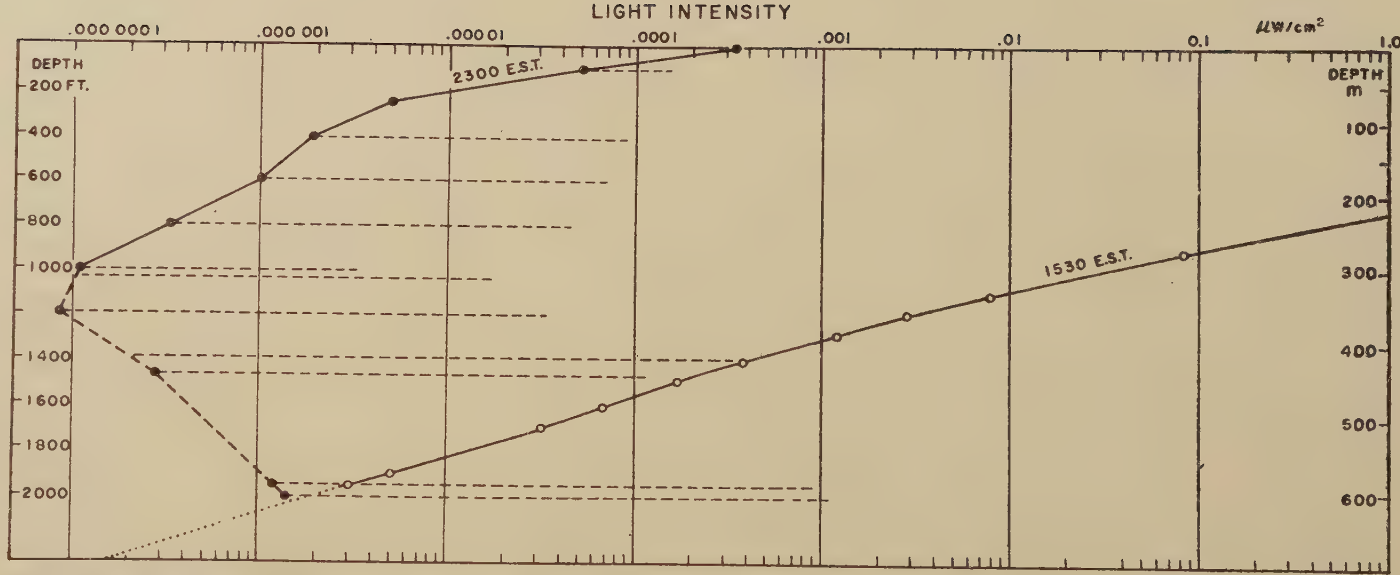

Fig. 9. The lower portion of daytime measurement (1530 E.S.T., Series 21) and entire extent of nighttime measurement (2300 E.S.T., Series 22) on 19 July at the same station 200 miles S.E. of New York. The dotted line is an extrapolation of the daytime curve assuming the same transparency. Dashed lines indicate the approximate magnitude of flashes from luminescent animals.

The only other deep measurements available for comparison with our observations in the slope water are our present Series 13 off Miami and the measurements of JERLOV (1951) and of JERLOV and KOCZY (1951) south of Bermuda – both in entirely different water masses and more than 800 miles away. Reference to Table 1 will show that the transparency of the deeper slope water is closely similar to that found off Miami. The value of JERLOV and KOCZY of $k = \cdot 041$ to $\cdot 043$ for the stratum from 100 to 200 m, obtained with a photo-electric photometer, and of $k = \cdot 039$ and ·038 for strata extending to 500 m, obtained photographically, are also in close agreement with our results. In addition, three deep observations by these investigators in the Pacific Ocean near Tahiti produced nearly the same extinction coefficients. Our measurements thus add to the areas of the sea which have been found to have a remarkably uniform and similar transparency from 100 m down to 400 m or to 600 m. The question of whether this uniformity extends to yet greater depths and to all regions of the ocean must await further investigation.

Observations at Night. Night measurements were made beginning in the evening of 19 July and extending past midnight (indicated as 2300 E.S.T. in figures). The upper portion of the night curve is shown in Fig. 8, where it can be seen that the night illumination at the surface was somewhat less than 10^{-8} of the daytime illumination. The moon had not risen, the sky was lightly overcast, and all externally visible lights of the ship were extinguished. The lower part of the daytime curve and the entire extent of the night observations are shown in Fig. 9.

The night measurements showed a diminution of light with depth through the upper 75 m at about the same rate as was observed during the day. At greater depths the rate of extinction became less. A few flashes of light, presumably from luminescent animals, were observed at 30 m, and flashing became more frequent, though irregular, at increasing depths, as was the case in the night observations off Miami. Below about 300 m flashing had become so frequent that the background illumination could be determined only with diffculty, and is indicated by a continuation of the curve as a broken line. At depths greater than 360 m the background illumination definitely increased, until at 600 m there was just about as much light at night as during the day. The approximate magnitude of the larger, individual flashes of bioluminescence is indicated by the horizontal broken lines. A tendency for the brightest flashes to occur at the greater depths is apparent ; some of these were 1,000 times the intensity of the background. During the daytime measurements occasional flashes, slightly above the background illumination, were noted (but not indicated on the figure) at about 400 m, and especially at depths greater than 460 m ; but these were not sufficiently frequent to interfere with the determination of the background illumination. However, if the amount of luminescence during the day is the same, or greater, below 600 m, then the general illumination will not decrease, and may even increase. No doubt the intensity and the degree of irregularity in the illumination will be found to vary greatly at different depths and in different regions of the sea, according to the type and abundance of luminescent animals present.

Some information exists on the vertical and horizontal distribution of deep-sea animals possessing photophores or other means of producing luminescence, but up to the present we have had little knowledge of the quantity, quality, or periodicity of the light produced. Graphical records of variations in luminescence at levels above 500 m at night are given by CLARKE and BACKUS (1956). During his descent in the bathysphere off Bermuda, Beebe (1934) could see no daylight from the surface at depths greater than 520 to 580 m, but he reported the occurrence of brilliantly luminescent animals at all depths down to 920 m, where he states ; " the jet blackness of the water was broken only by sparks and flashes and steadily glowing lamps of appreciable diameter, varied in colour and of infinite variety as regards size and juxtaposition." The blackening of a photographic plate at a depth of 1,000 m in the vincinity of the Azores, reported by Helland-Hansen (1912) and often referred to in the literature, may have been due in part to the light from passing luminescent animals. Methods are being considered for extending our light measurements to still greater depths, and for ascertaining the type, abundance, and activity of luminescent animals at deeper levels.

Acknowledgements—The authors are indebted to J. B. Hersey, S. T. Knott, W. Dow, E. T. Bunce, W. E. Witzell, and A. Vine for valuable suggestions and assistance in the design and construction of the bathyphotometer. We also wish to acknowledge the assistance of F. J. Shea, G. C. McLeod, and W. L. Clarke, especially in relation to the measurements at sea. We wish to thank the staff of the Marine Laboratory at the University of Miami for co-operation and facilities provided for the observations made off the coast of Florida.

The investigation was supported by funds from Research Grant G-796 of the National Science Foundation and Contract Nonr-1720 (00) NR-083-116 of the Office of Naval Research.

*Harvard University and Woods Hole Oceanographic Institution.**

Contribution No. 821 *from the Woods Hole Oceanographic Institution.*

REFERENCES

Atkins, W. R. G., Clarke, G. L., Pettersson, H., Poole, H. H., Utterback, C. L. and and Angstrom, A. (1938), Measurement of submarine daylight. *J. du Cons.*, **13**, 37-57.

Beebe, W. (1934), *Half Mile Down.* Harcourt Brace and Co., New York, 340 pp.

Clarke, G. L. (1936), On the depth at which fish can see. *Ecology*, **17**, 452-456.

Clarke, G. L. (1938), Light penetration in the Caribbean Sea and in the Gulf of Mexico. *J. Mar. Res.*, **1**, 85-94.

Clarke, G. L. (1939a), The utilization of solar energy by aquatic organisms. In : Problems in Lake Biology. *Publs. Amer. Assoc. Advance. Sci.*, **10**, 27-38.

Clarke, G. L. (1939b), Variation in the transparency of three areas of the Atlantic throughout the year. *Ecology*, **20**, 529-543.

Clarke, G. L. (1941), Observations on transparency in the southwestern section of the North Atlantic Ocean. *J. Mar. Res.*, **4**, 221-230.

Clarke, G. L. (1954), Elements of Ecology. John Wiley and Sons, New York, 534 pp.

Clarke, G. L. and Backus, R. H. (1956), Measurements of light penetration in relation to vertical migration and records of luminescence of deep sea animals. (In preparation).

Engstrom, R. W. (1947), Multiplier phototube characteristics. *J. Optical Soc., Amer.*, **37** (6), 420-431.

Hand, I. F. (1937), Review of the U.S. Weather Bureau solar radiation investigations. *Monthly Weather Rev.*, **65**, 415.

Helland-Hansen, Bjørn (1912), Physical Oceanography. In : *Depths of the Ocean.* (J. Murray and Johan Hjort), MacMillan & Co., London, 210-306.

Jerlov, N. G. (1951), Optical studies of ocean waters. *Repts. Swedish Deep-Sea Exped., Phys. Chem.*, 3 (1), 1-59.

---

*Present address of G. K. Wertheim *Bell Telephone Laboratories, Murray Hill, N.J.*

JERLOV, N. G. and KOCZY, F. (1951), Photographic measurements of daylight in deep water. *Repts. Swedish Deep-Sea Exped., Phys. Chem.*, 3 (2), 63-69.

KAMPA, E. M. and BODEN, B. P. (1954), Sonic scattering layer studies – an interim report. *Bermuda Biol. Sta. Rept.* (NR165-195). No. 1, 1-28. (Unpublished manuscript).

KNOTT, S. T. (1953), Design of depth meters for use with cable suspended hydrophones. *Woods Hole Oceanogr. Inst. Ref.* No. 53-44. (Unpublished manuscript).

MILLER, S. M., MOORE, H. B. and KVAMMEN, K. R. (1953), Plankton of the Florida Current. 1. General conditions. *Bull. Mar. Sci., Gulf and Caribbean*, **2**, 465-485.

OSTER, R. H. and CLARKE, G. L. (1935), The penetration of red, green and violet components of daylight into Atlantic waters. *J. Optical Soc., Amer.*, **25**, 84-91.

SWEET, M. H. (1946), Logarithmic photometer. *Electronics*, **19**, 106-109.

Prnetd in Great Britain by The Salisbury Press Ltd., Publicity House, Wilton Road, Salisbury, Wilts. (96500)

Contribution No. 823

Reprinted from Limnology and Oceanography
Vol. 1, No. 3, July, 1956
Printed in U.S.A.

A Dynamic Height Method for the Determination of Currents in Deep Lakes[1]

John C. Ayers

Department of Conservation, Cornell University and Woods Hole Oceanographic Institution

ABSTRACT

An adaptation of the oceanographer's dynamic height method to freshwater conditions, the method develops directly from the Smithsonian Tables of water density as a function of temperature and from Amagat's coefficients of compressibility. Pressure effects are handled by use of the decibar system. The calculated dynamic heights are plotted and contoured. Current directions are obtained by application of the geostrophic principle; current velocities are computed from the slopes of the surface topography. A table of specific volume anomalies, necessary for the height computation, has been developed. Sources of potential error are reviewed and assessed. The method has been applied to three synoptic surveys of Lake Huron, and the results obtained are both internally consistent and in good agreement with the behaviors of other parameters. When used with proper caution the method appears to be a promising technique for the study of certain circulation phenomena of large deep lakes.

INTRODUCTION

It is well known that freshwater is slightly compressed by pressure and expanded by temperatures above and below 4° Centigrade. For some decades the oceanographer has made use of similar phenomena to calculate current direction and velocity from density data, and from the reciprocal of density—specific volume. It appears that with certain modifications the oceanographer's dynamic height method of current determination can be applied to at least the deeper lakes.

The degree to which this application may be limited by the shallowness of lakes is not yet clear. The method depends upon the selection of a subsurface reference level at which currents are virtually absent. It is imperative that the reference level be below the depth of the turbulent mixing and return flow that result from wind action. It appears from the work of Mortimer (1951, 1954) that turbulent mixing and return may, under ordinary winds, attain two or three times the mean depth of the thermocline. The depth to which summer warming penetrates may also be used as a measure of the over-all depth of wind-caused mixing; the latter was used in Lake Huron (Table 3). On the basis of our present knowledge, the method appears to be applicable in lakes where the preponderance of depths is more than three times the mean depth to the thermocline.

It is strongly urged that currents determined by this method be checked against currents obtained by other means; lack of agreement may indicate that significant bottom currents are present and that bottom stress must be considered. The dynamic height method may be unsuccessful during periods of spring and fall turnover.

THE METHOD

The dynamic (or geopotential) height method deals with the calculated lengths of water columns which are considered to be standing upon the horizontal reference level. In each component segment of the water column at each station the resultant effect, on length, of compression due to hydrostatic pressure of overlying water and expansion due to temperatures above or below 4° C is determined. Summation of the resultant effects in all the component segments gives the column's length change resulting from the expansions and/or compressions of its parts. Addition of this length change to the theoretical length of the column under standard conditions gives the calculated height of the column top above the reference level under the prevailing conditions of pressure and temperature. The differing heights of the column tops at the various stations produce a "topography" of the water surface. From this dynamic or geopotential topography the current directions and velocities are obtained.

---

[1] Contribution No. 2 from the Great Lakes Research Institute and Contribution No. 823 from the Woods Hole Oceanographic Institution.

The freshwater method's primary length unit is the centimeter. Its use allows unusual convenience in operating with specific volume.

The effects of temperature on volume per unit mass have been obtained from the Smithsonian Tables as quoted in the *Handbook of Chemistry and Physics* (1949, Table of relative density and volume of water). The volume per unit mass is the specific volume.

Volume/unit mass = specific volume
$= a_{t,o}$ (at observed temperature (1)
and zero hydrostatic pressure)

The coefficients of compressibility used are those of Amagat (1893)[2] as given in the *Handbook of Chemistry and Physics* (*op. cit.*, Table of compressibility of liquids). Amagat's coefficients for 1 to 25 atmospheres pressure at 0, 10, and 20° C were graphed, and the graph extrapolated to 30° C; from the graph the coefficient at each degree was obtained (Table 1).

Amagat's unit "contraction in unit volume per atmosphere" (cm³/cm³/atm) when multiplied by the number of volumes involved becomes compression per atmosphere (cm³/atm); when one specific volume is used the compression is numerically the same as the coefficient and has the unit cm³/gm/atm.

TABLE 1. *Compressibility coefficients and compression in unit volume* (C_t) *at temperatures between 0 and 30 degrees Centigrade, based on Amagat* (*1893*)

°C	Compressibility coefficient* (cm³/cm³/atm)	Compression in 1 cm³ (C_t)* (cm³/atm)
	$\times 10^{-6}$	$\times 10^{-6}$
0	52.50	52.50
1	51.95	51.95
2	51.60	51.60
3	51.30	51.30
4	51.05	51.05
5	50.80	50.80
6	50.60	50.60
7	50.43	50.43
8	50.27	50.27
9	50.13	50.13
10	50.00	50.00
11	49.85	49.85
12	49.75	49.75
13	49.64	49.64
14	49.53	49.53
15	49.44	49.44
16	49.35	49.35
17	49.30	49.30
18	49.22	49.22
19	49.15	49.15
20	49.10	49.10
21	49.05	49.05
22	49.02	49.02
23	48.98	48.98
24	48.93	48.93
25	48.90	48.90
26	48.88	48.88
27	48.85	48.85
28	48.82	48.82
29	48.81	48.81
30	48.80	48.80

* Second decimal places only approximate.

Since one atmosphere of hydrostatic pressure = 1 bar = 10 decibars = the hydrostatic pressure of ten meters of water, and one meter of water produces one decibar of pressure, the depth in meters is therefore essentially numerically equal to the pressure in decibars. Also

Depth in meters/10
$= \text{atmospheres pressure} = p$ (2)

Compression at observed temperature, C_t, (Table 1) multiplied by the *in situ* pressure at depth gives compression *in situ*

$C_t \times p =$ compression *in situ* $= \Delta a_{t,p}$. (3)

It is assumed that a lake has constant surface area during the short period when data are being collected, i.e., the lake consists of a finite number of water columns each of constant 1 cm² cross section. Volume changes may then be considered as consisting entirely of changes in length, and each component specific volume of

---

[2] The author is aware of Beyer's (1954) conclusion that Amagat's coefficients are slightly too large. The use of Amagat's coefficients may introduce a small systematic error.

TABLE 2. *Specific volume anomaly* ($10^5\delta_{t,p}$)*
(Specific volume length anomaly when applied to columns of 1 cm² cross section)

Depth		Pressure, atmospheres	Temperature, °C							
feet	meters		0	1	2	3	4	5	6	7
0	0	0	13.0	7.0	3.0	1.0	0	1.0	3.0	7.0
	5	0.5	10.4	4.4	0.4	−1.6	−2.5	−1.5	0.5	4.5
	10	1.0	7.8	1.8	−2.2	−4.1	−5.1	−4.1	−2.1	2.0
	15	1.5	5.1	−0.8	−4.7	−6.7	−7.7	−6.6	−4.6	−0.6
50	15.2	1.52	5.0	−0.9	−4.8	−6.8	−7.8	−6.7	−4.7	−0.7
	25	2.5	−0.1	−6.0	−9.9	−11.8	−12.8	−11.7	−9.7	−5.6
100	30.5	3.05	−3.0	−8.8	−12.7	−14.6	−15.6	−14.5	−12.4	−8.4
	35	3.5	−5.4	−11.2	−15.1	−17.0	−17.9	−16.8	−14.7	−10.7
150	45.7	4.57	−11.0	−16.7	−20.6	−22.4	−23.3	−22.2	−20.1	−16.1
	50	5.0	−13.3	−19.0	−22.8	−24.7	−25.5	−24.4	−22.3	−18.2
	100	10.	−39.5	−45.0	−48.6	−50.3	−51.1	−49.8	−47.6	−43.4
	150	15.	−65.8	−70.9	−74.4	−76.0	−76.6	−75.2	−72.9	−68.7
	200	20.	−92.0	−96.9	−100.2	−101.6	−102.1	−100.6	−98.2	−93.9
	250	25.	−118.3	−122.9	−126.0	−127.3	−127.6	−126.0	−123.5	−119.1

Depth		Pressure, atmospheres	Temperature, °C							
feet	meters		7	8	9	10	11	12	13	14
0	0	0	7.0	12.0	19.0	27.0	37.0	48.0	60.0	73.0
	5	0.5	4.5	9.5	16.5	24.5	34.5	45.5	57.5	70.5
	10	1.0	2.0	7.0	14.0	22.0	32.0	43.0	55.0	68.0
	15	1.5	−0.6	4.5	11.5	19.5	29.5	40.5	52.6	65.6
50	15.2	1.52	−0.7	4.4	11.4	19.4	29.4	40.4	52.5	65.5
	25	2.5	−5.6	−0.6	6.5	14.5	24.5	35.6	47.6	60.6
100	30.5	3.05	−8.4	−3.3	3.7	11.8	21.8	32.8	44.9	57.9
	35	3.5	−10.7	−5.6	1.5	9.5	19.6	30.6	42.6	55.7
150	45.7	4.57	−16.1	−11.0	−3.9	4.2	14.2	25.3	37.3	50.4
	50	5.0	−18.2	−13.1	−6.1	2.0	12.1	23.1	35.2	48.2
	100	10.	−43.4	−38.3	−31.1	−23.0	−12.9	−1.8	10.4	23.5
	150	15.	−68.7	−63.4	−56.2	−48.0	−37.8	−26.6	−14.5	−1.3
	200	20.	−93.9	−88.5	−81.3	−73.0	−62.7	−51.5	−39.3	−26.1
	250	25.	−119.1	−113.7	−106.3	−98.0	−87.6	−76.4	−64.1	−50.8

Depth		Pressure, atmospheres	Temperature, °C							
feet	meters		14	15	16	17	18	19	20	21
0	0	0	73.0	87.0	103.0	120.0	138.0	157.0	177.0	198.0
	5	0.5	70.5	84.5	100.5	117.5	135.5	154.5	174.5	195.6
	10	1.0	68.0	82.1	98.1	115.1	133.1	152.1	172.1	193.1
	15	1.5	65.6	79.6	95.6	112.6	130.6	149.6	169.6	190.6
50	15.2	1.52	65.5	79.5	95.5	112.5	130.5	149.5	169.5	190.5
	25	2.5	60.6	74.6	90.7	107.7	125.7	144.7	164.7	185.7
100	30.5	3.05	57.9	71.9	88.0	105.0	123.0	142.0	162.0	183.0
	35	3.5	55.7	69.7	85.7	102.7	120.8	139.8	159.8	180.8
150	45.7	4.57	50.4	64.4	80.5	97.5	115.5	134.5	154.6	175.6
	50	5.0	48.2	62.3	78.3	95.4	113.4	132.4	152.5	173.5
	100	10.	23.5	37.6	53.7	70.7	88.8	107.9	127.9	149.0
	150	15.	−1.3	12.8	29.0	46.1	64.2	83.3	103.4	124.4
	200	20.	−26.1	−11.9	4.3	21.4	39.6	58.7	78.8	99.9
	250	25.	−50.8	−36.6	−20.4	−3.3	15.0	34.1	54.3	75.4

Depth		Pressure, atmospheres	Temperature, °C							
feet	meters		21	22	23	24	25	26	27	28
0	0	0	198.0	221.0	244.0	268.0	294.0	320.0	347.0	375.0
	5	0.5	195.6	218.6	241.6	265.6	291.6	317.6	344.6	372.6
	10	1.0	193.1	216.1	239.1	263.1	289.1	315.1	342.1	370.1
	15	1.5	190.6	213.7	236.7	260.7	286.7	312.7	339.7	367.7
50	15.2	1.52	190.5	213.6	236.6	260.6	286.6	312.6	339.6	367.6
	25	2.5	185.7	208.7	231.8	255.8	281.8	307.8	334.8	362.8
100	30.5	3.05	183.0	206.1	229.1	253.1	279.1	305.1	332.1	360.1
	35	3.5	180.8	203.8	226.9	250.9	276.9	302.9	329.9	357.9
150	45.7	4.57	175.6	198.6	221.6	245.6	271.7	297.7	324.7	352.7
	50	5.0	173.5	196.5	219.5	243.5	269.6	295.6	322.6	350.6
	100	10.	149.0	172.0	195.0	219.1	245.1	271.1	298.2	326.2
	150	15.	124.4	147.5	170.5	194.6	220.7	246.7	273.7	301.8
	200	20.	99.9	123.0	146.0	170.1	196.2	222.2	249.3	277.4
	250	25.	75.4	98.5	121.6	145.7	171.8	197.8	224.9	253.0

* Decimals are only approximate.

each column may be considered to contain unit mass in a 'cube' of 1 cm^2 cross section and variable length. Thus compression effects may be subtracted from the specific volume at temperature to obtain the resultant length of the specific volume 'cube' at *in situ* temperature and pressure

$$a_{t,o} - \Delta a_{t,p} = \text{specific volume length } \textit{in situ} = a_{t,p}. \quad (4)$$

To reduce the physical size of the numbers it is convenient to work with the specific volume length anomaly which, further, is multiplied temporarily by 10^5.

$$a_{t,p} - 1.000000 = \text{specific volume length anomaly} = \delta_{t,p} \quad (5)$$

The computations leading to the tabulated (Table 2) specific volume length anomaly of water at 15° C and 25 meters depth will serve as an example of the way the table was constructed.

$$a \text{ at } 15°, 0 \text{ hydrostatic pressure} = a_{t,o} = 1.00087 \text{ cm}^3/\text{gm} \quad \text{(Eq. 1)}$$

$$p = 25 \text{ meters} \div 10 \text{ meters/atm} = 2.5 \text{ atm} \quad \text{(Eq. 2)}$$

$$\Delta a_{15,2.5} = pC_t = 2.5 \text{ atm} \times 49.44 \times 10^{-6}\text{cm}^3/\text{gm/atm} = 123.6 \times 10^{-6}\text{cm}^3/\text{gm} \quad \text{(Eq. 3)}$$

$$a_{15,2.5} = (1.00087 \text{ cm}^3/\text{gm} \div 1 \text{ cm}^2/\text{gm}) - (123.6 \times 10^{-6}\text{cm}^3/\text{gm} \div 1 \text{ cm}^2/\text{gm}) = 1.00087 \text{ cm} - 123.6 \times 10^{-6} \text{ cm} = 1.000746 \text{ cm} \quad \text{(Eq. 4)}$$

$$\delta_{15,2.5} = 1.000746 \text{ cm} - 1 \text{ cm} = 0.000746 \text{ cm} \quad \text{(Eq. 5)}$$

$$10^5\delta_{15,2.5} = 74.6 \text{ cm}$$
(see $t = 15°$, $p = 2.5$ atm in Table 2)

The specific volume length anomalies ($10^5\delta_{t,p}$) for each degree between 0 and 28° C and at several pressure levels are given in Table 2. This table is of minimal size so far as numbers of pressure levels are concerned. The user is advised to expand it by adding other pressure levels in the depth (pressure) range which pertains to his lake.

Computation begins with a fairly detailed reading of the temperature profile, in which the profile is broken down into its essentially linear portions and the temperature and depth (pressure) of each inflection point recorded. Enough inflection points should be read to reproduce the profile well when these points on a graph are connected by straight lines.

The required specific volume length anomaly for the surface temperature is found by interpolation between the proper values of Table 2. Similarly the anomaly for each inflection point is found, by single interpolation when the depth (pressure) falls on a tabulated pressure level, or by double interpolation when observed temperature and pressure both fall between tabulated values.

The anomaly is determined for the surface, for each inflection point, and for the reference level. The anomalies are averaged by successive pairs and each average is multiplied by the depth interval (in centimeters) covered by that pair to give the calculated length anomaly, ΔD, of that segment of the water column. Each ΔD is divided by 10^5 to return it to actual value; the ΔD's are summed cumulatively from zero at the surface down to the reference level; and the cumulated sum at the reference level is converted to meters (see Table 3). The cumulated length anomaly added to the reference level's depth under standard conditions gives the calculated length of the existing unit-cross-section water column. The final calculated length of the water column is its dynamic height or geopotential height. In Table 3 the reference level was the 60-decibar surface whose depth under standard conditions would be 60 meters.

At stations where the depth is less than that of the chosen reference level it is permissible to substitute the lower parts of a near-by station of adequate depth, as in Figure 4. When this is done the isobaric surfaces become horizontal (slopeless and currentless) between the identical parts of the two stations. This device was suggested by Nansen and introduced by Helland-Hansen (1934). It is apparently satisfactory in places where bottom currents are virtually absent, but may be seriously in error in places where currents

TABLE 3. *Dynamic height computation, Station 40, survey* Synoptic II, *27 July 1954*

Depth cm	Temperature °C	$10^5\,\delta_{t,p}$ at temp. & depth	Average	Depth interval	Product	ΔD, cm	Cumulative ΔD, cm	60-decibar ΔD	
								cm	meters
0	18.6	149.4					0		
			141.5	520	73580	0.74			
520	17.9	133.6					0.74		
			99.4	520	51688	0.52			
1040	13.8	65.2					1.26		
			49.0	480	23520	0.24			
1520	11.3	32.7					1.50		
			9.2	1530	14076	0.14			
3050	5.1	−14.3					1.64		
			−16.7	760	−12692	−0.13			
3810	4.4	−19.0					1.51		
			−21.0	760	−15960	−0.16			
4570	4.3	−23.0					1.35		
			−26.7	1430	−38181	−0.38			
6000	4.3	−30.3					0.97	0.97	0.010
			add reference level depth at standard conditions						60.000 meters
			Dynamic height in dynamic meters						60.010

along the bottom are significant. This device should be used only with great caution at stations so shallow that major parts of the water column require substitution of values.

Current directions are obtained by plotting the dynamic height for each station and drawing height contours of the surface topography at regular intervals. Current-direction arrowheads may be drawn on the contour lines by application of the geostrophic principle: the currents are situated on the slopes of the topography, flow parallel to the contours, and flow in such direction that the topographic 'high' is on the right (in the Northern Hemisphere) when the observer looks in the direction of flow.

Current velocity between each pair of stations can be obtained from: $v = 10\ i_d/0.000145 \sin \phi$ (Sverdrup *et al.* 1942: 392) where i_d is the slope of the surface between the stations and $\sin \phi$ is the natural trigonometric function of the latitude of the mid-point between the station pair. If the slope is expressed in meters of height difference per meter of horizontal distance between the stations, the velocity will be in meters per second; if the slope is in cm/m, velocity will be in centimeters per second. LaFond (1951: 98) gives a similar method of calculating current velocity from the same parameters.

Since the distance between contours is inversely proportional to the velocity, it is convenient to determine the velocities of the fastest current, the slowest current, and of a few intermediate ones, then to construct a trumpet-shaped graph (see Figs. 1, 2, and 3) from which velocity may be read by transferring the intercontour distance with dividers.

APPLICATIONS OF THE METHOD

The dynamic height method has been used to determine the surface current patterns and velocities in Lake Huron at three different times in the summer of 1954. At the end of June the major part of the lake was still in essentially its spring condition —with no thermocline yet formed. At this time the current pattern (Fig. 1) was almost identical to that deduced by Harrington (1895) from drift bottles released by lake steamers throughout the entire shipping season, approximately late March to early December. It was also in agreement with the results of Millar (1952) who confirmed Harrington's current pattern by studies of intake-water temperatures on lake steamers throughout the shipping season. For these reasons it is believed that the pattern observed in June approximates the "fundamental" winter-to-winter circulation pattern of the lake.

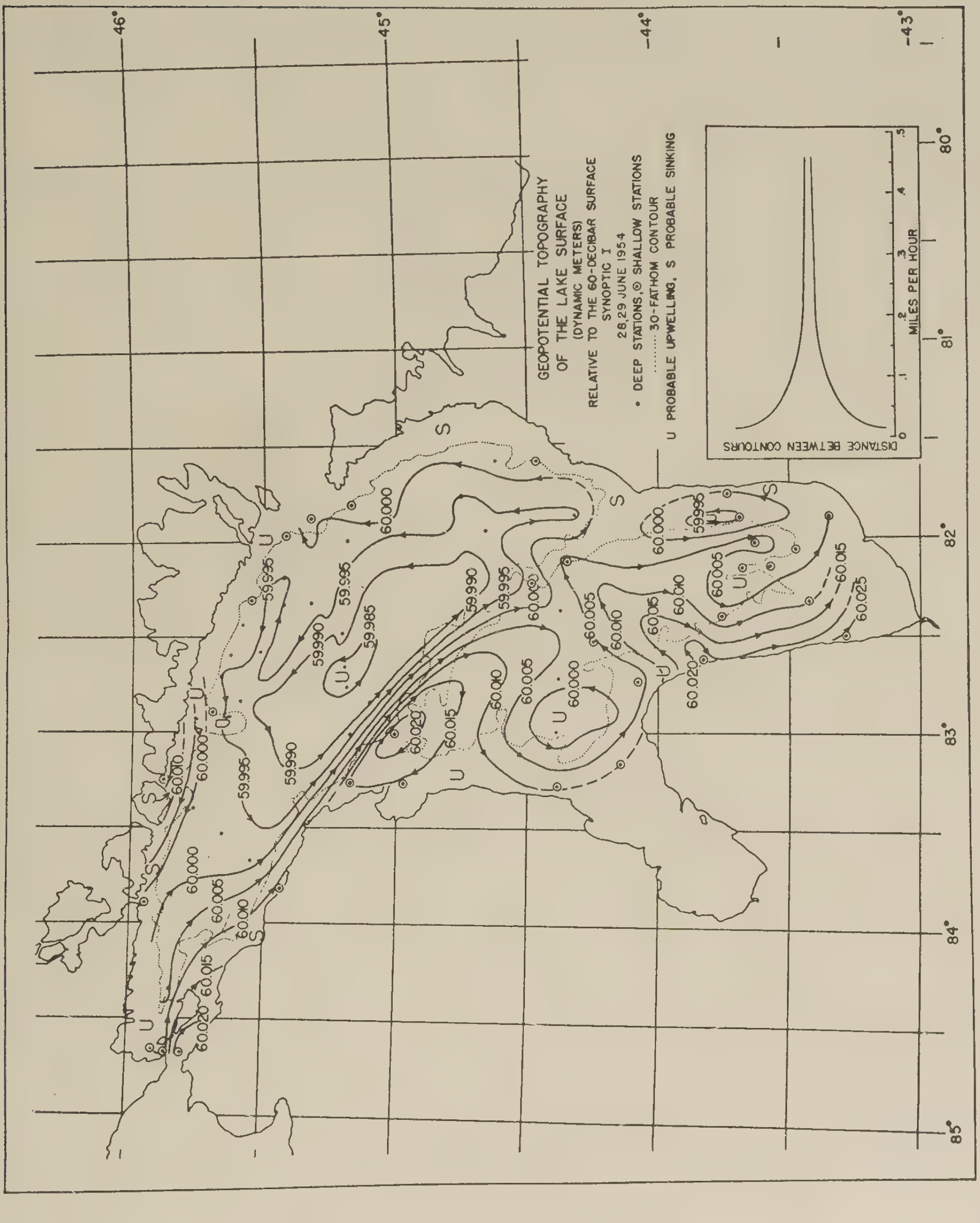
GEOPOTENTIAL TOPOGRAPHY
OF THE LAKE SURFACE
(DYNAMIC METERS)
RELATIVE TO THE 60-DECIBAR SURFACE
SYNOPTIC I
28,29 JUNE 1954
• DEEP STATIONS, ⊙ SHALLOW STATIONS
.... 30-FATHOM CONTOUR
U PROBABLE UPWELLING, S PROBABLE SINKING
DISTANCE BETWEEN CONTOURS
MILES PER HOUR
0
.1
.2
.3
.4
.5
46°
45°
44°
43°
80°
81°
82°
83°
84°
85°
59.985
59.990
59.995
60.000
60.005
60.010
60.015
60.020
60.025
U
S

FIG. 1. The currents of Lake Huron on 28-29 June 1954, in relation to the 60-decibar surface.

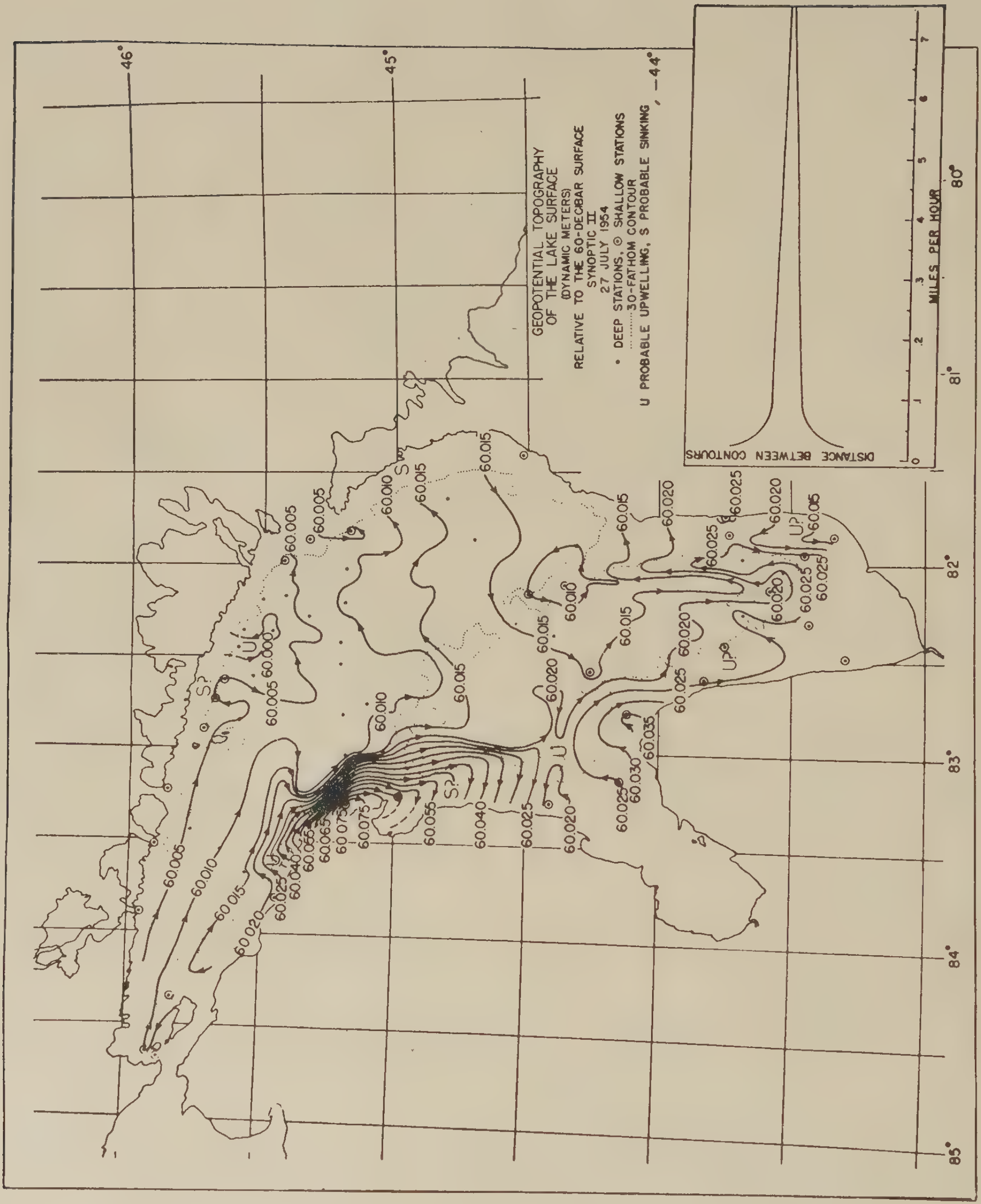
GEOPOTENTIAL TOPOGRAPHY
OF THE LAKE SURFACE
(DYNAMIC METERS)
RELATIVE TO THE 60-DECIBAR SURFACE
SYNOPTIC II
27 JULY 1954
• DEEP STATIONS, ⊙ SHALLOW STATIONS
......30-FATHOM CONTOUR
U PROBABLE UPWELLING, S PROBABLE SINKING
DISTANCE BETWEEN CONTOURS
0 1 2 3 4 5 6 7
MILES PER HOUR
46°
45°
44°
85°
84°
83°
82°
81°
80°
60.000
60.005
60.010
60.015
60.020
60.025
60.030
60.035
60.040
60.055
60.065
60.075
U
S

FIG. 2. The currents of Lake Huron on 27 July 1954, in relation to the 60-decibar surface.

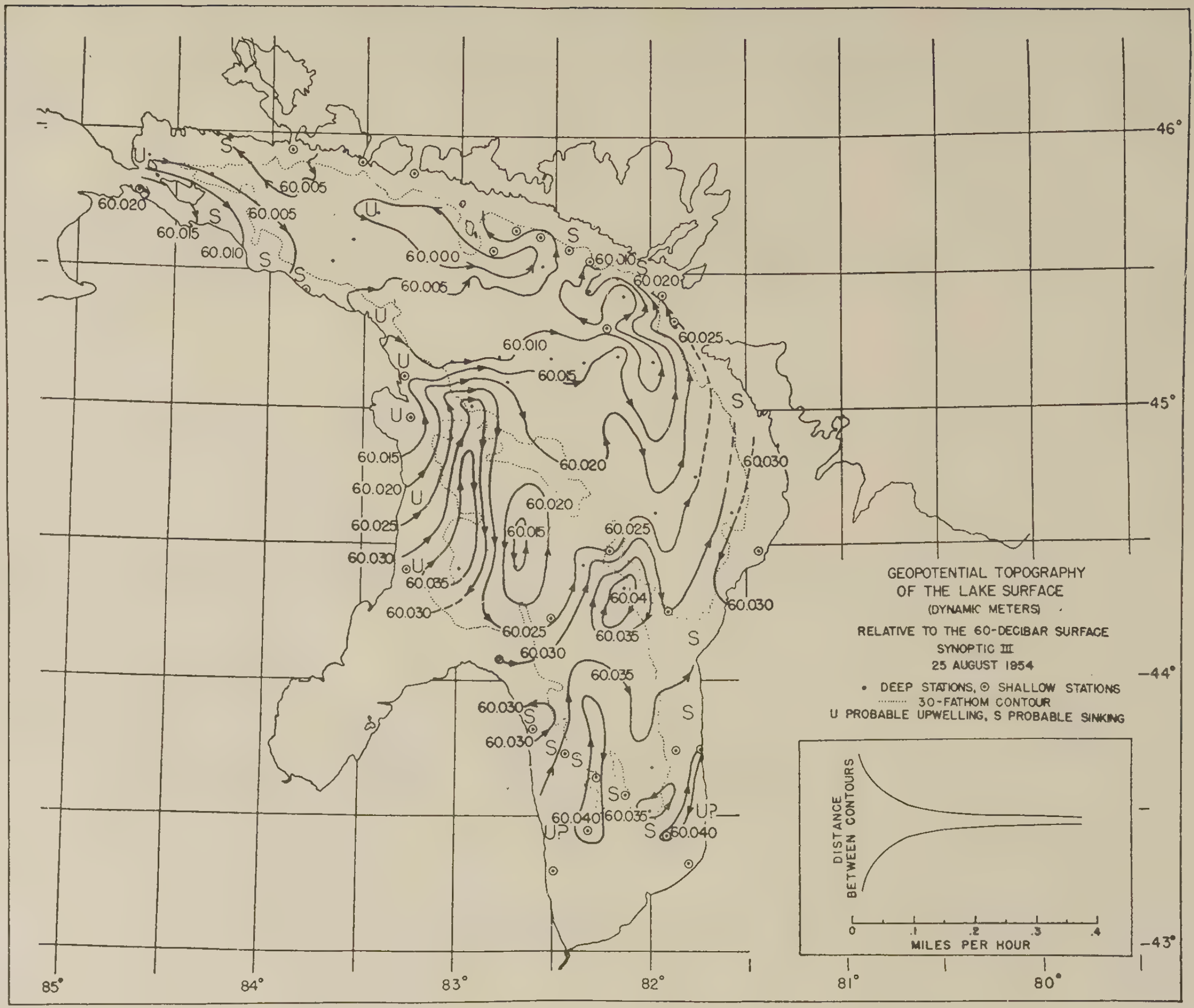
GEOPOTENTIAL TOPOGRAPHY
OF THE LAKE SURFACE
(DYNAMIC METERS)
RELATIVE TO THE 60-DECIBAR SURFACE
SYNOPTIC III
25 AUGUST 1954
• DEEP STATIONS, ⊙ SHALLOW STATIONS
.... 30-FATHOM CONTOUR
U PROBABLE UPWELLING, S PROBABLE SINKING
DISTANCE BETWEEN CONTOURS
0
.1
.2
.3
.4
MILES PER HOUR
60.000
60.005
60.010
60.015
60.020
60.025
60.030
60.035
60.04
60.040
46°
45°
44°
43°
85°
84°
83°
82°
81°
80°

FIG. 3. The currents of Lake Huron on 25 August 1954, in relation to the 60-decibar surface. This is apparently a non-equilibrium condition.

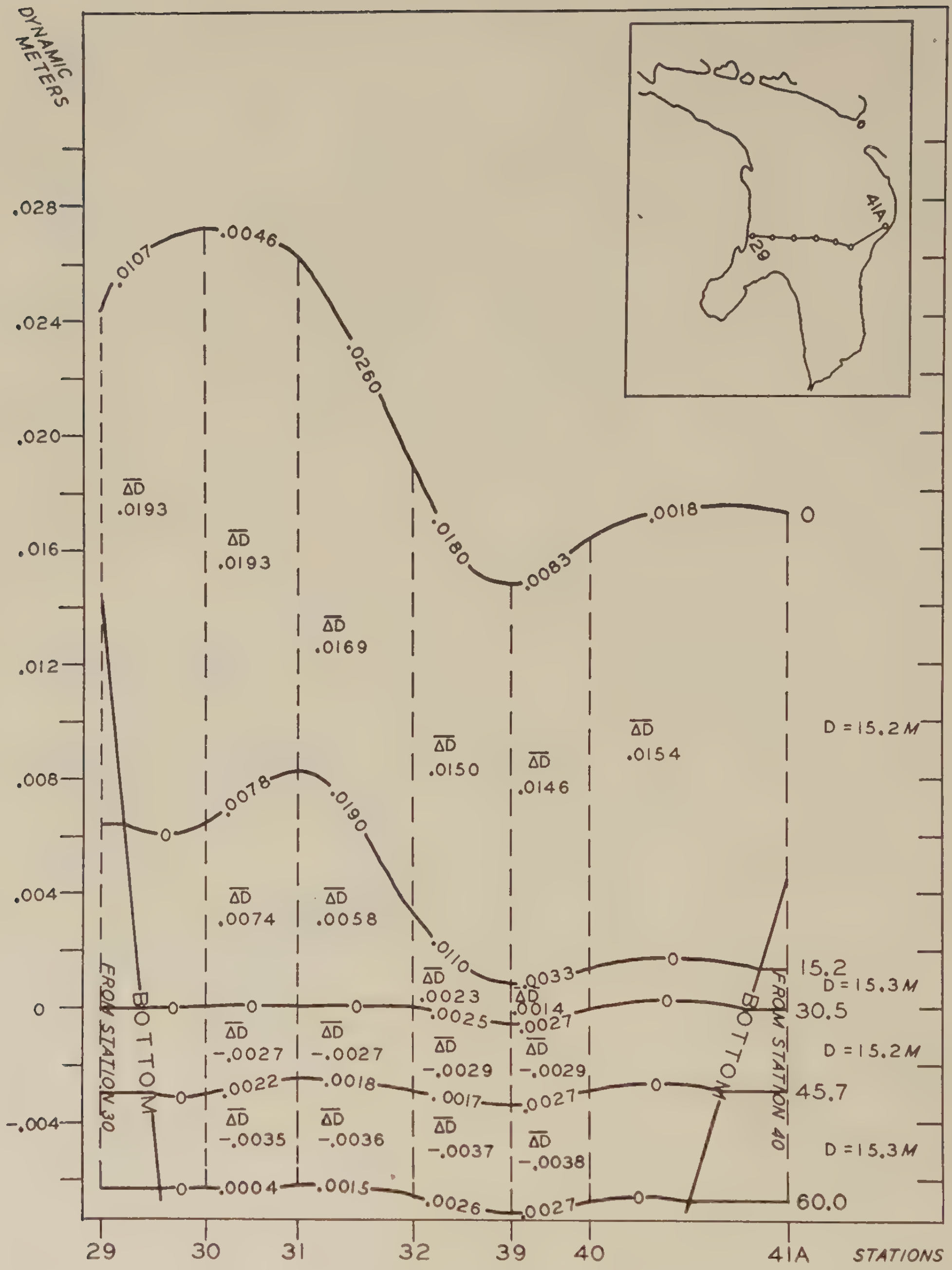

FIG. 4. The distribution of dynamic heights and current velocities in the Oscoda, Michigan-Southampton, Ontario section on 27 July 1954. Current velocities in meters/second are shown on the decibar surfaces. The ΔD values, in dynamic meters, in the between-station intercontour blocks are averages applying to those blocks. Interception of the isobaric surfaces by the bottom is indicated at each end. D values on the right are the intercontour intervals, in meters, under standard conditions. The insert shows the location of the section.

In the interval from late June to late July a strong thermocline developed over the whole lake. The survey of 27 July took place after winds from quarters more northerly than usual, and the current pattern (Fig. 2) appeared to be a wind-induced distortion of the fundamental pattern; the warm light surface water apparently responded rather readily to the wind shift.

Prior to the survey of 25 August 1954 (Fig. 3) the winds were from more nearly normal westerly quarters, and the current pattern appeared to indicate a partial return toward the June condition. The fact that the outflows from Lakes Michigan

TABLE 4. *Computation of water transport through the Oscoda-Southampton section, 27 July 1954*
Data for second and fourth columns are from Figure 4.

Isobaric surface pair, decibars	Intersurface depth $(\overline{D + \Delta D})$, dynamic m*	Intersurface area m²	Average velocity m/sec*	Transport m³/sec**	Transport sum m³/sec**
		Transport between stations 29 and 30, 23979 meters apart			
0–15.2	15.2193	364943	0.0054	1970 north	
15.2–30.5	—	—	0	0	
30.5–45.7	—	—	0	0	
45.7–60.0	—	—	0	0	
					1970 north
		Transport between stations 30 and 31, 21243 meters apart			
0–15.2	15.2193	323304	0.0016	517 north	
15.2–30.5	15.3074	325175	0.0039	1268 north	
30.5–45.7	15.1973	322836	0.0011	355 north	
45.7–60.0	15.2965	324944	0.0013	422 north	
					2562 north
		Transport between stations 31 and 32, 26393 meters apart			
0–15.2	15.2169	401620	0.0225	9036 south	
15.2–30.5	15.3058	403966	0.0095	3838 south	
30.5–45.7	15.1973	401102	0.0009	361 south	
45.7–60.0	15.2964	403718	0.0017	686 south	
					13921 south
		Transport between stations 32 and 39, 22048 meters apart			
0–15.2	15.2150	335460	0.0145	4864 south	
15.2–30.5	15.3023	337385	0.0068	2294 south	
30.5–45.7	15.1971	335066	0.0021	704 south	
45.7–60.0	15.2963	337253	0.0022	742 south	
					8604 south
		Transport between stations 39 and 40, 17703 meters apart			
0–15.2	15.2146	269344	0.0058	1562 north	
15.2–30.5	15.3014	270881	0.0030	813 north	
30.5–45.7	15.1971	269034	0.0027	726 north	
45.7–60.0	15.2962	270789	0.0027	731 north	
					3832 north
		Transport between stations 40 and 41A, 44096 meters apart			
0–15.2	15.2154	670938	0.0009	604 north	
15.2–30.5	—	—	0	0	
30.5–45.7	—	—	0	0	
45.7–60.0	—	—	0	0	
					604 north
				Net transport, m³/sec	13557 south

* Last decimal place only approximate.

** Last two places only approximate.

Contribution No. 824

(*Reprinted from Nature, Vol.* 177, *pp.* 454–455, *March* 10, 1956)

THE *ATLANTIS* MARINE GEOLOGICAL EXPEDITION TO PERU AND CHILE*

By Dr. PARKER D. TRASK

Department of Engineering, University of California

THE research vessel *Atlantis*, of Woods Hole Oceanographic Institution, explored the deep trenches that lie off the coast of Peru and northern Chile during November and December 1955. The expedition collected a hundred cores of sediments along twelve profiles between Talara in lat. 5° S. to a point eighty miles south of Antofagasta, Chile, in lat. 25° S. Continuous soundings of the water depth were made with the new Woods Hole sensitive sonic sounder whenever the ship was under way. In addition to the profiles on which sediments were collected, six traverses solely for sonic sounding were made across the deepest part of the trenches. Numerous bathythermograph readings were made of the Humboldt Current, and twelve runs were made with the geomagnetic electrokinetograph south of Iquique, Chile, in lat. 20° S. in an effort to determine the strength and character of the Humboldt Current. These are among the first runs of this character that have been made south of the magnetic equator, which passes near Lima, Peru. The results have not yet been calibrated to indicate the actual character of the current.

One of the most interesting features of the Expedition was the delineation, by means of the sonic sounder, of a trench 500 miles in length and one to three miles wide, and 24,000–26,000 ft.—mostly more than 25,000 ft.—deep extending between Arica in lat. 19° S. and lat. 25° S. The sides of this trench in each of the seven places where it was crossed are remarkably steep and range in height from 1,000 to 4,000 ft. In one place in lat. 25° S., the wall of the trench, as indicated by the fathometer trace, rose 1,500 ft. in a quarter of a mile. This trench was only forty miles from shore at this locality. The trench is balanced by mountains 20,000 ft. high scarcely 125 miles away. North of lat. 19° S. this trench is shallower and evidently is offset on echelon by a shallower trench to the west.

---

* Contribution No. 824 from the Woods Hole Oceanographic Institution.

The sea floor seaward from shore descended more or less progressively to the bottom of the trench. In many places remarkably flat benches were observed in water from a few hundred to several thousand feet deep. These benches in places were terminated by more or less pronounced scarps, some of which were steep and as much as 5,000 ft. in height. Seaward from the deepest part of the trench the bottom rises more or less progressively upward to a depth of 2,200–2,000 fathoms. The tracings of the sonic recorder give the impression that the deep trench represents a graben within other downfaulted blocks, such as is found in the Red Sea.

A profile was run parallel to the coast between lat. 12° S. and 26° S. in shallow water. One large submarine canyon with walls 3,000 ft. in height was found. It is located a short distance north of Arica, about lat. 18°. Elsewhere only occasional minor notches are observed in the profiles parallel to the coast.

The primary objective of the Expedition was to study the sediments. The deepness of the troughs suggests that the area represents a geosyncline in the making. The land that is the source of the sediments for the area is arid and supplies relatively little sediment to the sea. It is hoped that the results will throw light on the origin of greywackes. Details of sedimentation cannot yet be given as the sediments were kept in the core tubes until return to the laboratory ; but many of the samples, particularly in water of shallow and intermediate depth, consisted of muddy sands strongly suggestive of greywacke. Certainly the pattern of sedimentation does not accord with the concept of increasing fineness from shore. In many places the sediments at some distance from shore are much coarser than those nearer the coast. The deep samples consisted of clays in all cores except one, which was sandy. The cause of the variation in texture is not apparent from the field-observations. Perhaps bottom configuration is a factor.

Three cores were placed in a refrigerator as soon as collected to prevent decomposition of possible hydrocarbons. It is hoped that studies of the organic content of these frozen samples will throw light on the origin of oil.

The Expedition was conducted under the auspices of Woods Hole Oceanographic Institution of Woods Hole, Massachusetts. The Esso Research and Engineering Co. and Socony-Vacuum Laboratories have also contributed to the support of the project. The Esso Research and Engineering Co. hopes to assist with the studies of the hydrocarbon content of the sediments. Henry C. Stetson, research oceanographer of Woods Hole Oceanographic Institution and Alexander Agassiz Fellow in Oceanography, Museum of Comparative Zoology, Harvard University, was chief scientist in charge of the Expedition until his unfortunate death at sea on December 3. Parker D. Trask, research associate of Woods Hole Oceanographic Institution and lecturer in geologic engineering of the Department of Engineering of the University of California, was chief scientist for the remainder of the trip. Other members of the scientific staff included Bernhard Kummel, associate professor of stratigraphy and palæontology, Harvard University, and the following staff members of Woods Hole Oceanographic Institution: William D. Athearn, Robert Lufburrow, Herbert Small and John Zeigler. Victor Benavides, geologist of the International Petroleum Company of Peru, Lieut. Jose Carvajal of the Peruvian Navy, and Jose Stuardo of the Chilean Marine Laboratory at Valparaiso, also participated in the work.

This study was supported mainly by the Office of Naval Research.

Printed in Great Britain by Fisher, Knight & Co., Ltd., St. Albans.

Contribution No. 825

Reprinted from LIMNOLOGY AND OCEANOGRAPHY
Vol. 1, No. 2, April, 1956
Printed in U.S.A.

The Measurement of Primary Production[1]

JOHN H. RYTHER

Woods Hole Oceanographic Institution, Woods Hole, Mass.

ABSTRACT

A discussion is presented of the measurement of primary production by short-term experimental methods and by measurement of *in situ* environmental changes occurring over longer periods of time. The methods described include the measurement of photosynthesis by oxygen production, carbon dioxide assimilation and the associated pH change, and uptake of radioactive carbon (C^{14}). *In situ* changes in the standing crop and the concentration of inorganic plant nutrients are also discussed, and the possibility explored of relating the rate of uptake of radioactive inorganic tracers to primary production. The relationship between chlorophyll and photosynthesis is reviewed and some new experimental evidence is presented which indicates the possibility of using chlorophyll concentration as an index of primary production. In the discussions of each method emphasis is placed on sensitivity, reliability, and the interpretation of the data.

The production of organic matter is carried out in water, as elsewhere, by plants through the familiar process of photosynthesis. The problem of measuring primary production in natural waters then resolves itself, with certain reservations, to the measurement of the photosynthetic rates of aquatic plant communities.

The present paper will be concerned with the methods by which production may be measured. Emphasis will be placed on theoretical considerations rather than the applied aspects of such measurements. The actual techniques which may be employed are governed to a large extent by the particular environment to be studied and the producer populations living therein, and various details of the problem require unique solutions.

The productivity of natural waters is often judged on the basis of the quantity of organic matter which they support at any one moment. This instantaneous population or "standing crop" in itself is a rather poor index of production without some indication of the time factor involved in its formation. Large beds of eel grass, kelp, drifting *Sargassum*, etc. may consist of organic matter which has been synthesized over a period of months if not years. The actual production rate of such impressive populations may be quite low and may be overshadowed by that of relatively small standing crops of phytoplankton which are subject to decimation from many sources. Production must therefore be considered as a rate rather than a static quantity.

The most direct and in many cases the most satisfactory method of measuring production is simply by the increase or decrease in the standing crop over a measured interval of time. In this case production is measured in terms of biomass, and may be expressed variously as the increase in, 1) the area of bottom covered, 2) volume of producer organisms, 3) displacement volume, 4) wet or damp weight, 5) dry weight, 6) ash-free dry weight (i.e., loss on ignition).

This method, in one form or another, has been widely used in studying the production of macroscopic benthic populations which follow a regular seasonal pattern of growth and are relatively undisturbed by predation or other decimating factors. It is quite unsuitable for measuring production of the phytoplankton since changes in its biomass reflect merely the net change resulting both from production and removal by predation, water movement, sinking, etc.

In the latter case it is desirable to measure as nearly as possible the instantaneous production rate. In practice this means confining measurements to a few hours or, at most, days, rather than weeks or months. For this, one must turn to the reactions involved in organic production and the accompanying chemical changes which may be detected by more sensitive means. This leads to a brief consideration of photosynthesis.

---

[1] Contribution No. 825 from the Woods Hole Oceanographic Institution. This work was carried out with the aid of a research grant from the National Science Foundation.

In photosynthesis carbon dioxide is reduced to organic carbon with the evolution of free oxygen, the reaction utilizing the energy of solar radiation. Physiologists found early in their investigations of this process that the volume of oxygen liberated very nearly approximates the volume of CO_2 assimilated. These early workers reached the conclusion, still widely upheld, that the primary if not the sole product of photosynthesis is carbohydrate in nature. This then led to the familiar simplified equation for the overall reaction of photosynthesis:

$$CO_2 + H_2O \rightarrow CH_2O + O_2 \qquad (1)$$

The subsequent discovery that the photosynthetic oxygen is derived not from CO_2 but from H_2O, necessitating a modification of the equation to satisfy the stoichiometry, need not concern us here since the combining proportions of the various constituents remain the same in either case.

While equation (1) is a convenient expression for the reaction of photosynthesis, it by no means describes the complex process of growth in which the first products of photosynthesis are converted to fats, proteins, organic acids, etc. with the accompanying uptake and utilization of the mineral nutrients. Growth, which is more analogous to "primary production" than photosynthesis alone, probably cannot be expressed by any simple equation. However, an examination of the composition of the organisms will give some insight into the combining proportions of some of the major constituents involved in this process.

Table 1 gives the per cent of ash-free dry weight (% organic matter) of carbon, hydrogen, oxygen, nitrogen, and phosphorus for a variety of aquatic plants. The list is by no means complete, but probably adequate to illustrate consistencies or major variations in the relative composition of the five elements for the different groups represented. With this table for a guide, we may turn our attention to the applicability of the photosynthetic equation to the measurement of production. Before doing so, however, we may consider here briefly the effects of respiration upon such measurements.

TABLE 1. *Elementary composition of some aquatic plants in percent ash-free dry weight ± standard deviation*

Organism and Reference	No. Analyses	C	H	O	N	P
Diatoms	18	50.54	10.21	28.83	7.0	1.55
Brandt & Raben (1920)		±3.90	±1.90	±7.10	±3.7	±.88
Ketchum & Redfield (1949)						
Vinogradov* (1939)						
Peridineans	7	48.12	7.50	33.85	10.40	0.80
Brandt & Raben (1920)		±1.90	±1.70	±3.90	±1.40	±.36
Chlorophyceae	18	54.55	7.54	31.21	7.7	2.94
Ketchum & Redfield (1949)		±1.30	±.50	±4.35	±.56	±.83
Macroscopic algae	6	46.80	7.62	41.65	5.0	0.44
Brandt & Raben (1920)		±1.40	±1.90	±3.30	±2.40	±.37
Zostera	3	46.11	7.12	43.26	3.4	0.50
Brandt & Raben (1920)		±.60	±1.10	±1.70	±1.6	±.26

* N and P values only

The overall effect of respiration may be considered as the reverse reaction of photosynthesis. The organism exists in a state of equilibrium between these two processes, and changes in the standing crop or the related environmental factors reflect merely the product of this equilibrium.

Actually, ecologists are generally less concerned with the total photosynthesis or "gross production" than with the net effect of photosynthesis and respiration by the plant community, or "net production". The former is an intangible quantity; the latter represents the real production of organic matter which is added to the environment and hence is of ecological significance.

The rate of change of the standing crop, of course, measures "net production". Unfortunately the rate of change of the environment does not, for it reflects not only respiration of the producer population but also that of all other forms of life in the community.

If production is measured experimentally for short periods of time, the effects of respiration may be eliminated by performing parallel experiments in the dark in which respiration alone is measured. This practice is valid only if respiration is the same both in the light and dark. This assumption is obviously not correct if any appreciable growth occurs during the experiment. Thus one's purpose is defeated by the very thing he is attempting to measure and at best the value obtained is approximate and somewhat below the correct value for production.

Even disregarding the problem of differential growth in the light and dark control, the question of whether the process of respiration itself is the same in the light and dark has always bothered students of photosynthesis. The most recent investigation of this problem would indicate that it is. Brown (1953) studied respiration in *Chlorella* whose oxygen supply was enriched with O^{17} (heavy oxygen). By following the time course of the disappearance of O^{17} from the air in equilibrium with the culture, he could measure respiration independently of photosynthesis, since the photosynthetically produced oxygen contained none of the heavy isotope. His experiments show that respiration is essentially independent of light.

OXYGEN PRODUCTION

According to equation (1) for each mole of CO_2 reduced to organic carbon one mole of free oxygen is liberated. As mentioned earlier, this observation antedated and actually provided the basis for the photosynthetic equation. We have emphasized that the same relationships may not hold for both photosynthesis and growth. But if environmental changes are measured under the natural growing conditions of the plants they should reflect the effects of both processes simultaneously.

Table 2 shows some of the measurements which have been made of the photosynthetic quotient, defined here as the ratio of oxygen produced to carbon dioxide assimilated. While the values shown do not differ markedly from unity, it is obvious that they tend to be somewhat greater. The general opinion is that these values do not differ significantly from one, though some of the authors (cf. Barker) consider that the slight departure indicates the synthesis of substances slightly more reduced than carbohydrates.

TABLE 2. *Some measurements of the photosynthetic quotient (O_2/—CO_2) in aquatic plants*

Organism	Reference	PQ
Chlorella	Manning *et al* (1938)	0.98
Chlorella	Sargent (1940)	ca. 1.00
Chlorella	Wassink and Kersten (1944)	1.09–1.12
Diatoms	Wassink and Kersten (1944)	1.12–1.13
Nitzschia closterium	Barker (1935a)	1.05–1.08
Nitzschia palea	Barker (1935a)	1.03–1.05
Peridinium sp.	Barker (1935b)	1.03–1.11
Synechoccus sp.	Fraenkel *et al* (1950)	1.08±0.03
Homidium flaccidum	van der Paauw (1932)	0.92–1.07
Gelidium	Tseng and Sweeney (1946)	0.94±0.05
Gigartina	Emerson and Green (1934)	0.99–1.07
Raw seawater	Sargent and Hindman (1943)	1.09±0.23

From general considerations, the proximity of these values to unity seems rather surprising, for the organisms are certainly not composed of carbohydrates alone. The synthesis of either fats or proteins would result in values considerably in excess of one, and it would seem doubtful that they could be balanced by the few organic acids more highly oxidized than carbohydrate. When one examines the composition of aquatic plants, the observed PQ values are still more difficult to explain. This is illustrated in Table 3 showing the relative composition by atoms of carbon, hydrogen, and oxygen in a variety of aquatic plants. They are obviously more highly reduced than carbohydrate and their PQ, calculated from their composition, ranges from 1.09 to 1.48, averaging about 1.20.

If the plants obtain their nitrogen in the form of ammonia, the PQ may be somewhat smaller since the nitrogen is already fully reduced when it enters the cell. If, on the other hand, nitrate is the principal source of nitrogen, as is normally the case in most natural waters, then the PQ will be still higher than that indicated in Table 3. While the mechanism is not clear, it is

TABLE 3. *The relative composition by atoms of C, H, and O (C = 100), and the calculated photosynthetic quotient (O_2/—CO_2) in various aquatic plants*

Reference and Organism	No. analyses	C–H–O	PQ
Brandt & Rabin (1920)			
Diatoms	8	100–251–48	1.38
Peridians	7	100–184–54	1.16
Zostera	3	100–179–70	1.09
Chorda filum	1	100–186–72	1.10
Laminaria	1	100–182–68	1.11
Ascophyllum	1	100–170–64	1.10
Ulva	1	100–170–65	1.10
Enteromorpha	1	100–196–51	1.23
Rhodomela	1	100–315–60	1.48
Ketchum & Redfield (1949)			
Stichococcus bacillaria	6	100–160–46	1.17
Chlorella pyrenoidosa	8	100–168–41	1.21
Chlorella vulgaris	1	100–168–44	1.20
Scenedesmus obliquus 1	1	100–180–41	1.25
Scenedesmus obliquus 2	1	100–180–39	1.25
Scenedesmus basilensis	1	100–184–39	1.27
Nitzschia closterium	1	100–164–42	1.20

TABLE 4. *Variations in the relative composition and calculated photosynthetic quotient (O_2/—CO_2) in* Chlorella pyrenoidosa (from Spoehr and Milner 1949)

Relative composition by atoms (C = 100) C–H–O–N	Calculated PQ nitrogen source		
	Not consid.	NH_4^+	NO_3^-
100–165–61–16	1.11	0.99	1.22
100–162–45–16	1.18		
100–171–39–23	1.23		
100–160–38–16	1.21		
100–173–43–8	1.21		
100–178–36–16	1.22		
100–168–37–12	1.26		
100–172–33–6	1.28		
100–168–28–4	1.31		
100–177–27–2.2	1.33		
100–179–20–1.3	1.34		
100–180–19–1.7	1.35	1.34	1.37

generally agreed that plants must reduce nitrate to ammonia before it may be used. The subject has been reviewed recently by Syrett (1954). Whatever the process, the effect upon the PQ is the same. This was nicely demonstrated by Cramer and Myers (1948). *Chlorella* grown under their experimental conditions had the composition $C_{5.7}H_{9.8}O_{3.2}N_{1.0}$. With ammonia as their nitrogen source the PQ calculated from the composition was 1.10 while that determined experimentally was 1.06. With nitrate-nitrogen the calculated and measured PQ were respectively 1.45 and 1.47.

In a subsequent paper, the same authors (Myers and Cramer 1948) provided an explanation for the fact that most earlier measurements of PQ have approached values of unity. If they made their measurements at the same light intensity at which the organisms were grown they obtained quotients of 1.3–1.4 (with nitrate as a nitrogen source). If, however, the organisms were grown at a low light intensity and measured at light saturation, values of about 1.10 were obtained. These workers concluded that when *Chlorella* is transferred from low to high light intensity, its metabolism is temporarily shifted to one involving principally carbohydrate synthesis. Myers strongly maintains that the concept of a PQ of unity has resulted from experiments with organisms grown at sub-saturating light and measured, because of the requirements of the manometric techniques, at high intensity.

The photosynthetic quotient, of course, varies with the composition of the organisms. Table 4, taken from Spoehr and Milner (1949) illustrates the variation in composition which may occur in the single organism, *Chlorella pyrenoidosa,* shown in increasing order of its state of reduction. The calculated PQ, disregarding the effect of nitrogen assimilation, ranges from 1.11 to 1.35.

Since synthesis of fats increases with nitrogen deficiency (cf. Spoehr and Milner) the more highly reduced the organism the lower is its nitrogen content. Hence the state of reduction of the cells and nitrate reduction do not together produce a much greater effect upon the PQ than either one may have separately, as illustrated in Table 4.

In view of the preceding evidence it would appear that a photosynthetic quotient of one is largely an experimental artifact, and that values of 1.1 to 1.3 or higher are normal under natural conditions. While it is obviously impossible to choose the correct value for routine measurements of natural populations, the author suggests that a value of 1.25 is perhaps somewhat more realistic than that of unity.

The photosynthetic production of oxygen is usually studied in the laboratory by means of elaborate manometric techniques which are quite unsuitable for use in the field, particularly if one wishes to measure the process as it occurs *in situ*. Ecologists have generally employed the technique first described by Gaarder and Gran (1927) of measuring the rate of change of dissolved oxygen titrametrically by the Winkler method in samples enclosed in glass bottles. Since these may be returned to the same depth, maintained at the same temperature and receive the same illumination as the surrounding water, an approximation may be obtained of the natural production rate.

The dissolved oxygen concentration is influenced in such experiments by the respiration not only of the plants but of all other life including the large bacterial flora which develops in water enclosed in bottles, so that the net change in oxygen is meaningless. One normally employs a darkened bottle, therefore, to correct for respiration and thereby measure gross production.

Such "light and dark" bottle experiments are generally comparable in sensitivity to the more elegant manometric techniques; each is capable of detecting changes of a few hundredths of a milliliter of oxygen per liter. But where the physiologist may confine his measurements to a few minutes by using extremely dense cultures of organisms, the ecologist must take his populations as he finds them and, in an extremely oligotrophic environment, may require a matter of days to detect a measurable increase in oxygen.

Experiments by the author have indicated that photosynthesis in samples enclosed in glass bottles may proceed at a constant rate for 24 to 48 hours after which it almost invariably decreases. As a general practice such experiments should probably not exceed the daylight portion of one day. The sensitivity of Winkler titrations is approximately 0.02 ml of oxygen per liter. Since two such titrations are involved in a "light and dark" bottle experiment, the author has considered a difference of 0.05 ml per liter as the lower limit of sensitivity of the method. This is equivalent to carbon assimilation of approximately 0.02 mg per liter. The daily gross production of most natural waters normally exceeds this limit and therefore permits measurements not exceeding the time limit suggested above.

Before leaving the subject of oxygen production, mention should be made of Steemann Nielsen's objection to the "light and dark" bottle experiments of long duration as used by Riley *et al.* (1949 and ref.) for determining production in the open ocean. Steemann Nielsen (1952) first proposed that a differential growth of bacteria in the light and dark bottles due to the lethal effects of sunlight resulted in the over-correction for respiration and a corresponding overestimation of photosynthesis. Subsequent experiments by Vaccaro and Ryther (1954) disclosed no difference between the growth or respiration of bacteria in light and darkened bottles in experiments lasting for several days.

More recently Steemann Nielsen (1954) has postulated as a basis for the same result (i.e., a difference between respiration of bacteria in the two bottles) the bactericidal effects of substances produced by the phytoplankton in the light bottles in conjunction with photosynthesis. In a later paper (Steemann Nielsen 1955) the same author claims to have demonstrated this effect.

It is noteworthy, however, that Steemann Nielsen's experiments do not provide any direct demonstration of this phenomenon. On the other hand those of Vaccaro and Ryther give direct contradictory evidence. In samples of a natural plankton population enclosed in darkened and clear bottles exposed to sunlight, there was no difference in the growth of bacteria during a period of six days despite the vigorous photosynthetic activity in the light bottle (Vaccaro and Ryther 1954, pg. 23, exp. II).

Steemann Nielsen's stated objective was to demonstrate that production values obtained by long-term "light and dark" bottle measurements are many times too high. While experiments of long duration have many shortcomings, some of which have been discussed above, everything in the author's experience would indicate that values obtained by such experiments are too low.

CO_2 ASSIMILATION

The uptake of carbon dioxide is equivalent, mole for mole, to the production of organic carbon, and hence represents one of the most direct approaches to the measurement of primary production.

In all natural waters of alkaline pH, carbon dioxide exists in equilibrium with HCO_3^- and $CO_3^=$. Thus photosynthesis is not reflected by changes in concentration of CO_2 alone, but may be determined quantitatively only by following the level of the entire buffer system. Furthermore, there is evidence that at least some plants are capable of fixing bicarbonate ions directly. This subject has been reviewed by Steemann Nielsen (1947).

The only practical field method of measuring carbon assimilation from the entire buffer system is by pH change. The total CO_2 (that present in all forms in the buffer system) and its relation to pH may be determined for freshwater by the equations of Moore (1939) and for seawater by those of Buch, Grippenberg, Wattenberg, and Harvey, which have been conveniently summarized by Harvey (1945). This relationship breaks down in those areas, both freshwater and marine, in which photosynthetic activity is accompanied by the precipitation of calcium carbonate, and the method obviously cannot be used under such conditions.

Because of the buffering capacity of seawater and most freshwater, a relatively large uptake of CO_2 is necessary to produce a significant change in pH. With the equipment available in the average laboratory (i.e., a Beckman pH meter) a change of 0.1 pH unit probably represents the limit of sensitivity. This is equivalent to carbon assimilation between 0.1 and 0.5 mg/liter depending upon the alkalinity of the water. The lower limit would be typical of moderately soft freshwater, the upper limit representing seawater.

The daily photosynthetic rate of many freshwaters may exceed this lower limit and thus permit use of the method. But in lakes of high alkalinity and in the ocean a detectable pH change within 24 hours will occur only in such areas of high production as plankton blooms, vigorously-growing benthic populations, etc. Significant results may be obtained in more oligotrophic waters by artificially concentrating the organisms (cf. Verduin 1951) or extending the experimental period to more than one day. Either alternative represents a departure from natural conditions which should be avoided if possible. While pH changes of a few thousandths of a unit may be detected with fair accuracy by means of more sensitive potentiometers, it is doubtful if such instruments would prove reliable at their lower limit of sensitivity under field conditions.

THE FIXATION OF CARBON—14

The most recently developed experimental method of determining organic production is that of measuring the rate of uptake of radioactive carbon (C^{14}) by the plants. The method was first described by Steemann Nielsen (1952) and later reviewed by Ryther and Vaccaro (1954), and the technical details need not be repeated here. Although designed for measuring production of phytoplankton populations, it could easily be adapted for use with other aquatic plants.

Essentially the method consists of adding a small quantity of $C^{14}O_3^=$ to a sample of water containing its natural plankton population. After allowing photosynthesis to proceed for a suitable period, the plankton is filtered on filter paper capable of retaining all autotrophic organisms. The recently developed Millipore filter is particularly well suited for this purpose. The filter is then washed, dried, and its activity measured by standard counting techniques.

The assumption is made that the following relationship is true:

$$\frac{\text{Activity of phytoplankton}}{\text{Activity of } C^{14}O_3^= \text{ added}}(k) = \frac{\text{Total C assimilation}}{\text{Total C available}}$$

The constant (k) corrects for the isotope effect, since C^{14} is assimilated some 6% more slowly than C^{12} due to mass difference. The total available carbon may be calculated from the equations discussed earlier.

This method represents the most sensitive technique now in use for measuring photosynthesis under natural field conditions, and its sensitivity may be varied at will by simply adjusting the activity of the added C^{14}. For example, 10 μ-curies of C^{14} may be added to a 250 ml sample volume without increasing the carbon content by more than 0.03 mg/l, an insignificant amount even in soft freshwater. Assuming a 50% counting efficiency, this amount of C^{14} added to seawater will permit measurement of C^{14} uptake where photosynthesis is as low as 0.02 μg C/liter. In freshwater, with less available carbon, the sensitivity is correspondingly greater. There is probably no natural body of water in which photosynthesis does not exceed this limit within a few hours. The latest measurements of the author in the surface waters of the Sargasso Sea, a highly unproductive oceanic area, show a C^{14} uptake throughout the day equivalent to the assimilation of about 1.0 μg C/l.

In Steemann Nielsen's opinion the C^{14} method, as described above, measures the total or gross photosynthesis minus a small loss due to the respiration of the newly assimilated C^{14} during the course of the experiment. For a four-hour experiment, he placed this loss rather arbitrarily at 4%, and applied this correction to obtain values for gross production.

The present author (Ryther 1954) measured photosynthesis simultaneously by oxygen production and C^{14} assimilation in a pure culture of *Dunaliella euchlora*[2] which contained limiting quantities of nitrogen and phosphorus. In the early stages of growth, when cell division proceeded at an exponential rate, photosynthesis was about ten times as great as respiration. However, as a nutrient deficiency developed, photosynthesis decreased more rapidly than respiration until, under conditions of complete nutrient exhaustion and two weeks after growth had ceased, the P:R ratio was unity. In every case the uptake of C^{14} corresponded closely with the oxygen produced in excess of respiration. Use of a PQ of 1.25, as discussed earlier, would have made the agreement more striking. This led the author to conclude that C^{14} uptake provided a measurement of net production.

The objection has been raised (Steemann Nielsen, personal communication) that carbon dioxide rather than nitrogen and phosphorus was the limiting factor in these experiments, thus invalidating the results. This assumption was presumably the basis for his statement that these observations "seem obviously to be the result of unsatisfactory experimental techniques" (Steemann Nielsen 1955).

In this connection it may be pointed out that (1) pH in the experimental culture increased during the initial stages of rapid growth but thereafter decreased, ultimately reaching a value below that observed at the start of the experiment, and (2) addition of nitrogen and phosphorus to a duplicate culture two weeks after growth had ceased resulted, after a lag of 48 hours, in renewed exponential growth. Although the cultures were not continually agitated, it was felt that the use of an actively motile flagellate would prevent local deficiencies of CO_2 from developing immediately around the cells.

To further investigate the author's claim that C^{14} uptake measures net photosynthesis, a comparison was made of the two methods at different light intensities. Again a pure culture of *Dunaliella* was used, and gross and net oxygen production were compared with C^{14} assimilation.

Light intensity was measured incident to the experimental vessels (30 ml glass-stoppered bottles) with a calibrated Weston photoelectric cell. Graded light intensities were obtained with neutral density filters and illumination was provided by a bank of daylight fluorescent lamps. The light measurements were admittedly somewhat crude and the author does not pretend that the absolute values so obtained were exact.

---

[2] Originally described as *Chlamydomonas* sp. and correctly identified by Dr. Ralph Lewin.

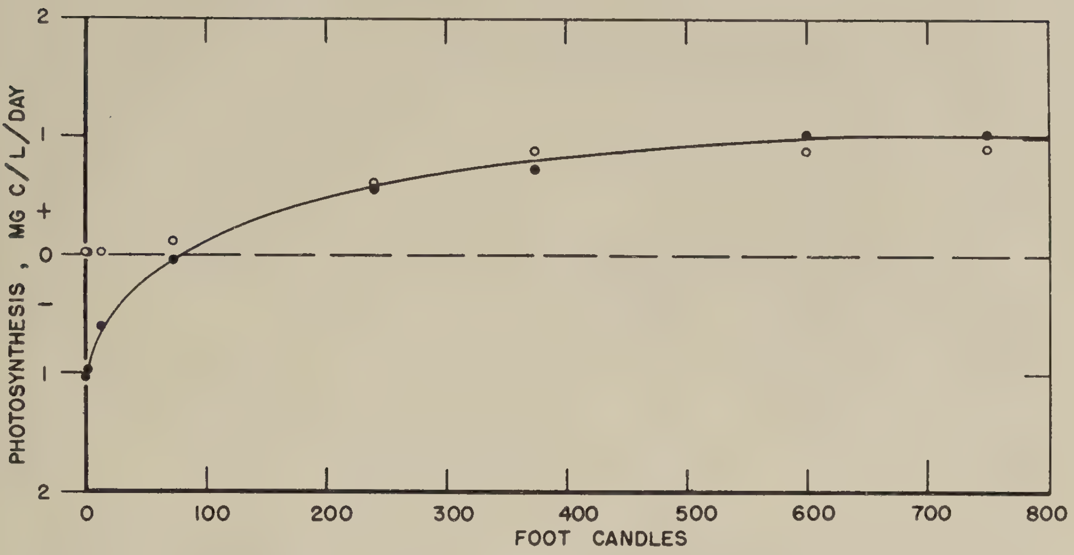

FIG. 1. Photosynthesis measured by oxygen production (filled circles) and C^{14} uptake (open circles) as a function of light intensity in a pure culture of *Dunaliella euchlora*. Values obtained from oxygen production represent the net change of oxygen at each light intensity.

For the purposes of this experiment it was considered sufficient merely to obtain a graded series of light intensities from saturation to values below compensation.

The results (Fig. 2) clearly show that C^{14} uptake agrees closely with the carbon equivalent of net oxygen production, in this case using a PQ of 1.25. Below the compensation intensity, where there was measurable photosynthesis but no net increase of oxygen, the uptake of C^{14} did not differ significantly from that which occurred in total darkness.

The reason that C^{14} uptake should correspond to net photosynthesis is not clear. It was originally suggested (Ryther 1954) that the plants may respire the newly formed products of their photosynthesis, and thus a portion of the assimilated C^{14} would be respired in the course of the experiment in the same ratio as normal P:R in the organism. However, it is rather difficult to believe that a complete equilibrium of this sort could be attained almost instantaneously, as would be required. Furthermore this hypothesis is not supported by the evidence of others (i.e., Calvin 1949, Weigl *et al.* 1951).

An alternative and perhaps more logical explanation is that the plants use respiratory CO_2 preferentially to external CO_2 for photosynthesis. In this case, the organisms would never assimilate external CO_2 in excess of their net photosynthesis. Some evidence for this is given in Warburg's (1920) experiments on the narcotization of photosynthesis by cyanide in which he found that only net photosynthesis was affected by the poison, the organism continuing to photosynthesize at a rate corresponding to its respiration. Supplementing this evidence Kok (1951) has recently found that the quantum yield of photosynthesis appears to be twice as great below the compensation point as that at light intensities above compensation. Both of these pieces of evidence appear to substantiate Franck's (1949) hypothesis that plants are capable of the photochemical reduction of respiratory intermediates. While Franck proposed that this occurs only below compensation light intensity, one need only extend his hypothesis to include the preferential use of these intermediates at all times to explain the situation reported above.

Whatever the correct physiological explanation, the empirical evidence seems clear that C^{14} uptake measures net photosynthesis. Upon first examination (including that of the present author) the

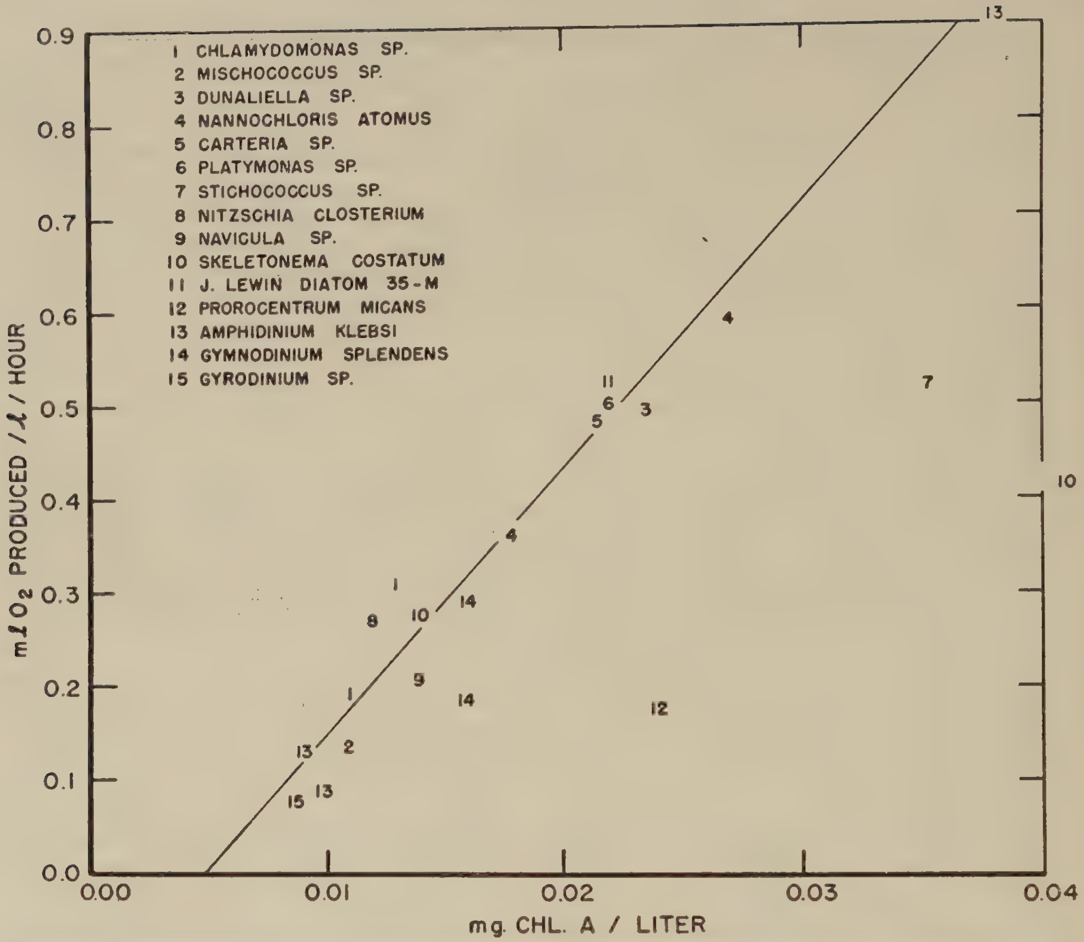

Fig. 2. The relationship between total photosynthesis at constant light intensity and chlorophyll "a" in some marine plankton algae.

method would appear to fulfill a long awaited need in providing the means for the direct measurement of net productivity. However, the fact must not be overlooked that net photosynthesis is thereby measured only during the course of the experiment (i.e., during the hours of the day when there is net photosynthesis to measure). The investigator would like to obtain values for overall net production on a daily basis. This information cannot be had from the uptake of C^{14}, for there is no way of estimating the additional respiratory loss of organic matter during the hours of darkness.

This fact greatly restricts the usefulness of the C^{14} method. While it remains a valuable tool for laboratory investigations and may provide interesting information pertaining to the relative fertility of natural waters, it does not provide, as currently employed, a quantitative measurement of either gross or net daily production.

The need is therefore apparent for a continued critical examination of the method and its physiological basis, and for the exploration of means to circumvent its shortcomings.

THE UPTAKE OF MINERAL NUTRIENTS

The uptake of nitrogen, phosphorus, and other mineral nutrients from the environment has been used in the past to estimate primary production. Since the changes involved are generally small, the method does not lend itself readily to experimental measurements by ordinary chemical methods. In areas where there is a marked seasonal growth of plants, usually in temperate waters where the regeneration and buildup of nutrients during the unproductive winter months is followed by a rapid utilization during the spring flowering, production has been calculated *in situ* over a period of weeks or months (Kreps and Verjbinskaya 1930, Atkins 1923, Cooper 1938, etc.).

The method is subject to the errors resulting from changes of these properties not associated with organic production. Furthermore, it does not account for the regeneration and reutilization of these substances during the growing season. Finally the ratio between the concentration of nitrogen, phosphorus, and undoubtedly the other mineral nutrients and the total organic matter is extremely variable (Tables 1 and 4).

In general, estimates of production based on such criteria have represented the attempted extension of investigations in which the chemical cycles of the water have been the primary object of interest. Values which have been obtained in this manner are given by Riley (1941) and Harvey (1945).

The short term uptake of many of the mineral nutrients may be measured experimentally by means of radioactive tracers. For instance, P^{32} is available with a specific activity of 1 μ-curie per 0.025 μg P. The addition of 10 μ-curies (0.008 μgA P) per liter would not significantly increase the phosphorus content of any natural waters. The uptake of less than 10^{-5} of the total available phosphate could then be detected by normal counting equipment. This is probably exceeded by the daily phosphorus assimilation of the poorest of producer populations.

The difficulty arises in trying to relate P uptake to organic production. The reader is again referred to Table 1 as an illustration of the inconsistency of the phosphorus content of aquatic plants, not only between various groups but also within the groups as indicated by the standard deviations. Several workers have shown that a large proportion of the assimilated phosphorus is loosely bound and freely exchanged (Goldberg *et al.* 1951, Rice 1953). This fraction cannot be quantitatively related to the organic content of the organism.

CHLOROPHYLL

Riley *et al.* (1949 and ref.) and others have attempted to relate the chlorophyll of aquatic plants to their total organic matter and, by following the change in the chlorophyll content of natural waters, thereby estimate production. However, many workers have shown that the chlorophyll content per cell may vary over a wide range depending upon the state of nutrition of the organisms, the quality and intensity of light in which they have grown, and other factors.

A much closer relationship appears to exist between chlorophyll and photosynthesis at a given light intensity. This fact was first demonstrated by plant physiologists who attempted to determine the smallest quantity of chlorophyll capable of reducing one mole of CO_2 to organic carbon (Emerson 1929, Arnold and Kohn 1934, Emerson and Arnold 1932, Gaffron and Wohl 1936). Fleischer (1935) showed that the photosynthesis:chlorophyll ratio remained constant even in cells whose chlorophyll content varied widely as a result of deficiencies of iron and nitrogen, though the relationship did not hold for magnesium deficient cells.

In a series of nine Wisconsin lakes, Manning and Juday (1941) found at the depth of maximum photosynthesis that 1.0 mg of chlorophyll related to the mean production of 6.7 mg of oxygen per hour with a standard deviation of only 0.60.

Edmondson (1955) observed a close correlation ($r = 0.86$) between photosynthesis per unit light and chlorophyll in a group of cement tanks at Woods Hole which contained phytoplankton populations resulting from the enrichment of natural seawater. This relationship was largely independent of changes in the species composition of the tanks.

Many plants develop more chlorophyll when grown in the shade than when exposed to bright light, and Sargent (1940)

TABLE 5. *Photosynthesis by* Dunaliella euchlora *grown at 350 foot candles (shade cultures) and 1500 foot candles (sun cultures) at different light intensities*

Intensity (foot candles)	Photosynthesis			
	mg carbon/4 hrs/10^8 cells		mg carbon/4 hrs/mg Chl. "a"	
	(shade cult.)	(sun cult.)	(shade cult.)	(sun cult.)
7000	0.34	0.06	2.30	1.80
4700	0.49	0.17	3.20	5.00
2400	1.30	0.28	8.70	8.00
950	1.50	0.42	10.00	12.00
280	0.73	0.17	4.80	4.80
126	0.36	0.07	2.40	2.10

observed this effect in *Chlorella*. He found, however, that his "sun cultures", though containing less chlorophyll per cell, carried on photosynthesis at any light intensity at a higher rate than the "shade cultures". In other words, photosynthesis per unit of chlorophyll appeared to vary according to the light intensity at which the organism was grown.

This was not the case in some recent experiments carried out at this laboratory. Duplicate cultures of *Dunaliella euchlora* were grown at light intensities of approximately 350 and 1500 foot candles under fluorescent lamps. After two weeks growth their chlorophyll "a" content was 1.5 mg and 0.35 mg per 10^8 cells respectively.

These cultures were diluted and C^{14} added to aliquots which were then lowered to various depths in Woods Hole Harbor. Photosynthesis was then measured over a four-hour, mid-day period, incident radiation was measured with a recording photoelectric cell calibrated in foot candles, and the extinction coefficient of visible light measured with a submarine photometer. The results of this experiment (Table 5) illustrate that, although the amount of chlorophyll per cell and the rate of photosynthesis per cell are extremely variable, the rate of photosynthesis per unit of chlorophyll remains relatively constant at any given light intensity regardless of the intensity at which the organisms grew.

Some preliminary experiments by the author and G. C. Fraser with 15 species of phytoplankton, including green algae, diatoms, and dinoflagellates, indicate a constant relationship between chlorophyll "a" and photosynthesis at a constant light intensity. Chlorophyll "a", determined from the equations of Richards with Thompson (1952), was considered rather than total chlorophyll since the accessory pigments (chlorophylls "b" and "c") vary widely among different taxonomic groups and do not participate directly in photosynthesis. Photosynthesis was determined by the difference in oxygen concentration between darkened and clear bottles exposed to a bank of fluorescent lamps for six hours. The experiments were made with stock cultures of the organisms without regard to their cell concentration, age, or physiological condition.

There was a considerable reduction and scatter in the photosynthesis:chlorophyll ratio in the denser cultures which is believed to have resulted from the reduction of light by the organisms themselves. At concentrations below 0.04 mg chlorophyll "a" per liter there was a rather good linear relationship observed (Fig. 2). Since neither light intensity nor cell concentrations were measured in these experiments, they lack any useful quantitative significance, but they are nevertheless valuable for demonstrating the constancy of the photosynthesis-chlorophyll "a" relationship among a wide variety of marine plankton algae.

The task remains, then, of obtaining precise quantitative measurements of chlorophyll "a" and photosynthesis at different light intensities for a few representative species of plankton algae. With that information, the measurement of a few variables such as daily surface radiation, the extinction coefficient of visible light, and chlorophyll "a" concentrations at various depths within the euphotic zone would provide adequate data for an estimate of total daily production within an entire body of water.

REFERENCES

ARNOLD, W., AND H. I. KOHN. 1934. The chlorophyll unit in photosynthesis. J. Gen. Physiol., **18:** 109–112.

ATKINS, W. R. G. 1923. Phosphate content of waters in relationship to growth of algal plankton. Mar. Biol. Assoc. U. K., **13:** 119–150.

Barker, H. A. 1935a. Photosynthesis in diatoms. Arch. f. Microbiol., **6:** 141–156.

———. 1935b. The culture and physiology of marine dinoflagellates. Ibid, **6:** 157–181.

Brandt, K., and E. Raben. 1919–22. Zur Kenntnis der chemischen Zusammensetzung des Planktons und einiger Bodenorganismen. Wiss. Meeruntersuch., **19:** 175–210.

Brown, A. H. 1953. The effects of light on respiration using isotopically enriched oxygen. Am. J. Bot., **40:** 719–729.

Calvin, M. 1949. The path of carbon in photosynthesis, VI. J. Chem. Ed. **26:** 639–657.

Cooper, L. H. N. 1938. Phosphate in the English Channel. J. Mar. Biol. Assoc. U. K., **23:** 181–195.

Cramer, M., and J. Myers. 1948. Nitrate reduction and assimilation in *Chlorella*. J. Gen. Physiol., **32:** 93–102.

Edmondson, W. T. 1955. Factors affecting productivity in fertilized salt water. Pap. Mar. Biol. & Oceanogr. Deep-Sea Res. Suppl. to Vol. **3:** 451–463.

Emerson, R. 1929. Relation between maximum rate of photosynthesis and chlorophyll concentration. J. Gen. Physiol., **12:** 609–622.

Emerson, R., and W. Arnold. 1932. The photochemical reaction in photosynthesis. Ibid, **16:** 191–205.

Emerson, R., and L. Green. 1934. Manometric measurements of photosynthesis in the marine alga, *Gigartina*. Ibid, **17:** 817–842.

Emerson, R., L. Green and J. L. Webb. 1940. Relation between quantity of chlorophyll and capacity for photosynthesis. Plant Physiol., **15:** 311–317.

Fleischer, W. E. 1935. The relation between chlorophyll content and rate of photosynthesis. J. Gen. Physiol., **18:** 573–597.

Franck, J. 1949. An interpretation of the contradictory results in measurements of the photosynthetic quantum yields and related phenomena. Arch. Biochem., **45:** 190–229.

Frenckel, A., H. Gaffron, and E. H. Battley. 1950. Photosynthesis and photoreduction by the blue green alga, *Synechococcus elongatus*, Nag. Biol. Bull., **99:** 157–162.

Gaarder, T., and H. H. Gran. 1927. Investigations of the production of plankton in the Oslo Fjord. Rapp. et Proc.-Verb., Cons. Internat. Explor. Mer., **42:** 1–48.

Gaffron, H., and K. Wohl. 1936. Zur Theorie der Assimilation. Naturwiss., **24:** 81–107.

Goldberg, E. J., T. J. Walker, and A. Whisenand. 1951. Phosphate utilization by diatoms. Biol. Bull., **101:** 274–284.

Harvey, H. W. 1945. The chemistry and biology of sea water. The University Press, Cambridge, pp. 1–164.

Ketchum, B. H., and A. C. Redfield. 1949. Some physical and chemical characteristics of algae grown in mass culture. J. Cell. & Comp. Physiol., **33:** 281–300.

Kok, B. 1951. Photo-induced interactions in metabolism of green plant cells. In, Carbon dioxide fixation and photosynthesis. Symp. Soc. Exp. Biol. *5*. Academic Press, Inc., New York.

Kreps, E., and N. Verjbinskaya. 1930. Seasonal changes in the Barents Sea. J. Cons. Internat. Explor. Mer, **5:** 329–346.

Manning, W. M., J. F. Stauffer, B. M. Duggar, and F. Daniels. 1938. Quantum efficiency of photosynthesis in *Chlorella*. J. Am. Chem. Soc., **60:** 266–274.

Manning, W. M., and R. E. Juday. 1941. The chlorophyll content and productivity of some lakes in northern Wisconsin. Trans. Wisconsin Acad. Sci, Arts & Let., **33:** 363–393.

Moore, E. W. 1939. Graphic determination of carbon dioxide and the three forms of alkalinity. Amer. Water Works Assoc. J., **31:** 51–66.

Myers, J., and M. Cramer. 1948. J. Gen. Physiol., **32:** 103–110.

Rice, T. R. 1953. Phosphorus exchange in marine phytoplankton. Bull. U. S. Fish & Wild. Ser., **54:** 77–89.

Richards, F. R., with T. G. Thompson. 1952. The estimation and characterization of plankton populations by pigment analysis. II. A spectrophotometric method for the estimation of plankton pigments. J. Mar. Res., **11:** 156–172.

Riley, G. A. 1941. Plankton studies. III. Long Island Sound. Bull. Bing. Oceanogr. Coll., **7** (art. 3): 1–93.

Riley, G. A., H. Stommel, and D. F. Bumpus. 1949. Quantitative ecology of the plankton of the western North Atlantic. Ibid. **12** (art. 3): 1–169.

Ryther, J. H. 1954. The ratio of photosynthesis to respiration in marine plankton algae and its effect upon the measurement of productivity. Deep-Sea Res., **2:** 134–139.

Ryther, J. H., and R. F. Vaccaro. 1954. A comparison of the oxygen and C^{14} methods of measuring marine photosynthesis. J. Cons. Internat. Explor. Mer., **20:** 25–37.

Sargent, M. C. 1940. Effect of light intensity on the development of the photosynthetic mechanism. Plant Physiol., **15:** 275–290.

Sargent, M. C., and J. C. Hindman. 1943. The ratio of carbon dioxide consumption to oxygen evolution in sea water in the light. J. Mar. Res., **2:** 131–135.

Spoehr, H. A., and H. W. Milner. 1949. The chemical composition of *Chlorella;* effect of environmental conditions. Plant Physiol., **24:** 120–149.

Steemann Nielsen, E. 1947. Photosynthesis of aquatic plants with special reference to the carbon-sources. Dansk. Botan. Arkiv., **12** (8): 1–71.

———. 1952. The use of radioactive carbon (C^{14}) for measuring organic production in the sea. J. Cons. Internat. Explor. Mer., **43:** 117–140.

———. 1954. On organic production in the ocean. Ibid., **49**: 309–328.

———. 1955. The production of antibiotics by plankton algae and its effect upon bacterial activities in the sea. Pap. Mar. Biol. & Oceanogr. Deep-Sea Res., Suppl. to Vol. **3**: 281–286.

Syrett, P. J. 1954. Ammonia and nitrate assimilation by green algae (Chlorophyceae). Chap. 4 in Autotrophic Micro-organisms. 4th Symp. Soc. Gen. Microbiol. The Univ. Press, Cambridge.

Tseng, C. K., and B. M. Sweeney. 1946. Physiological studies of *Gelidium cartilagineum.* I. Photosynthesis, with special reference to the carbon dioxide factor. Am. J. Bot., **33**: 706–715.

Vaccaro, R. F., and J. H. Ryther. 1954. The bactericidal effects of sunlight in relation to "light" and "dark" bottle photosynthesis experiments. J. Cons. Internat. Explor. Mer, **20**: 18–24.

Van der Paauw, F. 1932. The indirect action of external factors on photosynthesis. Rec. trav. botan. neerl., **29**: 497–620.

Verduin, J. 1951. Photosynthesis in naturally reared aquatic communities. Plant Physiol., **26**: 45–49.

Vinogradov, A. P. 1939. The chemical composition of plankton. III. Trav. Lab. Biogeochim U.S.S.R. **5**: 47. Quoted from Vinogradov, A. P. (1953) The elementary chemical composition of marine organisms. Mem. Sears Found. for Mar. Res. No. **2**: 1–647.

Warburg, O. 1920. Über die Geschwindigkeit der photochemischen Kohlensäurezetzung in lebenden Zellen. II. Biochem. Z., **103**: 188–217.

Wassink, E. C., and J. A. H. Kersten. 1943–5. Observations sur la photosynthese et la fluorescence chlorophylliene des diatomes. Enzymologia, **11**: 282–312.

Weigl, J. W., P. M. Warrington, and M. Calvin. 1951. The relation of photosynthesis to respiration. J. Am. Chem. Soc., **73**: 5058–5063.

Contribution No. 826

Reprinted for private circulation from
THE JOURNAL OF GEOLOGY
Vol. 64, No. 5, September 1956
PRINTED IN U.S.A.

TREND SURFACES: THEIR APPLICATION TO ANALYSIS AND DESCRIPTION OF ENVIRONMENTS OF SEDIMENTATION

1. THE RELATION OF SEDIMENT-SIZE PARAMETERS TO CURRENT-WAVE SYSTEMS AND PHYSIOGRAPHY[1]

ROBERT L. MILLER
University of Chicago

ABSTRACT

The problem of defining and analyzing contemporary environments of sedimentation is approached from the point of view of mapping "trend surfaces." In this way an objective, *continuous* pattern which avoids unrealistic definite boundaries can be established for each measurable property of an environment of sedimentation. A second, closely related, problem also considered is to examine measurable properties which will pass through the time-diagenetic zone unchanged in a statistical sense, in order to ascertain how much can be inferred about strictly contemporary properties. Application is made to the near-shore area off La Jolla, California, and good agreement is found between local wave-and-current systems and sorting. An appendix describes the method in detail.

INTRODUCTION

The purpose of this paper is twofold; it is concerned with presenting a way of thinking and a subsequent technique; it is also concerned with applying the philosophy and the method to a particular problem. The discussion of the particular problem in this paper is the first of a series in which the trend surfaces will be used. Recognition and analysis of environments of sedimentation introduce a class of problems of fundamental importance in many fields of the earth sciences from marine geology to the study of sedimentary rocks. This paper presents an approach to the general case. The specific thesis is to show that there exists a strong relationship between (1) *trend patterns* of the sediment properties of average size (md) and sorting (σ) and (2) the current-wave system and physiography in the environment in which the sediment is deposited.

Since the approach is new, much space is necessarily devoted in this preliminary paper to a discussion of the principles underlying the trend maps. In addition, a large section deals with the actual technique of computing the trends. This was done to make the method of "successive approximations" more easily understandable and to describe the modification used by the writer in the last stages of computation.

In what follows, the writer proposes a synthesis of field data which includes those advantages considered by him to be important for analysis and description of environments of sedimentation. Some of the criteria are satisfied, at least in part, by other approaches. The writer would like to call attention to a recent paper by Krumbein (1955) dealing with this problem from another point of view. No claim is made that the present proposition is the final answer to such a complicated problem. The criteria are as follows:

---

[1] Contribution No. 826 from the Woods Hole Oceanographic Institution. Manuscript received August 31, 1955.

1. Continuity
   The practice of drawing lines around "environments" introduces an unrealistic discreteness. Although sharp changes in sediment properties can and do occur in nature, a continuous merging is more common.
2. Objectivity
   The very process of using the discrete boundary introduces a certain element of subjectivity, particularly where there is a continuous merging of sediment types.
3. Simplicity
   Direct contouring of field data against map co-ordinates would satisfy the requirement of continuity. This has been done by Krumbein in his excellent study of the Barataria Bay sediments (Krumbein, 1937). However, it has been the experience of the writer that much field data are locally very irregularly distributed both in the values of the variables and in the location of the sampling points. Thus direct contouring does not in most cases satisfy the requirements of objectivity and simplicity. For example, a single sampling point may have an observed value so much higher or lower than its nearest neighbors as to dominate the freehand contouring in that section of the map. In addition, decision as to the path a contour will take, in areas of poor control, is often quite arbitrary.

The writer proceeded upon the premise that local irregularities in the distribution of sediment obscure rather than clarify the attempt to extract a diagnostic pattern from a particular region. It then seemed reasonable to suppose that a *trend pattern* of the area might more closely approach the underlying order of distribution of the sediment. Clearly, the large number of variables which operate in any particular region and the complications thus introduced are important factors which require careful consideration. A search for underlying regularity or patterning offers possibilities for recognizing and classifying environments of sedimentation in terms of both physiography and dynamics and thereby for bridging the present gap between field observation and theoretical knowledge.

TREND MAPPING

A trend is sought which adequately represents the distribution of the particular parameter of interest over a geographical region in which samples have been made. The simplest type of trend in such a situation is a plane (we are here dealing in three dimensions, namely, the two map co-ordinates and a third dimension representing various values of the variable). A plane is too great a simplification for many environments (consider, for example, the distribution of size of sediment on the continental shelf). Nevertheless, as a first approximation, a plane does present a simple gradient of the distribution of values. Least-squares methods are immediately available for fitting a plane and for further refinements in determining trend. Where irregularities are marked, the refinement referred to involves successive fittings of surfaces of higher degree to the data until a sufficiently close fit is obtained. Such a surface can be expressed analytically and points for contouring computed from the resulting equation. These points then form the basis for contouring the computed surface. The contours represent the pattern that is sought. Ambiguity in contouring is eliminated because as many close-spaced points as are required can be obtained from the equation.

The method of the least-squares fit of a polynomial to data distributed over a map has recently been discussed in various contexts in earth-science studies. Weather forecasting by fitting least-squares surfaces to meteorological data was presented by Gilchrist and Cressman (1954). Gravity maps have been analyzed by Simpson (1954) in the field of geophysics. In both the aforementioned papers, large-scale high-speed computers were used to facilitate the computations. An alternative method for obtaining a computed surface by using orthogonal polynomials was described by Oldham and Sutherland (1955), in which gravity data was analyzed for regional trend.

The present writer did not have high-speed computer service available for this initial study. The technique of fitting a polynomial to the field data used in this paper is based on the method described by Ezekial (1930) and involves a graphic method of successive approximations to arrive at the final surface to be contoured. In order to avoid the computational labor involved in solving for coefficients in higher-degree polynomials, the present writer has used the simplifying scheme of arbitrarily partitioning the final curves into sections requiring no greater than second-degree polynomials. This last proposition seems to give a reliability consistent with that attained by the sequence of graphic approximations used in Ezekial's method (see appendix for general discussion of error and reliability).

A short descriptive summary of the method is presented here, followed by a discussion of the final laborsaving device introduced by the author. Although using a high-speed computer has obvious advantages, the method independently discussed by Simpson at the Massachusetts Institute of Technology requires a rectangular spacing of the original field points. The method of Gilchrist and Cressman at the Princeton Institute for Advanced Studies avoids this difficulty, since their procedure includes an objective transition from irregularly spaced field data to a fixed final grid. Very commonly, geologic field data are irregularly spaced. The present method has the advantage of not requiring a rectangular distribution of field sample points but has strong subjective elements in the technique. The writer plans to search for an improved technique, as well as to extend the application of the principle to various environments.

We shall consider as an illustrative example a contemporary near-shore marine area in which samples of bottom sediment have been collected. For each sample the median size of sediment has been recorded. Figure 1 shows the distribution of the sampling points and gives the co-ordinates to be used throughout the rest of this discussion.

If we visualize the placing of points in space similar to *a* in figure 1 for each sampling point in the region under study, we then have a distribution of points which form the basis for the contouring of trend patterns. The first step in computation involves the fitting of a *plane* of best fit to these points. The plane may be regarded as a first approximation to the trend pattern. We desire to find a plane which is the "best fit" to the points in the sense that the sum of the squares of the differences between each observed value and its counterpart on the computed plane is at a minimum. This is illustrated in figure 2. Note that point *a* lies below its counterpart *a′* on the computed

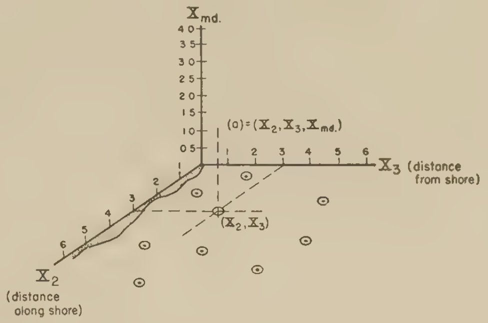
$X_{md.}$
40
35
30
25
20
15
10
05
(o)=(X_2,X_3,$X_{md.}$)
1
2
3
4
5
6
X_3 (distance from shore)
1
2
3
4
5
6
(X_2,X_3)
X_2 (distance along shore)

FIG. 1.—The co-ordinates in fig. 1 are as follows: X_2 is distance along shore, X_3 is distance from the shore, and X_{md} is median sediment size in phi units. Suppose that at sampling location $X_2 = 3$ and $X_3 = 3$, and the value of median sediment size is 2.5. Then the point *a* is located in space by reading up parallel to the X_{md} axis for a distance of 2.5.

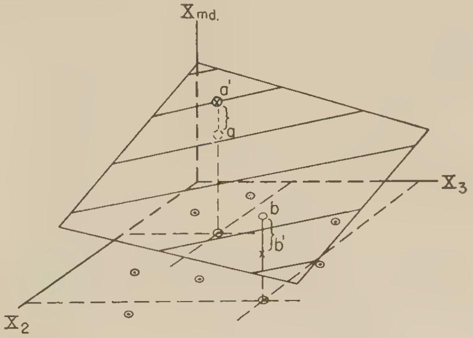

FIG. 2.—Plane of best fit to the three-dimensional data. Observed value *a* lies below its computed counterpart *a′* on the plane, and observed value *b* lies above its computed counterpart *b′* on the plane.

plane and that point b lies above its counterpart b' on the computed plane. If we consider an irregular distribution of values of md for the various sample points of the illustration, it is obvious that a plane cannot pass directly through all of them. We thus seek that plane so tilted in space that the sum of the squares of the "errors" in fit, $(a - a')^2 + (b - b')^2 + \ldots$, etc., are at a minimum. An excellent flow-sheet for computing the plane of best fit by least squares is given in Croxton and Cowden (1946, p. 748 and 757), and is described in the appendix of the present paper.

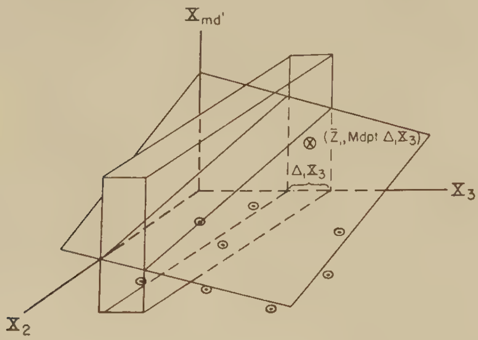

FIG. 3*a*.—Illustration of the geometrical relationships involved in computing the points $(\bar{Z}_i$, Mdpt $\Delta_i X_3)$ plotted on the X_{md}, X_3 plane. The width of the slab is determined by the width of the interval $\Delta_i X_3$ on the X_3 axis. All points $Z = (X_{md} - X_{md}^{plane})$ which fall in the slab then contribute to the average for the ith slab, namely, $\bar{Z}_i$.

We now proceed to complete the first approximation to a *surface* of best fit. The next step involves the computation of a value $Z = (X_{md} - X_{md}^{plane})$ for each observed value of X_{md}, where

X_{md} is the observed value ,

X_{md}^{plane} is the computed value on the plane,

$X_{md}^{plane} = a + bx_1 + cx_2$.

Then, for arbitrarily selected class intervals along the X_3 axis, we sum over X_2. Now, for each slab parallel to the X_2, X_{md} plane, compute a single value

$$\bar{Z}_i = \sum_{j=1}^{n_i} \frac{Z_{\Delta_i X_3}}{n_i} ,$$

where n_i is the number of Z's in the ith slab, and the subscript Δ_{iX_3} is the ith class interval on the X_3 axis. Figure 3*a* illustrates this procedure.

Summary points $(\bar{Z}_{\Delta iX_3}$, midpoint $\Delta_i X_3)$ are plotted on the X_{md}, X_3 plane as deviations from the net regression line, which is defined as $X_{md}^{net\ regr} = a + bX_2 + c(\bar{X}_3)$. By a similar procedure, analogous points are plotted on the X_{md}, X_2 plane, as shown in figure 3*b*. Curves are then drawn by eye to give as good a fit as possible to the summary points on both the X_{md}, X_3 and the X_{md}, X_2 plane. If we indicate the curve on the X_{md}, X_3 plane as $F'(X_3)$ and on the X_{md}, X_2 plane as $F'(X_2)$, we then have a first approximation *surface*, which may be expressed as follows:

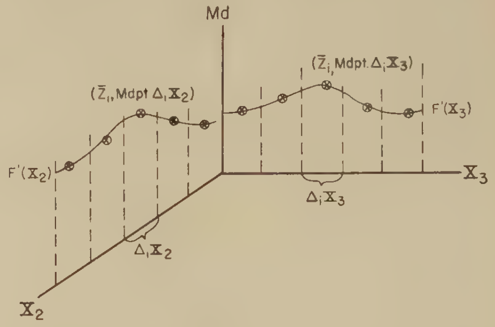
Md
$(\bar{Z}_i$ Mdpt $\Delta_i X_3)$
$(\bar{Z}_i$, Mdpt $\Delta_i X_2)$
$F'(X_3)$
$F'(X_2)$
X_3
$\Delta_i X_3$
$\Delta_i X_2$
X_2

FIG. 3*b*.—Each point on the X_{md}, X_3 plane computed as illustrated in fig. 3*a* represents an averaging for that slab. A similar procedure is followed for the X_{md}, X_2 plane. Curves are then drawn by eye through the points as shown in fig. 3*b*. These curves are then denoted by $F'(X_2)$ and $F'(X_3)$.

$$X'_{md} = a + F'(X_3) + F'(X_2) ,$$

where

$$a = \bar{X}_{md} - \frac{\sum_{j=1}^{n} [F'(X_{2j}) + F'(X_{3j})]}{n} ,$$

$$\bar{X}_{md} = \frac{\sum_{j=1}^{n} (X_{md})_j}{n} ,$$

n = Total sample size .

The first approximation to a surface is now completed. The polynomial is not expressed analytically, since we proposed to proceed to a second approximation directly from the graphs of $F'(X_3)$ and $F'(X_2)$.

The second-approximation trend surface proceeds as follows. Once again the "errors" are computed, this time reading directly from the graphs of figure *3b*. For each observed value of X_{md}, a new value X'_{md} is computed from the equation $X'_{\text{md}} = a + F'(X_3) + F'(X_2)$, where the individual values of $F'(X_2)$ and $F'(X_1)$ are read from the sketched curves. We expect that the sum of absolute values of terms $|X_{\text{md}} - X'_{\text{md}}| = Z'$ will be less than the previous sum $|X_{\text{md}} - X_{\text{md}}^{\text{plane}}| = Z$, since we have graphically improved the "fit" by introducing a curved surface instead of a plane. Figure 4 illustrates this. Note that the way in which the surface will curve is dependent upon high and low regions of values of the observed points of md.

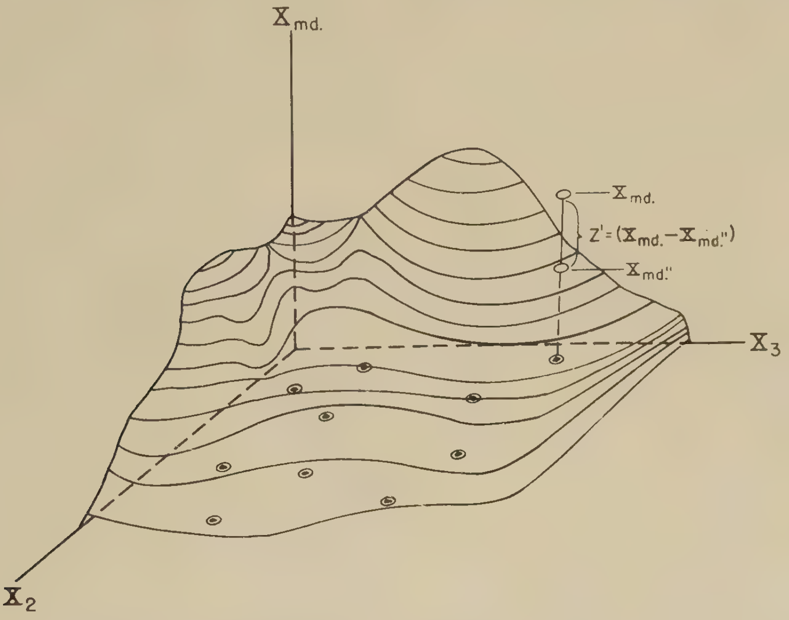

FIG. 4.—A curved surface representing a second-approximation trend pattern. The effect of high and low clusters of points is illustrated by high and low regions on the surface. $Z' = (X_{\text{md}} - X'_{\text{md}})$ illustrates the difference between an individual observed point and its computed counterpart on the surface.

As before, slabs whose width is determined by the arbitrarily selected class interval on the X_3 axis are averaged, to arrive at a $\bar{Z}'_i$ for each slab. As before, summary points ($\bar{Z}'_{\Delta_i X_3}$, midpoint $\Delta_i X_3$) are plotted on the X_{md}, X_3 plane and also on the X_{md}, X_2 plane.

We have now completed the graphic procedure for a second-approximation trend surface of best fit. The last step is to fit curves to the points ($\bar{Z}_{\Delta_i X_3}$, midpoint $\Delta_i X_3$) on the X_{md}, X_3 plane and similarly on the X_{md}, X_2 plane. However, actually to plot the surface in its second-approximation form, an analytical statement of the new curves $F''(X_2)$ and $F''(X_3)$ is needed. The following discussion covers the method as proposed by the present writer.

COMPUTATION OF THE EMPIRICAL FUNCTIONS

We desire to work out an empirical function from the sketched curves which were discussed previously. In order to reduce the labor and also the possibility of error in computation, the following method is used:

1. We shall apply the method of averages to equations of no higher than second degree, by partitioning the curve under study into subdivisions containing no more than one bend point (see figs. 5 and 6). $E''(X_3)$ is thus defined over the range o to p, $G''(X_3)$ over the range p to q, and $H''(X_3)$ over the range q to r.

2. Six[2] points are read from the first partition of the empirical curve and are substituted in the working second-degree equation, $X_{\text{md}} = a + bX_3 + cX_3^2$, resulting in six separate observation equations. Consecutive pairs of equations are then added to form three equations in three unknowns.

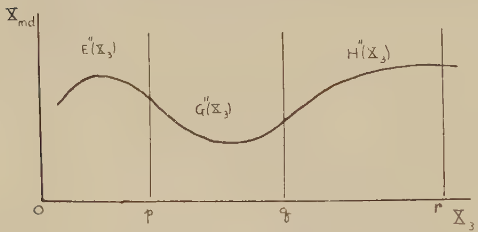

FIG. 5.—Illustration of the arbitrary partitioning of a function into segments of second degree or lower.

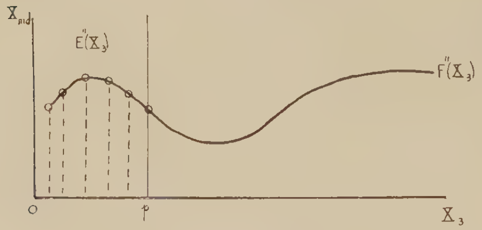

FIG. 6.—Illustration of selected points for empirical curve-fitting for segment of $F''(X_3)$ from o to p on X_3 axis.

3. The unknowns, which are the coefficients a, b, and c, are solved by using determinants.

In this way the function $F''(X_3)$ has been expressed in terms of successive functions which range over consecutive parts of $F''(X_3)$:

$$F''(X_3) = E''(X_3)\Big]_o^p , \quad G''(X_3)\Big]_p^q , \quad H''(X_3)\Big]_q^r$$

and

$$F''(X_2) = E''(X_2)\Big]_o^l , \quad G''(X_2)\Big]_l^m , \quad H''(X_2)\Big]_m^n .$$

Computation of values for purposes of contouring the final trend surfaces are made from the equation

$$X''_{\text{md}} = a'' + F''(X_3) + F''(X_2) ,$$

where

$$a'' = \bar{X}_{\text{md}} - \frac{\sum_{j=1}^{n} [F''(X_{3j}) + F''(X_{2j})]}{n} ,$$

$n =$ Total sample size ,

and $F''(X_3)$ and $F''(X_2)$, are computed from the previous equations.

APPLICATION

The technique of trend mapping is applied to the near-shore environment just off Scripps Beach at La Jolla, California. This region has been studied in great detail and is thus particularly suited for a preliminary application of trend mapping (see in particular Inman's excellent study, 1953; Inman and Quinn, 1952; Munk and Traylor, 1947; Scripps Institute of Oceanography, 1947; Miller, 1954; and Shepard and Inman, 1951).

The location of the sampling points and the values of the sediment parameters were taken from the August 24, 25, 1949, survey of the region as published by Inman (1953).

Before presentation of the trend maps, a preliminary discussion of source of sediment, wave-and-current systems, and the distribution of cut and fill of bottom will prove useful for later interpretation.

1. *Source of sediment.*—The following is quoted directly from Inman (1953, p. 7): "Scripps and La Jolla submarine canyons form a natural sediment barrier, so that any sand size material supplied to the intercanyon shelf and beach area must enter the area shoreward of the precipitous canyon heads. Since the erosion of cliffs along Scripps Beach does not provide a significant

---

[2] See appendix.

quantity of sand [Shepard and Inman, 1951], the major source of sediment must be from the north and must enter the area across a narrow 700 foot zone along range 'S' at the head of Scripps Canyon." Location of these points is given in figure 7, modified from Shepard and Inman (1950).

2. *Wave-and-current systems.*—A typical near-shore circulation pattern is illustrated in figure 7, modified from Shepard and Inman (1950). The waves tend to diverge over the submarine canyons and converge on the intercanyon shelf in the region shown by *Conv.* This convergence results in higher waves and a neutral or divergent current at *Conv.* Longshore currents flow away from this node in the directions shown.

During the period in which the data used in the present paper were collected, the predominant waves were of two general classes (Munk and Traylor, 1947; Scripps Institute of Oceanography, 1947; Shepard and Inman, 1950): (*a*) waves from a westerly direction; period 7–9 seconds, and (*b*) more abundant waves from a southerly direction; period 13–17 seconds.

3. *Sand-level changes on the bottom during a period which includes the time the present data were collected.*—Figure 8, modified from Inman (1953), shows the changes in sand level. A detailed discussion is to be found on pages 17–22 of Inman's paper. Note that the area of most marked fill occurs in the general vicinity of wave convergence shown in figure 7.

FIRST-APPROXIMATION TRENDS (PLANES) IN THE LA JOLLA AREA

Planes of best fit to the distribution of sediment size (md) and sorting (σ), in the area offshore from Scripps Beach, are shown in figures 9 and 10. In each case the arrow represents the gradient down the maximum slope of the plane.

In a crude sense there is a functional relationship between source of sediment, bottom topography, mass transport of water expressed as a single resultant, and the gradient directions shown on the two computed planes of best fit. It is interesting to note that the size and sorting gradients are both roughly normal to the best and almost parallel to each other. The apparent correlation between size and sorting shown on the trend planes may be due to the lack of weighing the σ values by size, in a form such as σ/md. The higher-approximation trend surface patterns, which will be discussed later, show no such close agreement.

It is possible to say, as a first approximation only, that size of sediment decreases and sorting becomes poorer seaward in this particular region. Although both gradients are nearly normal to the beach axis, there is a slight tilt in the plane of md from larger to the north to smaller to the south, which may partly reflect the effect of the localized source of sediment.

SECOND-APPROXIMATION TRENDS (SURFACE OF HIGHER DEGREE)

The computed surfaces of best fit for md and for σ are shown in contoured form in figures 11 and 12.[3] We shall refer briefly to the earlier discussion on source of sediment, waves and currents, and areas of cut and fill of bottom, in the following.

In figure 11, which shows the contours of the trend surface for sorting (σ), a number of features require discussion.

a) A local high of poor sorting coincides reasonably well with the region of wave convergence (see fig. 7) and also with the area of greatest fill of the sand on the bottom (see

---

[3] Estimates of how well the computed surfaces fit the observed points were made in two ways, with the following results:

$$a)\ \text{md:}\ \frac{\Sigma\,(X_{\text{obs}}-X_{\text{calc}})^2}{n}=0.0213;\qquad \frac{\Sigma\,|X_{\text{obs}}-X_{\text{calc}}|}{n}=0.1168;$$

$$b)\ \sigma:\ \frac{\Sigma\,(X_{\text{obs}}-X_{\text{calc}})^2}{n}=0.00401;\qquad \frac{\Sigma\,|X_{\text{obs}}-X_{\text{calc}}|}{n}=0.04727.$$

See appendix for a more detailed discussion of "error."

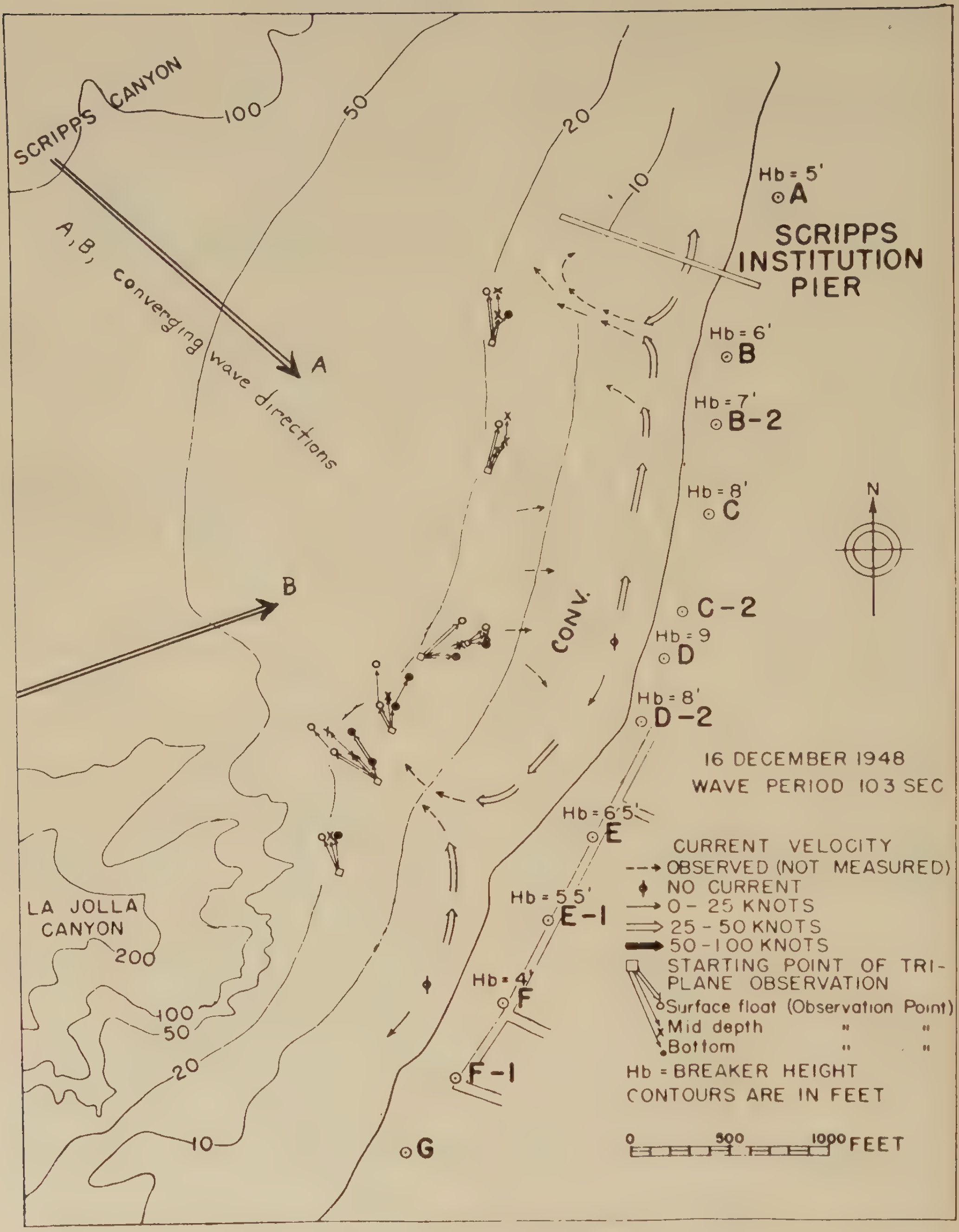
SCRIPPS CANYON
100
50
20
10
A, B, converging wave directions
A
B
Hb = 5'
A
SCRIPPS INSTITUTION PIER
Hb = 6'
B
Hb = 7'
B-2
Hb = 8'
C
N
C-2
CONV.
Hb = 9
D
Hb = 8'
D-2
16 DECEMBER 1948
WAVE PERIOD 10.3 SEC
Hb = 6.5'
E
Hb = 5.5'
E-1
Hb = 4'
F
F-1
G
LA JOLLA CANYON
200
100
50
20
10
CURRENT VELOCITY
OBSERVED (NOT MEASURED)
NO CURRENT
0 - 25 KNOTS
25 - 50 KNOTS
50 - 100 KNOTS
STARTING POINT OF TRI-PLANE OBSERVATION
Surface float (Observation Point)
Mid depth " "
Bottom " "
Hb = BREAKER HEIGHT
CONTOURS ARE IN FEET
0
500
1000 FEET

FIG. 7.—Wave-and-current system at Scripps Beach

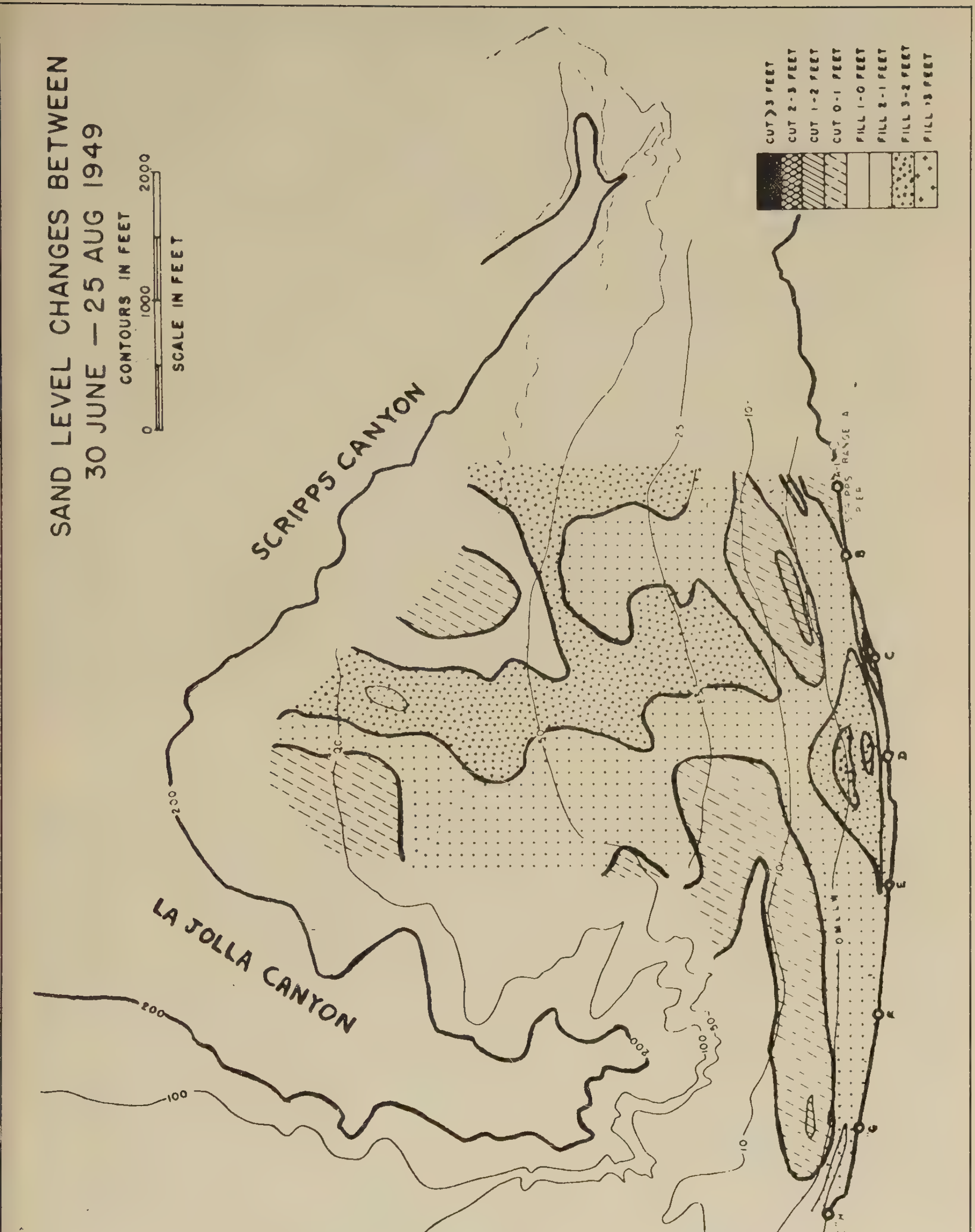
SAND LEVEL CHANGES BETWEEN
30 JUNE — 25 AUG 1949
CONTOURS IN FEET
0
1000
2000
SCALE IN FEET
SCRIPPS CANYON
LA JOLLA CANYON
CUT >3 FEET
CUT 2-3 FEET
CUT 1-2 FEET
CUT 0-1 FEET
FILL 1-0 FEET
FILL 2-1 FEET
FILL 3-2 FEET
FILL >3 FEET
SCRIPPS RANGE A
PIER
B
C
D
E
F
G
RANGE "H"
MLLW
N
10
25
50
100
200

Fig. 8

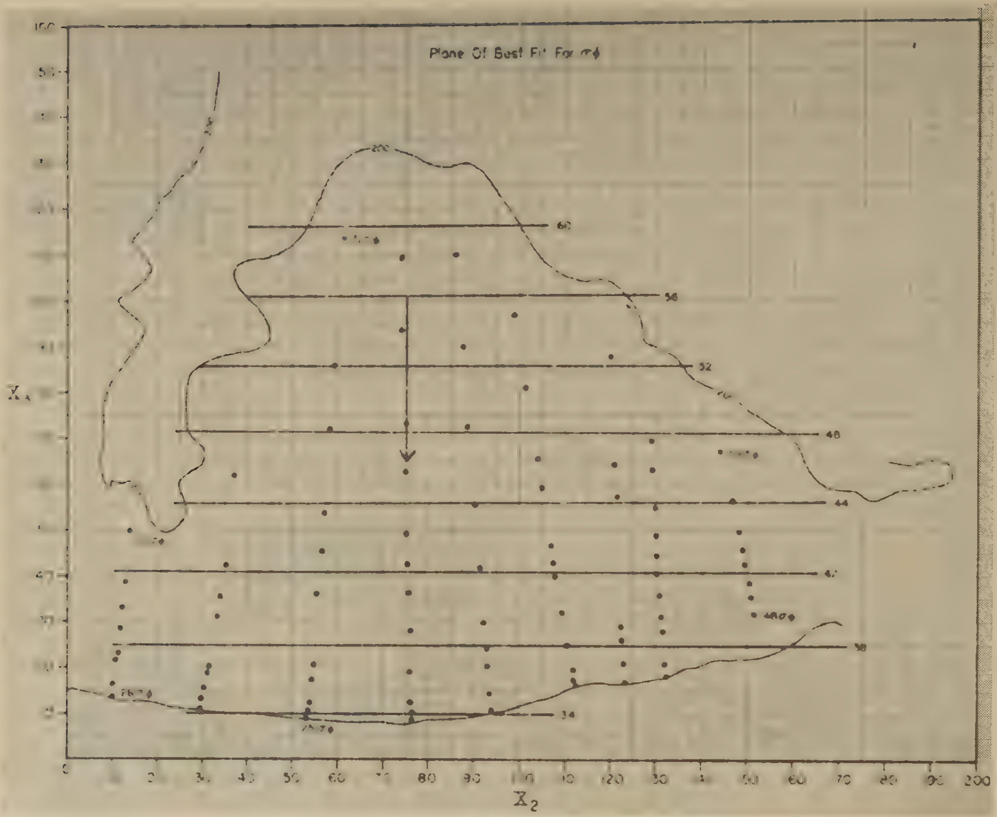
Plane Of Best Fit For σφ
200
60
56
52
48
44
40
36
34
48σφ
X_3
X_2
0
10
20
30
40
50
60
70
80
90
100
110
120
130
140
150
160
170
180
190
200

Fig. 9

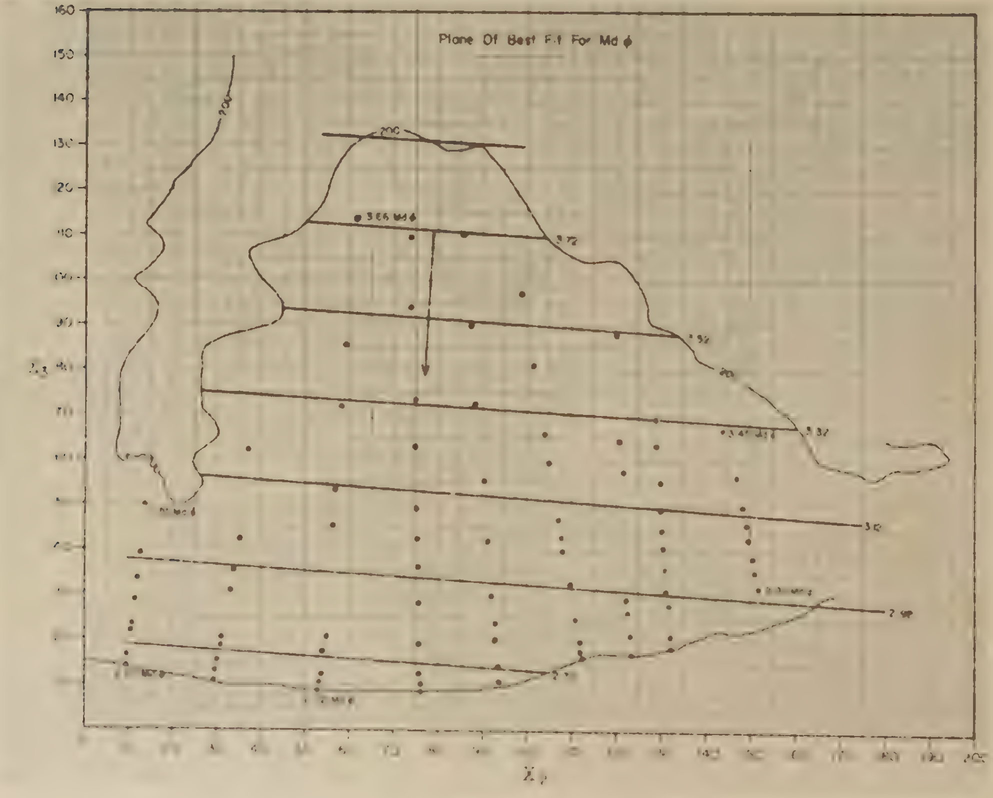
Plane Of Best Fit For Md φ
200
3.66 Md φ
3.72
3.52
3.32
3.12
2.92
2.72
160
150
140
130
120
110
100
90
80
70
60
50
40
30
20
10
X_3
X_2
0
10
20
30
40
50
60
70
80
90
100
110
120
130
140
150
160
170
180
190
200

Fig. 10

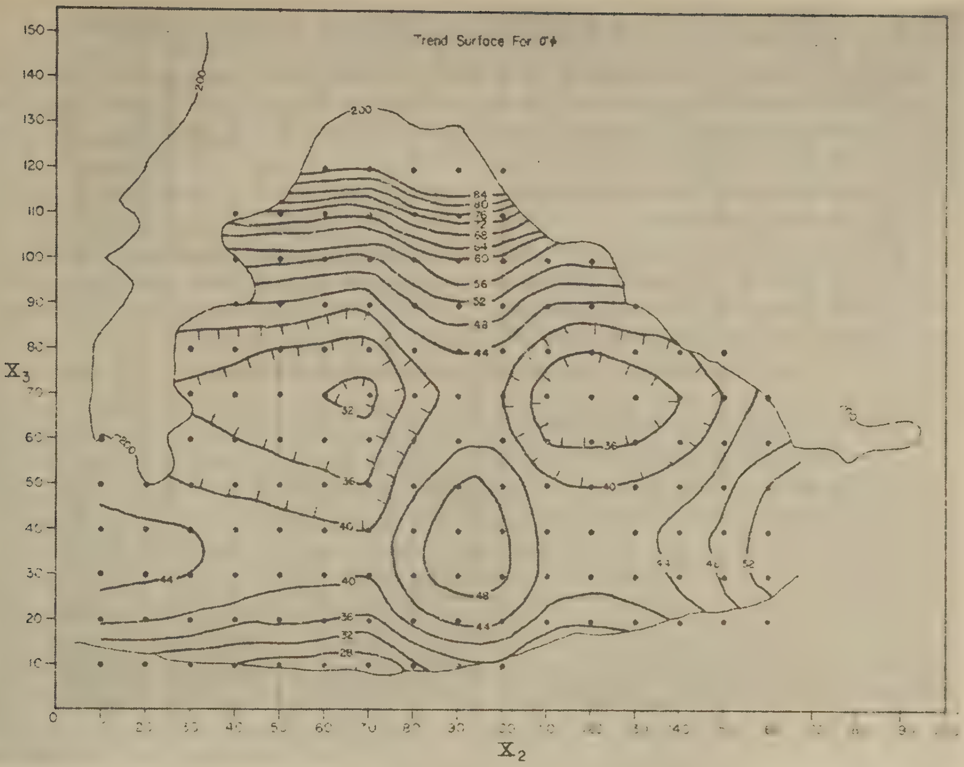
Trend Surface For σφ
X3
X2
150
140
130
120
110
100
90
80
70
60
50
40
30
20
10
0
10
20
30
40
50
60
70
80
90
100
110
120
130
140
150
160
170
180
190
200
200
84
80
76
72
68
64
60
56
52
48
44
32
36
40
44
48
40
36
32
28
44
48
52

FIG. 11

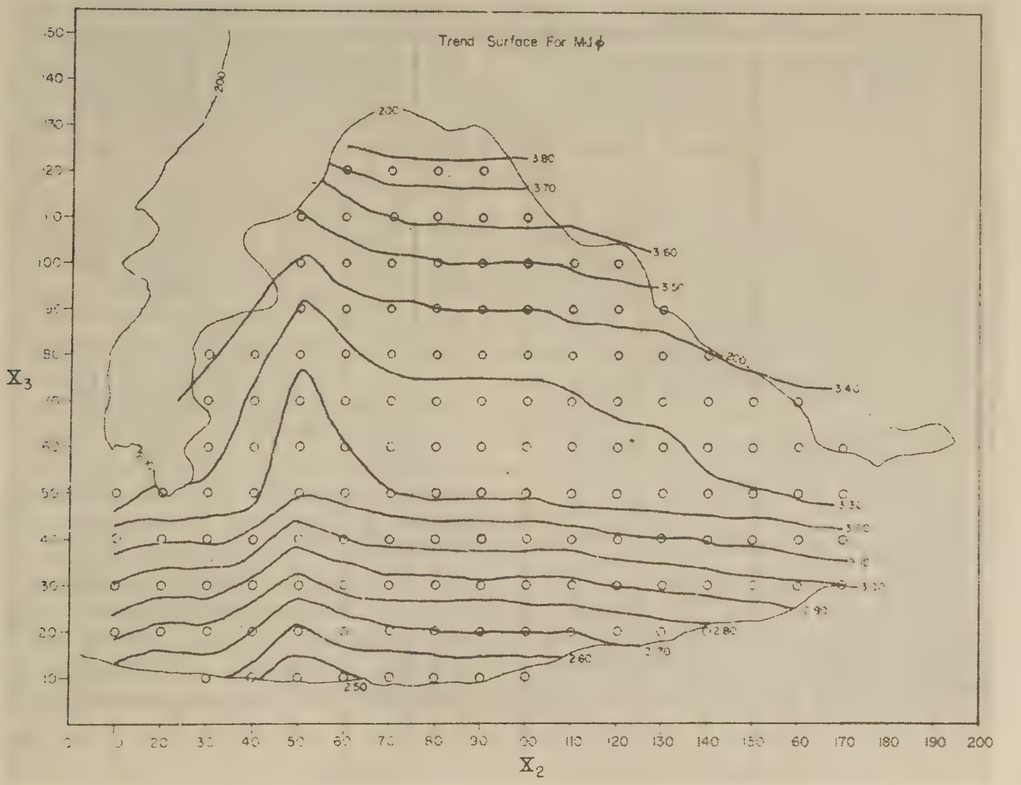
Trend Surface For Mdφ
X3
X2
150
140
130
120
110
100
90
80
70
60
50
40
30
20
10
0
10
20
30
40
50
60
70
80
90
100
110
120
130
140
150
160
170
180
190
200
200
3.80
3.70
3.60
3.50
3.40
3.30
3.20
3.10
3.00
2.90
2.80
2.70
2.60
2.50

FIG. 12

fig. 8), which indicates conditions of deposition rather than erosion.

b) The best sorting is on the beach side of the surf zone and on up the foreshore, where the water transport trends toward a thin sheet movement in the form of swash and backwash. Field observation by the writer with a Price-Gurley current meter on Cape Cod seemed to indicate that the movement of water on the foreshore more closely approached a unidirectional movement (both up and down the foreshore), with a markedly more powerful current than was noted just inside the breaker zone. This was particularly true in the backwash, where the runoff after a breaker was directed down the foreshore of the beach. In a qualitative sense the writer would expect the sorting to be very good in this zone.

c) Areas of good sorting shown by the two local depression-contoured regions on the trend map coincide with areas of "cut" of sediment on the bottom (see fig. 8). These areas are in the zone of refracted waves but on the sea-side of the zone of convergence.

d) Poorest sorting of all occurs at the apex of the triangle formed by the two submarine canyons with the beach as the base of the triangle. The regions of cut shown in figure 8, which extend back into the apex of the triangle, are not reflected in the trend patterns. This may be largely due to the smoothing effect of the trend surface.

e) There does appear to be a slight tendency to reflect the entry region of the sediment. A local gradient of sorting decreasing in the direction of the Scripps Beach region appears in the area where the sand enters from the source farther to the north. In this instance an extension of the sorting contours northward in the direction of source of the sediment would be very interesting.

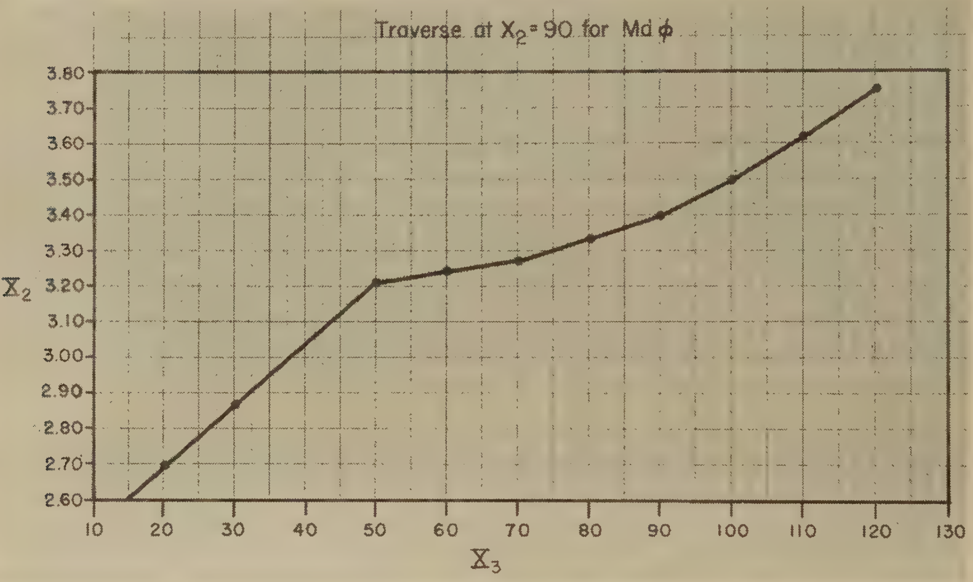

FIG. 12*a*

In summary, the trend pattern for σ shows strong agreement with movement of water as summarized in figures 7 and 8.

Figure 12, which shows the trend surface for median size (md), has several features which require discussion.

a) A sharp increase in size occurs toward the beach at a depth of 25–50 feet from a line roughly coinciding with the heads of the submarine canyons. The size then increases in almost linear fashion to the coarsest sediment, which is on the beach foreshore (see profile, figs. 12 and 12*a*).

b) A plateau of approximately uniform

median size occurs seaward of the canyon heads. This merges into a rapidly decreasing size, which is smallest at the apex of the triangular region.

c) The trend pattern of size of sediment does not reflect the source. However, there is an apparent physiographic and/or wave-and-current effect shown in the curved contours which almost parallel the axes of Scripps and La Jolla canyons and then curve around the canyon heads, becoming more closely parallel to the beach axis in shallower water.

A significant correlation of .368 between σ and md is indicated on a scattergram of these two variables, shown in Inman (1953, fig. 26*B*). However, when the geographical position of the sample points is taken into account, as in the trend surfaces presented in this paper, it is clear that in a *trend sense* md and σ show no apparent relationship (compare figs. 11 and 12). Further investigation of the apparent discrepancy between correlation in a linear-regression sense and correlation in a trend-surface sense seems indicated.

DISCUSSION

The writer believes that certain advantages have been demonstrated. The trend-pattern technique is independent of actual sizes of sediment, and it stresses, instead, the distribution pattern. This preliminary study indicates the possibility of establishing and analyzing the relationship between the current-and-wave system, whose parameters are not available to a geologist, and the distribution pattern of the sediment parameters, which are available for study in ancient rocks. Thus it may be possible by this means to gain information about "class A" parameters (which cannot be directly measured in the ancient rocks) from "class C" measurements, which are stable through the time-diagenetic zone (see Miller and Olson, 1955). Certain possibilities exist:

I. Several writers, notably Inman, Kuenen, Krumbein, and Doeglas have contended that sediment parameters should in some way reflect the hydrodynamic conditions involved in the transport and deposition of the sediment. Trend maps of the type presented here offer a simplified and objective summary pattern, free of local irregularities, which may be helpful in bridging the gap between the complexities of nature and the statements of experiment and theory.

II. The writer has now begun a collection of trend maps from areas which differ in the combination of water movements, type of sediment, and physiography that go to make up an offshore environment. With the belief that an underlying order must exist in various natural situations where sediments are deposited, it is the writer's hope that classes or types of environments of sedimentation may be ascertained by comparison of trend maps of many different present-day areas where contemporary sediments are being formed.

Trend maps may be made on core and outcrop data as well as on contemporary sediments. If the trend patterns are successful in discriminating contemporary environments, it is quite possible that patterns worked out on well-core and outcrop data may be compared with the collection of contemporary trend patterns. If such a plan is put into operation on a large scale, programming by the technique described previously or the use of one of the published programs and a high-speed computer would be required.

In the present study, only a restricted set of variables, namely, size and sorting of sediments, was mapped. In addition, no attempt was made to take into account the interaction of these two physically related variables (e.g., Miller, 1954). It would be a straightforward extension to compute a surface involving more than one variable in addition to the two map co-ordinates, although such a surface could not be contoured by conventional methods. This would at least offer a simultaneous approach to the problems of (1) interaction and (2) multivariate treatment. The writer feels, however, that extension of this sort would be very difficult to interpret in the present preliminary stage of this investigation.

A difficulty for which the writer has no present solution involves extrapolation versus interpolation. How closely should the points be spaced for "reliable" results? Suppose, for example, that a geographically large section of a basin actively receiving sediments has been sampled, but with sample points much farther apart than in Inman's study (see, for example, Stetson, 1953). Will trend contouring be justified? Accuracy of interpolation *between* sample points by the method of trend contouring is obviously a function of the spacing as well as the number of sample points. Situations where the sample points are dense in part of a geographical region and sparse in another part are special cases of this difficulty.

Extrapolation beyond the edges of the sampled area presents still another facet of the same difficulty. How far out beyond the edges of the area of control points can a trend surface be extended? As Hald (1952, p. 545) points out, "extrapolation implies an element of uncertainty which cannot be statistically evaluated." Since we do not have the empirical knowledge to make an educated guess as to the form the function should take beyond the region spanned by the sample points, extrapolation is a very dubious procedure, at least in our present state of knowledge about environments.

Application of statistical techniques in which population parameters are estimated by the sample statistics may prove useful, however, as the writer gets deeper into the general problem.

ACKNOWLEDGMENTS.—Part of the work involved in this paper was done while the writer held a fellowship at Woods Hole Institute of Oceanography during the summer of 1955. The writer wishes to express his appreciation for the opportunity to discuss the context of this paper with members of the staff at Woods Hole, especially J. Zeigler, H. C. Stetson, and W. Marks. Helpful comments and criticisms were also extended by D. L. Inman and G. Rusnak, of the Scripps Institute of Oceanography, and by S. M. Simpson, of the Massachusetts Institute of Technology. The drafting was done by E. B. Shykind, at the University of Chicago.

REFERENCES CITED

CROXTON, F. E., and COWDEN, D. J., 1946, Applied general statistics: New York, Prentice-Hall, Inc.

EZEKIAL, M., 1930, Methods of correlation analysis: 2d ed., New York, John Wiley & Sons, Inc.

GILCHRIST, B., and CRESSMAN, G. P., 1954, An experiment in objective analysis: Tellus, v. 6, no. 4.

HALD, A., 1952, Statistical theory with engineering applications, p. 545–546: New York, John Wiley & Sons, Inc.

INMAN, D. L., 1953, Areal and seasonal variations in beach and nearshore sediments at La Jolla, California: Beach Erosion Board Office of Chief of Engineers, Tech. Memo. 34.

——— and QUINN, W. H., 1952, Currents in the surf zone: Second Conf. Coastal Engin., Houston, Texas, 1951, Council on Wave Research, Proc.

KRUMBEIN, W. C., 1955, Statistical analysis of facies maps: Jour. Geology, v. 63, p. 452–470.

——— and ABERDEEN, E., 1937, The sediments of Barataria Bay: Jour. Sed. Petrology, v. 7, no. 1, p. 3–17.

MILLER, R. L., 1954, A model for the analysis of environments of sedimentation: Jour. Geology, v. 62, p. 108–113.

——— and OLSON, E. C., 1955, The statistical stability of quantitative properties as a fundamental criterion for the study of environments: Jour. Geology, v. 63, p. 376–387.

MUNK, W. H., and TRAYLOR, M.A., 1947, Refraction of ocean waves: a process linking underwater topography to beach erosion: Jour. Geology, v. 40, p. 1–26.

OLDHAM, C. H. G., and SUTHERLAND, D. B., 1955, Orthogonal polynomials: their use in estimating the regional effect: Geophysics, v. 20, no. 2, p. 295–306.

SCRIPPS INSTITUTE OF OCEANOGRAPHY, UNIV. OF CALIF., 1947, A statistical study of wave conditions at five open sea localities along the California coast: Wave Rept., no. 68.

SHEPARD, F. P., and INMAN, D. L., 1950, Nearshore water circulation related to bottom topography and wave refraction: Amer. Geophys. Union Trans., v. 31, no. 2, p. 196–212.

——— and ——— 1951, Sand movement on the shallow intercanyon shelf at La Jolla, California: Beach Erosion Board, Tech. Memo. 26, 29 p.

SIMPSON, S. M., 1954, Least squares polynomial fitting to gravitational data and density plotting by digital computors: Geophysics, v. 19, no. 2, p. 255–269.

STETSON, H. C., 1953, The sediments of the western Gulf of Mexico. Pt. I. The continental terrace of the western Gulf of Mexico: its surface sediments, origin and development: Papers in Physical Oceanography and Meteorology, v. 12, no. 4., published by Massachusetts Institute of Technology and Woods Hole Oceanographic Institute.

APPENDIX

Fifteen observations of median size of sediment taken in an area 1,500 yards square form the basis of the computing example in this appendix. Figure 13 shows the way these observations are distributed over the region. The first three columns in the computation sheet (table 1) give the median sediment size X_{md} corresponding to the map co-ordinates X_2 and X_3 in the second and third columns.

The first step involves computation of the plane of best fit to the X_{md} observations. The method is described in detail in Croxton and Cowden (1946, p. 748 and 757) but is given here so that the interested reader can follow through the method.[4]

The necessary sums and cross-products for computation of the plane are shown under the first three columns in table 1. The first entry in the column marked "X_{md}^{plane}" in table 1 is the value on the plane of best fit corresponding to the first observed value in the X_{md} column. We now calculate the difference between the observed X_{md} values and their analogues on the plane of best fit. These differences are entered in the column headed $Z = (X_{md} - X_{md}^{plane})$.

Note that the plane of best fit is much too high in some cases and much too low in others. See also the contours of the plane of best fit in figure 13 and compare with the observed values. It is apparent that a curved surface will greatly improve the fit of contours to the observed points. We now proceed to successive approximations of a curved surface.

The next five columns in table 1 are devoted to calculating average Z values for arbitrary class intervals, first, on X_2 for the $X_{md}X_2$ plane and then on X_3 for the X_3X_{md} plane. The column headed "Δ_i" gives the selected class intervals which will be used for both $X_{md}X_2$ and $X_{md}X_3$ planes.

Choice of class intervals is made on the basis of subdividing the X_2 (or X_3) axis into a number of partitions such that important bends in the rises and falls of the Z values will not be overlooked. On the other hand, each class interval should contain at least one observation. In the present example the X_2 and X_3 axes are divided into five equal class intervals. The average of all the Z values in each class interval is plotted as $\bar{Z}_{\Delta_i X_2}$ for the ith class interval at the midpoint of the ith class interval on the X_2 axis and as $\bar{Z}_{\Delta_i X_3}$ for the ith class interval at the midpoint of the ith class interval on the X_3 axis. Figures 14 and 15 show these averages plotted as *deviations from the respective "net regression lines" as a zero base.*

For example, the first $\bar{Z}$ entered in table 1 for the $X_{md}X_2$ plane is -0.343. This is plotted 0.343 units *down* from the net regression line and at midpoint of class interval 0.1 to 3.0. The co-ordinates are (1.85, 1.50), as shown in figure 14.

---

[4] Computation of plane of "best fit," $X_{md} = a + bX_2 + cX_3$:

$$\begin{array}{rr@{\qquad}rr@{\qquad}rr}
\Sigma X_2^2 = & 1118.00 & \Sigma X_2X_3 = & 963.00 & \Sigma X_2X_{md} = & 196.4 \\
\bar{X}_2\Sigma X_2 = & 866.40 & \bar{X}_3\Sigma X_2 = & 926.82 & \bar{X}_{md}\Sigma X_2 = & 213.18 \\
\hline
\Sigma x_2^2 = & 251.60 & \Sigma x_2x_3 = & 36.18 & \Sigma x_{md}x_2 = & -16.78
\end{array}$$

$$\begin{array}{rr@{\qquad}rr@{\qquad}rr}
\Sigma X_3^2 = & 1252.00 & \Sigma X_3X_{md} = & 200.50 & \Sigma X_{md}^2 = & 60.47 \\
\bar{X}_3\Sigma X_3 = & 991.86 & \bar{X}_3\Sigma X_{md} = & 228.45 & \bar{X}_{md}\Sigma X_{md} = & 52.55 \\
\hline
\Sigma x_3^2 = & 260.14 & \Sigma x_3x_{md} = & -27.95 & \Sigma x_{md}^2 = & 7.92
\end{array}$$

NOTE: $x_i = (X_i - \bar{X}_i)$. This is a laborsaving device and reduces the computations, since $\Sigma(x_2) = \Sigma(X_2 - \bar{X}) = 0$; similarly, Σx_3 and Σx_{md} vanish. The simplified normal equations are

$$\Sigma x_{md}x_2 = b\Sigma x_2^2 + c\Sigma x_2x_3 \, ,$$

$$\Sigma x_{md}x_3 = b\Sigma x_2x_3 + c\Sigma x_3^2 \, ;$$

substituting, $-16.78 = (b)\ 251.60 + (c)\ 36.18$ and, $-27.95 = (b)\ 36.18 + (c)\ 260.14$. Solving simultaneously for b and c, we find $b = -0.0523$ and $c = -0.1002$. The coefficient a is found from the equations $a = \bar{X}_{md} - b\bar{X}_2 - c\bar{X}_3$. Substituting, $a = 1.87 + 0.3975 + 0.8146 = 3.0821$. The final equation for the plane $X_{md} = a + bX_2 + cX_3$ becomes $X_{md} = 3.0821 - 0.0523X_2 - 0.1002X_3$.

TABLE 1

					z
X_{md}	X_2	X_3		X_{md}^{plane}	$X_{md}-X_{md}^{plane}$
1.9	2	3		2.677	−0.777
2.3	2	10		1.976	+0.324
1.1	2	13		1.675	−0.575
2.6	4	1		2.773	−0.173
2.2	5	8		2.019	+0.181
1.8	5	14		1.418	+0.382
3.5	7	3		2.415	+1.085
3.1	7	6		2.115	+0.985
1.3	8	11		1.561	−0.261
1.2	10	8		1.758	−0.558
1.4	11	13		1.204	+0.196
1.7	12	3		2.154	−0.454
1.8	12	6		1.853	−0.053
1.2	12	10		1.453	−0.253
1.0	15	13		0.995	+0.005
28.1	114	122	ΣX		
60.47	1,118	1,252	ΣX^2		
1.87	7.60	8.13	$\bar{X}$		

$\Sigma X_2X_3 = 963.0$
$\Sigma X_{md}X_3 = 200.5$
$\Sigma X_{md}X_2 = 196.4$

CALCULATION OF $\bar{Z}$'s

Δ_i	Z_{X_2}	Z_{X_3}	$Z_{\Delta_i X_2}$	$\bar{Z}_{\Delta_i X_3}$
0.1– 3	−0.777 + .324 −0.575 −1.030	−0.777 −0.173 +1.085 −0.454 −0.319	−0.343	−0.080
3.1– 6	−0.173 + .181 +0.382 +0.390	+0.985 −0.053 +0.932	+0.130	+0.466
6.1– 9	+1.085 +0.985 −0.261 +1.809	+0.181 −0.558 −0.377	+0.603	−0.188
9.1–12	−0.558 + .196 − .454 − .053 −0.253 −1.122	+0.324 − .261 −0.253 −0.190	−0.224	−0.063
12.1–15	+0.005	−0.575 + .382 + .196 +0.005 +0.008	+0.005	+0.002

TABLE 1—*Continued*

$f'(X_2)$	$f'(X_3)$	X_{md}	X'_{md}	Z' $X_{md}-X'_{md}$
1.89	2.62	1.9	2.559	−0.659
1.89	1.58	2.3	1.519	+ .781
1.89	1.42	1.1	1.359	− .259
2.14	2.40	2.6	2.589	+ .011
2.28	1.68	2.2	2.009	+ .191
2.28	1.30	1.8	1.629	+ .171
2.46	2.62	3.5	3.129	+ .371
2.46	2.29	3.1	2.799	+ .301
2.38	1.56	1.3	1.989	− .689
1.63	1.68	1.2	1.359	− .159
1.46	1.42	1.4	0.929	+ .471
1.46	2.62	1.7	2.129	− .429
1.46	2.29	1.8	1.799	+ .001
1.46	1.58	1.2	1.089	+ .111
1.70	1.42	1.0	1.169	−0.169
28.84	28.48		28.055	+0.045
57.32				

CALCULATION OF $\bar{Z}$'s

Δ_i	Z'_X	Z'_{X_3}	$\bar{Z}'_{\Delta_i X_2}$	$\bar{Z}_{\Delta_i X_3}$
0.1– 3	−0.659 + .781 −0.259 −0.137	−0.659 + .011 + .371 −0.429 −0.706	−0.046	−0.177
3.1– 6	+0.011 + .191 +0.171 +0.373	0.301 0.001 0.302	+0.124	+0.151
6.1– 9	+0.371 + .301 −0.689 −0.017	+0.191 −0.159 +0.032	−0.006	−0.016
9.1–12	−0.159 + .471 − .429 + .001 +0.111 −0.005	+0.781 − .689 +0.111 +0.203	−0.001	+0.068
12.1–15	−0.169	−0.259 + .171 + .471 −0.169 +0.214	−0.169	+0.0535

$'(X_2)$	$f''(X_3)$
1.92	2.67
1.92	1.64
1.92	1.44
2.25	2.16
2.39	1.69
2.39	1.30
2.53	2.67
2.53	2.35
2.37	1.63
1.64	1.69
1.46	1.44
1.40	2.67
1.40	2.35
1.40	1.64
1.41	1.44
28.93	28.78
57.71	

The "net regression line" on the $X_{md}X_2$ plane is given by the expression $X_{md}^{net\ regr} = a + bX_2 + c\bar{X}_3$, and on the X_mX_3 plane by the expression $X_{md}^{net\ regr} = a + b\bar{X}_2 + cX_3$. In this example the net regression line for the $X_{md}X_2$ plane is $3.0821 - 0.0523X_2 - 0.1002(8.13) = X_{md}^{net\ regr} = 2.2675 - 0.0523X_2$. Similarly, on the $X_{md}X_3$ plane the net regression line is $2.6846 - 0.1002X_3$.

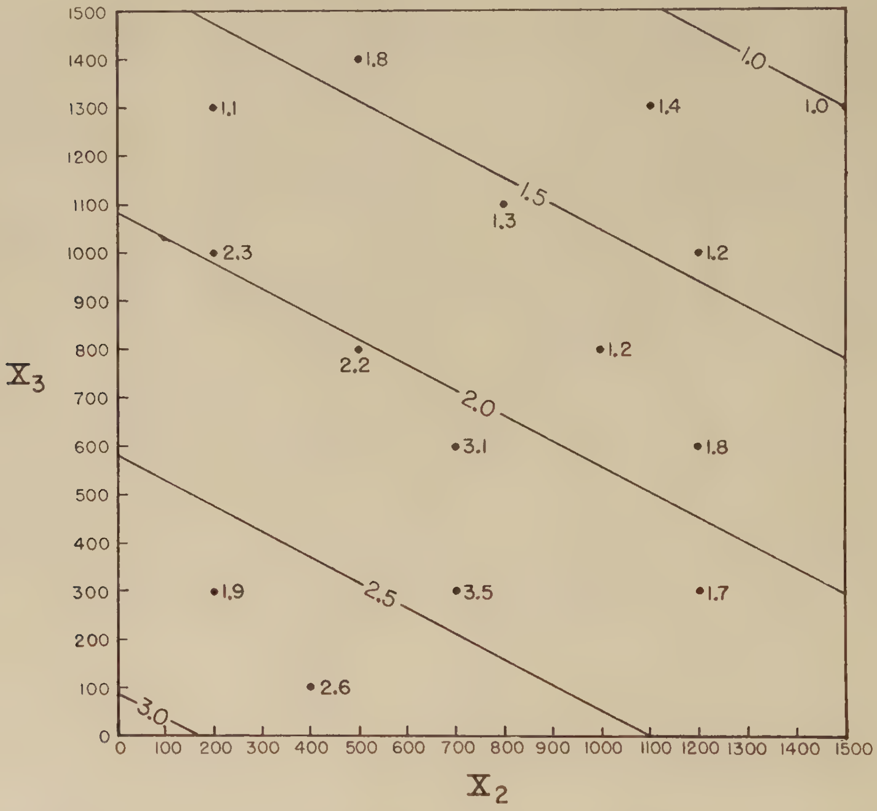
1500
1400
1300
1200
1100
1000
900
800
700
600
500
400
300
200
100
0
X_3
0
100
200
300
400
500
600
700
800
900
1000
1100
1200
1300
1400
1500
X_2
1.0
1.0
1.5
2.0
2.5
3.0
1.8
1.1
1.4
1.3
2.3
1.2
2.2
1.2
3.1
1.8
1.9
3.5
1.7
2.6

FIG. 13.—Map showing distribution of sample points of median sediment size in an area 1,500 yards square. The plane of "best fit" to these points is shown with 0.50 contour interval.

Next a curve is fitted to the $\bar{Z}$ points *by eye* [see the curve labeled $f'(X_2)$ in fig. 14 and $f'(X_3)$ in fig. 15]. Finally, we compute a', where

$$a' = \bar{X}_{md} - \frac{\Sigma\,[f'(X_2) + f'(X_3)]}{n}$$

and n = number of X_{md} entries. In this example $a' = 1.87 - (57.32/15) = -1.951$. The entries in the two columns headed $f'(X_2)$ and $f'(X_3)$ in table 1 are read directly from the graphs. For example, the first entry in the column $f'(X_2)$ is found as follows: at $X_2 \doteq 2$ on the abscissa of figure 14, read up to the $f'(X_2)$ curve and over the value of X_{md} on the ordinate, which is approximately 1.89.

The first approximation of a surface fit to the observed data is completed. It may be expressed as $X'_{md} = a' + f'(X_2) + f'(X_3)$. We shall proceed directly to a second approximation rather than compute analytical expressions for $f'(X_2)$ and $f'(X_3)$. The entries in table 1 in the column headed X'_{md} are taken from the expression $X'_{md} = a' + f'(X_2) + f'(X_3)$. For example, the first entry in this column is $X_{md} = -1.951 + 1.89 + 2.62 = 2.559$. The Z' entries are calculated next, where $Z' = X_{md} - X'_{md}$. The first entry on the computation sheet in the Z' column is $Z' = 1.900 - 2.559 = -0.659$.

The next five columns record the computations and entries necessary to calculate $\bar{Z}'$ values for both $X_{md}X_2$ and $X_{md}X_3$ planes. The procedure repeats that of calculating the $\bar{Z}$ values of the first approximation, and the same class intervals are used. As before, the $\bar{Z}'$ values are plotted as shown in figures 14 and 15. This time, however, the points in the columns headed $\bar{Z}'_{\Delta i X_2}$ and $\bar{Z}'_{\Delta i X_3}$ are plotted as *deviations from the first-approximation curve* $f'(X_2)$ *and* $f'(X_3)$.

The plan of successive approximations is thus shown, in that the first set of $\bar{Z}$'s is plotted as deviations from the planes (net regression lines) and the second set of $\bar{Z}$'s denoted by $\bar{Z}$'s is plotted as deviations from the curves drawn through the first set of $\bar{Z}$'s.

Having plotted the second set of points (the $\bar{Z}$'s) on both the $X_{md}X_2$ and the $X_{md}X_3$ plane, we now proceed to work out an analytic expression for the final curves, in order to plot contours. The following procedure is used:

1. Once again draw a smooth curve by eye through the Z' points, as shown in figures 14 and 15.

2. Partition the drawn curves denoted by $f''(X_2)$ and $f''(X_3)$ into subdivisions such that no more than one bend point appears in a given partition.

a) In figure 15 the partition was arbitrarily placed at $X_3 = 8$.

Six consecutive values are then read from the curve, so spaced that the curve is well represented. (The number six is arbitrary; see Smith, Gale, and Neeley, 1928, p. 228.)

TABLE 2

X_3	X''_{md} (from Curve)	X''_{md} (Computed)
1.50	2.32	2.22
3.00	2.67	2.67
4.50	2.85	2.74
5.50	2.57	2.58
7.00	1.85	2.01
8.00	1.69	1.43

Six equations in three unknowns are now available for obtaining an expression of the form $X''_{md} = a + bX_3 + cX_3^2]_0^8$ (the half-bracket indicates the range over which the function holds). These are summed over consecutive pairs to give three equations in three unknowns. Substituting from table 2 we have

$$\begin{array}{lll}
2.32 = a + 1.5b + 2.25c & 2.85 = a + 4.5b + 20.25c & 1.85 = a + 7.0b + 49.0c \\
\underline{2.67 = a + 3.0b + 9.00c} & \underline{2.57 = a + 5.5b + 30.25c} & \underline{1.69 = a + 8.0b + 64.0c} \\
4.99 = 2a + 4.5b + 11.25c & 5.42 = 2a + 10.0b + 50.50c & 3.54 = 2a + 15.0b + 113.0c
\end{array}$$

The three resulting sums in three unknowns are solved simultaneously by determinants to give $X'' = 1.3854 + 0.6820X_3 - 0.0846X_3^2]_0^8$. An empirical curve is also computed for the remainder of the drawn line in figure 15, ranging from 8 to 15, e.g., $X''_{md} = 0.2662 + 0.3127X_3 - 0.0168X_3^2]_8^{15}$. A similar procedure is followed on the $X_{md}X_2$ plane in figure 14 with these results: $X''_{md} = 0.830 + 0.5398X_2 - 0.0462X_2^2]_0^{11}$ and $X'' = 2.5906 - 0.1771X_2 + 0.0065X_2^2]_{11}^{15}$. The final computation is the constant a'', where $a'' = \bar{X} - \Sigma[f''(X_2) + f''(X_3)]/15$, and in this example $a'' = 1.87 - 3.847 = -1.977$.

In this example one partition was sufficient in both the $X_{md}X_2$ and the $X_{md}X_3$ plane.

As a result of the partitioning process, the map region of this example is divided into *four* parts, as shown in figure 16. In each of these subdivisions the computing equation for the surface is formed by substituting in the following general form, $X'' = a'' + f''(X_2)]_m^n + f''(X_3)]_p^q$ for the region ranging over the X axis from m to n and the X axis from p to q. Thus for the region in figure 16 from 0 to 8 on the X_3 axis and 0 to 11 on the X_2 axis we have $X''_{md} = -1.977 + (0.830 + 0.5398X_2 - 0.0462X_2^2) + (1.3854 + 0.6820X_3 - 0.0846X_3^2)$, which becomes $X''_{md} = 0.2384 + 0.6820X_3 + 0.5389X_2 - 0.0846X_3^2 - 0.0462X_2^2$. The computing equations for each of the partitions on the X_2X_3 plane are given in figure 16. Figure 17 shows computed points and contouring of the "second-approximation" surface.

ACCURACY OF RESULTS OF THE GRAPHIC METHOD OF SUCCESSIVE APPROXIMATIONS

1. The difference between the observed values of median sediment size and the corresponding points on the computed surface are given in table 3. This information is summed for convenience in two ways:

a) The sum of squares of the difference of the observed values from the calculated values is divided by the number of observations, to give an estimate of average deviation:

$$\frac{\Sigma\,(X_{md\,(obs)} - X_{md\,(calc)})^2}{n}.$$

In the present example we have 1.8225/15 = 0.1215.

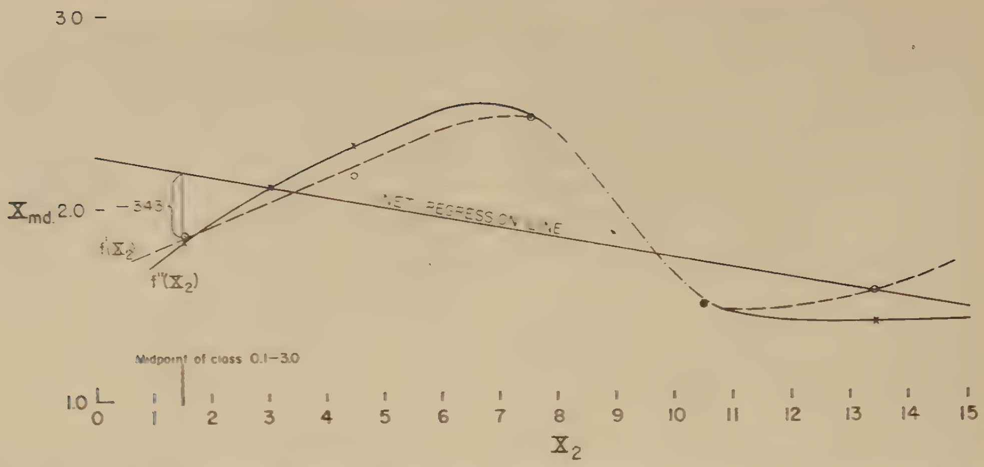

FIG. 14.—The work sheet used in the graphic method of successive approximations. This sheet represents the plane X_{md}, X_2. See also fig. 3*b*.

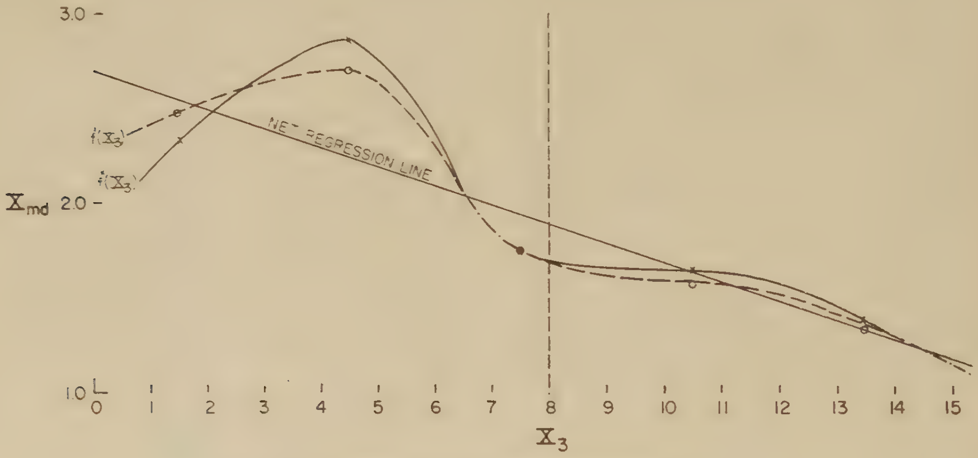

FIG. 15.—Same as fig. 14, but for the plane X_{md}, X_3

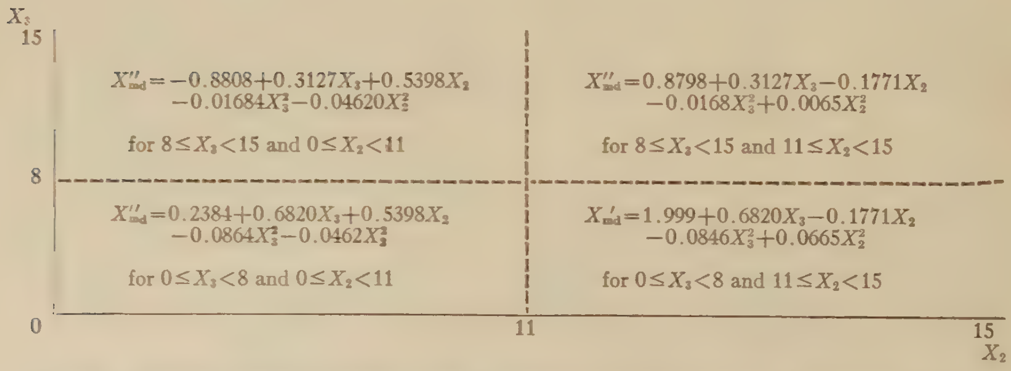

$$X''_{md} = -0.8808 + 0.3127X_3 + 0.5398X_2 - 0.01684X_3^2 - 0.04620X_2^2$$

for $8 \leq X_3 < 15$ and $0 \leq X_2 < 11$

$$X''_{md} = 0.8798 + 0.3127X_3 - 0.1771X_2 - 0.0168X_3^2 + 0.0065X_2^2$$

for $8 \leq X_3 < 15$ and $11 \leq X_2 < 15$

$$X''_{md} = 0.2384 + 0.6820X_3 + 0.5398X_2 - 0.0864X_3^2 - 0.0462X_2^2$$

for $0 \leq X_3 < 8$ and $0 \leq X_2 < 11$

$$X'_{md} = 1.999 + 0.6820X_3 - 0.1771X_2 - 0.0846X_3^2 + 0.0665X_2^2$$

for $0 \leq X_3 < 8$ and $11 \leq X_2 < 15$

FIG. 16.—Final partitioning of the map of fig. 13, showing the equations for the curved surface and the regions over which they are defined.

b) The absolute values of the deviations are summed and divided by n to give another estimate of average deviation:

$$\frac{\Sigma \mid X_{md\,(obs)} - X_{md\,(calc)} \mid}{n}.$$

In the present example we have 3.9606/15 = 0.2640.

The foregoing is not to be taken as statistical inference from sample to population but as a convenient way to measure how well the surface fits the observed data. The estimates of the fit of the computed surface to the observed data may be used as a criterion for the contour interval in the final map. In the present example the contour interval is 0.50, and the largest of the two ways of estimating fit is 0.2640. The contour interval chosen should not be smaller than the "error-term."

DISTRIBUTION AND NUMBER OF SAMPLING POINTS IN THE REGION STUDIED

It is obvious that the denser the point distribution, the more accurate will be the surface

TABLE 3

Observed			Computed	
X_{md}	X_2	X_3	X_{md}	$X_{obs}-X_{computed}$
1.9	2	3	2.4178	−0.5178
2.3	2	10	1.4610	+ .8390
1.1	2	13	1.2399	− .1399
2.6	4	1	2.2558	+ .3442
2.2	5	8	2.0896	+ .1104
1.8	5	14	1.7482	+ .0518
3.5	7	3	3.0378	+ .4622
3.1	7	6	2.7996	+ .3004
1.3	8	11	1.2859	+ .0141
1.2	10	8	1.3236	− .1236
1.4	11	13	0.9441	+ .4559
1.7	12	3	2.0944	− .3944
1.8	12	6	1.8562	− .0562
1.2	12	10	1.1376	+ .0624
1.0	15	13	0.9117	+0.0883

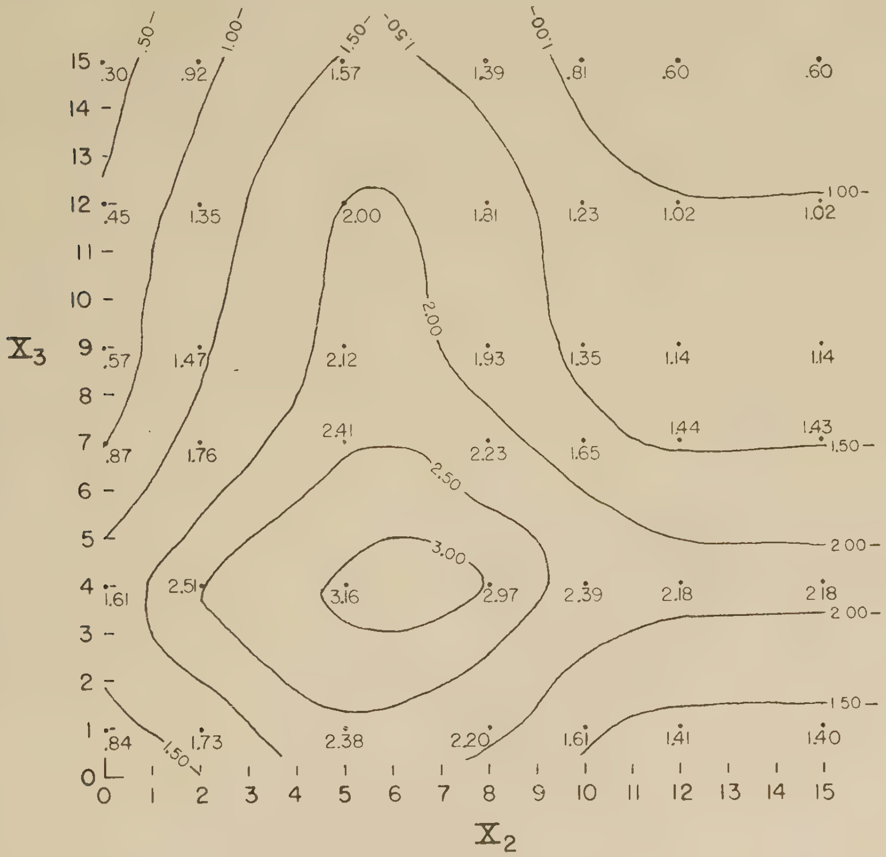

X3
X2
0
1
2
3
4
5
6
7
8
9
10
11
12
13
14
15
.30
.92
1.57
1.39
.81
.60
.60
.45
1.35
2.00
1.81
1.23
1.02
1.02
.57
1.47
2.12
1.93
1.35
1.14
1.14
.87
1.76
2.41
2.23
1.65
1.44
1.43
1.61
2.51
3.16
2.97
2.39
2.18
2.18
.84
1.73
2.38
2.20
1.61
1.41
1.40
.50
1.00
1.50
1.50
1.00
1.00
2.00
2.50
3.00
1.50
2.00
2.00
1.50
1.50

FIG. 17.—The final surface of best fit. Referred to as the *trend surface*. Compare with the plane of best fit in fig. 13.

fit to the points. The optimum density of points is relative, however, to the nature of the problem at hand. It seems to the writer that each case should necessarily be discussed independently, at least until we have reached the stage where the variability of the property measured is predictable from foot to foot or larger unit to larger unit in the specific environment under study. The particular kind of problem may be, for example, the effect of linear current on distributing sediment down-current from a fixed source for the sediment. How close should the sample points be spaced to bring out all the important peaks and valleys in the trend surface of median sediment size?

In such a case the proposal of a smoothed surface has merit. If the trend-surface contours in the studied region for a certain number of sample stations does not differ markedly in pattern from a second trend surface in the same region, but uses twice as many points, it would not be unreasonable to conclude that the first size of sample was enough.

A similar argument could be advance for the distribution of the points in the region, e.g., gaps versus clumps of points. This problem, however, is more difficult, since a good answer to the distribution problem would seem necessarily based on the information we are seeking to start with.

Mr. Ernest Kaarsberg carefully rechecked all computations in the appendix. However, all errors in appendix and text are the sole responsibility of the writer.

Contribution No. 827

Särtryck ur Tellus nr 3, 1956

On the Maintenance of the Trade Winds

By JOANNE STARR MALKUS, Woods Hole Oceanographic Institution[1]

(Manuscript received February 20, revised April 16, 1956)

Abstract

A relation between the large-scale features of the lower trade stream and the effects of small-scale convective motions is investigated. The small-scale processes impose constraints upon the over-all circulation through non-adiabatic heating and the production of shearing stresses. These constraints may be formulated in terms of a theoretical model describing the mean flow in a section along the northern portion of the Pacific trade, which has previously been studied observationally in some detail.

In a simplified frictionless model with non-adiabatic heating the flow exhibits qualitatively many of the important features of the trades, such as subsidence, and a downstream acceleration, increased vertical wind shear, and pressure drop. The motion and pressure fields become numerically related to the heating as observed, however, only upon the introduction of frictional stresses. It is found possible to describe the frictional stress distribution in the lower trades without resorting to direct measurements, which thus provide a later independent check of the model.

The last sections of the paper consider possible quasi-steady rearrangements between the fields of motion, heating, and stress which might be regarded as steps in the slow fluctuations of the system about its average condition. This is done to inquire whether changes in any one of these properties will produce readjustments in the others acting to restore the mean or to accelerate the departure from it. Although such an analysis is handicapped by lack of knowledge concerning the interaction between the heating and stress distributions, one sample calculation suggests that a reduction of heating acts to relieve the subsidence and might thus be expected to restore the convection and thereby the heating. A stable coupling between small- and large-scale motions in the low-level trades is thus indicated, which may play a role in maintaining the high steadiness of the flow. The fact that the wind steadiness vanishes rapidly above the convective layer is clarified if this model is acceptable.

1. Introduction

As the trade winds flow westward and equatorward they accumulate latent heat in the form of water vapor. This stored energy, when released and exported to distant places plays an important part in creating the temperature gradients which drive the general circulation. In the trades themselves, cumulus convection and convective turbulence below cloud base act as the upward distributors of the moisture, originally supplied to the lowest air by evaporation from the sea. These points were brought out in a budget study of the poleward half of the north-east Pacific trade (RIEHL, YEH, MALKUS, and LA SEUR, 1951), hereafter referred to as I. Energy-wise, and as far as mid-latitudes are concerned, vapor accumulation is perhaps the most important function of the trades. Nevertheless, they are also accumulating sensible heat in their low levels, as is evidenced by the increase in potential temperature along the air trajectories. Even in the rather northerly section studied in I, the non-adiabatic warming in the bottom 3 km amounts to 3° C in five days (or 2,500 km horizontal travel) and Riehl (1956) has recently shown that the consequent sensible heat accumulation amounts to about 25% that of the latent. It will be the purpose of this paper to illustrate the importance of this non-adiabatic heat source in the dynamics of the easterly circulation and to suggest the role played by convection in bringing about and distributing the heating. The concomitant role of convective elements in producing frictional stresses also proves important in constructing a theoretical model of the low-level trades.

---

[1] Contribution No. 827 from the Woods Hole Oceanographic Institution.

In order to set up the primary questions which any theoretical model must attempt to answer, we shall begin by reviewing briefly some of the outstanding features of the low-latitude circulation in the northern hemisphere. Between the equator and about 30° N, the existence of a meridional, Hadley-type circulation cell has been confirmed. The work of Pisharoty (1955) and others has shown that this cell operates in an energy-producing sense. Their figures show that it not only supplies enough energy to overcome its own losses and drive its own motions, but enough to overcome the net energy consumption in the westerlies. Their calculations provide evidence that large amounts of sensible heat and a significant quantity of kinetic energy are exported northward at high levels across latitude 35°. This "driving" cell differs from the other large branches of the general circulation in exhibiting far greater steadiness and relative freedom from travelling disturbances, particularly in the lower and more northerly portions. Its low-level winds, the northeast trades, are in fact the world's most constant wind system, exhibiting steadiness coefficients of 80—90%. The easterlies generally weaken at upper levels and their steadiness gives way to marked fluctuations aloft. The field of vertical motion is as expected, with subsidence in the poleward portions, giving way to ascent as latitude 15° is passed. North of 15°, interaction between the subsidence and counterworking convection from below produces the striking verticall layered structure which is one of the outstan ing features of tropical meteorology. T lower, convection-dominated layer is mois only slightly stable statically, and contai disturbances of small horizontal scale (fro eddies through trade cumuli to convectio cells) possessing marked vertical motions. T upper layer is dry, more stable, and contai disturbances of synoptic scale (such as easter waves) possessing much smaller vertical m tions. The upper limit of the convection co stitutes the boundary region; it is normally few hundred meters in thickness, much mo stable than either layer, and is called the "tra inversion".

Only that portion of the poleward bran of the Hadley cell will be treated here whi was examined in I. That cross section cover a horizontal distance of 2,500 km along t mean summer trajectory of the Pacific tra from 32° N 136° W to Honolulu, Haw (21° N 158° W). Vertically, it extended fro the sea surface to 3 km, including thus t bottom convective layer, the transition regio and the lowest part of the upper dry lay By this restricted choice we hope to ha selected a simple enough situation, and o covered by sufficient observational materi

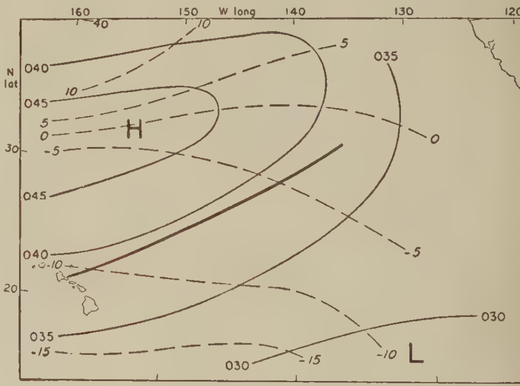

Fig. 1. Map showing orientation of trade-wind sectio studies. Four sounding stations were spaced out alo the heavy solid line, which closely follows the air tr jectory for the lowest 3 km. The Hawaiian Islands a shown at the downwind termination, while the U. west coast appears in the upper right-hand corner. T lighter solid lines are mean 700 mb contours (10's first digit omitted) while the dashed lines are isoplet of gradient wind speed (m/sec, positive values ha component toward east) and thus parallel the sea-lev isobars. (After Riehl et al., 1951.)

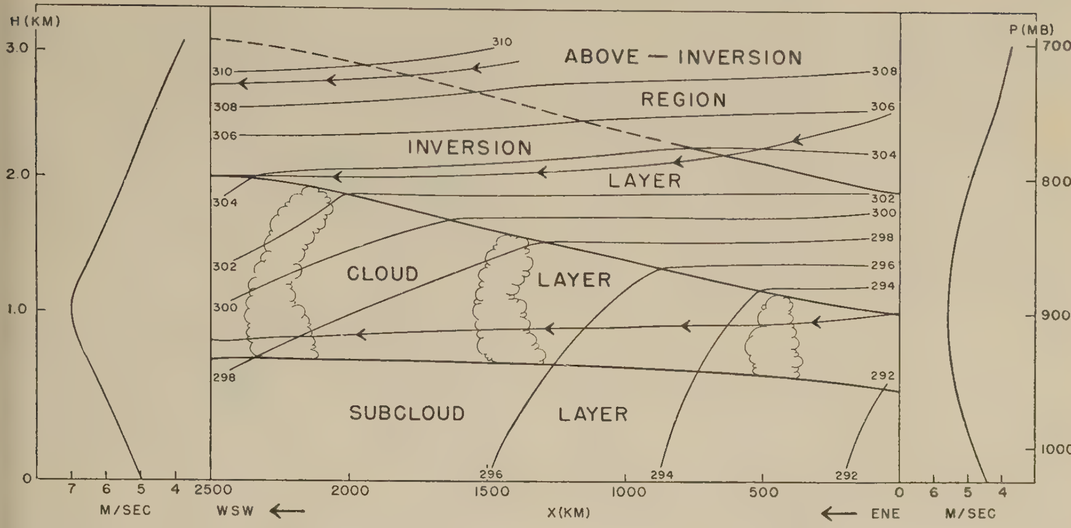

Fig. 2. Vertical structure of the air along the trajectory indicated in Fig. 1. Horizontal distance given in km downstream of entrance end. Vertical coordinate to right in mb, to left in km (approximate). The heavy lines separate the layers described in text. The lines with arrows are trajectories while the lighter solid lines are potential temperature isopleths labelled in degrees absolute. Trade cumulus clouds are entered schematically. To the right is the profile of wind speed (along the section) at the upstream end and to the left is the wind speed profile at the downstream end. Wind speeds are in m/sec.

to frame and test a theoretical model relating several of the predominant processes. To be specific, we shall inquire how the heating, the motions, and the pressure field are related within this section. These relations may in turn provide some clue concerning how this part of the Hadley cell manages to exhibit the structure and perform the transports which the observations tell us that it does. The procedure will be as follows: we shall examine what must happen within such a section to an airstream which has given properties upon entrance so that it comes out the other end changed in the observed manner. Most importantly, we shall relate the vertical motions to the heating and in so doing demonstrate that the latter is vitally necessary for this portion of the Hadley cell to show subsidence.

In the treatment of a limited section of a larger-scale circulation branch, some features of the over-all flow must be introduced as assumptions. We wish to find out how these over-all features are constrained by the processes going on within this section.

Figures 1—3 summarize the structure of the section, derived from the observations and analyses of I. Those properties which must eventually be related or predicted in a complete theoretical treatment are:

1. The nearly two-dimensional character of the flow. The curvature of the trajectory is not large, and the results of I strongly suggest that the cross-stream divergence is considerably smaller than the downstream divergence.

2. The vertically-layered stability structure. The static stability is close to neutral in the moist layer (nearly dry adiabatic below cloud base and close to moist adiabatic in the cloud layer) with strongest stability in the inversion region, decreasing again above but still positive.

3. The presence of non-adiabatic heating, indicated by the crossing of the parcel trajectories toward higher potential temperature.

4. Downstream increase of east wind speed at all levels below 3 km, with the greatest increase at about 1 km. A vertical profile showing maximum east wind just above cloud base, decreasing upwards and downwards.

5. Subsidence throughout the section, of the order of magnitude of 50 m/day.

6. Extreme wind steadiness in the low levels, decreasing markedly above the cloud tops. Weakness or absence of synoptic disturbances in the summer months. Unlike the westerlies,

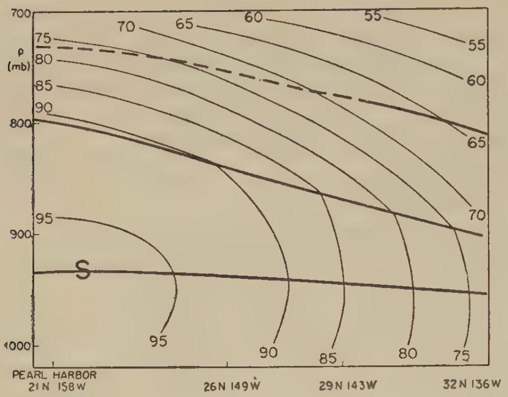

Fig. 3. Vertical cross section of wind steadiness (percent, as defined in I) for the section of Figs. 1 and 2. Heavy lines denote the layers, as in Fig. 2. The vertical coordinate is pressure in mb and the latitude and longitude of the sounding points appear along the bottom. (After Riehl et al., 1951.)

these can play no role in the maintenance of the flow.

7. A downstream drop in pressure of nearly 5 mb at the ground diminishing upward and disappearing entirely at 3 km. Relative to the trajectory (looking downstream) a counterclockwise rotation of the isobars with height, until they become parallel near the section top. This is another feature of the trades which distinguishes them sharply from the westerlies of middle latitudes.

The problem faced in this paper will be to relate as many as possible of these features theoretically using the hydrodynamic equations. In such a limited treatment as undertaken here, however, it will prove necessary to introduce the first two of the listed properties by assumption and the third, namely the non-adiabatic heating, by "plugging in" observed values. This will result in an over-specified situation, rendering superfluous one equation of motion. The key assumption of the work is probably that of two-dimensional motion, without which the problem would not be soluble. The observations in I, however, provide justification for this limited portion of the atmosphere. The extreme wind steadiness and relatively straight trajectory suggest that the divergence component parallel to the mean motion is very close to the total divergence. This hypothesis was tested in I when the mean vertical motion was computed from this component of the divergence and used satisfactorily in balancing the momentum and water vapor budgets. Estimations of the cross stream divergence (from the slight downstream fanning of trajectories) are in the same sense and about 10 % of the magnitude of the downstream divergence up to the level of the trade inversion, above which it may increase markedly. The reason, if any, for the nearly two-dimensional character of the lower trades must await more fundamental global treatments. Nevertheless, certain important aspects of their structure may be clarified using the restricted approach to be outlined. The types of questions we may hope to shed light upon include the following:

What is the role of the non-adiabatic heating in the dynamics and the thermodynamics of the section? What part do the clouds and smaller-scale turbulent elements play in releasing and distributing the heat? Is the heating vital in maintaining the flow against friction and in accelerating it downstream? Is it purely coincidental that the wind steadiness drops off so rapidly just above the cloud tops and coincidental that the maximum easterly wind is normally observed near cloud base? These questions may be combined in the following one which is tractable to theoretical analysis, namely: Does the heating produced by small-scale convection affect or constrain the larger-scale motions, and if so, is this a stable coupling? For example, if the convection is suppressed will the resulting changes in the large-scale motions be such as to restore it (i.e. perhaps weaken the subsidence rather than strengthen it)?

II. The Premises of the Theory

We are now going to set up a theoretical model for the two-dimensional mean flow in such a section, using the equations of motion, state, continuity, and the first law of thermodynamics containing non-adiabatic heating. Since the velocities solved for occur on a much larger space and time scale than those hypothesized to be responsible for the heating, the latter may, to first order, be introduced as a function of the coordinates only. The fact that the motions in the atmosphere ultimately regulate its heat sources and sinks is of course recognized (Malkus, 1955 a) and the interaction between motion and sources in maintaining the steadiness of the flow will be considered later. We will first show that the heating is necessary to specify the motion field in the average or steady-state condition. To get the observed motion field and pressure drop downstream related correctly to the observed values of the heating, it will also be necessary to include frictional stresses, as will be seen.

Of course, the necessity for subsidence in a broad, equatorward-flowing stream is obvious from other considerations. If the relative vorticity is small compared to the Coriolis parameter, potential vorticity conservation requires descent. But the rate of descent is not prescribed until the exact trajectory and rate of equatorward flow are known. That is to say, the constraint imposed by the requirement of potential vorticity conservation is not sufficient uniquely to determine the motions: we could, in fact, have an infinite number of equatorward trajectories all obeying it. The law of potential vorticity conservation is derived from combining the first two equations of motion and the equation of continuity. There is another constraint, to be derived here, essentially between the first and third equations of motion and the first law of thermodynamics, which will require a specified distribution of subsidence for a given distribution of heating. In other words, for the air to select between the infinite number of equatorward trajectories, each conserving potential vorticity, it is required to prescribe the relation between heating and vertical motion. *The air must pick an equatorward trajectory such that the heating is adequate to give the subsidence which potential vorticity conservation requires for that particular trajectory.* This conclusion is only quantitatively modified by the presence of friction, which in practice merely intensifies the amount of heating required.

To solve the problem in a truly general and complete manner, all these constraints should be applied to the air at once, without specifying the trajectory; and the trajectory, the steady condition, the two-dimensionality, pressure drop, wind-maximum, and so forth should all be derivable. The writer believes that this is beyond tractable analytical methods, at least at present, and that an experimental or numerical attack like that of PHILLIPS (1956) offers the best hope. The present, simple-minded approach may guide such future endeavors.

Here we shall treat the air flow along the *observed* trajectory of Figure 1, which we know from measurement obeys the vorticity conservation law. We shall relate the heating and motion field therein, to see if by assuming the first from observation we can construct a model giving the second. Thus the latitude does not enter explicitly as it would in a more general formulation, but only implicitly via the choice of coordinate axes.

III. The Frictionless Model

When the coordinates are chosen such that the x-axis points downstream along the surface trajectory (the trajectory rotates negligibly with height up to the top of the layer considered), the y-direction points cross stream, and the z-direction upward to form a right-handed system, the hydrodynamic equations of motion, continuity, and state for steady, two-dimensional flow on a rotating system are

$$u\frac{\partial u}{\partial x}+w\frac{\partial u}{\partial z}-fv=-\frac{1}{\varrho}\frac{\partial p}{\partial x} \qquad (1)$$

$$u\frac{\partial w}{\partial x}+w\frac{\partial w}{\partial z}=-\frac{1}{\varrho}\frac{\partial p}{\partial z}-g \qquad (2)$$

$$\frac{\partial u}{\partial x}+\frac{\partial w}{\partial z}=-\frac{1}{\varrho}\frac{d\varrho}{dt} \qquad (3)$$

$$p=\varrho RT \qquad (4)$$

where the symbols all have their conventional meanings. The non-adiabatic heating, V, in cal/gm sec, may be evaluated as follows:

$$\frac{V(x,z)}{c_p}\simeq\frac{d\Theta}{dt} \qquad (5)$$

where c_p is the specific heat of air at constant pressure and Θ is the potential temperature. Since the velocities appearing here to be solved for are steady or average values, the mean cross-trajectory velocity v is by definition zero and the Coriolis term in (1) drops out. A Coriolis term would remain in the y-equation of motion, which is, however, not needed because of the number of assumptions and parameters such as V specified from observations. The test of the presently derived results will be their agreement with the observed flow, which patently obeys the second equation of motion and the implied latitudinal relations.

Three final simplifications are made. The first is that of hydrostatic equilibrium, which is surely well approximated for motions of the scale considered. The second is the omission of the $1/\varrho\ d\varrho/dt$ term from the equation of continuity, which has been justified in detail by other writers on the steady-state heating problem (MALKUS and STERN, 1953; SMITH, 1955). The third permits linearization of the equations in this particular situation. This is done by noting that the changes in air properties within the section are small compared with the initial values at the entrance end, and in particular the horizontal windspeed, u, changes by only a fraction of itself (at most about 25 %) in the distance of travel considered. It will be assumed that a uniform wind u of 5 m/sec enters the section at the upstream end and that $u'(x, z)$ is the increment within the section. The other variables are similarly broken down into barred quantities referring to the properties of the current at the entrance end and primed quantities referring to the changes occurring within. The vertical velocity is of the magnitude of a primed quantity, being related to u' through the continuity equation. It can be proved[1] that linearization is not vital to the results presented and that these would be nearly identical were this simplification not made, and qualitatively the same for far longer sections where linearization is clearly not justified. The simplest mathematics is used here which brings out the essentials; more formality is not justified in view of the physical restrictions. With the approximations introduced, equations (1) – (4) become

$$\bar{u}\frac{\partial u'}{\partial x} = -\frac{1}{\bar{\varrho}}\frac{\partial p'}{\partial x} \qquad (1\,a)$$

$$-\frac{1}{\bar{\varrho}}\frac{\partial p'}{\partial z} = \frac{\varrho'}{\bar{\varrho}}g \qquad (2\,a)$$

$$\frac{\partial u'}{\partial x} + \frac{\partial w'}{\partial z} = 0 \qquad (3\,a)$$

$$\frac{\varrho'}{\bar{\varrho}} = -\frac{T'}{\bar{T}} \qquad (4\,a)$$

An additional small term has been left out of equation (4 a). This omission has also been justified in previous work on non-adiabatic heating (STERN, 1954) and its inclusion here gives results so little different from those actually shown that present-day observations could not test the difference.

The heating function V may now be related to the motion and temperature fields through the first law of thermodynamics, as follows:

$$\frac{V}{c_p} = \bar{u}\frac{\partial T'}{\partial x} + w'\ (\Gamma - \gamma) \qquad (5\,a)$$

where Γ is the adiabatic lapse rate and γ is the actual (average) lapse rate at the entrance end of the section. Elimination of all other dependent variables is now readily achieved and we obtain a simple differential equation for w', namely

$$\frac{d^2 w'}{dz^2} + \frac{gs}{\bar{u}^2}\,w' = \frac{gV}{c_p \bar{u}^2 \bar{T}} \qquad (6)$$

where s is $(\Gamma - \gamma)/\bar{T}$, the (average) stability at the upstream end. Since the observations show that $d\Theta/dt$ (and hence V) is very nearly independent of x along this section, the height derivative of w' may be written thus as a total derivative. It is readily shown that under conditions where hydrostatic equilibrium is realized, x-variations in w' would follow any x-variations in V exactly as prescribed by the solutions to this equation.

The heating function is evaluated using Figure 4, which was calculated from the observations of I. It shows the height distribution of the downstream rise in potential temperature along the parcel trajectories, which is readily converted into the individual rate of warming. The z-dependence of V is fairly well approximated by an exponential decay, where $V = V_0 e^{-z/h}$ and $h = 1.5$ km. It can be approximated to any higher desired degree of accuracy by a combination of exponential and sinusoidal functions. This was done, with so little difference in result that the added complexity did not justify the labor. If we use the simplest exponential, the differential equation becomes

---

[1] This has been demonstrated by Melvin Stern, to whom the writer is grateful for many helpful discussions. The formal proof will appear in Stern's Ph. D. dissertation.

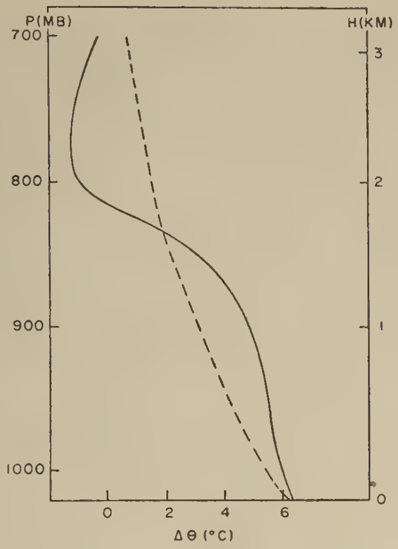

Fig. 4. Graph showing observed net downstream warming, $\Delta\Theta$, of the air parcels, calculated from Fig. 2 as a function of height. Can be converted to the rate of non-adiabatic heating by multiplying by c_p and dividing by the length of time required for the parcels to traverse the section (about 5 days). The potential temperature increment, $\Delta\Theta$, is given in degrees absolute. The dashed curve is the simple exponential function used in the theory to approximate the observed curve.

$$\frac{d^2w'}{dz^2}+B^2w' = Pe^{-z/h} \qquad (6\,\mathrm{a})$$

where

$$B^2=\frac{gs}{\bar{u}^2},\qquad P=\frac{gV_0}{c_p\bar{u}^2\bar{T}},$$

and where h is chosen as in Figure 4 to give the correct integrated heating for the layer as a whole and $\bar{T}$ is its mean temperature.

Smith (1955) has shown that the general solution to this equation for a deep air layer bounded below by the ground is given by the real part of the expression

$$\frac{P}{\frac{1}{h^2}+B^2}\left[e^{-z/h}-e^{-iBz}\right]$$

Since h, P, and B are all real, the general solution to (6 a) is

$$w'=\frac{P}{\frac{1}{h^2}+B^2}\left[e^{-z/h}-\cos Bz\right] \qquad (7)$$

The divergence field is prescribed as

$$-\frac{\partial w'}{\partial z}=\frac{\partial u'}{\partial x}=\frac{P}{\frac{1}{h^2}+B^2}\left[\frac{e^{-z/h}}{h}-B\sin Bz\right] \qquad (8)$$

Since the sine function is zero at the ground, the divergence must always be positive there. This means a downstream acceleration of the surface wind and subsidence in the low levels regardless of the value of B, just so long as the heating is positive and decays with height. Equation (1 a) also shows that the surface pressure must drop downstream. What happens to the motion field at higher levels clearly depends both qualitatively and quantitatively on the stability and wind structure through B. With windspeeds of about 5 m/sec in an atmosphere of very low stability, subsidence occurs through a several km-deep layer. For example, if $B=0.5\times10^{-5}$ cm^{-1}, the vertical distribution of w' in dimensionless units is shown in Table 1.

Since it might appear unrealistic to treat an air layer topped by an inversion as "infinitely" deep, we may alternatively investigate a layer in which the damping effect is simulated by a rigid lid placed somewhat higher than the inversion (this is done because the damping by the inversion is more gradual than that by a rigid surface; the precedents have been discussed by Malkus and Stern, 1953). The solu-

Table 1. Distribution of Vertical Velocity (Dimensionless) with Height for a Deep Layer of Low Stability

Height → (km)	0.2	0.5	1.0	1.5	2.0	2.5	3.0
$\frac{w'(1/h^2+B^2}{P}$	—.073	—.256	—.365	—.363	—.314	—.125	—.065

tion to (6 a) then contains a sine term with an amplitude about 6 % that of the cosine term and the results shown in Table 1 are imperceptibly altered.

Nevertheless, there are difficulties in applying these results directly to the trade winds. In the first place, the observed magnitude of the heating is much greater than necessary. Evaluating P using Figure 4, we find it to be about 1.7×10^{-10} cm^{-1} sec^{-1}, which would lead to rates of subsidence of 400 m/day! We also find faults in the divergence field, $\partial u'/\partial x$, and wind profile, $\bar{u}+u'$. In this theoretical section, the downstream-end wind profile and the divergence profile must have an exactly similar shape since the wind has a constant profile with elevation at the entrance end. Equation (8) tells us that $\partial u'/\partial x$ must be a maximum at the bottom and that the easterly winds will decrease from there upwards. The observations in I show, to be sure, divergence and wind profiles of similar shape but the maximum in both is well above the surface, at about 900 m. Another problem is that the value of B chosen for Table 1 is probably considerably less than the mean stability of the trade-wind moist layer would permit, if the major portion of the processes in the cloud layer are non-saturated.

The first two of the difficulties suggest that something must be working in opposition to the heat source. Examination of the pressure field provides the clue to what it is and what to do about it. Equation (1 a) tells us that a downstream surface pressure drop of only about 0.05 mb in the 2,500 km is required to produce the observed acceleration of the flow. The observations tell us that a pressure drop of nearly 5 mb in fact occurs. This gradient disappears toward the top of the section at 3 km, along which level the pressure is nearly constant. Using this fact and simple hydrostatic considerations, it is evident that the non-adiabatic heating accounts for 80 % of the observed pressure drop at the bottom surface. Adiabatic compression due to sinking accounts for the remainder of the rise of mean temperature in the layer. It seems that a "frictional drag" has been omitted from equation (1 a) which in practice uses up most of the pressure drop produced by the warming. The fact that the pressure gradient disappears at 3 km, at the top of the heated layer, indicates that the stresses may be provided by the same convective elements responsible for the heating. This suggests a method of introducing frictional stresses into the model, with which the next section will be occupied in detail. Even the present oversimplified analysis, however, illustrates the vital role of non-adiabatic heating in the structure, dynamics, and thermodynamics of the trade system. The refinements of the next section make the predicted numbers agree with measurements and tie some previously unrelated observations to the theory, thus providing independent checks of its plausibility.

IV. Model Including Frictional Stresses

If the frictional forces in the plane of the section are hypothesized to be due to the sea surface drag on the bottom and to vertical exchanges of horizontal momentum by small-scale convective elements within the layer, they may be expressed in terms of a shearing stress τ_{xz}. Equation (1 a) should then be written

$$\bar{u}\frac{\partial u'}{\partial x} = -\frac{1}{\bar{\varrho}}\frac{\partial p'}{\partial x} + \frac{1}{\bar{\varrho}}\frac{\partial \tau_{xz}}{\partial z} \qquad (1\text{ b})$$

Calculations (by SHEPPARD, 1954) from the observations in I and others made in the trades show that the term $1/\bar{\varrho}\ \partial\tau_{xz}/\partial z$ is of the same order of magnitude as $1/\bar{\varrho}\partial p'/\partial x$ and therefore about two orders of magnitude larger than $\bar{u}\partial u'/\partial x$. With the exception of a negligibly small term in the first law of thermodynamics, the remaining equations used here are unchanged. If the shearing stresses within the layer are produced by the same convective and turbulent elements also responsible for the heating, τ_{xz} and its derivatives may be considered functions of the coordinates only, and the elimination carried out as before. Eventually, of course, the shearing stress must be related to the mean wind profile, and be consistent with it.

After elimination, the modified differential equation for w' becomes

$$\frac{d^2 w'}{dz^2} + \frac{gs}{\bar{u}^2}w' = \frac{gV}{c_p\bar{u}^2\bar{T}} - \frac{1}{\bar{\varrho}\bar{u}}\frac{\partial^2\tau_{xz}}{\partial z^2} \qquad (9)$$

We could now proceed with this equation in the straightforward manner of attempting to evaluate $\partial^2\tau_{xz}/\partial z^2$ from the observations and expressing it in some simple functional form in the equation, as was done earlier for the heating function V. The results would be little better than guesswork, however, for the following combination of reasons: the best observational evidence to date indicates that the two inhomogeneous terms in (9) are very nearly the same size, and the small difference between them is the actual forcing function remaining to determine w'. Although the height distribution of τ_{xz} itself is fairly well depicted by recent measurements, its first derivative is not so certain, and its second derivative even less reliably specified. Therefore an indirect procedure will be followed which employs two independent calculations. Although each of these carries considerable uncertainty, consistency in the results of the two, if it occurs, would prove persuasive.

V. Two-Layer Model with Friction

It will be recalled that the trade-wind moist layer is itself subdivided vertically into two layers of quite different static stability. The subcloud layer, reaching from the sea up to about 650 m, has an average stability of zero. The cloud layer, although its lapse rate is steeper than moist adiabatic is almost surely stable on the average, since active clouds occupy only 10—20 % of the space. If we suppose that 78 % of the processes occurring within the layer are unsaturated, $gs/\bar{u}^2 = B^2 \simeq 2 \cdot 10^{-10}$ cm^{-2}. Applying equation (9) to this two-layer system will prove extremely illuminating. For the lower neutral region it takes the simple form

$$\frac{d^2 w'}{dz^2} = \frac{gV}{c_p \bar{u}^2 \bar{T}} - \frac{1}{\bar{\varrho} \bar{u}} \frac{\partial^2 \tau_{xz}}{\partial z^2} \qquad (10)$$

The two terms on the right are functions of z only and the left-hand term is related to the divergence through the equation of continuity. The height derivative of the divergence in the subcloud layer may thus be expressed as

$$\frac{d}{dz}\left(\frac{\partial u'}{\partial x}\right) = F_1(z) - F_2(z) = F(z) \qquad (11)$$

where

$$F_1(z) = \frac{1}{\bar{\varrho} \bar{u}} \frac{\partial^2 \tau_{xz}}{\partial z^2} \text{ and } F_2(z) = \frac{gV}{c_p \bar{u}^2 \bar{T}}.$$

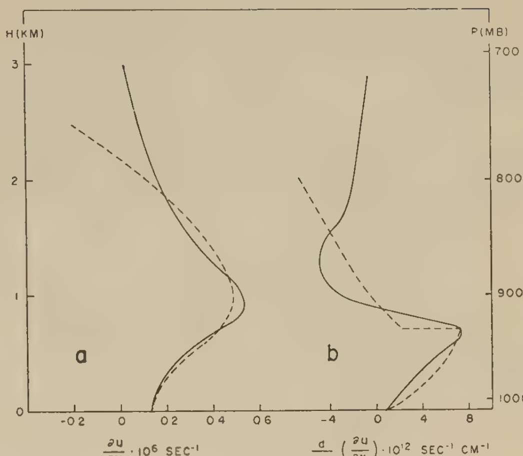

Fig. 5

a. Solid curve is the velocity divergence, $\partial u'/\partial x \cdot 10^6$ sec^{-1}, calculated from the observed wind profiles. It is the component of divergence along the trajectory and averaged over the whole length of the section. The dashed curve is the divergence calculated from the equations of the model.

b. Height derivative of divergence, $d/dz\,(\partial u'/\partial x) \cdot 10^{12}$ sec^{-1} cm^{-1}. The solid curve is calculated from the observed divergence (solid curve in 5a). The dashed curve up to 650 m is constructed (from two exponentials) to fit the observed curve. Its continuation above 650 m is calculated from the results of the model.

Now the observations in I led to a rather good profile of the mean divergence distribution in the section. It was calculated from several wind soundings daily over the four months and was used with consistent results in the previous paper in calculating w' and the transport budgets. This mean divergence profile and its first height derivative are plotted in Figure 5 and will be used here in the following outlined procedures:

(1) Recalling that we know $F_2(z)$ from the heating function, we will establish a functional form of $F(z)$ as a whole from the measurement-calculated profile of $d/dz\,(\partial u'/\partial x)$ in the subcloud layer (that part of the solid curve up to 650 m in Figure 5 b). We will apply the $F(z)$ so obtained to the entire two-layer system via equation (9) written for each layer with appropriate joining boundary conditions. We will solve for w', the divergence field, $d/dz(\partial u'/\partial x)$ above 650 m (not assumed as given), and the pressure field, and compare these with observations.

(2) We will then subtract from the $F(z)$ we took from Figure 5b and used, the $F_2(z)$ evaluated previously from the heating function. This will give a differential equation for τ_{xz}. We may then solve that differential equation and test the results for consistency, both with existing measurements of τ_{xz} in the trades and with the wind profiles.

VI. Solution for the Two-Layer Model

The height derivative of the divergence up to 650 m is well approximated by the dashed curve in Figure 5 b. It is the difference between two exponentials,

$$F(z) = A_1 e^{-z/a_1} - A_2 e^{-z/a_2} \qquad (12)$$

where $A_1 = 1.74 \times 10^{-10}$ cm^{-1} sec^{-1}, $a_1 = 1.715$ km; $A_2 = 1.73 \times 10^{-10}$ cm^{-1} sec^{-1}, $a_2 = 1.5$ km. This expression for $F(z)$ is substituted into equation (9) and the solution is carried out for the two-layered system. The boundary conditions are that w' is zero at the lower surface; that it and its height derivative are continuous at the interface between layers (giving a continuous divergence and wind profile); and that a rigid lid is placed at 4 km. It may be shown that the solution is nearly the same if the upper layer is allowed to be infinitely deep.

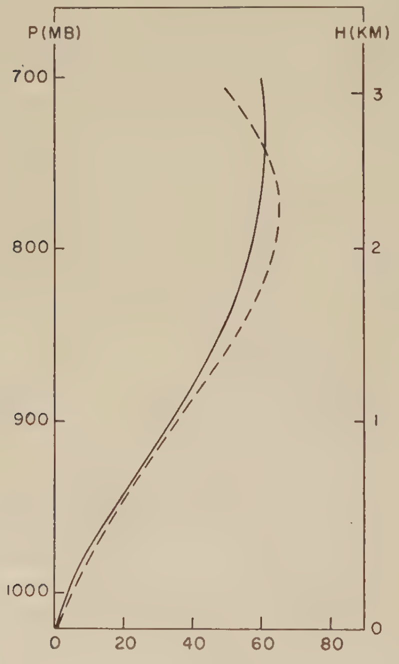

Fig. 6. Solid curve shows mean vertical motions (m/day) as a function of height and pressure calculated from the observed divergence distribution for the section. The dashed curve shows the corresponding vertical motion distribution given by the solution to the differential equation for the two-layer model.

The results for $\partial u'/\partial x$, $d/dz(\partial u'/\partial x)$, and w' are shown and compared with the observations in Figures 5 and 6. On the whole, the agreement is good, although the theoretical divergence shifts over to convergence above 2 km, while the observed curve trails off more slowly. This is believed to be due to the decrease in the two-dimensional character of the flow aloft as the wind steadiness falls off and thus the model begins to break down at higher levels. In practice, an increasing $\partial v'/\partial y$ probably accounts for the difference between the two curves above 2 km. Otherwise, many of the significant aspects of the flow are reproduced and elucidated by the model. Reserving discussion of the pressure field for the section below on shearing stresses, we can now call attention to some important features of the velocity structure: in particular the wind maximum and its location in the vertical.

Rewriting equation (9) in combination with (11), we have

$$\frac{d}{dz}\left(\frac{\partial u'}{\partial x}\right) = F(z) + \frac{gs}{u^2} w' \qquad (13)$$

In the subcloud layer $s \simeq 0$, $F(z)$ is positive, and the divergence increases rapidly upward. As the cloud base is reached stabilization rather suddenly occurs. The vertical velocity is negative and so a large term abruptly appears on the right to be subtracted from $F(z)$ which at this level is changing only very slowly with elevation. This means that the divergence must start decreasing upward instead of continuing to increase. This point is brought out clearly in Figure 5 b which shows $d/dz(\partial u'/\partial x)$ calculated from the observational curve of Figure 5 a, compared with $d/dz(\partial u'/\partial x)$ computed from the model. The sharp "knee" in the observationally-deduced curve is strikingly reproduced by the theory. It would seem that the average appearance of the trade-wind maximum near cloud base is no coincidence and, barring large changes in the forcing function,

$F(z)$, it would be tied there, at the level where the static stability rather suddenly becomes positive.

The latter conclusion is not sensitive to small changes in the amplitude and exact height dependence of $F(z)$ as a whole. The lower part of the solid curve in Figure 5 b may be approximated by other functions and the main features of the flow field, such as subsidence and wind maximum, derived within the same observational accuracy. The chosen $F(z)$, however, is composed of two subtractive terms and small changes in each individually lead to rather large alterations in their difference. An example is illustrated in Section X, following a discussion relating the components of $F(z)$ to physical processes.

VII. The Distribution of Shearing Stress

The total forcing function $F(z)$ for the differential equation (9) was seen earlier to be physically related to the heating and shearing stresses as follows

$$F(z) = F_1(z) - F_2(z) = \frac{1}{\bar{\varrho}\bar{u}}\frac{\partial^2 \tau_{xz}}{\partial z^2} - \frac{gV}{c_p \bar{u}^2 \bar{T}} \quad (14)$$

In solving the differential equation for w', however, this relation was temporarily ignored and a functional form of $F(z)$ was deduced from observations independent of the above. It was found to be well represented by the difference between two exponentials, as written out in equation (12). The second of these exponentials $A_2 e^{-z/a_2}$ is within computational accuracy the same as the heating term $Pe^{-z/h}$ of equation (6 a) evaluated previously in section III. Thus when we make the association between $gV/c_p\bar{u}^2\bar{T}$ in (14) with the $A_2 e^{-z/a_2}$ in (12), (14) becomes a differential equation for τ_{xz}, namely

$$F_1(z) = \frac{1}{\bar{\varrho}\bar{u}}\frac{\partial^2 \tau_{xz}}{\partial z^2} = A_1 e^{-z/a_1} =$$

$$= 1.74 \cdot 10^{-10}\, e^{-z/1.715} \quad (15)$$

Since $\bar{\varrho}$ varies rather little percentually through the height of the section, in most cases integration of this equation may be approximated by two simple quadratures. Two boundary conditions on τ_{xz} are, however, required. We will assume here that the shearing stress (or vertical transport of horizontal momentum) is zero at the height of the trade-wind maximum, a premise well justified by the work of SHEPPARD, CHARNOCK, and FRANCIS (1956), and we will take a value of $\tau_{xz} = 1.0$ dyne/cm² at the lower boundary. The latter is consistent with the values used in I for the drag of the sea surface on the lowest air. Under these conditions, τ_{xz}, the shearing stress, and $1/\bar{\varrho}\, \partial\tau_{xz}/\partial z$, the frictional force per unit mass are specified as functions of height. Introducing the latter into equation (1 b) the downstream pressure gradient is also determined. The results are given in Table 2 and Figure 7.

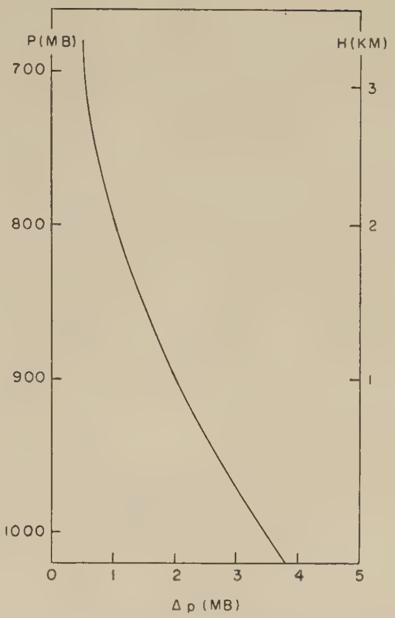

Fig. 7. Theoretical height distribution of downstream pressure drop, Δp, in mb. Δp is the difference between the pressure at the upstream end and that at the downstream end, or over a horizontal distance of 2 500 km along the flow. Observations show a surface pressure drop of just under 5 mb and little or no pressure drop at 3 km (see Fig. 1).

The next-to-last column tests the shearing stress by comparing it to the mean (observed) wind profile. It gives the eddy momentum exchange coefficient, defined as the ratio between the calculated shearing stress and the wind shear at the level considered. Beside it in the last column is shown the eddy coefficient which was required in I to balance the momentum budget. The agreement is within observational and computational error. The results in the two middle columns are also

Table 2. The Stress Distribution and Its Consequences

Height	Calculated τ_{xz}	Calculated $\partial\tau_{xz}/\partial z$	$\Delta p = p_{\text{upstream}} - p_{\text{downstream}}$	μ(from τ_{calc} and du/dz)	μ from momentum budget
m	dyne/cm²	dyne/cm² per 100 m	mb	c.g.s.	c.g.s.
0	1.0	—.149	3.8	330	
500	0.4	—.111	2.8	270	370
900	0	—.088	2.2	indeterminate	
1,500	—0.4	—.062	1.5	330	630
2,000	—0.7	—.046	1.1	700	680
2,500	—0.9	—.035	0.8	600	
3,000	—1.1	—.026	0.6	700	570

close to observational accuracy. The height derivative of shearing stress, $\partial\tau_{xz}/\partial z$, has a distribution similar to that described by SHEPPARD (1954). It falls off with height in a manner consistent with the hypothesis that the frictional drag is brought about by the same processes which distribute the heating. Due to the small contribution of $\bar{u}\ \partial u'/\partial x$ in equation (1 b), the downstream pressure drop is to all intents and purposes proportional to $\partial\tau_{xz}/\partial z$. It also decays exponentially and has nearly vanished at 3 km.

Although the model says nothing explicitly about the cross-stream pressure gradient (which is given by the y-equation of motion), the disappearance of the large downstream pressure gradient toward the top of the section means that the isobars are rotating with height into parallel orientation with the air trajectory, as observed. This conclusion has been arrived at without any *a priori* assumptions concerning the pressure field or of any simple relation between it and the wind field.

VIII. The Relation between Heating, Shearing Stress, and Convection

So far in this paper the relation between the small scales of motion in the trades and the heating and friction distributions has only been stated as an hypothesis. In the case of the shearing stresses, the hypothesis has received recent observational test in the western Atlantic trade-wind region (SHEPPARD, CHARNOCK, and FRANCIS, 1956; BUNKER, 1955). The shearing stresses contributed by turbulent and convective motions ranging in size from small eddies up to convection cells (10—50 km across) have been obtained and compared with mean wind profiles and the total stresses calculated therefrom. The agreement is sufficiently good to conclude that in the low-level easterlies the vertical transport of horizontal momentum is mainly achieved by scales of motion not larger than convection cells. The percentage contributed by the larger-scale systems apparently becomes greater with height, perhaps discontinuously rapidly through the trade inversion. The increased role played by synoptic systems (present in the trades with less regularity than smaller convective motions) in maintaining the momentum transports aloft may be related to the upward diminution of wind steadiness, as will become clearer in Sections IX—XI.

The production of the heating function V is somewhat more complex. The downstream rise in potential temperature represents a small net difference between opposing processes. Radiation is a heat sink throughout the free atmosphere. In the subcloud layer, the net warming is due to a slight excess of eddy flux convergence over outgoing radiation. In the cloud layer, although the potential temperature increases strongly upward, the direction of the eddy heat flux is not definitely known. In any case it probably plays a small role in the heat balance, which the evidence in I indicates is primarily achieved between a large precipitation source and radiation sink. Connecting the net warming throughout the moist layer to convective processes, therefore, implicitly assumes that the radiational heat sink varies relatively little.

IX. Fluctuations about the Steady State

The pronounced steadiness of the flow has been emphasized as one of the significant features of the trades. The over-all dynamic stability of a Hadley-type meridional cell in the low latitudes of a heated rotating system has been suggested by experimental (FULTZ, 1949) and theoretical (KUO, 1954) investigations of simplified planetary analogs. The present treatment of a limited portion of the real Hadley cell proposes consideration of another kind of stability, which may not be unrelated. The results of the preceding sections indicate a coupling between the small-scale motions occurring within a section along the easterlies and the modifications in the large-scale flow observed between the upstream and downstream ends. It has been shown that the transports effected by the small-scale systems impose a constraint upon the large-scale flow, or alternatively, that the large-scale flow must adjust itself to permit the development of those small scales which transport heat and momentum in the manner indirectly specified here. The response of either scale of motion to an alteration in the other is significant in determining the nature and amplitude of the system's fluctuations about its average condition. In the westerlies, disturbances of certain critical sizes are able, by drawing on stored energy, not only to grow in a self-accelerative fashion, but in so doing often to upset the entire structure of the flow, which thereby fluctuates so widely that an average picture has only very restricted meaning as a "steady state". In the easterlies, by contrast, the average and the daily picture bear a closer resemblance to one another. The infrequency of intense disturbances in the low-level trades, and the reliable presence of trade cumulus clouds suggests that the coupling between small- and large-scale processes is stable and perhaps contributes to the over-all dynamic stability of the meridional circulation.

In the framework of the present model, therefore, we might inquire what happens, for example, if the heating is weakened, presumably through a diminution of convective activity. A stable coupling of the type suggested would be substantiated if we could show that a weakening of the heat source would lead to decreased subsidence. It is well known that subsidence in the trades is one of the most effective brakes upon convection, and even a slight release of this brake would lead to renewed outbreaks of convective activity.

Any such approach, however, patently represents a drastic oversimplification, and its mathematical formulation must be preceded by several reservations. The present theoretical treatment cannot be interpreted to state that the heating within this limited section and the flow within it are cause and effect in a straightforward manner; it merely prescribes relations between the two which must, on the average, be satisfied. To deal with the complete, time-dependent behavior of the trades, the writer believes that much larger circulation branches must be considered.

The present theory can, on the other hand, tell us what other steady or quasi-steady configurations are possible and self-consistent for this section. If such configurations may be interpreted as describing the slow fluctuations about the mean seasonal picture discussed in the foregoing paragraphs, we may profitably inquire whether a given one of these exhibits a structure likely to restore the seasonal mean or to lead to even greater departures from it.

Re-examining equation (9) and temporarily ignoring variations in $gs/\bar{u}^2$, we see that the flow may be restored in two ways, either by a stable interaction between the forcing function as a whole and the motion field, or by readjustment between the two right-hand terms maintaining their difference the same. In both categories, only a few of the possible rearrangements will give a consistent relation between the resulting wind profile and stress distribution; the remainder are therefore excluded. Due to our inadequate knowledge of the dependence of the two right-hand terms both upon one another and upon external influences, only one illustrative calculation is worked out here.

X. An Example with Decreased Heating

Rainfall in the trade stream is the least reliable of its properties. Even casual observers have noted that a skyful of trade cumuli will on some days produce plentiful showers from clouds of all sizes, while on other apparently similar days with an apparently similar cloud distribution, no drop of rain appears. We have seen that the net non-adiabatic heating in the cloud layer is probably controlled by the

Table 3. Results of a 10 % Reduction in Heating

Height	w'	divergence · 10^6	calc. τ_{xz}	calc. $\frac{\partial \tau_{xz}}{\partial z}$	Δp
m	m/day	sec^{-1}	dyne/cm^2	dyne/cm^2 per 100 m	mb
0	0	— 1.1	2.2	—.19	4.8
300	+ 22	— 0.6	1.7	—.17	4.2
650	+ 23	— 0.2	1.2	—.14	3.5
1,000	+ 16	+ 0.6	0.7	—.12	3.0
1,500	— 23	+ 1.2			
1,600			0	—.10	2.6
2,000	— 65	+ 1.1	— 0.4	—.08	2.0
3,000	— 105	+ 0.3	— 1.2	—.07	1.8

amount of precipitation. The evidence in I suggests that precipitation heating in the cloud layer may also be of importance indirectly in the net warming of the air below cloud base (if the eddy heat transports are, in fact, down the potential temperature gradient). It is not impossible, therefore, that we might have significant changes in the V term in equation (9) while the frictional stresses produced by the convective and turbulent elements remain more or less the same. Thus we have chosen as the example case one in which just the net heating is reduced.

The situation is now considered where the amplitude of the heating function is cut by 10 % without altering its height dependence.

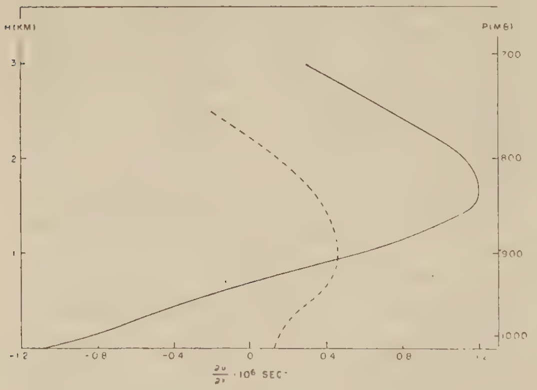

Fig. 8. Solid curve gives the theoretical divergence profile resulting when the heating is reduced by 10 % relative to that used for the average situation. The dashed curve reproduces the theoretical divergence curve for the average situation as a comparison (same as dashed curve of Fig. 5 a). Note that according to the model the wind profiles in the two cases would have shapes similar to the divergence profiles.

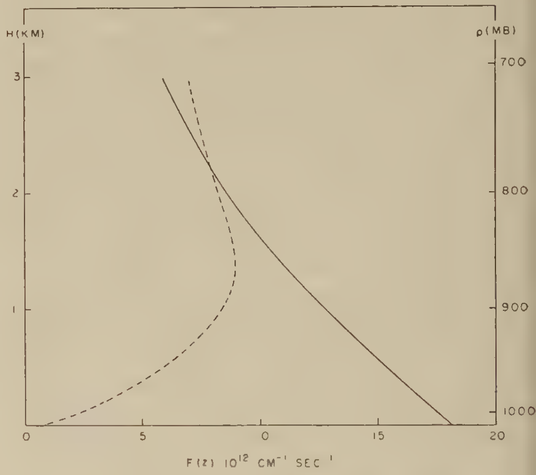

Fig. 9. Solid curve is the new forcing function $F(z)$ appearing (with a negative sign) on the right side of the differential equation for w' when the heating amplitude is reduced by 10 %. The dashed curve is the $F(z)$ used in the model of the mean flow with the heating distribution approximating that observed.

The only change in the corresponding stress term will be that its level of exponential decay is now taken as 1.6 instead of 1.7 km. This slight change is necessary to give consistent results throughout and would presumably allow for a small reduction of mean cloudiness. The solution of equation (9) is now carried through as previously, with the same stabilities in the two layers and the same boundary conditions on w'. The results are presented in Table 3 and Figures 8 and 9.

Since the wind (divergence) maximum now occurs at 1,600 m, the boundary conditions used here on τ_{xz} were that it be zero there and 2.2 dynes/cm^2 at the bottom surface. That choice of the lower boundary condition makes a self-consistent model because the surface wind now decreases downstream 2.8 m/sec (in the 2,500 km), while that at 1,600 m increases 3 m/sec, giving a positive wind shear of about 3.5 m/sec per km in the lower part of the section. The calculated τ_{xz} distribution in Table 3 requires an average eddy momentum exchange coefficient in the subcloud layer of about 500 c.g.s., or a substantial increase over the mean situation. This is plausible in view of the intensified eddying anticipated in consequence of replacing the former subsidence by comparable ascent in the low levels. The rate of wind shear up to the wind maximum and the height of the wind maximum are both at the upper limit of average daily values observed by Sheppard et al. in the western Atlantic trade. Thus Table 3 represents a realistic but rather extreme situation.

Although the heating has only been reduced slightly, a comparison of the new total forcing function (Figure 9) with that used previously shows that its average value has been altered by a factor of more than two in the lowest km. Apparently this is near the permissible limit of changes in the total forcing function still giving a flow field in the observed range. The new situation, however, does seem to contain restoring influences. Table 3 shows that sinking has been replaced by mean ascent up to 1 km and that the subsidence is much weaker than normal through most of the cloud layer. Weakening the descent in the cloud layer favors increased cloudiness and precipitation, while ascent in the subcloud layer aids upward transport of sensible heat, both directly and by destabilizing the already nearly neutral lapse rate. Recent observational studies (MALKUS, 1955 b) suggest that the processes in the tropical subcloud layer are critically sensitive to slight amounts of subsidence or its removal. In view of this it seems likely that the system would often restore its heating and return to normal even before departing so far as the conditions of Table 3.

XI. Concluding Remarks

Within the moist convective layer the trade stream seems to have at its disposal the mechanisms to adjust: it is able to meet the imposed constraints by mutual rearrangement between heating, stress, and motion field in such a way that the motion field is allowed to fluctuate little from the mean. Above the convective layer, these mechanisms are no longer available and we are not surprised that the steadiness vanishes.

Nevertheless, the reader familiar with the trade-wind system may be disturbed by the egregious unreliability of its precipitation. It was seen that only a 10 % reduction in heating produced, in one test situation, flow patterns in the outer range of those observed. Although the variation percentage-wise in the weekly or monthly rainfall along a 2,500 km oceanic section cannot even be estimated today, we may safely guess that it often exceeds 10 %. In conclusion of this work, therefore, we must briefly examine the consequences of larger variations in heating and inquire whether any plausible shearing stress field can conceivably maintain the flow for short periods. Thus the extreme limiting question to ask of our model is whether the total forcing function (and so the flow) can temporarily remain the same as given in Section VI, without any heating at all. This is readily tested by setting V equal to zero in equation (14) and solving for τ_{xz} under the boundary conditions originally used. An observationally possible distribution of τ_{xz} arises, provided that larger eddy coefficients are occasionally permitted near the section top than those required to balance the average budgets. We find, however, that the downstream pressure drop decreases much more slowly with height than before. Even allowing for the height variation of density in equation (14), Δp is about 3 mb at the bottom and 2 mb at the top of the section. Simple hydrostatic reasoning makes this inevitable, for if the lower column is warmed less, it can contribute proportionally less to a pressure fall along the bottom surface. Concomitantly, $\frac{\partial \tau_{xz}}{\partial z}$ shows $^2/_3$ of its surface value at 3 km. SHEPPARD (1954) has found that such situations are sometimes observed in the trades. It would be highly desirable to determine observationally whether occasions of abnormally slow vertical decay of frictional forces and pressure drop are associated with greatly diminished downstream warming, as the model suggests. This and other valuable tests of the relations between stress, motion field, and heating could be carried out were a series of weather ships or other sounding devices again placed along a trade-wind air trajectory.

Acknowledgments

The writer would like to acknowledge the enormous contribution made by Dr Herbert Riehl to every phase of this paper. Not only must any endeavor to advance our knowledge of the trades take account of his publications, but the specific lines pursued here largely arose from personal discussions and correspondence with him.

Most of the work described herein was carried out at the Imperial College, London, while the writer was on a Fellowship provided by the Munitalp and Guggenheim Foundations.

REFERENCES

Bunker, A. F., 1955: Turbulence and shearing stresses measured over the North Atlantic Ocean by an airplane-acceleration technique. *J. Meteor.*, **12**, pp. 445—455.

Fultz, D., 1949: A preliminary report on experiments with thermally produced lateral mixing in a rotating hemispherical shell of liquid. *J. Meteor.*, **6**, pp. 17—33.

Kuo, H.-L., 1954: Symmetrical disturbances in a thin layer of fluid subject to a horizontal temperature gradient and rotation. *J. Meteor.*, **11**, pp. 399—411.

Malkus, J. S., 1955 a: Meteorology: On the isolation of tractable problems and an example in variable heating. *Science Prog.*, **171**, pp. 461—475.

Malkus, J. S., 1955 b: The effects of a large island upon the trade-wind air stream. *Q. J. Roy. Met. Soc.*, **81**, pp. 538—550.

Malkus, J. S., and M. E. Stern, 1953: The flow of a stable atmosphere over a heated island, Part I. *J. Meteor.*, **10**, pp. 30—41.

Phillips, N. A., 1956: The general circulation of the atmosphere: A numerical experiment. Unpublished manuscript submitted under Contracts No. N-6-ori-139(01) and No. N-ONR-1358(02) with the U.S. Office of Naval Research and the Geophysics Research Directorate. To be published.

Pisharoty, P. R., 1955: The kinetic energy of the atmosphere. *Investigations of the general circulation of the atmosphere, final report*, Dept. Meteor. U. Calif. at Los Angeles.

Riehl, H., 1956: On the heat balance and maintenance of circulation of the trades. Unpublished manuscript.

Riehl, H., T. C. Yeh, J. S. Malkus, and N. E. La Seur, 1951: The north-east trade of the Pacific Ocean. *Q. J. Roy. Met. Soc.*, **77**, pp. 598—626.

Sheppard, P. A., 1954: The vertical transfer of momentum in the general circulation. *Archiv für Meteorologie, Geophysik und Bioklimatologie.* Serie A. Band 7, pp. 114—124.

Sheppard, P. A., H. Charnock, and J. R. D. Francis, 1956: An investigation of the lower atmosphere in the trades. Unpublished manuscript. To be published.

Smith, R. C., 1955: Theory of airflow over a heated land mass. *Q. J. Roy. Met. Soc.*, **81**, pp. 382—395.

Stern, M. E., 1954: Theory of the mean atmospheric perturbations produced by differential surface heating. *J. Meteor.*, **11**, pp. 495—502.

PRINTED IN SWEDEN
ESSELTE, STHLM 56

Contribution No. 830

Deep-Sea Research, 1956, Vol. 3, pp. 214 to 228. Pergamon Press Ltd., London.

The Cariaco Trench, an anaerobic basin in the Caribbean Sea

FRANCIS A. RICHARDS and RALPH F. VACCARO

(*Received* 8 *February*, 1956)

Abstract—The Cariaco Trench is a basin in the Caribbean Sea which is anaerobic below depths of about 375 metres to the bottom at 1,400 metres. Below ca. 250 metres the water is essentially isothermal at about 16·9°C. and has practically uniform salinity and density. Hydrogen sulphide reaches maximum concentrations of ·03 mgA sulphide S per litre, which is about 10% of the concentration found in the depths of the Black Sea. Inorganic phosphate is linearly related to the oxygen and sulphate consumption in a ratio equivalent to 235 atoms of oxygen utilized for the production of 1 atom of phosphate. The anaerobic zone is free of nitrate and nitrite, but some ammonia is present. It is suggested that most of the nitrogen arising from decomposition of organic matter is present as elementary N_2 in solution. The age of the water is estimated to be between 100 and 2,000 years. The physical properties of the trench are compared with those of other isolated basins.

THE Cariaco Trench is a depression about 1,390 metres deep in the continental shelf off the Venezuelan coast. It is separated from the Caribbean Sea to the north and east by a ridge which includes Islas Tortuga, Margarita, Cubagua, Coche, and Farallon Centinela. The sill is nowhere deeper than about 150 metres, thus shutting off the deeper water from that of the Caribbean (see Fig. 1), and enclosing a trench about 100 miles long (east to west) and 40 miles wide (north to south). The structure is superficially similar to the other island arcs with adjacent deep trenches characteristic of the West Indies, but it lies along the axis of the Venezuelan coastal range.

During a cruise of the *Atlantis* in December 1954, Mr. L. V. WORTHINGTON discovered that the trench water was anaerobic from about 500 metres to the bottom, and it was evident from the odour that hydrogen sulphide was present. The area was revisited in February 1955, at which time more extensive chemical observations were made.

CIRCULATION

Above sill depth, the waters of the Cariaco Trench are in free communication with the surface waters of the rest of the Caribbean. Currents of varying strength are reported (Hydrographic Offices, 1949) to enter the region between the islands to the east, and it is clear from salinity and temperature observations that the waters of the trench above sill depth exchange freely with the Caribbean.

Below sill depth, the trench is isolated from the off-lying waters, as shown by comparisons of the vertical distribution of salinity and temperature inside and just outside the sill (Fig. 2).

Within the trench, the temperature decreased rather steadily from surface values of 24° to 26°C to about 18°C just below sill depth. At 460 metres, the temperature had dropped to 17·00° ± ·02°C, and from that depth to 1320 metres remained remarkably constant. The lowest *in situ* temperatures, 16·85° ± ·02°C, were observed between 554 and 888 metres, while deeper observations were 16·88° ± ·02°C. This

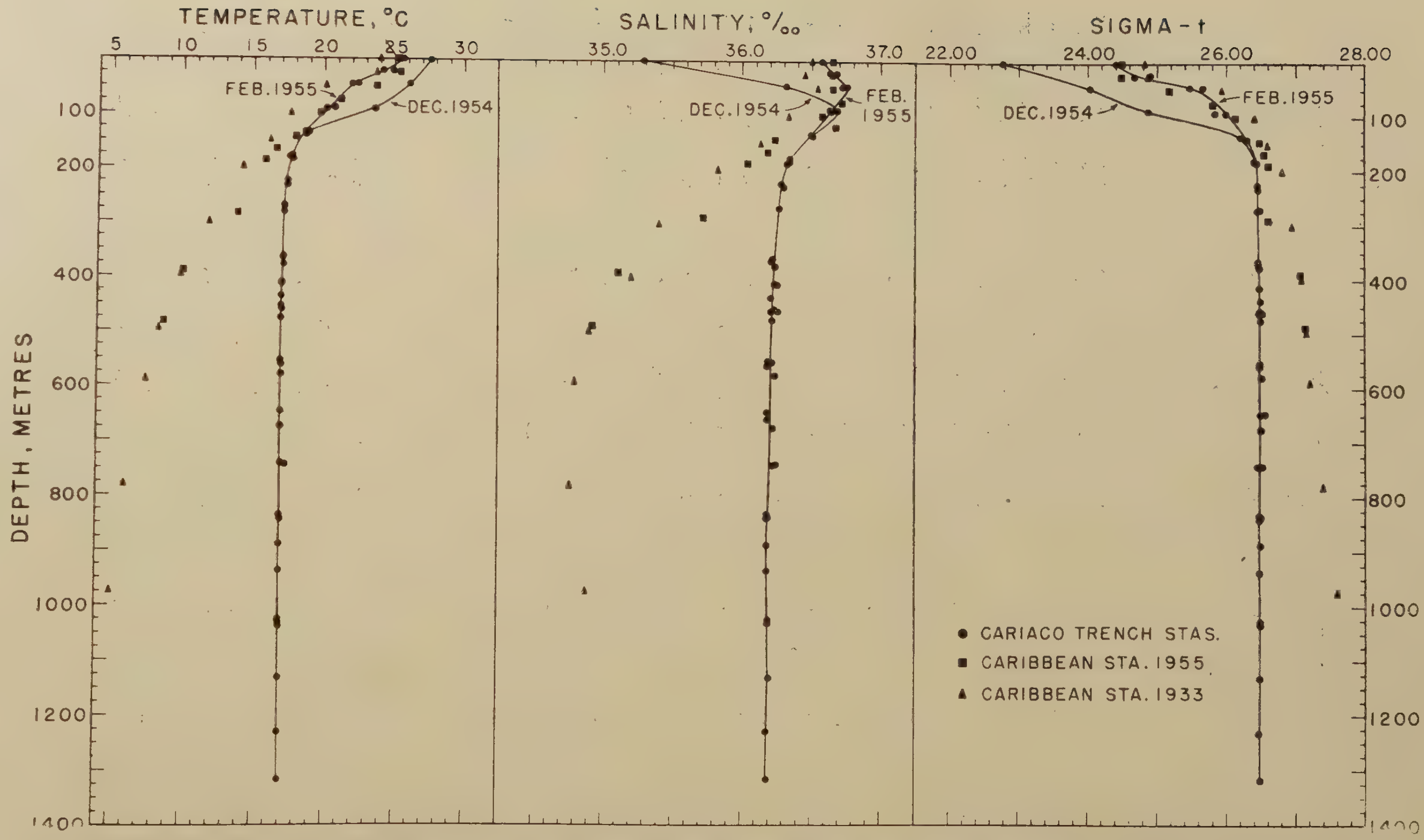

Fig. 2. Vertical distribution of salinity, temperature, and density in the Cariaco Trench and nearby Caribbean. Cariaco Trench stations: 5231, 10° 40′N, 65° 36′W., 5 Dec. 1954; 5268; 10° 41·5′N, 65° 40·5′W., 8 Feb. 1955; and 5269, 10° 37·5′N, 65° 24′W., 9 Feb. 1955. Caribbean stations: 1504, 12° 03′N, 64° 35′W., 15 March 1933; 5266, 11° 18′N, 65° 39′W., 8 Feb. 1955.

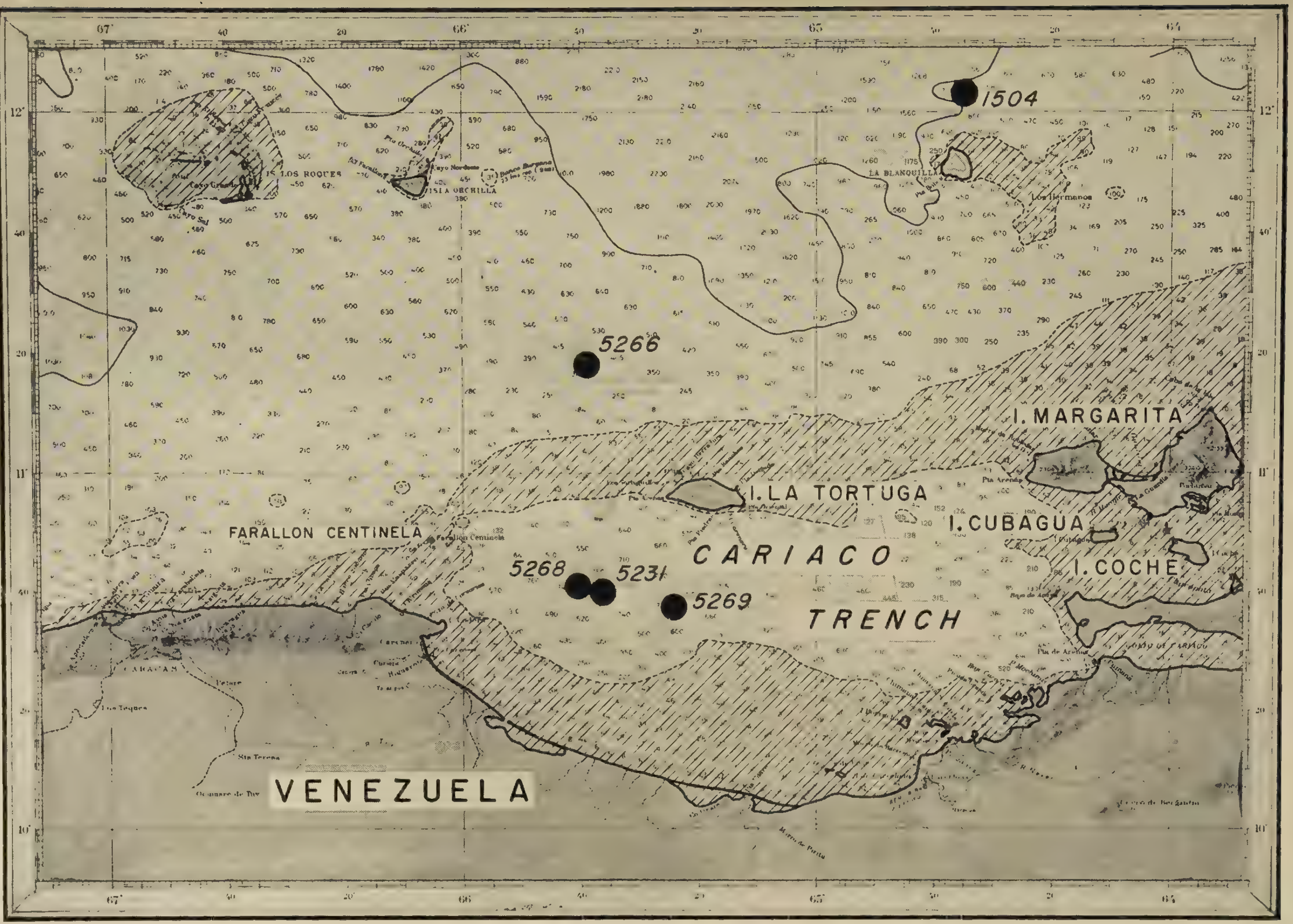
1504
IS LOS ROQUES
ISLA ORCHILLA
LA BLANQUILLA
Los Hermanos
5266
I. MARGARITA
I. LA TORTUGA
I. CUBAGUA
I. COCHE
FARALLON CENTINELA
CARIACO
TRENCH
5268
5231
5269
VENEZUELA
CARACAS
67°
66°
65°
64°
12°
11°
10°

Fig. 1. Location of Cariaco Trench and hydrographic stations, from U.S. Navy H.O. Chart No. 2319, April 1917. 13th Ed., 1950.

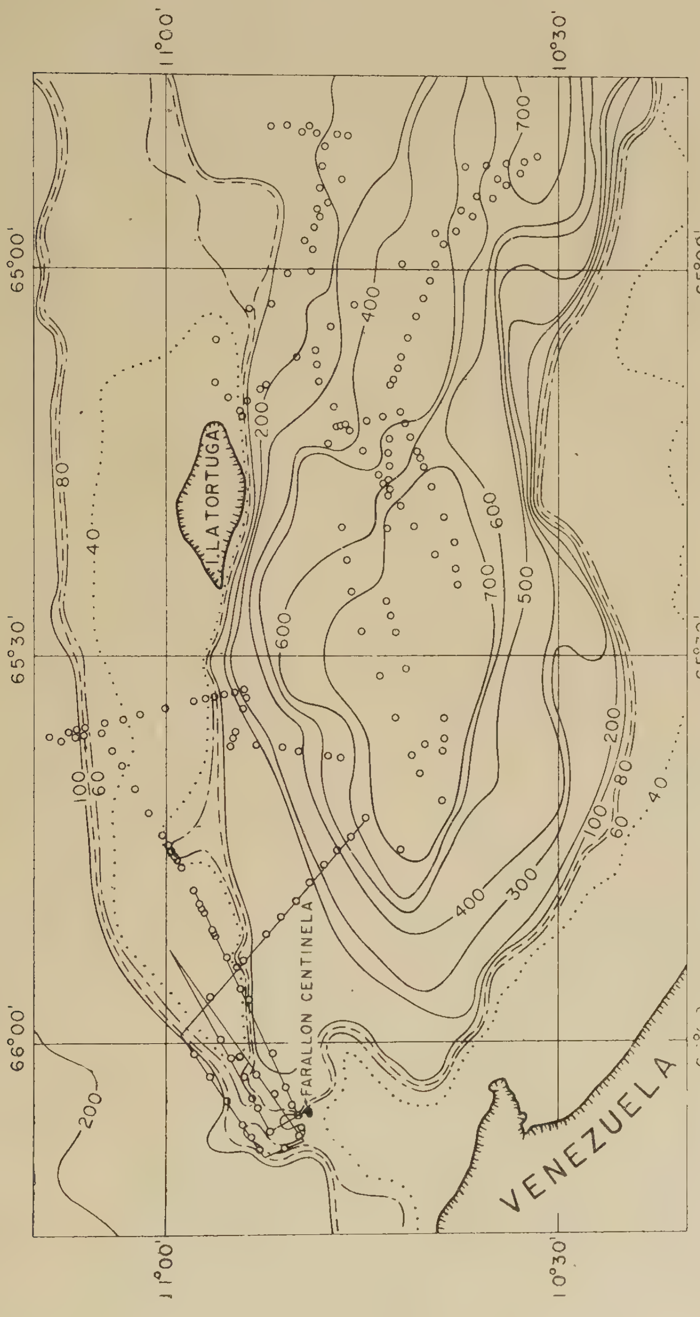
11°00'
10°30'
65°00'
65°30'
66°00'
I. LA TORTUGA
FARALLON CENTINELA
VENEZUELA
80
40
100
60
200
400
600
700
500
300

Fig. 3. Bathymetry in the Cariaco Trench, showing the track of the *Caryn* and location of discrete readings from the record of a high-precision echo-sounder.

temperature inversion is apparently the result of adiabatic heating[†]. Just north of the trench, the temperature was similar in distribution to that in the trench to sill depth, but continued to decrease at greater depth, falling to 8·60°C at 488 metres.

The salinity distribution likewise demonstrates the isolation of the water below sill depth. In December 1954 the surface salinity was 35·28‰, and in February 1955 36·57‰, but on both occasions at 180 metres it was 36·33‰. Between 180 and 520 metres the salinity decreased gradually to 36·20 ± ·02‰, and water of this salinity filled the trench below 520 metres. In the Caribbean north of the sill, the salinity continued to decrease steadily with depth to 34·91‰ at 488 metres.

The exchange of Caribbean Sea water with the deep water of the Cariaco Trench depends upon the density structure below sill depth off Farallon Centinela. The depth of the sill is close to 80 fathoms (146 metres) as disclosed by several fathometric traverses by CARYN *et al.* in February 1955 (Fig. 3). The potential density for the deepest water of the trench was 26·51 ± ·02. North of the sill (station 5266) a density of 26·51 was observed at a depth of 160 metres. At greater depths the density of the Caribbean water exceeded that of water within the trench, indicating that Caribbean water deeper than 160 metres is denied access to the trench. It is possible, however, that small variations in the external density structure may induce intermittant exchanges of such water across the sill.

BIOCHEMICAL PROPERTIES OF THE WATER

The biochemical properties of the water below sill depth also show that it is isolated from the rest of the Caribbean. The oxygen content in the trench water, determined by the Winkler titration, decreased rather regularly with depth to zero at about 475 metres, where hydrogen sulphide was first detected (Fig. 4A). Below this depth, hydrogen sulphide increased with depth to 800 metres below which concentrations of 0·03 mg A sulphide S per litre were found to the bottom[‡].

The total phosphorus concentration determined by HARVEY'S (1948) method increased with depth from about 0·1 microgram atoms per litre at the surface to 2·72 μgA per litre at 700 metres. It was impossible to make inorganic phosphate determinations at the time of sampling, and the analyses were made after four to sixteen weeks frozen storage in polyethylene bottles. During this time, the hydrogen sulphide disappeared from the samples and satisfactory determinations, as described by KETCHUM, CORWIN and KEEN (1955), were generally possible. Standards were made up with surface sea water so no salt error correction is necessary. Colour comparisons were made in the photoelectric colorimeter described by FORD (1950). Experience has shown that phosphates determined on frozen samples are somewhat erratic, and some analyses have been discarded because of discrepancies between samples taken at nearly the same depths. These analyses (Fig. 4B) show the same vertical distribution as the total phosphorous. At no depth was the inorganic phos-

---

[†] Heating by the adiabatic compression of sea water is usually insignificant at depths less than about 2,000 metres. However, the effect is directly proportional to the absolute temperature (PROUDMAN, 1953, pp. 197-201), so that in water having *in situ* temperature of the Cariaco Trench, the potential temperature is about 0·2°C lower than the *in situ* temperature of the deepest part of the trench.

[‡] Throughout this paper, hydrogen sulphide or sulphide is used to indicate the total sulphide sulphur content, *i.e.*, $H_2S + HS^- + S^{--}$. Sulphides were determined by spectrophotometric determination of the amount of methylene blue formed in the reaction between sulphides, para aminodimethylaniline, chloride and ferric ions. The method was adapted for use in sea water by Mr. SAYED ALI EL WARDANI.

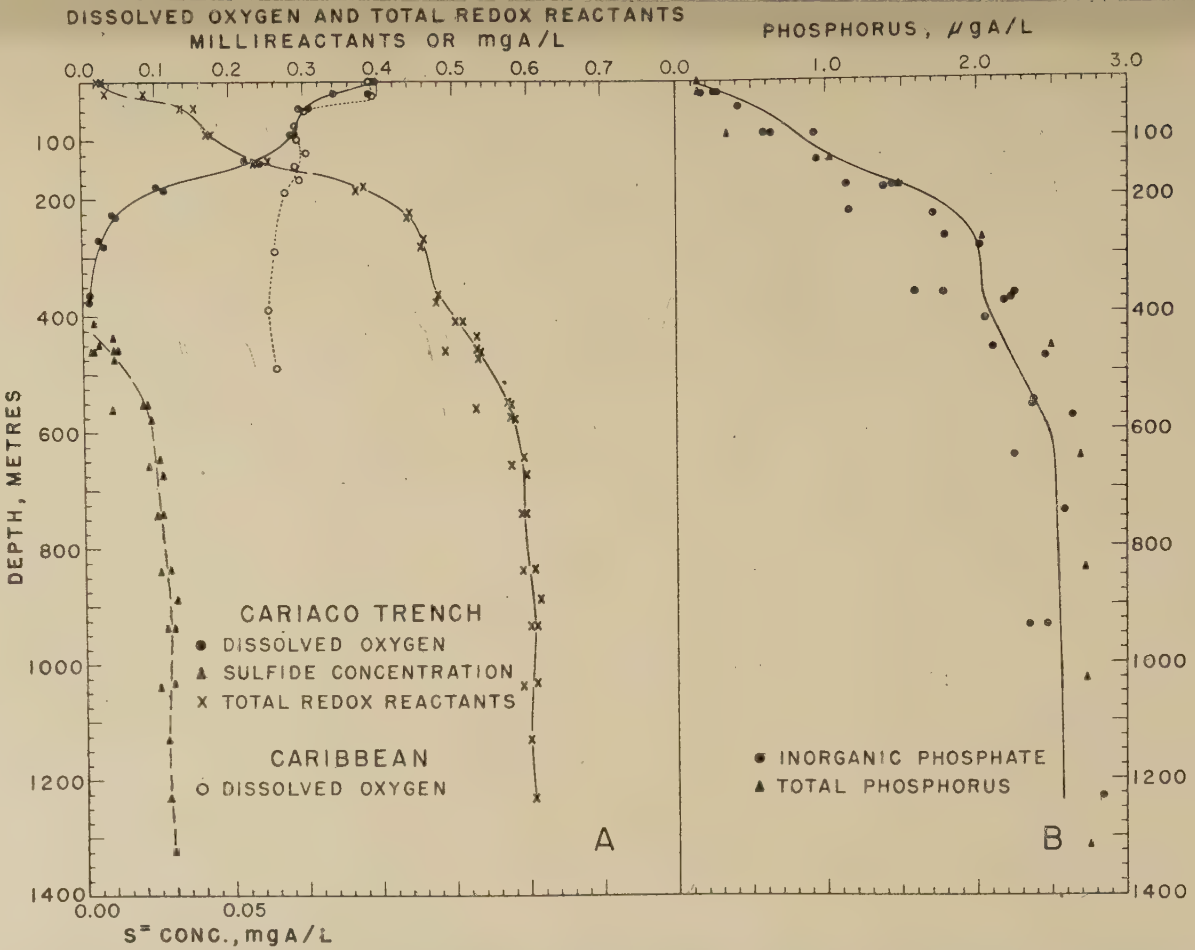

Fig. 4A. Dissolved oxygen in the Cariaco Trench and the nearby Caribbean, sulphide concentrations and total oxygen and sulphate consumed in the Cariaco Trench. The data are from stations 5266, 5268 and 5269. See Figs. 1 and 3 for these locations.

Fig. 4B. Vertical distribution of inorganic and total phosphorus in the Cariaco Trench. The line shows inorganic phosphate values predicted from the ratio $AOU + 4S^{=} : P = 235 : 1$ by atoms.

phate content sufficiently different from the total phosphorous to indicate significant amounts of organically bound phosphorous (KETCHUM, CORWIN, KEEN, 1955).

Nitrate, nitrite, and ammonia were determined on samples subjected to the same storage as the phosphate samples. These analyses showed that less than one microgram atom per litre of ammonia nitrogen, determined by the method of RILEY (1953), was present in the surface, but at 50 metres it had decreased to undetectably low concentrations. Ammonia again became detectable at 270 metres, and increased with depth to 8 to 9 microgram atoms per litre at about 550 metres and remained at this concentration through the rest of the anaerobic layer. Nitrate was very low in the surface and increased to a maximum of about 14 μgA/L at 180 metres. At greater depths, the concentration of nitrates decreased to traces (within the analytical sensitivity) in the anaerobic layer, essentially disappearing with the disappearance of oxygen and the appearance of hydrogen sulphide. Consistant analyses were obtained with ZWICKER and ROBINSON'S (1944) strychnidine method, and with MULLIN and RILEY'S (1955) hydrazine method, in which nitrate is reduced to nitrite with hydrazine and the latter determined by diazotization.

Only traces of nitrite, determined by the method of ROBINSON and THOMPSON (1948), were found throughout the water column, and it appears that the major inorganic nitrogen compound present in the anaerobic zone was ammonia.

Titration alkalinity was determined by the method of GRIPENBERG (1937), and the specific alkalinity (titration alkalinity $\times 10^3 \div \mathrm{Cl}‰$, HARVEY, 1955, pp. 160-161) was computed for eleven of the samples from the Cariaco Trench. Ten of these were from depths between the surface and 743 metres, and for all these the specific alkalinity was between 0·122 and 0·131. The value for the other sample, from 1231 metres, was 0·141, indicating a substantial increase in the titration alkalinity in the deep water of the trench. Approximate computations of the contribution of HS^- ions at the sulphide concentrations and pH found in the deep water of the trench indicate that the magnitude of change in alkalinity corresponds to the observed accumulation of bisulphide ions.

The pH, determined with a Beckman model G pH meter, decreased from a value of 8·2 at the surface to 7·8 at 375 metres, and remained approximately uniform at the latter value to the bottom. Some of the determinations in the deep part of the trench indicated that the pH dropped to 7·6, but these are believed to be in error, and were not substantiated by other determinations.

BIOCHEMICAL RELATIONSHIPS IN THE CARIACO TRENCH

In anaerobic waters, the oxidation of organic matter has consumed all the dissolved oxygen, and has led to the reduction of some of the sulphide ions with the production of sulphide. These reactions can be represented by the equations

$$2CH_2O + 2O_2 = 2CO_2 + 2H_2O$$

$$2CH_2O + SO_4^{=} = 2CO_2 + S^{=} + 2H_2O.$$

It can be seen from these equations that one sulphate ion as an oxidant is equivalent to four atoms of oxygen. The amount of oxygen consumed, the apparent oxygen utilization (AOU), is defined as

$$AOU = O_2' - O_2$$

in which O_2 is the observed concentration of oxygen and O_2' the concentration of oxygen dissolved in water having the observed salinity and temperature when in equilibrium with a water-saturated atmosphere (WHIPPLE and WHIPPLE, 1911; REDFIELD, 1948). The amount of sulphate ion consumed is assumed to equal the observed sulphide concentration. Therefore, when AOU and $S^=$ are expressed in milligram (or microgram) atoms per litre, $AOU + 4S^= =$ Total redox reactants.

Table 1. *Ratios of carbon, nitrogen, and phosphorus bound in organic matter, and of oxygen consumption to phosphate and inorganic nitrogen compounds formed upon its decomposition, by atoms.*

	Derivation	*O*	*C*	*N*	*P*	*Reference*
1.	Changes in sea water and analysis of plankton organisms. Phosphate analyses corrected for salt effect according to COOPER, 1938.	—	105	15	1	REDFIELD, 1934
2.	Ratios in line 1, assuming two atoms of oxygen consumed on oxidizing one atom of carbon.	210	105	15	1	
3.	Ratios in line 2, further assuming the oxidation of nitrogen compounds requires four atoms of oxygen for each atom of nitrogen.	270	105	15	1	GILSON, 1937
4.	Average composition of plankton organisms.	—	106	16	1	FLEMING, 1940
5.	Ratios in line 4, and the assumptions in lines 2 and 3 regarding consumption of oxygen and nitrogen.	276	106	16	1	
6.	Analyses of sea water, phosphate analyses corrected as in line 1.	180	—	15	1	REDFIELD, 1934 COOPER, 1938
7.	Cariaco Trench, 50 metres	235	—	15	1	
8.	Cariaco Trench, 50 metres to top of anaerobic layer.	235	—	15–3	1	
9.	Cariaco Trench, anaerobic layer.	235*	—	2–4	1	

*Total redox reactants, $AOU + 4S^=$

Two approximations are inherent in the method described above for calculating total redox reactants. The possible presence of intermediate products from the anaerobic reduction of sulphate is not taken into account, nor is any allowance made for the fraction of the observed hydrogen sulphide which originates directly from the anaerobic decomposition of organic sulphur compounds. The former approximation may result in high total redox reactants while the latter would tend to give low values. Both errors are probably small.

As calculated, the total redox reactants increase with depth to about 680 metres (Fig. 4A), and then remain constant at ca. 0·6 milliequivalents per litre to the bottom.

The ratios between the amounts of phosphorus, nitrogen, and carbon bound in organic matter, and the amount of oxygen consumed when organic matter decomposes with the release of phosphate, nitrate, nitrite, and ammonia, have been reported by

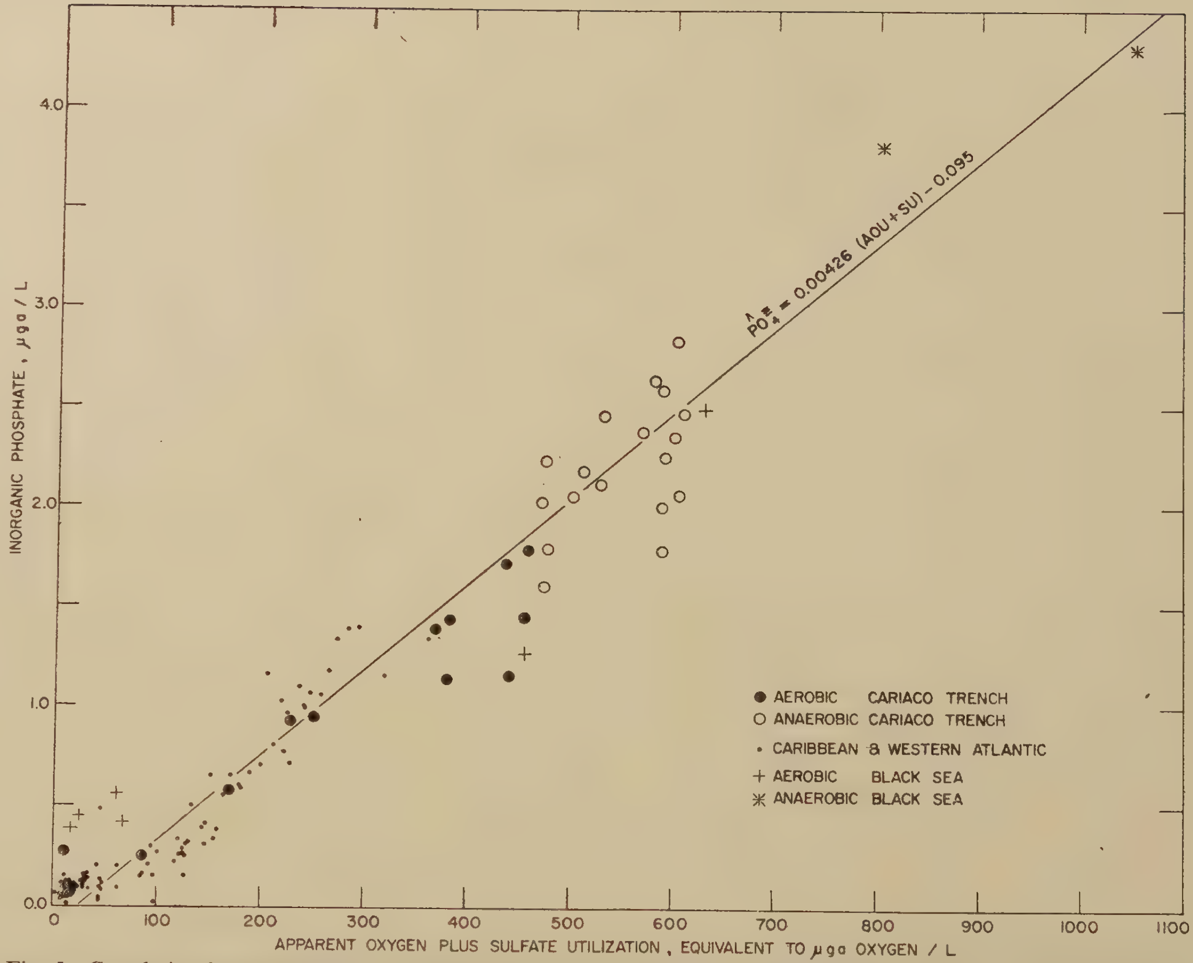

Fig. 5. Correlation between oxygen and sulphate utilization and inorganic phosphates in aerobic and anaerobic waters of the Cariaco Trench, Caribbean, western North Atlantic, and Black Sea. Two points for the anaerobic water of the Black Sea are not shown ; they are :

	$AOU + 4S^{=}$	$PO_4^{\equiv}$	$PO_4^{\equiv}$ predicted by the equation
500 m	1461	5·64	6·13
1,000 m	1717	5·91	7·22

several authors (Table 1). In the Cariaco Trench, the ratio between sulphate reduction and/or oxygen consumption and phosphorus release is shown by the data presented in Fig. 5, in which the line shown is the linear least-squares line of regression of phosphates on the sum of oxygen and sulphate utilized :

$$\widehat{PO_4}^{\equiv} = 0{\cdot}00426\,(AOU + 4S^{=}) - 0{\cdot}095.$$

The coefficient of correlation is 0·959. The standard error of estimate is 0·21 μgA phosphate-phosphorus per litre, showing that the departure of the intercept (0·095) from zero is insignificant. Thus, in the Cariaco Trench, the oxidation to phosphate regeneration ratio is 1/0·00426 = 235, in good agreement with the other ratios in Table 1, particularly since the nitrogen compounds in the anaerobic part of the Cariaco Trench are clearly not in their highest state of oxidation, and a number somewhere between 212 and 276 : 1 might well be expected. The vertical distribution of inorganic phosphate predicted from the oxygen and sulphate utilized by the 235 : 1 ratio (Fig. 4B) is in good agreement with the observed distribution of phosphate.

Estimates of the oxygen and sulphate utilized and phosphate concentrations in the Black Sea have been made from oxygen and hydrogen sulphide data reported from the *Thor* expedidition (SCHMIDT, 1912, p. 65, Station 172), and phosphate data reported by GOLOLOBOV (1949). In the Black Sea, the anaerobic zone begins at about 150 metres, and the hydrogen sulphide content increases much more rapidly with depth than it does in the Cariaco Trench, until at 1,000 metres it is approximately 10 times more concentrated. However, up to concentrations of 4·30 μgA phosphate phosphorus per litre, the same ratio of oxygen plus sulphate reduction to phosphate regeneration is found in both the aerobic and anaerobic layers of the Cariaco Trench and down to 300 metres in the Black Sea. The ratios are shown in Fig. 5 by distinctive symbols. At greater depths in the Black Sea this ratio attains a higher value, and it appears that mechanisms operate other than the oxidation of organic materials with the concurrent release of inorganic phosphate. Among the possible mechanisms are a) the direct assimilation of phosphate by bacteria as observed by RENN (1937) and others and b) the relatively more rapid decomposition of phosphatic organic compounds in the upper layers, permitting only residues low in phosphate to settle to greater depths. SEIWELL and SEIWELL (1938) and COOPER (1935) observed that phosphate was released more rapidly than the nonphosphatic residues when plankton organisms were oxidized. In favour of mechanism a), there are sufficient quantities of organic matter in the deeper layers of the Black Sea, reported by GOLOLOBOV (1949) as " oxidizability " to satisfy the phosphate deficit predicted by the linear relationship shown in Fig. 5, assuming that the C : P ratio is 235 : 1. In the Cariaco Trench the binding of phosphorous by anaerobic bacteria is not a predominant process, as shown by the absence of significant quantities of organic phosphorous.

NITROGEN REGENERATION

At the nitrate maximum in the aerobic layer of the Cariaco Trench (about 50 metres), the theoretical nitrate to phosphate ratio of 15 : 1 is realized, but at greater depths there is a relative deficiency of inorganic nitrogen compounds. From 50 metres to the top of the anaerobic layer the ratios decrease with depth to about 3 to 4 : 1, with similar ratios prevailing in the anaerobic layer. The maximum concentration of phosphate in the anaerobic layer is approximately 2·6 μgA/*l*. This amount of phosphorus regeneration should be accompanied by 39 μgA of nitrogen regeneration. Of this amount, only 8 μgA/l can be accounted for, as ammonia. This would leave 31 μgA/l of nitrogen to be accounted for. It is probable that the remaining nitrogen released by decomposition is present as molecular, uncombined dissolved N_2. This view is strengthened by the observations of Kriss (1949) that gaseous nitrogen increases toward the bottom of the Black Sea, and that the deep waters are supersaturated.

At the temperature and salinity of the Cariaco Trench, the quilibrium solubility of nitrogen in sea water is approximately 10 ml/l (RAKESTRAW and EMMEL, 1938a). The amount of nitrogen assumed to be of biological origin, 31 μgA or 0·35 ml per litre, is only 3·5% of the amount of atmospheric nitrogen ordinarily present in sea water. Even the careful work of RAKESTRAW and EMMEL (1939b) shows concentrations of nitrogen in sea water which vary from 100% saturation by as much as 7 to 8%, usually by 2 or 3%. Therefore, accumulations of gaseous nitrogen attributable to organic decomposition in the Cariaco Trench are probably too small for detection by a direct analysis of the nitrogen content of the water.

AGE OF THE WATER IN THE CARIACO TRENCH

Three methods can be used to estimate the time that the water has been sequestered in the deep part of the Cariaco Trench, provided the water is not overturning. At present it has not been definitely determined whether such is the case, partly because measurements of the sill depths and of the density structure outside the trench are too incomplete.

A minimum age can be estimated by comparing the quantity of organic matter decomposed below sill depth with the rate of organic production in the photic zone. This calculation involves the assumptions that a) all the organic matter formed in the upper layers rains into the basin and is there oxidized completely, with no deposition of organic detritus on the bottom ; b) there is no recycling of nutrients in the layer above the sill ; c) the same amount of organic matter enters and leaves the trench over the sill. Since two atoms of oxygen, either molecular or as sulphate, are required to oxidize one of carbon, the amount of carbon consumed below sill depth can be estimated by integrating the consumption of oxygen and sulphate. The carbon consumption thus estimated is $20{\cdot}55 \times 10^3$ gm C/M². The rate of organic production in the photic zone has been estimated by Dr. JOHN H. RYTHER to be about 0·48 gm C/M²/day, from a carbon-14 determination of the photosynthetic rate. Therefore,

$$\frac{20{\cdot}55 \times 10^3 \text{ gm C/M}^2}{0{\cdot}48 \text{ gm C/M}^2 \text{ days}^{-1}} = 40{\cdot}55 \times 10^3 \text{ days} = 111 \text{ years.}$$

Departures from assumptions a) and b) may be large but they would increase the age estimate, so 100 years is considered to be a minimum. Appreciable amounts of plankton pigments and up to about 4% of organic carbon in sediment cores from the trench prove that there is some departure from assumption a).

A maximum age of the water in the trench can be estimated by assuming that the trench was catastrophically filled with a mass of water having the uniform salinity and temperature now found below 650 metres. If present-day departures from uniform temperature have been caused solely by molecular conduction, it can be shown that it would take between 1,000 and 2,000 years to raise the temperature of the water column between sill depth and 650 metres to the observed temperatures. A much longer time, between 120,000 and 240,000 years, would be required for the present-day distribution of salt in this region to be accomplished by solely molecular diffusion.

These estimates are based on evaluation of the equation

$$TK_p \frac{\partial P}{\partial Z}\bigg|_{\text{sill}} = \int_{\text{isothermal layer}}^{\text{sill depth}} [P(Z) - P(i)]\, dz,$$

in which T is the time in seconds, K_p is the coefficient of molecular diffusion or conductivity for salt or heat, and $\partial P/\partial Z$ is the gradient of salt or heat existing across the sill. $P(Z)$ is the salinity or temperature at depth Z, $P(i)$ the temperature or salinity of the isothermal-isohaline layer. The integration was made graphically. Since it might be argued that the gradient $\partial P/\partial Z$ was zero at the time of catastrophic filling, it has been assumed that it increased linearly with time from zero to present-day values, so that the lesser age represents the time based on the existing gradient, the greater age the time based on $\frac{1}{2}$ of the present day gradient (the assumed average). Values of K_p are $1{\cdot}4 \times 10^{-3}$ cm^2 sec^{-1} for heat and 2×10^{-5} cm^2 sec^{-1} for salt (SVERDRUP, JOHNSON and FLEMING, 1942, pp. 61 and 69).

In a third method, the time required to achieve the observed temperature distribution by solar radiation is estimated. Within the limitations of the accuracy of the observations and of the constants for radiation and light penetration, it too should place an upper limit on the age.

The static model described above would require an estimated 160 years of heating by solar radiation alone to achieve the temperatures observed between sill depth and 650 metres. The heat involved is $1{\cdot}15 \times 10^4$ gram calories for the column under one square centimetre. The average total radiation from sun and sky reaching these latitudes is reported by Kimball to be 0·275 gm cal cm^{-2} minute^{-1} (SVERDRUP, JOHNSON and FLEMING, p. 103). If one half of this energy is in the visible light range, and since 0·1% of the visible energy reaches a depth of 150 metres in the Cayman Sea just west of Jamaica (CLARKE, 1937-8), then $0{\cdot}137 \times 0{\cdot}001 = 1{\cdot}37 \times 10^{-4}$ gm cal cm^{-2} reaches a depth of 150 metres every minute, is absorbed there or at some greater depth, and converted to heat. Therefore,

$$\frac{1{\cdot}15 \times 10^4 \text{ gm calories cm}^{-2}}{1{\cdot}37 \times 10^4 \text{ gm calories cm}^{-2}\text{ min}^{-1}} = 0{\cdot}84 \times 10^8 \text{ minutes} = 160 \text{ years.}$$

It is obvious that the temperature was not changed by insolation alone, because the salinity changes must also be accounted for. The evidence indicates that both heat and salt have been diffused downward mainly by eddy processes. Any eddy process should achieve the observed result more quickly than molecular processes, so we are inclined towards a shorter rather than a longer age estimate in the range between 100 and 2,000 years. The existing data do not justify more exact estimates.

COMPARISONS WITH OTHER ISOLATED BASINS

The Cariaco Trench differs from other anaerobic marine environments in respect to geomorphology, size, the amount of fresh water influx, the depth of the sill, the stability of the water column, and the degree of exchange of surface waters with the open ocean. The Norwegian and other fjords, the small semi-enclosed embayments which frequently become anaerobic in the summer, and the Black and Azov seas, all receive large influxes of fresh water which establish extreme density gradients preventing effective vertical mixing. Some of the Norwegian fjords and small embayments may overturn and flush with the advent of winter, but the density structure is essentially due to gradients in the salinity.

Table 2. Comparison of isolated basins.

	Sill depth, metres	*Stability[a] of water column near sill*		*Hydrogen sulphide accumulation, microgram atoms sulphide-sulphur per litre*	*Age estimate*
		Depth, metres	*Stability*		
Catalina Basin[b]	982	679 831 990 1143	92 31 13	nil	—
Santa Monica Basin[b]	737	579 701 792 884	33 44 22	nil	—
Santa Barbara Basin[b]	475	221 433 524 585	76 88 98	nil	2 to 20 years[b]
Kaoe Bay[c]	40–50	0 25 50 75	1920 520 240	13·4, maximum[e]	—
Cariaco Trench	146 (?)	100 125 150 175	680 440 320	30, at 1,200 M	greater than 100 years
Black Sea[d]	40–50	10 25 50 75	21,000 3,000 3,800	300, at 1,000 M	5,600 years[f]

[a] Stability $= \Delta \sigma_t \div \Delta D$ (metres) $\times 10^5$.
[b] Data from RITTENBERG, EMERY and ORR (1955).
[c] Data from VAN RIEL, HAMAKER ,and VAN EYCK (1950).
[d] Data from station at 43° 05′N. Lat., 38° 50′E. Long., 22 July 1925 (OBERKOMMANDO der KRIEGSMARINE, 1943).
[e] From VAN RIEL (1943).
[f] From GOLOLOBOV (1949).

The anaerobic Kaoe Bay in the East Indies (VAN RIEL, 1943) is about 500 metres deep, 18 miles across, and roughly circular. It is essentially land-locked, with limited access of the waters shallower than 45 to 50 metres to the ocean through a sound which is about six miles wide, 28 miles long, and 50 metres deep. Although there are over 80 inches of rainfall a year, the salinity in the bay is about the same as that found at comparable depths in the open Pacific, down to sill depth. It contains undiluted Pacific ocean water, in which there is no oxygen below 300 to 400 metres, and in which VAN RIEL observed a maximum of 13·4 microgram atoms of sulphide-sulphur per litre at 441 metres.

The Cariaco Trench differs from Kaoe Bay in that it is not land-locked, is much larger, and is considerably deeper. It differs from most small embayments, fjords, and the Black and Azov seas, in that it receives little or no fresh water run-off and is filled with typical, undiluted sea water. The density structures across the sills of Kaoe Bay and the Cariaco Trench result mostly from temperature differences in the water column, rather than to large salinity gradients.

The Cariaco Trench shows some interesting similarities to and contrasts with the basins off the California coast described by EMERY (1954) and RITTENBERG, EMERY and ORR (1955). Each of these basins is a depression in the continental shelf and each contains nearly isothermal and isohaline water from shortly below sill depth to the bottom. However, none of the California basins is anaerobic, and their oxygen content is essentially uniform from sill depth to the bottom. The authors indicate that constant flushing of the basin waters renews the oxygen at a rate which equals or exceeds the rate of oxygen consumption. Such is distinctly not the case in the Cariaco Trench.

One expression of differences in the ease of flushing such basins is the stability of the water column, expressed as the change in σ_t with depth (metres). This property, together with age estimates and sulphide accumulations, is shown in Table 2 for the trenches described by RITTENBERG, *et al.* for the Cariaco Trench, Kaoe Bay, and the Black Sea. The stability at about sill depth increases by one order of magnitude in comparing the California basins with the Cariaco Trench and Kaoe Bay, and by another order of magnitude in comparing the Cariaco Trench with the Black Sea. The age estimates and the amount of sulphide accumulation also change in a similar manner.

SUMMARY

The Cariaco Trench is filled with undiluted sea water, which appears to have been altered principally by the anaerobic reactions of bacteria. The surface waters exchange freely with the rest of the Caribbean, and vertical mixing is impeded more by thermal than by haline stratification. It represents an isolated marine environment in which the biochemical processes of decomposition of organic matter and the concurrent regeneration of its inorganic products have proceeded farther than in any other known place filled with typical oceanic water. It offers, therefore, a location where these phenomena can be observed, relatively isolated and uncomplicated by the sometimes confusing processes of circulation and mixing.

Acknowledgements—The authors wish to acknowledge that the original suggestion to study the Cariaco Trench was made by Dr. A. C. REDFIELD, who became interested in it because its geomorphology suggested to him that it might be a stagnant basin. Mr. SAYED ALI EL WARDANI, of Scripps Institution of Oceanography, made the determinations of sulphides and *pH* during the cruise, and his help is gratefully acknowledged. Suggestions by Dr. REDFIELD, Dr. B. H. KETCHUM, Mr. HENRY

STOMMEL, and Dr. J. H. RYTHER, and the technical assistance of Mr. NATHANIEL CORWIN, have been most helpful. Part of the work was supported by a grant from the National Science Foundation.

Contribution No. 830 *from the Woods Hole Oceanographic Institution.*

REFERENCES

CLARKE, G. L. (1938), Light penetration in the Caribbean Sea and in the Gulf of Mexico. *J. Mar. Res.*, **1** (2), 85-94, (4 figs.).
COOPER, L. H. N. (1938), Redefinition of the anomaly of the nitrate-phosphate ratio. *J. Mar. Biol. Ass. U.K.*, **23** (1), 179.
EMERY, K. O. (1954), Source of water in basins off Southern California. *J. Mar. Res.*, **13** (1), 1-21, (6 figs.).
FLEMING, R. H. (1940), The composition of plankton and units for reporting populations and production. *Proc., Sixth Pacific Sci. Congr.*, **3**, 535-540.
FORD, W. L. (1950), Seagoing photoelectric colorimeter. *Anal. Chem.*, **22** (11), 1431-1435.
GILSON, H. C. (1937), The nitrogen cycle. *Sci. Rept., John Murray Exped.*, 1933-34, **2** (8), 21-81.
GOLOLOBOV, Y. K. (1949), [Contribution to the problem of determining the age of the present stage of the Black Sea]. (In Russian). *Dokl. Akad. Nauk, S.S.S.R.*, **66**, 451-454.
GRIPENBERG, S. (1937), On the determination of excess base in sea water. *Comm., Fifth Hydrol. Conf., Helsingfors*, 1936, **10** (B), 15 pp.
HARVEY, H. W. (1948), The estimation of phosphate and total phosphorus in sea waters. *J. Mar. Biol. Assoc., U.K.*, **27** (2), 337-359.
HARVEY, H. W. (1955), *The Chemistry and Fertility of Sea Waters.* The University Press, Cambridge, viii + 224 pp.
KETCHUM, B. H., CORWIN, N., and KEEN, D. J. (1955), The significance of organic phosphorus determinations in ocean waters. *Deep-Sea Res.*, **2** (3), 172-181.
KRISS, A. E. (1949), [The role of microorganisms in the accumulation of hydrogen sulphide, ammonia and nitrogen in the depths of the Black Sea]. (In Russian). *Priroda*, 1949, (6), 35-46.
MULLIN, J. B., and RILEY, J. P. (1955), The spectrophotometric determination of nitrate in natural waters, with particular reference to sea water. *Analyt. Chim. Acta*, **12** (5), 464-480.
OBERKOMMANDO DER KRIEGSMARINE (1943), Schwarzes und Asowsches Meer. Beiheft zum *Handbuch für das Schwarze Meer*, Berlin, 72 pp.
PROUDMAN, J. (1953), *Dynamical Oceanography.* Methuen & Co., Ltd., London, and John Wiley & Sons, Inc., N.Y., xii + 409 pp.
RAKESTRAW, N. W., and EMMEL, V. M. (1938a), The solubility of nitrogen and argon in sea water. *Phys. Chem.*, **42** (9), 1211-1215.
RAKESTRAW, N. W., and EMMEL, V. M. (1938b), The relation of dissolved oxygen to nitrogen in some Atlantic waters. *J. Mar. Res.*, **1** (3), 207-216.
REDFIELD, A. C. (1934). On the properties of organic derivatives in sea water and their relation to the composition of plankton. In : *James Johnstone Memorial Volume*, University Press, Liverpool, 176-192.
REDFIELD, A. C. (1948), The exchange of oxygen across the sea surface. *J. Mar. Res.*, **7** (3), 347-361.
RENN, C. E. (1937), Bacteria and the phosphorus cycle in the sea. *Biol. Bull.*, **72** (2), 190-195.
RILEY, J. P. (1953), The spectrophotometric determination of ammonia in natural waters with particular reference to sea water. *Analyt. Chim. Acta*, **9** (6), 575-589.
RITTENBERG, S. C., EMERY, K. O., and ORR, W. L. (1955), Regeneration of nutrients in sediments of marine basins. *Deep-Sea Res.*, **3** (1), 23-45, (6 figs.).
ROBINSON, R. J., and THOMPSON, T. G. (1948), The determination of nitrites in sea water. *J. Mar. Res.*, **7** (1), 42-48.
SCHMIDT, J. (1912), Introduction, hydrography, deposits of the sea bottom. *Rept. Danish Oceanogr. Exped.*, 1908-1910 *to the Mediterranean and Adjacent Seas*, **1** (1-3), 269 pp., pls.
SEIWELL, H. R., and SEIWELL, G. E. (1938), The sinking of decomposing plankton and its relationship to oxygen consumption and phosphorus liberation. *Proc. Amer. Phil. Soc.*, **78** (3), 465-481.

SVERDRUP, H. U., JOHNSON, M. W., and FLEMING, R. H. (1942), *The Oceans.* Prentice-Hall Co., N.Y., x + 1087 pp.

U.S. NAVY HYDROGRAPHIC OFFICE (1949), Sailing directions for the West Indies, 2. *H. O. Pub.* 129 (6th Ed.) xxiii + 335 pp.

VAN RIEL, P. M. (1943), Oceanographic results, the bottom waters. Introductory remarks and oxygen content. *Snellius Exped.*, 1929-1930, **2** (5) (Ch. 1), 77 pp.

VAN RIEL, P. M. HAMAKER, H. C., and VAN EYCK, L. (1950), Oceanographic results, tables, serial and bottom observations, temperature, salinity and density. *Snellius Exped.*, 1929-1930, **2** (6), 44 pp.

WHIPPLE, G. C., and WHIPPLE, M. C. (1911), Solubility of oxygen in sea water. *J. Amer. Chem. Soc.*, **33** (3), 362-365.

ZWICKER, B. M. G., and ROBINSON, R. J. (1944), The photometric determination of nitrate in sea water with a strychindine reagent. *J. Mar. Res.*, **5** (3), 214-232.

Printed in Great Britain by The Salisbury Press Ltd., Publicity House, Wilton Road, Salisbury, Wilts. (96502)

Contribution No. 831

The Oceanography of Hebron Fjord, Labrador[1,2]

BY DAVID C. NUTT[3] AND LAWRENCE K. COACHMAN[4]
Dartmouth College, Hanover, N.H., U.S.A.

CONTENTS

		PAGE
I.	INTRODUCTION	710
	1. Bathymetry	712
	2. Climate	712
	3. Contributions of fresh water	713
	4. Tides and currents	715
II.	OCEANOGRAPHIC FACTORS	715
	1. Temperature	716
	2. Salinity	722
	3. Oxygen	724
	4. Inorganic phosphate (PO_4)	725
	5. Temperature–salinity relationships	726
	6. Long-term trends	732
III.	ICE	734
IV.	EXCHANGE	739
V.	VERTICAL MIXING BELOW SILL DEPTH	742
VI.	DYNAMIC COMPUTATIONS	746
VII.	SUMMARY	748
	REFERENCES	750
	STATION DATA SUMMARIES	753

ABSTRACT

Hebron Fjord, extending some 28 miles into the northeast coast of Labrador at about latitude 58°10′ N., and having a sill at depth of 59 m. across its mouth, was visited at various periods during 1949, 1952 and 1954. The present paper deals with the oceanographic regime and physical environment in the fjord and adjacent coastal waters. Data on tides and currents, and on contributions of fresh water from precipitation run-off and ice melting are given. Oceanographic factors discussed include temperature, salinity, dissolved oxygen, inorganic phosphate, temperature–salinity relationships, and long-term trends. Ice formation as an oceanographic phenomenon is considered. Computations of thermohaline convection are made, and the effects of ice formation and exchange in determining the winter oceanographic structure are discussed. Above sill depth exchange occurs principally by horizontal movements and a flushing

---

[1] Received for publication January 5, 1956.

[2] Contribution No. 831 from the Woods Hole Oceanographic Institution, Mass., U.S.A. The work on which this paper is based has been carried out under contracts between the Arctic Institute of North America and the United States Office of Naval Research. In addition co-operation and assistance have been received from the Woods Hole Oceanographic Institution, the United States Navy Hydrographic Office, the United States Air Force, Dartmouth College, and Dartmouth Medical School.

[3] Research Associate in Geography, Dartmouth College, Hanover, N.H.

[4] Research Assistant in Northern Studies, Dartmouth College, Hanover, N.H.

J. FISH. RES. BD. CANADA, 13(5), pp. 709–758, 1956.
Printed in Canada.

Contributions No. 831 from the Woods Hole Oceanographic Institution.

time of about 68 days is computed. Below sill depth exchange must involve vertical movements and occurs principally by convection in winter. Calculations of the A factors of eddy conductivity and eddy diffusivity are made. Dynamic computations of water transport are given. During winter a water temperature of −1.75°C. exists at all levels in the fjord, rising in summer only to −1.68° at 250 m. and −1.00° at 100 m., causing the bottom waters to remain an isolated pocket of high Arctic environment during the summer and fall seasons as contrasted with the disappearance of negative temperatures down to 120 m. by mid-October outside the fjord. Inorganic phosphate increases with depth; photosynthesis maintains oxygen at super-saturation above 30 m. during summer, and the rate of oxygen consumption and renewal by vertical transport below 80 m. is calculated.

I. INTRODUCTION

LABRADOR forms the easternmost extension of the North American continent. Its coast is much indented by bays and fjords of varying topographic arrangement. The cold Labrador Current flows south from Hudson and Davis Straits along the continental shelf and slope carrying with it extremely cold Arctic water to the relatively low latitudes off Labrador and Newfoundland and preventing true Atlantic water from reaching the coasts (Nutt, 1953). While earlier work has described or defined the Labrador Current (Iselin, 1932; Smith, Soule and Mosby, 1937; Bailey and Hachey, 1951b), our knowledge of the immediate coastal waters is restricted to the single observation of temperature in Nachvak Fjord made by the Brown Harvard Expedition of 1900 (Delabarre, 1902); the few hydrographic stations in Nachvak, Saglek, and Ekortiarsuk Fjords by the *Chance* in 1926 (Iselin, 1932); and the early studies of the *Blue Dolphin* (Nutt, 1953).

As a part of the extensive investigations of the Labrador coastal waters carried out by the research vessel *Blue Dolphin*, a specific study of the oceanography of Hebron Fjord, situated on the northeast coast of Labrador at latitude 58°10′ N., was completed in the fall of 1954. This detailed study had been prompted by the finding of an extremely low-temperature (−1.8°C.) marine environment at the lower levels of Hebron Fjord in 1949 which was believed to persist throughout the year. The adaptation and physiology of the marine bottom fauna in relation to this environment raised some interesting problems which were the subject of a detailed investigation of this fjord during 1954 and 1955. The physiological research has been conducted by Dr. Per F. Scholander[5] and his co-workers at the Woods Hole Oceanographic Institution and will be reported elsewhere. This paper deals with the oceanographic regime and physical environment in Hebron Fjord and in the adjacent coastal waters.

During the course of the *Blue Dolphin* Labrador Expeditions from 1949 to 1954 Hebron Fjord was examined at the following times: 1949, August 7–12; 1952, July 19, 23, 31; 1954, March 26 to April 6, July 9 to August 12, and October 15–26. On the occasion of each visit observations were taken for the determination of surface and subsurface temperatures, salinities and, at certain stations, for dissolved oxygen and inorganic phosphates. The station locations within Hebron Fjord and in the immediate coastal waters are given in Figure 1.

---

[5] Now at the Institute of Zoophysiology, University of Oslo, Norway.

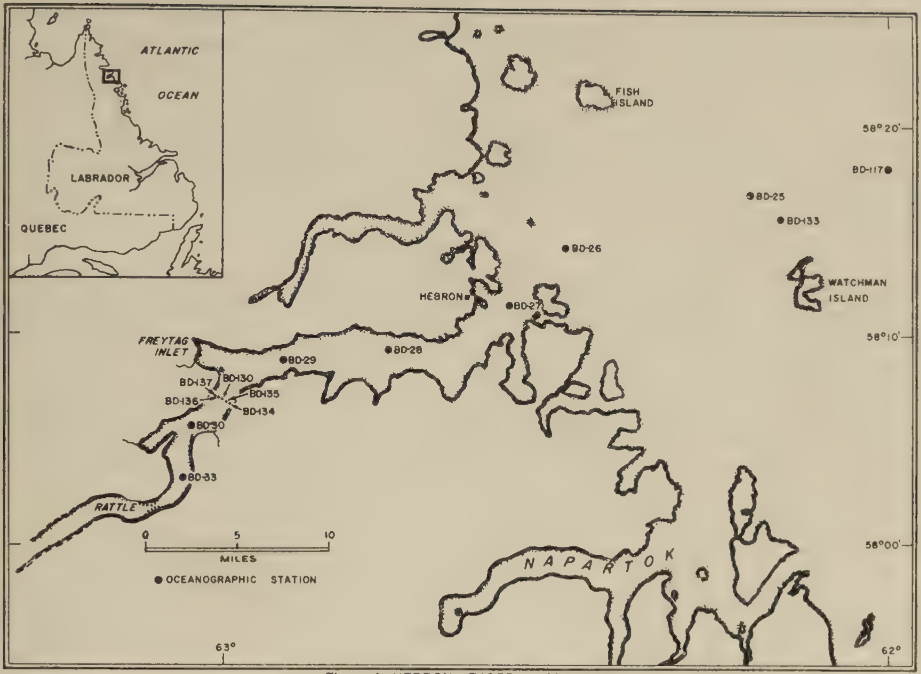
B
ATLANTIC
OCEAN
LABRADOR
QUEBEC
FISH ISLAND
58° 20'
BD-117
BD-25
BD-133
BD-26
WATCHMAN ISLAND
HEBRON
BD-27
58°10'
FREYTAG INLET
BD-29
BD-28
BD-137
BD-130
BD-136
BD-135
BD-134
BD-30
BD-33
RATTLE
0
5
10
MILES
● OCEANOGRAPHIC STATION
58°00'
NAPARTOK
63°
62°

Figure 1. HEBRON FJORD, LABRADOR.

Temperature observations were taken by means of both bathythermograph (BT) and protected deep-sea reversing thermometers. All instruments were calibrated at the Woods Hole Oceanographic Institution. As the depths involved were not great, the depth of observation was determined by the length of submerged wire × the cosine of the wire angle with the vertical.

Water samples were taken by means of Nansen bottles. Determinations for dissolved oxygen and inorganic phosphate were made in every case on board the vessel. The Winkler method was used for oxygen, while the phosphate determinations were made colorimetrically. In 1952 these were done by comparison with standards and the results are considered of only limited accuracy. In 1954 an electric eye photometer (EEP) was used.

The chlorinity titrations were made by the Knudsen method. In some cases these were done at the Woods Hole Oceanographic Institution and in some cases on board the *Blue Dolphin*. In cases where titrations were performed on board, certain selected samples were kept and returned for check titration at Woods Hole. In most cases substantial agreement was found between the shipboard results and the results at Woods Hole, so it is felt that shipboard titrations had a maximum probable error of ±0.05‰.

Observations during the summer months were made in a routine manner from the *Blue Dolphin*. The fall observations in 1954 were made from a motorboat with hand winch and temporary A-frame. Winter regime observations during March 1954 were made through the ice from a pyramidal tent, with the hand winch and metre wheel mounted on the specially designed tent frame (Nutt, 1952). It might be added that winter water samples were taken in the usual 6-ounce rubber-stoppered glass bottles which were filled only three-quarters full and allowed to freeze. No damage to the bottles was incurred and the validity of the samples is clearly indicated by the results, which show an almost completely isohaline structure within extremely narrow limits of ±0.01‰.

1. Bathymetry

Offshore from Hebron Fjord are very few islands and the bottom topography is quite irregular, varying in depth from 75 to 200 m. Between Hebron and Cape Chidley at the northern tip of Labrador there are large areas dotted with islands and shoal ground.

In the mouth of the fjord is Kingmiktok (Island), approximately 2 miles long; and between it and the mainland to the south is a very shallow channel ½ mile wide. The main entrance to the fjord is to the north of the island and is 2 miles wide. A sill with a maximum depth of approximately 59 m. lies across this entrance.

The fjord extends uniformly to the west about 18 miles and then to the southwest another 10 miles. The average width is 1.8 miles. The shores are regular and steep-to, and are indented by four bays on the south shore and three bays on the north.

The fjord bottom topography is shown in the vertical profiles of temperature and salinity (e.g. Fig. 2). Beyond the innermost station, BD-33, is an unexamined area approximately 8 miles long. The connection between this area and the fjord appears to be narrow and shallow.

The fresh water enters the fjord at various locations along either side. The major streams, none of which are large, enter the fjord at four points: in Freytag Inlet, on the south shore 20 miles from the mouth, in an inlet 23 miles from the entrance on the northwest shore, and at the head of the fjord.

2. Climate

The climate of northern Labrador shows considerable variation from season to season and from the coast to the interior. During the winter months Labrador lies between the Icelandic low and the North American continental high which produces a prevailing northwesterly airflow and low winter temperatures. However, easterly winds off the comparatively warm Labrador Sea provide a moderating influence on the temperatures and the possibility of short periods of near- or above-freezing temperatures during any month of winter. During summer the Icelandic low as well as the continental high dissipate, and a weak low appears over Hudson Strait and southern Baffin Island. Then the prevailing airflow is from the west and southwest which, with the continental heat of summer, can bring temperatures in Labrador into the 80's and 90's (Fahrenheit). However, due to intense land warming these westerly winds are often replaced along the immediate coastal fringe by a sea breeze that brings in cold air and fog from the ice pack and cold Labrador Current.

In Labrador the heaviest precipitation occurs in the southern part with an annual total of about 40 inches near Battle Harbour. Amounts of precipitation decrease regularly northward until at Resolution Island in Hudson Strait there is a total of only 16 inches.

Recent climatological observations at Hebron (Department of Transport, 1954) are based on only 4 years of record. Temperature data from this short period are deemed of sufficient accuracy for the purposes of this paper to indicate the general annual temperature regime.

On the other hand this 4-year period is not considered long enough in the case of the precipitation data on which freshwater run-off computations are based, especially as the general pattern of seasonal distribution of precipitation is in disagreement with that of the nearby stations of Nain, Hopedale, Indian House Lake and Resolution Island, where longer periods of observation are available. In order to arrive at a more representative picture for the precipitation in the Hebron area the following method has been used:

(a) Precipitation data from Hopedale (10 years of record) and from Resolution Island (19 years) have been averaged. Hebron is located approximately midway between these two stations.

(b) The figures arrived at from (a) are weighted 2.5:1 with respect to the actual Hebron data and a weighted average is thus obtained.

This computed precipitation is summarized with the temperature in Table I.

TABLE I.—Climatological data, Hebron Fjord area.

Month	Computed precipitation	Temperature
	inches	°*F.*
Jan.	1.77	0
Feb.	1.54	−3
Mar.	1.61	10
April	1.62	23
May	1.88	32
June	2.42	40
July	2.15	50
Aug.	2.28	50
Sept.	2.85	40
Oct.	1.52	34
Nov.	1.45	26
Dec.	1.97	14
For year	23.06	Average: 26

3. CONTRIBUTIONS OF FRESH WATER

Since the contribution of fresh water to the fjord water is one of the important factors influencing the hydrographic conditions, an attempt through analysis of precipitation data and watershed area is made to arrive at an approximate figure for the annual cycle of this contribution. The actual drainage area of Hebron Fjord has not been delimited, since certain sections of the interior are to date unmapped. However, an approximate watershed has been assumed and its area computed as $2{,}658 \times 10^6$ m^2. The area of Hebron Fjord itself is 224×10^6 m^2.

The following further assumptions are made:

(a) Precipitation is held in the form of snow from November 1 until May 15, and that the accumulated amount is released into the fjord from May 15 until July 15, by which time the larger part of the snow has been melted. This assumption means that fresh water is added in blocks and shut off suddenly on November 1, whereas actually the change in inflow varies progressively and likely fresh water is added in relatively small quantities well through November, December, and even into January.

(b) Run-off during May and June is equal to 80% of the actual precipitation and the run-off from July 1 until November 1 is equal to 60% of the actual precipitation. The Hebron Fjord drainage area is unforested, with rock outcroppings along the coast and permafrost in the interior. Although these percentages are arbitrary they are believed to be within reason for the area concerned.

(c) The melting of ice and snow cover in the fjord from May 15 to July 1 contributes an amount of fresh water equivalent to the melting of approximately one metre of ice of a salinity of 5‰.

This last assumption may or may not be valid, depending on the particular conditions prevailing in any particular year, but is an estimate of the average condition. At times all or part of the ice may melt in situ, or might break up and be carried outside the fjord to melt in the coastal waters, or as in July of 1954 pack ice from offshore might invade the fjord and make a contribution of fresh water.

The inherent inaccuracies in these assumptions together with the limitations of the available data are recognized, but it is believed that the figures for contributions of fresh water (Table II) present a reasonable picture of the volumes of fresh water involved.

TABLE II.—Contributions of fresh water, Hebron Fjord.

	Jan.	Feb.	Mar.	Apr.	May 1-15	May 15-31	June	July 1-15	July 15-31	Aug.	Sep.	Oct.	Nov. 1-15	Nov. 15-30	Dec.
Precipitation, *mm.*	45	39	41	41	24	24	61	28	27	58	72	39	18	19	50
Precip. accum. for run-off, *mm.*	0	0	0	0	0	87[c]	188[c]	91[c]	27	58	72	39	18	0	0
Run-off %	..	..	..	..	..	80	80	60	60	60	60	60	60	..	..
Fresh water to fjord by run-off[a], m^3 x 10^6	..	..	..	..	..	169.4	366.1	132.9	39.4	84.7	105.1	57.0	26.3	..	..
Fresh water direct[b], m^3 x 10^6	..	..	..	..	..	5.4	13.7	6.3	6.0	13.0	16.1	8.7	4.0	..	..
Melting of ice, m^3 x 10^6	..	..	..	..	..	63.5[d]	126.9[d]	..	.	..	..	.	.	.	..
Total fresh water, m^3 x 10^6	..	..	..	..	..	238.3	506.7	139.2	45.4	97.7	121.2	65.7	30.3	.	..

[a] Watershed less Fjord 2,434 x 10^6 m^2.

[b] Fjord 224 x 10^6 m^2.

[c] 25% of total winter accumulation of precipitation runs off during May 15-31, 50% in June and 25% in first half of July.

[d] One metre of ice of salinity 5‰ melts between May 15 and July 1.

4. TIDES AND CURRENTS

Along the greater part of the Labrador Coast the tidal range is from 3 to 6 feet. Only in the extreme northern part of the coast in the vicinity of Cape Chidley do the large tidal ranges that are well known in Ungava and Frobisher Bays begin to occur. Tidal observations were made at the village of Hebron from early July through the end of October 1954 and are summarized as follows:

	July (19 days)	Aug. (31 days)	Sept. (30 days)	Oct. (30 days)
HWI (hr.)	6.47	6.50	6.26	6.06
LWI (hr.)	12.63	12.73	12.70	12.35
MTL (ft.)	3.04	3.16	3.29	3.26
Mean (ft.)	4.18	3.92	4.04	3.81

The average flow of the Labrador Current has been estimated at some 10 miles per day (Iselin, 1932). Smith, Soule, and Mosby (1937) have calculated velocities as high as 38 miles per day. But information as to the nature and velocities of currents in the immediate coastal waters and inlets is conspicuously lacking. The movement of a cold water mass along the immediate coast near Hebron was traced during the summer of 1954 and its movement from north to south shown to be roughly 2 miles per day (see below). Within Hebron Fjord strong currents have never been noted. After a northeast storm on July 13 and 14 which drove pack ice some 20 miles into the fjord it took more than a day for the remnants of this ice to break up and move out to near the mouth of the fjord, which would show a net surface outflow of considerably less than 1 knot over this period. It is believed that velocities within the fjord seldom exceed 2 knots.

II. OCEANOGRAPHIC FACTORS

The oceanographic data show that during midwinter, which oceanographically occurs in April, the fjord water and the coastal water are virtually isothermal and isohaline. The coastal water appears to be very slightly colder than the fjord water, and a small progressive freshening from the coast toward the inner fjord is indicated. The average winter temperatures and salinities in 1954 were:

	Inner fjord	Mid fjord	Coastal
Average temperature, °C.	–1.76	–1.75	–1.78
Average salinity, ‰	32.73	32.75	32.76

These uniform midwinter conditions were altered during the course of the annual cycle by the seasonal changes in the Labrador Current, the climatic changes, and the contributions of fresh water from land drainage and melting ice. However, during the winter of 1955 it was expected that the conditions would again become uniform at very near the same point. (See later for discussion of longer-term trends.)

An examination of the various oceanographic factors now follows.

1. TEMPERATURE

Longitudinal profiles of Hebron Fjord showing the distribution of the temperature (°C.) for the times of observation during July, August and October 1954 are given in Figures 2, 3, and 4. As has been noted, the water in winter is isothermal and isohaline, and vertical convection processes are in progress.

The first heat of spring is used in the melting of ice, and heat is transferred to the fjord waters only when the ice surface becomes rotten and broken. However, by the time of the early summer observations on July 9 and 10 warming has taken place in the upper layers and is noticeable down to between 60 and 80 m. It is noted that the —1.5°C. isotherm slopes progressively down from the inner part of the fjord and disappears outside the fjord where heat has penetrated to the very bottom. At station BD-26 even with pack ice of concentration of 0.8 to 0.9 extending 100 miles offshore the temperature at 100 m. is as high as —1.29°C. At this depth the temperature within the fjord remains unchanged from that of winter. There then must be a greater mixing in the coastal waters, due to the greater movements and turbulence of the inner edge of the Labrador Current and associated coastal eddies as they pass over rough submarine topography. The downward mixing and transfer of heat below sill depth within the fjord is, as may be expected, much more restricted and is far less at BD-33 which lies inside of a 31-m. sill.

There are small temperature inversions at BD-26 and within the mouth of the fjord at BD-27 and BD-28, indicating a more vigorous exchange and mixing

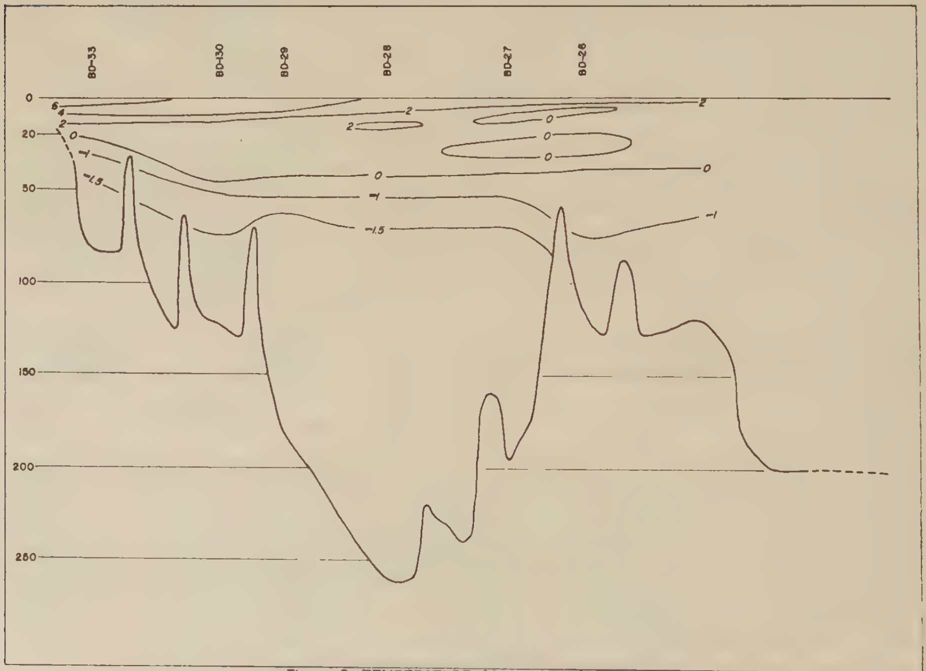

Figure 2. TEMPERATURE °C., July 9-10, 1954.

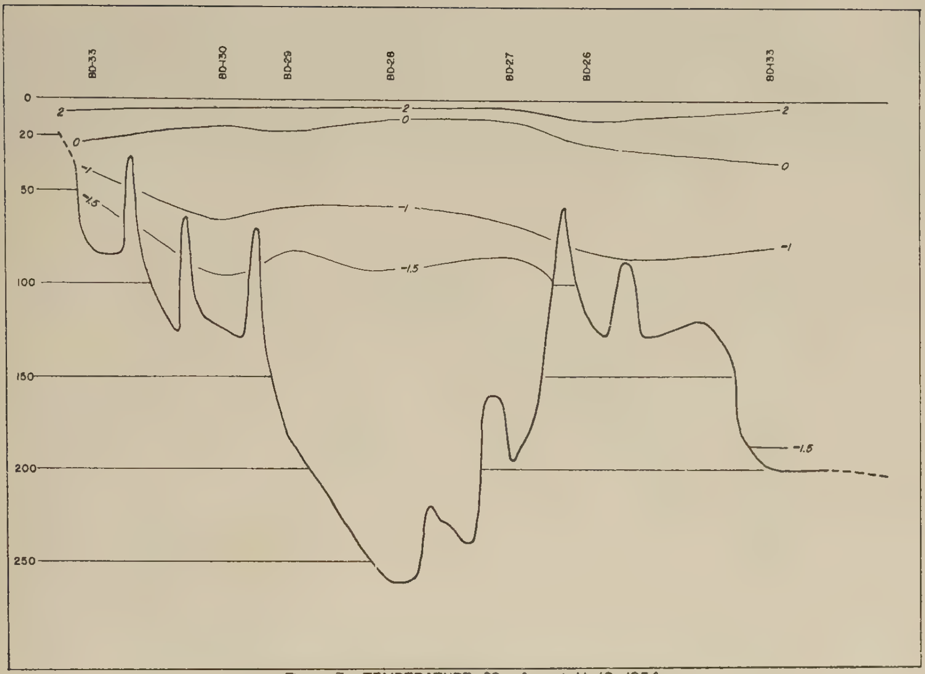

Figure 3. TEMPERATURE °C., August 11-12, 1954.

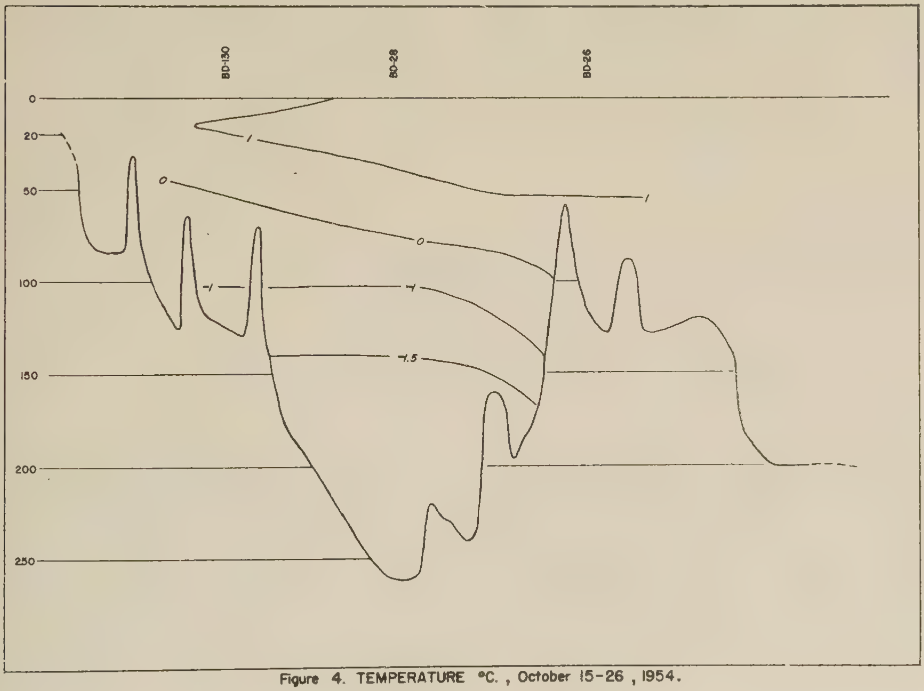

Figure 4. TEMPERATURE °C., October 15-26, 1954.

in this area than in the inner part of the fjord. However, the BT observations on July 15 taken at and near BD-130 show a large temperature inversion between 20 and 40 m. This is likely the result of the northeast storm of July 13–14 which filled the fjord with ice for a distance of 25 miles. The cooling effect of this ice was apparently small as quantitative heat calculations from the July 15 BT showed in fact a continued addition of heat (see below).

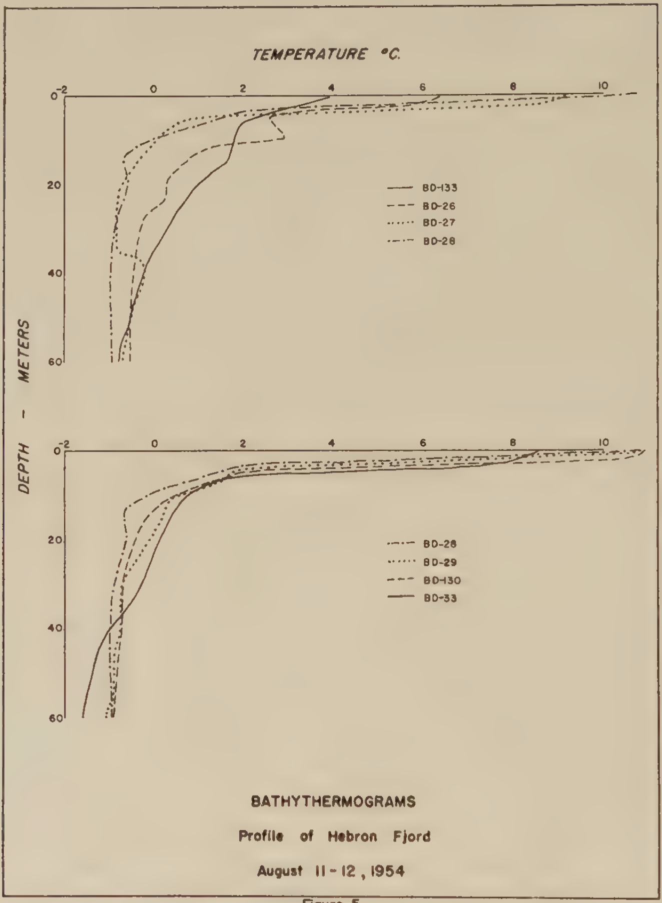

BATHYTHERMOGRAMS

Profile of Hebron Fjord

August 11 - 12, 1954

Figure 5.

On August 12 when the last summer observations were taken, unusual and apparently anomalous conditions are noted. The very surface waters show a continued warming, and so do the very bottom layers where heat has penetrated below 100 m. However, beween 5 and 50 m. a great drop in temperature can be seen. Since air temperatures and inflowing fresh water during the summer months are at all times above freezing (mean July and August temperatures are 50°F.), the only possible source of negative temperatures is the coastal water. But on August 11 at BD-26 and at BD-133 further offshore there is no evidence of low enough temperatures above sill depth to account for this cold water mass. It can only be supposed that at some time, perhaps during early August, a mass of cold water was present at the mouth of the fjord and that the reduced temperatures within the fjord are a result of exchange with this cold water mass. By the time of the August 11 observations evidence of this cold has been removed from the waters outside by the Labrador and coastal currents. The introduction of this cold water was quite rapid, and the re-establishment of what might be termed "normal conditions" (as indicated by the August 11 observations at BD-26) appears to have been equally rapid.

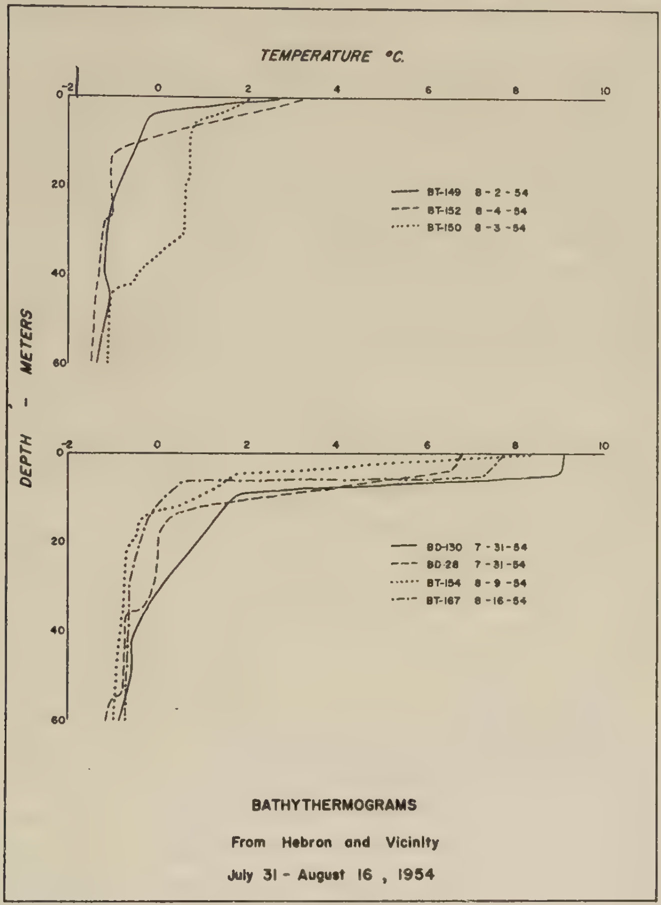

BATHYTHERMOGRAMS

From Hebron and Vicinity

July 31 - August 16, 1954

Figure 6.

The BT traces down to 60 m. for the seven stations of the August 11–12 profile are given as Figure 5. These illustrate clearly the nature and extent of this cold water mass that has penetrated the fjord. The offshore station, BD-133, shows no evidence of the cold water, and there is only slight evidence at BD-26 outside the mouth of the fjord. At BD-27 and BD-28 the upper layers are markedly colder than outside the fjord. BD-29 is similar in character but not as cold as BD-28. The same may be observed at BD-130 and BD-33, with the upper layers of each slightly warmer than the next station just outside. At BD-33 to 40- to 60-m. layer is, however, somewhat colder (about 0.5°C.) than at BD-130, a result of the 31-m. sill between the two stations. Thus in the process of exchange between the waters of the fjord and the coastal water, the cold water mass has been progressively tempered in penetrating the fjord. At the time of these observations its removal by exchange with the coastal water was taking place.

Various BT records from late July and the first two weeks of August are compared in Figure 6. BT-149 was taken August 2 about 2 miles WSW. of Fish Island and indicates the presence of a mass of cold water from 5 m. down. BT-152 was taken in the same place 2 days later, and the cold water mass was still present but surface warming has lowered the 0°C. point from 5 m. to 10 m., while the layers immediately beneath still contain water below —1.0°C. On the day between these observations (August 3) BT-150 was taken in conjunction with the occupation of BD-133 located approximately 10 miles farther offshore, and the cold water does not extend out this far. Shown also are the July 31 BT traces for BD-130 and BD-28 in the fjord. The cold water mass at this time has started to penetrate the fjord, as water of 0°C. may be noted below 15 m. at BD-28. The cold mass has not yet reached to BD-130. BT-154 was taken in Napartok to the south of Hebron on August 9, and by this time the cold water had to a certain extent penetrated this fjord. BT-167 taken August 16 in Mugford Tickle shows the remnant of the cold water mass at this time located 30 miles to the south of the Hebron area.

These BT records show that the cold water mass which so markedly influenced the fjord temperature structure at the time of the August 11–12 observations was very limited in size and passed quite rapidly from north to south off the entrance to Hebron fjord during the last few days of July and the first few days of August at a rate of approximately 2 miles per day.

Observations taken between October 15–26 show that autumnal cooling of the surface layers had begun, especially in the inner part of the fjord where the surface waters were practically at the freezing point and slob ice was observed along the shores. However, the maximum results of summer warming can now be noted in the intermediate and bottom layers. Outside the fjord negative temperatures have disappeared completely. Heat has penetrated to the very bottom water of the fjord as shown by the change of temperature at 250 m. at BD-28 from —1.76°C. in August to —1.68°C. in October.

In order to show more clearly the effects and magnitude of the annual thermal regime, computations of the quantities of heat in a column of water of 1 cm.^{2} cross-section at stations BD-26, BD-28 and BD-130[6] are given in Table

---

[6] Actually BD-30, located several miles further in the fjord, was occupied on April 7. Under the virtually isothermal and isohaline conditions of winter data from BD-30 and BD-130 may be considered identical. On several occasions in this paper, the April data from BD-30 have been compared with summer and fall data from BD-130.

III. The computation used is $Q = T \times c_p \times \rho_{s,\,v,\,p} \times h$ where Q is the heat in gram-calories, T is the average temperature, c_p is the specific heat, $\rho_{s,\,v,\,p}$ is the density in situ, and h the height of the column. The quantity of heat is shown for 0 to 50 m., which level lies entirely above the sill and will have free exchange with the coastal water; for 50 to 100 m., which level lies for the most part below sill depth; and for the total column 0 to 100 m. Below 100 m. the changes are quite small.

TABLE III.—Heat (in gram-calories) of a column of water one square centimetre in cross-section at various stations, 1954.

Depth *m.*						
			BD-26			
	March 26	July 10			Aug. 11	Oct. 15
0–50	−8,608	446			3,793	6,647
50–100	−8,625	−4,844			−3,489	3,533
0–100	−17,233	−4,398			304	10,180
			BD-28			
	March 29	July 10			Aug. 12	Oct. 18
0–50	−8,470	4,317			42	6,053
50–100	−8,481	−6,791			−5,820	969
0–100	−16,951	−2,474			−5,778	7,022
			BD-130			
	April 7	July 9	July 15	July 31	Aug. 12	Oct. 26
0–50	−8,517	7,491	10,064	8,476	1,500	2,166
50–100	−8,481	−7,510	− 5,959	−5,815	−5,819	−1,453
0–100	−16,998	−19	4,105	2,661	−4,319	713

Between March and July in the 0- to 50-m. level the greatest warming has taken place at BD-130 and the least at BD-26, while the opposite is true for the 50- to 100-m. level. In the total column the greatest heat increase in this period is at BD-130. This may be accounted for by the warmer climatic conditions within the fjord and that by July the inflow of fresh water is likely above 0°C., whereas at BD-26 the fresh water is largely from melting ice at 0°C. and the large ice cover offshore inhibits heat transfer from the atmosphere. Thus in July heat is being added more rapidly to the waters in the fjord than to the coastal waters and heat is being transferred above sill depth from the fjord to the coastal water through the processes of exchange.

The quantitative heat determinations for the August 11–12 observations show that the cooling of the intermediate layers is not possible by heat transfer with the atmosphere but must be caused by external exchange since there has been a considerable net loss of heat by the water mass in the fjord. As in July, BD-130 remains warmer than BD-28 but there is less difference. The cold water source has passed by BD-26 where it would appear that only a progressive summer warming has taken place.

After October 15 heat is being lost at the surface and at or just prior to this time of year the maximum warming is attained. In the 0- to 50-m. level there appears to be progressively less heat from BD-26 toward BD-130, but this might be due to the fact that BD-26 was occupied on October 15, while BD-28 was occupied on October 18, and BD-130 on October 26. At this time rapid cooling was taking place and ice was forming close to shore near BD-130. The water from 50 to 100 m. as well as the total 0- to 100-m. column is in every case warmer than in August, but considerably more heat is found in the coastal water than in the fjord water.

2. SALINITY

Longitudinal profiles of Hebron Fjord showing the distribution of salinity in ‰ for the times of observation in July, August, and October 1954 are given in Figures 7, 8, and 9. During the winter season virtually isohaline conditions prevail in the coastal water and within the fjord. As long as ice formation is in progress as well as the continuing exchange with the slightly more saline water from outside with the fjord by tidal action, salting of the fjord will continue.

When spring thaw commences, which is estimated as beginning about May 15, the snow and ice melt very rapidly, and within a relatively short period of time a large quantity of fresh water is introduced into the fjord. As this fresh water enters the upper layers, the convection of winter ceases immediately, and a stable density gradient is established.

By July 9 and 10 when the first observations of the summer were taken, the surface layers have freshened as deep as 80 to 100 m. while the large mass of bottom water remains largely unaffected. In Figure 7 the sloping of the 32.0 and 32.5‰ isohalines shows a greater downward mixing in the coastal and outer fjord water than in the inner. This confirms the evidence of the thermal regime

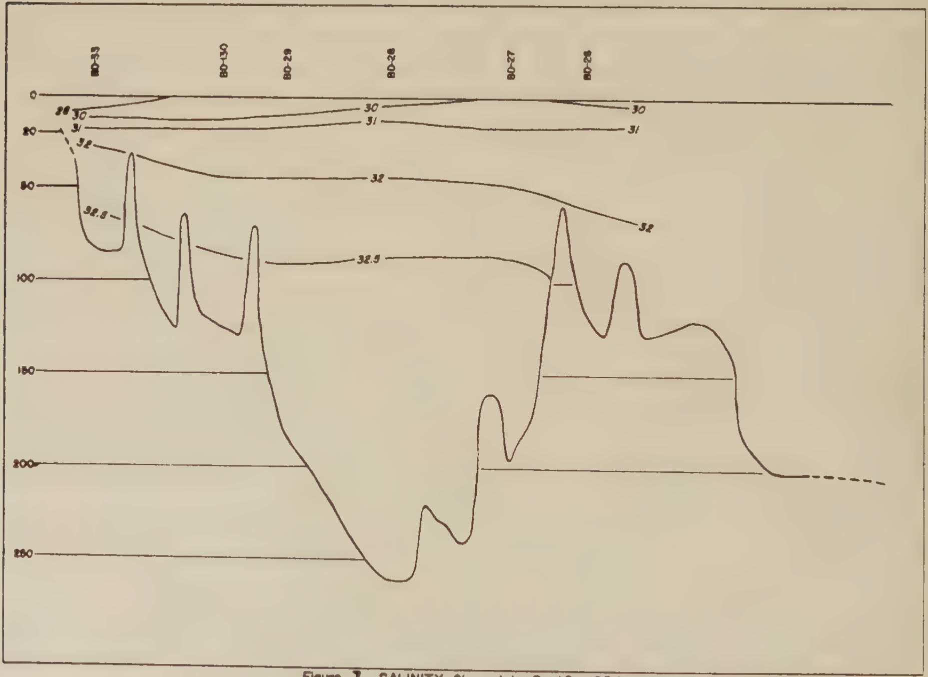

Figure 7. SALINITY ‰, July 9-10, 1954.

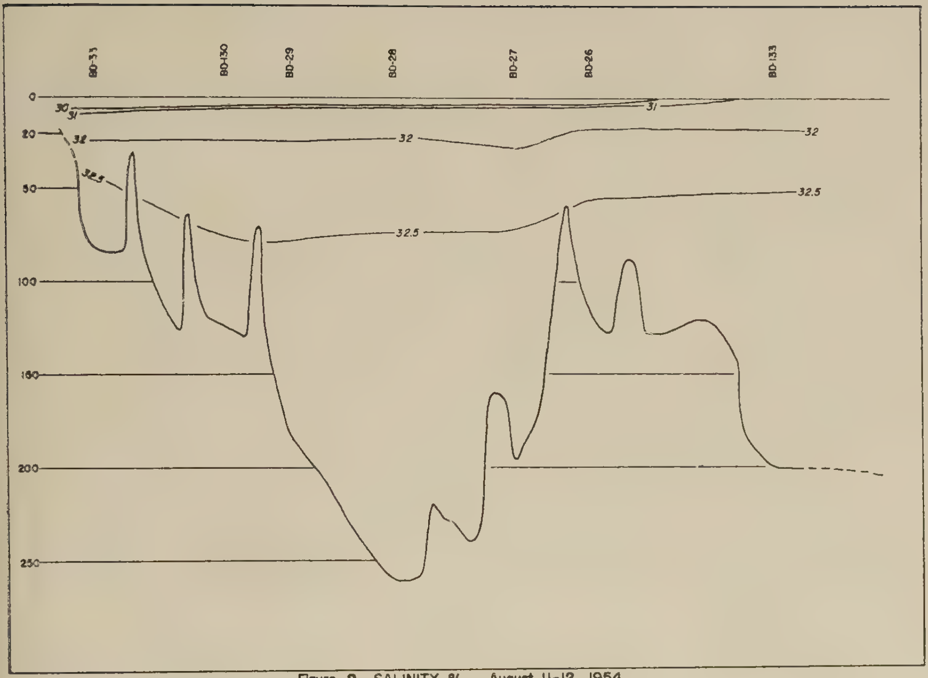

Figure 8. SALINITY ‰, August 11-12, 1954.

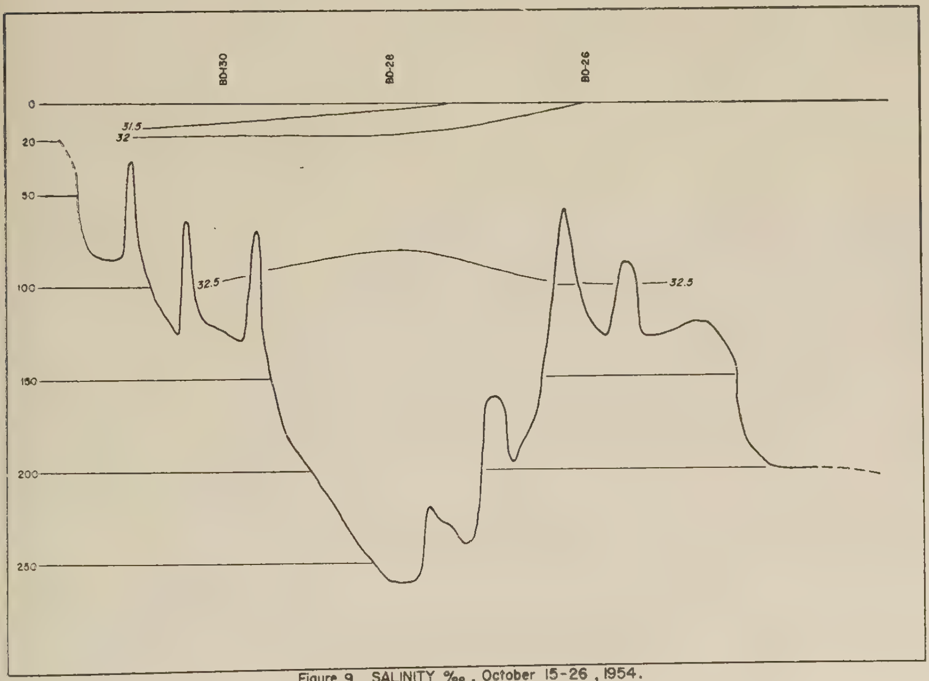

Figure 9. SALINITY ‰, October 15-26, 1954.

that there is greater turbulence and mixing in the coastal water likely due to the Labrador and associated coastal currents passing over the rough submarine topography of the continental shelf. More stable conditions and less vertical mixing prevail within the confines of the fjord. The transport of this more thoroughly mixed water into the fjord by tidal action can be seen by the progressively more stable stratification toward the inner part of the fjord.

As the summer progresses marked salting takes place in all but the very surface layers, particularly the intermediate layers above sill depth. The quantity of fresh water in the fjord responds to the volume inflow of fresh water, which by August is markedly less than the spring freshet effect noticeable in July. This salting is brought about by exchange with the coastal water and may be associated with the inflow of very cold water between observations noted previously. The observations at BD-130 taken July 31 show that an even greater freshening has taken place than earlier in July, so this sharp salting of the fjord must have been rapidly accomplished in the early days of August.

The October salinity profile (Fig. 9) shows a sharp salting of the 0- to 5-m. level due to the decreased run-off during the fall, and a continued slight freshening of the layers below sill depth due to the continued downward mixing of the comparatively fresher waters. The intermediate water of the fjord, below 5 m. and above sill depth, is quite similar to the August condition while salting has taken place outside the fjord at BD-26. The return to midwinter isohaline and isothermal conditions is accomplished by continued autumnal cooling, the formation of ice, and exchange with the Labrador Current.

3. OXYGEN

During the summer investigations in Hebron Fjord selected water samples were analysed for dissolved oxygen content. Essentially the same pattern of oxygen distribution is noted during each summer; and only the 1954 data is presented in Figure 10 for discussion.

The over-all high oxygen content of these waters is at once apparent. Photosynthetic activity appears to be producing an abundant supply of oxygen and the water above 30 m. is largely supersaturated. The water below 30 m. contains less oxygen, but there is always at least 6.0 ml./l. both offshore and within the main body of the fjord. The evidence of a reduced oxygen supply in the 50- and 75-m. levels at BD-33, which station is located inside a 31-m. sill, shows a reduced circulation and exchange in this inner basin.

The data from 100 m., which is well below the fjord sill depth and the euphotic zone, indicate a tendency toward progressively less oxygen from the coastal water toward the inner part of the fjord. Station data from BD-28 (with the exception of 250 m.) and to a lesser degree from BD-130 indicate also a slight tendency toward oxygen depletion as the season progresses.

Lack of oxygen data at seasons other than summer prevents more than a speculation concerning the annual cycle of oxygen distribution. It can be supposed that with the warming of the lower levels of the fjord during the fall, a greater metabolic rate and concurrent oxygen consumption among the animal

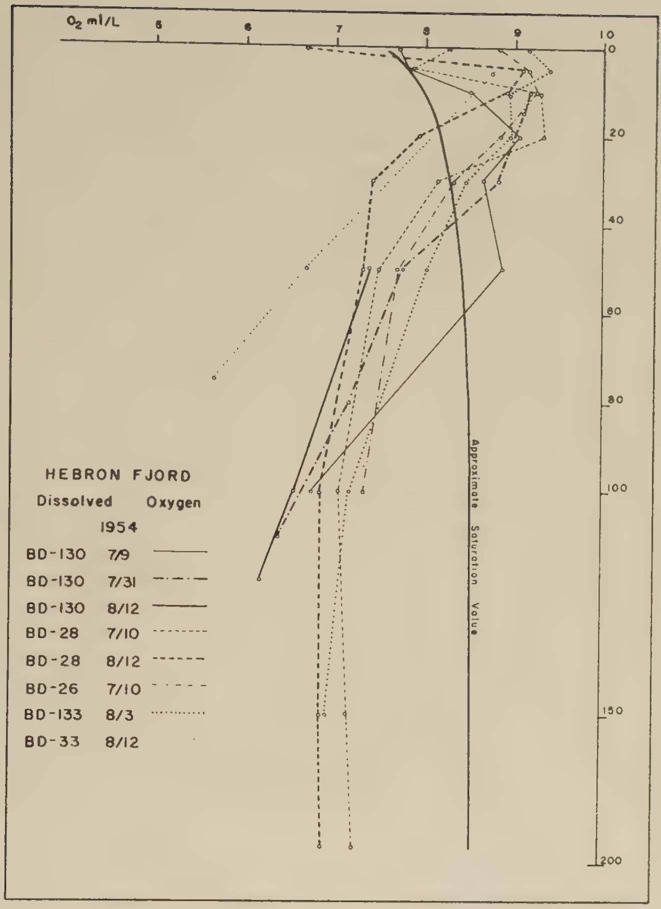

Figure 10.

populations may take place. However, at this time of year with the cooling and salting of the upper layers there is less density gradient, and exchanges and renewal are more rapid. After the formation of ice, through which the diffusion of atmospheric gases is nil (Scholander *et al.*, 1953), oxygen maintenance and renewal must take place through exchange above sill depth between the fjord and coastal waters and downward convection from the upper layers. In any case there would appear to be sufficient oxygen in all levels of Hebron Fjord throughout the year to support marine life.

4. INORGANIC PHOSPHATE (PO_4)

Determinations of inorganic phosphate content were made on samples of water from selected stations during the summers of 1952 and 1954 and are presented in Figure 11.

The 1954 data show in general an increase in phosphate with depth and it may reasonably be supposed that the reduction of phosphate in the upper layers is associated with photosynthetic activity. In comparing the data from July with those from August a tendency is noted at each individual station toward a general increase in phosphate content above 100 m. as the summer progresses.

Quite a different pattern is shown by the 1952 data. Since these were obtained by visual comparison to colour standards rather than by EEP, great reliance in the precision of these data is not warranted. There is, however, a strong indication that the available inorganic phosphate in 1952 was considerably less than in 1954, due perhaps to a greater depletion through productivity and/or to a smaller supply by renewal.

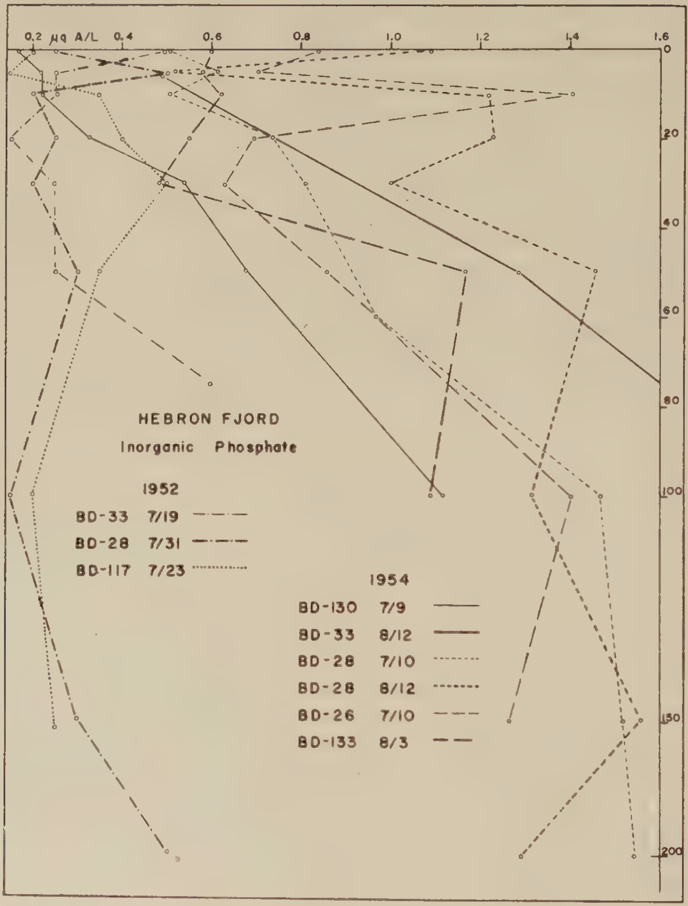

Figure 11.

5. Temperature–Salinity Relationships

Temperature–salinity (*T–S*) diagrams are useful in identifying water masses and determining their relationships. The uniform isothermal and isohaline conditions during winter in Hebron Fjord form a single point on the *T–S* diagram, which shows that a single uniform mass of water of the character of the Labrador

Current prevails at this season. This point on the diagram may vary from year to year within relatively narrow limits dependent on the Labrador Current, which is the controlling factor in the determination of the winter structure of Hebron Fjord.

The *T–S* relationships as observed in Hebron Fjord during the summer and fall of 1954 are given in Figures 12, 13, and 14. For simplification, observations showing extreme freshening and warming of the surface have been omitted.

In the course of the summer fresh water is added to the fjord. This fresh water must enter first at a temperature of 0°C. and later at temperatures as high as 10 to 15°C. If the water in the fjord were only a result of the mixing of this fresh water with the Labrador Current water of winter, the *T–S* plot would lie within the limits indicated in Figure 12. The actual plot is more upright, indicating the absorption and downward transfer of heat in the Labrador Current, coastal waters, and within the body of the fjord during summer.

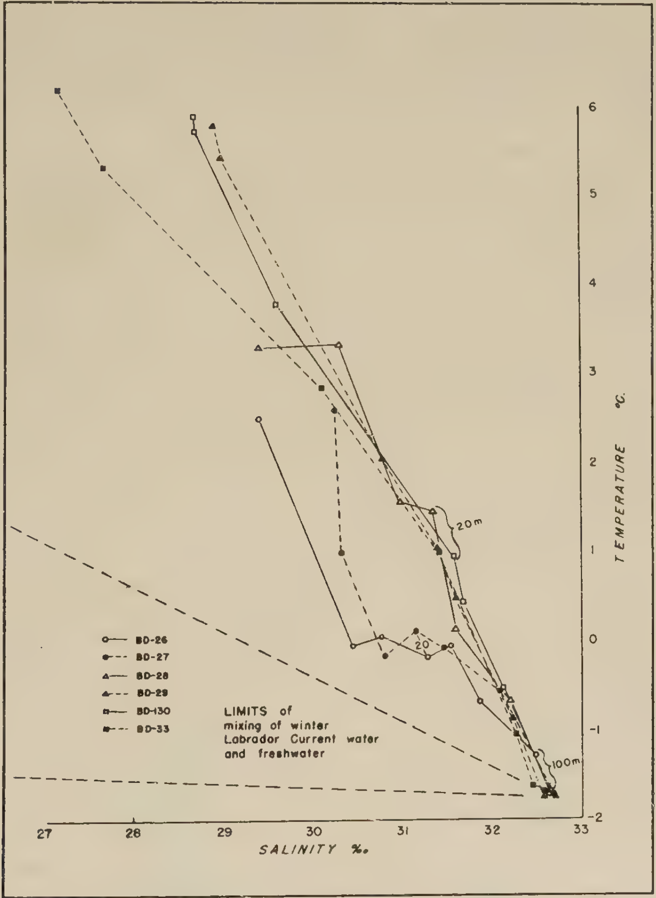

Figure 12. T-S DIAGRAM, July 9-10, 1954.

The influence of the ice cover on this downward transfer of heat can be seen from the July diagram (Fig. 12) in which BD-26 and BD-27, just offshore and within the mouth of the fjord, show a freshening with little warming, largely from melting ice, while in the inner part of the fjord much greater warming has taken place. At the time of the July observations, BD-33, BD-130, and BD-29 were all ice-free; scattered ice lay at BD-28, and BD-27 and BD-26 had 0.5 to 0.8 ice cover.

At the time of the August observations (Fig. 13) a decided salting and a continued warming has taken place in the coastal water where similar conditions exist at BD-26 and BD-133, some 10 miles further offshore. Relationships within the fjord are only slightly changed from those of July, which may be due in part to the influx of cold water noted at this time. From the *T–S* diagram (Fig. 13) we can determine more completely the character of this cold water mass. The temperature of the mass before it entered the fjord was —1.2 to

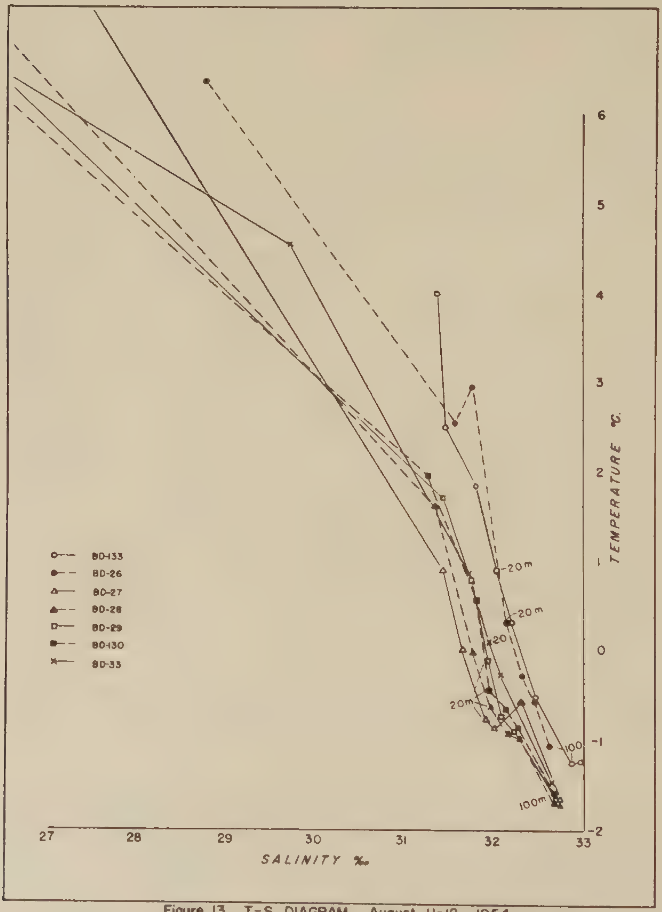

Figure 13. T-S DIAGRAM, August 11-12, 1954.

—1.3°C. (Fig. 6); and as it was coastal water, the salinity must have been 32.70 to 32.80‰.

The largest change in the character of the water masses occurs in late summer and fall, by which time all ice has melted, land drainage decreased, and surface cooling begun. At BD-130 the surface layers have cooled significantly to temperatures lower than the underlying layers where summer heat is still trapped. While the cooling and salting of the upper layers is taking place a continued slow reflection of summer warming and freshening in the bottom layers may be noted. As a result of the fall processes the water becomes more uniform, the density gradient becomes weaker and there is greater possibility of downward transport by turbulence. This can be seen in the continued freshening and warming of the bottom layers at this season. The changes in the very bottom layers, however, are of relatively little magnitude and virtually stable conditions prevail throughout the annual cycle.

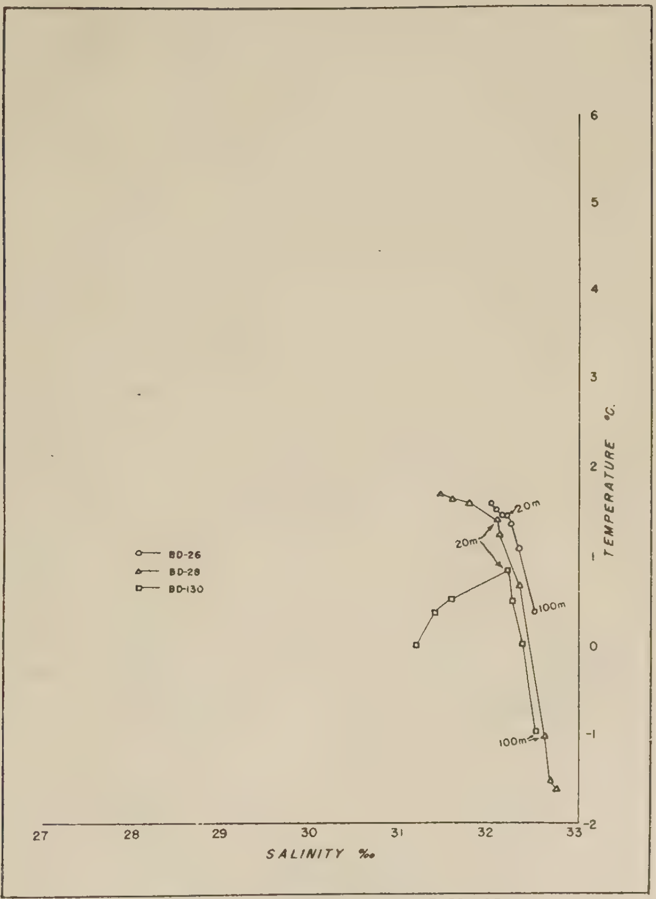

Figure 14. T-S DIAGRAM , October 15-26, 1954.

The *T–S* relationships show that in the course of the annual cycle the character of the water undergoes a considerable change. In the coastal waters the freshening takes place in advance of the warming while in the late summer and fall salting precedes the cooling. The same process occurs within the fjord, but varies within narrower limits. The late summer and fall changes show a lag of the fjord water in attaining through exchange the character of the coastal water. This, together with the rapid influx of the cold water mass in August, points out that conditions within the fjord are determined to a large degree by the conditions in the coastal waters. Finally the uniformity of the bottom water of the fjord with little variation throughout the annual cycle is emphasized in comparison to the more substantial warming that occurs in the bottom layers offshore.

So far only the seasonal cycle in 1954 has been considered. In Figure 15 are plotted the *T–S* relationships for the 1949 and 1952 observations together with the August 1954 observations, which were selected as being most nearly comparable. To show the year-to-year relationships more clearly a line plot of the average coastal and main fjord relationships is given (Fig. 16).

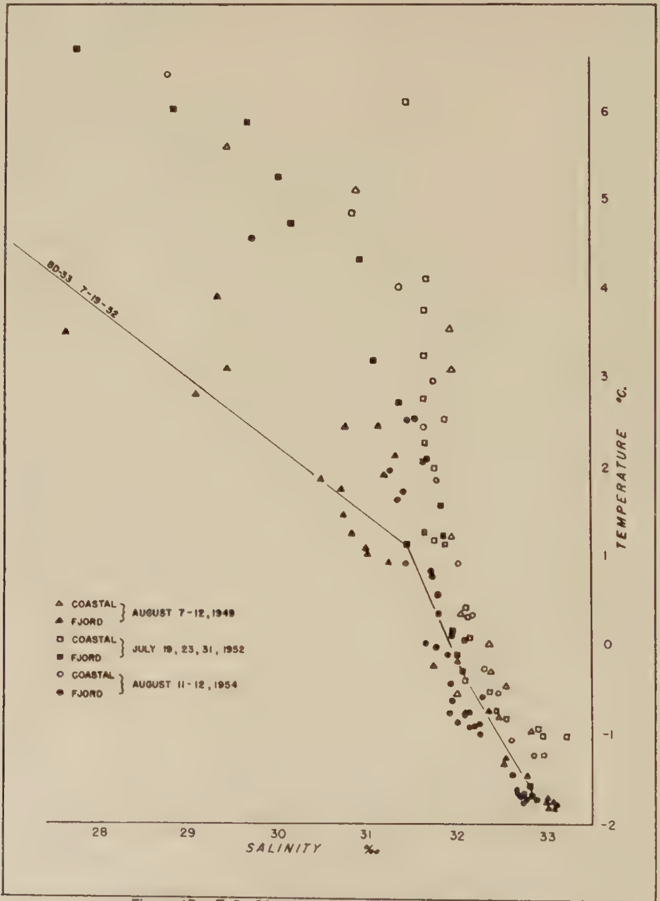

Figure 15. T-S COMPARISON, 1949, 1952, 1954.

One striking feature is the midsummer uniformity of the coastal water, with the exception of the surface where variations are bound to occur. A greater variation is noted within the fjord. The same conditions as described above in the seasonal analysis of the 1954 data seem to exist in 1949 and 1952. The coastal water in the upper layers is generally more saline. A greater difference between the coastal and fjord water in 1949 than in the other years is noted. In 1952 the fjord water is almost approaching the coastal water in character, which may be explained by the fact that the fjord observations were taken a week later, and as indicated in the seasonal cycle of 1954 the fjord water tends to attain the character of the coastal water. The single occupation of BD-33 on 19 July 1952 showed conditions much fresher and more characteristic of early summer (Fig. 15).

The 1952 coastal water observations were made at least 2 weeks earlier in the summer than were the observations in either 1949 or 1954, and the fjord water observations were made 8 to 12 days earlier. The fact that the 1952 relationships both within the fjord and in the coastal water are approaching a late

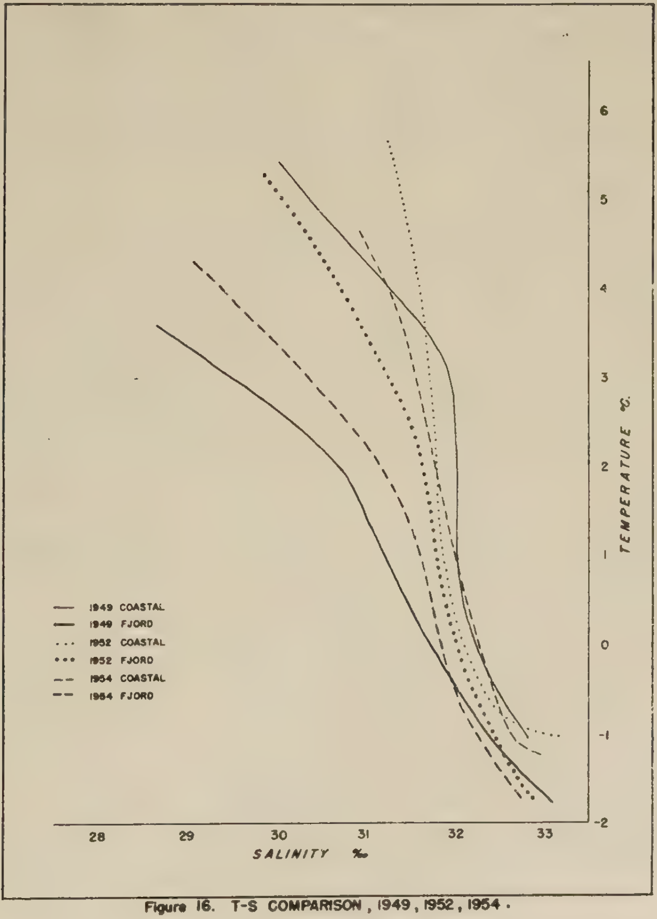

Figure 16. T-S COMPARISON, 1949, 1952, 1954.

summer condition at the earlier date suggests a more advanced season in 1952. This is borne out by the rather fine weather, early departure of ice, and the relatively little precipitation in 1952.

In the deeper layers there appears to be no specific relationship between the bottom water (below 100 m.) within the fjord and in the coastal waters. In each case slightly different *T–S* relationships are noted. The principal difference is the distinct warming of the very bottom water offshore while the bottom water within the fjord shows no change. Only very slowly does the summer heat and freshening penetrate to the levels below 100 m. inside the fjord, where no significant change is noted until late fall, at which time, because of the salting and cooling of the surface layers and the weaker density gradient, these effects can more readily be transported downward. That these effects are transported downward is clearly shown by the progressive freshening of the bottom water over the period from 1949–1954 (see Long-term Trends below). Unless the stable density gradient is overcome this freshening could not have taken place and the more saline water of an earlier year would have been trapped in the bottom with ensuing stagnation, of which there is no evidence.

It is at the same time quite evident from the March 1954 observations, with virtual isothermal and isohaline conditions within the fjord and coastal waters, that the character of the bottom water is determined by the conditions of the Labrador Current during the winter season and that this character is for all practical purposes retained well along toward late summer.

6. Long-term Trends

It is well known that the Arctic regions have been undergoing a period of climatic and oceanic warming (Dunbar, 1951; Jensen, 1939; Zubov, 1948). Off West Greenland water temperatures have risen 1.0 to 2.0°C. since 1920; but trends of such magnitude have not been measured in the Canadian eastern Arctic. Bailey and Hachey (1951a) reported an increasing Atlantic influence in Hudson Bay where between 1930 and 1948 there appeared to be a rise in temperature of the bottom waters of approximately 0.4°C. and an increase in salinity of 0.50‰. In comparing the 1949 *Blue Dolphin* data from 50 m. and below with corresponding 1926 *Chance* data, no apparent change seemed to have taken place (Nutt, 1953).

However, with the addition of the *Blue Dolphin* data of 1952 and 1954 and a better understanding of the oceanographic processes involved, a decided trend of small magnitude may now clearly be seen.

Observations in Hebron Fjord in 1954 show that by August the summer influences of warming and freshening have reached well below 50 m. These upper layers will be influenced by the amount and character of the run-off, the climatic conditions of the particular season, and the vagaries of the Labrador Current and coastal eddies.

However, in the lower levels seasonal changes are of small magnitude; and it is only in autumn that any significant changes can be noted below 100 m. The character of the very bottom layers would appear to be noticeably changed only within the period of a full annual cycle, particularly during the winter season at which time vertical convection takes place and the entire mass of fjord and coastal water becomes uniformly isothermal and isohaline with *T–S* characteristics of true Arctic water of the Labrador Current. It would therefore appear that this very bottom water assumes its *T–S* characteristics principally during this season and that the early and midsummer observations of these lower levels represent essentially conditions that had become established during the previous winter. Since winter observations have only been made once, any analysis of longer term trends must be made from the more numerous summer data. By restricting the analysis to the lower levels only, a reasonably valid picture which will not be obscured by irregular variations during summer may be obtained.

A *T–S* diagram showing a comparison of the 1926 *Chance*, and 1949, 1952, and 1954 *Blue Dolphin* data from 100 m. and below, is presented as Figure 17, and the *T–S* trends are summarized as follows:

Period	No. of years	Total warming	Warming per year	Total freshening	Freshening per year
		°C.	°C.	‰	‰
1929-49	23	0.03	0.0012	0.12	0.005
1949-52	3	0.05	0.017	0.24	0.08
1952-54	2	0.03	0.015	0.10	0.05

It must be pointed out that the *Chance* data are from Nachvak Fjord, while the *Blue Dolphin* data are from Hebron Fjord. Hebron and Nachvak Fjords are

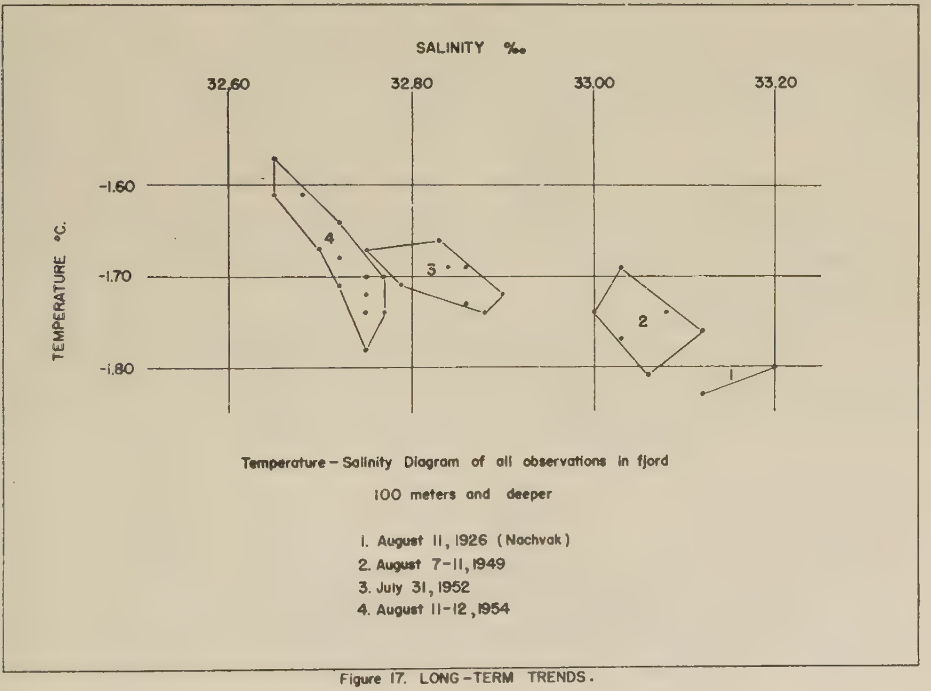

Figure 17. LONG-TERM TRENDS.

within 60 miles of each other and of quite similar bathymetric structure. It is believed that for the purposes of this paper a comparison of these data can reasonably be made.

A very slight warming trend and particularly a trend toward freshening can be readily noted. These trends would seem to be taking place at a more rapid rate in recent years during the period of the *Blue Dolphin* observations.

The 1926–49 trend is barely significant and the average per year rate of change of little meaning. However, from 1949 to 1954 a definite and regular trend is evident.

The coastal waters of Labrador lie on the "tail end" of the Arctic side of the over-all Atlantic–Arctic circulation. It is possible that the significant warming noted in the waters off West Greenland and elsewhere in the waters of the Northern Hemisphere is only in very recent years being felt in the Canadian waters of Labrador, and that the comparatively slight but definite trend, noted since 1949, is the beginning of a greater change as the Atlantic–Arctic circulation continues.

The freshening of the waters off Labrador is even more apparent. This freshening could be due to an increased annual precipitation with attendant increased land drainage. However, since the condition of the bottom water is determined largely during the winter period of vertical convection and exchange, when run-off plays no part, another explanation seems to be demanded.

A correlation with the recent changes in the Arctic Ocean is suggested. The decrease in general ice thickness, area of sea-ice cover, as well as the decrease in the thickness of the surface layer of Arctic water (Zubov, 1948) would result in the removal of a large quantity of fresh or low-salinity water from the Arctic Ocean and replacement by Atlantic water of higher salinity. This removal of fresh water would have to take place through the East Greenland and Canadian Currents, and the inner band of the Labrador Current. Freshening of the water of these currents tends to create a greater dynamic urge and a consequent greater volume of transport of Arctic water. It is also suggested that perhaps the Arctic water transported along the Labrador coast has served as the inhibiting restraint on any significant warming of the water (except summer processes) such as have occurred elsewhere in the Arctic.

A correlation between the increasing salinity in the bottom water of Hudson Bay and the decreasing salinity in the waters of the Labrador coast and fjords has not been established. Future investigations in Labrador and particularly in Hudson Bay are needed to clarify this problem.

III. ICE

Of all the oceanographic phenomena in Arctic and sub-Arctic areas, ice formation has perhaps the greatest practical significance, due to the limitations it imposes on navigation, aircraft landings, and surface transport. From December until June on the average Hebron Fjord is ice covered, which has several effects on the winter oceanographic processes.

Autumnal cooling and ice formation result in thermo-haline convection. Cooling and salting begins at the surface and progresses downward. The formation of ice has the actual net effect of adding salt to the water beneath, while the ice itself stores at the surface a substantial volume of fresh water to be returned to the fjord during spring thaw and break-up.

Ice thicknesses observed in Hebron Fjord during March and April 1954 were as follows:

Location	Ice thickness	Snow cover
	m.	*m.*
BD-26	0.41	0
Hebron Harbour	1 30	0.36
In fjord just off harbour	1.14	0.30
BD-28	0.84	0.25–0.30
BD-130	1.19	0.61

Essentially the same thicknesses were measured in the spring of 1955.[6]

Except for BD-26, where the station was purposely made in a newly frozen lead to lessen the work of cutting through the ice, the thicknesses are fairly representative of ice formation that might be expected with the greater amounts close to shore and in the inner fjord. In general one might estimate that an average of 1 m. of ice forms during a winter.

By computing the effects of the thermo-haline convection resulting from autumnal cooling and ice formation on the physical structure of the water it is possible to gain further insight into the oceanographic processes of winter. The method of Defant (1949) is followed except that for convenience σ_t is used instead of specific volume and the ice formed is assumed to have a salinity of 5‰. The method of computation is outlined briefly. A water column of 1 $cm.^2$ cross-section is divided into horizontal layers and the average temperature, salinity, and density of each layer are determined from the station data. As cooling takes place at the surface the upper layer becomes more dense until it has attained the density of the layer beneath, when the two layers mix. The point at which this takes place is determined from a T–S diagram with σ_t lines superimposed. The temperatures before and after mixing are then known; and from the temperature difference the quantity of heat Q_t lost due to atmospheric cooling may then be computed. The salinity of the mixed layer corresponds to the average of the salinities of the two separate layers before mixing.

One may then proceed to combine the third layer with the first two and so on. But dependent on the physical structure of the water, a point may be reached where the surface layer when cooled to its freezing point is not of a sufficient density to continue the process of thermal convection. Here ice forms. But as ice forms the average salinity of the column will increase because of this ice formation, and convection will in fact continue. By referring to the T–S–σ_t diagram it is possible to determine the increase in salinity due to ice formation; and the thickness e of ice formed and the amount of heat Q_e lost in the formation of ice (latent heat of fusion) may be computed. The total heat lost is the sum of the heat lost in cooling the water column and the heat lost in ice formation.

---

[6] P. F. Scholander, personal communication.

Computations of the thermo-haline convection resulting from autumnal cooling and ice formation have been made for stations BD-26, BD-28, and BD-130 based on the October 1954 observations, and have been carried on until the thickness of the ice formed is in reasonable agreement with what might be expected or until the bottom was reached, thus: BD-26 (62 cm. of ice), convection to bottom at 120 m.; BD-28 (96 cm. of ice), convection to 90 m.; BD-130 (120 cm. of ice), convection to bottom at 120 m. The results are summarized in Table IV.

Table IV.—Thermo-haline convection in Hebron Fjord, October 1954.

Layer	Layer thickness (*m.*)	Q_t	e	Q_e	ΣQ	Σe
BD-26 October 15						
1–2	10	0.48	....	....	0.48	....
1–3	20	0.60	....	....	1.08	....
1–4	30	1.77	....	....	2.85	....
1–5	40	2.98	....	....	5.83	....
1–6	50	5.00	....	....	10.83	....
1–7	60	6.15	....	....	16.98	....
1–8	70	3.39	1.4	0.10	20.47	1.4
1–9	80	2.32	9.8	0.71	23.50	11.2
1–10	90	2.09	10.9	0.78	26.37	22.1
1–11	100	2.03	16.2	1.17	29.57	38.3
1–12	110	2.02	8.9	0.64	32.23	47.2
1–13	120	1.97	14.6	1.05	35.25	61.8
BD-28 October 18						
1–2	10	1.02	....	....	1.02	....
1–3	20	5.34	4.1	0.30	6.66	4.1
1–4	30	2.99	2.5	0.18	9.83	6.6
1–5	40	2.75	3.3	0.24	12.82	9.9
1–6	50	2.42	20.5	1.48	16.72	30.4
1–7	60	2.32	12.2	0.88	19.92	42.6
1–8	70	2.10	14.2	1.02	23.04	56.8
1–9	80	1.86	9.7	0.70	25.60	66.5
1–10	90	1.40	29.1	2.10	29.10	95.6
BD-130 October 26						
1–2	10	1.93	0.8	0.06	1.99	0.8
1–3	20	2.34	10.8	0.78	5.11	11.6
1–4	30	2.35	24.6	1.77	9.23	36.2
1–5	40	2.05	6.5	0.47	11.75	42.7
1–6	50	1.80	8.1	0.58	14.13	50.8
1–7	60	1.69	2.4	0.17	15.99	53.2
1–8	70	1.76	5.7	0.41	18.16	58.9
1–9	80	1.54	6.5	0.47	20.17	65.4
1–10	90	1.31	14.6	1.05	22.53	80.0
1–11	100	0.97	12.1	0.87	24.37	92.1
1–12	110	0.64	13.3	0.96	25.97	105.4
1–13	120	0.58	14.5	1.04	27.59	119.9

Q_t = Heat lost to atmosphere in kg-cal./cm.^{2}
Q_e = Heat lost to ice formation in kg-cal./cm.^{2} (latent heat of fusion).
e = Ice thickness in cm.

The prediction of the date of freeze-up is of considerable practical importance. From these computations the quantity of heat that must be lost prior to ice formation can be determined. If we assume for the moment that from the date of observation the rate of effective heat loss to the atmosphere is 0.1

g-cal./cm.^{2}/min., it is then possible to obtain in advance some notion of the date of freeze-up. Applying this to the October data from Hebron Fjord, we have:

Station	Heat loss to ice formation	Date of observation	Number of days to freeze-up	Date of freeze-up
	kg-cal./cm.^{2}			
BD-26	20.37	Oct. 15, 1954	141	Mar. 5, 1955
BD-28	6.36	Oct. 18, 1954	44	Dec. 1, 1954
BD-130	1.93	Oct. 26, 1954	13	Nov. 8, 1954

From this it is possible to conclude that the inner fjords and bays of Labrador will freeze over first and the ice will gradually spread seaward. This is confirmed by local observation and knowledge. In 1954 slob ice was making along the shores of the inner fjord on October 26 at the time of occupation of BD-130, while the fjord, off the village of Hebron near its mouth, was reported to have frozen over on December 14. Of particular significance is the low "ice potential" at BD-26 in the coastal water as compared with the main body of the fjord. Ice is known to form here at an earlier date than that shown by the computations. In March 1954 off shore from the fjord, ice was forming rapidly in any open water, and the hydrographic structure was clearly favourable. Hence in the coastal waters in addition to convection resulting from atmospheric cooling some change in the physical structure of the water must also occur to hasten the ice formation.

With the relatively stable conditions that appear to exist in Hebron Fjord, particularly during the winter regime, it would seem reasonable for the purposes of this study to assume a return during the spring of 1955 to the same water structure and ice cover observed in 1954. It is then possible to compare the results predicted by the process of thermo-haline convection with the approximate conditions to be found.

Temperatures resulting from the convection are at the freezing point and in close agreement with the observed conditions; but in the salinity structure there is substantial disagreement. In order to obtain the observed salinity of approximately 32.75‰ it would be necessary to form approximately 2 m. of ice. This would seem quite unlikely in view of the none-too-severe winter climate of Labrador, and certainly untenable in view of the measured thicknesses in March and April, 1954 and 1955. It is thus apparent that the increase in salinity during the winter is not brought about alone by ice formation but must be due in part to the exchange with the Labrador Current and coastal waters. A summary of the winter haline processes as applied to a column of water of 1 cm.^{2} cross-section from the surface to the depth of computed convection is presented in Table V.

Greater ice growth and consequently a greater increase in salinity due to ice formation appears to be taking place progressively from the coastal water toward the inner part of the fjord, while conversely the effects on the salinity structure through the process of exchange appear to be of greater magnitude in the coastal water and progressively less within the fjord. The above breakdown

Table V.—Summary of winter haline processes in Hebron Fjord.

	BD-26	BD-28	BD-130
Average October salinity of water column, ‰	32.33	32.29	32.28
Average salinity of ice formed, ‰	5.00	5.00	5.00
Ice thickness computed as result of thermo-haline convection, *m.*	0.62	0.95	1.20
Ice thickness observed, *m.*	..	0.84	1.19
Depth to which convection computations carried, *m.*	120	90	120
Average salinity computed as result of ice formation, ‰	32.46	32.47	32.53
Observed March–April salinity, ‰	32.76	32.75	32.73
Increase in average salinity due to computed ice formation, ‰	0.13	0.18	0.25
Increase in average salinity due to exchange, ‰	0.30	0.28	0.20
Total increase of average salinity, ‰	0.43	0.46	0.45

has been shown as two separate processes, but it is implicit that they occur simultaneously.

Let us take a closer look at the thermal processes. The atmosphere must be the primary source of cooling during the autumn until ice formation commences. Atmospheric cooling most certainly accounts for the heat lost (latent heat of fusion) in the actual ice growth. After an ice cover has formed, atmospheric cooling of the water will be considerably reduced; and the process of exchange may play a greater part in further heat loss especially in the lower layers where the heat could not be removed except by exchange.

As the winter processes continue after ice begins to form, it may not be unreasonable to assume that, as the temperature and salinity approach the mid-winter equilibrium, the heat losses during this period due to ice formation and to exchange are proportional to the increases of average salinity due to these causes.

At the same time we are interested in the rates of heat loss. It is probable that the winter conditions of equilibrium are reached in early March. Uniform hydrographic conditions were observed in March 1954, and further increases in ice thickness will for all practical purposes be negligible. For purposes of computation it is assumed that the heat has been removed until some time in March, over a period of 150 days. Thus by dividing the heat losses by the period of time involved it is possible to determine the effective rate of heat loss.

In Table VI are summarized the winter thermal processes in Hebron Fjord as applied to a column of water of 1 cm.^{2} cross-section extending from the surface to the depth of computed convection. In the case of BD-26 the picture is obscured and complicated by the arrival during winter of the pack ice and its continual breaking up and refreezing. Therefore in this case only the totals are given, with no attempt at a breakdown.

It can be seen that in addition to the formation of ice and the associated convection, exchange plays a significant part in the winter oceanographic processes and is the ultimate determining factor in the oceanographic conditions. As we have seen from an analysis of the summer temperature regime, transports of a considerable magnitude can take place quite rapidly. Hence any long term prognosis of freeze-up date and ice thicknesses by computations of thermo-haline

TABLE VI.—Summary of winter thermal processes in Hebron Fjord.

	BD-26	BD-28	BD-130
Heat losses to atmosphere:			
Before ice formation, *kg-cal./cm.*^{2}	. .	6.36	1.93
Actual ice formation, *kg-cal./cm.*^{2}	. .	6.90	8.63
Proportion after ice formation, *kg-cal./cm.*^{2}	. .	6.20	9.26
Total heat losses to atmosphere, *kg-cal./cm.*^{2}	. .	19.46	19.82
Proportion to exchange after ice formation, *kg-cal.*	. .	9.64	7.77
Total heat loss, *kg-cal.*	35.25	29.10*	27.59
Average rate of loss to atmosphere, *g-cal./cm.*^{2}*/min.*	. .	0.090	0.092
Average rate of loss by exchange, *g-cal./min.*	. .	0.045	0.035
Total rate of heat loss, *g-cal./min.*	0.164	0.135*	0.127

*These values only apply to the depth of computed convection. Below this depth there is an additional quantity of residual heat of 4.30 kg-cal. that must be removed by exchange. For BD-28 the total rate of heat loss from the surface to the bottom would be 0.150 g-cal./min.

convection alone is liable to certain inherent inaccuracies; and along with any such studies the problems of transport and exchange between the fjords, bays, and coastal waters must be considered. Although the method used is crude, the results suggest that it gives a reasonably valid description of the actual winter processes.

IV. EXCHANGE

Exchange in an estuary with a deep basin and sill may be divided into two basically different parts; that taking place above the sill and that of the deeper layers. In Hebron Fjord exchange above the sill is essentially horizontal flows motivated by tidal action and fresh water transports. Below the sill exchange takes place by vertical convection in winter and during the other seasons, for the most part by turbulence. Although these two are related, we will discuss certain aspects of exchange primarily above the sill in this section and vertical mixing below sill depth in the following section.

By means of fresh-water fractions the actual quantities of fresh water in the various levels of the fjord for the times of observation in 1954 have been calculated and are presented in Table VII. The volumes of the levels used were determined by planimetry and the average salinity was calculated from the station data applied to appropriate segments within these levels. The fresh-water fraction (FWF) of each segment was obtained by the formula:

$$\text{FWF} = \frac{S_B - S_A}{S_B},$$

where S_A equals the base salinity of the source water and S_B equals the average observed salinity of the water in question. A base salinity of 32.79‰ was used for these calculations, which was the highest salinity observed in or just outside the fjord in 1954. By multiplying the FWF by the volume of each segment the actual quantity of fresh water in the segment was determined, and the total within each level obtained by summing the fresh water in each segment.

TABLE VII.—Fresh water in Hebron Fjord, 1954.

Level	March	July	August	October
m.	10^6 *cu. m.*	10^6 *cu. m.*	10^6 *cu. m.*	10^6 *cu. m.*
0–5	0.6	115.8	194.8	46.1
5–10	1.3	89.9	38.8	38.0
10–20	2.9	113.7	54.5	52.4
20–30	2.7	69.1	40.3	34.6
30–60	7.3	109.0	75.9	71.1
Vol. above sill:	14.8	497.5	404.3	242.2
60–100	6.6	29.9	31.7	43.0
100–150	4.4	13.2	5.5	14.3
150–200	2.6	6.5	2.0	4.6
200–250	1.1	2.6	0.8	0.8
Below 250	0.1	0.1	0.0	0.0
Total	29.6	549.8	444.3	304.9

From these data and the fresh water entering the fjord (Table II), the overall exchange of fresh water is summarized in Table VIII.

The total fresh water in the fjord reflects the annual cycle of the fresh-water contributions with the maximum observed fresh water in the fjord occurring in July after spring freshet. The total amount of fresh water decreases regularly throughout the late summer and fall as the fjord adjusts to the progressively reduced contributions of fresh water.

TABLE VIII.—Fresh water exchange, Hebron Fjord.

	May-July	July-Aug.	Aug.-Oct.	Oct.-Mar.
	10^8 *cu. m.*	10^8 *cu. m.*	10^8 *cu. m.*	10^8 *cu. m.*
Initial accumulation (start of period)	0.3	5.5	4.4	3.0
Fresh water added:	8.4	1.3	2.3	0.5
Total	8.7	6.8	6.7	3.5
Final accumulation (end of period)	5.5	4.4	3.0	0.3
Net fresh water exchanged	3.2	2.4	3.7	3.2
Period [a]	56 days	33 days	70 days	150 days[b]
Net exchange per day	0.057	0.073	0.053	0.021

[a] The beginning of spring freshet is estimated at May 15.

[b] 150 days is an arbitrary assumption of the time required for the return to isothermal and isohaline conditions of midwinter.

The change in fresh-water content of the levels below sill depth indicates that exchange is taking place with the upper levels. The intrusion during early August of the cold and more saline water mass is evident in the sharp salting of the fjord water from 5 m. to nearly the bottom, with an apparent damming up of the fresh-water contributions in the upper 5 m.

Calculations of flushing time, defined as the time necessary to renew the water within the estuary, have been made using fresh water as a tracer. For these calculations a false bottom has been assumed at 60 m. which is approximately sill depth. Below this depth during summer exchange must overcome the stable density gradient and is of small magnitude as compared to the exchange above sill depth.

The formula $F = \frac{Q}{R}$, where Q is the total accumulated fresh water, and R is the river flow (contribution of fresh water), has been used to calculate the flushing time (F) above sill depth (60 m.) at the times of observation in July, August, and October in the following tabulation:

	9-10 July	11-12 August	18-26 October
$Q \times 10^8$m.^{3}	4.98	4.04	2.42
R per day $\times 10^8$m.^{3}	0.090	0.031	0.021
F, days	55	130	115

This method presupposes a "steady state." In Figure 18 the annual cycles of the daily rate of R, R_e (fresh water exchanged out of the estuary), and Q are given. Q reaches a maximum where $R = R_e$. Prior to this time $R > R_e$ and the fresh water in the fjord is increasing; after this time $R < R_e$ and it is decreasing. In either case R is changing so that an adjustment to a steady state is never achieved. The point of crossing of these two curves is interesting, for at this time the conditions of no net exchange of either fresh or salt water exist momentarily.

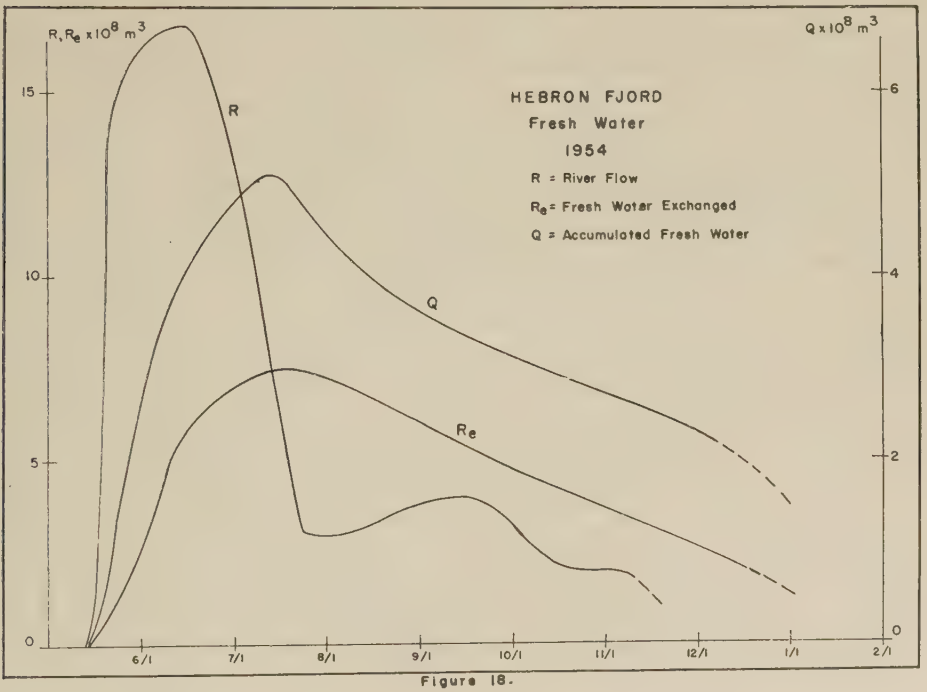

Figure 18.

Any computation of flushing time by $F = \frac{Q}{R}$ will yield too small a flushing time prior to the point where $R = R_e$, and too large a flushing time after. Therefore when $R = R_e$, the conditions of a steady state must momentarily exist. At no other time during the annual cycle is a steady state realized (except in the zero/zero relationship of midwinter).

If in such an estuary observations have not been obtained when $R = R_e$, it should be possible to solve graphically for values of Q and R at precisely this time. By so doing with the Hebron data a Q of 5.1×10^8 m.^{3} and an R of 0.075×10^8 m.^{3} are obtained, which yield a flushing time of 68 days. This time lies between the other values of 55 and 130 days and should be a reasonable representation of the actual flushing time. The value of 55, although obtained close to when $R = R_e$, would appear to be too rapid a flushing time. If the fjord were flushed in 55 days, a steady state would have been met or more nearly achieved during August, September or October when R is comparatively constant. This argues for perhaps an even greater flushing time than 68 days, but the present data do not permit a closer analysis.

Since it has been shown that the flushing time within a given estuary will remain constant in spite of large variations of R (Ketchum, Redfield and Ayers, 1951), we may conclude that at least during summer above sill depth the water in Hebron Fjord will be renewed regularly in a period of between two and three months.

V. VERTICAL MIXING BELOW SILL DEPTH

Exchange below sill depth must involve vertical movements, and may take place by convection and turbulence (used herein to mean eddy conductivity in the case of temperature and eddy diffusivity in the case of salinity). During winter when the water is isothermal and isohaline, exchange between the upper and lower levels occurs principally by convection. Turbulence is acting at all seasons simultaneously with the other processes, but would seem to be the dominant factor during summer when a stable density gradient must be overcome in any vertical movements. Within the body of the fjord below sill depth horizontal movements would appear to be restricted.

The source of energy for the turbulence is the tidal action and transports of fresh water through the fjord. In considering only the waters below sill depth turbulence should be greatest just at sill depth closest to the source of energy and progressively less toward the lower levels until it becomes inseparable from convection in the virtually uniform water that persists in the very bottom layers. It would therefore seem most advantageous to study the eddy coefficients for the levels at and just below sill depth during the summer season when a stable gradient exists.

From the 1954 data at station BD-130 some calculations of the "Austausch" A factor of eddy conductivity and eddy diffusivity have been made at and below sill depth at the 60-, 80- and 100-m. levels. The method of Saelen (1950) has been used:

$$\int_z^b (T_2 - T_1)\, dz = -\bar{A} \int_{t_1}^{t_2} \frac{\partial T}{\partial z}\, dt$$

$$\int_z^b (S_2 - S_1)\, dz = -\bar{A} \int_{t_1}^{t_2} \frac{\partial S}{\partial z}\, dt$$

where T_2, S_2, and T_1, S_1, are respectively the temperatures and salinities at the times t_2 and t_1, b is the depth at bottom, z is the depth of calculation, and $\bar{A}$ is a mean value of A during the time between t_1 and t_2. Values for $\bar{A}$ have been calculated over the periods between the various observations from the beginning of spring melting and the establishment of a stable density gradient (May 15) until the fall observations in October. The results are summarized in Table IX.

TABLE IX.—Calculations of eddy conductivity ($\bar{A}_T$) and ($\bar{A}_S$) diffusivity, Hebron Fjord, 1954.

	$\bar{A}_T$				
Depth	5/15–7/9	7/9–7/31	7/31–8/12	8/12–10/26	Mean
m.					*m.*
60	57	82	17	112	67
80	48	29	25	46	37
100	20	8.4	17	18.5	16
	$\bar{A}_S$				
60	111	48	(X)[a]	44	—
80	188	12	(X)[a]	32	—
100	108	(X)[a]	(X)[a]	21	—

[a] Negative values representing impossible solutions (see text).

There is a large variation between the individual values in each table and a variation between the $\bar{A}$ values obtained from temperature and from salinity. The theory implies that A_T should equal A_S; however it must be pointed out that in the determination of A_T only the transfer of a property is involved, while in the determination of A_S an actual transfer of mass is required.

In interpreting and evaluating these data we must consider the formula itself. $\frac{\partial T}{\partial z}$ and $\frac{\partial S}{\partial z}$ are obtained from the thermogram or halogram involved. Broadly speaking, in the course of the annual cycle $\frac{\partial T}{\partial z}$ and $\frac{\partial S}{\partial z}$ are zero at the beginning of spring freshet, increase to a maximum value during summer, and decrease again to zero during the ensuing winter. Thus regardless of the left-hand side of the equation $\bar{A}$ will range from infinity to a minimum during summer and again approach infinity in winter.

In Hebron Fjord $\frac{\partial T}{\partial z}$ and $\frac{\partial S}{\partial z}$ are always small and difficult to determine accurately. Greater precision may be expected from the thermogram which is obtained from a BT with reversing thermometer control, while the halogram is determined from the salinity data alone with the slope and nature of the curve determined by inference from the thermogram. The $\bar{A}$ values obtained become extremely tenuous as $\frac{\partial T}{\partial z}$ and $\frac{\partial S}{\partial z}$ approach zero. Particularly the May to July $\bar{A}_S$ values are likely invalid because of the very small $\frac{\partial S}{\partial z}$.

The rapid influx of the cold water mass between July 31 and August 12 has been discussed qualitatively earlier. Its effect upon the $\bar{A}$ computations is readily apparent. The character of this water mass as determined by the T–S relationships in the coastal water was approximately: temperature —1.2 to —1.3°C. and salinity 32.70 to 32.80‰. Thus it would seem likely that this water mass would interrupt the normal summer processes with a brief period of vertical convection. This convection might be visualized as taking place largely in the outer part of the fjord, the more saline water being transported to the inner part of the fjord by horizontal currents below sill depth. Evidence of some horizontal movement below sill depth is seen in the BT traces in Figure 5 which show the progressive intrusion of the cold water mass extending down to and projecting below the sill. $\bar{A}_S$ values designated (X) are negative and therefore represent an impossible solution to the equation. At the times of each observation a positive $\frac{\partial S}{\partial z}$ slope is obtained, yet there is a net increase of salinity which must therefore have been caused by some process other than eddy diffusivity and is undoubtedly due to the intrusion of the cold more dense water and the temporary convection that has upset the normal summer processes. In fact the negative $\bar{A}_S$ value and the low $\bar{A}_T$ for the period July 9–31 at 100 m. are likely indications of the first effects of this water mass. Therefore the only reliable A_S values are considered to be over the period August to October.

The intrusion of the cold dense water that disrupted the A_S picture does not similarly affect the $\bar{A}_T$ calculations. During the periods of observation $\frac{\partial T}{\partial z}$ is always negative with a normal corresponding rise in temperature of the bottom water. Since the temperature of this cold water was quite similar to that of the fjord water at the depths of calculation, the effects of the convection and horizontal currents are not apparent except in the case of the small $\bar{A}_T$ factor at 60 m. between July 9 and August 12. The high $\bar{A}_T$ value for the subsequent period may represent a compensating readjustment.

The unfortunate intrusion of the cold saline water mass at the time of the August observations, which has to a considerable extent obscured the turbulent processes, has limited the validity of the A calculations during this period. Of the values obtained it is felt that on the whole greater reliance may be placed on the temperature than on the salinity coefficients and that the A_T values obtained give us some general notion on the A factor as it applies to Hebron Fjord.

APPLICATION OF THE *A* FACTOR TO THE VERTICAL TRANSPORT OF DISSOLVED OXYGEN

During the summer months high oxygen content with supersaturation occurs in the upper layers with gradually decreasing amounts of oxygen toward the bottom. Therefore if downward mixing by turbulence occurs oxygen will be transported downward. However we note decreasing amounts of oxygen in the lower layers during the course of the summer. Thus the amount of oxygen consumed by biological respiration should equal the amount of oxygen transported downward by turbulence plus the net decrease of oxygen in these lower layers.

Calculations of the downward transport and consumption of dissolved oxygen have been made at station BD-130. A depth of 80 m. has been used in the calculations as it seems most suitable from the oxygen data available as well as the A_T values which are used, and it is below the euphotic zone. The quantity of oxygen (O) transported downward between the times t_1 and t_2 has been computed as follows:

$$O = -10^{-3} \int_{t_1}^{t_2} \bar{A} \frac{\partial O}{\partial z} \, dt$$

The results (upper two portions of Table X) are given in millilitres of oxygen transported through an area of cross-section of 1 cm.^{2} during the two periods July 9–31 and from July 31 to August 12, and the quantities of oxygen are in a column of water of 1 cm.^{2} cross-section from 80 m. to the bottom at 120 m.

The data in the upper two portions of Table X would appear to be of reasonable order of magnitude and indicate an uniform rate of oxygen consumption which might be expected with the uniformly cold water prevailing during the summer season in the lower levels. Biological activity may increase

TABLE X.—Calculations of vertical transport and consumption of oxygen in Hebron Fjord, 1954.

July 9 to July 31	
July 9 oxygen 80-120 m.	27.2 ml.
July 31 oxygen 80-120 m.	26.6 ml.
Net loss	0.6 ml.
Oxygen transported down ($A = 29$)	0.79 ml.
Total oxygen consumed	1.39 ml.
Av. rate of consumption	2.63×10^{-3} ml./hr.
July 31 to August 12	
July 31 oxygen 80-120 m.	26.6 ml.
Aug. 12 oxygen 80-120 m.	26.2 ml.
Net loss	0.4 ml.
Oxygen transported down ($A = 25$)	0.36 ml.
Total oxygen consumed	0.76 ml.
Av. rate of consumption	2.64×10^{-3} ml./hr.
August 12 to October 26	
Oxygen transported down ($A = 46$)	1.24 ml.
Total oxygen consumed (2.64×10^{-3} ml./hr.)	4.44 ml.
Net loss 80-120 m.	3.53 ml.
Reduction of oxygen 80-120 m. to	22.7 ml. or 5.67 ml./l.

somewhat during the late fall warming; however negative temperatures prevail in the lower levels throughout the annual cycle and such increase would likely be small.

The above calculations have been projected to October (lower portion of Table X), with the assumption that the uniform rate of oxygen consumption of summer is maintained throughout the fall.

Thus even if a greater oxygen consumption were encountered during the fall there would be no danger of oxygen depletion to a point of limiting biological activity, unless the process continues over a period of several years without any oxygen renewal. However, the uniformly high oxygen content observed over the several summers of observation suggests that complete renewal takes place during the winter processes of convection and exchange.

VI. DYNAMIC COMPUTATIONS

Some dynamic computations have been made from the Hebron station data. Specific volumes are expressed as the anomaly of the specific volume in situ and that of water of 35‰, 0°C. under atmospheric pressure ($\triangle a$). The dynamic height is then $D = \int_0^y \triangle a \, dp$. Various isobaric levels above 120 decibars, which was selected as a level of no motion, for the longitudinal section made August 11–12, 1954, are shown in Figure 19 as differences in dynamic millimetres as compared with station BD-133.

As would be expected the fjord water at this season lies at a higher level than the coastal water. The greatest height calculated is at BD-29 at all levels and not at the head of the fjord. This is easily explained by examining the principal fresh-water sources, which are not concentrated at the head of the fjord, but scattered from the head to Freytag Inlet; and hence the major proportion of run-off will pile up somewhere between BD-130 and BD-29.

On August 12 a section of five stations was made across the fjord including BD-130. The dynamic heights relative to 120 m. have been calculated, and the surface slope plotted (Fig. 20). Definite piling up of water is noted on the north shore, a lesser piling up on the south shore, and a low point at BD-135.

Calculation of the velocities at right angles to this section were made:

$$V - V_1 = \frac{10}{\lambda L}(D_A - D_B)$$

where D_A is the dynamic height for A, the left-hand, and D_B for B, the right-hand station, $\lambda = 2\omega \sin \phi$ (ω being the angular velocity of the earth's rotation and ϕ the mean latitude), and L is the distance between stations. Lines of equal velocity are plotted in Figure 20 where the negative values (solid lines) are into the paper and positive values (dashed lines) are out.

To calculate the transports through the section the approximation of Theisen (1946) was used: a line some 30 to 40 m. above the bottom was drawn on the

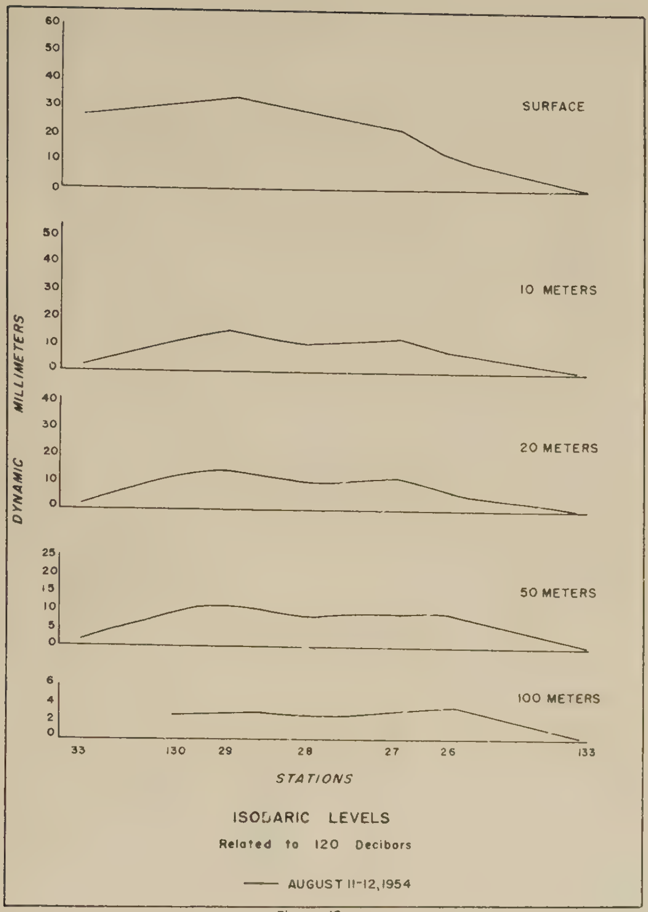

Figure 19.

velocity section, and the flows between this line and the bottom were neglected as being insignificant. The section was then planimetered, with the results:

Outflowing – 14,292 m.^{3}/sec.
Inflowing – 17,498 m.^{3}/sec.

Although the basic assumptions of no accelerations, no frictional forces, and a balance between pressure gradient and Coriolis force upon which dynamic computations are based, can at best only be partially fulfilled in confined coastal waters where fresh water mixing and tidal currents exist, it is interesting to see to what degree the dynamic picture agrees with the actual conditions as observed.

The pattern of velocity appears to indicate geostrophic movement with a strong inflow along the north shore and an outflow along the south shore. When the section was made, a sea breeze was blowing. Due to local topography the wind was only moderate along the south shore, while it freshened considerably

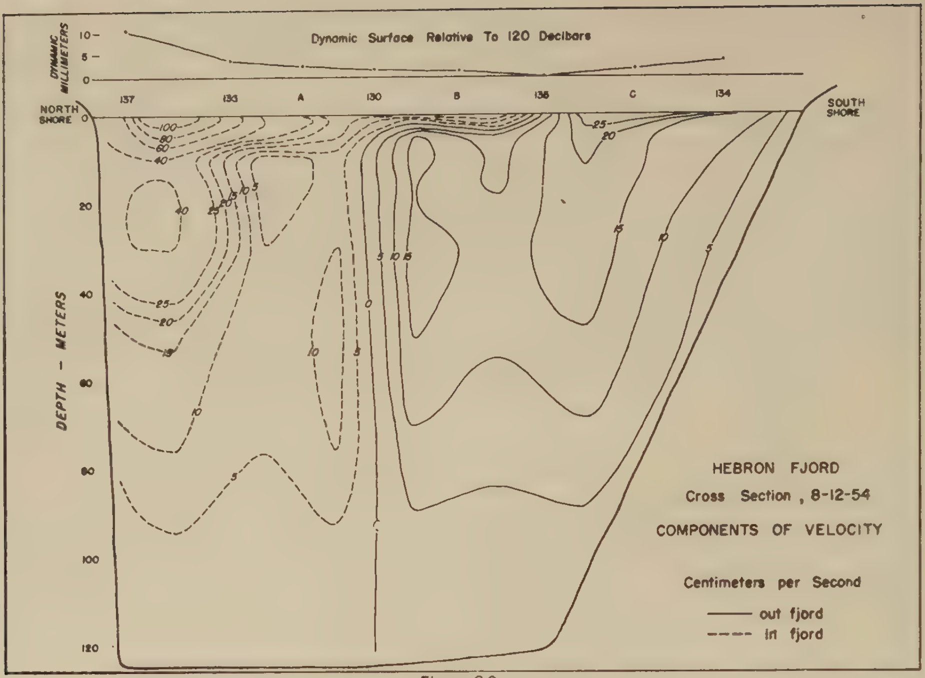

Figure 20.

toward the north shore. As the vessel was manoeuvered for the occupation of the three southern stations, little current was noted. During the occupation of the northern two stations, particularly BD-137 close by the north shore, a strong inflowing current was observed and estimated at about 2 knots, which is in reasonable agreement with the computed surface velocities.

At the time the section was made the tide was falling, which must have resulted in an actual seaward movement of water. The dynamic computations have shown a small net inflow. It would thus appear that although the values of transport obtained from the dynamic computations are not absolute, the qualitative description of the velocity pattern is in substantial agreement with the observed conditions.

VII. SUMMARY

1. Hebron Fjord, located at latitude 58° 10′ N. on the northeast coast of Labrador, is 255 m. deep with a 59-m. sill across its mouth. The climate and hydrological cycle of this area is sub-Arctic, with moderately cold winters which store all precipitation in the form of snow and ice, and moderately warm summers during which a large accumulation of fresh water from melting snow is released rapidly during the spring freshet. The volume of fresh-water contributions during the course of the annual cycle has been computed from the climatological data, watershed area. and ice cover.

2. During winter the waters within the fjord and immediate coastal water are uniformly isothermal and isohaline with a temperature of —1.76°C. and a salinity of 32.75‰. Soon after the advent of spring thaw about May 15 freshening and warming of the surface layers commence. The freshening takes place in advance of the warming and reaches a maximum in early July after which the fjord commences to salt. The maximum warming is not reached until sometime in September or early October. The drying up and freezing of the rivers in the fall, the formation of ice, and exchange with the coastal water lead to the re-establishment of isothermal and isohaline conditions during the ensuing winter.

During the last part of July and the first part of August 1954 a cold saline mass of water in passing along the coast from north to south invaded the fjord to upset the normal summer pattern.

3. A study of the temperature–salinity relationships more clearly defines the annual cycle and the relationships between the fjord and coastal water.

During winter the fjord and coastal waters become isothermal and isohaline with T–S relationships that may be identified as Arctic water of the Labrador Current. Due to the slow vertical exchange below sill depth after the establishment of a stable density gradient in summer the bottom water reflects essentially the conditions established during the preceding winter. Thus the condition of the bottom water during early and midsummer may be used as an indicator of the long-term trends of the Arctic water of the Labrador Current. The T–S relationships from the *Chance* data of 1926 and the *Blue Dolphin* data of 1949, 1952 and 1954 show a very slight warming trend, while a significant freshening is apparent. A correlation between these trends and recent changes in the Arctic Ocean and the Arctic–Atlantic circulation is suggested.

4. Ice formation as an oceanographic phenomenon is discussed. The thermohaline convection resulting from fall cooling and ice formation has been computed from the October 1954 data. It is shown that the inner fjord waters will freeze relatively early, while the freezing of the coastal water will be considerably delayed. In addition to the formation of ice a considerable exchange must take place between the fjord and coastal water to effect a return to the normal isothermal and isohaline conditions of mid winter. The thermal and haline cycles are considered in relation to both ice formation and exchange. It may be concluded that the formation and growth of ice is an important oceanographic feature of Arctic and sub-Arctic coastal waters.

5. The exchange mechanism and processes in Hebron Fjord may be described quite accurately qualitatively, but are difficult to determine quantitatively. Exchange is considered in essentially two parts, that above sill depth, which with free exchange between the fjord and coastal water involves principally horizontal movements, and that below sill depth which must involve vertical movements. Above sill depth, a slightly modified "steady state" concept is suggested which permits the calculation of a flushing time of approximately 68 days.

The bottom waters are not stagnant or dynamically dead, but enter into the exchange process at, however, a much slower rate. The waters below sill depth are renewed principally by vertical convection during winter. During summer any exchange must overcome a stable density gradient and is accomplished by turbulence. Computations of the "Austausch" A factor of eddy conductivity and eddy diffusivity at and below sill depth show generally a larger A in spring and fall with a minimum in summer. A decreases with depth and distance from the source of energy which is primarily tidal action. Average A values of 67, 37 and 16 were obtained at the 60-, 80- and 100-m. levels respectively.

6. Dynamic heights determined in a longitudinal section show a pile-up of fresh water in the area where the greatest river flow is concentrated. Dynamic calculations of velocities and transport in a cross-section indicate a geostrophic flow. The calculated volumes of transport are not absolute, but the velocity pattern is in substantial agreement with observed conditions.

7. In Hebron Fjord a high Arctic marine environment exists during winter at all levels with a uniform temperature of −1.75°C. This high Arctic environment prevails throughout the annual cycle in the lower levels. At 100 m. the maximum temperature attained is barely −1.00°C., while at 250 m. it has risen to only −1.68°C. In the upper levels above sill depth a significant seasonal amelioration takes place. This amelioration extends to greater depths in the coastal waters where negative temperatures have completely disappeared by mid-October down to 120 m., and likely deeper. Thus during the summer and fall seasons the bottom waters of Hebron Fjord become an isolated pocket of high Arctic marine environment.

Determinations of dissolved oxygen and inorganic phosphate content of the waters of Hebron Fjord have been made. In general there would appear to be an increase of phosphate content with depth. Photosynthetic activity maintains oxygen in the upper 30 m. at a level of supersaturation during the summer months. The rate of oxygen consumption below 80 m. has been computed from the amount of oxygen transported downward by eddy conductivity and the oxygen reduction observed in these levels during the summer months. It was found to be at a uniform rate of 2.64×10^{-3} ml./hr. in a column of water of 1 cm.^{2} cross-section from 80 m. to the bottom at 120 m.

REFERENCES

Bailey, W. B., and H. B. Hachey. 1951a. An increasing Atlantic influence in Hudson Bay. *Proc. Nova Scotian Inst. Sci.*, **22**(4): 17–33, (for 1949–50).

1951b. The vertical temperature structure of the Labrador Current. *Proc. Nova Scotian Inst. Sci.*, **22**(4): 34–48 (for 1949–50).

Defant, A. 1949. Konvektion und Eisbereitschaft in polaren Schelfmeeren. *Geografiska Annaler,* **31**: 25–35.

Delabarre, E. B. 1902. Report of the Brown Harvard Expedition to Nachvak, Labrador, in the year 1900. *Bull. Geog. Soc. Philadelphia,* **3**(4): 65–212.

Department of Transport. 1954. Climatic summaries for selected meteorological stations in Canada, Addendum to Vol. I. Average values of temperature and precipitation. Meteorological Div., Dept. Transport, Toronto, 29 pp.

Dunbar, M. J. 1951. Eastern Arctic waters. *Bull. Fish. Res. Bd. Canada,* No. 88, 131 pp.

Iselin, C. O'D. 1932. A Report on the coastal waters of Labrador, based on explorations of the *Chance* during the summer of 1926. *Proc. Amer. Acad. Arts and Sci.,* **66**(1): 1–37.

JENSEN, A. S. 1939. Concerning a change of climate during recent decades in the arctic and subarctic regions from Greenland in the west to Eurasia in the east, and contemporary biological and physical changes. *Kgl. Danske Vidensk. Selsk., Biol. Medd.,* **14**(8): 1-75.

KETCHUM, B. H., A. C. REDFIELD AND J. C. AYERS. 1951. The oceanography of the New York Bight. *Papers Phys. Oceanogr. and Meteor.,* **12**(1): 1-46.

NUTT, D. C. 1952. Blue Dolphin Labrador Expedition, winter project 1952, operational report, 15 June. (mimeographed).

1953. Certain aspects of oceanography in the coastal waters of Labrador. *J. Fish. Res. Bd. Canada,* **10**(4): 177–186.

SAELEN, O. H. 1950. The hydrography of some fjords in northern Norway: Balsfjord, Ulfsfjord, Grøtsund, Vengsøyfjord, and Malangen. *Tromsø Museums Arshefter, Naturhistorisk Avd.,* No. 38, Vol. 70 (1947), No. 1, pp. 1–102.

SCHOLANDER, P. F., W. FLAG, R. J. HOCK AND L. IRVING. 1953. Studies of the physiology of frozen plants and animals in the Arctic. *Jour. Cellular and Comparative Physiology,* **42**, Suppl. 1, 1–56.

SMITH, E. H., F. M. SOULE AND O. MOSBY. 1937. The *Marion* and *General Greene* Expeditions to Davis Strait and Labrador Sea; under the direction of the U.S. Coast Guard 1928, 1931, 1933, 1934, 1935. Scientific Results, Pt. 2, Physical Oceanography. *U.S. Treasury Dept., Coast Guard Bull.* No. 19, 259 pp.

THEISEN, E. 1946. Tanafjorden; en finnmarksfjords oseanografi. *Fiskeridirektoratets Skrifter, Serie Havundersøkelser,* 8(7): 1–77.

ZUBOV, N. N. 1948. Arctic ice and the warming of the Arctic; being ch. VI and VII of "In the Center of the Arctic", North Sea Route Directorate Press, Moscow–Leningrad, (translated by E. Hope, Defense Research Board of Canada).

STATION DATA SUMMARIES

STA. NO. BD-25 DATE 8/7/49 TIME 1220 ZONE + 2½
LAT. 58 ° 16.8'N LONG. 62 ° 12.5 'W. DEPTH 92 fm. BT NO. —
WEA. Fine AIR TEMP. 43.5 °F. WIND SSW 4 kts. SECCHI 42 ft.

DEPTH m	TEMP. °C.	SAL. °/oo	σ_t	O_2 ml/L	PO_4 µgA/L
0	5.1	30.89	24.44	5.96	
10	3.54	31.93	25.42	8.03	
20	—	32.18	—	9.66	
30	0.02	32.38	26.01	7.58	
50	- .42	32.56	26.17	6.29	
75	—	32.72	—	8.65	
100	- .96	32.83	26.42	7.61	

REMARKS:

STA. NO. BD-26 DATE 8/7/49 TIME 1730 ZONE + 2½
LAT. 58 ° 14.3 'N LONG. 62 ° 29.6 'W. DEPTH 58 fm. BT NO. —
WEA. Overcast AIR TEMP. 54.0 °F. WIND WxN - lgt kts. SECCHI 57 ft.

DEPTH m	TEMP °C.	SAL. °/oo	σ_t	O_2 ml/L	PO_4 µgA/L
0	5.6	29.44	23.25	5.86	
10	3.08	31.95	25.47	5.04	
20	1.21	31.95	25.60	5.63	
30	0.36	32.05	25.72	3.63	
50	- .29	32.40	26.05	7.20	
75	- .80	32.48	26.13	6.51	
100	- .96	—	—	5.16	

REMARKS:

STA. NO. BD-27 DATE 8/7/49 TIME 2040 ZONE + 2½
LAT. 58 ° 11.4 'N LONG. 62 ° 34.2 'W. DEPTH 95 fm. BT NO. —
WEA. Overcast AIR TEMP. 51.4 °F. WIND Calm kts. SECCHI 65 ft.

DEPTH m	TEMP °C.	SAL. °/oo	σ_t	O_2 ml/L	PO_4 µgA/L
0	7.8	24.71	19.28	4.89	
10	1.91	31.19	24.96	6.17	
20	—	31.64	---	8.09	
30	- .18	32.01	25.73	6.18	
60	- .73	32.36	26.03	3.35	
107.8	—	33.04	—	6.71	
154.3	-1.79	33.03	26.60	5.21	

REMARKS:

STA. NO. BD-28 DATE 8/8/49 TIME 1300 ZONE + 2½
LAT. 58 ° 09 'N LONG. 62 ° 45.7 'W. DEPTH 138 fm. BT NO. —
WEA. Overcast AIR TEMP. 43.7 °F. WIND ENE 5 kts. SECCHI — ft.

DEPTH m	TEMP. °C.	SAL. °/oo	σ_t	O_2 ml/L	PO_4 µgA/L
0	6.4	26.34	20.72	8.94	
10	0.91	31.27	25.08	11.90	
20	—	31.67	---	13.07	
30	- .53	32.01	25.74	11.98	
58	-1.31	32.54	26.18	9.27	
102	-1.73	33.00	26.57	10.68	
150	-1.75	33.08	26.63	6.32	
200	-1.81	33.06	26.61	9.87	

REMARKS:

STA. NO. BD-29 DATE 8/11/49 TIME 1200 ZONE + 2½
LAT. 58 ° 08.6 'N LONG. 62 ° 55.6 'W. DEPTH 93 fm. BT NO. —
WEA. Overcast AIR TEMP. 41.7 °F. WIND ENE 2 kts. SECCHI 36 ft.

DEPTH m	TEMP °C.	SAL. °/oo	σ_t	O_2 ml/L	PO_4 µgA/L
0	3.1	29.45	23.48	9.47	
10	2.44	30.76	24.58	7.90	
20	2.45	31.13	24.87	9.60	
30	2.12	31.32	25.05	5.91	
50	- .73	32.09	25.81	10.27	
100	-1.68	33.03	26.59	5.17	
150	-1.77	33.12	26.66	5.80	

REMARKS:

STA. NO. BD-30 DATE 8/11/49 TIME 1600 ZONE + 2½
LAT. 58 ° 04.7 'N LONG. 63 ° 06.0 'W. DEPTH 50 fm. BT NO. —
WEA. Overcast AIR TEMP. 44 °F. WIND NE - lgt. kts. SECCHI 18 ft.

DEPTH m	TEMP °C.	SAL. °/oo	σ_t	O_2 ml/L	PO_4 µgA/L
0	2.8	29.10	23.23	4.13	
10	1.85	30.49	24.42	3.59	
20	1.44	30.73	24.63	6.13	
28	1.03	31.00	24.86	7.11	
47	—	32.24	---	6.62	
70	-1.27	32.55	26.18	5.60	

REMARKS:

STA. NO. BD-33 DATE 8/12/49 TIME 1710 ZONE + 2½

LAT. 58 ° 01.5 'N LONG. 63 ° 08.0 'W. DEPTH 43 fm. BT NO. --

WEA. Fine AIR TEMP. 55 °F. WIND SW - lgt kts. SECCHI 30 ft.

DEPTH m	TEMP. °C.	SAL. °/oo	σ_t	O_2 ml/L	PO_4 µgA/L
0	3.5	27.62	22.00		
10	1.75	30.71	24.58		
20	1.27	30.82	24.70		
30	- .22	31.74	25.51		
50	—	32.91	---		
75	-1.81	33.01	26.57		

REMARKS:

STA. NO. BD-33 DATE 8/13/49 TIME 1020 ZONE + 2½

LAT. 58 ° 01.5 'N LONG. 63 ° 08.0 'W. DEPTH 43 fm. BT NO. —

WEA. Fine AIR TEMP. 53.6 °F. WIND Calm kts. SECCHI — ft.

DEPTH m	TEMP °C.	SAL. °/oo	σ_t	O_2 ml/L	PO_4 µgA/L
0	3.9	29.34	23.34	10.35	
10	—	30.54	---	6.48	
20	1.09	30.99	24.85	10.40	
30	—	31.55	---	13.21	
50	-1.46	32.79	26.40	6.63	
75	—	33.06	—	8.15	

REMARKS:

STA. NO. BD-33 DATE 7/19/52 TIME 1540 ZONE + 3

LAT. 58 ° 01.5 'N LONG. 63 ° 08 'W. DEPTH 44 fm. BT NO. BD 4, 274

WEA. Fine AIR TEMP. 51.4 °F. WIND lgt. var. kts. SECCHI 48 ft.

DEPTH m	TEMP °C.	SAL. °/oo	σ_t	O_2 ml/L	PO_4 µgA/L
0	6.8	24.49	19.23	8.01	0.50
5	4.76	26.71	21.16	8.17	0.25
10	1.12	31.46	25.22	9.35	0.25
20	0.36	31.80	25.53	9.14	0.15
30	- .28	32.07	25.78	8.75	0.25
49.5	-1.54	32.81	26.41	7.26	0.25
74.2	-1.73	32.90	26.48	6.55	0.60

REMARKS:

STA. NO. BD-117 DATE 7/23/52 TIME 0810 ZONE + 3

LAT. 58 ° 18 'N LONG. 62 ° 00 'W. DEPTH 110 fm. BT NO. BD 4, 276

WEA. Fine AIR TEMP. 50.0 °F. WIND SE 5 kts. SECCHI 80 ft.

DEPTH m	TEMP. °C.	SAL. °/oo	σ_t	O_2 ml/L	PO_4 µgA/L
0	4.1	31.67	25.17	8.10	0.20
5	3.75	31.65	25.18	8.19	0.15
10	2.42	31.64	25.28	8.28	0.35
20	2.28	31.65	25.30	8.20	0.40
30	- .39	32.10	25.80	8.26	0.50
50	- .76	32.45	26.10	8.00	0.35
100	- .92	32.90	26.47	7.46	0.20
150	-1.02	33.22	26.74	7.16	0.25

REMARKS:

STA. NO. BD-25 DATE 7/23/52 TIME 1055 ZONE + 3

LAT. 58 ° 16.8 'N LONG. 62 ° 12.5 'W. DEPTH 93 fm. BT NO. BD 4, 277

WEA. Fine AIR TEMP. 52.1 °F. WIND SE 5 kts. SECCHI 57 ft.

DEPTH m	TEMP °C.	SAL. °/oo	σ_t	O_2 ml/L	PO_4 µgA/L
0	6.1	31.44	24.76		
10	2.76	31.64	25.26		
20	1.14	31.89	25.56		
30	0.41	32.10	25.77		
50	0.09	32.16	25.84		
100	- .82	32.57	26.20		
150	-1.01	32.97	26.52		

REMARKS:

STA. NO. BD-26 DATE 7/23/52 TIME 2155 ZONE + 3

LAT. 58 ° 14.2 'N LONG. 62 ° 29 'W. DEPTH 62 fm. BT NO. BD 4, 278

WEA. Overcast AIR TEMP. 50.7 °F. WIND NExN 5 kts. SECCHI 66 ft.

DEPTH m	TEMP °C.	SAL. °/oo	σ_t	O_2 ml/L	PO_4 µgA/L
0	7.5	27.81	21.74		
5	4.82	30.82	24.42		
10	3.23	31.64	25.21		
20	2.52	31.89	25.47		
30	1.98	31.78	25.42		
50	1.18	31.74	25.45		
100	- .51	32.39	26.05		

REMARKS·

STA. NO. BD-27 DATE 7/31/52 TIME 0720 ZONE + 3

LAT. 58 ° 11.4 'N LONG. 62 ° 34.2 'W. DEPTH 92 fm. BT NO. BD 4, 280

WEA. Fine AIR TEMP. 48.1 °F. WIND N 5 kts. SECCHI 66 ft.

DEPTH m	TEMP. °C.	SAL. °/oo	σ_t	O_2 ml/L	PO_4 µgA/L
0	6.1	28.82	22.69		
5	5.86	29.69	23.42		
10	4.31	30.91	24.54		
20	2.08	31.69	25.34		
30	1.21	31.87	25.55		
50	0.08	32.10	25.79		
100	-1.69	32.84	26.44		
150	-1.72	32.90	26.49		

REMARKS:

STA. NO. BD-28 DATE 7/31/52 TIME 0920 ZONE + 3

LAT. 58 ° 09.5 'N LONG. 62 ° 45 'W. DEPTH 143 fm. BT NO. BD 4, 281 & 282

WEA. Fine AIR TEMP. 55.0 °F. WIND SSE 6 kts. SECCHI 65 ft

DEPTH m	TEMP °C.	SAL. °/oo	σ_t	O_2 ml/L	PO_4 µgA/L
0	7.5	27.83	21.75	7.56	0.25
5	5.26	30.01	23.73	7.96	0.50
10	3.19	31.08	24.77	8.26	0.20
20	2.09	31.69	25.34	8.38	0.25
30	1.57	31.82	25.48	8.29	0.20
50	0.15	31.94	25.61	8.47	0.30
100	-1.66	32.83	26.43	7.45	0.15
150	-1.73	32.86	26.46	7.40	0.30
200	-1.69	32.86	26.45	7.36	0.50
250	-1.74	32.88	26.48	7.39	0.25

REMARKS:

STA. NO. BD-29 DATE 7/31/52 TIME 1110 ZONE + 3

LAT. 58 ° 08.5 'N LONG. 62 ° 55.3 W. DEPTH 99 fm. BT NO. BD 4, 283 & 284

WEA. Fine AIR TEMP. 60.0 °F. WIND lgt. var kts. SECCHI 70 ft.

DEPTH m	TEMP °C.	SAL. °/oo	σ_t	O_2 ml/L	PO_4 µgA/L
0	6.7	27.75	21.81		
5	4.72	30.17	23.91		
10	2.71	31.38	25.05		
20	2.07	31.65	25.32		
30	1.27	31.64	25.36		
50	- .10	32.01	25.72		
100	-1.67	32.75	26.37		
150	-1.71	32.79	26.41		

REMARKS:

STA. NO. BD-26 DATE 3/26/54 TIME 1320 ZONE + 4

LAT. 58 ° 14.2'N LONG. 62 ° 29.0 'W. DEPTH 62 fm. BT NO. BD 12, 4

WEA. Fine AIR TEMP. 5 °F. WIND W 3 kts. SECCHI — ft.

DEPTH m	TEMP. °C.	SAL. °/oo	σ_t	O_2 ml/L	PO_4 µgA/L
0	-1.67	32.75	26.38		
5	-1.77	32.76	26.38		
10	-1.78	32.75	26.38		
20	-1.78	32.76	26.39		
30	-1.79	32.76	26.39		
50	-1.78	32.76	26.39		
100	-1.78	32.77	26.39		

REMARKS: Snow cover - 0 Ice thickness - 16"

STA. NO. BD-28 DATE 3/29/54 TIME 1330 ZONE + 4

LAT. 58 ° 09.5 'N LONG. 62 ° 45.0 'W. DEPTH 143 fm. BT NO. BD 12, 5

WEA. Blizzard AIR TEMP. 4 °F. WIND NE 5 kts. SECCHI — ft.

DEPTH m	TEMP °C.	SAL. °/oo	σ_t	O_2 ml/L	PO_4 µgA/L
0	-1.67	32.79	26.41		
5	-1.75	32.78	26.40		
10	-1.75	32.75	26.38		
20	-1.75	32.75	26.38		
30	-1.75	32.75	26.38		
50	-1.75	32.75	26.38		
100	-1.75	32.75	26.38		
150	-1.74	32.75	26.38		
200	-1.77	32.75	26.38		
250	-1.75	32.75	26.38		

REMARKS: Snow cover - 10" - 12" Ice thickness - 33"

STA. NO. BD-30 DATE 4/7/54 TIME 1930 ZONE + 4

LAT. 58 ° 04.7 'N LONG. 63 ° 06.0 'W. DEPTH -- fm. BT NO. BD 12, 6

WEA. Fine AIR TEMP. 8.5 °F. WIND W 5 kts. SECCHI — ft.

DEPTH m	TEMP °C.	SAL. °/oo	σ_t	O_2 ml/L	PO_4 µgA/L
0	-1.67	32.77	26.39		
5	-1.76	32.72	26.35		
10	-1.76	32.72	26.35		
20	-1.75	32.74	26.36		
30	-1.76	32.72	26.35		
50	-1.77	32.72	26.35		
100	-1.74	32.74	26.36		

REMARKS: Snow cover - 24" Ice thickness - 47"

STA. NO. BD-130 DATE 7/9/54 TIME 1600 ZONE + 3
LAT. 58 ° 06.6'N LONG. 63 ° 00.8 'W. DEPTH 66 fm. BT NO. BD 12, 107
WEA. Fine AIR TEMP. 50.1 °F. WIND E 5 kts. SECCHI 25 ft.

DEPTH m	TEMP. °C.	SAL. °/oo	σ_t	O$_2$ ml/L	PO$_4$ µgA/L
0	5.9	28.64	22.58	7.70	0.17
5	5.72	28.66	22.61	7.81	0.22
10	3.79	29.58	23.58	8.50	0.22
20	0.95	31.55	25.29	9.05	0.33
30	0.44	31.65	25.41	8.66	0.54
50	- .56	32.10	25.81	8.86	0.68
100	-1.72	32.65	26.29	6.73	1.12

REMARKS:

STA. NO. BD-33 DATE 7/9/54 TIME 1900 ZONE + 3
LAT. 58 ° 01.5 'N LONG. 63 ° 08.0 'W. DEPTH 43 fm. BT NO. BD 12, 108
WEA. Fine AIR TEMP. 55.8 °F. WIND NNW 7 kts. SECCHI 20 ft.

DEPTH m	TEMP °C.	SAL. °/oo	σ_t	O$_2$ ml/L	PO$_4$ µgA/L
0	6.2	27.11	21.33		
5	5.34	27.63	21.83		
10	2.84	30.08	24.01		
20	1.00	31.38	25.16		
30	-1.04	32.25	25.95		
50	-1.62	32.41	26.09		
75	-1.73	32.57	26.23		

REMARKS:

STA. NO. BD-29 DATE 7/10/54 TIME 0530 ZONE + 3
LAT. 58 ° 08.5 'N LONG. 62 ° 55.2 'W. DEPTH 100 fm. BT NO. BD 12, 109
WEA. Fine AIR TEMP. 45.0 °F. WIND W lgt. kts. SECCHI 22 ft.

DEPTH m	TEMP °C.	SAL. °/oo	σ_t	O$_2$ ml/L	PO$_4$ µgA/L
0	5.8	28.87	22.78		
5	5.44	28.93	22.85		
10	2.05	30.75	24.60		
20	1.04	31.38	25.16		
30	0.49	31.58	25.35		
50	- .87	32.21	25.91		
100	-1.74	32.57	26.23		
150	-1.76	32.70	26.33		
180	-1.76	32.70	26.33		

REMARKS:

STA. NO. BD-28 DATE 7/10/54 TIME 0800 ZONE + 3
LAT. 58 ° 09.5 'N LONG. 62 ° 45.0 'W. DEPTH 143 fm. BT NO. BD 12, 110
WEA. Fine AIR TEMP. 44.2 °F. WIND W lgt. kts. SECCHI 31 ft.

DEPTH m	TEMP. °C.	SAL. °/oo	σ_t	O$_2$ ml/L	PO$_4$ µgA/L
0	3.3	29.38	23.40	8.24	0.51
5	3.34	30.28	24.12	7.81	0.61
10	1.56	30.93	24.77	9.27	0.51
20	1.46	31.31	25.08	9.32	0.74
30	0.12	31.58	25.37	8.11	0.81
50	- .66	32.20	25.90	7.45	0.97
100	-1.71	32.66	26.30	7.03	1.47
150	-1.75	32.68	26.32	7.16	1.52
200	-1.76	32.70	26.33	7.22	1.55
250	-1.75	32.70	26.33	6.41	1.53

REMARKS:

STA. NO. BD-27 DATE 7/10/54 TIME 1215 ZONE + 3
LAT. 58 ° 11.5 'N LONG. 62 ° 34.2 'W. DEPTH 99 fm. BT NO. BD 12, 111
WEA. Fine AIR TEMP. 51.0 °F. WIND Calm kts. SECCHI 33 ft.

DEPTH m	TEMP °C.	SAL °/oo	σ_t	O$_2$ ml/L	PO$_4$ µgA/L
0	2.6	30.21	24.12		
5	1.00	30.30	24.29		
10	- .18	30.77	24.72		
20	0.20	31.11	24.99		
30	- .08	31.46	25.27		
50	- .57	32.09	25.80		
100	-1.71	32.68	26.32		
150	-1.74	32.70	26.33		
175	-1.73	32.74	26.36		

REMARKS: Moored to ice pan

STA. NO. BD-26 DATE 7/10/54 TIME 1415 ZONE + 3
LAT. 58 ° 14.2'N. LONG. 62 ° 29.0 'W. DEPTH 64 fm. BT. NO. BD 12, 112
WEA. Fine AIR TEMP. 49.1 °F. WIND Calm kts. SECCHI 20 ft.

DEPTH m	TEMP °C.	SAL. °/oo	σ_t	O$_2$ ml/L	PO$_4$ µgA/L
0	2.5	29.38	23.47	8.81	0.60
5	- .05	30.41	24.43	9.15	0.58
10	0.05	30.73	24.69	9.25	0.62
20	- .19	31.26	25.12	8.84	0.55
30	- .06	31.51	25.32	8.32	0.48
50	- .68	31.83	25.60	7.70	1.17
100	-1.29	32.48	26.14	7.32	1.09

REMARKS: Moored to ice pan

STA. NO. BD-130 DATE 7/31/54 TIME 1420 ZONE + 3

LAT. 58 ° 06.6 'N LONG. 63 ° 00.8 'W. DEPTH 68 fm. BT NO. BD 12, 147

WEA. Overcast AIR TEMP. 50.5 °F. WIND E 5 kts. SECCHI 26 ft.

DEPTH m	TEMP. °C.	SAL. °/oo	σt	O2 ml/L	PO4 µgA/L
0	9.0	---	---		
5	8.99	21.65	18.05		
10	1.70	30.73	24.77	9.19	
20	0.88	31.55	25.38		
30	0.11	31.80	25.56	8.80	
50	- .63	31.92	25.63	7.76	
80	-1.29	32.47	26.05	7.18	
110	-1.71	32.69	26.22	6.37	

REMARKS:

STA. NO. BD-133 DATE 8/3/54 TIME 1400 ZONE + 3

LAT. 58 ° 16 'N LONG. 62 ° 10 'W. DEPTH 115 fm. BT NO. BD 12, 150

WEA. Fine AIR TEMP. 41.4 °F. WIND Calm kts. SECCHI 13 ft.

DEPTH m	TEMP °C.	SAL °/oo	σt	O2 ml/L	PO4 µgA/L
0	2.2	30.88	24.94	9.15	0.84
5	1.21	31.58	25.43	9.40	0.71
10	0.71	31.74	25.53	8.95	1.41
20	0.59	31.82	25.59	8.75	0.69
30	0.53	31.85	25.62	8.46	0.63
50	-1.13	32.50	26.07	8.02	0.86
100	-1.30	32.84	26.34	7.16	1.41
150	-1.33	32.92	26.40	6.91	1.27

REMARKS:

STA. NO. BD-133 DATE 8/11/54 TIME 1045 ZONE + 3

LAT. 58 ° 16.0 'N. LONG. 62 ° 10.0 'W. DEPTH 110 fm. BT. NO. BD 12, 156

WEA. Fine AIR TEMP. 50.0 °F. WIND SSE lgt. kts. SECCHI 41 ft.

DEPTH m	TEMP °C.	SAL. °/oo	σt	O2 ml/L	PO4 µgA/L
0	4.0	31.38	24.93		
5	---	31.47	---		
10	1.83	31.80	25.45		
20	0.90	32.03	25.70		
30	0.31	32.20	25.85		
50	- .52	32.48	26.12		
100	-1.26	32.88	26.47		
150	-1.22	32.99	26.56		

REMARKS:

STA. NO. BD-26 DATE 8/11/54 TIME 1825 ZONE + 3

LAT. 58 ° 14.2 'N LONG. 62 ° 29.0 'W. DEPTH 64 fm. BT NO. BD 12, 157

WEA. Cloudy AIR TEMP. 49.2 °F. WIND SSE 5 kts. SECCHI 38 ft.

DEPTH m	TEMP. °C.	SAL. °/oo	σt	O2 ml/L	PO4 µgA/L
0	6.4	28.78	22.62		
5	2.53	31.56	25.21		
10	2.96	31.76	25.33		
20	0.30	32.14	25.80		
30	-0.28	32.32	25.98		
50	-0.53	32.48	26.12		
100	-1.06	32.61	26.24		

REMARKS:

STA. NO. BD-27 DATE 8/11/54 TIME 1935 ZONE + 3

LAT. 58 ° 11.5 'N LONG. 62 ° 34.2 'W. DEPTH 99 fm. BT NO. BD 12, 158

WEA. Cloudy AIR TEMP. 52.1 °F. WIND NNE 5 kts. SECCHI 49 ft.

DEPTH m	TEMP °C.	SAL °/oo	σt	O2 ml/L	PO4 µgA/L
0	9.2	26.29	20.32		
5	0.91	31.44	25.22		
10	0.01	31.65	25.43		
20	-0.76	31.92	25.68		
30	-0.87	32.01	25.75		
50	-0.58	32.30	25.97		
100	-1.64	32.72	26.35		
150	-1.71	32.72	26.35		
175	-1.70	32.77	26.39		

REMARKS:

STA. NO. BD-28 DATE 8/12/54 TIME 0645 ZONE + 3

LAT. 58 ° 09.5 'N. LONG. 62 ° 45.0 'W. DEPTH 143 fm. BT. NO. BD 12, 159

WEA. Fine AIR TEMP. 49.0 °F. WIND SE 5 kts. SECCHI 47 ft.

DEPTH m	TEMP °C.	SAL. °/oo	σt	O2 ml/L	PO4 µgA/L
0	10.8	23.30	17.75	6.67	1.09
5	1.62	31.35	25.09	9.08	0.52
10	-0.02	31.78	25.53	8.90	1.22
20	---	31.96	---	7.92	1.23
30	-0.92	32.16	25.88	7.40	1.00
50	-0.99	32.29	25.98	7.29	1.46
100	-1.68	32.72	26.35	6.84	1.32
150	-1.72	32.75	26.38	6.86	1.56
200	-1.74	32.77	26.39	6.88	1.29
250	-1.74	32.75	26.38	6.94	1.31

REMARKS:

STA. NO. BD-29 DATE 8/12/54 TIME 0915 ZONE + 3

LAT. 58 ° 08.5 'N LONG. 62 ° 55.2 'W. DEPTH 100 fm. BT NO. BD 12, 160

WEA. Cloudy AIR TEMP. 51.9 °F. WIND SE 5 kts. SECCHI 39 ft.

DEPTH m	TEMP. °C.	SAL. °/oo	σ_t	O_2 ml/L	PO_4 µgA/L
0	11.1	22.14	16.82		
5	1.71	31.42	25.15		
10	0.79	31.74	25.46		
20	- .10	31.92	25.65		
30	- .76	32.07	25.80		
50	- .90	32.21	25.91		
100	-1.67	32.70	26.33		
150	-1.74	32.75	26.38		
180	-1.78	32.75	26.38		

REMARKS:

STA. NO. BD-134 DATE 8/12/54 TIME 1015 ZONE + 3

LAT. 58 ° 06.1 'N LONG. 62 ° 59.5 'W. DEPTH 22 fm. BT NO. BD 12, 161

WEA. Fine AIR TEMP. 56.0 °F. WIND E 5 kts. SECCHI — ft.

DEPTH m	TEMP °C.	SAL °/oo	σ_t	O_2 ml/L	PO_4 µgA/L
0	11.1	22.07	16.76		
5	2.04	31.42	25.13		
10	0.24	31.69	25.45		
20	- .38	31.98	25.71		
30	- .60	32.12	25.83		

REMARKS:

STA. NO. BD-135 DATE 8/12/54 TIME 1040 ZONE + 3

LAT. 58 ° 06.3 'N. LONG. 63 ° 00.2 'W. DEPTH 66 fm. BT. NO. BD 12, 162

WEA. Fine AIR TEMP. 57.5 °F. WIND E 10 kts. SECCHI 41 ft.

DEPTH m	TEMP °C.	SAL. °/oo	σ_t	O_2 ml/L	PO_4 µgA/L
0	8.3	22.41	17.41		
5	1.55	31.38	25.13		
10	0.28	31.74	25.48		
20	- .37	32.00	25.72		
30	- .68	32.12	25.84		
50	- .81	32.25	25.95		
100	-1.57	32.65	26.28		

REMARKS:

STA. NO. BD-130 DATE 8/12/54 TIME 1105 ZONE + 3

LAT. 58 ° 06.6 'N LONG. 63 ° 00.8 'W. DEPTH 68 fm. BT NO. BD 12, 163

WEA. Fine AIR TEMP. 56.5 °F. WIND E 10kts. SECCHI 41 ft.

DEPTH m	TEMP. °C.	SAL. °/oo	σ_t	O_2 ml/L	PO_4 µgA/L
0	10.9	21.51	16.36		
5	1.96	31.27	25.03		
10	0.57	31.80	25.52		
20	- .42	31.94	25.68		
30	- .74	32.12	25.84		
50	- .88	32.29	25.98	7.40	
100	-1.61	32.68	26.31	6.52	
120	-1.70	32.75	26.38	6.18	

REMARKS:

STA. NO. BD-136 DATE 8/12/54 TIME 1135 ZONE + 3

LAT. 58 ° 06.8 'N LONG. 63 ° 01.3 'W. DEPTH 68 fm. BT NO. BD 12, 164

WEA. Fine AIR TEMP. 57.0 °F. WIND E 12 kts. SECCHI 41 ft.

DEPTH m	TEMP °C.	SAL °/oo	σ_t	O_2 ml/L	PO_4 µgA/L
0	9.9	21.82	16.72		
5	3.46	30.72	24.46		
10	0.48	31.80	25.52		
20	- .33	31.98	25.70		
30	- .63	32.14	25.85		
50	- .91	32.29	25.98		
100	-1.61	32.65	26.28		

REMARKS:

STA. NO. BD-137 DATE 8/12/54 TIME 1205 ZONE + 3

LAT. 58 ° 06.9 'N. LONG. 63 ° 01.8 'W. DEPTH 68 fm. BT. NO. BD 12, 165

WEA. Fine AIR TEMP. 55.7 °F. WIND E 10 kts. SECCHI — ft.

DEPTH m	TEMP °C.	SAL. °/oo	σ_t	O_2 ml/L	PO_4 µgA/L
0	8.8	21.58	16.73		
5	4.43	29.42	23.34		
10	0.22	31.87	25.60		
20	- .42	32.01	25.74		
30	- .65	32.10	25.81		
50	- .93	32.30	25.98		

REMARKS:

STA. NO. BD-33 DATE 8/12/54 TIME 1310 ZONE + 3

LAT. 58 ° 01.5 'N LONG. 63 ° 08.0 'W. DEPTH 43 fm. BT NO. BD 12, 166

WEA. Fine AIR TEMP. 64.6 °F. WIND N 7 kts. SECCHI 62 ft.

DEPTH m	TEMP. °C.	SAL. °/oo	σ_t	O_2 ml/L	PO_4 µgA/L
0	8.6	23.53	18.25		
5	4.57	29.72	23.57	8.75	0.49
10	0.82	31.71	25.43		
20	0.10	31.96	25.67		
30	- .29	32.07	25.78		
50	-1.46	32.63	26.27	6.68	1.29
75	-1.68	32.68	26.32	5.65	1.69

REMARKS:

STA. NO. BD-26 DATE 10/15/54 TIME 1300 ZONE + 3½

LAT. 58° 14.2 'N LONG. 62 ° 29.0 'W. DEPTH 64 fm. BT NO. BD 12, 254

WEA. Overcast AIR TEMP. 37.7 °F. WIND Calm kts. SECCHI -- ft.

DEPTH m	TEMP °C.	SAL °/oo	σ_t	O_2 ml/L	PO_4 µgA/L
0	1.6	----	----		
5	1.52	32.07	25.69		
10	1.48	32.12	25.73		
20	1.48	----	----		
30	1.36	32.23	25.83		
50	1.09	32.32	25.92		
100	0.38	---	----		

REMARKS:

STA. NO. BD-28 DATE 10/18/54 TIME 1230 ZONE + 3½

LAT. 58 ° 09.5 'N. LONG. 62 ° 45.0 'W. DEPTH 143 fm. BT. NO. BD 12, 255

WEA. Mild AIR TEMP. 43.4 °F. WIND W 5 kts. SECCHI -- ft.

DEPTH m	TEMP °C.	SAL. °/oo	σ_t	O_2 ml/L	PO_4 µgA/L
0	1.7	31.42	25.15		
5	1.67	31.58	25.28		
10	1.60	----	----		
20	1.41	32.08	25.70		
30	1.27	32.10	25.73		
50	0.68	32.33	25.94		
100	-1.01	32.62	26.25		
150	-1.51	32.69	26.32		
200	-1.63	32.75	26.38		
250	-1.68	32.76	26.39		

REMARKS:

STA. NO. BD-130 DATE 10/26/54 TIME 1430 ZONE + 3½

LAT. 58 ° 06.6 'N LONG. 63 ° 00.8 'W. DEPTH 68 fm. BT NO. BD 12, 257

WEA. Fine AIR TEMP. 30.8 °F. WIND WNW 10 kts. SECCHI -- ft.

DEPTH m	TEMP. °C.	SAL. °/oo	σ_t	O_2 ml/L	PO_4 µgA/L
0	0.00	31.16	25.03		
5	0.35	31.38	25.19		
10	0.51	31.57	25.35		
20	0.85	32.20	25.83		
30	0.50	32.25	25.88		
50	0.01	32.36	26.00		
100	- .96	32.51	26.16		

REMARKS:

STA. NO. DATE TIME ZONE +

LAT. ° 'N LONG. ° 'W. DEPTH fm. BT NO.

WEA. AIR TEMP. °F. WIND kts. SECCHI ft.

DEPTH m	TEMP °C.	SAL °/oo	σ_t	O_2 ml/L	PO_4 µgA/L

REMARKS:

STA. NO. DATE TIME ZONE +

LAT. ° 'N. LONG. ° 'W. DEPTH fm. BT. NO.

WEA. AIR TEMP. °F. WIND kts. SECCHI ft.

DEPTH m	TEMP °C.	SAL. °/oo	σ_t	O_2 ml/L	PO_4 µgA/L

REMARKS:

Contribution No. 832

B R E V I O R A

Museum of Comparative Zoology

Cambridge, Mass. April 6, 1956 Number 53

FOOD-FINDING BY A CAPTIVE PORPOISE (*TURSIOPS TRUNCATUS*)[1]

By William E. Schevill and Barbara Lawrence

Introduction 1
Experimental arrangements 2
Passive location 4
Active or echolocation 4
  Echolocation to determine presence of fish 6
  Echolocation to distinguish between alternate feeding places 7
Passive versus active location 8
Night tests 9
Vision 10
Discussion 12
Acknowledgments 14
References 14

INTRODUCTION

It soon appears on acquaintance with porpoises that these animals are well endowed with hearing and sight, and that they use both these senses in their normal environment. A captive *Tursiops truncatus* was confronted with the problem of finding unfamiliar food under varying and sometimes rather complicated circumstances, all unlike the normal hunting of his previous wild free existence. Experiments to find out which sense was relied on most and in what ways it was most useful have shown a wide and not unexpected variation in a single individual. Like man, the animal used all the clues he could get. Sometimes he listened, sometimes he looked, and sometimes he was so busy doing whatever he had last done that he missed perfectly obvious clues.

---

[1] Contribution No. 832 from the Woods Hole Oceanographic Institution.

Although there was such variation in his responses to similar circumstances that many experiments produced conflicting evidence, there was a certain pattern which makes possible a number of conclusions. When he was finding his food he was most eager, swift, and accurate in coming to the sound of a slap on the water. When he had no such clue he would find the fish, evidently by echolocation, if it was in a region where he expected to find food. His final searching for the fish was by eye, though he could not clearly distinguish his preferred butterfish from other offerings. His willingness to use clues, almost we might say his ability to notice them, depended on his memory and other psychological factors as well as hunger.

EXPERIMENTAL ARRANGEMENTS

Our laboratory on an island at Woods Hole was a pond 34 m. long, 23 m. wide, and 2.5 m. deep, cut off from the sea by a stony beach about 30 m. wide. Our subject was an old bull *Tursiops truncatus,* 203.6 kg. in weight and 267 cm. long, brought here from Florida especially for this experiment. Some injury had damaged his right eye, which we never observed him using, and towards the end of our work his left eye started to cloud over. Whatever the damage was, it did not affect his hearing, which was sharply directional. Temperamentally, he differed from our earlier subject (Lawrence and Schevill 1954), being bold and aggressive, and for this reason was often seen at the surface. Puzzling situations near at hand often caused him to thrust his head above the water, or ''souse out'' in this way to look, and when further off he would ''pitchpole'' straight up for a third or more of his length. He learned fast, and while his evident preference for doing as he pleased would make any formal analysis of his responses rather meaningless, this independence gave a much more varied and accurate picture of his inclinations and abilities than we could have obtained otherwise. Since he preferred going hungry to being forced into situations he disliked, the tests we devised were as simple as were consistent with getting reliable answers. Under these circumstances, it soon became clear that in many cases failure on his part to respond was due not to inadequacy of his senses, but to lack of hunger, temporary unwillingness to approach the feeder, or some other non-sensory reason.

The porpoise was ordinarily fed from a punt 3.6 m. long moored against the bank, usually at right angles, but sometimes parallel to it. In some experiments a small dinghy served as a second feeding station. The position of the feeder in the boat varied. The porpoise was fed dead butterfish (*Poronotus triacanthus*) about 8 to 23 cm. long, held in the water by hand, and was called by an acoustic signal made by slapping the water, or by hammer strokes on a partially immersed iron pipe, or by tones (ranging usually between 500 and 30,000 cycles per second) from an audio oscillator through an underwater sound projector; the pipe and oscillator signals were always remote from the feeding station.

Most of our work was done during daylight, so that we could watch where the animal was and how he responded under different conditions. It was not difficult to keep track of him because he frequently showed at the surface. Because porpoises see well both above and under water, we had to be sure than an apparently acoustic response was not in reality visual. This was the easier because his constant swimming kept the water stirred up and very murky. Transparency by Secchi disk from the surface was rarely as great as 70 cm. and often less than 45 cm.; the very unusual maximum was 85 cm. on 19 September. At 11 o'clock on a typical sunny day measurements made by diving after dark-adaptation gave a Secchi disk reading of 23 cm. from the diving mask at a depth of 2.4 m., and 61 cm. at the surafce. Underwater visibility will scarcely exceed the Secchi disk reading, and will be appreciably less for less bright objects.

This, and observations of the porpoise's behavior when he was finding fish by eye, led us to believe that we are conservative in saying that through the water he could not possibly have discerned with any clarity objects as much as 1 m. away from him. As a further check we repeated most of our tests at night.

We selected the pond because of its great freedom from noise-making animals; the beach protected us from most of the noises of the sea outside. Our listening gear included an AX58C Rochelle salt crystal hydrophone and a WHOI sound level meter (Suitcase), and was sensitive enough to pick up very plainly the noise of fine beach sand strewed into the water 20 m. from the hydrophone.

PASSIVE LOCATION

One of the most conspicuous traits of our porpoise was the accuracy and confidence with which he promptly made his way to the place where the water had been slapped. There was no uncertainty or hesitation in his response to such a signal; no matter where he was in the pond, he always came with alacrity when he was thus called unless he was not hungry or there were other obvious psychological reasons for his refusing to do so. While failure to reward response to a remote signal often made him ignore subsequent calls, this was never the case with a slap on the surface. As often as we repeated the slap he would return quickly, though we never called him more than four or five times in succession without giving him a fish.

Not only was he prompt in his response to this slap, but, when conditioned to it, he chose it in preference to other clues. If (as described on p. 8) a fish was slapped in one place and held in the water in another, he would choose to go to the place of the sound instead of to the fish, until he learned this clue was unreliable. His apparent reliance on this signal alone sometimes led him to miss a nearby fish entirely.

The porpoise's hearing was sharply directional and his estimates of range (distance) were very close, as is shown by his repeatedly homing directly on a single slap (with no fish in the water) to well within 20 cm. from ranges often as great as 20 to 25 m. through turbid waters and without coming up to look on the way.

ACTIVE OR ECHOLOCATION

The evidence that our porpoise was echolocating his fish was accumulated over eleven weeks of close observation of his behavior, when an increasing knowledge of what to expect from him under different circumstances made it possible to understand and to check his various capabilities with a fair degree of accuracy.

Early in our work we noticed that our porpoise usually made a characteristic sequence of ''creaks'' as he came in for a fish, and that in the last meter or so these sounds were matched to horizontal movements of his head. By ''creaks'' we mean a series of impulsive clicks made at widely varying repetition rates (from less than 10 to more than 400 per second), the slower ones sounding like knocks and the faster ones like snarls or whines. They have also been called ''barks'', ''snores'', ''rusty hinge'', or ''rasping and grating sounds,'' etc., by various authors, such as McBride and Hebb 1948, Kritzler 1952, and Wood 1954, and have been heard from several odontocetes. Some acoustic details of *Tursiops* calls have been given by Kellogg, Kohler, and Morris 1953. The other common odontocete sound, the whistle-like squeal, was evidently not employed in echolocation, and appears to be primarily communcative. The acoustic details of these sounds will be reported elsewhere.

Before long we noticed that when he was creaking he almost always swam directly to a fish held quietly in the water. When he was not creaking he would not do so. Though this suggested echolocation rather persuasively, we had to be sure that we were not inadvertently giving him other clues and that he was not using sight. His remarkably good hearing and his evident reliance on passive auditory clues made it especially important to make sure he was not coming because he heard us put a fish in water. Very occasionally it seemed highly likely this was just what he was doing, though we ourselves could never detect any sounds, even with our extremely sensitive listening gear. Responses at these few times were discounted. At other times when we were doubtful, we checked his behavior by dipping fish or fingers in and out or dabbling at the surface. This almost never brought him, nor could we get him to come unsignaled to a fish's nose in the water, even though he was coming accurately to a whole fish. Repeated checks also eliminated movements in the boat or the position of the feeder as clues.

The possibility that he was using sight to guide him to a fish had also to be investigated, and we did this in two ways. First of all we devised a series of daytime experiments which, because of the murkiness of the water (see Secchi disk readings), eliminated any possibility that he was using vision to locate his fish from a distance. These experiments are described in some detail below. After we had learned how he reacted to these different situations we repeated the tests at night, with similar results, which are also described below.

Two rather different sets of circumstances stimulated him to rely on echolocation alone in finding his food. Sometimes he used this means to discover whether or not a fish was waiting for him, and sometimes this was the way he distinguished between alternate feeding places.

Echolocation to Determine Presence of Fish

His reliance on echolocation to tell him whether or not a fish was waiting showed in a number of ways. Often, in the absence of an expected signal, he would circle the pond, creaking only as he passed the feeding station. This was anywhere from 1 to 5 meters away, and occasionally farther. If a fish were in the water as he passed, he would turn and swim directly to it; if there were no fish he would go on by. If a fish were slipped as silently as possible (and we believe inaudibly) into the water after he had passed when he was starting to circle away, he would usually turn and come back. We tried this many times on seven different days. Of these the first is especially significant. It was early in our work and was our first attempt to bring him to a fish without a signal, he being then conditioned to come only to the slap of a fish on the water. At first, although he passed nearby creaking, he did not come to the fish, but later that morning he was attracted some of the time. Five days later we tried again, and he had apparently learned not to wait for a signal. By now he would come in for a fish held silently in the water if he was creaking as he passed by; his decision to come on in seemed usually to be made at a distance of less than 5 but occasionally as much as 15 m. This was repeated a number of times during the next four days, and again two months later.

Our evidence that the porpoise was not seeing the fish before deciding to swim to it was partly his excessive distance when he turned toward it and partly the fact that he often had his bad eye towards the punt as he passed.

As well as using echolocation to find fish when he suspected fish should be available, he also used this means to confirm the reliability of a signal. While he almost never refused to come to the sound of a fish slapped on the water, various circumstances on several occasions made him uncertain about other signals. Early in his training he learned that an oscillator note or pipe-banging in various parts of the pond meant that he would get a fish at the feeding station, and, like our earlier porpoise, on being signaled with no fish in the water, he would make his way to the proper place to get it. Sometimes, however, he ignored the remote signal until there was a fish in the water as well. With this to convince him he would come unhesitatingly. This reaction was especially clear on four occasions when we had made changes which he did not like in the feeding station. These were all times when he was in good health and hungry, and the remote signal was one we knew he could hear. Until he was accustomed to the new arrangement, no matter how often we called, he always waited till there was a fish in the water before responding to the signal. The first time we had to signal six times with a fish in the water before he began to come on signal only. The other three occasions, at a much later date, were at successive feedings on two days. The first morning it took twelve fish, that afternoon three, and the following morning seven before he would come with no fish in the water. At these times he was creaking as he swam and for the most part responded to the signal by starting towards the feeding station, but with no fish in the water he usually turned away at 2½ meters or more, though sometimes he circled as near as a meter and a quarter. When he was thus relying on echolocation to tell him of the presence of a fish, he rarely troubled to look above the surface. Later, when he was coming on the remote signal with no fish held in, he often soused out of the water on the way in, eyeing the situation from a distance of ten or more meters.

His ability to arrive at a fish he could not see was further demonstrated one afternoon when his left eye failed. At that time, on a remote signal, he repeatedly swam directly to fish held anywhere over a 5½ m. radius.

Echolocation to Distinguish Between Alternate Feeding Places

To test his use of echolocation, two feeders slapped fish simultaneously on opposite sides of the punt and then one held a fish in the water while the other held a hand out over the water as if feeding. The distance between slaps was about 2 m., and a net projecting 2.5 m. from the end of the punt and hanging to the bottom of the pond prevented the porpoise from circling close to investigate by eye. We alternated feeding in irregular fashion and the feeders often exchanged places in order to eliminate any other clues. The first time we tried this he came to the correct side 24 times and the wrong side 11, the next time he made 45 correct responses and 13 wrong. His behavior was similar on both occasions. He never ignored a summons and always came directly and fast, creaking as he approached deep. The Secchi disk reading was 61 cm., and he was at the very least 2.5 m. from the fish when he had to decide which side of the net to go. In contrast to his behavior with a remote signal, he made no optical checks on the way in, though sometimes when feeding was slow he pitchpoled out, looking at us. We cannot say how often his wrong responses were caused by the net interfering with his sound patterns. We suspected this on some occasions, while other errors probably are evidence that his echolocation was not perfect.

PASSIVE VERSUS ACTIVE LOCATION

Experiments to find out what kinds of clues were most successful or preferred produced interesting results. One rather simple but very instructive one, here called the A-B experiment, consisted of slapping at A and putting a fish in the water at B or vice versa, with the distance between A and B farther than he could see. This, with minor variations, we tried many times on each of fifteen different occasions, and though his responses varied, they made a very neat pattern. The first time we tried it, and when we returned to it after a period of other work, he would always swim, creaking, directly to the point of slap, search diligently there, and usually swim away unrewarded. If, in leaving, he found the fish, he would thereafter search at the point of slap and then swim directly to the fish no matter how we varied the relation of these two places to each other. Finally, it was possible to destroy his confidence in the slap as a worthwhile clue, and then for the most part he would go directly to the fish. When he swam directly to the fish there was no possibility that memory could have guided him, because the fish might have been anywhere over a six meter stretch. Nor could vision have helped, because he was never nearer than 6½ meters when we signaled, and usually a great deal farther away. When he looked first at the point of slap and then went on to find the fish, not pausing on the way, the distance between the two places (minimum 1.3 m., usually more, sometimes as much as 5.2 m.) seemed to preclude the possibility of his being guided by sight, the more so because in this secondary finding of a fish it made no apparent difference whether he approached with his bad or his good eye towards it.

In one variation of the A-B experiment we fixed the points 2 m. apart. If we slapped at A with the fish in the water at B or vice versa, he went directly to the fish; if we slapped with no fish in the water, he searched at the point of slap but never investigated the alternate place as he left unrewarded; if we let him search at the point of slap and then eased a fish quietly into the water at the other place, he would immedately go to it. On a number of other occasions we tried this third modification, varying the place where we put the fish, and he always creaked his way to it. This is not entirely conclusive, as there is a small but unlikely possibility that he might have heard the fish put in, though our efforts to check this led us to believe that this was not passive location (cf. below, p. 11).

NIGHT TESTS

All of the experiments described above were carried out during the day. We also tried most of these same experiments on dark nights and found the results closely paralleled our daytime observations. On two nights when we tried to get him to take fish unsignaled, he came, apparently directly, making about ten successful runs each time, though he sometimes swam past, creaking, without coming in, and sometimes appeared to search near the fish without taking it. On two other nights we tried the A-B experiment, the first time feeding ten fish which he readily found, though it was too dark for us to see if he made a preliminary search at the point of slap. During the second and more prolonged A-B experiment he repeatedly came to the fish, not the point of slap, especially when he came from far down the pond. Occasionally he searched first at point of slap, and twice he missed the fish entirely. The last night feeding was partly from the dinghy in the middle of the pond. Two slaps informed him that fish were to be had in the vicinity; thereafter on remote signal he came directly and accurately seven times in a row to a fish held anywhere in a radius of 6 m. Later, when we fed from the punt, he responded to the correct side 6 times, to the wrong side 2, and did not respond at all 2 other times.

VISION

While sound was important to our animal, we have good evidence that he relied greatly on vision as well, both above and beneath the surface of the water. A bad if not completely blind right eye made him left-sided in his approach to things he wished to see. This was a convenient check when we could not see his eye rolled towards what interested him.

When on arrival from Florida he was dumped into the pond, his first check of his new surroundings was optical. As soon as he hit the water he swam off fast and silently, sousing high out of the water and blowing frequently, with his good eye towards the shore. It was three minutes before we heard him utter a single sound, and nearly two minutes more before he spoke up as loudly and persistently as he did for most of the rest of his stay. It was hard not to think that he was looking over his new surroundings, perhaps searching for a break in the beach. His obvious awareness of things on the shore showed in many ways. During his first two weeks in the pond there were often clusters of people working at different places along the bank. At such times he often blew near them, rolling a little on his right side so that his left eye cleared the surface. Soon he took his surroundings more for granted and his inspections of the shore were less frequent, though he quickly noticed changes. Possibly also with the passage of three or four weeks he became more accustomed to his blind eye; at all events he rolled more often on an even keel, and without bringing his good eye out of the water.

While this kind of check on his surroundings was not important in helping him find his food, it did have a bearing on his behavior at feeding time. Too many people on the bank near the feeding station made him shy, and he would come in deep and depart hastily. The presence of someone in the boat from which we fed aroused his interest, and he would blow nearby, looking. Sometimes it even seemed as if he reacted differently to different feeders.

When we actually called him to eat with the well-understood slap of a fish on the water, he rarely troubled to make an optical check on the way in as he did with a remote signal, but swam directly from wherever he was, to collect his morsel. At other times when he was less sure of the summons, or when we were slow sending signals, he rolled high, looking towards the feeder, or soused out to see what was going on. On occasions when he was more than ordinarily curious, he would pitchpole out of water as far as his flippers, with his good eye looking ventrad towards us.

In addition to keeping track of things above the water, under ordinary circumstances he relied on vision to a great extent in his final accurate taking of a fish from the feeder. Often we could see his eye rolled forward towards the fish. As with our earlier animal, space permitting he would turn over on his side when close, and in the eleven weeks we fed him he only once took a fish with his right eye up. When he lingered at the end of the boat waiting for a fish it was always with the left eye up. When we fed him in a sort of narrow stall 1.2 m. wide so that he did not roll over as he approached, he swung his head from side to side farther to the right than to the left, so that his left eye was in position to scan both sides of the stall as well as the end of the punt.

Fish put in on his blind side or above his head did not attract his attention unless they were splashed. Fish put in nearby and directly in front of him he also took in more fumbling fashion, and on at least two occasions actually bumped into them before seizing them. On the other hand, anything within his range of vision quickly caught his attention. When a fish was moved 15 cm. or so above the water he would follow it with his eye and when it was held lower would put his snout out to snatch it.

Repeatedly, we found a difference in his fish-taking when visibility was especially poor or he himself not seeing well. This usually meant that he would begin his search farther from the fish, nodding his head more widely as he approached slowly, and would be more hesitant about taking the fish, sometimes fumbling and dropping it. A few times, when the fish were small, he missed them entirely. This was true not only when the water was murky, but also when we held the fish deep.

These indications that vision is important in his ultimate locating of the fish were borne out by his behavior on two separate occasions when the salinity in the pond was down and the water dirty. At these times it appeared that his left eye also was not seeing well. On the first occasion, for three days his fish-finding was less accurate and his search wider than was usual. Once he even bit at the corner of the punt, though the fish was less than 50 cm. away. The other occasion was one afternoon when his left eye failed; then, he approached with it shut, and would lie left side up at the end of the punt, not noticing the fish when it was moved above the surface, but coming to grab it clumsily when it was put in the water. Once when he swam past a fish in the water, he worked his way back to it slowly with very exaggerated head noddings and took the fish awkwardly deep in his mouth. Though his sight recovered after this, he never seemed to see out of his left eye as well as in the beginning. A whitish spot began to form and he would partly close his eye against a low sun, whether because it hurt or dazzled was impossible to tell. At these times his fish-taking was again less accurate, and contrasted with a greater ease when the sun was not shining directly in his eye.

While taking the fish was easier if he could rely on seeing it, he apparently could not discriminate between objects very well. Squid and flattened tin cans don't resemble butterfish much, but even after he had found out he did not like the first two he repeatedly took them in his mouth when they were offered instead of fish. In the same way he would bite at floating vegetation near the boat, at bits of rope, or even at a rusty pail. Size seemed easier for him to tell, and he not infrequently appeared to inspect and then leave small butterfish, about which he was not enthusiastic.

DISCUSSION

In this study we took a gregarious free-ranging animal that in nature is almost always found at least in small groups and often in immense herds, and placed it in solitary confinement. Whereas wild porpoises hunt live food that occurs in schools, ours was obliged to take single dead fish from the hand. Moreover, the single fish was usually close to a boat or a bank, instead of in the more open water to which wild *Tursiops* are accustomed.

Perhaps the most striking result of our work is the great variation observed in the way our single animal sought his food. His primary reliance on passive auditory clues could have been due to the small size of his target and to the confused echo patterns in the pond. Nevertheless, evidence accumulated that he often echolocated the food we offered him, thus supporting the widespread supposition (for example, Kellogg, Kohler, and Morris 1953) that this was how cetaceans hunted. The sounds the porpoise made at these times were faint; indeed, only the very loudest were audible to a submerged man, and, in fact, were picked up by our sensitive listening gear only because we at last had a porpoise in a really quiet place. Thus we learned that the supposed taciturnity of solitary porpoises (Lawrence and Schevill 1954, pp. 229-231) is rather a relative matter; it appears that they merely speak very softly. The noisy listening conditions of our previous experiment had led us into error when we reported (op. cit., p. 229) ''the complete absence'' of evidence for echolocation although we cited some, unrecognized, at the bottom of page 227.[1] The only evidence we had been aware of was in McBride's posthumous note (in press) on net avoidance (what our porpoise taught us about this will be reported in another paper).

To demonstrate whether an animal is using echolocation, the most definite way is to show that acoustic intereference affects performance. Thus Griffin and Galambos (1941) and Griffin (1953) by deafening bats and nocturnal birds showed that these animals then collided with obstacles that, undeafened, they had avoided. It is of course necessary to make sure that other senses, such as smell (evidently not available to cetaceans) or sight, have been excluded. Furthermore, it must be shown that sounds suitable for echolocation are produced. This last point is abundantly proved for porpoises (e.g., Wood 1952, 1954). The role of sight in our porpoise's food-finding has been discussed under Vision. We did not deafen our animal or interfere with his sound production.

Therefore, our evidence for echolocation by the porpoise is essentially that he consistently found fish when we could convince ourselves that no other clue (sight or sound not made by the porpoise himself) was available.

---

[1] On page 414 of an article published while this paper was in press, Griffin (1956. Hearing and acoustic orientation in marine animals. Deep-Sea Research, *3*, Suppl. (1955), pp. 406-417) suggests that just such an improved signal-to-noise ratio might reveal evidence of echolocation by porpoises.

The porpoise's performance seemed poorer on targets behind him, particularly at the longer ranges. In general, the creaks with the higher repetition rate were heard at the shorter ranges, but this orderly arrangement was usually confused, perhaps because of additional targets. At close range the creaks were timed to a horizontal sweeping of the head (nodding when on his side). These observations may be interpreted as indicating directionality, presumably in his sound production. We have not investigated this arresting possibility further, except to consider that perhaps the pneumatic cephalic sinuses may modify the radiation of sound from the larynx.

Echolocation was evidently not a perfect method for our porpoise. Perhaps the fault lay in the special conditions in the pond, where the presence of multiple reflections from the stones in the banks and bottom must have confused the echoes. The primary target was a small fish; behind it was the punt, and behind that was the shore. We noticed that when being fed from the small dinghy (with so much less boat in the water to return an echo), he ordinarily came right to the fish with less hesitation than when feeding at the punt. These are indications that echolocation did not give him clear and unequivocal information (human users of this technique will sympathize).

ACKNOWLEDGMENTS

This work was supported by an Office of Naval Research contract with the Woods Hole Oceanographic Institution. The porpoise was generously supplied by Marine Studios, Marineland, Florida. We are most grateful also to the Naushon Trustees for hospitably permitting us to use and modify the pond and its immediate surroundings. And of course we were greatly dependent on the ever-ready support of many of our colleagues at Woods Hole, without whose help the maintenance of the pond and porpoise would have been impossible. We with to thank Drs. R. H. Backus and C. P. Lyman and Prof. D. R. Griffin for critically reading the manuscript.

REFERENCES

Griffin, D. R.
1953. Acoustic orientation in the oil bird, *Steatornis*. Proc. Nat. Acad. Sci., **39** (8): 884–893.

GRIFFIN, D. R., and GALAMBOS, R.
1941. The sensory basis of obstacle avoidance by flying bats. Jour. Exper. Zool., **86**: 481–506.

KELLOGG, W. N., KOHLER, R., and MORRIS, H. N.
1953. Porpoise sounds as sonar signals. Science, **117** (3036): 239–243.

KRITZLER, HENRY
1952. Observations on the pilot whale in captivity. Jour. Mamm. **33** (3): 321–334.

MCBRIDE, ARTHUR F.
(In press.) Evidence for echolocation by cetaceans. Deep-Sea Research, **3**: (2)

MCBRIDE, A. F., and HEBB, D. O.
1948. Behavior of the captive bottle-nose dolphin, *Tursiops truncatus*. Jour. Compar. Physiol. Psychol., **41** (2): 111–123.

LAWRENCE, B., and SCHEVILL, W. E.
1954. *Tursiops* as an experimental subject. Jour. Mamm. **35** (2): 225–232.

WOOD, F. G., JR.
1952. Porpoise sounds. A phonograph record of underwater sounds . . . *Tursiops truncatus* and *Stenella plagiodon*. Published by the Marineland Research Laboratory.

WOOD, F. G., JR.
1954. Underwater sound production and concurrent behavior of captive porpoises, *Tursiops truncatus* and *Stenella plagiodon*. Bull. Mar. Sci. Gulf and Caribbean, **3** (2): 120–133.

Contribution No. 8

Deep-Sea Research, 1956, Vol. 3, pp. 237 to 241. Pergamon Press Ltd., London.

Echo-sounder observations of midwater nets and their towing cables

RICHARD H. BACKUS and J. B. HERSEY

(*Received* 21 *March*, 1956)

Abstract—By echo-sounding from a following ship it has been possible to determine the shape of towing cables as well as the depth to a net with varying amounts of wire out. It was found that at 2·5 knots the depth to the Isaacs-Kidd midwater trawl can be closely approximated by computing it from the wire angle measured at the surface.

INTRODUCTION

ECHO-SOUNDERS have been put to many uses since their development for measuring water depth. A recent application was that of WOOD and PARRISH (1951) who observed ground and midwater trawls in action. They examined the dimensions of the mouths of nets being towed and the contact of ground trawls with the bottom.

A programme of fishing with two-metre stramin closing nets and the ten-foot Isaacs-Kidd midwater trawl (IKMT) was carried out by our institution during the summer of 1953. In the absence of a reliable depth meter it was suggested that the echo sounder be used to determine the relationship between length-of-wire and depth-of-net. At the same time a telemetering depth meter was being developed for use with nets (DOW, 1954) and it was proposed that echo soundings provide one of the checks on the performance of this meter. On the echo-sounder record of an exploratory run, portions of the towing cable were clearly detectable as well as the net itself. It was then decided that with suitable range information, the shape of the towing cable could be determined.

PROCEDURE

The IKMT is described by the Scripps Institution of Oceanography (1953). The two-metre net used is described by LEAVITT (1935 and 1938). These nets were towed by the research vessel *Blue Dolphin* on $\frac{3}{8}''$, 7 by. 7, galvanized aircraft cord at approximately 2·5 knots. The length of the towing cable was measured by a standard type meter wheel (similar to the G. M. Mfg. Co.'s # 400) made for $\frac{5}{32}''$ wire. A correction of 6% has been added to indications of wire out to allow for the use of $\frac{3}{8}''$ wire on this meter. The research vessel *Bear* made the echo-sounder observations with an Edo Corp. AN/UQN-1B 12-kc echo sounder.

Since the fishing gear did not tow directly astern of *Blue Dolphin* but slightly off the starboard quarter it was necessary to conn *Bear* by sighting along the towing cable and relaying instructions by radio telephone. Range between *Bear* and *Blue Dolphin* was determined by stadimeter. On *Bear*'s first echo-sounder contact with the fishing gear, range observations were begun. A series of " marks " from the stadimeter operator on *Blue Dolphin* were relayed to the echo-sounder operator on *Bear* by radio telephone. These marks were entered on the echo-sounder record and the corresponding ranges were logged on *Blue Dolphin*.

On 23 August, a total of seven echo-sounding runs was made. In these runs the IKMT depressor (without net) was fastened to the end of the towing cable. The telemetering depth meter was placed about five metres above the depressor and the two-metre stramin net was fastened to the wire about 5 metres above the depth meter. This gear was first set with 636 metres of wire out and Runs 1-3 were made. The gear was then retrieved and it was discovered that the net had not opened. The gear was then set as before save that 535 m of wire were paid out. Echo-sounding Runs 4-7 were then made. When the gear was retrieved it was found that the net had again failed to open and also that the frame that supported the depth meter was badly bent. This indicated that at some time during the haul the various parts of the gear did not tow in their proper relationship.

On August 24 a total of 21 echo-sounding runs was made on the IKMT (complete) alone. These runs were made with varying lengths of towing cable as follows: 320 metres – 2 runs, 530 – 2, 742 – 2, 903 – 1, 1007 – 8, 1113 – 2 and 1221 – 4.

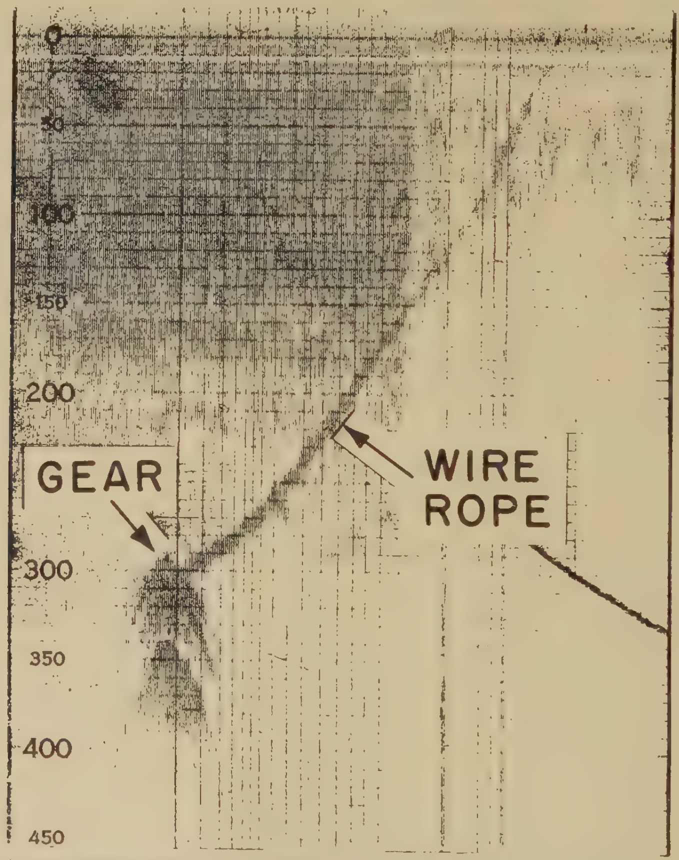

Fig. 1. Edo echo-sounder record of Run # 6, Aug. 23, 1953 on two-metre stramin, telemetering depth meter and 10-foot IKMT depressor.

ANALYSIS OF RECORDS

The following method has been used to interpret the echo-sounder records (Fig. 1) which resulted from these runs:

1. A time scale in arbitrary units was laid off on the echo-sounder record. The number of time units from some zero point (usually the trace of the net or " Mark " 1) to the successive range marks was plotted on graph paper against the corresponding range as determined by stadimeter. This relationship should be linear on the assumptions that *Bear*'s rate of closure with *Blue Dolphin* was constant and that the rate of paper advance of the echo sounder was constant. A straight line was fitted to these points and this graph was used to determine corrected ranges at any point on the record during an echo-sounder run.

2. At a number of points where the echo-sounder record could be clearly read the indicated depth to the cable or net was recorded. Zero correction, sound-velocity correction and transducer-depth correction were added in that order. Because the towing cable was in a sloping plane " up " which the *Bear* echo sounded, the depth values at a given range are too small because the shortest effective path between the transducer and the wire is not normal to the sea surface but normal to the wire. The amount of this correction is determined by the slope of the wire; the greater the slope, the greater the correction. For this purpose the echogram of the cable was divided into a few straight segments and the slope of these approximations calculated from the change in indicated depth and the change in corrected range. Once these slopes were known the suitable depth-correction factor was computed. This correction varies from about $\frac{1}{2}$ of 1% to about 6%.

An error for which one cannot correct is that which enters from the *Bear*'s echo sounder not being directly over the towing cable or net. Assuming an effective sound transmission and reception cone of 30° at the apex, the maximum error resulting from transmission along an hypotenuse would amount to about 4%. We have attempted to minimize the results of this error by showing some of the variation encountered in the more successful runs (in which the error would likely to be small).

Furthermore, we have previously noted errors in traveltime measurement by the Edo echo sounder as high as 6%. This error is due to friction in the belt drive of the recording styli and therefore the error is a negative one (depth indications too low), In the present case this error, if existent, was unknown and we have assumed it to be zero.

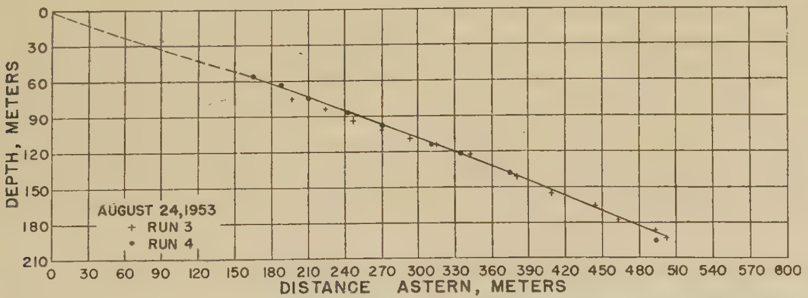

Fig. 2. Shape of the cable towing a 10-foot Isaacs-Kidd midwater trawl with 530 m of wire out. Speed about 2·5 knots.

RESULTS

Fig. 2 shows the shape of the lower two-thirds of the cable when the complete IKMT was being towed alone (Runs 3 and 4, 24 August). The values obtained for both runs are plotted but the minimum soundings are used to draw the line representing the cable. The part of the cable for which we have soundings is slightly concave downward. If the entire cable were of this shape the net should reach a greater depth than that computed from the wire angle measured at the surface. We find that the depth to the net, as determined by echo sounder, is always slightly less than that computed from the wire angle. Therefore we conclude that the upper one-third of the cable (for which we have no soundings) must be slightly concave upward and we have shown it as such in the figure. However, we might assume a negative error of 10% in depth measurement due to friction in the stylus belt of the echo sounder, and increase all soundings on the cable by this amount. Then, assuming the cable to be flat in the upper portion, the wire angle at the surface would necessarily be about 69°. Since this is within the limits of our observation (67° ± 2) a flat shape in the upper portion is a possibility.

We estimate from the data in SIO (1953) that the tension on the towing cable during these runs was about 1500 pounds.

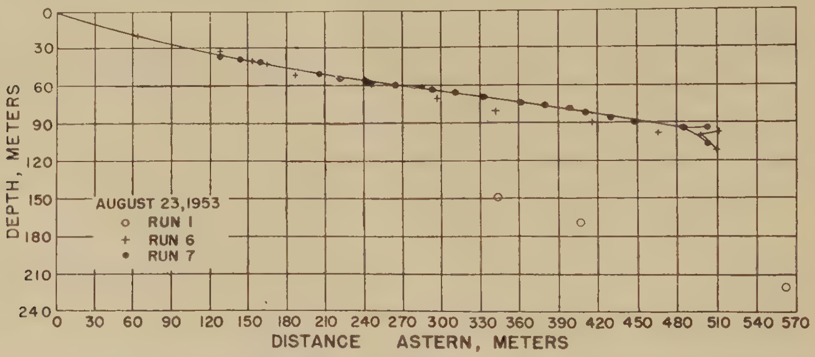

Fig. 3. Shape of the cable towing a closed two-metre stramin net, telemetering depth meter and 10-foot IMKT depressor. Gear is presumed to have been fouled during Runs 6 and 7 and clear during Run 1.

Fig. 3 shows the shape of the cable during Runs 6 and 7 on the 2-metre stramin net, depth meter and IKMT depressor on 23 August. On these runs the gear is presumed to have been fouled. Two soundings are shown at the very end of the cable for each run. These represent echoes from two parts of the gear, probably the rim of the net and the depressor. In this case the cable shape is slightly concave upward. The gear is probably behaving as any towed object in which the weight-drag ratio is less than that of the towing cable. Also shown are a few soundings on the cable during Run 1, 23 August, when the gear is presumed to have been towing properly. During this run the cable shape was probably the same as that when the complete IKMT was being towed.

It has been suggested to us by Mr. JOHN ISAACS, one of the designers of the IKMT, that the IKMT depressor should be very unstable when used without its net. This probably explains the observations in Runs 6 and 7 but the results of Run 1 show that this is not always so.

DEPTH-WIRE OUT RELATIONSHIP

The relationship between the length of the towing cable and the depth to the net from soundings on the IKMT itself is shown in Fig. 4. All soundings obtained are plotted but the minimum soundings are used to draw the line. The relationship is also shown that would obtain if the depth were computed from the wire angle read at the surface during the runs (67° ± 2 from the vertical). The latter values are about 6% higher than the former. These curves would lie even closer together if an error in the echo sounder, of the mechanical sort earlier described, of up to 6% existed. If the error exceeded 6% (a maximum of 10% seems reasonable) the actual depth would exceed the computed depth by some small amount (up to about 4%).

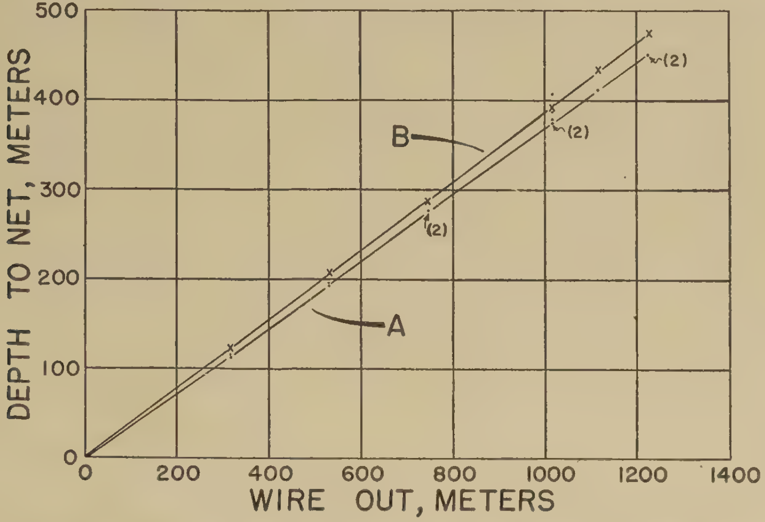

Fig. 4. A. Relationship between depth of 10-foot IKMT and length of towing cable at about 2·5 knots as observed by echo sounder. Figures in parentheses indicate number of observations at a particular point where more than one. B. Same relationship as in A. Computed from wire angle at surface.

Woods Hole Oceanographic Institution, Woods Hole, Mass., U.S.A.

Contribution No. 834 *of the Woods Hole Oceanographic Institution. The work was done under Contract NObsr*-43273 *with Bureau of Ships, U.S. Navy Department.*

REFERENCES

Dow, W. (1954), Underwater telemetering. A telemetering depth meter. *Deep-Sea Res.*, **2**, 145-151, 9 figs.

Leavitt, B. B. (1935), A quantitative study of the vertical distribution of the larger zoöplankton in deep water. *Biol. Bull.*, **68** (1) 115-130, 3 figs.

Leavitt, B. B. (1938), The quantitative vertical distribution of macrozoöplankton in the Atlantic Ocean basin. *Biol. Bull.* **74** (3) 376-394, 5 figs.

Scripps Institution of Oceanography (1953), Isaacs-Kidd midwater trawl. *SIO Ref.* 53-3 18 pp., 11 figs., 3 pls.

Wood, H. and Parrish, B. B. (1951), Echo sounding experiments on fishing gear in action. *J. Cons. Explor. Mer.* **17** (1) 25-36, 7 figs.

Printed in Great Britain by The Salisbury Press Ltd., Publicity House, Wilton Road Salisbury, Wilts. (27)

Contribution No. 837

(Reprinted from Nature, Vol. 178, pp. 253–255, August 4, 1956)

DIMORPHISM IN THE PORTUGUESE MAN-OF-WAR‡

By A. H. WOODCOCK
Woods Hole Oceanographic Institution, Mass.

THE interesting problems of the sailing of *Physalia* have been revived by Totton and Mackie[1] and Fontaine[2]. Since the publication of my observations on the predominance of the left-sailing *Physalia* in the North Atlantic[3], I have had numerous opportunities to observe them in various parts of the world. These observations continue to show that North Atlantic animals are predominantly right-handed. Observations of *Physalia* in the North Pacific show similar results. Unfortunately, the southern hemisphere data are not yet extensive enough to test fairly my original suggestion that most of the animals on the southern seas may be mirror images of those in the northern hemisphere.

The purpose of this communication is to present and discuss these additional observations (see Table 1) and to discuss further the suggestions of Wilson[4] and of Totton and Mackie[1] concerning the role of wind direction in altering the 'landfall' possibilities of the two differently-sailing *Physalia*.

First, it should be pointed out that the original observations showing the dominance of the right-handed (left-sailing) *Physalia* in the northern hemisphere were made on the open sea. These data are not subject to the local wind-direction errors of beach observations, a fact which Totton and Mackie seem to have overlooked. Beached animals do, however, show a clear and similar dominance of right-handedness in the northern hemisphere when the local winds are nearly directly on shore. For example, compare observations 1, 2 and 3 in Table 1.

The greater number of the right-handed animals on the open sea does not necessarily indicate that this condition existed at the time the animals changed from the larval form. However, the numerical dominance of the right-handed animals, which was evident among the smallest of the *Physalia* found on a Florida beach (see Fig. 1 and Table 1), suggests that this dominance is present at the start.

These Florida observations, and many of those in Hawaii as well, indicate that the selective processes favouring the left-sailing animals begin very early in the life of the animal, if one supposes, with Totton and Mackie, "that in each brood of *Physalia* the two forms are produced in rough equality . . .".

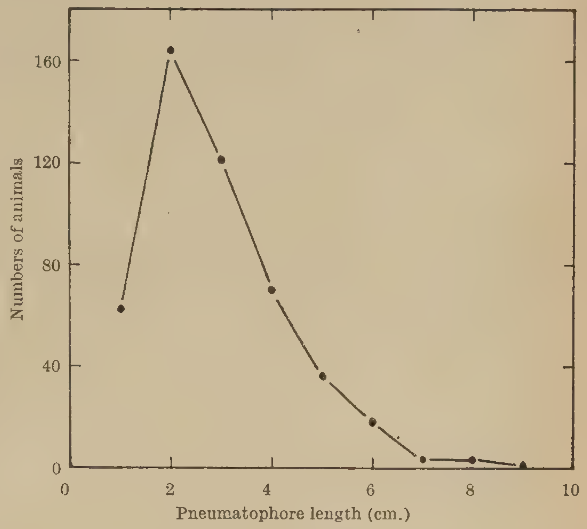

Fig. 1. A representative distribution of pneumatophore length among the *Physalia* seen during March, April and May 1944 on Ft. Pierce Beach, Florida. See Table 1 for total numbers

I have also measured roughly the sailing speed of a left-sailing North Atlantic *Physalia*, its angle of motion relative to the wind, and the approximate rate of down-wind drift of the upper 0·5 cm. of surface water. My results are about the same as those of Totton and Mackie, and are illustrated in Fig. 2.

Note in this figure that the number of animals which can land in unit time and on a unit length of beach (H) depends upon the angular relationship between their sailing-course line (for example, line BC) and the beach line (H). These lines control the angle α, and the length of line A. Thus the sine of the angle equals the ratio of the total possible landings on a section of beach (H) to the observed landings. This relationship is expressed in the following equation, and may be applied to all *Physalia* where α is known.

$$N_c = \frac{1}{\sin \alpha} N \qquad (1)$$

Table 1. OBSERVATIONS OF THE NUMBER OF RIGHT-HANDED (LEFT-SAILING) AND LEFT-HANDED (RIGHT-SAILING) *Physalia* SEEN ON THE SURFACE OF THE OPEN SEA AND ON VARIOUS SHORES. THE 'AT SEA' DATA INCLUDE THE ORIGINAL OBSERVATIONS FROM REF. 3

Data No.	Name	No. observed		Date	Location	Ratio of right-sailers to left-sailers	Average on-shore wind angle*	Position		Place name
		Right-handed	Left-handed					Lat.	Long.	
1	*Physalia physalis* L.	159	3	1939–45	at sea	0·02	—	25°–40° N.	46°–80° W.	North Atlantic
2	*Physalia physalis* L.	344	9	1942	at sea	0·03	—	26°–28° N.	84°–89° W.	Gulf of Mexico
3	*Physalia utriculus*, Esch.†	824	29	11/51–7/52	on beach	0·04	80–100	21° 23·5′ N.	157° 43′ W.	Hawaii
4	*Physalia physalis* L.	1,625	66	3/44–5/44	on beach	0·04	60–80	27° 18′ N.	80° 13′ W.	Ft. Pierce, Florida
5	*Physalia utriculus*, Esch.	694	0	18/12/51	on beach	0·00	90	21° 23·5′ N.	157° 43′ W.	Hawaii
6	?	314	306	8/52	on beach	0·98	45	33° 45·2′ S.	151° 17·9′ E.	Deewhy Beach, Sydney, Australia

* The 'average on-shore wind angle' is measured in a counter-clockwise direction from a line parallel to the beach.
† From ref. 5.

---

‡ Contribution No. 837 from the Woods Hole Oceanographic Institution.

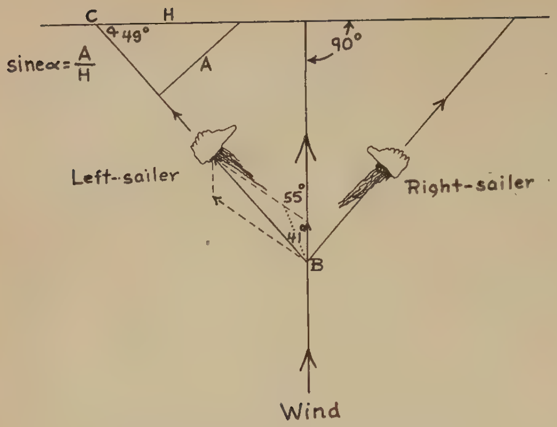

Fig. 2. Average sailing performance of a right-handed, left-sailing *Physalia physalis*, and further suggestions about effects of wind direction upon the number which will sail on to a shore (see text). A right-sailer is also shown in order to emphasize its markedly different sailing course in response to the same wind. Average speed of topmost 0·5 cm. of water = 9 cm. sec.$^{-1}$; average speed of wind = 680 cm. sec.$^{-1}$; average speed of *Physalia* = 26 cm. sec.$^{-1}$; pneumatophore length 17 cm., height 7 cm.

where N_c is the maximum possible number of arrivals in unit time and length of beach, and N is observed number of arrivals.

From Fig. 2 and the above equation it can be seen that the number of arrivals of the two forms of *Physalia* on a beach will represent the relative distribution on the sea only when the wind angle is 90° and the sailing angles α are equal.

The very small *Physalia*, such as most of those observed in Florida (see Table 1 and Fig. 1), sail much more slowly than the large *Physalia*. Their sailing course, assuming the same angular relationship to the wind as the large animal, would tend, therefore, to approach the shore at an angle which more nearly equalled that of the wind. For example, an animal sailing at one-fourth speed would follow a course from *B*, Fig. 2, shown by the dotted line. This may explain why the ratio of the right to the left-sailers on the Florida beach (see Table 1, observation 4) was so similar to this ratio among those observed on the open sea, despite the occasional obliquity of the wind.

On Lanikai Beach, Oahu, Hawaii, the north-east trade wind was almost always blowing from the sea and nearly normal to the beach. Hence the relative number of the two types of animals observed on this beach, as given in Table 1, observation 3, should represent their relative distribution on the open sea. During one exceptional period of several days, however, southerly or 'Kona' winds occurred, producing off-shore winds on the lee side of Oahu which carried the normal *Physalia* population far out to sea. Thus the lee side of the island became a 'shadow zone' for right-sailers (Fig. 3). For a period of about a day after the shift from southerly winds to the normal 'trades' occurred, only left-sailing *Physalia* were seen on the beach (see observation 5, Table 1). This result is explicable as illustrated in Fig. 3, the Kaiwi Channel producing a local separation of the two forms. (For convenience, equal numbers of lines are shown representing the differing sailing courses of the two forms during south-south-west winds. It is not intended to imply that an equality of number of the two forms exists at sea.) The first left-sailing *Physalia* to reach Lanikai beach after the wind shift to the north-east would presumably come from point *A*, while the first right-sailer would sail a greater distance from point *B*. Assuming the same sailing speed and sailing direction relative to the wind as that of the Atlantic *Physalia* (Fig. 2), the difference in the arrival time of *Physalia* from these two points would be about thirteen hours and may account for the observed complete dominance of the left-sailers among the first arrivals on the beach after the wind shift.

Observation 6, in Table 1, was made on the southern end of Deewhy Beach, Sydney, and seems to support the idea that most of the southern hemisphere animals sail to the right of the wind. On the only day when I was free to walk on the beach and to observe the stranded *Physalia*, the average wind angle was about 45° to the general trend of the irregular coast line of this region. According to equation (1), very few right-sailers should have been found on Deewhy Beach, since the angle α for the right-sailers would in this case become 4°, and the sine about 0·07. Actually, about one-half of the animals seen were right-sailers. These Deewhy Beach observations, when 'corrected' for the effects of the average sailing angle on the number of the right-sailers arriving on the beach, suggest a dominance of this form on the open sea of about ten to one of the left-sailers. This ratio agrees roughly with that among the southern hemisphere museum specimens discussed in the previous paper[3].

The above 'correction' is open to the serious objection that it is made using the sailing characteristics of the somewhat larger North Atlantic *Physalia*, which are given on Fig. 2. Also, in common with all beach observations of stranded animals, there are the added questions about the effects of coastal currents, and of changes in wind direction which may have occurred after they sailed ashore and before I arrived at the beach to observe them. It is hoped that someone will soon test these rather unsatisfactory southern hemisphere data by direct observation on the open sea in the Sydney region or elsewhere.

If further work proves the existence of a world-wide difference of *Physalia* form and sailing performance in the two hemispheres, we shall wish to know to what extent various physical factors may have produced this difference. Will such dominance of one form in each hemisphere be due to ecological factors acting selectively on each generation, to established genetic differences, or perhaps to 'tack' changes

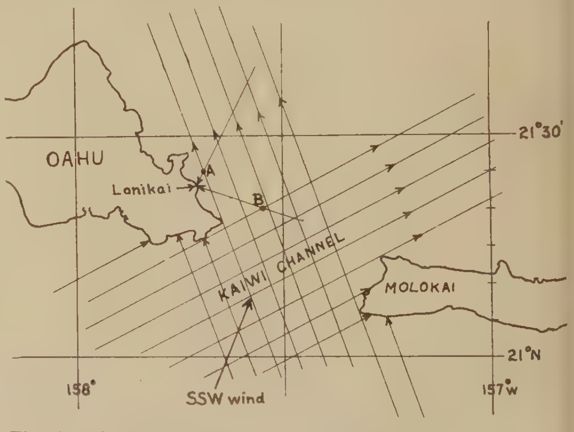

Fig. 3. Assumed separation of left-sailing and right-sailing *Physalia* in passing through Kaiwi Channel before a south-south-west wind. Note that the lee side of the islands is, in varying degree, a 'shadow zone' for either one or both forms. Following a wind shift to the normal east-north-east trades, the first animals of the two forms arriving on Lanikai Beach would sail different distances, along the new course lines shown, from points approximating intersections *A* and *B*

caused by migration of the tentacles on the pneumatophore? The answers to these questions will be interesting and perhaps useful in further studies.

My earlier proposal concerning a possible selective influence of small-scale wind-induced eddy motions in the surface waters[3] still seems reasonable to me. Larger-scale wind and water motions may be important, however. It is worth noting here that left-sailing *Physalia* in the average anti-cyclonic wind systems of the North Atlantic and the North Pacific[6] will move away from the centres of the systems, and often in the direction of coastal waters. The average wind systems of the oceans of the southern hemisphere tend to be cyclonic[6]. In cyclonic wind systems a right-sailer will also tend to sail away from the centres of the systems and in some cases toward coastal areas.

I am convinced that there is much that oceanographers can learn about the surface waters of the seas from detailed studies of the sailing of *Physalia*.

I am indebted to my young son, John B. Woodcock, for his enthusiastic help in collecting observations in Hawaii.

---

[1] Totton, A. K., and Mackie, G. O., *Nature*, **177**, 290 (1956).

[2] Fontaine, A., *Notes Nat. Hist. Soc. Jamaica*, **64**, 61 (1954).

[3] Woodcock, A. H., *J. Marine Res.*, **5**, 196 (1944).

[4] Wilson, D. P., *J. Mar. Biol. Assoc.*, **27**, 139 (1947–48).

[5] Bonnet, D. D., *Science*, **103**, 148 (1946).

[6] "Atlas of Climatic Charts of the Oceans", U.S. Wea. Bureau., Wash., D.C. (1938).

Printed in Great Britain by Fisher, Knight & Co., Ltd., St. Albans.

Contribution No. 840

Reprinted from "Geochimica et Cosmochimica Acta," 1956, Vol. 10, No. 4., pp 241–243.
Pergamon Press, London

On the state of our knowledge of trace elements in the ocean

(*Received* 10 *May* 1956)

THE concentrations of trace elements in the ocean are of considerable geochemical and biochemical significance. Workers in these fields have had recourse to published lists (for example, WATTENBERG, 1938, 1943; SVERDRUP *et al*,. 1942; HARVEY, 1945, 1955; RANKAMA and SAHAMA, 1950; MASON, 1952; and others) which sometimes tacitly imply that the reported concentrations are somehow representative of the whole ocean, either as averages or as typical concentration ranges. The purpose of this note is to suggest that such may be far from the case, and that most of the numbers shown in these tables cannot, even in the vaguest sense, be assumed to be representative of the oceans. Indeed it is readily conceivable that they miss the mark by orders of magnitude.

As examples of this point one might use the concentrations of the thirteen trace elements considered by KRAUSKOPF (1956) in his studies of factors determining their concentrations in the ocean. These concentrations, their original sources, and the number of samples analysed are shown in Table 1.

The concentrations of Ag, Bi, Cu, Zn, Co, and Ni from NODDACK and NODDACK (1940) are apparently based on the analysis of a single sample of surface water from the Gullmarfjord, Sweden. HABER'S (1927) many determinations of silver must all be questioned on the same basis that his gold determinations must be questioned, namely, that he failed to take into account the adsorption of these metals on the glass of the sample containers. BLACK and MITCHELL (1952) analysed three samples (Mo, Ni, V, and Cr in KRAUSKOPF'S table). One was from 20 metres depth 20 miles off Plymouth, England, and the other two were inshore surface samples. ERNST and HOERMANN (1936) (Mo, Ni, and V) analysed five samples from Heligoland and two North Atlantic samples, one from the Baltic current on the west central Norwegian coast; the sampling depths are not reported. (Ni was not determined on the two Atlantic samples, and Mo was not determined on one of the Heligoland samples.) The concentrations of Cd are the range of five samples of surface water from the Irish Sea (MULLIN and RILEY, 1954). BOURY (1938) analysed three surface samples from French coastal waters for Pb. STOCK and CUCUEL (1934) report on the analysis of Hg in water from Heligoland which appears to be a single sample of surface water. ISHIBASHI'S (1953) W figures are from a single sample taken offshore off Sirahama, Wakayama Prefecture, Japan; two samples from the same location were analysed for Cr and two samples from 31° N latitude, 135° W longitude were analysed for V.

As for copper, RILEY (1937) reports on a series of about twenty surface samples taken along the coast of the Gulf of Mexico near the mouth of the Mississippi River. ATKINS (1932) reported on the analysis of a single sample of surface water from a standard station of the Marine Biological Association (Plymouth, England). Even the ten samples reported from the subtropical North Atlantic by KALLE and WATTENBERG (1938) are from the surface; others taken at depth gave larger concentrations, but these were suspected of contamination from the water sampler.

A fairly thorough search of the literature indicates that there have been no valid analyses of deep water samples for Sb, Ba, Cd, Cs, Ce, Cr, Co, Ga, Ge, La, Pb, Hg, Mo, Ni, Sc, Se, Ag, Tl, Th, W, Sn, V, Y, and Zr, all of which are included in one or more of the cited tables. Moreover, the reported concentrations depend on not over a dozen analyses of surface or near surface samples. Critical examination of the analytical methods used by the various investigators might indicate that some of these data are not reliable, and that some of the subsurface analyses, notably that of Au, would have to be thrown out.

There is no doubt that marine organisms concentrate trace elements, impoverishing the ambient sea water. Surface concentrations of the nutrient salts are usually only a fraction of their concentrations at greater depths, which would more nearly represent the bulk of the ocean. For example, inorganic phosphate concentrations in the surface water of the Sargasso Sea are

Table 1. Determinations of the thirteen trace elements appearing in Krauskopf's (1956) Table 1.

Element	Concentration shown by Krauskopf (p.p.m.)	Original reports of the analyses	Deep-water samples included	Number of samples analysed
Ag	0·00015–0·003	Haber (1927)	Yes	Many
		Noddack and Noddack (1940)	No	One
Bi	0·0002	Noddack and Noddack (1940)	No	One
Mo	0·0003–0·0007	Ernst and Hoermann (1936)	?	Six
	(0·012–0·016)	Black and Mitchell (1952)	No	Three
Cd	0·000032–0·000075	Mullin and Riley (1954)	No	Five
Pb	0·003–0·008	Boury (1938)	No	Three
Hg	0·00003	Stock and Cucuel (1934)	No	One?
Cu	0·001–0·015	Atkins (1932)	No	One
		Riley (1937)	No	ca. 20
		Noddack and Noddack (1940)	No	One
		Kalle and Wattenberg (1938)	No	Ten
Zn	0·005–0·021	Noddack and Noddack (1940)	No	One
W	0·00009–0·0001	Ishibashi (1953)	No	One
Co	0·0001	Noddack and Noddack (1940)	No	One
Ni	0·0001–0·0005	Ernst and Hoermann (1936)	?	Five
		Noddack and Noddack (1940)	No	One
	(0·0015–0·006)	Black and Mitchell (1952)	No	Three
V	0·0003	Ernst and Hoermann (1936)	?	Seven
	(0·0024–0·007)	Black and Mitchell (1952)	No	Three
Cr	0·00004–0·00007	Ishibashi (1953)	No	Two
	(0·001–0·0025)	Black and Mitchell (1952)	No	Three

less than a few hundredths of a microgram atom per litre (0·01 microgram atom per litre of phosphorus is 0·0003 p.p.m.), but at greater depths the concentration is as much as 200 times this figure. Even greater discrepancies are found between surface and deep silicate concentrations, and nitrate concentrations follow the same rule. Harvey (1955) has listed several mechanisms by which trace elements are concentrated by organisms, and Noddack and Noddack (1940) list factors ranging between 300 and 280,000 by which various trace metals were more concentrated in marine organisms than in the surrounding water. Carritt and Goodgal (1955) and Krauskopf have demonstrated the importance of sorption phenomena in removing ions from free solution. The abundance of particulate matter in the upper layers (see, for example, Jerlov, 1953) could easily result in the removal of practically all the trace ions from surface waters, so that differences between filtered and unfiltered water may be large. Settling of particulate matter must effectively remove large fractions of these elements from the surface layers, to be returned to solution in deeper layers or to eventually be incorporated in the bottom sediments. It is most certainly conservative to state that there may be very little relationship between surface and deep-water concentrations of the trace elements. Yet, nearly all of the very few determinations of the trace elements to date have been made on surface samples, and their concentrations in deep water remain almost wholly unknown.

Probably too much emphasis has been placed on the uniformity of the composition of sea water, which has led to the assumptiom that a limited number of analyses suffices to characterize sea water in general. There is a constancy in the ratios of the major constituents (Na^+, Mg^{2+}, Ca^{2+}, K^+, Sr^+, Cl^-, SO_4^{2-}, Br^-, H_3BO_3, and HCO_3^- plus CO_3^{2-}) to one another, but it certainly does not extend to the nutrients and trace elements.

This note is not intended to be critical of Krauskopf's work. Criticism, if any, is due to oceanographers who have permitted the perpetuation of the notion that the concentrations of the trace elements in the sea are reasonably well-known. They are not.

Contribution No. 840 *from the*
Woods Hole Oceanographic Institution
Woods Hole, Massachusetts

Francis A. Richards

References

Atkins W. R. G. (1932) The copper content of sea water *J. Mar. Biol. Assoc., U.K.* **18,** 193–197.

Black W. A. P. and Mitchell R. L. (1952) Trace elements in the common brown algae and in sea water *J. Mar. Biol. Assoc., U.K.* **30,** 575–584.

Boury M. (1938) Le plomb dans le milieu marin *Rev. Trav. Off. Peches Marit.* **11,** 157–165.

Carritt D. E. and Goodgal S. (1954) Sorption reactions and some ecological implications *Deep-sea Res.* **1,** 224–243.

Ernst T. and Hoermann H. (1936) Bestimmung von Vanadium, Nickel, und Molybdän im Meerwasser *Nach. Ges. Wiss. Göttingen Math-Phys. Kl., Fach.* IV, *N.F.* **1,** 205–208.

Haber F. (1927) Das Gold im Meerwassers *Z. angew. Chem.* **40,** 303–317.

Harvey H. W. (1945) *Recent advances in the chemistry and biology of sea water* Cambridge University Press, London, viii + 164 pp.

Harvey H. W. (1955) *The chemistry and fertility of sea waters. ibid.* viii + 224 pp.

Ishibashi M. (1953) Studies on minute elements in sea water *Rec. Oceanogr Wks. Japan n. s.* **1,** 88–92.

Jerlov N. G. (1953) Particle distribution in the ocean *Rpts. Swedish Deep-Sea Exped.* 1947–1948, **3,** 73–97.

Kalle K. and Wattenberg H. (1938) Über Kupfergehalt des Ozeanwassers *Naturwiss.* **26,** 630–631.

Krauskopf K. B. (1956) Factors controlling the concentration of thirteen rare metals in sea water *Geochim. et Cosmochim. Acta.* **9,** 1–32B.

Mason B. (1952) *Principles of Geochemistry* John Wiley and Sons, N.Y., N.Y., vii + 276 pp.

Mullin J. B. and Riley J. P. (1954) Cadmium in sea water *Nature* **174,** 42.

Noddack I. and Noddack W. (1940) Die Haufigkeiten der Schwermetalle in Meerestieren *Ark. Zool.* **32**A (4), 35 pp.

Rankama K. and Sahama T. G. (1950) *Geochemistry* University of Chicago Press, Chicago, Ill., xvi + 912 pp.

Riley G. A. (1937) The significance of the Mississippi River drainage for biological conditions in the northern Gulf of Mexico *J. Mar. Res.* **1,** 60–74.

Stock A. and Cucuel F. (1934) Die Verbreitung des Quecksilbers *Naturwiss.* **22,** 390–393.

Sverdrup H. U., Johnson M. W., and Fleming R. H. (1942) *The Oceans* Prentice Hall, Inc., New York, N.Y., x + 1087 pp.

Wattenberg H. (1938) Zur Chemi des Meerwassers *Z. anorg. Chem.* **236,** 339–360.

Wattenberg H. (1943) Zur Chemie des Meerwassers. Über die in Spuren vorkommenden Elemente *ibid.* **251,** 86–91.

Contribution No. 841

Deep-Sea Research, 1956, Vol. 3, pp. 266 to 272. Pergamon Press Ltd., London.

Suspended echo-sounder and camera studies of midwater sound scatterers

HENRY R. JOHNSON, RICHARD H. BACKUS, J. B. HERSEY and DAVID M. OWEN

Abstract—Twelve-kilocycle-per-second echo sounders have been lowered in the sea to observe sound scatterers at short range. Once, an echo sounder was lowered to a point midway between the surface and a deep scattering layer to record the latter during its evening ascent. Individual scatterers moved upward at a rate of about 15 feet per minute. It was estimated that there was about one scatterer for each 650 m^3 of water at the time of the layer's passage by the transducer.

On another occasion a transducer was lowered at night by 35-fathom increments to a depth of about 400 fathoms. Counts of strong scatterers at the several levels were made save in the uppermost where scattering was too intense. Water volume per scatterer varied from about 800 to 2,000 m^3 depending on the depth of the observation.

A camera has also been used with the echo sounder to obtain simultaneous acoustic and photographic records of scatterers. The most successful experiments show a correlation between pictures of fishes and strong echoes.

INTRODUCTION

SINCE the discovery of deep scattering layers (DUVALL and CHRISTENSEN, 1946 ; EYRING, CHRISTENSEN and RAITT, 1948 ; RAITT, 1948) most observations of these layers have been made with single-frequency echo sounders operating from the surface (HERSEY and MOORE, 1948 ; DIETZ, 1948 ; MOORE, 1950 ; BODEN, 1950 ; BURD and LEE, 1951 ; HERDMAN, 1953 ; and others). If a broad-spectrum sound source is used, several layers may be detected in one locality, each layer having a different peak scattering frequency (HERSEY, JOHNSON and DAVIS, 1952). Furthermore, as some layers migrate in depth there is a gradual shift in their peak scattering frequency (HERSEY and BACKUS, 1954). This is interpreted as meaning that the scatterers change in size (resonant frequency) with changing depth (pressure) such as might be expected if the scatterers were the swimbladders of fishes. This observation supports the contention that bathypelagic fishes are the chief cause of deep scattering layers (MARSHALL, 1951). Furthermore, TUCKER (1951) has shown that there is a correlation between deeper, more intense scattering (at a single frequency), and the vertical distribution of fishes ; and shallower, less intense scattering, and the distribution of euphausiids. BURD and LEE (1951) though that some shallow scattering layers were caused by larval fishes. Arguments have also been advanced for euphausiids (MOORE, 1950 and BODEN, 1950) and squid (LYMAN, 1948) as the chief cause of the sound scattering.

Although the scattering layers on most echo-sounder recordings appear to have the character of reverberation (i.e., many unresolved echoes) rather than resolved, discrete echoes, there has long been unpublished evidence that this is not always the case. Some examples of the latter sort, made from a drifting vessel, were shown to HERSEY by R. S. DIETZ in 1950. Perhaps there are earlier examples of which we are unaware. KANWISHER and VOLKMANN (1955) demonstrated, with a cable-suspended transducer permitting short-range observation, that somewhat deeper scatterers could also be resolved. ANDERSON (1953) made essentially similar observations but by a very different technique. The present authors have suspended transducers to about 400 fathoms and more recently have used a camera with transducers to make simultaneous acoustic and photographic records of individual scatterers.

SUSPENDED ECHO-SOUNDER EXPERIMENTS

A UQN/1B Edo echo-sounder transducer was lowered in deep water north of Puerto Rico to study the vertical migration of a deep scattering layer at short range. A modified Bludworth recorder was used with the Edo transmitter and receiver. The system had a repetition rate of about 10 pings per second and a ping length of about two milliseconds. The transducer was lowered before sunset to 105 fathoms, the point of minimum sound scattering between the layer and the surface. The instrument was operated continuously until after the postsunset ascent of the layer (Fig. 1). The density of echo sequences† is low in this record until about 15 minutes after sunset (i.e., at 1845) when the scattering layer approached and moved upward past the transducer. At this time the population in the insonified‡ zone was much increased. The layer had moved past the transducer by about 1920 after which time there were markedly fewer echo sequences.

The upward progress of individual animals is recorded, it is believed, for the first time, previous observations having shown the vertical movement of the layer as a whole. The rate of ascent for these individuals was about 30 feet per minute as computed from the indicated change in depth with time on the record (Fig. 1). However, since the scatterers do not swim vertically up the axis of the sound cone nor even swim along paths that pass through the axis of the cone this method of computing the rate of ascent is incorrect. If it is assumed that the scatterers swim up along paths randomly distributed through the sound cone, a rate of ascent of about 15 feet per minute is obtained. This is in general agreement with the rate of ascent for layers as a whole as measured by surface echo sounders (JOHNSON, 1948, and DIETZ, 1948, as well as measurements of our own).

If the record (Fig. 1) is examined for echoes resulting from a single ping, during the maximum of the migration, about 20 discrete echoes may be counted. We assume here that each echo (and echo sequence) came from a single animal*. Furthermore the volume of water insonified by each ping in this record (Fig. 1) was about 45×10^4 ft^3 (13,000 m^3). Thus there was a single scatterer for about each $2{\cdot}3 \times 10^4$ ft^3 (650 m^3) of water. This may not represent the true population density within this scattering layer when at its midday depth, since there may be an expansion or compression of the layer during its ascent.

Essentially the same gear was used off the continental slope south of New England to test its usefulness in studying vertical distribution of scatterers at short range throughout a greater depth range. A brass ball 6·17 cm in diameter and of known target strength (— 38 db at 12 kc ; see SMITH, 1951) was used as a calibration device throughout the experiment. It was suspended 15 fathoms below the transducer on a fine nylon line. At each stage of the lowering, oscilloscope photographs of sound scattering were made, including that scattered by the ball. Thus target strengths of scatterers can be computed by comparison with the ball. A sequence of records was made during hours of darkness down to more than 400 fathoms by 35 fathom increments (Fig. 2)†. Many of the scatterers were comparable in target strength to the ball and a few showed a target strength greater than the ball‡. There is an apparent decrease in the number of scatterers with increasing depth (Fig. 2) with the great concentration of weak scatterers in the upper 35 fathoms being particularly noticeable. Echo sequences from individual strong scatterers are difficult to detect there.

---

†An echo sequence is the record of successive echoes from successive pings on a particular scatterer or small group of scatterers.

‡The useful verb to insonify, meaning to fill with sound, does not appear in the standard dictionaries, but is commonly employed in underwater acoustics. For another example of its use see MACHLUP and HERSEY (1955).

*We suppose an echo sequence coming from several animals to be characterized by an interference pattern of intense and faint bands of recording caused by the varying phase relationships as several echoes are received simultaneously at the transducer. There are few echo sequences of this sort on the present record, but see Figs. 4 and 6.

The distribution of scatterers as a function of depth cannot be read directly from Fig. 2 because of the decrease in ship's drift with increasing transducer depth*. This lessens the volume of water scanned per unit of time. The following assumptions were made in determining the rate of drift at various depths : (1) that the transducer was towed at 1 knot at the 34- to 69-fathom depth range and (2) that the movement of the scatterers was small compared with that of the ship during the period of observation. The average duration of echo sequences at the 34- to 69-fathom range was measured and made unity. To compute the rate of drift at the greater depths, the duration of echo sequences at these depths was measured and compared with that observed at the 34- to 69-fathom range. To determine the water volume scanned between 5 and 17·5 fathoms from the transducer during an 11-minute period, a transducer beam width of 30° was assumed. This volume was computed to be

Table 1. *Volume of water per strong sound scatterer at night in the deep ocean off southern New England.*

Depth fathoms	*No. of scatterers observed during* 11-*minute period*	*Drift knots*	*Vol. of water scanned, cubic feet*	*Vol. cubic feet per scatterer*	*Vol. cubic metres per scatterer*
39-51·5	100	1·0	3 × 10^6	3 × 10^4	850
68-80·5	28	·5	1·5 × 10^6	5·3 × 10^4	1500
107-119·5	16	·33	1 × 10^6	6·4 × 10^4	1800
139-151·5	12	·25	·75 × 10^6	6·4 × 10^4	1800
178-190·5	10	·25	·75 × 10^6	7·5 × 10^4	2100
212-224·5	21	·20	·60 × 10^6	2·9 × 10^4	820
250-262·5	9	·12	·375 × 10^6	4·2 × 10^4	1200
285-297·5	9	·11	·333 × 10^6	3·7 × 10^4	1050

---

†Because of failure of the gear this could not be repeated during daylight hours when maxima and minima in the vertical distribution would have been more pronounced. Failure was due to flooding of the electrical cable and the transducer through small cuts caused by the winding of the cable around the wire rope on which the gear was lowered. The winding was due to the torque of the wire rope as it was unrolled from the winch. This difficulty has since been overcome by the addition of an orienting fin which is effective providing the ship has sufficient drift.

‡In examining these data it was noticed that there is a systematic decrease in the sensitivity of the system as a function of increasing depth. This is not understood, but may have been due to slow flooding of the gear or possibly a change in the impedance of the transducer with increasing hydrostatic pressure.

*This is due to the increased sea-anchoring effect as more cable is paid into the water. Minor effects on the accuracy of the count are the loss of sensitivity of the system with increasing depth and receiver gain changes made during the experiment. These factors are not recoverable and are felt to be unimportant if the count of scatterers is made rather close to the transducer.

3×10^6 cubic feet at 1 knot (39-51·5 fathom range), and volumes scanned at other depths were reduced in accordance with the reduced rate of drift.

The number of scatterers in the region from 5 to 17·5 fathoms from the transducer was counted during an 11-minute period for each depth range observed.

The water volumes per scatterer at various depths thus computed are summarized in Table 1, which shows a decrease in population density with increasing depth down to the 212-224·5 fathom depth range where there is a sharp increase in population. This increase actually begins at about 193 fathoms (Fig. 2) but as no count was made of scatterers from 190·5 to 212 fathoms this is not recorded in Table 1. Since a prominent scattering layer is observed in this locality in the daytime at approximately 200 fathoms, it appears that some of the scatterers in it do not migrate.

SUSPENDED ECHO SOUNDER – CAMERA EXPERIMENTS

A camera was added to the suspended echo-sounder system to make simultaneous photographic and acoustic records of sound scatterers (Fig. 3). The intent was to design the system so that a scatterer appearing at a certain range on the echo-sounder record would also be within the purview of the camera and in focus ; at this point the camera could be triggered by the echo-sounder operator. A 35-mm Edgerton repeating-flash shutterless deep-sea camera (EDGERTON and HOADLEY, 1955) was used. It could only be operated where an electronic flash was the sole source of light.

Two schemes of lighting have been used. At first, it was thought necessary to use side lighting to reduce the amount of extraneous light reflected to the camera by particulate matter in the water. However, it was found that this reflection was negligible in the clear water of the high seas. Direct lighting does not have the disadvantage of side lighting, which causes the eclipse of one side of the scatterer, making identification difficult. An orienting fin was attached to the rig to prevent the winding of the electrical cable around the wire suspension rope.

The first cruise with this gear indicated that the minimum distance at which the echo sounder could operate was too great to give large enough images in the photographs. This was due to paralysis of the receiving system for a period of several milliseconds after the emission of each ping. To remedy this situation an independent receiving transducer (QBG) was installed. The receiving transducer was fed to the driving amplifier of a high-resolution travel-time recorder. This change made it possible to record echoes from scatterers at ranges as short as five feet†.

Two major deficiencies have controlled the experiments that we have performed with this gear. It was soon apparent that, contrary to expectations, the acoustic field of the echo-sounder system was much larger than the optical field of the camera. From a series of rough measurements we have seen that good echoes can be obtained throughout a field having an angle at the apex of about 90°. The camera lenses used have angles of 20° × 30° (50 mm focal length) or 30° × 40° (35 mm focal length) in water. The discrepancy is in fair agreement with the average percentage of " misses " (40%) obtained in the photographs when strong scatterers are indicated on the acoustic record. An acoustic system with greater directionality appears to be a logical improvement.

---

†At such short ranges the driver amplifier must be operated at low gain which results in inability to record scatterers except at rather short range.

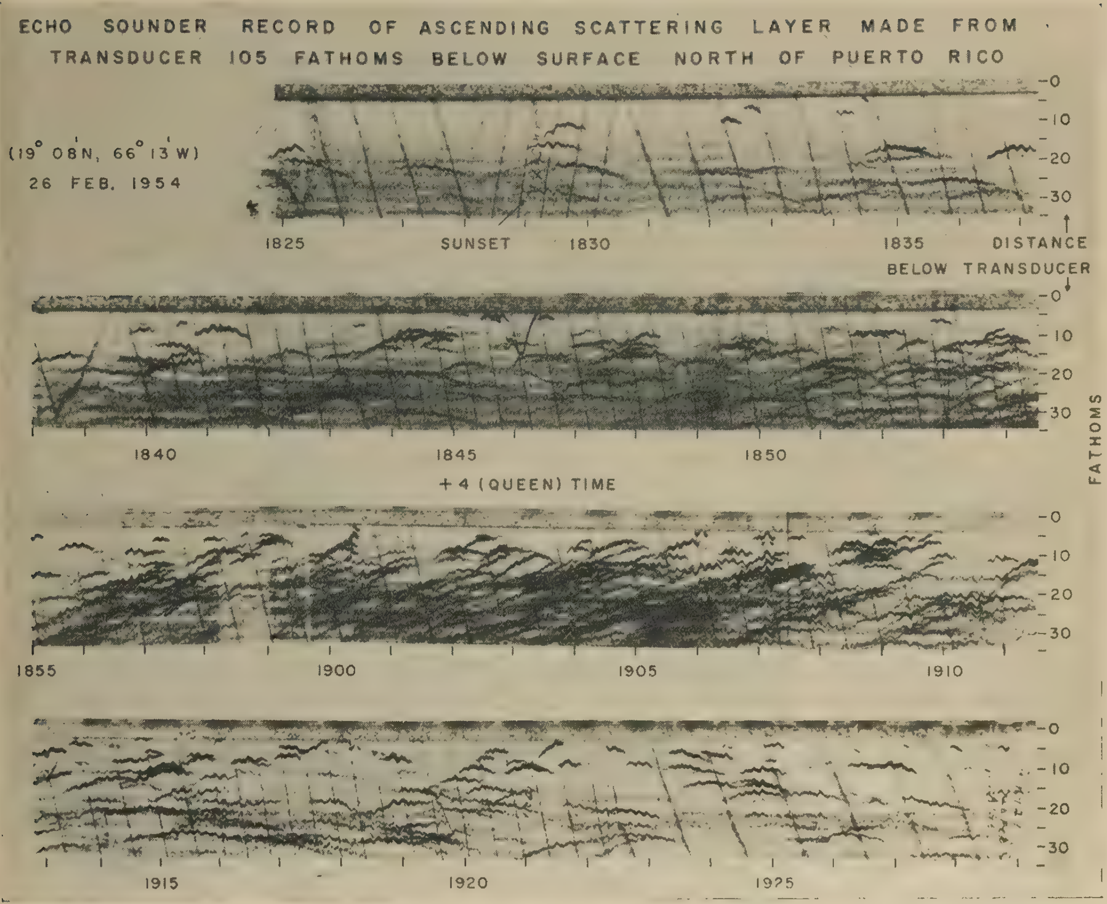

Fig. 1. Suspended echo-sounder record of scattering layer ascent. The roll of the vessel is apparent from the sinuous shapes of the echo sequences as the scatterer's distance from the transducer is alternately increased and decreased. The diagonal traces across the record are time marks from a break-circuit chronometer. Their changes in slope reflect fluctuations in power-line frequency.

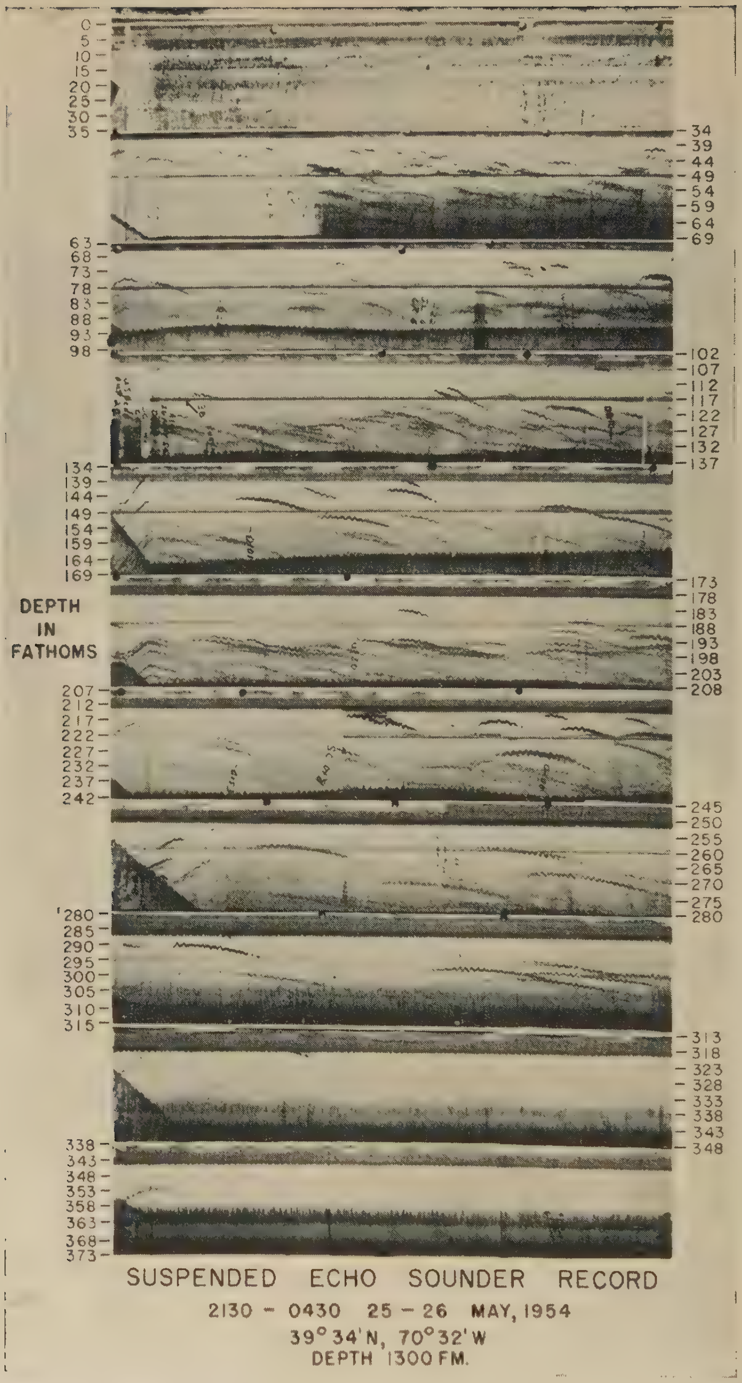

Fig. 2. Echo-sounder record made by lowering transducer by 35-fathom increments (the width of the echo-sounder record). The downward slant from left to right of the echo sequences is due to the cant of the transducer as it is being towed by the drifting ship. The increasing time during which individual scatterers remain in the sound field as the depth of the gear is increased is probably due to the reduction of the speed of the ship's drift as more cable is paid into the water. The continuous constant-depth stripe along the record about 15 fathoms from the transducer is the echo sequence from the brass calibration ball. The solid dark zone of scattering with a sinuous upper margin towards the bottom of each section of the record represents scattering from the sea surface via the back lobe of the transducer. Because of this the depth to the gear could be computed.

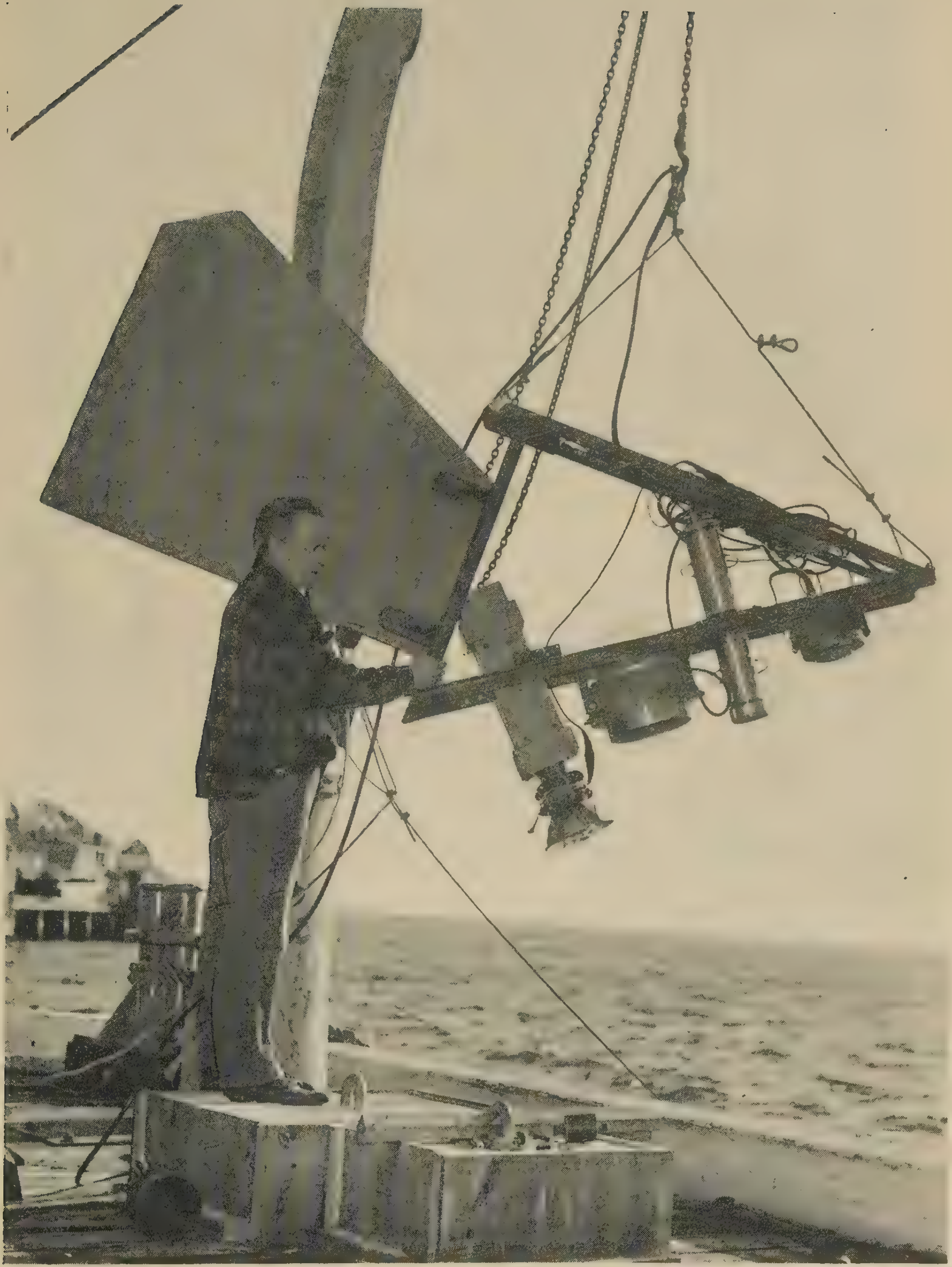

Fig. 3. The most recent echo sounder-camera apparatus. Left to right on the iron frame are the electronic flash, Edo transducer (transmit), camera, and QBG transducer (receive). The orienting fin is to the left. The suspension bridle allows either vertically or obliquely downward orientation of the camera and echo sounder. It has been mostly used in the former position since this allows the calibration ball to be suspended on the axis of the acoustic field ; however, this is disadvantageous in that the camera photographs the backs of fishes etc., making precise identification difficult.

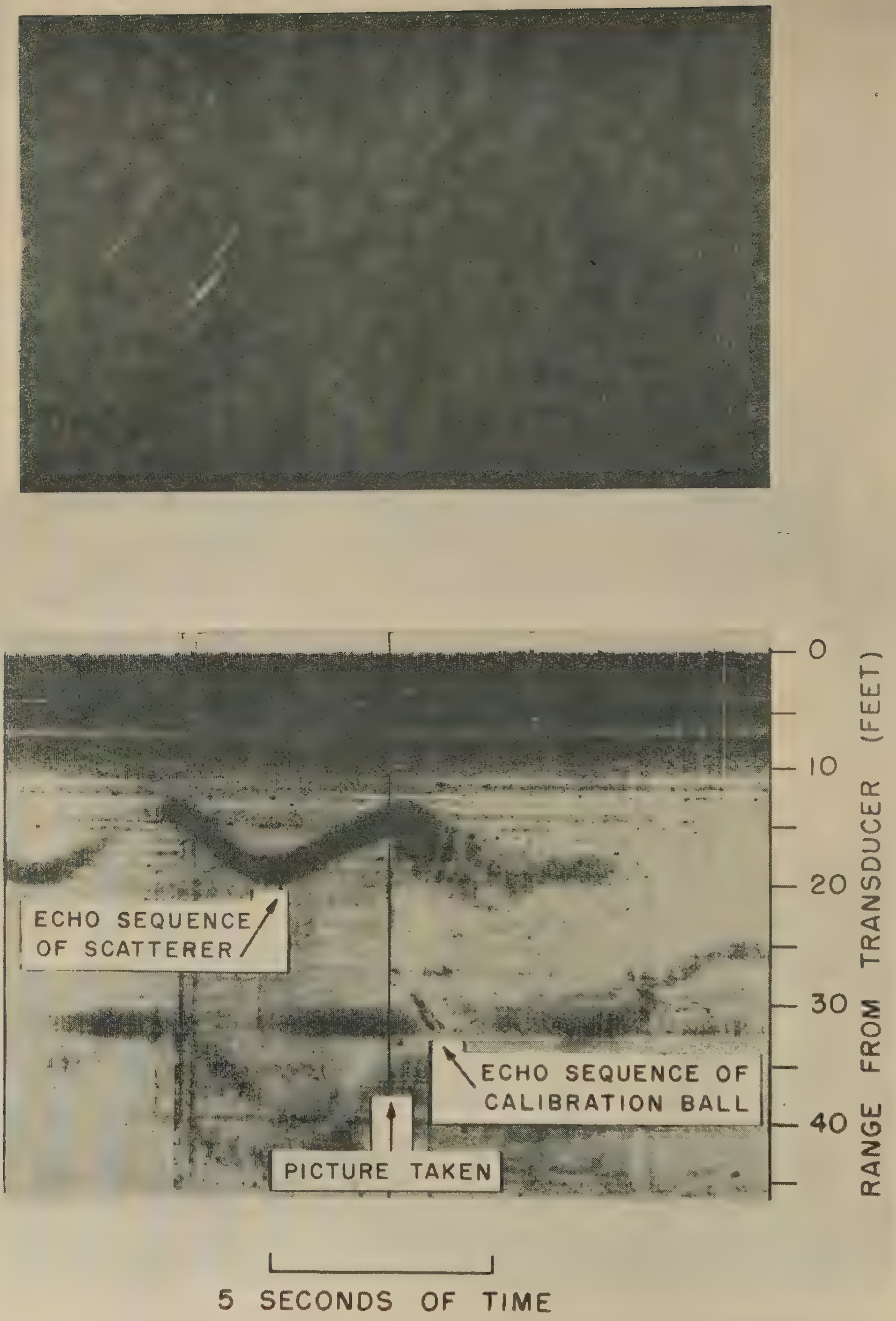

Fig. 4. Photograph and simultaneous acoustic record of 8 unidentified fish made at a depth of 30 metres on 27 February, 1955 at 12° 05′N, 60° 25′W in a water depth of about 1,000 fm. The echo-sounder record shows the scatterer (in this case a school) at a range of 12·5 feet. The 50-mm-focal-length lens was focused for a distance of 8 feet in water (depth of focus from about 7 feet to 9 feet at *f* 6·3, the iris opening used) ; thus this picture is somewhat out of focus. By computing the length of the field of the photograph at the 12·5-foot range and multiplying by the proportionate length of the image of the fish we estimate the fish to be about seven inches long.

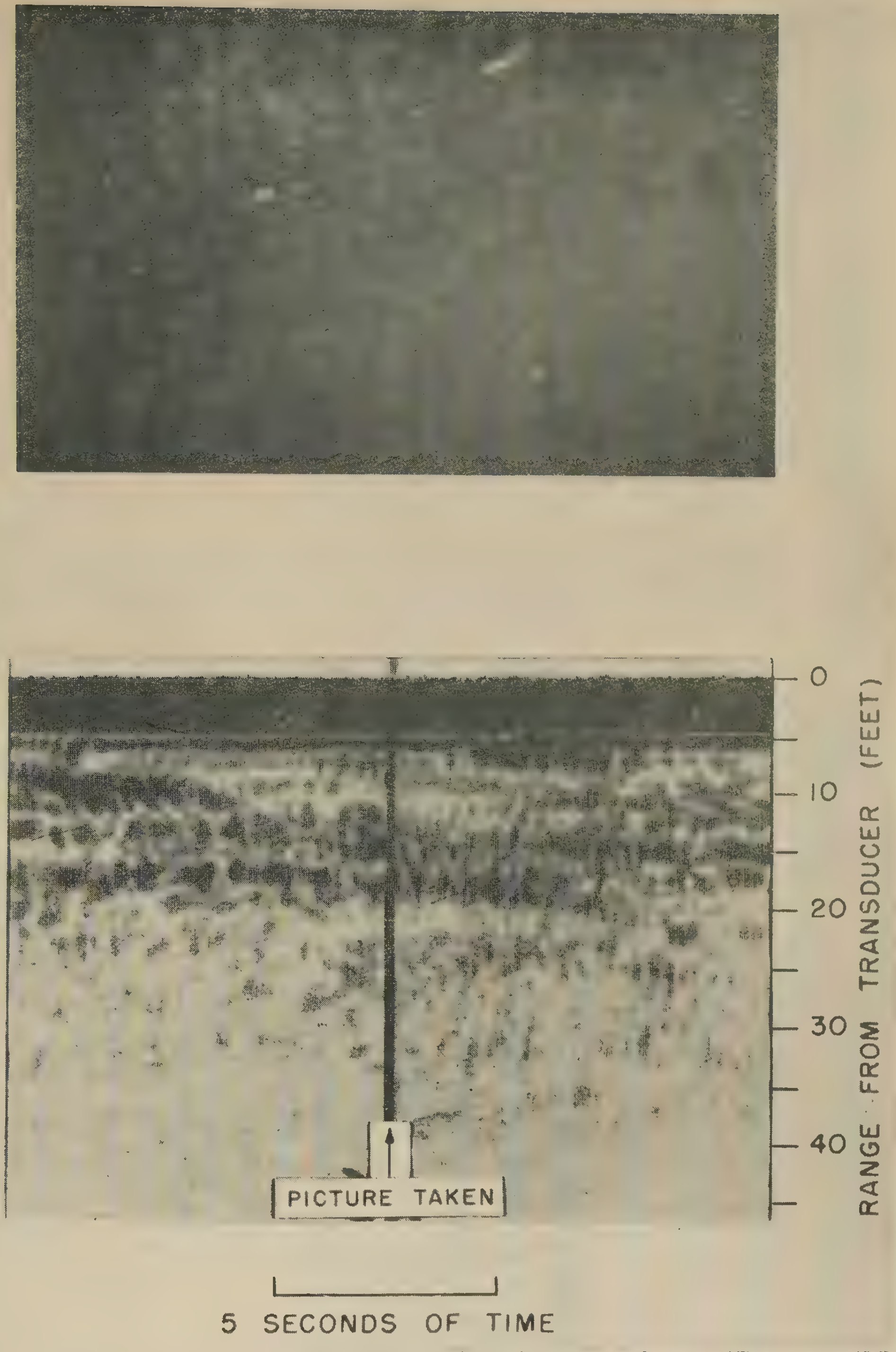

Fig. 5. Salps are seen in a photograph from a lowering made at a depth of 30 metres on 21 July, 1955 at 38°20′N, 69°05′W in a water depth of about 2000 fm. The associated acoustic record shows no well-resolved echo sequences within camera range at the time the picture was taken.

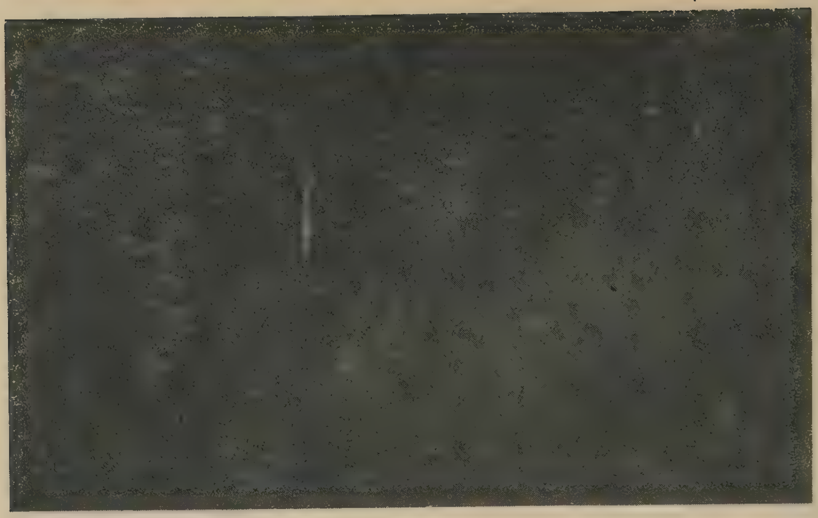

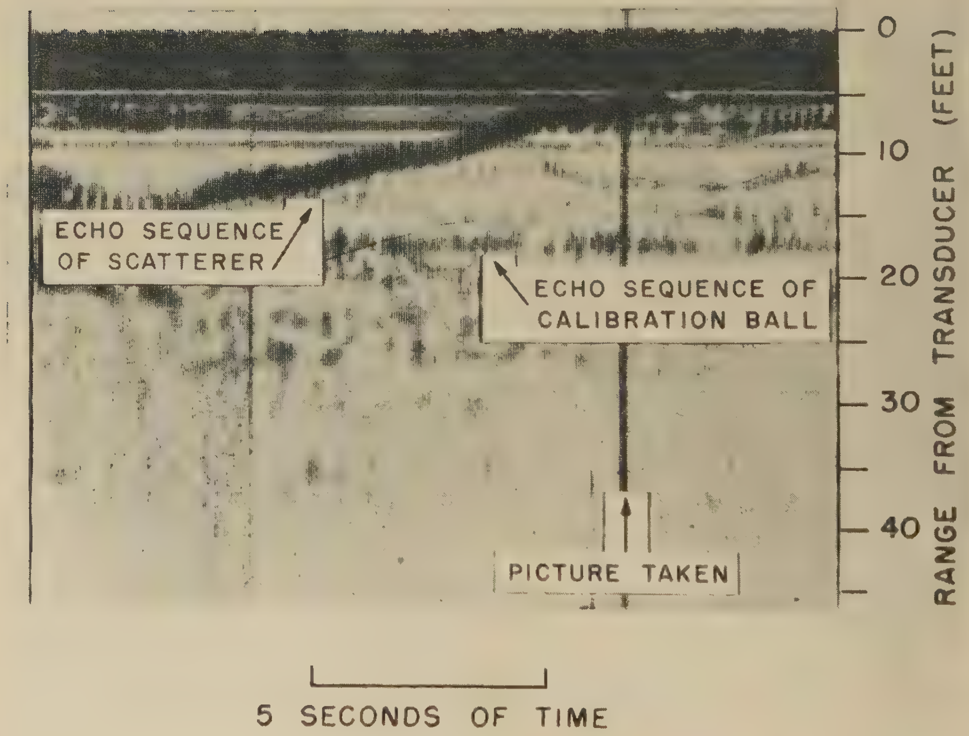
0
10
20
30
40
RANGE FROM TRANSDUCER (FEET)
ECHO SEQUENCE OF SCATTERER
ECHO SEQUENCE OF CALIBRATION BALL
PICTURE TAKEN
5 SECONDS OF TIME

Fig. 6. This couplet was chosen from the same lowering as that in Fig. 5. The fish in the photograph is *Nealotus tripes* Johnson, a trichiuroid fish related to the snake mackerel. The associated acoustic record shows a strong echo sequence. The 35-mm-focal-length lens was focused for a distance of six feet in water (depth of focus from about five feet to eight feet at *f* 6·3). The echo-sounder record shows the fish to have been about five and one half feet from the camera. If the proportionate length of the image of the fish is multiplied by the length of the field of the frame for this range the length of the fish would be about six inches (150 mm).

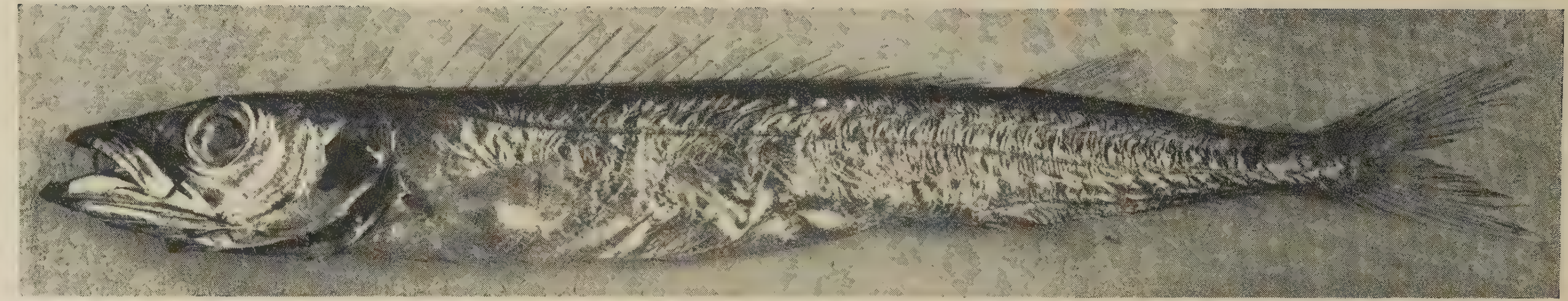

Fig. 7. *Nealotus tripes* Johnson. Length about five and one-half inches (140 mm). The same species as that in Fig. 6. One of about 15 specimens dipnetted at the surface on the evening on which the records in Fig. 6 were made and on the preceding evening. According to MATSUBARA and IWAI (1952), only eight specimens of this widely distributed fish have been previously recorded.

Secondly, the observed decrease in sensitivity of the acoustic system with increasing hydrostatic pressure has limited our observations of deep scattering layers to hours of darkness when the layers are near the surface. This has the obvious disadvantage of having nonmigrating, near-surface scatterers mixed in with the population in which we are particularly interested.

About 40% of the photographs accompanying strong echo sequences show nothing. It is unlikely that the sound scatterers in such cases are too small or too transparent to be revealed on the film, but that they lie outside the purview of the camera. Until this technical difficulty is overcome various objects cannot be associated with a certain echo quality. On the contrary, given an object, its echo can be loosely described. The data in Table 2 summarize the results of a lowering made on 21 July, 1955. In describing this lowering we do not imply that this experiment is representative of our experience so far. In a half-dozen earlier lowerings in which reasonable success might have been expected, only images of blobs were found in the photographs. In these earlier experiments we mostly operated at a much higher recorder amplifier gain which probably accentuated the disparity between the acoustic and optical fields as well as decreased our ability to distinguished between echoes of different amplitudes on the echo-sounder record.

The photographs made during the 21 July lowering have been classified as blank, blobs, unidentified objects, salps, and fishes (Table 2). The echoes recorded at the time of the photographic exposures have been classified as poor, 20% ; and as good, 63% of the total. 16% of the time no echoes were recorded[‡]. If there is no correlation between a class of object and the quality of its echo, each class of object photographed should be accompanied by echoes of the three kinds in the same proportion as they occur in the total. Departures from the expected percentages

Table 2. Summary of the results of an echo sounder-camera lowering.

	Echo sequence								
	None			*Poor*			*Good*		
Picture	*No.*	*Expected*	*Observed*	*No.*	*Expected*	*Observed*	*No.*	*Expected*	*Observed*
Blank	2	16%	40%[*]	1	20%	20%	2	63%	40%[*]
Blobs[†]	4	16%	14%	9	20%	31%	16	63%	55%
Unident. irregular objects	2	16%	14%	4	20%	28%	8	63%	58%
Salps	8	16%	18%	9	20%	20%	28	63%	62%
Fishes	0	16%	0%[*]	0	20%	0%[*]	18	63%	100%[*]

[‡] In thus " classifying " echoes we have in mind only qualitative judgements about the amplitude and general clarity (signal-to-noise ratio) of the individual echoes. With the possible exception of recognizing multiple scatterers from interference patterns in an echo sequence we do not regard descriptions of echo " quality " of further use in identifying scatterers.

[*] See text.

[†] All picture classes are self-explanatory save blobs. The latter images have appeared in all of our lowerings. These are round images, small when in focus and larger when out of focus. Often, when they occur along the edges of our pictures they are somewhat elongated and are so oriented as to point towards the centre of the frame (Fig. 4). These, then, are the so-called coma, originating from objects acting as point sources of light when seen by uncorrected lenses. They are familiar in astronomical photography. In the present case we presume them to be caused by particulate matter of a small size. However, in the case of large blobs, larger, out-of-focus objects could be the source of these images.

indicate a correlation between class of object and echo category. The departures in Table 2 that are deemed possibly significant are few and are marked with an asterisk. In the case of pictures showing nothing there are more such pictures than expected when there is no echo and fewer than expected when there is a good echo. If, with such a small sample, anything is indicated it is that a correlation exists between some of the remaining classes of objects and the category of the echo. With respect to blobs, unidentified objects, and salps, the observed percentages are close to the expected percentages for all echo categories indicating no correlation for these object classes. For fishes, however, the observed values are very different from the expected values. There are no pictures of fishes accompanied by no echo or poor echoes ; rather, all pictures of fishes are accompanied by strong echoes. Thus this experiment adds to earlier evidence that fishes are important sources of strong deep-ocean sound scattering.

Acknowledgments—We are greatly indebted to Professor HAROLD E. EDGERTON of the Massachusetts Institute of Technology for arranging the loan of a deep-sea camera and electronic flash belonging to the National Geographic Society. Mr. LLOYD D. HOADLEY of the Woods Hole Oceanographic Institution helped us to incorporate the camera with the echo-sounding system. We are also grateful to many members of the underwater acoustics group and ships' companies of the Woods Hole Oceanographic Institution who helped us ashore and at sea, particularly Mr. S. T. KNOTT and Mr. HERBERT SMALL. The work was done under Contract NObsr-43270 with Bureau of Ships, U.S. Navy Department.

Contribution No. 841, *Woods Hole Oceanographic Institution, Woods Hole, Massachusetts.*

REFERENCES

ANDERSON, V. C. (1953), Wide band sound scattering in the deep scattering layer. *SIO Ref.* 53-36, 1-35. (Unpublished manuscript).
BODEN, B. P. (1950), Plankton organisms in the deep scattering layer. *Rept. U.S. Navy Electronics Laboratory* 186, 1-29. (Unpublished manuscript).
BURD, A. C. and LEE, A. J. (1951), The sonic scattering layer in the sea. *Nature*, **167** (4251), 624.
DIETZ, R. S. (1948), Deep scattering layer in the Pacific and Antarctic Oceans. *J. Mar. Res.* **7** (3), 430-442.
DUVALL, C. E. and CHRISTENSEN, R. J. (1946), Stratification of sound scatterers in the ocean. *J. Acous. Soc. Amer.* **18** (1), 254.
EDGERTON, H. E. and HOADLEY, L. D. (1955), Cameras and lights for underwater use. *J. Mot. Pict. Tel. Eng.* **64**, 345-350.
EYRING, C. F., CHRISTENSEN, R. J. and RAITT, R. W. (1948), Reverberation in the sea. *J. Acous. Soc. Amer.* **20** (4), 462-475.
HERDMAN, H. F. P. (1953), The deep scattering layer in the sea : Association with density layering. *Nature* **172** (4372), 275-276.
HERSEY, J. B. and BACKUS, R. H. (1954), New evidence that migrating gas bubbles, probably the swimbladders of fish, are largely responsible for scattering layers on the continental rise south of New England. *Deep-Sea Res.* **1** (3), 190-191.
HERSEY, J. B., JOHNSON, H. R. and DAVIS, L. C. (1952), Recent findings about the deep scattering layer. *J. Mar. Res.* **11** (1), 1-9.
HERSEY, J. B. and MOORE, H. B. (1948), Progress report on scattering layer observations in the Atlantic Ocean. *Trans. Amer. Geophys. Un.* **29**, 341-354.
JOHNSON, M. W. (1948), Sound as a tool in marine ecology, from data on biological noises and the deep scattering layer. *J. Mar. Res.* **7** (3), 443-458.

KANWISHER, J. and VOLKMANN, G. (1955), A scattering layer observation. *Science* **121** (3134), 108-109.

LYMAN, J. (1948), The sea's phantom bottom. *Sci. Month.* **66** (1), 87-88.

MACHLUP, S. and HERSEY, J. B. (1955), Sound-scattering observations of scatterers in the ocean. *Deep-Sea Res.* **3**, 4, par. 1, line 7.

MARSHALL, N. B. (1951), Bathypelagic fishes as sound scatterers in the ocean. *J. Mar. Res.* **10**, 1-17.

MATSUBARA, K. and IWAI, T. (1952), Studies on some Japanese fishes of the family Gempylidae. *Pacif. Sci.* 6, 193-212.

MOORE, H. B. (1950), The relation between the scattering layer and the Euphausiacea. *Biol. Bull.* **99** (2), 181-212.

RAITT, R. W. (1948), Sound scatterers in the sea. *J. Mar. Res.* 7 (3) 393-409.

SMITH, P. F. (1954), Further measurements of the sound scattering properties of several marine organisms. *Deep-Sea Res.* **2**, 71-79.

TUCKER, G. H. (1951), Relation of fishes and other organisms to the scattering of underwater sound. *J. Mar. Res.* **10** (2), 215-238.

Printed in Great Britain by The Salisbury Press Ltd., Publicity House, Wilton Road, Salisbury, Wilts. (99080)

Contribution No. 842

(*Reprinted from Nature, Vol.* 178, *pp.* 861–862, *October* 20, 1956)

Interrelation between Photosynthesis and Respiration in the Marine Flagellate, *Dunaliella euchlora**

THE photosynthetic assimilation of carbon-14 from the external medium by unicellular algae appears to proceed at a rate which is equivalent to the plants' net photosynthesis (the difference between photosynthesis and respiration). This was demonstrated in experiments in which the assimilation of carbon-14 was compared simultaneously with the evolution of oxygen[1], and was most apparent under conditions of low light intensity or nutrient depletion where respiration approached or equalled photosynthesis. For example, at or below the compensation-level no significant uptake of carbon-14 could be detected in 24 hr. despite the occurrence of measurable photosynthesis by oxygen production.

Two possible physiological explanations for this behaviour have been considered. These are : (1) that newly assimilated carbon serves as an immediate substrate for respiration ; (2) that respiratory carbon dioxide is used preferentially to external carbon dioxide for photosynthesis. The first of these explanations appears to be contradictory to the findings of Calvin[2] and Weigl *et al.*[3], who have reported that newly assimilated carbon-14 does not immediately enter the respiratory cycle as long as the plants are photosynthesizing.

The second possibility may be investigated by a simple experiment in which organisms are grown in a medium containing carbon-14 for a sufficient number of generations so that essentially all their carbon becomes uniformly labelled with the tracer. If the cells are then removed from their external carbon-14 source and resuspended in fresh medium, any respiratory loss of carbon must be accompanied by a loss of carbon-14 activity by the organisms. The failure to detect such a loss during photosynthesis would clearly demonstrate the re-assimilation of respiratory carbon dioxide. The details of such an experiment are as follows.

A bacteria-free culture of *Dunaliella euchlora* was inoculated into 1·5 litres of enriched sea water medium deficient in nitrogen (0·001 per cent potassium nitrate), giving an initial cell concentration of 1,500 cells/ml. 10 μc. of $^{14}CO_3$ were added and the cultures exposed to approximately 800 foot-candles of illumination at 20° C. At the same time a duplicate culture containing no carbon-14 was inoculated. After two days the cultures contained 21,000 cells/ml. and, for practical purposes, all the carbon of the cells in the isotope-enriched culture was uniformly labelled with the tracer. Exponential growth continued for four days and growth stopped after the fifth day. During the growth period sufficient carbon dioxide was added daily to keep the *p*H below 8·0. This was not necessary after growth had stopped. The growth-curve for the two duplicate cultures is shown in Fig. 1, each point representing the mean concentration of cells in the two cultures.

* Contribution No. 842 from the Woods Hole Oceanographic Institution.

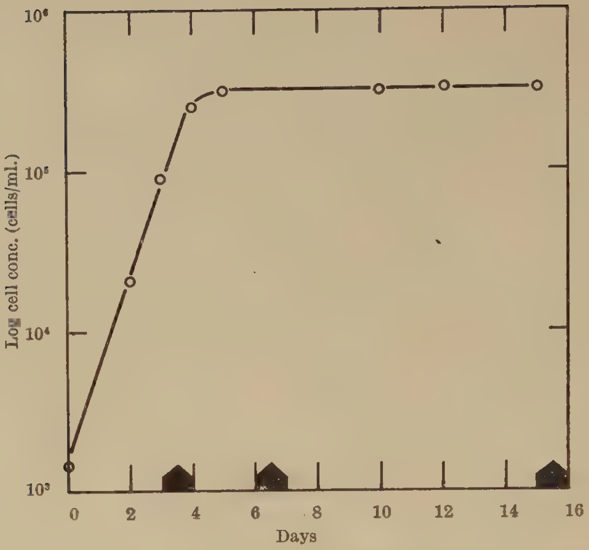

Fig. 1. Growth curve of duplicate *Dunaliella* cultures. Arrows denote days on which experiments were performed.

Table 1. THE LOSS OF ACTIVITY IN *Dunaliella* TAGGED WITH CARBON-14 IN THE LIGHT AND DARK IN RELATION TO PHOTOSYNTHESIS AND RESPIRATION

Age of culture (days) (see Fig. 1)	P	R	$P : R$	% Loss activity/ 24 hr.	
		(ml. O_2/l./hr.)		Light	Dark
3	0·36	0·03	12·0 : 1	−0·3*	20·9
6	0·09	0·02	4·5 : 1	1·6*	22·9
15	0·03	0·015	2·0 : 1	1·5*	20·0

* Attributable in each case to random counting error.

On the third, sixth and fifteenth days aliquots of the culture tagged with carbon-14 were centrifuged. The cells were then washed in filtered sea water and resuspended in the filtered medium of the culture containing no carbon-14, adjusting the density to give 25,000 cells/ml. The tagged cells were thereby removed from their external source of carbon-14 but retained in a medium physiologically identical with that in which they had grown. The *p*H was adjusted to 7·0–7·5 by the addition of carbon dioxide and the new cell suspension siphoned into 35-ml. glass-stoppered bottles.

Half the bottles were used for the determination of photosynthesis and respiration by measuring the change in dissolved oxygen concentration (Winkler method) in the light (800 f.c.) and in the dark after six hours. The increase in oxygen in the light represents net photosynthesis ($P-R$), the decrease in the dark represents respiration (R) and the difference between the two is considered equivalent to total photosynthesis (P).

Of the remaining bottles, one-third were filtered immediately, one-third exposed to 800 foot-candles illumination for 24 hr. and filtered, and one-third kept in the dark for 24 hr. and filtered. The filters were then dried and their radioactivity determined. All the above measurements were made in triplicate, and the mean values are given in Table 1. The data show that the cells tagged with carbon-14 did not lose a significant amount of carbon during 24 hr. of exposure to light, while those kept in the dark for the same length of time lost approximately 20 per cent of their carbon.

Measurements of the oxygen assimilation of *Dunaliella* following its removal from light have shown that respiration proceeds at a rapid and constant rate during the first 24 hr., after which the process slows down markedly. Kok[4] observed the same behaviour in *Chlorella*, which respired as much as 15 per cent of its dry weight (or a comparable fraction of its carbon) in 20 hr., following which the rate of oxygen uptake "declined to a low and steady level of endogenous respiration".

The loss of 20 per cent of the carbon-14 content of the cells in the dark over 24 hr. may therefore be reasonably attributed to respiration. Since the rate of oxygen uptake remains constant throughout that period, it also seems reasonable to assume that respiration occurred at essentially the same rate in the organisms exposed to the light, particularly in view of the evidence presented by Brown[5] that respiration is independent of light.

Since all carbon in the organisms was tagged with carbon-14, any measurable respiration would result in a loss of activity to the cells. The fact that such a loss was not detected in the light must be interpreted to mean that somewhere within the respiratory cycle the carbon was re-assimilated by photosynthesis. This process appears to have occurred with 100 per cent efficiency regardless of the rate of photosynthesis or the ratio of $P : R$. It is noteworthy that the respiratory carbon dioxide was preferentially used despite an external partial pressure of carbon dioxide more than four times as great as that of normal sea water. Even during the period of maximum photosynthesis (on the third day) carbon dioxide assimilation did not exceed 15 per cent of the total carbon dioxide available in the medium.

These experiments provide no clue as to the biochemical state of the recycled respiratory carbon. They recall the suggestion of Franck[6], Gaffron[7] and others of a common intermediate pool for photosynthesis and respiration. However, a case may also be made on purely physical grounds for the successful competition of respiratory versus external carbon dioxide at the chloroplast. The latter is perhaps more compatible with the observations of Brown[5], who was able to neglect the preferential utilization of photosynthetically produced oxygen in his respiration experiments with *Chlorella*, indicating that the two processes are not universally linked at an intermediate level.

JOHN H. RYTHER

Woods Hole Oceanographic Institution,
Woods Hole, Mass.
June 11.

---

[1] Ryther, J. H., *Deep-Sea Res.*, **2**, 134 (1954); *Limnol. and Oceanogr.*, **1** (2), 72 (1956).

[2] Calvin, M., *J. Chem. Ed.*, **26**, 639 (1949).

[3] Weigl, J. W., Warrington, P. M., and Calvin, M., *J. Amer. Chem. Soc.*, **73**, 5058 (1951).

[4] Kok, B., *Acta Bot. Néerl.*, **1**, 445 (1952).

[5] Brown, A. H., *Amer. J. Bot.*, **40**, 719 (1953).

[6] Franck, J., *Arch. Biochem.*, **45**, 190 (1953).

[7] Gaffron, H., 4th Symp. Soc. Gen. Microbiol., 152 (Camb. Univ. Press, 1954).

Printed in Great Britain by Fisher, Knight & Co., Ltd., St. Albans.

Contribution No. 846

Deep-Sea Research, 1956, Vol. 3, pp. 273 to 278. Pergamon Press Ltd., London.

On the determination of the depth of no meridional motion

HENRY STOMMEL

(*Received* 29 *May* 1956)

Abstract—The depth of no meridional geostrophic velocity is determined from a pair of hydrographic stations in the Sargasso Sea, on the premise that the deep flow is frictionless. Certain implications regarding the eddy and advective flux of heat in the deep water are also discussed.

WE WILL consider the consequences of EKMAN's classical concept of dividing the central ocean circulation into a shallow wind-driven surface layer of frictional influence, and a deeper frictionless geostrophic flow, when it is applied to actual hydrographic data, rather than to an abstract homogeneous ocean. We proceed to define a rectangular co-ordinate system, with origin at the sea surface, with x directed eastward, y northward, z upward, and u, v, and w representing the corresponding velocity components. The Coriolis parameter is f. Denote pressure by p, density by ρ, the x and y components of shearing stresses across horizontal planes by τ_x and τ_y; and the acceleration due to gravity by g. In central oceanic regions we assume that the hydrographic-station data are representative of a time-averaged steady density field, and we assert that the inertial terms are negligible. The system is then described by the following equations

$$-f\rho v = -\frac{\partial p}{\partial x} + \frac{\partial \tau_x}{\partial z} \tag{1}$$

$$f\rho u = -\frac{\partial p}{\partial y} + \frac{\partial \tau_y}{\partial z} \tag{2}$$

$$g\rho = -\frac{\partial p}{\partial z} \tag{3}$$

$$\frac{\partial}{\partial x}(\rho u) + \frac{\partial}{\partial y}(\rho v) + \frac{\partial}{\partial z}(\rho w) = 0 \tag{4}$$

Elimination of pressure by cross-differentiation leads to the following three relations

$$\frac{\partial}{\partial z}(\rho v) = -\frac{g}{f}\frac{\partial \rho}{\partial x} - \frac{1}{f}\frac{\partial^2 \tau_x}{\partial z^2} \tag{5}$$

$$-\frac{\partial}{\partial z}(\rho u) = -\frac{g}{f}\frac{\partial \rho}{\partial y} - \frac{1}{f}\frac{\partial^2 \tau_y}{\partial z^2} \tag{6}$$

$$\frac{\partial}{\partial z}(\rho w) = \frac{\beta}{f}\rho v - \frac{1}{f}\frac{\partial}{\partial z}\left[\frac{\partial \tau_y}{\partial x} - \frac{\partial \tau_x}{\partial y}\right] \tag{7}$$

where $\beta = \partial f/\partial y$.

The quantity ρv can be eliminated between equations (5) and (7).

$$\frac{d^2\, \rho w}{dz^2} = -\frac{\beta g}{f^2}\frac{\partial \rho}{\partial x} - \frac{d^2}{dx^2}F(z) \tag{8}$$

where

$$F(z) \equiv \frac{\partial}{\partial x}\left(\frac{\tau_y}{f}\right) - \frac{\partial}{\partial y}\left(\frac{\tau_x}{f}\right).$$

Equation (8) is written as a total differential equation because $\partial\rho/\partial x$ is known (from a pair of hydrographic stations both on the same latitude circle) along a vertical as a function of z, and $F(z)$ is to be regarded as a more or less undeterminable function of z, into whose detailed structure we will not inquire, but merely suppose that, following EKMAN, it differs from zero only in a thin upper layer extending from $z = 0$ to $z = -D$, the depth of frictional influence. The value of $F(0)$ is known explicitly in terms of the distribution of wind stress on the sea surface in the neighbourhood of the pair of hydrographic stations. The ocean bottom is at $z = -B$. A first integral of equation (8) can now be obtained.

$$\frac{d}{dz}\rho w = \frac{\beta}{f}[\phi(z) + C] - \frac{dF}{dz}\Big|_{-B}^{z} \tag{9}$$

where we define

$$\phi(z) \equiv -\frac{g}{f}\int_{-B}^{z}\frac{\partial\rho}{\partial x}\,dz$$

and C is a constant of integration. The meaning of the function $\phi(z)$ is familiar, because for purely geostrophic flow (from equation 5) we have simply

$$\rho v = \phi(z) + C$$

and the constant C is the undetermined reference velocity. This amounts, of course, to the traditional method of *dynamic computation* and the undetermined constant of integration is the undetermined meridional mass flux ρv at the bottom. Thus we see that the determination of C is equivalent to determining the *depth of no motion*, i.e. the depth at which ρv vanishes. We will henceforth avoid both italicized terms because they are misleading; indeed we will find that the level of no meridional motion coincides with the maximum vertical motion, and that the level of no zonal motion does not necessarily coincide with either.

Since in the real ocean time-averaged bottom currents are weak, we may write, by hypothesis, $\frac{dF}{dz}\Big|_{-B}^{z} = \frac{dF}{dz}$, and equation (9) may be integrated once again between the limits z and $-B$, and taking $F(-B) = 0$, $\rho w(-B) = 0$, the following expression for ρw is obtained.

$$\rho w = \frac{\beta}{f}\left[\int_{-B}^{z}\phi(z)\,dz + C(z + B)\right] - F(z) \tag{10}$$

At the surface $z = 0$, ρw vanishes (or is fixed by some small known mean evaporation-precipitation correction). The quantity $F(0)$ is simply the well-known net convergence of the Ekman wind-driven layer as computed for ocean areas (MONTGOMERY, 1936). Thus the constant C is determined by the following relation

$$C = \frac{1}{B}\left[\frac{f}{\beta}F(0) - \int_{-B}^{0}\phi(z)\,dz\right] \tag{11}$$

The depth at which $\phi(z) + C$ vanishes is the depth of no meridional motion. The same analysis cannot be applied to determine the zonal component of velocity ρu.

The velocity component ρu is determined, in principle, however, from equation (4), because the fields of ρv and ρw are determined. From a practical point of view a very detailed network of hydrographic stations would be necessary to develop the field of the quantity ρu.

In physical terms the method which we have discussed above in formal terms can be loosely described as follows. At any geographical position in the ocean the distribution of the winds produces a net convergence (or divergence) of surface waters. The only place for this water to escape (or come from) in the steady state is downward (upward) through the bottom of the surface frictional layer. In the deep frictionless (by hypothesis) geostrophic flow, water elements stretch (or shrink) vertically if they move poleward (equatorward). The cumulative effect of such stretching and shrinking, added up over the entire vertical column from the ocean bottom to the bottom of the frictional layer, leads to a vertical component of velocity which must, by mass conservation, equal that induced at the bottom of the frictional layer by the winds. This matching occurs only for a specific choice of reference level and the latter is thereby determined.

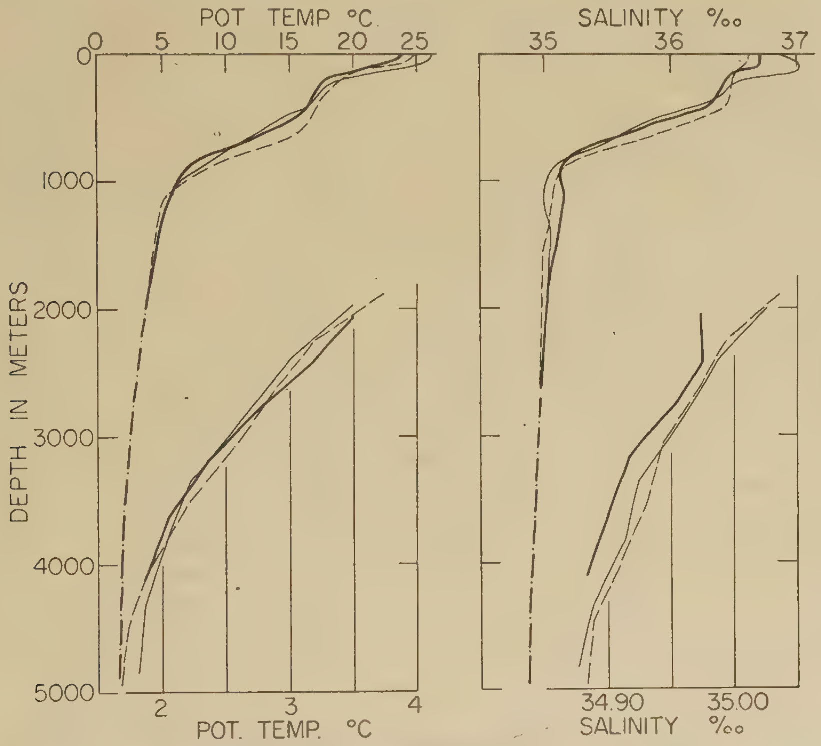

Fig. 1. Potential temperature and salinity at *Atlantis* Stations 5203 (dashed) 5210 (solid) and 5215 (light solid). Below 2,000 metres the abscissae are shown expanded ten times, in order to exhibit detail.

If the hypothetical elements of this analysis obtain in nature, we now have a way of computing the actual vertical profile of meridional velocity – except in the frictional layer itself, where there is some ambiguity due to our lack of knowledge of the distribution of eddy viscosity. We also have computed the actual vertical distribution of the vertical component of velocity (equation 10). We cannot determine the reference level of the zonal velocity from the data of a pair of hydrographic stations, as computed from equation (6). In principle, however, for an ocean area well covered by hydrographic data, the zonal component of velocity is determined through equation (4) and a coastal boundary condition because the other components are known by the above theory.

In order to illustrate the method and its implications, a numerical example is presented here. Three of WORTHINGTON's recent *Atlantis* stations in the Sargasso Sea are used: 5203, 5210, and 5215. The vertical distribution of potential temperature and salinity is illustrated in Fig. 1.

Table 1. *Numerical Examples*

Atlantis Stations 5203 32°00′N 63°03′W
5210 32°00′N 50°41′W

Depth m	*Specific Volume Anomaly* 5203 10^{-5} cm³ gm⁻¹	5210	$\phi(z)$ cm sec⁻¹	$\int_{-B}^{z} \phi(z)\,dz$ 10^4 cm² sec⁻¹	$\rho w + F(z)$ 10^5 cm sec⁻¹	ρv cm sec⁻¹
0			− 2·587	− 20·58	− 9	− 2·2
50	331.5	298·3	− 2·402	− 19·33	− 6	− 2·1
100	265·0	240·0	− 2·263	− 18·16	− 4	− 1·9
150	200·0	184·5	− 2·176	− 17·06	− 1	− 1·8
200	180·2	173·6	− 2·140	− 15·97	+ 1	− 1·8
250	176·6	168·6	− 2·095	− 14·92	3	− 1·7
300	174·0	166·5	− 2·053	− 13·88	5	− 1·7
350	172·3	165·0	− 2·013	− 12·86	7	− 1·7
400	171·4	162·0	− 1·960	− 11·87	9	− 1·6
450	170·8	157·3	− 1·885	− 10·91	11	− 1·5
500	168·6	150·5	− 1·784	− 9·99	13	− 1·5
600	159·5	138·8	− 1·553	− 8·32	16	− 1·2
700	142·8	120·5	− 1·305	− 6·89	19	− 1·0
800	123·8	96·9	− 1·005	− 5·74	21	− 0·7
900	99·9	77·0	− 0·749	− 4·86	22	− 0·4
1000	79·7	62·9	− 0·562	− 4·21	22	− 0·2
1200	61·9	54·8	− 0·404	− 3·24	23	− 0·1
1400	51·3	49·0	− 0·352	− 2·49	24	− 0·02
1600	48·5	45·9	− 0·294	− 1·84	24	+ 0·04
1800	46·7	44·9	− 0·254	− 1·29	23	0·08
2000	46·3	44·4	− 0·212	− 0·84	23	0·12
2500	46·3	43·6	− 0·061	− 0·14	20	0·27
3000	44·5	43·9	− 0·028	− 0·09	17	0·31
3500	43·4	43·5	− 0·033	+ 0·25	13	0·30
4000	43·0	43·4	0·000	+ 0·33	9	0·34
4500	43·9	42·8	0·061	+ 0·18	5	0·40
5000	43·7	44·6	0·011	0·00	0	0·34

Other numerical values used: $f = 0{\cdot}773 \times 10^{-4}$ sec⁻¹
$\beta = 1{\cdot}9 \times 10^{-13}$ cm⁻¹ sec⁻¹
$F(0) = -9 \times 10^{-5}$ cm sec⁻¹ (from MONTGOMERY, 1936)
Distance between stations $= 1{\cdot}16 \times 10^8$ cm
Value found: $C = 0{\cdot}338$ cm sec⁻¹

The calculation of the meridional and vertical velocity distributions is carried out in Table 1. The depth of no meridional motion is found to be about 1,500 metres. The maximum value of vertical velocity, 24×10^{-5} cm/sec, is also found at this depth. This is also very nearly the depth of the centre of the high-salinity anomaly water from the Mediterranean.

In order to carry the investigation further, for example into the question of heat fluxes, etc., the reference level for the zonal velocity component is, in general, needed. Since we do not have this information we can only discuss heat fluxes where zonal advection appears to be inconsiderable. For example, in the divergence of heat flux equation (θ denotes temperature)

$$\frac{\partial \theta}{\partial t} + u\frac{\partial \theta}{\partial x} + v\frac{\partial \theta}{\partial y} + w\frac{\partial \theta}{\partial z} = K\frac{\partial^2 \theta}{\partial z^2}$$

we are forced to estimate $\partial\theta/\partial t$ and u in the left-hand member. In the water below 1,000 metres (Table 2) it seems probable that the last term of the left-hand member dominates entirely, for any reasonable estimates of the first two terms, and hence must be balanced by the vertical conduction divergence on the right-hand side. In this way we compute the vertical eddy coefficient of thermal conductivity K. Of course little confidence can be placed in the exact numerical values of K, but the order of magnitude is defensible. A consideration of the salt flux divergence leads to similar values of the eddy diffusivity. Unless the eddy coefficient of viscosity is three or four orders of magnitude greater than K, there is no inconsistency in taking $F(z) = 0$ in the deep water. Finally there are some comments which I would like to make:

Table 2. Evaluation of Terms in the Divergence of Heat Flux Equation

Depth *m*	* $\frac{\partial\theta}{\partial t}$ 10^{-8} *sec*$^{-1}$	† $u\frac{\partial\theta}{\partial x}$ 10^{-8} *sec*$^{-1}$	$v\frac{\partial\theta}{\partial y}$ 10^{-8} *sec*$^{-1}$	$w\frac{\partial\theta}{\partial z}$ 10^{-8} *sec*$^{-1}$	$\frac{\partial^2\theta}{\partial z^2}$ 10^{-8} *cm*$^{-2}$	K *cm*^{2} *sec*$^{-1}$
1000	(0·02)	0.25	0·06	1·00	0·10	8
1500	(0·02)	(– 0·10)	0·00	0·46	0·06	8
2000	(0·02)	(± 0·05)	< 0·01	0·28	0·02	14
3500	(0·02)	(± 0·05)	0·00	0·13	0·01	13

* Based on estimated maximum probable long-term trend of 0·2°C per 30 years.
† Based on estimated maximum probable value of ρu, ± 0·5 cm sec^{-1}.

(1) The idea that friction is dynamically unimportant in the deep water is purely hypothetical, and will have to be justified eventually by its results.

(2) The concept of a hydrodynamical situation in which mixing is important, but friction unimportant, is an odd one, and deserves further study.

(3) There is nothing in this treatment to imply that the ocean is entirely wind-driven; indeed in another place (STOMMEL, 1956, Chap. xi) I have given reasons for supposing that a large portion of the ocean circulation is thermohaline in origin.

(4) The relatively large values of vertical velocity and diffusivity in the Sargasso Sea indicate that the deep water cannot be much more than 200 years older than the surface water – in contradiction to the tenfold greater age reported by KULP (1953) from carbon-14 measurements.

(5) The depth of no meridional motion in the Sargasso Sea determined by the the above method nearly coincides with that inferred by DEFANT (1941) from intuitive considerations. One hopes that eventually there will be a direct observational check.

(6) The notion that there is a *level of no motion* in the ocean, where all three

velocity components vanish, is not substantiated; indeed maximum upward velocity is found to occur at the depth of no meridional velocity.

(7) The method is not unrelated to SVERDRUP's (1947) vertically integrated transport functions, but differs in that the vertical density structure is considered in detail. Like SVERDRUP's theory, *the method is restricted to central oceanic areas*, well removed from high-velocity boundary currents like the Gulf Stream. Another previous attempt to match the flow from the frictional layer to deeper geostrophic flow is the rather different discussion by MONTGOMERY (1938, pp. 38-40).

(8) A reviewer has recommended that, in order to avoid confusion, I should state explicitly that vertical velocities in the steady state do not necessarily imply mixing. For example, flow along sloping isothermal surfaces, in which the dominant terms in the heat-divergence equation are the last three terms of the left-hand member, does not necessarily do so. Indeed, in the upper layers of the Sargasso Sea this latter condition seems to occur; and it is for this reason that the calculations in Table 2 are limited to 1,000 metres and deeper.

Contribution No. 846 *from the Woods Hole Oceanographic Institution. This work was supported by the Office of Naval Research under Contract Nonr*-769(00) (*NR* 083-069).

REFERENCES

DEFANT, A. (1941), Die absolute Topographie des physikalischen Meeresniveaus und der Druckflächen, sowie die Wasserbewegungen im Atlantischen Ozean. *Deutsche Atlantische Exped.* "*Meteor*" 1925-27, *Wiss. Erg.*, **6**, 191-260.

KULP, J. L. (1953), Climatic change and radioisotope dating, pp. 201-8, in *Climatic change*, edited by A. H. SHAPLEY, Harvard Univ. Press (1953), 318 pp.

MONTGOMERY, R. B. (1936), On the momentum transfer at the sea surface, III, transport of surface water due to the wind system over the North Atlantic. *Pap. Phys. Oceanogr. Meteorol.*, **4** (3), 23-30.

MONTGOMERY, R. B. (1938), Circulation in the upper layers of southern North Atlantic deduced with use of isentropic analysis. *Pap. Phys. Oceanogr. Meteorol.*, **6** (2), 1-55.

STOMMEL, H. (1956), *The Gulf Stream*, Univ. of California Press (in press).

SVERDRUP, H. U. (1947), Wind-driven Currents in a Baroclinic Ocean; with Application to the Equatorial Currents of the Eastern Pacific. *Pro. Nat. Acad. Sci.*, **33**, 318-326.

Contribution No. 847

[REPRINTED FROM *The Geographical Review,* Vol. XLVI, No. 4, October, 1956]

The Geographical Review

VOLUME XLVI *October, 1956* *NUMBER 4*

CONTROL OF THE WORLD ENVIRONMENT*

ATHELSTAN SPILHAUS

ONE essential difference between man and the lesser animals is that man strives to change his environment to meet his peculiar needs, whereas other forms of life in the course of time submissively adapt themselves to the whims of their surroundings. Man began to alter his environment to his needs when, in his primitive state, he found himself a shelter to keep out rain, wind, and sun; when he discovered fire to warm himself against the chill; when he herded animals and cultivated plants instead of merely hunting and gathering them; when he stored fresh water against times of drought and thirst. From these beginnings of his ancient forebears, man has continually applied his increasing knowledge of Nature toward his better living. We now control to our liking, in our ordinary dwellings, the physical things that we sense—cold and heat, darkness and light, noise and silence, and odors. We do this by heating in winter and air conditioning in summer, by illuminating or darkening our rooms without regard to night or day, by acoustical conditioning, and by ventilating. We also eliminate disease-carrying animals such as rats and mosquitoes, and we control within our own bodies viruses, germs, and other living organisms that undermine our well-being. We breed animals and plants selectively for better and more abundant food, and we condition the spaces in which they grow by animal shelters and greenhouses, and by fertilizing and irrigating open tracts. There is no question that as the population of the earth increases, the need to utilize

---

*Expanded and revised from an address delivered at the Twentieth Executives' Conference, Institute of Paper Chemistry, at Appleton, Wis., May 10, 1956. (Contribution No. 847 from the Woods Hole Oceanographic Institution.)

➤ DR. SPILHAUS is dean of the Institute of Technology at the University of Minnesota, Minneapolis, and a member of the staff and of the trustees of the Woods Hole Oceanographic Institution. He also represents the United States on the Executive Board of UNESCO. Dr. Spilhaus' most recent contribution to the *Geographical Review* concerned "Sea and Air Resources" and appeared in the issue for July, 1954.

Copyright © 1956, by the American Geographical Society of New York

the presently uncomfortable empty areas of its surface will give impetus to making them more suitable for supporting human life.

There are, of course, many pitfalls and errors into which man can fall in exercising his new-found scientific strength because of his incomplete understanding of the complex interrelationships of the physical and living components on the earth. Lack of understanding and the inability to foresee the results of his actions have sometimes led man to make changes in his surroundings that were for the worse. The Buddhists believe that if Nature is tampered with too much she takes her revenge, and there are numerous examples from the past of endeavors which were carried out without adequate consideration of future implications and as a result of which it would seem that Nature has indeed taken her revenge. The denuding of forest lands, as, for example, long ago in Spain, more recently in our own country, and most recently in Korea, leads to changes in the local climate and causes erosion of the land, with dire consequences. But we are now learning to borrow from Nature and not to rob her. In our enthusiasm about industrialization, we have on occasion polluted the atmosphere, the rivers, and the ocean fringes. Here again Nature sometimes takes her revenge, as by the smog in Los Angeles. The increasing use of our new power from atomic energy confronts us with a waste we can neither bury in the ground nor dump in the sea nor burn so that it is diffused harmlessly into the atmosphere. The long half-life waste products that result from the use of nuclear fuels are not disposed of so easily. If we dilute the radioactive waste and spread it around, natural concentrating mechanisms, both in living plants and animals and by geophysical processes, defeat our purpose. If we concentrate it and put it in containers, the containers will not last as long as the longest half-lives of the wastes. If we drop the containers into the ocean, where sedimentation takes place fast enough to build up an adequate depth of shielding sediment before the containers deteriorate, it would seem as though we had the solution. But we must remember that the sea itself is a source of valuable nutrients, which are lost to man's use when they settle to the bottom, and within the period of time of the longer half-lives of the nuclear wastes the need may arise, and the ways be found, to mine or stir the bottom sediments for elements useful to man. It may conceivably be necessary to shoot these wastes off the earth into the truly plentiful space in rocket-type radioactive garbage scows. These few examples suffice to indicate that if we are to turn Nature to our better service, much thought and planning will be needed to ensure that we do not jeopardize the well-being of ourselves or of future generations.

Interplay of Knowledge and Application

The aim of our learning in science, both natural and social, and in the arts and humanities should be to maximize improvement of our living conditions, including the constant raising of human values, with the minimum exhaustion of real resources. If this ideal is kept in mind, I believe that the next half century will see an explosion of world engineering, dedicated to the welfare of man, on a much greater scale than that of the hydrogen bomb devised for his destruction. To give some credibility to the world engineering projects that may be carried out in the next fifty years, the fantastic advances of the last fifty years must be borne in mind. Also, it is necessary to recall the interdependence between basic science and engineering and industry, and the mutually supporting interplay between different technologies. Engineering advances depend on basic scientific discoveries, but in their turn they provide the great tools for further advancement of science—cyclotrons, linear accelerators, research reactors, electronic computers, and the like. This is the chain reaction that leads to the explosion of technology. A nice example of this chain reaction has been given by Dr. Alexander King[1] to show what happened at the beginning of the Industrial Revolution. James Watt's newly invented steam engine required, for its manufacture, more and better iron, and therefore more coal. The engine itself was put to work producing the blast for the iron furnaces and for pumping water from coal mines. Thus more coal was produced, more iron was produced, and more steam engines were produced. And the cycle goes on in an ever-expanding spiral.

For the thoughtful engineering of our world environment on the scale on which I believe it will take place in the next few decades, we shall need to increase many times our knowledge of our physical environment—the land, the sea, the atmosphere, and the space above it, including such extraterrestrial phenomena as the sun and cosmic rays. It is for this purpose that the International Geophysical Year, 1957–1958, has been planned. It is without doubt the greatest international scientific effort ever undertaken. The study of geophysics is essentially international because it deals with phenomena—such as the earth's atmosphere, its oceans, magnetism, gravity, solar activity, and cosmic-ray effects—which are problems of such scope that they transcend international boundaries and thrust aside curtains, even if made of iron. That is why 55 nations are taking part in this enormous cooperative effort to understand the physics of the earth. To many persons it may seem that the information gathered will be of purely scientific interest, but, in fact, the observations and studies made during the Geophysical Year will provide the basic data on which the vast world engineering projects of the future will be founded.

---

[1] Alexander King: Science and the Changing Face of Industry: The Social Phase, *Impact of Science on Society*, Vol. 7, 1956, pp. 3–33.

Scientists, engineers, and industrialists, each busy with their own concerns, perhaps lose sight of the fact that much of their effort relates (though sometimes in an indirect way) to a better understanding and use of four simple but wonderful things that contribute to mankind's well-being: fire, shelter, sweet water, and wholesome food.

Fuel

Fire is power, whether it comes directly or indirectly from nuclear sources on our planet or on the sun. Fossil fuel originated from the nuclear power that came to us as sunshine, was concentrated by Nature and stored for millions of years. Wood fuel is similar, except that the time between the arrival of the sunshine and its utilization is shorter. The time interval for hydroelectric power is shorter still: the atmosphere's sun-powered heat engine evaporates water from the sea, and the winds bring it to the land and deposit it on high places, where its potential energy can be converted to our use.

To obtain nuclear fuel directly on our planet, we expend power to extract it from rocks and ores just as we do to extract coal from mines. Nuclear fuel is not yet competitive where fossil fuels still exist, but upon the exhaustion, or in the absence, of other fuels nuclear fuel will be useful as long as less energy needs to be expended in its extraction than it will itself release. Sober estimates show that perhaps half of our common rock can in the future be utilized for nuclear power in this way. Power is the basic currency of all civilizations, and this abundant new power will lessen dependence on the more familiar sources. Thus abundant nuclear power can become a leveler among nations, raising living conditions in those areas which were poor in the older natural resources and reducing tensions caused by the contrast of haves and have-nots.

Shelter

The need for shelter for an ever-increasing world population will lead, through advances in the development of new materials, to enclosure of larger and larger spaces, perhaps whole cities. All around us the provision of shelter is already moving in this direction. More and more space is being enclosed under one roof; indeed, in the Arctic, where the rigors of climate render it economical, we find a town under one roof.

In intemperate climates huge areas may be enclosed in the future for the growing of foods. Greenhouses may be much larger, cheaper space enclosures in which soil moisture, atmospheric humidity, carbon dioxide content, soil temperature, heat, and the necessary light for photosynthesis are automatically balanced for optimum growth. Such structures, at first justified only for crops with a high value per unit area, will with increased yields and increased demand be used for the production of more and more foodstuffs. One can also envisage in arid regions the re-use of water within enclosures to prevent it from being lost to the open atmosphere. A small-scale artificial hydrologic cycle could be produced by which the water necessary to carry nutrients up into the plant would be transpired into the controlled atmosphere and circulated artificially to a cooler space, where it would condense and could be re-used. In this kind of greenhouse one would merely put plant nutrients in and take human nutrients out—it would be, as it were, a photosynthetic converter. This is an intermediate step toward automatic food factories based on algae culture (*Chlorella*) or on the growing of yeast animals, the beginnings of which are already here, unappetizing though they may seem.

WATER

Fresh-water demands will increase steadily with increasing population and industrialization. Regions that yesterday had fresh water in ample supply are today limited in their industrial development by its shortage; for example, in southern California. As pressures arise to inhabit the more arid regions of the world, means of bringing plentiful fresh water to these regions must and will be found. Imaginative engineering must discover economical ways to supplement natural distillation from the sea and find means of using the fresh-water ice that Nature provides in abundance in polar latitudes. The conservation of fresh water by repeated re-use and by prevention of wastage and runoff to the sea will become the rule. Larger and larger engineering projects to carry water from areas of plenty to areas of shortage and storage systems to hold the water from times of abundance to times of scarcity will be necessary. Nature will be emulated in conduits that copy her rivers and in great surface reservoirs that copy her lakes, and perhaps her lead will be followed in stimulating and adding to the storage of water underground. The effect of all this on man's living will be to make available the use of vast regions of the earth hitherto uninhabitable.

Food

For food production, scientists and engineers will join more and more with agriculturists in efforts to improve the environment of edible plants and animals, not only as now by the use of fertilizers and irrigation but perhaps even by removing the periodic interruption of the growing season through artificial heat or stored sunshine. Food production will tend to become a continuous-flow, chemical-engineering-type process rather than the present batch process. As population increases, there must be a tendency toward the growing of those organisms and plants which transform sunshine into food fuel with maximum efficiency; that is, with the fewest number of changes from the initial utilization of the sunshine to the final food: there will be an increasing use of the prey for food rather than the predator, and of the cereal rather than the animal that grazes upon it. Here, too, advanced and complex applications of science have a simple objective—the provision of enough wholesome food for the world.

Geotechnology

Vast though such engineering projects may seem, there are more subtle ways of turning our natural environment to our benefit. These more sophisticated schemes are further in the future and may have to await a better understanding of geophysical processes than we have yet attained. It is to this end that the studies of the International Geophysical Year will contribute mightily. Observations will be made of the sun's radiation, not only outside the atmosphere by means of artificial satellites but also from the earth's surface on the mechanism of how the sunlight is absorbed and how it is reflected, and indeed on all the elements of its utilization. These observations will provide the basic scientific data for the extensive developments that involve the interrelations of engineering and farming. An immediate and almost naïve use of solar energy, which may be of enormous importance, is already being worked on. This is the replacement by little solar cookstoves of the cow-dung fuel used for cooking in huge areas of the world, such as India and Africa. The effect of this simple development would be profound. The valuable organic material now burned could be returned to the soil and the land would soon be brought back into productivity. In Korea, too, solar cooking could reduce the demand for wood fuel and aid reforestation and reconditioning of the land.

Conditioning of Open Spaces

The increasing understanding of the mechanism of the utilization of the sun's energy and of related processes in the atmosphere leads to the idea of conditioning spaces that are not enclosed. The artificial stimulation and prevention of rainfall is just one example of how the plentiful but unevenly distributed fresh water of the world may be better shared in the future. The devastation wrought by hurricanes will not be lessened by the brute force released by the explosion of nuclear bombs to dissipate them. The force of even the largest nuclear bomb is so tiny in comparison with the violence of a natural storm as to be like that of a mosquito pitted against an elephant. If, however, the elephant can be caught in embryo—that is, if the hurricane can be treated in its formative stages—control may be exercised. Perhaps this will come about by regulating the absorption or reflection of sunshine at the ocean surfaces, or by the control of nuclei of condensation in the atmosphere, in the regions where the hurricanes are born. In these ways the instability may be dissipated *in situ* before devastating potentials are reached. Absorption of sunlight may be controlled in water and on ice surfaces by the addition of dyes; hence it may be possible to influence the growth or shrinking of large ice deposits. One could even speculate that conditioning of open spaces may ultimately include the stimulation of the nighttime air glow sufficiently to illuminate the night sky. There is a natural faint glow in the sky at night, which comes from the energy of the recombination of oxygen atoms broken up from the molecules during the periods of sunshine. Experiments have already been carried out which indicate that by increasing a catalyst in the high atmosphere the night glow could be increased. Careful thought would have to be given to the social and psychological implications of such an action, as well as to its effect on other scientific work. Certainly we should not want to increase materially the light in the night sky if this would prevent the further study and understanding of the universe by astronomers. Perhaps we shall need to wait until astonomers have their observatories on satellites above the atmosphere!

In all these approaches the engineer will not supply the enormous power to accomplish the result directly but will seek ways to catalyze or stimulate the immense natural forces to man's best use.

Control of the Ocean Environment

Even the unruly oceans which cover three-quarters of the earth's surface and which have such a huge volume will be susceptible to some measure of control, at least of their harvest. The mining and artificial introduction of the proper nutrients where we want optimum fish production in the ocean would be an improvement over the fortuitous natural leaching by rivers, which, while providing some elements valuable for ocean plants and fish, robs the land unnecessarily of useful materials. There is a scientist in this country who is devoting his time to studying the noises that a porpoise makes. By studying the noises made at feeding, mating, and other times, he may ultimately be able to "talk back" to the porpoise as a man speaks to his dog. This, in turn, could lead to the training of porpoises as fish herders, just as collies are trained as sheep dogs. Here would be one possible simple beginning toward the more controlled farming of the sea. This somewhat fanciful illustration does serve to emphasize that artificial devices may not necessarily be the best way of concentrating and gathering things from Nature for our use. There are efficient natural concentrating mechanisms, both animal and plant, and the scientist and the engineer must know these too and utilize them when they promise a better result than a purely physical device. Who knows whether the efficiency of the solar electric converter will be increased faster than an understanding of the fundamental process of photosynthesis might enable us to increase the efficiency of the natural process of solar food-fuel conversion?

Engineering Tools

It is the better understanding of the basic sciences that will lead to fantastic engineering applications such as these, but it is the great modern engineering tools that make it possible to uncover still more knowledge of the earth's environment. About five years ago, in the "Compendium of Meteorology,"[2] I suggested that, in order to obtain a satisfactory distribution of meteorological data for weather prediction to feed to the electronic computers (which were then in an early stage of development), buoys and artificial islands would be needed to fill in the vast gaps in our weather network caused by the oceans. We now have the "Texas Towers"—platforms far out in the Atlantic. Twenty years ago meteorologists added a third dimension to their knowledge of the atmosphere by the use of airplanes and then of balloons that radioed back information on conditions in the upper air. Today, although we still use balloons, the need to go higher and higher has made the use of rockets common enough to be referred to as the "conventional rocket" program. But conventional rockets spend only a little time at high altitudes before they fall back to earth, and for many investigations a much longer time is needed. It is for this reason that the artificial satellite has been devised. In contradistinction to the conventional rocket, the satellite has been christened the "LPR," the "long-playing rocket." It will add immeasurably to our knowledge of the high atmosphere and extraterrestrial influences. Its orbit will circle the earth, and because of its longer time aloft it will make geophysical measurements at greater leisure, even though it hurtles along at 18,000 miles an hour! Although the Texas Towers and the rockets are for military defense (an element of shelter, if you will), they are engineering tools with no intrinsic immorality and may serve equally to promote peaceful living. The huge Antarctic program of the IGY, in which 13 nations will participate, is no longer the dangerous adventure of former times but a calmly planned *occupation* by scientists using every boon of modern engineering to overcome the rigors of Nature in that inhospitable part of the world. These are examples of engineering tools which resulted from earlier scientific discoveries and which in their turn permit us to extend further the frontiers of our understanding of Nature.

---

[2] Athelstan Spilhaus: World Weather Network, *in* Compendium of Meteorology, edited by T. F. Malone (Boston, 1951), pp. 705–710.

This interaction of basic discovery and application, leading to new instruments for the further probing of the unknown, suggests that practical applications of new knowledge will increase logarithmically, and it is for this reason that I expect the mushrooming of engineering development on a world scale in the next fifty years.

The Human Aspect

The most difficult problems in this expanding technology will not, I think, be technical ones. They will be problems of supplying sufficient wisdom in the leadership and management of projects of this scale and of this complexity. If speculations such as those I have advanced here materialize, more thought and education must be directed toward the proper use of leisure, because the fraction of every man's time over which he is master will continue markedly to increase. There is therefore ever-increasing importance in finding ways for people to invest this time so as to promote tranquillity of mind and satisfaction rather than merely spending it in ways that sometimes lead to frustration. A stronger emphasis on the social sciences and on the employment of this greater leisure in contemplative and creative ways will prevent the tempestuous advance of technology from having uncontrolled ill effects.

It seems clear that scientists, engineers, and industrialists must do more than contribute to the freedom from want that I have symbolized by the four simple material needs: fire or power, shelter, fresh water, and wholesome food. Because they can understand better than others what the future complex technology to meet these needs has in store for mankind, they must also give thought to what is perhaps the greatest problem of all—how fundamental human values can be retained in the face of an increasingly "engineered" and artificial world.

Contribution No. 852

Reprinted from LIMNOLOGY AND OCEANOGRAPHY
Vol. 1, No. 4, October, 1956
Printed in U.S.A.

Some Oceanographic Applications of Recent Determinations of the Solubility of Oxygen in Sea Water[1]

FRANCIS A. RICHARDS AND NATHANIEL CORWIN

Woods Hole Oceanographic Institution, Woods Hole, Mass.

ABSTRACT

The solubility of oxygen in fresh and sea water has recently been redetermined by Truesdale, Downing, and Lowden (1955), who found that the data of Fox (1909), long considered definitive, are in substantial error. The old and new data are compared, and the new are used to recompute the percentage saturation in the surface layer of the South Atlantic and equatorial North Atlantic Oceans from the METEOR observations. It is shown that most of the surface waters are in equilibrium with the atmosphere. The effects of the error on computations of oxygen consumption and of oxygen tension are discussed.

A new nomogram relating the equilibrium oxygen concentration, the temperature, and the salt content of the water is presented.

Truesdale, Downing, and Lowden (1955) have recently redetermined the solubility of oxygen in fresh and sea water, and have found that the data of C. J. J. Fox (1909), long considered definitive, are in substantial error.

Fox's data have been widely used in oceanography, limnology, estuary and sewerage studies to estimate the amount of oxygen in solution when equilibrium is established with a dry atmosphere at a total pressure of 760 mm of mercury. Whipple and Whipple (1911), recognizing that in nature the atmosphere at water surfaces is more apt to be saturated with water vapor than to be dry, published tables for the solubility of oxygen in fresh and sea water in equilibrium with moist air. They had begun their own determinations at the time Fox's data came into their hands, but since their figures were in substantial agreement with his they abandoned their experiments and based their tables on Fox's experimental work, thus lending authority to his data.

Truesdale, Downing, and Lowden (1955) were led to suspect that the accepted figures were in error by observations of rates of solution that departed from the Adeney and Becker (1919) law of aeration. They undertook new determinations after carefully establishing conditions which assured that the final solutions were in true equilibrium, neither under- nor super-saturated. They found solubilities appreciably smaller than Fox reported, and therefore presumed that both Fox and the Whipples were working with supersaturated solutions.

Kalle (1939) published a nomogram widely used in oceanography, based on Fox's dry air data, for making the computation of oxygen solubility. Other nomograms and tables have been published (e.g. Tully 1949), which relate the salt content, temperature, and oxygen solubility, based either on Fox's data or Whipple and Whipple's tables derived from them. We have prepared a nomogram, based on the new data, as a supplement to this paper (Fig. 1). It should be emphasized that the data are for equilibrium established under an atmosphere saturated with water vapor at the temperature in question. The solubility is expressed in parts per million (actually milligrams per liter: Truesdale, personal communication), and in milliliters at STP per liter. The scale for milligram atoms per liter printed on the nomogram may be cut off and substituted for either the ppm or ml/L scale if the user prefers this expression of concentration.[2]

A comparison of solubility values according to a) Fox's data, b) Whipple and

---

[1] Contribution No. 852 from the Woods Hole Oceanographic Institution.

[2] Copies of this nomogram, 13″ x 14″, are available on request from the Director, Woods Hole Oceanographic Institution, Woods Hole, Massachusetts.

TABLE 1. *Comparison of values of O_2' (ml. O_2/liter) from Fox's (1909) dry air data (Col. 1), his data corrected for moist air according to Whipple and Whipple (1911) (Col. 2), and the new data for moist air of Truesdale, Downing, and Lowden (1955) (Col. 3)*

Temp. °C	S = 0 ‰			S = 20 ‰			S = 40 ‰		
	1	2	3	1	2	3	1	2	3
0	10.29	10.29	9.92	9.02	9.00	8.74	7.71	7.69	7.56
5	9.03	8.95	8.65	7.95	7.87	7.65	8.86	6.80	6.64
10	8.02	7.92	7.65	7.10	7.01	6.78	6.17	6.09	5.94
15	7.22	7.10	6.84	6.42	6.33	6.08	5.62	5.53	5.35
20	6.57	6.43	6.18	5.87	5.73	5.52	5.17	5.03	4.87
25	6.04	5.85	5.67	5.40	5.23	5.07	4.74	4.59	4.47
30	5.57	5.32	5.27	4.90	4.77	4.70	4.33	4.17	4.13

Whipple's tables, and c) the new data of Truesdale *et al.* (Table 1), shows that the discrepancies are greatest in low-salinity, low-temperature water and least at high salinities and temperatures. In sea water having a salinity 35‰, the discrepancy between Fox's values corrected for moist air and the new values vary from 0.16 ml O_2/liter at 0°C. to 0.04 ml O_2/liter at 30°C. However, most oceanographers have computed oxygen solubility from Fox's dry air data, and these discrepancies vary from 0.18 ml O_2/liter at 0°C. to 0.33 ml O_2/liter at 30°C. The values in Table 1 were read from nomograms prepared by Kalle (1939) for Col. 1, A. C. Redfield (1948) for Col. 2, and that which accompanies the present paper for Col. 3.

APPLICATION OF OXYGEN SOLUBILITY DATA

In the following discussion, O_2 will be used to designate the actual oxygen content of a water sample. O_2' is the solubility of oxygen in water having the observed salinity and temperature when in equilibrium with a standard atmosphere of 760 mm of mercury. O_2'' is the solubility in water at the observed salinity and temperature when in equilibrium with an atmos-

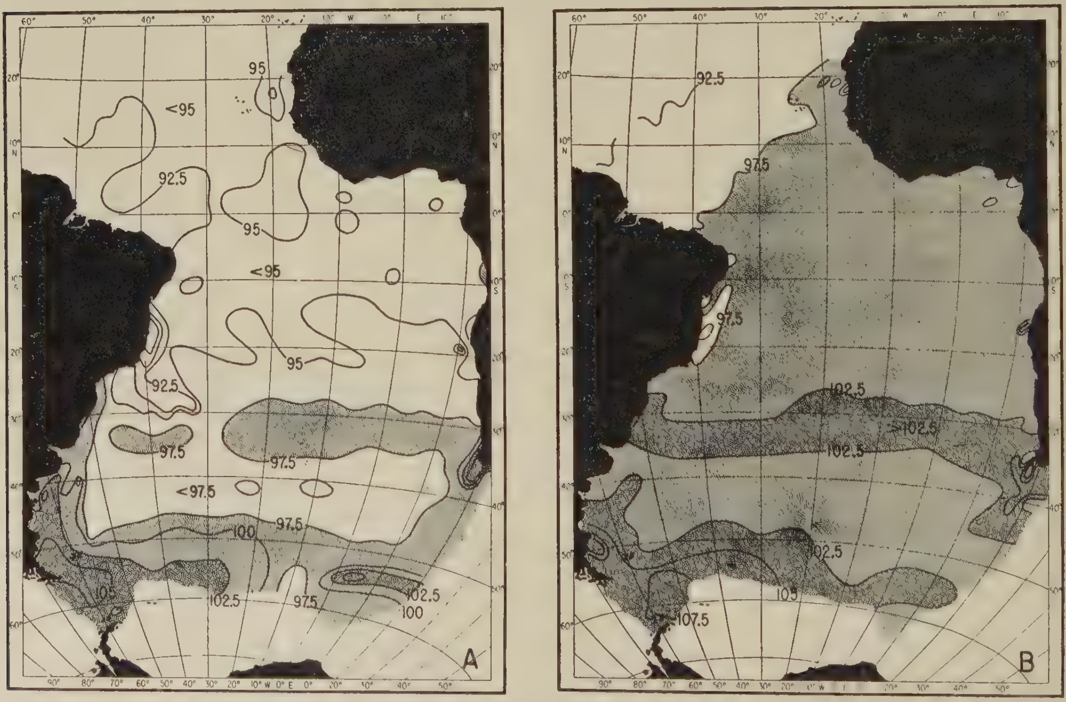

FIG. 2. Percentage saturation of oxygen in the surface layer of the equatorial North and South Atlantic Ocean. *A*. Redrawn from Wattenberg (1939), computed from the solubility data of Fox (1909). *B*. Recomputed from the METEOR data of Wüst (1932) and Wattenberg (1933, 1938), using the solubility data of Truesdale *et al.* (1955). The unshaded areas are less than 97.5% saturated, the lighter shading is in areas between 97.5 and 102.5% saturation, and the darker shading indicates greater than 102.5% saturation.

phere having the observed total barometric pressure and relative humidity.

In oceanography, values of O_2' have been used, *inter alia*, to compare with the observed oxygen concentration (O_2) in the computation of percentage saturation, *i.e.*, $\% \text{ saturation} = \frac{O_2}{O_2'} \times 100$; the oxygen deficit (Brennecke 1909) or apparent oxygen utilization (Redfield 1942 *et seq.*), *i.e.*, $AOU = O_2' - O_2$; and the partial pressure or oxygen tension according to Henry's law, $p = P\frac{O_2}{O_2'}$, in which p is the partial pressure of oxygen in solution and P is the oxygen pressure in the atmosphere.

Wattenberg (1939, Beilage L) prepared a chart showing the percentage saturation of oxygen in the surface layer of the South Atlantic Ocean from the METEOR expedition data. This chart has been somewhat puzzling, showing, as it does, large areas of the surface to be 5 to 10% deficient in oxygen. In some regions one might expect the surface to be somewhat undersaturated, by virtue of the upwelling of undersaturated waters or by a high oxygen demand in the upper mixed layer in regions of high organic productivity. However, the distribution and the magnitude of the departures from 100% saturation shown by Wattenberg could not well be explained as results of these phenomena. Wattenberg's data have been recomputed and are shown, with a redrawing of his original chart for comparison in Figure 2. The most striking features of the revised chart are a) that in most of the South Atlantic Ocean the surface waters are essentially in equilibrium with the atmosphere, *i.e.*, 100% ± 2.5% saturated, b) that the surface is undersaturated in the region north of the equator, except in the eastern part, which is rich in phytoplankton and animal life (Hentschel 1936), and c) that the surface is supersaturated in the Subtropical Convergence, a region of high normal barometric pressures, and in the Antarctic Convergence, a region of large phytoplankton populations (Hentschel 1936). Conclusion a) is in marked contrast with Wattenberg's original findings, and the quantitative aspects of b) and c) are probably more accurately fixed by using the new oxygen solubility data.

Only some 10% of Wattenberg's computations were 100% ± 1%; the new data yield over 44% in this range. Appreciable undersaturation is still evident in the region north of the equator, and is apparently a manifestation of upwelling off the coast of Africa and of high oxygen demands resulting from high organic production farther to the west.

Significant supersaturation in the surface waters occurs across the ocean just north and south of 30° S. latitude and at the far-southern METEOR stations. These are regions of known convergence and/or of high phytoplankton growth and *in situ* production of dissolved oxygen. Other conditions, such as the warming of surface layers, departures of the total barometric pressure from normal (760 mm of mercury), and departures of the relative humidity from 100% (water saturated air) could result in values of the apparent percentage saturation departing from 100, even though equilibrium with the atmosphere exists. The METEOR data have been examined for these last two effects by computing the partial pressure of air in the atmosphere from the barometric pressure and relative humidity data of Kuhlbrodt and Reger (1938). These computations were made by application of the equation

$$O_2'' = O_2' \left[\frac{\left(P - p_t \frac{h}{100}\right)}{(760 - p_t)} \right]$$

O_2'' is the solubility of oxygen in water in equilibrium with an atmosphere having a total pressure of P mm of mercury and a relative humidity of h%.

O_2' is the solubility of oxygen in water in equilibrium with a water saturated atmosphere having a total pressure of 760 mm of mercury (the solubility data of Truesdale *et al.*).

p_t is the vapor pressure of water at t °C.

$(P - p_t\, h/100)$ is the partial pressure of air in the atmosphere.

These corrections make few qualitative changes in the data shown in Figure 2*B*: undersaturation and supersaturation are

TABLE 2. *Effect of total barometric pressure on apparent oxygen saturation from a water-saturated atmosphere at various temperatures*

Barometric pressure, mm of mercury	Apparent per cent saturation		
	0°C	20°C	35°C
720	94.68	94.48	94.12
740	97.33	97.27	97.07
760	100.00	100.00	100.00
780	102.64	102.76	102.93

Apparent saturation is $\frac{O_2''}{O_2'} \times 100$, in which O_2'' is the oxygen solubility under the specified conditions, and O_2' is the oxygen solubility from a water-saturated atmosphere having a total pressure of 760 mm of mercury.

TABLE 3. *Effect of relative humidity on apparent oxygen saturation at various temperatures*
Total atmospheric pressure = 760 mm.

Relative humidity, %	0°C	20°C	35°C
50	100.30	101.17	102.94
60	100.23	100.93	102.34
70	100.18	100.70	101.77
80	100.12	100.47	101.18
90	100.07	100.23	100.60
100	100.00	100.00	100.00

found in practically the same locations. The separate effects of barometric pressure and relative humidity are shown in Tables 2 and 3 for sea water having a salinity of 35‰. It will be noted that, in waters in equilibrium with the atmosphere, relative humidities of less than 100% would result in apparent saturations $\left(\frac{O_2''}{O_2'} \times 100\right)$ of more than 100%, as would barometric pressures of greater than 760 mm. In this connection it is noteworthy that the zone of high oxygen saturation extending across the ocean at about 30°S. latitude coincides with the region of highest normal barometric pressures in the South Atlantic, as shown by Brunt (1939, Figs. 7 and 8). However, there is a poor correlation between apparent per cent saturations and the partial pressure of air in the atmosphere observed at the time of sampling. This might be expected, since the concentration of dissolved oxygen in surface samples would not be expected to respond immediately to changes in relative humidity and barometric pressure; it is more likely to be correlated with the integrated effect of these two parameters operating over some time preceding the sampling. Other factors, such as wind, the regime of warming and cooling and related differences between air and water temperatures, etc., would also be expected to have their effects on the oxygen content of the surface layer. The biological processes of photosynthesis and respiration and diurnal variations in them probably have an even more pronounced influence on the oxygen content at the moment.

The apparent oxygen utilization has been related to the regeneration of inorganic compounds of nitrogen and phosphorus and to *in situ* production of carbon dioxide by Redfield (1938, 1942) and others. The ratios in which oxygen is consumed and carbon dioxide, phosphate, and nitrate are regenerated have been reviewed by Richards and Vaccaro (1956). Since the consumption of oxygen has been estimated from equilibrium solubility data, $O_2' - O_2$, the new values of O_2' make revisions of these ratios necessary. Preliminary computations indicate that these corrections will be moderately small, but improved analytical methods for the other variables may make them important.

Recomputations of the values of the oxygen tension in the Gulf of Maine used by Redfield (1938) to examine the processes of oxygen exchange across the sea surface in that region indicate that his results are unchanged in a qualitative way, but their magnitude is appreciably altered. He evaluated the equation

$$P - p = P(O_2' - O_2)/O_2'$$

in which P is the oxygen pressure in the atmosphere, p the oxygen tension in the water, and O_2' and O_2 have their previous meanings. When $P - p$ is negative, the oxygen pressure in the water is greater than in the atmosphere, and oxygen will tend to pass from the liquid to the gas phase. Since O_2' is smaller than Redfield estimated, values of $P - p$ are smaller, in a positive sense, and it follows that conditions favoring the escape of oxygen from sea water are more pronounced and prevail during a larger part of the year than Redfield estimated.

Since the errors in Fox's data are greater in low salinity water than in fully saline sea water, it is evident that the new data of Truesdale, Downing, and Lowden may be even more important in limnology and investigations of inshore waters and estuaries.

REFERENCES

Adeney, W. E., and H. G. Becker. 1919. The determination of the rate of solution of atmospheric nitrogen and oxygen by water. Part 1. Phil. Mag., **38**: 317–337.

Brennecke, W. 1909. Ozeanographie: Forschungsreise S. M. S. PLANET 1906/07. **3**: 153 pp.

Brunt, D. 1939. Physical and dynamical meteorology. Cambridge Univ. Press, Cambridge. 2nd Ed. xxiv + 428 pp.

Fox, C. J. J. 1909. On the coefficients of absorption of nitrogen and oxygen in distilled water and sea water, and of atmospheric carbonic acid in sea water. Trans. Faraday Soc., **5**: 68–87.

Hentschel, E. 1936. Allgemeine Biologie des südatlantischen Ozeans. Wiss. Ergeb. Deutsch. Atlant. Exped. METEOR, 1925–1927, **11**: 1–344 + 42 Beilagen.

Kalle, K. 1939. Einige Verbesserungen zur Bestimmung des gelösten Sauerstoffs im Meerwasser. Annal. Hydrogr. Marit. Meteorol., **67**: 267–269.

Kuhlbrodt, E., and J. Reger. 1938. Die meteorologischen Beobachtungen. Methoden der Bordbeobachtungen, Beobachtungen und Ergebnisse. Wiss. Ergeb. Deutsch. Atlant. Exped. METEOR, 1925–1927, **14**: 1–392.

Redfield, A. C. 1934. On the proportions of organic derivatives in sea water and their relation to the composition of plankton. *In* James Johnston Memorial Vol. Univ. Press, Liverpool. pp. 179–192.

——— 1942. The processes determining the concentration of oxygen, phosphate, and other organic derivatives within the depths of the Atlantic Ocean. Pap. Phys. Oceanogr. Meteorol., **9**(2): 1–22.

——— 1948. The exchange of oxygen across the sea surface. J. Mar. Res., **7**(3): 347–361.

Richards, F. A., and R. F. Vaccaro. 1956. The Cariaco Trench, an anaerobic basin in the Caribbean Sea. Deep-Sea Res., **3**: 214–228.

Truesdale, G. A., A. L. Downing, and G. F. Lowden. 1955. The solubility of oxygen in pure water and sea water. J. Appl. Chem., **5**(2): 53–62.

Tully, J. P. 1949. Oceanography and prediction of pulp mill pollution in Alberni Inlet. Bull. Fish. Res. Bd. Canada, No. 83, 169 pp.

Wattenberg, H. 1933. Das chemische Beobachtungsmaterial und seine Gewinnung. Wiss. Ergeb. Deutsch. Atlant. Exped. METEOR, 1925–1927, **7**: 333 pp.

——— 1938. Die Verteilung des Sauerstoffs und des Phosphats im atlantischen Ozean. *Ibid.*, **9**: 132 pp.

——— 1939. Atlas zu: Die Verteilung des Sauerstoffs im atlantischen Ozean. *Ibid.*, **9**: 72 Beilagen.

Whipple, G. C., and M. C. Whipple. 1911. Solubility of oxygen in sea water. J. Am. Chem. Soc., **33**: 362–365.

Wüst, G. 1932. Das ozeanographische Beobachtungsmaterial (Serienmessungen). Wiss. Ergeb. Deutsch. Atlant. Exped. METEOR, 1925–1927, **7**: 290 pp.

Contribution No. 853

ON THE NATURE AND ORIGIN OF THE SOUTHERN OSCILLATION

By Irving I. Schell

Tufts University and Woods Hole Oceanographic Institution[1]

(Original manuscript received 18 August 1955; revised manuscript received 23 March 1956)

ABSTRACT

A physical explanation is given of the nature and origin of the June–August Southern Oscillation and of its relationships with the contemporary, and following September–November and December–February, air and sea temperatures. The variations in the Southern Oscillation are attributed to solar activity, in part directly and in part through the variations in the Antarctic circulation.

1. Preface

The Southern Oscillation, as it was originally derived by Walker and Bliss (1932; 1937) and less formally by earlier investigators, is a statistical expression reflecting certain large-scale interrelations in the atmosphere. It is the purpose of this article to explain this oscillation on physical grounds, insofar as seems possible at present.

2. Introduction

An oscillation, in the sense generally understood in research on long-range weather phenomena, consists of a circulation system dominating a certain area during a definite time interval (as a season) which is in balance with a like system dominating another area during the same time interval. As is well known, an oscillation prevails over the North Atlantic in the following sense: when the subtropical high is better developed than usual (pressure above normal over the Azores and Bermuda), the Icelandic low is also better developed than usual. Such a state involves a back-and-forth pulsation of the air from one area to another and owes to this its name: oscillation. Expressed statistically, one group of pressures, *etc.*, in the combination acts in a phase opposite to that of the other group, both groups together defining the oscillation and forming a single statistical unit.

The various oscillations derived so far lend themselves to interrelations with other circulation systems and, further, exhibit marked stability with respect to time. The latter is shown when their relationships are recomputed with new data (Schell, 1947; Willett and Bodurtha, 1952). By gaining a better understanding of the nature and origin of the oscillations, we can, therefore, expect to obtain a better insight into the general circulation.

3. The Southern Oscillation

Nature of the oscillation. — Of the three major oscillations in the atmosphere determined thus far, the most important by reason of the size of the area it encompasses and the wide influence it apparently exerts on the subsequent weather, is the so-called Southern Oscillation. Its name is somewhat a misnomer, since in both summer and winter it reaches deep into the northern hemisphere. The oscillation, in its simplest form, is a mass pulsation of air between the tropical Indian Ocean and adjacent land areas on the one hand, and the South Pacific Ocean and adjacent land and ocean areas on the other (Walker and Bliss, 1932).

Although we cannot be expected to deal fully with the physical basis of the Southern Oscillation until we have accumulated more data, especially from the southern hemisphere, it appears that this vast circulation system owes its existence largely to the deep northward flow of cool subantarctic water along the west coast of South America. The latter is made possible in a large measure by the southerly extension of the South American continent into high latitudes, causing a portion of the cool subantarctic water in the South Pacific to be diverted from an easterly set towards the north. The result is that the temperatures are lower, and the pressures higher, over the eastern South Pacific than over the western South Pacific and the Indian Oceans. A mass difference is established between the generally warmer Indian Ocean and adjacent land areas on the one hand, and the generally cooler South Pacific and adjacent land areas on the other.

Thus, we may assume that the changes in the Southern Oscillation must greatly depend on the fluctuations in the northward flow of the subantarctic water. A weakened northward transport, for example, could be expected to lead to warmer-than-usual sea-surface temperatures and to lower pressures over the

---

[1] Contribution No. 853 from the Woods Hole Oceanographic Institution. The work was supported in part by the Geophysics Research Directorate, Air Force Cambridge Research Center.

South Pacific and, therefore to a smaller pressure difference between it and the Indian Ocean (a weaker Southern Oscillation).

The degree to which the Southern Oscillation can either weaken or strengthen appears to be limited, however. Following a period of weak or strong Southern Oscillation, there must come a period of reversed activity (Berlage, 1952). Thus, given a diminished northward transport of subantarctic water into the eastern South Pacific following a weaker circulation, higher sea-surface temperatures will develop first over the eastern South Pacific and next along the equatorial zone and farther west over the Indian Ocean. The higher temperatures over the Indian Ocean area will call for a fall in pressure and for an outflow of air to the South Pacific, leading to higher pressures and to a stronger circulation in that area. This, in turn, would lead to a greater northward flow of subantarctic water northward and to lower temperatures[2] eventually also along the equatorial zone and over the Indian Ocean, and back to a weaker Southern Oscillation.

That the above sequence probably does take place is shown by the results of a correlation by Walker and Bliss (1932) of the winter (summer) Southern Oscillation with the subsequent spring and summer (fall and winter) sea-surface temperatures in the equatorial Indian Ocean area: 10°N to 10°S, and 70 to 90°E. Although the data available to them were rather meager, the fact that all 16 correlation coefficients involved had a minus sign, and the absolute values of ten equalled or exceeded 0.6 (one was −0.9), would seem to bear out the mechanism postulated by Berlage (1952): a weakening of the South Pacific circulation and a diminished northward flow of cool water, lead-

---

[2] With a stronger South Pacific circulation, for example, the development of lower sea-surface temperatures in the eastern equatorial Pacific would be due in part to the greater upwelling of water as the thin warm layer at the top is driven off, in part to the less-warm air originally from higher latitudes. In the western equatorial Pacific and farther west, where the top layer is fairly thick, the lowering of the temperature with an intensified South Pacific high would be due only to the less-warm air reaching that area.

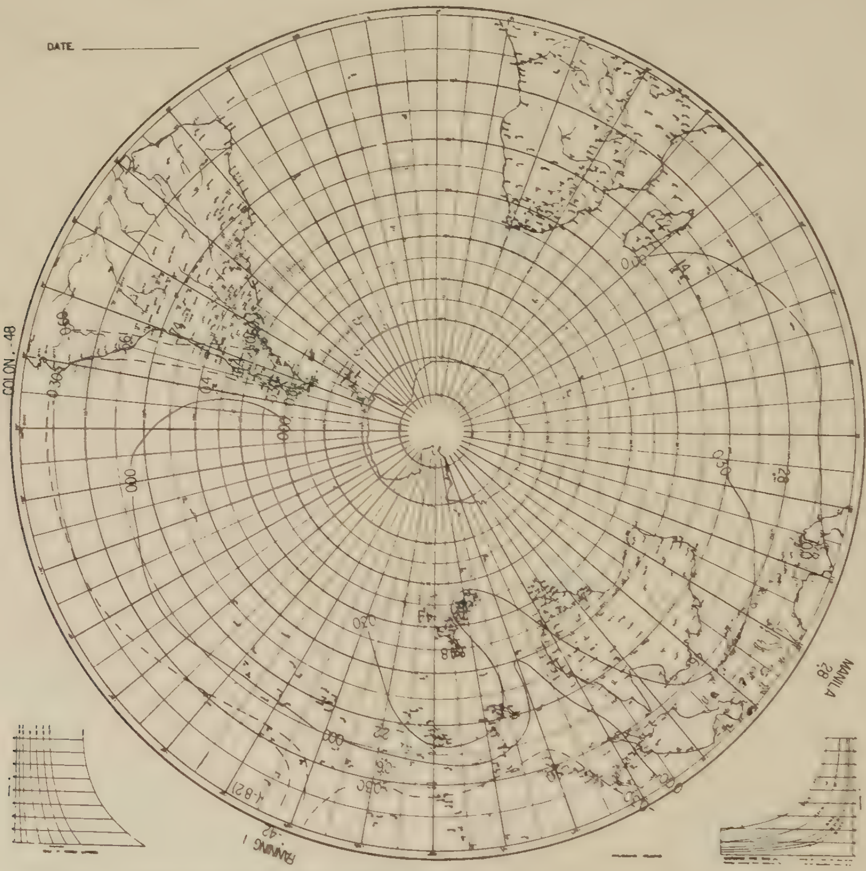

Fig. 1. Correlation of June–August Southern Oscillation with contemporary air temperatures. (After Walker and Bliss, 1932.)

ing to higher sea-surface temperatures first to the north and then to the west.

We can also expect the effects of a stronger or weaker Southern Oscillation to appear in the observed variations of air temperatures within the influenced areas. Since, with a stronger Southern Oscillation, cooler air may be expected to reach the west coast of South America, we should expect negative correlation coefficients between the Southern Oscillation and the air temperature in that area. Also, we should expect the field of negative correlation coefficients gradually to spread westward during the following seasons, after it has reached the equatorial zone. Thus, the correlations of the June–August Southern Oscillation with the contemporary-quarter temperatures on the west coast of South America, obtained by Walker and Bliss (1932), are as follows: Iquique, −0.74; Arequipa, −0.56; Mocha, −0.44. Similarly, farther north, near the equator, values are as follows: Fanning Island, −0.42; Malden Island, −0.82. But westward at Manila, the correlation coefficient has a positive sign (0.28, fig. 1), indicating that the influence of a stronger or weaker Southern Oscillation ceases at a line well to the east of the Philippines during the contemporary June–August quarter.

Again, with an intensified June–August Southern Oscillation, we might expect the area lying in the western sector of the South Pacific high and south of the equator to be subject to a greater flow of air from the north, in accordance with the circulation character of the South Pacific high. Hence, a greater flow of warmer air would be expected to reach the east coast of Australia and adjacent areas. Thus, the correlation coefficients of the June–August Southern Oscillation with the contemporary air temperatures in that region (Walker and Bliss, 1932) are positive in sign as follows: Suva, 0.44; Alofi, 0.22; Chatham Island, 0.44; Auckland, 0.48 (fig. 1).

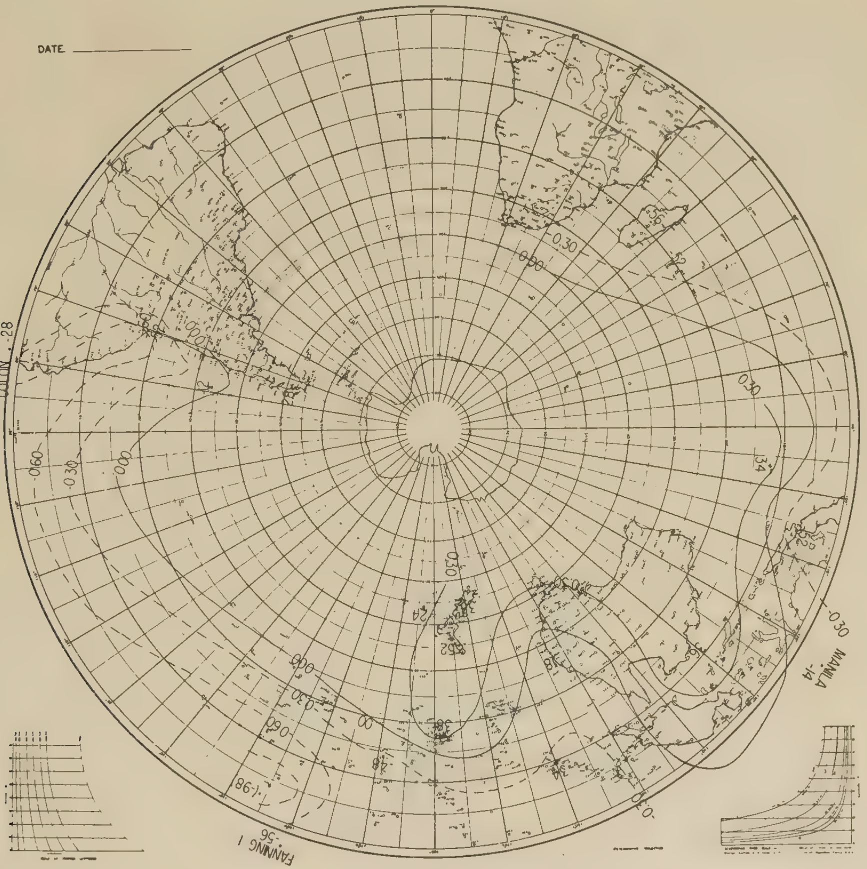

FIG. 2. Correlation of June–August Southern Oscillation with following September–November air temperatures. (After Walker and Bliss, 1932.)

Next, by reason of the very considerable persistence of the June–August Southern Oscillation into the following September–November and December–February quarters (Walker and Bliss, 1937), we might expect: first, a continuation of the correlation pattern between the Southern Oscillation and the air temperatures over the west coast of South America *etc.*; second, as the effects of a stronger circulation over the eastern South Pacific penetrate farther and farther north and then west, a westward extension of the negative coefficients in the tropical sector of the South Pacific high and the replacement of some of the positive coefficients by negative ones.

Thus, the correlation coefficient of the June–August Southern Oscillation with September–November Manila temperature (fig. 2) has changed from a positive sign during June–August (0.28) to one with a negative sign (−0.14), and the coefficients with the Batavia and Samoa temperatures, formerly negligible in value, have become marked and taken on negative sign (−0.52 and −0.48, respectively). It would also appear that the influence of an intensified South Pacific circulation has reached, for example, as far west as Madagascar and Mauritius, the correlation coefficients with the temperatures at these stations having become marked in value and negative in sign (−0.56 and −0.52, respectively).

Continuing our study of the impact of a stronger June–August circulation over the South Pacific into the following December–February quarter (fig. 3), we find, as before, a continuation of the negative coefficients at the stations on the west coast of South America and in the equatorial area. Also, Madagascar and Mauritius continue to show negative correlation coefficients (−0.60 and −0.58, respectively) during the December–February quarter.

The only exception to the trend here noted is the assumption of positive values by Evangelists Island

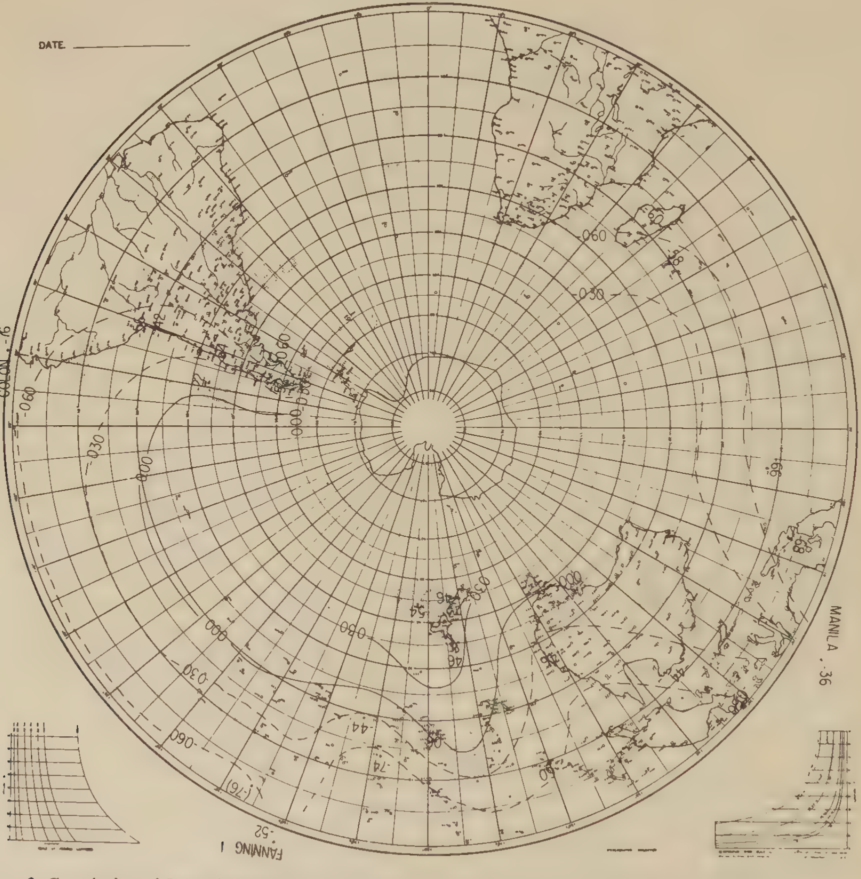

Fig. 3. Correlation of June–August Southern Oscillation with following December–February air temperatures. (After Walker and Bliss, 1932.)

and Mocha, off the west coast of South America, during the September–November quater (fig. 2); however, they have reassumed negative values during the following December–February quarter (fig. 3). Significant, also, appears the change from a positive to a negative coefficient at Port Darwin and at Cocos or Keeling Island from the June–August and September–November quarters to the December–February quarter under the culminating effect of the fluctuation in the Southern Oscillation during the preceding June–August.

Origin of the Southern Oscillation. — We have indicated that the variations in the Southern Oscillation are in a large measure due to the variations in the South Pacific high, which drives the cool subantarctic water along the west coast of South America and brings the cool air from the higher latitudes of the South Pacific Ocean northward. But since the South Pacific high is a prominent component of the Southern Oscillation, variations of the former cannot be used to "explain" the variations in the latter. Another agency must be involved; we may seek to identify it with solar activity.

The pressure over the tropical Indian Ocean, which figures prominently in the Southern Oscillation, has been earlier shown to correlate with the sunspot number (Walker, 1915; Clayton, 1926), The negative sign and the magnitude of the coefficients obtained shows a marked tendency for a fall of pressure, for example, to occur with higher sunspot numbers, as demanded by an expansion of the atmosphere over the low latitudes with a generally hotter sun. Were it not for the oscillation of air between the Indian and South Pacific Oceans demanded by the variations in temperature and pressure differences between these two areas, a fall in pressure with increased sunspot activity would be expected to occur also over the tropical Pacific Ocean. But because of the compensation over the Pacific of solar pressure-reduction by inflow from the Indian Ocean, correlation of pressure and sunspot activity would not expect to be marked in this area. The correlation coefficients actually obtained (Walker, 1915; Clayton, 1926) between the annual pressure over the tropical Pacific Ocean and adjacent areas and the corresponding sunspot number were positive and small. This indicates that the reaction of the tropical Pacific Ocean to an outflow of air from over the Indian Ocean is greater than to an increase in solar activity.

It must follow that a correlation of solar activity with the Indian Ocean and Pacific Ocean pressures taken together, which broadly speaking constitute the Southern Oscillation, would yield a rather small value somewhere between the values obtained for each area separately. This, in fact, was shown from the small negative correlation of the Southern Oscillation with the sunspot number obtained by Walker and Bliss (1932), which lead them to conclude that the great Southern Oscillation is only to a small degree *directly* influenced by changes in solar activity. By far the greater direct control of the changes in the Southern Oscillation would appear to lie elsewhere (see below). This conclusion is not inconsistent when the changes in the Southern Oscillation and in the general circulation are viewed from a different standpoint.

Because the general circulation continually seeks the level of least differences within itself, it is in conflict with the relatively steady demand for an increased and then a decreased circulation due to the periodic character of solar variations. The apparent lack of a consistent 11-yr periodicity in the general circulation, including the Southern Oscillation, suggests that the critical level of differences which the latter can comfortably sustain is very often reached in less than the average span of 11 yr of the sunspot cycle.

Again, the general circulation can respond in a simple and direct manner to the marked abnormalities in the sun only when it is in a state of equilibrium. Actually it never achieves this state, because the various systems within the general circulation continually react upon each other. On the other hand, the larger and more stable systems would act more clearly upon the smaller and less stable systems than *vice versa*. Therefore, the relationships between solar changes and the general circulation would be expected to be more readily traceable with respect to the major stable systems.

The Southern Oscillation, especially during the southern winter, is probably very markedly influenced by the Antarctic circulation through a great and persistent outflow of cold air from the Antarctic and by the flow of subantarctic water. The slowness and steadiness of these flows no doubt contribute to the great persistence of the Southern Oscillation, especially from the southern winter to the following spring and summer (Walker and Bliss, 1937), and to the influence which the Southern Oscillation exerts on the following weather.

The significance of the persistence character of the Southern Oscillation for an understanding of its observed time-lag relationships compels us to dwell further on this property of the Southern Oscillation and of the atmosphere in general.

It appears, from a recent autocorrelation of annual sea-level pressures over the northern hemisphere by Schumann (1952), that the tendency towards persistence in the sea-level pressure is at least twice as great as the tendency towards a change. Also, from a recent study by Namias (1954), persistence is marked in the pressure at upper levels. From a necessarily limited study by Wiese (1925), it seems that persistence in the ocean is very considerable. And, from the work of Walker (1924), Landsberg *et al* (1943), Elliott *et al* (1949), and others, it appears that persistence generally is much better developed in the tropics than in other latitudes.

The outstanding characteristics of the tropics, from the standpoint of persistence, are:

1. Roughly three-fourths of the area is ocean surface;
2. The horizontal temperature and pressure gradients are generally quite weak, as are their changes from month to month, season to season, *etc.*; and
3. They possess a surplus of radiation.

In view of the very considerable heat-storage capacity of the water, the tropics must act as a large reservoir of heat. As this heat is being lost slowly, they must exert a steadying influence on the circulation. The small horizontal temperature and pressure gradients operate against a disruption of any trends that may develop in the circulation and further contribute to the maintenance of persistence in the tropics.

As between the two hemispheres, the southern, with its greater preponderance of ocean over land than in the northern (81 *versus* 61 per cent), would be expected to contribute more to persistence in the general circulation than the northern hemisphere. Further, greater contribution toward persistence by the southern hemisphere would result from the less broken-up character of its water surface, stretching almost uninterruptedly over a wide zone (35 to 65°S), which makes for more stable movements of both air and water. Another very probable factor in the greater contribution to persistence by the southern hemisphere is, as we have earlier suggested, the Antarctic anticyclonic circulation.

Thus, the net result of these factors is a powerful urge towards persistence, which explains why the Southern Oscillation, in the main a phenomenon of the South Pacific, the Indian Ocean and, we suspect the Antarctic as well, exhibits (particularly in winter) great persistence and marked control of the following weather over wide areas.

In stating earlier that the Southern Oscillation appears little influenced by variations in solar activity, we based this conclusion on the correlations of mean seasonal values of the Southern Oscillation with corresponding mean seasonal values of the sunspot number. It is well known, however, that the pressure in the tropics frequently fails to reveal weak waves that often later grow into major storms. It is equally true that the sunspot number is not as sensitive a parameter of solar activity as we might wish to have. From this, we may infer that some better correlation may exist between more representative measures of solar activity and the weather in the tropics and the Southern Oscillation.

Yet, the manner in which changes in solar radiation could affect the observed changes in the Southern Oscillation may be quite obscure. The suggestion variously made that the pressure changes in the troposphere could be brought about through temperature changes in the very high layers, initially produced by changes in ultraviolet radiation, is difficult to reconcile with the smallness of the masses of air at those heights. An addition or subtraction of a mass of air near the top of the atmosphere cannot be expected to transform, say, a high-pressure system into a low-pressure one at the surface, though it might produce a significant effect over a diffuse pressure field. Thus, in areas where as a rule no well-defined circulation systems exist, increases in ultraviolet radiation could conceivably lead to small wave disturbances resulting from pressure changes at high levels, which in turn result either from a direct increase of temperature or through the presence of water vapor in large amounts extending high up in the manner suggested by Palmer (1953). The latter can occur where a warm and moist marine layer has direct access to the upper part of the troposphere, as in the region of the equatorial convergence. As this region is intimately involved in the Southern Oscillation, solar changes might conceivably play a greater role in the variations in the Southern Oscillation than we were first led to believe.

However, the responses of the Southern Oscillation to variations in solar activity would in a certain measure not be expected to be instantaneous. This follows from the fact that, while both have very marked persistence, there appears no marked relationship between them.

The writer suspects that the Southern Oscillation is intimately related to the Antarctic circulation; but this cannot be the final answer to its origin. It is difficult to see that the variations in the Southern Oscillation are ultimately determined other than by variations in solar activity, whether through increases in ultraviolet radiation acting directly over the equatorial latitudes, or through changes in corpuscular radiation reaching deep into the Antarctic circulation.

As the key to the variations in the Southern Oscillation may in a large measure depend on a sufficiency of special observations of solar activity and on observations from the Antarctic that are equally unavailable at present, we cannot expect a broad answer to their origin in the near future. Fortunately, the task of affirming the Southern Oscillation, and its relationships with following conditions over wide areas, on strong physical and synoptic grounds is in many respects a feasible one.

REFERENCES

Berlage, H. P., 1952: Solar activity and air pressure fluctuations over the South Pacific Ocean. *Proc. 7th Pacific Sci. Cong., Meteor. Oceanogr.*, **3**, 1–4.

Clayton, H. H., 1926: Solar activity and long-period weather changes. *Smiths. misc. Coll.*, **78**, No. 4, 62 pp.

Elliott, R. D., *et al*, 1949: *On world-wide weather studies.* (Part II), Pasadena, Amer. Inst. aerol. Res.

Landsberg, H., *et al*, 1943: *Studies on pressure, temperature and precipitation.* (Unpubl. Rep., Military Climat. Project), Chicago, Univ. Chicago.

Namias, J., 1954: Further aspects of month to month persistence in the mid-troposphere. *Bull. Amer. meteor. Soc.*, **35**, 112–117.

Palmer, C. E., 1953: The impulsive generation of certain changes in the tropospheric circulation. *J. Meteor.*, **10**, 1–9.

Schell, I. I., 1947: Dynamic persistence and its application to long-range foreshadowing. *Harvard meteor. Stud.*, No. 8, 80 pp.

Schumann, T. E. W., 1952: Auto-correlation of annual atmospheric pressures. *Weather*, **7**, 370–371.

Walker, G. T., 1915: Correlations in seasonal variations of weather, VI. Sunspots and pressure. *Mem. India meteor. Dept.*, **21**, 91–118.

——, and E. W. Bliss, 1932: World weather, V. *Mem. r. meteor. Soc.*, **4**, 53–84.

——, 1937: World weather, VI. *Mem. r. meteor. Soc.*, **4**, 85–139.

Wiese, W., 1925: Studien über die Erhaltungstendenz der mittleren monatlichen Temperatur-Anomalien. *Meteor. Z.*, **42**, 217–225.

Willett, H. C., and F. T. Bodurtha, 1952: An abbreviated Southern Oscillation. *Bull. Amer. meteor. Soc.*, **33**, 429–430.

Contribution No. 855

Deep-Sea Research, 1956, Vol. 4, pp. 23 to 31. Pergamon Press Ltd., London.

A β-plane analysis of free periods of the second class in meridional and zonal oceans

A. B. ARONS and HENRY STOMMEL

Abstract—Quasigeostrophic free oscillations (or barotropic seiches) of meridional and zonal oceans are analysed for plane oceans of uniform depth and nonuniform rotation (the approximation of the β plane). These motions have been denoted " motions of the second class " by tidal theorists. An attempt is made to clarify the physical nature of such oscillations and to calculate periods and wavelengths which give an idea of the orders of magnitude which are involved.

INTRODUCTION

TIDAL theorists have long recognized* that rotation of a globe covered with a thin fluid layer of uniform depth and density not only introduces changes in the frequencies of free long-wave standing oscillations which exist on the globe even in the absence of rotation (so-called oscillations of the first class), but also converts certain motions which are steady in the absence of rotation into long-period oscillations (so-called oscillations of the second class). In the terrestrial atmosphere and oceans, waves of the first class are usually spoken of as tidal waves. On the other hand, waves of the second class are nearly in geostrophic balance, and therefore appear as moving wind systems for example, planetary waves (ROSSBY, 1939), or moving current systems in the ocean. The ordinary method of oceanographic-current determination – dynamic computation – reveals only internal modes of second class motions. The external mode of second class motion in the ocean must appear as a relatively long-period oscillation of the free surface, and as we will show in this paper is quite possibly excited by atmospheric storms. A study of observations has not been made. In the spherical system, the introduction of meridional walls or coasts makes the mathematics rather difficult, although GOLDSBROUGH (1933) has been able to obtain approximations for the free periods in an ocean of uniform depth (12,880 ft) bounded by meridians 60° apart (to approximate the Atlantic) including the second-class period (7·1 sidereal days). However, there are a number of physical questions that remain somewhat obscure. For example, planetary waves all have westwardly directed phase velocity, and in compounding free second-class waves to produce a standing wave between two walls, we do not have any waves that move toward the east. In what sense, then, can a second-class wave (or planetary wave) reflect from a meridional barrier ? In order to clarify some of these questions we have transferred the problem to the dynamical system of the beta plane : that is, instead of treating the rotating globe, we study the dynamics of waves on a plane ocean of uniform depth with nonuniform rotation. Our results are therefore not exact, but they are more easily manipulated, and we feel that certain physical features of second-class waves undergoing reflection at a barrier, and of the eigenvalue problem of standing waves between two barriers, emerge more clearly than from the more exact but more complicated dynamical system. In fact, that is our only excuse for dealing with the inexact beta

* For example see LAMB's (1932, p. 350 ff) discussion of HOUGH's tidal studies.

plane, rather than the exact rotating sphere. A brief derivation of the fundamental equations involved is given in the Appendix.

PROPERTIES OF PLANETARY WAVES

A brief derivation of the fundamental equation describing the propagation of plane planetary waves in the x (east-west) direction in an ocean of uniform depth D_0 is given in the Appendix. This equation has the form:

$$\lambda^2 \frac{\partial^3 \eta}{\delta t\, \partial \chi^2} - \frac{\partial \eta}{\partial t} + \beta \lambda^2 \frac{\partial \eta}{\partial x} = 0 \tag{1}$$

where η is the displacement of the free surface from its unperturbed level. Also:

$$\beta \equiv \partial f / \partial y,$$

where f is the Coriolis parameter $2\Omega \sin \phi$, and

$$\lambda^2 \equiv g D_0 / f^2$$

λ is ROSSBY's "radius of deformation."

Consider plane-wave solutions of the form:

$$\eta = A e^{i(\omega t - k\chi)} \tag{2}$$

representing wave trains of angular frequency ω and wave number k propagating in the positive x (easterly) direction.

Substitution of equation (2) into equation (1) gives the characteristic equation:

$$\omega = \frac{-\beta k \lambda^2}{1 + k^2 \lambda^2}. \tag{3}$$

The negative sign in equation (3) has to do with the direction of the phase velocity of the wave train. If we denote phase velocity by c, we have:

$$c = \frac{\omega}{k} = \frac{-\beta \lambda^2}{1 + k^2 \lambda^2}. \tag{4}$$

Thus the phase velocity is inherently negative, i.e. always in the westerly direction, as originally demonstrated by ROSSBY.

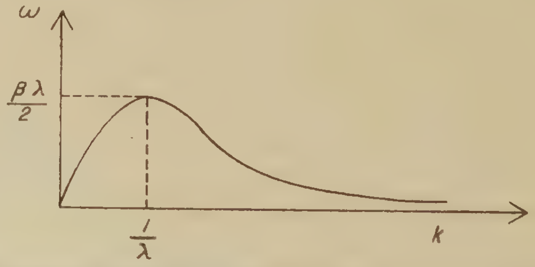

Fig. 1. Sketch of the dispersion relation for planetary waves (equation 3) without regard for the negative sign.

In a dispersive wave system such as that being dealt with in this analysis, energy is propagated at the *group* rather than the *phase* velocity. Denoting the group velocity by U, we have

$$U = \frac{d\omega}{dk} = \beta\lambda^2 \left[\frac{k^2\,\lambda^2 - 1}{(k^2\,\lambda^2 + 1)^2}\right] \tag{5}$$

by differentiation of equation (3).

The functional relationship between ω and k (without regard to the algebraic sign of equation (3) is sketched in Fig. 1.

Equation (5) shows that ω has a maximum at $k = 1/\lambda$. At this wave number, ω has the value $\beta\lambda/2$, and U is equal to zero. Then from equation (5):

$$\begin{aligned} &\text{(a)}\quad \text{For } k < 1/\lambda,\ U < 0;\ \text{group velocity westward,} \\ &\text{(b)}\quad \text{For } k > 1/\lambda,\ U > 0;\ \text{group velocity eastward.} \end{aligned} \tag{6}$$

Restating conditions (6) verbally: For wavelengths greater than $2\pi\lambda$, energy will always be propagated in the westward direction; while for wavelengths shorter than $2\pi\lambda$, energy will always be propagated in the eastward direction despite the westwardly directed phase velocity.

The waves being described have pressure gradients in the east-west direction, very small particle velocity (u) in this direction, and substantial particle velocities (v) in the north-south direction.

These physical properties of planetary waves suggest examination of the free oscillations (standing waves) of an ocean bounded by meridional walls in simple terms of incident and reflected wave trains superposed to satisfy the boundary conditions:

$$u = 0 \text{ at } x = 0 \text{ and at } x = L \tag{7}$$

where L is the width of the meridional ocean.

STANDING PLANETARY WAVES IN A MERIDIONAL OCEAN

From equation (A15) in the Appendix and condition (7) above, we have the requirement that:

$$\frac{\partial^2 \eta}{\partial t\, \partial x} = 0 \qquad \text{at} \qquad x = 0 \qquad \text{and} \qquad x = L \tag{8}$$

Consider the superposition of two westwardly propagating wave trains:

$$\eta = A_1\, e^{i(\omega_1 t + k_1 x)} + A_2\, e^{i(\omega_2 t + k_2 x)} \tag{9}$$

Equation (8) requires that:

$$- A_1\, \omega_1\, k_1\, e^{i(\omega_1 t + k_1 x)} - A_2\, \omega_2\, k_2\, e^{i(\omega_2 t + k_2 x)} = 0 \quad \text{at} \quad x = 0 \quad \text{and} \quad x = L \tag{10}$$

To satisfy equation (10) at $x = 0$ for all values of t we have the requirements that:

$$\omega_1 = \omega_2 = \omega$$

$$A_1\, k_1 = - A_2\, k_2$$

We then have the requirement at $x = L$

$$A_1\, k_1 \left[e^{i(\omega t + k_1 L)} - e^{i(\omega t + k_2 L)}\right] = 0 \tag{11}$$

Equation (11) is satisfied for all values of t if:

$$k_{2n} L = k_{1n} L + n(2\pi) \quad . \tag{12}$$

where $n = 0, 1, 2, 3, \ldots\ldots$

The case $n = 0$ represents a trivial or degenerate solution in which two wave trains of the same ω and k but of opposite phase cancel each other. The other cases represent possible planetary modes of the meridional ocean.

EVALUATION OF PERIODS OF THE ALLOWABLE MODES

Because of the double-valued nature of the dispersion relation (equation 3), it is possible to find two values of k corresponding to the same ω and simultaneously satisfying equation (12).

If we drop the negative sign in equation (3) and solve for the roots of the equation, setting the smaller root equal to k_1, we obtain:

$$\begin{aligned} k_1 &= \frac{\omega_0}{\omega\lambda}\left\{1 - \left[1 - \left(\frac{\omega}{\omega_0}\right)^2\right]^{\frac{1}{2}}\right\} \\ k_2 &= \frac{\omega_0}{\omega\lambda}\left\{1 + \left[1 - \left(\frac{\omega}{\omega_0}\right)^2\right]^{\frac{1}{2}}\right\} \end{aligned} \tag{13}$$

where

$$\omega_0 \equiv \beta\lambda/2$$

Imposing on equations (13) the simultaneous restriction of equation (12), we obtain the periods of the allowable modes:

$$\frac{\omega_0}{\omega_n} = \frac{T_n}{T_0} = \left(1 + n^2 \frac{\pi^2 \lambda^2}{L^2}\right)^{\frac{1}{2}} \tag{14}$$

or, alternatively, in terms of primary parameters:

$$T_n = \frac{4\pi f}{\beta (g\, D_0)^{\frac{1}{2}}} \left[1 + n^2 \frac{\pi^2 g D_0}{L^2 f^2}\right]^{\frac{1}{2}} \tag{15}$$

Thus the mode or standing wave pattern is set up by the superposition of two wave trains of westward phase velocity and different wave number. Since the wave numbers lie on opposite sides of the maximum in Fig. 1, one train (that of lower wave number and longer wavelength) is associated with a westward *group* velocity and propagation of energy, while the wave train of higher wave number and lower wavelength is associated with an *eastward* propagation of energy. One wave train may be considered an incident wave, and the other train is then the reflection which occurs at the meridional boundaries.

The wavelengths corresponding to the two trains making up a mode of oscillation are given by:

$$\Lambda_{1n} = \frac{2\pi\lambda}{\dfrac{T_n}{T_0} - n\dfrac{\pi\lambda}{L}} \tag{16}$$

$$\Lambda_{2n} = \frac{2\pi\lambda}{\dfrac{T_n}{T_0} + n\dfrac{\pi\lambda}{L}} \tag{17}$$

where Λ_{1n} and Λ_{2n} are the wavelengths associated with the wave numbers k_{1n} and k_{2n} respectively.

Rossby (1939) gives a convenient table of values for f and β for use in computations of this kind. A sample set of computed results for the first mode ($n = 1$) is given in Table 1, illustrating the orders of magnitude of period and wavelength and the effects of such parameters as latitude ϕ, ocean depth D_0, and ocean width L. A plot of the period results is shown in Fig. 2.

Table 1. Periods and wavelengths associated with first mode of standing planetary waves in an ocean with meridional boundaries.

Ocean width $L \times 10^{-3}$ km	Ocean depth D_0 km	Latitude $\phi = 30°$			Latitude $\phi = 45°$			Latitude $\phi = 60°$		
		T_1 days	$\Lambda_1 \times 10^{-3}$ km	$\Lambda_2 \times 10^{-3}$ km	T_1 days	$\Lambda_1 \times 10^{-3}$ km	$\Lambda_2 \times 10^{-3}$ km	T_1 days	$\Lambda_1 \times 10^{-3}$ km	$\Lambda_2 \times 10^{-3}$ km
2	2	12·2	75·2	1.95	15·6	38·4	1·90	22·9	26·2	1·86
4		6·92	40·2	3·65	9·63	21·7	3·39	15·1	15·4	3·18
6		5·42	29·4	4·98	8·08	16·6	4·42	13·2	12·2	4·02
8		4·78	24·4	6·02	7·47	14·3	5·13	12·4	10·7	4·57
12		4·27	19·6	7·45	7·00	12·1	6·03	11·9	9·32	5·25
18		4·02	16·9	8·70	6·77	10·8	6·78	11·6	8·50	5·78
2	4	11·9	147	1·98	14·9	75·2	1·95	21·5	49·4	1·92
4		6·36	77·0	3·81	8·44	40·2	3·65	12·8	27·9	3·49
6		4·70	53·7	5·40	6·61	29·4	4·98	10·45	20·9	4·66
8		3·95	43·3	6·76	5·83	24·4	6·02	9·48	17·7	5·52
12		3·32	33·1	8·82	5·22	19·6	7·45	8·73	14·7	6·61
18		2·99	27·1	10·8	4·91	16·9	8·70	8·36	13·0	7·53
2	6	11·7	222	2·00	14·6	112	1·96	21·0	75·2	1·95
4		6·16	113	3·86	8·02	58·5	3·74	11·9	40·2	3·65
6		4·42	78·6	5·58	6·06	41·8	5·23	9·36	29·4	4·98
8		3·53	70·2	7·18	5·20	33·9	6·47	8·26	24·4	6·02
12		2·92	46·0	9·50	4·48	26·5	8·27	7·40	19·6	7·45
18		2·54	36·4	12·0	4·12	22·1	9·87	6·95	16·9	8·70

In Table 1 it will be noted that the wavelength associated with the Λ_1 component is generally substantially greater than the ocean width L. This leads one to speculate about a physical situation in which the shorter Λ_2 component might be excited by essentially random meteorological processes, etc. with reflections at the boundaries introducing Λ_1. The ocean level would then rise and fall with period T_1, in some cases with very little phase difference between the opposite boundaries. (In the β plane model of infinite north-south canal, the apparent continuity paradox is resolved by the divergence of the north-south flow.)

Table 2. Periods of first and second modes for various specific cases.

Ocean	North Atlantic		South Atlantic	North Pacific		South Pacific	Indian
Latitude	30°	45°	30°	30°	45°	30°	30°
Avg. $L \times 10^{-3}$ km	5·8	3·5	5·8	11·5	6·7	9·6	7·8
Avg. D_0 km	4·5	3·5	4·0	5·5	5·0	4·5	4·0
T_1 (days)	4·7	9·6	4·8	3·0	6·0	3·5	4·0
T_2 (days)	8·2	16·6	8·3	4·6	9·5	5·3	6·6

Table 2 shows a number of periods (T_1 and T_2) computed for specific oceanic conditions, with rough average values of L and D_0 estimated from the charts.

In the case of the North Atlantic, the values of T_1 (4·7 and 9·6 days at 30° and 45° respectively) straddle GOLDSBROUGH's (1933) value of 7·1 days for the fundamental spherical mode cited in the Introduction above. Thus one might expect to observe long wave motions in the North Atlantic, with associated north-south particle velocities, having periods in the range indicated. Similarly one might expect to observe periods of about 4 or 5 days in the North Pacific.

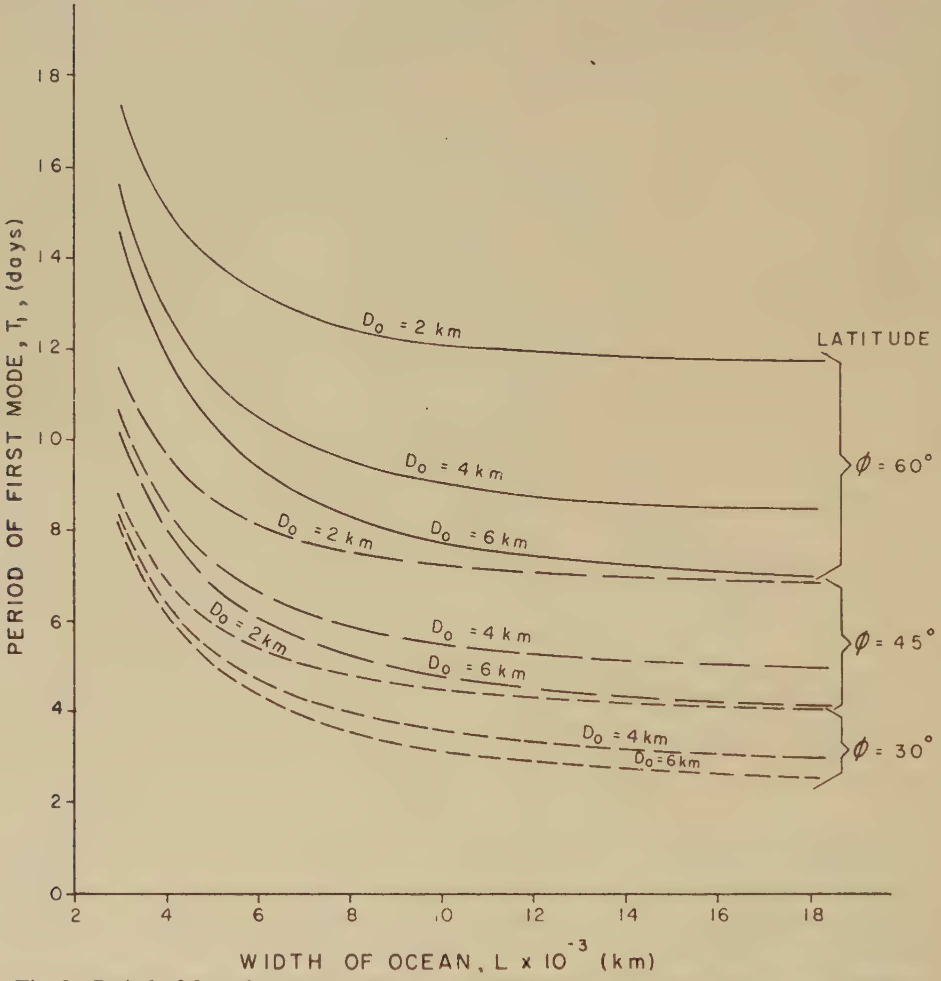

Fig. 2. Period of first planetary mode vs. ocean width for various ocean depths and latitudes.

FREE PERIODS OF A ZONAL OCEAN

In the case of a zonal ocean (such as the Antarctic Circumpolar), standing waves must divide the ocean length or circumference into an integral number of wavelengths, giving the condition:

$$L = n\,\Lambda_n = n\frac{2\pi}{k_n} \tag{18}$$

where $n = 1, 2, 3, \ldots\ldots$

Substitution of equation (18) into equation (3), dropping the negative sign of the latter, gives:

$$\frac{T_n}{T_0} = \frac{\omega_0}{\omega_n} = \frac{\tau_n}{2}\left(1 + \frac{1}{\tau_n^{\,2}}\right) \tag{19}$$

where

$$\tau_n \equiv n\,(2\pi\lambda/L)$$

or, in terms of primary parameters:

$$T_n = \frac{4\pi^2 n}{\beta L}\left[1 + \frac{L^2 f^2}{4\pi^2 n^2 g D_0}\right] \tag{20}$$

Modes calculated for the Antarctic Ocean are given in Table 3.

Table 3. *Free periods for the Antarctic Ocean. Assumed parameters:* $\phi = 55°$; $L = 25{,}000$ km; $D_0 = 4{\cdot}0$ km.

n	T_n (*days*)	$\Lambda_n \times 10^{-3}$ (*km*)
1	9·33	25·0
2	6·75	12·5
3	6·82	8·33
4	7·53	6·25
5	8·53	5·00
6	9·68	4·17
7	10·9	3·57
8	12·1	3·13
9	13·4	2·78
10	14·7	2·50

The results of Table 3 show an interesting clustering of periods in the neighbourhood of the maximum of the dispersion curve (Fig. 1). For this case, the wavelength associated with the dispersion maximum ($k = 1/\lambda$) is 10,500 km. The first two periods have smaller wave number (larger wavelength) and fall at positions to the left of the maximum in Fig. 1. The higher modes all have wave numbers to the right of the maximum. This relation among the parameters accounts for the initial decrease and subsequent increase in the periods and for their clustering – which takes place in the neighbourhood of the dispersion maximum. The calculations imply that there might be a fairly strong weekly period in the surface levels and north-south particle velocities of the Antarctic Ocean.

SUMMARY

Although this treatment of second-class motions on the β plane is obviously unsophisticated, we feel that it clarifies the physical nature of the model being invoked and of the phenomena taking place, thus deepening our insight into the meaning of the more abstract results obtained by the tidal theorists. It seems quite possible that motions of this type might be excited by meteorological as well as tidal forces and that the motions thus induced in the ocean depths might play a significant role in affecting the history of the oceanic water masses.

APPENDIX

The equation for planetary waves in an ocean of uniform depth.

Given the hydrodynamic equations of motion in a right-handed co-ordinate system with x directed to the east, y to the north, and z upward:

$$\frac{Du}{Dt} - fv + (2\Omega \cos \phi)\, w = -\frac{1}{\rho}\frac{\partial p}{\partial x} \tag{A1}$$

$$\frac{Dv}{Dt} + fu = -\frac{1}{\rho}\frac{\partial p}{\partial y} \tag{A2}$$

$$\frac{Dw}{Dt} - (2\Omega \cos \phi)\, u = -\frac{1}{\rho}\frac{\partial p}{\partial t} - g \tag{A3}$$

where $f = 2\Omega \sin \phi$, and u, v, w are the x, y, z components of velocity respectively. ϕ is the angle of latitude, Ω the angular velocity of the earth, ρ the density, p the pressure.

Dropping inertial terms and assuming hydrostatic equilibrium in the vertical direction, we have:

$$\frac{\partial u}{\partial t} - fv = -\frac{1}{\rho}\frac{\partial p}{\partial x} \tag{A4}$$

$$\frac{\partial v}{\partial t} + fu = -\frac{1}{\rho}\frac{\partial p}{\partial y} \tag{A5}$$

$$0 = -\frac{1}{\rho}\frac{\partial p}{\partial z} - g \tag{A6}$$

where ρ will be taken as constant through the body of the fluid and u and v constant with depth.

Consider a body of fluid with a free surface and a uniform unperturbed depth D_0. If η denotes displacements of the surface from the unperturbed level, equations (A4) and (A5) take the following form after making use of equation (A6):

$$\frac{\partial u}{\partial t} - fv = -g\frac{\partial \eta}{\partial x} \tag{A7}$$

$$\frac{\partial v}{\partial t} + fu = -g\frac{\partial \eta}{\partial y} \tag{A8}$$

The equation of continuity for this case takes the form:

$$\frac{\partial u}{\partial x} + \frac{\partial v}{\partial y} = -\frac{1}{D_0}\frac{\partial \eta}{\partial t} \tag{A9}$$

Cross differentiating equations (A7) and (A8) with respect to y and x respectively, and subtracting to eliminate the second derivatives of η, we obtain:

$$\frac{\partial^2 v}{\partial x\, \partial t} - \frac{\partial^2 u}{\partial y\, \partial t} + f\left(\frac{\partial u}{\partial x} + \frac{\partial v}{\partial y}\right) + \beta v = 0 \tag{A10}$$

where

$$\beta \equiv \partial f / \partial y$$

We now make a quasigeostrophic approximation by setting

$$v \simeq \frac{g}{f}\frac{\partial \eta}{\partial x}; \qquad u \simeq \frac{g}{f}\frac{\partial \eta}{\partial y} \tag{A11}$$

in the first, second, and fourth terms of equation (A10), and utilize the continuity equation (A9) to make a substitution for the third term. The resulting equation in η is:

$$\frac{g}{f}\frac{\partial^3\eta}{\partial t\,\partial x^2}+\frac{g}{f}\frac{\partial^3\eta}{\partial t\,\partial y^2}+\frac{g\beta}{f^2}\frac{\partial^2\eta}{\partial t\,\partial y}-\frac{f}{D_0}\frac{\partial\eta}{\partial t}+\frac{g\beta}{f}\frac{\partial\eta}{\partial x}=0. \tag{A12}$$

We shall concern ourselves with the propagation of plane waves in the x direction and therefore drop the second and third terms, leaving the fundamental equation:

$$\lambda^2\frac{\partial^3\eta}{\partial t\,\partial x^2}-\frac{\partial\eta}{dt}+\beta\lambda^2\frac{\partial\eta}{\partial x}=0 \tag{A13}$$

where

$$\lambda^2 \equiv g\,D_0/f^2 \tag{A14}$$

Equation (A13) is an equation for free oscillations of a medium subject to the restrictions and quasigeostrophic approximation used above. It describes planetary waves identical with those originally identified by Rossby (1939) in a somewhat more complicated context.

For the case of plane waves propagating in the x direction, equations (A8) and (A11) yield the following expression for the particle velocity u:

$$u=-\frac{g}{f^2}\frac{\partial^2\eta}{\partial t\,\partial x} \tag{A15}$$

Contribution No. 855 *from the Woods Hole Oceanographic Institution; this work was done under Contract with the Division of Biology and Medicine of the Atomic Energy Commission.*

REFERENCES

GOLDSBROUGH G. R. (1933) The Tides in Oceans on a Rotating Globe, Part IV. *Proc. Roy. Soc. London.* **A140**, 241-253.

LAMB H. (1952) *Hydrodynamics* 6th ed. Cambridge Univ. Press, p. 350 ff.

ROSSBY C.-G. (1939), Relation between variations in the intensity of the zonal circulation of the atmosphere and the displacements of the semi-permanent centres of action. *J. Mar. Res.* **2** (1), 38-55.

Printed in Great Britain by The Salisbury Press Ltd., Publicity House, Wilton Road Salisbury, Wilts. (1108)

Contribution No. 856

Vol. 37, No. 5 Transactions, American Geophysical Union October 1956

The Use of Parachute Drogues in the Measurement of Subsurface Ocean Currents*

Gordon Volkmann, John Knauss, and Allyn Vine

Abstract—A technique for the measurement of subsurface currents is described in which a standard parachute is used at depth as a sea anchor for a small surface float. By tracing a series of drogues set at various depths, a current profile may be obtained. Hydrodynamic corrections (amounting to about ten per cent of the shear) have been computed and other refinements incorporated which make this a feasible method for measuring the main structure of the major ocean currents down to depths where the current is five to ten per cent that of the surface current.

Introduction—There have been few measurements of subsurface currents in the open ocean, as indicated by *Bowden* [1954] in his survey of the literature. On the other hand there is no shortage of papers describing current-measuring devices. *Böhnecke* [1954] listed some half a hundred different instruments and ended by quoting *Fleming* [1952] who suggested that what was needed were fewer new instruments and more measurements. The present technique has been developed over a period of three cruises in three years, and has been used for a relatively large number of subsurface current observations by ourselves and others, the results of which will be published in the future. Like other methods it has certain limitations, but it is a cheap and easy technique which has been successfully used.

The method is that of the free-floating drogue which is one of the oldest, having been used by the *Challenger* Expedition, 1873–1876 [*Thomson* and *Murray*, 1885, p. 79]. It also appears to be one of the least used, since in Bowden's summary of subsurface-current observations in deep water, all measurements were made with propeller-type instruments. However, the drogue technique has been used in recent years by *Stommel* [1954] and by *Cromwell* and others [1954].

In brief the drogue system consists of a standard aviator's parachute suspended by a weighted wire from a surface float (Fig. 1). The ideal subsurface drogue is one in which the ratio of drogue surface area to float and wire surface area is infinitely large since, as described below, a correction must be applied to the trajectory of the drogue system based on the drag of these appendages. In this respect the recent work of *Swallow* [1955], who has devised a neutrally buoyant drogue with no surface float, is the ideal. Our drogue system was designed with three points in mind. (1) The drag of the wire and surface floats should be small compared to the drag of the sea anchor. (2) The parachute must be given every chance to open and to remain open under water, and the other components and the techniques should be reliable enough so that they could be used with a high percentage of successes. When possible, positive identification of a proper or malfunctioning drogue should be provided. (3) The drogue system should be cheap enough to be considered expendable.

The work reported on was started by Vine, in March and April 1951, on R/V *Atlantis* in the Cayman Sea and continued in April 1953 on R/V *Spencer F. Baird* off Southern California and on EASTROPIC in October to December 1955 on R/V *Horizon* and *Spencer F. Baird*.

Parachute—The standard flat circular aviators' parachutes used as drogues were obtained from the armed forces over-age supply. They are also available on the civilian surplus market, although care should be taken with the latter source because parachutes are sometimes sold without shrouds to prevent re-use. The parachutes used have an effective cross section of 200 sq ft when completely open, and they are almost weightless in water, making it possible to use a relatively small surface float. Furthermore they can be launched unopened (our technique was to stuff them into large mailing tubes and 'pour' them over the side). The problem of launching an already opened or rigid frame-work type of drogue of similar cross section is formidable.

Very few pounds of force are required to open a parachute in the air, and once open it stays open. The same appears to be true when parachutes are used as deep-sea drogues. To check this, parachutes were observed underwater by SCUBA-equipped divers. The only difficulty was the tendency for the

---

* Contribution from the Scripps Institution of Oceanography, New Series No. 881. Contribution Number 856 of the Woods Hole Oceanographic Institution.

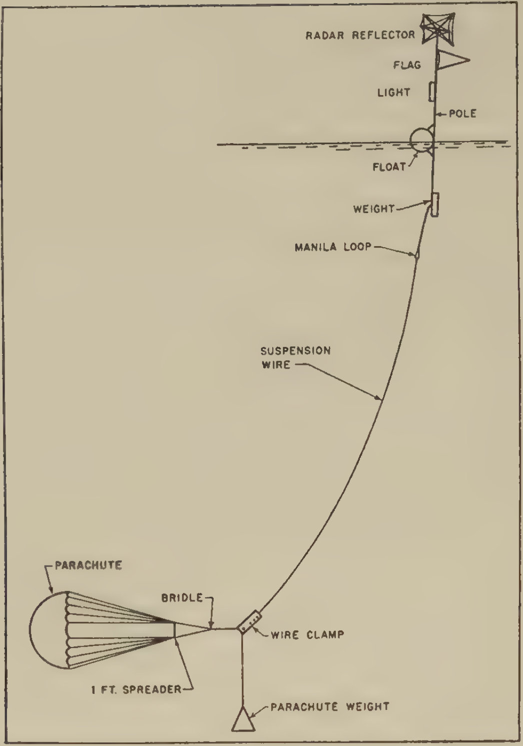

FIG. 1 – The parachute drogue system

shrouds to twist before the parachute opened as it fell through the water. In the tests conducted the parachute never failed to open, but the opening time was delayed by twisting, and a greater initial force was required. This difficulty was alleviated by inserting a spreader bar between the two groups of shrouds. Any twisting was taken up by the line which ran from the spreader bar to the wire (Fig. 1).

Wire and rigging—The suspension wire used was 0.030- or 0.040-in music wire, and while it has definite disadvantages, it was satisfactory for these purposes. The disadvantages are that it kinks easily, and, when it does, it only has about 20 pct of its original strength. It also corrodes quickly, as may be seen from the fact that 0.030-in wire generally parted after 24 hr with about a 30-lb pull on it. The advantages are that it is cheap, light, non-twisting under tension, and available in long lengths. If a laid wire is used, a good ball bearing swivel at the parachute end is recommended. The wire was in our instance the limiting factor in the length of life of the drogue, which was 24 to 36 hr. The use of either heavier wire or galvanized wire would lengthen this life considerably.

Since there is no need to reel in on this type of rig, a simple spindle and brake suffice as a winch. On two of the three cruises the front axle of an automobile complete with brake was used with great success. On the last cruise the music wire was supplied on wheel rims purchased to fit the automobile axle. The addition of small plywood flanges to prevent the wire from slipping off this drum makes a cheap and effective rig. The purchase of wire on drums rather than coils is strongly recommended because rewinding from coils requires special equipment and is lengthy and tedious.

A few of the many methods of holding music wire are shown in Figure 2. The cheek clamp is the strongest and most convenient, since it can be applied while the wire is under tension. It can also be clamped quickly, an asset when wire tension is high and mounting rapidly.

To ease the strain on the wire during drogue launching, the surface buoy with wire attached was put over first. The ship then steamed away until the proper amount of wire was out and then stopped while the parachute was 'poured.' This eliminated any tendency to sea-anchor the ship on 0.040-in music wire to an open parachute. Since music wire has a tendency to fatigue when bent on a short radius, manila leaders were used whenever practicable. Manila, marline, and friction tape were used copiously to prevent chafing and to lash the components together.

Floats—A different type of float was used on each of the three cruises: extra strong meteorological balloons in gunny sacks, canvas-covered balsa wood floats (Navy dan-buoys), and 14-inch Japanese glass fishing floats. The balloons are the cheapest and easiest to stow but are the least durable. The

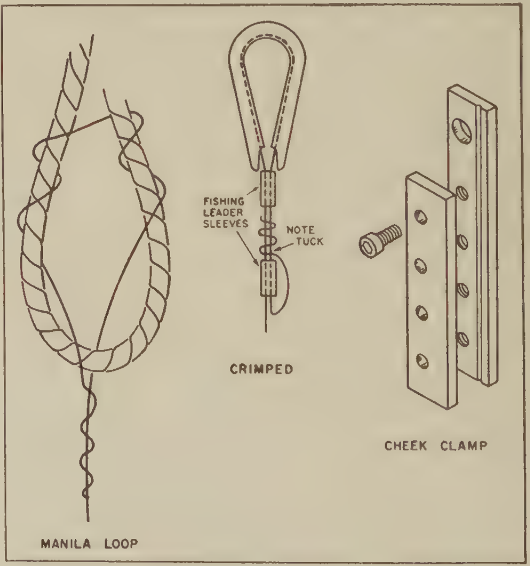

FIG. 2 – Various techniques for securing music wire

fishing floats proved the most satisfactory, but the storage of a hundred or more glass floats on a small ship can be a problem. Usually a single glass float provided enough buoyancy. The float was lashed to a bamboo pole, to the top of which were attached flags, a light, and a radar reflector. The suspension wire was attached to the bottom of the pole, and it was necessary for the parachute with its attached 20-lb weight to sink to its full depth before the pole would stand completely upright. The pole was so weighted that before the addition of the 20-lb load, it would lie at an angle of about 30° with the surface. Thus one could tell when the drogue system was properly set by watching the pole swing to an upright position, and one could also tell when something was amiss (usually a parted wire) when the pole flopped down. This type of positive identification of the fact that the drogue was properly set or that it had broken loose saved considerable time on the most recent cruise.

It can take as long as an hour for a parachute drogue and 20-lb attached weight to sink to 200 m. To eliminate the long time required for an open parachute to sink to the greater depths, additional weights were secured by means of a simple time release to the apex of the chute, which then descended closed. Here as a signalling device an additional float was attached between the upper end of the wire and the surface buoy. When the parachute was at depth, this float would be submerged under the additional weight of the release weights, but it would reappear when these weights were released. Also, when something parted, this second float would pop high out of the water and thus give a positive signal that something was amiss.

Measurement techniques—Currents at various depths were measured by tracing the movements of the various floats. Of the two general ways in which this can be done, neither is completely satisfactory: one is to measure the movement of the drogue over the surface by standard navigational techniques, that is, celestial fixes or Loran; the second is to measure the movement relative to some reference point, that is, an anchored ship, buoy, or some other easily observable reference.

The conditions were different on each of the three cruises and different techniques were used to solve this problem. Loran coverage was inadequate in each area as it is over most of the oceans of the world, and celestial navigation has certain obvious limitations with respect to accuracy, time between fixes, and the uncertainties of cloud formation. In the Cayman Sea, where we were often within sight of land, piloting techniques were used. When land fixes were not available the same surface-float, piano-wire rig was attached to an anchor and used as a reference buoy. The circular area of possible positions created by the necessary scope (we used a wire-length to water-depth ratio of 1.1 to 1) is reduced to a segment of a circle by a steady current, and this uncertainty can be considerably reduced by time averaging.

During the 1953 cruise of the *Spencer F. Baird* off Lower California where the currents were weak a slightly heavier version of the anchored buoy was used, and celestial navigation was employed to check possible lifting or dragging of the anchor.

On the EASTROPIC Expedition into the eastern part of the Equatorial Current and Countercurrent system a parachute drogue at 2000 m was used as the reference buoy. In this area of strong currents, it was felt that any slight drift of the water at 2000 m could be tolerated. An upper limit of this drift was established by celestial fixes but was never found to be more than predicted (see next section) and may have been less.

The range and bearing from the reference point to the other drogues was measured by one of three methods: (1) By timing the vessel up and down current along an average fixed course, taking bow and beam bearings or angles of depression from the horizon to establish the distance of the buoys from this course. (2) By timing the vessel from the reference buoy to each buoy and return, along a course parallel to the visual bearing between the two. (3) By standing by the reference-buoy and measuring range and bearing by radar.

The last method is, of course, the most efficient and the most accurate. Unfortunately the radar was not working properly on any of the three ships used by the authors. (EASTROPIC was a two-ship cruise and radar was used by Townsend Cromwell on the other vessel to great advantage.)

Corrections to observations—Since the velocity of the surface water is in general different from that of the water at the depth of the parachute, there is a flow of water past the surface buoy. This implies a slower flow of water by the parachute, since there must be a balance of the horizontal forces on the drogue system. These horizontal forces are given by

$$F = \tfrac{1}{2}\rho C_D A V^2 \qquad (1)$$

where F is the force, C_D a non-dimensional drag coefficient, ρ the density of the fluid, A the cross sectional area, and V the relative velocity of the fluid.

(The equation for the horizontal force created by a sinusoidal motion, for example, surface waves, of

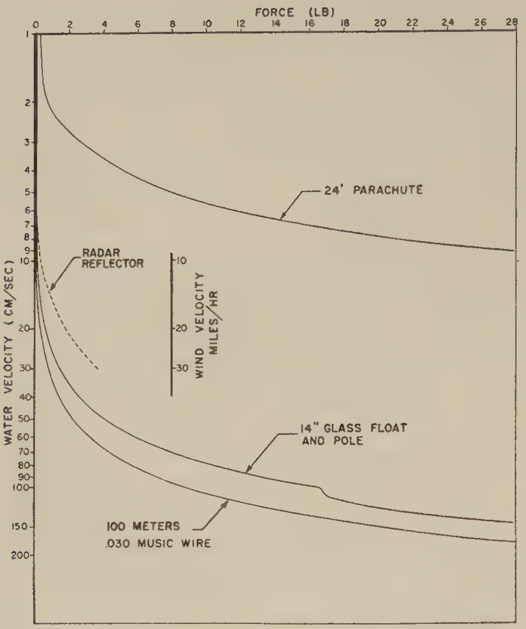

FIG. 3 – Drag forces on various components of the drogue system (note different scale for radar reflector in air)

orbital velocity U superimposed on a steady current V and integrated over one cycle is $F = (\frac{1}{2})\ \rho\ C_D A\ (V^2 + U^2/2)$. For the shallower depths the parachute may be within the region of wave motion and complicate the picture phase-wise. For the greater depths it is not clear how much of the oscillatory force is transmitted down the wire to the parachute.)

Figure 3 has a plot of force as a function of speed through the water for a 24-ft circular flat parachute computed from (1). The area of such a parachute is 200 sq ft. (The diameter must be reduced by a third in calculating the area of the parachute, according to the USAF *Parachute Handbook*, 1951.) The drag coefficient was assumed to be 1.5, although this may be subject to some error. The coefficient is a function of the porosity of the material as well as the geometry. For a completely imporous chute, it is 1.7; for a standard chute in air it is 1.3 [*Heinrich*, 1954]. The porosity of the parachute material is less for sea water than for air, but no measurements have been made of its effect on the drag coefficient.

Also plotted in Figure 3 are the forces at different speeds computed for a surface float consisting of a 14-in float and 8 ft of bamboo pole, both submerged, 100 m of 0.030-in music wire, and a two-ft Navy lifeboat radar reflector in air. The curves for the float and wire were calculated using the appropriate drag coefficients in *Rouse* [1946]; the curve for the radar reflector (type MX-138/A) is based upon measured values of drag.

To calculate completely the forces on the parachute and hence the speed at which it moves through the water, it is necessary to know exactly the forces on the float and wire. This is in general not possible, nor in many cases is it necessary if the ratio of drogue to float area is large enough. From Figure 3 one can see that a current which flows at 50 cm/sec to a depth of 100 m will drag a parachute at 200 m through the water at about 4.5 cm/sec, assuming no current at 200 m. It has been our experience that a first-order correction such as this will correct the measurements to a couple of centimeters per second and that both the uncertainties in observation as well as short-period changes in the current make it impracticable to try to reduce the error any more.

The standard flat parachute is unstable. As it falls through the air it falls at an angle of about 22° with the vertical. This angle of stability is again a function of the porosity of the chute and is 45° for a completely imporous parachute [*Heinrich*, 1954]. Hence the direction of the 4.5 cm/sec correction of the previous example could be as much as 22° to 45° in error. It is believed, however, that this directional correction is negligible. In the first place an uncertainty of even 45° on a 5 cm/sec correction to a 50 cm/sec current does not change the resultant by more than ±4°. Secondly, underwater observations of parachutes used as drogues indicate that if there is a directional preference for the towed parachute it is in the downward direction.

The actual depth of the parachute drogue can be estimated by assuming the wire to be a rigid member and the forces in equilibrium (hence the depth of the 200-m drogue with a 20-lb weight and pulled by a 6-lb force would be $d = 200 \cos \phi$ where $\phi = \tan^{-1} 6/20$ so that $d = 191$ m), or by the more rigorous method of *Pode* [1951], where the forces on the flexible wire are also considered. In this example, assuming 0.030-in wire, the calculated depth is 189 m. As long as ϕ is a relatively small angle the two methods give about the same results.

Discussions and conclusions—The techniques and equipment described have been used successfully in the measurement of surface and subsurface ocean currents in both the Atlantic and the Pacific. On EASTROPIC, continual tracking of as many as five drogues at various depths with reference to the 2000-m drogue was done by radar, and up to four drogues were tracked at once by continuously running between them and the reference drogue. It was nearly always possible to get a satisfactory picture of the vertical current structure down to several hundred m during the daylight hours.

The shear measured in these cruises was nearly always between 10 and 100 cm/sec. The little experience we had in three-knot (150 cm/sec) shear indicated that perhaps the drogue system would have to be sturdier to be used in the Kuroshio or the Gulf Stream.

It seems clear from the force computations in Figure 3 that in areas of even modest surface currents the correction which must be applied due to shear may easily exceed the velocities which other workers have shown to exist at greater depths. This suggests that the usefulness of this technique may be limited to depths where the current is more than 5 to 10 pct that of the surface current.

However, for the task of measuring the structure of the major ocean currents where an error of a few centimeters per second can be accepted, it is believed that the technique as described is a useful one.

Acknowledgment—This paper represents results of work carried out by the University of California and the Woods Hole Oceanographic Institution under contract with the Office of Naval Research.

REFERENCES

BÖHNECKE, G., Principles of measuring currents, International Association of Physical Oceanography, IUGG, General Assembly at Rome. *Procès-Verbaux* **6**, Sep., 1954.

BOWDEN, K. F., The direct measurement of subsurface currents in the oceans, *Deep Sea Research*, **2**, 33–47, 1954.

CROMWELL, T., R. B. MONTGOMERY, AND E. D. STROUP, Equatorial undercurrent in the Pacific Ocean revealed by new methods, *Science*, **119**, 648–649, 1954.

FLEMING, R. H., Discussion in *Symposium on Oceanographic Instrumentation*. Nat. Res. Counc. Pub. 309, 231 pp., 1952.

HEINRICH, H. G., *The effects of porosity of design and performance characteristics of parachutes*, USAF Equipment Lab., Wright Air Dev. Center. 11 pp., 1954.

PODE, L., *Tables for computing the equilibrium configuration of a flexible cable in a uniform stream*, USN David Taylor Model Basin Rep. 687, 33 pp., 1951.

ROUSE, H., *Elementary mechanics of fluids*, John Wiley and Sons, 376 pp., 1946.

STOMMEL, H., Serial observations of drift currents in the central North Atlantic Ocean, *Tellus*, **6**, 203–214, 1954.

SWALLOW, J. C., A neutral-buoyant float for measuring deep currents, *Deep-Sea Research*, **3**, 74–81, 1955.

THOMSON, C. WYVILLE, AND JOHN MURRAY, *Report on the Scientific Results of the Voyage of HMS Challenger*, Narrative, 1110 pp., 1885.

USAF Parachute Handbook, ATI 35 532, 78 pp., 1951.

Scripps Institution of Oceanography (G. V. and J. K.). *La Jolla, California, and Woods Hole Oceanographic Institution* (A. V.), *Woods Hole, Massachusetts.*

(Manuscript received April 18, 1956; presented at the Thirty-Seventh Annual Meeting, April 30, 1956; open for formal discussion until March 1, 1957).

Contribution No. 858

Deep-Sea Research 1956, Vol. 4, pp. 1 to 14. Pergamon Press Ltd., London.

Measurements of light penetration in Relation to Vertical Migration and Records of Luminescence of Deep-Sea Animals

GEORGE L. CLARKE and RICHARD H. BACKUS

Abstract—Direct measurements of the intensity of light at the levels of certain deep scattering layers were made using a bathyphotometer capable of responding to illumination as low as 10^{-7} μw/cm^2 or about 10^{-12} of full sunlight. The vertical migration of the scattering layers was recorded by means of an echo sounder. During the middle of the day a single scattering layer was found and the top of this remained below the 0·01-μw/cm^2 isolume. In the late afternoon the layer split into two and both parts rose more rapidly than the isolumes with the result that at sunset the top of the upper layer was 40 m above the 0·1-μw/cm^2 isolume. Reactions other than the following of a certain light intensity were thus involved in the vertical migration of these layers.

Flashes from luminescent animals detected by the bathyphotometer were recorded on a Brush pen recorder. The intensity and frequency of luminescent flashes varied greatly with depth and with time and presented differing patterns in coastal and slope waters.

INTRODUCTION

MOST pelagic animals in the ocean and in lakes are limited in their vertical distribution to definite ranges of depth, and many kinds of zooplankton and fishes are known to undertake characteristic vertical migrations downward to lower levels in the early morning with a return to higher levels in the evening. This diurnal migration appears to be more closely correlated with changes in the strength of the light penetrating from the surface than with any other known factor of the environment (CUSHING, 1951). In certain instances in which the migration was confined to relatively shallow depths, measurements of the illumination in the water have been made at the same time that the vertical distribution of the animal populations was determined by means of plankton hauls (CLARKE, 1933, 1934a). However, photometers of the usual type containing photovoltaic cells are not reliable for the measurement of intensities less than about 0·01 per cent of sunlight. Accordingly, with this type of photometer, the relation between light as an ecological factor and the activities of migrating animals cannot be directly investigated at depths greater than about 60 to 80 m even in clear waters (CLARKE, 1954). At greater depths or in less transparent water a more sensitive photometer is required, or else reliance must be placed on an extrapolation of the diminution of light assuming that the extinction rate in the deeper water is the same as that actually measured near the surface – an assumption which may lead to highly erroneous results (KAMPA, 1955).

Off the continental shelf, net hauls have shown that certain species of Crustacea carry out diurnal migrations the lower limits of which are as great as 800 m (WATERMAN *et al.*, 1939). In addition, echo sounder records have revealed the widespread occurrence of " deep scattering layers," commonly at depths of 400 to 600 m during the daytime but also sometimes as deep as 1,000 m (MOORE, 1950). These layers typically migrate vertically several hundred metres each day. Although the kinds of animals primarily responsible for these sound-scattering layers are not precisely known, it seems probable that euphausids and fishes are involved in at least some of these layers (Moore, 1950; Boden, 1950; Tucker, 1951; Marshall, 1951; Hersey and Backus, 1954). No doubt concentrations of other animals, some of which do not reflect sufficient sound to be recorded by present equipment, are living at various levels in the ocean and are carrying out similar or perhaps even more extensive migrations, as yet undetected.

The construction of photometers containing extremely sensitive photomultiplier tubes has made possible the direct measurement of light at depths at which the deep scattering layers are found in the oceans and hence permit a more exact study of the role of light in the control of diurnal migration. Observations with the bathyphotometer (Clarke and Wertheim, 1956) not only provided measurements of transparency to depths as great as 610 m but also revealed the fact that luminescent flashing of deep-sea animals may be of an intensity comparable to the daylight reaching the lower part of this range. Off southern California, Kampa and Boden (1954) undertook simultaneous observations of illumination and the movements of a sound-scattering layer. The observations reported in the present paper were made in the slope water southeast of New York and yielded somewhat different results. Our direct reading bathyphotometer was employed during the day to measure the light penetrating from the surface to the level of the scattering layers as observed on the echo sounder. In addition, during the night the bathyphotometer and strip recorder were used to compare the strength and frequency of the flashes of luminescent animals at various depths as well as to record the changes with time of the luminescence at the same level.

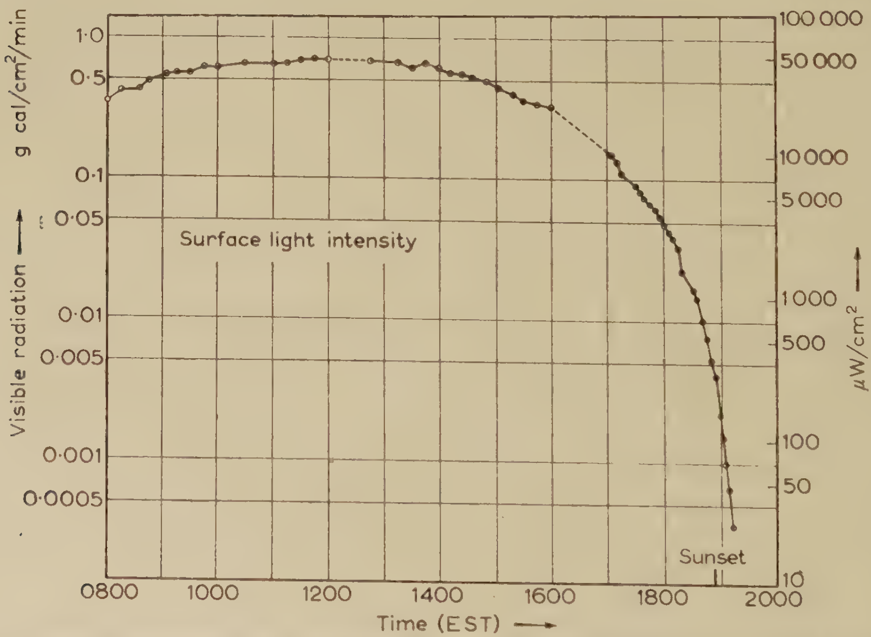

Fig. 1. Light recorded by deck photometer containing Weston photronic cell. 21 July 1955. Position 38°21′N, 69°09′W.

SUBMARINE DAYLIGHT AND VERTICAL MIGRATION

Observations. The relation between intensity of illumination and the vertical migrations of certain scattering layers was investigated from the research vessel

Atlantis on July 20 and 21, 1955 at the stations 200 miles SE of New York for which transparency values were reported by Clarke and Wertheim (1956, Table 1, Series 23, 24 and 25). Since the stations were only about four miles apart with closely similar surface light, transparency, and scattering layer behaviour, the results of the two days' observations are considered together.

During the day-time periods measurement of the light at the sea surface were made by means of a deck photometer containing a Weston photronic cell provided with a diffusing surface of semitranslucent plexiglas and mounted in gimbals. The record of surface light intensity reveals the relatively steady illumination during the middle of the day and the precipitous drop near sunset (Fig. 1). From this record and measurements of transparency to a depth of 554 m (Clarke and Wertheim, 1956) a family of curves was drawn showing the depth of the isolumes ranging from 10,000 to 0·00001 μw/cm² (Fig. 2). In conformity with the changes in surface light the isolumes remain at a relatively constant depth during the middle of the day but later move rapidly upward especially at sunset.

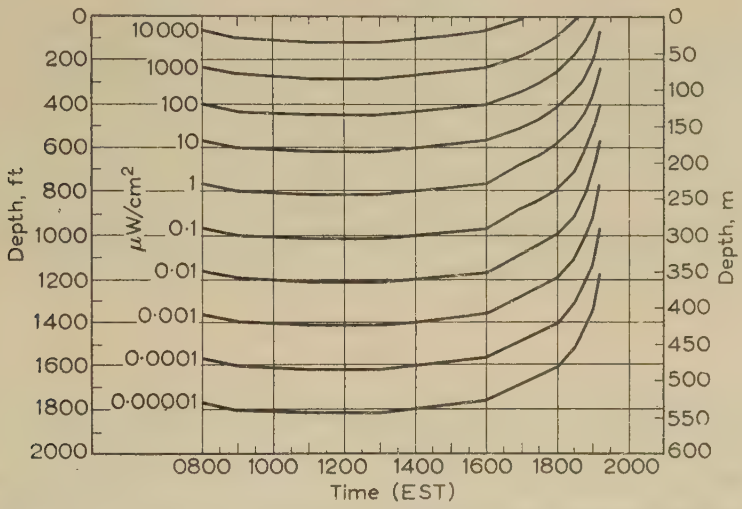

Fig. 2. Isolumes for 21 July calculated from surface light using the extinction coefficient measured for the water column.

Scattering layer observations were made with an Edo Corporation UQN/1B 12 kc transducer and electronic system coupled with a high-resolution recorder (Knott and Hersey, 1956). Sample sections of the record obtained on 21 July (Figs. 3 and 4) show the presence of a single pronounced scattering layer the top of which was found at a depth of about 300 m at 1700 hours. This layer moved upward slowly during the first hour and then at 1810 began to divide into two layers.

To obtain a direct measure of the light at the level of the scattering layers the bathyphotometer was lowered beginning at 1700 hours. The echoes from the bathyphotometer were immediately discernible on the echo-sounder record in the ship's laboratory and this echo sequence is seen as a downwardly sloping trace labelled " photometer " (Fig. 3). When the bathyphotometer was observed to have reached the level of the top of the scattering layer, lowering was halted and measurements of light intensity were begun. By 1836 hours two scattering layers were apparent and the upper one had moved to a position above the photometer. Accordingly, the instrument was raised until its level again conformed with the top of the upper layer. In the succeeding 20 minutes this scattering layer moved up past the photometer and soon thereafter the echoes from it became diffuse and merged with the surface "noise."

The bathyphotometer was lowered again at 1854 hours until it reached the level of the top of the lower scattering layer. At this time the lower layer had become dense and was moving rapidly toward the surface. As the trace from this layer moved up past the photometer (Fig. 4), the instrument was again raised, and subsequently this process was repeated until about 1927 hours when the trace merged with the surface "noise."

By the foregoing procedure the moments could be directly observed on the echo sounder when the depth of the photometer coincided with the depth of the scattering layer under study, and the illumination at that depth immediately determined by readings made in the ship's laboratory. From these direct measurements the depths of the 0·1- and 0·01-μw/cm^2 isolumes were calculated using the values of the extinction coefficient of the water measured earlier in the day. In this way the position of these isolumes, which were never far from the depths of the attendant photometer readings, was determined with greater assurance than if calculations had been made from the surface light values.

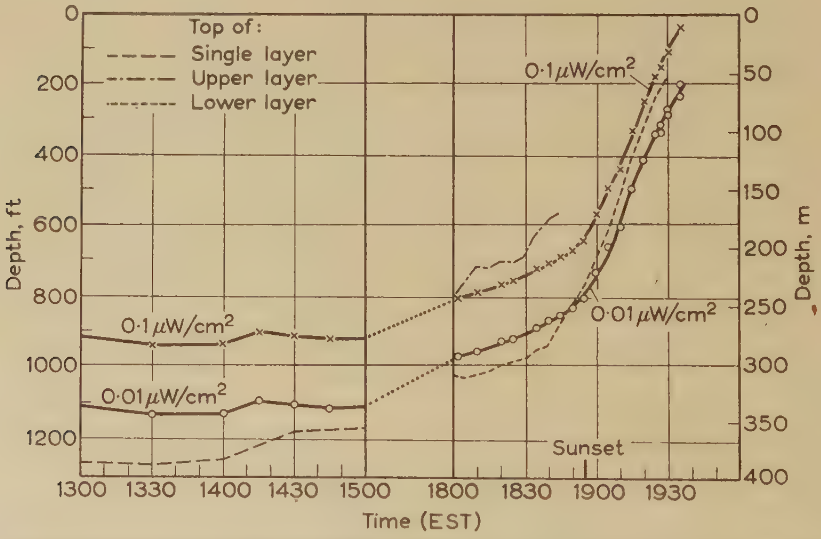

Fig. 5. Plot of the position of the tops of certain scattering layers in relation to the indicated isolumes for the indicated periods on 20 July.

The changes in level of the scattering layers have been compared with the changes in the intensity of illumination in the water for certain periods on 20 July (Fig. 5). During the afternoon only a single scattering layer was discernible. The top of this layer was at 390 m at 1300 hours and about 50 m below the 0·01-μw/cm^2 isolume. By 1500 hours the layer had risen to 355 m although the isolume had not changed position appreciably.

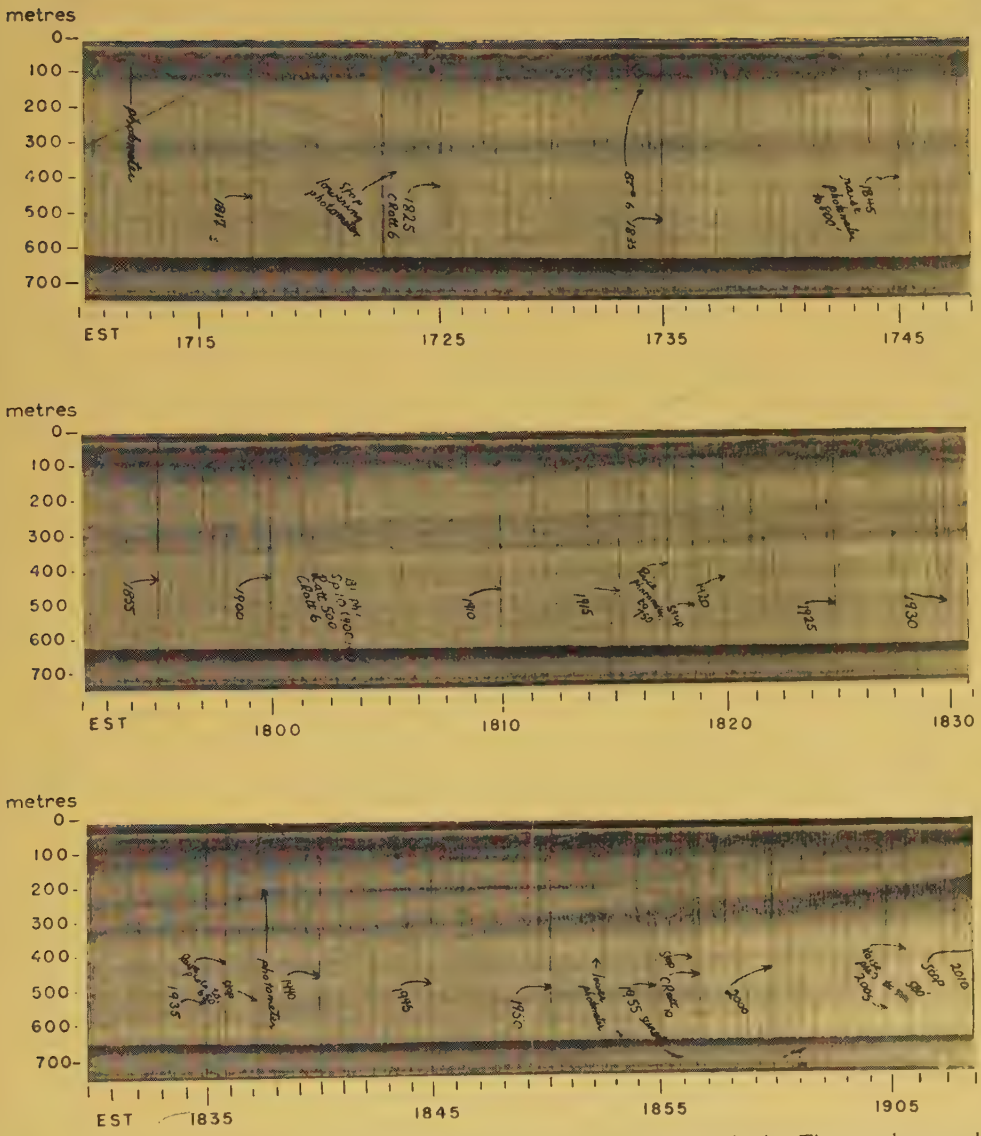

Fig. 3. Echo-sounder record on 21 July for the hours indicated (Daylight Saving Time on the record and Eastern Standard Time in the bottom margins). Zero depth in this and the succeeding figure represents the depth of the transducer which is about 5·5 m below the surface. Near-surface reverberation appears as a broad black band at top. The bottom echoes show as a heavy black band near the lower margin during the fifth traverse of the record and indicate a depth of 3,840 m.

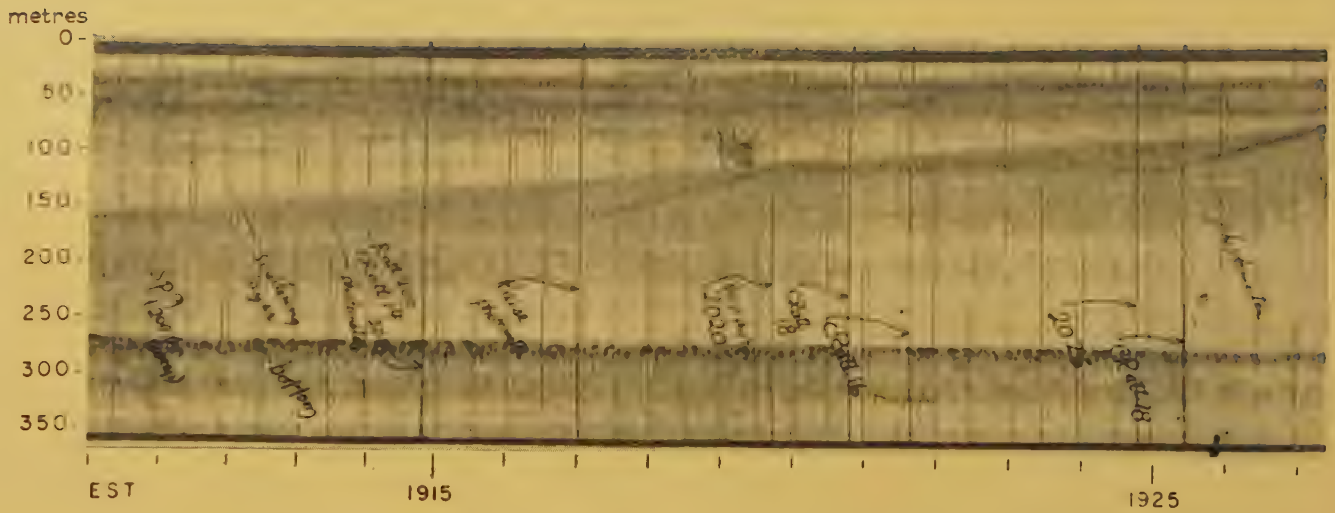

Fig. 4. Continuation of the echo-sounder record on 21 July, but with an enlarged scale.

During the evening two scattering layers were recorded. At 1800 hours the top of the upper layer was found at 240 m and corresponded in depth very closely to the position of the 0·1-μw/cm^2 isolume. At the same time the top of the lower layer was observed at 315 m which was about 15 m below the level of the 0·01-μw/cm^2 isolume. The upper scattering layer rose rapidly, although irregularly, from 1800 to 1845 hours at which time it was found at a depth of 170 m or 40 m above the 0·1-μw/cm^2 isolume. The lower scattering layer moved upward slowly at first but more rapidly after 1840 hours, rising from 286 to 54 m in the ensuing 50 minutes, or at an average rate of 4·6 m vertical rise per minute.

A similar comparison for 21 July showed that the top of the upper scattering layer, although fluctuating in position, followed in a general way the upward movement of the 0·1-μw/cm^2 isolume from 1730 to 1830 hours (Fig. 6). At 1800 the depth of the layer and the isolume was 250 m as on the previous evening. In the 20 minutes following 1830 the upper scattering layer moved to a position 40 m above the isolume. The densest portion of the upper scattering layer was located midway between the isolumes at 1730 hours but moved to a position above the 0·1-μw/cm^2 isolume at 1840.

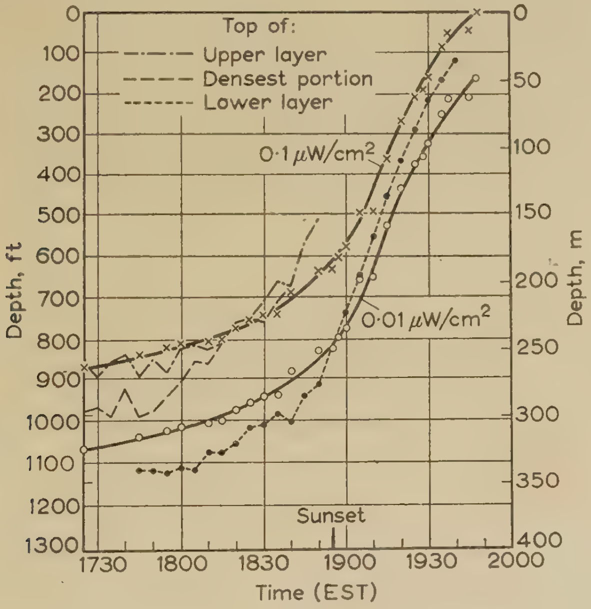

Fig. 6. Plot of the position of scattering layers and isolumes on 21 July.

At 1800 hours on 21 July the lower scattering layer was found at 340 m, or 30 m below the 0·01-μw/cm^2 isolume. It was thus 30 m below its depth at the same time on the previous evening, whereas the isolume was only 10 m below its previous level. As before the lower scattering layer moved gradually upward during the next 40 minutes, parallelling the rise of the isolume. At about the same time as on the previous evening the scattering layer accelerated its upward migration, reaching a depth of 65 m at 1930 with an average rate of rise of 4·4 m per minute. As before, this scattering layer rose more rapidly than the 0·01-μw/cm^2 isolume after 1830 hours and at 1940 was located at 36 m, or 30 m above the isolume.

Discussion. The general features of the depth distribution and migration of the scattering layers observed in this investigation are essentially similar to observations earlier reported. The separation of the principal layer into two layers during the sunset ascent has been reported by BODEN (1950) and by TUCKER (1951). DIETZ (1948) reported a layer that was double during the morning descent but remained unsplit during the evening migration. TUCKER (1951) associated shallower, less intense sound scattering with euphausids and deeper, more intense scattering with fishes, but he does not state whether he considers this conclusion to apply to layers which split during the evening and morning migrations.

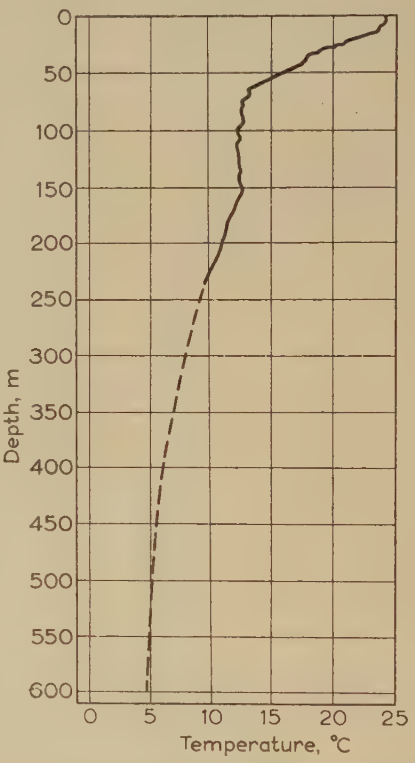

Fig. 7. Temperature section for 21 July, 1955. Solid line from bathythermograph slide made at the time; broken line from measurements taken in previous years in this area and season. Bathythermograms made on 20 July 1955 show essentially the same temperature structure in the upper 240 m.

The present observations on light made simultaneously with the records of the vertical distribution of the scattering layers make possible a further study of the manner in which light acts to control the diurnal migration. On the two successive days the relation with time of ascent, depth, and light intensity was remarkably similar for both upper and lower scattering layers. This suggests that the control of vertical position may be rather precise, and also uniform over considerable areas, since the ship had drifted for several miles between the two evening observations.

Our observations agree with previous findings in showing that the diurnally migrating plankton tends in general to follow the vertical movements of certain isolumes (CLARKE, 1934a; WATERMAN *et al.*, 1939; MOORE, 1950; KAMPA and BODEN, 1954). However, the details of the relation with light and the degree of modification of behaviour that is brought about by other factors vary in different instances. In the Gulf of Maine the upward migration of copepods was found to be stopped by the summer thermocline on one occasion (CLARKE, 1933) but not on another occasion (CLARKE, 1934a). Temperature, and perhaps also pressure, may affect the vertical position of zooplankton (MOORE, 1955). Recent laboratory studies of the effects of light intensity on the phototaxis and photokinesis of certain plankton animals are summarized by HARRIS and WOLFE (1955), and modifications of these reactions by changes in *p*H and other factors have been investigated by E. R. BAYLOR (private communication) and others.

In the locality where the present observations were made the temperature gradient apparently did not cause a significant change in the pattern of the vertical migration of the scattering layers. The temperature profile (Fig. 7) showed a sharp decline from 24°C near the surface to 13°C at 65 m. The temperature remained essentially unchanged from this depth to 150 m and then gradually dropped off to about 4·5°C at 600 m. During the two evening observations reported here the deeper scattering layer was observed to move upward without an abrupt change of rate from about 300 m to 55 m and 36 m respectively, thus undergoing a temperature change of 8°C or more. The animals may have continued to rise still nearer to the surface, but if so, their echoes were obscured by the surface " noise."

The present observations indicate the extent to which the migrating animals tend to maintain themselves at an " optimal " intensity of light – that is, one at which they tend to congregate by a phototactic, photokinetic, or other reaction. During the early afternoon of 20 July the top of the single scattering layer was located at a depth where the light was little more than 0·001-μw/cm^2 but the layer moved upward toward the 0·01-μw/cm^2 isolume at 1430 hours (Fig. 5). Since the two scattering layers distinguishable at a later hour appear to have arisen by a continuous process from the single layer, it seems probable that the two sets of animals in the separated layers had already been present in the single layer. The animals that formed the top of the single layer presumably continued in the vanguard of the upward moving population and formed the top of the upper layer. If this was the case, then these animals crossed the isolumes for 0·01 and 0·1-μw/cm^2 and continued moving upward into light which was more than 100 times brighter than that existing at their midday level. Assuming that the animals in the lower part of the single scattering layer formed the lower of the two separated layers, these individuals similarly moved up into much more intense illumination. Thus both scattering layers moved upward faster than the isolumes did, particularly in the period beginning about one half hour before sunset.

The same tendency for the animals to accelerate their migration and to move into brighter light was observed on the evening of 21 July (Fig. 6). On this occasion the depth of the top of the densest portion of the upper scattering layer was also plotted during the period when this differed markedly from the depth of the uppermost limit of this layer. The depth of the top of the densest portion changed from about midway between the depths of the tops of the upper and lower layers to a level nearly the same as the top of the upper layer. This change might have resulted from a shift in the concentration of the animals in the upper layer or from the presence of more than one type of animal in this layer.

Frequently zooplankton populations have been reported to descend to their maximum depths early in the day and to rise to levels nearer the surface during midday or early afternoon where light intensity is higher. This is interpretated as a manifestation of light adaptation resulting in an increase in the intensity of illumination which is reacted to as optimal by the animals concerned. As the isolumes move toward the surface during the evening, those animal populations which tend to congregate at a certain intensity would move upward at a corresponding rate provided that their powers of locomotion were sufficient to enable them to keep up. Off southern California during the early part of the migration the scattering layer lagged behind the ascending isolume with which it had been associated earlier in the afternoon (Kampa and Boden, 1954). During this period the upward movement was slow and there seems no reason to believe that the animals could not keep up; rather the investigators suggest that the threshold intensity of migration may be slightly lower than the intensity of the optimal illumination. The fact that the receiving surface of the photometer used by Kampa and Boden was vertical may have introduced some differences in the light values recorded, as compared with the changes in underwater intensities recorded when employing the usual horizontal receiving surface (Clarke and Wertheim, 1956).

During the period of most rapid ascent observed by Kampa and Boden the scattering layer and the isolume with which it was associated moved upward together at the rate of 5·1 m per minute. This rate of rise is about the same as that observed in the present investigation but considerably higher than values of about 1 m per minute reported by Clarke (1934b) for copepod populations in the Gulf of Maine and by Hardy and Bainbridge (1954). Scatterers that can move upwards at rates faster than 4 m/minute are presumably strong swimmers such as fishes or the larger crustaceans.

If we accept the idea that photic reactions cause animal populations to move away from high light intensities during the day and that their day-time level is determined by that intensity which causes no negative response, we should not expect the animals to move upward faster than their optimal illumination and thus pass into brighter light. Since such behaviour was clearly observed in the present investigation, we must conclude that other factors have entered the picture. One possible explanation is that the upward migration is initiated primarily by the *change* in light and that once the stimulus has been received from a sufficient reduction in light, the animals swim steadily toward the surface even though this means moving into higher intensities. This type of response to a reduction in light has been observed in the laboratory particularly with fresh-water plankton, such as *Daphnia* (Clarke, 1932; Harris and Wolfe, 1955). The present observations thus provide additional evidence for the occurrence in vertically migrating animals of tactic or kinetic responses that may considerably modify the general tendency to remain at the level of a certain intensity of illumination.

RECORDS OF LUMINESCENCE

Observations. During the measurements of transparency made in July 1955 (Clarke and Wertheim, 1956) flashes of light were observed during the day-time at levels near the maximum depth attained (610 m) and at all levels down to 610 m at night but particularly at the deeper levels. These flashes are interpreted as the luminescent activity of fishes or invertebrates and may be due to intermittent discharges of the photophores of certain animals or may result from the movement of steadily luminescing forms past the receiving surface of the photometer. In order to determine in a preliminary way the variation in the amount and type of luminescence at different depths and at different times, observations were made from the research vessel *Bear* on 6 September 1955 in the coastal water about 40 miles south of Martha's Vineyard, and on 8 September 80 miles farther south in the slope water between the continental shelf and the Gulf Stream and about 80 miles northwest of the area studied on 20 and 21 July, 1955.

The records of flashes were made by connecting an Edin AC amplifier in parallel with the microammeter reporting the light response of the bathyphotometer. The amplifier was in turn connected to a Brush pen recorder (Clarke and Wertheim, 1956, Fig. 2). This system was used to resolve more satisfactorily the flashes originally observed on the microammeter and to obtain a graphical record. It was intended only to show the frequency of occurrence of flashes brighter than the background. Since the recorder did not report the level of steady background illumination, little

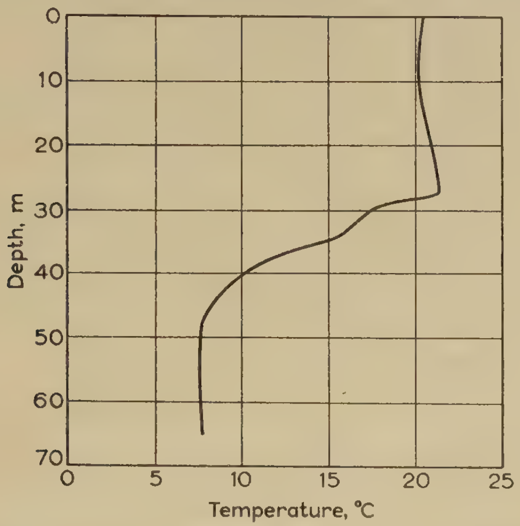

Fig. 8. Temperature section for 6 September 1955, made from bathythermograph slide.

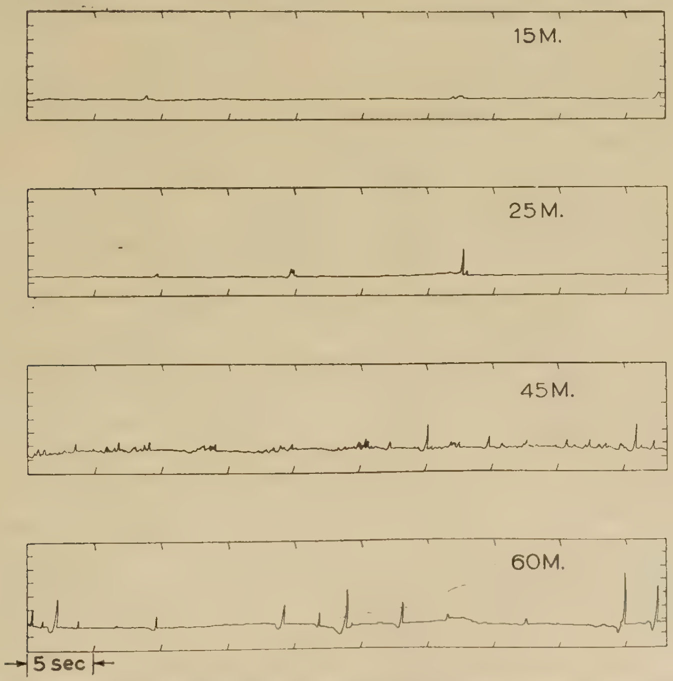

Fig. 9. Sections of records, made with Brush pen recorder, of luminescent flashes at the indicated depths at 1915-2035 EST. 6 September 1955, position: 40°37′N, 71°03′W. No moon or stars visible. (Bathyphotometer circuit voltage: Position 9, scale 50). Abscissa: time; ordinates: see text.

can be said about the relative intensity of the flashes recorded. In any event the actual relative intensities of the sources could not be deduced since their distances from the photometer are unknown. The background illumination is probably composed of numerous flashes dimmer than those recorded but might consist of light from continuously luminescing organisms. Because of the relationship between the band pass of the recording system and the duration of the flashes the recorder has given a fairly accurate portrayal of the "shape" of the flashes.

The coastal water station was occupied early in the evening of 6 September in 70 m of water. A bathythermogram made at this station showed that the temperature was relatively uniform in the upper 28 m at 20·2 to 21·°5C, dropped in a sharp thermocline to 7·5°C at 48 m, and thence remained about the same to the bottom (Fig. 8). Strip records of luminescent flashing were made at 15, 25, 45, and 60 m (Fig. 9). At 15 m the flashes typically were small and infrequent. Somewhat more luminescent activity was detected at 25 m. Animals near the bottom of the thermocline at 45 m produced very frequent but small flashes, whereas at 60 m irregularly spaced medium to large flashes were recorded.

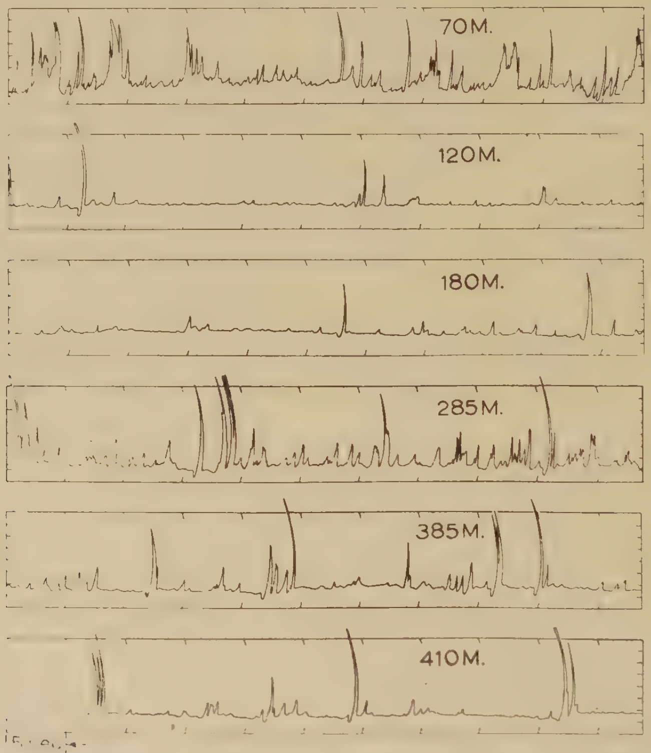

Fig. 10. Sections of record made with Brush pen recorder showing luminescent flashes at the indicated depths at 1945-2130 EST., 8 September 1955, position: 39 23′N, 70 16′W. No moon but faint stars visible. (Bathyphotometer circuit: voltage position 9, scale 5). Abscissa: time; ordinates; see text.

The station in the slope water was occupied at about the same time in the evening of 8 September in about 2,560 m of water. The thermal structure in the upper 600 m was similar to that recorded for the slope water station occupied on 21 July. The sample sections of the strip record reproduced in Fig. 10 show an even greater variation in luminescent activity with depth. At the shallowest level of 70 m, which was only

10 m deeper than the deepest level observed in the coastal water station, almost incessant but very irregular flashing occurred with both small and very large individual flashes. At 120 and at 180 m luminescent activity dropped to a few minor flashes with an occasional large one and contrasted very sharply with the conditions above and below these levels. The record of luminescence at 285 m shows intense activity with repeated flashes of moderate size and many large individual outbursts of light. The picture at 385 m is one of many fewer minor discharges with occasional very large flashes; at 410 m the large flashes are of about the same intensity, but there is a further reduction of the frequency and size of the smaller flashes.*

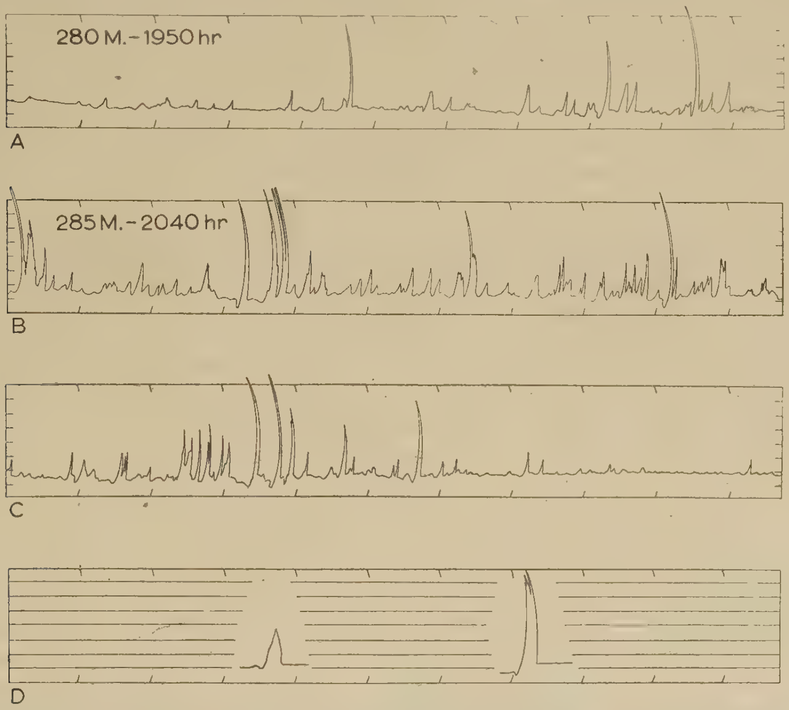

Fig. 11. Sections of record made with Brush pen recorder (bathyphotometer circuit: voltage position 9, scale 5) showing: (a and b) change in pattern of luminescent flashing at 1950 and at 2040 hours EST. at 280-285 m on 8 September, 1955; (c) change in luminescence while photometer was being raised at 2110 EST at a depth of about 130 m; and (d) two flashes from a 35-mm *Mnemiopsis leidyi* placed 50 cm from the receiving surface of the bathyphotometer in the Laboratory at Woods Hole on 14 September 1955.

Changes in time at the same level at this station were observed and samples of the record for periods beginning at 1950 and 2040 hours are shown in Fig. 11 (a and b). The pronounced differences may be due to a change in the behaviour of the animals or to a replacement of one set of animals by another either vertically or horizontally. We know that the vertical migration of certain animal groups takes place at earlier hours and probably other types of animals, undetected by the echo sounder, are changing level at these later hours. Variations in flashing might also be produced by the drift of the ship into or out of patches of animals. An example of a pronounced change in the amount of luminescence during an actual observation was recorded at 2110 hours at a depth of about 130 m while the bathyphotometer was being reeled in at a rate of approximately 30 m/minute and the ship was drifting at about 60 m/minute (Fig. 11 c). Abrupt increase in flashing may result from the photometer moving either horizontally or vertically into a concentration of animals and in some instances luminescent discharge may be caused by the actual contact of animals with the photometer or its supporting cables. Conversely, abrupt decrease in flashing may be caused by the instrument moving away from the luminescent animals.

---

* Following the preparation of this report records and quantitative measurements of luminescence were obtained in this general area during July 1956, at depths down to about 1,700 m and these will be fully presented in a subsequent report.

It was desired to obtain records with the Brush pen recorder of flashes of a known animal at a known distance from the photometer, although these cannot be compared quantitatively with the other records because of the characteristics of the circuits employed and the differences in the intensity of the background light, as explained above. Such records were obtained in the laboratory by placing the bathyphotometer in a light-tight box with the receiving surface of the instrument 50 cm from a glass dish containing sea water and a freshly caught 35-mm specimen of the ctenophore, *Mnemiopsis leidyi*. The ctenophore was caused to luminesce by applying a momentary charge of about 8 volts from a transformer to copper electrodes immersed in the water on each side of the animal (Fig. 11 d). Simultaneous reading of the micro-ammeter in the bathyphotometer circuit showed that the intensity of light received at 50 cm was about $0{\cdot}00005 \mu w/cm^2$ for the first flash shown and off scale at $0{\cdot}000075 \mu w/cm^2$ for the second flash. The only previous measurement of the strength of luminescence of this type of animal known to us is that of Nichols (1924) in which the investigator using an optical pyrometer found the brightness of *Mnemiopsis leidyi* to be 0·116 to 0·30 millilambert. Although exact comparison of this value with ours is not possible because of the differences in the methods, rough calculation indicates that it is of the same order of magnitude.

Discussion. There is very little information on the vertical distribution of bioluminescence in the sea. The direct observations in the deep ocean by Beebe (1934) from the bathysphere and by Monod (1954) from the French bathyscaphe are of great interest but report little more than the presence of bioluminescence at all depths down to the greatest depths reached. Monod found much less luminescence near the bottom at 1,400 m than at depths above this. Boden and Kampa (private communication) undertook similar observations with an underwater photometer off Hawaii and off southern California. They found that when the spectral sensitivity of the photometer was limited, differences in the vertical distribution of bioluminescence were recorded as a function of wavelength. They also reported that a correlation seemed to exist between the depth of luminescent activity and the position of a deep scattering layer during the evening migration of the latter.

The present observations show that at the coastal water station the luminescent activity is almost entirely restricted to the cold water beneath the thermocline (Fig. 9). The intensity of the flashes below the thermocline as observed on the microammeter makes it certain that flashes of like intensity would have been observed on the Brush pen recorder at the near-surface level, had they existed, in spite of the much higher background there due to surface illumination.

The maxima of luminescent activity shown for the slope water station (Fig. 10) are at 70 m and 285 m. The observation at 70 m probably represents luminescence activity from euphotic zone inhabitants together with scattering layer animals which are at this and higher levels at the hour of the observation. The maximum at the 285 m level may be partly caused by the non-migrating members of the deep scattering layer (JOHNSON *et al.*, 1956) which is near this depth during daylight hours. The similarity of the records at 70 and 285 m does not indicate equal luminescent activity at these levels since that at 70 m is being displayed against a much higher background of light due not only to surface illumination but to the luminescent activity itself.

The commonest pelagic and bathypelagic sources of bioluminescence are probably found among the protozoans, ctenophores, euphausids, decapod crustaceans, cephalopods, salps, and fishes (HARVEY, 1952). Both intermittent luminescence and the steady condition of luminescence are found among the animals in these groups although the limited information available suggests that the former is the commoner condition. Of the types of animals mentioned we consider the protozoans, ctenophores, and salps the most likely sources at our coastal water station, whereas members of all of the first-mentioned groups might be important at the slope water station.

HARVEY (1952) summarizes what is known about the spectral distribution, intensity, periodicity, and other aspects of bioluminescence in animals. Certain more recent investigations are presented in the volume edited by JOHNSON (1955). However, aside from several fairly well-studied animals, such as the ostracod *Cypridina* and the firefly *Photinus*, precise quantitative information is scarce, particularly for oceanic forms. Thus it appears that we need not only to make further measurements of bioluminescence as a function of depth in the ocean but also to study the luminescent properties of representative individual species from the deep-sea fauna.

Acknowledgements—The authors are indebted to WILLARD DOW and A. L. CARTER for help in combining the Brush pen recording system with the bathyphotometer and to LINCOLN BAXTER II and EARL E. HAYS for help in evaluating the recorder's performance. We also wish to acknowledge the assistance of G. C. MCLEOD and W. L. CLARKE during the measurements at sea and of C. V. MACCOY during the tests of luminescence in the laboratory. Drs. E. NEWTON HARVEY and J. B. HERSEY helpfully criticized the manuscript.

The investigation was supported by funds from Research Grant G-1686 of the National Science Foundation and Contract Nonr 1720(00)(NR-083-116) with the Office of Naval Research and the Bureau of Aeronautics.

Harvard University and Woods Hole Oceanographic Institution. Contribution No. 858 from the Woods Hole Oceanographic Institution.

REFERENCES

BEEBE W. (1934) *Half Mile Down.* Harcourt Brace and Co., New York, 340 pp.

BODEN B. P. (1950) Plankton organisms in the deep scattering layer. *Rept. U.S. Navy Electronics Laboratory* 186, 1-29 (unpublished manuscript).

CLARKE G. L. (1932) Quantitative aspects of the change of phototropic sign in *Daphnia. J. Exp. Biol.* **9**, 180-211.

CLARKE G. L. (1933) Diurnal migration of plankton in the Gulf of Maine and its correlation with changes in submarine irradiation. *Biol. Bull.* **65** (3), 402-436.

CLARKE G. L. (1934a) Further observations on the diurnal migration of copepods in the Gulf of Maine. *Biol. Bull.* **67**, 432-455.

Clarke G. L. (1934b) Factors affecting the vertical distribution of copepods. *Ecol. Mon.*, **4**, 530-540.

Clarke G. L. (1954) *Elements of Ecology*. Ch. 6 Light. John Wiley and Sons, New York, 534 pp.

Clarke G. L. and Wertheim G. K. (1956) Measurements of illumination at great depths and at night in the Atlantic Ocean by means of a new bathyphotometer. *Deep-Sea Res.* **3**, 189-205.

Cushing D. H. (1951) The vertical migration of planktonic crustacea. *Biol. Reviews* **26**, 158-192.

Dietz R. S. (1948) Deep scattering layer in the Pacific and Antarctic Oceans. *J. Mar. Res.* **7**, 430-442.

Hardy A. C. and Bainbridge R. (1954) Experimental observations on the vertical migrations of plankton animals. *J. Mar. Biol. Assoc. U.K.* **33**, 409.

Harris J. E. and Wolfe U. K. (1955) A laboratory study of vertical migration. *Proc. Roy. Soc.* **B144** (916), 329-354.

Harvey E. N. (1952) *Bioluminescence*. New York Academic Press, 632 pp.

Hersey J. B. and Backus R. H. (1954) New evidence that migrating gas bubbles, probably the swim-bladders of fish, are largely responsible for scattering layers on the continental rise south of New England. *Deep-Sea Res.* **1**, 190-191.

Hersey J. B., Johnson H. R. and Davis L. C. (1952) Recent findings about the deep scattering layer. *J. Mar. Res.* **11**, 1-9.

Johnson F. H. (Editor) (1955) The luminescence of biological systems. *Amer. Assoc. Advanc. Sci.*, Washington, D.C., 452 pp.

Johnson H. R., Backus R. H., Hersey J. B. and Owen D. M. (1956) Suspended echo sounder and camera studies of midwater sound scatterers. *Deep-Sea Res.* **3**, 266-272.

Kampa E. M. (1955) A discrepancy between calculation and measurement of submarine illumination. *Proc. Nat. Acad. Sci.* **41**, 938.

Kampa E. M. and Boden B. P. (1954) Submarine illumination and the twilight movements of a sonic scattering layer. *Nature* **174**, 869.

Knott S. T. and Hersey J. B. (1956) High resolution echo sounding techniques and their use in bathymetry, marine geophysics, and biology. *Deep-Sea Res.* **4**, 36.

Marshall N. B. (1951) Bathypelagic fishes as sound scatterers in the ocean. *J. Mar. Res.* **10**, 1-17.

Monod T. (1954) Oceanographie biologique-sur un premier essai d'utilisation scientifique du bathyscaphe F.N.R.S.3. *C. R. Acad. Sci., Paris* **238**, 1951.

Moore H. B. (1950) The relation between the scattering layer and the Euphausiacea. *Biol. Bull.* **99**, 181-212.

Moore H. B. (1955) Variations in temperature and light response within a plankton population. *Biol. Bull.* **108**, 175-181.

Nichols E. L. (1924) The brightness of marine luminescence. *Science* **60**, 592-593.

Tucker G. H. (1951) Relation of fishes and other organisms to the scattering of underwater sound. *J. Mar. Res.* **10**, 215-238.

Waterman T. H., Nunnemacher, R. F., Chace, F. A., Jr. and Clarke, G. L. (1939) Diurnal vertical migration of deep water plankton. *Biol. Bull.* **76**, 256-279.

Printed in Great Britain by The Salisbury Press Ltd., Publicity House, Wilton Road, Salisbury, Wilts. (1106)

Contribution No. 859

G. VERONIS and HENRY STOMMEL

THE ACTION OF VARIABLE WIND STRESSES ON A STRATIFIED OCEAN

Reprint from:

SEARS FOUNDATION: JOURNAL OF MARINE RESEARCH

Volume 15, Number 1, October 15, 1956. P. 43–75

THE ACTION OF VARIABLE WIND STRESSES ON A STRATIFIED OCEAN[1, 2]

BY

G. VERONIS AND HENRY STOMMEL

Institute for Advanced Study, Princeton, N. J.

ABSTRACT

The forced response of a horizontally infinite ocean on a rotating earth to a transient wind system is investigated. In an equilibrium state, the ocean consists of two homogeneous layers of fluid of finite depth, the fluid in the lower layer being slightly denser than that in the upper. The wind system is periodic in space, and its time-dependence is periodic or is given by a step function.

Little energy goes into the inertio-gravity waves for winds that blow longer than a half pendulum day; most of the energy appears as geostrophically balanced Rossby (planetary) waves. Wind systems with periods from a day to a year excite motions which are in part barotropic and in part baroclinic. Winds of long period (100 years or more) excite the (internal) baroclinic Rossby mode, in which the currents are confined to the upper layer. The applicability and oceanographic implications of the model are discussed quantitatively.

1. INTRODUCTION

This paper treats the response of a stratified ocean to time-dependent wind stress systems of various dimensions. The model of the ocean is infinite horizontally, but the wind systems are of finite dimensions.

We anticipate that the density stratification of the ocean will play an important role in the response of ocean to wind. To account for the effect of density variation, a highly idealized structure is introduced, viz., a two-layer ocean with each layer homogeneous in density. This structure is supposed to correspond roughly to the two masses of water above and below the main thermocline in the real ocean.

In accordance with the theoretical framework for the dynamics of

---

[1] Work was sponsored by the Office of Naval Research under Contract No. N-6-ORI-139, Task Order I. Reproduction in whole or in part is permitted for any purpose of the U. S. government.

[2] Contribution No. 859 of the Woods Hole Oceanographic Institution.

Note added in proof. In a recent publication (Veronis, 1956) it was pointed out that this article in the *Journal of Marine Research* contained a wrong conclusion. The mistake referred to has been corrected in this article subsequent to publication of the Veronis (1956) article in *Deep Sea Research.*

Reprint from SEARS FOUND. JOURN. MAR. RES.

currents in central oceanic areas as given by Sverdrup (1947) and Reid (1948), we will neglect horizontal friction due to large scale lateral turbulent processes.

Cases where the effects of coastal boundaries are involved are not considered because of the complexity of the general problem. It is not generally possible therefore to apply the results of this paper to the real ocean in an enclosed basin in the same satisfactory way that theories of the mean steady-state circulation (e. g. Munk, 1950) have been applied. Application of theoretical results must be limited to types of motion (or initial stages of certain types) in which boundaries or coasts do not exert an immediate influence.

Essentially, what we have sought is an understanding of how the two-layer ocean responds to changes in the applied wind. Is the wind-induced velocity (a) confined to the upper layer, (b) nearly the same throughout the depth of the ocean, or (c) a combination of a and b? Correspondingly, how does the interface between the two layers respond in relation to the free surface? (a) Does it respond in such fashion as to keep the horizontal pressure gradients (and hence velocities) negligible in the deep layer? (b) Does it remain essentially unaffected, hence permitting the horizontal pressure gradients to be nearly equal in both layers? (c) Or does it respond as a combination of a and b?[3] From a practical oceanographic point of view, a clear picture as to which of these alternative modes of motion is probable is of great importance in any attempt to relate changes of oceanic circulations to changes in the applied wind stress.

The surface wind-drift currents within the top 100 m are almost always in equilibrium with the wind stress and are measured directly by discrepancies in navigation of ships, while currents in deeper portions of the ocean are inferred from dynamic computations only. It is well known that the latter method fails to detect the barotropic component of velocity.

Despite the fact that there are no satisfactory *direct* measurements of velocity distribution in deep waters beneath the main thermocline, it is quite obvious from a study of the distribution of certain properties such as salinity and dissolved oxygen that these deep waters do not move with the same high mean velocity of the water masses above the main thermocline. Therefore, so far as the mean circulation is concerned, it is certain that the time-mean velocity is essentially baroclinic, and one may be sure that any theory which results in a barotropic mean circulation has some essential physical feature lacking. Barotropic mean currents are excluded by observation; but time-periodic barotropic currents are permissible provided they do not involve horizontal displacements large enough to confuse the picture of the mean distribution of deep ocean properties. For example, ordinary tidal currents are barotropic, but, since the amplitude of the periodic horizontal displacement associated with them is of the order of one kilometer, they produce unobservably small periodic variations in the mean distribution of deep water properties at any fixed point. It is necessary to examine the theoretical implications of any time-variable barotropic flow which might result from the passage of storms, from prolonged disturbances to the circulation, or even from seasonal variations in wind. If the theoretical result requires barotropic modes with periodic horizontal displacements of the deep water of more than, say, 300 km, then it seems safe to say that such a result is in conflict with observation.

---

[3] Motion of the type (a) will be called baroclinic or internal; motion of the type (b) will be referred to as barotropic or external.

Finally, one further test by observation should be mentioned. Barotropic currents set up by a storm might involve a permanent displacement of the deep water in addition to the periodic displacements. The passage of a number of storms, more or less at random, would then result in deep water particles executing horizontal "random walks." This type of mixing process can then be expressed in terms of a coefficient of eddy diffusivity. If theoretically predicted motions of the deep water layers imply an eddy coefficient of much more than 10^8 cm^2 sec^{-1} (Sverdrup, 1939), they are in conflict with observational material.

The history of previous theoretical work on this subject goes back to Rossby (1938) who, in a pioneer theoretical investigation, came to the conclusion that the ocean responds barotropically to variable applied wind stress. Because this result was so surprising and since it might lead to contradictions with observation in some one of the ways mentioned above, Rossby re-examined his results by means of several different models. In addition to the simple case of two homogeneous layers with an abrupt density discontinuity, he studied a case where the density stratification was continuous in the lower layer; and he even considered the effect of placing another thick homogeneous layer beneath the layer of constant stability. Despite these elaborations he was unable to escape the disconcerting conclusion that currents produced by changes in wind stress are almost independent of depth and are not affected significantly by density stratification.

Since Rossby's conclusion is independent of frequency of applied stress (except that it must be less than the inertial frequency), it seems that one must infer that even seasonal fluctuations of winds produce barotropic changes in the circulation, although in this case the boundaries must certainly have some influence on the circulation.

However, if the boundary conditions are *linear*, then they would change only the horizontal distribution of the velocity field, not the fact that velocity is independent of depth. Finally, it is impossible, on the basis of Rossby's model, to account for the fact that the observed mean wind-induced circulation is confined to the upper layer of the ocean. In the latter case, one can point out that bottom friction, which is not included in Rossby's model, might well be important in preventing the mean wind-induced circulation from extending to the bottom, but it could hardly be effective on a time scale such as that of a storm. Despite difficulties in interpreting Rossby's model for long-period wind variations, in which a completely naïve application of the model leads to results that contradict observation, the theoretical conclusions regarding short-period wind variations seemed quite inescapable.

Rossby's model involves a uniform Coriolis parameter. It is important to see what effect the introduction of a *variable* Coriolis parameter would have on Rossby's conclusions, on the grounds that the variable Coriolis parameter is a vital feature of the steady-state wind-driven circulation theories (Sverdrup, Reid, Stommel, Munk, et al.). Its presence in the vorticity equation might modify the response of the ocean to a variable wind system.

A number of other theoretical studies on the time-response of the ocean have been published in the intervening time, and it may be helpful to the reader to see explicitly the relation of the present study to some of the previous ones. A brief summary of the essential characters of these studies is given in Table I.

The theories of Sverdrup (1947), Reid (1948), Stommel (1948), and Munk (1950) are steady-state theories of the circulation set up by a steady wind system. They provide the justification for neglecting horizontal frictional forces in the interior of the ocean.

The theories of Ichiye (1951) and of Veronis and Morgan (1955) are concerned with changes in the total circulation in an enclosed basin due to variations in wind. The papers deal with a homogeneous ocean.

A recent study by Groves (1954) shows some of the features produced in the Rossby (1938) type of model in the presence of a coast, but since the influence of boundaries is not included in the present study, there will be no further occasion to refer to the Groves paper.

An equation for predicting the change in depth of the seasonal thermocline, in terms of the applied wind-stress field alone, has recently been published (Freeman, 1954); this is based on the assumption that the induced velocity field is baroclinic. In view of the fact that no reason has been formed to dismiss Rossby's 1939 demonstration that

TABLE I.

	Boundaries	*Variation of Coriolis parameter*	*Time variability of wind*	*Stratification*
Sverdrup, 1947	+(one)	+	−	−
Stommel, 1948	+	+	−	−
Reid, 1948	+(one)	+	−	+
Stockmann, 1946	+	+	−	+
Munk, 1950; and other similar theories	+	+	−	−
Ichiye, T., 1951	+	+	+	−
Veronis & Morgan, 1955	+	+	+	−
Rossby, 1938	−‡	−	+	+
Cahn, 1945	−‡	−	+	−
Bolin, 1953	−‡	−	+	+
Groves, 1954	+(one)	−	+	+
Charney, 1955	+(two)†	+†	+	+
Freeman, 1954	−	−	+	−*
Present study	−	+	+	+

‡ No fixed boundaries, but initial stream restricted in extent.

† Charney does consider variation of Coriolis parameter with latitude in one portion of his study, but not in the model with boundaries.

* In this case the response of the interface is specified, not determined.

short-period response must be barotropic, such an assumption seems unsubstantiable.

During the latter half of 1954, when J. G. Charney (1955) was preparing a contribution for The Convocation held at Woods Hole in connection with the dedication of the new U. S. Navy Laboratory of Oceanography at Woods Hole, we had an opportunity to read his manuscript and to discuss it at length with him; we are indebted to Dr. Charney for many valuable suggestions. His paper uses the quasigeostrophic approximation throughout. Starting with Rossby's two-layer model, he studies the effects of coastal boundaries and of the variation of Coriolis parameter with latitude. The presence of a coastal boundary tends to favor the baroclinic mode (even in the absence of the variation of Coriolis parameter with latitude), a result which may be of fundamental importance in future theoretical studies of such coastal currents or of the Gulf Stream.

Finally, mention should be made of two papers, by Cahn (1945) and Bolin (1953), in which particular attention is paid to the dispersal of energy from an initially concentrated current system by means of inertio-gravitational waves. Whereas the present study does include gravitational and inertial waves, it cannot produce many of the interesting features of the Cahn and Bolin models. This shortcoming arises from the periodic spatial distribution of applied wind stress in the present study.

2. THE VORTICITY EQUATIONS IN NORMAL MODES

The model which will be considered in the subsequent analysis consists of a horizontally infinite rotating ocean which is of constant depth in the equilibrium state. The density stratification, an idealization of the observed (continuous) density distribution of the ocean, consists of two layers of homogeneous water separated by a surface of discontinuity which corresponds to the mean thermocline. It is assumed that the motions are quasihydrostatic and that no momentum is transmitted across the interface by friction. If the motions are small, the equations may be linearized. Thus

$$\frac{\partial u_1}{\partial t} - fv_1 = -g\frac{\partial \eta_1}{\partial x} + \frac{\tau'}{D_1}, \tag{2.1}$$

$$\frac{\partial v_1}{\partial t} + fu_1 = -g\frac{\partial \eta_1}{\partial y} + \frac{\tau}{D_1}, \tag{2.2}$$

$$\frac{\partial}{\partial t}(\eta_1 - \eta_2) + D_1\left(\frac{\partial u_1}{\partial x} + \frac{\partial v_1}{\partial y}\right) = 0 \quad , \tag{2.3}$$

$$\frac{\partial u_2}{\partial t} - fv_2 = -g\left[a\frac{\partial \eta_1}{\partial x} + b\frac{\partial \eta_2}{\partial x}\right], \tag{2.4}$$

$$\frac{\partial v_2}{\partial t} + fu_2 = -g\left[a\frac{\partial \eta_1}{\partial y} + b\frac{\partial \eta_2}{\partial y}\right], \tag{2.5}$$

$$\frac{\partial \eta_2}{\partial t} + D_2\left(\frac{\partial u_2}{\partial x} + \frac{\partial v_2}{\partial y}\right) = 0 \quad , \tag{2.6}$$

where x (directed eastward) and y (directed northward) are the horizontal co-ordinates; t is time; u_i and v_i ($i = 1, 2$) are the velocities in the x and y directions respectively; D_1 is the equilibrium thickness of the upper layer;[4] η_1 is the deviation of the free surface from its equilibrium position; g is gravity; $f = 2\,\Omega \sin$ (latitude) is the Coriolis parameter; Ω is the angular speed of the earth's rotation; $a = \rho_1/\rho_2$, $b = (\rho_2 - \rho_1)/\rho_2$; ρ_1 is the density of the upper layer; and τ' and τ are stresses in the x and y directions, respectively, exerted on the ocean surface by a wind. Charney (1955) has shown in some detail that it is justifiable to treat the wind stress, which is, of course, actually applied

[4] The terms with subscript $_2$ define similar quantities in the lower layer.

at top surface, as a body force distributed evenly with depth over the entire top layer.

If

$$\eta = \eta_1, \phi = \eta_1 - \eta_2 \tag{2.7}$$

are substituted above, one finds

$$\frac{\partial u_1}{\partial t} - fv_1 = -g\frac{\partial \eta}{\partial x} + \frac{\tau'}{D_1}, \tag{2.8}$$

$$\frac{\partial v_1}{\partial t} + fu_1 = -g\frac{\partial \eta}{\partial y} + \frac{\tau}{D_1}, \tag{2.9}$$

$$\frac{\partial \phi}{\partial t} + D_1\left(\frac{\partial u_1}{\partial x} + \frac{\partial v_1}{\partial y}\right) = 0 \quad , \tag{2.10}$$

$$\frac{\partial u_2}{\partial t} - fv_2 = -g\left[\frac{\partial \eta}{\partial x} - b\frac{\partial \phi}{\partial x}\right], \tag{2.11}$$

$$\frac{\partial v_2}{\partial t} + fu_2 = -g\left[\frac{\partial \eta}{\partial y} - b\frac{\partial \phi}{\partial y}\right], \tag{2.12}$$

$$\frac{\partial}{\partial t}(\eta - \phi) + D_2\left(\frac{\partial u_2}{\partial x} + \frac{\partial v_2}{\partial y}\right) = 0 \quad . \tag{2.13}$$

In the subsequent analysis we propose to take account of the variability of the Coriolis parameter by writing $df/dy = \beta =$ constant whenever f appears in differentiated form. Otherwise f will be assumed constant. Cross differentiating (2.8) and (2.9) and (2.11) and (2.12), we obtain the vorticity equations

$$\frac{\partial \zeta_1}{\partial t} - \frac{f}{D_1}\frac{\partial \phi}{\partial t} + \beta v_1 = \frac{1}{D_1}\left(\frac{\partial \tau}{\partial x} - \frac{\partial \tau'}{\partial y}\right), \tag{2.14}$$

$$\frac{\partial \zeta_2}{\partial t} - \frac{f}{D_2}\frac{\partial}{\partial t}(\eta - \phi) + \beta v_2 = 0\,, \tag{2.15}$$

where $\zeta_1 = \partial v_1/\partial x - \partial u_1/\partial y$ and $\zeta_2 = \partial v_2/\partial x - \partial u_2/\partial y$ are the relative vorticities of the upper and lower layers respectively.

At this point it is assumed that the motions are independent of the y co-ordinate. The effect of β is thereby incorporated into the equations of the simple one-dimensional model. Care must be exercised, however, in the choice of equations which describe the system; otherwise the trivial and uninteresting condition $\beta \equiv 0$ results. Thus, in eliminating all but a single dependent variable, one must not include the curl operation, since now $\partial/\partial y \equiv 0$, and the only possible consequence is $\beta \equiv 0$.

The only set of equations which is consistent with the above remarks is:

$$\frac{\partial^2 v_1}{\partial x \partial t} - \frac{f}{D_1}\frac{\partial \phi}{\partial t} + \beta v_1 = \frac{1}{D_1}\frac{\partial \tau}{\partial x}, \tag{2.16}$$

$$\frac{\partial u_1}{\partial t} - f v_1 = -g\frac{\partial \eta}{\partial x}, \tag{2.17}$$

$$\frac{\partial \phi}{\partial t} + D_1\frac{\partial u_1}{\partial x} = 0, \tag{2.18}$$

$$\frac{\partial^2 v_2}{\partial x \partial t} - \frac{f}{D_2}\frac{\partial}{\partial t}(\eta - \phi) + \beta v_2 = 0, \tag{2.19}$$

$$\frac{\partial u_2}{\partial t} - f v_2 = -g\left[\frac{\partial \eta}{\partial x} - b\frac{\partial \phi}{\partial x}\right], \tag{2.20}$$

$$\frac{\partial}{\partial t}(\eta - \phi) + D_2\frac{\partial u_2}{\partial x} = 0 \quad . \tag{2.21}$$

Eliminating u_1 from (2.17) and (2.18) and substituting the value of v_1 in (2.16) we find for the upper layer

$$r\lambda^2\eta_{xxxt} - \frac{\phi_{xttt}}{f^2} - \phi_{xt} + r\beta\lambda^2\eta_{xx} - \frac{\beta}{f^2}\phi_{tt} = \frac{\tau_{xx}}{f}, \tag{2.22}$$

where $r = D_1/D_2$ and $\lambda^2 = gD_2/f^2$; λ is the quantity Rossby called the radius of deformation.

A similar procedure in the last three equations results in the following equation for the lower layer

$$\lambda^2(\eta - b\,\phi)_{xxxt} - \frac{(\eta - \phi)_{xttt}}{f^2} - (\eta - \phi)_{xt}$$
$$+ \beta\lambda^2(\eta - b\,\phi)_{xx} - \frac{\beta}{f^2}(\eta - \phi)_{tt} = 0 \quad . \tag{2.23}$$

The two equations (2.22) and (2.23) may be used for a detailed study of the response of η and ϕ to the variable wind stress τ, but from an analytical point of view it is much simpler to introduce normal modes, which enable one to separate the two dependent variables in the two vorticity equations without increasing the order of the differential form. Equation (2.23), multiplied by the arbitrary constant α, is added to (2.22) to obtain

$$\lambda^2\Big[(r+\alpha)\,\eta-\alpha b\phi\Big]_{xxxt}-\frac{1}{f^2}\Big[(1-\alpha)\,\phi+\alpha\eta\Big]_{xttt}$$
$$-\Big[(1-\alpha)\,\phi+\alpha\eta\Big]_{xt}+\beta\lambda^2\Big[(r+\alpha)\,\eta-\alpha b\phi\Big]_{xx}$$
$$-\frac{\beta}{f^2}\Big[(1-\alpha)\,\phi+\alpha\eta\Big]_{tt}=\frac{\tau_{xx}}{f}\quad. \qquad (2.24)$$

The conditions

$$(1+\alpha)\,\phi+\alpha\eta=R \quad \text{and} \quad (r+\alpha)\,\eta-\alpha b\phi=kR\,, \qquad (2.25)$$

where k is a constant of proportionality, are sufficient to reduce the equations to a single variable. The above conditions determine α and k by the necessity that

$$k=-\frac{\alpha b}{1-\alpha}=\frac{r+\alpha}{\alpha}\quad. \qquad (2.26)$$

Therefore

$$\alpha=\frac{1-r\pm\sqrt{(1+r)^2-4rb}}{2(1-b)}\,,$$

and

$$\alpha_1\approx\frac{1+r-rb}{(1+r)\,(1-b)}\,,\qquad \alpha_2\approx\frac{-r\,(1+r-b)}{(1+r)\,(1-b)}\,,$$
$$k_1\approx 1+r\,,\qquad k_2\approx\frac{rb}{1+r}\,. \qquad (2.27)$$

The two values of R (two normal modes corresponding to the two values of α) are

$$R_i=(1-\alpha_i)\,\phi_i+\alpha_i\eta \qquad (i=1,2)\,. \qquad (2.28)$$

Thus (2.24) may be written

$$\lambda^2 k_i\,R_{ixxxt}-\frac{1}{f^2}R_{ixttt}-R_{ixt}+\beta\lambda^2 k_i\,R_{ixx}-\frac{\beta}{f^2}R_{itt}=\frac{\tau_{xx}}{f}\quad. \qquad (2.29)$$

These will be referred to as the equations of normal modes. Once the normal modes have been determined, it is possible to obtain other more primitive quantities, such as elevation of the free surface and interface, as well as the velocities in each layer from definitions (2.27), (2.28) and equations (2.17), (2.18), (2.20), (2.21); e.g.,

$$\phi=\frac{\alpha_2\,R_1-\alpha_1\,R_2}{\alpha_2-\alpha_1}\,, \qquad (2.30)$$

$$\eta = \frac{(\alpha_2 - 1)\,R_1 - (\alpha_1 - 1)\,R_2}{\alpha_2 - \alpha_1} \quad . \tag{2.31}$$

3. FREE WAVES

In subsequent sections we shall have occasion to refer to various wave motions which are induced by the action of a transient wind stress on the sea surface. It is appropriate therefore to consider the free waves which are inherent in the normal mode equations and to study thereby the behavior of the solutions. A clear picture of the free wave motions is also desirable because it helps in visualizing certain resonance phenomena which occur in cases where the wind stress is periodic in time.

Consider a normal mode of the form

$$R_i = S_i \sin (lx + \omega_i t) \quad , \tag{3.1}$$

where S_i = const. and where l is the wave number associated with the wave length L, i.e. $l = 2\pi/L$. The assumed form of the normal mode is therefore a wave progressing in the negative x direction when the frequency ω_i is positive. Substituting R_i into (2.29), we find that the equations reduce to a pair of frequency equations of the form

$$\left(\frac{\omega_i}{f}\right)^3 - \frac{\beta}{fl}\left(\frac{\omega_i}{f}\right)^2 + (1 + \mu_i^2)\,\frac{\omega_i}{f} + \frac{\beta \mu_i^2}{lf} = 0 \quad (i = 1, 2)\,, \tag{3.2}$$

where $\mu_i^2 = k_i\, l^2 \lambda^2$. The solutions of the algebraic equations (3.2) give the frequency ω_i in terms of the wave number l.

From an oceanographic point of view, only a limited range of values of l is of interest, and it will be demonstrated that the approximate roots of the cubic equation within this range of values of l are:

$$\omega_{i1} = \frac{\beta}{l}\,\frac{\mu_i^2}{\gamma_i}\,, \tag{3.3}$$

$$\omega_{i2} = \frac{\beta}{2l\gamma_i} + \sqrt{\left(\frac{\beta}{2\gamma_i l}\right)^2 + \frac{4\beta^2\mu_i^2}{l^2\gamma_i^2} + 4f^2\gamma_i}\,, \tag{3.4}$$

$$\omega_{i3} = \frac{\beta}{2l\gamma_i} - \sqrt{\left(\frac{\beta}{2\gamma_i l}\right)^2 + \frac{4\beta^2\mu_i^2}{l^2\gamma_i^2} + 4f^2\gamma_i}\,, \tag{3.5}$$

where $\gamma_i = 1 + \mu_i^2$. In order to indicate the degree of approximation involved in these expressions for the roots, the original cubic equation may be compared with the expression

$$\frac{1}{f^3}\,(\omega_i - \omega_{i1})\,(\omega_i - \omega_{i2})\,(\omega_i - \omega_{i3}) = 0$$

or

$$\left(\frac{\omega_i}{f}\right)^3 - \frac{\beta}{fl}\left(\frac{\omega_i}{f}\right)^2 - (1 + \mu_i^2)\left(\frac{\omega_i}{f}\right) + \frac{\beta\mu_i^2}{fl}(1 + \varepsilon_i) = 0\,,$$

where $\varepsilon_i = \dfrac{\beta^2\mu_i^2}{l^2 f^2 \gamma_i^3}$. The original cubic frequency equation is distinguished from the approximate equation only by the absence of the term ε_i. In order to ascertain the limitations of the approximations, we consider an ocean model with the following properties

$$\begin{aligned} D_1 &= 500\ \text{m} & \beta &= 2 \times 10^{-11}\text{m}^{-1}\text{sec}^{-1} \\ D_2 &= 3500\ \text{m} & f &= 10^{-4}\text{sec}^{-1} \\ r &= 1/7 & b &= 2 \times 10^{-3}. \end{aligned}$$

Then

$$\begin{aligned} \lambda^2 &= 3.5 \times 10^{12}\text{m}^2 & \varepsilon_1 &\leq .16 \text{ for all } l \\ k_1 &\approx 8/7 & \varepsilon_2 &\leq 4 \times 10^{-6} \text{ for all } l\,. \\ k_2 &\approx 2.5 \times 10^{-4} \end{aligned}$$

The largest values of ε_i occur for $l = 0$, i.e., for an infinite wave length L. Since L will be restricted by $L \leq 12{,}000$ km, the practical upper limit of ε_1 is .02. Therefore the approximate roots are actually close to the real ones.

The phase velocity and frequency of these various waves are shown in Fig. 1 for the range of wave lengths 10 km $\leq L \leq$ 12,000 km.

The six wave motions may be separated into two categories. The waves with frequency ω_{11} and ω_{21} represent the geostrophically balanced current motions; ordinarily they contain the measurable flow in the ocean. The remaining four waves arise from a completely different source, viz., the unbalance between Coriolis and pressure forces. These inertio-gravitational motions will often be referred to as "transient" motions, since in a nonperiodic model their energy would be rapidly dispersed into the outlying regions (see Cahn, 1945).

Specifically, the waves with frequency ω_{11} and ω_{21} are barotropic and baroclinic Rossby waves, respectively, moving toward the west. They determine the external and internal geostrophic response of the ocean to an applied wind stress. For scales of motion most often encountered in the ocean, i.e. $L \geq 1{,}000$ km, the isostatic Rossby wave merges into a nondispersive type of wave.

For the smaller wave lengths ($L \leq 2{,}000$ km), the ω_{12} and ω_{13} waves are barotropic gravity waves of the familiar nondispersive type moving to the west and east respectively. For larger wave lengths, the waves become dispersive waves of the Sverdrup type (Sverdrup, 1926), although this characteristic of their behavior is practically unnoticeable except for long waves, $L \geq 6{,}000$ km. In

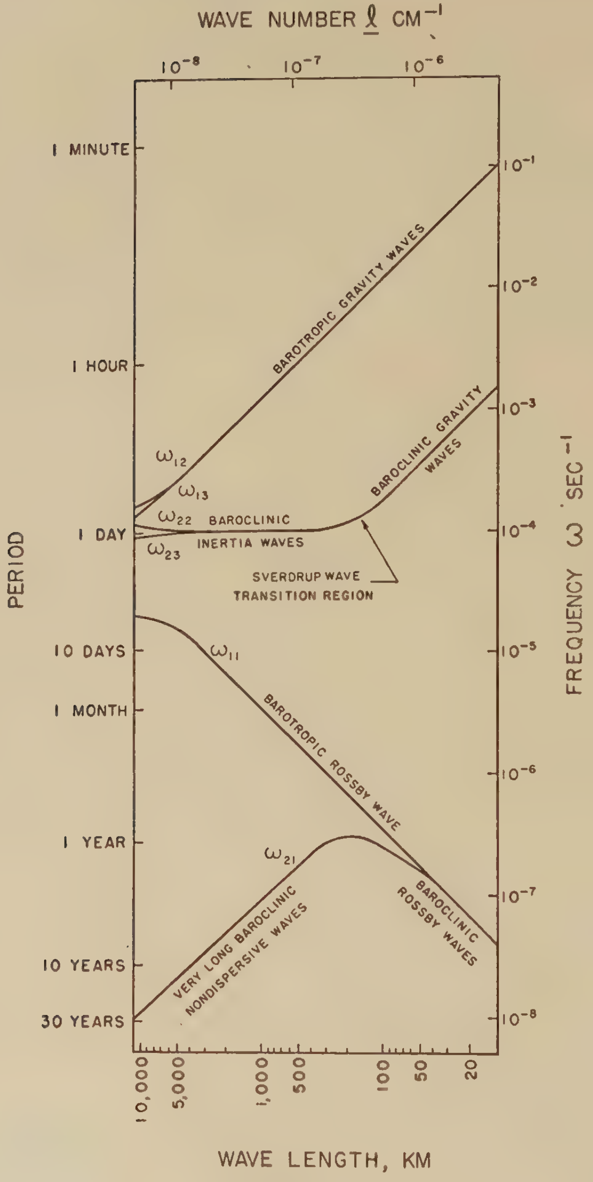
WAVE NUMBER ℓ CM⁻¹
10⁻⁸
10⁻⁷
10⁻⁶
1 MINUTE
1 HOUR
1 DAY
10 DAYS
1 MONTH
1 YEAR
10 YEARS
30 YEARS
PERIOD
10⁻¹
10⁻²
10⁻³
10⁻⁴
10⁻⁵
10⁻⁶
10⁻⁷
10⁻⁸
FREQUENCY ω SEC⁻¹
BAROTROPIC GRAVITY WAVES
BAROCLINIC GRAVITY WAVES
ω12
ω13
ω22
BAROCLINIC
INERTIA WAVES
ω23
SVERDRUP WAVE
TRANSITION REGION
ω11
BAROTROPIC ROSSBY WAVE
ω21
VERY LONG BAROCLINIC
NONDISPERSIVE WAVES
BAROCLINIC
ROSSBY WAVES
10,000
5,000
1,000
500
100
50
20
WAVE LENGTH, KM

Figure 1

the latter range, both the earth's rotation and the variation of the Coriolis parameter affect the velocities of propagation; thus the westward moving waves ω_{12} move faster than long gravity waves and the eastward moving waves ω_{13} move more slowly.

The waves ω_{22} and ω_{23} are baroclinic waves moving to the west and east respectively. For extremely small scale motions ($L \leq 100$ km), they take the form of internal long gravity waves (speed $\sqrt{bgD_1}$). For somewhat larger wave lengths (100 km $\leq L \leq$ 400 km) they are of the Sverdrup type. For the more realistic values $L > 400$ km they are essentially inertial waves with a period of a half pendulum day.

Since the properties of the various types of waves have been discussed in the literature they will not be considered here in any more detail. Baroclinic and barotropic long gravity, Sverdrup, and inertial waves are discussed in Proudman (1953). Barotropic Rossby waves are discussed by Rossby (1949) and Yeh (1949).

4. MOTIONS CAUSED BY MOVING WIND SYSTEM

As the simplest case of a time-dependent wind stress, consider the y component of wind stress to be of the form

$$\tau = W \sin (lx + \nu t).\text{[5]} \tag{4.1}$$

The modes excited by the present form of τ are

$$R_i = S_i \sin (lx + \nu t) \quad , \tag{4.2}$$

where frequency and wave number of the forced motion are the same as those of the stress field. The amplitudes S_i of the normal modes are determined from the vorticity equations (2.29) and are

$$S_i = \frac{Wl}{f^2 \mathfrak{D}_i(\nu, l)} , \tag{4.3}$$

where

$$\mathfrak{D}_i(\nu, l) = \left(\frac{\nu}{f}\right)^3 - \frac{\beta}{lf}\left(\frac{\nu}{f}\right)^2 - (1 + \mu_i^2)\frac{\nu}{f} + \frac{\beta}{lf}\mu_i^2 . \tag{4.4}$$

From S_i, the physical quantities may be determined immediately by means of relations

---

[5] In this case, τ could be interpreted as wind stress caused by (slowly) moving large-scale wind systems such as those obtained from five-day-mean weather charts. Reasonable values for the frequency ν and for the wave-number l are $\nu = -5 \times 10^{-5}$ sec^{-1} and $l = 10^{-6}\ m^{-1}$. These correspond to a period of about two weeks and to a wave-length of 6,000 km. The system moves toward the east and ν is therefore negative. W, the amplitude of stress, is constant.

$$\begin{aligned}
\phi &= \frac{rS_1 + S_2}{1 + r} & u_1' &= -\frac{\nu}{D_1 l}\phi' \\
\eta_1' &= S_1 + \frac{b}{(1 + r)^2} S_2 & u_2' &= -\frac{\nu}{D_2 l}\eta_2' \\
\eta_2' &= \frac{S_1 - S_2}{1 + r} & v_1' &= \frac{\nu}{f}u_1 + \frac{gl}{f}\eta_1'
\end{aligned} \tag{4.5}$$

$$v_2' = \frac{\nu}{f}u_2' + \frac{gl}{f}(\eta_1' - b\phi') ,$$

where

$$\begin{aligned}
(\phi, \eta_1, \eta_2, u_1, u_2) &= (\phi', \eta_1', \eta_2', u_1', u_2') \sin (lx + \nu t) \\
(v_1, v_2) &= (v_1', v_2') \cos (lx + \nu t) .
\end{aligned} \tag{4.6}$$

The exact forms for the solutions will not be written here since they will not be used.

It is apparent that resonance will occur in the present system where the denominator $\mathfrak{D}_i(\nu, l)$ vanishes. Specifically, the resonant frequencies correspond to those of the various free waves (Section 3). An eastward moving wind system can excite resonance only for the internal and barotropic inertio-gravity waves since there are no eastward moving Rossby waves. Since natural wind systems rarely move to the west, there is no point in considering the cases $\nu > 0$.

In footnote 4 we noted that the present form of the wind stress could correspond to slowly moving patterns of ridges and troughs in the atmosphere. The frequencies of these atmospheric motions correspond to periods of the order of several weeks. If such low frequencies are assumed, the quantities $\mathfrak{D}_i(\nu, l)$ are given approximately by

$$\begin{aligned}
\mathfrak{D}_1(\nu, l) &= -(1 + \mu_1^2)\frac{\nu}{f} + \frac{\beta}{lf}\mu_1^2 \\
\mathfrak{D}_2(\nu, l) &= -(1 + \mu_2^2)\frac{\nu}{f} + \frac{\beta}{lf}\mu_2^2 ,
\end{aligned} \tag{4.7}$$

where ν/f is negative.

Consider the case where $l = 10^{-6}\text{m}^{-1}$ (corresponding to a wave length of approximately 6 000 km). If we use here the values of the physical quantities D_1, D_2, etc. which were perscribed in Section 3, then $\mu_1^2 = 4$ and $\mu_2^2 = .88 \times 10^{-3}$. It is apparent, therefore, that the $\mathfrak{D}_i(\nu, l)$ given by (4.7) can be further simplified for certain ranges of ν/f. Thus

$$
\begin{array}{ll}
\left.\begin{array}{r}\text{Range 1: } 10^{-2} \leq -\dfrac{\nu}{f} \leq 10^{-1} \\ \text{or } 70 \text{ days} \geq T \geq 7 \text{ days}\end{array}\right\} \text{yields} & \left\{\begin{array}{l}\mathfrak{D}_1(\nu, l) = -(1+\mu_1^2)\dfrac{\nu}{f} + \dfrac{\beta}{lf}\mu_1^2 \\ \mathfrak{D}_2(\nu, l) \approx -\dfrac{\nu}{f}\ ,\end{array}\right. \\[3ex]
\left.\begin{array}{r}\text{Range 2: } 2 \times 10^{-3} \leq -\dfrac{\nu}{f} < 10^{-2} \\ \text{or 1 year} \geq T > 70 \text{ days}\end{array}\right\} \text{yields} & \left\{\begin{array}{l}\mathfrak{D}_1(\nu, l) \approx \dfrac{\beta}{lf}\mu_1^2 \\ \mathfrak{D}_2(\nu, l) \approx -\dfrac{\nu}{f}\ ,\end{array}\right. \\[3ex]
\left.\begin{array}{r}\text{Range 3: } 0 \leq -\dfrac{\nu}{f} \leq 2 \times 10^{-5} \\ \text{or T} \geq 100 \text{ years}\end{array}\right\} \text{yields} & \left\{\begin{array}{l}\mathfrak{D}_1(\nu, l) \approx \dfrac{\beta}{lf}\mu_1^2 \\ \mathfrak{D}_2(\nu, l) \approx \dfrac{\beta}{lf}\mu_2^2\ ,\end{array}\right.
\end{array}
\tag{4.8}
$$

where $T = -2\pi/\nu$ is the period.

The first range, corresponding to periods which are considerably longer than those of the inertio-gravitational motions, is still comparable to the period of the barotropic Rossby wave; this initial range contains magnitudes that are comparable to observed phenomena in the atmosphere (see footnote 4). Range 2 represents periods which are much longer than the barotropic but shorter than the baroclinic Rossby wave period. The final range exceeds the internal Rossby wave period by at least a factor of 10.

In Range 1, the crosswind velocity component in the upper layer u_1 is simply the Ekman frictional wind-drift velocity directed to the right of the applied wind stress. It is independent of period. This is depicted in Fig. 2, which contains the amplitudes of the four velocities as well as the two surface heights for Range 1, with the magnitude of the wind-stress $W = 1$ cm²/sec². Since the crosswind velocity in the upper layer is independent of period, its total effect on the mass distribution is increased with increasing period. Thus the divergences are larger and the thermocline is displaced further. Fig. 2 shows that the thermocline response is linearly proportional to the period. The free surface deviation is small in this range (less than 2 cm), and for larger periods in the range it is also proportional to the period. The crosswind velocity in the lower layer u_2 tends to compensate for the divergence caused by u_1 in the upper layer. Since it is a function of the free surface deviation as well as of the thermocline response, it is not exactly constant in this range.

The downwind velocities, mainly geostrophic in the large period end of this range, are proportional to period there. It is interesting to note that, for the small periods, the accelerative (nongeostrophic)

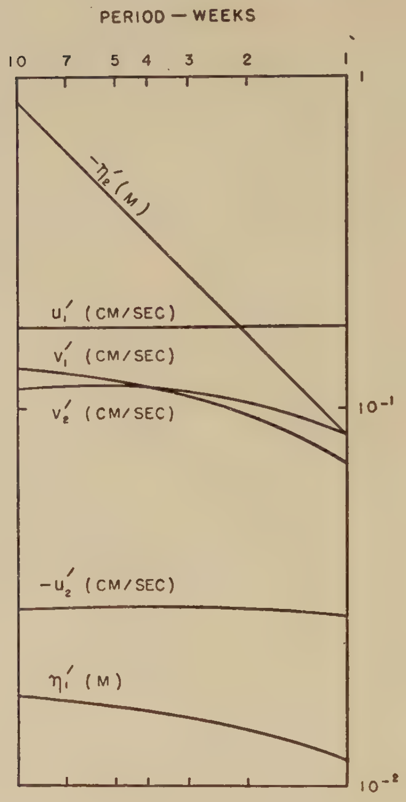

Figure 2

effects which tend to retard the motion are quite prominent, representing roughly 20% of the contribution to the downstream velocity. Since these effects are considerably stronger in the upper layer (where wind stress is a direct cause of the unbalanced state), the downwind velocity of the upper layer is actually smaller than that of the lower layer. The accelerative effects become negligible for a period longer than four weeks. It is evident also that the principal response of the system throughout Range 1 is barotropic. Near the large period end of the range, internal effects become important.

The periods contained in Range 2 represent the seasonal to yearly variations in the wind stress systems. Although boundary effects must certainly become important for such long periods, the results of the present investigation yield some features which are of interest and which will therefore be given here.

The solutions of the two modes are

$$S_1 = \frac{Wf}{\beta g(D_1 + D_2)}, \qquad S_2 = -\frac{Wl}{f^2(\nu/f)}, \tag{4.9}$$

and the physical variables become (approximately)

$$\eta_1{}' = \frac{Wf}{\beta g(1+r)D_2} - \frac{Wlb}{(1+r)^2 f^2(\nu/f)}, \tag{4.10}$$

$$\eta_2{}' = \frac{Wl}{(1+r)\, f^2(\nu/f)}, \tag{4.11}$$

$$u_1{}' = \frac{W}{(1+r)\, D_1 f}, \tag{4.12}$$

$$u_2{}' = -\frac{W}{(1+r)\, D_2 f}, \tag{4.13}$$

$$v_1{}' = \frac{Wgl}{(1+r)f}\left[\frac{f}{\beta g D_2} - \frac{bl}{(1+r)\, f^2(\nu/f)}\right], \tag{4.14}$$

$$v_2{}' = \frac{Wl}{(1+r)\beta D_2} \quad . \tag{4.15}$$

When interpreting results for the present range, one must keep in mind the fact that Range 2 corresponds to periods which are considerably longer than the barotropic Rossby wave period but shorter than the baroclinic Rossby wave period. However, in $\eta_1{}'$ and $v_1{}'$ the effect of the internal Rossby wave period appears. The longer the period, the larger the effect of this internal wave.

The following facts are evident from an inspection of (4.10) to (4.15):

(a) The crosswind velocity component in the upper layer is simply the Ekman frictional wind-drift current and is independent of the period. In the lower layer there is a compensating (baroclinic) counterflow.

(b) The thermocline response is directly proportional to the period.

(c) The downwind lower layer velocity, essentially constant, is unaffected by variations in the period.

The free surface deviation $\eta_1{}'$ and the downwind upper layer velocity $v_1{}'$ are dependent on the period. In each case the variable has a constant value upon which is superposed the baroclinic Rossby wave effect (proportional to period). The velocity $v_1{}'$ exceeds the lower layer velocity $v_2{}'$ by the amount $-\dfrac{bgl^2W}{(1+r)f^3(\nu/f)} = 1.53 \times 10^{-4}$

(f/ν) cm sec^{-1}. For the longest period in this range, i.e., $T \approx$ one year, this excess value is approximately half of the constant value $\dfrac{Wl}{(1+r)D_2\beta}$. The baroclinic effect has therefore become quite important for this extreme value.

For Range 3, the periods are much longer than the internal Rossby wave period. Both D_1 and D_2 and consequently all of the coefficients of the physical quantities are independent of frequency. The flow in this range is now a quasisteady flow. Thus

$$\begin{aligned}
\eta_1' &= -\frac{1}{r}\frac{Wl^2}{\beta f \mu_1^2},\\
\eta_2 &= \frac{1}{rb(1+r)}\frac{Wl^2}{\beta f \mu_1^2},\\
v_2' &= u_1' = u_2' = 0\,,\\
v_1' &= \frac{Wl}{\beta D_1}\,.
\end{aligned}$$

The velocities are all contained in the upper layer. The total transport Wl/β is equal to that given by Munk (1950) for the steady-state model $\nu/f \to 0$. In this range of long period variations the flow is geostrophic.

5. MOTIONS CAUSED BY STORMS

We shall consider next a simple transient model, i.e., one in which all of the wave motions discussed in Section 3 are present. It is assumed that the ocean is initially at rest and that a wind stress begins to act on the ocean surface at time $t = 0$. The y-component of the stress is

$$\begin{aligned}
\tau &= 0\,, & t &< 0\,,\\
\tau &= W\cos lx\,, & t &> 0\,.
\end{aligned} \tag{5.1}$$

The effect of a storm on oceanic motions can be investigated with the present model by the simple expedient of adding the new condition $\tau = 0$ for $t > t_0$, where t_0 is, say, four or five days. A more realistic wind stress resulting from the passage of a storm is a moving wave which starts at $t = 0$, i.e.

$$\begin{aligned}
\tau &= 0\,, & t &< 0\,,\\
\tau &= W\cos(lx + \nu t)\,, & t &> 0\,.
\end{aligned} \tag{5.2}$$

Except for possible resonance effects, the progressive storm, as opposed to a fixed storm, reduces the importance of the inertio-gravitational motions. However, since we are primarily interested in the qualitative effect of the initial unbalance and since the moving storm adds nothing new to the qualitative behavior, we shall confine our attention to the wind stress defined by (5.1).

The solution of the normal mode equations (2.29), with the wind stress τ given by (5.1), is[6]

$$R_1 = Wlf \left\{ \frac{\cos lx - \cos (lx + \omega_{11} t)}{\frac{\beta}{l} f^2 \mu_1^2} + \frac{\cos (lx + \omega_{12} t)}{2f^3 [1 + \mu_1^2]^{3/2}} - \frac{\cos (lx + \omega_{13} t)}{2f^3 [1 + \mu_1^2]^{3/2}} \right\}, \tag{5.3}$$

$$R_2 = Wlf \left\{ \frac{\cos lx - \cos (lx + \omega_{21} t)}{\frac{\beta}{l} f^2 \mu_2^2} + \frac{\cos (lx + \omega_{22} t)}{2f^3 (1 + \mu_2^2)^{3/2}} - \frac{\cos (lx + \omega_{23} t)}{2f^3 (1 + \mu_2^2)^{3/2}} \right\}, \tag{5.4}$$

where

$$\omega_{11} = \frac{\beta \mu_1^2}{l (1 + \mu_1^2)}, \quad \omega_{12} = \frac{\beta \mu_2^2}{l (1 + \mu_2^2)},$$

$$\omega_{12} = f \sqrt{1 + \mu_1^2} + \frac{\beta}{2l (1 + \mu_1^2)}, \quad \omega_{22} = f \sqrt{1 + \mu_2^2} + \frac{\beta}{2l (1 + \mu_2^2)}, \tag{5.5}$$

$$\omega_{13} = - f \sqrt{1 + \mu_1^2} + \frac{\beta}{2l (1 + \mu_1^2)}, \quad \omega_{23} = - f \sqrt{1 + \mu_2^2} + \frac{\beta}{2l (1 + \mu_2^2)}.$$

The velocities and surface heights can now be determined from (2.30), (2.31), (2.8), (2.10), (2.11), (2.13)

---

[6] The solution is approximate, terms of order $\beta^2 k_i^2 \lambda^2 / f^2 \gamma_i^3$ having been considered small when compared to unity. This restriction is the same as the one used in Section 3 for the approximate roots of the frequency equation. The simpler forms for the frequencies, as given below, are also subject to the same approximation within the range of wave lengths of interest.

$$
\begin{aligned}
\phi = \frac{Wlf}{r+1}\Bigg\{ & \frac{l}{\beta f^2}\left[\frac{r}{\mu_1{}^2}+\frac{1}{\mu_2{}^2}\right]\cos lx - \frac{lr\cos(lx+\omega_{11}t)}{\beta f^2\mu_1{}^2} \\
& - \frac{l\cos(lx+\omega_{21}t)}{\beta f^2\mu_2{}^2} + \frac{r}{2f^3(1+\mu_1{}^2)^{3/2}}\Big[\cos(lx+\omega_{12}t) \\
& - \cos(lx+\omega_{13}t)\Big] + \frac{1}{2f^3(1+\mu_2{}^2)^{3/2}}\Big[\cos(lx+\omega_{22}t) \\
& - \cos(lx+\omega_{23}t)\Big]\Bigg\} \quad ,
\end{aligned} \tag{5.6}
$$

$$
\begin{aligned}
\eta = \eta_1 = Wl\Bigg\{ & \frac{l\cos lx}{\beta fr\,(r+1)\,\mu_1{}^2} - \frac{l\cos(lx+\omega_{11}t)}{\beta f\mu_1{}^2} - \frac{l\cos(lx+\omega_{21}t)}{\beta rf\mu_1{}^2} \\
& + \frac{1}{2f^2(1+\mu_1{}^2)^{3/2}}\Big[\cos(lx+\omega_{12}t) - \cos(lx+\omega_{13}t)\Big] \\
& + \frac{b}{2f^2(1+r)^2(1+\mu_2{}^2)^{3/2}}\Big[\cos(lx+\omega_{22}t) - \cos(lx+\omega_{23}t)\Big]\Bigg\} \quad ,
\end{aligned} \tag{5.7}
$$

$$
\begin{aligned}
\eta_2 = \frac{Wla}{1+r}\Bigg\{ & \frac{l}{\beta f}\left(\frac{1}{\mu_1{}^2}-\frac{1}{\mu_2{}^2}\right)\cos lx - \frac{l\cos(lx+\omega_{11}t)}{\beta f\mu_1{}^2} \\
& + \frac{l\cos(lx+\omega_{21}t)}{\beta f\mu_2{}^2} + \frac{\cos(lx+\omega_{12}t) - \cos(lx+\omega_{13}t)}{2f^2(1+\mu_1{}^2)^{3/2}} \\
& - \frac{\cos(lx+\omega_{22}t) - \cos(lx+\omega_{23}t)}{2f^2(1+\mu_2{}^2)^{3/2}}\Bigg\} \quad ,
\end{aligned} \tag{5.8}
$$

$$
\begin{aligned}
u_1 = -\frac{W}{D_1(1+r)}\Bigg\{ & -\frac{l\omega_{11}\,r\cos(lx+\omega_{11}t)}{\beta f\mu_1{}^2} - \frac{l\omega_{21}\cos(lx+\omega_{21}t)}{\beta f\mu_2{}^2} \\
& + \frac{r}{2f^2(1+\mu_1{}^2)^{3/2}}\Big[\omega_{12}\cos(lx+\omega_{12}t) - \omega_{13}\cos(lx+\omega_{13}t)\Big] \\
& + \frac{1}{2f^2(1+\mu_2{}^2)^{3/2}}\Big[\omega_{22}\cos(lx+\omega_{22}t) - \omega_{23}\cos(lx+\omega_{23}t)\Big] \quad ,
\end{aligned} \tag{5.9}
$$

$$
\begin{aligned}
u_2 = -\frac{Wa}{D_2(1+r)}\Bigg\{ & -\frac{l\omega_{11}\cos(lx+\omega_{11}t)}{\beta f\mu_1{}^2} + \frac{l\omega_{21}\cos(lx+\omega_{21}t)}{\beta f\mu_2{}^2} \\
& + \frac{\omega_{12}\cos(lx+\omega_{12}t) - \omega_{13}\cos(lx+\omega_{13}t)}{2f^2(1+\mu_1{}^2)} \\
& - \frac{\omega_{22}\cos(lx+\omega_{22}t) - \omega_{23}\cos(lx+\omega_{23}t)}{2f^2(1+\mu_2{}^2)^{3/2}}\Bigg\} \quad ,
\end{aligned} \tag{5.10}
$$

$$\begin{aligned} v_1 = &- \frac{W}{(1+r)D_1} \left\{ \frac{\omega_{11}^2 rl \sin(lx + \omega_{11}t)}{\beta f^2 \mu_1^2} + \frac{l\omega_{21}^2 \sin(lx + \omega_{21}t)}{\beta f^2 \mu_2^2} \right. \\ &+ \frac{r}{2f^3(1+\mu_1^2)^{3/2}} \left[-\omega_{12}^2 \sin(lx + \omega_{12}t) + \omega_{13}^2 \sin(lx + \omega_{13}t) \right] \\ &\left. + \frac{1}{2f^3(1+\mu_2^2)^{3/2}} \left[-\omega_{22}^2 \sin(lx + \omega_{22}t) + \omega_{23}^2 \sin(lx + \omega_{23}t) \right] \right\} \\ &+ Wl^2g \left\{ \frac{-l(1+r)\sin lx}{\beta f^2 r \mu_1^2} + \frac{l \sin(lx + \omega_{11}t)}{\beta f^2 \mu_1^2} + \frac{l \sin(lx + \omega_{21}t)}{\beta f^2 r \mu_1^2} \right. \\ &- \frac{1}{2f^3(1+\mu_1^2)^{3/2}} \left[\sin(lx + \omega_{12}t) - \sin(lx + \omega_{13}t) \right] \\ &\left. - \frac{b}{2f^3(1+r)^2(1+\mu_2^2)^{3/2}} \left[\sin(lx + \omega_{22}t) - \sin(lx + \omega_{23}t) \right] \right\} , \end{aligned} \tag{5.11}$$

$$\begin{aligned} v_2 = &- \frac{Wa}{(1+r)D_2} \left\{ \frac{l\omega_{11}^2 \sin(lx + \omega_{11}t)}{\beta f^2 \mu_1^2} - \frac{l\omega_{21}^2 \sin(lx + \omega_{21}t)}{\beta f^2 \mu_2^2} \right. \\ &- \frac{\omega_{12}^2 \sin(lx + \omega_{12}t) - \omega_{13}^2 \sin(lx + \omega_{13}t)}{2f^3(1+\mu_1^2)^{3/2}} \\ &\left. + \frac{\omega_{22}^2 \sin(lx + \omega_{22}t) - \omega_{23}^2 \sin(lx + \omega_{23}t)}{2f^3(1+\mu_2^2)^{3/2}} \right\} \\ &+ Wl^2g \left\{ \frac{-l \sin(lx + \omega_{21}t) + l \sin(lx + \omega_{11}t)}{\beta f^2 \mu_1^2} \right. \\ &- \frac{\sin(lx + \omega_{12}t) - \sin(lx + \omega_{13}t)}{2f^3(1+\mu_1^2)^{3/2}} \\ &\left. + \frac{br\left[\sin(lx + \omega_{22}t) - \sin(lx + \omega_{23}t)\right]}{2f^3(1+r)^2(1+\mu_2^2)^{3/2}} \right\} . \end{aligned} \tag{5.12}$$

From the above form of the solutions it can be seen that the various contributions consist of a stationary meridional flow and/or the six progressive waves discussed in Section 3. Comparison of the upper and lower layer velocities shows that amplitudes of the barotropic waves in the lower layer are essentially equal to those of the upper layer. The amplitude of the internal wave contributions of the lower layer differ by the factor $-r$. The stationary wave is not present in the lower layer since it is a direct consequence of wind action. With these facts in mind, only upper layer velocities and surface heights will be discussed in the remaining portion of this section.

As stated earlier, the waves with second subscript equal to unity are the geostrophically balanced Rossby waves (see also Charney, 1955). Representing the geostrophic current motions, they are the features of flow which are ordinarily measurable. The remaining four terms are accelerative effects and have periods of less than a half pendulum day. Thus, for studies of motions with a sufficiently large time scale (say, two weeks or longer), the Rossby waves represent the essential form of the solution.

TABLE II.

Values of ω_i for three values of L.

	L = 200 km	L = 2000 km	L = 8000 km
ω_{11}	6.32×10^{-7} sec^{-1}	6.17×10^{-6} sec^{-1}	1.81×10^{-5} sec^{-1}
ω_{12}	6.22×10^{-3} sec^{-1}	6.3×10^{-4} sec^{-1}	1.91×10^{-4} sec^{-1}
ω_{13}	-6.22×10^{-3} sec^{-1}	-6.3×10^{-4} sec^{-1}	-1.83×10^{-4} sec^{-1}
ω_{21}	2.95×10^{-7} sec^{-1}	5.53×10^{-8} sec^{-1}	1.38×10^{-8} sec^{-1}
ω_{22}	1.37×10^{-4} sec^{-1}	1.03×10^{-4} sec^{-1}	1.13×10^{-4} sec^{-1}
ω_{23}	-1.37×10^{-4} sec^{-1}	$-.97 \times 10^{-4}$ sec^{-1}	$-.87 \times 10^{-4}$ sec^{-1}

The coefficients of the various wave contributions of η_1, η_2 and u_1. The three (vertical) values given for each coefficient are for L = 200, 2000, and 8000 km.

Coefficient of	η_1 (in m)	η_2 (in m)	u_1 (in cm/sec)
$\cos lx$	.3	−150	—
	.3	−150	—
	.3	−150	—
$\cos(\omega_{11}t+lx)$	.0375	3.3×10^{-2}	1.9×10^{-5}
	.0375	3.3×10^{-2}	1.8×10^{-3}
	.0375	3.3×10^{-2}	2.1×10^{-2}
$\cos(\omega_{21}t+lx)$	.2625	150	.276
	.2625	150	.54
	.2625	150	.153
$\cos(\omega_{12}t+lx)$	1.8×10^{-6}	1.65×10^{-6}	-9.2×10^{-6}
	1.8×10^{-6}	1.6×10^{-4}	-9×10^{-4}
	1.8×10^{-6}	-1.6×10^{-4}	-1.1×10^{-2}
$\cos(\omega_{13}t+lx)$	-1.8×10^{-6}	-1.65×10^{-6}	-9.2×10^{-6}
	-1.8×10^{-6}	-1.6×10^{-4}	-9×10^{-4}
	-1.8×10^{-6}	-1.6×10^{-4}	-1.1×10^{-2}
$\cos(\omega_{22}t+lx)$	2.8×10^{-4}	1.6×10^{-1}	− .11
	7.3×10^{-5}	4.1×10^{-2}	− .27
	1.8×10^{-5}	1.0×10^{-2}	− .30
$\cos(\omega_{23}t+lx)$	-2.8×10^{-4}	-1.6×10^{-1}	− .11
	-7.3×10^{-5}	-4.1×10^{-2}	− .27
	-1.8×10^{-5}	-1.0×10^{-2}	− .23

TABLE II. *(Continued)*

The coefficients of the various wave contributions of v_1. The first column represents the $\partial u_1/\partial t$ (or acceleration) contribution to the v_1 term, the second column gives the geostrophic or $g\ \partial \eta/\partial x$ contribution to v_1.

Coefficient of:	v_1 (in cm/sec) ($\partial u_1/\partial t$ contribution)	v_1 (in cm/sec) ($g\ \partial \eta/\partial x$ contribution)
$\sin lx$	—	-96
	—	-9.6
	—	-2.4
$\sin(\omega_{11}t+lx)$	-1.2×10^{-7}	12
	-1.1×10^{-4}	1.2
	-4×10^{-3}	.3
$\sin(\omega_{21}t+lx)$	-8.4×10^{-4}	84
	-3×10^{-4}	8.4
	-7.2×10^{-5}	2.1
$\sin(\omega_{12}t+lx)$	5.7×10^{-4}	$-.6 \times 10^{-4}$
	5.7×10^{-3}	-5.7×10^{-3}
	2.1×10^{-2}	-1.4×10^{-2}
$\sin(\omega_{13}t+lx)$	-5.7×10^{-4}	6×10^{-4}
	-5.7×10^{-3}	5.7×10^{-3}
	-1.9×10^{-2}	1.4×10^{-2}
$\sin(\omega_{22}t+lx)$	.19	-9×10^{-2}
	.28	-2.1×10^{-3}
	.34	-1.4×10^{-4}
$\sin(\omega_{23}t+lx)$	$-.19$	9×10^{-2}
	$-.25$	2.1×10^{-3}
	$-.20$	1.4×10^{-4}

Table II gives compilations of the amplitudes of the various wave motions for three separate values of l corresponding to wave lengths of 200, 2000 and 8000 km. The 200 km wave length does not represent any actual wind-driven motions, but it does give a picture of the type of motion which can be expected for such a scale length. The other two cases, i.e., wave lengths of 2,000 and 8,000 km, represent the practical scale limits of wind-driven oceanic motions. The numerical values shown in Table II are based on the physical properties of the ocean (D_1, D_2, b, etc.) prescribed in Section 3. The wind-stress amplitude, taken as 3 dynes/cm^2, corresponds to wind velocities commonly found in storms.

In interpreting the results of Table II, it is necessary to consider the frequencies of the various waves. For example, in the values for surface heights η_1, η_2 and downstream velocity v_1, the amplitudes of the internal Rossby wave and of the standing wave are much larger than any of the other individual amplitudes. However, these two amplitudes differ in sign and, because of the low frequency of the baroclinic

Rossby wave, their net effect is small (comparable in magnitude to the external Rossby wave amplitude) for quite a long period of time. On the other hand, the barotropic Rossby wave, which has a considerably smaller amplitude, actually attains its maximum value after just a few days. For practical purposes, therefore, the geostrophic response of the ocean is a combination of the barotropic and baroclinic modes.

In order to extend the results to storms of finite duration, it is necessary to subtract from the above form of the solution a similar contribution with t replaced by $t - t_0$, where t_0 is the length of time during which the wind acts. From the values of the frequencies it is then clear that the internal Rossby wave does not attain its maximum amplitude for storms of, say, five days duration. The remaining terms execute at least a fourth of one oscillation in that time—that is, their maximum values are attained.

Note that the barotropic long gravity wave amplitude in the velocity terms is always at least an order of magnitude smaller than that of the baroclinic inertial wave. In the lower layer the internal amplitudes are reduced by a factor of $-r = -1/7$ and the two terms may become comparable.

We have separated the magnitudes of the various waves of the downstream velocity v_1 into two sections that correspond to the contributions from the acceleration term $\partial u_1/\partial t$ and the pressure term $g\ \partial\eta/\partial x$ in the first equation of motion:

$$v_1 = \frac{1}{f}\left(\frac{\partial u_1}{\partial t} + g\,\frac{\partial \eta}{\partial x}\right).$$

The purpose of this separation is to compare the relative effects of acceleration and pressure in building up the downwind velocity. As one would expect, the pressure terms are the dominant forces in producing the barotropic and internal Rossby waves, since these motions are essentially geostrophically balanced. However, the high frequency inertio-gravitational motions present an entirely different picture. These motions result primarily from acceleration effects.

Separation of acceleration and pressure terms has resulted in a rather surprising characteristic of the baroclinic inertio-gravitational motions. Rossby (1938) presented an intuitive picture of inertial motions in a homogeneous ocean. He suggested that an unbalanced stream is shifted to the right (in the northern hemisphere) of its downstream direction and that its inertia carries it beyond the equilibrium position to a point where the pressure gradients caused by the resultant piling up of mass force it back again. The stream thus oscillates about its equilibrium position with a period of a half pendulum day. This intuitive picture was confirmed by the quantitative results of Cahn (1945). In a note following Cahn's paper, Starr (1945) suggested that the extension to a stratified system was relatively simple—that one can extend the results to a baroclinic ocean with relatively minor changes. Inspection of the internal inertial wave amplitudes for v_1 in Table I shows that such an extension is unjustified. It is seen that the Coriolis force is almost completely balanced by the acceleration terms and that neither the free surface nor the interface changes much in this contribution to the flow. *Thus the transient internal motion is purely an inertial motion* of the type such as a bead may execute when constrained to move on a rotating frictionless sphere.

At the outset of the investigation we had the impression that a possible indication of distant storms would be a measure of the change of the interface and that the period of oscillation would be roughly a half pendulum day. However, unless other effects, such as sloping bottom or resonance, contribute to amplification of the interface changes, this quantity would be quite unmeasurable. The velocities[7] resulting from such storms at distant regions are also quite small. Possibly the only noticeable effect would be the amplitude of the barotropic Rossby wave contribution to the free surface height. Perhaps such measurements could be made with tide gauges on isolated oceanic islands.

As stated earlier, the "permanent" current velocity is a combination of the barotropic and internal Rossby wave contributions to the downwind velocity. Rossby's conclusion, viz., that changes in the winds must produce motions which extend to the ocean bottom, is verified here. These velocities are so small, however, that they are comparable only to the slow deep-water drift which results from large sources of heating and cooling. For example, a storm with a scale of 2,000 km, applying a wind stress of 3 dynes/cm^2 to the sea surface, gives rise to a maximum velocity of approximately 1 cm/sec in the deep layers of the ocean (result of barotropic Rossby wave contribution). The maximum value is attained in a period of three days. Thus the maximum possible mixing length attributable to such a storm is approximately 3×10^5 cm. This leads to a coefficient of lateral eddy diffusivity considerably smaller (3×10^5cm^{2}sec^{-1}) than the one assumed by Sverdrup (1939), viz. 10^8cm^{2}sec^{-1}. His justification for using such a value is found in the following quotation from his paper (Sverdrup,

---

[7] Frictionally wind-driven surface velocities would be measurable. However, these are in the direct vicinity of the storm area.

1939: 196): "Rossby (1938) has, however, shown that changes in the winds over the ocean may produce currents reaching from the surface to the greatest depths. All such motions will be directed at random and Rossby's conclusions, therefore, can be interpreted as showing that changing wind conditions may produce variable currents in the deep water, but no flow in a definite direction. If this is the case, a large scale lateral mixing may take place." His reasoning is probably based on the following excerpt from Rossby (1938: 262): "However, since the large scale atmospheric wind systems which drive the ocean circulation change from day to day and from season to season, it is permissible to state with a reasonable degree of assurance, that it is entirely inappropriate to consider the homogeneous bottom water as inert beyond the slow thermal circulation maintained by antarctic cooling."

Both of these statements are qualitatively correct. However, from quantitative considerations these statements appear to be misleading. The deep lateral mixing due to storms is probably negligible on the basis of the present investigation.

A few remarks should probably be made concerning the effect of the change of the Coriolis parameter with latitude. An investigation of a model with constant Coriolis parameter reveals that the geostrophically balanced downwind velocities must increase linearly with time. The essential effect of β is to keep the velocities finite (in the form of moving waves). The two solutions become comparable for sufficiently small values of t (less than a day) where the sinusoidal time-dependent Rossby wave terms can be linearized. In none of the inertio-gravitational wave frequencies does the β term contribute an effect of more than two percent. Therefore the effect of β on inertial oscillations is essentially negligible, whereas its effect on the geostrophically balanced motions is such as to alter the solution completely (from a linear function of time to a moving wave form) for time scales larger than the inertial period.

An important question which has been raised by various authors in the past concerns the amount of energy absorbed by the inertial oscillations when a transient wind blows over the ocean. This question may be partially answered by the present model, although a complete investigation would necessarily embrace many more features than those included here. By restricting our attention to the initial stages of the motion, say, to the first day or so, we may investigate the case of $\beta = 0$ as a good approximation to the present model. The total energy E of the flow between the limits $-L \leq X \leq L$ and per unit thickness in the y direction may be derived from a combination of equations (2.1) to (2.6) (with $\beta = 0$)

$$D_1 \frac{\rho_1}{2} \int_0^t \int_{-L}^{L} \frac{\partial}{\partial t}\left(u_1^2 + v_1^2 + \frac{g\eta_1^2}{D_1}\right) dydt + \frac{D_2\rho_2}{2} \int_0^t \int_{-L}^{L} \frac{\partial}{\partial t}\left(u_2^2 + v_2^2 + \frac{\Delta\rho g}{D_2}\eta_2^2\right) dydt = \rho_1 \int_0^t \int_{-L}^{L} \tau v_1 dydt .$$

The term on the left represents the total (kinetic and potential) energy of the flow. The right-hand term, the energy input, can be evaluated directly

$$\rho_1 \int_{-L}^{L} \int_0^t \tau v_1 dtdy = \frac{W^2\rho_1 L}{D_1} \left\{ \frac{f^2 D_2}{D p_1^4}(1 - \cos p_1 t) + \frac{f^2 D_1}{D p^4}(1 - \cos pt) + \frac{1}{2}\left[1 - \frac{f^2 p_2^2}{p^2 p_1^2}\right] t^2 \right\} ,$$

where $p^2 = f^2 + gDl^2$, $p_1^2 = f^2 + \dfrac{bgD_1D_2l^2}{D}$, $p_2^2 = f^2 + gD_2l^2$, and $D = D_1 + D_2$. The two sinusoidal terms represent the input energy which is absorbed by the inertio-gravitational motions; the remaining term (t^2) is the geostrophic current energy. For a wave length of 2,000 km, the term $\dfrac{f^2D_1}{Dp^4}(1 - \cos pt)$ (corresponding to the barotropic inertio-gravitational motions) is negligible as compared to either of the other terms. Hence a comparison of inertio-gravitational energy with geostrophic current energy is afforded by the ratio

$$\frac{E_i}{E_g} = \frac{\dfrac{f^2D_2}{Dp_1^4}(1 - \cos p_1 t)}{\dfrac{1}{2}[1 - f^2p_2^2/p^2p_1^2]t^2} .$$

Time t in this expression is to be interpreted as the time during which energy is added to the system by a wind stress. If the length of time is considerably shorter than a half pendulum day, most of the energy is absorbed by transient oscillatory motions. For times longer than a half pendulum day, the maximum amount of energy is contained in the geostrophic current field. These facts are shown in Fig. 3, which gives the ratio E_i/E_g as a function of time of wind duration for $t < 1$ pendulum day. The graph cannot be carried any further as a function of time because linearization of the Rossby waves is no longer valid. The tendency, however, is clearly indicated even for the short period shown in Fig. 3.

The case which we have chosen is conducive to strong inertial oscillations. If the wind system were moving with a speed of 10 m/sec, the reverse action of the wind after a day or so would have a destructive influence on the inertio-gravitational motions. However, the transient motions will dominate in the initial period (< 1/2 pendulum day) regardless of whether the wind system is moving, unless the frequency of the moving system is unrealistically large. Therefore, for motions with a sufficiently large time scale (> 1 pendulum day), the flow may be considered as essentially quasigeostrophic (Charney, 1955).

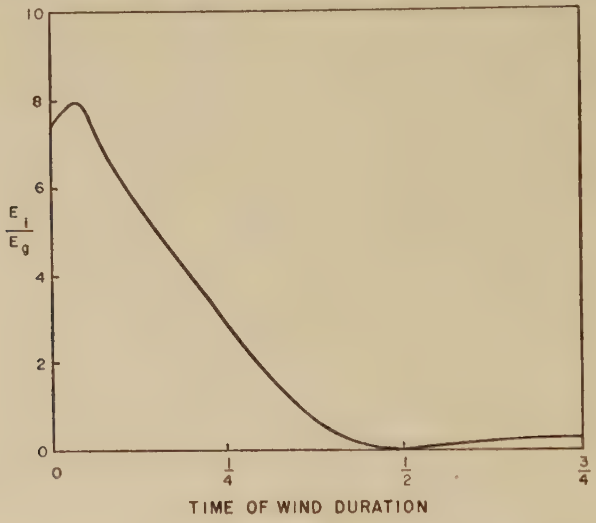

Figure 3

6. APPLICABILITY OF THE MODEL TO THE OCEAN

There are several questions concerning the applicability of the present model to the ocean which merit particular consideration: (1) To what extent are variable motions in the ocean independent of the presence of boundaries? (2) How justifiable is the neglect of friction? (3) Are other forces such as atmospheric pressure important in setting up oceanic currents? and (4) What are the effects of bottom topography on the induced motions?

(1) The disturbance set up by an instantaneous change in wind is propagated toward the boundaries in the form of waves. The length of time required for the influence of the boundaries to become evident at an interior point of the ocean therefore depends upon the time required for a wave to move from that point to the boundary. Since the wave velocities differ for each mode of motion, strict application of the model is limited by the time it takes the fastest wave (barotropic gravity wave) to reach the coast (a matter of a few hours). However, there are two reasons for assuming that the essential results of this model would not be affected by coastal influences for a considerably longer period. First, there is no interaction between the various modes in the interior of the ocean and there is no reason to suppose that there is any interaction between the transient and Rossby modes at the coast. Therefore, so far as the balanced motion is concerned, the model may be used in the interior of the oceans for the time it takes a barotropic Rossby wave to reach the coast (a matter of a few days). Second, the amount of energy contained in the transient motions is considerably smaller than that in the balanced motions. The reflection of this energy from the coasts would exert a relatively negligible influence on any observable motions. It seems likely, therefore, that the geostrophically balanced motion of the real ocean should respond to a three or five day storm much like the theoretical model—that is, during the "active phase" or life time of a central oceanic storm, the effect of coastal boundaries should be negligible.

It is clear that, for periods longer than a week, the barotropic Rossby mode of motion may be strongly influenced by the coasts. The length of time over which the internal Rossby mode is unaffected by the coasts could be as much as several years were it not for the uncertainty as to whether the two Rossby modes can interact at the coasts. There is a possibility that the proper boundary conditions are nonlinear in a coastal current such as the Gulf Stream, in which case there might be an interaction between the barotropic and baroclinic Rossby modes. This is the reason why we hesitate to extend the discussion of the internal Rossby mode to wind fluctuations of a seasonal time scale.

If there is, in fact, no interaction between Rossby modes at the coasts, this model leads us to the conclusion that equilibrium adjustment of the main thermocline in the central ocean does not occur even in response to wind variations with periods as long as a year.

(2) The effect of friction is neglected in the model under discussion, and it is important to form some estimate of the frictional force. For bottom friction, Proudman (1953) gives the frictional force on the ocean

bottom as $F = - k \rho u^2$, where $k = 2 \times 10^{-3}$. The bottom velocities involved in the models under discussion are less than those due to deep sea tides. The amplitude of the tidal velocity U may be regarded as purely periodic, in which case the resultant frictional force due to a long period deep sea velocity component u is simply $F = -2k\ U\ u$. If the bottom layer is of depth D, then the time constant K of the frictional damping of the lower layer velocity is $K = kU/D$. Taking representative values $k = 2 \times 10^{-3}$, $U = 2$ cm sec^{-1}, $D = 4 \times 10^5$ cm, one calculates $K = 10^{-8}$sec^{-2}. Thus the length of time necessary for destruction of the velocity of the bottom layer by bottom friction is approximately three years.

The time constant involved in lateral friction is $K' = Al^2$, where l is the wave number and A the coefficient of lateral eddy viscosity. For the largest scale phenomena in the deep sea (Sverdrup, 1939), it appears that a largest possible limit of A is 10^8cm^{2}sec^{-1}. Taking $l = 1/2 \times 10^{-8}$cm^{-1}, the time constant becomes $K' = 0.25 \times 10^{-8}$. Thus lateral friction of the most intense sort can destroy motion in these models in the bottom layer only after 12 years. The conclusion is that the frictionless models are justified only for periods up to about one year, and that physically they should include friction explicitly for longer periods.

(3) There are other surface stresses which may affect the response of the ocean also. These are the variations of atmospheric pressure and the divergence of the wind stress. (The latter term is approximately an order of magnitude smaller than the curl of the wind stress.) Neither of these driving terms contributes to the current motions, but they tend only to increase the transient motions in the ocean. For this reason they have not been considered, although any thorough study of inertial oscillations would necessarily entail a detailed study of these effects.

(4) The effect of bottom topography has been neglected altogether. Perhaps there is no other justification for excluding this feature than the fact that the analysis is quite complex when it is included. It is conceivable that its effect may be important, particularly for the stratified ocean.

7. SUMMARY AND CONCLUSIONS

We have investigated the response of an infinite rotating ocean of finite depth to a transient wind stress applied at the sea surface. The density structure, an idealization of the observed stratification, consists of two layers of homogeneous water. The variation β of the Coriolis parameter f with latitude is included in the equations by taking $\beta = df/dy =$ constant; elsewhere, f is assumed to be constant.

By using normal modes, the equations of motion of a two layer system can be reduced to a vorticity equation in a single variable whose highest order derivative is of the same order as that in the homogeneous system. The vorticity equation contains two separate types of motion corresponding to the two modes of oscillation in the system. In the barotropic case the motion is uniform vertically. The second type, baroclinic motion, occurs when the lower layer responds in such a manner as to offset the pressure gradient caused by deviations of the free surface from its equilibrium position.

Substitution of a moving wave solution in the homogeneous vorticity equation yields a frequency equation which shows that six different types of waves may be excited in the system. Two of the waves, the barotropic and baroclinic Rossby waves, represent the motions which are in geostrophic balance. The remaining four waves (two barotropic and two baroclinic) represent inertio-gravitational motions which result from incomplete balance between pressure and Coriolis forces. Behavior of the latter waves is dependent on both the Coriolis parameter and the static parameters (depth, density, gravity) of the system. Generally, however, the barotropic waves are pure gravity waves travelling with speed $\sqrt{gD}$, and the internal waves are pure inertial waves with a period of a half pendulum day, $2\pi/f$.

Two types of wind-driven motions are treated. The forced motions caused by a moving wave system with a scale comparable to atmospheric patterns as given by five-day mean charts are investigated by assuming a driving force of the type $W \sin (lx + \nu t)$, with $W = 1 \text{ cm}^2 \text{ sec}^{-1}$. The resultant motions may be studied by considering three separate ranges of period of the driving wind.

For periods of one to seven weeks (comparable to the barotropic Rossby wave period), the ocean responds principally as a homogeneous body of water. The baroclinic effects increase in importance with longer period.

For longer periods (up to a year, thus lying between the barotropic and baroclinic Rossby wave period) the motion is partly barotropic although the effects of baroclinity are more prominent. The upper layer downwind velocity is approximately half barotropic-half baroclinic when the wind period is a year for the scale chosen. The other variables are effected less by the baroclinity.

When the wind period is long (at least 100 years) the motion is purely baroclinic. The flow is geostrophic and the total transport is equal to that given by Munk for the steady-state model.

The second type of wind-driven motions treated here is that caused by a nonmoving wind which varies sinusoidally in space and which begins impulsively at some time. In this case all of the possible free wave motions of the system occur, and one can study the relative importance of the inertio-gravitational and geostrophically balanced motions.

When the wind acts for a period of time comparable to the life of a storm, the geostrophically balanced motion is partially external and partially internal. The precise partition of the energy between the two modes depends on the scale of the motion. The thermocline therefore responds to the action of the wind stress and may be measurable (of the order of 10 to 20 m) when the wind blows for three days or more. The currents set up in the deep layers are small and are probably no stronger than the slow thermal currents resulting form antarctic cooling. Consequently, as a result of storms there is probably no mechanism for the formation of large-scale lateral mixing in the oceanic stratosphere.

The isostatic inertio-gravitational motions are much larger than the barotropic inertio-gravitational motions. However, they are not accompanied by any measurable movement of the thermocline; instead, they are purely horizontal inertial motions. In a stratified ocean, therefore, the observed inertial oscillation is not accompanied by pressure gradients resulting from excess piling up of water. Instead, it is mainly a lateral movement with an oscillation caused by the earth's rotation only.

From the present simple analysis, the essential effect of β in a transient problem is to amplify the baroclinic mode for large periods.

A simple investigation of the relative amounts of energy contained in the inertio-gravitational and geostrophically balanced flow indicates that, so long as the wind blows for more than a half pendulum day, most of the energy is contained in the geostrophically balanced flow. For winds of shorter duration the energy is expended in inertio-gravitational motions.

BIBLIOGRAPHY

Bolin, B.

1953. The adjustment of a non-balanced velocity field towards geostrophic equilibrium in a stratified fluid. Tellus, *5* (3): 373–385.

Cahn, A.

1945. An investigation of the free oscillations of a simple current system. J. Meteor., *2* (2): 113–119.

Charney, J. G.

1955. The generation of ocean currents by wind. J. Mar. Res., *14* (4): 477–498.

Freeman, J. C.

1954. Note on a prediction equation for the surface layer of a two-layer ocean. Trans. Amer. geophys. Un., *35* (4): 585–587.

GROVES, G. W.
1954. Dynamic model of a two-layer ocean under influence of atmosphere and coastal boundary. Tech. Rept. No. 54–22, Scripps Institution of Oceanography, 27 pp.

ICHIYE, T.
1951. On the variation of oceanic circulation. Oceanogr. Mag., *3* (2): 79–82.

MUNK, W. H.
1950. On the wind-driven ocean circulation. J. Meteorol., *7* (2): 79–93.

PROUDMAN, J.
1953. Dynamical Oceanography. London Methuen, London. 409 pp.

REID, R. O.
1948. The equatorial currents of the eastern Pacific as maintained by the stress of the wind. J. Mar. Res., *7* (2): 74–99.

ROSSBY, C. G.
1938. On the matual adjustment of pressure and velocity distribution in certain simple current systems, II. J. Mar. Res., *1:* 239–263.
1949. On the dispersion of planetary waves in a barotropic atmosphere. Tellus, *1:* 54–58.

STARR, J.
1945. Note on inertial oscillations. J. Meteorol., *2* (2): 120–122.

STOCKMANN, W. B.
1946. Equations of the field of integrated currents caused by the wind in a nonhomogeneous ocean. Doklady Akad. Nauk. SSSR, *54* (5): 403–406.

STOMMEL, HENRY
1948. The westward intensification of wind-driven ocean currents. Trans. Amer. geophys. Un., *29* (2): 202–206.

SVERDRUP, H. U.
1926. Dynamic of tides on the North Siberian shelf. Geofys. Publ., *4* (5): 75 pp.
1939. Lateral mixing in the deep water of the South Atlantic Ocean. J. Mar. Res., *2* (3): 195–207.
1947. Wind-driven currents in a baroclinic ocean; with application to the equatorial currents of the eastern Pacific. Proc. Nat. Acad. Sci., *33* (11): 318–326.

VERONIS, G.
1956. Partition of energy between geostrophic and non-geostrophic oceanic motions. Deep-Sea Res., *3* (3): 157–177.

VERONIS, G. AND G. W. MORGAN
1955. A study of the time-dependent wind-driven ocean circulation. Tellus, *7* (2): 232–242.

YEH, T.
1949. On energy dispersion in the atmosphere. J. Meteor., *6* (1): 1–16.

Contribution No. 862

Reprinted from Biological Bulletin, Vol. 111, No. 3, 393–398, December, 1956
Printed in U. S. A.

INFLUENCING THE CALLING OF SEA ROBINS (PRIONOTUS SPP.) WITH SOUND[1, 2, 3]

JAMES M. MOULTON

Bowdoin College, Brunswick, Maine

Despite abundant evidence that fishes hear and produce sounds (Fish, 1948, 1954; Griffin, 1955; von Frisch, 1938), a review of the literature (Moulton and Backus, 1955) on attempts to influence fish movements with man-made sounds has uncovered reports only of quickened movements of fishes during production of such sounds. Nor has a biological significance of any sound known to stem from a fish, whether produced by stridulation of skeletal parts or by the air bladder, been clearly demonstrated. However, the apparent relationship between sound-production by some species of fishes and their respective breeding seasons has been noted by a number of authors (Fish, 1954, pp. 51, 83; Goode, 1888, p. 137; Marshall, 1954, p. 254), and the possible significance of fish calls in bringing individuals of the same species together has been suggested. Sounds are also produced during defensive spine raising of such fishes as groupers, grunts, squirrel fishes and sea robins.

During the summer of 1954, it was accidentally discovered that the production of certain fish calls, later identified as the calls of sea robins, could be stimulated by transmission of certain sounds into the water, and that the calling could be suppressed by other sounds (Moulton, 1955). The study resulting from this finding was pursued further during the summer of 1955. The observations yielded evidence that calls produced during the breeding season of two species of sea robins (*Prionotus carolinus* L. and *P. evolans* L.) are produced as responses to calls of the same species, and that by the transmission of appropriate sounds, some degree of control over the calling of sea robins may be exercised.

The sound-generating equipment employed in the experiments here described consisted of a Hewlett-Packard audio oscillator Model LAJ or a Magnecorder tape recorder Model PT6J; either an Altec Type A-323B or a Craftsman Model C550 amplifier, and a QBG transducer. The monitoring system was an AX-120 ADP or an AX-58-C Rochelle salt hydrophone and a Woods Hole Suitcase amplifier. Recordings were made on the Magnecorder tape recorder at a speed of 15 in./sec. and were analyzed on a Vibralyzer vibration analyzer. The experiments were performed from a raft anchored over 72 feet of water in Great Harbor, Woods Hole, Massachusetts.

---

[1] Contribution No. 862 from the Woods Hole Oceanographic Institution.

[2] The work was performed while the author was a Research Fellow at the Woods Hole Oceanographic Institution during the summers of 1954 and 1955.

[3] This study was supported in part by a grant from the Bowdoin College Faculty Research Fund, established by the Class of 1928.

THE SOUNDS OF SEA ROBINS

The sound-producing air bladder of the sea robin has been described by Fish (1954). It is the apparent source of two different calls. One of these calls is a vibrant grunt produced when a sea robin is handled in or out of water, and when a sea robin is brought to the surface by net or by hook and line. The grunt accompanies fin erection.

As determined by vibration analysis, the sea robin grunt is a single burst of noise lasting about $\frac{1}{10}$ second. The upper frequency limit is approximately 1.7 kc., the lower below 44 cps. The grunt is audible to the unaided ear above the water when a sea robin is submerged four feet beneath the surface. Noises of frequency characteristics similar to those of the grunt may be obtained by pressing the air bladder through the ventral body wall of the intact fish, and by stimulation of the nerves to the drumming muscles located on the lateral surfaces of the bilobed air bladder.

The onset of the breeding season of the sea robins at Woods Hole is marked by the production by these fishes of a staccato call. Although this call has been monitored from sea robins contained within a live car at the surface of Great Harbor, no single fish has been identified as the source of an individual call. This call is not produced under conditions that bring forth the grunt already described, and it is much more frequently produced by fishes in the Harbor than by caged specimens.

The breeding season of the sea robins at Woods Hole extends from June to September, with July and August the height of the season (Bigelow and Schroeder, 1953). In 1955, listening began on 29 June. The first staccato calls were heard on 5 July, and calls were heard on each day of listening thereafter until work terminated for the summer on 30 August. The number of outbursts of calling and the number of calls comprising a single outburst increased rapidly during the first half of July (compare Tables I and II). During the latter part of August calling became more infrequent.

TABLE I

Responses of sea robins to audio oscillator signals in Great Harbor, 15 July, 1955

Time	Number of signal transmissions	Response
1415	1	2 calls
1420	1	No calls
1430	1	No calls
1440	1	No calls
1450	1	No calls
1500	2	1 call after first signal
1510	3	1 call after first signal
1520	2	No calls
1530	2	No calls
1540	2	1 call after first signal
1550	3	1 call after second signal
1600	2	No calls
1610	4	1 call after signals one and two
1620	3	No calls
1630	3	No calls

Table II

Responses of sea robins to recordings of the staccato call and to audio oscillator signals, Great Harbor, 20 July, 1955

Time	Number and type of signal transmission	Response
1425	1 recording	2 calls
1430	1 signal	No calls
1435	1 recording	No calls
1440	1 signal	No calls
1445	1 recording	4 calls
1450	1 signal	No calls
1455	1 recording	No calls
1500	1 signal	2 calls
1505	1 recording	No calls
1510	1 signal	No calls
1515	1 recording	No calls
1520	1 signal	6 calls
1525	1 recording	No calls
1530	1 signal	No calls
1535	1 recording	No calls
1540	1 signal	No calls
1545	1 recording	No calls
(5 spontaneous calls during this interval)		
1550	1 signal	No calls
1555	1 recording	No calls
1600	1 signal	No calls
1605	1 recording	No calls
(12 spontaneous calls during this interval)		
1610	1 signal	No calls
1615	1 recording	No calls
1620	1 signal	No calls
1625	1 recording	No calls
1630	4 signals	1 call after No. 2
1635	3 recordings	No calls
1640	3 signals	No calls

The staccato calls consist of pulses of noise usually produced in pairs, at an average rate of 22 pulses/second. The paired arrangement of the pulses in a typical call is probably due to a slightly asynchronous contraction of the drumming muscles on the two lobes of the air bladder. The pairing of the pulses is not distinguishable to the ear, but can be seen on vibration analysis. Absence of the double pulses in a portion of some calls and, rarely, throughout a call suggests that one lobe of the air bladder may be silent during sound production by the other lobe.

The individual pulses of the staccato call lie between 500 cps and 4 kc. The frequencies of greatest intensity lie between 700 cps and 2.5 kc. The respective intensity peaks of the paired pulses are at different frequencies on the vibragrams, separated by approximately 1 kc. This is presumably related to a differential resonance of the two air bladder lobes which generally differ somewhat in size. It is possible to obtain sounds of similar frequency and intensity characteristics by palpitation of the dissected air bladder.

INFLUENCING PRODUCTION OF THE STACCATO CALL

With the sound-generating equipment employed, it is possible to transmit a series of sound pulses crudely imitative of the staccato call of the sea robin when the audio oscillator is set at 17 to 40 cps. (The QBG emits a considerably distorted wave train when driven with a sine wave at these frequencies.) With transmissions timed to correspond to the duration of an average call, 2½ to 3 seconds, production of the staccato call by free sea robins was repeatedly incited during July and August of 1954 and 1955.

Tables I and II present the results of two experiments extending over 2 hours and 15 minutes on 15 and 20 July, 1955. On 15 July (Table I) from one to three imitations of the staccato call were transmitted at ten-minute intervals, except for the second trial which followed the first by five minutes. Of the 15 trials, 6 were followed immediately by calling of free sea robins. There was no calling during the listening period other than immediately following signal transmissions.

On 20 July (Table II), playing of recordings of the sea robin staccato calling into the harbor water was alternated with transmission of imitations of the calling at five-minute intervals. During the 28 tests of 20 July, the calling of free sea robins was heard five times immediately following transmissions, twice after playing recordings of the calling and three times following transmissions of the imitations. Two spontaneous outbursts, frequent by 20 July, were heard during the period of the experiment. As Table II also indicates, outbursts of several calls were the rule by 20 July, whereas earlier in the month single or double calls comprised the characteristic outburst in 1955.

SUPPRESSING OF THE STACCATO CALL

Signals of 200 to 600 cps transmitted for the approximate duration of a staccato call interrupt the production of this call by sea robins. (Again the QBG signal is considerably distorted as at the lower frequency.) Signals above 2 kc. have never been effective in suppressing the calling. Signals from 600 cps to 2 kc. are variable in effectiveness. Sea robins confined in a live car and sea robins on the bottom of Great Harbor, observed by an aqualung diver, Mr. Robert Weeks of the Woods Hole Oceanographic Institution, show no obvious change in behavior during transmission of signals effective in suppressing the staccato call.

DISCUSSION

Conditions bringing forth the grunting of sea robins suggest that this sound is part of a general alarm reaction. It may be of value in nature as an adjunct to the spiny armor of the species in discouraging enemies, but no evidence is available on this point.

That the staccato calling reaches its climax near the peak of the sea robin breeding season is strongly suggestive of a relation of this calling to breeding activities, and the possibility cannot be overlooked that the calls serve as a species recognition device in waters where visibility is rather poor. Mr. Robert Weeks has informed me that visibility on the bottom of Great Harbor beneath the raft was a little over 6 feet on 10 July, 1955, and that sea robins could be seen clearly within that distance moving over the bottom of the harbor. The calling is heard at night, as well as in the daytime. In a few instances during the summer, production of the staccato call was heard to follow various sharp percussive sounds—the discharge of a high-energy spark into the water, the explosion of a detonating cap in the harbor, and the slamming of the live car lid on the raft.

Since the first staccato calls of 1955 were heard from fishes caged at the surface, while sea robins characteristically feed on the bottom, it was thought that warming of surface waters might have initiated calling from surface specimens earlier than their calling would ordinarily have commenced. However, temperatures taken with a bathythermograph during July and August of 1955 showed that there was a thorough mixing of water over the 72-foot depth under the raft, and no records obtained showed over a two-degree F. variation in temperature from the surface to the bottom.

While the significance of the calling behavior of the sea robin to its survival and normal behavior is as yet undetermined, the observations reported have demonstrated that sound is significant to the behavior of sea robins. The work has demonstrated that it is possible to control sound production by these marine fishes with man-made sounds. The findings stand as an exception to the general rule (Moulton and Backus, 1955) that production of man-made sounds causes only quickened swimming movements of fishes.

It should also be of interest to students of marine animal noises that it is possible to incite, without handling or trapping, the calling of marine fishes by transmission of appropriate signals, thus making it possible to move experiments to the natural environment from the confines of laboratory tanks, which under the best of conditions suppress and may otherwise modify calling behavior.

I am grateful for highly valued criticism to Dr. J. B. Hersey, Mr. William Schevill and Dr. R. H. Backus of the Woods Hole Oceanographic Institution, who read the manuscript of this paper. I am much indebted to Mr. Willard Dow, as to many others of the Institution, for their generous technical advice.

Summary

1. A vibrant grunt and a staccato call of sea robins in the Woods Hole area are described. Sounds similar to these can be obtained by manipulation of the air bladder and by stimulation of the nerves to the drumming muscles.

2. It is suggested that the sea robin grunt is part of a general alarm reaction, and that the staccato call is related to the breeding behavior of the sea robin. It is suggested that the staccato call may serve as a species recognition device in waters where visibility is relatively poor.

3. A method of controlling production of the staccato call is described. Production of the call can be initiated by playing into the water imitations of the call and recordings of the call itself. The calling can be suppressed by playing of signals of 200 to 600 cps, and, less consistently, by playing of signals of 600 cps to 2 kc.

4. The results obtained furnish an exception to the general rule that sound production causes only quickened swimming movements of free fishes, and demonstrate the possibility of exercising some degree of control over the behavior of fishes in nature with man-made sounds.

LITERATURE CITED

BIGELOW, H. B., AND W. C. SCHROEDER, 1953. Fishes of the Gulf of Maine. First revision. *Fish and Wildlife Service, Fish. Bull.*, **53**.

FISH, M. P., 1948. Sonic fishes of the Pacific. Project NR 083-003. Contr. N6 ori-195, t.o. i, between ONR and Woods Hole Oceanographic Institution, Tech. Report No. 2.

FISH, M. P., 1954. The character and significance of sound production among fishes of the western North Atlantic. *Bull. Bingham Oceanographic Collection,* **14**, Art. 3.

VON FRISCH, K., 1938. The sense of hearing in fish. *Nature,* **141**: 8–11.

GOODE, G. B., 1888. American fishes. Standard Book Co., New York.

GRIFFIN, D. R., 1955. Hearing and acoustic orientation in marine animals. Papers Mar. Biol. and Oceanogr., Deep-Sea Research, suppl. to Vol. 3, pp. 406–417.

MARSHALL, N. B., 1954. Aspects of deep sea biology. Hutchinson's, London.

MOULTON, J. M., 1955. The eliciting and suppressing of a marine biological sound. *Bull. Ecol. Soc. Amer.,* **36**: 80.

MOULTON, J. M., AND R. H. BACKUS, 1955. Annotated references concerning the effects of man-made sounds on the movements of fishes. Fisheries Circ. No. 17, Dep't of Sea and Shore Fisheries, Augusta, Maine.

Contribution No. 863

Deep-Sea Research, 1956, Vol. 4, pp. 36 to 44. Pergamon Press Ltd., London.

Interpretation of high-resolution echo-sounding techniques and their use in bathymetry, marine geophysics, and biology

S. T. KNOTT and J. B. HERSEY

Abstract—Experience in making observations with commercially available correlation recorders designed for sounding ocean depths has suggested design modifications which would combine the capabilities of both shallow- and deep-water sounders in one instrument as well as improve their general performance for research. The design and construction of such a recorder is described. Some examples are given of its application to the study of smaller-scale bottom features ; to the echolocation of fish schools, individual fishes, and other aggregations of marine animals ; and for locating instruments in depth and range.

Occasionally echo-sounder pings penetrate the bottom to reflect from deeper horizons ; the recorder then presents a continuous-structure section. By using a sound source having a broad spectrum instead of the usual single-frequency ping, and by extending the receiver design to record in two or more filter bands, shallow structures have been observed which could not be recorded with the high frequency of the conventional echo sounder.

INTRODUCTION

FOR many years the acoustic signals from an echo sounder have been recorded in such a way that the echoes from one sound pulse can conveniently be correlated with those of neighbouring pulses by the familiar device of moving a recording stylus across the short dimension of a long strip of recording paper, the latter moving along its length under the stylus carriage. The time of the outgoing sound pulse is controlled by the position of the stylus and is usually made to occur when the stylus has just started its traverse across the recording paper. Thus all initial pulses are recognized by their position relative to the edge of the paper, and successive echoes from the ocean bottom or objects in the water may readily be correlated. Such a recording technique is generally accepted as a very powerful method for studying echoes from a bottom varying rapidly in depth, weak echoes against a noisy background and scattering from discrete reflectors over which the ship passes rapidly. This technique has made detailed investigations of submarine topography a practical venture, and has converted the taking of general ocean-depth soundings from a laborious task to an easy and continuous process.

Echo sounders providing this sort of information have been widely used since World War II. While the resulting soundings have greatly increased our knowledge of oceanic topography, these instruments have generally been less precise than is required for several problems. LUSKIN *et al.* (1954) have discussed these inadequacies and have described a recording system which corrects them by providing very accurate travel-time measurements. The recording system described below provides accurate travel-time measurements as LUSKIN's instrument does, and in addition provides considerably higher resolution for the purpose of studying the smaller-scale bottom-roughness features. For general bathymetric surveying we have also provided writing rates and ping lengths similar to existing deep-sea echo sounders. As this instrument was being developed several functions were also incorporated which make it useful for other marine-research problems involving acoustic travel-time measurements.

Among these is the tantalizing possibility of mapping subbottom structures at least to shallow depths, which has been repeatedly suggested by echo-sounder recordings showing excellent evidence of echoes from extended reflecting horizons below the bottom (e.g., see MURRAY, 1947). HERSEY and EWING (1949) have demonstrated the usefulness of distinguishing between reflections from the bottom and from subbottom horizons by filtering in several frequency bands ; the lower frequencies will penetrate the sediments to deeper horizons with far less attenuation than higher frequencies, so that deep reflections can be identified by the relative lack of high-frequency content. Thus a multichannel correlation recorder filtered in two or more frequency bands can be used to record reflections of complex pulses to provide a continuous section of subbottom structure just as single-frequency sounders provide a profile of the bottom.

Echo sounders have been used extensively to study the behaviour and occurrence of fish schools in shallow water (HODGSON and FRIDRIKSSON, 1955) and to study the animal populations of the open ocean by observing the characteristics of the deep scattering layers (DIETZ, 1948 ; HERSEY and MOORE, 1948 ; TUCKER, 1951 ; HERDMAN, 1953 ; and others). For these studies two different instruments are needed: one which will examine large volumes of water with each observation and possibly enhance the weak return from a sparse population, and a second having high enough resolution to single out individuals. The first requires slow writing rates on extended depth scales and, for echo enhancement, a long ping length. The second requires a very high writing rate and a very short ping length. It has been shown that scattering layers and individual fishes have frequency-dependent scattering ; hence multichannel recording is as useful in these studies as it is for reflection seismography. Thus the salient requirements for a recorder are similar in both fields.

THE RECORDER

Writing Speeds

Shallow-water instruments have high writing speeds (scales less than 100 feet across about 8 inches of recorded sweep, or ·005 seconds per inch), whereas deep echo sounders have medium to low speeds (100 to 6000 fathoms across 8 to 10 inches, ·025 to 1·5 seconds per inch). But no recording system has been available incorporating a range of choice between the two extremes. The writing rates of the first model of this recorder cover much of this overall range, while a second model provides only the slower writing rates needed for routine sounding (Table 1).

Stylus and Paper Drive

For a " stylus " we used a helical wire wound on a drum which rotates under a straight edge which is provided by an Aldin facsimile recorder. A positive-gear train driven by synchronous motors turns the helix drum by means of a cog-timing belt and also powers a simple friction paper-drive mechanism. Writing rates are selected by a multiposition switch which controls the speed and rotation sense of the motors, and shifts gears by means of magnetic clutches. The sixteen useable speeds of the first model were achieved by employing a differential at the output of two motors and their gear trains, while the second model employs only a single motor shaft (two speeds) and appropriate gear shift (Fig. 1). The paper drive has two speeds, one which advances the paper about the width of the recording trace per helix revolution, and a second somewhat slower speed which has been found useful for integrating successive weak echoes or for aiding the correlation of echoes recorded when gated recording is used. We now feel that a third somewhat faster paper drive would be useful occasionally to permit the arrival time of single transient pulses to be unequivocally identified.

Table 1. *Recording speeds of the* 16-*speed drive* (*echo depth ranges based on sound velocity of* 4800′/*sec*).

Speed selection	*Depth range*		*Helix* (*r.p.m.*)	*Sweep time interval* (*seconds*)	*Writing rates* 19″ *recorder* (*sec/in.*)	*Pulse lengths* (*seconds*)
	(*fms.*)	(*ft.*)				
1	20		1,200	1/20	·0027	·0003 to ·005
2	25		960	1/16	·0030	
3		200	720	1/12	·0044	Increasing
4	40		600	1/10	·0053	to
5	50		480	1/8	·0066	
6		400	360	1/6	·0084	
7	100		240	1/4	·013	
8	200		120	1/2	·026	·003 to ·05
9	400		60	1	·053	Increasing
10	500		48	1 1/4	·067	
11		4,000	36	1 2/3	·084	to
12	800		30	2	·106	
13	1,000		24	2 1/2	·13	·03 to ·5
14		8,000	18	3 1/3	·18	
15	2,000		12	5	·26	
16	4,000		6	10	·53	
			Recording speeds of the 6-*speed drive*			
1	200		120	1/2	·026	
2	400		60	1	·053	(See corresponding speeds above)
3	500		48	1 1/4	·067	
4	1,000		24	2 1/2	·13	
5	1,500		16	3 3/4	·2	
6	3,000		8	7 1/2	·4	

This sweep system has now been used on several ships on extended cruises, and has operated for periods of many days without adjustment.

Precision power source

For this purpose we have used a tuning-fork-controlled oscillator feeding a power amplifier. This equipment has scarcely been standardized ; the Ampex Model 375 and alternatively the Time Products, Inc. precision-power supplies have supplied precision 60 c.p.s. frequency control, while the Altec Model A287W 250-watt, and the MacKintosh K107 200-watt power amplifiers, have been used to drive the synchronous motors.

Recording Paper and Depth Scales

Both wet chemical-dye process papers and Teledeltos recording paper (a sandwich paper in which the carbonized inner layer is exposed by a spark discharge through the top layer) have been commonly employed. Recently Teledeltos paper has been greatly improved, but the grades employed in echo sounders smudge badly with handling and will not display variations in sound intensity well. A further difficulty was the necessity for frequent readjustment of the stylus on several commercial models we used with the Teledeltos paper. Some of the wet chemical papers are apt to fade unless very carefully treated as they dry. However, a damp chemical-recording paper, ferrous-ion-deposit type (Alfax type A), had earlier shown promise for this sort of instrumentation since it does not fade and displays good response (several distinguishable tonal shades) to recording current changes ; consequently we experimented with it in this recording system. We used paper widths of 8 and 19 inches, but prefer the latter since it provides a wider recording surface and also feeds with less tracking problems in paper drive. Since the paper is damp and also since it changes dimensions (though linearly) upon drying, scales cannot be readily printed on it prior to use ; hence we record the depth scale simultaneously with the sounding data. The scale is printed by electrical pulses derived from the same precision source as the stylus and paper drive. Thus, these lines also indicate recorder synchronism, but calibration is accomplished by introducing a signal from a break-circuit chronometer and by the use of periodical time checks with a radio time standard.

Ping-Length Adjustment and Gating

The effectiveness of the recording technique depends in part on the choice of writing rates. However, the resolution is further dependent on the ping length, and the unambiguous identification of signals depends on the ability to gate or select a particular depth interval. For use with an echo sounder, the ping length is controlled by mechanical contactors on the recorder, the period of contact being adjustable between wide limits independent of writing rates (a minimum of about 0·3 milliseconds at the fastest writing rate in Table 1 and a maximum of 0·5 sec at the slowest). Thus at the fast rate, scatterers whose range differs by 1·5 ft. can be resolved ; at the slowest rate such a ping length as 0·05 sec is adequate for enhancing a weak signal by integration.

For gating, the outgoing pulse is actuated by the keying contacts which close once each revolution of the helix drum, and a second " selector switch " consisting of a twelve-contact commutator which rotates at one twelfth the speed of the helix drum. These contacts are, in turn, connected to the pinging circuit of the echo sounder through individual switches, so that any of twelve successive drum revolutions may be accompanied by a ping, or may not, as the operator desires. Similarly the helix wire may be connected to or disconnected from the amplifier which supplies the recording signal over the same twelve drum revolutions by another commutator. Thus it is possible to disregard reverberation from shallow scatterers in deep water by sending out pulses on only a fraction of the twelve sweeps, and recording only for the depth intervals where the bottom echo is expected. Conversely, the bottom echo can be disregarded and only the near-surface scattering recorded.

Multichannel Recording

Multichannel recording can be accomplished in three ways; (1) by providing as many helix wires on the same drum as there are channels of information; (2) by bridging the output of the several channels on to one helix all the time (this we already do when we record bottom echoes, depth scales, and time signals simultaneously) ; or (3) by causing the several channels to share time on the same helix. As a first design for recording information filtered in several frequency bands we chose the last method and made a four-channel recorder simply by adding a quadrant commutator to the shaft of the helix drum, each quadrant being connected to one of four separate preamplifiers connected to the filters, which are connected, in turn, to the recorder driver amplifier. The four outgoing pings are actuated by four switches on the same shaft which close just as the recording circuit is switched from one channel to the next. Suitable interconnecting arrangements are made to provide one, two, or three channels, if desired. Also any of the four ping positions can be used singly.

This last feature is a great convenience when the recorder is used for conventional echo sounding. It is soon discovered in deep-water sounding that a particular depth of water will frequently occur near an integral multiple of the smaller depth scales (by the law of maximum unhappiness) thus placing the echo near one edge of the paper. By switching the ping to a quadrant that lies near the middle of the paper the echo is moved there as well.

APPLICATIONS

During its development the recording system was employed in a variety of ways which show its range of usefulness to marine science. These are described below with illustrative material, some of which was recorded at times when the design objectives had not been wholly achieved.

Travel-Time Measurement

The precision of travel-time measurements by the recorder depends on the precision with which the position of a recorded pulse can be determined relative to the timing lines recorded at the same time, as well as on the constancy of the sweep rate of the helix. The quality of both is shown in a recording of pulses one second apart from the time signal of Station *WWV* and from a break circuit chronometer (Fig. 2a). The beginning of each pulse can be determined readily to ·02 parts of the spacing between adjacent timing lines (0·05 sec apart) while the start of pulses from *WWV* form a line closely parallel to the time grid. Thus the record indicates that the power frequency in this case was constant and estimated to be within one part in 10^6 of 60 c.p.s. Thus for the time scales shown ($\frac{1}{2}$ sec across the record) a precision of ± ·0005 sec can be expected. Proportionately higher precision is available on the more expanded scales; with some writing rates, oscillations of the driving-gear train reduce the precision of the measurement below the limit set by resolution. Our power frequency has often differed from 60 c.p.s. by more than this (Fig. 2b), but holds a constant rate over long periods. Travel times can readily be corrected in such instances by measuring the slope of the chronometer trace (usually quite sufficient) or a radio time signal.

The accuracy of a given travel-time measurement depends on the shape and spectrum of the sound pulse and the signal-to-noise ratio as well as the precision of the recorder, and can be estimated only when these are known. Of course, the accuracy of any distance measurement (as depth in echo sounding) depends on one's knowledge of the travel path and sound velocity and is beyond the scope of this paper.

Application as an Echo-Sounding Recorder

There are several commonly observed features of bottom echoes. These include echoes having the same length as the outgoing pulse which occur either as long sequences of closely correlated echoes (Fig. 3a), or shorter crescent-shaped sequences of echoes. The crescent sequences are interpreted as series of echoes from reflecting highlights on a rough bottom, the shape of the crescent being partly determined by motion of the ship relative to the highlight (Fig. 3b). These discrete echoes are usually accompanied by fainter, much more indistinct echoes as shown ; these signals sound like distinct echoes with very faint reverberation. Other bottom echoes have an intense portion equal in length to the outgoing pulse, which terminates more gradually. These sound like sharp echoes followed by reverberation of comparable intensity (Fig. 3c). Still other bottom echoes bear no resemblance to the outgoing pulse, and show little or no detailed correlation with each other. To the ear such echoes sound like a series of reverberations.

On a bottom appearing smooth when using the more usual recording speeds, we have recorded bottom echoes from shorter pulses and with higher resolution (e.g. Fig. 3a and c). In these examples the roll of the ship imposes its pattern, but, in addition (see especially Fig. 3c) the intense part of the echo sequence breaks up into more or less well-defined crescent sequences, and these are followed by fainter, rather patchy reverberation. The depth range of echo sequences having roughly the same darkness together with the approximate water depth can be used to compute the solid angle within which the strong highlights occur, and thus set a crude limit to bottom roughness. (Echoes from strong shoaler highlights, whose travel time is equal to or less than that of the principal group of bottom echoes, should reveal themselves by prolonged crescents like those in Fig. 3b). For Fig. 3a the ping length is roughly one fathom in a depth of about 500 fathoms. This record is somewhat complicated because the ship was under way and rolling, but crescents appear to form strongly over distances of, at most, about a fathom in depth, which corresponds to a cone of about 7 degrees. In 500 fathoms this corresponds to a circular patch of about 120 yards diameter from which echoes would not be completely resolved. However, the bottom echo is seldom strong for much longer than the pulse length. Hence the patch is probably even smaller ; a shorter ping length is needed to demonstrate how much smaller it may be. Similarly for Fig. 3c at a depth of 2752 fathoms the depth range encompassing the onset of all intense echoes is at most 6 or 7 fathoms, corresponding to a cone of about 8 degrees or a patch 1300 yards in diameter. Here again a shorter pulse would yield a more satisfactory estimate.

In a recording at moderately high resolution taken over a flat portion of the Puerto Rico Trench (Fig. 4a), the character of bottom roughness is especially interesting because of its great depth and its striking flatness. A 100-fathom gated scale was used with a ping length of about 3 fathoms. Here the undulations of the trace are due to the roll and pitch of the sounding ship, but the trace shows a clear bottom echo having the same length as the outgoing pulse, and is followed mostly by relatively weak reverberation. The variations in intensity suggest that an even shorter ping length and higher recording speeds would have brought out evidence of bottom roughness here.

Over a bottom recorded at 3 different resolutions (Fig. 4b) the 100-fathom scale shows a strong pulselike echo with complicated reverberation, and the more expanded scales show the principal reflection to consist of resolved echo sequences within the 3-fathom range covered by the ping length on the 100-fathom scale. Here the accom-

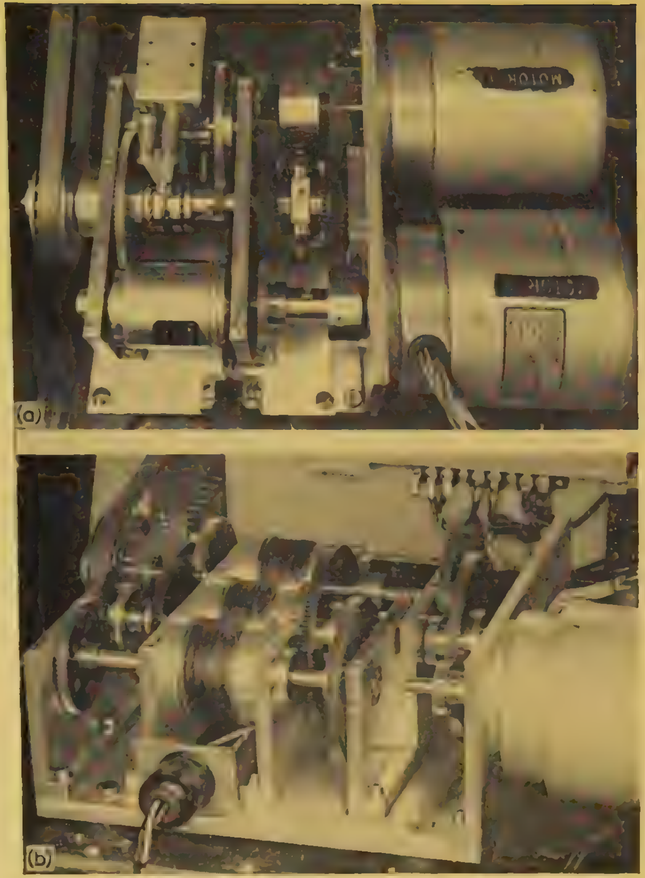

Fig. 1. Multispeed recorder drives :
(a) 16-speed gear assembly, (b) 6-speed gear assembly.

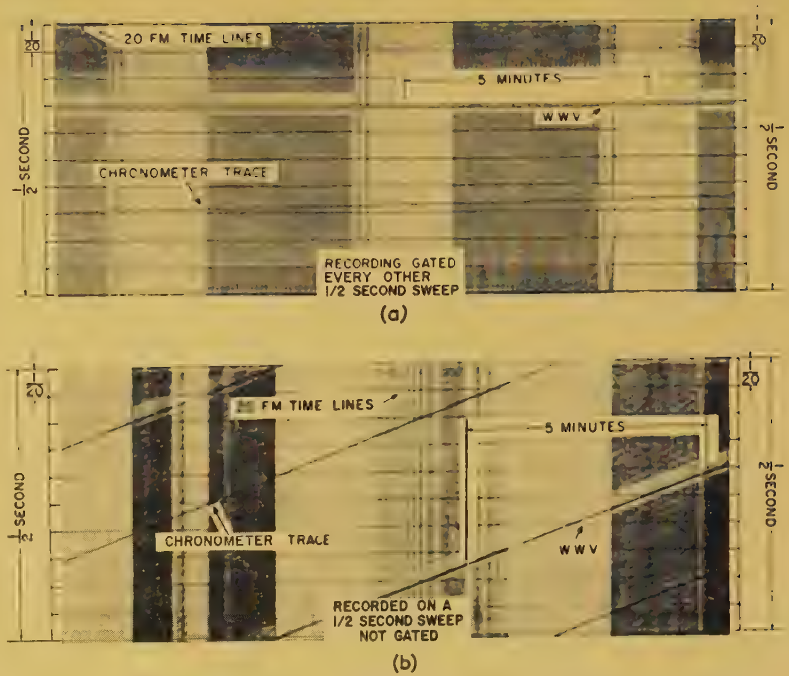

Fig. 2. Records of the timing grid and its calibration with a radio time signal and break circuit chronometer : (a) Precision power source close to 60 cycles, (b) Source constant but not at 60 cycles.

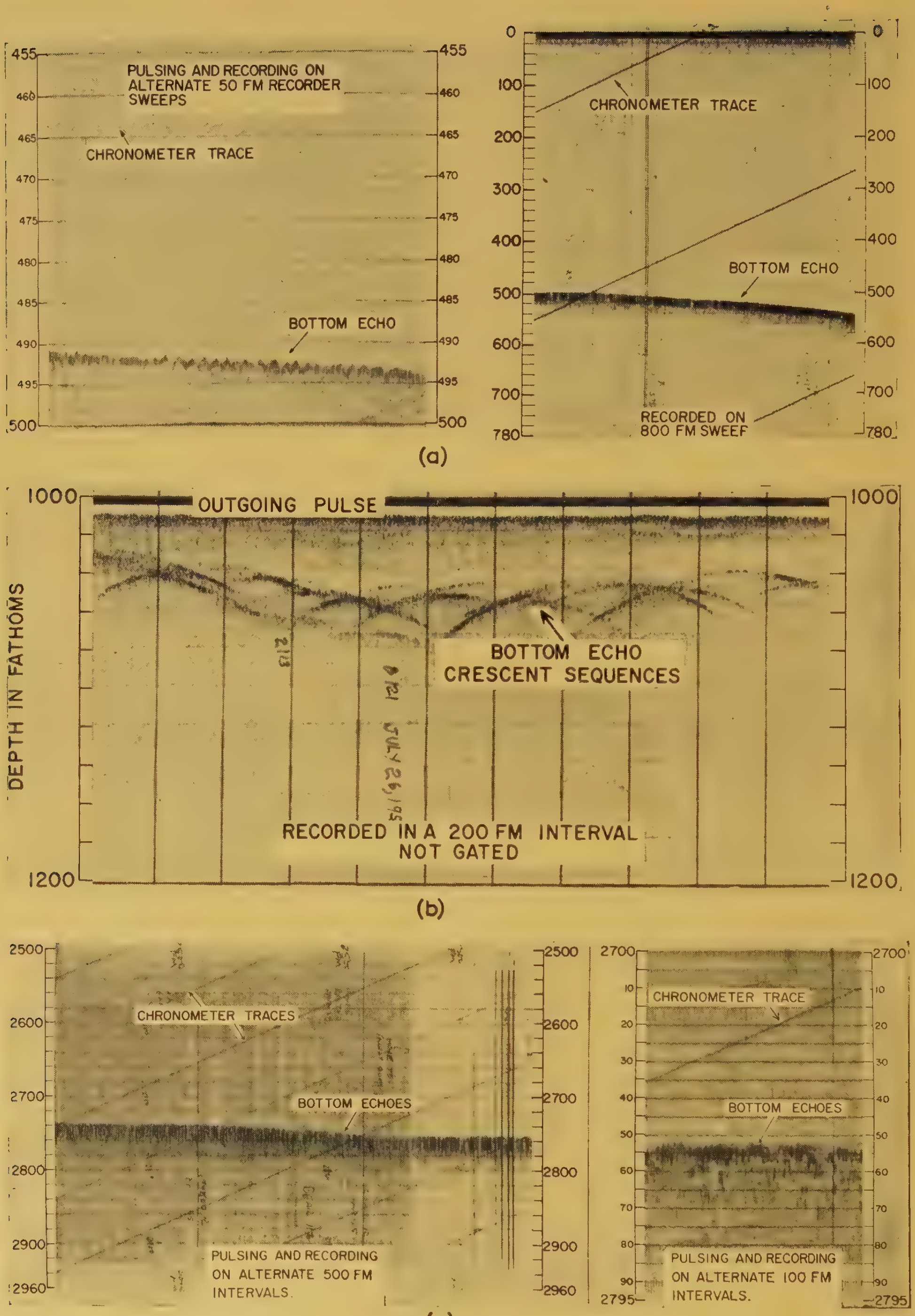

Fig. 3. Three examples of bottom roughness revealed by high resolution in various water depths. (a) 500 fm. – left, with an expanded scale, right, the same at lower resolution. (b) 1,000 fm. – with moderate resolution. (c) 2,700 fm. – left, low resolution ; right, the same with an expanded scale.

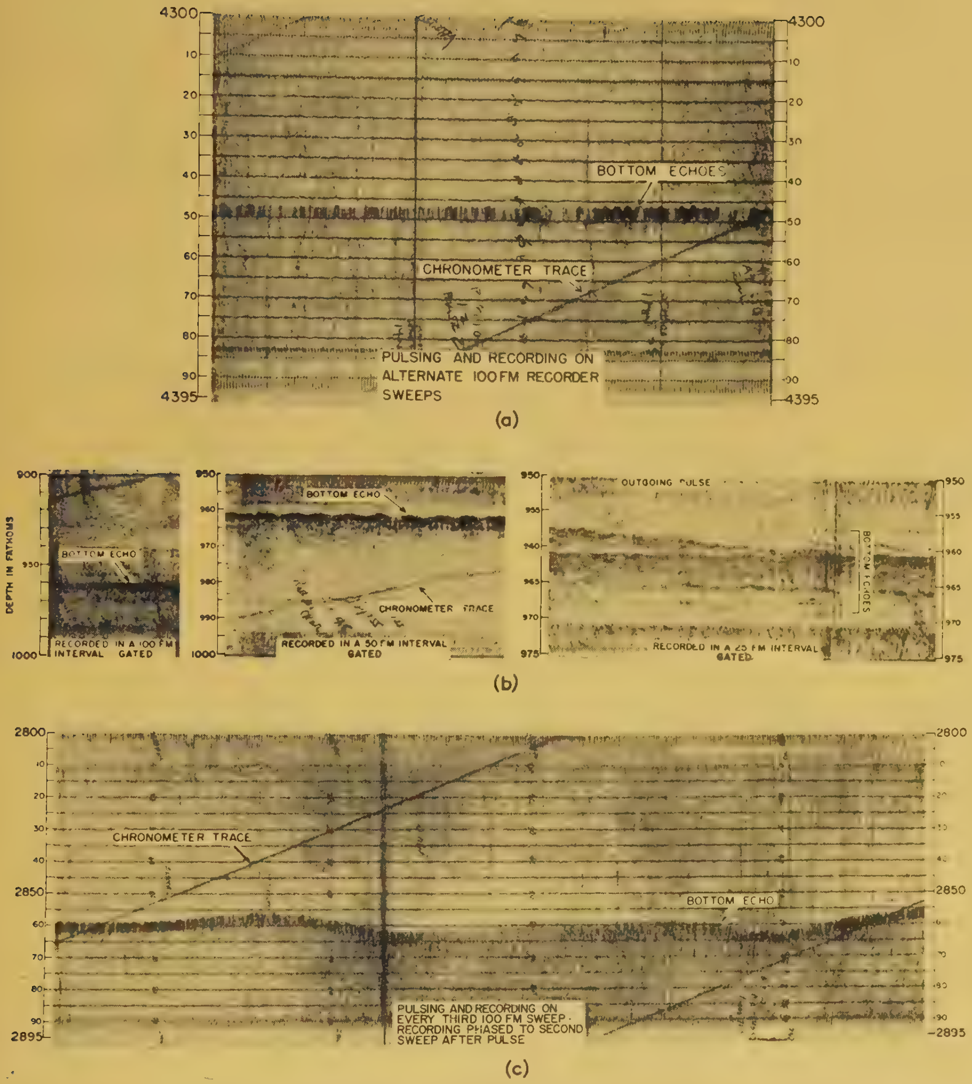

Fig. 4. Examples of high-resolution recording: (a) in the Puerto Rico Trench, (b) on a continental rise, (c) in an ocean basin.

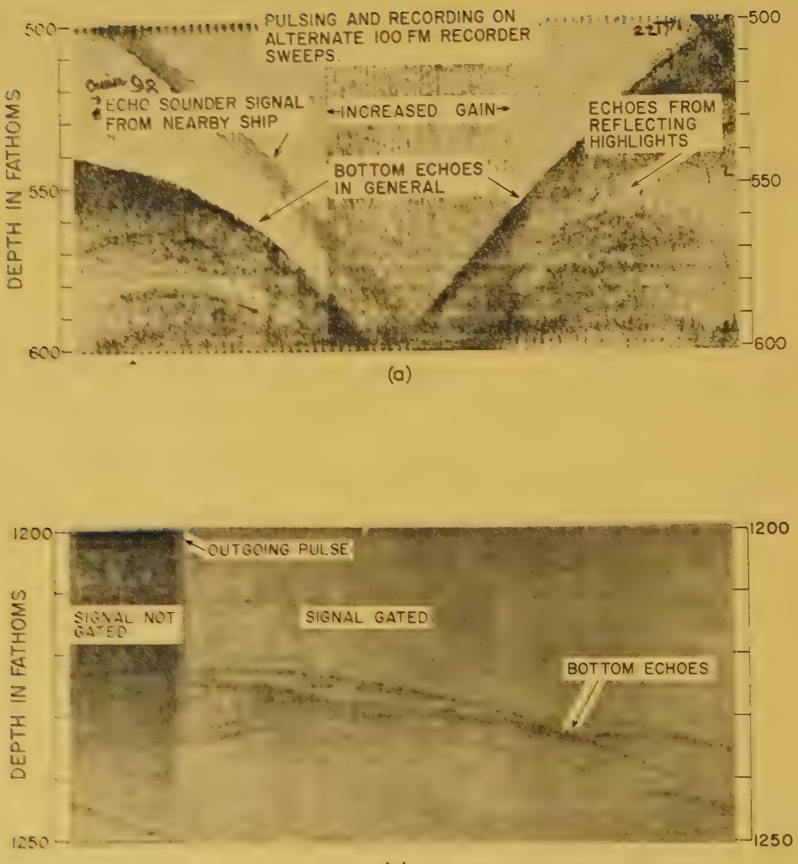

(a)

(b)

Fig. 5. High-resolution recordings in Block Canyon: (a) a traverse of the canyon using the 100-fm. writing rate. (b) a portion of the canyon bottom on a similar crossing using the 25-fm. writing rate.

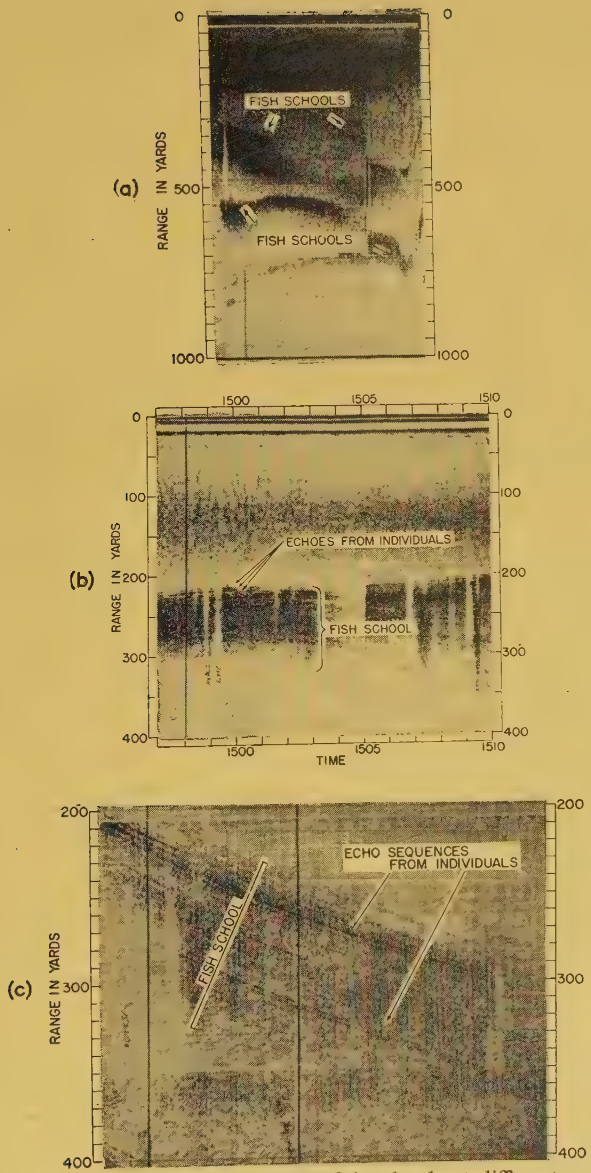

Fig. 6. (a), (b) and (c). Echo ranging on fish schools at different writing rates.

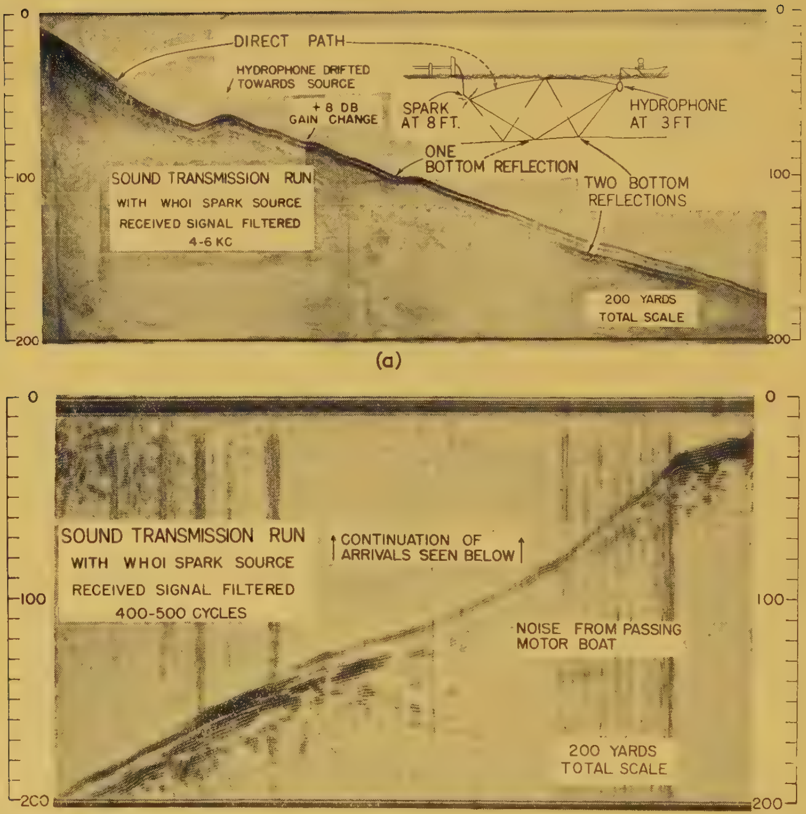

Fig. 7. (a) and (b). A sound transmission study in Great Harbor, Woods Hole.

panying patchy reverberation is frequently comparable to the principal echo. The usually fainter echoes whose travel times are shorter than the main group may have reflected from rough topography out to the side, or the whole complicated series could contain echoes from below the bottom ; with the present technique we cannot distinguish between these alternatives.

Study of the geomorphology of the ocean basin frequently hinges on reliably observing small changes of depth. High-resolution recording may reveal (Fig. 4c) these small changes in bottom depth and character even in very deep water. This recording was made east of the Bahamas, and possibly could be a depositional feature caused by density currents from the slope of the banks.

High-resolution techniques were used in an experimental study of Block Canyon in two cruises in 1954. The two recordings (Fig. 5) show the typical crescent-shaped highlights. The one at higher resolution shows how completely the echoes from the canyon floor are composed of highlights from individual reflectors. In an unpublished study of the crescent shapes of these canyon records, WILLIAM MOSS was able to show that some individual crescents come from reflectors of little horizontal extent while others are from extensive surfaces. We have been unable to return to this study since, but it appears that much could be deduced about the detailed shape of submarine canyons with a high-resolution echo sounder and very accurate navigation. An obvious extension of such observations would be to lower the echo sounder nearer to the bottom.

Applications to Echo Ranging

The application of this mode of recording to echo ranging is straight forward ; it has been described in naval applications and is increasingly being employed for exploration by the fishing industry. We have made a series of observations in waters near Woods Hole on fish schools which illustrate the kind of information made available by high-resolution recording. The EDO echo sounder was used with the recorder as in the echo-sounding applications above, but with its transducer trained horizontally. Several fish schools were recorded over a smooth bottom in shallow water (Fig. 6). By suitable gating one of the schools was singled out for recording with a short pulse at high resolution (Fig. 6b). The rather formless mass (Fig. 6a) becomes a series of discrete echoes (Fig. 6b and c) that can be correlated over minutes of time.

Applications to Scattering-Layer Studies

Recordings of the scattering layers of the deep ocean have appeared many times in the literature, but in most instances from a transducer at the surface and with only the resolution required to show the layered character. KANWISHER and VOLKMANN (1955) have described observations using an EDO echo sounder with the transducer lowered below the ship. They observed some individuals that could be resolved even with the 100-fathom scale of the EDO recorder. JOHNSON *et al.* (1956) have continued this line of investigation through several stages in the development of the Woods Hole Oceanographic Institution recorder, and have been successful in observing the movement of individuals in a layer during its migration, using high resolution. They have also photographed individuals which had first been " located " by means of the echo sounder.

Applications with a Sound Source having a Broad Spectrum

The applications described thus far have employed a single-frequency sound source. We have incorporated an electric spark discharged under water as a sound source in order to study frequency-dependent effects. The output of the sparker is usable over the range from 0.1 to 50 kc, and offers the possibility of studying in a more detailed way a range of problems which have been studied in the past, using explosives as sound sources. Typical examples are geologic structures at shallow depths below the bottom ; details of multiple-path transmission through the water where the travel times involved are nearly, but not quite, equal ; and the frequency-dependent properties of marine sound scatterers. The combination of the spark with the recorder is a powerful method for observing both short- and long-period variations in these phenomena. It can also be used in conjunction with an A-scan oscilloscope and camera for sound-intensity measurements, with the recorder acting as continuous observer for determining when 'scope photographs should be taken.

A recording was made of the underwater transmission from the sparker at the institution's dock to a hydrophone towed by a rowboat to distances of the order to 200 yards (Fig. 6). The spark sound pulse is emitted when the helix starts its sweep near the edge of the paper, and sound received over various paths is recorded as it arrives at the hydrophone. The first recording (Fig. 7a) was made through a 4-to-6-kc band-pass filter. The first arrival noted at the shorter ranges is transmitted directly through the water, and it is double owing to the bubble pulse from the spark. The second group of arrivals is a single bottom reflection which is somewhat complicated, the principal features being four arrivals near its leading edge. Two of the arrivals are the initial sound and bubble pulse, while the others are related to them by travel-time differences to be expected from bottom-reflected travel paths directly from the spark and, after one reflection, from the surface near the spark. (The spark was 8 feet below the surface ; the hydrophone, 3 feet). The third group of arrivals corresponds to paths involving two reflections from the bottom ; they are seen to be weakly developed over most of the experiment, but do come in strongly at certain ranges. Subsequent repeats of the same test showed this intensification to be reproducible. A similar run was recorded through a 400-to-500-c.p.s. band-pass filter (Fig. 7b). While the same general features can still be seen, they are not as readily resolved because of the lower frequency, but the more striking contrast between the two frequency bands is the appearance of a complicated set of arrivals at the lower frequency, which come in later than those mentioned above and which have no counterpart in the higher-frequency recording. These may well be reflections from below the bottom where the higher frequencies are very rapidly attenuated. In other test observations we have recorded scattering from fish schools in Vineyard Sound at both low and high frequencies, and have recorded consistent low-frequency echoes having no high-frequency counterpart, which have the appearance of coming from a reflecting surface below the bottom. On another occasion off the coast of South Carolina a subbottom echo was recorded with the multichannel recorder described above ; it appeared strongly on a low frequency channel, but not at all on a high-frequency channel.

From these two observations and other tests we find the recorder satisfactory, but the spark source rather too weak for any other than short range phenomena.

Applications to the Locations of Instruments

BACKUS and HERSEY (1956) determined the shape of a trawl wire with a standard Edo echo sounder. Similarly other objects of sufficient target strength have been tracked to depths of several hundred fathoms. Sonobuoys have been located for retrieving at a range of three miles by pointing the Edo transducer horizontally and recording the radio transmission of the sound received at the buoy. The buoy used was not intended for this purpose ; a sonobuoy of suitable design could be located at considerably greater ranges.

Acknowledgements—We are indebted to several members of the staff of the Woods Hole Oceanographic Institution for suggestions and assistance in the design, construction, and testing of the recorder. We are especially indebted to the instrument-shop staff of The Woods Hole Oceanographic Institution for their interest in the construction of the gear drives and their help in meeting cruise deadlines. MR. WARREN WITZELL made many valuable contributions to the mechanical design, and MR. HERBERT SMALL developed the principal electronic components such as the pre-amplifiers and power amplifier feeding the recording stylus, and the timing-grid generator.

The recorder was developed and tested at sea under Contract NObsr-43270 and NObsr-72521 with the Bureau of Ships.

Contribution No. 863 *of the Woods Hole Oceanographic Institution.*

REFERENCES

BACKUS R. H. and HERSEY, J. B. (1956), Echo-sounder observations of midwater nets and their towing cables. *Deep-Sea Res.* **3** (4), 237-241.

DIETZ R. S. (1948), Deep scattering layer in the Pacific and Antarctic Oceans. *J. Mar. Res.* **7** (3), 430-442.

HERDMAN H. F. P. (1953), The deep scattering layer in the sea ; association with density layering. *Nature* **4372**, 275-276.

HERSEY J. B. and MOORE H. B. (1948), Progress report on scattering layer observations in the Atlantic Ocean. *Trans. Amer. Geophys. Union* **29**, 341-354.

HERSEY J. B. and EWING M. (1949), Seismic reflections from beneath the ocean floor. *Trans., Amer. Geophys. Union* **30**, (1), 5-14.

HODGSON W. C. and FRIDRIKSSON A. (1955), Report on echo-sounding and asdic for fishing purposes. *Rapp. Proc. Verb., Cons. Perm. Int. Expl. Mer.* **139**, 1-49.

JOHNSON H. R., BACKUS R. H., HERSEY J. B. and OWEN D. M. (1956), Suspended echo-sounder and camera studies of midwater sound scatterers. *Deep-Sea Res.* **3** (4), 266-272.

KANWISHER J. and VOLKMANN G. (1955), A scattering layer observation. *Science* **121** (3134), 108-109.

MURRAY H. W. (1947), Topography of the Gulf of Maine. Field season of 1940. *Bull. Geol. Soc. Amer.* **58**, 153-196.

LUSKIN B., HEEZEN B. C., EWING M., and LANDISMAN M. (1954), Precision measurement of ocean depth. *Deep-Sea Res.* **1** (3), 131-140.

TUCKER G. H. (1951), Relation of fishes and other organisms to the scattering of underwater sound. *J. Mar. Res.* **10** (2), 212-238.

Printed in Great Britain by The Salisbury Press Ltd., Publicity House, Wilton Road, Salisbury, Wilts. (1111)

Contribution No. 864

Reprinted from
BULLETIN OF MARINE SCIENCE
OF THE GULF AND CARIBBEAN
Vol. 6, No. 4, pp. 273-287
DECEMBER, 1956

THE EFFECTS OF TEMPERATURE, ILLUMINATION AND PRESSURE ON THE VERTICAL DISTRIBUTION OF ZOOPLANKTON[1, 2]

H. B. MOORE AND E. G. CORWIN
The Marine Laboratory, University of Miami

ABSTRACT

Thirteen 24-hour plankton stations were worked in the Florida Current and counts made for four species of siphonophores. Depth, temperature and illumination data accompanied all net hauls. An equation is developed relating the depth of each species at any given time to external conditions of temperature, illumination and pressure. This involves null value of each at which there is no stimulus to vertical movement, and factors giving relative response to each of the three environmental influences. The nulls are not solved here; the factors show a diurnal rhythm and also a progressive change from predominance of light control in the upper part of the population to predominance of temperature control in the lower part.

INTRODUCTION

In earlier studies (Moore, 1953, 1955; Moore, et al, 1953) it was shown that changes in the temperature and illumination are reflected in corresponding changes in the noon vertical distribution of various kinds of oceanic zooplankton. A balance appears to be attained, such that the stimulus to move upwards into warmer water just counteracts the stimulus to move downwards to a lower level of illumination. Furthermore, the deeper-living individuals in a population are more influenced by a given temperature change than the shallower ones while the latter are more influenced by a given change of illumination. That there is such a gradation of reaction through a population is to be expected since all individuals are not concentrated at a single depth but rather are spread over a wide range of external conditions.

In an attempt to relate, mathematically, the depth occupied and the external conditions, the general conditions of temperature and

---

[1] Contribution No. 161 from The Marine Laboratory, University of Miami.
[2] Contribution No. 864 from the Woods Hole Oceanographic Institution.

illumination were expressed as the depths of a selected isotherm and isolume, and all data were translated into deviations from annual mean values of these depths at noon. Similarly the depth of the organism in question at noon was expressed as deviation from its annual mean noon depth. This had the advantage of allowing results for a number of different species to be grouped together and thus increasing the significance of results based on somewhat inadequate data. When the depths, temperatures and illuminations had been converted to deviations, partial regressions were calculated, and it was in this form that the plankton behavior was expressed. The population was separately analyzed at nine levels from 10% to 90%, the percentage representing the proportion of the population above that level. For each such level we solved the equation

$$d = T \text{ fac. } t + I \text{ fac. } i \qquad (1)$$

where the factors are obtained as partial regressions and t, i, and d are the deviations from the mean of isotherm, isolume and plankton depth respectively.

This equation, in effect, related vertical movement of the animals to vertical movements of a given temperature and illumination level, and as such gave a close prediction of where the plankton would be found under widely varying conditions. At a test of its applicability, the equation predicted that the plankton at a station 40 miles east of Miami should be at least twice as deep as at a ten mile station. Roane (1954) verified this for the siphonophores, the mean day level, averaged for eight species, being 79 meters at the 10 mile station and 253 meters at the 40 mile station.

The type of equation given above yielded good values for the depth of the organism in terms of the displacement of isolines but proved useless in trying to relate depths with actual temperatures and illuminations *in situ*. Furthermore, some of the partial regressions obtained were greater than 1.0, suggesting an over-compensation by the animals. The present paper presents a modified equation which allows the actual values to be used rather than the deviations and appears to come closer to representing the actual mechanism involved.

Since we commence with counts of organisms in net hauls whose sampling variation is unknown, it seems valueless to attempt to determine the significance of the final figures arrived at. It must therefore be strongly emphasized that these figures should be considered as establishing certain general trends but not as being accurate

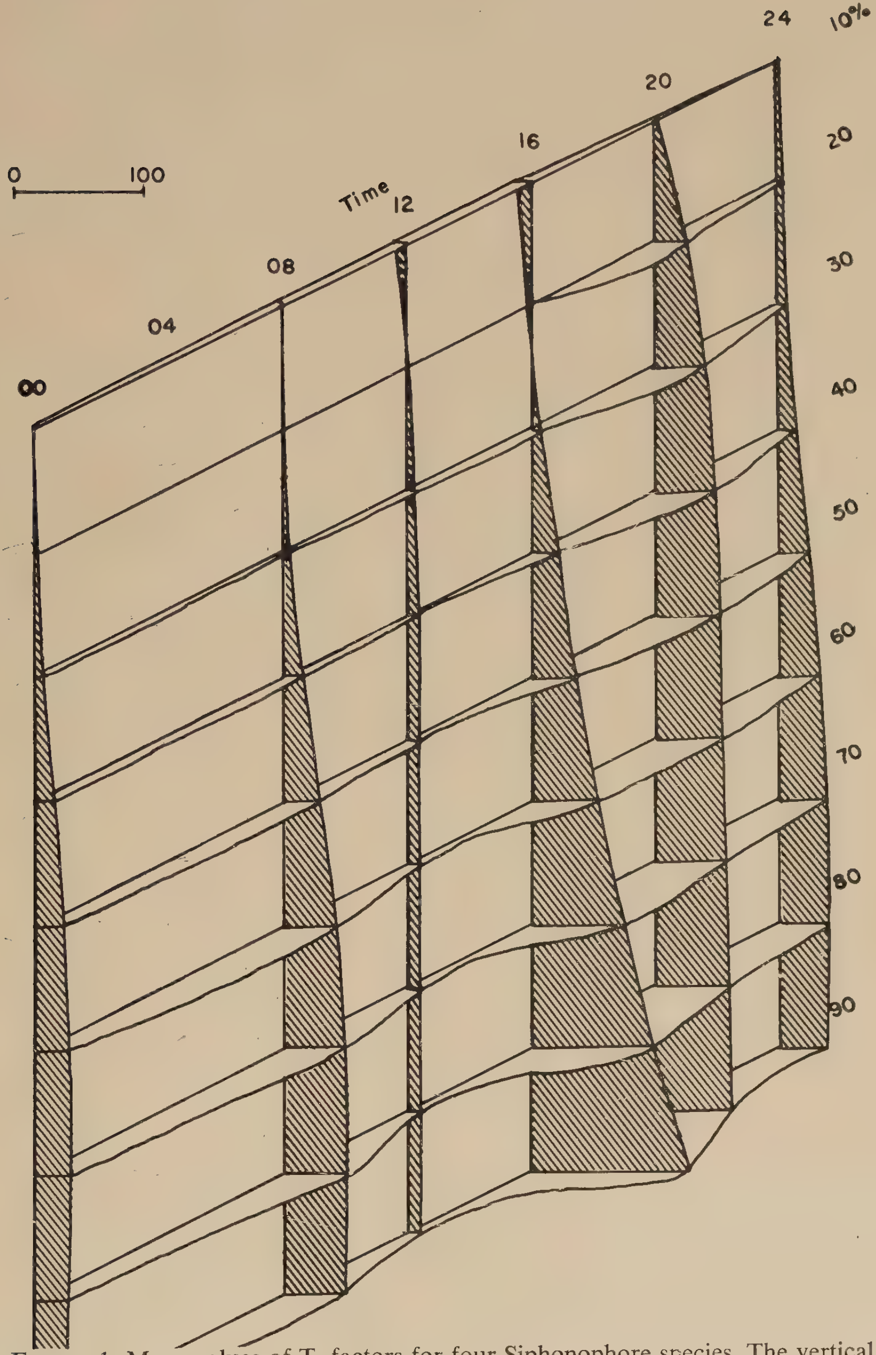

FIGURE 1. Mean values of T. factors for four Siphonophore species. The vertical coordinates represent percentage levels in the population. The horizontal coordinates are time and strength of factor. A vertical section (hatched) shows, for a given time, the variation in factor strength through the population. A horizontal section shows the diurnal change in the factor at a given percentage level.

in detail. It should be stated that the data used have served mainly for the development of methods. The diurnal rhythms found were considered questionable until more material had been collected and analyzed. Analysis of copepod behavior, based on a new and larger series of hauls, has confirmed the general pattern of these rhythms and has justified the presentation of the present series.

MATERIAL AND METHODS

Net hauls were available from thirteen stations at different locations in the Florida Current off Miami. At each, from six to nine hauls were made at different depths, and this series was repeated through a 24 hour period. However, weather and other conditions sometimes curtailed operation so that the number of stations usable varies with time of day. The collecting methods were those previously described. All counts were reduced to the equivalent of a one-mile tow and are accompanied by depth, temperature and illumination data. The full series of nets could not be towed simultaneously, so values have been interpolated at standard times at four hour intervals through the 24 hours.

The present treatment does not apply to conditions of complete darkness. We have therefore omitted those night hours when there was no moonlight. Unfortunately, these were mostly at 0400 hours so that the remaining data for this hour is insufficient for analysis.

The material was drawn from samples, collected for other purposes, in part under a joint program of the Marine Laboratory of the University of Miami and the National Geographic Society, in part under the contract number NObsr-57146 for the Office of Naval Research and in part under a grant from the Rockefeller Foundation. The analyses were carried out under contracts listed above and also under a National Science Foundation grant and under contract number NObsr-43270 at Woods Hole Oceanographic Institution.

EQUILIBRIUM EQUATION

The only formulation which would account for the observed facts required the inclusion of a third factor which was correlated linearly with depth. This is assumed to be pressure, and there is some evidence that pressure may control vertical movement of plankton (Hardy and Bainbridge, 1951; Knight-Jones and Quasim, 1955). Since our assumed pressure factor is derived from depths, the unit used is meters

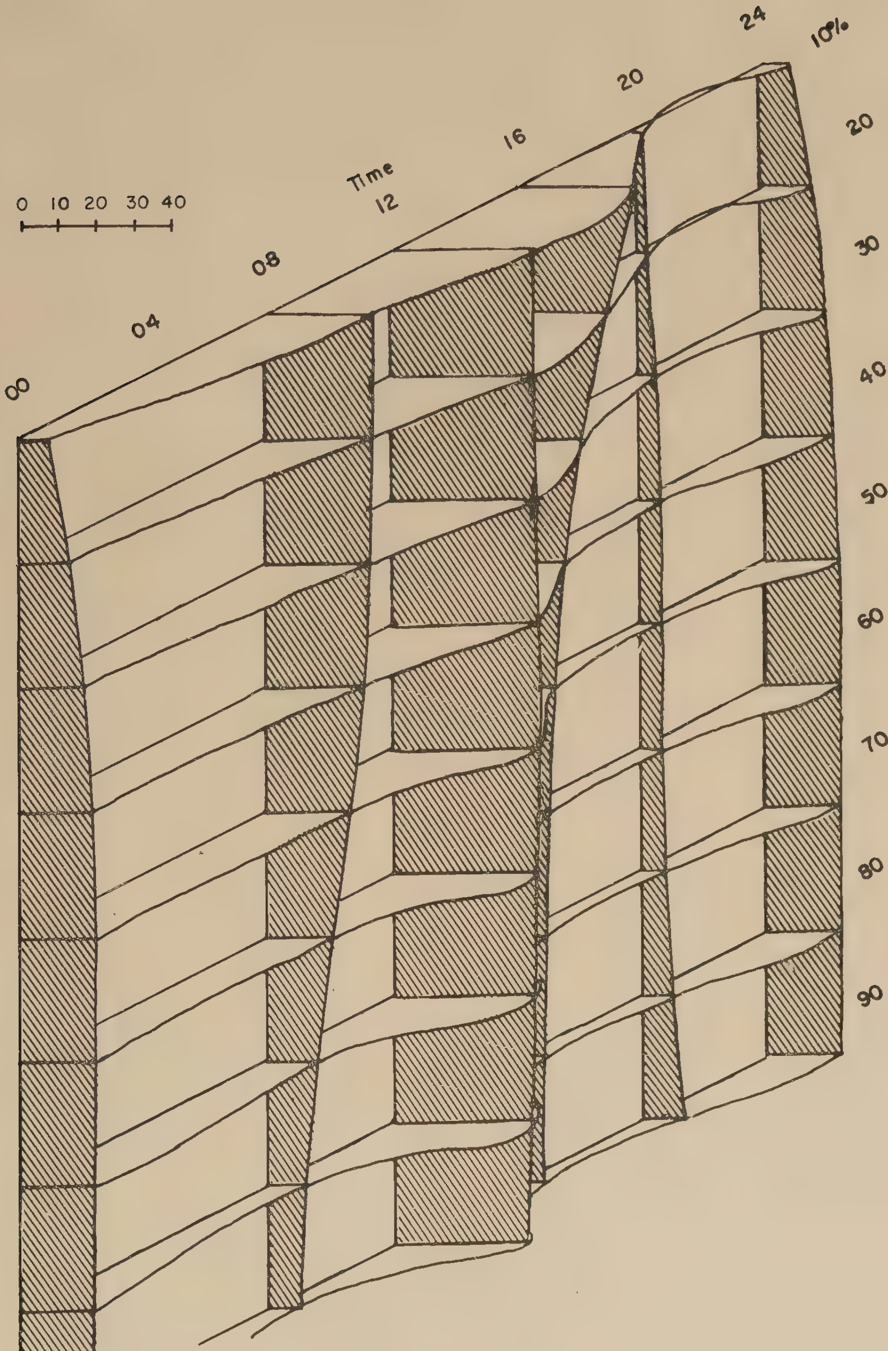

FIGURE 2. Mean values of I. factors for four Siphonophore species, represented as in Fig. 1.

of water. The light unit is the exponent to the base ten with full sunlight rated at 10^2. Temperatures are in degrees centigrade.

It is assumed that there are null values of temperature, illumination and pressure (T_n, I_n and P_n) at which an animal has no tendency to move upwards or downwards. This does not exclude the possibility of their oscillating between two limiting values since the null would represent the mean of these. It is further assumed that the strength of the animal's response is linearly proportional to the difference between the null values and the *in situ* values of the condition to which the animal is exposed. While this is improbable, it is necessary as an approximation if the solution is not to become impossibly complex at the present stage.

We may therefore represent the strengths of the stimuli to vertical movement as $T\text{-}T_n$, $I\text{-}I_n$ and $P\text{-}P_n$ where T, I, and P are the temperature, illumination and pressure *in situ,* and T_n, I_n and P_n, the null values of each. To equate relative responses to the three stimuli, it is necessary to designate three factors, T. fac., I. fac., and P. fac. Since these are determined relatively and not absolutely, one of them, P. fac., is assumed to be always equal to one. If it varies, certain changes are implied, which will be discussed later.

If the animals of a given part of the population, and at a given time, have achieved an equilibrium between their responses to the three stimuli, then

$$\text{T fac. }(T\text{-}T_n) + \text{I fac. }(I\text{-}I_n) + \text{P fac. }(P\text{-}P_n) = 0 \qquad (2)$$

It is initially assumed that the organisms at different percentage levels of the population may differ in their responses and in their nulls. There may also be differences in diurnal rhythm. There may be some delay in response to changing conditions but both net hauls and scattering layer records have frequently demonstrated the ability of plankton to keep pace in its vertical movements with the rapidly changing illumination at sunrise and sunset. Thus, for each time and percentage level we have an array of occasions with different, known values of T, I and P. With these it is possible to obtain a solution to part of the equation, namely the three factors. Equation 2 may be rewritten:

$$\text{T fac. } T + \text{I fac. } I + \text{P fac. } P = \text{T fac. } T_n + \text{I fac. } I_n + \text{P fac. } P_n \quad (3)$$

and the sum of the right hand part may be temporarily designated Tot. fac.

Solution by partial regressions gives us the best fitting values of T fac., I fac. and Tot. fac.; P fac. is assumed to equal one. The values for T and I factors are given in Tables 5-8, while Figures 1 and 2 are smoothed curves drawn from the mean value for the four. The 0400 hour series, as stated above, is missing, and the 2000 hour means are based on two species only. The other two being inadequately represented.

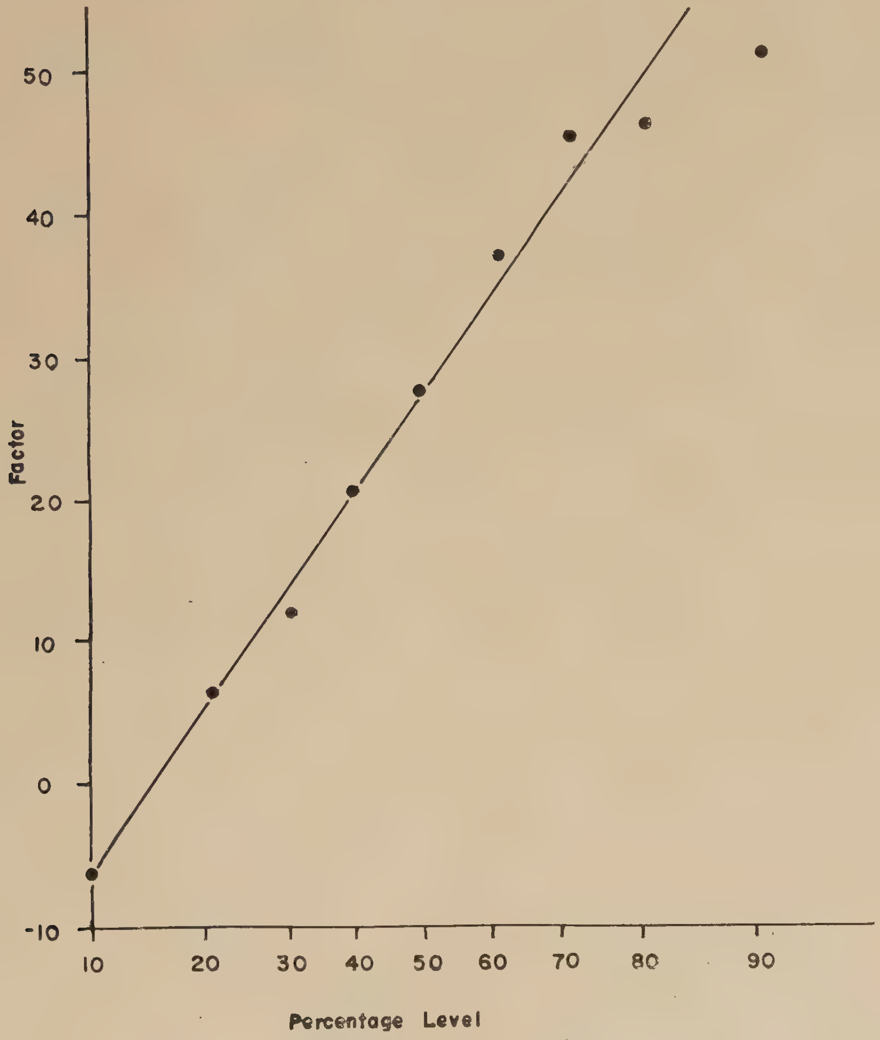

FIGURE 3. Mean of T. factors for four Siphonophore species, taking all times, in relation to percentage level. These are plotted on linear probability paper.

Bearing in mind that only generalizations, and not details, should be taken from these results, one or two particular aspects may be considered. In the first place, earlier work indicated a change from dominant illumination sensitivity in the upper part of the population to dominant temperature sensitivity in the lower part. If we take the means for all hours for the present data we find this to be true here also. In the earlier work it was stated that the partial regressions, which were not strictly equivalent to the present ones, seemed to vary linearly with percentage level. The present values approach a straight line on linear probability paper (Figs. 3, 4) which suggest that they represent a more or less normal distribution of the two factors through the population. Again we must not draw too detailed inferences from the data. The misfit of the 90% values, particularly for the I factor, may well be due to the inadequacy of the original sampling since this is the sparsest part of the population.

We originally assumed that the pressure factor was constant with a value of one. In view of the variation in the other two factors it seems probable that the pressure factor also varies. Since they are measured in units relative to the pressure factor at any given time and percentage level, the values shown in Figures 1 and 2 would have to be correspondingly modified. This might result in a change in the gradient of a factor through the population or in its diurnal rhythm in itself or one of the other two factors. Changes in the pressure factor could, however, in no way modify the diurnal and percentage level changes in the relative strengths of the temperature and illumination factors. In other words the change from shallow illumination sensitivity to deep temperature sensitivity is real, as is the diurnal change in their relations.

The second generalization which may be made from the data is that there is a marked diurnal rhythm in the factors. In general there is a marked noon drop in the temperature factor with a corresponding increase in the illumination factor. The 1600 hours series appears to indicate an over-compensation following the noon condition. The 2000 hours and 0800 hours conditions are so similar that it seems unlikely that the missing 0400 hours series would be much different.

It can be shown that, even if the pressure factor varies, there will still be a diurnal rhythm in the relative strengths of the temperature and illumination factors. The ratio $\frac{\text{T fac}}{\text{I fac}}$ can be calculated, and expressed as the mean for all percentage levels. To eliminate the effects of the few negative values for the factors, a constant can be added throughout which makes all values positive. This does not affect the general trend of the means. Table 1 shows the mean values of $\frac{\text{T fac.} + 14}{\text{I fac.} + 3}$

TABLE 1

Time	00	04	08	12	16	20
Ratio	17.73	—	3.06	0.45	4.66	10.22

Discussion

At an earlier stage in these studies it was shown that there was a very similar pattern of response to temperature and illumination in widely different groups of plankton animals (Moore, et al, 1953). An average siphonophore (mean of 8 species) was very similar to an average chaetognath (9 species), pteropod (6 species) or copepod (18 species). The depth at which they were found most closely reflected isolume movements in the upper part of the population and isotherm movement in the lower part. This was later confirmed in more detail for siphonophores and chaetognaths (Moore 1955). Coming to individual species, the pattern is the same, although here we are relating depth to actual temperature and illumination, and not to movements of isotherms and isolumes. If we take, for each species, the mean value of temperature and illumination factor for all percentage levels, and exclude 2000 hours, for which only two of the species were analyzed, we obtained the following values:

TABLE 2
Mean Values of Factors

	T fac.	I fac.
Abylopsis eschscholtzii	20.7	21.1
A. tetragona	17.3	19.9
Eudoxoides mitra	23.6	20.0
Chelophyes appendiculata	24.9	20.1

The differences are very small and perhaps not even significant. Yet these species characteristically live at very different levels. The following mean day levels are given by Roane (loc. cit.). In the Florida Current the cold water comes closer to the surface at the 10 mile than at the 40 mile station. Depths at the 40 mile station are the means of Roane's values for the two generations.

TABLE 3
MEAN DAY LEVELS. DEPTHS IN METERS

		Florida Current	
	Bermuda	10 Mile	40 Mile
Abylopsis eschscholtzii	40	58	171
A. tetragona	55	104	188
Eudoxoides mitra	125	134	270
Chelophyes appendiculata	75	74	221

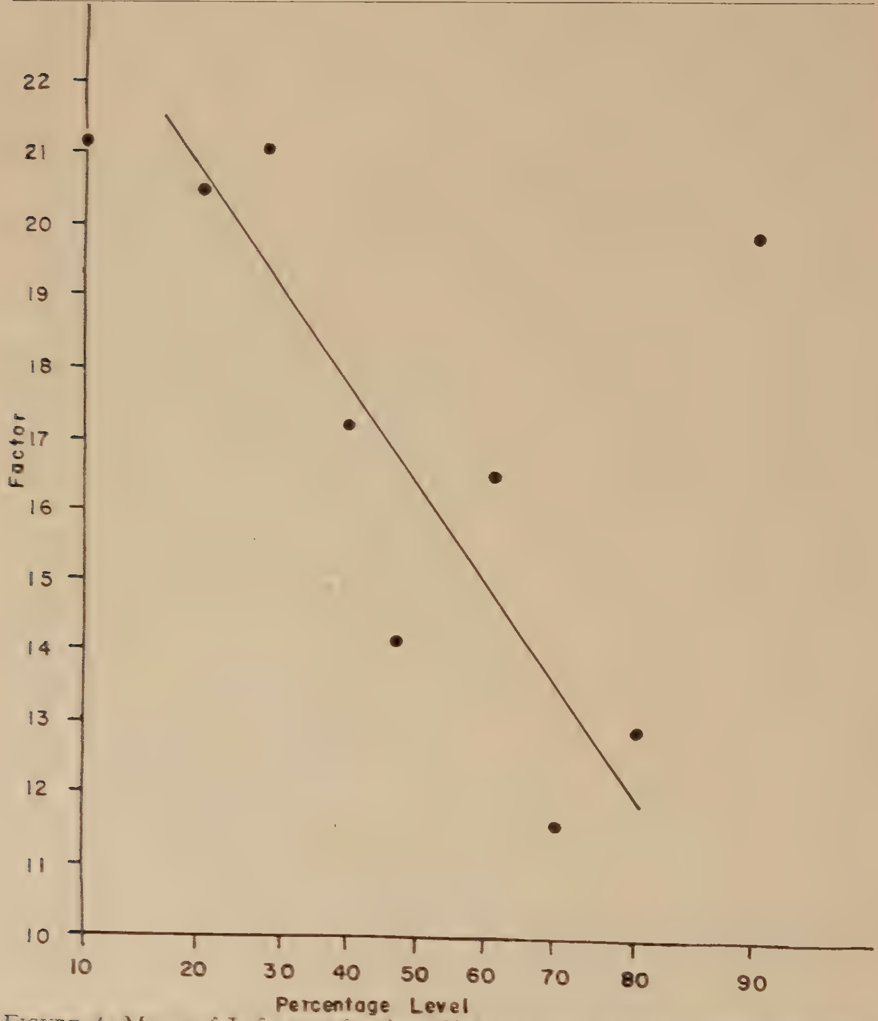

FIGURE 4. Mean of I. factors for four Siphonophore species, taking all times, in relation to percentage level. These are plotted on linear probability paper.

The present paper does not present the analysis of the second part of the equation, which yields the null values of temperature, etc., at which the animals are not stimulated to vertical movement. The similarity of their responses to unit change of temperature, etc., suggests that the difference in the levels characteristically occupied is more likely to reflect specific differences in their null values.

It is not surprising that there should be a regular change through the population in the relative strength of temperature and illumination response. It is true that random movement about an optimal depth would result in vertical spread but it is hard to believe that animals with identical behavior characteristics would tolerate the wide range of external conditions which they would encounter. Roane (loc. cit.) gives the following vertical spreads between the 25% and 75% levels. For the entire population, 0% - 100%, these would be still greater.

TABLE 4

VERTICAL SPREAD IN METERS

		Florida Current	
	Bermuda	10 Mile	40 Mile
Abylopsis eschscholtzii	80	51	219
A. tetragona	25	63	234
Eudoxoides mitra	105	65	209
Chelophyes appendiculata	130	81	134

If such spreads are not due to random movement they must represent a sorting of the population resulting from individually different behavior characteristics.

The existence of a diurnal rhythm in degree of response to the same stimulus is also in accord with the numerous examples of rhythms known in other animals. While some of these are timed by varying external conditions, many others are known to be timed by an internal "clock." It has been suggested that the observed rhythm reflects a conditioning to the much more intense light in the middle of the day or is even an effect of the response scale not being linearly related to the illumination scale. This at first sounds reasonable, since the light changes many million-fold diurnally, whereas the temperatures and pressures encountered have a far smaller range. However, the animals to a great extent regulate their level so as to follow a constant illumination and the actual light changes they encounter during their diurnal movement are of comparable magnitude with the temperature and pressure changes.

It is interesting to make a tentative comparison of the relative effects of the three environmental conditions considered. A change of one light unit represents a ten-fold change in light. Temperature is in degrees centigrade and one pressure unit is equivalent to one meter of water or about a tenth of an atmosphere. Both temperature and illumination factors have mean values of about twenty, so a ten-fold light change, or a 1°C temperature change is equivalent to about two atmosphere. Dr. P. F. Scholander suggested that it would be more logical to consider volume changes rather than pressure changes and that the reciprocal of the pressure might yield better correlation than the pressure istelf. This was tested, but found not to be true.

We wish to express our indebtedness to many people for assistance. The Captain, crew and various scientists on board made possible the extensive collecting at sea. This work was done from The Marine Laboratory R/V PHYSALIA. Illumination and temperature data were worked up by various members of the Laboratory staff. The counting was done partly by the senior author and partly by D. C. Roane (1954). Thanks are due to various members of Woods Hole Oceanographic Institution for helpful criticism and suggestions. Finally invaluable assistance in statistics was received from Dr. F. Smith of the University of Michigan, Dr. C. C. Taylor of the U. S. Fish and Wildlife Service in Woods Hole, Mrs. Helen Roberts of Woods Hole Oceanographic Institution, and Miss A. Feinstein, of The Marine Laboratory, University of Miami.

TABLE 5

Abylopsis eschscholtzii

	TEMPERATURE FACTORS			
%	00.00	08.00	12.00	16.00
10	+3.8	—5.1	—3.3	—17.0
20	+8.0	—11.9	—15.1	—18.7
30	+9.4	—11.8	—1.2	+0.6
40	+13.6	+1.9	+16.3	+20.5
50	+12.1	+6.7	+37.7	+38.2
60	+47.8	+36.0	—4.6	+57.4
70	+178.4	+25.6	—3.3	+52.5
80	+12.3	+42.4	+22.5	+63.6
90	+15.3	+41.8	+3.3	+69.8

TABLE 5 (Cont.)

ILLUMINATION FACTORS

%	00.00	08.00	12.00	16.00
10	+2.0	+21.0	+38.2	+37.9
20	+6.7	+37.9	+47.3	+23.9
30	+21.3	+43.5	+40.8	+12.8
40	+16.0	+33.7	+26.6	+5.4
50	—0.6	+33.6	+3.4	+13.9
60	+2.2	+36.2	+65.3	+11.2
70	—58.1	+15.1	+53.6	+20.7
80	+32.2	+4.8	+11.9	+12.7
90	+30.7	+7.9	+44.6	+4.6

TABLE 6

Abylopsis tetragona

TEMPERATURE FACTORS

%	00.00	08.00	12.00	16.00
10	—5.3	+11.7	+8.8	—9.8
20	—1.4	+16.2	—0.9	+0.9
30	+6.9	+2.8	—0.5	+4.6
40	+26.9	+15.3	+5.8	+11.4
50	+12.4	+30.3	—3.8	+31.0
60	+24.6	+46.1	—4.1	+37.3
70	+22.7	+46.2	—2.6	+43.8
80	+25.1	+52.0	—1.7	+40.7
90	+33.1	+33.9	—2.8	+62.7

ILLUMINATION FACTORS

%	00.00	08.00	12.00	16.00
10	+7.2	+16.6	+25.5	+36.4
20	+20.6	+21.4	+38.7	+26.1
30	+21.5	+28.3	+38.1	+22.8
40	+12.9	+16.9	+21.3	+18.1
50	+21.3	+10.1	+38.9	+10.4
60	+16.0	+4.0	+40.0	+7.5
70	+15.2	+5.4	+37.6	+4.7
80	+16.2	+1.1	+37.0	+11.9
90	+15.3	+13.7	+37.5	+2.1

TABLE 7

Eudoxoides mitra

Temperature Factors

%	00.00	08.00	12.00	16.00	20.00
10	+4.8	—13.3	—2.8	—7.0	—0.1
20	+5.0	—6.7	—3.4	—6.0	+36.2
30	+6.8	+15.8	—9.7	+9.9	+39.7
40	+21.5	+29.6	—3.4	+19.5	+56.5
50	+31.3	+45.5	—4.2	+34.2	+55.1
60	+36.6	+58.6	—2.7	+56.7	+72.0
70	+42.7	+65.6	—7.2	+99.8	+73.2
80	+63.2	+71.6	—5.5	+105.2	+79.2
90	+34.7	+46.1	—2.0	+4.6	+67.7

Illumination Factors

%	00.00	08.00	12.00	16.00	20.00
10	+25.5	+25.5	+37.9	+30.8	+1.6
20	+24.4	+26.0	+38.6	+29.1	+3.8
30	+24.6	+17.1	+45.4	+19.5	—3.3
40	+21.0	+11.6	+37.1	+15.5	+7.1
50	+19.5	+5.5	+38.0	+10.7	+7.8
60	+18.5	+0.8	+37.0	+4.7	+9.4
70	+16.7	+0.0	+37.0	—8.1	—2.7
80	+5.6	—1.5	+36.4	—17.4	+6.1
90	+15.3	+13.3	+38.5	+21.0	+7.3

TABLE 8

Chelophyes appendiculata

Temperature Factors

%	00.00	08.00	12.00	16.00	20.00
10	+5.3	—	—	—	—
20	+8.3	+6.9	+31.2	+17.4	+12.5
30	+10.5	+3.8	+17.3	+25.6	+38.2
40	+18.7	+0.6	+13.4	+27.6	+30.0
50	+26.2	+34.1	+26.9	+40.1	+26.4
60	+36.5	+24.9	+9.7	+58.9	+42.0
70	+33.8	+33.0	+8.2	+68.9	+31.6
80	+30.9	+37.7	+19.2	+72.5	+64.7
90	+54.2	+35.3	+5.6	—	+34.9

TABLE 8 (Cont.)

ILLUMINATION FACTORS

%	00.00	08.00	12.00	16.00	20.00
10	—7.4	——	——	——	——
20	—6.7	+24.1	+22.8	+20.3	—1.8
30	+15.4	+25.9	+32.2	+14.4	—0.1
40	+14.5	+26.3	+33.1	+12.0	+4.7
50	+12.6	+9.5	+25.6	+6.4	+4.8
60	+11.6	+13.2	+35.4	+1.4	+3.3
70	+15.6	+10.2	+36.9	+6.3	+8.7
80	+21.2	+8.6	+31.1	+11.2	+11.6
90	+13.8	+12.8	+35.8	——	+17.6

REFERENCES

HARDY, A. C. AND R. BAINBRIDGE
1951. Effect of pressure on the behavior of decapod larvae (Crustacea). Nature, *167* (4244): 354-355.

KNIGHT-JONES, E. W. AND S. Z. QUASIM
1955. Response of some marine plankton animals to change in hydrostatic pressure. Nature, *175*: 941-942.

MOORE, H. B.
1953. Plankton of the Florida Current. II. Siphonophora. Bull. Mar. Sci. Gulf and Caribbean, *2* (4): 559-573.
1955. Variations in temperature and light response within a plankton population. Biol. Bull., *108* (2): 175-181.

MOORE, H. B., H. OWRE, E. C. JONES, AND T. DOW
1953. Plankton of the Florida Current. III. The control of the vertical distribution of zooplankton in the daytime by light and temperature. Bull. Mar. Sci. Gulf and Caribbean, *3*: 83-95.

ROANE, D. C.
1954. A study of some siphonophores of the Florida Current. Thesis for Masterate of the University of Miami, 1-77.

Contribution No. 865

Deep-Sea Research, 1956, Vol. 4, pp. 65 and 66. Pergamon Press Ltd., London.

INSTRUMENTAL NOTE

A Bottom-Water Sampler

The device described herein enables one to take water samples with one to six water bottles at predetermined depths from one to sixty metres from the bottom. It is essentially a Nansen bottle holder which trips the attached bottles at predetermined heights above the sea floor. These heights are measured from the bottom up instead of from the sea surface down as is common practice in taking water samples.

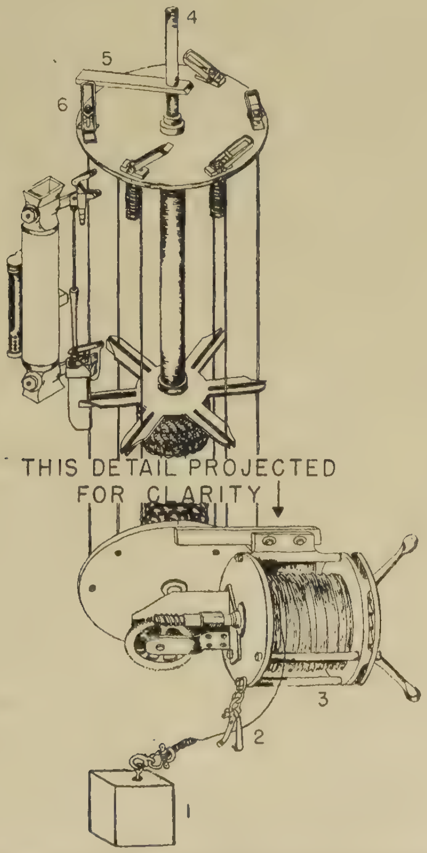

Fig. 1. Instrument viewed from above. Detail of bottom below lettering portion viewed from below.

The device consists of the following major parts shown in the accompanying sketch: (1) weight, (2) weight release, (3) wire storage spool, (4) central column, (5) tripping arms (five are used but only one is shown in Fig. 1), (6) spring-loaded plungers. Various enclosures are possible to protect the working parts and to facilitate handling on board ship. We used a regular tetrahedron, seven feet on each side, constructed of $\frac{1}{2}$ in. galvanised pipe. The bottle holder was mounted with its top at an apex; the opposite side of the tetrahedron served as the base.

The apparatus is lowered by a hydrographic winch to the sea bottom, and the sounding of an imploding glass ball is used to indicate the bottom rest position. At this point the weight (1) is automatically released, tripping the first bottle with a flexible wire lanyard. The hydrographic wire is retrieved slowly (at about 20 m./min.) unreeling the wire from the spool. The slow rotation of the arms trips the plungers in turn and hence the remaining bottles are released. After hauling in a length of hydrographic wire equal to the length of the wire on the spool the apparatus is retrieved at normal speed. The apparatus was used on *Atlantis* cruise A-213 in the vicinity of the Cariaco Trench. The following data from three lowerings indicate the attached thermometers reach equilibrium. It is important to note that time spent at each depth is probably not enough to assure equilibrium except in such cases as the Cariaco Trench where independent measurements show that the temperature gradient near the bottom is nearly adiabatic. The depths were (a) estimated from the corrected sonic depth and the positioning of the tripping arms and (b) determined with protected and unprotected deep-sea reversing thermometers.

Station			Estimated Depth	Thermometric Depth
5278	12°36′N		1852 m	1856 m
	58°34′W	Bottom (sonic)	1853 m	
5279	12°41′N		1111 m	1112 m
	59°40′W		1121 m	1116 m
			1166 m	1166 m
		Bottom (sonic)	1167 m	
5280	11°29′N		394 m	394 m
	60°46′W		416 m	416 m
			449 m	445 m
		Bottom (sonic)	450 m	

The agreements between the estimated and thermometric depths are all within the errors expected from our experience with the particular thermometer pairs used.

RICHARD S. EDWARDS
FRANCIS A. RICHARDS

Woods Hole Oceanographic Institution, Contribution No. 865

Printed in Great Britain by The Salisbury Press Ltd., Publicity House, Wilton Road, Salisbury, Wilts. (1116)

Contribution No. 867

Reprinted from LIMNOLOGY AND OCEANOGRAPHY
Vol. 1, No. 4, October, 1956
Printed in U.S.A.

The Deuterium Balance of Lake Maracaibo[1]

IRVING FRIEDMAN, DANIEL R. NORTON
U. S. Geological Survey, Washington, D. C.
DOUGLAS B. CARTER
Drexel Institute of Technology, Laboratory of Climatology, Centerton, N. J.
AND ALFRED C. REDFIELD
Woods Hole Oceanographic Institution, Woods Hole, Mass.

ABSTRACT

A balance sheet for the gains and losses of deuterium from Lake Maracaibo, using estimates based on climatological data for the exchanges of water and measurements of the deuterium content of lake water, rainfall, river flow, and Caribbean Sea water to obtain the volumes of the deuterium exchange, indicates that the relations are qualitatively satisfactory, although not numerically exact.

The concentration of deuterium, present chiefly as HDO, differs in various natural waters (Friedman 1953). Deuterium consequently promises to provide a tracer useful in the study of the water cycle of the earth. The differences are presumed to arise from the different vapor pressures of H_2O and HDO which cause fractionation when natural waters evaporate, from the differential behavior of these water substances in the condensation of rain or snow, and from the mixing of waters of different deuterium content in the sea or elsewhere.

Lake Maracaibo provides a favorable situation in which to compare the deuterium content of the intercommunicating waters and thus to examine the theory of the physical relations responsible for the deuterium cycle in nature. The lake lies in a watershed sharply delineated by mountains, its hydrography is adequately known, water balance has been deduced from analysis of the climatological data, and analyses of the deuterium content of samples of the natural waters involved have been made. The combined data available from these sources permit a tentative balance sheet to be drawn for the lake, and thus permit a critical scrutiny of the factors on which the balance seems to depend.

The hydrography has been studied by the Woods Hole Oceanographic Institution, working under contract with the Creole Petroleum Corporation. This study confirms and extends the earlier observations of Gessner (1953). The climatological data have been analyzed by Carter, employing methods outlined by Thornthwaite (1948), to obtain estimates of the mean annual runoff from the watershed, rainfall on the lake, and evaporation from its surface. Consideration of the salt content of lake water allowed the water balance to be completed by the addition of estimates of the inflow of sea water and the outflow of lake water into the Caribbean Sea. Deuterium

---

[1] Contribution Number 867 from the Woods Hole Oceanographic Institution. Publication authorized by the Director of the U. S. Geological Survey.

TABLE 1. *Analyses of deuterium in natural waters of and adjacent to Lake Maracaibo*

Station	Date	Latitude °N.	Longitude °W.	Depth ft	Temperature °C	Chloride ppm	Deuterium mole per cent
			Lake Maracaibo				
87	Mar. 24, 1954	9°17′	71°12′	1	29.80	638	0.01527
87	Mar. 24, 1954	9°17′	71°12′	15	29.51	642	—
87	Mar. 24, 1954	9°17′	71°12′	20	29.53	638	—
87	Mar. 24, 1954	9°17′	71°12′	40	29.48	650	0.01527
87	Mar. 24, 1954	9°17′	71°12′	55	29.46	633	0.01527
70	Mar. 18, 1954	9°24′	71°43′	10	29.31	735	0.01529
70	Mar. 18, 1954	9°24′	71°43′	42	29.42	732	0.01527
70	Mar. 18, 1954	9°24′	71°43′	63	29.27	720	0.01526
72	Mar. 19, 1954	9°40′	71°35′	10	29.07	756	0.01521
72	Mar. 19, 1954	9°40′	71°35′	21	28.97	760	0.01526
72	Mar. 19, 1954	9°40′	71°35′	63	28.62	835	0.01529
72	Mar. 19, 1954	9°40′	71°35′	74	28.54	1,039	0.01527
72	Mar. 19, 1954	9°40′	71°35′	84	28.52	1,110	0.01527
11	May 30, 1953	9°44′	71°14′	10	31.16	690	0.01521
21	Jun. 1, 1953	9°44′	71°43′	1	30.55	670	0.01518
21	Jun. 1, 1953	9°44′	71°43′	98	28.52	1,540	0.01523
90	Mar. 3, 1954	9°46′	71°38′	60	28.49	1,312	0.01530
90	Mar. 3, 1954	9°46′	71°38′	88	28.39	2,020	0.01527
80	Mar. 23, 1954	9°55′	71°21′	1	29.80	720	—
74	Mar. 19, 1954	9°56′	71°27′	1	29.84	740	—
74	Mar. 19, 1954	9°56′	71°27′	10	29.59	735	—
74	Mar. 19, 1954	9°56′	71°27′	21	29.07	732	—
74	Mar. 19, 1954	9°56′	71°27′	53	28.99	731	—
74	Mar. 19, 1954	9°56′	71°27′	63	28.96	749	—
74	Mar. 19, 1954	9°56′	71°27′	86	28.81	1,009	—
10	May 30, 1953	10°02′	71°26′	1	31.00	670	0.01513
10	May 30, 1953	10°02′	71°26′	20	30.11	660	0.01516
10	May 30, 1953	10°02′	71°26′	40	29.44	665	0.01518
10	May 30, 1953	10°02′	71°26′	80	29.42	660	0.01520
10	May 30, 1953	10°02′	71°26′	98	29.12	1,265	0.01520
79	Mar. 3, 1954	10°07′	71°24′	1	29.80	684	—
94	Mar. 27, 1954	10°10′	71°22′	1	29.74	670	—
9	May 30, 1954	10°20′	71°36′	1	30.13	670	0.01523
			Strait of Maracaibo and Channel				
28	Mar. 14, 1954	10°26′	71°34′	39	27.37	8,340	0.01542
76	Mar. 22, 1954	10°42′	71°34′	5	28.14	2,160	0.01536
76	Mar. 22, 1954	10°42′	71°34′	15	28.16	2,535	0.01533
76	Mar. 22, 1954	10°42′	71°34′	25	27.75	4,190	0.01532
76	Mar. 22, 1954	10°42′	71°34′	35	27.05	8,710	0.01542
76	Mar. 22, 1954	10°42′	71°34′	42	26.94	14,700	0.01548
5	May 27, 1953	10°48′	71°38′	1	30.02	840	0.01521
8	May 28, 1953	10°59′	71°36′	1	30.06	2,800	0.01529
			Gulf of Venezuela				
5239	Dec. 8, 1954	11°09′	71°46′	1	27.32	7,130	0.01524
5239	Dec. 8, 1954	11°09′	71°46′	9	27.78	14,650	0.01542
5240	Dec. 8, 1954	11°19′	71°43′	1	27.56	13,210	0.01542
5240	Dec. 8, 1954	11°19′	71°43′	19	28.16	18,080	0.01546
5245	Dec. 8, 1954	11°28′	71°06′	1	27.87	16,700	0.01545
5245	Dec. 8, 1954	11°28′	71°06′	13	28.02	18,190	0.01544
5242	Dec. 8, 1954	11°38′	71°40′	1	27.63	9,320	0.01531
5242	Dec. 8, 1954	11°38′	71°40′	8	27.74	13,100	0.01540
5251	Dec. 9, 1954	11°58′	70°44′	1	27.22	19,630	0.01545
5251	Dec. 9, 1954	11°58′	70°44′	50	25.43	20,140	0.01548
			Caribbean Sea				
5237	Dec. 7, 1954	12°19′	69°56′	1	27.56	19,710	0.01545
5237	Dec. 7, 1954	12°19′	69°56′	99	22.00	20,360	0.01551
5256	Dec. 9, 1954	12°34′	71°01′	1	27.35	19,750	0.01547
5256	Dec. 9, 1954	12°34′	71°01′	65	23.49	20,310	0.01543
	Mar. 30, 1954	10°30′	68°3′	1	—	20,340	0.01550

analyses were made at the U. S. Geological Survey using methods described by Friedman (1953). The results are expressed as mole per cent HDO/H_2O and are believed to be accurate to at least 0.00015 mole per cent which is 1% of the quantity usually present. Samples of rain water were obtained through the courtesy of Mr. Earlston Doe of the Creole Petroleum Corporation.

This work was sponsored by the Woods Hole Oceanographic Institution and the U. S. Geological Survey—the Survey part of the study having been conducted on behalf of the Division of Research of the U. S. Atomic Energy Commission.

LAKE WATER

The volume of the lake when divided by the estimated mean annual outflow indicates that the water remains in the lake about ten years. The chloride content shows that the lake water is a mixture of 1 part of sea water and 30 parts of fresh water; this provides an index of its homogeneity. The water is thoroughly mixed vertically to the bottom at depths of 100 feet, except for a relatively limited pool of more saline water over the bottom near the center of the basin. Otherwise the water is nearly homogeneous in all parts because of a rapid, cyclonic circulation.

The deuterium content of 23 scattered samples of lake water is recorded in Table 1. It has a mean value of 0.01525 mole per cent, the individual measurements ranging from 0.01513 to 0.01530. No significant difference can be detected between samples from different parts of the lake nor from different depths. The representative deuterium content of lake water is 0.0152 mole per cent.

EXCHANGE WITH THE SEA

The water lost to the sea is lake water to which a deuterium content of 0.0152 has

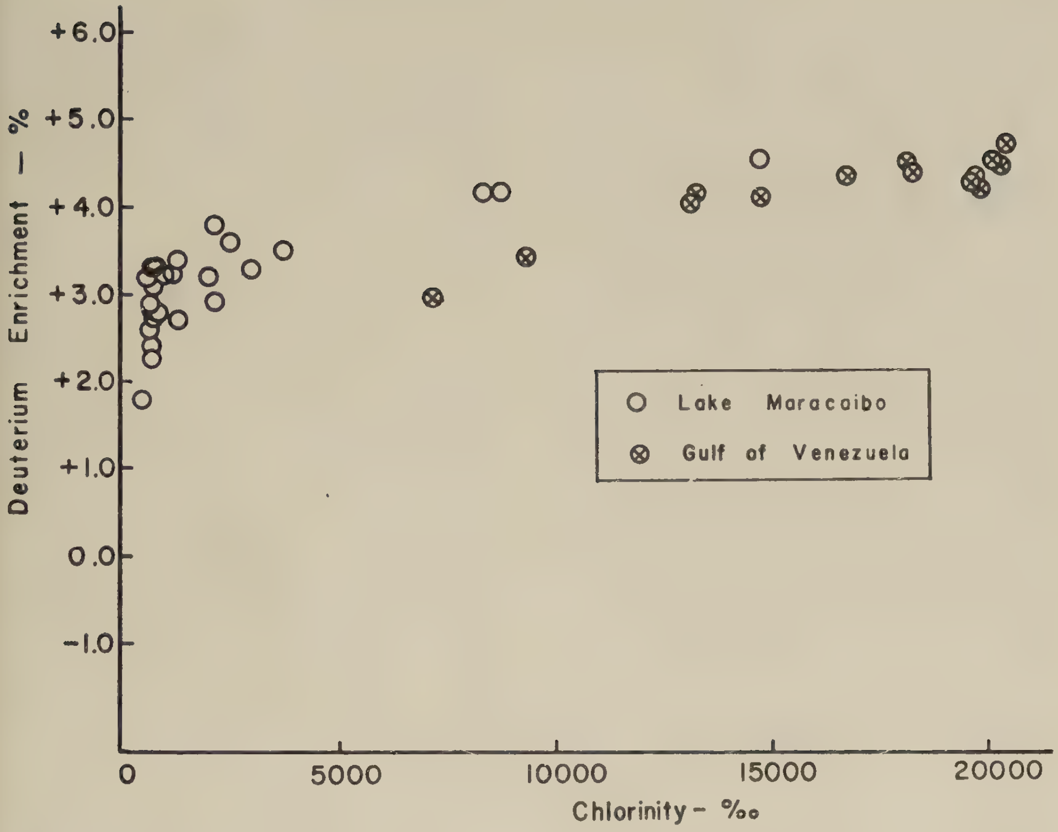

FIG. 1. Relation of deuterium content and chloride content of water samples from Lake Maracaibo and the Gulf of Venezuela.

been assigned. A relatively small quantity of sea water of Caribbean origin enters the lake, chiefly during the dry season (in winter) to provide the observed chloride content. Caribbean water, sampled off the approaches to the Gulf of Venezuela, has a deuterium content of 0.01550.

In the Strait of Maracaibo, in the inner part of the Gulf of Venezuela, and in the connecting channel across Tablazo Bay, mixtures of lake water and Caribbean water are found in various proportions. Figure 1 shows the relation between the chloride content and the deuterium content of water samples from this region. The linear relationship indicates that the varied deuterium content is the simple result of physical admixture of the two source waters.

LAND DRAINAGE

The Maracaibo basin varies from semi-arid desert along the coast to tropical rain forest along the southern margin of the lake. The surrounding mountains rise to elevations of 15,000 feet above sea level. Much of the area is inaccessible and unsettled, and consequently the integration of the climatic factors determining the water balance of the uplands was difficult. Records were available of temperatures from 23 stations and of precipitation from 68 stations for varying periods.

From these data an accounting of the monthly gains, losses, and storage of moisture at each climatological station was made according to the procedures devised by Thornthwaite and his associates.[2] The estimated monthly values of runoff obtained by the method were mapped, using altitude as a guide to the distribution. The map

[2] The basic method is described by Thornthwaite (1948); however, the method has since been modified and presented in relation to its applications in Thornthwaite and Mather (1955).

areas were integrated by planimetry, and the monthly volumes of runoff from the upland were computed.

Deuterium analyses of samples from 8 rivers are shown in Table 2. Probably three-quarters of the drainage into the lake is carried by the Rio Catatumbo and the lesser streams which drain the swampy jungles along the southwestern quarter of the basin. Rio Catatumbo water collected in the wet season contained 0.01461 mole per cent deuterium. This value agrees well with a sample collected in the dry season from Rio Motatan, a clear running river draining mountainous terrain in the southeastern quarter, which gave a value of 0.01468. A deuterium content 0.0146 is consequently assigned to the mean annual land drainage.

The other samples are of interest in showing the increase in deuterium content of the river water at the end of the dry season northward into the semiarid region, and the decrease in the samples collected from streams at high altitudes in the mountains. The extreme range is from 0.01393 mole per cent in Rio Poco del Aquila flowing at an altitude of 4130 meters to 0.01572 in a stagnant pool in the bed of the otherwise dry Rio Pueblo Viejo, a difference of 13 per cent. The latter sample was probably concentrated by evaporation.

PRECIPITATION

The average monthly volumes of precipitation onto the lake and its associated marshes were determined from precipitation records at more than 20 climatic stations situated on the periphery of the water area. Isohyetal maps were drawn and the monthly volumes were integrated by planimetry.

Samples of rain water collected at various locations and seasons have been analyzed (Table 2). The deuterium content of these samples varied between 0.01411 and 0.1546 mole per cent and averaged 0.01495. Accordingly a value of 0.0150 is taken as repre-

TABLE 2. *Analyses of deuterium in water of rivers tributary to Lake Maracaibo and in rain*

	Date	Latitude °N.	Longitude °W.	Deuterium mole per cent	Remarks
River water					
Rio Catatumbo	May 31, 1953	9°19.5′	71°47′	0.01461	4 miles above mouth
Rio Motatan	Mar. 29, 1954	9°38′	70°43′	0.01468	running freely
Rio San Juan	Mar. 29, 1954	9°45′	70°50′	0.01479	running freely
Rio San Piedro	Mar. 29, 1954	9°52′	70°53′	0.01495	scarcely flowing
Rio Pueblo Viejo	Mar. 29, 1954	10°02′	71°10′	0.01572	stagnant pool
Rio Merida	Feb. 3, 1956	Trib. of Rio Escalante		0.01460	2,000 meters altitude
Rio Poco del Aquila	Apr. 9, 1955	Near divide between Maracaibo and Orinoco		0.01393	4,130 meters altitude
Rio Poco del Aquila	Feb. 4, 1956	Near divide between Maracaibo and Orinoco		0.01397	4,130 meters altitude
Rio La Mesa	Apr. 9, 1955	Rio Motatan system		0.01437	1,800 meters altitude
Rio La Mesa	Apr. 9, 1955	Rio Motatan system		0.01416	3,000 meters altitude
Rain water					
Off Santa Maria	Sep. 20, 1955	9°05′	71°22′	0.01411	
Central Lake Maracaibo	Mar. 25, 1954	9°27′	71°22′	0.01546	heavy shower
Off La Ceiba	Dec. 1, 1955	9°29′	71°06′	0.01452	
La Salina	Apr. 25, 1955	10°23′	71°27′	0.01524	
La Salina	Aug. 15, 1955	10°23′	71°27′	0.01509	
La Salina	Sep. 16, 1955	10°23′	71°27′	0.01515	
La Salina	Jan. 3, 1956	10°23′	71°27′	0.01516	
Maracaibo	Jun. 29, 1955	10°39′	71°37′	0.01483	

senting the deuterium content of average rain falling on the lake.

The interpretation of the variable deuterium content of the rain samples requires some review of the physics of the fractionation of deuterium in the evaporation and precipitation of water and of the observations in nature that may be interpreted by the resulting theory. It can be expected on physical grounds that the moisture evaporated from a water surface will contain about 6 per cent less deuterium than the source water (Epstein, Friedman, and Urey, in press). If evaporation and precipitation are strictly reciprocal aspects of the fractional distillation process, the *initial* precipitate from air immediately over the water surface should have a deuterium content similar to that of the source water. The precipitate, however, will contain relatively more deuterium than the moist air from which it separates. Consequently the remaining moisture in the air will be left with relatively less deuterium than the original evaporate from the water surface. Subsequent precipitation from such air will yield a rain having a lower deuterium content than the initial precipitate.

The expectations raised by these considerations are that rain precipitated from air immediately over the sea will have a deuterium content similar to the surface sea water, whereas that precipitated at higher altitudes, during the later stages in the ascent of air in convective rain storms, in the course of the ascent of moist air over mountains, or after a long period of drift across continental masses, will have lower deuterium content.

These expectations are supported by observations made in Hawaii where it was found that rain collected near sea level approached the surface sea water in deuterium content, whereas that collected at higher altitudes contained a smaller quantity, 0.0003 mole per cent less (Friedman and Woodcock, in press). Substantial evidence has also accumulated from the analysis of ice from mountain glaciers and of other natural waters at high altitudes that the precipitation at altitude has a low deuterium content. In contrast, river water from the southeastern United States yields higher values compatible with a relatively immediate origin from the precipitation of gulf air (Friedman 1953).

The variable deuterium content of the Maracaibo rains can be interpreted as follows. The samples from La Salina, at the seaward extremity of the lake, (content $\simeq$ 0.0152 mole per cent) represents the initial precipitation of maritime air derived from the Caribbean (surface deuterium $\simeq$ 0.0154). A similar origin may be assigned to the sample from the central lake, which was obtained at a period when strong trade winds blew into the basin. The contribution that moisture evaporated directly from the lake's surface may have made to these rains cannot be assessed since the lake water contains only 0.0002 mole per cent less than the surface water of the Caribbean. The samples from off Santa Maria and La Cieba, at the southern end of the lake, contain substantially less deuterium (0.0141–0.0145 mole per cent). These samples are interpreted as having originated from maritime air after depletion in deuterium by previous precipitation, either as a result of convection to high altitude or a longer history of movement over the continent. The low value of the Maracaibo specimen may be similarly explained.

It should be noted that the low deuterium content of the samples from Santa Maria and La Cieba approaches the low values obtained from mountain streams at altitudes of 3,000–4,000 meters in the nearby mountains. The fact that the average value of the deuterium content assigned to the land drainage, based on analyses of river waters, is lower than the average value assigned to the lake rain seems to arise from the preponderance of rainfall of low deuterium content over the southern part of the Maracaibo drainage basin.

It is clear that much more detailed information on the origin and movements of the air masses which occupy the Maracaibo basin, of the deuterium content of their contained moisture and the mechanisms by which it is precipitated is required before the data on the deuterium content of the rainfall into the lake can be evaluated so as to provide an accurately weighted mean value. The attribution of 0.0150 mole per cent to the rainfall on the lake is unsatisfactory but is made in lieu of a more certain figure.

EVAPORATION

Monthly averages of evaporation and evapotranspiration were estimated for each climatological station near the shore of Lake Maracaibo and its marshes. From monthly maps of this distribution, the average loss from the lake was reckoned by the same methods used in estimating precipitation over the lake.

The deuterium content of the evaporate is estimated from physical considerations to be 6 per cent less than that of the lake water, or 0.0143 mole per cent (Epstein, Friedman, and Urey, in press).

THE BALANCE SHEET

Table 3 gives the tentative balance sheet for the mean annual gains and losses of ordinary water and deuterium for Lake Maracaibo.

The items for the water balance are based on the climatological estimates. These estimates are not considered very precise, and it should be noted that the perfection of the balance is the result of estimating the loss to the sea from the difference between the gains and the evaporation, there being no independent measure of this loss.

The source of the deuterium concentration assigned to the items and their reliability have been discussed. The quantities of deuterium in the items are obtained by multiplying the quantity of water by the moles per cent deuterium $\times 10^{-2}$.

The gains and losses in deuterium agree to about 1 per cent. This is of the same order of accuracy as the individual deuterium determinations. When it is considered that the total deuterium concentrations do not differ among themselves by more than 8 per cent, and that the water balance has an arbitrary perfection, this agreement is not as impressive as it seems. All that is claimed is that the various estimates and measurements fall together in a consistent and theoretically reasonable relationship.

TABLE 3. *Tentative balance sheets, Lake Maracaibo*

Gains	Water balance $10^9 m^3$/yr.	Source	HDO	
			Concentration mole per cent	Quantity $10^7 m^3$/yr.
Land drainage	32.2	Rio Catatumbo	0.0146	0.470
Rainfall	22.0	Lake rain	0.0150	0.330
Sea water	.7	Caribbean Sea	0.0155	0.011
	54.9			0.811
A. Losses				
To sea	22.0	Lake Maracaibo	0.0152	0.335
Evaporation	32.9	Physical estimate	0.0143	0.470
	54.9			0.805
B. Losses—adjusted to obtain deuterium balance				
To sea	28.0	Lake Maracaibo	0.0152	0.426
Evaporation	26.9	Physical estimate	0.0143	0.385
	54.9			0.811

Of the deuterium concentrations, the value assigned to rainfall is the most questionable. A large number of collections in time and position would be necessary to fix this value with greater certainty.

Permissible adjustments in the values of the water balance items would serve to correct the discrepancy in the heavy water balance. In the lower part of Table 3 the losses have been re-estimated so as to secure a balance of deuterium by readjusting the estimates of evaporation. The evaporation must be reduced by 18 per cent with a compensating increase in the loss to the sea to bring the items into balance. Smaller adjustments more generally applied would serve the same purpose and would be permitted by the precision of the estimates, but there is no rational basis for making such adjustments.

DISCUSSION

The deuterium balance and the water balance provide complimentary procedures for estimating our hydrologic economy. Although the physical processes that determine the circulation of H_2O and of HDO in nature are the same, differences in the physical properties of these molecules are sufficient to cause recognizable differences in natural waters, which depend upon their history and which could not be detected otherwise. This important fact is illustrated by the discussion of the origin of the Maracaibo rains. The purpose of this paper will be met if, in spite of the admitted limitations of its conclusions, it draws attention to the value of deuterium as a tool for examining the natural processes on which the distribution and behavior of natural waters depend.

It is obvious that for technical reasons the deuterium cycle cannot be examined separately from the water cycle, and the results would be of minor interest if it could.

Lake Maracaibo has provided a promising water mass for the present study, not only because information is available on its hydrography and water balance but because its volume is sufficient relative to its water exchange to justify the use of long-term averages in estimating the balance of water movement. It should be pointed out, however, that the balances are shifting, both seasonally and over the years.

Records extending over 20 years show that the chloride content of the lake water increased gradually from 425 ppm in 1938 to a maximum of nearly 1200 ppm in 1948. Since that time the chlorides have diminished and at present approximate the earlier value. There are substantial reasons to believe that these changes were due to variation in the accessions of fresh water as rainfall and runoff. The data used in estimating the water balance for the lake, however, represent fairly the average over this period.

The Maracaibo basin experiences a marked annual cycle of precipitation. From January through April, when northeast trade winds thoroughly permeate the Lake Maracaibo basin, there is a general reduction in rainfall. During the remainder of the year, when the Maracaibo basin is a meeting place for air streams from the Caribbean and the interior of the continent, the wet season occurs. The effect of the seasonal variation in rainfall on the water balance of the lake is illustrated in Table 4. The rate of gain of water by runoff and precipitation is greatly increased during the wet season and is balanced by increased losses of lake water to the sea. The return of water to atmosphere by evaporation is little changed by the season. During the dry season evaporation exceeds the gains that depend on rainfall, and a net inflow of sea water into the lake results. Consequently there is a reversing movement of water to and from the atmosphere in the course of the year that is not brought out by the annual water balance.

TABLE 4. *Tentative water balance sheets for the months of dry and wet season, expressed as the mean monthly gain and loss averaged for the periods January through April, and May through December, respectively*

	Dry season 10^9m^3/month	Wet season 10^9m^3/month
Gains		
Runoff	1.078	3.488
Precipitation	1.125	2.188
Inflow	0.579	0
Total	2.782	5.676
Losses		
Evaporation	2.578	2.820
Outflow	0.205	2.856
Total	2.783	5.676

The gains and losses in deuterium must vary in a similar way with the season. They cannot be calculated in the absence of data on the seasonal changes in the deuterium content of the several items.

The Maracaibo basin provides an excellent example of the great significance of the atmospheric transport of moisture. During the dry season evaporation persistently exceeds precipitation, and moisture is lost from the basin by the transport of moisture in the atmosphere. Even in the wet season there are many times when precipitation over the basin is less than evaporation, although the excess precipitation during the whole period is so great that as much as half the precipitated water reaching the lake is returned directly to the sea. It is likely that both the total water and the deuterium which enter the basin and leave it as vapor without being precipitated are a much larger quantity than all that enters into the cycle of exchange revealed by the balance of the lake itself.

REFERENCES

Epstein, S., I. Friedman, and H. C. Urey. In press. J. Chem. Phys.

Friedman, Irving. 1953. Deuterium content of natural water and other substances. Geochemica et Cosmochemica Acta, **4**: 89–103.

Friedman, I., and A. H. Woodcock. In press. Determination of deuterium-hydrogen ratios in Hawaiian waters. Am. Meteorological Soc. Monogr.

Gessner, Fritz. 1953. Investigaciones hidrograficas en al Lago de Maracaibo. Acta Cientifica Venezolana, **4**: 173–177.

Thornthwaite, C. W. 1948. An approach toward a rational classification of climate. Geographical Review, **38**: 55–94.

Thornthwaite, C. W., and J. R. Mather. 1955. The water balance. Publications in Climatology, **8**(1): 1–104. The Drexel Institute of Technology, Centerton, N. J.

Contribution No. 869

Reprinted from BIOLOGICAL BULLETIN, Vol. 111, No. 3, 410–414, December, 1956
Printed in U. S. A.

ON THE ECOLOGY OF THE LOWER MARINE FUNGI

HELEN S. VISHNIAC

Department of Microbiology, Yale University, New Haven 11, Connecticut

ON THE ECOLOGY OF THE LOWER MARINE FUNGI[1, 2]

HELEN S. VISHNIAC[3]

Department of Microbiology, Yale University, New Haven 11, Connecticut

The lower marine fungi (*i.e.*, Myxomycetes and aquatic Phycomycetes) have generally been described as occurring on plant and animal hosts. While several forms have been described as saprophytes, the only genus known to occur on debris is *Labyrinthula* (Sparrow, 1936). All other described species are endobiotic or epibiotic with rhizoids penetrating living or dead host cells. They are also sporadic in occurrence. The application of a semi-quantitative plating technique to sea water has now established that lower fungi are far more common in littoral waters than previous studies indicate, and has suggested a new ecological niche for these fungi.

The plating technique which we used consisted of spreading samples of sea water with a bent glass rod on the surface of a solid isolation medium (Table I).

TABLE I

Isolation Medium

Sea water	80 ml./100 ml.
Gelatin hydrolysate	0.1%
Glucose (added aseptically)	0.1%
Liver 1:20	0.001%
B-vitamins	
Agar	1.5%
	adjusted to pH 7.5

Marine mineral base (Vishniac, 1955) was sometimes substituted for sea water. Gelatin hydrolysate and the B-vitamin mixture were prepared as by Vishniac and Watson (1953). Liver extract concentrate 1:20 was obtained from the Nutritional Biochemicals Co.

The moisture content of the medium is critical: the agar plates should be dried overnight, but not allowed to stand for more than two days. Just before use the plates are spread with 2000 units of Penicillin G (Squibb, buffered) and 0.5 mg. of dihydrostreptomycin sulfate (Wyeth) in concentrated aqueous solution. These plates will then absorb a 0.2-ml. sea water sample in an hour or two. After inoculation, the plates were incubated at 20 degrees or less. Such plates support the growth of lower fungi, yeasts, molds, and some diatoms, but few or no bacteria. We have found unfortunately incomplete suppression of bacterial growth when water samples taken from City Point, New Haven, near the sewage disposal plant,

---

[1] Contribution No. 869 from The Woods Hole Oceanographic Institution.

[2] It is a pleasure to acknowledge the hospitality of Dr. J. Ryther and other members of The Woods Hole Oceanographic Institution, the kindness of Dr. W. R. Taylor in identifying *Polysiphonia urceolata*, and the excellent technical assistance of Miss E. A. Adair. This study was aided by a contract between Yale University and the Office of Naval Research, Department of the Navy, NR 135-241. Reproduction in whole or part is permitted for any purpose of the United States Government.

were plated. Colonies of lower fungi visible to the naked eye appear in a week or ten days. Colonies were counted at 30 × and further examined at 100 ×.

The results of spreading triplicate 0.2-ml. samples of sea water taken in June, 1956 from waters in and around Woods Hole, Mass. are given in Table II. The number of species represented is probably a minimum figure, since only colonies which were markedly distinct in color, texture, or size of thallus were picked for further study. Yeasts, molds and diatoms were not counted regularly. Yeasts were rare. From 0–5 colonies of molds, mainly *Penicillium* spp. of uncertain provenance, were found on those plates for which molds were counted. The presence of molds was not correlated with the presence of lower fungi.

It is evident from the poor agreement between triplicate platings in Table II that this technique is quantitative only within an order of magnitude. The procedure suffers from the following defects:

Table II

Occurrence of lower fungi in sea water

Origin of sample	Colonies/plate	No. species
1. Sea water tap, W.H.O.I.	0, 0, 0	0
2. Great Harbor	0, 0, 0	0
3. Eel Pond	94, 34, 20	7
Tap water, from bowls with algae		
4. Algae washed ca. 5 hrs.	23, 8, 20	5
5. Algae washed ca. 24 hrs. (another collection)	15, 10, 1	6
Water expressed from algae		
6. Pilings, U. S. Fish and Wildlife Station	62, 5, 56	2
7. Rocks, Red Spindle (Grassy Island)	66, 214, 35	7

(1) Spreading the sample, necessitated by the aerobic nature and poor temperature tolerance of the desired forms, entails the loss of 3 to 8% of a 0.2-ml. sample. The amount of sample remaining on the glass rod was determined by weighing the salt remaining on the glass rod after spreading a 20% NaCl solution.

(2) Either a thallus or a spore may give rise to a colony. The ecologic implications of the presence of a thallus or a spore in the sample are quite different.

(3) A thallus may produce zoospores in the interval between spreading and drying of the sample, giving rise to several colonies. The occasional appearance of groups of colonies of the same form on a plate was presumed to have this cause.

(4) Not every viable spore or thallus present in the sample may give rise to a colony. The conditions provided for growth were chosen after study of a limited number of marine forms—members of the genera *Labyrinthula, Sirolpidium, Thraustochytrium,* and three unidentified isolates. Obviously, forms with other requirements may exist. We have been particularly interested in assessing the probable extent of the selective action of the medium.

It is probable that forms with additional nutritional requirements would grow sufficiently on the medium used to form a countable colony. The ability of an individual organism, previously well nourished, to form a colony in the absence of required nutrients is inversely proportional to the quantity of nutrient required. Generally, absence of a suitable carbon source is felt first, amino acids required as growth factors next, and lastly the absence of added vitamins—some of which may be stored in quantities sufficient for many generations. It is highly improbable that suitable carbon sources for any of the fungi with which we were concerned were lacking. As a source of amino acids, gelatin hydrolysate is inferior, since it is poor in methionine and in the aromatic amino acids. Nevertheless, we have maintained methionine-requiring Phycomycetes on gelatin hydrolysate media for over a year of semi-monthly transfers. The feasibility of isolating forms requiring growth factors not present in this medium was demonstrated by the isolation of sterol-requiring *Labyrinthulas* from two of the sea water samples used in this study (4 and 7, Table II). Syntrophism may occur (though no obvious examples were seen) on these plates.

An experimental approach to this problem was made by plating a sample of sea water from *Ulva* colonies on pilings at City Point, New Haven, in triplicate on the isolation medium, on the isolation medium without liver extract, on the isolation medium without liver extract, vitamins, or glucose, and on a medium containing glucose, glutamate, and thiamine as its only organic constituents. At the same time isolates known to require liver extract and known to require glucose, amino acids, and vitamins were plated on these media. Of the media used, only the glucose-glutamate-thiamine agar gave significantly lower sea water counts. This medium also failed to support typical colony formation by isolates known to require growth factors. The isolates requiring liver extract failed to form typical colonies on the medium from which liver, glucose, and vitamins were omitted also, though the omission of liver extract alone did not affect their growth under the conditions used.

It is, on the other hand, quite possible that fungi exist which did not form recognizable colonies because they were inhibited by the ingredients of the medium. Representative colonies were picked from the isolation plates made at Woods Hole into tubes of semi-solid (0.1% agar) isolation medium for further study. It then developed that, in semi-solid media, each of the organic constituents of the medium was somewhat inhibitory to some of the fungi isolated. The results of the comparative plating of City Point sea water outlined above and of similarly plating isolates known to be inhibited by ingredients of the isolation medium indicated that, for these fungi, the inhibitions are relieved by growth on a solid agar surface. The validity of this conclusion must be restricted to the fungi examined.

In principle, these defects are not unique to our procedure; they require restatement here because this is the first application of plating techniques to the lower marine fungi, indeed to ecologic studies of any aquatic Phycomycetes, and because they bear on the conclusions to be drawn from our results. The results of Table II suggest, first, that the presence of these fungi is correlated with the organic content of the water examined, since the highly polluted Eel Pond is richer than Great Harbor (on the incoming tide). Second, in Great Harbor (and in the Hole), fungi are associated with algae: they may be isolated from water taken from finger bowls in which algae were being kept under a constant drip of previously fungus-free tap water. They may be isolated from water squeezed by hand from masses of attached algae growing on rocks and pilings.

The organic content of polluted waters, such as those of the Eel Pond, could reasonably be expected to support a population of free-living non-filamentous fungal saprophytes, just as of bacterial saprophytes. We have calculated, from cell counts of representative cultures, that the amount of soluble organic material required to produce a single thallus of the common holocarpic or monocentric marine Phycomycetes is of the order of 1 $m\mu$ g. But the development of techniques for establishing directly the presence of a free-living fungus population would be very desirable. Two instances of association with organic debris were noted. One colony of a monocentric Phycomycete was found on a plate on a stray grain of pine pollen. One species (an undescribed myxoid form here referred to as isolate "S"), of which 1–22 colonies were found on every plate containing lower fungi, formed colonies which were as often as not centered on a microscopic bit of nondescript organic debris.

In view of the known endo- and epibiotic habit of marine fungi, the apparent association with algae required further investigation. The algae with which the sea water samples of Table II were associated were examined microscopically for the presence of fungal thalli. As might have been expected from the experience of previous investigators (see Petersen, 1905; Sparrow, 1934, 1936; Kobayashi and Ookubo, 1953), recognizable thalli were rare. The one species which Sparrow (1936) found epidemic later in the summer—*Ectrogella perforans* in *Licmophora*—was conspicuously absent. The only form found during these examinations was *Petersenia lobata* (?) on *Polysiphonia urceolata* (*fide* W. R. Taylor) collected at the Red Spindle and allowed to rest for 12 days in a finger bowl under dripping sea water (as suggested by Sparrow). Five days later the infection had disappeared.

TABLE III

Fungi associated with algal surfaces

	No. fragments	No. species fungi/fragment
1. Algae from rocks at Red Spindle (Grassy Island)		
Ectocarpus	1	2
Antithamnion	8	1–3
Polysiphonia	4	1–3
Ceramium	3	1–3
2. Algae from rocks of Pine Island		
Ectocarpus	4	1–2
Elachistea	5	1
Punctaria	2	2
Chorda filum	1	3
Callithamnion	18	1–3
Antithamnion	4	2
	1	0
Polysiphonia	3	0
Bryopsis	10	1–2
	4	0

The results of plating small pieces of algae showed, in marked contrast, that the algal surface not contaminated by lower fungi was rare. Bits of algae, usually strands approximately one cm. long, were cut from the collected plants, drawn gently over the edge of a petri dish to remove water and placed on the surface of the usual antibiotic-isolation medium agar. No fungal thalli (possibly because of their small size) could be recognized at 100 × on the algal fragments at the time of plating. Neither fungal thalli nor rhizoids were seen within the cells of these algae at any time, though the specimens were examined at 430 × at the end of the incubation period. The association of lower fungi with fragments of algae collected at the Red Spindle (Grassy Island) in Great Harbor and at Pine Island (off Nonamesset Island, in the Hole) is shown in Table III. Molds and yeasts were observed fairly frequently; specimens in this series which were obscured by such forms have been omitted from the tabulation.

Are these fungi on the algal surface or in the surface film of water surrounding the algal fragment? If the surface film of water is, at a guess, about 0.01 ml., one would expect to find of the order of 1–10 viable units of lower fungi in it. The results of Table III are not inconsistent with this estimate, but are unfortunately not quantitative, because discrete colonies are rarely formed around algal fragments. But we are inclined to consider, for two reasons, that the fungi found in association with algal fragments resemble many of the marine bacteria in being present, as thalli, on the surface of the alga. First, we have attempted (in a limited number of trials) to wash the fungi away with sterile sea water. The results, even with such algae as *Bryopsis plumosa* and *Polysiphonia urceolata* which were free of the forest of hairs and epiphytes found on most marine algae, were poor. No more fragments were free of fungi after washing than before, and essentially the same type of fungi was present. Secondly, although both holocarpic and eucarpic Phycomycetes were among the forms associated with algal surfaces, the predominant form was, as in sea water samples, the myxoid surface-loving "S." Every algal fragment listed in Table III as having associated fungi had "S" associated with it. The association of "S" with bits of organic debris has already been noted. "S" was also found to be associated with two of six copepods plated as part of a rather unproductive plankton haul from Great Harbor. Another surface-loving form, *Labyrinthula* sp., occurred less frequently on *Polysiphonia, Ceramium*, and *Ectocarpus*.

CONCLUSIONS AND SUMMARY

Our data therefore suggest that the lower marine fungi occupy essentially the same ecologic niche as the marine saprophytic bacteria. These fungi can be found in suitably polluted sea water in numbers of the order of 1–500,000 viable units/liter but less than 5000/liter in more open waters of Woods Hole. The fungus count increases, as has long been noted for bacteria (Gazert, 1906), in the presence of macroscopic algae. They also resemble marine bacteria in their association with surfaces. As a group, these fungi differ from marine bacteria in being strongly aerobic. One may justifiably wonder as to the basis of their success in competition with bacteria in this niche. Studies, now in progress, of the individual species of fungi concerned may clarify this question.

LITERATURE CITED

GAZERT, H., 1906. Untersuchungen über Meeresbakterien und ihren Einfluss auf den Stoffwechsel im Meere. *Deutsche Südpolar-Expedition, 1901–03, Berlin,* **7**: 235–296.

KOBAYASHI, Y., AND M. OOKUBO, 1953. Studies on the marine Phycomycetes. *Bull. Nat. Sci. Mus., Tokyo,* **33**: 53–65.

PETERSEN, H. E., 1905. Contributions à la connaissance des Phycomycetes marins (Chytridinae Fischer). *Oversigt k. dansk. vidensk. Selskabs Forhandl.,* **1905**: 439–488.

SPARROW, F. K., JR., 1934. Observations on marine phycomycetes collected in Denmark. *Dansk. bot. Ark.,* 8 (6): 1–24.

SPARROW, F. K., JR., 1936. Biological observations on the marine fungi of Woods Hole waters. *Biol. Bull.,* **70**: 236–263.

VISHNIAC, H. S., 1955. Marine mycology. *Trans. N. Y. Acad. Sci.,* **17**: 352–360.

VISHNIAC, H. S., AND S. W. WATSON, 1953. The steroid requirements of *Labyrinthula vitellina* var. *pacifica. J. Gen. Microbiol.,* **8**: 248–255.

Contribution No. 876

The Commonwealth of Massachusetts

DEPARTMENT OF NATURAL RESOURCES
Arthur T. Lyman, Commissioner
DIVISION OF MARINE FISHERIES
Francis W. Sargent, Director

EIGHTH REPORT ON

INVESTIGATIONS OF THE SHELLFISHERIES OF MASSACHUSETTS

Prepared by the
WOODS HOLE OCEANOGRAPHIC INSTITUTION
In Accordance with Contract
Effective July 1, 1955

PREFACE

The following report, prepared by Harry J. Turner, Jr., Marine Biologist of the Woods Hole Oceanographic Institution is a summary of the investigations or methods of improving the shellfish resources of Massachusetts which were carried out in 1955 by the Woods Hole Oceanographic Institution under contract with the Division of Marine Fisheries, Massachusetts Department of Natural Resources.

The investigations were conducted under the leadership of Mr. Turner. Those participating were Joseph H. Connell and Carl J. George. The work was greatly aided by counsel from Dr. David L. Belding, former Biologist for the Massachusetts Department of Fisheries and Game who is now a member of the consultant staff of the Woods Hole Oceanographic Institution.

The Institution has worked in close cooperation with the U.S. Fish and Wildlife Service which is conducting investigations in other parts of New England under a Federal appropriation for the improvement of the soft and hard clam fisheries. Members of the Institution have served on the Committee of Clam Technicians sponsored by The Atlantic States Marine Fisheries Commission.

The Woods Hole Oceanographic Institution wishes to express its appreciation to Mr. Francis W. Sargent, Director of the Division of Marine Fisheries, and to Mr. Charles L. Wheeler, Assistant Director and Biologist of the Division for their valuable suggestions and close cooperation.

Bostwick H. Ketchum
Senior Oceanographer

December 31, 1955

EIGHTH REPORT ON INVESTIGATIONS OF THE SHELLFISHERIES OF MASSACHUSETTS *

BY

HARRY J. TURNER

INTRODUCTION

During the year 1955 the Woods Hole Oceanographic Institution has conducted biological investigations of the larvae of the bay quahaug, *Venus mercenaria,* and of the zonation of the soft clam, *Mya arenaria.* The investigations of the biology of the larvae of the quahaug were undertaken for two purposes: (1) to determine aspects of the behavior and physiology of the larvae that may account for the erratic and unpredictable occurences of new sets of quahaugs, and (2) to determine the possibility of using larvaculture as a predictable and reliable source of "seed" quahaugs to populate barren areas within the normal geographic range of the species and also other areas north of the range where quahaugs are known to survive but not propagate.

The investigations of the zonation of the soft clam were undertaken to determine if this species occurs in random or aggregated distributions in any one bed. The importance of this information stems from recent works in Europe where it has been shown that certain sedentary marine organisms exhibit the phenomenon of "gregariousness" which means that larvae tend to settle near members of their own species and form aggregated distributions. When this occurs, excessive exploitation of a species may so reduce the attractiveness of a locality that no setting will occur even when plenty of swimming larvae are present.

The investigations of the behavior of the quahaug larvae required the construction of apparatus to provide a supply of running water at elevated temperatures. A modified Loosanoff unit which consisted of a fifty-gallon drum with four 2-kw electric heating units inserted into the bottom was assembled. A coil of 1-inch lead pipe was placed in the drum and the drum was then filled with fresh water. Suitable thermoregulators were installed to maintain the fresh water at the desired temperature. Sea water taken from the laboratory salt water supply was then circulated through the coil of a lead pipe and the thermoregulators were adjusted to produce the desired temperature in the sea water effluent. In this way spring and summer water conditions could be simulated to cause the reproductive products of the quahaugs to mature out of season so that spawning could be induced. Other apparatus included a large constant temperature water bath to maintain optimal temperatures for the cultures of larvae, various earthenware, glass and plastic containers in which the larvae were cultured, and assorted stainless steel sieves for removing larvae from the culture media.

---

* Contribution No. 876 Woods Hole Oceanographic Institution.

In addition, it was necessary to provide food in the form of phytoplankton in considerable quantity. Facilities for growing dense cultures of various species of phytoplankton were made available in the Institution's microbiological laboratory so that various kinds of food organisms could be obtained in known densities.

After a number of preliminary trials, a routine procedure was established so that cultures of larvae could be maintained in various stages of development to the limit of the available facilities. Mortality was usually low up to the time of setting so that ample material was available for observations on aspects of behavior that might influence distribution and survival in the natural environment. These observations are discussed in a later section of this report.

The experiments indicated that the use of larvaculture as a seed source has considerable promise. A number of broods that were not expended during experiments have been reared beyond the setting stage. At the present time, however, there is insufficient knowledge as to how large "seed" should be before it can be planted in the natural environment with reasonable expectancy of a high survival rate. This must be investigated thoroughly before it will be possible to determine the kind of facilities that would be necessary to establish larvaculture on a commercial basis.

The author wishes to express his appreciation to Dr. Victor L. Loosanoff and his associates at the U.S. Fish and Wildlife Service Laboratory at Milford, Connecticut for their extensive correspondence and personal interviews which have aided substantially in the development of routine larvaculture at the Institution. Thanks are also due to Dr. John Ryther, Microbiologist of the Woods Hole Oceanographic Institution who provided facilities for growing food organisms and aided in the maintenance of food cultures. In addition, the cooperation of Mr. John Glude of the U.S. Fish and Wildlife Laboratory at Boothbay Harbor, Maine, is duly appreciated.

SOME ASPECTS OF THE BEHAVIOR OF THE QUAHAUG, *VENUS MERCENARIA,* DURING THE EARLY STAGES

BY

HARRY J. TURNER, JR. AND CARL J. GEORGE

INTRODUCTION

Efforts to expand production of commercial shellfish have been hampered by the failure of natural sets to occur regularly and predictably. The past history of the shellfish industry clearly shows that the survival of large sets is an exceptional rather than a regular occurence in any one locality. As a result the industry generally has depended on single large generations of clams or quahaugs to supply the commercial catch for long periods of time during which no significant repopulation took place. With the increased popularity and value of shellfish products, there has been a tendency to exploit such generations so intensely that individual areas have been rapidly dug out and have remained barren until other sets have appeared. Consequently, shellfishing can no longer be depended upon to provide a steady remunerative occupation.

The causes for the erratic natural propagation of commercial molluscs have never been adequately determined. It is generally believed that the free-swimming larval stage is critical and that the tiny helpless larvae are subjected to destruction by numerous unspecified predators, or are affected favorably or adversely by unspecified physical and chemical environmental conditions. These accidental combinations of complex circumstances either drastically reduce survival or, in rare instances, permit such a high degree of survival that a dominant year class (unusually successful generation) occurs.

Determination of the factors that favor or discourage the appearance of a successful generation of commercial molluscs has been hampered by a number of technical problems. However, the advances made by Dr. Victor L. Loosanoff and his associates at the U.S. Fish and Wildlife Service Laboratory at Milford, Connecticut, have provided a method by which the ecology and physiology of the early stages of commercial molluscs can be investigated. At the Milford Laboratory, methods of inducing the spawning and rearing the larvae of a number of commercial molluscs have reached such a high degree of perfection that an abundance of material can be available at all seasons.

Within the past year equipment and facilities have been constructed at the Woods Hole Oceanographic Institution for larval studies. The methods employed are the same as those described in the numerous publications from the Milford Laboratory. Briefly, the molluscs are subjected to an accellerated conditioning to cause the reproductive products to mature. Spawning is induced by the application of suitable stimuli and the larvae which develop from the fertilized eggs are provided with optimal quantities of suitable food. In this way cultures of larval and juvenile molluscs in various stages of development have been maintained for the study of their behavior.

The purpose of this report is to describe a number of our observations on the larval and juvenile stages of the bay quahaug, *Venus mercenaria,* and to attempt to correlate certain events with the behavior of this mollusc in its natural environment. We are well aware that there are inherent dangers in attempting to draw conclusions about the natural ecology of an organism on the basis of laboratory experiments in which conditions are maintained at a more constant level than ever occurs in the open marine environment. We hope, however, that these observations may be related in some way to the normal reactions of the organisms in nature, although our conclusions are necessarily tentative. We have endeavored to emphasize those behavioral peculiarities which are significant to the well-being and survival of mollusc larvae in their natural environment as well as in laboratory cultures. Also we wish to make it clear that many of these observations cannot be claimed as original, since other investigators undoubtedly have observed various aspects of the behavior of larvae and juvenile quahaugs not directly applicable to the particular problems under investigation and thus not included in the published reports.

The bay quahaug, *Venus mercenaria*, has been used exclusively in our experiments because the adults are hardy and the larvae are relatively easy to rear. The breeding stocks were established in the spring by sending several bushels of large quahaugs to Boothbay Harbor, Maine, where summer temperatures did not ordinarily reach the spawning temperature (Loosanoff 1954) Through the courtesy of the U.S. Fish and Wildlife Service, Clam Investigations, these quahaugs were held in the open water and were shipped to Woods Hole in such quantities as were needed during the summer. In the fall the entire stock was returned after the water temperature at Woods Hole had fallen below 18°C.

Spawning was induced by placing large quahaugs in warm water (26°C) for several hours and then adding a small quantity of reproductive products, either male or female, stripped from a single individual. In every instance a number of individuals spawned within a short time after exposure to the stimulating substance. In general the first specimens to spawn were males with the females spawning a short time later. When males and females were in the same container we found it expedient to collect the eggs by aspirating them into a large flask through a rubber tube placed near the excurrent siphon. This prevented losses by the accidental intake of eggs into the incurrent siphons of their own parents. There were always enough sperm accompanying the eggs to insure nearly 100% fertilization. The eggs were then passed through a coarse seive to remove debris, and were then concentrated on a #325 stainless steel screen where they were washed with filtered sea water to remove excess sperm. Finally they were placed in containers of filtered sea water in a constant temperature bath at 25°C. Earthenware, glass and plastic containers were used with equal success. At first the water was changed every other day although methods of maintaining the cultures in good condition for several days in the same water were developed later.

Food in the form of microscopic algae was grown in 3 gallon pyrex bottles according to the methods described by Ketchum and Redfield (1938). Several species were found to be suitable as food for the early larvae, but of these a small diatom-like plant, *Nitzschia closterium*, was found to be the easiest to raise in quantity. In high densities this species lacked the toxic properties that have been found in certain of the *Chlorella*-like plants (Loosanoff 1954), and could thus be fed to the larval cultures in large quantities without danger.

Observations on the reactions of the larvae to light, gravity, salinity gradients, and other factors were made in various containers and accessory apparatus under experimental conditions.

SPAWNING AND THE FERTILIZED EGG

Spawning of the quahaug in the natural environment has seldom been observed. The laboratory method of inducing spawning indicates that both thermal and chemical stimuli are involved. It is clear that the reproductive products, either male or female, will induce spawning after properly conditioned quahaugs have been held at a temperature of 25°C for a few hours. In the natural environment at least one individual in a bed must spawn spontaneously to trigger the spawning of others. Loosanoff (1954) has reported that spontaneous spawning often occurs as the temperature falls after the quahaugs have been subjected to a high temperature, and we have noticed the same thing. In the natural environment this condition generally occurs in a bay or estuary on a hot day just as the tide begins to rise. During low tide, exposed flats and shallow waters become intensely heated and the temperature falls rapidly as the cooler waters flow in with the rising tide. Therefore, it is highly likely that spawning often occurs just after low tide under natural conditions, and that the eggs are carried up the bay or estuary with the incoming tide.

The lunar phase theory of Korringa may apply in this connection. Korringa (1947) observed that swarming of the larvae of the European oyster generally occurs at certain phases of the moon. He interpreted this phenomenon to mean that changes in hydrostatic pressure with the approach of the spring tides triggered the spawning. However, during the spring tides when the expanse of uncovered flats is greatest the absorption of solar heat is most pronounced. For this reason the thermal stimulus would be greatest during the spring tides and least at the neaps.

Spawning during the spring tides would undoubtedly be advantageous to any estuarine organism because the inward tidal excursion is maximal and the eggs would be carried farthest up the estuary. This initial advantage would occur, however, only if the eggs remain in suspension. We have determined that they tend to settle out of sea water with a salinity of 31°/₀₀ at 23°C, but, the rate of settling is so slow that even the weak convective currents produced by differential warming of culture jars in the temperature bath tends to keep the eggs in suspension. In any estuary where currents, waves and thermal convections are always present quahaug eggs are undoubtedly distributed throughout the water column.

One subject of practical importance that has not as yet been investigated is the influence of the distance between individuals in a breeding stock on spawning and fertilization. There is some reason to believe that exploitation may reduce the density of a population to a point where individuals are so widely spaced that the stimulus of the reproductive products of a spawning individual fails to reach the others. There is also a possibility that sperm suspensions may become too dilute to affect adequate fertilization. In laboratory practice it has been found that very dilute suspensions of sperm give satisfactory fertilization but no quantitative data have been secured.

THE EARLY LARVAL STAGE

During the first 12 to 24 hours the fertilized quahaug egg undergoes a series of developmental stages that transform it into a swimming larva. The early swimming larva, called the trochophore, has rudimentary internal organs but does not feed, nutrition being provided by the yolk. At this time the larva is a vigorous swimmer and migrates rapidly toward the surface. In laboratory cultures the majority of the 24-hour-old larvae are concentrated in the upper half inch of the water in the culture jar even when there is a considerable amount of convection. We have determined that the larvae of this age, when held at a temperature of 22°C, swim upwards at a rate of 7 to 8 centimeters per minute and show no detectable reaction to light. They are indifferent to a considerable range of salinity gradients. We have experimentally introduced larvae into the bottom of a glass tube in which layers of diluted sea water were placed one above the other. The early larvae passed through the sharp gradients that separated layers differing by as much as 5‰ with no loss in velocity until the salinity was reduced to 15‰. After crossing a boundary between a layer of 20‰ sea water and 15‰ sea water the swimming velocity decreased so that the larvae could no longer swim upward. Instead they swam slowly in a circular pattern just above the interface.

It is not apparent at first how this behavior aids the survival of the larvae, but the investigations of Cerrutti (1941) provide a possible clue. While studying the failure of oyster sets near Taranto, Italy, Cerrutti determined that toxic hydrogen sulphide sometimes accumulated in the lower waters. Furthermore he discovered that numerous bottom-dwelling and pelagic organisms either preyed directly on larvae or accidentally entrapped them in their filtering organs so that losses from these sources were considerable. In view of Cerrutti's findings we suggest that the tendency of quahaug larvae to congregate at the surface may have some survival value, since it keeps them out of the lower levels where toxic conditions may occur and where bottom-dwelling predators are usually present.

Under certain conditions, swarming at the surface may be disadvantageous. Studies of estuarine circulation have shown that the upper levels of highly stratified estuaries move seaward more rapidly than the lower layers and this movement is accentuated by wind blowing in the same direction. Thus some failures in propagation may result when a strong seaward breeze arises during the first 24 hours of larval existence and sweeps the surface layers containing the larvae out of the estuary.

THE FEEDING STAGE

The digestive organs of the quahaug larva become functional as soon as the primitive shell is formed, usually 24 to 48 hours after fertilization depending on the temperature. The swimming behavior then becomes altered so that the larvae become uniformly distributed throughout the water column in laboratory culture jars. We have not been able to determine exactly what changes take place although there is some evidence that the larvae swim somewhat slower. They still tend to swim upward in a clockwise spiral propelled by the beating of cilia on a trumpet-shaped organ called the velum protruded outward between the shells in the anterior ventral region. At this time they become sensitive to various disturbances and will retract the swimming organ and sink if they collide with an object. We have observed, however, that under ordinary circumstances the larvae seldom collide with each other even when crowded as as thickly as 50 per cubic centimeter. The currents provided by the swimming organ seem to act like the slip-stream of an aeroplane. It is not unusual to see two larvae swimming in close proximity to each other, one caught in the slipstream of the other.

The tendency to distribute themselves throughout the water column undoubtedly has some advantage in food gathering. Naturally, if the larval population continues to swarm at the surface after the need for food occurs, the immediate food supply would be rapidly exhausted.

Loosanoff (1954) determined that the rate of growth and duration of the larval period in laboratory cultures depends on the concentration and quality of available food. Development can proceed as far as the early shelled stage in filtered water without the addition of food. However, after the primitive shells are formed growth does not occur although the larvae continue to survive. We have maintained such starved cultures for twelve days and observed normal development when suitable food was again provided. We have also determined that larvae which have developed as far as the early umbo stage on an optimal diet usually die when food is withheld. For instance, in one of our experiments at a temperature of 25°C, larvae were provided with food in suitable quantity for two days after feeding commenced and were then starved. Few survived the following 24 hours.

Loosanoff (1954) has also shown that a certain strain of *Chlorella* is a suitable food for quahaug larvae when present in relatively low concentrations, but has toxic properties which prevent growth and cause heavy mortalities of larvae when supplied in excess. We have found that *Nitzschia* does not have these toxic qualities and will support optimal growth in concentrations as high as a million cells per cubic centimeter.

The capricious manner in which blooms of planktonic algae of various kinds arise and decline under natural conditions undoubtedly has a profound affect on the survival of quahaug larvae. The experimental evidence supports the idea of Thorson (1946) that a sub-optimal concentration of food affects survival indirectly by prolonging larval life and thus exposing the population to a greater period of predation and to the additional possibility of transportation to unfavorable localities. Our observations on the fatal effects of starvation on partially grown larvae suggest that the elimination of the food supply by competing organisms may contribute directly to failures of propagation. In addition, mass mortalities may result from excessive growth of algae which are toxic in high densities. On the other hand, it appears probable that optimal concentrations of food of suitable quality are essential to promote a high degree of survival during the free swimming period.

METAMORPHOSIS AND SETTING

In the literature on the setting of a wide variety of marine invertebrates, which has been reviewed by Thorson (1946), there are few references to the behavior of commercial molluscs. Carriker (1951) has described a transitional phase in the quahaug, during which the foot develops although the swimming organ is retained so that the organism can both swim and crawl. He reports that during this transitional phase there is considerable activity as if the organism were testing out various surfaces, and even after the swimming organ degenerates exploratory movements continue for a long time. According to Carriker, the preferred substratum for the set is a hard surface overlain with a layer of fine silt, to which the tiny quahaug attaches its byssus and remains suspended in the silt.

Our own observations are in substantial agreement with those of Carriker's. The onset of metamorphosis is indicated by the development of the foot and gills when the well nourished quahaug larva is approximately 200 microns long. Contrary to popular opinion, the swimming activity appears to increase and the larvae have a stronger tendency to congregate at the surface rather than settle. In glass dishes they appear to crawl around on the bottom for a short time and then rise rapidly to the surface of the water where they often remain for some time, suspended by the beating of the cilia of the swimming organ. Alternate swimming and crawling may persist for one or more days until the swimming organ degenerates and the internal reorganization that accompanies metamorphosis is completed.

We have made a number of unsuccessful attempts to determine if the quahaug exhibits a special preference for a specific kind of substratum when it sets. We have placed dishes of sieved sand of varying grain sizes in the bottom of culture jars and have not been able to detect any preference. Instead the larvae appear to set at random in the dishes of sand, and also on the bottom of the jar between the dishes, although the mobility of the larvae allows them free choice. It must be noted that the sand was freed from organic matter so that it could be sieved successfully and that this experiment was designed only to test the effect of the size of sand grains.

In the event that a preferred type of substratum is discovered, it would be desirable to determine if it has any stimulating effect on the rate of metamorphosis. Wilson (1953) has shown that certain marine worm larvae will not metamorphose unless provided with a special kind of sand, characteristic of the adult habitat. It is conceivable that such a mechanism to a lesser degree might occur with the quahaug so that the previously-described transitional phase would terminate whenever the organism comes in contact with a suitable surface. At the present time however there is so little known about the composition of sediments that it is difficult to set up experimental procedures to determine their effect on setting. Geologists classify sediments according to the sizes of the particles, the mineral composition, and the degree of roundness or angularity. Little is known about the composition of associated organic matter except the amount as determined by loss on ignition. Benthic ecologists discuss sands, muds, and silts, with, or more often without, qualitative and quantatative explanations as to what is meant. It is essential that many details of the physical and chemical composition of sediments be ascertained before logical experiments on the effect of sediments on larval metamorphosis in molluscs can be designed.

THE EARLY JUVENILE STAGE

The early juvenile stage is defined as the period between setting and the time when the young quahaug is easily visible to the unaided eye. Few fishermen and investigators have ever seen juveniles smaller than half an inch long so that little is known about the factors that affect their survival, growth, or distribution.

Our observations on the activities of the juvenile quahaug immediately after metamorphosis are in substantial agreement with those of Carriker (1951). In glass dishes they will crawl about actively until they find a clump of algal detritus where they can imbed themselves in an upright position. We have been unable to determine if the clean glass surface has any repelling action, but our observations to date suggest that young quahaugs prefer an upright position and that clumps of detritus aid in maintaining that position.

When placed in containers with a substratum of sand, very young juveniles crawl about, sometimes wedging themselves between the sand grains but more often grouping in clumps of detritus. We have never seen a juvenile less than three-quarters of a millimeter long completely bury itself and even after the ability to dig becomes well developed the tendency to crawl about persists.

The effect of shifting sand on early juvenile quahaugs was studied by placing them in large flat dishes of sand where they were subjected to various actions simulating current, wave motions, etc. Preliminary results indicate that there is little likelihood of burial or breakage of the tiny quahaugs even when conditions are violent. When newly-set quahaugs, sand, and sea water are stirred with sufficient violence to move the surface of the sand, the quahaugs tend to remain above the sand grains in the agitated water and as the motion of the water subsides the sand settles out first so that the quahaugs remain on the surface. Juveniles asociated with clumps of algal detritus are carried along with the algae which slows down the settling rate in a parashoot-like manner so that the quahaugs again remain on the surface of the sand. The only way that juvenile quahaugs can be buried to a fatal depth is to pour sand directly over them in still water. It appears therefore, that normal conditions along the substratum of the natural quahaug habitat tend to keep the young juveniles from being buried and also that the shells of the juveniles are capable of withstanding considerable rough treatment.

Our observations indicate that hydrographic features undoubtedly play a considerable part in distributing or concentrating the young juveniles after metamorphosis. Their location on the surface of the substratum or their association with fine detritus places them in a situation where any current strong enough to move the detritus or the sand grains to which they are attached would carry the tiny quahaugs various distances. Since currents tend to sort sand grains according to size and density in the same way a winnowing machine sorts grain and chaf, there is good evidence that juvenile quahaugs are affected similarly. Smith (1952) and Turner (1953) have suggested that movements after setting, both directive and by hydrographic agencies, may be of considerable importance in determining the localities where concentrated populations develop. At present there is need for more study of the reactions of juvenile quahaugs of various sizes to turbulent water conditions such as occur from time to time in the natural environment.

The habitat assumed by the newly-set quahaug, either in a layer of silt or associated with algal detritus would seem to place it in a situation where it would be exposed to the direct and accidental attacks of predators. Sanders (in press) has shown that the normal inhabitants of certain types of bottom include a variety of species that feed indiscriminately by taking in the surface ooze and digesting the organic matter. It seems likely that any organism capable of ingesting particles as large as 250 microns may be a potential predator of young juvenile quahaugs. Shellfishermen have repeatedly suggested that the common mud snail *Nassa,* which often becomes abundant on potential shellfish flats may include young commercial shellfish in its diet. The literature on the natural history of the mud snail is meager in spite of its common abundance. Minor (1950) states that it is essentially carnivorous and can drill through the shells of other molluscs and even another snail. However, Dr. Charles Jenner (personal communication) who has studied the stomach contents of hundreds of mud snails has come to the conclusion that they are essentially omnivorous and the main item of their diet is ordinarily mud of high organic content. We have attempted to determine if starved mud snails feed on young juvenile quahaugs both in the presence and absence of other types of food. Our observations indicate that mud snails never take in juvenile quahaugs one-half millimeter long, although algal detritus and bits of clam meats are readily attacked. The activities of other suspected predators have not been studied.

SUMMARY

The foregoing account has discussed a number of observed properties and behavior patterns of the young stages of the bay quahaug which may interreact with physical, chemical and biological conditions in the natural environment to determine the success or failure of any one generation in a particular locality. In summary, we propose to describe a sequence of events, based on these properties, that might occur during the early stages of the life of a brood of quahaugs in an attempt to make clear how the interrelationships with the environment may affect survival.

In our account of the hypothetical situation, let us assume that there is a parent stock in the lower part of an estuary, a characteristic habitat (Turner 1953). If one or more individuals should spawn just after low tide the reproductive products thus liberated would trigger spawning in the entire bed, and the flooding tidal currents would then sweep the fertilized eggs toward the head of the estuary. This sequence seems probable in view of the tendency for spontaneous spawning to occur under experimental conditions when the temperature is reduced after a brief period of warming. However, if some unknown stimulus should cause spawning on an ebbing tide, the eggs would be carried out to sea and no repopulation of the estuary would occur in the estuary from that particular spawning.

Several hazards would reduce the survival of fertilized eggs. Slow currents with little turbulence would carry them near the bottom where benthic filter feeders could destroy large numbers, since those passing near the incurrent siphons of adult members of their own species as well as clams, mussels and other filter feeders would be sucked in and entangled in mucous threads. Swift currents would mix the waters and distribute the eggs throughout the water column and make them available to free swimming predators. Thus many of the original millions of eggs may be eliminated before completion of the flood tide excursion.

If vertical mixing becomes attenuated at slack high water, the developing eggs would settle toward the bottom. The seaward traverse of the developing eggs on the ebb tide would thereby be slightly delayed so that the full excursion of the ebb tide would not carry them out of the estuary.

At the end of one tidal cycle, the larvae would be situated near the mouth of the estuary and the site of their origin. Under favorable temperature conditions they should begin to swim under their own power at this time and migrate toward the surface. Here they would be immune to predations of bottom dwelling organisms. Now however, the wind direction may be critical since a strong seaward breeze could accellerate the surface currents enough to sweep the entire population out to sea. On the other hand, a landward breeze would decrease the seaward velocity of the surface currents and retain the surviving members of the brood in the estuary.

Under favorable conditions, feeding would begin sometime during the third and fourth tidal cycle and the larvae would distribute themselves throughout the water column. At this time the quality and quantity of the food supply would be critical. Inadequate concentrations of suitable planktonic algae would retard growth and extend the duration of the larval period. The disappearance of suitable food after a few days of larval development would decimate the population by starvation, and the development of unusual densities of unsuitable or toxic food would cause serious losses.

Additional losses would occur from other agencies. If the lower layer of a stratified body of water were anaerobic, all larvae entering these layers would die. Predators, including species of many groups from hydroid medusae to small fish, would take their toll.

Throughout the larval period, the mixing processes of our hypothetical estuary would tend to break up the swarm of quahaug larvae, to dilute them, and to carry some out to sea on each tidal cycle. The vertical distribution of the larvae in the water column would modify the transport. At the present time, field data are inconclusive and observations in the laboratory have not indicated whether or not the organisms are endowed with a behavior pattern that might keep them together and within the estuary. Such behavior patterns have been demonstrated in oyster larvae (Carriker 1951a) which tend to remain in swarms or lanes, dropping to the bottom on the ebb tide and swimming actively on the flood, so that the net drift carries them toward the headwaters of the estuary. Similarly Bousfield (1955) has demonstrated vertical movements of barnacle larvae which change with the larval stage so that they first drift seaward in the upper layers, but at later larval stages they migrate downward into the deeper water and are transported up the estuary again as they approach metamorphosis. It is possible that quahaug larvae are equipped with some similar mechanism to aid retention in estuaries but that remains to be demonstrated.

At the onset of metamorphosis the quahaug larvae develop a foot, byssal gland, and gills but still retain their swimming ability. We suspect that this transitional phase permits them to test various surfaces until a suitable substratum is found. We do not know what kind of substrata are suitable but suspect that thin layers of ooze or clumps of algal detritus may be preferred. We also suspect that the finding of a suitable surface may stimulate the termination of the crawling-swimming stage. At the end of their swimming stage the larvae can still swim vigorously and have also developed a foot with which they can crawl. We suspect that they spend one or more days testing various surfaces until a suitable place is found. Our observations indicate that such places may include hard surfaces covered with thin layers of ooze or clumps of algal detritus.

Newly-set quahaugs are probably not adversely affected by minor disturbances of the substratum. On the other hand it seems likely that such disturbances may be one of the factors that tends to concentrate them in the same way that sand grains of uniform size are selectively sorted. We suspect that numbers of newly-set juvenile quahaugs are destroyed by direct predation and accidental ingestion by various benthic organisms but have not observed any typical cases in the laboratory. However, we have not made enough extensive observations as yet. The entire question of survival of the early juveniles is now under study.

This account of a sequence of events in the early life of a hypothetical brood of quahaugs is undoubtedly over-simplified and may contain a number of incorrect assumptions in cases where organisms in their natural habitat act differently from those in laboratory cultures. However the account indicates how a succession of events may permit a high degree of survival or that a single event may be so disasterous that the generation may fail completely. It would appear that the probability of a succession of events, all of which favor survival is so low as to explain the rare appearance of dense sets of quahaugs.

REFERENCES

Carriker, M. R.
1951 Preliminary studies on field culture, behavior and trapping of the larvae of hard clams, *Venus* (*Mercenaria*) *mercenaria.* Nat. Shellfish Ass'n., Convention. Addresses.
1951a Ecological observations on the distribution of oyster larvae in New Jersey estuaries. Ecol. Mon, 21.
Cerruti, A.
1941 Osservazioni ed esperimenti sulle cause di distruzione delle larve d'ostrica nel Mar Piccolo e nel Mar Grande di Taranto. Arch. di Oceanog. Limnol., Roma. Vol. 1.
Ketchum, B. H. and A. C. Redfield
1938 A method of maintaining a continuous supply of marine diatoms bv culture. Bio. Bull., Vol. 75, No. 1.
Korringa, P.
1947 Relations between the moon and periodicity in the breeding of marine animals. Ecol. Mon. 17.
Loosanoff, V. L.
1954 New advances in the study of bivalve larvae. American Scientist, Vol. 42, No. 4
Loosanoff, Victor L. and Harry C. Davis
1950 Conditioning *V. mercenaria* for spawning in winter and breeding its larvae in the laboratory. Bio. Bull., Vol. 98, No. 1.
Minor, R. W.
1950 Field Book of Seashore Life. G. P. Putnam's Sons, New York.
Sanders, H. L.
(in press) The biology of marine bottom communities.
Smith, O. R.
1952 The wanderings of soft clams. Nat. Shellfish Ass'n. Convention Addresses.
Thorson, G.
1946 Reproduction and larval development of Danish marine bottom invertebrates. Medd. fra Komm. for. Danm. Fisk. Ser. Plank. B. 1, Nr 1.
Turner, H. J., Jr.
1953 A review of the biology of some commercial molluscs of the east coast of North America. Sixth Rept. Invest. Shellfish. Mass. Div. Mar. Fish., Dep. Nat. Res. Com. Mass., Boston.
Wilson, D. P.
1953 The settlement of *Ophelia bicornis,* Savigny larvae. J. Mar. Biol. Ass'n., Vol. 32.

SPATIAL DISTRIBUTION OF TWO SPECIES OF CLAMS *MYA ARENARIA L.* AND *PETRICOLA PHOLADIFORMIS LAMARCK,* IN AN INTERTIDAL AREA.

BY

JOSEPH H. CONNELL

INTRODUCTION

It is well known that the distribution of soft clams, *Mya arenaria* is extremely variable in any locality within their normal habitat. It is not known whether this variability is due entirely to discontinuities in the substratum, some portions being more favorable than others, or due to "social" influences between the organisms themselves. An example of social influence is gregariousness, a tendency for organisms to settle near others of the same species and form local aggregations. Another is competition which causes animals to space themselves so that each individual will have adequate living space or food supply. In either case the distribution of organisms shows a departure from randomness which can be analyzed quantitatively.

In the case of the soft clam, the presence or absence of social behavior may be of importance in the regulation of commercial exploitation. If this species exhibits a gregarious tendency on setting, we may suspect that depletion of a local area might discourage subsequent repopulation of that area. On the other hand if individual clams exert negative influences on each other so that they space out, we may suspect that some degree of exploitation would encourage repopulation by providing additional living space as mature individuals are removed

In addition there is the possibility that one species of clam may influence distribution of another when both are living together in the same area. Since the "double-neck" *Petricola pholadiformis* commonly occurs in the same habitat as the soft clam its distribution is included in this study.

METHODS

The spatial distribution of the soft clam and the double-neck clam was studied in a strip two feet wide and fourteen feet long at right angles to the shore line on the east side of Eel Pond, Woods Hole, Massachusetts. Here the tidal amplitude was about 2½ feet producing an intertidal beach about 30 feet wide with a slope of 8%. The bottom consisted of muddy sand, dark grey, below the depth of about one inch. The surface of the shells of the clams was partly black when they were first dug up; this color disappeared when the clams were kept overnight in the laboratory in running sea water. This suggested anerobic conditions, the oxygen probably being depleted by the decomposition of the organic matter present in the Eel Pond. The dark color, probably iron sulfide formed anaerobically by sulfur bacteria, would be expected to disappear when aerated. A continuous transect strip was excavated from average low water upward until no more clams were found above the level of mid-tide. The transect was excavated in segments, each two feet in length, by pushing a square metal frame, 2′x2′, with vertical sides 3″ high, into the sand on the transect. Then the sand inside was carefully removed to a depth of 6 inches, working across from one side. A strip about two inches wide was dug on either side outside the frame so that any neighbors to clams near the border might be found. As each clam was found its distance from the top and left hand sides of the square was recorded, so establishing its grid position. The depth of the top edge of the shell below the surface and the length of the clam were also recorded. Dead paired valves, which were found in the normal position of living clams and all rocks and other solid objects over one inch in diameter were also mapped.

For the purpose of analysis of different levels, the mapped portion of the transect was divided into four portions as shown in Figure 1: the lowest one is shorter than the others. In the analysis of size and density the clams collected from the foot below the mapped part of the transect were included in level IV. Levels III and IV were dug in mid September and early October, while the upper levels were dug in late October and early November. The excavation of each of the densely occupied squares took two to three low tide periods.

The method of Clark and Evans (1954) was used to describe the distribution. This consists in measuring the distance of each individual to its nearest neighbor. The average of these measurements is then compared to the average distance which would be expected to occur in a random distribution of points. In such a random distribution of points on a plane surface with a density d, the average distance to nearest neighbor r/E is given by the formula r E is equal to 0.5 divided by the square root of the density. This formula had been derived independently by Hertz (1909) and G. M. Spooner quoted in Holme (1950). The ratio, R, of the average distance to nearest neighbor in the observed distribution to that calculated by the formula gives the degree or departure from randomness. In a population where most of the points are aggregated in groups, the average distance will normally be smaller than would be expected in a random pattern so that the ratio, R, will be less than one. Where the points are spaced out more uniformly than random, the ratio will be greater than unity.

Clark and Evans give a method for testing the significance of the observed departure from randomness. A random distribution of points in space is defined as one in which neither the nature of the space nor the position and nature of the points has any influence on the position of any point. Thus any significant departure from such a distribution must be caused by discontinuities in the space or by some influence of the points on one another.

POPULATION DENSITY, SIZE AND MORTALITY

It is necessary to describe the population density and size distribution of the individual clams with respect to the various sections of the transect before it is possible to present meaningful analysis of the spatial relationships. In addition, the presence or absence of paired shells of dead clams situated upright as in life gives some indication as to whether or not the population has been disturbed in the recent past.

The population density at each level is given in Table 1. The greatest densities occurred at the middle levels for both species. The proportion of live to dead shells is also given for each level. The pairs of valves occurring in the vertical position of living clams at similar depths are assumed to be clams which died in place. Any single valves or pairs out of position near the surface were not included. None of the shells had been bored, and the natural position made it unlikely that crabs or birds had killed these individuals.

The proportion of these dead shells increased toward the low tide level. This may have been due either to an increase in the mortality rate or to a decrease in the rate of shell dissolution lower down the shore. The shells of living Mya at higher levels seemed to be much smoother and thinner than lower down. This fact suggests that faster disintegration rather than lower mortality may account for the lower proportion of shells at high levels.

The great number of dead shells *in situ* and the existence of the larger sizes seems to indicate that this is an undisturbed, established population.

A frequency distribution of measurements of *Mya* at each level is given in Table 2A. The mean size increases progressively toward the low tide line although there is little difference between the lower two levels. The differences between levels other than these were judged to be significant, the tests of significance being given in Table 2B. Intertidal barnacles have faster initial growth rates at low levels (Hatton, 1938, Barnes and Powell, 1953) and it is possible that this is also true of the clams in this area, the faster growth rate presumably being due to the longer period of immersion with its greater possible feeding time. However, the possibility of greater mortality among small individuals at low levels, or the converse at high levels cannot be eliminated.

SPATIAL RELATIONSHIPS

An analysis of the spatial relationships of the two species of clam was made to determine if they were distributed in a random pattern or in aggregate groups. This was done because it seemed probable that a random pattern would result if the clams had set on a uniform surface with no influence of one individual on another in choice of site, or survival of subsequent generations. On the other hand aggregate groupings or other non-random patterns would indicate that either the substratum was variable or that the clams had some influence on each other either in selecting the site.

The analysis of the spacing of Mya arenaria alone is given in Table 3A. At all levels R was less than 1.0, indicating that *Mya* was clumped, but was significant only at levels I and III. However, level III contained many large rocks, so that a recalculation was made for this level, the area covered by the rocks being subtracted from the total area in the calculation of density. The distribution was then found to be not significantly different from a random one. Thus the aggregation observed in the first analysis of this level was a result of discontinuities in the substratum. The aggregation indicated at level I is based on too few animals to be considered reliable.

A similar analysis of the *Petricola pholadiformis* distribution, in the lower three-quarters of level III and in level IV also resulted in values of R significantly lower than unity (Table 3B). This aggregation was probably due to unknown discontinuities in level IV, since only level III was considered in the following analysis, the distribution resembled a random one.

It was decided to combine the *Mya* and *Petricola* populations, and to measure the distance to nearest neighbor, irrespective of species. For this, only the lower ¾ of level III was used, since the density remained fairly constant, and most of the *Petricola* were concentrated in this area (Figure 1). The results of this analysis are given in Table 4. First the *Mya* and *Petricola* were analyzed separately for this area, then together. The only significant grouping was one of clams, rather than of either species. Since any social behavior leading to grouping would be expected to be greater within a species than between species, except in a symbiotic association, this evidence seems to rule out the action of any social influences. Discontinuities in the bottom must then cause the aggregation. The aggregations observed after removal of the obvious discontinuities were of *Mya* in level I, *Petricola* when levels III and IV were combined, and both species together in level III. Past discontinuities, such as the attacks of predators, might account for these observations.

VARIATION OF DEPTH BELOW THE SURFACE

During the course of this study, observations were made on the depth at which the clams were situated in the substratum, and these are reported here because the depths varied somewhat according to the level of the beach as well as with the size of the clams.

The analysis of the depth measurements is given in Table 5. This depth was measured as the distance from the sand surface to the upper edge (posterior) of the shell. At each level the larger *Mya* were deeper. However, when comparing the same sized clams at different levels, the smaller ones (less than 45 mm) seem to be slightly deeper at low levels, while those over 65 mm were deeper at higher shore levels. However, the numbers, especially of the smaller individuals, are too small to draw conclusions from. The few measurements of *Petricola* indicate that the larger individuals were buried deeper. Several instances were noted where a smaller *Mya* occurred almost directly above a larger one; the small clam lay alongside the siphon of the latter.

DISCUSSION

The evidence suggests that where the soft clam and double-neck clam tend to be aggregated in their distribution, the aggregations are caused by variations in the substratum. Within favorable areas of the substratum, however, the distribution is random. Nothing in the study indicates a gregarious tendency in either species nor is there any evidence of even spacing. Likewise it is apparent that both species may live together in a random distribution with no apparent influence of one species on the other. It is suggested that this may be a fundamental property of sedentary, bottom-dwelling, filter-feeders that obtain their food from the waters above and have little ability to move except downwards.

In contrast, a small deposit-feeding English clam exhibits a different behavior which generally results in even spacings as reported by Holme (1950). This small clam, *Tellina tenuis* lives near the surface and feeds on surface ooze which it sucks in through the inhalent siphon operating over the surface like a vacuum cleaner. In addition this clam has a well developed foot and is capable of directional movement. Holme found that *Tellina* exhibited a spacing that was more even than random. For comparison with *Mya* and *Petricola* his data have been analyzed in the present method and the results given in Table 3c. A significant degree of uniformity in spacing is confirmed. Holme suggested that in moderate densities each *Tellina* has a territory delineated by the feeding activities of the inhalent siphon. He demonstrated this by placing 100 clams around the inside of a metal circle 22 inches in diameter and found that the clams had spaced themselves out evenly when the experiment was terminated eight weeks later. See Table 3c. However, when the experiment was tried at a much higher density the spacing became random. Holme suggested that the territorial behavior broke down due to the confusion of the number of siphons meeting each other when the density were too high.

It is apparent from these studies that the type of spacing exhibited by some bottom-dwelling marine clams depends on the uniformity of the substratum the feeding and mechanisms of the different species, and the density of the organisms. Aggregate distributions of the filter feeding clams *Mya* and *Petricola* occur in the more favorable portions of a variable substratum but within these the distributions are fundamentally random. In the deposit feeders however, there tends to be a more even spacing so that each individual will have an area of its own from which to obtain its food. In *Tellina,* however, the territoriality breaks down when too many individuals are confined in a small space.

The determination of random distribution of the soft clam within the favorable areas of the substratum does not definitely indicate the lack of a gregarious tendency at the time of the setting. Other factors such as washing out the redistribution of the very young juveniles, and also variable mortality during early life may produce random distributions even though there is an original gregarious tendency at the time of setting. Similarly, the failure of the soft clam to exhibit even spacing does not indicate that it does not occur at some time during early life. The feeding mechanism of the soft clam does not appear to require territoriality such as occurs in *Tellina,* but Turner (1948) has shown that the growth rate is depressed as the density of clams increases. This is a clear indication that spacing would be advantageous although the locomotory mechanism of the adult soft clam is too poorly developed to permit it. If territoriality occurs at all in this species, it must take place when the clams are very young and active.

REFERENCES

Barnes, H., and Powell, H. T.
1953 The growth of *Balanus balanoides* (L.) and *Balanus crenatus* Brug. under varying conditions of submersion. J. Mar. Bio. Ass. U. K., 32: 107-128.

Clark, Philip J. and Francis C. Evans
1954 Distance to nearest neighbor as a measure of spatial relationships in populations. Ecology, 35. 445-453.

Hertz, P.
1909 Uber den geigenseitigen durchschnittlichen Abstand von Punkten, die mit bekannter mittlerer Dichte im Raume angeordnet sind. Mathematische Annalen 67: 387-398.

Holme, N. A.
1950 Population-dispersion in *Tellina tenuis* Da Costa. J. Mar. Biol. Ass. U.K., 29: 267-280.

Turner, H. J., Jr.
1948 Report on investigations of the propagation of the soft-shell clam, *Mya arenaria.* Div. Mar. Fish., Dept. Conservation, Commonwealth of Mass., Boston. (Contribution No. 462, Woods Hole Oceanographic Institution.)

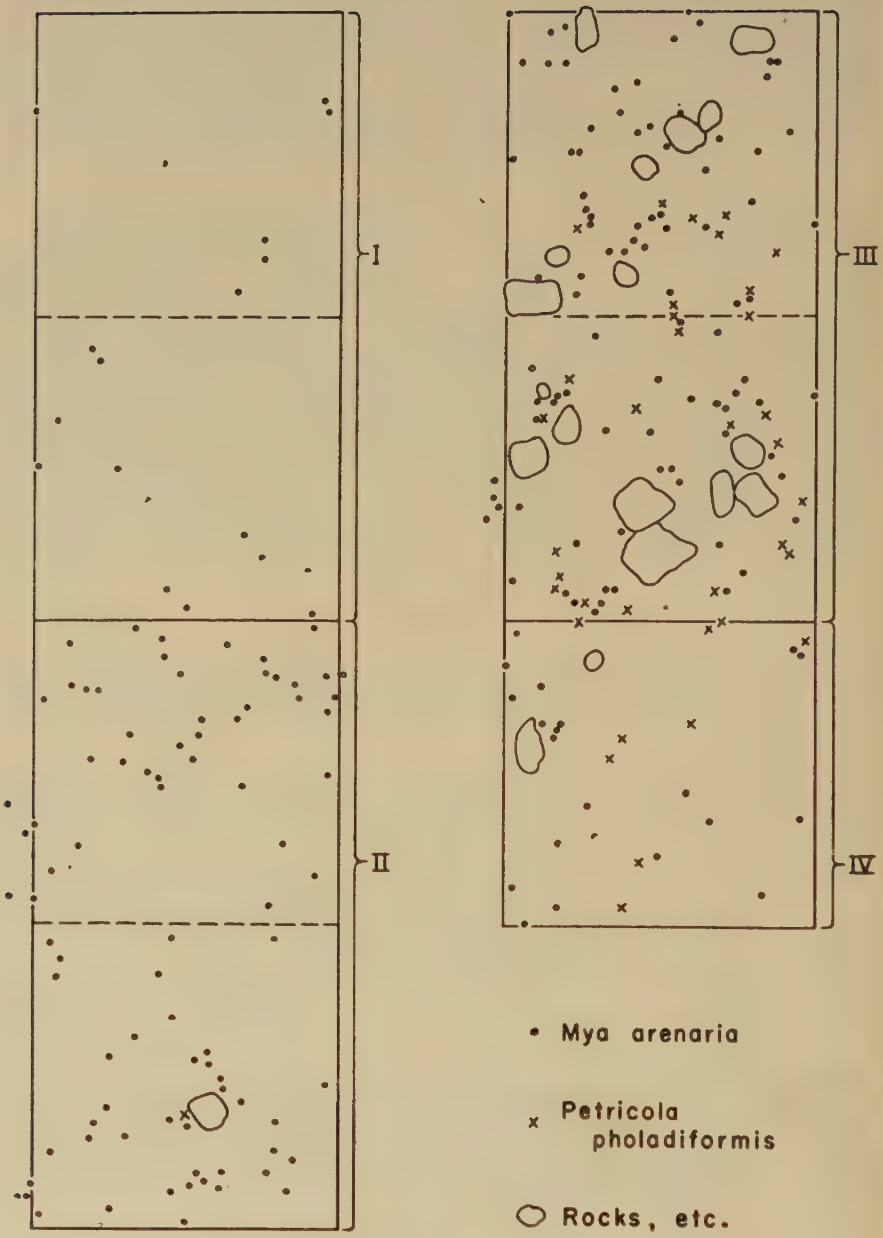
I
II
III
IV
● Mya arenaria
× Petricola pholadiformis
Rocks, etc.

Figure 1

Table 1. Variations in density of living clams and in the proportion of dead pairs of valves found *in situ* at different levels of the shore.

Level	Density (no. sq. ft.) live clams	No. of live clams	No. of dead pairs of valves	Total no. of live and dead	% dead
		Mya arenaria			
I	2.4	22	2	24	8.
II	10.0	86	42	128	33.
III	10.9	91	88	179	49.
IV	5.3	30	124	154	80.
		Petricola pholadiformis			
II	0.1	1	2	3	67.
III	4.3	26	17	43	39.
IV	1.7	10	38	48	74.

Table 2A. Frequency distribution of lengths of *Mya arenaria* at the different levels of the transect.

Length mm.	Level I	II	III	IV
16-20	1			
21-25		1	1	
26-30		1	1	
31-35	1	1		
36-40	4	3	1	3
41-45	2	5	2	
46-50	5	12	4	
51-55	1	13	11	3
56-60	4	11	15	3
61-65	3	15	20	4
66-70		11	12	5
71-75	1	9	11	5
76-80		1	6	4
81-85			2	1
86-90			1	1
91-95			1	
No.	22	83	87	29
Mean length	48.4	57.1	64.0	65.0
Standard Deviation	12.6	10.7	6.7	12.8

Table 2B. Tests of the significance of the differences of the average lengths of *Mya arenaria* between the levels of the transect.

A. Between levels I and II, "t" test, t=3.22, p less than .01.

B. Between levels II, III, IV, Analysis of Variance:

Source of variation	Sum of squares	Degrees of freedom	Variance estimate
Between levels	2525.	2	1262.5
Within levels	18071.	196	92.2
Total	20596.	198	

F=13.69
p less than .01

Table 3. The spatial distribution of two species of clam from the Eel Pond transect and one from southwest England, analyzed by the method of Clark and Evans (1954). Distances are given in inches.

		3A. *Mya arenaria*					3B. *Petricola pholadiformis*		3C. *Tellina tenuis* Southwest England		
	Symbol	Whole area				Less rocks	Whole area	Less rocks	(Holme, 1950)		
Level		I	II	III	IV	III	III-IV	III-IV	Sta. F	Sta. G	Exp. I
No. of measurements	N	17	77	82	18	82	32	32	65	29	30
Density (no./in.^{2})	d	.016	.069	.075	.035	.083	.024	.026	.119	.142	.296
Average dis. to nearest neighbor, OBSERVED	r/A	2.51	1.73	1.60	2.29	1.60	2.42	2.42	1.69	1.62	1.20
Average dis., calculated for a random distribution	r/E	4.00	1.91	1.83	2.68	1.74	3.25	3.13	1.45	1.33	0.92
Ratio, $\frac{\text{observed dis.}}{\text{random dis.}}$	R	.628	.906	.874	.854	.920	.745	.774	1.17	1.22	1.30
Standard variate of normal curve	c	2.93	1.58	2.17	1.18	1.40	2.76	2.45	2.55	2.25	3.22
Significance		**		*			**	*	*	*	**

Note: The significance limits for c are as follows:

c=1.96, p=.05, judged significant: *
c=2.58, p=.01, judged highly significant: **

Table 4. The spatial distribution of *Mya arenaria* and *Petricola pholadiformis* in the lower three-quarters of level III, considered apart and together.

	Symbol	*Mya* alone	*Petricola* alone	Both species
No. of measurements	N	57	27	84
Density ,(no./in.^{2})	d	.078	.035	.115
Average dis. to nearest neighbor, OBSERVED	r/A	1.61	2.22	1.29
Average dis., calculated for a random distribution	r/E	1.79	2.66	1.47
Ratio, $\frac{\text{Observed dis.}}{\text{Random dis.}}$	R	.900	.835	.878
Standard variate of the normal curve	c	1.45	1.64	2.14
Significance				*

Note: See Table 3 for explanation of significance symbols.

Table 5. The depth in inches from the sand surface to the top of the shell, for different sizes of *Mya arenaria* and *Petricola pholadiformis*.

		Mya arenaria Size-classes, mm.							
		15-24	25-34	35-44	45-54	55-64	65-74	75-84	85-94
Level I	Number of meas.	1		2	4	5	2		
	Ave. depth	0.5		1.9	2.7	3.3	4.2		
Level II	Number of meas.		1	4	23	25	16	3	
	Ave. depth		2.0	2.7	3.4	4.0	4.3	5.4	
Level III	Number of meas.	1	1	2	13	29	27	10	2
	Ave. depth	1.0	2.0	3.1	2.9	3.6	4.0	4.6	4.5
Level IV	Number of meas.			1	3	4	6	3	
	Ave. depth			3.0	3.0	3.5	3.7	4.0	
		Petricola pholadiformis							
		45-49	50-54	55-59					
Levels III & IV	Number of meas.	4	13	6					
	Ave. depth	2.4	2.5	3.2					

Kendall Printing Co., Falmouth, Mass.

Contribution No.

Reprinted from the JOURNAL OF CELLULAR AND COMPARATIVE PHYSIOLOGY
Vol. 48, No. 3, December 1956

MICRO GASOMETRIC DETERMINATION OF OXYGEN IN FISH BLOOD[1]

P. F. SCHOLANDER AND L. VAN DAM
Woods Hole Oceanographic Institution

ONE FIGURE

The micro gasometric method for oxygen determination in blood by Roughton and Scholander ('43) works well with the blood from humans, dogs, rabbits, and rats, but may be difficult, sometimes impossible, to use on the blood of cats, birds, or fishes, where the reagents do not properly break up the blood proteins into a flocculate precipitate, but produce a viscid foam. By increasing the acidity of the final blood mixture, with due changes in technique, this difficulty has been overcome. With the present method we believe determinations can be made on a much wider range of animal material than was possible before. For details in procedure and equipment the basic papers by Scholander and Roughton ('42) and Roughton and Scholander ('43) should be consulted.

APPARATUS

The syringe analyzer and the calibrated blood pipette, with a capacity of about 40 mm^3, are described by Scholander and Roughton ('42). The strong acid used in the present modification of the method produces a rapid CO_2 evolution, which makes it necessary to close the analyzer with a special wire clip, instead of with the finger (fig. 1). The clip has a polyethylene tip made by pressing a piece of polyethylene tubing into the lumen of a piece of drawn out warm glass tubing. The plug is self-holding, and closes the capillary gas tight.

---

[1] Contribution no. 879 from the Woods Hole Oceanographic Institution. This work was supported by a grant from the National Science Foundation.

REAGENTS

1. Distilled water.

2. Isotonic saline. Dissolve 11.7 gm NaCl in 1 liter of water (= 0.20 M).

3. Caprylic alcohol.

4. Ferricyanide solution. Dissolve 12.5 gm $K_3Fe(CN)_6$, 3 gm $KHCO_3$, and 0.5 gm saponin in 50 ml water.

5. Acid sulfate solution. Dissolve 30 gm Na_2SO_4 anhydrous in 100 ml water and add 5 ml concentrated H_2SO_4.

6. NaOH solution. Dissolve 10 gm NaOH in 50 ml H_2O and add 5 gm Na_2SO_4 anhydrous.

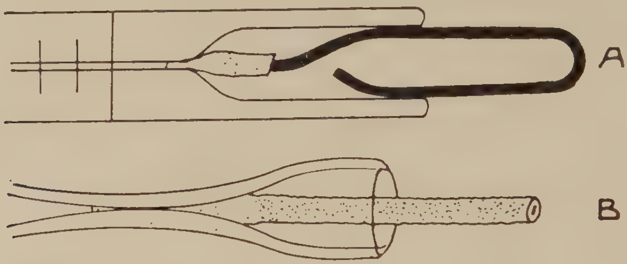

Fig. 1 A. Wire clip with polyethylene tip sealing the capillary of the analyzer. B. Method of forming the polyethylene tip in warm glass tubing.

7. Pyrogallol solution. Add 15 gm pyrogallol to 100 ml of 20% NaOH and cover with a layer of oil 2 cm thick. Dissolve under the oil by stirring with a glass rod.

Store the above solutions in 2–5 ml syringes provided with drawn out glass tips.

PROCEDURE

Clean the analyzer and blood pipette with dichromate H_2SO_4 cleaning solution, and rinse them thoroughly with water. Dry the warm pipette by suction. Rinse the capillary and barrel of the analyzer twice with ferricyanide solution. Fill the cup with the solution to the mark and draw it down into the capillary. Rinse the cup with saline, and empty. Place a drop of caprylic alcohol in the bottom of the cup. Expel any trapped air bubbles.

Fill the blood pipette with the blood to be analyzed and transfer the sample into the analyzer in the usual way. Discharge the air bubble that is on top of the blood through the caprylic alcohol. Draw in the caprylic alcohol to the zero mark, and remove the rest by suction. Fill the cup with acid sulfate solution to the mark.

Place the metal plug in position in the bottom of the cup, so that the plastic tip almost closes the capillary. Draw the acid sulfate solution into the barrel, and close the capillary by immediately seating the plug. Shake the analyzer horizontally for two minutes. At short intervals loosen the plunger arresting clip to equalize the pressure.

Adjust the gas pressure to atmospheric with the plunger. Remove the plug carefully, while manipulating the plunger so as to maintain the liquid seal in the capillary. Attach the NaOH cup and fill it with NaOH solution. Eject the air trapped in the capillary, and draw some NaOH into the barrel, letting the plunger up during the absorption. Towards the end of the absorption move the bubble up into the capillary, where it is protected against reabsorption.

Remove the NaOH cup, and empty the analyzer cup by suction. Clean the upper part of the capillary where the readings will be taken by twirling a fine stainless steel wire. Temperature equilibrate the analyzer in a beaker containing water of room temperature for half a minute. Dry the analyzer by wiping it lightly with cheesecloth, and read the volume of the bubble (V_1).

Fill the glass cup with pyrogallol solution. Draw it down slowly over the bubble in the barrel. Read the volume of the bubble (V_2).

The oxygen content in volume per cent equals $(V_1 - V_2 - c) \times f$, where c is the blank correction for oxygen in the reagents (about 0.9 vol. %), and f is the STP correction.

ACCURACY

Duplicate analyses in a variety of fishes usually agreed within 0.2 to 0.3 volume per cent. The gasometric method checks linearly with an optical method (Scholander and van Dam, '54), and when samples of tautog blood of different oxygen contents were mixed anaerobically in syringes the results agreed well with the calculated value.

LITERATURE CITED

ROUGHTON, F. J. W., AND P. F. SCHOLANDER 1943 Micro gasometric estimation of the blood gases. I. Oxygen. J. Biol. Chem., *148:* 541–550.

SCHOLANDER, P. F., AND L. VAN DAM 1954 Secretion of gases against high pressures in the swimbladder of deep sea fishes. I. Oxygen dissociation in blood. Biol. Bull., *107:* 247–259.

SCHOLANDER, P. F., AND F. J. W. ROUGHTON 1942 A simple microgasometric method of estimating carbon monoxide in blood. J. Industrial Hygiene Toxicology, *24:* 218–221.

Contribution No.

Reprinted from the JOURNAL OF CELLULAR AND COMPARATIVE PHYSIOLOGY
Vol. 48, No. 3, December 1956

OBSERVATIONS ON THE GAS GLAND IN LIVING FISH[1]

P. F. SCHOLANDER
Woods Hole Oceanographic Institution and
Lerner Marine Laboratory, Bimini

In spite of all the information available regarding the function of the gas gland in fishes, one may safely say that none of the three cardinal feats of the gland can as yet be explained; namely, the production of 100–200 atmospheres of oxygen, of 10–20 atmospheres of nitrogen, and of 0.1–0.2 atmospheres of argon. It is believed that some advance towards solving these problems can be gained by studying the secretion more closely on the intact gland itself.

This paper presents some observations on the gas gland in living fish, giving analyses of the gas bubbles secreted by the gland of cod and of the oxygen content and capacity of the blood leaving the active gland in barracuda. In these two species it is relatively easy to expose the swimbladder gland and to induce gas secretion for studies *in situ.* After deflation, about half the number of barracudas examined continued to secrete gas on the operating table, and deflated codfish, when treated with yohimbine (Fänge, '53), would do the same.

The barracudas *(Sphyraena barracuda)* were obtained at the Lerner Marine Laboratory, Bimini, Bahamas, in January, 1955, and the codfish *(Gadus callarias)* were procured through the courtesy of Mr. David F. Ryder, of Chatham, Massachusetts. The cod were kept in live cars near the laboratory in Woods Hole.

---

[1] Contribution No. 880 from the Woods Hole Oceanographic Institution. This investigation was supported by a grant from the National Science Foundation.

PRESS OF THE WISTAR INSTITUTE OF ANATOMY AND BIOLOGY
Printed in the United States of America

Composition of the gas bubbles secreted by the gland of cod

The codfish was deflated by puncture and given 5–10 mg yohimbine per kilogram. After one or two hours the fish was lifted onto a V board, lashed in place, and provided with a rubber tube and mask, through which the water passed into its mouth and out under the gill covers. A rubber collar behind the gills prevented the water from flowing back over the body. The tail end of the fish was covered with a plastic apron and was kept irrigated with cold water. The swimbladder was exposed and opened along one side, so as not to sever the gland. Part of the gland was exposed by turning over the ventral swimbladder wall. The bubble foam which usually covered the gland was wiped off with a fine glass rod, or if necessary rinsed off with 0.17 M saline. A small square of household Saran wrapping film was placed on the gland, without trapping any air bubbles. In a few minutes an active gland would produce masses of bubbles under the Saran, which slowly coalesced into larger ones. Under the binocular microscope small bubbles could be removed from beneath the Saran film, by means of a mercury pipette with a hair-fine tip bent at an angle. They were handled and analyzed according to a micro gasometric technique described by Scholander and Evans ('47).

The composition of the gas bubbles secreted under the Saran film is given in table 1. There is a considerable variability. The carbon dioxide averages some 9% and the oxygen some 63%. These figures, including the spread, agree well with the gas composition found in the swimbladder of fish treated with yohimbine, where the bladder had been completely emptied (cp. Scholander, van Dam, and Enns, '56).

These analyses are significant in that the composition of the gas has not been modified by a differential elimination of gas by the oval, but represents what is actually being secreted. In the codfish the oxygen secretion is accompanied by a carbon dioxide tension which seems exceptionally high. A great variety of fishes have been found to secrete oxygen with a much lower CO_2 concentration, sometimes only a small fraction of 1%. This should, however, be verified by analyses of bubbles taken directly from the gland.

It is an interesting fact that the bubbles secreted into the mucus covering the gland or into crevices between the cells are formed only on the outside of the gland cells; i.e., towards the swimbladder lumen. As the gas pressure in a bubble, due to surface tension, is inversely proportional to the diameter, considerable pressures are necessary for the formation of bubbles *de novo*. If the primary tension build-up were in the blood of the capillary loops one might ask why the bubbles do not form there, rather than on the outer side of the large gland cells. Unfortunately, because of the complexity of bubble formation, this cannot be taken as an indication of how the tension gradients run in relation to the epithelium.

TABLE 1

Composition of gas bubbles secreted under Saran film by the gas gland of codfish treated with yohimbine; sample 0.5 mm^3

FISH NO.	SAMPLE	% CO_2	% O_2	% N_2
I	1	8.6	81.1	10.3
	2	5.0	70.3	24.7
II	1	15.8	76.6	7.6
III	1	6.9	49.5	43.6
	2	6.8	61.1	32.1
	3	5.9	66.5	27.6
	4	13.9	30.1	56.0
IV	1	7.2	69.2	23.6
Average	—	8.8	63.1	28.1

Blood analyses in barracuda

A living barracuda was lashed to a V board and irrigated with water. The swimbladder was exposed, as described for the cod. Part of the gland was covered with a piece of

Saran film, through which the gas secretion could be clearly observed. Blood samples were taken directly from the gland vein with a fine, heparinized glass pipette, and were at once analyzed for oxygen content. In one large secreting barracuda enough blood could be collected from the gland vein to determine both oxygen content and capacity. For the latter the blood was rotated with air in a 5 cm³ vial, shielded against evaporation loss. Normal oxygen capacity was determined in blood obtained by heart puncture. Three independent series (IIIa, b, and c in table 2) were performed on this fish at intervals of about one hour. All samples were analyzed by a micro gasometric method (Scholander and van Dam, '56).

TABLE 2

Oxygen in blood from heart and secreting gas gland in three barracudas. Oxygen saturation is calculated by taking air-equilibrated heart blood as 100%

FISH NO.	GLAND BLOOD				HEART BLOOD			
	Content		Capacity		Content		Capacity	
	Vol. %	Sat.	Vol. %	Sat.	Vol. %	Sat.	Vol. %	Sat.
I	9.7	98%					9.9	100%
IIa	9.3	88%					10.6	100%
IIb	10.0	94%					10.6	100%
IIIa	11.9	92%	13.2	102%	5.9	46%	12.9	100%
IIIb	11.7	91%	13.2	102%	5.0	39%	12.9	100%
IIIc	10.9	89%	12.7	104%	5.0	41%	12.2	100%

With fishes II and III the set of determinations was repeated at intervals of approximately one hour, as long as the fish secreted. There is evidence of a slight anemia in IIIc.

The oxygen capacity of the barracuda blood was usually between 10 and 13 volume per cent. In table 2 the capacity of the heart blood has been set at 100%. Relative to this the blood leaving the secreting gland had an oxygen content averaging 92%. This is a very high figure, considering that the normal arterial saturation could hardly be expected to be more than perhaps 95%. The oxygen capacity of the blood leaving the gland was not lower than that of heart blood, but possibly slightly higher. The oxygen saturation of the heart blood was low, as would be expected, averaging 42%.

There are two striking points in these results: (1) that oxygen secretion took place with a hardly measurable A-V difference in the gland blood, and (2) that the blood leaving the gland had apparently lost none of its oxygen carrying capacity.

We know from oxygen[18] experiments on codfish that the oxygen secreted by the gland is derived directly from the dissolved oxygen in the sea water, and is hence transported to the gland via the blood stream (Scholander, van Dam, and Enns, '56). We would therefore feel safe in making the generalization that whenever oxygen is being secreted the gas gland must have a positive A-V difference. That this difference may be surprisingly low was evident from mere inspection of the *retes* in the barracuda. They are multiple in this species, and can readily be observed under a binocular. While secreting, they are hyperemic and of bright arterial color, but when there is no secretion they are poorly circulated and cyanotic. If CO_2 and fixed acids poured into the *rete* blood during secretion, the concentration in barracuda must have been quite low, since it did not visibly reduce the blood. Again, if fixed acid were the cause of oxygen secretion via the Bohr or Root effect, it would show up as a diminished oxygen capacity in the leaving blood, which however was not indicated by our analyses. Even in the codfish, with its high CO_2 tension in the secreted gas, it has not been conclusively demonstrated so far that there is a rise in lactic acid associated with the secretion (Fänge, '53). One might also mention here, for whatever it may be worth, that indicator paper placed on the mucus of the secreting gland in codfish gave a pH of 7 ± 0.2, and the same very trifling acidity was also found in a wreckfish caught near Bimini at a depth of 600 meters.

From theoretical considerations of the *rete* as a counter current exchange system, one may calculate that a very minute primary increment in the CO_2 tension at the glandular pole of the *rete* could easily be multiplied to tensions of such magnitude as are commonly found at this site. The swimbladder gas secreted by 4 deflated barracudas contained 3.6 to 5.2% CO_2, but nevertheless the blood which left the secreting gland had almost full arterial oxygen saturation. This strongly indicates a low CO_2 tension in the leaving blood. Such a tension drop along the *rete* is in accordance, of course, with the assumed function of this structure.

SUMMARY

Gas bubbles secreted under a Saran film by the intact gas gland of cod contained 5–16% CO_2 and 30–81% oxygen. The blood leaving the secreting gland of barracuda had an average oxygen saturation of 92%, i.e.; nearly arterial. Secretion in barracuda can therefore take place with a very low A-V difference. The *retes,* while secreting, were hyperemic and of bright arterial color, but cyanotic and poorly circulated when there was no secretion. There was no measurable loss in oxygen combining capacity of the blood leaving the active gland.

I wish to express my gratitude to Dr. C. M. Breder, Jr., of the American Museum of Natural History, for arranging my stay at Bimini, and to Mr. and Mrs. Michael Lerner for their help in getting barracuda alive. For assistance in the studies on barracuda, I am much indebted to Dr. L. A. Krumholz, of the Lerner Marine Laboratory, and to Mrs. Susan I. Scholander.

LITERATURE CITED

Fänge, R. 1953 The mechanisms of gas transport in the euphysoclist swimbladder. Acta Physiol. Scandinavica, vol. 30, suppl. 110, 133 pp.

Scholander, P. F., and L. van Dam 1956 Micro gasometric determination of oxygen in fish blood. J. Cell. and Comp. Physiol., *48:* 529–532.

Scholander, P. F., L. van Dam, and T. Enns 1956 The source of oxygen secreted into the swimbladder of cod. J. Cell. and Comp. Physiol., *48:* 517–522.

Scholander, P. F., and H. J. Evans 1947 Microanalysis of fractions of a cubic millimeter of gas. J. Biol. Chem., *169:* 551–560.

Contribution No. 88

Reprinted from the JOURNAL OF CELLULAR AND COMPARATIVE PHYSIOLOGY
Vol. 48, No. 3, December 1956

THE SOURCE OF OXYGEN SECRETED INTO THE SWIMBLADDER OF COD[1]

P. F. SCHOLANDER, L. VAN DAM AND THEODORE ENNS
Woods Hole Oceanographic Institution, and Department of Medicine, Johns Hopkins University

ONE FIGURE

In vitro studies of blood from several species of deep sea fish revealed that neither a high CO_2 tension nor a low pH could unload the oxygen from the hemoglobin against such high oxygen pressures (100–200 atmospheres) as are known to exist in the swimbladder (Scholander and van Dam, '54). This cast serious doubt on the theory that either the Bohr or the Root effect is the cause of the high oxygen pressures produced in live fish, and made it desirable to endeavor to find out what exactly is the source of the oxygen secreted into the swimbladder. We describe tracer experiments below, where codfish were induced to secrete oxygen while breathing oxygen^{18} dissolved in ordinary sea water. These experiments were designed to show whether the oxygen was derived directly from the molecular oxygen dissolved in the water, or whether it came from other sources.

APPARATUS AND MATERIAL

An experimental fish chamber was made from a 100 l metal container fitted with a window and coated on the inside with beeswax. Synthetic air could be recirculated through the chamber by means of a gear pump, which drove the air through a CO_2 absorber and down into a 15 cm long cloth hose which

---

[1] Contribution No. 881 from the Woods Hole Oceanographic Institution. This investigation was supported by a grant from the National Science Foundation.

acted as a bubbler for the fish tank. The gas returned to a 40 l spirometer, and from there back to the pump (fig. 1). By introducing some oxygen into the system while recirculating, it was established by gas analysis that a complete equilibration with the water phase took place within 20 minutes. Water containing > 1.4 atom per cent 0^{18} was obtained on allocation by the U. S. Atomic Energy Commission from the Stuart Oxygen Company, San Francisco. Oxygen^{18} labeled oxygen was produced by electrolysis of the water on platinum electrodes, with sulfuric acid added.

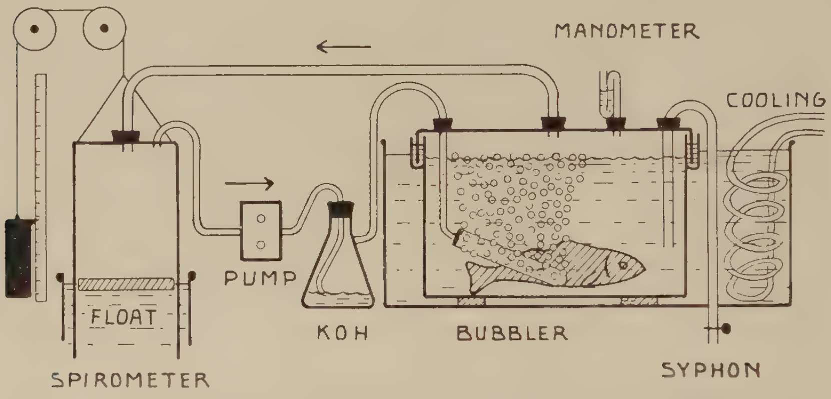

Fig. 1 Fish chamber and closed circuit arrangement for circulating oxygen^{18}.

Codfish *(Gadus callarias)* were used in these experiments, since they secrete oxygen relatively quickly. They were obtained through the courtesy of Mr. David F. Ryder, of Chatham, Massachusetts. In order to make them secrete while confined in the relatively cramped space of the fish chamber, it was necessary to administer yohimbine (Fänge, '53), in addition to deflating the swimbladder. In the course of 10 hours after a complete deflation they would then fill their swimbladders to almost normal buoyancy.

EXPERIMENTAL PROCEDURE

The spirometer was filled with 9.5 l of electrolyzed tagged oxygen and 30 l tank nitrogen. The fish tank was filled to the top with sea water, the apparatus closed, and recirculation continued for an hour, after which the circulation was stopped, all hoses were clamped, and the lid was opened.

Meanwhile the swimbladder gas had been removed from the codfish by puncture, and the traces of oxygen left were washed out with nitrogen, all of which was drawn out. Analysis of this gas showed that no more than 0.2–0.4 cm^3 of air oxygen remained in the bladder. Yohimbine was given intramuscularly (about 0.8 mg/kg), and the fish was slipped into the fish tank. All handling was done with the fish submerged or with its gills irrigated. Additional fish were prepared in the same way. The tank was closed and connected with the spirometer. Twenty liters of water were siphoned out of the tank to keep foam from spreading, and recirculation was started. The gas phase maintained an oxygen concentration between 20 and 21%, with CO_2 less than 0.1%. After a run of 10 hours, the now buoyant fishes were taken out. Gas was withdrawn from their swimbladders and stored in 20 cm^3 syringes, which had been lubricated with concentrated lithium chloride. Checks showed that the system was completely air tight, and that the dilution of the introduced O^{18} enriched oxygen checked exactly with the dilution calculated from the amount of normal oxygen which was added to the system by introducing the fish.

The isotope determinations were performed on a mass spectrometer at the Johns Hopkins University School of Medicine (Chinard and Enns, '54).

RESULTS

Table 1 shows the results of two experiments with deflated codfish treated with yohimbine. The amount of gas secreted by each fish was between 40 and 50 cm^3. Both carbon dioxide and oxygen concentrations are high, and correspond well with the composition of the gas which the gland itself secretes (Scholander, '56).

It will be seen from the almost identical figures for the $oxygen^{18}$ concentration in the gas phase of the water and in the swimbladder that the fish deposits only the molecular oxygen dissolved in the sea water into the swimbladder. No other source of any significance is involved. Consequently, we know now that the oxygen is picked up through the gills, and is transported by the hemoglobin to the *rete*-gland system of the swimbladder. It is then deposited into the swimbladder, sometimes against pressures of 100 atmospheres or more. There is no knowledge as to how such high pressures are attained. At the very low partial pressures of oxygen prevailing in our tracer experiments (less than one atmosphere) a Root effect, caused by 10–14% CO_2, would undoubtedly liberate oxygen from the red cells. But whether enough of this excess tension of CO_2 could be transmitted to the proximal end of the *rete* to effect an oxygen secretion is a question which must await experimental evidence (cp. Scholander, '54).

TABLE 1

Oxygen secretion in deflated codfish treated with yohimbine

Water temperature, 5°C. 0^{18} in air found as 0.204 atom %. Time, 10 hours

EXP. NO.	FISH NO.	CHAMBER GAS		SWIMBLADDER GAS			
		O_2	O^{18}	O_2	O^{18}	CO_2	CO_2
		vol. %	*atom %*	*vol. %*	*atom %*	*vol. %*	*atom % O^{18}*
I	1	21.0	1.13	78.0	1.12	10.0	
II	1	20.0	1.11; 1.10	44.8	1.15	14.2	0.44
	2			68.8	1.13	11.5	0.44
	3			69.3	1.14	11.3	0.37

Spectro photometry of the blood of several deep sea fishes indicated that the limiting dissociation pressure via excessive acidification of oxyhemoglobin was often less than 40–50 atmospheres, falling short by 2–5 times of the oxygen pressure which the gland produces. One is therefore led to assume that some additional process must be responsible for the ultimate step-up of the pressure. One may wonder whether the secreting cells covering the capillary loops of the gas gland can actively take molecular oxygen from the plasma and secrete it into the swimbladder. Some such arrangement may be responsible for the nitrogen and argon deposition (cp. Scholander, van Dam, and Enns, '56). Or it may be that some as yet undiscovered means exists for dissociating off oxygen from the hemoglobin to yield the very high pressures required, in which case the nitrogen secretion must be an entirely different process.

In the codfish oxygen secretion takes place accompanied by high CO_2 tensions (table 1). In many fishes this apparently is not so (cp. Scholander, '54). It can be seen from table 1 that the O^{18} atom fraction of CO_2 in the swimbladder was only about 0.4%, against 0.2% in air and 1.1% in the oxygen dissolved in the chamber water, i.e. only about one quarter of the CO_2 was labeled. The respiratory CO_2 formed in the fish during the experiment would be O^{18} labelled and would exchange with the large unlabeled bicarbonate pool in the fish and sea water. The accumulation of CO_2 in the swimbladder would therefore always involve both labeled and unlabeled CO_2 and it would be very difficult from the isotope ratio to conclude how the CO_2 was formed. Copeland ('52) and Fänge ('53) found that glycogen disappears from the gland during secretion and Ball, Strittmatter and Cooper ('55) found that gland tissue *in vitro* produces a rapid breakdown of glucose to lactic acid. It is therefore possible that the high CO_2 tension found in the swimbladder during secretion is caused by lactic acid production in the gland, but if so it must be very slight, inasmuch as Fänge ('53) failed to find it.

SUMMARY

Codfish treated with yohimbine after complete deflation were kept in ordinary sea water containing dissolved O^{18} labeled oxygen. In 10 hours the swimbladder filled with oxygen, all of which was labeled and was hence derived from the dissolved oxygen in the water. The *rete*-gland system accordingly transfers molecular oxygen from the blood into the swimbladder. There is at the present time no known mechanism which can account for the resultant extremely high pressures. Of the 10–14% CO_2 deposited with the oxygen, only one quarter was labeled. Possible causes of the elevated CO_2 tension are discussed.

We are greatly indebted to Dr. V. T. Bowen, of the Woods Hole Oceanographic Institution, for his help and advice.

LITERATURE CITED

Ball, E. G., C. F. Strittmatter and O. Cooper 1955 Metabolic studies on the gas gland of the swimbladder. Biol. Bull., *108:* 1–17.

Chinard, F. P., and T. Enns 1954 Relative rates of passage of deuterium and tritium oxides across capillary walls in the dog. Amer. Jour. Physiol., *178:* 203–205.

Copeland, D. E. 1952 The histophysiology of the teleostean physoclistous swimbladder. J. Cell. and Comp. Physiol., *40:* 317–334.

Fänge, R. 1953 The mechanisms of gas transport in the euphysoclist swimbladder. Acta Physiol. Scandinavica, vol. 30, suppl. 110, 133 pp.

Scholander, P. F. 1954 Secretion of gases against high pressures in the swimbladder of deep sea fishes. II. The *rete mirabile*. Biol. Bull., *107:* 260–277.

——— 1956 Observations on the gas gland in living fish. J. Cell. and Comp. Physiol., *48:* 523–528.

Scholander, P. F., and L. van Dam 1954 Secretion of gases against high pressures in the swimbladder of deep sea fishes. I. Oxygen dissociation in blood. Biol. Bull., *107:* 247–259.

Scholander, P. F., L. van Dam and T. Enns 1956 Nitrogen secretion in the swimbladder of whitefish. Science, *123:* 59–60.

Report for the year 1956

THE
WOODS HOLE OCEANOGRAPHIC INSTITUTION

REPORT FOR THE YEAR
1956

1957

TABLE OF CONTENTS

PAGE

I. Trustees, as of December 31, 1956 4

II. Members of the Corporation, as of December 31, 1956 . 5

III. Research Staff 7

IV. Director's Report 10

V. Treasurer's Report 26

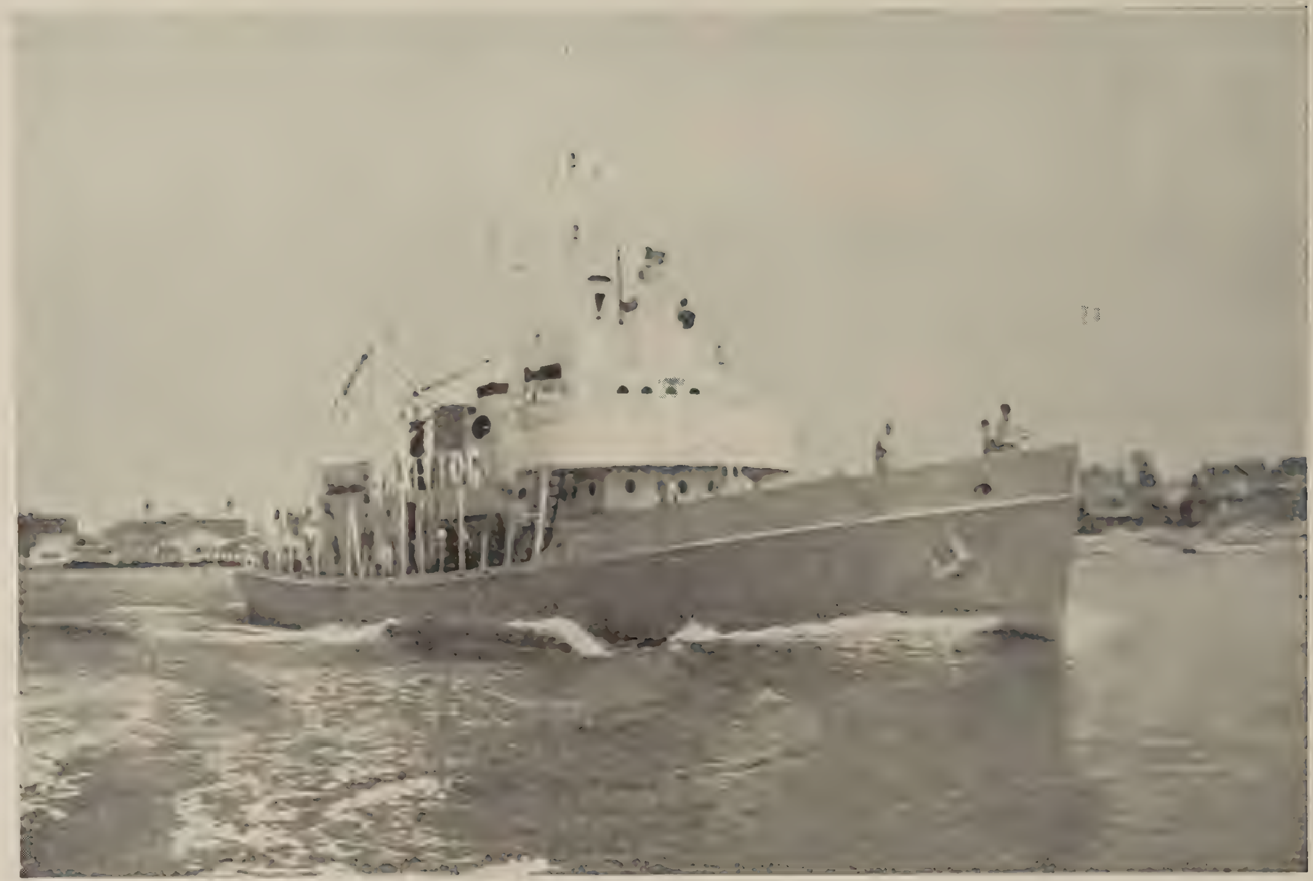

RESEARCH VESSEL "CRAWFORD"

I. TRUSTEES

(As of December 31, 1956)

Honorary Trustees

Henry B. Bigelow, Museum of Comparative Zoology, Cambridge 38, Mass.
L. O. Colbert, 4408 29th Street, N. W., Washington, D. C.
Marion Eppley, 510 Park Avenue, New York, N. Y.
Alexander Forbes, 610 Harland Street, Milton, Mass.
Lawrason Riggs, Riggs, Ferris and Geer, Room 1201, 74 Trinity Place, New York 6. N. Y.
Henry L. Shattuck, 10 Milk Street, Boston, Mass.

To serve until 1960

Detlev W. Bronk, The Rockefeller Institute of Medical Research, 66th Street and York Avenue, New York 21, N. Y.
Noel B. McLean, Edo Corporation, College Point 56, New York
Daniel Merriman, Bingham Oceanographic Laboratory, Yale University, New Haven, Conn.
Emanuel R. Piore, Avco Manufacturing Company, 420 Lexington Avenue, New York, N. Y.
Alfred C. Redfield, Woods Hole, Mass.
Gerard Swope, Jr., c/o International General Electric Co., 570 Lexington Avenue, New York, N. Y.

To serve until 1959

J. S. Coles, Bowdoin College, Brunswick, Maine
Carl H. Eckart, Scripps Institution of Oceanography, La Jolla, Calif.
Ross G. Harrison, Osborn Zoological Laboratory, Yale University, New Haven, Conn.
Milford R. Lawrence, Siders Pond Road, Falmouth, Mass.
Harlow Shapley, Sharon Cross Road, Peterborough, N. H.
Francis C. Welch, 73 Tremont Street, Boston, Mass.

To serve until 1958

Charles Francis Adams, Raytheon Manufacturing Company, 138 River Street, Waltham 54, Mass.
Horace S. Ford, 77 Massachusetts Avenue, Cambridge 39, Mass.
Arnaud C. Marts, 521 Fifth Avenue, New York, N. Y.
Albert E. Parr, American Museum of Natural History, Central Park West at 79th Street, New York, N. Y.
Athelstan F. Spilhaus, Institute of Technology, University of Minnesota, Minneapolis 14, Minnesota
Selman A. Waksman, Institute of Microbiology, Rutgers University, New Brunswick, N. J.
Eric G. Ball, Department of Biological Chemistry, Harvard Medical School, Boston, Mass.
Frank A. Howard, 30 Rockefeller Plaza, New York, N. Y.
Carl-G. Rossby, Woods Hole Oceanographic Institution, Woods Hole, Mass.
Edward H. Smith, Woods Hole, Mass.
Raymond Stevens, c/o Arthur D. Little, Inc., 30 Memorial Drive, Cambridge 42, Mass.
E. Bright Wilson, Jr., Department of Chemistry, Harvard University, Cambridge 38, Mass.

Ex Officio

Edwin D. Brooks, Jr., P. O. Box 1135, Boston 3, Mass.
Mary Sears, Woods Hole Oceanographic Institution, Woods Hole, Mass.
Columbus O'D. Iselin, Woods Hole Oceanographic Institution, Woods Hole, Mass.

Officers

Raymond Stevens, President of the Corporation, c/o Arthur D. Little, Inc., 30 Memorial Drive, Cambridge 42, Mass.
Henry B. Bigelow, Chairman of the Board of Trustees, Museum of Comparative Zoology, Cambridge 38, Mass.
Edwin D. Brooks, Jr., Treasurer, P. O. Box 1135, Boston 3, Mass.
Mary Sears, Clerk of the Corporation, Woods Hole Oceanographic Institution, Woods Hole, Mass.

II. MEMBERS OF THE CORPORATION

Charles Francis Adams, Raytheon Manufacturing Company, 138 River Street, Waltham, 54, Mass.
Oliver Ames III, North Easton, Mass.
Philip Armstrong, Medical Center of Syracuse, State University of New York, Syracuse, N. Y.
Eric G. Ball, Harvard Medical School, Shattuck Street, Boston, Mass.
Henry B. Bigelow, Museum of Comparative Zoology, Cambridge 38, Mass.
Lindsay Bradford, 215 East 72nd Street, New York, N. Y.
Detlev W. Bronk, The Rockefeller Institute of Medical Research, 66th Street and York Avenue, New York 21, N. Y.
Edwin D. Brooks, Jr., P. O. Box 1135, Boston 3, Mass.
C. Lloyd Claff, Single Cell Research Foundation, Inc., 5 Van Beal Road, Randolph, Mass.
L. O. Colbert, 4408 29th Street, N. W., Washington, D. C.
Kenneth S. Cole, National Institute of Health, Bethesda 14, Md.
J. S. Coles, Bowdoin College, Brunswick, Maine
Henry B. DuPont, E. I. duPont de Nemours & Company, Wilmington 98, Delaware
Ferdinand Eberstadt, 39 Broadway, New York 6, N. Y.
Carl H. Eckart, Scripps Institution of Oceanography, La Jolla, Calif.
Harrison P. Eddy, c/o Metcalf & Eddy, 1300 Statler Building, Boston, Mass.
Marion Eppley, 510 Park Avenue, New York, N. Y.
Alexander Forbes, 610 Harland Street, Milton, Mass.
Horace S. Ford, 77 Massachusetts Avenue, Cambridge, Mass.
John A. Gifford, 14 Wall Street, New York 5, N. Y.
Ross G. Harrison, Osborn Zoological Laboratory, Yale University, New Haven, Conn.
Hudson Hoagland, Worcester Foundation for Experimental Biology, 222 Maple Avenue, Shrewsbury, Mass.
Frank A. Howard, 30 Rockefeller Plaza, New York, N. Y.
Columbus O'D Iselin, Woods Hole Oceanographic Institution, Woods Hole, Mass.
Augustus B. Kinzel, Union Carbide and Carbon Corporation, 30 East 42nd Street, New York 17, N. Y.
Milford R. Lawrence, Siders Pond Road, Falmouth, Mass.
Lamar R. Leahy, 910 Park Avenue, New York, N. Y.
Alfred L. Loomis, Room 2420, 14 Wall Street, New York, N. Y.
Arnaud C. Marts, 521 Fifth Avenue, New York, N. Y.
Robert E. McConnell, 230 Park Avenue, New York, N. Y.
Noel B. McLean, Edo Corporation, College Point 56, N. Y.
Daniel Merriman, Bingham Oceanographic Laboratory, Yale University, New Haven, Conn.
Henry S. Morgan, 2 Wall Street, New York, N. Y.
Frank A. Pace, General Dynamics Corporation, 445 Park Avenue, New York 22, N. Y.
Albert E. Parr, American Museum of Natural History, Central Park West at 79th Street, New York, N. Y.
Emanuel R. Piore, Avco Manufacturing Co., 420 Lexington Avenue, New York N. Y.
Alfred C. Redfield, Woods Hole, Mass.
Lawrason Riggs, Riggs, Ferris and Geer, Room 1201, 74 Trinity Place, New York 6, N. Y.
George H. Richards, 68 William Street, New York, N. Y.
Carl-G. Rossby, Woods Hole Oceanographic Institution, Woods Hole, Mass.

Francis C. Ryder, Massachusetts Institute of Technology, Cambridge 39, Mass.
Mary Sears, Woods Hole Oceanographic Institution, Woods Hole, Mass.
Athelstan F. Spilhaus, Institute of Technology, University of Minnesota, Minneapolis 14, Minn.
Lyman Spitzer, Jr., Princeton University Observatory, 14 Prospect Avenue, Princeton, N. J.
Harlow Shapley, Sharon Cross Road, Peterborough, N. H.
Henry L. Shattuck, 10 Milk Street, Boston, Mass.
Edward H. Smith, Woods Hole, Mass.
Raymond Stevens, c/o Arthur D. Little Inc., 30 Memorial Drive, Cambridge 42, Mass.
Julius A. Stratton, Massachusetts Institute of Technology, Cambridge 39, Mass.
Gerard Swope, Jr., c/o International General Electric Co., 570 Lexington Avenue, New York, N. Y.
J. H. Van Vleck, Lyman 332, Harvard University, Cambridge 38, Mass.
Selman A. Waksman, Institute of Microbiology, New Brunswick, N. J.
Thomas J. Watson, Jr., International Business Machines Corporation, 590 Madison Avenue, New York 22, N. Y.
Francis C. Welch, 73 Tremont Street, Boston, Mass.
E. Bright Wilson, Jr., Department of Chemistry, Harvard University, Cambridge 38, Mass.

III. RESEARCH STAFF

(As of December 31, 1956)

Arnold B. Arons, Professor of Physics, Amherst College; Associate in Physical Oceanography.

William D. Athearn, Research Associate in Geology.

John C. Ayers, Associate Professor, Great Lakes Research Institute, and Associate Professor of Zoology, Department of Zoology, University of Michigan; Associate in Marine Biology.

Richard H. Backus, Research Associate in Marine Biology.

Lincoln Baxter II, Research Associate in Electronics.

David L. Belding, Professor of Bacteriology and Experimental Pathology (Emeritus), Boston University; Consultant, U. S. Fish and Wildlife Service; Associate in Marine Biology.

Henry B. Bigelow, Professor of Zoology (Emeritus), Harvard University; Research Oceanographer, Museum of Comparative Zoology; Associate in Oceanography.

Duncan C. Blanchard, Research Associate in Meteorology.

Vaughan T. Bowen, Lecturer in Zoology, Yale University; Geochemist.

Robert R. Brockhurst, Research Associate in Physics.

John G. Bruce, Jr., Research Associate in Physics.

Dean F. Bumpus, Oceanographer.

Elizabeth T. Bunce, Research Associate in Physics.

Andrew F. Bunker, Meteorologist.

Cornelia L. Carey, Associate Professor in Botany (retired), Barnard College; Associate in Marine Bacteriology.

Charles E. Carver, Jr., Research Associate in Hydraulics.

Joseph Chase, Research Associate in Meteorology.

George L. Clarke, Associate Professor of Zoology, Harvard University; Marine Biologist.

L. A. Earlston Doe, Associate in Physical Oceanography.

Willard Dow, Electronics Engineer.

Maurice Ewing, Professor of Geology, Columbia University; Director, Lamont Geological Observatory; Associate in Geophysics.

Alan J. Faller, Research Associate in Meteorology.

Harlow G. Farmer, Jr., Research Associate in Hydraulics.

Charles J. Fish, Professor of Marine Biology, University of Rhode Island; Director, Narragansett Marine Laboratory; Associate in Marine Biology.

David H. Frantz, Jr., Research Associate in Engineering.

Frederick C. Fuglister, Physical Oceanographer.

Robert H. Gibbs, Jr., Research Associate in Marine Biology.

Bernhard Haurwitz, Professor of Meteorology and Chairman of the Department of Meteorology and Oceanography, New York University; Associate in Meteorology.

John B. Hersey, Geophysicist.

Edward M. Hulburt, Research Associate in Marine Biology.

Louis W. Hutchins, Associate in Marine Biology.

Laurence Irving, Biologist, Arctic Health Research Center; Associate in Physiology.

Columbus O'D. Iselin, Associate Professor of Physical Oceanography, Harvard University and Research Oceanographer, Museum of Comparative Zoology; Senior Oceanographer.

Henry R. Johnson, Research Associate in Underwater Acoustics.

John W. Kanwisher, Research Associate in Biophysics.

Bostwick H. Ketchum, Senior Oceanographer.

Sydney T. Knott, Jr., Research Associate in Engineering.

Bernhard Kummel, Associate Professor of Geology, Harvard University; Associate in Submarine Geology.

Benjamin B. Leavitt, Associate Professor of Biological Sciences, University of Florida; Associate in Marine Biology.

Robert A. Lufburrow, Research Associate in Physics.

Joanne S. Malkus, Meteorologist.

Willem V. R. Malkus, Physical Oceanographer.

Wilbur Marks, David Taylor Model Basin; Research Associate in Physical Oceanography.

Frank J. Mather III, Research Associate in Oceanography.

William G. Metcalf, Research Associate in Physical Oceanography.

Arthur R. Miller, Research Associate in Physical Oceanography.

Raymond B. Montgomery, Associate Professor of Oceanography, Chesapeake Bay Institute, Johns Hopkins University; Associate in Physical Oceanography.

Hilary B. Moore, Professor in Marine Biology and Assistant Director, Marine Laboratory, University of Miami; Associate in Marine Biology.

James M. Moulton, Assistant Professor of Biology, Bowdoin College; Associate in Marine Biology.

Jerome Namias, Chief, Extended Forecast Section, U. S. Weather Bureau; Associate in Meteorology.

Daniel R. Norton, Research Chemist, Sprague Electric Company, North Adams, Mass.; Associate in Chemical Oceanography.

Charles B. Officer, Jr., Associate Professor of Geology, Rice Institute; Geophysicist.

David M. Owen, Research Associate in Underwater Photography.

Mary Alys Plunkett, Associate Professor of Chemistry, Vassar College; Associate in Chemistry.

Roy L. Rather, Jr., Associate in Underwater Acoustics.

Alfred C. Redfield, Professor of Physiology, Harvard University; Senior Oceanographer.

Charles E. Renn, Professor of Sanitary Engineering, School of Engineering, Johns Hopkins University; Associate in Engineering.

Francis A. Richards, Chemical Oceanographer.

William S. Richardson, Physical Chemist.

Gordon A. Riley, Associate Director, Bingham Oceanographic Laboratory, Yale University; Associate in Marine Biology.

Helen M. Roberts, Assistant Professor of Mathematics, University of Connecticut; Associate in Mathematics.

F. Claude Ronne, Research Associate in Photography.

Carl-G. Rossby, Director, Institute of Meteorology, University of Stockholm, Meterorologist.

John H. Ryther, Marine Biologist.

Howard L. Sanders, Research Associate in Marine Biology.

Harold E. Sawyer, Research Engineer.

Marshall Schalk, Associate Professor of Geology and Geography, Smith College; Associate in Geology.

Irving I. Schell, Research Associate Department of Geology, Tufts University; Associate in Meteorology.

William E. Schevill, Research Associate in Zoology, Museum of Comparative Zoology; Associate in Oceanography.

Karl E. Schleicher, Research Associate in Physics.

Per F. Scholander, Professor of Physiology, University of Oslo; Director, Institute of Zoophysiology; Associate in Physiology.

William C. Schroeder, Associate Curator of Fishes, Museum of Comparative Zoology, Harvard University; Ichthyologist.

George T. Scott, Professor of Zoology, Oberlin College; Associate in Physiology.

Mary Sears, Planktonologist.

Herbert Small, Research Associate in Electronics.

Paul Ferris Smith, Electronics Engineer, Rockefeller Institute for Medical Research; Associate in Physical Oceanography.

Floyd M. Soule, Oceanographer, U. S. Coast Guard; Associate in Physical Oceanography.

Allard, T. Spencer, Research Associate in Engineering.

Athelstan F. Spilhaus, Dean, Institute of Technology, University of Minnesota; Associate in Physical Oceanography.

Henry M. Stommel, Physical Oceanographer.

Thomas T. Sugihara, Assistant Professor of Chemistry, Clark University; Associate in Geochemistry.

Parker D. Trask, Professor of Geological Engineering, University of California; Associate in Submarine Geology.

Harry J. Turner, Jr., Lecturer in Zoology, University of New Hampshire; Marine Biologist.

Ralph F. Vaccaro, Research Associate in Microbiology.

George Veronis, Research Associate in Mathematics.

Allyn C. Vine, Physical Oceanographer.

William S. von Arx, Physical Oceanographer.

Robert G. Walden, Research Associate in Electronics.

Edmond E. Watson, Professor of Physics, Queen's University, Kingston, Ontario; Associate in Physical Oceanography.

Raymond Wexler, Meteorologist.

Geoffrey G. Whitney, Jr., Research Associate in Physical Oceanography.

Alfred H. Woodcock, Oceanographer.

George P. Woollard, Professor of Engineering Geology and Geophysics, University of Wisconsin; Associate in Geophysics.

L. Valentine Worthington, Research Associate in Physical Oceanography.

John M. Zeigler, Research Associate in Marine Geology.

ADMINISTRATIVE STAFF

Columbus O'D. Iselin	Director
Alfred C. Redfield	Associate Director
Richard G. Leahy	Assistant to the Director
Ronald A. Veeder	Assistant to the Director
John McGilvray	Bsuiness Manager
Jan Hahn	Public Information
Norman T. Allen	Administrator
Harvey MacKillop	Controller
John F. Pike	Port Captain
Delmar R. Jenkins	Purchasing Agent
Otis E. Hunt	Laboratory Services

IV. DIRECTOR'S REPORT

Introduction

In his report to the Trustees in August the retiring director, Admiral Edward H. Smith, stressed the following accomplishments of the past year: a considerable increase in the number of papers published; the acquisition and reconditioning of the 125-foot diesel-powered Crawford which marked a major investment in research vessels comparable to the building of the Atlantis 25 years ago; and the strengthening of the educational character of the Institution through an increased budget for lectureships, seminars, and fellowships. To this I would only like to add that we have also gradually become aware of the great importance of the future of oceanography of the International Geophysical Year. In fact, this was the main reason why I reluctantly agreed to resume temporarily the administrative responsibility for our research program.

While field observations will not officially start until July 1957, much effort has been devoted to planning and to preparatory observations during 1956. At this writing it is evident that with more than 60 vessels from 23 nations taking part, the International Geophysical Year could indeed become a milestone in oceanography.

When this major event in the earth sciences was first announced, most members of our staff, including myself, were not very enthusiastic. Individual researchers are more interested in short-term progress than in programs that will require the passage of several 25-year periods before the main objectives can bear much fruit. Why should we interrupt our present program to help gain a worldwide set of observations in the hope that 25 years from now a repeated survey will be possible? Surely by then interests and problems in oceanography will have very much changed. Can we today plan so large an operation and hope that the next generation of oceanographers will think that our objectives were wisely conceived.

Only gradually during the past year have most of us begun to realize that 25 years from now the Institution and the science of oceanography will still be in their infancy, and that we owe it to the future to help gain information on the long-period changes in geophysical phenomena. Furthermore, we have been slow to grasp what could be accomplished in the near future through real international cooperation in oceanography. During the past year it has finally become clear that the prospects are indeed exciting.

The following account of our activities during 1956 is about half taken from the report of Admiral Smith, which he prepared for the Annual Meeting of the Trustees in August. To this basic material, to which Dr. Alfred C. Redfield and I had also contributed, I have merely added some new paragraphs to make the account more or less complete to the end of the calendar year.

It cannot be overemphasized how much the whole staff regrets the decisions of both Admiral Smith and Dr. Redfield to retire from full-time participation in the affairs of the Institution. As Trustees the help of both will continue to be available to us, but we will all miss their wise counsel on a day-by-day basis.

Research

So far as physical oceanography and submarine geology are concerned there are not many new achievements to be reported since the last printed Annual Report. This does not mean that we have been idle, either in the field or in the laboratory. In general we have been casting around for new leads, digesting old data, and preparing the instrumentation for new assaults.

Dr. J. B. Hersey and his many co-workers were at sea during most of the winter. The ATLANTIS and the BEAR were much assisted by the PBY plane under the vigorous direction of Dr. William Richardson and Dr. Joanne Malkus. Thus, marine meteorology and underwater acoustics achieved a sort of marriage during the winter months in the Caribbean area. What emerged from this rather major effort is provocative but inconclusive. So far as the airplane is concerned it would "see" many "hot" streaks on the sea surface and nearly always the formation of cumulus clouds could be associated with the existence of these streaks or patches of slightly warmer water with sharp thermal boundaries. The vessels were able to show that these abrupt changes in surface temperature extended downward 100 feet or more, but neither ship nor airplane was able to map the full three-dimensional characteristics of these slight thermal boundaries. The net result is that on a microthermal scale the wind-stirred surface layer of the winter sea in the subtropics has much more structure than we had supposed and that the warmer patches may be the real thermal "roots" of the clouds. However, the finer points of these processes that might lead to a better understanding of the exchange of energy between the ocean and the atmosphere remain obscure. It is evident that towing strings of sensitive thermistors from a ship, which is advised about surface temperature distributions by a plane, can be profitable, but we can only conclude for the moment that the surface layer of the sea is much more complicated than we thought it was and that no doubt this complexity plays a part in near-surface sound transmission. Such is the inevitable outcome of advances in measuring techniques. We have been several years in achieving these advances.

Many people have contributed to these refinements in temperature measuring techniques. The sea surface radiation recorder in the PBY has been steadily improved by Dr. Richardson and his group. The basic means of towing a string of thermistors from a ship has stemmed from the work of Mr. A. C. Vine. The underwater equipment is still rather crude and difficult to handle, but the rig is more sensitive by a whole order of magnitude than a bathythermograph. Additional equipment is being prepared for our other vessels.

Dr. Hersey and his assistants again took advantage of the voyage home in the spring from the West Indies to engage in seismic refraction observations over and along the margins of the Blake Plateau. Several long cores of the bottom sediments were also obtained. This is the third geophysical attack on the Blake Plateau. In time we will be able to report substantial advances in the understanding of the deep geology of the area.

Another strong team of students in geology and geophysics cruised in the Caribbean area during the early summer under the leadership of Dr. Charles B. Officer and Dr. John Ewing.

In preparation for the summer cruises of the CRAWFORD in the northern equatorial current Mr. F. C. Fuglister made a thorough review of the accumulated temperature measurements at the 100-meter level. Not only are the data entirely inadequate when subdivided on a monthly basis, but it is even difficult to show changes in the current pattern between winter and summer. The fact that so few vessels have visited the area during the summer months is strong justification for the recent operations of the CRAWFORD, even if no problems concerning hurricanes existed.

After many thousands of miles of cruising and after overcoming a considerable number of minor mechanical and electrical difficulties, during October in the central Caribbean the crew of the CRAWFORD finally witnessed the early stages of the development of a hurricane. The upper air observations were successful because the winds were light and the sea calm, but we have still to work out a satisfactory means of observing the winds aloft under more normal sea conditions.

Mr. L. V. Worthington, Mr. W. G. Metcalf, and Mr. David H. Frantz made a cruise during the early spring on the CARYN to the northern Caribbean. They were unsuccessful in establishing the sill depth of the Windward Passage due to rough weather, but other objectives of the cruise were fully achieved. An especially fine hydrographic section across the Yucatan Channel was secured. On the way home the axis of the Gulf Stream was followed from the Florida Staits to a point south of Woods Hole.

During the late autumn months in the ATLANTIS Mr. Worthington and his most skillful assistants accomplished the impossible; namely, a complete north-south profile of temperature, salinity, and dissolved oxygen from the Grand Banks to the equator. At all 56 stations observations were successful down to within a few meters of the bottom. It has taken many years of patient effort to learn how to do this and we are now confident that we can carry out our share of gathering similar very deep observations over even wider areas during the International Geophysical Year.

During the autumn months also we benefited greatly through the extended visits of Professor Georg Wüst and Dr. C. -G. Rossby. The former gave us a notable series of lectures on the circulation of the South Atlantic as deduced from the classical survey of the METEOR and the latter, as always, greatly stimulated our efforts to develop more satisfactory mathematical models of oceanic circulations.

As far as new instrumentation is concerned, the importance of two different lines of development has been fully demonstrated. The two new salinity bridges designed and constructed by Mr. Alvin L. Bradshaw and Mr. Karl E. Schleicher have been at sea enough to demonstrate not only that salinities can be determined by one man on shipboard as rapidly as the samples are collected, but also an accuracy of approximately one more decimal place can be maintained. The new radio-telemetering drift buoys, developed by Mr. Robert G. Walden and Mr. David H. Frantz, have been given a thorough trial in the Gulf of Maine under the energetic leadership of Mr. Dean F. Bumpus. They survived and functioned well during late autumn weather in the Bay of Fundy. They could be relocated frequently, either from a vessel or a plane. It is clear that such equipment can greatly aid in the solution of the many baffling problems of coastal currents. Basically we have achieved a practical "drift bottle" whose movements can be followed on a day-to-day basis, and which can be set out in sufficient number to reveal quite small-scale patterns in the horizontal water movements.

Work in the new hydraulics laboratory has been pursued vigorously by Mr. Allan J. Faller and Dr. W. S. von Arx. Unfortunately the very ingenious drive for the large rotating basin has to some extent lost one of its best features due to a slow sinking of the westerly end of the building. The loss of fill through the bulkhead seems to be a slow, continuous process. To correct this situation will be expensive and in any case would greatly delay the results. Dr. von Arx is carrying on as best he can until it becomes more evident how best to correct the situation. As account of this experimental program follows.

Reconstruction of the torsion balance for the measurement of wind stress on smooth water surfaces is well along toward completion. The revised apparatus consists of an annular trough 10 cm. wide and of 1-meter mean radius, over which a succession of hexagonal cells (louvers for fluorescent lighting fixtures) are supported, with 2 mm. clearance, by cars and motor-truck assembles for model electric trains running on a circular track. The model train drive permits the tangential velocity of the cells to reach 1 meter per second. The entire apparatus will be enclosed in a pliofilm envelope so that the effects of different mixing ratios and temperature contrast across the air-water interface can be studied. Miss Betty Ann Morse spent the summer months running this apparatus.

In addition to the evaluation runs performed to determine the stability and suitability of the 4-meter main tank and its accessories, three preliminary experiments have been completed which are directed toward a study of the ocean circulation. These have involved the circulation within generalized ocean compartments separated by four meridional barriers forming apex angles of 30, 60, 90, and 180°, respectively. The experiments have concerned the barotropic mode of motion under the influence of a monotonic wind field and that occurring with the addition of trade winds. This change amounts to an increase in the wind curl which was adjusted to be maximum at latitude 30°. The experiments differed in the manner in which the tracers were introduced. It was found that detailed motions could be traced by simply allowing droplets of dye to fall into the model at rates of between 1 and 5 per second at each of four latitudes equatorward of the latitude of maximum wind curl. A magenta color produced by potassium permanganate solution and a blue color produced by fountain pen ink were introduced in alternate rings so that the streamlines produced after the droplets had lost their identity could be traced throughout an entire circuit of the circulation in each compartment.

The relationships were discerned; namely, that the velocity of motion in the zone of westward intensification was proportional to the apex angle of the compartment, that the westward intensified circulation separated from the coast line poleward of the latitude of maximum wind curl at a latitude inversely related to the apex angle, and that for the first time countercurrents were produced along the seaward margin of the westward intensified currents. These experiments were interesting in one other respect in that the water moving eastward from countercurrents neighboring the zone of westward intensification developed waves which apparently remained nearly fixed in longitude but increased in amplitude as time passed. The motions of and within these waves are so slow that special experiments will be necessary to determine their exact behavior and identity, (for example, are they Rossby waves?).

During the autumn work began on preparing the large tank for studies of the circulation of the southern hemisphere oceans. Since during the International Geophysical Year for the first time many vessels will be operating south of the equator, these tank experiments could become an important aid in the analysis of the field observations.

The initial atmospheric experiments have largely been directed toward evaluation of the symmetric heating and cooling mechanisms, their calibrations, and qualitative results. Of particular significance is the determination that the heating by radiation is independent of the temperature of the water and of the circulation. This is because the net radiative transfer is governed principally by the temperature of the spot lamps and at normal temperatures a variation of the temperature of the copper plate produces an insignificant variation of the back radiation. However, the correction for conduction to the air cannot be neglected.

Another preliminary result of significance is that the two methods of cooling by the flush cold source and by evaporation lead to fundamentally different patterns of circulation. The former produces a stratification with relatively strong zonal winds resembling a wintertime circulation, and the latter results in a less stable vertical profile with weak meridional temperature gradients and a correspondingly weak zonal circulation.

Although the resistance wire temperature elements have proven satisfactory for gross measurements of the zonally averaged temperature distribution, the maximum sensitivity of the elements has not been utilized because of apparent changes of calibration during the course of an experiment. The cause of this difficulty is as yet undetermined but is being systematically investigated. An accuracy of better than 0.1 °C should be possible.

A program of investigation will be systematically carried out to study the following:

(*a*) The response of the model atmosphere to varied distributions of zonally symmetric heating and cooling.

(*b*) The response of the model to slowly and rapidly varying heat sources and sinks resembling seasonal variation.

(*c*) Particular attention will be paid to the presence or absence of index cycle phenomena and the response of the system to small changes in the applied energy distribution.

(*d*) Comparisons will be made between the atmosphere and the model to point out regions of similarity and essential differences in the physical make-up of the two systems, in the application of the energy sources and sinks, and in the resulting circulations.

In addition to the principal efforts mentioned above there are two byproducts. First, in connection with his course work at the Massachusetts Institute of Technology, Mr. Faller conducted an experimental study of the heights of surface wavelets determined through an analysis of the absorption of light in a dyed liquid illuminated from below. The method seems capable of high precision provided the efforts of refraction and the added path length due to the obliquity of marginal rays can be kept small. Secondly, it seemed expedient to assist the hurricane reconnaissance program to be undertaken by the CRAWFORD by applying the wide-field photographic techniques to the problems of cloud development photography and apparatus for automatic weather registration from shipboard. The optical system of the latter permits a camera to photograph through a zenith angle of 120° thereby recording the appearance of the whole sky and of the sea surface to a level 30° below the horizon and at the same time to include in the field of view a clock, aneroid barometer, compass, wet and dry bulb thermometers, and a wind speed indicator. The apparatus is turned on and off each day by the rising and setting of the sun and the record of one week's daytime weather is recorded on about 100 feet of 16 mm. film.

The development of atomic energy has raised new problems for the oceanographer. These problems include the present effects of weapons testing programs, and the possible future effects of the accidental or intentional discharge of atomic wastes into the oceans. Dr. B. H. Ketchum and Mr. Allyn C. Vine served as members of a committee of the National Academy of Sciences to consider the effects of atomic radiations on oceanography and fisheries. Among the conclusions of the committee was that studies of the biological and geochemical processes which would affect the distribution of radioisotopes are imperative; that studies of the age, degree of isolation and rate of exchange of water masses, especially in the deeper regions of the sea, should be accelerated; and that the use of radioisotopes to study problems of mixing and exchange, the biological productivity and transfer of materials in the sea should be encouraged. Several members of our staff are conducting research which will provide the basic information essential to the solution of these problems.

Drs. B. H. Ketchum and V. T. Bowen have received a grant from the Atomic Energy Commission to study the biology and chemistry of coastal plankton populations. The program will permit the coordination of interests in the coastal circulation, in the productivity and development of the planktonic populations, in the biochemical cycles of nutrients, and in the chemical exchanges between the water and the bottom deposits. Drs. Sears, Ryther, and Richards will participate in the investigation. Mr. Vaccaro and Mr. Yentsch who are working under National Science Foundation grants will have increased opportunities to conduct their work at sea.

From data published by the Atomic Energy Commission one can estimate for several long-lived radioisotopes the amounts delivered to unit areas of sea surface as fallout following the various atomic tests. It is established that the strontium and cesium fallout are in soluble form and it seems most probable that this is also true for antimony. Thus there are radioactive tracers whose distributions in the sea can give invaluable information on the vertical movements of surface waters. Since differences in the rates of movement of the tracers can be produced only by differences in the sea-water chemistry of the pertinent elements, comparisons of their vertical distributions would also give information on their chemistry. Dr. Bowen and Dr. Sugihara have been developing methods for the determination of these long-lived radioactive fission products in the sea. Determinations of strontium 90 in several surface water samples have been made; a method for the measurement of cesium 137 is being developed; and work will shortly start on cerium 144 and on antimony 125.

The physiology of marine plants is being actively studied, aided in great part by the use of radioactive tracers. Dr. John H. Ryther has continued his investigations on the discrepancy between the rates of photosynthesis obtained by measuring oxygen production and C^{14} assimilation. He has discovered the physiological basis for this difference and has shown that the C^{14} method alone cannot be used to determine the productivity of sea water.

These technical advances have enabled Dr. Ryther to define more exactly than heretofore the relation between light intensity and photosynthesis for a number of marine phytoplankton species. In collaboration with Mr. Charles S. Yentsch, Dr. Ryther has also made a study of the relationship between photosynthesis and the chlorophyll content of the phytoplankton. From the interrelationships of chlorophyll, light, and photosynthesis, a practical and reliable method has been developed for estimating productivity of the open sea.

Dr. Joyce C. Lewin is studying the physiology of silica deposition in the diatom skeleton. With Dr. Bowen, she is investigating further the organic phosphorus produced by marine algae.

The study of the distribution of deuterium in the ocean, in which the Institution has been collaborating for several years with Dr. Irving Friedman of the U. S. Geological Survey, is now bearing fruit. This heavy isotope of hydrogen promises to provide a tracer for the movement of water in its worldwide cycle. It has been found that the deep water of the Atlantic, from the Arctic Basin to the Antarctic Continent, is practically uniform in deuterium content, which is apparently determined by equilibrium with atmospheric moisture at the sites of deep-water formation in high latitudes. The surface waters of the Atlantic in mid-latitude are enriched in deuterium as the result of the excess evaporation in these regions; while in the Arctic Basin and along the coasts the deuterium concentration is reduced by the dilution of sea water with runoff from the land, which is characteristically of low deuterium content.

These findings appear to explain in a reasonable way the general distribution of deuterium in the ocean. Two discoveries are, however, of special interest. The first is that the melt-water of sea ice is high in deuterium compared to that from atmospheric precipitation. It is thus possible in polar regions to determine whether the sea water is being diluted by melting ice or the products of atmospheric precipitation. The second is that the deep water of the Caribbean Sea and the Gulf of Mexico contains less deuterium than the supposed source waters from the Atlantic. This observation may have critical value in connection with the origin of the Caribbean water, concerning which Mr. Worthington has recently raised some provocative questions.

Dr. Francis A. Richards and Mr. Ralph Vaccaro have published an account of the preliminary study of the water in the Cariaco Trench. This is a deep basin on the continental shelf of northern Venezuela, in which the deep water appears to be isolated from the surface and from the surrounding deeps for at least 100 years. Their paper extends our knowledge of the biochemistry of the deep sea, especially as it is affected by the decomposition of organic matter sinking from the surface. Perhaps more important are the problems which remain to be examined in this isolated basin. These relate to rate of circulation of deep water, the determination of heat flux in the deeper layers of the continental sea bottom, and the chemistry of sediments laid down in deep anerobic waters. The latter problem is already under attack by Dr. Mary Alys Plunkett.

Dr. Richards has recently prepared several interesting reviews of aspects of chemical oceanography which are not adequately covered by recent publications. One of these serves to emphasize the totally inadequate knowledge which exists of the minor elements in truly representative ocean water. A second is a re-examination of the saturation of the ocean surface with oxygen, required by new determination of the solubility of oxygen in sea water. With Mr. Ralph Vaccaro, Dr. Richards is developing a much needed improvement on the methods for the determination of the nitrogen in sea water.

Perhaps the most striking accomplishment in marine zoology has been the development by Dr. George L. Clarke of a supersensitive instrument for measuring light in the deep sea. This bathyphotometer is capable of measuring and recording light intensities as small as 1/1,000,000,000,000 of full sunlight. The instrument is so sensitive that it has been advantageous to work at night in order to reach depths where no surface light can be detected. During the past year an improved model has been perfected, with the assistance of Mr. Charles J. Hubbard, which can be lowered to very great depths. On a recent cruise of the CARYN it was used successfully to depths of more than a mile. Even at these depths there is a detectable illumination attributed to the luminescence of animals. Against this background frequent brighter flashes are recorded as individual animals light up when close to the photometer.

A very active group interested in the fauna of the sea bottom has been working more or less in association with the shellfish project being conducted by Mr. Harry J. Turner for the Commonwealth of Massachusetts. In addition to a number of men working on summer fellowships these included Mr. Joseph Connell, who came to us a year ago from the Millport Laboratory in Scotland and who left in the Fall to take an Assistant Professorship at Santa Barbara College, and Dr. Howard L. Sanders.

Mr. Connell has been examining the spatial distribution of a number of sedentary animals which live between tide lines to determine whether they distribute themselves at random in areas suitable to them, or whether some biological factor causes them to be aggregated or to be spaced more evenly than chance would dictate. Examples of all three were discovered, soft-shell clams being distributed at random, several other mollusks appeared to be aggregated, while the burrows of fiddler crabs were uniformly spaced owing to the behavior of these animals in keeping other crabs away from the territory around their homes.

Dr. Sanders is making a very detailed survey of the fauna which inhabits the sediments at the bottom of Buzzards Bay. The objective is to discover how each species obtains its food and to understand the competition between the different species for sources of nourishment and, finally, to compute the quantities of organic matter produced by each kind of animal. The bottom fauna is a very important part of the marine environment which is difficult to study and Dr. Sanders' investigations should add much to our knowledge of its economy. In the course of this work he has discovered a small crustacean, *Hutchinsoniella macracantha*, which represents an entirely new subclass intermediate in character between other modern crustaceans and the ancient Trilobites. It is thus a missing link in the evolution of the crustacea.

One of the greatest difficulties in the propagation of shellfish is in obtaining an adequate supply of "seed" for cultivation. Small stages of mollusks must be found in natural situations from which they are moved to places suitable for their subsequent growth. Dr. Loosanoff of the U. S. Fish and Wildlife Service had shown that the common quahog, *Venus mercenaria*, may be induced to spawn in the laboratory and reared until the adult stage is reached. Mr. Turner is now attempting to determine whether seed quahogs can be reared in sufficient numbers to provide a practical source of "seed" for quahog farming. This work requires the detailed study of many aspects of the physiology of these mollusks during their early stage which, in themselves, will be of value to zoology quite apart from the practical objective.

Dr. John W. Kanwisher has been engaged in an investigation of the effects of freezing on marine organisms under a contract with the Arctic Institute of North America. He has recently completed papers on the ability of the seaweeds of Labrador to survive being frozen into the ice during the arctic winter and on the oxygen consumption of marine algae in the frozen state. He has found that more than three-quarters of the water in a frozen organism separates to form ice. This leads to a great concentration of salt in the remaining tissue fluids. The effects of freezing consequently closely resemble those of desiccation.

During the summer Dr. Laurence Irving of the U. S. Public Health Service and Dr. J. L. Hart of the University of Toronto were at the laboratory engaged in a study of the physiological mechanisms which enable seals to conserve body heat when in cold water or air and to dissipate heat when it is warm. Six seals spent what for them was apparently a comfortable summer in a pen constructed in the boat basin while awaiting experimentation. The newly-installed cold room, in which temperatures of –40°C. can be maintained, found its first use in this work.

Mr. William C. Schroeder now has in preparation a paper on the offshore lobster population and the fishery which has developed as the result of his exploratory cruises, which have been described in previous reports. He now has in prospect further exploration aimed particularly at seeking information on the spawning place of the bluefish and the early stages in the development of this important species—a matter on which there is complete ignorance.

Mr. Frank J. Mather III, who has been developing studies of the pelagic fish of interest to sport fishermen, is now on leave of absence in the Virgin Islands where he is looking into fishery possibilities for the government. Dr. Robert H. Gibbs, Jr., has joined the staff and is carrying on with the work in which Mr. Mather was formerly engaged in association with Mr. Schroeder.

Dr. Henry B. Bigelow and Mr. Schroeder have completed a paper on the sharks of the suborder Squaloidea, based in part on material collected by the Institution's vessels, while Dr. Richard H. Backus has recorded a number of interesting observations on the distribution of various fish picked up in the course of our explorations.

Publications

During 1956, 56 papers bearing contribution numbers were published:

	Contr. No.
Worthington, L. V., 1956. The temperature increase in Caribbean deep water since 1933. *Deep-Sea Res.*, 3(3): 234–235	666
Von Arx, W.S., 1956. Some techniques for laboratory study of the primary ocean circulation. *Fluid Models in Geophysics, Proc. First Symposium on Use of Models in Geophysical Fluid Dynamics, Johns Hopkins Univ.*, Sept. 1–4, 1953: 89–99	681
Bunker, A. F., 1956. Measurements of counter-gradient heat flows in the atmosphere. *Australian J. Physics*, 9(1): 133–143	682

	Contr. No.
Schell, I. I., 1956. Interrelationship of Arctic ice with the atmosphere and the ocean in the North Atlantic-Arctic and adjacent areas. *J. Meteorol.*, 13(1): 46–58	745
Faller, Alan J., 1956. A demonstration of fronts and frontal waves in atmospheric models. *J. Meteorol*, 13(1): 1–4	754
Hulburt, E. M., 1956. The phytoplankton of Great Pond, Massachusetts. *Biol. Bull.*, 110(2): 157–168	764
Ayers, J. C., 1956. Population dynamics of the marine clam, *Mya arenaria*. *Limnol. and Oceanogr.*, 1(1): 26–34	766
Bullis, H. R., Jr. and F. J. Mather, 1956. Tunas of the genus *Thunnus* of the northern Caribbean. *Amer. Mus. Novitates*, No. 1765: 12 pp.	774
Lawrence, Barbara and W. E. Schevill, 1956. The functional anatomy of the delphinid nose. *Bull. Mus. Comp. Zool., Harvard Coll.*, 114(4): 103–151	793
Schell, I. I., 1956. Further evidence of dynamic persistance and of its application to foreshadowing. *J. Meteorol.*, 13(5): 471–481	797
Fairbank, N. G., 1956. Methods and preliminary results in a study of minerals from the eastern Gulf of Mexico. *J. Sed. Petr.*, 26(3): 268–275	798
Stommel, Henry, A. B. Arons and D. C. Blanchard, 1956. An oceanographical curiosity: the perpetual salt fountain. Ltr. to the Editors. *Deep-Sea Res.*, 3(2): 152–153	799
Soule, F. M. and J. E. Murray, 1956. Physical oceanography of the Grand Banks and the Labrador Sea in 1955. *U. S. Coast Guard Bull.*, No. 41: 59–114	801
Malkus, W. V. R., 1956. Outline of a theory of turbulent shear flow. *J. Fluid Mech.*, 1(6): 521–539	804
Mackiewicz, John and R. H. Backus, 1956. Oceanic records of *Lasionycteris noctivagans* and *Lasiurus borealis*. *J. Mammal.*, 37(3): 442–443	805
Schleicher, K. E. and A. Bradshaw, 1956. A conductivity bridge for measurement of the salinity of sea water. *J. du Cons.*, 22(1): 9-20	810
Morgan, G. W., 1956. On the wind-driven ocean circulation. *Tellus*, 8(3): 301–320	811
Holmes, R. W., 1956. The annual cycle of phytoplankton in the Labrador Sea, 1950–51. *Bull. Bingham Ocean. Coll.*, 16(1): 1–74	813
Backus, R. H., Stewart Springer and E. L. Arnold, Jr., 1956. A contribution to the natural history of the white-tip shark, *Pterolamiops longimanus* (Poey). *Deep-Sea Res.*, 3(3): 178–188	814
Schevill, W. E., 1956. *Lagenorhynchus acutus* off Cape Cod. *J. Mammal.*, 37(1): 128–129	815
Scholander, P. F., L. van Dam and T. Enns, 1956. Nitrogen secretion in the swimbladder of whitefish. *Science* 123(3185): 59–60	816
Scholander, P. F., J. W. Kanwisher and D. C. Nutt, 1956. Gases in icebergs. *Science*, 123(3186): 104–105	818

	Contr. No.
Ryther, J. H., 1956. Photosynthesis in the ocean as a function of light intensity. *Limnol. and Oceanogr.*, 1(1): 61–70	819
Clarke, G. L. and G. K. Wertheim, 1956. Measurements of illumination at great depths and at night in the Atlantic Ocean by means of a new bathyphotometer. *Deep-Sea Res.*, 3(3): 189–205	821
Ayers, J. C., 1956. A dynamic height method for the determination of currents in deep lakes. *Limnol. and Oceanogr.*, 1(3) :150–161	823
Trask, P. D., 1956. The *Atlantis* marine geological expedition to Peru and Chile. *Nature*, 177(4506): 454–455	824
Ryther, J. H., 1956. The measurement of primary production. *Limnol. and Oceanogr.*, 1(2): 72–84	825
Miller, R. L., 1956. Trend surfaces: their application to analysis and description of environments of sedimentation: I The relation of sediment size parameters to current-wave systems and physiography. *J. Geol.*, 64(5): 425–446	826
Malkus, J. S., 1956. On the maintenance of the Trade Winds. *Tellus*, 8(3): 335–350	827
Richards, F. A. and R. F. Vaccaro, 1956. The Cariaco Trench, an anaerobic basin in the Caribbean Sea. *Deep-Sea Res.*, 3(3): 214–228	830
Nutt, D. C. and L. K. Coachman, 1956. The oceanography of Hebron Fjord, Labrador. *J. Fish. Res. Bd., Canada*, 13(5): 709–758	831
Schevill, W. E. and Barbara Lawrence, 1956. Food-finding by a capitive porpoise (*Tursiops truncatus*). *Breviora* No. 53: 15 pp.	832
Backus, R. H. and J. B. Hersey, 1956. Echo-sounder observations of midwater nets and their towing cables. *Deep-Sea Res.*, 3(4): 237–241	834
Woodcock, A. H., 1956. Dimorphism in the Portuguese man-of-war. *Nature*, 178(4527): 253–255	837
Richards, F. A., 1956. On the state of our knowledge of trace elements in the sea. Ltr. to the Editor. *Geochimica et Cosmochimica Acta*, 10(4): 241–243	840
Johnson, H. R., R. H. Backus, J. B. Hersey and D. M. Owen, 1956. Suspended echo-sounder and camera studies of midwater sound scatterers. *Deep-Sea Res.*, 3(4): 266–272	841
Ryther, J. H., 1956. Interrelation between photosynthesis and respiration in the marine flagellate, *Dunaliella euchlora*. *Nature*, 178(4538): 861–863	842
Stommel, H., 1956. On the determination of the depth of no meridional motion. *Deep-Sea Res.*, 3(4): 273–278	846
Spilhaus, A. F., 1956. Control of the world environment. *Geogr. Rev.*, 46(4): 451–459	847

	Contr. No.
Richards, F. A. and N. Corwin, 1956. Some oceanographic applications of recent determinations of the solubility of oxygen in sea water. *Limnol. and Oceanogr.*, 1(4): 263–267	852
Schell, I. I., 1956. On the nature and origin of the Southern Oscillation. *J. Meteorol.*, 13(6): 592–598	853
Arons, A. B. and H. Stommel, 1956. A β-plane analysis of free periods of the second class in meridional and zonal oceans. *Deep-Sea Res.*, 4(1): 23–31	855
Volkmann, Gordon, John Knauss and A. C. Vine, 1956. The use of parachute drogues in the measurement of subsurface currents. *Trans. Amer. Geophys. Union*, 37(5): 573–577	856
Clarke, G. L. and R. H. Backus, 1956. Measurements of light penetration in relation to vertical migration and record of luminescence of deep-sea animals. *Deep-Sea Res.*, 4(1): 1–14	858
Veronis, George and Henry Stommel, 1956. The action of variable wind stresses on a stratified ocean. *J. Mar. Res.*, 15(1): 43–75	859
Moulton, J. M., 1956. Influencing the calling of sea robins (*Prionotus* spp.) with sound. *Biol. Bull.*, 111(3): 393–398	862
Knott, S. T. and J. B. Hersey, 1956. Interpretation of high-resolution echo-sounding techniques and their use in bathymetry, marine geophysics and biology. *Deep-Sea Res.*, 4(1): 36–44	863
Moore, H. B. and E. G. Corwin, 1956. The effects of temperature, illumination and pressure on the vertical distribution of zooplankton. *Bull. Mar. Sci., Gulf and Caribbean*, 6(4): 273–287	864
Edwards, R. S. and F. A. Richards, 1956. A bottom-water sampler. *Deep-Sea Res.*, 4(1): 65–66	865
Friedman, I., D. R. Norton, D. B. Carter and A. C. Redfield, 1956. The deuterium balance of Lake Maracaibo. *Limnol. and Oceanogr.*, 1(4): 239–246	867
Vishniac, Helen S., 1956. On the ecology of the lower fungi. *Biol. Bull.*, 111(3) 410–414	869
Coachman, L. K., E. Hemmingsen and P. F. Scholander, 1956. Gas enclosures in a temperate glacier. *Tellus* 8(4): 415–423	873
Turner, H. J., Jr., J. H. Connell and C. J. George 1955 (1956). Eighth report on investigations of the shellfisheries of Massachusetts. Comm. Mass., Dept. Nat. Res., Div. Mar. Fish.: 25 pp.	876
Scholander, P. F. and L. van Dam, 1956. Micro gasometric determination of oxygen in fish blood. *J. Cell. Comp. Physiol.*, 48(3): 529–532	879
Scholander, P. F., 1956. Observations on the gas gland in living fish. *J. Cell. Comp. Physiol.*, 48(3): 523–528	880
Scholander, P. F., L. van Dam and Theodore Enns, 1956. The source of oxygen secreted into the swimbladder of cod. *J. Cell. Comp. Physiol.*, 48(3): 517–522	881

Personnel

At their twenty-seventh Annual Meeting the Members of the Corporation elected the following Trustees to serve until 1960; namely,

Detlev W. Bronk	Daniel Merriman	Alfred C. Redfield
Noel B. McLean	Emanuel R. Piore	Gerard Swope, Jr.

The Board re-elected Dr. Henry B. Bigelow as Chairman of the Board, and the following were elected as new members of the Corporation:

Carl-G. Rossby	Emanuel R. Piore

It is with pleasure that we record the appointment of the following persons to the Research Staff for a period of one year beginning September 1:

Lincoln Baxter II	Research Associate in Electronics
Robert H. Gibbs, Jr.	Research Associate in Marine Biology
Edward M. Hulburt	Research Associate in Marine Biology
Laurence Irving	Associate in Physiology
Bernhard Kummel	Associate in Submarine Geology
Charles E. Renn	Associate in Engineering
George Veronis	Research Associate in Mathematics
Raymond Wexler	Meteorologist

Reappointments for one- and three-year terms, as authorized by the Board of Trustees, were made to all Staff Members whose terms expired on September 1.

The following Visiting Investigators spent considerable time at the laboratory during the past year:

Angeles Alvariño de Leira	Spanish Institute of Oceanography (Navy Ministry), Spain
Richard Fay	U. S. Weather Bureau
Malcolm S. Gordon	Yale University
Alister C. Hardy	University Museum, Oxford, England
Laurence Irving	Arctic Health Research Center, Alaska
Allen Milne	Pacific Naval Laboratory, British Columbia
Edward W. Moore	Harvard University
T. S. Satyanarayana Rao	Andhra University, India
George Shor	Scripps Institution of Oceanography
S. Wennerberg	Research Institute of National Defence, Sweden

The following persons were awarded grants, honoraria, or fellowships during the year:

Spencer Appolonio	Bowdoin College
Harold Barnes	Marine Station, Millport, Scotland
Duncan C. Blanchard	Woods Hole Oceanographic Institution
Hubert Caspers	Zoologisches Staatsinstitut, Germany
John Chronic	University of Colorado
R. F. Clippinger	Datomatic Corporation
George M. Cresswell	Harvard University
R. M. Cunningham	Air Force Cambridge Research Center
Herbert Curl, Jr.	A & M College of Texas
George E. R. Deacon	National Institute of Oceanography, England
Roberta C. Eike	Harvard University
Helen B. Fink	Harvard University
El Sayed Mohamed Hassan	New York University
Gerald J. Holton	Harvard University
W. W. Howells	Harvard University
Borje Kullenberg	Oceanographic Institute, Sweden
J. B. Lucke	University of Connecticut
Robert L. Miller	University of Chicago
Yasuo Miyake	Meteorological Research Institute, Japan
James M. Moulton	Bowdoin College
Leonard K. Nash	Harvard University
Erik Palmén	Academy of Finland
Roderic B. Park	California Institute of Technology
Jacques Piccard	Paris, France
W. H. Pinson	Massachusetts Institute of Technology
Mary Alys Plunkett	Vassar College
E. G. Pringsheim	Pflanzenphysiologisches Institut, Germany
Arthur G. Randall	Marine Station, Millport, Scotland
Herbert Riehl	University of Chicago
Gordon A. Riley	Yale University
W. Rodhe	University of Uppsala, Sweden
Hartley Rogers, Jr.	Harvard University
Alfred S. Romer	Harvard University
Rudolf S. Scheltema	Harvard University
Harlow Shapley	Harvard University
B. K. Skinner	Harvard Observatory
Parmatma Srivastava	New York University
Edward D. Stroup	University of Hawaii
Ken Sugawara	Nagoya University, Japan
Parker D. Trask	University of California
P. L. R. S. Welander	University of Stockholm, Sweden
George C. Williams	Michigan State University
D. P. Wilson	Marine Biological Laboratory, England
Georg Wüst	Institut fur Meereskunde der Universitat, Germany
E-an Zen	Harvard University
Stetson Memorial Fund	

V. TREASURER'S REPORT

The accounts for the year 1956 have been audited by Lybrand, Ross Bros. & Montgomery.

The book value of endowment funds, at December 31, 1956 was $3,238,878, of which $818,357 represents accumulated net gains from sales of investments, and $2,420,521 the original value of endowment funds. The market value of endowment assets on the same date was $4,550,357. Endowment fund investments and income received therefrom are summarized in Schedule D. The first addition to endowment funds, since the original Rockefeller grants, came in December of this year in the form of a gift by a member of The Associates of 10 shares of Amerada Petroleum Corp. at a valuation of $1,101.

Income received on endowment assets, including interest charged on the advance to current funds, was $167,380 for the year ended December 31, 1956, compared with $158,743 the previous year. This income represents a return on endowment fund assets of 3.7% at year-end market quotations, 5.2% on the book amount, and 6.9% on the original amount of the endowment fund.

Endowment income was allocated for 1956 operating expenses at the rate of 5.3% of the book amount of original endowment funds, or $128,229; the rate was the same as that of the previous year. The balance of endowment income, $39,151, was transferred to the income and salary stabilization reserve.

The advance to current funds from endowment funds was paid off during the year.

Deferred charges amounting to $247,272 represent expenditures for the benefit of future years. The deferred portion of the costs of reconditioning the Crawford amounting to $228,969 comprise the major part of such charges at December 31, 1956. A proportionate part of these charges will be added to current costs, or other appropriate accounts, as the benefits accrue.

The details of unexpended balances of gifts and receipts for research, other than government, are shown in Schedule C. The income from Woods Hole Oceanographic Associates for the year amounted to $73,189, from which were made expenditures and allocations to specific projects of $33,936. The balance, amounting to $39,253, added to the balance on hand December 31, 1955, totals the $71,549 shown on the balance sheet. The above total of Associates' income for the year was made up of $54,700 corporate and individual dues, $8,000 of life memberships, and $10,489 of miscellaneous contributions by Associates.

The Institution's 1956 contribution to the Woods Hole Oceanographic

Institution Employees Retirement Trust amounted to $60,750. The Trust is administered by three trustees. The balance remaining in the old retirement fund, which is in the custody of the Treasurer, amounted to $62,893 as at December 31, 1956.

In the financial statements that follow it is interesting to note that for each dollar spent 79.5 cents were spent for direct costs of research activity, 15.6 cents for general and administration expenses and 4.9 cents for plant operation and miscellaneous. Total administrative salaries amounted to only 6.3 cents of each dollar of total expense.

BALANCE SHEET

As at December 31, 1956

ASSETS

ENDOWMENT FUND ASSETS:		
Investment securities (Schedule D):		
Bonds (market quotations $1,863,083)		$1,975,696
Stocks (market quotations $2,642,334)		1,218,242
		3,193,938
Cash		44,940
		3,238,878
PLANT ASSETS (note):		
Laboratory plant and equipment		552,145
Vessels and equipment		364,983
Other property		161,541
		1,078,669
CURRENT FUND ASSETS:		
Cash		35,793
Accounts receivable:		
U. S. Government	$364,462	
Other	15,176	379,638
Unbilled costs on research contracts:		
U. S. Government	269,596	
Other	5,267	274,863
Supply inventories		23,199
Deferred charges:		
Reconditioning boat Crawford	228,969	
Other	18,303	247,272
		960,765
		$5,278,312

LIABILITIES

ENDOWMENT FUNDS:		
Unrestricted		$2,001,101
For upkeep of plant		419,420
Accumulated net gain on sale of investments		818,357
		3,238,878
FUNDS INVESTED IN PLANT		1,078,669
CURRENT LIABILITIES AND FUNDS:		
Accounts payable and accrued expenses		150,022
Contribution payable to employees' retirement plan and trust		60,750
Unexpended balances of gifts and grants:		
For research:		
Government	$332,579	
Other (Schedule C)	21,707	354,286
Oceanographic Associates		71,549
General Fund:		
General plant and equipment reserve	183,574	
Income and salary stabilization reserve	114,324	
Unappropriated	26,260	324,158
		960,765
		$5,278,312

Note — Since 1945 the Institution has provided for depreciation of plant assets other than vessels at annual rates of 2% on buildings and 5% to 33⅓% on equipment, carrying the amounts to general plant and equipment reserve.

STATEMENT OF INCOME, OPERATING EXPENSES AND UNAPPROPRIATED GENERAL FUND

For the Year Ended December 31, 1956

INCOME:		
Reimbursement of sponsored research activity:		
For direct costs		$1,641,986
For indirect costs		512,204
		2,154,190
Endowment income after amortization of bond premiums (Schedule D)	$167,380	
Less amount added to income and salary stabilization reserve	39,151	128,229
Miscellaneous		337
Total income availed of		2,282,756
OPERATING EXPENSES:		
Direct costs of research activity (Schedule A):		
Salaries and wages		807,336
Vessel operations		498,648
Materials and services		380,537
Travel		74,649
		1,761,170
Indirect costs:		
General and administration (Schedule B)	346,831	
Plant operation (Schedule B)	104,118	
Miscellaneous	4,500	455,449
Total operating expenses		2,216,619
EXCESS OF INCOME		66,137
Additions to plant from current funds — books and equipment purchased		31,053
		35,084
DEFICIT IN UNAPPROPRIATED GENERAL FUND, JANUARY 1, 1956		8,824
UNAPPROPRIATED GENERAL FUND, DECEMBER 31, 1956		$26,260

Schedule A

DIRECT COSTS OF RESEARCH ACTIVITY

For the Year Ended December 31, 1956

	Salaries and Wages	Vessel Operations	Materials and Services	Travel	Total
U.S. Government Contracts	$707,310	$471,212	$299,232	$63,799	$1,541,553
Other Sponsored Research	37,056	13,590	43,669	6,118	100,433
Total direct costs of sponsored research ...	744,366	484,802	342,901	69,917	1,641,986
Institution Research......	62,970	13,846	37,636	4,732	119,184
Total direct costs of research . .	$807,336	$498,648	$380,537*	$74,649	$1,761,170

* Includes grants and fellowships:

Other sponsored research	$11,250
Institution research	13,785
	$25,035

Schedule B

GENERAL AND ADMINISTRATION EXPENSES AND EXPENSES FOR PLANT OPERATION

For the Year Ended December 31, 1956

GENERAL AND ADMINISTRATION

General Expenses:		
Staff benefits:		
Contributions to retirement plan..............................		$60,750
Social security taxes..		20,952
Group insurance		2,137
		83,839
Shop services...		69,005
Housing, net..		2,571
Administration Expenses:		
Salaries and wages..................................	$140,285	
Insurance, travel, supplies and other....................	51,131	191,416
		$346,831

PLANT OPERATION

Salaries and Wages..		$41,754
Provision for Depreciation (credited to general plant and equipment reserve)		24,377
Other Repair Costs..................................	$13,408	
Heat, Light and Power................................	17,978	
Other...	6,601	37,987
		$104,118

SCHEDULE C

SUMMARY OF GIFTS AND RECEIPTS FOR RESEARCH

Year Ended December 31, 1956

	Unexpended Balance January 1, 1956	Received	Expended		Other Charges or (Credits)	Unexpended Balance December 31, 1956
			Direct Costs	Indirect Costs		
American Bureau of Shipping — sea keeping hulls .	$443		$270	$173		
American Society of Limnology and Oceanography		$600	410	190		
Arctic Institute of North America:						
Buoyancy control in fish.		6	(11)	17		
Freezing of living tissue.	2,392	2,500	3,605	1,287		
Barataria Bay model.	45	60	105			
Bermuda Biological Station for Research		519	519			
Bigelow volume.	2,748	45	2,793			
Blue Dolphin.		1,497	1,468	29		
Commonwealth of Massachusetts—shellfish propogation.	14,203	20,000	18,620	10,483		$5,100
Esso Research and Engineering Company:						
Foraminifera cataloging	2,213	5,300	4,794	2,719		
Peruvian samples analysis		5,000	3,000			2,000
Gordon project		137	126	11		
Hudson Laboratory		4,990	4,990			
Manufacture, sale, and calibration of instruments .		2,001	4,012	2,188	($4,199) (2)	
Massachusetts Institute of Technology — pressure pump	35		31	4		
Munitalp Foundation — atmospheric chemistry . . .		8,000	8,000			
National Academy of Sciences:						
Operation Piccard.		4,514	4,514			
Project Nobska		1,180	761	419		
National Lead Company		2,944	2,591	353		
Oceanographic Associates:						
Deuterium studies	404	2,325	2,478	251		
Peruvian core analysis.	5,478	10,500	6,169	827	(1,500) (3)	10,482
Other (including fellowships, lectureship, and pelagic fish studies)		20,018	19,140	878		
Outside work done for others		2,518	1,831	687		
Research Corporation — instrument fund	2,220	2,000	1,150	512		2,558
Rockefeller Brothers Fund Incorporated — motion picture on oceanography.		6,141	6,141			
Socony-Mobil Laboratories — Peruvian expedition	2,500	2,500	2,500		1,500 (3)	1,000
Town of Islip, New York — Great South Bay Survey		1,000	333	100		567
U.S. Coast Guard Oceanographic unit		1,655	93	30	1,532 (4)	
	$32,681 (1)	$107,950	$100,433	$21,158	($2,667)	$21,707

(1) Omitting $7,681, National Science Foundation, classified as goverment in 1956.

(2) Charged to other projects. (3) Transfers. (4) Credited to income.

SCHEDULE D

SUMMARY OF INVESTMENTS

As at December 31, 1956

	Book Amount	% of Total	Market Quotation	% of Total	Income
BONDS:					
U.S. Government	$610,919	19.13	$598,854	13.29	$12,384
Railroad	546,904	17.12	508,227	11.28	21,759
Public utility	187,743	5.88	162,095	3.60	7,305
Industrial	293,037	9.17	263,776	5.85	10,232
Financial and investment	337,093	10.56	330,131	7.33	10,697
Total bonds	1,975,696	61.86	1,863,083	41.35	62,377
STOCKS:					
Preferred	305,349	9.56	307,443	6.82	15,980
Common:					
Public utility	293,218	9.18	478,216	10.61	20,392
Industrial	441,601	13.83	1,562,252	34.68	53,668
Miscellaneous	178,074	5.57	294,423	6.54	13,011
Total common stocks	912,893	28.58	2,334,891	51.83	87,071
Total stocks	1,218,242	38.14	2,642,334	58.65	103,051
Total investments	$3,193,938	100.00	$4,505,417	100.00	165,428
INTEREST ON ADVANCE TO CURRENT FUNDS CHARGED TO MISCELLANEOUS OPERATING EXPENSE					1,952
TOTAL ENDOWMENT FUND INCOME					$167,380

WOODS HOLE OCEANOGRAPHIC INSTITUTION
WOODS HOLE, MASSACHUSETTS

We have examined the balance sheet of Woods Hole Oceanographic Institution as at December 31, 1956 and the related statement of income, operating expenses and unappropriated general fund for the year then ended. Our examination was made in accordance with generally accepted auditing standards, and accordingly included such tests of the accounting records and such other auditing procedures as we considered necessary in the circumstances.

In our opinion, the accompanying financial statements present fairly the position of Woods Hole Oceanographic Institution at December 31, 1956 and the results of its operations for the year then ended, on a basis consistent with that of the preceding year.

LYBRAND, ROSS BROS. & MONTGOMERY

Boston, Massachusetts
June 4, 1957

List of Contributions

LIST OF CONTRIBUTIONS
FROM THE WOODS HOLE OCEANOGRAPHIC INSTITUTION

See Author Index in *Collected Reprints* 1950 for a complete list up to that year.

No. 366. Bostwick H. Ketchum. Plankton Algae and their Biological Significance. In: Manual of Phycology — an Introduction to the Algae and their Biology, Ch. 17, pp. 335–346. Gilbert M. Smith, Editor. Published by The Chronica Botanica Co., Waltham, Mass. 1951.

No. 401. W. S. Butcher. A New Species of *Nonion* (Foraminifera) from the Woods Hole Region. *Contr. Cushman Lab. Foram. Res.*, Vol. 24, (1), No. 308, pp. 21–23. 1948.

No. 402. Edward S. Deevey, Jr. On the Date of the Last Rise of Sea Level in Southern New England, with Remarks on the Grassy Island Site. *Amer. Jour. Sci.*, Vol. 246, pp. 329–352. 1948.

No. 403. Charles M. Weiss. The Abnormal Development of Tunicates Attached to Glass Surfaces Adjacent to Antifouling Paints. *Ecology*, Vol. 29, No. 2, pp. 215–218. 1948.

No. 404. Charles M. Weiss. The Seasonal Occurrence of Sedentary Marine Organisms in Biscayne Bay, Florida. *Ecology*, Vol. 29, No. 2, pp. 153–172. 1948.

No. 405. R. B. Montgomery. Vertical Eddy Flux of Heat in the Atmosphere. *Jour. Meteorology*, Vol. 5, No. 6, pp. 265–274. 1948.

No. 406. Hilary B. Moore. The Zooplankton of the Upper Waters of the Bermuda Area of the North Atlantic. *Sears Found., Jour. Mar. Res.*, Vol. 12, Art. 2, pp. 1–97. 1949. (Not included in *Collected Reprints*.)

No. 407. H. R. Seiwell. Evaluation of Sea-Surface Roughness from Underwater-Pressure Recordings. *Trans. Amer. Geophys. Union*, Vol. 29, No. 2, pp. 197–201. 1948.

No. 408. Henry Stommel. The Westward Intensification of Wind-Driven Ocean Currents. *Trans. Amer. Geophys. Union*, Vol. 29, No. 2, pp. 202–206. 1948.

No. 409. Sidney C. Hsiao. The Simple Micromethod for Rapid Extraction of Lipids. *Science*, Vol. 107, No. 2766, pp. 24–25. 1948.

No. 410. Austin H. Clark. Some Interesting Starfishes and Brittle-Stars Dredged by the *Atlantis* in the Mid-Atlantic. *Jour. Wash. Acad. Sci.*, Vol. 38, No. 2, pp. 75–78. 1948.

No. 411. Alfred C. Redfield and Charles M. Weiss. The Resistance of Metallic Silver to Marine Fouling. *Biol. Bull.*, Vol. 94, No. 1, pp. 25–28. 1948.

No. 412. J. B. Hersey and H. B. Moore. Progress Report on Scattering Layer Observations in the Atlantic Ocean. *Trans. Amer. Geophys. Union*, Vol. 29, No. 3, pp. 341–354. 1948.

No. 413. Gardner Emmons. Vertical Distributions of Temperature and Humidity over the Ocean between Nantucket and New Jersey. *Papers in Physical Oceanography and Meteorology*, Vol. 10, No. 3, pp. 1–89. 1947.

No. 414. W. T. Edmondson and Yvette H. Edmondson. Measurements of Production in Fertilized Salt-Water. *Sears Found., Jour. Mar. Res.*, Vol. 6, No. 3, pp. 228–245. 1947.

No. 415. J. Lamar Worzel and Maurice Ewing. Propagation of Sound in the Ocean: Explosion Sounds in Shallow Water. *Mem. Geol. Soc. Amer.*, 27, pp. i–vi, 1–53. 1948.

C. L. Pekeris. Propagation of Sound in the Ocean: Theory of Propagation of Explosive Sound in Shallow Water. *Mem. Geol. Soc. Amer.*, 27, pp. i–viii, 1–117. 1948.

Maurice Ewing and J. Lamar Worzel. Propagation of Sound in the Ocean: Long-Range Sound Transmission. *Mem. Geol. Soc. Amer.*, 27, pp. i–v, 1–35. 1948. (Not included in *Collected Reprints*.)

No. 416. Sidney Cornell. The Collapse of Long Cylindrical Shells under External Pressure. *Soc. Exper. Stress Analysis*, Vol. 6, No. 1, pp. 111–114. 1948.

No. 417. Alfred H. Woodcock. The Swimming of Dolphins. *Nature*, Vol. 161, p. 602. 1948.

No. 418. J. M. Richardson, A. B. Arons and R. R. Halverson. Hydrodynamic Properties of Sea Water at the Front of a Shock Wave. *Jour. Chem. Physics*, Vol. 15, No. 11, pp. 785–794. 1947.

No. 419. Bostwick H. Ketchum and Jean Keen. Unusual Phosphorus Concentrations in the Florida "Red Tide" Sea Water. *Sears Found., Jour. Mar. Res.*, Vol. 7, No. 1, pp. 17–21. 1948.

No. 420. C. A. Barnes, D. F. Bumpus and John Lyman. Ocean Circulation in Marshall Islands Area. *Trans. Amer. Geophys. Union*, Vol. 29, No. 6, pp. 871–876. 1948.

No. 421. William S. von Arx. The Circulation Systems of Bikini and Rongelap Lagoons. *Trans. Amer. Geophys. Union*, Vol. 29, No. 6, pp. 861–870. 1948. Revised and published as *Geol. Survey Prof. Pap.* No. 260-b. In: Bikini and nearby Atolls. Pt. 2, Oceanography (Physical), pp. 265–273. 1954.

No. 422. William L. Ford. Radiological and Salinity Relationships in the Water at Bikini Atoll. *Trans. Amer. Geophys. Union*, Vol. 30, No. 1, pp. 46–54. 1949.

No. 423. R. B. Montgomery. Ivory's Psychrometric Formula and the Concepts of Equivalent Temperature and Wet-Bulb Temperature. *Jour. Meteorology*, Vol. 5, No. 3, pp. 113–115. 1948.

No. 424. Parker D. Trask, Fred B Phleger, Jr., and Henry C. Stetson. Recent Changes in Sedimentation in the Gulf of Mexico. *Science*, Vol. 106, No. 2759, pp. 460–461. 1947.

No. 425. George L. Clarke and David W. Bishop. The Nutritional Value of Marine Zooplankton with a Consideration of its Use as an Emergency Food. *Ecology*, Vol. 29, No. 1, pp. 54–71. 1948.

No. 426. J. Lamar Worzel. Ocean Bottom Sampler for Ships Under Way. *Geophysics*, Vol. 13, No. 3, pp. 452–456. 1948.

No. 427. Clinton M. Osborn. Factors Influencing the Growth of Integumentary Pigment in Fishes. I. The Role of Light. *Proc. Soc. Exper. Biol. and Med.*, Vol. 67, pp. 440–445. 1948.

No. 428. A. W. Jacobson. An Instrument for Recording Continuously the Salinity, Temperature, and Depth of Sea Water. *Trans. Amer. Inst. Elec. Eng.*, Vol. 67, pp. 1–9. 1948.

No. 429. Fred B Phleger, Jr. Foraminifera of a Submarine Core from the Caribbean Sea. *Kungl. Vet.-o. Vittern. Samh. Handl.*, F. 6, Ser. B, Bd. 5, No. 14, pp. 1–9. 1948.

No. 430. A. B. Arons, J. P. Slifko and A. Carter. Secondary Pressure Pulses due to gas Globe Oscillation in Underwater Explosions. I. Experimental Data. *Jour. Acoust. Soc. Amer.*, Vol. 20, No. 3, pp. 271–276. 1948.

No. 431. A. B. Arons. Secondary Pressure Pulses due to Gas Globe Oscillation in Underwater Explosions. II. Selection of Adiabatic Parameters in the Theory of Oscillation. *Jour. Acoust. Soc. Amer.*, Vol. 20, No. 3, pp. 277–282. 1948.

No. 432. Talbot H. Waterman. Studies on Deep-Sea Angler-Fishes (Ceratioidea). III. The Comparative Anatomy of *Gigantactis longicirra* Waterman. *Jour. Morphology*, Vol. 82, No. 2, pp. 81–149. 1948.

No. 433. L. N. Liebermann. Reflection of Sound from Coastal Sea Bottoms. *Jour. Acoust. Soc. Amer.*, Vol. 20, No. 3, pp. 305–309. 1948.

No. 434. Charles M. Weiss. Seasonal and Annual Variations in the Attachment and Survival of Barnacle Cyprids. *Biol. Bull.*, Vol. 94, No. 3, pp. 236–243. 1948.

No. 435. H. R. Seiwell. Sea Surface Roughness Measurements in Theory and Practice. *Annals N. Y. Acad. Sci.*, Vol. 51, Art. 3, pp. 483–501. 1949.

No. 436. H. R. Seiwell. Results of Research on Surface Waves of the Western North Atlantic. I. Investigation of Bottom Pressure Fluctuations and Surface Waves. II. Results of Sea Roughness Determinations in the Vicinity of Woods Hole, Massachusetts and Bermuda. *Papers in Physical Oceanography and Meteorology*, Vol. 10, No. 4, pp. 1–56. 1948.

No. 437. A. B. Arons and R. H. Cole. Design and Use of Piezoelectric Gauges for Measurement of Large Transient Pressures. *Review of Sci. Instruments*, Vol. 21, No. 1, pp. 31–38. 1950.

No. 438. Arthur A. Klebba. Details of Shore-Based Wave Recorder and Ocean Wave Analyzer. *Annals N. Y. Acad. Sci.*, Vol. 51, Art. 3, pp. 533–544. 1949.

No. 439. Athelstan F. Spilhaus. Drop Size, Intensity and Radar Echo of Rain. *Jour. Meteorology*, Vol. 5, No. 4, pp. 161–164. 1948.

No. 440. Athelstan F. Spilhaus and Arthur R. Miller. The Sea Sampler. *Sears Found., Jour. Mar. Res.*, Vol. 7, No. 3, pp. 370–385. 1948.

No. 441. Gordon A. Riley and Samy Gorgy. Quantitative Studies of Summer Plankton Populations of the Western North Atlantic. *Sears Found., Jour. Mar. Res.*, Vol. 7, No. 2, pp. 100–121. 1948.

No. 442. Alfred C. Redfield. The Exchange of Oxygen across the Sea Surface. *Sears Found., Jour. Mar. Res.*, Vol. 7, No. 3, pp. 347–361. 1948.

No. 443. Patricia A. Langwell. Inhomogeneities of Turbulence, Temperature, and Moisture in the West Indies Trade-wind Region. *Jour. Meteorology*, Vol. 5, No. 5, pp. 243–246. 1948.

No. 444. Fred B. Phleger, Jr. Origin and Deposition of Deep Sea Sediments. *Trans. Amer. Geophys. Union*, Vol. 30, No. 2, pp. 180–182. 1949.

No. 445. B. Haurwitz. The Effect of Ocean Currents on Internal Waves. *Sears Found., Jour. Mar. Res.*, Vol. 7, No. 3, pp. 217–228. 1948.

No. 446. Bostwick H. Ketchum, Cornelia L. Carey and Margaret Briggs. Preliminary Studies on the Viability and Dispersal of Coliform Bacteria in the Sea. *In* Limnological Aspects of Water Supply and Waste Disposal. Ed. F. R. Moulton and and Florence Hitzel. *Publ. Amer. Assoc. Adv. Sci.*, pp. 64–73. 1949.

No. 447. Henry B. Bigelow and William C. Schroeder. New Genera and Species of Batoid Fishes. *Sears Found., Jour. Mar. Res.*, Vol. 7, No. 3, pp. 543–566. 1948.

No. 448. Hilary B. Moore. A Camera for Producing One-Dimensional Reduction in Narrow Records. *Sears Found., Jour. Mar. Res.*, Vol. 8, No. 1, pp. 21–23. 1949.

No. 449. A. B. Arons and D. R. Yennie. Energy Partition in Underwater Explosion Phenomena. *Rev. Modern Physics*, Vol. 20, No. 3, pp. 519–536. 1948. (Not included in *Collected Reprints*.)

No. 450. J. B. Hersey and Maurice Ewing. Seismic Reflections from beneath the Ocean Floor. *Trans. Amer. Geophys. Union*, Vol. 30, No. 1, pp. 5–14. 1949.

No. 451. C. O'D. Iselin and Frederick C. Fuglister. Some Recent Developments in the Study of the Gulf Stream. *Sears Found., Jour. Mar. Res.*, Vol. 7, No. 3, pp. 317–329. 1948.

No. 452. Norris W. Rakestraw and Dayton E. Carritt. Some Seasonal Chemical Changes in the Open Ocean. *Sears Found., Jour. Mar. Res.*, Vol. 7, No. 3, pp. 362–369. 1948.

No. 453. Henry Stommel. The Theory of the Electric Field Induced in Deep Ocean Currents. *Sears Found., Jour. Mar. Res.*, Vol. 7, No. 3, pp. 386–392. 1948.

No. 454. Parker D. Trask. Oceanography and Geosynclines. *Sears Found., Jour. Mar. Res.*, Vol. 7, No. 3, pp. 679–685. 1948.

No. 455. L. N. Liebermann. Reflection of Underwater Sound from the Sea Surface. *Jour. Acoust. Soc. Amer.*, Vol. 20, No. 4, pp. 498–503. 1948.

No. 456. Lewis F. Richardson and Henry Stommel. Note on Eddy Diffusion in the Sea. *Jour. Meteorology*, Vol. 5, No. 5, pp. 238–240. 1948.

No. 457. Joanne Starr Malkus. Effects of Wind Shear on Some Aspects of Convection. *Trans. Amer. Geophys. Union*, Vol. 30, No. 1, pp. 19–25. 1949.

No. 458. Alfred H. Woodcock and Mary M. Gifford. Sampling Atmospheric Sea-Salt Nuclei over the Ocean. *Sears Found., Jour. Mar. Res.*, Vol. 8, No. 2, pp. 177–197. 1949.

No. 459. William L. Ford. The Field Use of a Salinity-Temperature-Depth Recorder. *Sears Found., Jour. Mar. Res.*, Vol. 8, No. 1, pp. 84–96. 1949.

No. 460. William E. Schevill and Barbara Lawrence. Underwater Listening to the White Porpoise (*Delphinapterus leucas*). *Science*, Vol. 109, No. 2824, pp. 143–144. 1949.

No. 461. H. R. SEIWELL and GEORGE P. WADSWORTH. A New Development in Ocean Wave Research. *Science*, Vol. 109, No. 2829, pp. 271–274. 1949.

No. 462. HARRY J. TURNER, JR., JOHN C. AYERS and CHARLES L. WHEELER. Report on Investigations of the Propagation of the Soft-Shell Clam, *Mya arenaria*. *Com. Mass., Dept. Cons., Div. Mar. Fish.*, pp. 1–61. 1948.

No. 463. FLOYD M. SOULE and E. R. CHALLENDER. Discussion of some of the Effects of Winds on Ice Distribution in the Vicinity of the Grand Banks and the Labrador Shelf. *U. S. Coast Guard Bull.*, No. 33, pp. 59–61. 1949.

No. 464. GORDON A. RILEY, HENRY STOMMEL and D. F. BUMPUS. Quantitative Ecology of the Plankton of the Western North Atlantic. *Bull. Bingham Oceanographic Coll.*, Vol. 12, Art. 3, pp. 1–169. 1949. (Not included in *Collected Reprints*.)

No. 465. A. F. BUNKER, B. HAURWITZ, J. S. MALKUS and H. STOMMEL. Vertical Distribution of Temperature and Humidity over the Caribbean Sea. *Papers in Physical Oceanography and Meteorology*, Vol. 11, No. 1, pp. 1–82. 1949.

No. 466. DAVID M. PRATT. Experiments in the Fertilization of a Salt Water Pond. *Sears Found., Jour. Mar. Res.*, Vol. 8, No. 1, pp. 36–59. 1949.

No. 467. FLOYD M. SOULE, H. H. CARTER and L. A. CHENEY. Oceanography of the Grand Banks Region and Labrador Sea, 1948. *U. S. Coast Guard Bull.*, No. 34, pp. 67–118. 1950.

No. 468. RICHARD A. CRAIG. Vertical Eddy Transfer of Heat and Water Vapor in Stable Air. *Jour. Meteorology*, Vol. 6, No. 2, pp. 123–133. 1949.

No. 469. HENRY STOMMEL. Trajectories of Small Bodies Sinking Slowly through Convection Cells. *Sears Found., Jour. Mar. Res.*, Vol. 8, No. 1, pp. 24–29. 1949.

No. 470. HENRY W. MENARD, JR. Synthesis of Sand Mixtures. *Jour. Sed. Petrology*, Vol. 19, No. 2, pp. 71–77. 1949.

No. 471. AUSTIN H. CLARK. Echinoderms from the Mid-Atlantic Dredged by the *Atlantis* in the Summer of 1948. *Jour. Wash. Acad. Sci.*, Vol. 39, No. 11, pp. 371–377. 1949.

No. 472. GORDON A. RILEY and RUTH VON ARX. Theoretical Analysis of Seasonal Changes in the Phytoplankton of Husan Harbor, Korea. *Sears Found., Jour. Mar. Res.*, Vol. 8, No. 1, pp. 60–72. 1949.

No. 473. BOSTWICK H. KETCHUM, LOIS LILLICK and ALFRED C. REDFIELD. The Growth and Optimum Yields of Unicellular Algae in Mass. Culture. *Jour. Cell. and Comp. Physiol.*, Vol. 33, No. 3, pp. 267–279. 1949.

No. 474. BOSTWICK H. KETCHUM and ALFRED C. REDFIELD. Some Physical and Chemical Characteristics of Algae Grown in Mass. Culture. *Jour. Cell. and Comp. Physiol.*, Vol. 33, No. 3, pp. 281–299. 1949.

No. 475. JOANNE STARR MALKUS. Cumulus, Thermals and Wind. *Soaring*, Vol. 13, Nos. 9–10, pp. 6–9, 12. 1949.

No. 476. HENRY W. MENARD. Transportation of Sediment by Bubbles. *Jour. Sed. Petrology*, Vol. 20, No. 2, pp. 98–106. 1950.

No. 477. B. HAURWITZ. Internal Waves of Tidal Character. *Trans. Amer. Geophys. Union*, Vol. 31, No. 1, pp. 47–52. 1950.

No. 478. Richard A. Craig and R. B. Montgomery. Evaporation (Measured) from Ocean into Hydrostatically Stable Air. *Jour. Meteorology*, Vol. 6, No. 6, pp. 426-427. 1949.

No. 479. Athelstan F. Spilhaus, A. Ehrlich and Arthur R .Miller. Hydrostatic Instability in the Ocean. *Trans. Amer. Geophys. Union*, Vol. 31, No. 2, pp. 213–215. 1950.

No. 480. Maurice Ewing, J. L. Worzel, N. C. Steenland and Frank Press. Geophysical Investigations in the Emerged and Submerged Atlantic Coastal Plain. Part V: Woods Hole, New York, and Cape May Sections. *Bull. Geol. Soc. Amer.*, Vol. 61, pp. 877–892. 1950.

No. 481. Mary Sears. Notes on Siphonophores. I. Siphonophores from the Marshall Islands. *Sears Found., Jour. Mar. Res.*, Vol. 9, No. 1, pp. 1–16. 1950.

No. 482. R. B. Montgomery. The Taylor Diagram (Temperature against Vapor Pressure) for Air Mixtures. *Arch. Meteorol. Geoph. u. Bioklim.*, Ser. A: Meteorol. und Geoph., Band II, Heft 2–3, pp. 163–183. 1950.

No. 483. Maurice Ewing, J. L. Worzel, J. B. Hersey, Frank Press and G. R. Hamilton. Seismic Refraction Measurements in the Atlantic Ocean Basin. (Part I). *Bull. Seismol. Soc. Amer.*, Vol. 40, No. 3, pp. 233–242. 1950.

No. 484. Fred B. Phleger. The Foraminifera. *In* The Boylston Street Fishweir II. *Papers Robert S. Peabody Found. Archaeol.*, Vol. 4, No. 1, pp. 99–108. 1949.

No. 485. Fred B. Phleger. Submarine Geology and Pleistocene Research. A Review by the Members of the Committee on Interrelations of Pleistocene Research, National Research Council. 8. Submarine Geology and Pleistocene Research. *Bull. Geol. Soc. Amer.*, Vol. 60, pp. 1457–1461. 1949.

No. 486. H. R. Seiwell. The Principles of Time Series Analyses Applied to Ocean Wave Data. *Proc. Nat. Acad. Sci.*, Vol. 35, No. 9, pp. 518–528. 1949.

No. 487. Henry C. Stetson. The Sediments and Stratigraphy of the East Coast Continental Margin: Georges Bank to Norfolk Canyon. *Papers in Physical Oceanography and Meteorology*, Vol. 11, No. 2, pp. 1–60. 1949.

No. 488. Martin J. Pollak. Notes on Determining the Depths of Sampling in Serial Oceanographic Observations. *Sears Found., Jour. Mar. Res.*, Vol. 9, No. 1, pp. 17–20. 1950.

No. 489. Alfred H. Woodcock. Subsurface Pelagic Sargassum. *Sears Found., Jour. Mar. Res.*, Vol. 9, No. 2, pp. 77–92. 1950.

No. 490. A. B. Arons and D. R. Yennie. Phase Distortion of Acoustic Pulses Obliquely Reflected from a Medium of Higher Sound Velocity. *Jour. Acoust. Soc. Amer.*, Vol. 22, No. 2, pp. 231–237. 1950.

No. 491. Rushdi Said. Foraminifera of Narragansett Bay. *Contr. Cushman Found. Foram. Res.*, Vol. 2, (3), pp. 75–86. 1951.

No. 492. William L. Ford. Seagoing Photoelectric Colorimeter. *Analytical Chemistry*, Vol. 22, No. 11, pp. 1431–1435. 1950.

No. 493. Henry W. Menard. Current-Ripple Profiles and their Development. *Jour. Geology*, Vol. 58, No. 2, pp. 152–153. 1950.

No. 494. Jack L. Hough. Pleistocene Lithology of Antarctic Ocean-Bottom Sediments. *Jour. Geology*, Vol. 58, No. 3, pp. 254–260. 1950.

No. 495. Martin J. Pollak. The Water Structure in the Brownson Deep. *Trans. Amer. Geophys. Union*, Vol. 31, No. 3, pp. 393–397. 1950.

No. 496. Henry Stommel. Horizontal Diffusion Due to Oceanic Turbulence. *Sears Found., Jour. Mar. Res.*, Vol. 8, No. 3, pp. 199–225. 1949.

No. 497. David M. Pratt. Experimental Study of the Phosphorus Cycle in Fertilized Salt Water. *Sears Found., Jour. Mar. Res.*, Vol. 9, No. 1, pp. 29–54. 1950.

No. 498. Ivan Tolstoy and Maurice Ewing. North Atlantic Hydrography and the Mid-Atlantic Ridge. *Bull. Geol. Soc. Amer.*, Vol. 60, pp. 1527–1540. 1949.

No. 499. William S. von Arx. An Electromagnetic Method for Measuring the Velocities of Ocean Currents from a Ship Under Way. *Papers in Physical Oceanography and Meteorology*, Vol. 11, No. 3, pp. 1–62. 1950.

No. 500. Floyd M. Soule and C. A. Barnes. Physical Oceanography of the Ice Patrol Area in 1941. *U. S. Coast Guard Bull.*, No. 31, pp. 1–62. 1950.

No. 501. Alfred H. Woodcock. Condensation Nuclei and Precipitation. *Jour. Meteorology*, Vol. 7, No. 2, pp. 161–162. 1950.

No. 502. Andrew F. Bunker. Fluctuations of the Vertical Component of the Wind Associated with the Outflow of Cold Air from a Thunderstorm. *Bull. Amer. Meteorol. Soc.*, Vol. 31, No. 5, pp. 178–180. 1950.

No. 503. Henry Stommel. The Gulf Stream. A Brief History of the Ideas Concerning Its Cause. *The Scientific Monthly*, Vol. 70, No. 4, pp. 242–253. 1950.

No. 504. H. R. Seiwell. A New Mechanical Autocorrelator. *Review of Sci. Instruments*, Vol. 21, No. 5, pp. 481–484. 1950.

No. 505. H. R. Seiwell. Problems in Statistical Analyses of Geophysical Time Series. *Science*, Vol. 112, No. 2905, pp. 243–246. 1950.

No. 506. Ralph F. Vaccaro, Margaret P. Briggs, Cornelia L. Carey and Bostwick H. Ketchum. Viability of *Escherichia coli* in Sea Water. *Amer. Jour. Public Health*, Vol. 40, No. 10, pp. 1257–1266. 1950.

No. 507. Fred B. Phleger and William R. Walton. Ecology of Marsh and Bay Foraminifera, Barnstable, Mass. *Amer. Jour. Sci.*, Vol. 248, pp. 274–294. 1950.

No. 508. Jan Hahn. Some Aspects of Deep Sea Underwater Photography. *Jour. Photo. Soc. Amer.*, Sect. B. Phot. Sci. Tech., Vol. 16, No. 6, pp. 27–29. 1950.

No. 509. William S. von Arx. Some Current Meters Designed for Suspension from an Anchored Ship. *Sears Found., Jour. Mar. Res.*, Vol. 9, No. 2, pp. 93–99. 1950.

No. 510. Harry J. Turner, Jr. Report on Investigations of Methods of Improving the Shellfish Resources of Massachusetts. *Com. Mass., Dept. Cons., Div. Mar. Fish.*, pp. 1–22. 1949. (Included in *Collected Reprints* for 1950.)

No. 511. Henry B. Bigelow and William C. Schroeder. New and Little Known Cartilaginous Fishes from the Atlantic. *Bull. Mus. Comp. Zool.*, Vol. 103, No. 7, pp. 385–408. 1950.

No. 512. Henry W. Menard. Sediment Movement in Relation to Current Velocity. *Jour. Sed. Petrology*, Vol. 20, No. 3, pp. 148–160. 1950.

No. 513. B. Haurwitz and H. A. Panofsky. Stability and Meandering of the Gulf Stream. *Trans. Amer. Geoph. Union*, Vol. 31, No. 5, pp. 723–731. 1950.

No. 514. Alfred C. Redfield. Some Applications of Oceanography to Engineering Problems. *Jour. Boston Soc. Civil Eng.*, Vol. 37, No. 3, pp. 275–295. 1950.

No. 515. Bostwick H. Ketchum. Hydrographic Factors Involved in the Dispersion of Pollutants Introduced into Tidal Waters. *Jour. Boston Soc. Civil Eng.*, Vol. 37, No. 3, pp. 296–314. 1950.

No. 516. Bostwick H. Ketchum. The Exchanges of Fresh and Salt Waters in Tidal Estuaries. *Sears Found., Jour. Mar. Res.*, Vol. 10, No. 1, pp. 18–38. 1951.

No. 517. Alfred H. Woodcock. Impact Deposition of Atmospheric Sea Salts on a Test Plate. *Amer. Soc. for Testing Materials*, Vol. 50, pp. 1151–1166. 1950.

No. 518. Arthur R. Miller. A Study of Mixing Processes over the Edge of the Continental Shelf. *Sears Found., Jour. Mar. Res.*, Vol. 9, No. 2, pp. 145–160. 1950.

No. 519. Vern O. Knudsen, Alfred C. Redfield, Roger Revelle, and Robert R. Shrock. Education and Training for Oceanographers. *Science*, Vol. 111, No. 2895, pp. 700–703. 1950.

No. 520. George L. Clarke. Conservation and the Productivity of the Sea. *The Gamma Alpha Record*, Vol. 40, No. 4, pp. 95–101. 1950.

No. 521. H. R. Seiwell. Ocean Wave Analyses. In: Symposium on Applications of Autocorrelation Analysis to Physical Problems, Woods Hole, Massachusetts, 13–14 June 1949, *Office of Naval Research*, NAVEXOS–P–735, pp. 74–79. 1950.

No. 522. Alfred H. Woodcock and A. F. McBride. Wave-riding Dolphins. *Jour. Exper. Biol.*, Vol. 28, No. 2, pp. 215–217. 1951.

No. 523. John Northrop and Bruce C. Heezen. An Outcrop of Eocene Sediment on the Continental Slope. *Jour. Geology*, Vol. 59, No. 4, pp. 396–399. 1951.

No. 524. Henry Stommel. An Example of Thermal Convection. *Trans. Amer. Geophys. Union*, Vol. 31, No. 4, pp. 553–554. 1950.

No. 525. Alfred C. Redfield. Hemocyanin. In: Copper Metabolism, A Symposium on Animal, Plant and Soil Relationships, W. D. McElroy and B. Glass, Editors, Johns Hopkins University Press, pp. 174–190. 1950.

No. 526. William S. von Arx. Dead Reckoning by Surface Current Observation. *Jour. Inst. Navigation* (London), Vol. 4, No. 2, pp. 117–125. 1951.

No. 527. Patricia A. Langwell. Forced Convection Cell Circulation in Clear Air. *Trans. Amer. Geophys. Union*, Vol. 32, No. 1, pp. 7–14. 1951.

No. 528. Alfred H. Woodcock. Sea Salt in a Tropical Storm. *Jour. Meteorology*, Vol. 7, No. 6, pp. 397–401. 1950.

No. 529. Alfred C. Redfield. The Analysis of Tidal Phenomena in Narrow Embayments. *Papers in Physical Oceanography and Meteorology*, Vol. 11, No. 4, pp. 1–36. 1950.

No. 530. G. L. Clarke and D. F. Bumpus. The Plankton Sampler — An Instrument for Quantitative Plankton Investigations. *Amer. Soc. Limnol. and Oceanogr.*, Spec. Publ. No. 5 (revised), pp. 1–8. 1950.

No. 531. H. R. Seiwell. Experimental Correlogram Analyses of Artificial Time Series (with Special Reference to Analyses of Oceanographic Data). In: Proc. Second Berkeley Symposium on Mathematical Statistics and Probability, Univ. Calif. Press, pp. 639–666. 1951. (Published posthumously.)

No. 532. Henry Stommel. An Elementary Explanation of Why Ocean Currents are Strongest in the West. *Bull. Amer. Meteorol. Soc.*, Vol. 32, No. 1, pp. 21–23. 1951.

No. 533. Henry Stommel. Entrainment of Air into a Cumulus Cloud II. *Jour. Meteorol.*, Vol. 8, No. 2, pp. 127–129. 1951.

No. 534. Joanne Starr Malkus, Andrew F. Bunker and Kenneth McCasland. A Formation of Pileus-like Veil Clouds over Cape Cod, Massachusetts. *Bull. Amer. Meteorol. Soc.*, Vol. 32, No. 2, pp. 61-66. 1951.

No. 535. Hilary B. Moore. The Relation between the Scattering Layer and the Euphausiacea. *Biol. Bull.*, Vol. 99, No. 2, pp. 181–212. 1950.

No. 536. Bostwick H. Ketchum. The Flushing of Tidal Estuaries. *Sewage and Industrial Wastes*, Vol. 23, No. 2, pp. 198–209. 1951.

No. 537. Henry Stommel. Streaks of Natural Water Surfaces. In: International Symposium on Atmospheric Turbulence in the Boundary Layer. Mass. Inst. Tech., 4–8 June, 1951. *Geophys. Res. Pap., Air Force Cambridge Research Center*, No. 19, pp. 145–154. 1952.

No. 538. Henry Stommel. Streaks on Natural Water Surfaces. *Weather*, Vol. 6, No. 3, pp. 72–74. 1951.

No. 539. Edward S. Castle. Electrical Control of Marine Fouling. *Ind. Eng. Chem.*, Vol. 43, No. 4, pp. 901–904. 1951.

No. 540. Rushdi Said. Organic Origin of some Calcareous Sediments from the Red Sea. *Science*, Vol. 113, No. 2940, pp. 517–518. 1951.

No. 541. Rushdi Said. Preliminary Note on the Spectroscopic Distribution of Elements in the Shells of some Recent Calcareous Foraminifera. *Contr. Cushman Found. Foram. Res.*, Vol. 2, Pt. 1, pp. 11–13. 1951.

No. 542. Gordon A. Riley. Oxygen, Phosphate and Nitrate in the Atlantic Ocean. *Bull. Bingham Oceanographic Coll.*, Vol. 13, Art. 1, pp. 1–126. 1951. (Not included in *Collected Reprints.*)

No. 543. J. Lamar Worzel and Maurice Ewing. Gravity Measurements at Sea, 1947. *Trans. Amer. Geophys. Union*, Vol. 31, No. 6, pp. 917–923. 1950.

No. 544. Arnold B. Arons and Henry Stommel. A Mixing-length Theory of Tidal Flushing. *Trans. Amer. Geophys. Union*, Vol. 32, No. 3, pp. 419–421. 1951.

No. 545. Arthur A. Klebba and Henry Stommel. A Simple Demonstration of Coriolis Force. *Amer. Jour. Physics*, Vol. 19, No. 4, p. 247. 1951.

No. 546. Henry W. Menard and A. J. Boucot. Experiments on the Movement of Shells by Water. *Amer. Jour. Sci.*, Vol. 249, No. 2, pp. 131–151. 1951.

No. 547. E. W. Roelofs and D. F. Bumpus. The Hydrography of Pamlico Sound. *Bull. Mar. Sci. Gulf and Caribbean*, Vol 3, No. 3, pp. 181–205. 1953.

No. 548. Frederick C. Fuglister and L. V. Worthington. Some Results of a Multiple Ship Survey of the Gulf Stream. *Tellus*, Vol. 3, No. 1, pp. 1–14. 1951.

No. 549. Bostwick H. Ketchum, Alfred C. Redfield and John C. Ayers. The Oceanography of the New York Bight. *Papers in Physical Oceanography and Meteorology*, Vol. 12, No. 1, pp. 1–46. 1951.

No. 550. Floyd M. Soule. Physical Oceanography of the Grand Banks Region, the Labrador Sea and Davis Strait in 1949. *U. S. Coast Guard Bull.*, No. 35, pp. 49–116. 1951.

No. 551. Floyd M. Soule. Physical Oceanography of the Grand Banks Region and the Labrador Sea in 1950. *U. S. Coast Guard Bull.*, No. 36, pp. 61–127. 1951.

No. 552. Henry Stommel. Determination of the Lateral Eddy Diffusivity in the Climatological Mean Gulf Stream. *Tellus*, Vol. 3, No. 1, p. 43. 1951.

No. 553. Henry Stommel and Alfred H. Woodcock. Diurnal Heating of the Surface of the Gulf of Mexico in the Spring of 1942. *Trans. Amer. Geophys. Union*, Vol. 32, No. 4, pp. 565–571. 1951.

No. 554. Henry B. Bigelow and William C. Schroeder. A New Genus and Species of Anacanthobatid Skate from the Gulf of Mexico. *Journ. Wash. Acad. Sci.*, Vol. 41, No. 3, pp. 110–113. 1951.

No. 555. Henry B. Bigelow and William C. Schroeder. Three New Skates and a New Chimaerid Fish from the Gulf of Mexico. *Journ. Wash. Acad. Sci.*, Vol. 41, No. 12, pp. 383–392. 1951.

No. 556. Martin J. Pollak. The Sources of the Deep Water of the Eastern Mediterranean Sea. *Sears Found., Jour. Mar. Res.*, Vol. 10, No. 1, pp. 128–152. 1951.

No. 557. Frederick C. Fuglister. Annual Variations in Current Speeds in the Gulf Stream System. *Sears Found., Jour. Mar. Res.*, Vol. 10, No. 1, pp. 119–127. 1951.

No. 558. Donald Parson and Andrew F. Bunker. A Recording Computer for the Direct Measurement of the Turbulent Heat Exchange in the Atmosphere. In: International Symposium on Atmospheric Turbulence in the Boundary Layer. Mass. Inst. Tech., 4–8 June, 1951. *Geophys. Res. Pap., Air Force Cambridge Research Center*, No. 19, pp. 369–379. 1952.

No. 559. Ivan Tolstoy. Submarine Topography in the North Atlantic. *Bull. Geol. Soc. Amer.*, Vol. 62, No. 5, pp. 441–450. 1951.

No. 560. Hilary B. Moore. The Seasonal Distribution of Oceanic Birds in the Western North Atlantic. *Bull. Mar. Sci. Gulf and Caribbean*, Vol. 1, No. 1, pp. 1–14. 1951.

No. 561. Bostwick H. Ketchum, John C. Ayers and Ralph F. Vaccaro. Processes Contributing to the Decrease of Coliform Bacteria in a Tidal Estuary. *Ecology*, Vol. 33, No. 2, pp. 247–258. 1952.

No. 562. J. B. Hersey, H. R. Johnson and L. C. Davis. Recent Findings about the Deep Scattering Layer. *Sears Found., Jour. Mar. Res.*, Vol. 11, No. 1, pp. 1–9. 1952.

No. 563. Alfred H. Woodcock. Atmospheric Salt Particles and Raindrops. *Jour. Meteorol.*, Vol. 9, No. 3, pp. 200–212. 1952.

No. 564. Harry J. Turner, Jr., David B. Sawyer, Carl N. Shuster, Jr., and Julius A. Posgay. Third Report on Investigations of Methods of Improving the Shellfish Resources of Massachusetts. *Com. Mass., Dept. Cons., Div. Mar. Fish.*, pp. 1–31. 1951.

No. 565. Fred B. Phleger. Ecology of Foraminifera, Northwest Gulf of Mexico. Part I. Foraminifera Distribution. *Mem. Geol. Soc. Amer.*, No. 46, pp. 1–88. 1951. (Not included in *Collected Reprints*.)

No. 566. Fred B. Phleger and Frances L. Parker. Ecology of Foraminifera, Northwest Gulf of Mexico. Part II. Foraminifera Species. *Mem. Geol. Soc. Amer.*, No. 46, pp. 1–64. 1951. (Not included in *Collected Reprints*.)

No. 567. Bostwick H. Ketchum and William L. Ford. Rate of Dispersion in the Wake of a Barge at Sea. *Trans. Amer. Geophys. Union*, Vol. 33, No. 5, pp. 680–684. 1952.

No. 568. Patricia A. Langwell. The Onset of Rain from Cumuli. *Jour. Meteorol.*, Vol. 8, No. 5, pp. 354–356. 1951.

No. 569. Stefan Machlup. A Theoretical Model for Sound Scattering by Marine Crustaceans. *Jour. Acoust. Soc. Amer.*, Vol. 24, No. 3, pp. 290–293. 1952.

No. 570. Henry B. Bigelow and William C. Schroeder. Fishes of the Western North Atlantic. Sawfishes, Guitarfishes, Skates and Rays. *Mem. Sears Found. Mar. Res.*, No. 1, Pt. 2, Ch. 1, pp. 1–514. 1953. (Not included in *Collected Reprints*.)

No. 571. Henry B. Bigelow and William C. Schroeder. Fishes of the Western North Atlantic. Chimaeroids. *Mem. Sears. Found. Mar. Res.*, No. 1, Pt. 2, Ch. 2, pp. 515–562. Index to Chs. 1 and 2, pp. 563–588. 1953. (Not included in *Collected Reprints*.)

No. 572. Andrew F. Bunker. Recognition of the Presence of Convective Currents within a Nonsaturated Turbulent Layer of the Atmosphere. In: International Symposium on Atmospheric Turbulence in the Boundary Layer. Mass. Inst. Tech., 4–8 June, 1951. *Geophys. Res. Pap., Air Force Cambridge Research Center*, No. 19, pp. 309–322. 1952.

No. 573. John Northrop. Ocean-bottom Photographs of the Neritic and Bathyal Environment South of Cape Cod, Massachusetts. *Bull. Geol. Soc. Amer.*, Vol. 62, No. 12, pp. 1381–1384. 1951.

No. 574. I. I. Schell. Stability and Mutual Compensation of Relationships with the Iceberg Severity off Newfoundland. *Trans. Amer. Geophys. Union*, Vol. 33, No. 1, pp. 27–31. 1952.

No. 575. D. B. Ericson, Maurice Ewing and Bruce C. Heezen. Deep-sea Sands and Submarine Canyons. *Bull. Geol. Soc. Amer.*, Vol. 62, No. 8, pp. 961–965. 1951.

No. 576. R. B. Montgomery. The Present Position of the Study of Exchange across the Ocean-Atmosphere Interface. In: International Symposium on Atmospheric Turbulence in the Boundary Layer. Mass. Inst. Tech., 4–8 June, 1951. *Geophys. Res. Pap., Air Force Cambridge Research Center*, No. 19, pp. 131–140. 1952.

No. 577. Gordon A. Riley. Parameters of Turbulence in the Sea. *Sears Found., Jour. Mar. Res.*, Vol. 10, No. 3, pp. 247–256. 1951.

No. 578. Gordon A. Riley. Hydrography of the Long Island and Block Island Sounds. *Bull. Bingham Oceanographic Coll.*, Vol. 13, Art. 3, pp. 5–39. 1952.

No. 579. Gordon A. Riley. Phytoplankton of Block Island Sound, 1949. *Bull. Bingham Oceanographic Coll.*, Vol. 13, Art. 3, pp. 40–64. 1952.

No. 580. Woods Hole Oceanographic Institution. Marine Fouling and its Prevention. U. S. Naval Inst., Annapolis, Md. 388 pp. 1952. (Not included in *Collected Reprints*.)

No. 581. Hilary B. Moore. Physical Factors Affecting the Distribution of Euphausids in the North Atlantic. *Bull. Mar. Sci. Gulf and Caribbean*, Vol. 1, No. 4, pp. 278–305. 1952.

No. 582. Henry A. Kierstead. Bottom Pressure Fluctuations due to Standing Waves in a Deep, Two-Layer Ocean. *Trans. Amer. Geophys. Union*, Vol. 33, No. 3, pp. 30–9 396. 1952.

No. 583. J. B. Hersey, Charles B. Officer, H. R. Johnson, and S. Bergstrom. Seismic Refraction Observations North of the Brownson Deep. *Bull. Seismol. Soc. Amer.*, Vol. 42, No. 4, pp. 291–306. 1952.

No. 584. Frederick C. Fuglister. Multiple Currents in the Gulf Stream System. *Tellus*, Vol. 3, No. 4, pp. 230–233. 1951.

No. 585. Gerald B. Collins. Factors Influencing the Orientation of Migrating Anadromous Fishes. Fish and Wildlife Service, Vol. 52, *Fish. Bull.* 73, pp. 375–396. 1952.

No. 586. Alfred C. Redfield and Lionel A. Walford. A Study of the Disposal of Chemical Waste at Sea. Report of the Committee for Investigation of Waste Disposal. *Nat. Res. Council*, Publ. 201, 49 pp. 1951.

No. 587. Henry Stommel and Harlow G. Farmer. Control of Salinity in an Estuary by a Transition. *Sears Found., Jour. Mar. Res.*, Vol. 12, No. 1, pp. 13–20. 1953.

No. 588. Rushdi Said. Foraminifera of Great Pond, East Falmouth, Massachusetts. *Contr. Cushman Found. Foram. Res.*, Vol. 4, Pt. 1, pp. 7–14. 1953.

No. 589. Frances L. Parker. Foraminifera Species off Portsmouth, New Hampshire. *Bull. Mus. Comp. Zool.*, Vol. 106, No. 9, pp. 391–423. 1952.

No. 590. Frances L. Parker. Foraminiferal Distribution in the Long Island Sound-Buzzards Bay Area. *Bull. Mus. Comp. Zool.*, Vol. 106, No. 10, pp. 427–473. 1952.

No. 591. Fred B. Phleger. Foraminifera Ecology off Portsmouth, New Hampshire. *Bull. Mus. Comp. Zool.*, Vol. 106, No. 8, pp. 315–390. 1952.

No. 592. Henry B. Bigelow and William C. Schroeder. Fishes of the Gulf of Maine. Fish and Wildlife Service, Vol. 53, *Fish. Bull.* 74, pp. i–viii, 1–577. 1953. (Not included in *Collected Reprints.*)

No. 593. Bostwick H. Ketchum and D. Jean Keen. The Exchanges of Fresh and Salt Waters in the Bay of Fundy and in Passamaquoddy Bay. *Jour. Fish. Res. Bd. Canada*, Vol. 10, No. 3, pp. 97–124. 1953.

No. 594. I. I. Schell. The Problem of the Iceberg Population in Baffin Bay and Davis Strait and Advance Estimate of the Berg Count off Newfoundland. *Jour. Glaciology*, Vol. 2, No. 11, pp. 58–59. 1952.

No. 595. Joanne Starr Malkus. Recent Advances in the Study of Convective Clouds and their Interaction with the Environment. *Tellus*, Vol. 4, No. 2, pp. 71–87. 1952.

No. 596. Henry B. Bigelow, William C. Schroeder and Stewart Springer. New and Little Known Sharks from the Atlantic and from the Gulf of Mexico. *Bull. Mus. Comp. Zool.*, Vol. 109, No. 3, pp. 213–276. 1953.

No. 597. George T. Scott and Hugh R. Haywood. Sodium and Potassium Regulation in *Ulva lactuca* and *Valonia macrophysa*. In: Electrolytes in Biological Systems, pp. 35–64. 1955.

No. 598. Bostwick H. Ketchum. Relation between Circulation and Planktonic Populations in Estuaries, *Ecology*, Vol. 35, No. 2, pp. 191–200. 1954.

No. 599. Frank J. Mather, III. Three Species of Fishes, Genus *Seriola*, in the Waters of Cape Cod and Vicinity. *Copeia*, No. 3, pp. 209–210. 1952.

No. 600. Jeffries Wyman, Jr., P. F. Scholander, G. A. Edwards and L. Irving. On the Stability of Gas Bubbles in Sea Water. *Sears Found., Jour. Mar. Res.*, Vol. 11, No. 1, pp. 47–62. 1952.

No. 601. Floyd M. Soule, P. S. Branson and R. P. Dinsmore. Physical Oceanography of the Grand Banks Region and the Labrador Sea in 1951. *U. S. Coast Guard Bull.*, No. 37, pp. 17–85. 1952.

No. 602. Mary Sears. Notes on Siphonophores. 2. A Revision of the Abylinae. *Bull. Mus. Comp. Zool.*, Vol. 109, No. 1, pp. 1–119. 1953. (Not included in *Collected Reprints*.)

No. 603. I. I. Schell. On the Role of the Ice off Iceland in the Decadal Air Temperatures of Iceland, and some other Areas. *Jour. du Conseil*, Vol. 18, No. 1, pp. 11–36. 1952.

No. 604. D. B. Ericson, Maurice Ewing and Bruce C. Heezen. Turbidity Currents and Sediments in the North Atlantic. *Bull. Amer. Assoc. Petrol. Geol.*, Vol. 36, No. 3, pp. 489–511. 1952.

No. 605. Andrew F. Bunker. On the Determination of Moisture Gradients from Radiosonde Records. *Bull. Amer. Meteorol. Soc.*, Vol. 34, No. 9, pp. 406–409. 1953.

No. 606. Frank J. Mather, III and Howard A. Schuck. Additional Notes on the Distribution of the Blackfin Tuna (*Parathunnus atlanticus*). *Copeia*, No. 4, p. 267. 1952.

No. 607. Mary Sears. Notes on Siphonophores. 3. *Nectopyramis spinosa* n. sp. *Breviora*, No. 3, pp. 1–4. 1952.

No. 608. W. V. R. Malkus and M. E. Stern. Determination of Ocean Transports and Velocities by Electromagnetic Effects. *Sears Found., Jour. Mar. Res.*, Vol. 11, No. 2, pp. 97–105. 1952.

No. 609. Joanne Starr Malkus. The Slopes of Cumulus Clouds in Relation to External Wind Shear. *Quart. Jour. Roy. Meteor. Soc.*, Vol. 78, No. 338, pp. 530–542. 1952.

No. 610. Henry B. Bigelow and William C. Schroeder. A New Species of the Cyclostome Genus *Paramyxine* from the Gulf of Mexico. *Breviora*, No. 8, pp. 1–10. 1952.

No. 611. Frank J. Mather, III. Sport Fishes of the Vicinity of the Gulf of Honduras, certain Caribbean Islands, and Carmen, Mexico. *Proc. Gulf and Caribbean Fish. Inst.*, pp. 118–129. 1952.

No. 612. C. O'D. Iselin. The Gulf Stream System. *Proc. Amer. Philos. Soc.*, Vol. 96, No. 6, pp. 660–662. 1952.

No. 613. Frederick B. Laidlaw. The History of the Prevention of Fouling. *U. S. Naval Inst. Proc.*, Vol. 78, No. 7, Whole No. 593, pp. 768–779. 1952.

No. 614. Gary Felsenfeld. The Binding of Copper by Hemocyanin. *Jour. Cell. and Comp. Physiol.*, Vol. 43, No. 1, pp. 23–38. 1954.

No. 615. Harry J. Turner, Jr. Fourth Report on Investigations of the Shellfisheries of Massachusetts. *Com. Mass., Dept. Cons., Div. Mar. Fish.*, pp. 1–21. 1951.

No. 616. Henry Stommel and Harlow G. Farmer. Abrupt Change in Width in Two-Layer Open Channel Flow. *Sears Found., Jour. Mar. Res.*, Vol. 11, No. 2, pp. 205–214. 1952.

No. 617. Joanne Starr Malkus and Andrew F. Bunker. Observational Studies of the Air Flow over Nantucket Island during the Summer of 1950. *Papers in Physical Oceanography and Meteorology*, Vol. 12, No. 2, pp. 1–50. 1952.

No. 618. Andrew F. Bunker. Measurements of the Vertical Water Vapor Transport and Distribution within Unstable Atmospheric Ground Layers and the Turbulent Mass Exchange Coefficient. *Papers in Physical Oceanography and Meteorology*, Vol. 12, No. 3, pp. 1–42. 1952.

No. 619. William L. Ford and A. R. Miller. The Surface Layer of the Gulf Stream and Adjacent Waters. *Sears Found., Jour. Mar. Res.*, Vol. 11, No. 3, pp. 267–280. 1952.

No. 620. Willem V. R. Malkus. The Heat Transport and Spectrum of Thermal Turbulence. *Proc. Roy. Soc.*, A, Vol. 225, pp. 196–212. 1954. (Not included in *Collected Reprints.*)

No. 621. William S. von Arx. Notes on the Surface Velocity Profile and Horizontal Shear across the Width of the Gulf Stream. *Tellus*, Vol. 4, No. 3, pp. 211–214. 1952.

No. 622. William S. von Arx. A Laboratory Study of the Wind-driven Ocean Circulation. *Tellus*, Vol. 4, No. 4, pp. 311–318. 1952.

No. 623. Helen S. Vishniac and S. W. Watson. The Steroid Requirements of *Labyrinthula vitellina* var. *pacifica*. *Jour. Gen. Microbiol.*, Vol. 8, No. 2, pp. 248–255. 1953.

No. 624. Joanne Starr Malkus and Melvin E. Stern. The Flow of a Stable Atmosphere over a Heated Island, Part I. *Jour. Meteorology*, Vol. 10, No. 1, pp. 30–41. 1953.

No. 625. Melvin E. Stern and Joanne Starr Malkus. The Flow of a Stable Atmosphere over a Heated Island, Part II. *Jour. Meteorology*, Vol. 10, No. 2, pp. 105–120. 1953.

No. 626. William E. Schevill. On the Nomenclature of the Pacific Gray Whale. *Breviora*, No. 7, pp. 1–3. 1952.

No. 627. Alfred C. Redfield. The Flushing of Harbors and other Hydrodynamic Problems in Coastal Waters. In: *Hydrodynamics in Modern Technology*, Mass. Inst. Tech., pp. 127–135, December 1951.

No. 628. L. V. Worthington. Oceanographic Results of Project Skijump I and Skijump II in the Polar Sea, 1951–1952. *Trans. Amer. Geophys. Union*, Vol. 34, No. 4, pp. 543–551. 1953.

No. 629. Charles B. Officer, Jr. The Refraction Arrival in Water Covered Areas. *Geophysics*, Vol. 18, No. 4, pp. 805–819. 1953.

No. 630. Harry J. Turner, Jr. The Drilling Mechanism of the Naticidae. *Ecology*, Vol. 34, No. 1, pp. 222–223. 1953.

No. 631. Andrew F. Bunker. Diffusion, Entrainment and Frictional Drag Associated with Non-Saturated, Buoyant Air Parcels rising through a Turbulent Air Mass. *Jour. Meteorology*, Vol. 10, No. 3, pp. 212–218. 1953.

No. 632. P. F. Scholander and L. van Dam. Composition of the Swimbladder Gas in Deep Sea Fishes. *Biol. Bull.*, Vol 104, No. 1, pp. 75–86. 1953.

No. 633. L. van Dam and P. F. Scholander. Concentration of Hemoglobin in the Blood of Deep Sea Fishes. *Jour. Cell. and Comp. Physiol.*, Vol. 41, No. 3, pp. 522–524. 1953.

No. 634. Willem V. R. Malkus. A Recording Bathypitotmeter. *Sears Found., Jour. Mar. Res.*, Vol. 12, No. 1, pp. 51–59. 1953.

No. 635. A. B. Arons and C. F. Kientzler. Vapor Pressure of Sea Salt Solutions. *Trans. Amer. Geophys. Union*, Vol. 35, No. 5, pp. 722–728. 1954.

No. 636. Alfred C. Redfield. Interference Phenomena in the Tides of the Woods Hole Region. *Sears Found., Jour. Mar. Res.*, Vol. 12, No. 1, pp. 121–140. 1953.

No. 637. Floyd M. Soule. Physical Oceanography of the Grand Banks Region and the Labrador Sea in 1952. *U. S. Coast Guard Bull.*, No. 38, pp. 31–100. 1953.

No. 638. Harlow G. Farmer and George W. Morgan. The Salt Wedge. *Proc. Third Conf. on Coastal Engineering*, Cambridge, Mass., October 1952, pp. 54–64. 1953.

No. 639. J. R. D. Francis. A Note on the Velocity Distribution and Bottom Stress in a Wind-Driven Water Current System. *Sears Found., Jour. Mar. Res.*, Vol. 12, No. 1, pp. 93–98. 1953.

No. 640. Henry Stommel. Computation of Pollution in a Vertically Mixed Estuary *Sewage and Industrial Wastes*, Vol. 25, No. 9, pp. 1065–1071. 1953.

No. 641. Jack L. Hough. Pleistocene Climatic Record in a Pacific Ocean Core Sample. *Jour. Geology*, Vol. 61, No. 3, pp. 252–262. 1953.

No. 642. Bostwick H. Ketchum. Circulation in Estuaries. *Proc. Third Conf. on Coastal Engineering*, Cambridge, Mass., October 1952, pp. 65–76. 1953.

No. 643. A. H. Woodcock. Salt Nuclei in Marine Air as a Function of Altitude and Wind Force. *Jour. Meteorology*, Vol. 10, No. 5, pp. 362–371. 1953.

No. 644. Henry Stommel, W. S. von Arx, D. Parson and W. S. Richardson. Rapid Aerial Survey of Gulf Stream with Camera and Radiation Thermometer. *Science*, Vol. 117, No. 3049, pp. 639–640. 1953.

No. 645. Henry Stommel. Examples of the Possible Role of Inertia and Stratification in the Dynamics of the Gulf Stream System. *Sears Found., Jour. Mar. Res.*, Vol. 12, No. 2, pp. 184–195. 1953.

No. 646. Henry C. Stetson. The Sediments of the Western Gulf of Mexico. Part I. The Continental Terrace of the Western Gulf of Mexico: its Surface Sediments, Origin and Development. *Papers in Physical Oceanography and Meteorology*, Vol. 12, No. 4, pp. 1–45. 1953.

No. 647. Parker D. Trask. The Sediments of the Western Gulf of Mexico. Part II. Chemical Studies of Sediments of the Western Gulf of Mexico. *Papers in Physical Oceanography and Meteorology*, Vol. 12, No. 4, pp. 47–120. 1953.

No. 648. William E. Schevill and Barbara Lawrence. Auditory Response of a Bottle-nosed Porpoise, *Tursiops truncatus*, to Frequencies above 100 kc. *Jour. Exper. Zool.*, Vol. 124, No. 1, pp. 147–165. 1953.

No. 649. William S. von Arx. Cartographic Principles Applied to Wide-Field Photography. *Photogr. Engineering*, Vol. 4, No. 2, pp. 60–73. 1953.

No. 650. Betty Lee Gealy. Topography of the Continental Slope in Northwest Gulf of Mexico. *Bull. Geol. Soc. Amer.*, Vol. 66, No. 2, pp. 203–227. 1955.

No. 651. Frank J. Mather III and C. Godfrey Day. Observations of Pelagic Fishes of the Tropical Atlantic. *Copeia*, No. 3, pp. 179–188. 1954.

No. 652. Joseph Chase. A Comparison of Certain North Atlantic Wind, Tide Gauge and Current Data. *Sears Found., Jour. Mar. Res.*, Vol. 13, No. 1, pp. 22–31. 1954.

No. 653. Barbara Lawrence and William E. Schevill. *Tursiops* as an Experimental Subject. *Jour. Mammalogy*, Vol. 35, No. 2, pp. 225–232. 1954.

No. 654. William E. Schevill. Sight Records of the Gray Grampus, *Grampus griseus* (Cuvier). *Jour. Mammalogy*, Vol. 35, No. 1, pp. 123–124. 1954.

No. 655. Henry Stommel. The Role of Density Currents in Estuaries. *Proc. Minnesota Int. Hydraulics Conv.*, Sept. 1–4, 1953, pp. 305–312. 1953.

No. 656. Harry J. Turner, Jr. Fifth Report on Investigations of the Shellfisheries of Massachusetts. *Com. Mass., Dept. Cons., Div. Mar. Fish.*, pp. 1–37. 1952.

No. 657. Henry B. Bigelow and William C. Schroeder. A New Family, a New Genus, and Two New Species of Batoid Fishes from the Gulf of Mexico. *Breviora*, No. 24, 16 pp. 1954.

No. 658. Duncan C. Blanchard. Raindrop Size-Distribution in Hawaiian Rains. *Jour. Meteorology*, Vol. 10, No. 6, pp. 457–473. 1953.

No. 659. Duncan C. Blanchard. A Simple Recording Technique for Determining Raindrop Size and Time of Occurrence of Rain Showers. *Trans. Amer. Geophys. Union*, Vol. 34, No. 4, pp. 534–538. 1953.

No. 660. A. H. Woodcock. Hawaii as a Cloud Physics Laboratory. *Pacific Science*, Vol. 7, No. 4, pp. 522–524. 1953.

No. 661. Daniel R. Norton, Mary A. Plunkett and Francis A. Richards. Spectrophotometric Determination of Uric Acid and Some Redeterminations of its Solubility, *Analytical Chemistry*, Vol. 26, No. 3, pp. 454–457. 1954.

No. 662. C. B. Officer, Jr. and Maurice Ewing. Geophysical Investigations in the Emerged and Submerged Atlantic Coastal Plain. *Bull. Geol. Soc. Amer.*, Vol. 65, pp. 653–670. 1954.

No. 663. William E. Schevill and Barbara Lawrence. High-Frequency Auditory Response of a Bottlenosed Porpoise, *Tursiops truncatus* (Montagu). *Jour. Acoust. Soc. Amer.*, Vol. 25, No. 5, pp. 1016–1017. 1953.

No. 664. R. B. Montgomery. Analysis of a Hugh M. Smith Oceanographic Section from Honolulu Southward across the Equator. *Sears Found., Journ. Mar. Res.*, Vol. 13, No. 1, pp. 67–75. 1954.

No. 665. C. H. Keith and A. B. Arons. The Growth of Sea-Salt Particles by Condensation of Atmospheric Water Vapor. *Jour. Meteorology*, Vol. 11, No. 3, pp. 173–184. 1954.

No. 666. L. V. Worthington. The Temperature Increase in Caribbean Deep Water since 1933. *Deep-Sea Research*, Vol. 3, pp. 234–235. 1956.

No. 667. Joanne Starr Malkus. Some Results of a Trade-Cumulus Cloud Investigation. *Jour. Meteorology*, Vol. 11, No. 3, pp. 220–237. 1954.

No. 668. F. C. Fuglister. Average Temperature and Salinity at a Depth of 200 Meters in the North Atlantic. *Tellus*, Vol. 6, No. 1, pp. 46–58. 1954.

No. 669. Hilary B. Moore, Harding Owre, Everett C. Jones and T. Dow. Plankton of the Florida Current. III. The Control of the Vertical Distribution of Zooplankton in the Daytime by Light and Temperature. *Bull. Mar. Sci. Gulf and Caribbean*, Vol. 3, No. 2, pp. 83–95. 1953.

No. 670. Willem V. R. Malkus. Discrete Transitions in Turbulent Convection. *Proc. Roy. Soc.*, A, Vol. 225, pp. 185–195. 1954. (Not included in *Collected Reprints*.)

No. 671. Mary Sears. Notes on the Peruvian Coastal Current. 1. An Introduction to the Ecology of Pisco Bay. *Deep-Sea Research*, Vol. 1, pp. 141–169. (Also published as: Notas sobre la Corriente Costanera del Peru. 1. Introduccion a la Ecologia de la Bahia de Pisco. *Bol. Cient. Cia. Admora. Guano*, Lima, Peru, Vol. 1, No. 2, pp. 133–179). 1954.

No. 672. Ralph F. Wyrick. Observations on the Movements of the Pacific Gray Whale *Eschrichtius glaucus* (Cope). *Journ. Mammalogy*, Vol. 35, No. 4, pp. 596–598. 1954.

No. 673. A. H. WOODCOCK, C. F. KIENTZLER, A. B. ARONS and D. C. BLANCHARD. Giant Condensation Nuclei from Bursting Bubbles. *Nature*, Vol. 172, No. 4390, pp. 1144–1145. 1953.

No. 674. HARRY J. TURNER, JR. An Improved Method of Staining the External Organelles of Hypotrichs. *Jour. Protozoology*, Vol. 1, No. 1, pp. 18–19. 1954.

No. 675. FLOYD M. SOULE, A. J. BUSH and J. E. MURRAY. Physical Oceanography of the Grand Banks Region and the Laborador Sea in 1953. *U. S. Coast Guard Bull.*, No. 39, pp. 45–138. 1955.

No. 676. J. B. HERSEY and R. H. BACKUS. New Evidence that Migrating Gas Bubbles, Probably the Swimbladders of Fish, are Largely Responsible for Scattering Layers on the Continental Rise South of New England. *Deep-Sea Research*, Vol. 1, pp. 190–191. 1954.

No. 677. ILMO HELA, HILARY B. MOORE and HARDING OWRE. Seasonal Changes in the Surface Water Masses and in their Plankton in the Bermuda Area. *Bull. Mar. Sci. Gulf and Caribbean*, Vol. 3, No. 3, pp. 157–167. 1953.

No. 678. B. HAURWITZ. The Occurrence of Internal Tides in the Ocean. *Arch. Meteorol. Geoph. u. Bioklim.*, Ser. A, Meteorol. und Geoph., Band 7, pp. 406–424. 1954.

No. 679. GUNTHER K. WERTHEIM. Studies of the Electric Potential between Key West, Florida, and Havana, Cuba. *Trans. Amer. Geophys. Union*, Vol. 35, No. 6, pp. 872–882. 1954.

No. 680. JOHN C. AYERS. A Method for Rendering Wood Resistant to Marine Borers. *Bull. Mar. Sci. Gulf and Caribbean*, Vol. 3, No. 4, pp. 297–304. 1954.

No. 681. WILLIAM S. VON ARX. Some Techniques for Laboratory Study of the Primary Ocean Circulation. Fluid Models in Geophysics. In: Proc. First Symp., Models in Geophysical Fluid Dynamics, The Johns Hopkins University, Sept. 1–4, 1953, pp. 89–99. 1956.

No. 682. A. F. BUNKER. Measurements of Counter-Gradient Heat Flows in the Atmosphere. *Australian Jour. Physics*, Vol. 9, No. 1, pp. 133–143. 1956.

No. 683. R. F. VACCARO and J. H. RYTHER. The Bactericidal Effects of Sunlight in Relation to "Light" and "Dark" Bottle Photosynthesis Experiments. *Jour. du Conseil*, Vol. 20, No. 1, pp. 18–24. 1954.

No. 684. J. H. RYTHER and R. F. VACCARO. A Comparison of the Oxygen and 14C Methods of Measuring Marine Photosynthesis. *Jour. du Conseil*, Vol. 20, No. 1, pp. 25–34. 1954.

No. 685. JOHN H. RYTHER. The Ecology of Phytoplankton Blooms in Moriches Bay and Great South Bay, Long Island, New York. *Biol. Bull.*, Vol. 106, No. 2, pp. 198–209. 1954.

No. 686. E. E. WATSON. An Experiment to Determine the Hydrodynamic Forces on a Cable Inclined to the Direction of Flow. *Sears Found., Jour. Mar. Res.*, Vol. 12, No. 3, pp. 245–248. 1953.

No. 687. BOSTWICK H. KETCHUM. Mineral Nutrition of Phytoplankton. *Ann. Rev. Plant Physiol.*, Vol. 5, pp. 55–74. 1954.

No. 688. FRANCIS A. RICHARDS and ALFRED C. REDFIELD. Oxygen-Density Relationships in the Western North Atlantic. *Deep-Sea Research*, Vol. 2, pp. 182–199. 1955.

No. 689. WILLIAM S. VON ARX. Measurements of the Oceanic Circulation in Temperate and Tropical Latitudes. In: Oceanographic Instrumentation. *National Research Council Publ.*, No. 309, pp. 13–35. 1954.

No. 690. M. S. LONGUET-HIGGINS, M. E. STERN and HENRY STOMMEL. The Electrical Field Induced by Ocean Currents and Waves, with Applications to the Method of Towed Electrodes. *Papers in Physical Oceanography and Meteorology*, Vol. 13, No. 1, pp. 1–37. 1954.

No. 691. C. F. KIENTZLER, A. B. ARONS, D. C. BLANCHARD and A. H. WOODCOCK. Photographic Investigation of the Projection of Droplets by Bubbles Bursting at a Water Surface. *Tellus*, Vol. 6, No. 1, pp. 1–7. 1954.

No. 692. HENRY B. BIGELOW and WILLIAM C. SCHROEDER. Deep Water Elasmobranchs and Chimaeroids from the Northwestern Atlantic Slope. *Bull. Mus. Comp. Zool.*, Vol. 112, No. 2, pp. 37–87. 1954.

No. 693. HENRY STOMMEL. Exploratory Measurements of Electrical Potential Differences between Widely Spaced Points in the North Atlantic Ocean. *Arch. Meteorol., Geoph. u. Bioklim.*, Ser. A, Meteorol. und Geoph., Band 7, pp. 292–304. 1954.

No. 694. L. V. WORTHINGTON. Three Detailed Cross-Sections of the Gulf Stream. *Tellus*, Vol. 6, No. 2, pp. 116–123. 1954.

No. 695. FRANCIS A. RICHARDS and ALFRED C. REDFIELD. A Correlation between the Oxygen Content of Sea Water and the Organic Content of Marine Sediments. *Deep-Sea Research*, Vol. 1, pp. 279–281. 1954.

No. 696. ALLYN C. VINE. Oceanographic Instruments for Measuring Temperature. In: Oceanographic Instrumentation. *National Research Council Publ.*, No. 309, pp. 55–69. 1954.

No. 697. J. B. HERSEY. Acoustic Instrumentation as a Tool in Oceanography. In: Oceanographic Instrumentation. *National Research Council Publ.*, No. 309, pp. 101–122. 1954.

No. 698. A. B. ARONS. Underwater Explosion Shock Wave Parameters at Large Distances from the Charge. *Jour. Acoust. Soc. Amer.*, Vol. 26, No. 3, pp. 343–346. 1954.

No. 699. P. F. SCHOLANDER and L. VAN DAM. Secretion of Gases against High Pressures in the Swimbladder of Deep Sea Fishes. I. Oxygen Dissociation in Blood. *Biol. Bull.*, Vol. 107, No. 2, pp. 247–259. 1954.

No. 700. P. F. SCHOLANDER. Secretion of Gases against High Pressures in the Swimbladder of Deep Sea Fishes. II. The Rete Mirabile. *Biol. Bull.*, Vol. 107, No. 2, pp. 260–277. 1954.

No. 701. R. B. MONTGOMERY. Convection of Heat. *Arch. Meteorol., Geoph. u. Bioklim.*, Ser. A, Meteorol. und Geoph., Band 7, pp. 125–132. 1954.

No. 702. FRANK J. MATHER III. Northerly Occurrences of Warm Water Fishes in the Western Atlantic. *Copeia*, No. 4, pp. 292–293. 1954.

No. 703. C. W. NEWTON. Analysis and Data Problems in Relation to Numerical Prediction. *Bull. Amer. Meteorol. Soc.*, Vol. 35, No. 7, pp. 287–294. 1954.

No. 704. GEORGE L. CLARKE. Elements of Ecology. John Wiley & Sons, Inc., New York 534 pp. 1904. (Not included in *Collected Reprints*.)

No. 705. L. VAN DAM. On the Respiration in Scallops (Lamellibranchiata). *Biol. Bull.*, Vol. 107, No. 2, pp. 192–202. 1954.

No. 706. JOANNE STARR MALKUS and R. S. SCORER. The Erosion of Cumulus Towers. *Jour. Meteorol.*, Vol. 12, No. 1, pp. 43–57. 1955.

No. 707. Athelstan F. Spilhaus. Sea and Air Resources. *Geogr. Rev.*, Vol. 44, No. 3, pp. 346–351. 1954.

No. 708. Charles J. Fish and Mary Curtis Cobb. Noxious Marine Animals of the Central and Western Pacific Ocean. Fish and Wildlife Service, *Research Report* 36, 45 pp., 1954.

No. 709. P. F. Scholander, Warner E. Love and John W. Kanwisher. The Rise of Sap in Tall Grapevines. *Plant Physiol.*, Vol. 30, No. 2, pp. 93–104. 1955. (Not included in *Collected Reprints.*)

No. 710. P. F. Scholander, L. van Dam and Susan I. Scholander. Gas Exchange in the Roots of Mangroves. *Amer. Jour. Bot.*, Vol. 42, No. 1, pp. 92–98. 1955.

No. 711. Duncan C. Blanchard. A Simple Method for the Production of Homogenouse Water Drops down to 1 Micron Radius. *Jour. Colloid Sci.*, Vol. 9, No. 4, pp. 321–328. 1954.

No. 712. John H. Ryther. Ecology of Autotrophic Marine Dinoflagellates with Refence to Red Water Conditions. In: The Luminescence of Biological Systems, F. H. Johnson, Edit., Publ. by Amer. Assoc. Adv. Sci., Washington, pp. 387–414. 1955.

No. 713. Henry Stommel. Serial Observations of Drift Currents in the Central North Atlantic Ocean. *Tellus*, Vol. 6, No. 3, pp. 203–214. 1954.

No. 715. Harry J. Turner, Jr. and J. Arthur Posgay. Sixth Report on Investigations of the Shellfisheries of Massachusetts. *Com. Mass., Dept. Nat. Res., Div. Mar. Fish.*, pp. 1–74. 1953.

No. 716. Joanne Starr Malkus and Claude Ronne. On the Structure of Some Cumulonimbus Clouds which Penetrated the High Tropical Troposphere. *Tellus*, Vol. 6, No. 4, pp. 351–366. 1954.

No. 717. L. V. Worthington. A Preliminary Note on the Time Scale in North Atlantic Circulation. *Deep-Sea Research.* Vol. 1, pp. 244–251. 1954.

No. 718. Arthur R. Miller. Some Suggestions for more precise Loran Navigation. *Navigation*, Vol. 3, Nos. 1 and 2, pp. 23–29. 1951. (Included in *Collected Reprints* for 1953.)

No. 719. Henry B. Bigelow and Isabel Pérez Farfante. Fishes of the Western North Atlantic. Lancelets. *Mem. Sears Found. Mar. Res.*, No. 1, Pt. 1, Ch. 1, pp. 1–28. 1948. (Not included in *Collected Reprints.*)

No. 720. Henry B. Bigelow and William C. Schroeder. Fishes of the Western North Atlantic. Cyclostomes. *Mem. Sears Found. Mar. Res.*, No. 1, Pt. 1, Ch. 2, pp. 29–58. 1948. (Not included in *Collected Reprints.*)

No. 721. Henry B. Bigelow and William C. Schroeder. Fishes of the Western North Atlantic. Sharks. *Mem. Sears Found. Mar. Res.*, No. 1, Pt. 1, Ch. 3, pp. 59–576. 1948. (Not included in *Collected Reprints.*)

No. 722. Arthur H. Clarke, Jr. Some Mollusks from the Continental Slope of Northeastern North America. *Breviora*, No. 40, 11 pp. 1954.

No. 723. C. W. Newton. Frontogenesis and Frontolysis as a Three-Dimensional Process. *Jour. Meteorology*, Vol. 11, No. 6, pp. 449–461. 1954.

No. 724. Charles B. Officer. Southwest Pacific Crustal Structure. *Trans. Amer. Geophys. Union*, Vol. 36, No. 3, pp. 449–459. 1955.

No. 725. K. G. Wilson and A. B. Arons. Osmotic Pressures of Sea Water Solutions Computed from Experimental Vapor Pressure Lowering. *Sears Found., Jour. Mar. Res.*, Vol.14, No. 2, pp. 195–198. 1955.

No. 726. Joanne Starr Malkus. On the Formation and Structure of Downdrafts in Cumulus Clouds. *Jour. Meteorol.*, Vol. 12, No. 4, pp. 350–354. 1955.

No. 727. Joanne Starr Malkus. The Effects of a Large Island upon the Trade-Wind Air Stream. *Quart. Jour. Roy. Meteor. Soc.*, Vol. 81, No. 350, pp. 538–550. 1955.

No. 728. Paul Ferris Smith. Further Measurements of the Sound Scattering Properties of Several Marine Organisms. *Deep-Sea Research*, Vol. 2, pp. 71–79. 1954.

No. 729. Willard Dow. Underwater Telemetering. *Deep-Sea Research*, Vol. 2, pp. 145–151 (erroneously dated 1954). 1955.

No. 730. John H. Ryther. Inhibitory Effects of Phytoplankton upon the Feeding of *Daphnia magna* with Reference to Growth, Reproduction, and Survival. *Ecology*, Vol. 35, No. 4, pp. 522–533. 1954.

No. 731. Charles B. Officer. A Deep-Sea Seismic Reflection Profile. *Geophysics*, Vol. 20, No. 2, pp. 270–282. 1955.

No. 732. Henry B. Bigelow and William C. Schroeder. Occurrence off the Middle and North Atlantic United States of the Offshore Hake *Merluccius albidus* (Mitchill) 1818, and of the Blue Whiting *Gadus (Micromesistius) poutassou* (Risso) 1826. *Bull. Mus. Comp. Zool.*, Vol. 113, No. 2, pp. 205–226. 1955.

No. 733. John H. Ryther. The Ratio of Photosynthesis to Respiration in Marine Plankton Algae and its Effect upon the Measurement of Productivity. *Deep-Sea Research*, Vol. 2, pp. 134–139 (erroneously dated 1954). 1955.

No. 734. Duncan C. Blanchard. Bursting of Bubbles at an Air-Water Interface. *Nature*, Vol. 173, p. 1048. 1954.

No. 735. Joseph Chase. Winds and Temperatures in Relation to the Brood-Strength of Georges Bank Haddock. *Jour. du Conseil*, Vol 21, No. 1, pp. 17–24. 1955.

No. 736. Grace I. Creitz and Francis A. Richards. The Estimation and Characterization of Plankton Populations by Pigment Analysis. III. A Note on the use of "Millipore" Membrane Filters in the Estimation of Plankton Pigments. *Sears Found., Jour. Mar. Res.*, Vol. 14, No. 3, pp. 211–216. 1955.

No. 737. Charles J. Fish. Preliminary Observations on the Biology of Boreo-Arctic and Subtropical Oceanic Zooplankton Populations. In: Symposium on Marine and Fresh-Water Plankton in the Indo-Pacific, Bangkok, Jan. 25–26, 1954, FAO-UNESCO, Sect. 1, No. 1, pp. 1–7, 1955. (Not included in *Collected Reprints.*)

No. 739. William G. Metcalf. On the Formation of Bottom Water in the Norwegian Basin. *Trans. Amer. Geophys. Union*, Vol. 36, No. 4, pp. 596–600. 1955.

No. 740. Andrew F. Bunker. Turbulence and Shearing Stresses Measured over the North Atlantic Ocean by an Airplane-Acceleration Technique. *Jour. Meteorol.*, Vol 12, No. 5, pp. 445–455. 1955.

No. 741. Wilbur Marks and F. Claude Ronne. Aerial Stereo-Photography and Ocean Waves. *Photogr. Engineering*, March 1955, pp. 107–110. 1955.

No. 742. Malcolm S. Gordon. Summer Ecology of Oceanic Birds off Southern New England. *The Auk*, Vol 72, pp. 138–147. 1955.

No. 743. Charles B. Officer. Geologic Interpretation of a Series of Seismic Reflection Profiles from Bermuda to the Continental Margins. *Deep-Sea Research*, Vol. 2, pp. 253–260. 1955.

No. 744. J. W. Kanwisher and Gordon Volkmann. A Scattering Layer Observation. *Science*, Vol. 121, No. 3134, pp. 108–109. 1955.

No. 745. Irving I. Schell. Interrelations of Arctic Ice with the Atmosphere and the Ocean in the North Atlantic — Arctic and Adjacent Areas. *Jour. Meteorol.*, Vol. 13, No. 1, pp. 46–58. 1956.

No. 746. H. G. Farmer, W. Marks, R. G. Walden and G. G. Whitney, Jr. A Technique for Ocean Wave Measurements. In: Proc. First Conf., Ships and Waves, Oct. 1954, Counc. Wave Res. and Soc. Naval Arch. and Mar. Eng., pp. 11–32. 1955.

No. 747. Duncan C. Blanchard. Electrified Droplets from the Bursting of Bubbles at an Air-Sea Water Interface. *Nature*, Vol. 175, No. 4451, pp. 334–336. 1955.

No. 749. F. C. Fuglister. Alternative Analyses of Current Surveys. *Deep-Sea Research*, Vol. 2, pp. 213–229. 1955.

No. 750. Gilbert L. Voss. The Cephalopoda Obtained by the Harvard-Havana Expedition off the Coast of Cuba in 1938–39. *Bull, Mar. Sci., Gulf and Caribbean*, Vol. 5, No. 2, pp. 81–115. 1955.

No. 751. Frank S. Essapian. Speed-Induced Skin Folds in the Bottle-Nosed Porpoise, *Tursiops truncatus*. *Breviora*, No. 43, 4 pp., 9 Pls. 1955.

No. 753. John P. Barlow. Physical and Biological Processes Determining the Distribution of Zooplankton in a Tidal Estuary. *Biol. Bull.*, Vol. 109, No. 2, pp. 211–225. 1955.

No. 754. Alan J. Faller. A Demonstration of Fronts and Frontal Waves in Atmospheric Models. *Jour. Meteorol.*, Vol. 13, No. 1, pp. 1–4. 1956.

No. 755. P. F. Scholander. Evolution of Climatic Adaptation in Homeotherms. *Evolution*, Vol. 9, No. 1, pp. 15–26. 1955.

No. 756. Hilary B. Moore. Variations in Temperature and Light Response within a Plankton Population. *Biol. Bull.*, Vol. 108, No. 2, pp. 175–181. 1955.

No. 757. A. H. Woodcock and W. A. Mordy. Salt Nuclei, Wind and Daily Rainfall in Hawaii. *Tellus*, Vol. 7, No. 3, pp. 291–300. 1955.

No. 758. Floyd M. Soule and J. E. Murray. Physical Oceanography of the Grand Banks Region and the Laborador Sea in 1954. *U. S. Coast Guard Bull.*, No. 40, pp. 79–168. 1955.

No. 759. Bostwick H. Ketchum, Nathaniel Corwin and D. Jean Keen. The Significance of Organic Phosphorus Determinations in Ocean Waters. *Deep-Sea Research*, Vol. 2, pp. 172–181. 1955.

No. 760. Dean F. Bumpus and E. Lowe Pierce. The Hydrography and the Distribution of Chaetognaths over the Continental Shelf off North Carolina. Pap. Mar. Biol. and Oceanogr., *Deep-Sea Research*, Suppl. to Vol. 3, pp. 92–109. 1955. (Included in *Collected Reprints* for 1955, Part II.)

No. 761. A. H. Woodcock. Bursting Bubbles and Air Pollution. *Sewage and Industrial Wastes*, Vol. 27, No. 10, pp. 1189–1192. 1955.

No. 762. Gordon A. Riley. Review of the Oceanography of Long Island Sound. Pap. Mar. Biol. and Oceanogr., *Deep-Sea Research*, Suppl. to Vol. 3, pp. 224–238. 1955. (Included in *Collected Reprints* for 1955, Part II.)

No. 763. Talbot H. Waterman. Polarization of Scattered Sunlight in Deep Water. Pap. Mar. Biol. and Oceanogr., *Deep-Sea Research*, Suppl. to Vol. 3, pp. 426–434. 1955. (Included in *Collected Reprints* for 1955, Part II.)

No. 764. E. M. Hulburt. The Phytoplankton of Great Pond, Massachusetts. *Biol. Bull.*, Vol. 110, No. 2, pp. 157–168. 1956.

No. 765. C. O'D. Iselin. Recent Advances in our Understanding of the Circulation Problem and their Implications. *Sears Found., Jour. Mar. Res.*, Vol. 14, No. 4, pp. 315–322. 1955.

No. 766. John C. Ayers. Population Dynamics of the Marine Clam, *Mya arenaria*. *Limnol. and Oceanogr.*, Vol. 1, No. 1, pp. 26–34. 1956.

No. 767. Edward M. Thorndike. Hydroscopes. *Trans. Amer. Geophys. Union*, Vol. 36, No. 3, pp. 470–472. 1955.

No. 768. A. H. Woodcock and D. C. Blanchard. Tests of the Salt-Nuclei Hypothesis of Rain Formation. *Tellus*, Vol. 7, No. 4, pp. 437–448. 1955.

No. 770. C.-G. Rossby and H. Egnér. On the Chemical Climate and its Variation with Atmospheric Circulation Pattern. *Tellus*, Vol. 7, No. 1, pp. 118–133. 1955.

No. 771. Stefan Machlup and J. B. Hersey. Analysis of Sound-Scattering Observations from Non-Uniform Distributions of Scatterers in the Ocean. *Deep-Sea Research*, Vol. 3, pp. 1–22. 1955.

No. 772. Bostwick H. Ketchum. Distribution of Coliform Bacteria and other Pollutants in Tidal Estuaries. *Sewage and Industrial Wastes*, Vol. 27, No. 11, pp. 1288–1296. 1955.

No. 773. Susan I. Scholander. Land Birds over the Western North Atlantic. *The Auk*, Vol. 72, pp. 225–239. 1955.

No. 774. Harvey R. Bullis, Jr. and F. J. Mather, III. Tunas of the Genus *Thunnus* of the Northern Caribbean. *Novitates*, No. 1765, 12 pp. 1956.

No. 775. Bostwick H. Ketchum and D. Jean Keen. The Accumulation of River Water over the Continental Shelf between Cape Cod and Chesapeake Bay. Pap. Mar. Biol. and Oceanogr., *Deep-Sea Research*, Suppl. to Vol. 3, pp. 346–357. 1955. (Included in *Collected Reprints* for 1955, Part II.)

No. 776. Alfred C. Redfield. The Hydrography of the Gulf of Venezuela. Pap. Mar. Biol. and Oceanogr., *Deep-Sea Research*, Suppl. to Vol. 3, pp. 115–133. 1955. (Included in *Collected Reprints* for 1955, Part II.)

No. 777. Harry J. Turner, Jr. How Clam Drills Capture Razor Clams. *The Nautilus*, Vol. 69, No. 1, pp. 20–22. 1955.

No. 778. J. W. Kanwisher. Freezing in Intertidal Animals. *Biol. Bull.*, Vol. 109, No. 1, pp. 56–63. 1955.

No. 779. Ruth D. Turner. Scaphopods of the *Atlantis* Dredgings in the Western Atlantic with a Catalogue of the Scaphopod Types in the Museum of Comparative Zoology. Pap. Mar. Biol. and Oceanogr., *Deep-Sea Research*, Suppl. to Vol. 3, pp. 309–320. 1955. (Included in *Collected Reprints* for 1955, Part II.)

No. 780. E. STEEMANN NIELSEN. The Production of Antibiotics by Plankton Algae and its Effect upon Bacterial Activities in the Sea. Pap. Mar. Biol. and Oceanogr., *Deep-Sea Research*, Suppl. to Vol. 3, pp. 281–286. 1955. (Included in *Collected Reprints* for 1955, Part II.)

No. 781. W. T. EDMONDSON. Factors Affecting Productivity in Fertilized Water. Pap. Mar. Biol. and Oceanogr., *Deep-Sea Research*, Suppl. to Vol. 3, pp. 451–464. 1955. (Included in *Collected Reprints* for 1955, Part II.)

No. 782. HENRY C. STETSON. Patterns of Deposition at the Continental Margin. Pap. Mar. Biol. and Oceanogr., *Deep-Sea Research*, Suppl. to Vol. 3, pp. 298–308. 1955. (Included in *Collected Reprints* for 1955, Part II.)

No. 783. HARRY J. TURNER, JR. and STANLEY SCHER. Seventh Report on Investigations of the Shellfisheries of Massachusetts. *Com. Mass., Dept. Nat. Res., Div. Mar. Fish.*, 35 pp. 1954.

No. 785. EARL BARRETT and GUNNAR BRODIN. The Acidity of Scandinavian Precipitation. *Tellus*, Vol. 7, No. 2, pp. 251–257. 1955.

No. 786. T. F. GOREAU and V. T. BOWEN. Calcium Uptake by a Coral. *Science*, Vol. 122, No. 3181, pp. 1188–1189. 1955.

No. 787. HENRY B. BIGELOW, WILLIAM C. SCHROEDER and STEWART SPRINGER. Three New Shark Records from the Gulf of Mexico. *Breviora*, No. 49, 12 pp. 1955.

No. 788. DEAN F. BUMPUS. The Circulation over the Continental Shelf South of Cape Hatteras. *Trans. Amer. Geophys. Union*, Vol. 36, No. 4, pp. 601–611. 1955.

No. 789. DONALD R. GRIFFIN. Hearing and Acoustic Orientation in Marine Animals. Pap. Mar. Biol. and Oceanogr., *Deep-Sea Research*, Suppl. to Vol. 3, pp. 406–417. 1955. (Included in *Collected Reprints* for 1955, Part II.)

No. 790. WILLIAM C. SCHROEDER. Report on the Results of Exploratory Otter-Trawling along the Continental Shelf and Slope between Nova Scotia and Virginia during the Summers of 1952 and 1953. Pap. Mar. Biol. and Oceanogr., *Deep-Sea Research*, Suppl. to Vol. 3, pp. 358–372. 1955. (Included in *Collected Reprints* for 1955, Part II.)

No. 791. L. V. WORTHINGTON. A New Theory of Caribbean Bottom-Water Formation. *Deep-Sea Research*, Vol. 3, pp. 82–87. 1955.

No. 792. C. O'D. ISELIN. Coastal Currents and the Fisheries. Pap. Mar. Biol. and Oceanogr., *Deep-Sea Research*, Suppl. to Vol. 3, pp. 474–478. 1955. (Included in *Collected Reprints* for 1955, Part II.)

No. 793. BARBARA LAWRENCE and WILLIAM E. SCHEVILL. The Functional Anatomy of the Delphinid Nose. *Bull. Mus. Comp. Zool.*, Vol. 114, No. 4, pp. 103–151. 1956. (Not included in *Collected Reprints*.)

No. 794. WILLIAM S. VON ARX and W. S. RICHARDSON. On the Fine-Structure of the Gulf Stream Front. *Deep-Sea Research*, Vol. 3, pp. 46–65. 1955.

No. 795. P. F. SCHOLANDER, L. VAN DAM, C. LLOYD CLAFF and J. W. KANWISHER. Micro Gasometric Determination of Dissolved Oxygen and Nitrogen. *Biol. Bull.*, Vol. 109, No. 2, pp. 328–334. 1955.

No. 796. HENRY STOMMEL. Lateral Eddy Viscosity in the Gulf Stream System. *Deep-Sea Research*, Vol. 3, pp. 88–90. 1955.

No. 797. Irving I. Schell. Further Evidence of Dynamic Persistence and of its Application to Foreshadowing. *Jour. Meteorol.*, Vol. 13, No. 5, pp. 471–481. 1956.

No. 798. Nora Gladwin Fairbank. Methods and Preliminary Results in a Study of Minerals from the Eastern Gulf of Mexico. *Jour. Sed. Petrol.*, Vol. 26, No. 3, pp. 268–275. 1956.

No. 799. Henry Stommel, Arnold B. Arons and Duncan Blanchard. An Oceanographical Curiosity: the Perpetual Salt Fountain. *Deep-Sea Research*, Vol. 3, pp. 152–153. 1956.

No. 801. Floyd M. Soule and J. E. Murray. Physical Oceanography of the Grand Banks and the Labrador Sea in 1955. *U. S. Coast Guard Bull.*, No. 41, pp. 59–114. 1956.

No. 802. James M. Moulton and Richard H. Backus. Annotated References Concerning the Effects of Man-Made Sounds on the Movements of Fishes. *Dept. Sea and Shore Fish.*, Augusta, Maine, Fish. Circ. No. 17, 8 pp. 1955.

No. 804. W. V. R. Malkus. Outline of a Theory of Turbulent Shear Flow. *Jour. Fluid Mech.*, Vol. 1, Pt. 5, pp. 521–539. 1956.

No. 805. John Mackiewicz and Richard H. Backus. Oceanic Records of *Lasionycteris noctivagans* and *Lasiurus borealis*. *Jour. Mammalogy*, Vol. 37, No. 3, pp. 442–443. 1956.

No. 806. Allyn C. Vine. Oceanographic Instrumentation. *Science*, Vol. 122, No. 3173, pp. 748–751. 1955.

No. 807. P. F. Scholander and William E. Schevill. Counter-Current Vascular Heat Exchange in the Fins of Whales. *Jour. Appl. Physiol.*, Vol. 8, No. 3, pp. 279–282. 1955.

No. 808. E. Steemann Nielsen. The Interaction of Photosynthesis and Respiration and its Importance for the Determination of ^{14}C-Discrimination in Photosynthesis. *Physiologia Plantarum*, Vol. 8, pp. 945–953. 1955.

No. 810. Karl E. Schleicher and Alvin Bradshaw. A Conductivity Bridge for Measurement of the Salinity of Sea Water. *Jour. du Conseil*, Vol. 22, No. 1, pp. 9–20. 1956.

No. 811. G. W. Morgan. On the Wind-Driven Ocean Circulation. *Tellus*, Vol. 8, No. 3, pp. 301–320. 1956.

No. 814. Richard H. Backus, Stewart Springer and Edgar L. Arnold, Jr. A Contribution to the Natural History of the White-Tip Shark, *Pterolamiops longimanus* (Poey). *Deep-Sea Research*, Vol. 3, pp. 178–188. 1956.

No. 815. William E. Schevill. *Lagenorhynchus acutus* off Cape Cod. *Jour. Mammalogy*, Vol. 37, No. 1, pp. 128–129. 1956.

No. 816. P. F. Scholander, L. van Dam and Theodore Enns. Nitrogen Secretion in the Swimbladder of Whitefish. *Science*, Vol. 123, No. 3185, pp. 59–60. 1956.

No. 817. Harold E. Edgerton and Lloyd D. Hoadley. Cameras and Lights for Underwater Use. *Jour. Soc. Motion Pic. and Tel. Eng.*, Vol. 64, pp. 345–350. 1955.

No. 818. P. F. Scholander, John W. Kanwisher and D. C. Nutt. Gases in Icebergs. *Science*, Vol. 123, No. 3186, pp. 104–105. 1956.

No. 819. John H. Ryther. Photosynthesis in the Ocean as a Function of Light Intensity. *Limnol. and Oceanogr.*, Vol. 1, No. 1, pp. 61–70. 1956.

No. 821. George L. Clarke and Gunther K. Wertheim. Measurements of Illumination at Great Depths and at Night in the Atlantic Ocean by Means of a New Bathyphotometer. *Deep-Sea Research*, Vol. 3, pp. 189–205. 1956.

No. 822. P. F. Scholander. Hydrostatic Pressure in Coconuts. *Plant Physiol.*, Vol. 30, No. 6, pp. 560–561. 1955.

No. 823. John C. Ayers. A Dynamic Height Method for the Determination of Currents in Deep Lakes. *Limnol. and Oceanogr.*, Vol. 1, No. 3, pp. 150–161. 1956.

No. 824. Parker D. Trask. The *Atlantis* Marine Geological Expedition to Peru and Chile. *Nature*, Vol. 177, pp. 454–455. 1956.

No. 825. John H. Ryther. The Measurement of Primary Production. *Limnol. and Oceanogr.*, Vol. 1, No. 2, pp. 72–84. 1956.

No. 826. Robert L. Miller. Trend Surfaces: Their Application to Analysis and Description of Environments of Sedimentation. 1. The Relation of Sediment-Size Parameters to Current-Wave Systems and Physiography. *Jour. Geology*, Vol. 64, No. 5, pp. 425–446. 1956.

No. 827. Joanne Starr Malkus. On the Maintenance of the Trade Winds. *Tellus*, Vol. 8, No. 3, pp. 335–350. 1956.

No. 830. Francis A. Richards and Ralph F. Vaccaro. The Cariaco Trench, an Anaerobic Basin in the Caribbean Sea. *Deep-Sea Research*, Vol. 3, pp. 214–228. 1956.

No. 831. David C. Nutt and Lawrence K. Coachman. The Oceanography of Hebron Fjord, Labrador. *Jour. Fish. Res. Bd. Canada*, Vol. 13, No. 5, pp. 709–758. 1956.

No. 832. William E. Schevill and Barbara Lawrence. Food-Finding by a Captive Porpoise (*Tursiops truncatus*). *Breviora*, No. 53, 15 pp. 1956.

No. 834. Richard H. Backus and J. B. Hersey. Echo-Sounder Observations of Midwater Nets and their Towing Cables. *Deep-Sea Research*, Vol. 3, pp. 237–241. 1956.

No. 837. A. H. Woodcock. Dimorphism in the Portuguese Man-of-War. *Nature*, Vol. 178, No. 4527, pp. 253–255. 1956.

No. 840. Francis A. Richards. On the State of our Knowledge of Trace Elements in the Ocean. *Geochimica et Cosmochimica Acta*, Vol. 10, No. 4, pp. 241–243. 1956.

No. 841. Henry R. Johnson, Richard H. Backus, J. B. Hersey and D. M. Owen. Suspended Echo-Sounder and Camera Studies of Midwater Sound Scatterers. *Deep-Sea Research*, Vol. 3, pp. 266–272. 1956.

No. 842. John H. Ryther. Interrelation between Photosynthesis and Respiration in the Marine Flagellate, *Dunaliella euchlora*. *Nature*, Vol. 178, pp. 861–862. 1956.

No. 846. Henry Stommel. On the Determination of the Depth of No Meridional Motion. *Deep-Sea Research*, Vol. 3, pp. 273–278. 1956.

No. 847. Athelstan Spilhaus. Control of the World Environment. *Geogr. Rev.*, Vol. 46, No. 4, pp. 451–459. 1956.

No. 852. Francis A. Richards and Nathaniel Corwin. Some Oceanographic Applications of Recent Determinations of the Solubility of Oxygen in Sea Water. *Limnol. and Oceanogr.*, Vol. 1, No. 4, pp. 263–267. 1956.

No. 853. Irving I. Schell. On the Nature and Origin of the Southern Oscillation. *Jour. Meteorol.*, Vol. 13, No. 6, pp. 592–598. 1956.

No. 855. A. B. Arons and Henry Stommel. A β-Plane Analysis of Free Periods of the Second Class in Meridional and Zonal Oceans. *Deep-Sea Research*, Vol. 4, pp. 23–31. 1956.

No. 856. Gordon Volkmann, John Knauss and Allyn Vine. The Use of Parachute Drogues in the Measurement of Subsurface Ocean Currents. *Trans. Amer. Geophys. Union*, Vol. 37, No. 5, pp. 573–577. 1956.

No. 858. George L. Clarke and Richard H. Backus. Measurements of Light Penetration in Relation to Vertical Migration and Records of Luminescence of Deep-Sea Animals. *Deep-Sea Research*, Vol. 4, pp. 1–14. 1956.

No. 859. G. Veronis and Henry Stommel. The Action of Variable Wind Stresses on a Stratified Ocean. *Sears Found., Jour. Mar. Res.*, Vol. 15, No. 1, pp. 43–75. 1956.

No. 862. James M. Moulton. Influencing the Calling of Sea Robins (*Prionotus* spp.) with Sound. *Biol. Bull.*, Vol. 111, No. 3, pp. 393–398. 1956.

No. 863. S. T. Knott and J. B. Hersey. Interpretation of High-Resolution Echo-Sounding Techniques and their Use in Bathymetry, Marine Geophysics, and Biology. *Deep-Sea Research*, Vol. 4, pp. 36–44. 1956.

No. 864. H. B. Moore and E. G. Corwin. The Effects of Temperature, Illumination, and Pressure on the Vertical Distribution of Zooplankton. *Bull. Mar. Sci., Gulf and Caribbean*, Vol. 6, No. 4, pp. 273–287. 1956.

No. 865. Richard S. Edwards and Francis A. Richards. A Bottom-Water Sampler. *Deep-Sea Research*, Vol. 4, pp. 65–66. 1956.

No. 867. Irving Friedman, Daniel R. Norton, Douglas B. Carter and Alfred C. Redfield. The Deuterium Balance of Lake Maracaibo. *Limnol. and Oceanogr.*, Vol. 1, No. 4, pp. 239–246. 1956.

No. 869. Helen S. Vishniac. On the Ecology of the Lower Marine Fungi. *Biol. Bull.*, Vol. 111, No. 3, pp. 410–414. 1956.

No. 873. Lawrence K. Coachman, E. Hemmingsen and P. F. Scholander. Gas Enclosures in a Temperate Glacier. *Tellus*, Vol. 8, No. 4, pp. 415–423. 1956. (Not included in *Collected Reprints*.)

No. 876. Harry J. Turner, Carl J. George and Joseph H. Connell. Eighth Report on Investigations of the Shellfisheries of Massachusetts. *Com. Mass., Dept. Nat. Res., Div. Mar. Fish.*, 25 pp. 1955.

No. 879. P. F. Scholander and L. van Dam. Micro Gasometric Determination of Oxygen in Fish Blood. *Jour. Cell. and Comp. Physiol.*, Vol. 48, No. 3, pp. 529–532. 1956.

No. 880. P. F. Scholander. Observations on the Gas Gland in Living Fish. *Jour. Cell. and Comp. Physiol.*, Vol. 48, No. 3, pp. 523–528. 1956.

No. 881. P. F. Scholander, L. van Dam and Theodore Enns. The Source of Oxygen Secreted into the Swimbladder of Cod. *Jour. Cell. and Comp. Physiol.*, Vol. 48, No. 3, pp. 517–522. 1956.